Journal Pre-proof



Photoperiod strategies to increase microalgae-pigment content: A new level-up to natural food colorants production

Tatiele Casagrande do Nascimento, Pricila Nass Pinheiro, Mariany Costa Deprá, Rafaela Basso Sartori, Maria Roca, Eduardo Jacob-Lopes, Leila Queiroz Zepka

PII: S2211-9264(25)00296-6

DOI: https://doi.org/10.1016/j.algal.2025.104185

Reference: ALGAL 104185

To appear in: *Algal Research*

Received date: 27 February 2025

Revised date: 17 June 2025

Accepted date: 1 July 2025

Please cite this article as: T.C. do Nascimento, P.N. Pinheiro, M.C. Deprá, et al., Photoperiod strategies to increase microalgae-pigment content: A new level-up to natural food colorants production, *Algal Research* (2024), https://doi.org/10.1016/j.algal.2025.104185

This is a PDF file of an article that has undergone enhancements after acceptance, such as the addition of a cover page and metadata, and formatting for readability, but it is not yet the definitive version of record. This version will undergo additional copyediting, typesetting and review before it is published in its final form, but we are providing this version to give early visibility of the article. Please note that, during the production process, errors may be discovered which could affect the content, and all legal disclaimers that apply to the journal pertain.

© 2025 Published by Elsevier B.V.

Journal Pre-proof

Photoperiod Strategies to Increase Microalgae-Pigment Content: A New Level-Up to Natural Food Colorants Production

Tatiele Casagrande do Nascimento[a], Pricila Nass Pinheiro[a], Mariany Costa Deprá[a], Rafaela Basso Sartori[a], Maria Roca[b], Eduardo Jacob-Lopes[a], Leila Queiroz Zepka[a*]

[a]Food Science and Technology Department, Federal University of Santa Maria, Santa Maria, RS, Brazil.

[b]Food Phytochemistry Department, Instituto de la Grasa, Consejo Superior de Investigaciones Científicas, University Campus, Sevilla, Spain.

*Corresponding author: zepkaleila@yahoo.com.br

Abstract: This study investigates the influence of different photoperiods on the pigment profiles of the microalgae *Scenedesmus obliquus*, focusing on maximizing the production of carotenoids and chlorophylls. Experiments were conducted under three photoperiod regimes:(i) Long-term (h:h) – light:dark cycles of 10:14, 12:12, 18:6, 20:4, 22:2, and 24:0 hours; (ii) Frequencies (t/d): based on a previously defined optimal light/dark cycle of 22:2 h – in this setup, the 2 h of darkness were subdivided into 2, 4, 8, 12, 24, and 48 times per day, resulting in increasingly frequent light/dark transitions; and (iii) Short-term (s:s) – light:dark cycles in on second with ratios of 0.91:0.09, 0.83:0.17, 0.75:0.25, and 0.50:0.50. The short-term photoperiod of 0.91:0.09 proved to be the most effective condition for the overall maximization of pigments, standing out especially for the accumulation of all-*trans*-lutein (7.14 g/kg), and chlorophyll *a* (46.32 g/kg). In contrast, long-term photoperiods favored the accumulation of chlorophyll *b'*, and pheophytin *b* (12:12 h), 9-*cis*-violaxanthin (18:6 h), and antheraxanthin (20:4 h). On the other hand, the application of frequencies proved to be, in general, an unfavorable strategy for the total accumulation of pigments. However, productivity metrics revealed that the 4 t/d frequency was the most efficient for volumetric biomass production (3.85 mg/L), while the 0.91:0.09 h photoperiod provided the best results for carotenoid (31.84 mg/L) and total chlorophyll (165.11 mg/L). Finally, it is suggested that specific adjustments to the lighting

Journal Pre-proof

regime can optimize the accumulation and productivity of natural pigments for industrial application, especially in conditions of very rapid light:dark alternations.

Keywords: *Scenedesmus obliquus*, Natural Colorants, Chlorophylls, Carotenoids, Foods.

1. Introduction

In an era of impending ecocide, microalgae are promising microscopic organisms that represent a disruptive solution to supply the ingredients production demanded by the food industry [1]. Their multifaceted role allows for improving product quality while meeting the demands for a more conscious, balanced, and eco-friendly diet [2]. Rich in bioactive compounds, they offer a robust nutritional profile capable of meeting global trends for healthier and more functional foods that, unlike conventional sources, are independent of climate conditions [3].

To address global concerns about the current mass environmental degradation [4], potential cultivation methods that require fewer natural resources can be carried out under harsh conditions, and can significantly contribute to environmental sustainability from microalgae. Furthermore, these microorganisms are considered excellent biofactories of natural pigments and thus align with the trend of replacing synthetic colorants with natural alternatives [5]. A wide range of pigments, such as carotenoids and chlorophylls, are abundant in microalgae and provide not only specific colors but also noteworthy bioactive characteristics [6–12].Thus, when utilized as natural food colorants, these pigments, besides enhancing the visual appeal of food items, they contribute to positive health impacts.

The photoperiod regime is one of the key parameters that can regulate pigment production in microalgae [13–16]. Microalgae pigment profiles can be optimized by varying these light-dark cycles, enabling the yield and quality of colorants that can be

used in a variety of food applications. However, the relationship between the application of light and pigment production is complex, involving intricate biological responses that can affect both the quantity and composition of pigments [9].

Among the exploited microalgae species, *S. obliquus* is a recognized robust strain that is highly used in bio-based processes [17,18]. Technologically important pigments such as lutein and chlorophyll *a* are reported to be predominant in the biomass of *S. obliquus*. However, the pigment profile can be changed according to the cultivation configuration used [11,19,20].

Given the above, it is believed that knowledge of these dynamics can establish solid foundations for the productive cultivation of microalgae colorants that meet the food industry's demands under the precepts of health and sustainability. Thus, this study aimed to explore the impact of different photoperiods (long-term, frequencies, and short-term) on the pigments produced by *S. obliquus*, focusing on identifying conditions that improve the production of pigments with high potential for use as natural food colorants.

2. Material and Methods

2.1. Chemicals and reagents

All chemical compounds used for the BG-11 medium, sodium chloride, ammonium acetate (98%), and tetrabutylammonium acetate were supplied by Sigma-Aldrich Chemical Co. Acetonitrile was supplied by Panreac Química SLU (Barcelona, Spain). N, N-dimethylformamide (DMF) was provided by Scharlab (Barcelona, Spain). Other reagents were supplied by VWR BDH Chemicals (United States of America). Chlorophyll pigment standards: chlorophyll *a* and *b*, pheophorbide *a*, pheophytin *a* and *b* were provided by Cymit SL (Barcelona, Spain). The remaining standards were

obtained following a previous protocol [21]. The β-carotene standard was obtained from Extrasynthese (Genay Cedex, France), while other carotenoid standard solutions were obtained from natural sources following the procedures described by [22].

2.2. Microorganisms and culture media

Axenic cultures of *S. obliquus* (CPCC05) were obtained from the Canadian Collection of Psychocultural Culture at the University of Toronto, Canada. Stock cultures were propagated on solidified agar-agar (20 g/L) containing synthetic BG-11 medium [23]. Incubation conditions were 26°C, photon flux density of 30 μmol $m^{-2}.s^{-1}$, and a photoperiod of 12 h.

2.3. Photobioreactor design

Microalgal cultures were conducted in a bubble column photobioreactor (Tecnal, Piracicaba, Brazil). The system was constructed of 4 mm thick glass with an internal diameter of 7.5 cm, a height of 75 cm, and a nominal working volume of 2.0 L. The dispersion system for the reactor consisted of a 1.5 cm diameter air diffuser located in the center of the column. The reactor was illuminated with forty-five 0.23 W LED lamps (total consumption of 0.01125 kWh), located in a photoperiod chamber. The CO_2/air mixture was adjusted to achieve the desired concentration of carbon dioxide in the air stream, by means of three rotameters that measured the flow rates of carbon dioxide, air, and gas mixture, respectively.

2.4. Experimental conditions

Experiments were conducted in a batch mode bioreactor (photobioreactor bubble column -Tecnal, Piracicaba-SP, Brazil) fed with 2.0 L of synthetic BG-11 medium. The

experimental conditions were: isothermal reactor operating at a temperature of 26°C, photon flux density of 150 μmol /m^2s^1, continuous aeration of 1VVM (volume of air per volume of culture per minute) with the injection of air enriched with 15% carbon dioxide, and initial cell concentration of 100 mg/L [24]. The culture pH was initially adjusted to 7.6 and remained stable throughout the experiment, ranging from 7.0 to 8.0 ± 0.2, due to the natural buffering capacity of the microalga. Different photoperiods were evaluated, including short- and long-duration cycles, as well as the effect of varying frequencies of light/dark transitions on pigment production. The study was carried out with consideration for the work cycle and the photosynthetic photon flux density (PPFD).

For the long-term photoperiod assays, the light:dark cycles applied were 24:0, 22:2, 20:4, 18:6, 12:12, and 10:14 (h:h). In the frequency-modulated light/dark experiments, cells were exposed to 22 hours of light and 2 hours of darkness (previously identified as the optimal condition), with the 2-hour dark period distributed across six different frequencies: 2, 4, 8, 12, 24, and 48 transitions per day (t/d). For the short-term photoperiod assays, four different cycles were tested on a per-second basis: 0.91:0.09, 0.83:0.17, 0.75:0.25, and 0.50:0.50 (light:dark). A diagram summarizing the experimental design is provided in Supplementary Material 1.

The experiments with long-term photoperiods were (h:h): 10:14, 12:12, 18:6, 20:4, 22:2, 24:0 (light:dark). In experiments of light/dark cycle frequency, cells were exposed to 22 hours of light and 2 hours of darkness (previously defined optimal condition). These 2 hours were divided into six frequencies: 2, 4, 8, 12, 24, and 48 times per day (t/d). To study the effects of short-term photoperiods (s/s), four different cycles of 0.91:0.09, 0.83:0.17, 0.75:0.25, and 0.50:0.50 (light:dark) were defined every second.

The biomass was collected at the end of the stationary phase, with cultivation times ranging from 144 to 192 hours (all kinetic parameters are available in Supplementary Material 2). The biomass was separated from the culture medium by centrifugation at 1500× g, 10°C, for 10 min (model D-37520, Thermo, Langenselbold, Germany). Afterward, the obtained paste was frozen at -18°C for 24 hours and lyophilized for 24 hours at -50°C above -175 μm Hg. Samples were stored under refrigeration until the pigment extraction step.

2.5. Pigments extraction

The lyophilized microalgae biomass (10 mg) was extracted with 50 mL of DMF saturated with Mg_2CO_3 to exhaustion. Afterward, the remaining biomass was re-extracted with 50 mL of methanol to exhaustion again. The obtained extracts were mixed with 100 mL of diethyl ether and 400 mL of 10% NaCl solution (w/v) in a separation funnel. The mixture was shaken and then left to rest until complete separation of the organic layer was observed. Then, the solvent phase was washed three times with 400 mL of 10% NaCl solution (w/v). In sequence, pigments were transferred to diethyl ether and NaCl, and the same protocol described above was applied. The extracts were concentrated in a rotary evaporator under vacuum at 30°C to dryness, and the dry residue was dissolved in acetone for immediate HPLC analysis.

2.6. Pigments identification by liquid chromatography/electrospray-APCI ionization/high-resolution-time-of-flight mass spectrometry.

Chromatographic separation was performed in a Dionex Ultimate3000RS UHPLC (Thermo Fisher Scientific, Waltham, MA, USA). The column used was a Mediterranea Sea18 column (200 × 4.6 mm, 3 μm particle size) (Teknokroma,

Journal Pre-proof

Barcelona, Spain), protected by a guard column (10 × 4.6 mm) filled with the same material. Chromatographic separation was performed using the elution gradient described by [21,25] with the mobile phases: A, water/1 M ammonium acetate in water/methanol (1/1/8, v/v/v) and B, methanol/acetone (1/1, v/v). Online UV–Visible spectra were recorded from 350 to 800 nm with the photodiode array detector, and sequential detection was performed at 410, 430, 450, and 666 nm. The HPLC/ESI-HRQqTOF operated for mass analysis using a micrOTOF-QII High-Resolution Time-of-Flight mass spectrometer (HR-TOF) with Qq-TOF geometry (Bruker Daltonics, Bremen, Germany) equipped with electrospray ionization (ESI) interface for polar chlorophylls and with an APCI interface for non-polar chlorophylls and carotenoids. The instrument control was performed using Bruker Daltonics HyStar 3.2. Mass spectra were acquired in bbCID mode and data were used to perform multitarget-screening using TargetAnalysis 1.2 software (Bruker Daltonics, Bremen, Germany). Data evaluation was performed with Bruker Daltonics DataAnalysis 4.1. The experimental values of mass to charge ratio and isotopic pattern corresponding to those elemental compositions were compared with the theoretical data, obtaining the mass error and mSigma values, which should be below the tolerance limits (mass error < 5 ppm, and mSigma value < 50). The consistency of the elemental composition and formulas of the experimental product ions was checked by applying the same procedure to the product ions and with the assistance of the SmartFormula3D algorithm [25].

2.7. Pigments quantification by HPLC-UV-Visible

Identified carotenoids and chlorophylls were quantified by reverse-phase HPLC using Agilent 1260 liquid chromatograph after the chromatographic separation described above. Subsequently, data were collected and processed with an OpenLab

CDS software (C.01.07; Santa Clara, CA, USA). Pigment quantification was performed with corresponding calibration curves (quantity × integrated peak area). Calibration equations were obtained by least squares linear regression analysis over a concentration range according to the observed levels of these pigments in the samples. Triplicate injections were made for five different volumes of each standard solution.

2.8. Productivity Metrics

Productivity metrics were estimated based on the relationship between the pigment content of the biomass and the maximum cell concentration (X_{max}) achieved in each experimental condition (refer to supplementary material). Productivity results are expressed in milligrams of pigment per liter of microalgae culture (mg/L).

2.9. Statistical analysis

The analysis was performed using Statistica 10.0 software (Statsoft, Tulsa-OK, USA). The significance of the experimental data was determined using one-way ANOVA followed by Tukey's test ($p < 0.05$). In addition, all data were submitted to Principal Component Analysis (PCA) in the same software. The experiments were performed in triplicate, and the data refer to the mean value of the six repetitions.

3. Results and discussion

3.1. Pigment profile under different photoperiod conditions

The characteristics of the chromatographic and mass spectrometric data for the carotenoids and chlorophylls analyzed in the present study are shown in Table 1. A total of 26 compounds were separated in all experiments (15 chlorophylls and 11 carotenoids). The identification of pigments was based on chemical evidence provided

Journal Pre-proof

by chromatographic analysis, such as elution order, UV-Visible spectra, and MS high-accuracy measurements, including mass error, isotopic pattern, and the featured product ions. This chemical evidence was compared with authentic standards or those isolated from natural sources. Furthermore, the pigments were identified considering a detailed description previously reported in the literature [20,21,26,27].

[Insert Table 1]

The microalgae *S. obliquus* presents a chlorophyll profile characteristic of the *Chlorophyta* taxon, generally composed of chlorophyll *a* and *b* series [18,28]. A total of nine and six chlorophylls of the *a* and *b* series were identified, respectively. Additionally, a detailed analysis revealed the presence of metabolites such as chlorophyllides (peaks 1-3), pheophorbide (peak 4), hydroxychlorophylls (peaks 15, 18, 21), pheophytins (peaks 21-24), oxidized derivative (peak 14) and epimers (peaks 3, 17, 20, 24). Among the metabolites, mainly in algae, chlorophyllides can be considered a precursor of chlorophylls [29]. The other metabolites are a consequence of the degradation pathway or may result of oxidative stress derived from different cultivation conditions and extraction methods [9].

Regarding the carotenoid profile, the main component identified in all experiments was all-*trans*-lutein (peak 12). Smaller amounts were detected — varying according to the photoperiod condition used — of carotenes (peaks 25 and 26) and xanthophylls, including neoxanthin (peaks 5 and 6), violaxanthin (peaks 7 and 9), luteoxanthin (peak 8), antheraxanthin (peak 10), *cis*-lutein (peak 13) and mutatoxanthin (peak 11), which represents another recurrent characteristic for this taxonomic group of green algae.

3.2. Global pigment content and impact on coloration

Journal Pre-proof

Measuring the overall content of carotenoids and chlorophylls is crucial for understanding microalgae adaptation to light and, more importantly, for optimizing industrial processes such as the production of natural colorants.

In terms of total chlorophyll content (Figure 1A), total chlorophylls of *a* (Figure 1B) and *b* (Figure 1C) series, the short-term photoperiod 0.91:0.09 (63.74 g/kg) yielded the highest amounts, differing statistically ($\rho<0.05$) from all other tested photoperiods. In contrast, the 12t/d (8.10 g/kg) frequency exhibited the lowest total chlorophyll levels.

[Insert Figure 1]

This trend is also observed when examining total degradation metabolites (Figure 1D). Except for the high total of oxidized chlorophylls (1.27 g/kg) obtained for the long-term photoperiod (12:12), the 0.91:0.09 resulted in the highest content of pheophytins (10.92 g/kg) and pheophorbide (0.89 g/kg).

Regarding colorant effects, this information is extremely relevant since these derivatives exhibit coloration that varies according to their structural characteristics. Consequently, when fractionated, they may have distinct applications in the food industry, such as coloring bakery products, confectionery, beverages, and dairy items, for example. As shown in Figure 1D, as chlorophyll undergoes structural changes, the green color also varies. The introduction of a hydroxyl group at $C13^2$ does not modify the UV-Vis spectrum. However, when the central Mg^{+2} is substituted by hydrogen (pheophytins and pheophorbides), the color shifts to an olive tone (characteristic of cooked vegetables).

In addition to color changes, the bioactivity of the chlorophyll structure is also affected by structural modifications [30]. Despite conflicting results, various chlorophyll derivatives have demonstrated health-promoting activities superior to those

of intact chlorophyll and copper chlorophyll, which is commonly used in the food industry [31,32]. Among the bioactive properties, antioxidant and anticancer activities have been the most frequently cited.

The degradation pathway of these tetrapyrrolic structures in microalgae is not fully understood, but it is known to occur in response to different biotic and abiotic stresses [32]. In this study, it is evident that the application of light in the form of rapid pulses induced significant abiotic stress, as indicated by the high levels of degradation compounds. On the other hand, this light-dark configuration may have stimulated the activity of key enzymes responsible for specific reactions, as the highest levels of chlorophyll *a* and *b* were found alongside the degradation metabolites, for example.

Similarly, the total contents of carotenoids (Figure 2a), carotenes (Figure 2b), and xanthophylls (Figure 2c) appeared to follow the same trend, showing significant increases under the application of very rapid light pulses (0.91:0.09), reaching 14.47, 1.55, and 12.92 g/kg, respectively. As observed with chlorophylls, the photoperiod with a frequency of 12f/d yielded the lowest total carotenoid content (1.58 g/kg).

[Insert Figure 2]

Among the carotenes obtained during the experiment, all-*trans*-β-carotene (Figure 2d) was undoubtedly the most significant. In addition to its characteristic intense orange color, which is due to its chemical structure (chromophore with 11 conjugated double bonds (CDBs); two within the β-ionone terminal rings), this carotene has 100% provitamin A activity, making it suitable for use in fortifying foods deficient in this vitamin [33]. In contrast, the xanthophylls (Figure 2d) identified in this study exhibit yellow coloration, with intensity varying according to structural characteristics, particularly the size of the chromophore and whether it extends to the acyclic ends or not [34]. Generally, as the chromophore size decreases, the yellow color becomes less

intense, with the exception of mutatoxanthin (10 CDBs and 1 epoxy group with a double bond), where the light-yellow results from the unsaturation of the epoxy group. Considering the chromophore, for example, the intensity of the yellow color decreases in the following order: lutein and antheraxanthin (10 CDBs) > violaxanthin (9 CDBs) > neoxanthin and luteoxanthin (8 CDBs). As with chlorophylls, fractionating this carotenoid extract could enable different food-related coloring applications.

In addition to their role as natural colorants, microalgal carotenoids and chlorophylls are recognized for their bioactive properties, which require adequate bioavailability to be effective [35]. Studies indicate that their bioaccessibility varies with the associated matrix and is enhanced when consumed as isolated extracts, highlighting the importance of extraction and fractionation [20,36,37]. This approach not only aids in understanding their biological mechanisms but also broadens their potential applications. Therefore, developing biotechnological strategies, such as manipulating light cycles, is essential to maximize pigment yield and tailor their profiles for specific functional uses, ultimately enhancing their commercial and functional value. In this context, the present study demonstrated that, under optimal conditions (0.9:0.09), chlorophyll levels were about twice as high and total carotenoid concentrations up to 8 times higher than those reported in previous studies for *S. obliquus* [9,18,38,39], highlighting the relevance of the tested photoperiod strategies.

3.3. Effects of long-term, frequency, and short-term photoperiods on chlorophylls *a* content

The metabolism of photosynthetic organisms is closely linked to the amount of light energy received and stored by their cells, which influences the accumulation of various biocompounds [13]. Chlorophyll *a* is the primary photosynthetic pigment, and

its concentration is influenced by light exposure. In this context, the present study investigated the effects of different photoperiod regimes (long-term, frequency, and short-term) on the production of chlorophyll *a* series pigments in *S. obliquus* (Figure 3). Nine chlorophyll *a*-related compounds were identified across all treatments, with chlorophyll *a* consistently emerging as the predominant pigment across all conditions tested.

[Insert Figure 3]

These findings are consistent with the central role of chlorophyll *a* in the photochemical reactions of both photosystem I (PSI) and photosystem II (PSII). In green algae, chlorophyll *a* is the most important pigment, as it regulates the light-harvesting antennae and the reaction centers of these systems. One of the pathways for the accumulation of this pigment involves the phytylation of protochlorophyllide *a* into protochlorophyll *a*, followed by its photochemical reduction to chlorophyll *a* [29]. When protochlorophyllide *a* is enzymatically reduced to chlorophyllide *a* using light as an energy source, the process is light-dependent. Alternatively, in a light-independent pathway, protochlorophyllide *a* can be reduced to chlorophyllide *a* and subsequently enzymatically phytylated to form chlorophyll *a* [40].

This became evident during the long-term photoperiod experiment. This study demonstrated that the microalga *S. obliquu*s is capable of sustaining its photosynthetic machinery during long periods without light. Among long-term photoperiods, the 18:6 accumulated a higher content of chlorophyll *a* series (31.67 g/kg). However, an increasing trend in chlorophyll *a* concentration was observed as the dark period decreased up to a certain point [10:14 (27.72 g/kg), 12:12 (27.72 g/kg), 18:6 (31.68 g/kg)]. In contrast, under the conditions 20:4 (22.72 g/kg) and 22:2 (16.28 g/kg), this

trend reversed, with a slight increase observed under constant light conditions, 24:0 (20.59 g/kg).

This leads us to believe that there is a metabolic threshold for chlorophyll *a* accumulation during certain long-term photoperiods, where, under specific conditions, increasing the duration of the light fraction may induce the reduction of this pigment. This can be explained by the hypothesis that, under higher light conditions, the photosynthetic apparatus is more active, supporting the increased synthesis of carbon compounds (e.g., lipids). This elevated activity can lead to greater turnover or degradation of chlorophyll *a*, either due to photooxidative stress or as part of a regulatory adjustment in the pigment-protein complexes involved in light harvesting [41].

Another possibility is that microalgae produce chlorophyll antennas of smaller size and less chlorophyll *a* content at high light intensity as a protective mechanism to minimize photon absorption and reduce photoinhibition [42].

From a biochemical perspective, chlorophyll metabolism can be divided into synthesis, the chlorophyll cycle, and degradation, and these processes are regulated independently [43]. Therefore, another hypothesis is that long periods of light can trigger degradative processes, altering the original structure of chlorophyll *a* and resulting in a greater accumulation of pheophytin *a* (2.20 g/kg), pheophorbide *a* (0.17 g/kg), and pheophytin *a'* (0.12 g/kg), as observed in experiments with constant light (24:0).

In this sense, the proportion of pheophytin *a*, a metabolite of the chlorophyll degradation pathway [44], increases as long as the hours of light grows. Pheophytin *a* represents 1% of the total chlorophyll content in 10:14 and 12:12 photoperiod regime reaches 4-5% when the light increases up to 20 and 22 hours and rises to 10% when

microalgae are in continuous light. Additionally, under the condition where the dark time equals the light time (12:12), higher levels of epimer (chlorophyll *a'*: 4.92 g/kg) and 13^2-OH-pheophytin *a* (0.69 g/kg) are accumulated.

An interesting result observed in the chlorophyll profile is that chlorophyllide *a* significantly increases with longer light exposure. From 10 to 20 hours of light, chlorophyllide *a* accounts for less than 0.5% of the total chlorophyll content. However, when the photoperiod reaches 22 and 24 hours of light, its proportion rises to as much as 3%. Chlorophyll turnover is a natural phenomenon for which there is not much information. For example, in *Chlamydomonas reinhardtii* [45], it has been determined that the half-live for chlorophyll *a* is 24.1 hours, and by the time the enyme responsible for such turnover was identified [46]. The authors determined that chlorophyllide *a* was the first metabolite formed during chlorophyll turnover. The higher accumulation of chlorophyllide in light-stressing conditions (22 and 24 hours of light) can then be interpreted as a signal of the high repair of the PSII system under damage by irradiation.

A strategy used to improve process performance is to increase the frequency of the light and dark cycles [47]. As shown in previous experiments [24], a 22:2 h photoperiod was ideal for long-term biomass production. Therefore, the current study aimed to verify whether different frequencies of this light/dark cycle would also have a positive impact on pigment content. However, in terms of chlorophylls of *a* series, this condition was not quantitatively satisfactory.

Under the frequency conditions tested, six chlorophyll *a* series compounds were identified. Among these, the 8t/d regime (eight light/dark transitions per day) resulted in the highest accumulation of chlorophyll *a* series pigments (28.74 g/kg), with chlorophyll *a* alone accounting for 26.64 g/kg. Although the overall pigment yields

were lower than those observed under long- and short-term photoperiods, the frequency treatments exhibited minimal pigment degradation.

Notably, degradation markers such as pheophorbides were not detected. These compounds typically arise through successive degradative reactions, such as the loss of phytol and magnesium from the chlorophyll structure, leading to a brown coloration in contrast to the characteristic green pigment [48]. The absence of such markers suggests that frequent light/dark alternation may reduce photooxidative stress and help preserve pigment integrity.

While frequency-based light regimes contributed only to chlorophyll stability, short-duration photoperiods or intermittent light exposure significantly increased photosynthetic efficiency, a result of the very rapid alternations between light and darkness. characteristic of this type of regime [16].

Although an increase in derivative compounds was observed, there was a significant preservation and enhancement of the original pigment structures, particularly under extremely brief light/dark cycles. This was especially evident with the 0.9:0.09 photoperiod, which yielded the highest chlorophyll *a* concentration (46.33 g/kg) among all conditions evaluated. This value represents a 1.5- and 1.7-fold increase compared to the best results observed under the long-term photoperiod (18:6) and frequency-based (8t/d) regimes, respectively.

Among all photoperiods evaluated, the most efficient condition for the production of the chlorophyll *a* series was 0.9:0.09, which presented the highest concentrations and the largest number of detected compounds. Under this condition, seven of the nine pigments of the *a* series stood out in relation to the other conditions: chlorophyll *a* (46.32 g/kg), pheophytin *a* (9.16 g/kg), pheophytin *a´*(1.73 g/kg),

Journal Pre-proof

chlorophyllide *a* (1.14 g/kg), pheophorbide *a* (0.89 g/kg), 13^2-OH-chlorophyll *a* (0.72 g/kg) and chlorophyllide *a´*(0.10 g/kg).

Collectively, the results indicate that the light regime was decisive for maximizing chlorophyll *a* content. In general, short-duration photoperiods with rapid light/dark alternations were most effective (except in the 0.75:0.25 condition), while frequency-based regimes minimized pigment degradation, and long-duration cycles provided relevant insights into the metabolic thresholds associated with pigment synthesis and turnover.

3.4. Effects of long-term, frequency and short-term photoperiods on chlorophyll *b* content

Chlorophyll *b* is the second most abundant pigment in nature and is an important accessory pigment in the light-harvesting apparatus during photosynthesis [49]. To adapt their photosynthetic apparatus to the level of irradiance, photosynthetic organisms utilize a mechanism for the interconversion of chlorophylls *a* and *b* through the chlorophyll cycle [50]. Therefore, the content of chlorophylls in *b* series obtained in all experiments is shown in Figure 4. In total, six chlorophylls of this series were discriminated, with chlorophyll *b* (peak 16) being the predominant compound in all photoperiods tested, followed by its epimer (peak 17).

[Insert Figure 4]

Among the long-term photoperiods analyzed, the 18:6 accumulated the highest chlorophyll a content (5.22 g/kg), while the condition with the highest irradiance, 22:2 (2.50 g/kg), showed the lowest quantitative content. The 12:12 condition stood out for the abundance of metabolites, such as chlorophyll *b'* (1.13 g/kg), pheophytin *b* (0.25 g/kg), and 15^1-hydroxylactone chlorophyll *b* (0.15 g/kg).

Journal Pre-proof

Partly, this accumulation of chlorophylls in series *b* under conditions of longer dark periods can be explained by the effect of radiance on the antenna complexes of the photosynthetic apparatus. These antenna complexes are also rich in chlorophyll *b*, which, at high illumination levels, is reduced to avoid excess photons and minimize the production of ROS. As a result, the relative amounts of chlorophyll *b* decrease.

In addition, excessive periods of light (20 to 24 hours) induce greater chlorophyll *a* degradation. Following the chlorophyll catabolic pathway, the first step is the transformation of chlorophyll *b* into chlorophyll *a* (chlorophyll cycle). Therefore, under such circumstances, chlorophyll *b* forms chlorophyll a directly, without being degraded into pheophytin.

On the other hand, under shaded or low-light conditions, it is hypothesized that the organism compensates for reduced photon availability by expanding its light-harvesting antenna complexes, which are rich in chlorophyll *b* [9]. However, to support these hypotheses, future studies that include specific analyses, such as reactive oxygen species (ROS) quantification or gene expression by qPCR, would be necessary.

These adjustments may lead to an increase in chlorophyll *b* levels relative to chlorophyll *a*, reflected in a higher chlorophyll *b/a* ratio. This ratio is often considered an indicator of antenna size and could be a useful parameter for assessing photoacclimation responses in microalgae. In the present study, this ratio (1.76, 1.78, 1.79, 1.73, 1.66, and 1.76 for 10:14, 12:12, 18:6, 20:4, 22:2, and 24:0, respectively) demonstrated the ability of the microalgae to adapt reversibly under different light conditions, optimizing photosynthetic efficiency.

Only five chlorophylls of this series were detected in the frequency experiment. The 8 t/d proved to be the best frequency option for producing chlorophyll *b* (3.73 g/kg), while the 12 t/d conditions proved less satisfactory, as they produced the lowest

quantitative content for all compounds in this series. Metabolites such as chlorophyllide *b*, and oxidized chlorophyll *b* were not detected under these experimental conditions. Additionally, insignificant amounts of hydroxyl-lactones *b* or pheophytins (less than 0.08 g/kg) were detected in this regime of light.

Again, among all the photoperiods evaluated, the short-term ones proved to be more efficient for the production of microalgae pigments. The rapid alternation of 0.91:0.09 resulted in the highest chlorophyll *b* content (9.90 g/kg). This short photoperiod presented 1.9 and 2.7 times more chlorophyll *b* than the best conditions established for long-term and frequencies, respectively. Except for the 0.75:0.25 photoperiod, all short-term conditions presented higher values of chlorophyll *b* when compared to the best conditions listed for the other photoperiods. There was also maximum production of hydroxylated compounds, such as hydroxylactone *b*, by regime 0.50:0.50 (0.28 g/kg).

These findings support the strategic use of short-term 0.91:0.09 photoperiod as a possible biotechnological approach for increasing chlorophyll *b* content in microalgae, targeting commercial and functional applications.

3.5. Effects of long-term, frequency and short-term photoperiods on carotenoids content

During photosynthesis, carotenoids play a fundamental role, helping chlorophylls capture light energy and provide photoprotection. This assistance occurs by capturing light energy and transferring it to chlorophylls through singlet-singlet excitation. Additionally, they absorb excess energy from chlorophylls via triplet-triplet transfer (higher energy state) and release the excess energy through vibration of the

polyene chain. This mechanism is essential for photoprotection as it neutralizes ROS produced from oxygen and light during photosynthesis [51].

Consequently, as can be seen in Figure 5, the carotenoid content can be altered due to light variations during microalgae cultivation. Throughout all experiments, 11 carotenoids were identified, with all-*trans*-lutein (peak 12), its isomer 9-*cis* (peak 13), all-*trans*-neoxanthin (peak 5), and all-*trans*-β-carotene (peak 26) being the most abundant.

[Insert Figure 5]

Among the long-term photoperiods, the 18:6 demonstrated the best performance, as evidenced by the highest production of all-*trans*-lutein (5.88 g/kg), 9-*cis*-lutein (1.07 g/kg), all-*trans*-β-carotene (1.03 g/kg), *cis*-neoxanthin (0.59 g/kg), 9-*cis*-α-carotene (0.27 g/kg), and 9-*cis*-violaxanthin (0.27 g/kg) compared to the other long-duration periods. The 12:12 and 10:14 resulted in the highest accumulation of all-*trans*-neoxanthin (1.26 g/kg; 1.25 g/kg), while the 20:4 cycle accumulated the highest levels of all-*trans*-antheraxanthin (0.23 g/kg) and all-*trans*-mutatoxanthin (0.06 g/kg). Under constant light conditions (24:0), only the content of all-*trans*-luteoxanthin (0.06 g/kg) stood out among the other long-term photoperiods.

A tendency to accumulate lutein and β-carotene is observed as the light period increases up to 6 hours, indicating that structural reactions of cyclization are favored under these conditions. According to Rodrigues et al. [52], the cyclization of tetraterpenoids increases their capacity to absorb energy. On the other hand, as the light period is extended (20 to 24 hours), epoxidation reactions (producing antheraxanthin, mutatoxanthin, and luteoxanthin) and acetylation (resulting in neoxanthin) are promoted. These modifications are associated with a greater capacity for energy dissipation in high-light environments.

Journal Pre-proof

The application of different frequencies influenced the detection of eight tetraterpene structures. Among the frequencies tested, the 8 t/d condition resulted in the highest accumulation of all-*trans*-lutein (4.48 g/kg), 9-*cis*-lutein (0.58 g/kg), and all-*trans*-β-carotene (0.73 g/kg). Lower frequencies, such as 4 t/d and 2 t/d, favored the accumulation of all-*trans*-neoxanthin (0.19 g/kg) and *cis*-neoxanthin (0.09 g/kg), respectively. On the other hand, increasing the frequency to 48 t/d stimulated the production of all-*trans*-violaxanthin (0.29 g/kg), *cis*-violaxanthin (0.07 g/kg), and 9-*cis*-α-carotene (0.22 g/kg). However, this condition showed the lowest total carotenoid accumulations compared to the other photoperiods tested.

Unlike the use of frequency, the application of short-term photoperiods positively impacted carotenoid production. Similar to chlorophylls, rapid light cycles maximized carotenoid content compared to long-term and frequency photoperiods. Of the 11 tetraterpenoid structures identified throughout the study, nine had their best production with short-term photoperiods. Of these overproductions, seven were obtained for the 0.91:0.09 (14.47 g/kg), including all-*trans*-lutein (7.14 g/kg), 9-*cis*-lutein (1.95 g/kg), all-*trans*-neoxanthin (1.56 g/kg), all-*trans*-β-carotene (1.06 g/kg), all-*trans*-violaxanthin (1.36 g/kg), all-*trans*-luteoxanthin (0.18 g/kg), and all-*trans*-mutatoxanthin (0.08 g/kg). The other two noteworthy productions were the short photocycles 0.83:0.17 and 0.50:0.50 with the highest productions of the *cis*-neoxanthin isomers (0.61 g/kg) and *cis*-α-carotene (0.59 g/kg), respectively.

In *S. obliquus*, carotenoid production was strongly influenced by the different photoperiod regimes evaluated. Similar to chlorophylls, photoperiod manipulation represents a valuable biotechnological strategy to increase carotenoid synthesis. Short photoperiods produced the highest overall carotenoid levels, particularly increasing the content of bioactive tetraterpenoids, such as lutein. In contrast, long-term photoperiods

favored the accumulation of specific compounds, suggesting that prolonged light exposure may be a useful tool to selectively increase carotenoids such as antheraxanthin. These findings highlight the potential of photoperiod control to maximize and tailor carotenoid production.

3.6. Productivity Metrics and PPFD

Although the pigment content in the biomass is an important parameter for evaluating each specific condition, it is not sufficient on its own to estimate total pigment productivity. For this, determining the amount of biomass obtained under each experimental condition is also essential, as well as establishing correlations with the photosynthetic photon flux density (PPFD) received can offer valuable insights into optimizing natural pigment production via photosynthesis. In light of these considerations, Figure 6 presents pigment productivity data, including biomass concentration and the PPFD applied in each photoperiod.

[Insert Figure 6]

As shown in the graph, the highest biomass productions were obtained under the frequency cycles of 4t/d (3.85 g/L), 8t/d (3.71 g/L), and 2t/d (3.70 g/L). In contrast, a remarkable increase in the volumetric production of carotenoids and chlorophylls was observed under the pulsed light condition of 0.91:0.01, reaching 31.84 mg/L and 165.11 mg/L, respectively, along with the highest total pigment productivity (196.95 mg/L). When specifically compared to the carotenoid content reported for another chlorophyte grown under phototrophic conditions (2.9 mg/L), this photoperiod strategy resulted in an increase of more than 10-fold [53].

Regarding the total amount of PPFD received, it varied throughout the experiment, a consequence of the determination based on the different light cycles and

generation times characteristic of each experimental condition (see supplementary material). The condition with the longest light period (24:0) received the highest accumulated photosynthetic photon flux density (116.64 mol/m²), but did not stand out in any productivity parameter.

When analyzing long-term photoperiods, for instance, no clear trend was observed between the received PPFD and the production of biomass or pigments. The 12:12 and 18:6 conditions received the same photon dose (58.32 mol/m²), but resulted in distinct biomass and pigment yields, reduced by 42% and 36%, respectively for 18:6. Under frequency cycles, biomass and pigment production increased in line with PPFD up to the limit of four dark periods per day. However, it ceased to exist after 8t/d.

On the other hand, under short photoperiods, biomass production increased proportionally with the increment in PPFD. Although this pattern was not consistently reflected in pigment production, the condition 0.91:0.01, which received the highest PPFD dose among the short photoperiods (94.35 mol/m²), stood out by simultaneously achieving the highest biomass productivity (2.20 g/L) and pigments (196.95 mg/L) within this experimental block.

Overall, the data indicate that light cycle modulation had distinct effects on pigment and biomass productivity, which were little influenced by the amount of PPDF received. Although accumulated PPFD had a greater influence on biomass accumulation under short photoperiods, its effect on pigment production was limited. Therefore, the frequency of 4 t/d and the use of pulsed light (0.91:0.01) emerge as key variables to optimize *S. obliquus* productivity.

3.7. Exploratory Multivariate Analysis

Journal Pre-proof

To better visualize the effect of different light-dark cycles (cases) on pigment accumulation (variables), a principal component analysis (PCA) was performed. This statistical analysis, applied to multiple variables, reduces the original spatial dimensions (with minimal information loss) while also establishing or highlighting the intrinsic relationships between variables and cases, thereby enhancing data interpretability [54].

[Insert Figure 7]

Figure 7 (a and b) presents the scores (samples) and loadings (compounds) of principal components I (PCI, 65.3%) and II (PCII, 13.7%), which together accounted for 79.0% of the total variance in the results. Based on these two PCs, samples that are further from the origin are considered the most relevant for data discrimination.

As observed in Figure 7(a), four photoperiods were clearly discriminated from the others. The 0.91:0.09 and 12t/d were discriminated by PCI, while 12:12 and 18:6 were discriminated by PCII. These discriminations result from the clustering of certain groups or isolated pigments (see Figure 7b). Specifically, 0.91:0.09 and 12t/d were discriminated by PCI, while 12:12 and 18:6 were discriminated by PCI.

Firstly, in terms of chlorophyll, samples cultivated under very rapid light pulses (0.91:0.09) correlated with the totals of this pigment class, particularly with the total pheophytins (*a* and *a'*), pheophorbide *a*, and total chlorophyll (*a* and *b*), as well as chlorophyllide *a* content. In contrast, long-term photoperiods (12:12) correlated with the degradation metabolite of chlorophyll series *b* (pheophytin *b*). Regarding carotenoids, the factor that most influenced the discrimination of the short-term photoperiod was the high production of luteoxanthin and mutatoxanthin compared to the other conditions.

Meanwhile, the use of frequencies (12t/d) was discriminated by the reduced content of compounds obtained for the vast majority of all pigments evaluated in the

Journal Pre-proof

study. This can be observed through the opposition of the compounds projected in the factorial space opposite to this frequency photoperiod.

4. Conclusions

This study demonstrated that photoperiod modulation has a significant impact on the pigment profile and productivity of *S. obliquus*. A total of 26 compounds were identified, including chlorophylls, carotenoids, and their degradation derivatives. Short photoperiods (0.91:0.09) maximized total pigment productivity, particularly enhancing the accumulation of chlorophylls *a* and *b*, lutein, and β-carotene, indicating a metabolic adaptation to rapid light–dark alternations, while long photoperiods (20:4) promoted the selective accumulation of compounds like antheraxanthin. Although increased biomass productivity does not necessarily correlate with higher pigment yields, the results highlight light regime modulation as an effective strategy for optimizing the biosynthesis of natural pigments. In addition, the resulting color gradient, shaped by the structural diversity of the pigments, further supports their potential application in the food industry.

In summary, by emphasizing the role of photoperiod control in enhancing the yield of industrially relevant pigments, this study contributes valuable insights into microalgal pigment biosynthesis. These findings validate microalgae as a sustainable source of food colorants and open new avenues for the development of cultivation strategies focused on targeted pigment production.

Acknowledgements

This study was financially supported by the FAPERGS/CNPq 07/2022 (23/2551-0001879-9) and the project PID2021-12799OB-I00 funded by MCIN/AEI/10.13039/501100011033 and by "ERDF A way of making Europe".

Author contributions

Conceptualization, T.C.N. and L.Q.Z.; methodology, P.N.P., R.B.S, and M.C.D.; software, P.N.P.; validation, R.B.S, and M.C.D; formal analysis, L.Q.Z., M.R., P.N.P. and T.C.N; investigation T.C.N; resources, T.C.N.; data curation, E.J.-L. and, M.R.; writing—original draft preparation, T.C.N.; writing—review and editing, T.C.N, M.R., and L.Q.Z.; visualization, M.R., E.J.-L. and L.Q.Z.; supervision, E.J.-L. and L.Q.Z.; project administration, E.J.-L. and L.Q.Z.; funding acquisition, L.Q.Z.

Conflict of interest

The authors have no conflicts of interest to report.

Declaration

During the preparation of this work, the author(s) used ChatGPT to improve language and readability. After using this tool/service, the author(s) reviewed and edited the content as necessary and assume full responsibility for the content of the publication.

References

[1] M. Bühler, P. Hollenbach, L. Köhler, R. Armstrong, Unlocking resilience and sustainability with earth-based materials: a principled framework for urban transformation, Front. Built Environ. 10 (2024) 1385116.

Journal Pre-proof

https://doi.org/10.3389/FBUIL.2024.1385116/BIBTEX.

[2] A. Ahmad, S.S. Ashraf, Sustainable food and feed sources from microalgae: Food security and the circular bioeconomy, Algal Res. 74 (2023) 103185. https://doi.org/10.1016/J.ALGAL.2023.103185.

[3] B. Naik, R. Mishra, V. Kumar, S. Mishra, U. Gupta, S. Rustagi, A.K. Gupta, M.S. Preet, S.C. Bhatt, S. Rizwanuddin, Micro-algae: Revolutionizing food production for a healthy and sustainable future, J. Agric. Food Res. 15 (2024) 100939. https://doi.org/10.1016/J.JAFR.2023.100939.

[4] F. Yamin, Why I broke the law for climate change, Nat. 2021 5737774 573 (2019) 337–339. https://doi.org/10.1038/d41586-019-02736-9.

[5] A.K. Molina, R.C.G. Corrêa, M.A. Prieto, C. Pereira, L. Barros, Bioactive Natural Pigments' Extraction, Isolation, and Stability in Food Applications, Molecules 28 (2023). https://doi.org/10.3390/MOLECULES28031200.

[6] M. Roca, K. Chen, A. Pérez-Gálvez, Chlorophyll, in: Encycl. Food Heal., 2015: pp. 37–41. https://doi.org/10.1016/B978-0-12-384947-2.00147-1.

[7] E. Jacob-Lopes, M.M. Maroneze, M.C. Deprá, R.B. Sartori, R.R. Dias, L.Q. Zepka, Bioactive food compounds from microalgae: an innovative framework on industrial biorefineries, Curr. Opin. Food Sci. 25 (2019) 1–7. https://doi.org/10.1016/j.cofs.2018.12.003.

[8] M. Manzoni Maroneze, E. Jacob-Lopes, L. Queiroz Zepka, M. Roca, A. Pérez-Gálvez, Esterified carotenoids as new food components in cyanobacteria, Food Chem. 287 (2019) 295–302. https://doi.org/10.1016/j.foodchem.2019.02.102.

[9] M.M. Maroneze, L.Q. Zepka, E.J. Lopes, A. Pérez-Gálvez, M. Roca, Chlorophyll Oxidative Metabolism During the Phototrophic and Heterotrophic Growth of Scenedesmus obliquus, Antioxidants (Basel, Switzerland) 8 (2019).

Journal Pre-proof

https://doi.org/10.3390/ANTIOX8120600.

[10] T.C. Nascimento, C.B.B. Cazarin, M.R. Maróstica, A.Z. Mercadante, E. Jacob-Lopes, L.Q. Zepka, Microalgae carotenoids intake: Influence on cholesterol levels, lipid peroxidation and antioxidant enzymes, Food Res. Int. 128 (2020). https://doi.org/10.1016/j.foodres.2019.108770.

[11] T.C. Nascimento, P.P. Nass, A.S. Fernandes, K.R. Vieira, R. Wagner, E. Jacob-Lopes, L.Q. Zepka, Exploratory data of the microalgae compounds for food purposes, Data Br. 29 (2020). https://doi.org/10.1016/j.dib.2020.105182.

[12] M. Herrera, M. Roca, Microalgal chlorophylls for food/feed applications, Handb. Food Feed from Microalgae Prod. Appl. Regul. Sustain. (2023) 147–160. https://doi.org/10.1016/B978-0-323-99196-4.00041-3.

[13] E. Jacob-Lopes, C.H.G. Scoparo, L.M.C.F. Lacerda, T.T. Franco, Effect of light cycles (night/day) on CO2 fixation and biomass production by microalgae in photobioreactors, Chem. Eng. Process. Process Intensif. 48 (2009) 306–310. https://doi.org/10.1016/J.CEP.2008.04.007.

[14] M. Janssen, P. Slenders, J. Tramper, L.R. Mur, R.H. Wijffels, Photosynthetic efficiency of Dunaliella tertiolecta under short light/dark cycles, Enzyme Microb. Technol. 29 (2001) 298–305. https://doi.org/10.1016/S0141-0229(01)00387-8.

[15] Q. Zhou, P. Zhang, G. Zhang, M. Peng, Biomass and pigments production in photosynthetic bacteria wastewater treatment: Effects of photoperiod, Bioresour. Technol. 190 (2015) 196–200. https://doi.org/10.1016/J.BIORTECH.2015.04.092.

[16] S. Abu-Ghosh, D. Fixler, Z. Dubinsky, D. Iluz, Flashing light in microalgae biotechnology, Bioresour. Technol. 203 (2016) 357–363. https://doi.org/10.1016/J.BIORTECH.2015.12.057.

Journal Pre-proof

[17] M.C. Deprá, L.G.R. Mérida, C.R. de Menezes, L.Q. Zepka, E. Jacob-Lopes, A new hybrid photobioreactor design for microalgae culture, Chem. Eng. Res. Des. 144 (2019) 1–10. https://doi.org/10.1016/j.cherd.2019.01.023.

[18] R.G. Vendruscolo, M.B. Fagundes, M.M. Maroneze, T.C. do Nascimento, C.R. de Menezes, J.S. Barin, L.Q. Zepka, E. Jacob-Lopes, R. Wagner, Scenedesmus obliquus metabolomics: effect of photoperiods and cell growth phases, Bioprocess Biosyst. Eng. 42 (2019). https://doi.org/10.1007/s00449-019-02076-y.

[19] A. Erdoğan, A. Çağır, M.C. Dalay, A.E. Eroğlu, Composition of Carotenoids in Scenedesmus protuberans: Application of Chromatographic and Spectroscopic Methods, Food Anal. Methods 8 (2015) 1970–1978. https://doi.org/10.1007/s12161-015-0088-8.

[20] A.S. Fernandes, T.C. Nascimento, P.N. Pinheiro, V. V. de Rosso, C.R. de Menezes, E. Jacob-Lopes, L.Q. Zepka, Insights on the intestinal absorption of chlorophyll series from microalgae, Food Res. Int. 140 (2021) 110031. https://doi.org/10.1016/J.FOODRES.2020.110031.

[21] K. Chen, J.J. Ríos, M. Roca, A. Pérez-Gálvez, Development of an accurate and high-throughput methodology for structural comprehension of chlorophylls derivatives. (II) Dephytylated derivatives, J. Chromatogr. A 1412 (2015) 90–99. https://doi.org/10.1016/J.CHROMA.2015.08.007.

[22] G. Britton, Structure and properties of carotenoids in relation to function, FASEB J. 9 (1995) 1551–1558. https://doi.org/10.1096/FASEBJ.9.15.8529834.

[23] R. Rippka, J. Deruelles, J.B. Waterbury, Generic assignments, strain histories and properties of pure cultures of cyanobacteria, J. Gen. Microbiol. 111 (1979) 1–61. https://doi.org/10.1099/00221287-111-1-1.

Journal Pre-proof

[24] M.M. Maroneze, S.F. Siqueira, R.G. Vendruscolo, R. Wagner, C.R. de Menezes, L.Q. Zepka, E. Jacob-Lopes, The role of photoperiods on photobioreactors – A potential strategy to reduce costs, Bioresour. Technol. 219 (2016) 493–499. https://doi.org/10.1016/j.biortech.2016.08.003.

[25] K. Chen, J.J. Ríos, A. Pérez-Gálvez, M. Roca, Development of an accurate and high-throughput methodology for structural comprehension of chlorophylls derivatives. (I) Phytylated derivatives, J. Chromatogr. A 1406 (2015) 99–108. https://doi.org/10.1016/J.CHROMA.2015.05.072.

[26] M.G. Ferruzzi, M.L. Failla, S.J. Schwartz, Assessment of degradation and intestinal cell uptake of carotenoids and chlorophyll derivatives from spinach puree using an in vitro digestion and Caco-2 human cell model, J. Agric. Food Chem. 49 (2001) 2082–2089. https://doi.org/10.1021/JF000775R.

[27] I. Viera, K. Chen, J.J. Ríos, I. Benito, A. Pérez-Gálvez, M. Roca, First-Pass Metabolism of Chlorophylls in Mice, Mol. Nutr. Food Res. 62 (2018). https://doi.org/10.1002/MNFR.201800562.

[28] I. Viera, M. Roca, Analytical Protocols in Chlorophyll Analysis, Pigment. from Microalgae Handb. (2020) 127–149. https://doi.org/10.1007/978-3-030-50971-2_6.

[29] J.C. da Silva, A.T. Lombardi, Chlorophylls in Microalgae: Occurrence, Distribution, and Biosynthesis, Pigment. from Microalgae Handb. (2020) 1–18. https://doi.org/10.1007/978-3-030-50971-2_1.

[30] Y.R. Kang, J. Park, S.K. Jung, Y.H. Chang, Synthesis, characterization, and functional properties of chlorophylls, pheophytins, and Zn-pheophytins, Food Chem. 245 (2018) 943–950. https://doi.org/10.1016/J.FOODCHEM.2017.11.079.

[31] U.M. Lanfer-Marquez, R.M.C. Barros, P. Sinnecker, Antioxidant activity of

chlorophylls and their derivatives, 38 (2005) 885–891. https://doi.org/10.1016/j.foodres.2005.02.012.

[32] L.Q. Zepka, E. Jacob-Lopes, M. Roca, Catabolism and bioactive properties of chlorophylls, Curr. Opin. Food Sci. 26 (2019) 94–100. https://doi.org/10.1016/j.cofs.2019.04.004.

[33] A.P. Miller, J. Coronel, J. Amengual, The role of β-carotene and vitamin A in atherogenesis: Evidences from preclinical and clinical studies, Biochim. Biophys. Acta. Mol. Cell Biol. Lipids 1865 (2020). https://doi.org/10.1016/J.BBALIP.2020.158635.

[34] D.B. Rodriguez-amaya, A guide to carotenoid analysis in foods, 2001.

[35] R.E. Kopec, M.L. Failla, Recent advances in the bioaccessibility and bioavailability of carotenoids and effects of other dietary lipophiles, J. Food Compos. Anal. 68 (2018) 16–30. https://doi.org/10.1016/j.jfca.2017.06.008.

[36] T.C. Nascimento, P.N. Pinheiro, A.S. Fernandes, D.C. Murador, B. V. Neves, C.R. de Menezes, V. V. de Rosso, E. Jacob-Lopes, L.Q. Zepka, Bioaccessibility and intestinal uptake of carotenoids from microalgae Scenedesmus obliquus, LWT 140 (2021) 110780. https://doi.org/10.1016/J.LWT.2020.110780.

[37] P.P. Nass, T.C. do Nascimento, A.S. Fernandes, P.A. Caetano, V. V. de Rosso, E. Jacob-Lopes, L.Q. Zepka, Guidance for formulating ingredients/products from Chlorella vulgaris and Arthrospira platensis considering carotenoid and chlorophyll bioaccessibility and cellular uptake, Food Res. Int. 157 (2022) 111469. https://doi.org/10.1016/J.FOODRES.2022.111469.

[38] L.D. Patias, A.S. Fernandes, F.C. Petry, A.Z. Mercadante, E. Jacob-Lopes, L.Q. Zepka, Carotenoid profile of three microalgae/cyanobacteria species with peroxyl radical scavenger capacity, Food Res. Int. 100 (2017) 260–266.

Journal Pre-proof

https://doi.org/10.1016/j.foodres.2017.06.069.

[39] T.C. do Nascimento, C.B.B. Cazarin, M.R. Maróstica, A.Z. Mercadante, E. Jacob-Lopes, L.Q. Zepka, Microalgae carotenoids intake: Influence on cholesterol levels, lipid peroxidation and antioxidant enzymes, Food Res. Int. 128 (2020) 108770. https://doi.org/10.1016/J.FOODRES.2019.108770.

[40] E. Gálová, I. Šalgovičová, V. Demko, K. Mikulová, A. Ševčovičová, L. Slováková, V. Kyselá, J. Hudák, A short overview of chlorophyll biosynthesis in algae, Biologia (Bratisl). 63 (2008) 947–951. https://doi.org/10.2478/S11756-008-0147-3/MACHINEREADABLECITATION/RIS.

[41] R.B. Sartori, R.G. Vendruscolo, S.R. Ribeiro, V.J.M. Furlan, R. Wagner, L.Q. Zepka, E. Jacob-Lopes, The Role of Photo-Cycles in the Modulation of Growth and Biochemical Profile of Microalgae: Part I—Food Interest Compounds, Life 2022, Vol. 12, Page 462 12 (2022) 462. https://doi.org/10.3390/LIFE12030462.

[42] X. Chen, Q.Y. Goh, W. Tan, I. Hossain, W.N. Chen, R. Lau, Lumostatic strategy for microalgae cultivation utilizing image analysis and chlorophyll a content as design parameters, Bioresour. Technol. 102 (2011) 6005–6012. https://doi.org/10.1016/J.BIORTECH.2011.02.061.

[43] M. Roca, A. Pérez-Gálvez, Metabolomics of Chlorophylls and Carotenoids: Analytical Methods and Metabolome-Based Studies, Antioxidants 2021, Vol. 10, Page 1622 10 (2021) 1622. https://doi.org/10.3390/ANTIOX10101622.

[44] S. Schelbert, S. Aubry, B. Burla, B. Agne, F. Kessler, K. Krupinska, S. Hörtensteiner, Pheophytin pheophorbide hydrolase (pheophytinase) is involved in chlorophyll breakdown during leaf senescence in Arabidopsis, Plant Cell 21 (2009) 767–785. https://doi.org/10.1105/TPC.108.064089.

[45] S.A. Stopka, T.R. Mansour, B. Shrestha, É. Maréchal, D. Falconet, A. Vertes,

Journal Pre-proof

Turnover rates in microorganisms by laser ablation electrospray ionization mass spectrometry and pulse-chase analysis, Anal. Chim. Acta 902 (2016) 1–7. https://doi.org/10.1016/J.ACA.2015.08.047.

[46] Y.P. Lin, M.C. Wu, Y.Y. Charng, Identification of a Chlorophyll Dephytylase Involved in Chlorophyll Turnover in Arabidopsis, Plant Cell 28 (2016) 2974–2990. https://doi.org/10.1105/TPC.16.00478.

[47] I. Krzemińska, B. Pawlik-Skowrońska, M. Trzcińska, J. Tys, Influence of photoperiods on the growth rate and biomass productivity of green microalgae, Bioprocess Biosyst. Eng. 37 (2014) 735–741. https://doi.org/10.1007/S00449-013-1044-X.

[48] H. Vergara-Domínguez, M. Roca, B. Gandul-Rojas, Thylakoid peroxidase activity responsible for oxidized chlorophyll accumulation during ripening of olive fruits (Olea europaea L.), Food Res. Int. 65 (2014) 247–254. https://doi.org/10.1016/J.FOODRES.2014.04.030.

[49] A.B. Cahoon, M.P. Timko, Biochemistry and Regulation of Chlorophyll Biosynthesis, (2003) 95–131. https://doi.org/10.1007/978-94-007-1038-2_6.

[50] R. Tanaka, A. Tanaka, Chlorophyll cycle regulates the construction and destruction of the light-harvesting complexes, Biochim. Biophys. Acta 1807 (2011) 968–976. https://doi.org/10.1016/J.BBABIO.2011.01.002.

[51] T. Maoka, Carotenoids as natural functional pigments, J. Nat. Med. 74 (2020) 1–16. https://doi.org/10.1007/S11418-019-01364-X/FIGURES/15.

[52] E. Rodrigues, L.R.B. Mariutti, R.C. Chisté, A.Z. Mercadante, Development of a novel micro-assay for evaluation of peroxyl radical scavenger capacity : Application to carotenoids and structure – activity relationship, Food Chem. 135 (2012) 2103–2111. https://doi.org/10.1016/j.foodchem.2012.06.074.

Journal Pre-proof

[53] P.A. Caetano, P.P. Nass, M.C. Deprá, T.C. do Nascimento, E. Jacob-Lopes, L.Q. Zepka, Trade-Off Between Growth Regimes in Chlorella vulgaris: Impact on Carotenoid Production, Color. 2024, Vol. 3, Pages 282-297 3 (2024) 282–297. https://doi.org/10.3390/COLORANTS3040020.

[54] I.T. Jollife, J. Cadima, Principal component analysis: a review and recent developments, Philos. Trans. A. Math. Phys. Eng. Sci. 374 (2016). https://doi.org/10.1098/RSTA.2015.0202.

Journal Pre-proof

Figure 1. Total chlorophylls and derivatives of *Scenedesmus obliquus* obtained with different photoperiods. Different letters indicate statistical differences ($p<0.05$).
Figure 2. Total carotenoids of *Scenedesmus obliquus* obtained with different photoperiods. Different letters indicate statistical differences ($p<0.05$).
Figure 3. Chlorophyll content of series *a* from *Scenedesmus obliquus* under different photoperiod conditions. Different letters in the column indicate statistical differences ($p<0.05$).
Figure 4. Chlorophyll content of series *b* from *Scenedesmus obliquus* under different photoperiod conditions. Different letters in the column indicate statistical differences ($p<0.05$).
Figure 5. Carotenoids content from *Scenedesmus obliquus* under different photoperiod conditions. Different letters in the column indicate statistical differences ($p<0.05$).
Figure 6. Volumetric pigment productivity, biomass concentration (X_{max}), and PPFD available under different photoperiod regimes.

Figure 7. Graphs of scores (samples) (a) and loadings (variables) (b) showing principal components 1 (PCI) and 2 (PCII) of *Scenedesmus obliquus* cultivated with different photoperiods.

Journal Pre-proof

Journal Pre-proof

Table 1. Chromatographic and mass spectrometry characteristics of pigments identified in *Scenedesmus obliquus* under different photoperiod conditions.

Peak	Compound MS	t_R[a]	Elemental composition	$[M + H]^+$ (*m/z*) Exact mass	mSigma	Error (ppm)	Main product ions (*m/z*)
1	Chlorophyllide *b*	1.5	$C_{35}H_{33}MgN_4O_6$	629.2259	33.2	-2.2	569.2083
2	Chlorophyllide *a*	5.3	$C_{35}H_{34}MgN_4O_5$	615.2482	16.6	-4.8	555.2216
3	Chlorophyllide *a´*	6.9	$C_{35}H_{34}MgN_4O_5$	615.2440	13.8	2.0	555.2231
4	Pheophorbide *a*	8.0	$C_{35}H_{36}N_4O_5$	593.2760	26.9	-0.2	533.2530
5	all-*trans*-neoxanthin	9.0	$C_{40}H_{56}O_4$	601.4273	36.5	-3.7	583.4168
6	9-*cis*-neoxanthin	9.2	$C_{40}H_{56}O_4$	601.4260	49.9	-1.5	583.4199
7	all-*trans*-violaxanthin	10.1	$C_{40}H_{57}O_4$	601.4272	23.4	-3.5	583.4200
8	all-*trans*-luteoxanthin	10.5	$C_{40}H_{57}O_4$	601.4228	25.1	4.0	583.4205
9	9-*cis*-violaxanthin	10.7	$C_{40}H_{56}O_4$	601.4269	23.0	-3.0	583.4216
10	all-*trans*-antheraxanthin	11.2	$C_{40}H_{56}O_3$	585.4394	43.4	1.4	567.4197
11	all-*trans*-mutatoxhanthin	11.4	$C_{40}H_{56}O_3$	585.4384	20.5	3.1	567.4189
12	all-*trans*-lutein	12.5	$C_{40}H_{56}O_2$	569.4354	23.6	-0.1	551.4243
13	*cis*-lutein	13.3	$C_{40}H_{56}O_2$	569.4353	36.8	0.9	551.4233
14	15^1-OH lactone-chlorophyll *b*	15.0	$C_{55}H_{70}MgN_4O_8$	939.5145	12.3	-3.0	585.1902
15	13^2-OH-chlorophyll *b*	15.9	$C_{55}H_{70}MgN_4O_7$	923.5187	45.7	-2.1	569.1890
16	Chlorophyll *b*	17.2	$C_{55}H_{70}MgN_4O_6$	907.5221	41.9	-0.2	569.1995
17	Chlorophyll *b´*	17.8	$C_{55}H_{70}MgN_4O_6$	907.5204	27.3	1.6	569.1995
18	13^2-OH-chlorophyll *a*	18.1	$C_{55}H_{73}MgN_4O_6$	909.5344	12.3	3.5	555.2225
19	Chlorophyll *a*	19.6	$C_{55}H_{72}MgN_4O_5$	893.4505	34.9	2.3	555.2196
20	Chlorophyll *a´*	20.6	$C_{55}H_{72}MgN_4O_5$	893.5409	36.9	1.8	555.2196
21	13^2-OH-pheophytin *a*	25.2[d]	$C_{55}H_{74}N_4O_6$	887.5673	23.9	0.9	593.2721
22	Pheophytin *b*	22.5	$C_{55}H_{37}N_4O_6$	885.5498	34.8	3.0	547.2347
23	Pheophytin *a*	27.3	$C_{55}H_{74}N_4O_5$	871.5703	32.0	3.4	593.2730
24	Pheophytin *a´*	28.2	$C_{55}H_{74}N_4O_5$	871.5732	7.9	2.4	593.2743
25	9-*cis*-α-carotene	28.4	$C_{40}H_{57}$	537.4455	24.9	-0.1	457.3745
26	all-*trans*-ß-carotene	28.6	$C_{40}H_{57}$	537.4436	12.9	3.3	413.3241

[a]Retention time in minutes: HPLC and MS

Journal Pre-proof

Journal Pre-proof

Graphical abstract

Highlights

- Photoperiod modulations influenced the yield of microalgae colorants.
- Very short-term photoperiods enhanced pigment productivity.
- Different light:dark cycle conditions increased chlorophyll derivatives.
- Long light times increased epoxy carotenoid.
- Pigment productivity was uncoupled from biomass, except under short photoperiods.

Journal Pre-proof

processes

MDPI

Review

Tackling Old Challenges in Microalgal Biotechnology: The Role of Photobioreactors to Advance the Technology Readiness Level

Mariany Costa Deprá *, Rosangela Rodrigues Dias, Leila Queiroz Zepka and Eduardo Jacob-Lopes *

Bioprocess Intensification Group, Federal University of Santa Maria, UFSM, Roraima Avenue 1000, Santa Maria 97105-900, RS, Brazil; ro.rosangelard@gmail.com (R.R.D.); zepkaleila@yahoo.com.br (L.Q.Z.)
* Correspondence: marianydepra@gmail.com (M.C.D.); ejacoblopes@gmail.com (E.J.-L.); Tel.: +55-55-3220-8822 (M.C.D. & E.J.-L.)

Abstract: Microalgae biotechnology has taken the world by storm. However, despite its great potential promise, it still cannot be considered a fully consolidated technology due to a crucial challenge: the low rates of biomass productivity. To overcome this hurdle, photobioreactors have been developed as an innovative solution, promising to increase the efficiency of microalgae cultures by providing optimized conditions. However, the results obtained with these systems do not always meet initial expectations, and their large-scale implementation faces complex technical challenges. In light of this, the present review addresses the main aspects related to the design and engineering of photobioreactors, highlighting their potentialities and limitations in overcoming the critical challenges of microalgal biotechnology. Furthermore, we discuss the current technological readiness level and the commercial readiness index of microalgae-based bioproducts from the perspective of industrial-scale production.

Keywords: abiotic/biotic aspects; bioreactor parameters; commercial readiness index; microalgae-based bioproducts; technology readiness level

check for updates

Academic Editors: Serena Lima and Francesca Scargiali

Received: 10 December 2024
Revised: 20 December 2024
Accepted: 24 December 2024
Published: 29 December 2024

Citation: Deprá, M.C.; Dias, R.R.; Zepka, L.Q.; Jacob-Lopes, E. Tackling Old Challenges in Microalgal Biotechnology: The Role of Photobioreactors to Advance the Technology Readiness Level. *Processes* **2025**, *13*, 51. https://doi.org/10.3390/pr13010051

Copyright: © 2024 by the authors. Licensee MDPI, Basel, Switzerland. This article is an open access article distributed under the terms and conditions of the Creative Commons Attribution (CC BY) license (https://creativecommons.org/licenses/by/4.0/).

1. Introduction

Industrial biotechnology has been portrayed as providing revolutionary solutions to some of the world's biggest challenges [1]. Its purposes range from mitigating climate changes to decreasing health issues, promoting renewable alternative energy sources, and developing new sustainable manufacturing routes [2]. However, biofabrication is not just about creating cheaper or more environmentally friendly materials. It is also about bringing new and innovative products to the market that surpass the best products that conventional chemistry can offer [3].

Given the widespread attention surrounding industrial biotechnology, researchers realized that microalgae could be used as a photosynthesis-powered expression chassis. Indeed, the substantial interest in microalgal biotechnology is not random. Its metabolic versatility that assimilates high carbon dioxide loads under the light, resulting in biomass with a high level of exploration, positions microalgae in a prominent place today [4]. They are emerging as new, attractive, promising, and scalable platforms for the production of various biomolecules while contributing to cleaner industrial processes. Among them, a non-exhaustive list includes some primary and secondary metabolites, such as proteins [5–7], essential fatty acids [8,9], and pigments, including carotenoids, chlorophylls, and phycocyanins [10–12]. Microalgae have gained a competitive space in the global market due to their nutritional properties, bioaccessibility, and cellular absorption [13,14]. Consequently, microalgae biotechnology has proven to be an essential strategic enabler for

marketing associated with One Health principles, resulting in an indispensable driving force for a strong and vibrant bioeconomy.

Although future market projections push decision-makers to open the doors to the industrialization of microalgae-based bioproducts, success remains doubtful. It is due to deep technical and operational hurdles that, despite their magnitude, continue to demand innovation and improvement, stemming from one of the higher bottlenecks to microalgal biotechnology: photobioreactors. Essential for large-scale operations, these devices function as the core of bioprocesses. Nevertheless, their full efficiency, which should catalyze industrial expansion, is still far from being achieved [15,16].

Given this background, the research gap to address with this publication is to examine why microalgae photobioreactors have not yet reached the greatest industrial-scale advancements despite more than 140 years of extensive and intensive investigations. Other sub-objectives of this publication consist of elucidating whether there is a combination of existing strategies in the biotechnological core that can identify these weaknesses and collectively address them to overcome these drawbacks. Also, to the best knowledge of the authors, this is the first literature review that analyzes, through concepts of technological readiness level and commercial readiness index, paths to strengthen microalgal biotechnology. Therefore, this publication is intended for all stakeholders in microalgal biotechnology, with a particular focus on addressing the pitfalls associated with the research fragmentation, development, and innovation of photobioreactors. We aim to foster a more integrative approach with industrial market players, helping to overcome past setbacks in microalgal production and positioning it as a major big win for the global community's future.

2. Biomass Production—The Death Valley of Microalgal Biotechnology

Successful technology transfer for microalgae-based processes and products depends on overcoming several hurdles. However, it is understood that the key driving force for its achievement is tied to its starting point—biomass production in cultivation systems. In this way, the consolidation of microalgae-based facilities has been limited by losses in cellular productivity, which are sharply perceived in the transition from projects on a laboratory scale to an industrial scale. Thus, biomass production has turned into a bottleneck for crowning microalgal biotechnology [17].

Scalability and trouble are terms that seem to go together. And for a long time, this has been the rule. However, for the modern researcher, although many biotechnological processes have come off the drawing board, the research and discovery pathway for large-scale production has rarely been direct and easy, especially in microalgae cultivation systems [18]. On the whole, bioprocess development occurs on three scales: laboratory, pilot, and industrial. On the laboratory scale, also known as the bench scale, the working volumes are reduced (~0.5 to 10 L), and microorganisms are inoculated for conditions and tests aimed at process optimization. Once the process parameters are established, they are only gradually transferred to larger volumes (pilot scale ~50 to 500 L) until, with all the optimal conditions determined, they can be transferred to industrial scale (>500 L), with scale factors ranging from thousands to millions (Figure 1). However, as larger work volumes are obtained, a proportional reduction in process control is observed. This is fundamentally attributed to an insufficient understanding of the principles that govern the expansion requirements [19,20].

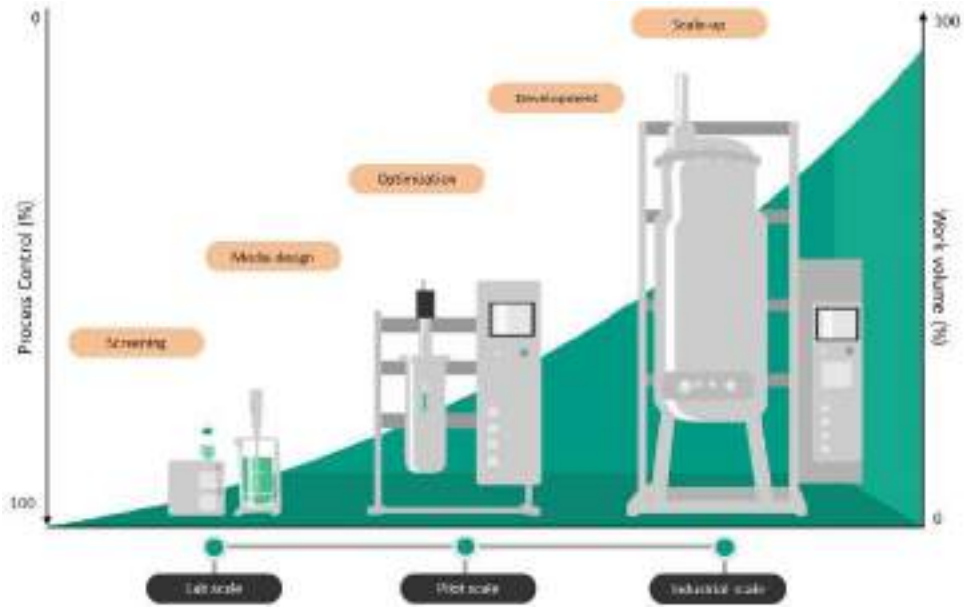


Figure 1. Tradicional principles of scale-up for microalgal bioprocesses. Note that process control is inversely proportional to the increase in the volume of work. Adapted from [21].

Indeed, it is well known that empirical engineering approaches based on the similarity principle and dimensional analysis for scale-up are always implemented under the general principle of keeping specific parameters constant. Among these aspects, factors such as specific energy consumption rate, mass transfer coefficient, impeller tip speed, shear forces, and mixing time and efficiency are considered, for example [22]. However, one cannot simply duplicate the scale conditions when scaling up equipment from the laboratory scale. After all, any process involving living microorganisms is unique and complex; therefore, the changes in the environment caused by a change in scale result in interactions and unforeseen responses, placing the efficiency and profitability of bioprocesses at risk [23].

Given these particularities, the scaling-up design of microalgal biotechnology begins, above all, with the numerous research efforts regarding the development of cultivation systems. Initially, large-scale cultivation was investigated in open systems led by raceway pond models due to primitive intuition compared to the way they were found in their natural habitat, as well as low installation cost [24]. However, with the need to achieve higher productivity under precisely controlled operational environments, engineering design developed closed systems known as photobioreactors. These systems are primarily designed and configured to achieve the following: (i) the highest surface-to-volume ratio; (ii) provide an adjusted level of nutrients; (iii) maintain balanced mass transfer rates; (iv) ensure appropriate photon absorption supply; and (v) sustain the ideal concentration of microalgal cells in combination with the extent of their cell multiplication phase [15].

Although a large number of photobioreactors have been investigated and have reached a somewhat satisfactory technological maturity, only detailed knowledge about hydrodynamic characteristics, mass transfer, shear stress, and scalability has not been enough to turn a silver bullet to the challenges of microalgal biotechnology [25]. Even the best-designed photobioreactor configuration requires considerable additional optimization work to achieve the necessary concentrations, rates, and yields for the adoption of these systems by industry. In this way, for the effective development of photobioreactors, your projects must integrate parameters that vary over time and on different spatial scales, considering the interaction of physical, chemical, and biological phenomena that affect microalgae cells [26]. Abiotic factors play a fundamental role in understanding how organisms interact with their physical–chemical environment, especially during the complex chemical

reactions involved in photosynthesis, which act as a cornerstone in nutrient conversion in microalgal biomass; these include (i) light supply—intensity, distribution, and spectrum quality of light, (ii) temperature, and (iii) mass transfer [27].

As is known, the light intensity that microalgae cells receive during cultivation has a substantial impact on cellular metabolism and growth since photosynthesis directly depends on the available light energy. Thus, it can be stated that the efficiency of the photobioreactors is intrinsically linked to the efficiency of the light supply, a key factor for the overall system performance [28,29]. However, one of the primary challenges associated with this principle arises from the fact that light, as it passes through the interior of photobioreactors, experiences attenuation due to absorption, scattering, and shielding effects induced by the microalgal cells. This phenomenon leads to unwanted light gradients throughout the system, thereby compromising the efficiency of photosynthesis within the photobioreactors [30]. Therefore, when managing and projecting parameters such as flow regimes within a photobioreactor configuration, it is often assumed that turbulent flows are ideal, as they favor greater homogenization of the culture, reducing light gradients and increasing uniformity of exposure to light. However, the implementation of high hydrodynamic forces can present a dilemma: while turbulent flow improves homogeneity, it can hinder the movement of the liquid between the dark zone (bottom) and the light zone (surface), limiting the exposure of cells to the light required for efficient photosynthesis. Furthermore, the resulting shear stress can become excessive, leading to increased cell mortality and decreased growth rates. This adverse effect may, therefore, reduce the effectiveness of the photosynthetic process, becoming a bottleneck in the photobioreactor performance [31].

As strategies to increase cellular exposure without rupture damage, the choice of an optimized design, such as the use of bioreactors with cylindrical or helical geometry, can help control the intensity of turbulent forces. Bioreactors with several flow zones can also be designed to dissipate excessive turbulence in certain areas, ensuring better energy distribution in the system [32]. More recently, flux and luminosity sensor use coupled with automatic control systems allows for constant monitoring and the dynamic adjustment of operating conditions. These systems can adjust the pumping speed and the rotation of the agitators or others in real time, depending on the conditions inside the photobioreactor, ensuring a balance between the efficiency of the light supply and the protection of the microalgae cells [33].

Simultaneously, light distribution efficiency can be intensified or attenuated depending on the surface-to-volume (S/V) and the height-to-diameter (H/D) ratio. The light distribution path in a photobioreactor can be divided into three zones: photo-inhibition, light-limited, and stagnation. In zones with short light paths, the light intensity is generally higher than the photosynthetic demand of the cells. It originates in a zone with the largest photo-inhibition potential, resulting in the inhibition of microalgae cell growth and, in some more extreme cases, potentially leading to cellular death. Insofar as the light path increases, the light intensity decreases, and a balance state is reached between light entry and cellular absorption at a specific point. In this position, the microalgae cells achieve their maximum growth rate. However, in zones with a longer light path, the light intensity is very low for supporting the growth of algae cells, and these, consequently, will stagnate in this area [34]. In this context, when the transition from bench photobioreactors to pilot and industrial scale occurs, the increase in work volume does not accompany the pre-established performance of the light distribution paths, and, therefore, operational problems arise in the search for illumination and space [35]. According to the literature, a height/diameter ratio suitable for the optical path to reach the reactor core without interference from cell density is set to values lower than 2. However, these configurations on an

industrial scale—today—generally present values equal to or greater than 10, as in the case of tubular photobioreactors and flat plates (~14.0 m^2/m^3). To try to circumvent this gap, in recent years, models of hybrid photobioreactors have been designed to provide a high work volume while maintaining an adequate height/diameter ratio (H/D = 1.5). For example, studies conducted by Jacob-Lopes et al. [36,37] developed a lighting platform for hybrid photobioreactors that requires only 0.22 m^2/m^3 since the largest reactor compartment is not dependent on light. However, these systems must be used in cultures with highly resistant strains due to the risk of contamination [38].

Maximizing light penetration in the photobioreactor not only involves adjusting the appropriate flow regime and surface-to-volume ratio but is also closely linked to the quality of the materials used in its construction. As is known, the type of material influences the transmission, dispersion, and reflection of light and can optimize the intensity and spectrum of light that affects microalgae, directly impacting the efficiency of photosynthesis and, consequently, the microalgae growth. Furthermore, the material's durability against UV radiation and internal cooling also plays a crucial role in choosing the most suitable material for the photobioreactor [39]. Meanwhile, the advancement of this objective has been confronted with a significant additional challenge: biofouling on the internal walls of photobioreactors. Biofouling compromises the penetration of solar radiation, reduces the useful life of materials, harms the quality of culture, and amplifies the risk of contamination. As a result, frequent interruptions are necessary to carry out physical and chemical cleaning, apart from the eventual replacement of coatings, which results in an increase in operating costs [40]. In this context, choosing materials for the construction of photobioreactors must prioritize not only high transparency but also essential characteristics, such as flexibility, durability, non-toxicity, and resistance to chemicals and metabolites generated by microorganisms, as well as resistance to climatic conditions and, always if possible, low cost [41].

Currently, the traditional materials used in photobioreactor construction include glass and polymers, such as polymethylmethacrylate (PMMA) and polycarbonate (PC), which stand out for their high luminous transmittance. The common glass potential generally varies between 80–90%; however, high-quality glass, such as tempered or ultra-clear glass, can achieve more than 90% transmittance [42]. In comparison, the luminous transmittance of PMMA can vary from 90 to 92%, depending on the quality and thickness of the material [43]. Polycarbonate, in turn, has a slightly lower luminous transmittance, varying from 85 to 90%. Nevertheless, polycarbonate stands out for its greater impact resistance and better thermal performance, properties that render it especially suitable for applications demanding high mechanical durability and resistance to extreme conditions [44].

Regarding the potential for biofouling, the three materials in question have extremely smooth surfaces, which could make it difficult for microorganisms to adhere. However, considering the minimum Vogler interval ($20 < \tau_0 < 40$ mJ/m^2), which defines the surface tension level in which surfaces are only less prone to the microorganisms' adherence, it is observed that these materials are not ideally placed in this parameter [45]. The surface tension of polymethylmethacrylate (PMMA) and polycarbonate (PC) is between 40 and 45 mJ/m^2, while the glass presents a surface tension that varies from 50 to 70 mJ/m^2 [46]. Thus, to consider the trade-off between luminous transmittance, mechanical resistance, and biofouling potential, the optimal choice for the construction of photobioreactors seems to be polycarbonate due to its combination of high transmittance and higher resistance to biofouling in comparison with other materials.

Although light is the most studied parameter in photobioreactor design due to its impact on photosynthetic efficiency, temperature is also a crucial factor, albeit less understood and explored [47]. Each microalgae species has an optimal growth temperature that

allows the cell to photosynthesize without altering essential biochemical or physiological parameters. The temperatures that promote maximum growth rates vary between 20 and 25 °C for mesophilic species but can reach around 40 °C for thermophilic strains or reduce to around 15 °C for psychrophilic strains [48]. However, when temperatures are adjusted to these ideal conditions, the levels of cellular productivity can be affected on three levels: (i) cellular, (ii) molecular, and (iii) physical–chemical. From a cellular point of view, temperature oscillations affect enzymatic processes, mainly the kinetics of ribulose-1,5-bisphosphate adjustment (Rubisco). Rubisco is an enzyme responsible for carbon fixation and is a fundamental part of photosynthesis, catalyzing photosynthesis in two concurrent physiological pathways—photosynthesis and photorespiration—with a dual activity of carboxylase and oxygenase, respectively [49,50]. At temperatures above 30 °C, the affinity of the enzyme (Rubisco) for the substrate (carbon dioxide) is reduced, becoming a limiting factor for photosynthesis and, therefore, reducing the levels of cellular productivity. At temperatures below 15 °C, the reduced activity of Rubisco can slow down cellular metabolism, prejudging processes such as energy production and synthesis of microalgal biomass [51]. As for molecular damage, high temperatures induce protein degradation, leading to cellular mortality. Furthermore, the activation mechanisms of cellular stress strongly affect the oxygen–reactive species dynamics, causing progressive oxidative damage and, finally, cellular death. Under physical–chemical optics, temperature influences the mass transfer rates of gases, such as CO_2 and O_2, beyond affecting the gas solubility in the medium, which influences the equilibrium and the reaction kinetics [52].

It is generally known that hot and sunny regions (tropical and subtropical zones) are ideal for photobioreactor installations because they offer favorable natural conditions, such as adequate temperature and high-intensity sunlight for microalgae cultures. Most of the commercial production of microalgae is carried out in external environments with little or no humidity control over the climate [53,54]. The result of this practice is the overheating of cultures in the absorption and conversion of excess solar energy into heat. In the absence of active temperature control systems, depending on the geospatial position of the facilities, the internal temperatures of culture systems can easily reach temperatures of >50 °C, making it impossible for any mesophilic species of commercially cultivated microalgae to thrive under these conditions [55]. Therefore, temperature control becomes a vital resource for cell survival in extreme oscillations [56].

The temperature control systems active in photobioreactors must be designed to facilitate heat exchange and maintain a rigorous adjustment to the temperature suitable for cell development during the bioprocess [57]. The industry has developed two main control methods: (i) passive evaporative cooling and (ii) heat exchangers [58]. The operational mechanism of evaporative passive cooling consists of the utilization of water evaporated to reduce the temperature. Meanwhile, heat exchangers operate through thermal energy exchange for heat absorption by cold fluid that passes around the equipment, maintaining the equipment at temperatures around 25 °C [59]. In a decision-making process, the passive evaporative cooling method has the advantage of being a more economical device for large-scale cultures. However, from an environmental point of view, this statement is not supported. This is because the system requires the distribution and consumption of a considerable water volume: 8000 m^3/ha/year of water to reduce the PBR temperature from 40 °C to 25 °C (equivalent to removing 18,000 GJ/ha/year of heat) [60]. Additionally, it is important to highlight that since all places with high solar radiation are ideal for the production of microalgae, water is a finite resource, which makes these systems economically and environmentally unsustainable. Likewise, heat exchanger systems for photobioreactors are expensive for industrial photobioreactors, especially when initial installation investments are a concern. Also, the environmental challenges regarding energy efficiency and the use

of natural resources (freshwater) are aspects that must be improved for this equipment [61]. Given the existing technological gap, significant advancements have been made in research focused on sustainable alternatives for temperature control in photobioreactors, with the aim of achieving greater energy efficiency and reducing environmental impact. Various passive approaches have already been investigated, such as thermal ground exchangers, the use of phase change materials, and light filtering [62–65]. Light filtering, for example, can use the principle of hot mirrors to selectively reflect ultraviolet (UV) and infrared (IR) radiation, which account for approximately 50% of solar energy, thus preventing system overheating. Additionally, a more innovative approach involves the use of semi-transparent photovoltaic (PV) panels placed on the optical surface of photobioreactors, which absorb and convert specific wavelengths into electricity while allowing the remaining light to pass through for microalgal cell growth. This solution not only reduces water consumption and energy needs for thermal control but also contributes to the additional production of electricity from the conversion of UV and IR radiation, improving the overall efficiency of solar light conversion and promoting the sustainable co-production of biomass and electricity [66].

Although the mass transfer characteristics are also strongly correlated with hydrodynamic parameters, such as mixing time, liquid velocity, gas ball velocity, and gas retention, the main parameter evaluated is the mass transfer coefficient [67]. Mass transfer refers to the diffusion rates of components, such as carbon dioxide, between the gas and liquid phases. In photobioreactors, bioprocesses are characterized by multiphase interactions, mainly involving gaseous exchangers for the fixation and generation of carbon dioxide and oxygen, respectively. Furthermore, it involves microalgae cell interaction in solution with substances excreted by the cells (mostly exopolymers) [68]. Likewise, improving the mass transfer coefficient between the CO_2 bubbles and the microalgae solution allows a higher rate of CO_2 fixation for microalgae and, consequently, the proliferation of microalgal biomass [69].

To better understand these aspects, it is essential to understand the reactivity of carbon dioxide in aqueous solutions. Carbon dioxide establishes various balances in its contact with water. The first equilibrium refers to the dissolution of gas in water to form carbonic acid. Carbonic acid undergoes almost instantaneous dissociation in bicarbonate and carbonate ions, with the concentration of total inorganic carbon given by total carbonic acid (H_2CO_3), bicarbonate (HCO_3^-), and carbonate (CO_3^{2-}), which needs to be considered in the transient response [70,71]. As elucidated by Cuaresma et al. [72], how microalgae cells adapt to use CO_2 as a carbon source is related to carbon concentration mechanisms (CCMs). The photosynthetic mechanism developed by these organisms enables the transport of free CO_2 and bicarbonate ions through a thin plasma membrane after having accumulated in the cell as a carbon reserve, making it possible to assimilate inorganic carbon in the form of bicarbonate or free CO_2 [73,74]. Thus, to provide these elements efficiently throughout the process, it is necessary to understand the solubility rates of the two gases present in the system. In terms of solubility, CO_2 is much more soluble in water than O_2. However, both have low solubility at optimal cell growth temperatures of most microalgae species. To ensure a continuous supply of nutrients and high volumetric coefficients, photobioreactor projects depend mainly on the physical properties of the fluid, flow, system, and gas injector geometry. It is worth highlighting that, to improve mass transfer, reducing the size of the CO_2 bubbles leads to a faster dissolution, slower rise, and a higher surface/volume ratio, facilitating gas exchange [75].

Simultaneously with the increase in carbon dioxide fixation rates, the photosynthetic response of microalgae results in the generation of oxygen. When the gas bubbles are released during the culture process, they coalesce, forming an interface between the liquid

and gas phases and the walls of the photobioreactors. This phenomenon is mainly caused by oxygen accumulation. It is estimated that the concentration of dissolved oxygen cannot exceed 400% of the saturation value, or it leads to a reduction in the surface area available for mass transfer between the gas and the liquid [76]. Mass transfer rates can be quite prejudicial, resulting in low efficiency of the process. This inefficiency in mass transfer directly affects biomass productivity, as it can induce photorespiration and oxidative damage to cells. A high oxygen concentration favors the activity of oxygenase enzymes, which use O_2 instead of CO_2, harming cell growth. This phenomenon is particularly common in tubular configuration photobioreactors. To mitigate this problem, many tubular photobioreactors incorporate degassing systems, which use devices based on air transport to remove excess oxygen from the air [77]. Another alternative is to manipulate secondary factors, such as activating turbulence in the system, which can increase the efficiency of the gas exchange. Furthermore, the introduction of air flows enriched with CO_2 and O_2 in controlled concentrations can optimize mass transfer, improving the efficiency of the photosynthetic process and, consequently, biomass productivity [78].

As discussed here, a deep knowledge of aspects related to the rational core of microorganisms is crucial to informing various decisions in photobioreactor project design development. However, understanding the biotic factors that influence biomass production is equally essential because, with the metabolic characteristics of strains, we can optimize growth processes, promote the production of specific metabolites, and strengthen the composition of the desired microalgal biomass [79]. Thus, biotic factors mainly involve the conditions that affect microalgae metabolism and their interactions with the environment.

Microalgae species selection is one of the main determinants for the success of any industrial cultivation operation. The taxonomic classification, which organizes the microalgae according to their lines and classes, offers a fundamental understanding of the biological characteristics and performance of the species, allowing the selection of the most suitable ones for different cultivation conditions and production objectives [80]. This process is crucial because each species has unique characteristics that directly influence its efficiency in growth, carbon fixation, biomass production, and added value in industrial processes. For example, species belonging to the class *Chlorophyceae*, such as *Chlorella vulgaris* and *Scenedesmus obliquus*, are widely used due to their high photosynthetic taxes and high efficiency in carbon fixation. These characteristics become particularly advantageous for large-scale production, as they can reach cell productivity rates of 0.50–2.11 g/L/d and give a final biomass concentration of 3.0–20.0 g/L [81,82]. These species are frequently chosen when the main objective is to prioritize biomass, especially in controlled photobioreactors, where environmental conditions can be rigorously adjusted to optimize their growth. However, *Chlorella vulgaris* has been more prominently studied for biofuel research due to its ability to accumulate lipids (~0.20 g_{lipids}/L/d), whereas *Scenedesmus obliquus* is primarily investigated for carbon capture and storage (~0.44 $g_{dioxide\ carbon}$/L/d), with a focus on biomass utilization [83,84]. On the other hand, the species of the *Cyanophyceae* class represented by *Arthrospira platensis* (popularly known as *Spirulina*) stand out for high biomass production, especially with high protein content (>50% dry weight). This characteristic makes this microalgal species of great nutritional interest, being widely used in the food industry and the production of food supplements [85]. Thus, the identification and taxonomic classification of microalgae are essential, allowing us to select the species most suitable for specific production objectives. Species selection not only impacts the efficiency of culture productivity but also determines the economic viability and sustainability of the industrial process. Depending on the objective—whether to maximize biomass or key biocomposts—the correct species selection allied to the cultivation domain conditions is crucial for the operation's success.

Another relevant factor is the identification and management of the cell cycle of microalgal growth. In terms of life cycle, microalgae microorganisms can develop (i) vegetatively or (ii) reproductively. During the vegetative phase, these microorganisms reproduce by cell division, which results in rapid growth and is the most efficient phase for biomass production. The reproductive phase, which occurs with the gamete's formation, is generally associated with the spore's formation or resistant structures, which may be less productive in biomass [86]. Therefore, the controlled adjustment of culture parameters is important and should be used to optimize biomass production in large-scale cultures. For example, the controlled supply of nutrients, such as nitrogen and phosphorus, must be abundant in cultivation systems once we induce the vegetative phase, resulting in higher biomass production. Scarcity, on the other hand, tends to induce microorganisms to enter the reproductive phase, which may be useful, in some cases, for spore production but is not desirable for maximizing biomass [87]. This same effect induces sexual reproduction and has also been observed in conditions of environmental stress, such as intensive use in extreme light temperatures in some microalgae species, as a form of survival or resistance.

Simultaneously, certain physiological stress conditions impose microalgae microorganisms in need of environmental adaptability, which occurs through changes in their genetic expression. Some species, such as *Haematococcus pluvialis*, possess physiological mechanisms that allow them to adapt to these adverse conditions. This adaptation process can result in the production of secondary metabolites, such as astaxanthin, which have various industrial applications, especially in the pharmaceutical, food, and cosmetic industries. This is a promising alternative in the context of advances in genetic engineering, which aims to understand in more detail the metabolism and the pathways responsible for the multiplication of these microorganisms [88]. The genetic sequence not only helps in the identification of new species with exploration potential but also opens possibilities for the genetic improvement of microalgae [89]. Genetic improvement may represent a great advance for microalgae-based process consolidation, allowing the characterization of important biosynthetic pathways. An example is the chlorophyll-binding proteins, which are directly associated with the photosynthetic apparatus. The genes that encode these proteins play a crucial role in increasing microalgal biomass production [90]. Furthermore, microalgae genetic modification has been optimized for various applications, mainly in the bioenergy field, with the aim of improving lipid yields and increasing amino acid conversions. In parallel, studies focused on genetic modification during the cultivation stages have sought to increase the nutritional biocompounds, such as carotenoids [91,92].

Microalgae are subject to multiple ecological interactions that can significantly influence cell multiplication. Among them, symbiosis is one of the main mutualistic relationships in which microalgae species build with other microorganisms, such as bacteria [93]. These consortia can be beneficial once they help in essential nutrient fixation, beyond providing protective barriers against strenuous external conditions, resulting in better metabolic efficiency for cell multiplication. On the other hand, microalgae also face competition from other microalgae species or microorganisms present in the environment, which can negatively affect their productivity. When abiotic resources are limited, competition intensifies, resulting in a reduction in microalgae growth and a decrease in biomass production. This competition is especially accentuated in environments where the supply of resources is restricted, such as in intensive cultures. Likewise, microalgae are subject to the influence of pathogens and predators, which can further impact their productivity. Infections by viruses, bacteria, or fungi can reduce health and microalgae growth, negatively affecting biomass production. In open or closed systems, interactions with predators, such as zooplankton and other aquatic organisms that feed on microalgae, also represent a

challenge. These predators can directly reduce available biomass, prejudicing the success of the culture [94].

Given the current scenario, a deep understanding of abiotic factors related to the design, configuration, and operation of photobioreactors and biotic factors that regulate the physiological conditions of microalgae cells is essential to optimize microalgae cultivation. This understanding becomes even more relevant when considering the critical challenges that characterize microalgal biotechnology. In this context, a common denominator to be highlighted is that the success of industries based on microalgae intrinsically depends on the efficiency of process control systems. The relationship between process control and microalgal biomass productivity is profoundly influenced by seasonal oscillations, daily fluctuations, biotic and abiotic factors, microbiome variability, various cultivation practices, and applied regimes. These factors contribute such that the processes are, at times, highly controlled, at other times managed in an intermediary manner, and, in many situations, vulnerable to unexpected variations (Figure 2). In this way, these factors require rigorous and constant management of the cultivation parameters to ensure that ideal conditions are maintained. As reported in the literature, on bench scales, the precise control of cultivation parameters allows the productivity of some microalgae to exceed 2–5 g/L/d. However, in industrial environments, where the conditions are the most challenging, the maximum productivity of photobioreactors tends to vary between 1.5 and 2.0 g/L/d for microalgae cultures. In open systems, such as raceway ponds, with insufficient or substantially uncontrollable control, these estimates can be even more reduced (~0.5 g/L/d), seriously compromising the process viability and resulting in industrial operations with less-than-expected performance. Therefore, rigorous control and effective management of the processes represent the backbone of ensuring the stability and productivity of large-scale cultures. The dynamic implementation of control strategies, which continually adjust the operational parameters in response to changes in the growing conditions, thus becomes the main differential between industrial systems that have not yet succeeded and those that have failed to achieve their full potential.

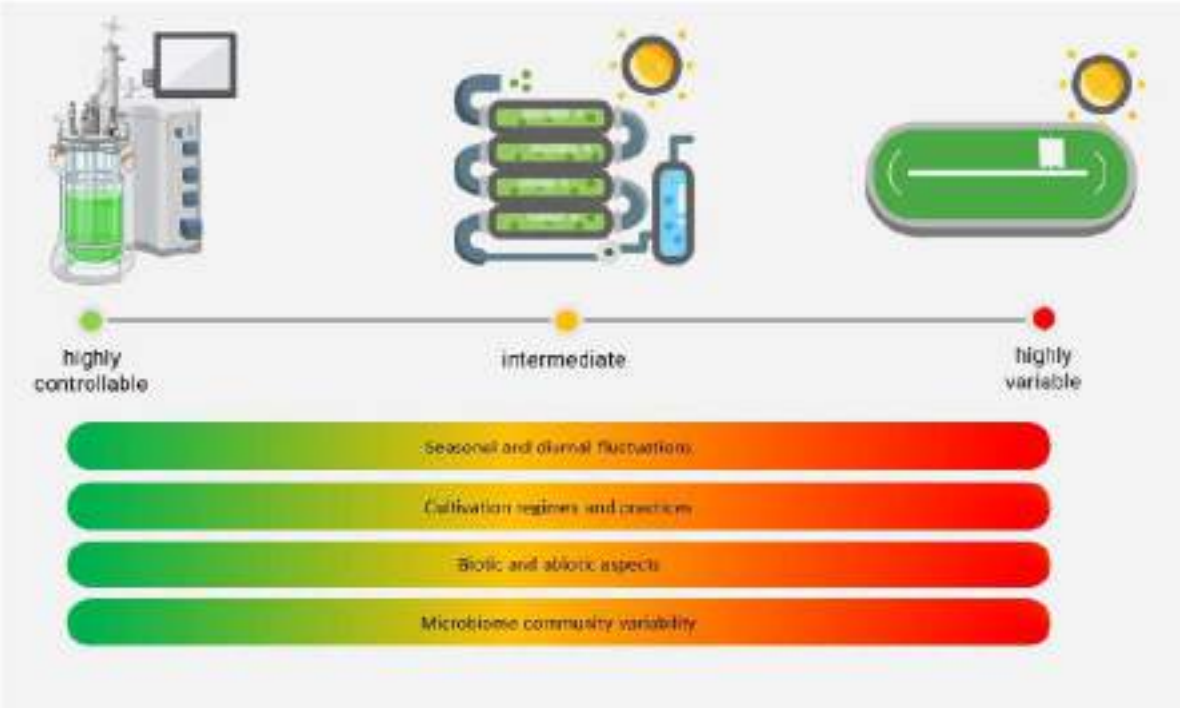


Figure 2. Relation between process control effects and microalgal biomass productivity. Adapted from [95].

3. It Takes Two to Tango: Analyzing the Technological Readiness Level and Market Demand of Microalgae-Based Bioproducts

Before any bioprocess can be implemented and raised in the laboratory on an industrial scale, it is not enough to carry out extensive research, development, and evaluation of its performance. It is also imperative to optimize and model the processes precisely and estimate the financial demands and the potential returns, in addition to deeply considering the social and environmental impacts involved [20]. Only when all these elements are meticulously aligned can the transition to large-scale production be truly feasible. Therefore, a crucial stage in the investment decision-making process for the commercialization of innovative products is to evaluate their current technological readiness level (TRL) [96]. Initially developed by NASA in the 1970s, technological readiness level is a globally recognized benchmarking tool to measure progress and support development from basic research—including blue sky research, which represents the early, exploratory phases of the innovation process—through to reaching practical implementation in real-world applications [97,98].

Structurally, the technological readiness level (TRL) scale can be divided into three major stages: (i) idea conception, (ii) death valley, and (iii) acceptance (Figure 3). The first stage, dedicated to conception and research, encompasses TRLs 1 to 3. This is technology at its most incipient stage. O TRL 1, the initial level, represents the starting point of the technological journey, where scientific research begins to transition from theory to practical application. TRL 2 marks the moment when the possibility of transforming concepts into tangible applications arises, initiating the development and the first investigations. O TRL 3 is achieved when applied research advances in laboratory experiments and the tests validate the first hypotheses, confirming the technology viability. The second phase, which encompasses TRLs 4 to 6, is characterized by intensive development and is commonly known as the death valley. At this stage, the technology begins to take shape but still faces significant challenges before reaching maturity. TRL 4 involves the integration of several components, after being individually tested, to ensure their compatibility and functionality in a controlled laboratory environment. In TRL 5, the functionality of these components begins to be validated in tangible conditions, an essential step to approximate the technology of its application potential. Upon reaching TRL 6, the technology starts to be tested in a relevant environment, bringing it closer to practical application yet still distant from large-scale production. Finally, the demonstration stage includes TRLs 7 to 9, representing the transition to commercialization and acceptance. In TRL 7, the technology consists of a crucial framework, with functional prototype implementation in a real environment that simulates and reflects the intended operating conditions. O TRL 8 denotes the final technology validity, which is now fully functional and ready to be operated within the conditions and parameters for which it was designed. Finally, TRL 9 represents the apex of the technological trajectory: full innovation commercialization, with technology fully accepted and implemented in the global market [99,100].



Figure 3. Technology readiness level (TRL) and commercial readiness index (CRI) scale. Adapted from [101].

However, for a technology to be readily available on the market, it is not enough for it to be just technically ready. It is equally crucial that there is market demand for products derived from technology [102]. Both factors—technology and market—must be aligned to ensure their commercial consolidation. Once the technology advances to the demonstration and implementation phases, a new set of variables is introduced to validate the commercial readiness of the technology [103]. The commercial readiness index (CRI), sometimes called a marketing pathway, encompasses a series of stages that enable us to identify the barriers that a given industrial sector may face. This parameter offers a rigorous structure to assess these obstacles and facilitates the financial support organization through a systematic approach, aiming to reduce risks and overcome barriers in the various phases of the marketing process [101].

In light of the above, when we analyze the different models of photobioreactors and their technological maturity, the tubular photobioreactors stand out as the most advanced, with an estimated TRL between 7 and 9 (Table 1). This level reflects the technology consolidation in commercial production, especially in areas such as fine chemicals. Due to their robustness and efficiency, tubular photobioreactors have achieved success in microalgal facilities and continue to be a pillar for large-scale biotechnology applications. Models such as flat-plate photobioreactors and bubble columns (airlift), however, fall within the pilot or semi-industrial phase, with estimated TRLs ranging from 6 to 8. These systems are in

intermediate development levels, where the cultivation and scale production efficiency are still being optimized. Although these photobioreactors show great potential in light distribution and energy economy, they still face technical and economic challenges to being competitively implemented on a large scale. Moreover, hybrid photobioreactors present an estimated TRL of 5–7, indicating that they are in the initial development stage, with some prototypes still in experiments or integration tests. These systems combine different types of photobioreactors, seeking optimization of both performance and operational cost, but also need more validation to achieve full technological maturity. Finally, plastic bag photobioreactors are in the very early stages of development, with TRL estimated between 4 and 6. This application is predominantly restricted to academic research and small-scale testing due to its simple and low-cost structure but is still limited in production scale-up and energy efficiency. These systems, with promise for certain applications, need further evolution before they are considered suitable for large-scale adoption.

Table 1. Estimation of the technological readiness level for the main photobioreactor models intended for microalgae-based facilities.

Photobioreactor Design	Technological Readiness Level	Implementation Costs (kUSD/m^3)	Status	Bottlenecks
Tubular	TRL 7–9	40.0–50.0	Industrial scale	Light efficiency and nutrient distribution
Flat plate	TRL 6–8	~150.0	Pilot and semi-industrial scale	Culture maintenance and flow control
Bubble column (airlift)	TRL 6–8	5.0–10.0	Pilot and semi-industrial scale	Light efficiency and culture homogeneity
Hybrid	TRL 5–7	4.0–15.0	Pilot and semi-industrial scale	Integration between systems and operating costs
Plastic bags	TRL 4–6	1.0–3.0	Laboratory and pilot scale	Fragility of materials and temperature control

Moreover, it is important to highlight that the large-scale consolidation of the technological maturity of photobioreactors is often associated with the cost–benefit of their installation and their scalability potential. The implementation cost of photobioreactors is closely linked to the quality of materials required by each configuration, as well as the specific area requirements. As shown in Table 1, tubular photobioreactors, with the highest level of technological maturity, have implementation costs in the range of 40–50 kUSD/m^3, significantly lower than flat-plate photobioreactors (~150 kUSD/m^3) [104]. This substantial difference can be attributed to the amount of material required for construction, with rectangular configurations requiring more material than cylindrical tubes. Furthermore, tubular photobioreactors, which produce higher value-added products, help balance the initial investments, justifying their higher cost when compared to models with lower technological maturity [105]. In contrast, models with intermediate technological maturity, such as bubble columns and hybrid systems, have lower implementation costs but still face considerable challenges in terms of productivity and engineering setups (scale-up), hindering their full consolidation.

Additionally, when we analyze microalgal biotechnology in a broad manner, it is possible to observe that microalgal biomass exploitation for commercial purposes is not a recent idea. In fact, this field has developed consistently over the years, especially as a food source and in supplements, with technologies that have already reached levels of TRL 8–9 and CRI 4 (Figure 4). These food bioresources have been traditionally consumed across various cultures, with established markets in Asia, Europe, and North America [106]. The sustained

growth in demand for these products is closely linked to the perception of microalgae as a healthy food source, making them particularly attractive as dietary supplements due to their high protein content and overall nutritional value [107]. Additionally, fine chemical products, such as β-carotene and astaxanthin, exhibit the highest technological readiness level (TRL 8–9). These bioproducts, with CRI 6, demonstrate a high commercial readiness level, being widely recognized and distributed globally. They can be marketed under various brands, which attests to both their formal registration and proven market success. Their market leadership is further emphasized by the absence of alternative natural sources, as is the case with phycocyanin, which only has a synthetic countertype. This factor further strengthens their established position in the market [108].

Microalgae-based feeds for animal nutrition, especially for aquaculture and pets, are already a reality [109]. These bioproducts are used as essential nutrient sources, reflecting a market in the maturation process, and are classified with CRI 4. Also, although there is a growing interest in microalgae as livestock feed, this market is still in development but not as established as the aquaculture sector. While some operational trials and commercial activities are underway, they remain in an early stage (CRI 3) [110]. On the other hand, microalgae-based biofertilizers and other intermediate-volume biomaterials, such as bioplastics, are classified with TRL levels between 4 and 6, reaching CRI indices between 2 and 3. These products are in the testing and preparation phase, with a commercial adoption that is still growing but not fully consolidated [111]. In contrast, microalgae-based biofuels and bioenergy sources, recognized as potential commodities, are found in a more initial phase of development (TRL 3–5), with commercial readiness levels varying between 2 and 3. Some authors have reported TRL levels that have reached around 6 [112]. However, it is worth noting that competition with fossil fuels, especially petroleum, represents a significant challenge for full biofuel commercialization.

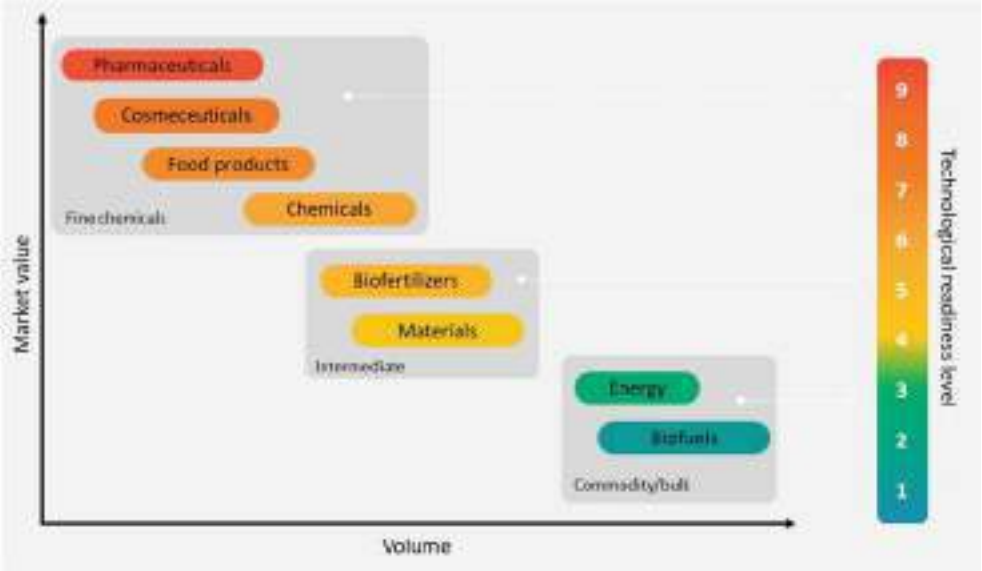


Figure 4. Technological readiness level of microalgae-based products from a market value and volume perspective. Adapted from [113].

4. Future Directions

In order for photobioreactors to advance from their current levels of technological readiness to more advanced stages, stakeholders should adopt a comprehensive and multifaceted approach that integrates operational optimization, technological innovation, technical capacity building, infrastructure investments, and a thorough analysis of eco-

nomic and environmental feasibility. In this context, fostering collaborative research and development among academia, industry, and government is the starting point for optimizing photobioreactor designs and facilitating the transition from laboratory-scale to commercial-scale systems. Furthermore, the implementation of tax incentives for pilot-scale demonstrations is vital to assess photobioreactor performance under real operational conditions. Process optimization and standardization will significantly contribute to enhancing efficiency, reducing operational costs, and promoting broader adoption of this technology.

Precise control of parameters, such as temperature, pH, light intensity, and nutrient supply, maintains the stability and productivity of the system. The integration of real-time monitoring sensors and automated systems allows for dynamic and accurate adjustments, ensuring that the cultivation environment remains within optimal conditions. Currently, companies such as Solazyme (TerraVia) employ sophisticated computational systems, such as the SCADA system, that enable the capture of all environmental and culture parameters for data analysis while simultaneously monitoring and controlling these factors in real time, thus ensuring ideal growth conditions for their microalgae [114]. Other companies also utilize laboratory information management software to document process control and batch validation, enabling quick access and facilitating the predictive control of the photobioreactor. These technologies enable rapid research on process variables to achieve the desired production, thereby contributing to the scalability of algae-based products once environmental conditions can be instantly adjusted to maintain high productivity.

Furthermore, it is recommended to select microalgal strains with rapid growth and greater resistance to adverse environmental conditions, as this enables shorter cultivation cycles and, consequently, higher productivity. By applying advanced genetic engineering techniques, such as CRISPR, microalgal strains can be made more productive, resilient, and adaptable to various environmental conditions. Examples like those from ExxonMobil-Viridos demonstrate the success of the genetic modification of strains and optimizing the production of biofuels and other high-value compounds while simultaneously improving yield and environmental performance [115]. These technological innovations, despite requiring an expensive initial investment, must be adopted because they do not merely increase productivity but also reduce long-term operational costs, improving the robustness and efficiency of the systems and making microalgae production more economically viable.

Additionally, the efficient operation and success of photobioreactors require continuous training for staff. Training programs should focus on new technologies, data analysis, process control, and applied engineering solutions, preparing operators to manage ongoing innovations in the field. Collaboration with universities and specialized research centers is strongly recommended to enhance operational practices and ensure a qualified workforce. Through the integration of academia and industry, the adoption of risk management practices, including the development of contingency protocols for operational failures and periodic testing, will facilitate the identification of vulnerabilities, thereby promoting the continuous advancement of photobioreactors.

In economic terms, effective strategies for decision-makers involve optimizing operational costs through automation to reduce dependence on labor-intensive work. The adoption of innovative technologies, such as hybrid systems, can increase productivity and reduce land requirements, resulting in lower costs. Environmentally, it is essential to prioritize the use of renewable energy sources to power the systems, minimizing the carbon footprint. Integrating photobioreactors in locations near sources of wastewater or excess CO_2 can enhance the sustainability of the process, utilizing waste as resources and creating a closed-loop system that prevents pollutant emissions. Companies like Algenol exemplify this approach by optimizing the conversion of CO_2 into valuable products, reducing carbon emissions [116]. Solazyme (TerraVia), in turn, uses a combination of photobioreactors and

conventional bioreactors to improve process efficiency and reduce costs while also utilizing agricultural waste and by-products as nutrient sources for algae, promoting a circular economy [114]. Therefore, integrative and practical strategies like these, grounded in solid scientific principles, not only enhance economic efficiency but also promote more sustainable operations, driving photobioreactors and microalgal biotechnology to a new industrial level where innovation and sustainability intertwine synergistically. Undoubtedly, it is essential to emphasize that the initial implementation of these strategies can be substantially costly, presenting a significant challenge for their large-scale adoption. However, in the long term, these integrative approaches hold the potential to boost productivity rates, enhance efficiency in resource consumption, and optimize the overall economics of the process, paving the way for overcoming the bottlenecks in microalgal biotechnology.

5. Conclusions

Photobioreactors represent a crucial component for the advancement of microalgal biotechnology, as they are essential for maximizing cellular productivity and optimizing the use of both biotic and abiotic resources. Their capacity for customization is a determining factor, as different types of microalgae and their bioproducts require specific operational conditions. This necessitates technical innovations and sophisticated engineering to ensure process efficiency, directly influencing the scalability, viability, and competitiveness of photobioreactors.

In addition to the technical aspects, optimizing the cost–benefit ratio and aligning with market demand are key elements in ensuring that photobioreactors become competitive not only in the production of fine chemicals for the food and pharmaceutical industries but also in emerging sectors such as biofuels. In this context, the continuous improvement of these systems, with a focus on reducing operational costs and increasing productivity, will be essential for their global integration.

By overcoming the technological and economic challenges that still hinder the engineering of photobioreactors, coupled with progress in research and continuous innovations, as well as the experience gained from various photobioreactor configurations, these systems have the potential to establish themselves as robust and scalable solutions for the industrial production of microalgal-based bioproducts. Undoubtedly, photobioreactors will play a strategic role in sustainable and innovative industries, contributing decisively to a greener and more technologically advanced future.

Author Contributions: Writing—review and editing, writing—original draft, visualization, investigation, conceptualization: M.C.D.; formal analysis and data curation: R.R.D.; supervision and project administration: L.Q.Z.; conceptualization, project administration, writing—review and editing: E.J.-L. All authors have read and agreed to the published version of the manuscript.

Funding: This research received no external funding.

Conflicts of Interest: The authors declare no conflicts of interest.

References

1. Razzak, S.A.; Bahar, K.; Islam, K.O.; Haniffa, A.K.; Faruque, M.O.; Hossain, S.Z.; Hossain, M.M. Microalgae cultivation in photobioreactors: Sustainable solutions for a greener future. *Green. Chem. Eng.* **2024**, *5*, 418–439. [CrossRef]
2. Amarakoon, I.I.; Hamilton, C.L.; Mitchell, S.A.; Tennant, P.F.; Roye, M.E. Biotechnology: Principles and applications. In *Pharmacognosy*, 2nd ed.; McCreath, S.B., Clement, Y.N., Eds.; Academic Press: London, UK, 2024; Volume 1, pp. 627–645.
3. Filippi, M.; Mekkattu, M.; Katzschmann, R.K. Sustainable biofabrication: From bioprinting to AI-driven predictive methods. *Trends Biotechnol.* **2024**, *1*, 1–14. [CrossRef] [PubMed]
4. Yap, J.K.; Sankaran, R.; Chew, K.W.; Munawaroh, H.S.H.; Ho, S.H.; Banu, J.R.; Show, P.L. Advancement of green technologies: A comprehensive review on the potential application of microalgae biomass. *Chemosphere* **2021**, *281*, 130886. [CrossRef] [PubMed]

5. Hong, X.; Fan, L.; Yan, X.; Li, J. Structural and functional properties of proteins isolated from four species of microalgae and their application in air-water interface stabilization. *Int. J. Biol. Macromol.* **2024**, *283*, 137531.
6. Nunes, E.; Odenthal, K.; Nunes, N.; Fernandes, T.; Fernandes, I.A.; de Carvalho, M.A.P. Protein extracts from microalgae and cyanobacteria biomass. Techno-functional properties and bioactivity: A review. *Algal Res.* **2024**, *82*, 103638. [CrossRef]
7. Thakur, A.; Sharma, D.; Saini, R.; Suhag, R.; Thakur, D. Cultivating Blue Food Proteins: Innovating Next-Generation Ingredients from Macro and Microalgae. *Biocatal. Agric. Biotechnol.* **2024**, *60*, 103278. [CrossRef]
8. Williamson, E.; Ross, I.L.; Wall, B.T.; Hankamer, B. Microalgae: Potential novel protein for sustainable human nutrition. *Trends Plant Sci.* **2024**, *29*, 370–382. [CrossRef]
9. Jadhav, H.B. Functional triacylglycerols from microalgae and their use in the formulation of functional foods—Review. *Food Chem. Adv.* **2024**, *4*, 100695. [CrossRef]
10. Lim, H.R.; Khoo, K.S.; Chew, K.W.; Tao, Y.; Xia, A.; Ma, Z.; Show, P.L. Upstream bioprocessing of Spirulina platensis microalgae using rainwater and recycle medium from post-cultivation for C-phycocyanin production. *J. Taiwan Inst. Chem. Eng.* **2023**, *166*, 104986. [CrossRef]
11. Shokrkar, H.; Nedaei, L. Chlorophyll and carotenoid extraction from mixed microalgae; experimental and kinetic study. *Biomass Convers. Biorefinery* **2024**, *14*, 17891–17903. [CrossRef]
12. Jorge, A.M.; Pedroso, P.R.; Pereira, J.F. Sustainable extraction and utilization of chlorophyll from microalgae for eco-friendly wool dyeing. *J. Clean. Prod.* **2024**, *451*, 142009. [CrossRef]
13. Sharma, C.; Kamle, M.; Kumar, P. Microbial-Derived Carotenoids and Their Health Benefits. *Microbiol. Res.* **2024**, *15*, 1670–1689. [CrossRef]
14. Duan, X.; Xie, C.; Hill, D.R.; Barrow, C.J.; Dunshea, F.R.; Martin, G.J.; Suleria, H.A. Bioaccessibility, bioavailability and bioactivities of carotenoids in microalgae: A review. *Food Rev. Int.* **2024**, *40*, 230–259. [CrossRef]
15. Novoveská, L.; Nielsen, S.L.; Eroldoğan, O.T.; Haznedaroglu, B.Z.; Rinkevich, B.; Fazi, S.; Einarsson, H. Overview and challenges of large-scale cultivation of photosynthetic microalgae and cyanobacteria. *Mar. Drugs* **2023**, *21*, 445. [CrossRef]
16. Palladino, F.; Marcelino, P.R.F.; Schlogl, A.E.; José, Á.H.M.; Rodrigues, R.D.C.L.B.; Fabrino, D.L.; Rosa, C.A. Bioreactors: Applications and Innovations for a sustainable and healthy future—A critical review. *Appl. Sci.* **2024**, *14*, 9346. [CrossRef]
17. Smith, V.H.; Crews, T. Applying ecological principles of crop cultivation in large-scale algal biomass production. *Algal Res.* **2014**, *4*, 23–34. [CrossRef]
18. Noorman, H. An industrial perspective on bioreactor scale-down: What we can learn from combined large-scale bioprocess and model fluid studies. *Biotechnol. J.* **2011**, *6*, 934–943. [CrossRef]
19. Xia, J.; Wang, G.; Fan, M.; Chen, M.; Wang, Z.; Zhuang, Y. Understanding the scale-up of fermentation processes from the viewpoint of the flow field in bioreactors and the physiological response of strains. *Chin. J. Chem. Eng.* **2021**, *30*, 178–184. [CrossRef]
20. de Mello, A.F.M.; de Souza Vandenberghe, L.P.; Herrmann, L.W.; Letti, L.A.J.; Burgos, W.J.M.; Scapini, T.; Soccol, C.R. Strategies and engineering aspects on the scale-up of bioreactors for different bioprocesses. *Syst. Microbiol. Biomanuf.* **2024**, *4*, 365–385. [CrossRef]
21. PharSol—Pharmaceutical Solutions. Available online: https://pharsol.com/knowledge-hub/blog/scaling-up-or-out (accessed on 17 December 2024).
22. Xu, P.; Shao, S.; Qian, J.; Li, J.; Xu, R.; Liu, J.; Zhou, W. Scale-up of microalgal systems for decarbonization and bioproducts: Challenges and opportunities. *Bioresour. Technol.* **2024**, *398*, 130528. [CrossRef] [PubMed]
23. Legrand, J.; Artu, A.; Pruvost, J. A review on photobioreactor design and modelling for microalgae production. *React. Chem. Eng.* **2021**, *6*, 1134–1151. [CrossRef]
24. Peixoto, M.L.; Brito, M.S.; Santos, R.J.; Vilar, V.J. Kinetic model implementation in raceway pond reactors with hydrodynamic and radiation fields. *Chem. Eng. Res. Des.* **2024**, *210*, 150–162. [CrossRef]
25. Barboza-Rodríguez, R.; Rodríguez-Jasso, R.M.; Rosero-Chasoy, G.; Aguado, M.L.R.; Ruiz, H.A. Photobioreactor configurations in cultivating microalgae biomass for biorefinery. *Bioresour. Technol.* **2024**, *394*, 130208. [CrossRef]
26. Penloglou, G.; Pavlou, A.; Kiparissides, C. Recent Advancements in Photo-Bioreactors for Microalgae Cultivation: A Brief Overview. *Processes* **2024**, *12*, 1104. [CrossRef]
27. Pandey, S.; Narayanan, I.; Selvaraj, R.; Varadavenkatesan, T.; Vinayagam, R. Biodiesel production from microalgae: A comprehensive review on influential factors, transesterification processes, and challenges. *Fuel* **2024**, *367*, 131547. [CrossRef]
28. Li, S.; Xing, D.; Sun, C.; Jin, C.; Zhao, Y.; Gao, M.; Guo, L. Effect of light intensity and photoperiod on high-value production and nutrient removal performance with bacterial-algal coupling system. *J. Environ. Manag.* **2024**, *356*, 120595. [CrossRef]
29. Sartori, R.B.; Deprá, M.C.; Dias, R.R.; Fagundes, M.B.; Zepka, L.Q.; Jacob-Lopes, E. The Role of Light on the Microalgae Biotechnology: Fundamentals, Technological Approaches, and Sustainability Issues. *Recent Pat. Biotechnol.* **2024**, *18*, 22–51.

30. Ahangar, A.K.; Yaqoubnejad, P.; Divsalar, K.; Mousavi, S.; Taghavijeloudar, M. Design a novel internally illuminated mirror photobioreactor to improve microalgae production through homogeneous light distribution. *Bioresour. Technol.* **2023**, *387*, 129577. [CrossRef] [PubMed]
31. Chiarini, A.; Quadrio, M. The light/dark cycle of microalgae in a thin-layer photobioreactor. *J. Appl. Phycol.* **2021**, *33*, 183–195. [CrossRef]
32. Luzi, G.; McHardy, C. Modeling and simulation of photobioreactors with computational fluid dynamics—A comprehensive review. *Energies* **2022**, *15*, 3966. [CrossRef]
33. Brzychczyk, B.; Giełżecki, J.; Kijanowski, K.; Hebda, T.; Rzepka, F. Automation of the Photobioreactor Lighting System to Manage Light Distribution in Microalgae Cultures. *Energies* **2023**, *16*, 7183. [CrossRef]
34. Wang, S.K.; Stiles, A.R.; Guo, C.; Liu, C.Z. Microalgae cultivation in photobioreactors: An overview of light characteristics. *Eng. Life Sci.* **2014**, *14*, 550–559. [CrossRef]
35. Huang, Q.; Jiang, F.; Wang, L.; Yang, C. Design of photobioreactors for mass cultivation of photosynthetic organisms. *Engineering* **2017**, *3*, 318–329. [CrossRef]
36. Jacob-Lopes, E.; Zepka, L.Q.; Mérida, L.G.R.; Maroneze, M.M.; Neves, C. Bioprocess of Conversion of Carbon Dioxide from Industrial Emissions, Bioproducts, Their Uses and Hybrid Photobioreactor. Patent WO 2014/2014000333, September 2014.
37. Jacob-Lopes, E.; Zepka, L.Q.; Mérida, L.G.R.; Maroneze, M.M.; Neves, C. Bioprocess for the Conversion of Carbon Dioxide from Industrial Emissions, Bioproducts Use Thereof and Hybrid Photobioreactor. Patent WO 2016/041028 A1, 24 March 2016.
38. Deprá, M.C.; da Motta Pacheco, L.F.C.; Rossi, R.; Nunes, M.; Goldemberg, S.; Suzuki, S.; Jacob-Lopes, E. Hybrid photobioreactors: The success-to-failure experiences on pilot scale. In *3rd Generation Biofuels*, 1st ed.; Jacob-Lopes, E., Zepka, L.Q., Severo, I.A., Maroneze, M.M., Eds.; Woodhead Publishing: Cambridge, UK; Elsevier Science Ltd.: Amsterdam, The Netherlands, 2022; Volume 1, pp. 1019–1035.
39. Yen, H.W.; Hu, I.C.; Chen, C.Y.; Nagarajan, D.; Chang, J.S. Design of photobioreactors for algal cultivation. In *Biofuels from Algae*, 2nd ed.; Pandey, A., Chang, J.-S., Soccol, C.R., Lee, D.-J., Chisti, Y., Eds.; Elsevier: London, UK, 2019; Volume 1, pp. 225–256.
40. Zeriouh, O.; Reinoso-Moreno, J.V.; López-Rosales, L.; Cerón-García, M.D.C.; Sánchez-Mirón, A.; García-Camacho, F.; Molina-Grima, E. Biofouling in photobioreactors for marine microalgae. *Crit. Rev. Biotechnol.* **2017**, *37*, 1006–1023. [CrossRef]
41. Posten, C. Design and performance parameters of photobioreactors. *TATuP-J. Technol. Assess. Theory Pract.* **2012**, *21*, 38–45. [CrossRef]
42. Haghanifar, S.; Gao, T.; Rodriguez De Vecchis, R.T.; Pafchek, B.; Jacobs, T.D.; Leu, P.W. Ultrahigh-transparency, ultrahigh-haze nanograss glass with fluid-induced switchable haze. *Optica* **2017**, *4*, 1522–1525. [CrossRef]
43. Wu, W.; Ouyang, Q.; He, L.; Huang, Q. Optical and thermal properties of polymethyl methacrylate (PMMA) bearing phenyl and adamantyl substituents. *Colloids Surf. A Physicochem. Eng.* **2022**, *653*, 130018. [CrossRef]
44. Wu, X.; Wang, X.; Qin, Z.; Zhang, W. Polycarbonate composites with high light transmittance, haze, and flame retardancy based on a series of incomplete-cage oligomeric silsesquioxanes. *J. Mater. Sci.* **2021**, *56*, 428–441. [CrossRef]
45. Vogler, E.A. A thermodynamic model of short-term cell adhesion in vitro. *Colloids Surf.* **1989**, *42*, 233–254. [CrossRef]
46. Soriano-Jerez, Y.; Gallardo-Rodríguez, J.J.; López-Rosales, L.; García-Camacho, F.; Bressy, C.; Molina-Grima, E.; Cerón-García, M.C. Preventing biofouling in microalgal photobioreactors. *Bioresour. Technol.* **2024**, *407*, 131125. [CrossRef] [PubMed]
47. Serra-Maia, R.; Bernard, O.; Gonçalves, A.; Bensalem, S.; Lopes, F. Influence of temperature on *Chlorella vulgaris* growth and mortality rates in a photobioreactor. *Algal Res.* **2016**, *18*, 352–359. [CrossRef]
48. Pires, J.C.; Alvim-Ferraz, M.C.; Martins, F.G. Photobioreactor design for microalgae production through computational fluid dynamics: A review. *Renew. Sustain. Energy Rev.* **2017**, *79*, 248–254. [CrossRef]
49. Boyd, R.A.; Cavanagh, A.P.; Kubien, D.S.; Cousins, A.B. Temperature response of Rubisco kinetics in Arabidopsis thaliana: Thermal breakpoints and implications for reaction mechanisms. *J. Exp. Bot.* **2019**, *70*, 231–242. [CrossRef]
50. Gurrieri, L.; Sparla, F.; Zaffagnini, M.; Trost, P. Dark complexes of the Calvin-Benson cycle in a physiological perspective. *Semin. Cell Biol.* **2024**, *155*, 48–58. [CrossRef]
51. Ras, M.; Steyer, J.P.; Bernard, O. Temperature effect on microalgae: A crucial factor for outdoor production. *Rev. Environ. Sci. Biotechnol.* **2013**, *12*, 153–164. [CrossRef]
52. Garcia-Ochoa, F.; Gomez, E. Bioreactor scale-up and oxygen transfer rate in microbial processes: An overview. *Biotechnol. Adv.* **2009**, *27*, 153–176. [CrossRef] [PubMed]
53. Dias, R.R.; da Silva, P.A.; Deprá, M.C.; Deprá, B.; Wagner, R.; Zepka, L.Q.; Jacob-Lopes, E. Mapping the performance of photobioreactors for microalgae cultivation. Part III: Subtropical and mid-latitudes climate zone. *J. Chem. Technol. Biotechnol.* **2023**, *98*, 1497–1519. [CrossRef]
54. Gharib, A.; Djema, W.; Fernández, P.M.; Chin-On, R.; Janssen, M.; Bernard, O. Validation of an adaptive temperature model for closed microalgae cultivation systems. *Algal Res.* **2024**, *in press*. [CrossRef]
55. Kato, H.; Suzuki, H.; Wijffels, R.H.; Schulze, P.S.; Hulatt, C.J. Thermal responses of *Tetradesmus obliquus* for industrial outdoor cultivation. *Bioresour. Technol. Rep.* **2024**, *27*, 101909. [CrossRef]

56. Alonso-Bastida, A.; Franco-Nava, M.A.; Adam-Medina, M.; López-Zapata, B.; Álvarez-Gutiérrez, P.E.; García-Morales, J. Mathematical modeling of thermal interactions in a self-cooling pilot-scale photobioreactor. *Case Stud. Therm. Eng.* **2022**, *31*, 101825. [CrossRef]
57. Androga, D.D.; Uyar, B.; Koku, H.; Eroglu, I. Dynamic modeling of temperature change in outdoor operated tubular photobioreactors. *Bioprocess. Biosyst. Eng.* **2017**, *40*, 1017–1031. [CrossRef]
58. Nwoba, E.G.; Parlevliet, D.A.; Laird, D.W.; Alameh, K.; Moheimani, N.R. Pilot-scale self-cooling microalgal closed photobioreactor for biomass production and electricity generation. *Algal Res.* **2020**, *45*, 101731. [CrossRef]
59. Medrano, M.; Yilmaz, M.O.; Nogués, M.; Martorell, I.; Roca, J.; Cabeza, L.F. Experimental evaluation of commercial heat exchangers for use as PCM thermal storage systems. *Appl. Energy* **2009**, *86*, 2047–2055. [CrossRef]
60. Béchet, Q.; Shilton, A.; Fringer, O.B.; Muñoz, R.; Guieysse, B. Mechanistic modeling of broth temperature in outdoor photobioreactors. *Environ. Sci. Technol.* **2010**, *44*, 2197–2203. [CrossRef] [PubMed]
61. Nwoba, E.G.; Parlevliet, D.A.; Laird, D.W.; Vadiveloo, A.; Alameh, K.; Moheimani, N.R. Can solar control infrared blocking films be used to replace evaporative cooling for growth of *Nannochloropsis* sp. in plate photobioreactors? *Algal Res.* **2019**, *39*, 101441. [CrossRef]
62. Uyar, B.; Kapucu, N. Passive temperature control of an outdoor photobioreactor by phase change materials. *J. Chem. Technol. Biotechnol.* **2015**, *90*, 915–920. [CrossRef]
63. Endres, C.H.; Roth, A.; Brück, T.B. Thermal reactor model for large-scale algae cultivation in vertical flat panel photobioreactors. *Environ. Sci. Technol.* **2016**, *50*, 3920–3927. [CrossRef] [PubMed]
64. Nwoba, E.G.; Parlevliet, D.A.; Laird, D.W.; Alameh, K.; Moheimani, N.R. Light management technologies for increasing algal photobioreactor efficiency. *Algal Res.* **2019**, *39*, 101433. [CrossRef]
65. Alshammari, O.; Basem, A.; Hameed, A.I.; Agarwal, D.; Shawabkeh, A.; Kenjrawy, H.A.; Jerbi, H. Advanced eco-friendly power and cooling cogeneration-thermal energy storage utilizing phase change materials and chemisorption in renewable-based configurations. *Therm. Sci. Eng. Prog.* **2024**, *54*, 102813. [CrossRef]
66. Louveau, J.; Titica, M.; Moheimani, N.R.; Pruvost, J. Coupling semi-transparent PV PANELS with thin-film PBRs for sustainable microalgal biomass production. *Chem. Eng. Res. Des.* **2024**, *205*, 722–732. [CrossRef]
67. Ugwu, C.U.; Aoyagi, H.; Uchiyama, H. Photobioreactors for mass cultivation of algae. *Bioresour. Technol.* **2008**, *99*, 4021–4028. [CrossRef] [PubMed]
68. Zhou, Y.; Cui, X.; Wu, B.; Wang, Z.; Liu, Y.; Ren, T.; Rittmann, B.E. Microalgal extracellular polymeric substances (EPS) and their roles in cultivation, biomass harvesting, and bioproducts extraction. *Bioresour. Technol.* **2024**, *406*, 131054. [CrossRef] [PubMed]
69. Guo, W.; Song, Y. Improvement of mass transfer in microalgal photobioreactors. In *Sustainable Industrial Processes Based on Microalgae*, 1st ed.; Lafarga, T., Acién, G., Eds.; Elsevier: London, UK, 2024; Volume 1, pp. 41–57.
70. Cabello, J.; Morales, M.; Revah, S. Carbon dioxide consumption of the microalga *Scenedesmus obtusiusculus* under transient inlet CO_2 concentration variations. *Sci. Total Environ.* **2017**, *584*, 1310–1316. [CrossRef]
71. Hajinajaf, N.; Fallahi, A.; Eustance, E.; Sarnaik, A.; Askari, A.; Najafi, M.; Varman, A.M. Managing carbon dioxide mass transfer in photobioreactors for enhancing microalgal biomass productivity. *Algal Res.* **2024**, *80*, 103506. [CrossRef]
72. Cuaresma, M.; Garbayo, I.; Vega, J.M.; Vílchez, C. Growth and photosynthetic utilization of inorganic carbon of the microalga Chlamydomonas acidophila isolated from Tinto River. *Enzym. Microb. Technol.* **2006**, *40*, 158–162. [CrossRef]
73. Li, P.; Wang, D.; Hu, Z.; Chen, D.; Wang, Y.; Wang, M.; Song, C. Insight into the potential mechanism of bicarbonate assimilation promoted by mixotrophic in CO_2 absorption and microalgae conversion system. *Chemosphere* **2024**, *349*, 140903. [CrossRef] [PubMed]
74. Deprá, M.C.; Dias, R.R.; Severo, I.A.; de Menezes, C.R.; Zepka, L.Q.; Jacob-Lopes, E. Carbon dioxide capture and use in photobioreactors: The role of the carbon dioxide loads in the carbon footprint. *Bioresour. Technol.* **2020**, *314*, 123745. [CrossRef] [PubMed]
75. Silva, J.; Arias-Torres, L.; Carlesi, C.; Aroca, G. Use of Nanobubbles to Improve Mass Transfer in Bioprocesses. *Processes* **2024**, *12*, 1227. [CrossRef]
76. Kishi, M.; Tanaka, K.; Tagawa, M.; Akizuki, S.; Toda, T. Energy-efficient algal culture through aeration-less oxygen removal in a gas-permeable bag photobioreactor. *Algal Res.* **2023**, *69*, 102959. [CrossRef]
77. Trentin, G.; Barbera, E.; Bertucco, A.; Sforza, E. Role of oxygen in tubular photobioreactors: Model-Based design and operating conditions to minimize productivity losses. *Chem. Eng. Process. Process Intensif.* **2020**, *157*, 108151. [CrossRef]
78. Assunção, J.; Malcata, F.X. Enclosed "non-conventional" photobioreactors for microalga production: A review. *Algal Res.* **2020**, *52*, 102107. [CrossRef]
79. Kang, N.K.; Baek, K.; Koh, H.G.; Atkinson, C.A.; Ort, D.R.; Jin, Y.S. Microalgal metabolic engineering strategies for the production of fuels and chemicals. *Bioresour. Technol.* **2022**, *345*, 126529. [CrossRef]
80. B-Béres, V.; Naselli-Flores, L.; Padisák, J.; Borics, G. Trait-based ecology of microalgae. *Hydrobiologia* **2024**, *851*, 713–732. [CrossRef]

81. Fu, W.; Gudmundsson, O.; Feist, A.M.; Herjolfsson, G.; Brynjolfsson, S.; Palsson, B.Ø. Maximizing biomass productivity and cell density of *Chlorella vulgaris* by using light-emitting diode-based photobioreactor. *J. Biotechnol.* **2012**, *161*, 242–249. [CrossRef] [PubMed]
82. Lukyanov, V.; Gorbunova, S.; Avsiyan, A. Biotechnological and economic assessment of the productivity of *Chlorella vulgaris* IBSS-19 microalgae under different cultivation regimes. *Bioresour. Technol. Rep.* **2024**, *27*, 101907. [CrossRef]
83. Leong, W.H.; Saman, N.A.M.; Kiatkittipong, W.; Assabumrungrat, S.; Najdanovic-Visak, V.; Wang, J.; Lim, J.W. Photoperiod-induced mixotrophic metabolism in *Chlorella vulgaris* for high biomass and lipid to biodiesel productions using municipal wastewater medium. *Fuel* **2022**, *313*, 123052. [CrossRef]
84. Cao, W.; Yu, H.; Dong, W.; Rong, Z.; Peng, D.; Chen, F.; Li, L. Comparison of *Scenedesmus obliquus* in CO_2 Capture, Biolipid Production and Nutrient Removal. *Separations* **2024**, *11*, 218. [CrossRef]
85. Muys, M.; Cámara, S.J.G.; Arnau, C.; García, D.; Peiro, E.; Gòdia, F.; Vlaeminck, S.E. Light regime, harvesting time and operation mode can optimize the productivity of nutritional protein in *Chlorella* and *Spirulina* biomass. *Algal Res.* **2024**, *79*, 103443. [CrossRef]
86. Gastineau, R.; Davidovich, N.A.; Hallegraeff, G.M.; Probert, I.; Mouget, J.L. Reproduction in microalgae. In *Reproductive Biology of Plants, USA*; Springer: Berlin/Heidelberg, Germany, 2014; Volume 1, pp. 1–28.
87. Procházková, G.; Brányiková, I.; Zachleder, V.; Brányik, T. Effect of nutrient supply status on biomass composition of eukaryotic green microalgae. *J. Appl. Phycol.* **2014**, *26*, 1359–1377. [CrossRef]
88. Patra, P.; Disha, B.R.; Kundu, P.; Das, M.; Ghosh, A. Recent advances in machine learning applications in metabolic engineering. *Biotechnol. Adv.* **2023**, *62*, 108069. [CrossRef] [PubMed]
89. Brar, A.; Kumar, M.; Soni, T.; Vivekanand, V.; Pareek, N. Insights into the genetic and metabolic engineering approaches to enhance the competence of microalgae as biofuel resource: A review. *Bioresour. Technol.* **2021**, *339*, 125597. [CrossRef]
90. Ramanna, L.; Rawat, I.; Bux, F. Light enhancement strategies improve microalgal biomass productivity. *Renew. Sustain. Energy Rev.* **2017**, *80*, 765–773. [CrossRef]
91. Gupta, A.; Kang, K.; Pathania, R.; Saxton, L.; Saucedo, B.; Malik, A.; Mayfield, S.P. Harnessing genetic engineering to drive economic bioproduct production in algae. *Front. Bioeng. Biotechnol.* **2024**, *12*, 1350722.
92. Ahmad Kamal, A.H.; Mohd Hamidi, N.F.; Zakaria, M.F.; Ahmad, A.; Harun, M.R.; Chandra Segaran, T.; Jusoh, M. Genetically engineered microalgae for enhanced bioactive compounds. *Discov. Appl. Sci.* **2024**, *6*, 482. [CrossRef]
93. Fuentes, J.L.; Garbayo, I.; Cuaresma, M.; Montero, Z.; González-del-Valle, M.; Vílchez, C. Impact of microalgae-bacteria interactions on the production of algal biomass and associated compounds. *Mar. Drugs* **2016**, *14*, 100. [CrossRef] [PubMed]
94. Nordio, R.; Belachqer-El Attar, S.; Clagnan, E.; Sánchez-Zurano, A.; Pichel, N.; Viviano, E.; Acién, G. Exploring microbial growth dynamics in a pilot-scale microalgae raceway fed with urban wastewater: Insights into the effect of operational variables. *J. Environ. Manag.* **2024**, *369*, 122385. [CrossRef] [PubMed]
95. Jebali, A.; Sanchez, M.R.; Hanschen, E.R.; Starkenburg, S.R.; Corcoran, A.A. Trait drift in microalgae and applications for strain improvement. *Biotechnol. Adv.* **2022**, *60*, 108034. [CrossRef] [PubMed]
96. Dębowski, M.; Świca, I.; Kazimierowicz, J.; Zieliński, M. Large scale microalgae biofuel technology—Development perspectives in light of the barriers and limitations. *Energies* **2022**, *16*, 81. [CrossRef]
97. Sadin, S.R.; Povinelli, F.P.; Rosen, R. The NASA technology push towards future space mission systems. In *Space and Humanity*, 1st ed.; Napolitano, L.G., Ed.; Pergamon: Oxford, UK, 1989; Volume 1, pp. 73–77.
98. Salvador-Carulla, L.; Woods, C.; de Miquel, C.; Lukersmith, S. Adaptation of the technology readiness levels for impact assessment in implementation sciences: The TRL-IS checklist. *Heliyon* **2024**, *10*, e29930. [CrossRef]
99. Bukar, A.M.; Asif, M. Technology readiness level assessment of carbon capture and storage technologies. *Renew. Sustain. Energy Rev.* **2024**, *200*, 114578. [CrossRef]
100. Yfanti, S.; Sakkas, N. Technology Readiness Levels (TRLs) in the Era of Co-Creation. *Appl. Syst. Innov.* **2024**, *7*, 32. [CrossRef]
101. Animah, I.; Shafiee, M. A framework for assessment of technological readiness level (TRL) and commercial readiness index (CRI) of asset end-of-life strategies. In *Safety and Reliability—Safe Societies in a Changing World*, 1st ed.; CRC Press: London, UK, 2018; Volume 1, pp. 1767–1773.
102. Lähteenmäki, J.; Töyli, J. Industry consolidation as a strategy: An acquisition program perspective. *J. Strategy Manag.* **2023**, *16*, 492–515. [CrossRef]
103. Capatina, A.; Bleoju, G.; Kalisz, D. Falling in love with strategic foresight, not only with technology: European deep-tech startups' roadmap to success. *J. Innov. Knowl.* **2024**, *9*, 100515. [CrossRef]
104. Ramiréz-Mérida, L.G.; Zepka, L.Q.; Jacob-Lopes, E. Current production of microalgae at industrial scale. In *Microalgae as a Source of Bioenergy: Products, Process and Economics*, 1st ed.; Pires, J.C., Ed.; Betham Science Publishers: Amsterdam, The Netherlands, 2017; pp. 278–292.
105. Acién, F.G.; Fernández, J.M.; Magán, J.J.; Molina, E. Production cost of a real microalgae production plant and strategies to reduce it. *Biotechnol. Adv.* **2012**, *30*, 1344–1353. [CrossRef]

106. Weinrich, R.; Elshiewy, O. A cross-country analysis of how food-related lifestyles impact consumers' attitudes towards microalgae consumption. *Algal Res.* **2023**, *70*, 102999. [CrossRef]
107. Yang, S.; Fan, Y.; Cao, Y.; Wang, Y.; Mou, H.; Sun, H. Technological readiness of commercial microalgae species for foods. *Crit. Rev. Food Sci. Nutr.* **2024**, *64*, 7993–8017. [CrossRef] [PubMed]
108. Thomassen, G.; Van Dael, M.; You, F.; Van Passel, S. A multi-objective optimization-extended techno-economic assessment: Exploring the optimal microalgal-based value chain. *Green Chem.* **2019**, *21*, 5945–5959. [CrossRef]
109. Kusmayadi, A.; Leong, Y.K.; Yen, H.W.; Huang, C.Y.; Chang, J.S. Microalgae as sustainable food and feed sources for animals and humans–biotechnological and environmental aspects. *Chemosphere* **2021**, *271*, 129800. [CrossRef]
110. Bature, A.; Melville, L.; Rahman, K.M.; Aulak, P. Microalgae as feed ingredients and a potential source of competitive advantage in livestock production: A review. *Livest. Sci.* **2022**, *259*, 104907. [CrossRef]
111. Samoraj, M.; Chojnacka, K.; Skrzypczak, D.; Mikula, K.; Mironiuk, M.; Calis, D. Microalgae as biobased fertilizers for sustainable agriculture. In *Advances in Sustainable Applications of Microalgae*, 1st ed.; Pires, J.C.M., Esteves, A.F.C., Salgado, E.M.A.C., Eds.; Elsevier: London, UK, 2025; Volume 1, pp. 263–281.
112. Rumin, J.; Nicolau, E.; Gonçalves de Oliveira Junior, R.; Fuentes-Grünewald, C.; Picot, L. Analysis of scientific research driving microalgae market opportunities in Europe. *Mar. Drugs* **2020**, *18*, 264. [CrossRef]
113. Severo, I.A.; Deprá, M.C.; Dias, R.R.; Jacob-Lopes, E. Process integration applied to microalgae-based systems. In *Handbook of Microalgae-Based Processes and Products*, 1st ed.; Jacob-Lopes, E., Maroneze, M.M., Queiroz, M.I., Zepka, L.Q., Eds.; Academic Press: London, UK, 2020; Volume 1, pp. 709–735.
114. Corbion-AlgaVia™ Culinary Algae Oils. Available online: https://www.corbion.com/products/algae-ingredients-products/algavia (accessed on 17 December 2024).
115. ExxonMobil. Available online: https://corporate.exxonmobil.com/what-we-do/transforming-transportation/advanced-biofuels/advanced-biofuels-and-algae-research#Algaeforbiofuelsproduction (accessed on 17 December 2024).
116. Algenol. Available online: https://www.algenol.com/ (accessed on 17 December 2024).

Disclaimer/Publisher's Note: The statements, opinions and data contained in all publications are solely those of the individual author(s) and contributor(s) and not of MDPI and/or the editor(s). MDPI and/or the editor(s) disclaim responsibility for any injury to people or property resulting from any ideas, methods, instructions or products referred to in the content.

processes

MDPI

Review

Microalgae Cultivation in Wastewater: How Realistic Is This Approach for Value-Added Product Production?

Rosangela Rodrigues Dias, Mariany Costa Deprá, Cristiano Ragagnin de Menezes, Leila Queiroz Zepka and Eduardo Jacob-Lopes *

Bioprocess Intensification Group, Federal University of Santa Maria, UFSM, Roraima Avenue 1000, Santa Maria 97105-900, RS, Brazil; ro.rosangelard@gmail.com (R.R.D.); marianydepra@gmail.com (M.C.D.); cristiano.ufsm@gmail.com (C.R.d.M.); zepkaleila@yahoo.com.br (L.Q.Z.)
* Correspondence: ejacoblopes@gmail.com; Tel.: +55-55-3220-8822

Abstract

Microalgae cultivation in wastewater is a production approach that combines wastewater treatment with biomass generation for various applications. This strategy aligns with the concept of a circular bioeconomy, which aims to transform waste into valuable resources. However, although this is true, this synergy's potential bumps into obstacles that still limit the consolidation of the commercial cultivation of microalgae using wastewater. This review analyzed how close or far we are from achieving the successful integration of commercial microalgae cultivation with wastewater treatment for the production of value-added products. The analysis of the scientific literature highlighted that certain strains, such as *Chlorella*, *Arthrospira*, and *Scenedesmus*, can remove up to 90% of nitrogen and phosphorus from effluents while maintaining productivities of up to 45 g/m^2/day. The techno-economic analyses presented here indicate that production costs range between 1.98 and 9.69 EUR/kg, depending on the effluent composition and biomass productivity. From an environmental perspective, replacing synthetic media with wastewater can significantly reduce input use, but the environmental impacts associated with energy consumption remain a challenge. This paper also discusses the technological readiness level (TRL), which currently remains between levels 4 and 6, concentrated on demonstration and pilot scales. By gathering and critically analyzing the current literature, this work seeks to answer how realistic and sustainable this integration is today.

Keywords: algae; raceway pond; residual resources; phycoremediation; value-added products; technology readiness level; technical-economic; environmental impact

check for updates

Academic Editors: Marcos Alberto Coronado Ortega and José Ramón Ayala Bautista

Received: 28 April 2025
Revised: 21 June 2025
Accepted: 24 June 2025
Published: 28 June 2025

Citation: Dias, R.R.; Deprá, M.C.; de Menezes, C.R.; Zepka, L.Q.; Jacob-Lopes, E. Microalgae Cultivation in Wastewater: How Realistic Is This Approach for Value-Added Product Production? *Processes* **2025**, *13*, 2052. https://doi.org/10.3390/pr13072052

Copyright: © 2025 by the authors. Licensee MDPI, Basel, Switzerland. This article is an open access article distributed under the terms and conditions of the Creative Commons Attribution (CC BY) license (https://creativecommons.org/licenses/by/4.0/).

1. Introduction

The increasing generation of waste shows that the more we advance, the more complex and voluminous the industrial, agricultural, and urban waste streams we produce become [1]. It is estimated that more than 380 trillion liters of wastewater are generated globally each year, of which only a fraction is treated adequately [2]. Besides that, it is worth highlighting that inadequate sanitation and the use of contaminated water are responsible for a high rate of waterborne morbidities—such as cholera, diarrhea, hepatitis A, and others [3]. The direct and indirect costs of waterborne diseases (WBD) amount to hundreds of millions of dollars per year, reflecting the impact of the lack of access to potable water and basic sanitation—one of the Sustainable Development Goals (SDG 6) [4].

As a result, disruptive measures aimed at treating wastewater and promoting reuse perspectives have gained prominence [5]. Thus, waste—previously considered an environmental liability—has been reinterpreted as a strategic input for generating value [6–8]. This paradigm shift aligns with the precepts of the circular economy, closing cycles in which material and energy flows are optimized to maximize value and minimize waste [9]. In this scenario, microalgae emerge as disruptive agents, capable of reconfiguring the linear logic of disposal. Studies show that some microalgae strains, such as *Chlorella*, *Arthrospira*, and *Scenedesmus*, not only remove nutrients such as nitrogen and phosphorus from wastewater with efficiencies higher than 80–90% but also produce biomass rich in proteins, lipids, and carbohydrates [10–15]. This phycoremediation approach is a high-value biotransformation technology for organic and inorganic residues present in wastewater.

Considering this, it is important to highlight that the scientific relevance of phycoremediation can be observed through bibliometric analyses in the Web of Science and ScienceDirect databases. By way of example, searching for the term "phycoremediation" reveals over 220 research and review articles indexed from 2010 to 2020 and more than 450 articles from 2021 to 2024, showing consistent annual growth. Besides that, combining the keywords "microalgae" and "wastewater" resulted in over 12,800 research articles and more than 4600 review articles from 2010 to 2024, with approximately 62% and 75% published in the last five years, respectively (Figure 1). These quantitative data illustrate the growing efforts of the scientific community to advance the integration of microalgae cultivation with wastewater.

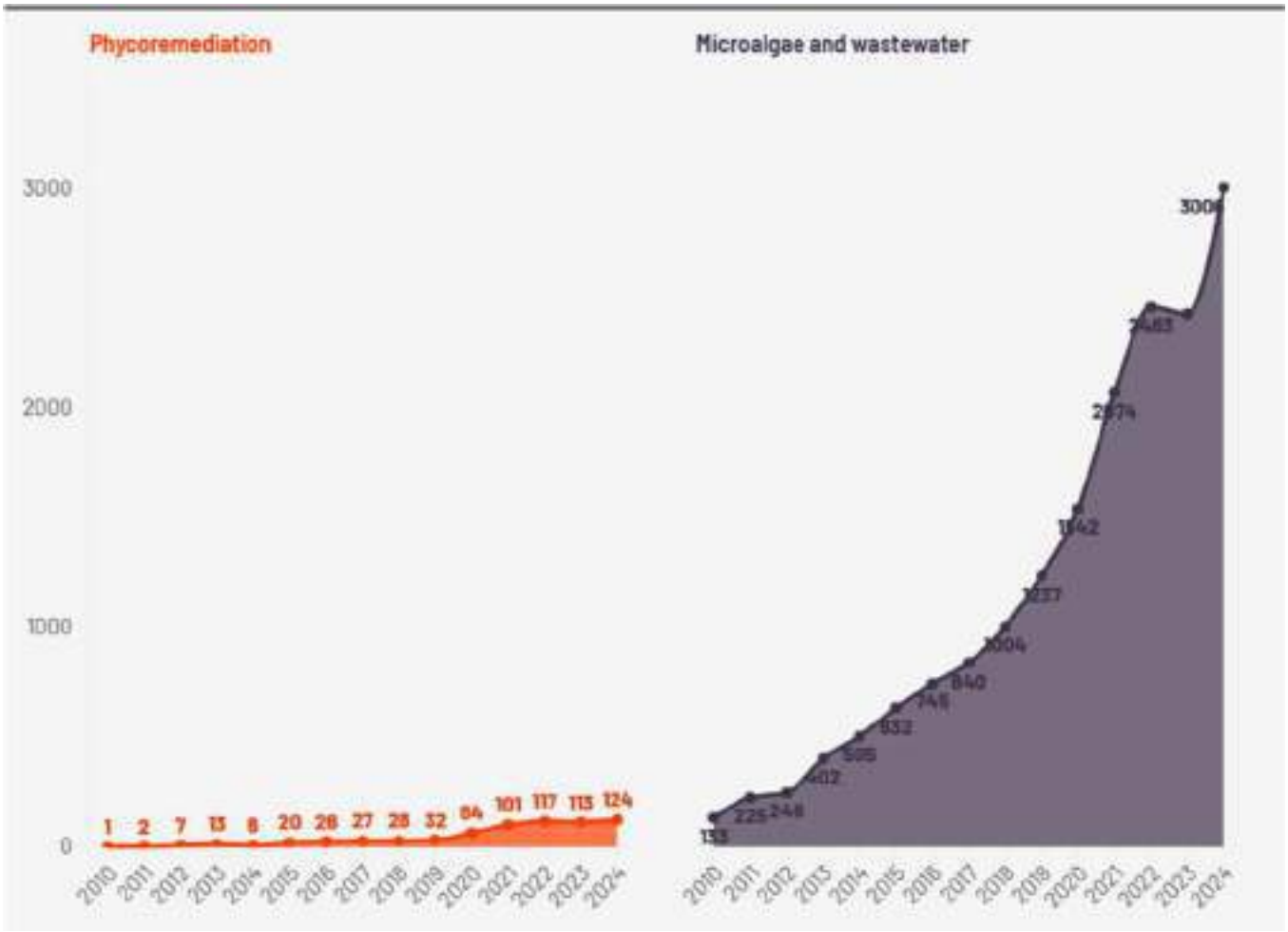


Figure 1. Number of target articles published in the last fourteen years.

However, despite the enthusiasm surrounding the integration of microalgae cultivation with wastewater, this approach still occupies a marginal space in waste treatment and valorization strategies. This is due, in part, to the fact that biomass cultivated under these conditions may not meet the rigorous standards required for high-value products—such as nutraceuticals—without an additional purification process. The additional costs of these processes can lead to a mismatch between cost and market price. Furthermore, even if biomass is suitable for applications without security requirements or with minimum security requirements—such as bioenergy, biofertilizer, biostimulant, biopesticide, bioplastic, and animal feed—the low added value of these applications becomes the main bottleneck. In both cases, the costs do not seem to be offset, calling into check not only the technical-economic viability but also the environmental sustainability of this approach, which remains on the margins of progress [16–18].

Thus, in a scenario where the potential is palpable but practical solutions are still uncertain, it is essential to revisit the microalgae role in wastewater phycoremediation and the limitations—technical, economic, or environmental—that keep this approach from achieving the highest levels of commercial readiness. This article offers a critical analysis of this topic, examining the technoeconomics involved, the associated environmental impacts, and the degree of maturity of this technology. Despite the increasing number of publications on microalgae cultivation in wastewater, most studies still focus on isolated proofs of concept [19–24], failing to progress toward integrated analyses that consider the technical, economic, environmental, and technological maturity aspects simultaneously [25–30]. Moreover, most research articles and reviews are restricted to discussing nutrient removal efficiency [31–36], phycoremediation mechanisms [37–43], or biomass valorization potential [44–48], neglecting the articulation between them and their implications for commercial viability. Therefore, an important gap in the literature is identified: the absence of works that systematically integrate acquired knowledge with an explicit focus on the feasibility of industrial-scale application today. By articulating knowledge about the potential of microalgae for removing and biotransforming pollutants from wastewater with technical-economic and environmental analyses, as well as the level of technological maturity achieved by this proposal, this article provides a holistic and realistic view of how close—or far—this strategy is to becoming a scalable solution within the scope of the circular bioeconomy. The originality of this work lies in consolidating scattered evidence into an analytical framework that enables a critical analysis of what remains as a promise and what is already translated into practice.

2. Microalgae-Based Phycoremediation

Phycoremediation with microalgae emerged as a promising alternative for industrial, agricultural, and urban effluent treatment in the 1960s and 1980s, with emphasis on the pioneering studies conducted by William J. Oswald and collaborators in the United States [49–51]. However, this approach only gained a great boost from the 2000s onwards, with research demonstrating the synergy between effluent treatment and biomass production for various value-added applications [52–59].

The advantages of phycoremediation with microalgae are multiple. First, microalgae have a remarkable metabolic capacity to capture and biotransform a wide range of organic and inorganic contaminants, including heavy metals [60–62], phenolic compounds [63–65], pesticides [66–68], textile dyes [69,70], radionuclides [71,72], polycyclic aromatic hydrocarbons [73], antibiotics [46,74–76], and pharmaceuticals [77]. This action occurs through photosynthesis and mechanisms, such as bioadsorption and bioabsorption (Figure 2) [37,78,79]. Furthermore, microalgae serve as significant biological carbon sinks, capturing atmospheric CO_2 during photosynthesis, which aids in strategies for mitigating climate change [80–82].

Additionally, compared to conventional wastewater treatment methods, such as activated sludge, microalgae-based phycoremediation offers a complementary and multifunctional alternative that is more aligned with circularity, waste valorization, and sustainability goals [83–85]. Another relevant aspect is that the biomass produced can be used in the production of multiple value-added products [17,30,86].

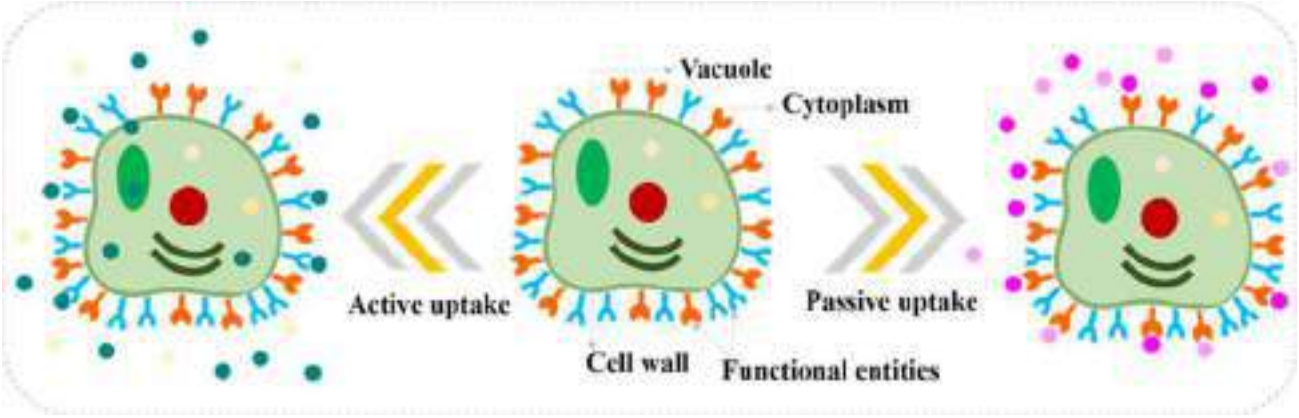


Figure 2. Microalgae bioremediation mechanisms. The active mechanisms are demonstrated by bioabsorption in the presence of living cells and the passive mechanisms are demonstrated by bioadsorption to the surface of non-living or living cells [87,88].

Another important advantage is the diversity of microalgae strains available for phycoremediation [89]. However, it is worth noting that, sometimes, unique efficiency in removing specific contaminants, such as heavy metals, pharmaceuticals, and persistent organic pollutants. This can lead to targeted selection of species with high affinity for certain compounds. For example, strains from the genera *Chlorella* and *Scenedesmus* are notable for their efficacy in eliminating nitrogenous compounds, such as ammonia and nitrate [10,90–96], while *Arthrospira* shows great potential for removing heavy metals [60,97–99]. However, it is important to recognize that the diversity of microalgae strains is a double-edged sword: on the one hand, it expands the application possibilities and process specialization; on the other, it complicates standardization, increases development costs, and may restrict scalability.

Furthermore, so that the wastewater can be used safely and efficiently for microalgae cultivation, some purification or pretreatment methods are commonly applied. Sieving or filtration is used to remove coarse solids that could compromise the cultivation systems [100–102]. Then, decantation or sedimentation can be used to separate sludge and settleable particles [103,104]. In some cases, partial disinfection, such as UV radiation or ozonation, is used to reduce the microbial load of competing organisms [7,15,105]. pH adjustment is often necessary, as is controlled effluent dilution, especially in cases of high ammonia concentrations [106]. Adsorption may be necessary and highly effective when contaminants, such as heavy metals, are present in wastewater intended for microalgae cultivation [101]. These treatments, applied alone or in combination, allow the safe use of wastewater as a culture medium. However, often, especially in circular bioeconomy approaches, the objective is to use the effluent without any treatment to minimize material and energy costs. However, minimal pretreatment, such as sieving or filtration, is almost always necessary.

But, regardless of this, it is important to highlight that research on microalgae cultivation in wastewater has evolved significantly, with results that reinforce the potential of integrating microalgae cultivation with wastewater. On a pilot scale, Morillas-España et al. [107] operated 3600 L and 2400 L thin-layer cascade photobioreactors using domestic wastewater collected from the sewerage of the University of Almería (Almeria,

Spain) without any treatment other than solids removal. The average annual productivity of the microalgae *Scenedesmus* sp. was 24.8 g/m^2/day (82.0 t/ha/year), with peaks of 32.8 g/m^2/day in summer and significant nitrogen and phosphorus removals of up to 2383.4 mg N/m^2/day and 111.8 mg P/m^2/day. In parallel, Abraham et al. [108] cultivated natural consortia of microalgae and cyanobacteria in 1000 L open raceway ponds using wastewater from the ammunition industry, achieving an average biomass productivity of up to 23.9 g/m^2/day. These biomass productivity data converge with those presented by Fernández et al. [109], who, when evaluating the production cost of biomass cultivated in wastewater—using average productivity of 20 g/m^2/day—found values of 4.45 EUR/kg. This value, as discussed in the following topic, is well above the value necessary for competitive insertion in low-value markets, such as biofuels. However, these concrete and scalable results, obtained under real operational conditions, demonstrate that the field has already advanced beyond proof-of-concept studies.

However, despite the documented potential of microalgae-based phycoremediation, the implementation of this synergy on a commercial scale remains a promise, with challenges related to process optimization, separation, and valorization of biomass [109,110]. The advances made since the launch of this proposal have allowed the development of initiatives on a demonstration and pilot scale; however, these experiences have not yet translated into operationally robust and consolidated solutions on an industrial scale [107,108,111–118]. First, the heterogeneity in the wastewater composition directly affects the microalgae productivity, requiring the selection of tolerant strains. Second, the strains' diversity, although advantageous, complicates standardization. Besides that, the biomass produced in these systems may require purification steps, especially when intended for applications for human consumption, such as food or cosmetics, which increases costs and reduces the competitiveness of the technology. Another relevant bottleneck is the harvesting of biomass, generally highly diluted, making the process technologically and economically onerous. These are some of the specific challenges that help explain why, despite its conceptual alignment with the circular bioeconomy, phycoremediation has not yet achieved the same degree of robustness, standardization, and technological consolidation observed in conventional wastewater debugging methods.

Despite this, given the obstacles, it is inevitable not to ask: why has an approach with so much potential— disseminated for more than half a century —not yet reached the highest levels of technological readiness? Are we overestimating its potential or underinvesting in disruptive innovations that could make it viable? This leads us to reflect on the path that is being taken—and what is really preventing us from moving forward.

3. Technoeconomics of Microalgae Production Using Wastewater

The use of wastewater in microalgae cultivation is promising, especially for low-value-added applications, such as bioenergy and biofertilizer—segments in which profit margins are traditionally narrow [119]. Beyond promoting the circular economy, microalgae cultivation in wastewater is an approach that aims to reduce operational costs associated with water and nutrient (fertilizer and CO_2) consumption. However, there are bottlenecks in both upstream and downstream processes, which compromise the technical and economic viability of this large-scale operation [120]. In upstream processes, obstacles, such as heterogeneity in wastewater quality and composition, the need to select tolerant microalgae strains and control biological contaminants, as well as ideal cultivation conditions, stand out [121–123]. On the other hand, in downstream processes, the challenges are concentrated in biomass harvesting—normally diluted in large volumes of water—and in biomass separation from contaminants present in wastewater, which is especially critical when biomass is destined for applications that require greater safety requirements, such as food ingredients [124,125].

Notably, although the integration of microalgae cultivation with wastewater use has not been validated on a commercial scale, demonstrative experiments at relevant scales have already provided real data on biomass productivity, cost savings, and nutrient removal efficiency. The FP7 All-Gas project, for example, demonstrates low-cost microalgae production using municipal wastewater, with a biomass productivity close to 100 t/ha/year [126]. In parallel, other pilot-scale studies, such as those by Morillas-España et al. [107], Abraham et al. [108], Rossi et al. [115], and Morillas-España et al. [117] have demonstrated the technical feasibility of using untreated or minimally treated wastewater to produce microalgae biomass at rates comparable to those obtained when produced using freshwater and commercial fertilizers. These efforts represent the current state of the art, in which techno-economic assessments have been based on relevant operational scales. Furthermore, it is worth emphasizing that there is a growing consensus in the literature that the integration of microalgae cultivation with wastewater represents one of the most promising strategies for the production of low-cost biomass—to promote applications with lower added value. However, although the technology has progressed beyond laboratory proofs of concept, its transposition to industrial contexts has not yet occurred [127].

A close look at the data extracted from technical-economic analyses also reveals a complex and, at times, contradictory scenario [128,129]. While some studies indicate that the use of effluents does not significantly compromise microalgae growth, maintaining productivities comparable to those obtained in synthetic media [130], others reveal considerable variations—both increases and decreases in productivity [128,129,131]. This disparity is strongly related to the intrinsic heterogeneity of wastewater, whose composition varies widely in terms of nutrient concentration, presence of heavy metals, toxic compounds, and microbiological agents [132,133]. These variations shape the physiological response of microalgae in a species-specific manner. Conclusively, the replacement of synthetic media by wastewater is not a linear equation, and converting an unstable substrate into a reliable input continues to represent a major challenge for this approach [134].

Besides that, it is important to emphasize that biomass productivity influences virtually all aspects of a techno-economic analysis. Improving—or at least maintaining—biomass productivity is what allows for the dilution of fixed costs, the optimization of resource use efficiency, and the reduction of the payback period of invested capital. In this sense, to provide an applied perspective, this paper presents, in Table 1, a preliminary techno-economic analysis, elaborated by the authors, for the microalgae cultivation using wastewater collected from an oil and gas facility. This case study comprehensively represents the results of research on microalgae production using wastewater, clearly illustrating the negative impact that reductions in productivity—caused by effluent use—can have on the technical-economic viability of the process. This case directly dialogues with the evidence that biomass productivity is a key variable in any economic analysis of microalgae production in wastewater. The specific characteristics of the effluent, as well as the assumptions adopted for the techno-economic analysis, are detailed in references [109,128,135].

According to the case study data (Table 1) carried out following the methodology of Acién et al. [135] and the results of Acién et al. [109] and Rahman et al. [128], the biomass production cost reaches 5.57 EUR/kg when using freshwater and nutrients (fertilizers and CO_2). However, when replacing these inputs with wastewater (5% WW), the cost is reduced to 4.45 EUR/kg. This slightly lower value is due to the elimination of freshwater and nutrient costs and productivity comparable to the control (base case). In this regard, it is worth highlighting that the annual productivity of 60 t/ha/year adopted in the base case is not an idealized overestimation but rather a conservative value based on the technical literature. Fernández et al. [109] consider this value representative for raceway pond systems, and studies on a relevant scale, such as the one conducted by the European project

FP7 All-Gas, demonstrated productivities close to 100 t/ha/year in ponds operating with municipal wastewater [126]. In parallel, Morillas-España et al. [107] reported an average annual productivity of 82 t/ha/year in thin-layer cascade photobioreactors operating with domestic effluent.

However, following the data in Table 1 and according to the data of Rahman et al. [128], at wastewater concentrations of 10% and 20%, there is a decrease in biomass productivity of 35% and 54%, respectively. Under these conditions, biomass production costs are increased to 6.87 and 9.69 EUR/kg, respectively. These values confirm that biomass productivity directly impacts the economic viability of the process.

These costs are also comparable to those reported by Norsker et al. [136], who when evaluating the cost of producing microalgae biomass in open ponds, reported a cost of 6.63 EUR/kg (data corrected for inflation). In parallel, Rossi et al. [115], when conducting a pilot-scale study under real conditions for wastewater treatment, identified a variation in the production cost between 1.9 and 10.3 EUR/kg.

Table 1. Parameters for microalgae cultivation in a raceway pond using wastewater. Acronyms: WW, Wastewater. Adapted from [109,128].

Case Study		Base Case	5% WW	10% WW	20% WW
Biomass productivity	$g/m^2/day$	20	20	12.97	9.19
CO_2 usage	kg/kg biomass	2	2	2	2
Water evaporation	$L/m^2/day$	7.5	7.5	7.5	7.5
Mixing power consumption	W/m^3	10	10	10	10
Labor	people/ha	1	1	1	1
Production days	days	300	300	300	300
Land area	ha	5	5	5	5
Ratio V/S	m^3/m^2	0.2	0.2	0.2	0.2
CO_2 fixation efficiency		0.9	0.9	0.9	0.9
Dilution rate	1/day	0.2	0.2	0.2	0.2
Total culture volume	m^3	10,000	10,000	10,000	10,000
Total biomass production	t/ha/year	60	60	38.91	27.57
Total CO_2 consumption	t/ha/year	120	120	77.82	55.14
Total water evaporation	t/ha/year	22,500	22,500	22,500	22,500
Water and nutrients cost	EUR/kg	1.1			
Power cost	EUR/kWh	0.12	0.12	0.12	0.12
Power for harvesting and others	kWh/m^3 harvest	0.1	0.1	0.1	0.1
Bioreactor cost	EUR/m^3	61.87	61.87	61.87	61.87
Biomass sludge production cost	EUR/kg	5.57	4.45	6.87	9.69

[1] The biomass productivity of 20 $g/m^2/day$ is a conservative but representative value for raceway pond systems, which currently represent more than 90% of commercial microalgae production. [2] Cost data have been corrected for inflation, when needed, and thus, provide a reasonable estimate of the current costs.

However, all these values are above the estimated critical value of 1.24 EUR/kg for low-value applications, such as bioenergy [109]. The biomass production cost needs to reach values equal to or below 1.24 EUR/kg to compete with commodities, such as cereals and vegetable oils. To achieve this baseline, it would be necessary not only to maintain high biomass productivity but also to adopt other measures to reduce operational costs, such as direct manpower. However, for the case study (Table 1), even if it were possible to reduce from 1 to 0.1 person/ha, costs would remain between 3.22 and 7.05 EUR/kg—still far from the target.

Additionally, from a wastewater treatment perspective, the situation is also challenging. Average treatment costs with microalgae exceed those observed in optimized or medium-sized conventional systems (0.2 to 0.7 EUR/m^3) [137,138]. For example, Rossi et al. [115] reported a cost for piggery wastewater treatment in the range of 6.3–34.2 EUR/m^3, which is in line with the

values reported for microalgae-based phycoremediation but still high compared to conventional processes. Despite that, it is reported in the literature that the costs of treating wastewater with microalgae can be competitive with smaller-scale or low-efficiency systems [25,109,139].

On the other hand, despite the data presented above, more encouraging results are also found in the literature. Table 2 presents a techno-economic analysis for the microalgae cultivation using wastewater collected from a dairy industry. The case study comprehensively demonstrates the most positive results found in the literature for the cultivation of microalgae in wastewater, illustrating the impact that significant productivity increases—caused by effluent use—can have on the technical-economic viability. The specific characteristics of the effluent, as well as the assumptions adopted for the techno-economic analysis, are detailed in references [109,129,135].

Table 2. Parameters for the microalgae cultivation in a raceway pond using wastewater from the dairy industry. Acronyms: WW, Wastewater. Adapted from [109,129].

Case Study		Base Case	75% WW
Biomass productivity	$g/m^2/day$	14.2	45
CO_2 usage	kg/kg algae biomass	2	2
Water evaporation	$L/m^2/day$	7.5	7.5
Mixing power consumption	W/m^3	10	10
Labor	people/ha	1	1
Production days	days	300	300
Land area	ha	5	5
Ratio V/S	m^3/m^2	0.2	0.2
CO_2 fixation efficiency		0.9	0.9
Dilution rate	1/day	0.2	0.2
Total culture volume	m^3	10,000	10,000
Total biomass production	t/ha/year	42.6	135
Total CO_2 consumption	t/ha/year	85.2	270
Total water evaporation	t/ha/year	22,500	22,500
Water and nutrients cost	EUR/kg	1.1	
Power cost	EUR/kWh	0.12	0.12
Power for harvesting and others	kWh/m^3 harvest	0.1	0.1
Bioreactor cost	EUR/m^3	61.87	61.87
Biomass sludge production cost	EUR/kg	7.84	1.98

[1] Cost data have been corrected for inflation, when needed, and thus, provide a reasonable estimate of the current costs.

In this new scenario (Table 2), when cultivating microalgae with synthetic media, a conservative biomass productivity of 14.2 $g/m^2/day$ was achieved, equivalent to 42.6 t/ha/year, resulting in a cost of 7.84 EUR/kg. With wastewater use, however, beyond the nutrient costs being zero, productivity has increased considerably, reducing the production cost to 1.98 EUR/kg. For the same surface area of 5 ha, up to 675 t/year of microalgae biomass are produced when using wastewater, whereas this production capacity decreases to 213 t/year when using synthetic media. With the manpower reduction, the cost can fall to 1.44 EUR/kg. This value approaches the target of 1.24 EUR/kg, providing greater competitiveness for lower value-added markets and effluent treatment in specific contexts (smaller-scale or low-efficiency systems).

In sum, although the integration of microalgae cultivation with wastewater use has proven to be technically feasible and economically promising, it is worth mentioning that its consolidation remains restricted to laboratory, semi-controlled, and, ultimately, pilot-scale environments [107–109,115,117,140]. Thus, transposing these advances to an industrial scale cannot be seen simply as a matter of incremental improvement but as a systemic challenge that requires a paradigm shift; it is necessary to design large-scale operations

without off-season periods, breaking with the logic of seasonality and operational fragility. Posteriorly, from this basis, the true technological frontier lies in efficiency—not only in photosynthetic efficiency or the biomass volumetric productivity, but in the efficiency of the economic conversion of available inputs. In a scenario of tight margins, such as the markets for bioenergy, biofertilizers, biostimulants, biopesticides, bioplastics, and, ultimately, aquaculture feed, efficiency is not a differentiator but a condition for technological survival. Furthermore, at the state-of-the-art, the real challenge is no longer proving that the technology works but making it efficient enough to compete with conventional wastewater treatment processes and, in terms of value-added product production, efficient enough to compete with commodities from conventional agriculture and fossil fuel-based industries.

4. Environmental Impact of Microalgae Production Using Wastewater: Environmental Sustainability Metrics and Indicators

As studies on the feasibility of integrating microalgae production with wastewater intensify, the need to understand and qualify the environmental impacts of this technology through life cycle assessment (LCA) also grows [141,142]. The objective is to quantify and analyze metrics associated with several environmental impact indicators—such as global warming potential, fossil resource scarcity, human toxicity, soil and water eutrophication, soil, water, and air acidification, and soil and water ecotoxicity—in different operational scenarios to guide decisions and promote improvements in production systems [143]. Here, particular emphasis is placed on the influence of wastewater composition, biomass productivity, and energy consumption on the technical-environmental performance of the system. By documenting these factors and their interactions, this analysis seeks to clarify the environmental tradeoffs and opportunities involved in the phycoremediation strategy, supporting its alignment with the logic of the circular bioeconomy.

Many studies on the environmental sustainability of microalgae production find, at their core, two critical variables that strongly condition the performance of the systems evaluated: energy consumption and biomass productivity [144–150]. When related to cultivation with wastewater, a third variable emerges: wastewater composition, which can positively or negatively impact the indicators, especially due to its influence on biomass productivity [151–153]. Both are interconnected in an intricate way and decisively determine the metrics applied in environmental analyses [154].

Energy consumption during the harvesting and drying phases, and especially during the cultivation stage, is high, and when it comes from non-renewable sources, such as coal, the environmental impacts are significant [155] (Table A1). Among the most reported impact categories with expressive values are freshwater eutrophication, marine eutrophication, terrestrial acidification, and human toxicity, with most of these impacts being strongly associated with intensive energy consumption, especially in systems powered by fossil matrices [150,156–158].

Additionally, the cultivation system, classified as open (such as a raceway pond) and closed (such as tubular photobioreactors), also exerts influence. Magalhães et al. [159] recently compared the techno-environmental feasibility of both systems for microalgae biomass production in agro-industrial wastewater and observed that although the closed system presented greater productivity and efficiency in nutrient removal, its environmental impacts were greater than those of the open system, whose lower productivity was offset by lower energy requirements. Although closed systems allow greater operational control, favoring both biomass productivity and nutrient removal from wastewater, they demand greater energy consumption and, consequently, can present more significant environmental impacts [149,160]. In this sense, to what extent is the efficiency of these systems compatible with environmental sustainability? In contexts in which energy matrices are predominantly

fossil, this virtue can become ambiguous, but environmental sustainability will depend directly on the balance between biomass productivity and energy consumption [161].

In parallel, under the same cultivation system, such as a raceway pond, biomass productivity is a key variable capable of diluting resource use and environmental impacts. By way of example, Table 3 shows an analysis based on data extracted from the literature, structured in the form of a life cycle inventory for microalgae production using wastewater. The base case considers the use of standard culture media, and the 10% WW and 20% WW scenarios consider the use of wastewater from an oil and gas facility [128], while the 75% WW scenario considers the use of wastewater from a dairy industry [129]. As can be seen in Table 3, to achieve a standardized functional unit of 1 kg of dry biomass, as productivity decreases (10% WW and 20% WW) or increases (75% WW), the energy consumption is proportionally different. In summary, productivity and resource consumption are closely related, and the lower the productivity, the greater the impact on the consumption of these resources [162].

Table 3. Life cycle inventory for microalgae production using wastewater [109,128,129]. Acronyms: WW, Wastewater.

		Base Case	10% WW	20% WW	75% WW
Raceway pond	m^3	10	15.41	21.76	4.44
Electric energy for paddle wheel	kWh	129.60	199.71	282.01	57.54
Electric energy for water pumping	kWh	24.00	36.98	52.22	10.66
Electric energy for CO_2 injection	kWh	79.20	122.05	172.34	35.16
CO_2 consumption	kg/kg biomass	2.00	2.00	2.00	2.00
Biomass productivity	$g/m^2/day$	20.00	12.97	9.19	45
Energy consumption centrifugation	kWh	12.50	19.26	27.20	5.55
Spray-dryer	kWh	8.52	8.52	8.52	8.52
Output					
Whole dried biomass	kg	1	1	1	1
Electricity	kWh	253.82	386.53	542.30	117.44

The greater or lesser impact on resource consumption is reflected in the metrics of the main environmental performance indicators (Table A1). Although the use of wastewater can reduce or eliminate the need for fertilizer inputs, the process continues to demand energy, and when production is sometimes limited, the impacts per functional unit increase. Thus, even well-intentioned processes—such as effluent reuse—can present unsatisfactory metrics if they fail to, at least, maintain productivity. More than a kinetic parameter, biomass productivity assumes the role of a structuring variable in the metrics of environmental sustainability indicators, as can be seen in Figure 3.

Figure 3 presents the compact and comparative contribution of the different categories of environmental impact associated with the production of 1 kg of microalgae biomass cultivated in wastewater (base case, 10% WW, 20% WW, and 75% WW scenarios), considering the use of energy from coal, according to the data in Table A1. Among the categories evaluated, the most impactful are human non-carcinogenic toxicity (HnCT) and global warming potential (GWP), followed by terrestrial ecotoxicity (TEC) and fossil resource scarcity (FRS) [150,156–158]. The HnCT varied between 284 and 1312 kg 1,4-DCB eq./kg of biomass, while the values of GWP, TEC, and FRS oscillated between 127 and 586 kg CO_2 eq./kg of biomass, 41.7 and 193 kg 1,4-DCB eq./kg of biomass, and 27.8 and 129 kg oil eq./kg of biomass, respectively. These results confirm that such impacts are strongly conditioned by the biomass productivity and the intensity of electricity consumption—non-renewable.

The nature of the energy matrix used to feed microalgae-based processes plays an important role, capable of amortizing environmental impacts by more than an order of

magnitude (Table A1). The replacement of fossil energy sources by renewable ones emerges as the backbone for operations with significantly lower emissions. Arbour et al. [163] found in their study that electricity use was the main environmental critical point of microalgae-based wastewater treatment and proposed replacing the predominantly fossil-based electricity matrix with renewable sources. The replacement was shown to reduce the environmental impact in all impact categories, with reductions ranging from 90% to 99%. This finding is in full agreement with the results presented in Figure 4, which summarizes part of the data described in Table A1, reinforcing the centrality of the energy transition for the sustainability of the process.

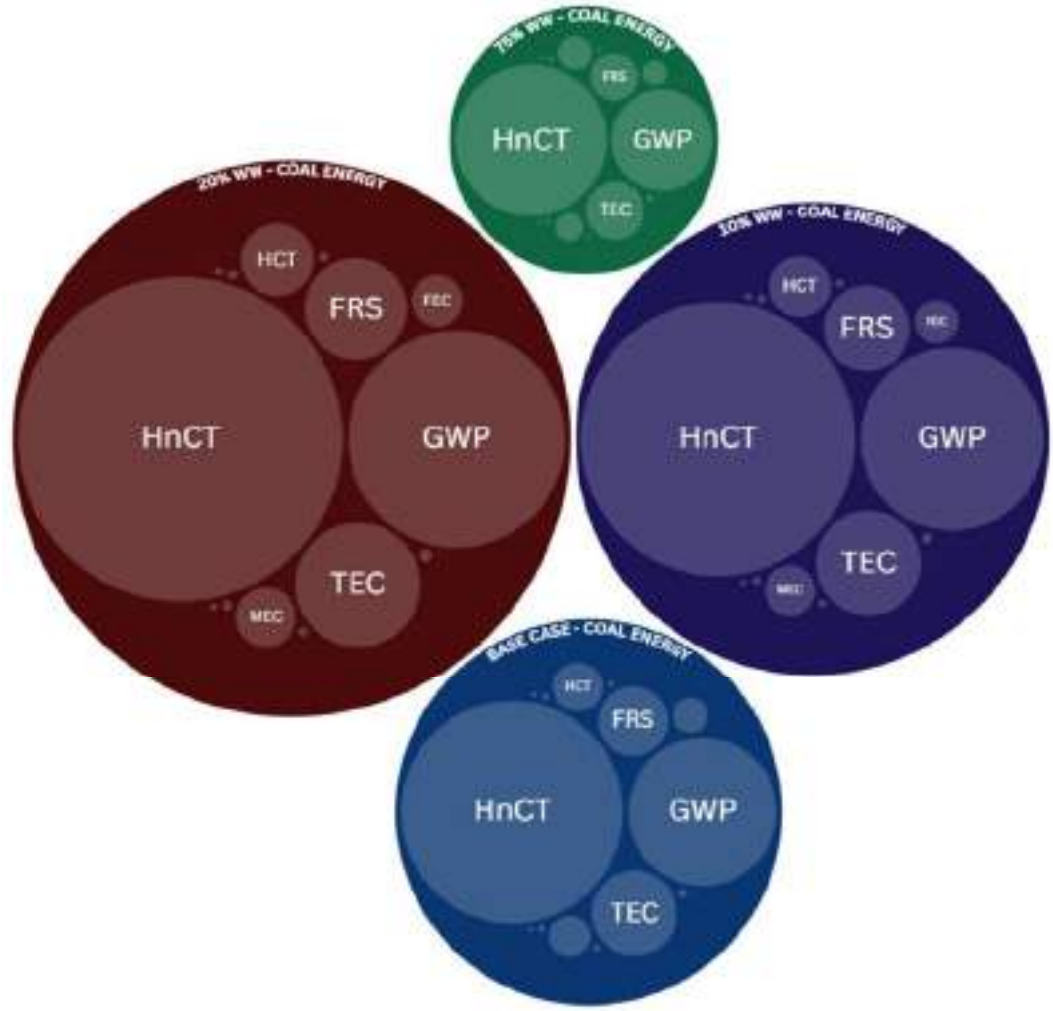


Figure 3. Compact contribution of each environmental impact category to emissions from microalgae production using wastewater. Note: Processes powered by coal-based energy. Figure 3 was created using the Flourish Studio platform without the use of artificial intelligence tools. Acronyms: WW, Wastewater; FPMF, Fine particulate matter formation (kg $PM_{2.5}$ eq.); FRS, Fossil resource scarcity (kg oil eq.); FEC, Freshwater ecotoxicity (kg 1,4-DCB); FEU, Freshwater eutrophication (kg P eq.); GWP, Global warming potential (kg CO_2 eq.); HCT, Human carcinogenic toxicity (kg 1,4-DCB); HnCT, Human non-carcinogenic toxicity (kg 1,4-DCB); IR, Ionizing radiation (kBq Co-60 eq.); LU, Land use (m^2a crop eq.), MEC, Marine ecotoxicity (kg 1,4-DCB); MRS, Mineral resource scarcity (kg Cu eq.); OFTE, Ozone formation affecting terrestrial ecosystems (kg NOx eq.); SOD, Stratospheric ozone depletion (kg CFC_{11} eq.); TAC, Terrestrial acidification (kg SO_2 eq.); TEC, Terrestrial ecotoxicity (kg 1,4- DCB); TWC, Total water consumption (m^3).

Figure 4 shows the compact and comparative contribution of the different categories of environmental impact associated with the production of 1 kg of microalgae biomass grown in wastewater (scenario: 75% WW), considering the use of energy from coal, hydropower, photovoltaic, and wind, as per the data in Table A1. While the impacts considering the fossil matrix were high in all categories, the adoption of renewable sources—especially hydropower and wind—demonstrated substantial reductions. While the GWP drops from 127 kg CO_2 eq./kg of biomass (coal) to 0.77 kg CO_2 eq./kg of biomass with hydropower and 1.82 kg CO_2 eq./kg of biomass with wind power, the HnCT is reduced from 284 to only 0.56 kg 1,4-DCB/kg of biomass with hydropower. Likewise, FRS decreases from 27.8 to 0.13 kg oil eq./kg biomass, and TEC decreases from 41.7 to 2.6 kg 1,4-DCB/kg biomass.

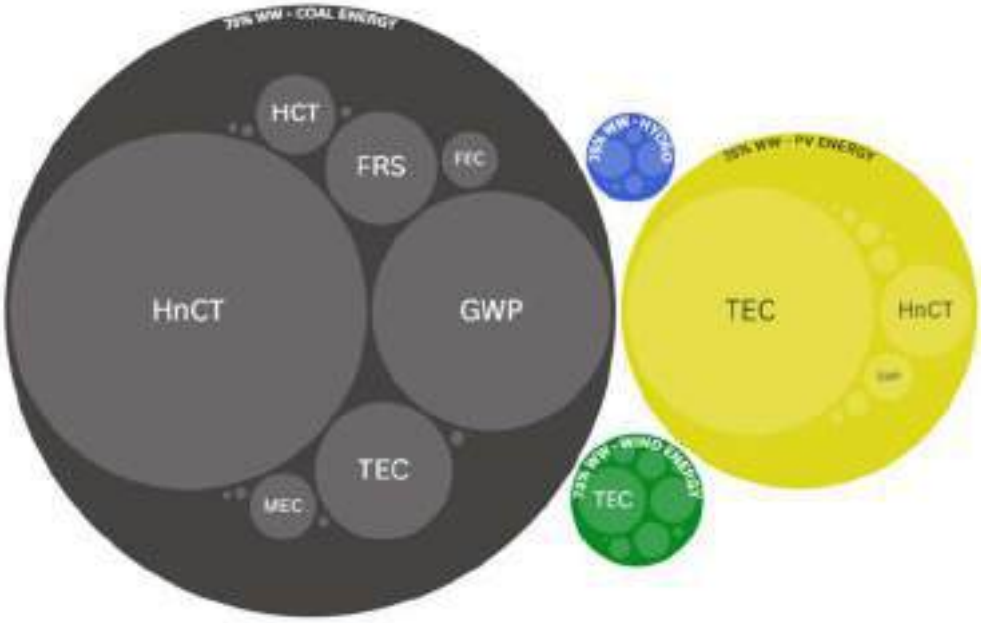


Figure 4. Compact contribution of each environmental impact category to emissions from microalgae production using wastewater. Note: Processes powered by coal, hydro, photovoltaic, and wind-based energy. Figure 4 was created using the Flourish Studio platform without the use of artificial intelligence tools. Acronyms: WW, Wastewater; FPMF, Fine particulate matter formation (kg $PM_{2.5}$ eq.); FRS, Fossil resource scarcity (kg oil eq.); FEC, Freshwater ecotoxicity (kg 1,4-DCB); FEU, Freshwater eutrophication (kg P eq.); GWP, Global warming potential (kg CO_2 eq.); HCT, Human carcinogenic toxicity (kg 1,4-DCB); HnCT, Human non-carcinogenic toxicity (kg 1,4-DCB); IR, Ionizing radiation (kBq Co-60 eq.); LU, Land use (m^2a crop eq.), MEC, Marine ecotoxicity (kg 1,4-DCB); MRS, Mineral resource scarcity (kg Cu eq.); OFTE, Ozone formation affecting terrestrial ecosystems (kg NOx eq.); SOD, Stratospheric ozone depletion (kg CFC_{11} eq.); TAC, Terrestrial acidification (kg SO_2 eq.); TEC, Terrestrial ecotoxicity (kg 1,4- DCB); TWC, Total water consumption (m^3).

However, it is worth mentioning that access to these sources is not always trivial, especially for those who depend on electricity supplied by the electrical grids without having autonomous power generation systems. But, in this scenario, it is noteworthy that the advancement in photovoltaic (PV) systems stands out as a concrete opportunity to mitigate the environmental impacts associated with energy consumption. The proposal to implement PV systems in microalgae installations has proven to be economically viable, capable of improving environmental sustainability metrics, and strengthening the long-term economic viability of facilities—reducing the vulnerability to electricity prices [164,165].

Finally, environmental sustainability does not depend on a single factor but on a balance between interdependent pillars—such as wastewater composition, productivity, and energy consumption. Connecting these pillars requires more than coexistence: it requires integration, intensification, and systemic articulation. However, in practice, they do not always converge spontaneously and, often, tense up mutually. For example, prioritizing circularity—such as wastewater use—can impose limitations on productivity and operational predictability. Furthermore, life cycle analysis—although a powerful tool—may not capture all the nuances of the system due to the multiple variables in constant interaction. Therefore, first, it is important to recognize that the fragility of sufficiently robust support systems to deal with the systemic complexity of microalgae-based biotechnological processes is also one of the main hidden bottlenecks that contribute to the inefficiency of innovative and potentially sustainable technologies.

5. Technological Readiness Level of Microalgae Cultivation Using Wastewater

This topic aims to close the discussion developed throughout the work, showing the Technological Readiness Level (TRL) of the integration between microalgae cultivation and wastewater use. Although the previous topics have already indicated, based on several studies, that most of the experiences are at the laboratory or pilot scale, here we seek to consolidate this evidence in a clear diagnosis of the technology's development stage. The TRL scale, widely used to measure the evolution of technologies towards their commercial application [166,167], indicates that this approach is predominantly between levels 4 and 6, concentrated in validation stages in a laboratory environment and a relevant operational environment, such as pilot plants (Figure 5).

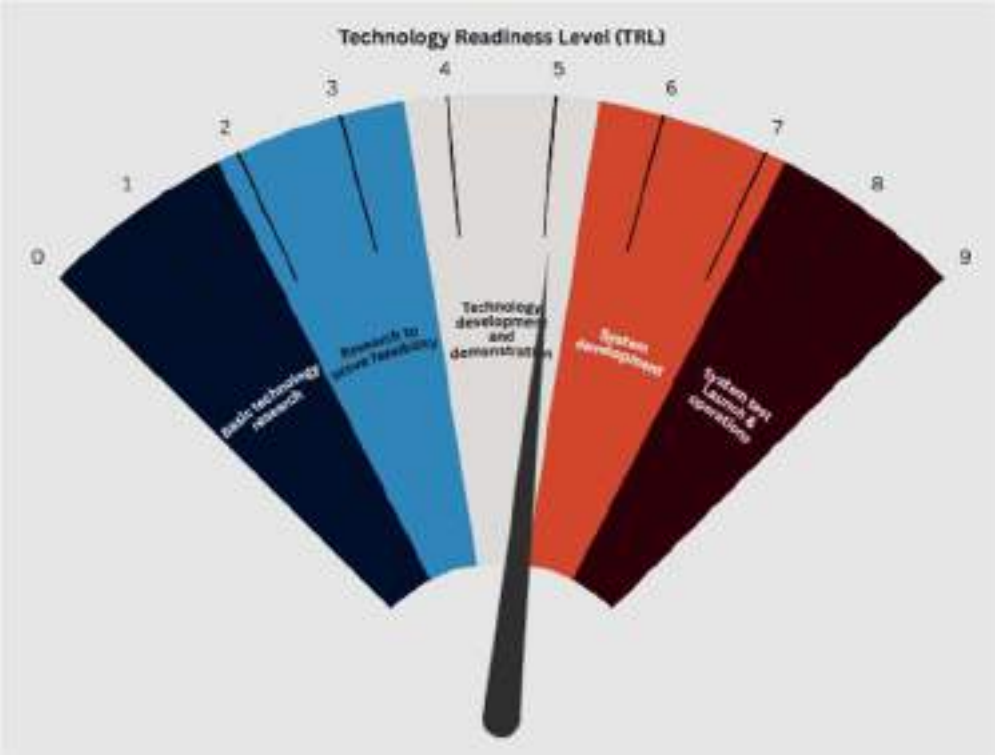


Figure 5. TRL for microalgae cultivation using wastewater. Adapted from [63].

At TRL scale 1 to 4, which corresponds to hypotheses, proof of concept, and validation in a laboratory environment, studies, such as those by Matamoros et al. [39], Petrini et al. [168], Krishnamoorthy et al. [169], Moondra et al. [170], Xu et al. [171], Azam et al. [172], Noshadi and Nouripour [173], and Moondra et al. [174], can be cited. At TRL scales 5 and 6, which correspond to more advanced experiments and prototypes tested in a relevant operational environment, the studies by Morillas-España et al. [107], Abraham et al. [108], Matamoros et al. [111], Ovis-Sánchez et al. [112], Goswami et al. [113], Yu et al. [114], Rossi et al. [115], Mantovani et al. [116], Morillas-España et al. [117], Dalvi et al. [118], and Blanco-Vieites et al. [175] can be cited. In these studies, the experiments were conducted in pilot systems with volumes ranging from 10, 100, 1000, and even 10,000 L, demonstrating important advances towards scalability. However, the transition to higher levels (NRT 7-9), corresponding to the implementation of the technology in a real operational environment with proven success under the desired conditions and subsequent commercialization—the apex of the technological trajectory—does not yet count on consolidated reports or robust evidence in the literature to date [127,176,177].

In sum, the typical technological symbiosis of a microalgae-based biorefinery, which integrates nutrient capture, CO_2 sequestration, and biomass production, has already been identified as a key solution to consolidate the technical and economic viability of value-added products, whose competitiveness depends heavily on reducing operating costs [178–180]. However, beyond the technical obstacles related to the cultivation operation in heterogeneous wastewater that require highly adaptive strains [181], there are economic, environmental, logistical, and regulatory issues [83,182–184]. The production systems lack greater scalability and competitive costs compared to conventional technologies [185]. Integration with effluent-generating industries is incipient, and, associated with this, the lack of clear regulatory frameworks for wastewater use in biomass production, especially for high value-added applications, creates a gap that inhibits investments [186].

Furthermore, fragmented research—focused on proofs of concept—is also not enough to achieve a paradigm shift. In truth, the integration of microalgae cultivation with wastewater depends less on isolated new discoveries and more on the systemic articulation between science, technology, market, and policy. Strategic vision, targeted funding, and, above all, the breaking of obsolete industrial paradigms could crown this approach. However, the field remains, for the most part, in a repetitive cycle of identifying bottlenecks and promises that rarely translate into concrete solutions. This symptomatic stagnation may reflect how disconnected fundamental research is from the real dynamics of technological implementation.

Finally, the actions needed to break the cycle of stagnation and advance to higher levels of technological readiness are already widely discussed in the literature. Therefore, it is time to stop simply mapping obstacles and start structuring collaborative projects at relevant scales (TRL 6-8), guided by economic, environmental, and social performance metrics. Shaping the technological maturity of the integration of microalgae cultivation with wastewater requires an intersectoral commitment, as the challenges go beyond the technical field and involve issues that require coordination between academia, the productive sector, and the public power.

6. Conclusions

The integration of microalgae cultivation with wastewater is a tangible approach within the circular bioeconomy paradigm. The findings show that this strategy can reduce biomass production costs to as little as EUR 1.98/kg, especially when combined with effluents with a favorable composition and high productivity. However, economic viability remains strongly conditioned by the quality of the effluent and the stability of biomass

productivity, which, in turn, is also a determining variable of the environmental performance of the system. Drops in productivity intensify energy consumption per biomass unit, compromising the environmental gains associated with the reuse of residual resources. On the other hand, the replacement of fossil sources with renewable energy has proven to be the backbone for significantly mitigating the environmental impacts of the process. From a technological point of view, the data indicate that most initiatives remain between technology readiness levels 4 and 6, which reveals a still incipient stage of transition from the bench to the industry. In summary, the results presented confirm that the technology has already surpassed the proof-of-concept stage, but high costs and limited technological maturity continue to stifle the potential of this approach. Applications on modest scales, but real, indicate that prioritizing products with medium added value—such as aquaculture feed—that emerge in an intermediate zone between complexity and viability is a viable alternative to promote the gradual consolidation of the technology. In conclusion, transit through small victories can attract investments in research that, in the future, will support applications with lower added value, such as bioenergy. Furthermore, disruptive leaps will not be achieved without the patient construction of a solid base.

Author Contributions: R.R.D.: Conceptualization, investigation, writing—review and editing, writing—original draft. M.C.D.: Writing—review and editing. C.R.d.M.: Project administration. L.Q.Z.: Project administration, writing—review and editing. E.J.-L.: Conceptualization, project administration, writing—review and editing. All authors have read and agreed to the published version of the manuscript.

Funding: This research was funded by the Coordination for the Improvement of Higher Education Personnel (CAPES) (grant number 001) and the National Council for Scientific and Technological Development (CNPq).

Data Availability Statement: The original contributions presented in this study are included in the article. Further inquiries can be directed to the corresponding authors.

Conflicts of Interest: The authors declare no conflicts of interest.

Abbreviations

The following abbreviations are used in this manuscript:

TRL	Technology Readiness Level
WW	Wastewater
PV	Photovoltaic
FPMF	Fine particulate matter formation
FRS	Fossil resource scarcity
FEC	Freshwater ecotoxicity
FEU	Freshwater eutrophication
GWP	Global warming potential
HCT	Human carcinogenic toxicity
HnCT	Human non-carcinogenic toxicity
IR	Ionizing radiation
LU	Land use
MEC	Marine ecotoxicity
MRS	Mineral resource scarcity
OFTE	Ozone formation affecting terrestrial ecosystems
SOD	Stratospheric ozone depletion
TAC	Terrestrial acidification
TEC	Terrestrial eco-toxicity
TWC	Total water consumption

Appendix A

Table A1. Characterized values of environmental impact categories associated with the production of 1 kg of dry biomass using wastewater based on the energy source. Acronyms: WW, Wastewater; FPMF, Fine particulate matter formation; FRS, Fossil resource scarcity; FEC, Freshwater ecotoxicity; FEU, Freshwater eutrophication; GWP, Global warming potential; HCT, Human carcinogenic toxicity; HnCT, Human non-carcinogenic toxicity; IR, Ionizing radiation; LU, Land use; MEC, Marine ecotoxicity; MRS, Mineral resource scarcity; OFTE, Ozone formation affecting terrestrial ecosystems; SOD, Stratospheric ozone depletion; TAC, Terrestrial acidification; TEC, Terrestrial eco-toxicity; TWC, Total water consumption.

Base Case				
	Coal	Photovoltaic	Onshore wind	Hydropower
FPMF (kg $PM_{2.5}$ eq.)	3.00×10^{-1}	2.64×10^{-2}	7.41×10^{-3}	2.51×10^{-3}
FRS (kg oil eq.)	6.02×10^{1}	2.74×10^{0}	1.07×10^{0}	2.77×10^{-1}
FEC (kg 1,4-DCB)	1.53×10^{1}	2.94×10^{0}	2.02×10^{0}	5.56×10^{-2}
FEU (kg P eq.)	6.22×10^{-1}	9.59×10^{-3}	1.83×10^{-3}	3.40×10^{-4}
GWP (kg CO_2 eq.)	2.74×10^{2}	1.12×10^{1}	3.93×10^{0}	1.66×10^{0}
HCT (kg 1,4-DCB)	3.07×10^{1}	1.06×10^{0}	5.94×10^{0}	8.07×10^{-1}
HnCT (kg 1,4-DCB)	6.14×10^{2}	4.14×10^{1}	9.70×10^{0}	1.21×10^{0}
IR (kBq Co-60 eq.)	6.42×10^{-1}	1.04×10^{0}	2.26×10^{-1}	6.78×10^{-2}
LU (m^2a crop eq.)	4.85×10^{-1}	3.12×10^{-1}	4.59×10^{-1}	5.36×10^{-2}
MEC (kg 1,4-DCB)	2.11×10^{1}	3.88×10^{0}	2.49×10^{0}	7.77×10^{-2}
MRS (kg Cu eq.)	3.15×10^{-2}	1.41×10^{-1}	9.32×10^{-2}	1.83×10^{-2}
OFTE (kg NOx eq.)	4.21×10^{-1}	2.67×10^{-2}	1.23×10^{-2}	4.95×10^{-3}
SOD (kg CFC_{11} eq.)	4.24×10^{-5}	5.23×10^{-6}	1.72×10^{-6}	8.10×10^{-7}
TAC (kg SO_2 eq.)	9.75×10^{-1}	5.61×10^{-2}	1.35×10^{-2}	4.11×10^{-3}
TEC (kg 1,4- DCB)	9.01×10^{1}	2.97×10^{2}	2.11×10^{1}	5.66×10^{0}
TWC (m^3)	5.51×10^{-1}	3.43×10^{-1}	4.87×10^{-2}	7.44×10^{0}
10% WW				
	Coal	Photovoltaic	Onshore wind	Hydropower
FPMF (kg $PM_{2.5}$ eq.)	4.56×10^{-1}	4.02×10^{-2}	1.13×10^{-2}	3.82×10^{-3}
FRS (kg oil eq.)	9.16×10^{1}	4.17×10^{0}	1.62×10^{0}	4.21×10^{-1}
FEC (kg 1,4-DCB)	2.33×10^{1}	4.48×10^{0}	3.08×10^{0}	8.47×10^{-2}
FEU (kg P eq.)	9.47×10^{-1}	1.46×10^{-2}	2.78×10^{-3}	5.18×10^{-4}
GWP (kg CO_2 eq.)	4.17×10^{2}	1.71×10^{1}	5.99×10^{0}	2.53×10^{0}
HCT (kg 1,4-DCB)	4.68×10^{1}	1.61×10^{0}	9.04×10^{0}	1.23×10^{0}
HnCT (kg 1,4-DCB)	9.35×10^{2}	6.30×10^{1}	1.48×10^{1}	1.84×10^{0}
IR (kBq Co-60 eq.)	9.78×10^{-1}	1.58×10^{0}	3.44×10^{-1}	1.03×10^{-1}
LU (m^2a crop eq.)	7.38×10^{-1}	4.75×10^{-1}	7.00×10^{-1}	8.16×10^{-2}
MEC (kg 1,4-DCB)	3.21×10^{1}	5.91×10^{0}	3.79×10^{0}	1.18×10^{-1}
MRS (kg Cu eq.)	4.79×10^{-2}	2.14×10^{-1}	1.42×10^{-1}	2.79×10^{-2}
OFTE (kg NOx eq.)	6.42×10^{-1}	4.06×10^{-2}	1.87×10^{-2}	7.54×10^{-3}
SOD (kg CFC_{11} eq.)	6.46×10^{-5}	7.96×10^{-6}	2.61×10^{-6}	1.23×10^{-6}

Table A1. *Cont.*

TAC (kg SO_2 eq.)	1.48×10^{0}	8.54×10^{-2}	2.06×10^{-2}	6.26×10^{-3}
TEC (kg 1,4- DCB)	1.37×10^{2}	4.52×10^{2}	3.22×10^{1}	8.62×10^{0}
TWC (m^3)	8.39×10^{-1}	5.22×10^{-1}	7.42×10^{-2}	1.13×10^{1}
20% WW				
	Coal	Photovoltaic	Onshore wind	Hydropower
FPMF (kg $PM_{2.5}$ eq.)	6.40×10^{-1}	5.64×10^{-2}	1.58×10^{-2}	5.36×10^{-3}
FRS (kg oil eq.)	1.29×10^{2}	5.86×10^{0}	2.28×10^{0}	5.91×10^{-1}
FEC (kg 1,4-DCB)	3.28×10^{1}	6.29×10^{0}	4.32×10^{0}	1.19×10^{-1}
FEU (kg P eq.)	1.33×10^{0}	2.05×10^{-2}	3.90×10^{-3}	7.27×10^{-4}
GWP (kg CO_2 eq.)	5.86×10^{2}	2.40×10^{1}	8.41×10^{0}	3.55×10^{0}
HCT (kg 1,4-DCB)	6.56×10^{1}	2.26×10^{0}	1.27×10^{1}	1.72×10^{0}
HnCT (kg 1,4-DCB)	1.31×10^{3}	8.84×10^{1}	2.07×10^{1}	2.58×10^{0}
IR (kBq Co-60 eq.)	1.37×10^{0}	2.21×10^{0}	4.83×10^{-1}	1.45×10^{-1}
LU (m^2a crop eq.)	1.04×10^{0}	6.67×10^{-1}	9.82×10^{-1}	1.14×10^{-1}
MEC (kg 1,4-DCB)	4.50×10^{1}	8.30×10^{0}	5.31×10^{0}	1.66×10^{-1}
MRS (kg Cu eq.)	6.72×10^{-2}	3.00×10^{-1}	1.99×10^{-1}	3.92×10^{-2}
OFTE (kg NOx eq.)	9.00×10^{-1}	5.69×10^{-2}	2.63×10^{-2}	1.06×10^{-2}
SOD (kg CFC_{11} eq.)	9.06×10^{-5}	1.12×10^{-5}	3.67×10^{-6}	1.73×10^{-6}
TAC (kg SO_2 eq.)	2.08×10^{0}	1.20×10^{-1}	2.89×10^{-2}	8.79×10^{-3}
TEC (kg 1,4- DCB)	1.93×10^{2}	6.34×10^{2}	4.52×10^{1}	1.21×10^{1}
TWC (m^3)	1.18×10^{0}	7.32×10^{-1}	1.04×10^{-1}	1.59×10^{1}
75% WW				
	Coal	Photovoltaic	Onshore wind	Hydropower
FPMF (kg $PM_{2.5}$ eq.)	1.39×10^{-1}	1.22×10^{-2}	3.43×10^{-3}	1.16×10^{-3}
FRS (kg oil eq.)	2.78×10^{1}	1.27×10^{0}	4.93×10^{-1}	1.28×10^{-1}
FEC (kg 1,4-DCB)	7.09×10^{0}	1.36×10^{0}	9.35×10^{-1}	2.57×10^{-2}
FEU (kg P eq.)	2.88×10^{-1}	4.44×10^{-3}	8.46×10^{-4}	1.57×10^{-4}
GWP (kg CO_2 eq.)	1.27×10^{2}	5.20×10^{0}	1.82×10^{0}	7.69×10^{-1}
HCT (kg 1,4-DCB)	1.42×10^{1}	4.90×10^{-1}	2.75×10^{0}	3.73×10^{-1}
HnCT (kg 1,4-DCB)	2.84×10^{2}	1.91×10^{1}	4.49×10^{0}	5.59×10^{-1}
IR (kBq Co-60 eq.)	2.97×10^{-1}	4.79×10^{-1}	1.05×10^{-1}	3.14×10^{-2}
LU (m^2a crop eq.)	2.24×10^{-1}	1.44×10^{-1}	2.13×10^{-1}	2.48×10^{-2}
MEC (kg 1,4-DCB)	9.75×10^{0}	1.80×10^{0}	1.15×10^{0}	3.59×10^{-2}
MRS (kg Cu eq.)	1.46×10^{-2}	6.51×10^{-2}	4.31×10^{-2}	8.48×10^{-3}
OFTE (kg NOx eq.)	1.95×10^{-1}	1.23×10^{-2}	5.70×10^{-3}	2.29×10^{-3}
SOD (kg CFC_{11} eq.)	1.96×10^{-5}	2.42×10^{-6}	7.94×10^{-7}	3.75×10^{-7}
TAC (kg SO_2 eq.)	4.51×10^{-1}	2.60×10^{-2}	6.26×10^{-3}	1.90×10^{-3}
TEC (kg 1,4- DCB)	4.17×10^{1}	1.37×10^{2}	9.78×10^{0}	2.62×10^{0}
TWC (m^3)	2.55×10^{-1}	1.59×10^{-1}	2.25×10^{-2}	3.44×10^{0}

References

1. Plöhn, M.; Spain, O.; Sirin, S.; Silva, M.; Escudero-Oñate, C.; Ferrando-Climent, L.; Funk, C. Wastewater treatment by microalgae. *Physiol. Plant.* **2021**, *173*, 568–578. [CrossRef]
2. Tariq, A.; Mushtaq, A. Untreated wastewater reasons and causes: A review of most affected areas and cities. *Int. J. Chem. Biochem. Sci* **2023**, *23*, 121–143.
3. Ahmed, S.F.; Mofijur, M.; Parisa, T.A.; Islam, N.; Kusumo, F.; Inayat, A.; Ong, H.C. Progress and challenges of contaminate removal from wastewater using microalgae biomass. *Chemosphere* **2022**, *286*, 131656. [CrossRef] [PubMed]
4. Pratap, B.; Kumar, S.; Nand, S.; Azad, I.; Bharagava, R.N.; Ferreira, L.F.R.; Dutta, V. Wastewater generation and treatment by various eco-friendly technologies: Possible health hazards and further reuse for environmental safety. *Chemosphere* **2023**, *313*, 137547. [CrossRef]
5. Wollmann, F.; Dietze, S.; Ackermann, J.U.; Bley, T.; Walther, T.; Steingroewer, J.; Krujatz, F. Microalgae wastewater treatment: Biological and technological approaches. *Eng. Life Sci.* **2019**, *19*, 860–871. [CrossRef] [PubMed]
6. Su, Y. Revisiting carbon, nitrogen, and phosphorus metabolisms in microalgae for wastewater treatment. *Sci. Total Environ.* **2021**, *762*, 144590. [CrossRef] [PubMed]
7. Kaloudas, D.; Pavlova, N.; Penchovsky, R. Phycoremediation of wastewater by microalgae: A review. *Environ. Chem. Lett.* **2021**, *19*, 2905–2920. [CrossRef]
8. Singh, V.; Mishra, V. Evaluation of the effects of input variables on the growth of two microalgae classes during wastewater treatment. *Water Res.* **2022**, *213*, 118165. [CrossRef]
9. Guerra-Rodríguez, S.; Oulego, P.; Rodríguez, E.; Singh, D.N.; Rodríguez-Chueca, J. Towards the implementation of circular economy in the wastewater sector: Challenges and opportunities. *Water* **2020**, *12*, 1431. [CrossRef]
10. Göncü, S.; Şimşek Uygun, B.; Atakan, S. Nıtrogen and phosphorus removal from wastewater usıng *Chlorella vulgarıs* and *Scenedesmus quadrıcauda* mıcroalgae wıth a batch bıoreactor. *Int. J. Environ. Sci. Technol.* **2025**, 1–16. [CrossRef]
11. Prabhath, G.P.W.A.; Shukla, S.P.; Srivastava, P.P.; Kumar, K.; Sawant, P.B.; Verma, A.K.; Nuwansi, K.K.T. Downstream processing of biomass produced in aquaculture wastewater for valuable pigments from the cyanobacterium *Spirulina* (*Arthrospira*) *platensis*: A green and sustainable approach. *Aquac. Int.* **2022**, *30*, 3081–3106. [CrossRef]
12. Mesa, A.P.; Grattz, P.A.C.; Vargas, J.J.V.; Ríos, L.A.; Echeverri, D.O.; Parra, A.M.M. Feasibility of nitrogen and phosphorus removal from treated wastewater using microalgae and potential microalgae use as biofertilizer. *J. Water Process Eng.* **2025**, *70*, 107023. [CrossRef]
13. Papadopoulos, K.P.; Economou, C.N.; Markou, G.; Nicodemou, A.; Koutinas, M.; Tekerlekopoulou, A.G.; Vayenas, D.V. Cultivation of *Arthrospira platensis* in brewery wastewater. *Water* **2022**, *14*, 1547. [CrossRef]
14. Tan, Y.H.; Chai, M.K.; Na, J.Y.; Wong, L.S. Microalgal growth and nutrient removal efficiency in non-sterilised primary domestic wastewater. *Sustainability* **2023**, *15*, 6601. [CrossRef]
15. Amaro, H.M.; Salgado, E.M.; Nunes, O.C.; Pires, J.C.; Esteves, A.F. Microalgae systems-environmental agents for wastewater treatment and further potential biomass valorisation. *J. Environ. Manag.* **2023**, *337*, 117678.
16. Morais, E.G.; Cristofoli, N.L.; Maia, I.B.; Magina, T.; Cerqueira, P.R.; Teixeira, M.R.; Gouveia, L. Microalgal systems for wastewater treatment: Technological trends and challenges towards waste recovery. *Energies* **2021**, *14*, 8112. [CrossRef]
17. Nobre, M.L.; Tavares, D.; Fraga, C.; Oliveira, B.; Dias, M.; Mesquita, S.; Pires, J.C. Techno-economic analysis of a circular microalgal approach for enhanced wastewater treatment and resource recovery in Northern Portugal. *J. Clean. Prod.* **2024**, *434*, 140389. [CrossRef]
18. Álvarez-González, A.; Uggetti, E.; Serrano, L.; Gorchs, G.; Casas, M.E.; Matamoros, V.; Díez-Montero, R. The potential of wastewater grown microalgae for agricultural purposes: Contaminants of emerging concern, heavy metals and pathogens assessment. *Environ. Pollut.* **2023**, *324*, 121399. [CrossRef]
19. Osman, M.E.; Abo-Shady, A.M.; Gheda, S.F.; Desoki, S.M.; Elshobary, M.E. Unlocking the potential of microalgae cultivated on wastewater combined with salinity stress to improve biodiesel production. *Environ. Sci. Pollut. Res.* **2023**, *30*, 114610–114624. [CrossRef]
20. Ali, M.; Masood, A.; Saleem, M. Microalgae cultivation in wastewater for simultaneous nutrients removal and biomass production. *Int. J. Energy Environ. Eng.* **2021**, *12*, 475–485. [CrossRef]
21. Bhuyar, P.; Trejo, M.; Dussadee, N.; Unpaprom, Y.; Ramaraj, R.; Whangchai, K. Microalgae cultivation in wastewater effluent from tilapia culture pond for enhanced bioethanol production. *Water Sci. Technol.* **2021**, *84*, 2686–2694. [CrossRef] [PubMed]
22. Khalid, A.A.H.; Yaakob, Z.; Abdullah, S.R.S.; Takriff, M.S. Assessing the feasibility of microalgae cultivation in agricultural wastewater: The nutrient characteristics. *Environ. Technol. Innov.* **2019**, *15*, 100402. [CrossRef]
23. de Souza Leite, L.; Hoffmann, M.T.; Daniel, L.A. Coagulation and dissolved air flotation as a harvesting method for microalgae cultivated in wastewater. *J. Water Process Eng.* **2019**, *32*, 100947. [CrossRef]

24. Daneshvar, E.; Zarrinmehr, M.J.; Koutra, E.; Kornaros, M.; Farhadian, O.; Bhatnagar, A. Sequential cultivation of microalgae in raw and recycled dairy wastewater: Microalgal growth, wastewater treatment and biochemical composition. *Bioresour. Technol.* **2019**, *273*, 556–564. [CrossRef]
25. Chaudry, S. Integrating microalgae cultivation with wastewater treatment: A peek into economics. *Appl. Biochem. Biotechnol.* **2021**, *193*, 3395–3406. [CrossRef] [PubMed]
26. Nur, M.M.A.; Buma, A.G. Opportunities and challenges of microalgal cultivation on wastewater, with special focus on palm oil mill effluent and the production of high value compounds. *Waste Biomass Valorization* **2019**, *10*, 2079–2097. [CrossRef]
27. Aron, N.S.M.; Khoo, K.S.; Chew, K.W.; Veeramuthu, A.; Chang, J.S.; Show, P.L. Microalgae cultivation in wastewater and potential processing strategies using solvent and membrane separation technologies. *J. Water Process Eng.* **2021**, *39*, 101701. [CrossRef]
28. Melo, J.M.; Ribeiro, M.R.; Telles, T.S.; Amaral, H.F.; Andrade, D.S. Microalgae cultivation in wastewater from agricultural industries to benefit next generation of bioremediation: A bibliometric analysis. *Environ. Sci. Pollut. Res.* **2022**, *29*, 22708–22720. [CrossRef]
29. Purba, L.D.A.; Susanti, H.; Admirasari, R.; Praharyawan, S.; Iwamoto, K. Bibliometric insights into microalgae cultivation in wastewater: Trends and future prospects for biolipid production and environmental sustainability. *J. Environ. Manag.* **2024**, *352*, 120104. [CrossRef]
30. Fal, S.; Smouni, A.; El Arroussi, H. Integrated microalgae-based biorefinery for wastewater treatment, industrial CO_2 sequestration and microalgal biomass valorization: A circular bioeconomy approach. *Environ. Adv.* **2023**, *12*, 100365. [CrossRef]
31. Zhuang, L.L.; Li, M.; Ngo, H.H. Non-suspended microalgae cultivation for wastewater refinery and biomass production. *Bioresour. Technol.* **2020**, *308*, 123320. [CrossRef] [PubMed]
32. de Souza Leite, L.; Hoffmann, M.T.; Daniel, L.A. Microalgae cultivation for municipal and piggery wastewater treatment in Brazil. *J. Water Process Eng.* **2019**, *31*, 100821. [CrossRef]
33. Garbowski, T.; Pietryka, M.; Pulikowski, K.; Richter, D. The use of a natural substrate for immobilization of microalgae cultivated in wastewater. *Sci. Rep.* **2020**, *10*, 7915. [CrossRef] [PubMed]
34. Vaz, S.A.; Badenes, S.M.; Pinheiro, H.M.; Martins, R.C. Recent reports on domestic wastewater treatment using microalgae cultivation: Towards a circular economy. *Environ. Technol. Innov.* **2023**, *30*, 103107. [CrossRef]
35. Wang, Q.; Wang, X.; Hong, Y.; Liu, X.; Zhao, G.; Zhang, H.; Zhai, Q. Microalgae cultivation in domestic wastewater for wastewater treatment and high value-added production: Species selection and comparison. *Biochem. Eng. J.* **2022**, *185*, 108493. [CrossRef]
36. Han, W.; Jin, W.; Li, Z.; Wei, Y.; He, Z.; Chen, C.; Zhou, X. Cultivation of microalgae for lipid production using municipal wastewater. *Process Saf. Environ. Prot.* **2021**, *155*, 155–165. [CrossRef]
37. Abdelfattah, A.; Ali, S.S.; Ramadan, H.; El-Aswar, E.I.; Eltawab, R.; Ho, S.H.; Sun, J. Microalgae-based wastewater treatment: Mechanisms, challenges, recent advances, and future prospects. *Environ. Sci. Ecotechnol.* **2023**, *13*, 100205. [CrossRef]
38. Prosenc, F.; Piechocka, J.; Škufca, D.; Heath, E.; Bulc, T.G.; Istenič, D.; Buttiglieri, G. Microalgae-based removal of contaminants of emerging concern: Mechanisms in *Chlorella vulgaris* and mixed algal-bacterial cultures. *J. Hazard. Mater.* **2021**, *418*, 126284. [CrossRef]
39. Matamoros, V.; Uggetti, E.; García, J.; Bayona, J.M. Assessment of the mechanisms involved in the removal of emerging contaminants by microalgae from wastewater: A laboratory scale study. *J. Hazard. Mater.* **2016**, *301*, 197–205. [CrossRef]
40. Liu, R.; Li, S.; Tu, Y.; Hao, X. Capabilities and mechanisms of microalgae on removing micropollutants from wastewater: A review. *J. Environ. Manag.* **2021**, *285*, 112149. [CrossRef]
41. Liu, L.; Lin, X.; Luo, L.; Yang, J.; Luo, J.; Liao, X.; Cheng, H. Biosorption of copper ions through microalgae from piggery digestate: Optimization, kinetic, isotherm and mechanism. *J. Clean. Prod.* **2021**, *319*, 128724. [CrossRef]
42. Zhou, J.L.; Yang, L.; Huang, K.X.; Chen, D.Z.; Gao, F. Mechanisms and application of microalgae on removing emerging contaminants from wastewater: A review. *Bioresour. Technol.* **2022**, *364*, 128049. [CrossRef]
43. Yadav, G.; Shanmugam, S.; Sivaramakrishnan, R.; Kumar, D.; Mathimani, T.; Brindhadevi, K.; Rajendran, K. Mechanism and challenges behind algae as a wastewater treatment choice for bioenergy production and beyond. *Fuel* **2021**, *285*, 119093. [CrossRef]
44. Cinq-Mars, M.; Bourdeau, N.; Marchand, P.; Desgagné-Penix, I.; Barnabé, S. Characterization of two microalgae consortia grown in industrial wastewater for biomass valorization. *Algal Res.* **2022**, *62*, 102628. [CrossRef]
45. de Morais, E.G.; da Silveira, J.T.; Schüler, L.M.; de Freitas, B.C.B.; Costa, J.A.V.; de Morais, M.G.; Barreira, L. Biomass valorization via pyrolysis in microalgae-based wastewater treatment: Challenges and opportunities for a circular bioeconomy. *J. Appl. Phycol.* **2023**, *35*, 2689–2708. [CrossRef]
46. Morillas-España, A.; López-Serna, R.; Chikri, L.Y.R.; Jiménez, J.J.; Lafarga, T.; Uggetti, E.; González-López, C.V. Microalgae wastewater treatment: Pharmaceutical removal and biomass valorization. *J. Environ. Manag.* **2025**, *380*, 124942. [CrossRef] [PubMed]
47. Singh, P.K.; Bhattacharjya, R.; Saxena, A.; Mishra, B.; Tiwari, A. Utilization of wastewater as nutrient media and biomass valorization in marine *Chrysophytes-Chaetoceros* and *Isochrysis*. *Energy Convers. Manag. X* **2021**, *10*, 100062.

48. Kumar, N.; Banerjee, C.; Chang, J.S.; Shukla, P. Valorization of wastewater through microalgae as a prospect for generation of biofuel and high-value products. *J. Clean. Prod.* **2022**, *362*, 132114. [CrossRef]
49. Oswald, W.J.; Golueke, C.G. Harvesting and processing of waste-grown microalgae. *Algae Man Environ.* **1968**, *1*, 371–389.
50. Oswald, W.J. Productivity of algae in sewage disposal. *Sol. Energy* **1973**, *15*, 107–117. [CrossRef]
51. Oswald, W.J.; Benemann, J.R. A critical analysis of bioconversion with microalgae. In *Biological Solar Energy Conversion*; Academic Press: New York, NY, USA, 1977; pp. 379–398.
52. Craggs, R. Energy from wastewater treatment. *Water Atmos* **2005**, *13*, 20.
53. Benemann, J.R.; Van Olst, J.C.; Massingill, M.J.; Carlberg, J.A.; Weissman, J.C.; Brune, D.E. The controlled eutrophication process: Using microalgae for CO_2 utilization and agricultural fertilizer recycling. In *Greenhouse Gas Control Technologies—6th International Conference*; Elsevier: Amsterdam, The Netherlands, 2003; pp. 1433–1438.
54. Park, J.B.K.; Craggs, R.J.; Shilton, A.N. Wastewater treatment high rate algal ponds for biofuel production. *Bioresour. Technol.* **2011**, *102*, 35–42. [CrossRef] [PubMed]
55. Pittman, J.K.; Dean, A.P.; Osundeko, O. The potential of sustainable algal biofuel production using wastewater resources. *Bioresour. Technol.* **2011**, *102*, 17–25. [CrossRef] [PubMed]
56. Cho, S.; Luong, T.T.; Lee, D.; Oh, Y.K.; Lee, T. Reuse of effluent water from a municipal wastewater treatment plant in microalgae cultivation for biofuel production. *Bioresour. Technol.* **2011**, *102*, 8639–8645. [CrossRef]
57. Craggs, R.J.; Lundquist, T.J.; Benemann, J.R. Wastewater treatment and algal biofuel production. In *Algae for Biofuels and Energy*; Springer: Dordrecht, The Netherlands, 2012; pp. 153–163.
58. Zhou, W.; Chen, P.; Min, M.; Ma, X.; Wang, J.; Griffith, R.; Ruan, R. Environment-enhancing algal biofuel production using wastewaters. *Renew. Sustain. Energy Rev.* **2014**, *36*, 256–269. [CrossRef]
59. Sutherland, D.L.; Howard-Williams, C.; Turnbull, M.H.; Broady, P.A.; Craggs, R.J. Enhancing microalgal photosynthesis and productivity in wastewater treatment high rate algal ponds for biofuel production. *Bioresour. Technol.* **2015**, *184*, 222–229. [CrossRef]
60. Singh, U.; Tiwari, G.L.; Tandon, R.; Tandon, R. Bioremediation of Heavy Metals Mediated by Cyanobacteria. In *Biodegradation of Toxic and Hazardous Chemicals*; CRC Press: Boca Raton, FL, USA, 2024; pp. 135–147.
61. Goswami, R.K.; Agrawal, K.; Shah, M.P.; Verma, P. Bioremediation of heavy metals from wastewater: A current perspective on microalgae-based future. *Lett. Appl. Microbiol.* **2022**, *75*, 701–717. [CrossRef]
62. Sarma, U.; Hoque, M.E.; Thekkangil, A.; Venkatarayappa, N.; Rajagopal, S. Microalgae in removing heavy metals from wastewater–An advanced green technology for urban wastewater treatment. *J. Hazard. Mater. Adv.* **2024**, *15*, 100444. [CrossRef]
63. Surkatti, R.; Al-Zuhair, S. Microalgae cultivation for phenolic compounds removal. *Environ. Sci. Pollut. Res.* **2018**, *25*, 33936–33956. [CrossRef]
64. Lindner, A.V.; Pleissner, D. Removal of phenolic compounds from olive mill wastewater by microalgae grown under dark and light conditions. *Waste Biomass Valorization* **2022**, *13*, 525–534. [CrossRef]
65. Lindner, A.V.; Pleissner, D. Utilization of phenolic compounds by microalgae. *Algal Res.* **2019**, *42*, 101602. [CrossRef]
66. Goh, P.S.; Lau, W.J.; Ismail, A.F.; Samawati, Z.; Liang, Y.Y.; Kanakaraju, D. Microalgae-enabled wastewater treatment: A sustainable strategy for bioremediation of pesticides. *Water* **2022**, *15*, 70. [CrossRef]
67. Martínez-Burgos, W.J.; Pozzan, R.; da Silva Vale, A.; de Carvalho, J.C.; Iwamoto, H.; de Souza Vandenberghe, L.P.; Soccol, C.R. Bioremediation of Microalgae-Based Pesticides. In *Algae as a Natural Solution for Challenges in Water-Food-Energy Nexus: Toward Carbon Neutrality*; Springer Nature Singapore: Singapore, 2024; pp. 903–929.
68. Castellanos-Estupiñan, M.A.; Carrillo-Botello, A.M.; Rozo-Granados, L.S.; Becerra-Moreno, D.; García-Martínez, J.B.; Urbina-Suarez, N.A.; Zuorro, A. Removal of nutrients and pesticides from agricultural runoff using microalgae and cyanobacteria. *Water* **2022**, *14*, 558. [CrossRef]
69. Premaratne, M.; Nishshanka, G.K.S.H.; Liyanaarachchi, V.C.; Nimarshana, P.H.V.; Ariyadasa, T.U. Bioremediation of textile dye wastewater using microalgae: Current trends and future perspectives. *J. Chem. Technol. Biotechnol.* **2021**, *96*, 3249–3258. [CrossRef]
70. Sudarshan, S.; Harikrishnan, S.; RathiBhuvaneswari, G.; Alamelu, V.; Aanand, S.; Rajasekar, A.; Govarthanan, M. Impact of textile dyes on human health and bioremediation of textile industry effluent using microorganisms: Current status and future prospects. *J. Appl. Microbiol.* **2023**, *134*, lxac064. [CrossRef]
71. Pradhan, D.; Sukla, L.B. Removal of radon from radionuclide-contaminated water using microalgae. In *The Role of Microalgae in Wastewater Treatment*; Springer: Berlin/Heidelberg, Germany, 2019; pp. 75–86.
72. Kim, T.Y.; Hong, J.E.; Park, H.M.; Lee, U.J.; Lee, S.Y. Decontamination of low-level contaminated water from radioactive cesium and cobalt using microalgae. *J. Radioanal. Nucl. Chem.* **2020**, *323*, 903–908. [CrossRef]
73. Ramirez, K.D.R.; Ñañez, K.B.; Gomez, C.L.G.; Moreira, Í.T.A. Efficient PAHs removal and CO_2 fixation by marine microalgae in wastewater using an airlift photobioreactor for biofuel production. *Environ. Res.* **2024**, *261*, 119672. [CrossRef] [PubMed]

74. Zhao, C.; Lu, B.; Wang, Z.; Wei, J.; Zhao, Y.; Wang, S. Enhanced antibiotics and antibiotics resistance genes removal from aquaculture wastewater by microalgae-based system induced with plant hormones. *Int. Biodeterior. Biodegrad.* **2025**, *200*, 106045. [CrossRef]
75. Michelon, W.; Matthiensen, A.; Viancelli, A.; Fongaro, G.; Gressler, V.; Soares, H.M. Removal of veterinary antibiotics in swine wastewater using microalgae-based process. *Environ. Res.* **2022**, *207*, 112192. [CrossRef]
76. Xiong, Q.; Hu, L.X.; Liu, Y.S.; Zhao, J.L.; He, L.Y.; Ying, G.G. Microalgae-based technology for antibiotics removal: From mechanisms to application of innovational hybrid systems. *Environ. Int.* **2021**, *155*, 106594. [CrossRef]
77. Pereira, A.; de Morais, E.G.; Silva, L.; Pena, A.; Freitas, A.; Teixeira, M.R.; Barreira, L. Pharmaceuticals removal from wastewater with microalgae: A pilot study. *Appl. Sci.* **2023**, *13*, 6414. [CrossRef]
78. Mokrani, S.; Houali, K.; Yadav, K.K.; Arabi, A.I.A.; Eltayeb, L.B.; AwjanAlreshidi, M.; Nabti, E.H. Bioremediation techniques for soil organic pollution: Mechanisms, microorganisms, and technologies-A comprehensive review. *Ecol. Eng.* **2024**, *207*, 107338. [CrossRef]
79. Abuhasheesh, Y.; Ghazal, A.; Tang, D.Y.Y.; Banat, F.; Hasan, S.W.; Show, P.L. Advances in *Chlorella* Microalgae for Sustainable Wastewater Treatment and Bioproduction. *Chem. Eng. J. Adv.* **2025**, *22*, 100715. [CrossRef]
80. Prasad, R.; Gupta, S.K.; Shabnam, N.; Oliveira, C.Y.B.; Nema, A.K.; Ansari, F.A.; Bux, F. Role of microalgae in global CO_2 sequestration: Physiological mechanism, recent development, challenges, and future prospective. *Sustainability* **2021**, *13*, 13061. [CrossRef]
81. Reisoglu, Ş.; Aydin, S. Microalgae as a promising candidate for fighting climate change and biodiversity loss. In *Microalgae—Current and Potential Applications*; IntechOpen: Rijeka, Croatia, 2023.
82. Aljabory, M.N.; Alhaboubi, N.A. Green Solutions for CO_2 Mitigation: Exploring Microalgae-Based Carbon Capture and Utilization Technologies. *J. Biotechnol. Res. Cent.* **2025**, *19*, 52–64. [CrossRef]
83. Santos, B.; Freitas, F.; Sobral, A.J.; Encarnação, T. Microalgae and circular economy: Unlocking waste to resource pathways for sustainable development. *Int. J. Sustain. Eng.* **2025**, *18*, 2501488. [CrossRef]
84. Loaiza-González, J.M.; Rubio-Clemente, A.; Peñuela, G.A. Removal of contaminants through microalgae: Towards the development of a circular economy. *Rev. UIS Ing.* **2024**, *23*, 123–132. [CrossRef]
85. Srivastava, N.; Maurya, V.K.; Bee, Z.; Singh, N.; Khare, S.; Singh, S.; Rai, P.K. Green Solutions for a blue planet: Harnessing bioremediation for sustainable development and circular economies. In *Biotechnologies for Wastewater Treatment and Resource Recovery*; Elsevier: Amsterdam, The Netherlands, 2025; pp. 283–296.
86. Singh, S.K.; Shukla, L.; Singh, R.P.; Yadav, P.; Kumar, A. Microalgae mediated wastewater treatment and its production for biofuels and bioproducts. In *Advances in Chemical Pollution, Environmental Management and Protection*; Elsevier: Amsterdam, The Netherlands, 2023; Volume 9, pp. 153–165.
87. Saldarriaga-Hernandez, S.; Hernandez-Vargas, G.; Iqbal, H.M.; Barceló, D.; Parra-Saldívar, R. Bioremediation potential of *Sargassum* sp. biomass to tackle pollution in coastal ecosystems: Circular economy approach. *Sci. Total Environ.* **2020**, *715*, 136978. [CrossRef]
88. Dias, R.R.; Deprá, M.C.; Zepka, L.Q.; Jacob-Lopes, E. Microalgae-Based Bioremediation. *Appl. Water Sci. Remediat. Technol.* **2021**, *2*, 357–380.
89. Mahlangu, D.; Mphahlele, K.; De Paola, F.; Mthombeni, N.H. Microalgae-mediated biosorption for effective heavy metals removal from wastewater: A review. *Water* **2024**, *16*, 718. [CrossRef]
90. He, Z.; Fan, X.; Qu, L.; Zhou, X.; Jin, W.; Hatshan, M.R.; Wang, Q. Cultivation of *Chlorella pyrenoidosa* and *Scenedesmus obliquus* in swine wastewater: Nitrogen and phosphorus removal and microalgal growth. *Process Saf. Environ. Prot.* **2023**, *179*, 887–895. [CrossRef]
91. Acebu, P.I.G.; de Luna, M.D.G.; Chen, C.Y.; Abarca, R.R.M.; Chen, J.H.; Chang, J.S. Bioethanol production from *Chlorella vulgaris* ESP-31 grown in unsterilized swine wastewater. *Bioresour. Technol.* **2022**, *352*, 127086. [CrossRef]
92. Cheng, P.; Chu, R.; Zhang, X.; Song, L.; Chen, D.; Zhou, C.; Ruan, R. Screening of the dominant *Chlorella pyrenoidosa* for biofilm attached culture and feed production while treating swine wastewater. *Bioresour. Technol.* **2020**, *318*, 124054. [CrossRef]
93. Carneiro, M.; Ranglová, K.; Lakatos, G.E.; Manoel, J.A.C.; Grivalský, T.; Kozhan, D.M.; Masojídek, J. Growth and bioactivity of two chlorophyte (*Chlorella* and *Scenedesmus*) strains co-cultured outdoors in two different thin-layer units using municipal wastewater as a nutrient source. *Algal Res.* **2021**, *56*, 102299. [CrossRef]
94. Kisielewska, M.; Zieliński, M.; Dębowski, M.; Kazimierowicz, J.; Romanowska-Duda, Z.; Dudek, M. Effectiveness of *Scenedesmus* sp. biomass grow and nutrients removal from liquid phase of digestates. *Energies* **2020**, *13*, 1432. [CrossRef]
95. Ansari, F.A.; Hassan, H.; Gani, K.M.; Rawat, I.; Gupta, S.K.; Bux, F. Influence of nitrogen sources on growth and biochemical composition of *Chlorella sorokiniana*. *Biomass Bioenergy* **2025**, *197*, 107832. [CrossRef]
96. Guo, C.; Chen, J.; Ma, Y.; Lin, S.; Dong, R.; Ruan, R.; Liu, S. Enhanced Tolerance and Growth of *Chlorella vulgaris* and *Scenedesmus quadricauda* in Anaerobic Digestate Food Waste Effluent. *Appl. Biochem. Biotechnol.* **2025**, *197*, 4131–4156. [CrossRef]

97. Singh, V.P.; Godara, P.; Srivastava, A. Sustainable Microalgal Bioremediation of Heavy Metals and Dyes from Synthetic Wastewater: Progressing Towards United Nations Sustainable Development Goals. *Waste Manag. Bull.* **2024**, *2*, 123–135. [CrossRef]
98. Abd El-Reheem Mohammed, A.; Muhammad, S.S.; Mohamed, H.A.; El-Agamy, H.H. Potentiality of *Spirulina platensis* in zirconium ions biosorption and removal from aqueous solution as an eco-friendly process. *Sep. Sci. Technol.* **2025**, *60*, 1101–1112. [CrossRef]
99. Osuna Barreto, M.P. Remediación de Suelos Contaminados con Cadmio a Partir de Mezclas de Enmiendas-*Spirulina platensis*. Diploma Thesis, Universidad de los Andes, Santiago, Chile, 2024.
100. Nakarmi, K.J.; Daneshvar, E.; Mänttäri, M.; Bhatnagar, A. Removal and recovery of nutrients from septic tank wastewater using microalgae: Key factors and practical implications. *J. Environ. Manag.* **2023**, *345*, 118922. [CrossRef]
101. López-Rosales, L.; López-García, P.; Benyachou, M.A.; Molina-Miras, A.; Gallardo-Rodríguez, J.J.; Cerón-García, M.C.; García-Camacho, F. Treatment of secondary urban wastewater with a low ammonium-tolerant marine microalga using zeolite-based adsorption. *Bioresour. Technol.* **2022**, *359*, 127490. [CrossRef]
102. Aguiar Severo, I.; Azevedo, O.G.D.A.; da Silva, P.A.S.; Jacob-Furlan, B.; Mariano, A.B.; Ordonez, J.C.; Vargas, J.V.C. Wastewater treatment process using immobilized microalgae. *Water Sci. Technol.* **2024**, *90*, 1306–1320. [CrossRef]
103. Liu, Z.; Gao, Z.; Lu, X. Advanced treatment of pharmaceutical wastewater with a combined Fe-C micro-electrolysis/EGSB system assisted by microalgae. *Sep. Sci. Technol.* **2021**, *56*, 2826–2837. [CrossRef]
104. Nunes, N.S.P.; de Almeida, J.M.O.; Fonseca, G.G.; de Carvalho, E.M. Clarification of sugarcane (*Saccharum officinarum*) vinasse for microalgae cultivation. *Bioresour. Technol. Rep.* **2022**, *19*, 101125.
105. Svierzoski, N.D.S.; Matheus, M.C.; Bassin, J.P.; Brito, Y.D.; Mahler, C.F.; Webler, A.D. Treatment of a slaughterhouse wastewater by anoxic–aerobic biological reactors followed by UV-C disinfection and microalgae bioremediation. *Water Environ. Res.* **2021**, *93*, 409–420. [CrossRef]
106. Nagi, M.; He, M.; Li, D.; Gebreluel, T.; Cheng, B.; Wang, C. Utilization of tannery wastewater for biofuel production: New insights on microalgae growth and biomass production. *Sci. Rep.* **2020**, *10*, 1530. [CrossRef]
107. Morillas-España, A.; Lafarga, T.; Acién-Fernández, F.G.; Gómez-Serrano, C.; González-López, C.V. Annual production of microalgae in wastewater using pilot-scale thin-layer cascade photobioreactors. *J. Appl. Phycol.* **2021**, *33*, 3861–3871. [CrossRef]
108. Abraham, J.; Abimbola, T.; Braida, W.J.; Terracciano, A.; Su, T.L.; Christodoulatos, C.; Lawal, A. On-site pilot-scale microalgae cultivation using industrial wastewater for bioenergy production: A case study towards circular bioeconomy. *Bioengineering* **2023**, *10*, 1339. [CrossRef]
109. Fernández, F.A.; Sevilla, J.M.F.; Grima, E.M. Costs analysis of microalgae production. In *Biofuels from Algae*; Elsevier: Amsterdam, The Netherlands, 2019; pp. 551–566.
110. Rafa, N.; Ahmed, S.F.; Badruddin, I.A.; Mofijur, R.M.; Kamangar, S. Strategies to produce cost-effective third-generation biofuel from microalgae. *Front. Energy Res.* **2021**, *9*, 749968. [CrossRef]
111. Matamoros, V.; Gutiérrez, R.; Ferrer, I.; García, J.; Bayona, J.M. Capability of microalgae-based wastewater treatment systems to remove emerging organic contaminants: A pilot-scale study. *J. Hazard. Mater.* **2015**, *288*, 34–42. [CrossRef]
112. Ovis-Sánchez, J.O.; Perera-Pérez, V.D.; Buitrón, G.; Quintela-Baluja, M.; Graham, D.W.; Morales-Espinosa, R.; Carrillo-Reyes, J. Exploring resistomes and microbiomes in pilot-scale microalgae-bacteria wastewater treatment systems for use in low-resource settings. *Sci. Total Environ.* **2023**, *882*, 163545. [CrossRef]
113. Goswami, R.K.; Mehariya, S.; Verma, P. Sub-pilot scale sequential microalgal consortium-based cultivation for treatment of municipal wastewater and biomass production. *Environ. Pollut.* **2024**, *348*, 123796. [CrossRef]
114. Yu, Z.; Hou, Q.; Liu, M.; Xie, Z.; Ma, M.; Chen, H.; Pei, H. From lab to application: Cultivating limnetic microalgae in seawater coupled with wastewater for biodiesel production on a pilot scale. *Water Res.* **2023**, *229*, 119471. [CrossRef]
115. Rossi, S.; Pizzera, A.; Bellucci, M.; Marazzi, F.; Mezzanotte, V.; Parati, K.; Ficara, E. Piggery wastewater treatment with algae-bacteria consortia: Pilot-scale validation and techno-economic evaluation at farm level. *Bioresour. Technol.* **2022**, *351*, 127051. [CrossRef]
116. Mantovani, M.; Marazzi, F.; Fornaroli, R.; Bellucci, M.; Ficara, E.; Mezzanotte, V. Outdoor pilot-scale raceway as a microalgae-bacteria sidestream treatment in a WWTP. *Sci. Total Environ.* **2020**, *710*, 135583. [CrossRef]
117. Morillas-España, A.; Lafarga, T.; Sánchez-Zurano, A.; Acién-Fernández, F.G.; Rodríguez-Miranda, E.; Gómez-Serrano, C.; González-López, C.V. Year-long evaluation of microalgae production in wastewater using pilot-scale raceway photobioreactors: Assessment of biomass productivity and nutrient recovery capacity. *Algal Res.* **2021**, *60*, 102500. [CrossRef]
118. Dalvi, V.; Chawla, P.; Malik, A. Year-long performance assessment of an on-site pilot scale (100 L) photobioreactor on nutrient recovery and pathogen removal from urban wastewater using native microalgal consortium. *Algal Res.* **2021**, *55*, 102228. [CrossRef]
119. Hussain, F.; Shah, S.Z.; Ahmad, H.; Abubshait, S.A.; Abubshait, H.A.; Laref, A.; Iqbal, M. Microalgae an ecofriendly and sustainable wastewater treatment option: Biomass application in biofuel and bio-fertilizer production. A review. *Renew. Sustain. Energy Rev.* **2021**, *137*, 110603. [CrossRef]

120. Molinuevo-Salces, B.; Riaño, B.; Hernández, D.; Cruz García-González, M. Microalgae and wastewater treatment: Advantages and disadvantages. In *Microalgae Biotechnology for Development of Biofuel and Wastewater Treatment*; Springer: Berlin/Heidelberg, Germany, 2019; pp. 505–533.
121. Li, K.; Liu, Q.; Fang, F.; Luo, R.; Lu, Q.; Zhou, W.; Ruan, R. Microalgae-based wastewater treatment for nutrients recovery: A review. *Bioresour. Technol.* **2019**, *291*, 121934. [CrossRef]
122. Chai, W.S.; Tan, W.G.; Munawaroh, H.S.H.; Gupta, V.K.; Ho, S.H.; Show, P.L. Multifaceted roles of microalgae in the application of wastewater biotreatment: A review. *Environ. Pollut.* **2021**, *269*, 116236. [CrossRef]
123. Do, C.V.T.; Pham, M.H.T.; Pham, T.Y.T.; Dinh, C.T.; Bui, T.U.T.; Tran, T.D.; Nguyen, V.T. Microalgae and bioremediation of domestic wastewater. *Curr. Opin. Green Sustain. Chem.* **2022**, *34*, 100595. [CrossRef]
124. Li, L.; Gao, K.; Yang, M.; Zheng, Q.; Zhang, M.; Deng, X. Challenges and potential solutions of microalgae-based systems for wastewater treatment and resource recovery. *Front. Bioeng. Biotechnol.* **2023**, *11*, 1210228. [CrossRef]
125. Priya, A.K.; Jalil, A.A.; Vadivel, S.; Dutta, K.; Rajendran, S.; Fujii, M.; Soto-Moscoso, M. Heavy metal remediation from wastewater using microalgae: Recent advances and future trends. *Chemosphere* **2022**, *305*, 135375. [CrossRef]
126. All-Gas. A Major Step Forward Towards Sustainability. Available online: https://www.all-gas.eu/ (accessed on 14 April 2025).
127. Valchev, D.; Ribarova, I. A review on the reliability and the readiness level of microalgae-based nutrient recovery technologies for secondary treated effluent in municipal wastewater treatment plants. *Processes* **2022**, *10*, 399. [CrossRef]
128. Rahman, A.; Pan, S.; Houston, C.; Selvaratnam, T. Evaluation of *Galdieria sulphuraria* and *Chlorella vulgaris* for the Bioremediation of Produced Water. *Water* **2021**, *13*, 1183. [CrossRef]
129. Sudhanthiran, M.C.; Perumalsamy, M. Bioremediation of dairy industry wastewater and assessment of nutrient removal potential of *Chlorella vulgaris*. *Biomass Convers. Biorefinery* **2024**, *14*, 10335–10346.
130. Amaya-Santos, G.; Ruiz-Nieto, Á.; Sánchez-Zurano, A.; Ciardi, M.; Gómez-Serrano, C.; Acién, G.; Lafarga, T. Production of *Chlorella vulgaris* using urban wastewater: Assessment of the nutrient recovery capacity of the biomass and its plant biostimulant effects. *J. Appl. Phycol.* **2022**, *34*, 2971–2979. [CrossRef]
131. Li, F.; Amenorfenyo, D.K.; Zhang, Y.; Zhang, N.; Li, C.; Huang, X. Cultivation of *Chlorella vulgaris* in membrane-treated industrial distillery wastewater: Growth and wastewater treatment. *Front. Environ. Sci.* **2021**, *9*, 770633. [CrossRef]
132. Molazadeh, M.; Ahmadzadeh, H.; Pourianfar, H.R.; Lyon, S.; Rampelotto, P.H. The use of microalgae for coupling wastewater treatment with CO_2 biofixation. *Front. Bioeng. Biotechnol.* **2019**, *7*, 42. [CrossRef]
133. You, X.; Yang, L.; Zhou, X.; Zhang, Y. Sustainability and carbon neutrality trends for microalgae-based wastewater treatment: A review. *Environ. Res.* **2022**, *209*, 112860. [CrossRef] [PubMed]
134. Aravantinou, A.F.; Barkonikou, E.F.; Manariotis, I.D. Microalgae biomass and lipid production using primary treated wastewater. *Desalination Water Treat.* **2017**, *91*, 228–234. [CrossRef]
135. Acién, F.G.; Fernández, J.M.; Magán, J.J.; Molina, E. Production cost of a real microalgae production plant and strategies to reduce it. *Biotechnol. Adv.* **2012**, *30*, 1344–1353. [CrossRef]
136. Norsker, N.H.; Barbosa, M.J.; Vermuë, M.H.; Wijffels, R.H. Microalgal production—A close look at the economics. *Biotechnol. Adv.* **2011**, *29*, 24–27. [CrossRef] [PubMed]
137. Gouveia, L.; Graça, S.; Sousa, C.; Ambrosano, L.; Ribeiro, B.; Botrel, E.P.; Silva, C.M. Microalgae biomass production using wastewater: Treatment and costs: Scale-up considerations. *Algal Res.* **2016**, *16*, 167–176. [CrossRef]
138. Pajares, E.M.; Valero, L.G.; Sánchez, I.M.R. Cost of urban wastewater treatment and ecotaxes: Evidence from municipalities in southern Europe. *Water* **2019**, *11*, 423. [CrossRef]
139. Suwanu Europe. Available online: https://suwanu-europe.eu/project/dam-recharge-irrigation-municipal/ (accessed on 14 April 2025).
140. Liu, X.Y.; Hong, Y. Microalgae-based wastewater treatment and recovery with biomass and value-added products: A brief review. *Curr. Pollut. Rep.* **2021**, *7*, 227–245. [CrossRef]
141. Bhatt, A.; Prajapati, S.K.; Arora, P. Assessing algae-based wastewater treatment—A life cycle assessment approach. In *Clean Energy and Resource Recovery*; Elsevier: Amsterdam, The Netherlands, 2022; pp. 137–154.
142. Sangma, C.B.; Chalie-u, R. Life cycle assessment of wastewater treatment by microalgae. In *Valorization of Microalgal Biomass and Wastewater Treatment*; Elsevier: Amsterdam, The Netherlands, 2023; pp. 137–178.
143. Jacob-Lopes, E.; Zepka, L.Q.; Deprá, M.C. *Sustainability Metrics and Indicators of Environmental Impact: Industrial and Agricultural Life Cycle Assessmen*; Elsevier: Amsterdam, The Netherlands, 2021.
144. Gurreri, L.; Rindina, M.C.; Luciano, A.; Lima, S.; Scargiali, F.; Fino, D.; Mancini, G. Environmental sustainability of microalgae-based production systems: Roadmap and challenges towards the industrial implementation. *Sustain. Chem. Pharm.* **2023**, *35*, 101191. [CrossRef]
145. Togarcheti, S.C.; kumar Mediboyina, M.; Chauhan, V.S.; Mukherji, S.; Ravi, S.; Mudliar, S.N. Life cycle assessment of microalgae based biodiesel production to evaluate the impact of biomass productivity and energy source. *Resour. Conserv. Recycl.* **2017**, *122*, 286–294. [CrossRef]

146. Porcelli, R.; Dotto, F.; Pezzolesi, L.; Marazza, D.; Greggio, N.; Righi, S. Comparative life cycle assessment of microalgae cultivation for non-energy purposes using different carbon dioxide sources. *Sci. Total Environ.* **2020**, *721*, 137714. [CrossRef]
147. Ferreira, J.; de Assis, L.R.; de Sousa Oliveira, A.P.; de Siqueira Castro, J.; Calijuri, M.L. Innovative microalgae biomass harvesting methods: Technical feasibility and life cycle analysis. *Sci. Total Environ.* **2020**, *746*, 140939. [CrossRef]
148. Yaashikaa, P.R.; Devi, M.K.; Kumar, P.S.; Pandian, E. A review on biodiesel production by algal biomass: Outlook on lifecycle assessment and techno-economic analysis. *Fuel* **2022**, *324*, 124774. [CrossRef]
149. Pechsiri, J.S.; Thomas, J.B.E.; El Bahraoui, N.; Fernandez, F.G.A.; Chaouki, J.; Chidami, S.; Gröndahl, F. Comparative life cycle assessment of conventional and novel microalgae production systems and environmental impact mitigation in urban-industrial symbiosis. *Sci. Total Environ.* **2023**, *854*, 158445. [CrossRef]
150. Santurbano, V.; Marangon, B.; Castro, J.; Calijuri, M.L.; Leme, M.; Assemany, P. Enhancing environmental performance in biogas production from wastewater-grown microalgae: A life cycle assessment perspective. *J. Environ. Manag.* **2024**, *362*, 121251. [CrossRef]
151. D'Imporzano, G.; Veronesi, D.; Salati, S.; Adani, F. Carbon and nutrient recovery in the cultivation of *Chlorella vulgaris*: A life cycle assessment approach to comparing environmental performance. *J. Clean. Prod.* **2018**, *194*, 685–694. [CrossRef]
152. Magalhães, I.B.; Ferreira, J.; de Siqueira Castro, J.; de Assis, L.R.; Calijuri, M.L. Technologies for improving microalgae biomass production coupled to effluent treatment: A life cycle approach. *Algal Res.* **2021**, *57*, 102346. [CrossRef]
153. Song, Y.; Wang, L.; Qiang, X.; Gu, W.; Ma, Z.; Wang, G. The promising way to treat wastewater by microalgae: Approaches, mechanisms, applications and challenges. *J. Water Process Eng.* **2022**, *49*, 103012. [CrossRef]
154. Dasan, Y.K.; Lam, M.K.; Yusup, S.; Lim, J.W.; Lee, K.T. Life cycle evaluation of microalgae biofuels production: Effect of cultivation system on energy, carbon emission and cost balance analysis. *Sci. Total Environ.* **2019**, *688*, 112–128. [CrossRef]
155. Gurreri, L.; Rindina, M.C.; Luciano, A.; Falqui, L.; Fino, D.; Mancini, G. Microalgae production in an industrial-scale photobioreactors plant: A comprehensive Life Cycle assessment. *Sustain. Chem. Pharm.* **2024**, *39*, 101598. [CrossRef]
156. Zuorro, A.; García-Martínez, J.B.; Barajas-Solano, A.F.; Rodríguez-Lizcano, A.; Kafarov, V. Environmental Footprint of Inland Fisheries: Integrating LCA Analysis to Assess the Potential of Wastewater-Based Microalga Cultivation as a Promising Solution for Animal Feed Production. *Processes* **2023**, *11*, 3255. [CrossRef]
157. Ferreira, J.; Braga, M.Q.; da Gama, R.C.N.; Magalhães, I.B.; Marangon, B.B.; de Siqueira Castro, J.; Calijuri, M.L. Carotenoids from wastewater-grown microalgae biomass: Life cycle assessment and techno-economical analysis. *J. Clean. Prod.* **2024**, *434*, 140526. [CrossRef]
158. Arashiro, L.T.; Montero, N.; Ferrer, I.; Acién, F.G.; Gómez, C.; Garfí, M. Life cycle assessment of high rate algal ponds for wastewater treatment and resource recovery. *Sci. Total Environ.* **2018**, *622*, 1118–1130. [CrossRef] [PubMed]
159. Magalhães, I.B.; Ferreira, J.; de Siqueira Castro, J.; de Assis, L.R.; Calijuri, M.L. Agro-industrial wastewater-grown microalgae: A techno-environmental assessment of open and closed systems. *Sci. Total Environ.* **2022**, *834*, 155282. [CrossRef]
160. Abu-Ghosh, S.; Fixler, D.; Dubinsky, Z.; Iluz, D. Energy-input analysis of the life-cycle of microalgal cultivation systems and best scenario for oil-rich biomass production. *Appl. Energy* **2015**, *154*, 1082–1088. [CrossRef]
161. Pérez-López, P.; De Vree, J.H.; Feijoo, G.; Bosma, R.; Barbosa, M.J.; Moreira, M.T.; Kleinegris, D.M. Comparative life cycle assessment of real pilot reactors for microalgae cultivation in different seasons. *Appl. Energy* **2017**, *205*, 1151–1164. [CrossRef]
162. Lopes, A.C.; Valente, A.; Iribarren, D.; González-Fernández, C. Energy balance and life cycle assessment of a microalgae-based wastewater treatment plant: A focus on alternative biogas uses. *Bioresour. Technol.* **2018**, *270*, 138–146. [CrossRef]
163. Arbour, A.J.; Bhatt, P.; Simsek, H.; Brown, P.B.; Huang, J.Y. Life cycle assessment on environmental feasibility of microalgae-based wastewater treatment for shrimp recirculating aquaculture systems. *Bioresour. Technol.* **2024**, *399*, 130578. [CrossRef]
164. Dias, R.R.; Deprá, M.C.; Severo, I.A.; Zepka, L.Q.; Jacob-Lopes, E. Smart override of the energy matrix in commercial microalgae facilities: A transition path to a low-carbon bioeconomy. *Sustain. Energy Technol. Assess.* **2022**, *52*, 102073. [CrossRef]
165. Morales, M.; Hélias, A.; Bernard, O. Optimal integration of microalgae production with photovoltaic panels: Environmental impacts and energy balance. *Biotechnol. Biofuels* **2019**, *12*, 1–17. [CrossRef]
166. Sandoval, D.P. Environmental Impact Extrapolation of Environmental Processes at Low Technology Readiness Level (TRL): Application to Microalgae-Based Processes. Ph.D. Dissertation, Université Côte d'Azur, Nice, France, 2024.
167. Lanjekar, P.R.; Panwar, N.L. A review on hydrogen production from biomass and commercialization assessment through technology readiness levels (TRLs). *BioEnergy Res.* **2024**, *17*, 912–931. [CrossRef]
168. Petrini, S.; Foladori, P.; Andreottola, G. Laboratory-scale investigation on the role of microalgae towards a sustainable treatment of real municipal wastewater. *Water Sci. Technol.* **2018**, *78*, 1726–1732. [CrossRef]
169. Krishnamoorthy, S.; Manickam, P.; Muthukaruppan, V. Evaluation of distillery wastewater treatability in a customized photobioreactor using blue-green microalgae–Laboratory and outdoor study. *J. Environ. Manag.* **2019**, *234*, 412–423. [CrossRef] [PubMed]
170. Moondra, N.; Jariwala, N.D.; Christian, R.A. Microalgae based wastewater treatment: A shifting paradigm for the developing nations. *Int. J. Phytoremediation* **2021**, *23*, 765–771. [CrossRef]

171. Xu, K.; Zou, X.; Xue, Y.; Qu, Y.; Li, Y. The impact of seasonal variations about temperature and photoperiod on the treatment of municipal wastewater by algae-bacteria system in lab-scale. *Algal Res.* **2021**, *54*, 102175. [CrossRef]
172. Azam, R.; Kothari, R.; Singh, H.M.; Ahmad, S.; Sari, A.; Tyagi, V.V. Cultivation of two *Chlorella* species in open sewage contaminated channel wastewater for biomass and biochemical profiles: Comparative lab-scale approach. *J. Biotechnol.* **2022**, *344*, 24–31. [CrossRef]
173. Noshadi, M.; Nouripour, R. Urban wastewater treatment by microalgae, bacteria and microalgae–bacteria system (Laboratory-scale study). *Urban Water J.* **2022**, *19*, 161–172. [CrossRef]
174. Moondra, N.; Jariwala, N.; Christian, R. Impact of Microalgae in Domestic Wastewater Treatment: A Lab-Scale Experimental Study. *Pollution* **2023**, *9*, 211–221.
175. Blanco-Vieites, M.; Álvarez-Gil, M.; Delgado, F.; García-Ruesgas, L.; Rodríguez, E. Livestock wastewater bioremediation through indigenous microalgae culturing as a circular bioeconomy approach as cattle feed. *Algal Res.* **2024**, *78*, 103424. [CrossRef]
176. Deprá, M.C.; Dias, R.R.; Zepka, L.Q.; Jacob-Lopes, E. Tackling Old Challenges in Microalgal Biotechnology: The Role of Photobioreactors to Advance the Technology Readiness Level. *Processes* **2024**, *13*, 51. [CrossRef]
177. Liberti, D.; Pinheiro, F.; Simões, B.; Varela, J.; Barreira, L. Beyond bioremediation: The untapped potential of microalgae in wastewater treatment. *Water* **2024**, *16*, 2710. [CrossRef]
178. Bhujade, R.; Chidambaram, M.; Kumar, A.; Sapre, A. Algae to economically viable low-carbon-footprint oil. *Annu. Rev. Chem. Biomol. Eng.* **2017**, *8*, 335–357. [CrossRef]
179. Blanco-Vieites, M.; Casado, V.; Battez, A.H.; Rodríguez, E. Culturing *Arthrospira maxima* in mining wastewater: Pilot-scale culturing and biomass valorisation into C-phycocyanin and crude lipid extract. *Environ. Technol. Innov.* **2023**, *29*, 102978. [CrossRef]
180. Mohit, A.; Mishel, V.K.; Remya, N. Life cycle assessment and technoeconomic analysis of biofuels produced from polyculture microalgae cultivated in greywater. *J. Environ. Manag.* **2024**, *356*, 120711. [CrossRef]
181. Gondi, R.; Kavitha, S.; Kannah, R.Y.; Kumar, G.; Banu, J.R. Wastewater based microalgae valorization for biofuel and value-added products recovery. *Sustain. Energy Technol. Assess.* **2022**, *53*, 102443. [CrossRef]
182. Al Ketife, A.M.; Almomani, F.; Muftah, E.N.; Judd, S. A technoeconomic assessment of microalgal culture technology implementation for combined wastewater treatment and CO_2 mitigation in the Arabian Gulf. *Process Saf. Environ. Prot.* **2019**, *127*, 90–102. [CrossRef]
183. Arashiro, L.T.; Josa, I.; Ferrer, I.; Van Hulle, S.W.; Rousseau, D.P.; Garfí, M. Life cycle assessment of microalgae systems for wastewater treatment and bioproducts recovery: Natural pigments, biofertilizer and biogas. *Sci. Total Environ.* **2022**, *847*, 157615. [CrossRef]
184. Verdelho Vieira, V.; Cadoret, J.P.; Acien, F.G.; Benemann, J. Clarification of most relevant concepts related to the microalgae production sector. *Processes* **2022**, *10*, 175. [CrossRef]
185. De Francisci, D.; Su, Y.; Iital, A.; Angelidaki, I. Evaluation of microalgae production coupled with wastewater treatment. *Environ. Technol.* **2018**, *39*, 581–592. [CrossRef] [PubMed]
186. Zheng, Q.; Ning, R.; Zhang, M.; Deng, X. Biofuel production as a promising way to utilize microalgae biomass derived from wastewater: Progress, technical barriers, and potential solutions. *Front. Bioeng. Biotechnol.* **2023**, *11*, 1250407. [CrossRef] [PubMed]

Disclaimer/Publisher's Note: The statements, opinions and data contained in all publications are solely those of the individual author(s) and contributor(s) and not of MDPI and/or the editor(s). MDPI and/or the editor(s) disclaim responsibility for any injury to people or property resulting from any ideas, methods, instructions or products referred to in the content.

foods

MDPI

Article

The Cecal Distribution of Microalgal Pigments in Rats: Do Carotenoids and Chlorophylls Play a Pharmacobiotic Role?

Tatiele Casagrande do Nascimento [1], Patrícia Acosta Caetano [1], Marcylene Vieira da Silveira [2], Luiz Eduardo Lobo [1], Uashington Da Silva Riste [1], Mariany Costa Deprá [1], Maria Rosa Chitolina Schetinger [2], Cristiano Ragagnin de Menezes [1], Roger Wagner [1], Eduardo Jacob-Lopes [1] and Leila Queiroz Zepka [1,*]

[1] Food Science and Technology Department, Federal University of Santa Maria, Santa Santa Maria 97105-900, RS, Brazil; tatielecasagrande@gmail.com (T.C.d.N.); pati.caetano98@gmail.com (P.A.C.); uashington03@gmail.com (U.D.S.R.); rogerwag@gmail.com (R.W.)
[2] Department of Biochemistry and Molecular Biology, Federal University of Santa Maria, Santa Maria 97105-900, RS, Brazil
* Correspondence: zepkaleila@yahoo.com.br; Tel.: +55-55-3220-8822

Abstract

This study investigated the cecal distribution of lipophilic pigments (carotenoids and chlorophylls) from *Scenedesmus obliquus* and their effects on the activity of the intestinal microbiota in rats. Oleoresins containing different concentrations of microalgal pigments (from 0 to 600 μg·kg^{-1}bw·d^{-1}), previously characterized by chromatographic and spectrometric analyses, were administered for four weeks. At the end of the intervention, cecal content samples were collected and analyzed for their pigment composition, short-chain fatty acids (SCFAs), and probiotic microbiota. Nine pigments were identified in the cecal samples, with all-*trans*-zeaxanthin and pheophytin being the most abundant in all groups. Furthermore, 15-*cis*-lutein, all-*trans*-β-cryptoxanthin, and 9-*cis*-β-carotene—found exclusively in microalgal oleoresin—were detected only in animals receiving doses above 300 μg·kg^{-1}bw.day^{-1}, indicating a link with the SCFA modulation. These supplementations significantly increased the levels of acetate (300 and 450 μg·kg^{-1}bw·d^{-1} −13% and 14%), butyrate (300 μg kg^{-1}bw·d^{-1} −19%), and propionate (600 μg·kg^{-1}bw·d^{-1} −16%). Notably, 300 μg·kg^{-1}bw·d^{-1} significantly increased *Bifidobacterium* and *Lactobacillus* populations. Overall, the pigment supplementation positively influenced the gut microbiota composition and SCFA production in a dose-dependent manner, particularly at 300 μg·kg^{-1}bw·d^{-1}. These results support the potential application of microalgal pigments as functional food ingredients or supplements with gut health benefits.

Keywords: bioactive pigments; gut microbiota; oleoresin supplementation; *Scenedesmus obliquus*; short-chain fatty acids

check for updates

Academic Editor: Bin Zhang

Received: 14 May 2025
Revised: 17 June 2025
Accepted: 19 June 2025
Published: 21 June 2025

Citation: Nascimento, T.C.d.; Caetano, P.A.; da Silveira, M.V.; Lobo, L.E.; Riste, U.D.S.; Deprá, M.C.; Schetinger, M.R.C.; de Menezes, C.R.; Wagner, R.; Jacob-Lopes, E.; et al. The Cecal Distribution of Microalgal Pigments in Rats: Do Carotenoids and Chlorophylls Play a Pharmacobiotic Role? *Foods* **2025**, *14*, 2172. https://doi.org/10.3390/foods14132172

Copyright: © 2025 by the authors. Licensee MDPI, Basel, Switzerland. This article is an open access article distributed under the terms and conditions of the Creative Commons Attribution (CC BY) license (https://creativecommons.org/licenses/by/4.0/).

1. Introduction

The gut microbiota is a central component of the intestinal ecosystem and fulfills critical functions in maintaining human well-being, including the protection against pathogenic microorganisms, modulation of the immune system, metabolic regulation, and absorption of nutrients and drugs. Imbalances in the gut microbiota are associated with a variety of gastrointestinal disorders. This microbial community can be affected by several variables, including the intake of compounds initially labeled as prebiotics, which are known to contribute to intestinal health maintenance [1,2].

However, the traditional definition of prebiotics—as indigestible food ingredients that support the host by specifically promoting the proliferation or function of specific bacteria—has recently been revised. The updated concept broadens the scope to include any fermentable compound capable of selectively promoting beneficial microorganisms within the gut microbiota, resulting in positive health outcomes. In this context, the term "pharmacobiotics" emerged to describe substances with therapeutic potential mediated by the modulation of the intestinal microbiota [3].

Non-digestible carbohydrates are the most extensively studied compounds in this field. However, bioactive phytochemicals such as carotenoids and chlorophylls—well known for their antioxidant properties—have been modestly explored regarding their potential role in promoting intestinal homeostasis [4–6].

Within this framework, microalgae such as *Scenedesmus obliquus*, rich in carotenoids and chlorophylls, stand out as promising functional sources of these compounds, particularly due to their demonstrated bioaccessibility, bioavailability, and bioactivity in oleoresin matrices, as shown in both in vitro and in vivo assays [7–9]. Nevertheless, studies evaluating the contribution of microalgae to gut health remain scarce and are largely limited to in vitro models or the use of the whole biomass [10,11].

Short-chain fatty acids (SCFAs), such as acetic, propionic, and butyric acids, are the main metabolic products of the intestinal microbiota—especially *Bifidobacterium* and *Lactobacillus*—and have been shown to support glucose and lipid metabolism, energy expenditure, and the regulation of immune responses and inflammation [12]. Consequently, SCFA levels serve as important markers of intestinal ecosystem health. However, no reports link the microalgal pigment intake to SCFA production. Specific activities on the levels of these cecal microbiota metabolites make the cecum a more optimized sampling site for determining environmental/dietary effects on the microbiota [13,14]

Given this background, the current research sought to examine the cecal distribution of microalgal carotenoids and chlorophylls in rats following a supplementation with oleoresin containing different concentrations of these pigments. Additionally, this study sought to evaluate their potential association with changes in the gut microbiota composition and SCFA production. This work contributes to addressing a knowledge gap regarding the uncertain ability of microalgal carotenoids and chlorophylls to exert direct "pharmacobiotic" effects.

2. Materials and Methods

2.1. Chemicals

All chemical compounds used for the BG-11 medium, sodium chloride, ammonium acetate (98%), tetrabutylammonium acetate, and all solvents for extraction and chromatography analysis were purchased from Sigma-Aldrich Chemical Co. (St. Louis, MO, USA). The standards all-*trans*-β-carotene, all-*trans*-lutein, and chlorophyll a (with purities ranging from 95.0% to 99.9%) were purchased from Sigma-Aldrich (Darmstadt, Germany).

2.2. Microalgal Strain and Biomass Production

The *S. obliquus* (CPCC05) strain was utilized for the production of whole-cell dried powder in a hybrid photobioreactor model, with the setup details, operating parameters, and downstream procedures previously outlined by Deprá et al. [15]. The biomass was isolated from the cultivation medium through centrifugation (Hitachi, Tokyo, Japan) at 1500× *g* for 10 min. The supernatant was discarded, and the remaining biomass was frozen at −18 °C for 24 h. Subsequently, it was freeze-dried for 24 h at −50 °C under a pressure below −175 µm Hg and then stored under refrigeration until further analysis.

2.3. Microalgal Pigments Extraction

The microalgal biomass (10 mg) was exhaustively extracted with 50 mL of dimethylformamide (DMF) saturated with magnesium carbonate (Mg_2CO_3). Afterward, the remaining biomass was re-extracted with 50 mL of methanol to exhaustion again. The obtained pigment extracts were mixed with 100 mL of diethyl ether and 400 mL of a 10% (*w*/*v*) sodium chloride solution (NaCl) in a separation funnel. The mixture was agitated and subsequently allowed to stand until the organic phase had fully separated. Then, the solvent phase was rinsed three times using 400 mL of a 10% NaCl solution (*w*/*v*). In sequence, pigments were transferred to diethyl ether and NaCl, and the above protocol was applied. The extracts were concentrated in a rotary evaporator under vacuum at 30 °C to dryness, and the dry residue was dissolved in the mobile phase for immediate HPLC analysis.

2.4. HPLC-PDA-MS/MS Pigments Analysis

The pigments were evaluated using high-performance liquid chromatography (HPLC) (Shimadzu, Kyoto, Japan) equipped with binary pumps (model LC-20AD), an inline degasser, and an automated sample injector (Rheodyne, Rohnert Park, CA, USA). The chromatographic system, featuring a photodiode array detector (PDA) (model SPD-M20A), was coupled in series to an atmospheric pressure chemical ionization (APCI) source (Shimadzu America, Columbia, MD, USA) and a Shimadzu 8040 triple quadrupole mass spectrometer. The pigments separation was performed on a C30 YMC column (5 µm, 250 × 4.6 mm) (Waters, Wilmington, DE, USA). HPLC-PDA analysis was performed in accordance with Rodrigues et al. [15]. Prior to HPLC-PDA analysis, the carotenoid extract was dissolved in a methanol (MeOH) and methyl tert-butyl ether (MTBE) solution at a 70:30 (*v*/*v*) ratio and filtered through Millipore membranes of 0.22 µm. The mobile phases—A (MeOH) and B (MTBE)—were obtained using a linear gradient program as follows: from 0 to 30 min 5% B; from 30 to 40 min, 5 to 30% B; from 40 to 41 min, 30 to 50% B; and from 41 to 50 min, 50 to 5% B. The flow rate was maintained at 0.9 mL·min^{-1}, with an injection volume of 20 µL. The column temperature was controlled at 25 °C. UV-Vis spectra were acquired over the range of 220–700 nm, and chromatographic detection was carried out at 450 nm.

The MS/MS analysis was carried out in accord with Giuffrida et al. [16] with modifications; the APCI source operated in positive (+) ionization mode; detector voltage was set at 4.5 kV; interface temperature maintained at 350 °C; DL temperature at 250 °C; heat block temperature at 200 °C; nebulizing gas flow (N_2) at 3.0 L·min^{-1}; drying gas flow (N_2) at 5.0 L·min^{-1}; collision-induced dissociation (CID) gas pressure at 23 kPa (argon); and event time of 0.5 s. To enhance identification accuracy, MS/MS was simultaneously performed in SIM (Selected Ion Monitoring) and MRM (Multiple Reaction Monitoring) modes.

Identification was carried out based on the following combined criteria: elution order on a C30 HPLC column, co-chromatography with authentic standards, UV-Vis spectrum, and mass characteristics (protonated molecule ([M+H]+) and MS/MS fragments). And it was compared with information reported in the literature [9,17–20]. Individual quantification of the pigment content was performed by HPLC-PDA using calibration curves constructed from five-point concentration. Analytical curves of all-*trans*-lutein, all-*trans*-β-carotene, and chlorophyll *a* were employed to quantify the xanthophylls, carotenes, and chlorophylls, respectively. Results were expressed as micrograms per gram of sample (µg·g^{-1}).

2.5. In Vivo Experimental Design

This study was approved by the Animal Ethics Committee (CEUA) of the Federal University of Santa Maria under number 2662070222. Male Wistar rats (150–250 g) were obtained from the Animal Facility of the Federal University of Santa Maria and kept in the

Pharmacology sector animal facility. The animals were kept under controlled temperature (23 ± 1 °C), light–dark cycle (12/12 h), and humidity conditions (50 ± 10%), with free access to water and commercial diet Puro Lab 22PB® (see composition in Table 1). The animals were randomly distributed into six groups (n = 10 per group). The sample n value was determined according to the test curve of Dressler et al. [21]. The control group received 300 µL of 0.9% saline solution by oral gavage (without pigments), while the other groups received different doses of microalgal pigments suspended in sunflower oil (oleoresin), at concentrations of 75, 150, 300, 450, and 600 µg kg^{-1} day^{-1}, respectively. Given the lack of official guidelines on the recommended daily intake of microalgal pigments, the doses used in this study were selected based on concentrations previously shown to be safe and beneficial in eutrophic animal models using lipophilic *S. obliquus* extracts [7]. These doses were then converted for use in rats through allometric scaling, using a JavaScript-based calculator (http://clymer.altervista.org/minor/allometry.html, accessed on 15 April 2025) that estimates interspecies dosages by accounting for body weight differences on an exponential scale. After four weeks, the animals were euthanized with 100% isoflurane (DCB no.: 05082/CAS no.: 26675-46-7). The intestine was retired, and fecal samples (cecum) were collected to analyze pigments, short-chain fatty acids, and total probiotic microbiota.

Table 1. The composition of the commercial diet Puro Lab 22PB®.

Composition *
Folic acid
Nicotinic acid
Antioxidant additive (BHA and BHT)
Biotin
Calcitic limestone
Choline chloride
Sodium chloride (Common salt)
Soybean meal (GMO from Agrobacterium SP.)
Wheat bran
Dicalcium phosphate
Calcium iodate
Lysine
Methionine
Ground whole corn (GMO from *Bacillus thuringiensis*, *Streptomyces* sp.)
Calcium pantothenate
Sodium selenite
Ground whole soybean (GMO from *Agrobacterium* sp./Pressure treatment)
Cobalt sulfate
Copper sulfate
Iron sulfate
Manganese sulfate
Zinc sulfate
Whole wheat
Vitamin A, B1, B12, B2, B6, C, E, K3

* Source: https://www.purotrato.com.br/produtos/Puro-Lab-22PB accessed on 15 April 2025.

2.5.1. Eutrophic Status

To assess the eutrophy of the animals, water intake (mL) and feed intake (g) were measured daily. Body weight (g) was recorded on days 1, 3, 7, 10, 14, 17, 21, and 28 of the experiment. After euthanasia, abdominal fat was collected and weighed (g). Additionally, the animals were monitored throughout the experiment for any clinical signs of toxicity.

2.5.2. Determination of Pigments in Commercial Diet and Fecal Samples

The pigments in the commercial diet (1 g) and fecal samples (1 g) were extracted and analyzed according to Sections 2.3 and 2.4, respectively. Quantitative results were shown as micrograms per gram of sample ($\mu g \cdot g^{-1}$).

2.5.3. Determination of Short-Chain Fatty Acids (SCFAs) and Total Microbiota (*Bifidobacterium* and *Lactobacillus*)

The microbiota samples were thawed to 5 °C and agitated manually to homogenize them. Then, 250 mg of samples and 750 µL of methanol were added into a 1.5 mL polypropylene microtube and then shaken with a vortex for 1 min. Then 250 µL of the supernatant was removed and transferred to a new microtube containing 250 µL of formic acid. The mixture was manually stirred and subjected to centrifugation for 3 min. After centrifugation, 250 µL of the supernatant of the mixture was collected in another polypropylene tube previously containing 500 µL of isoamyl alcohol solution (692.40 µg mL^{-1} in methanol), used as an internal standard, and was homogenized and centrifuged again. Then, 650 µL of sample was inserted into a 2 mL injection vial, and 1 µL of extract was injected into a gas chromatograph equipped with a flame ionization detector (GC-FID; Varian Star 3400, Palo Alto, CA, USA) and an autosampler (Varian 8200CX, Palo Alto, CA, USA) in split mode (1:10) at 250 °C. Hydrogen was employed as the carrier gas at a constant pressure of 12 psi. The analytes (acetic, propionic, butyric, valeric, and isovaleric acids) were resolved using a CP-Wax 52CB capillary column (50 m × 0.32 mm; 0.20 µm film thickness of the stationary phase). The initial column temperature was set at 60 °C for 1 min and increased to 90 °C at a rate of 10 °C min^{-1}, then to 110 °C for 5 °C min^{-1}, and, lastly, to 230 °C at a rate of 20 °C min^{-1}, where it remained for 1 min. The detector was operated at a temperature of 250 °C. Method validation included the evaluation of selectivity, linearity, linear range, repeatability, precision, limit of detection (LOD), and limit of quantification (LOQ) for acetic, propionic, butyric, and isovaleric acids. Linearity was determined by constructing a regression equation based on the least squares method. LOD and LOQ values were obtained by sequential dilutions up to signal-to-noise ratios of 3:1 and 6:1, respectively. Precision was assessed by analyzing the repeatability of six replicated samples. Accuracy was evaluated by measuring the recovery of known quantities of standard compounds spiked into a diluted sample. The results were expressed in mol 100 mol^{-1} of each SCFA in the samples.

For determination of microbiota, serial dilutions were transferred to triplicate sterile Petri plates containing MRS agar (Himedia Curitiba, Paraná, Brazil), for total *Bifidobacterium* and *Lactobacillus* counts. Plates were incubated at 37 °C for 72 h. The dilution of the microparticles involved weighing 1 g of microparticles and adding 9 mL of sterile phosphate buffer solution (pH 7.5), according to the procedure outlined by Sheu et al. [22]. Results were shown as log colony-forming units per gram (log $CFU \cdot g^{-1}$).

2.6. Statistical Analysis

Statistical analysis was performed using GraphPad Prism 5.0 software (GraphPad Software Inc., La Jolla, CA, USA). Data normality criteria were assessed by the Shapiro–Wilk test. Subsequently, the significance of the experimental data was determined using one-way ANOVA followed by Tukey's test ($p < 0.05$). Data were expressed as mean ± standard deviation of the mean (SMD).

3. Results and Discussion

3.1. Eutrophic Status Analysis

Data on the food and water intake, body weight, and abdominal fat were collected to analyze the rats' eutrophy status in the experimental period. As shown in Figure 1, the food intake (A, B, and C) among the groups that received different concentrations of microalgal pigments (0, 75, 150, 300, 450, and 600 $\mu g \cdot kg^{-1} bw \cdot d^{-1}$) did not differ throughout the experiment, except for the 75 $\mu g \cdot kg^{-1} \cdot bw \cdot d^{-1}$ group on the 18th day. However, by day 28, this difference was no longer observed. Likewise, no statistical differences were found between the groups for water intake (Figure 1D–F). Furthermore, Figure 1G shows that the body weight gain in the experimental groups followed the same variation pattern as the control group (0 $\mu g \cdot kg^{-1} bw \cdot d^{-1}$) throughout the experiment (from day 1 to day 28).

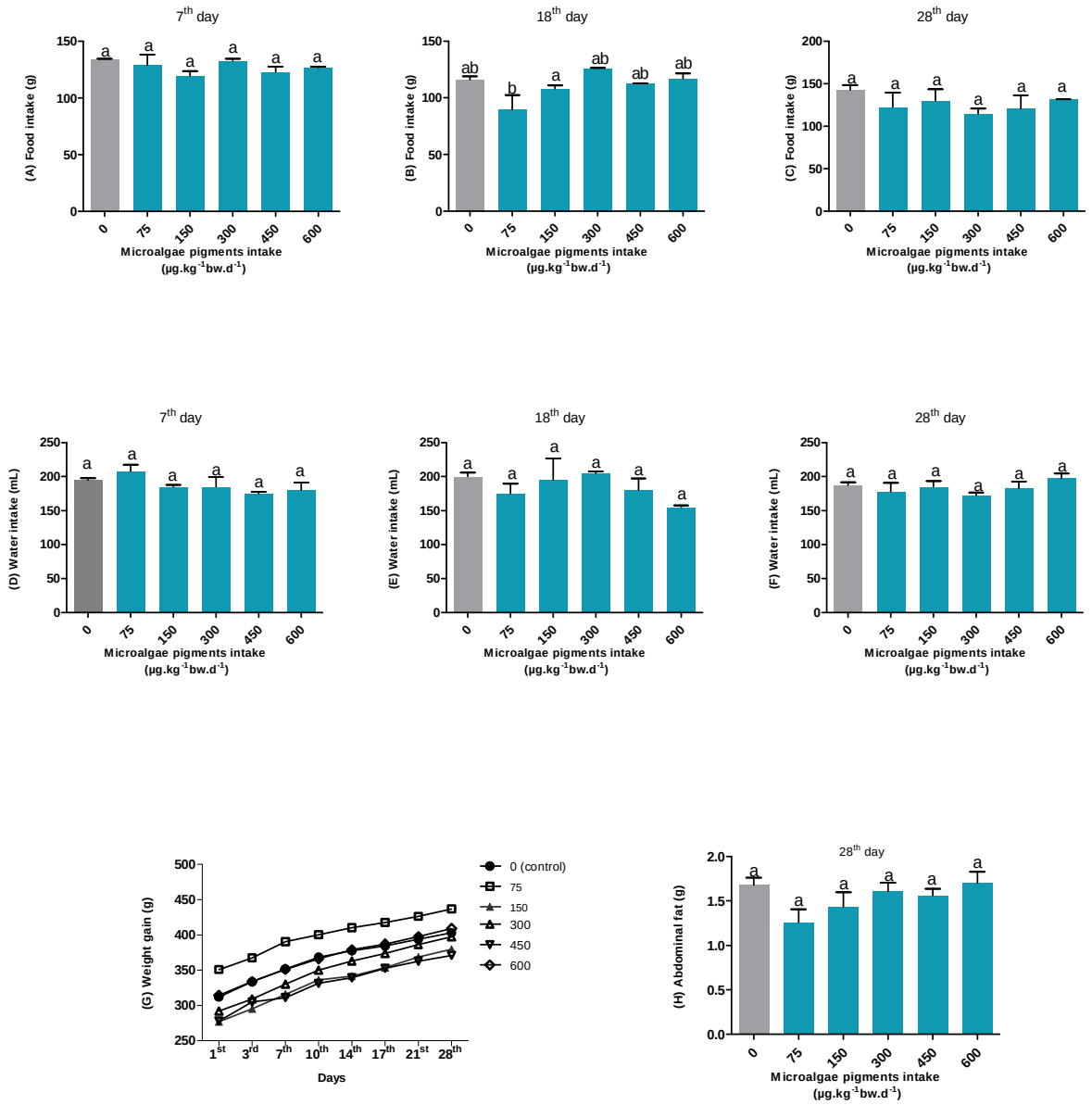


Figure 1. The food intake (**A**–**C**), water intake (**D**–**F**), body weight (**G**), and abdominal fat (**H**) of rats. Different letters between the columns indicate statistical differences ($p < 0.05$).

The abdominal fat content was also evaluated (Figure 1H), given the purely lipophilic nature of the extract administered—which was rich in carotenoids—which could influence

the lipid accumulation metabolism [23]. Nevertheless, no statistically significant differences were observed among the groups at the end of the experiment.

The compilation of these results indicates that the different concentrations of carotenoids and chlorophylls from *S. obliquus* provided in the oleoresin during the study did not interfere with the healthy development or growth of the rats. Moreover, no clinical signs of toxicity or mortality were observed throughout the entire experiment.

3.2. Carotenoids and Chlorophylls Identification by HPLC-PDA-MS/MS

The chromatographic and spectrometric characteristics of carotenoids and chlorophylls analyzed in the present study (oleoresin containing the lipophilic extract of *S. obliquus*, commercial diet, and fecal content samples) are presented in Table 2. The pigment identification was based on the chemical evidence obtained through the chromatographic analysis, including the elution order, UV-visible features, and MS/MS experiments, which confirmed the assignment of the protonated molecule ($[M+H]^+$) to the peaks identified through the expected fragments for each compound. Furthermore, the identification was based on a detailed description previously reported in the literature [9,17,18,20,24].

Twenty-two pigments were identified throughout the trial (sixteen carotenoids and six chlorophylls). Of these compounds, twenty-one were present in the microalgal oleoresin, including sixteen carotenoids (all-*trans*-violaxanthin—peak 1, 9-*cis*-violaxanthin—peak 2, 15-*cis*-lutein—peak 3, 13-*cis*-lutein—peak 6, all-*trans*-lutein—peak 7, all-*trans*-zeaxanthin—peak 8, 9-*cis*-lutein—peak 10, canthaxanthin—peak 11, 9-*cis*-zeaxanthin—peak 13, 2′-dehydrodeoxymyxol—peak 14, 5,6-epoxy-β-carotene—peak 15, all-*trans*-β-cryptoxanthin—peak 16, all-*trans*-echinenone—peak 17, 9-*cis*-echinenone—peak 19, all-*trans*-β-carotene—peak 20, and 9-*cis*-β-carotene—peak 22) and five chlorophylls (hydroxychlorophyll—peak 4, chlorophyll *b*—peak 5, chlorophyll *a*—peak 9, chlorophyll *a*′—peak 12, and pheophytin *a*—peak 21). This pigment profile is a recurring characteristic of the taxonomic group of green algae, such as *S. obliquus* [25,26]. Moreover, the profile found is similar to previous characterizations carried out for this same microalga [9,17,19].

In contrast, only five compounds (three carotenoids and two chlorophylls) were detected in the commercial diet, all-*trans*-lutein—peak 7, all-*trans*-zeaxanthin—peak 8, 9-*cis*-zeaxanthin—peak 13, hydroxypheophytin *a*—peak18, and pheophytin *a*—peak 21, and were probably xanthophylls and chlorophylls from ingredients that make up the commercial diet, such as corn and soy, for example [27,28]. Likewise, these pigments were also detected in fecal samples from the control group and the groups that ingested 75 and 150 $\mu g \cdot kg^{-1} bw \cdot d^{-1}$ of pigments.

In addition to these five compounds, the 300 and 450 groups also showed the 15-*cis*-lutein (peak 3), 9-*cis*-lutein (peak 10), all-*trans*-β-cryptoxanthin (peak 16), and 9-*cis*-β-carotene (peak 22), totaling nine pigments. Similarly, these nine pigments were detected in the fecal content of animals that received a daily dose of 600 $\mu g \cdot kg^{-1} bw \cdot d^{-1}$. Still, for this same dosage, the isomer 13-cis-lutein (peak 6) was detected, increasing the total to ten pigments.

It is worth noting that only in the fecal content of the groups that received daily concentrations above 300 $\mu g \cdot kg^{-1} bw \cdot d^{-1}$ of pigments was it possible to detect isomers of lutein, 9-*cis*-β-carotene, and all-*trans*-β-cryptoxanthin. Among these, the latter two are present only in the *S. obliquus* oleoresin, which indicates that this is the source of their accumulation. In contrast, hydroxypheophytin *a*, which is absent in the microalgal oleoresin, was detected in all experimental groups. Although this chlorophyll derivative is present in the commercial diet, its presence in the fecal content may result from microbial biotransformations occurring in the intestine [5]. Similarly, it has been proposed that *cis* isomers of carotenoids may also originate from gastrointestinal conditions [29].

Table 2. Chromatographic characteristics, UV-vis spectrum, and mass obtained by HPLC–PDA–MS/MS of pigments from *S. obliquus* oleoresin, commercial diet, and cecal samples from rats after ingestion of oleoresin with different concentrations of microalgae pigments.

Peak	Pigments	tR (min) [a]	UV–Vis Characteristics			Fragment Ions (Positive Mode) (*m*/*z*)	
			λmáx (nm) [b]	III/II (%) [c]	AB/II (%) [d]	$[M+H]^+$	MS/MS
1	all-*trans*-violaxanthin	8.1	415,438,468	85	0	601	583 $[M+H–18]^+$, 565 $[M+H–18–18]^+$, 509 $[M+H–92]^+$
2	9-cis-violaxanthin	9.0	326, 411, 435,464	72	18	601	584 $[M+H–18]^+$, 565 $[M+H–18–18]^+$, 509 $[M+H–92]^+$
3	15-*cis*-lutein	11.2	328,412,439,464	16	24	569	551 $[M+H–18]^+$, 533 $[M+H–18–18]^+$
4	hydroxychlorophyll *a*	11.2	430, 664	na [e]	na	909	631 $[M+H–278]^+$
5	chlorophyll *b*	11.7	465,654	na	na	907	629 $[M+H–278]^+$, 569 $[M+H–278–60]^+$
6	13-*cis*-lutein	12.4	415,440,465	37	nc [f]	569	551 $[M+H–18]^+$, 533 $[M+ –18–18]^+$
7	all-*trans*-lutein	13.6	420, 445, 472	50	0	569	551 $[M+H–18]^+$, 533 $[M+H–18–18]^+$
8	all-*trans*-zeaxanthin	15.8	425,451, 476	22	0	569	551 $[M+H-18]^+$, 533 $[M+H-18-18]^+$, 495, 477 $[M+H-92]^+$, 459
9	chlorophyll *a*	15.7	431, 664	na	na	893	615 $[M+H-278]^+$, 583 $[M+H-278-31]^+$, 555 $[M+H–278–59]^+$
10	9-*cis*-lutein	16.4	418, 440, 470	50	nd [g]	569	550 $[M+H-18]^+$, 533 $[M+H-18-18]^+$
11	canthaxanthin	17.0	460	nc	nd	565	547 $[M+H-18]^+$
12	chlorophyll *a*′	17.4	430, 664	na	na	893	615 $[M+H–278]^+$, 583 $[M+H–278–31]^+$, 555 $[M+H–278–59]^+$
13	9-*cis*-zeaxanthin	20.9	420, 446, 471	25	nc	569	551 $[M+H-18]^+$, 533 $[M+H-18-18]^+$, 495, 477 $[M+H-92]^+$, 459
14	2′-dehydrodeoxymyxol	22.0	445,474,504	63	0	567	549 $[M+H-18]^+$
15	5,6-epoxy-β-carotene	22.9	420,446,471	50	0	553	535 $[M+H-18]^+$, 461 $[M+H-92]^+$, 205
16	all-*trans*-β-cryptoxanthin	24–24.6	425,450,476	25	0	553	535 $[M+H-18]^+$
17	all-*trans*-echinenone	25.1	461	nc	0	551	533 $[M+H-18]^+$, 427, 203
18	hydroxypheophytin *a*	26–27.2	408,666	na	na	887	869 $[M+H-18]^+$; 803 $[M+H-63]^+$; 609 $[M+H-278]^+$; 591 $[M+H-278-18]^+$; 531 $[M+H-278-18-60]^+$
19	9-*cis*-echinenone	27.6	454	nc	nc	551	533 $[M+H-18]^+$, 427, 203
20	all-*trans*-β-carotene	33.6	425, 451, 476	25	0	537	444 $[M+H-92]^+$, 399, 355
21	pheophytin *a*	34.4–36.0	408,666	na	na	871	593 $[M+H-278]^+$; 533 $[M+H-278-60]^+$
22	9-*cis*-β-carotene	36.6	425, 451, 476	30	nc	537	444 $[M+H-92]^+$, 399, 355

[a]: The retention time (linear gradient in methanol and methyl tert-butyl ether); [b]: the spectral fine structure; [c]: the ratio of the height of the longest wavelength absorption peak (III) and that of the middle absorption peak (II); [d]: the ratio of the *cis* peak (AB) and the middle absorption peak (II); [e]: not applicable; [f]: not calculated; and [g]: not detected.

3.3. Carotenoids and Chlorophylls Quantification

The carotenoid and chlorophyll content ($\mu g \cdot g^{-1}$) of the *S. obliquus* oleoresin, commercial diet, and fecal content samples from the experimental trial (groups 0 (control), 75, 150, 300, 450, and 600 $\mu g \cdot kg^{-1} bw \cdot d^{-1}$) is presented in Table 3.

Considering the carotenoid profile, all-*trans*-lutein (622.98 ± 1.20 $\mu g \cdot g^{-1}$) followed by all-*trans*-zeaxanthin (290.13 ± 0.33 $\mu g \cdot g^{-1}$) and all-*trans*-β-carotene (264.66 ± 0.27 $\mu g \cdot g^{-1}$) were the major constituents in the microalgal oleoresin. With the exception of all-*trans*-β-carotene, the same occurred in the commercial diet (all-*trans*-lutein: 1.60 ± 0.25 $\mu g \cdot g^{-1}$ and all-*trans*-zeaxanthin: 1.46 ± 1.10 $\mu g \cdot g^{-1}$). Despite this, all-*trans*-zeaxanthin was the most abundant carotenoid in the cecal content of the experimental groups, totaling 1.52 ± 1.03, 1.65 ± 1.60, 2.03 ± 0.23, 1.80 ± 1.78, 2.48 ± 1.09, and 3.15 ± 1.10 $\mu g \cdot g^{-1}$ for the control, 75, 150, 300, 450, and 600 groups, respectively.

Pigments such as 15-*cis*-lutein (0.20 ± 0.24, 0.21 ± 0.31, and 0.22 ± 0.99 $\mu g \cdot g^{-1}$), all-*trans*-β-cryptoxanthin (0.27 ± 0.51, 0.28 ± 0.69, and 0.42 ± 0.50 $\mu g \cdot g^{-1}$), and 9-*cis*-β-carotene (0.19 ± 0.92, 0.21 ± 0.31, and 0.32 ± 0.60 $\mu g \cdot g^{-1}$) were quantifiable only in animals supplemented with higher pigment concentrations (300, 450, and 600 $\mu g \cdot kg^{-1} bw \cdot d^{-1}$). In addition, 13-*cis*-lutein was detected exclusively in the 600 $\mu g \cdot kg^{-1}$ group (0.21 ± 0.30 $\mu g \cdot g^{-1}$). This fact reinforces the idea that the presence of several carotenoids in higher concentrations tends to decrease the intestinal cellular uptake of some structures, and consequently these compounds follow the intestinal transit [30,31].

Considering a previous study of in vitro intestinal digestion and absorption, 15-*cis*-lutein, all-*trans*-β-cryptoxanthin, and 9-*cis*-β-carotene showed a good bioaccessibility (74%, 36%, and 22%) but were not satisfactorily absorbed by Caco-2 cells in the intestinal model [18], which may justify their presence in the fecal samples analyzed in this study. On the other hand, canthaxanthin, despite presenting a 99% bioaccessibility and also not having been absorbed by the intestinal mucosa in the same in vitro study, was not detected in the fecal content of the present study, which is consistent with the possible degradation, bioconversion, or microbial metabolism during intestinal transit. The same may have occurred for the other carotenoids present in the oleoresin and not detected in the analyzed samples.

As illustrated in Figure 2, carotenoids, once ingested, are released from the food matrix through mechanical and enzymatic actions during digestion. Due to their lipophilic nature, they associate with co-ingested lipids, forming emulsions that are subsequently digested by lipases with the aid of bile salts in the small intestine. Lipid digestion leads to the formation of mixed micelles—structures responsible for solubilizing and transporting carotenoids through the aqueous environment of the intestine to the enterocytes. In this form, carotenoids become bioaccessible, meaning they are available for absorption by intestinal cells [32].

From this point, three potential routes may be followed: Route 1—carotenoids are absorbed and transported via chylomicrons into the lymphatic system, then to the liver, where they may be stored, metabolized, or redistributed to target tissues to exert health-promoting effects. Route 2—provitamin A carotenoids are converted into retinyl esters within enterocytes before entering the bloodstream. Route 3—unabsorbed carotenoids proceed to the colon, where they may be beneficially utilized by the gut microbiota [6,33]. Once in the colon, possible microbial processing pathways include catabolism, fermentation, or biotransformation.

Table 3. The carotenoid and chlorophyll content of the *S. obliquus* oleoresin, commercial diet, and cecal content of rats after the intake of oleoresin with different concentrations of microalgae pigments. Different superscript letters on the same line indicate statistical differences ($p < 0.05$) between the experimental groups.

Peak	Pigments	The Pigment Content of the Fecal Sample (μg·g^{-1})							
		***S. oliquus* Oleoresin**	**Commercial Diet**	**0 (Control)**	**75 ***	**150 ***	**300 ***	**450 ***	**600 ***
1	all-*trans*-violaxanthin	61.52 ± 0.52	nd	nd	nd	nd	nd	nd	nd
2	9-*cis*-violaxanthin	49.53 ± 0.39	nd	nd	nd	nd	nd	nd	nd
3	15-*cis*-lutein	81.30 ± 1.19	nd	nd	nd	nd	0.20 ± 0.24	0.21 ± 0.31	0.22 ± 0.99
4	hydroxychlorophyll *a*	136.43 ± 0.41	nd	nd	nd	nd	nd	nd	nd
5	chlorophyll *b*	84.87 ± 1.26	nd	nd	nd	nd	nd	nd	nd
6	13-*cis*-lutein	65.25 ± 1.48	nd	nd	nd	nd	nd	nd	0.21 ± 0.30
7	all-*trans*-lutein	622.98 ± 1.20	1.60 ± 0.25	0.46 ± 0.36	0.48 ± 0.60	0.45 ± 0.49	1.18 ± 0.30	0.93 ± 0.33	2.53 ± 0.14
8	all-*trans*-zeaxanthin	290.13 ± 0.33	1.46 ± 1.10	1.52 ± 1.03	1.65 ± 1.60	2.03 ± 0.23	1.80 ± 1.78	2.48 ± 1.09	3.15 ± 1.10
9	chlorophyll *a*	4459.81 ± 2.17	nd						
10	9-*cis*-lutein	52.53 ± 0.30	nd	nd	nd	nd	0.13 ± 0.08	0.17 ± 0.20	0.23 ± 0.89
11	canthaxanthin	49.46 ± 0.40	nd	nd	nd	nd	nd	nd	nd
12	chlorophyll *a*′	136.14 ± 6.8	nd	nd	nd	nd	nd	nd	nd
13	9-*cis*-zeaxanthin	70.74 ± 1.37	0.80 ± 0.29	0.28 ± 0.83	0.30 ± 0.58	0.24 ± 47	0.33 ± 0.99	0.34 ± 0.70	0.87 ± 0.81
14	2′-dehydrodeoxymyxol	125.32 ± 0.24	nd	nd	nd	nd	nd	nd	nd
15	5,6-epoxy-β-carotene	56.60 ± 0.33	nd	nd	nd	nd	nd	nd	nd
16	all-*trans*-β-cryptoxanthin	55.49 ± 0.17	nd	nd	nd	nd	0.27 ± 0.51	0.28 ± 0.69	0.42 ± 0.50
17	all-*trans*-echinenone	309.93 ± 0.31	nd	nd	nd	nd	nd	nd	nd
18	hydroxypheophytin *a*	nd	0.18 ± 0.51	0.33 ± 0.39	0.24 ± 1.87	0.25 ± 1.03	0.31 ± 0.60	0.64 ± 0.84	0.84 ± 0.77
19	9-*cis*-echinenone	121.31 ± 0.23	nd	nd	nd	nd	nd	nd	nd
20	all-*trans*-β-carotene	264.66 ± 0.27	nd	nd	nd	nd	nd	nd	nd
21	pheophytin *a*	162.21 ± 6.53	0.14 ± 0.82	1.73 ± 0.13	1.75 ± 0.86	1.86 ± 0.38	2.03 ± 1.98	2.51 ± 0.39	3.17 ± 0.19
22	9-*cis*-β-caroten	73.09 ± 0.26	nd	nd	nd	nd	0.19 ± 0.92	0.21 ± 0.31	0.32 ± 0.60
	Total carotenoids	2349.77 ± 1.11	3.85 ± 0.57	1.98 ± 0.62 ^{a}	2.43 ± 1.04 ^{b}	2.72 ± 0.07 ^{c}	4.09 ± 1.01 ^{d}	4.62 ± 0.30 ^{e}	7.94 ± 0.60 ^{f}
	Total chlorophylls	4979.45 ± 2.28	0.32 ± 0.55	2.06 ± 0.17 ^{a}	1.98 ± 0.50 ^{a}	2.11 ± 0.59 ^{b}	2.34 ± 0.49 ^{c}	3.15 ± 0.22 ^{d}	4.01 ± 0.31 ^{e}
	Total pigments	7329.09 ± 1.56	4.17 ± 0.68	4.04± 0.82 ^{a}	4.44 ± 0.54 ^{b}	4.83 ± 0.19 ^{c}	6.43 ± 0.60 ^{d}	7.77 ± 0.70 ^{e}	11.95 ± 0.34 ^{f}

*: Concentration of microalgae pigments present in oleoresin ingested daily (μg·kg^{-1}bw·d^{-1}). nd: not detected.

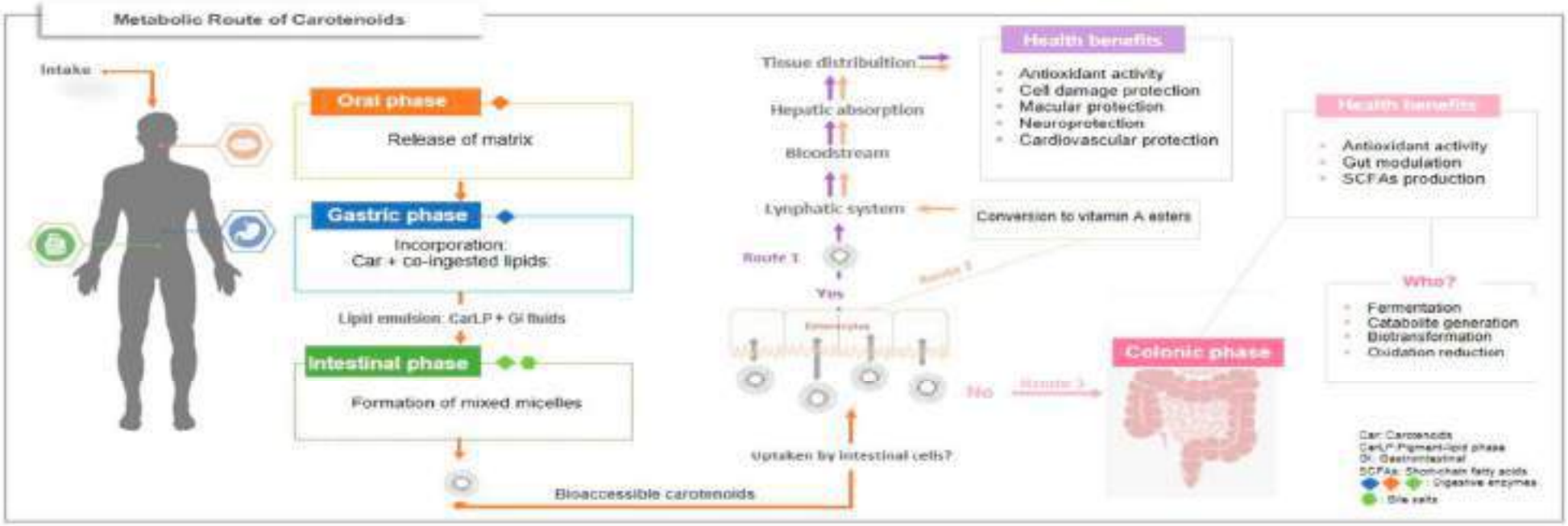


Figure 2. Metabolic routes of carotenoids after intake.

To date, the specific mechanisms governing carotenoid–microbiota interactions remain unclear, and few studies have directly or indirectly investigated this relationship. An investigation conducted by Kaulmann et al. [34] demonstrated the generation of novel compounds during fermentation by the intestinal microbiota and inferred that tetraterpenoids were effectively metabolized. It is known that carotenoids can be cleaved by oxygenases present in various organisms, including those in the gut microbiome, supporting the hypothesis that unabsorbed compounds may be locally metabolized by gut microbes [35]. Among the resulting metabolites, apocarotenoids have been identified as potential modulators of the gut microbiota, contributing to intestinal health benefits [36].

Regarding the chlorophyll fraction, although chlorophyll *a* was the main tetrapyrrole in the oleoresin (4459.81 ± 2.17 $\mu g \cdot g^{-1}$), at the end of the in vivo administrations, pheophytin *a* was more abundant in the cecal content of all groups. Furthermore, an increase was observed in the following order 1.75 ± 0.86, 1.86 ± 0.38, 2.03 ± 1.98, 2.51 ± 0.39, and 3. 7 ± 0.19 $\mu g \cdot g^{-1}$ for groups 75, 150, 300, 450, and 600, respectively.

It is believed that the pheophytin content may originate from the loss of the central magnesium from the chlorophyll a structure (see Figure 3). This transformation is common due to the structural vulnerability of chlorophyll at an acidic pH, which is a normal biological condition of the gastric phase (pH close to 3.0) during the digestive process [9].

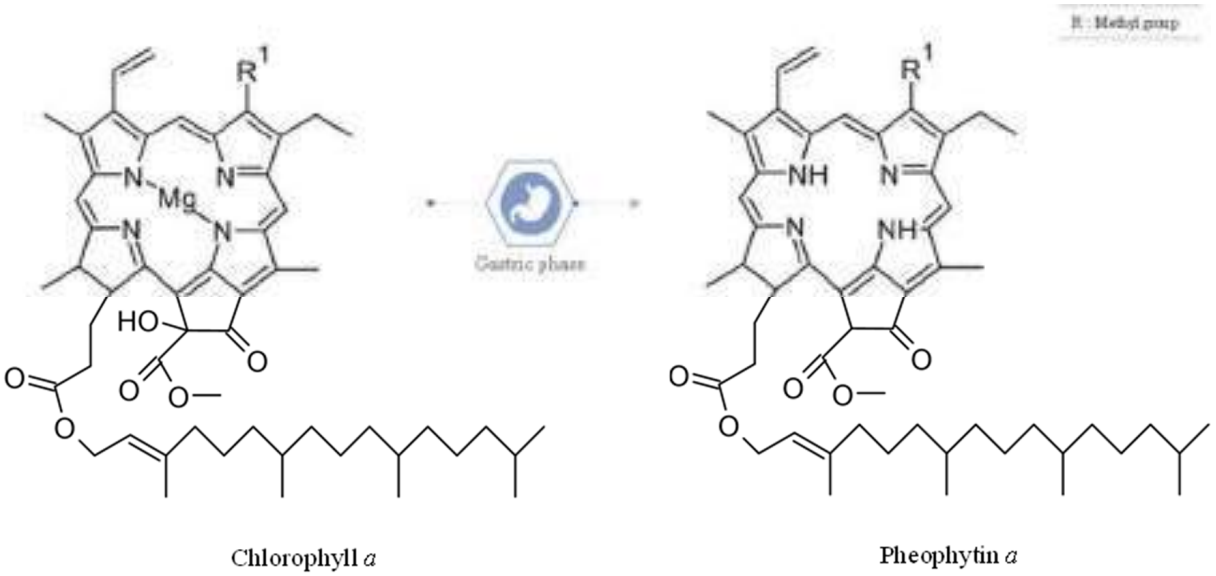


Figure 3. Chemical structure of chlorophyll *a* and pheophytin *a*.

Other hypotheses arise when observing the content of chlorophyll derivatives present in the control group. Although this group exclusively consumed the commercial diet, which contained reduced amounts of hydroxypheophytin *a* (0.18 ± 0.51 $\mu g \cdot g^{-1}$) and pheophytin *a* (0.14 ± 0.82 $\mu g \cdot g^{-1}$), it is notable that the fecal samples presented significantly higher concentrations of these compounds—approximately twelve times more pheophytin a and twice as much hydroxypheophytin *a*. Thus, the accumulation of these derivatives in the cecum would be another tangible hypothesis. However, the free access to the commercial diet during the experimental trial weakens this possibility. According to Li et al. [5], there is also the possibility of chlorophylls being biotransformed during the in vitro digestion or colonic fermentation.

Analyzing the totality, the twenty-one compounds identified in the oleoresin of *S. obliquus* amounted to 7329.09 ± 1.56 $\mu g \cdot g^{-1}$ of pigments. Of this amount, approximately 68% (4979.45 ± 2.28 $\mu g \cdot g^{-1}$) and 32% (2349.77 ± 1.11 $\mu g \cdot g^{-1}$) corresponded to chlorophylls and carotenoids, respectively. On the other hand, the compounds found in the commercial

diet totaled 4.17 ± 0.68 μg·g^{-1}, which is approximately two thousand times lower than the content contained in the microalgal oleoresin. Furthermore, unlike microalgal oleoresin, the largest fraction of pigments found in the diet was carotenoids (3.85 ± 0.57 μg·g^{-1}), while chlorophylls accounted for approximately 8% (0.32 ± 0.55 μg·g^{-1}).

In contrast, in fecal samples the proportion varied according to the concentration ingested. Interestingly, the group that did not ingest pigments (control) presented approximately 50% carotenoids and chlorophylls. In the experimental groups (75, 150, 300, 450, and 600), the total amount of carotenoids (55–66%) stood out in relation to chlorophylls (35–45%). This increase in the relative proportion of carotenoids compared to chlorophylls can be attributed to the higher carotenoid content in the oleoresin, combined with the lower structural stability of chlorophylls, which are more prone to degradation due to the pH variation, oxidative environment, and enzymatic reactions [37].

In general, a dose-dependent relationship was observed in the global distribution of carotenoids and chlorophylls in the fecal content, since the concentration of these pigments in the cecum increased proportionally to the amount present in the administered oleoresin.

3.4. SCFA Levels and Microbiota

The results regarding the SCFA profile, as well as the total microbiota, obtained from the cecal samples of the experimental groups are presented in Figure 4.

As shown in Figure 4A, acetic acid levels in the groups supplemented with 300 and 450 μg·kg^{-1} bw·d^{-1} increased by 13% and 14%, respectively, compared to the control group, showing statistically significant differences ($p < 0.05$). The other groups did not differ statistically from the control. However, a significant reduction of 11% in acetic acid levels was observed for the supplementation of 600 μg·kg^{-1} bw·d^{-1}, compared to that of 450 μg·kg^{-1} bw·d^{-1} of pigments.

Among all the AGCCs analyzed in this study, acetic acid was the most abundant. This finding is relevant, since high levels of acetate are associated with beneficial effects, including a decreased appetite, improved glucose metabolism, reduced inflammatory processes, and lipid accumulation in adipose and liver cells [3,38].

Regarding propionate levels (Figure 4B), only the animals that received 600 μg·kg^{-1} bw·d^{-1} of microalgal pigments showed a statistically significant difference compared to the control group ($p < 0.05$), with an increase of 16%. The other experimental groups did not differ significantly from each other regarding this SCFA.

In contrast, in relation to butyric acid levels (Figure 4C), a statistically significant increase (19%) was observed only in animals supplemented with 300 μg·kg^{-1}bw·d^{-1} of microalgal pigments ($p < 0.05$). As observed for propionic acid levels, there were no statistical differences between the other experimental groups.

When analyzing the acetic acid/propionic acid ratio (Figure 4D), it is observed that no concentration of pigments provided to the animals presented a statistically significant difference from the control ($p < 0.05$). Considering that the acetic acid/propionic acid ratio is an important indicator of the functional balance of the intestinal microbiota [39], the similarity observed in relation to the control group proposes the maintenance of this balance.

Overall, an overall increase of 11–21% in SCFA levels (Figure 4E) was observed in the pigment-supplemented groups, compared to the control group. This increase indicates a positive modulation of the intestinal microbial activity. According to Agus et al. [40], the increase in the levels of these metabolites is essential because, in addition to regulating the immune system and inflammatory responses, they can also contribute to improving the glycemic and lipid metabolism, as well as controlling the energy intake.

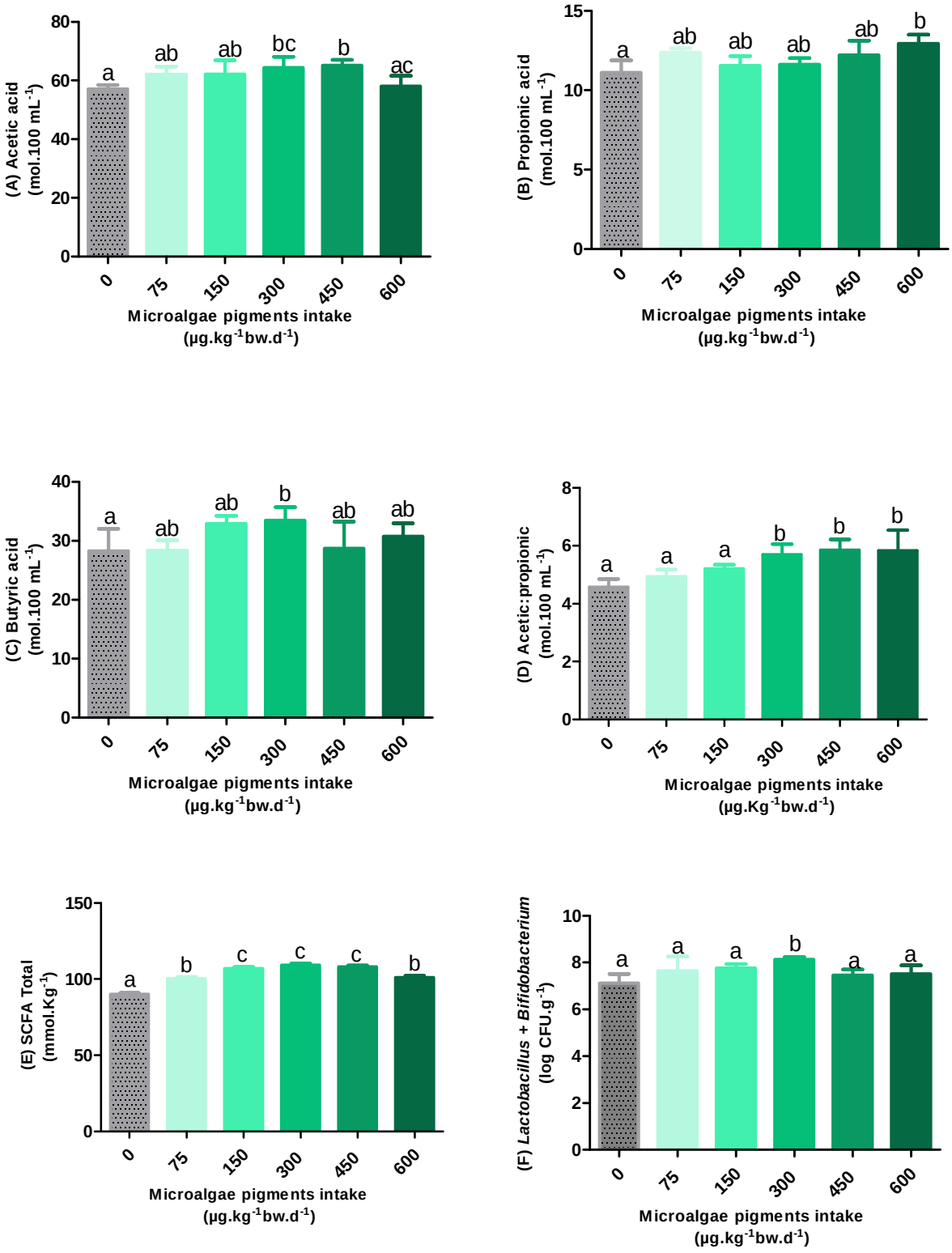


Figure 4. The short-chain fatty acid content (**A**–**E**) and total microbiota (**F**) after the intake of oleoresin with different concentrations of microalgae pigments. Different letters between the columns indicate statistical differences ($p < 0.05$).

Despite the significant increase compared to the control, a downward trend in total levels was observed after the supplementation with 300 µg/kg body weight·d^{-1}, being more pronounced at the concentration of 600 µg·kg^{-1}bw·d^{-1}, which presented a statistically significant difference among the groups of 150, 300, and 450 µg·kg^{-1}bw·d^{-1}. This

corroborates the evidence that higher concentrations of pigments may be associated with a reduction in the abundance of the intestinal microbiota. This assumption is plausible since high doses of carotenoids can exert a pro-oxidant effect, which results in cellular damage that compromises the microbial activity. However, the lack of a broader microbiome profile limits the robustness of this hypothesis. A more accurate interpretation could be achieved in future studies through the inclusion of genetic sequencing, intestinal histology, inflammatory cytokine measurements, and gut permeability markers.

The data related to the total microbiota (Figure 4F) showed a significant increase in the microbial population only in the group treated with the oleoresin containing 300 $\mu g \cdot kg^{-1} bw \cdot d^{-1}$ of pigments, which reinforces the potential prebiotic effect of this concentration. However, it is important to highlight that the microbiota analyzed in this study refers exclusively to the total *Bifidobacterium* and *Lactobacillus*. This indicates that the significant increases in SCFA levels observed in groups 450 (acetic acid) and 600 (propionic acid) may be associated with the activity of other bacterial groups not contemplated in the quantification performed, such as the phylum Bacteroidetes (acetic acid), *Clostridium ramosum* (propionic acid), and *Bacteroides thetaiotaomicron* (acetic acid/propionic acid) [41].

In support of the results of this study, Table 4 presents comparisons between pigments of a non-microalgal origin and biomass. Previous research demonstrates that pigments such as β-carotene and lutein from other sources contributed to intestinal homeostasis. Scientific evidence indicates that xanthophylls like lutein and zeaxanthin exert a more pronounced effect on gut microbiota modulation compared to carotenes [42]. Nevertheless, β-carotene has also shown significant contributions to intestinal homeostasis by increasing the abundance of *Bacteroidetes* and *Proteobacteria*, while reducing harmful bacteria and promoting the growth of beneficial strains such as *Bifidobacterium*, *Collinsella* (at intermediate doses), and *Lactobacillus* (at higher doses) [43]. Lycopene, another carotene, has also demonstrated the ability to inhibit the Proteobacteria proliferation and increase the abundance of *Bifidobacterium and Lactobacillus* [44].

Table 4. Effects of non-microalgal origin pigments and biomass on gut microbiota.

Pigments/Biomass	Effects	Reference
Lutein; zeaxanthin	Pronounced effect on gut microbiota modulation	[42]
β-Carotene	↑ Bacteroidetes, ↑ Proteobacteria, ↓ harmful bacteria, ↑ Bifidobacterium, Collinsella (intermediate), and Lactobacillus (high doses)	[43]
Lycopene	↓ Proteobacteria, ↑ Bifidobacterium, and Lactobacillus	[44]
Carotenoids (fruits and vegetables)	↑ SCFAs in gut and feces; ↑ butyrate production; modulate IgA production; and prevent/delay dysbiosis	[6,45,46]
β-Cryptoxanthin	No significant changes after 8 weeks of supplementation (3 mg/day)	[47]
Carotenoids (general)	↑ Butyrate production	[6]
Carotenoids (general)	Regulation of immunoglobulin A (IgA) production and the prevention or delay of dysbiosis	[48]
Chlorophylls	↓ Firmicutes and ↑ Bacteroidetes	[4]
Chlorophyll-rich extract	↑ Akkermansia (linked to glucose metabolism)	[49]
Spirulina biomass	↑ SCFAs (acetate, propionate, butyrate, hexanoate, isovalerate, and isobutyrate); ↑ Lachnospiraceae, Lactobacillus, and Bifidobacterium (due to fiber and phenolics)	[50]
Pigments (general)	↑ Antioxidant activity in intestinal lumen; beneficial microbiota modulation	[51,52]
Pigments (general)	May modulate GI transit time, pH, antimicrobial peptides, and secretory IgA	[36]

In addition, diets rich in fruits and vegetables with high carotenoid contents have been associated with increased levels of SCFAs in the gut and feces [45,46]. Consistent with the results of the present study, findings from Rocha et al. [6] reported a marked increase in butyrate production following a carotenoid administration. Other studies have also demonstrated that carotenoids contribute to intestinal immune homeostasis through

the regulation of the immunoglobulin A (IgA) production and the prevention or delay of dysbiosis [48].

Studies on the influence of β-cryptoxanthin on the gut microbiota remain limited. The only available investigation found no significant changes after eight weeks of supplementation with 3 $mg \cdot d^{-1}$ [47]. Similarly, the evidence regarding chlorophylls is scarce. However, the negative regulation of the Firmicutes phylum and the positive modulation of Bacteroidetes was observed [4]. Additionally, the supplementation with a chlorophyll-rich extract was found to increase the Akkermansia abundance, a microorganism associated with the glucose metabolism [49].

Among the few studies available on microalgae, the reported beneficial effects have mainly been attributed to whole biomass consumption. Spirulina, for example, was recently investigated for its potential to stimulate the production of short-chain fatty acids (SCFAs), such as acetate, propionate, butyrate, hexanoate, isovalerate, and isobutyrate, and to promote the growth of beneficial bacteria, like *Lachnospiraceae*, *Lactobacillus*, and *Bifidobacterium*. However, these effects have been largely attributed to the fiber and phenolic compounds naturally present in the biomass [50].

Unlike prebiotic carbohydrates, whose benefits are primarily derived from microbial fermentation, the beneficial effects observed with pigments are also attributed to their accumulation in the intestinal lumen. This local presence may enhance antioxidant activity and positively influence the composition and functionality of the gut microbiota [52,53]. Additionally, pigments may indirectly affect the gut microbiota by modulating the gastrointestinal transit time, the pH, and the synthesis and release of antimicrobial peptides and secretory immunoglobulins, all of which play a crucial role in maintaining intestinal homeostasis [36].

Overall, the microalgal pigments present in the *S. obliquus* oleoresin were detected in the cecal content and demonstrated the ability to stimulate SCFA production and promote the growth of *Bifidobacterium* and *Lactobacillus*, indicating a positive effect on the gut microbiome, especially at concentrations of 300, 450, and 600 $\mu g \cdot kg^{-1} bw \cdot d^{-1}$. Furthermore, the data suggest that this beneficial effect may be associated with the presence of specific carotenoids, such as all-*trans*-β-cryptoxanthin, 15-*cis*-lutein, and 9-*cis*-β-carotene, since these compounds were quantified exclusively in the groups supplemented with oleoresin. To the best of our knowledge, this is the first study to evaluate such effects using pigments extracted from microalgae, thereby expanding our understanding of their functional potential. Combined with the already well-established antioxidant properties of these compounds, this set of effects highlights the multifunctional role of S. obliquus in health promotion. This functional versatility underscores the value of this microalga as a promising bioactive matrix whose integrated physiological impact warrants further investigation.

4. Conclusions

The results of this study provide relevant insights into the interactions between microalgal pigments and the activity of the intestinal microbiota. The supplementation with oleoresins containing different concentrations of *S. obliquus* pigments did not adversely affect the eutrophy of the animals. All-*trans*-zeaxanthin and pheophytin *a* were the most abundant pigments in all experimental groups. Additionally, pigments exclusive to microalgal oleoresin, such as 15-*cis*-lutein, all-*trans*-β-cryptoxanthin, and 9-*cis*-β-carotene, were detected only in animals that received doses equal to or greater than 300 $\mu g \cdot kg^{-1} bw \cdot d^{-1}$, which proposes a possible association with the modulation of SCFA levels. These supplements promoted significant increases in the levels of acetate (300 and 450 $\mu g \cdot kg^{-1} bw \cdot d^{-1}$), butyrate (300 $\mu g \cdot kg^{-1} bw \cdot d^{-1}$), and propionate (600 $\mu g \cdot kg^{-1} bw \cdot d^{-1}$). In addition, the dose of 300 $\mu g \cdot kg^{-1} bw \cdot d^{-1}$ significantly increased the populations of *Bifidobacterium* and

Lactobacillus. In general, the supplementation positively influenced both the composition of the intestinal microbiota and the production of SCFAs, in a dose-dependent manner, with an emphasis on the dose of 300 $\mu g \cdot kg^{-1} bw \cdot d^{-1}$. This supports the possibility that pigments may function as pharmacobiotic modulators, with positive implications for intestinal health. The differential distribution of carotenoids in the cecal contents and the conversion or accumulation of chlorophylls into derivatives, such as pheophytins, indicate that gastrointestinal transit and the microbiota play a central role in the transformation or elimination of these compounds, which deserves further investigation. Taken together, these findings support the use of microalgal pigments as promising functional ingredients in foods or supplements aimed at promoting intestinal health.

Author Contributions: Conceptualization, T.C.d.N. and L.Q.Z.; methodology, T.C.d.N., M.V.d.S., L.E.L., U.D.S.R., M.C.D., M.R.C.S., R.W. and C.R.d.M.; software, P.A.C.; validation, P.A.C.; formal analysis, L.Q.Z., P.A.C. and T.C.d.N.; investigation T.C.d.N.; resources, T.C.d.N.; data curation, E.J.-L. and L.Q.Z.; writing—original draft preparation, T.C.d.N.; writing—review and editing, T.C.d.N., M.C.D., E.J.-L. and L.Q.Z.; visualization, E.J.-L. and L.Q.Z.; supervision, E.J.-L. and L.Q.Z.; project administration, M.R.C.S., E.J.-L. and L.Q.Z.; funding acquisition, L.Q.Z. and M.R.C.S. All authors have read and agreed to the published version of the manuscript.

Funding: This study was financially supported by the FAPERGS/CNPq 07/2022 (23/2551-0001879-9) and the project PID2021-12799OB-I00 funded by MCIN/AEI/10.13039/501100011033 and by "ERDF A way of making Europe".

Institutional Review Board Statement: This study was approved by the Animal Ethics Committee (CEUA) of the Federal University of Santa Maria under number 2662070222 (approval: 1 August 2022)

Informed Consent Statement: Not applicable.

Data Availability Statement: The original contributions presented in the study are included in the article, further inquiries can be directed to the corresponding author.

Conflicts of Interest: The authors declare no conflicts of interest.

References

1. Fusco, W.; Lorenzo, M.B.; Cintoni, M.; Porcari, S.; Rinninella, E.; Kaitsas, F.; Lener, E.; Mele, M.C.; Gasbarrini, A.; Collado, M.C.; et al. Short-Chain Fatty-Acid-Producing Bacteria: Key Components of the Human Gut Microbiota. *Nutrients* **2023**, *15*, 2211. [CrossRef]
2. Ficagna, C.A.; Silva, A.S.d.; Rofino, R.D.; Zatti, E.; Esposito, T.; Xavier, A.C.H.; Wagner, R.; Bissacotti, B.F.; Seghetto, R.B.; Ternus, E.M.; et al. Effects on Performance, Immunological Response and Short-Chain Fatty Acid Profile in Feces of Nursery Piglets Fed with Organic Acids and Yeast Wall. *Animals* **2025**, *15*, 1051. [CrossRef]
3. Jamar, G.; Santamarina, A.B.; Casagrande, B.P.; Estadella, D.; de Rosso, V.V.; Wagner, R.; Fagundes, M.B.; Pisani, L.P. Prebiotic Potencial of Juçara Berry on Changes in Gut Bacteria and Acetate of Individuals with Obesity. *Eur. J. Nutr.* **2020**, *59*, 3767–3778. [CrossRef] [PubMed]
4. Zheng, H.; You, Y.; Hua, M.; Wu, P.; Liu, Y.; Chen, Z.; Zhang, L.; Wei, H.; Li, Y.; Luo, M.; et al. Chlorophyllin Modulates Gut Microbiota and Inhibits Intestinal Inflammation to Ameliorate Hepatic Fibrosis in Mice. *Front. Physiol.* **2018**, *9*, 1671. [CrossRef] [PubMed]
5. Li, Y.; Lu, F.; Wang, X.; Hu, X.; Liao, X.; Zhang, Y. Biological Transformation of Chlorophyll-Rich Spinach (*Spinacia oleracea* L.) Extracts Under In Vitro Gastrointestinal Digestion and Colonic Fermentation. *Food Res. Int.* **2021**, *139*, 109941. [CrossRef]
6. Rocha, H.R.; Pintado, M.E.; Gomes, A.M.; Coelho, M.C. Carotenoids and Intestinal Harmony: Exploring the Link for Health. *Foods* **2024**, *13*, 1599. [CrossRef]
7. Nascimento, T.C.; Cazarin, C.B.B.; Maróstica, M.R.; Mercadante, A.Z.; Jacob-Lopes, E.; Zepka, L.Q. Microalgae Carotenoids Intake: Influence on Cholesterol Levels, Lipid Peroxidation and Antioxidant Enzymes. *Food Res. Int.* **2020**, *128*, 108770. [CrossRef] [PubMed]

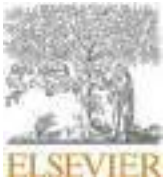
8. Fernandes, A.S.; Nascimento, T.C.; Pinheiro, P.N.; Vendruscolo, R.G.; Wagner, R.; de Rosso, V.V.; Jacob-Lopes, E.; Zepka, L.Q. Bioaccessibility of Microalgae-Based Carotenoids and Their Association with the Lipid Matrix. *Food Res. Int.* **2021**, *148*, 110596. [CrossRef]
9. Fernandes, A.S.; Nascimento, T.C.; Pinheiro, P.N.; de Rosso, V.V.; de Menezes, C.R.; Jacob-Lopes, E.; Zepka, L.Q. Insights on the Intestinal Absorption of Chlorophyll Series from Microalgae. *Food Res. Int.* **2021**, *140*, 110031. [CrossRef]
10. Guo, B.; Oliviero, T.; Fogliano, V.; Ma, Y.; Chen, F.; Capuano, E. Gastrointestinal Bioaccessibility and Colonic Fermentation of Fucoxanthin from the Extract of the Microalga Nitzschia Laevis. *J. Agric. Food Chem.* **2020**, *68*, 1844–1850. [CrossRef]
11. de Medeiros, V.P.B.; de Souza, E.L.; de Albuquerque, T.M.R.; da Costa Sassi, C.F.; dos Santos Lima, M.; Sivieri, K.; Pimentel, T.C.; Magnani, M. Freshwater Microalgae Biomasses Exert a Prebiotic Effect on Human Colonic Microbiota. *Algal Res.* **2021**, *60*, 102547. [CrossRef]
12. Zhang, Q.; Guan, G.; Liu, J.; Hu, W.; Jin, P. Gut Microbiota Dysbiosis and Decreased Levels of Acetic and Propionic Acid Participate in Glucocorticoid-Induced Glycolipid Metabolism Disorder. *mBio* **2024**, *15*, e02943-23. [CrossRef]
13. Livingston, D.B.H.; Sweet, A.; Chowdary, M.; Demissie, M.S.; Rodrigue, A.; Gedara, K.P.; Kishore, L.; Mahmoodianfard, S.; Power, K.A. Diet Alters the Effects of Lipopolysaccharide on Intestinal Health and Cecal Microbiota Composition in C57Bl/6 Male Mice. *J. Nutr. Biochem.* **2025**, *144*, 109951. [CrossRef] [PubMed]
14. Ericsson, A.C.; Gagliardi, J.; Bouhan, D.; Spollen, W.G.; Givan, S.A.; Franklin, C.L. The Influence of Caging, Bedding, and Diet on the Composition of the Microbiota in Different Regions of the Mouse Gut. *Sci. Rep.* **2018**, *8*, 4065. [CrossRef] [PubMed]
15. Rodrigues, D.B.; Menezes, C.R.; Mercadante, A.Z.; Jacob-lopes, E.; Zepka, L.Q. Bioactive Pigments from Microalgae *Phormidium autumnale*. *Food Res. Int.* **2015**, *77*, 273–279. [CrossRef]
16. Giuffrida, D.; Zoccali, M.; Giofrè, S.V.; Dugo, P.; Mondello, L. Apocarotenoids Determination in *Capsicum chinense* Jacq. Cv. Habanero, by Supercritical Fluid Chromatography-Triple-Quadrupole/Mass Spectrometry. *Food Chem.* **2017**, *231*, 316–323. [CrossRef]
17. Patias, L.D.; Fernandes, A.S.; Petry, F.C.; Mercadante, A.Z.; Jacob-Lopes, E.; Zepka, L.Q. Carotenoid Profile of Three Microalgae/Cyanobacteria Species with Peroxyl Radical Scavenger Capacity. *Food Res. Int.* **2017**, *100*, 260–266. [CrossRef]
18. Nascimento, T.C.; Pinheiro, P.N.; Fernandes, A.S.; Murador, D.C.; Neves, B.V.; de Menezes, C.R.; de Rosso, V.V.; Jacob-Lopes, E.; Zepka, L.Q. Bioaccessibility and Intestinal Uptake of Carotenoids from Microalgae *Scenedesmus obliquus*. *LWT* **2021**, *140*, 110780. [CrossRef]
19. Do Nascimento, T.C.; Pinheiro, P.N.; Fernandes, A.S.; Caetano, P.A.; Jacob-Lopes, E.; Zepka, L.Q. Insights on the Bioaccessibility of Natural Pigments from Diatom Chaetoceros Calcitrans. *Molecules* **2022**, *27*, 3305. [CrossRef]
20. Nass, P.P.; do Nascimento, T.C.; Fernandes, A.S.; Caetano, P.A.; de Rosso, V.V.; Jacob-Lopes, E.; Zepka, L.Q. Guidance for Formulating Ingredients/Products from Chlorella Vulgaris and Arthrospira Platensis Considering Carotenoid and Chlorophyll Bioaccessibility and Cellular Uptake. *Food Res. Int.* **2022**, *157*, 111469. [CrossRef]
21. Dressler, V.L.; Ogunmodede, O.T.; Heidrich, G.M.; Neves, V.M.; Schetinger, M.R.C.; Morsch, V.M. Investigative Analysis of Lanthanum Oxide Nanoparticles on Elements in Bone of Wistar Rats After 30 Days of Repeated Oral Administration. *Biol. Trace Elem. Res.* **2020**, *196*, 153–167. [CrossRef]
22. Sheu, T.Y.; Marshall, R.T.; Heymann, H. Improving Survival of Culture Bacteria in Frozen Desserts by Microentrapment. *J. Dairy Sci.* **1993**, *76*, 1902–1907. [CrossRef]
23. Bonet, M.L.; Ribot, J.; Galmés, S.; Serra, F.; Palou, A. Carotenoids and Carotenoid Conversion Products in Adipose Tissue Biology and Obesity: Pre-Clinical and Human Studies. *Biochim. Biophys. Acta-Mol. Cell Biol. Lipids* **2020**, *1865*, 158676. [CrossRef]
24. De Rosso, V.V.; Mercadante, A.Z. Identification and Quantification of Carotenoids, by HPLC-PDA-MS/MS, from Amazonian Fruits. *J. Agric. Food Chem.* **2007**, *55*, 5062–5072. [CrossRef] [PubMed]
25. Erdoğan, A.; Çağır, A.; Dalay, M.C.; Eroğlu, A.E. Composition of Carotenoids in Scenedesmus Protuberans: Application of Chromatographic and Spectroscopic Methods. *Food Anal. Methods* **2015**, *8*, 1970–1978. [CrossRef]
26. Vendruscolo, R.G.; Fagundes, M.B.; Maroneze, M.M.; do Nascimento, T.C.; de Menezes, C.R.; Barin, J.S.; Zepka, L.Q.; Jacob-Lopes, E.; Wagner, R. *Scenedesmus obliquus* Metabolomics: Effect of Photoperiods and Cell Growth Phases. *Bioprocess Biosyst. Eng.* **2019**, *42*, 727–739. [CrossRef]
27. Gebregziabher, B.S.; Zhang, S.R.; Azam, M.; Qi, J.; Agyenim-Boateng, K.G.; Feng, Y.; Liu, Y.T.; Li, J.; Li, B.; Sun, J.M. Natural Variations and Geographical Distributions of Seed Carotenoids and Chlorophylls in 1167 Chinese Soybean Accessions. *J. Integr. Agric.* **2023**, *22*, 2632–2647. [CrossRef]
28. da Silva, J.C.; Lombardi, A.T. Chlorophylls in Microalgae: Occurrence, Distribution, and Biosynthesis. In *Pigments from Microalgae Handbook*; Springer: Cham, Switzerland, 2020; pp. 1–18. [CrossRef]
29. Tao, W.; Ye, X.; Cao, Y. Isomerization and Degradation of All-Trans-β-Carotene During In-Vitro Digestion. *Food Sci. Hum. Wellness* **2021**, *10*, 370–374. [CrossRef]

30. Kopec, R.E.; Failla, M.L. Recent Advances in the Bioaccessibility and Bioavailability of Carotenoids and Effects of Other Dietary Lipophiles. *J. Food Compos. Anal.* **2018**, *68*, 16–30. [CrossRef]
31. Mapelli-Brahm, P.; Margier, M.; Desmarchelier, C.; Halimi, C.; Nowicki, M.; Borel, P.; Meléndez-Martínez, A.J.; Reboul, E. Comparison of the Bioavailability and Intestinal Absorption Sites of Phytoene, Phytofluene, Lycopene and β-Carotene. *Food Chem.* **2019**, *300*, 125232. [CrossRef]
32. Garrett, D.A.; Failla, M.L.; Sarama, R.J. Estimation of Carotenoid Bioavailability from Fresh Stir-Fried Vegetables Using an in Vitro Digestion/Caco-2 Cell Culture Model. *J. Nutr. Biochem.* **2000**, *11*, 574–580. [CrossRef] [PubMed]
33. Rocha, H.R.; Coelho, M.C.; Gomes, A.M.; Pintado, M.E. Carotenoids Diet: Digestion, Gut Microbiota Modulation, and Inflammatory Diseases. *Nutrients* **2023**, *15*, 2265. [CrossRef]
34. Kaulmann, A.; André, C.M.; Schneider, Y.J.; Hoffmann, L.; Bohn, T. Carotenoid and Polyphenol Bioaccessibility and Cellular Uptake from Plum and Cabbage Varieties. *Food Chem.* **2016**, *197*, 325–332. [CrossRef]
35. Rodriguez-Concepcion, M.; Avalos, J.; Bonet, M.L.; Boronat, A.; Gomez-Gomez, L.; Hornero-Mendez, D.; Limon, M.C.; Meléndez-Martínez, A.J.; Olmedilla-Alonso, B.; Palou, A.; et al. A Global Perspective on Carotenoids: Metabolism, Biotechnology, and Benefits for Nutrition and Health. *Prog. Lipid Res.* **2018**, *70*, 62–93. [CrossRef]
36. Eroglu, A.; Al'Abri, I.S.; Kopec, R.E.; Crook, N.; Bohn, T. Carotenoids and Their Health Benefits as Derived via Their Interactions with Gut Microbiota. *Adv. Nutr.* **2023**, *14*, 238–255. [CrossRef] [PubMed]
37. Viera, I.; Chen, K.; Ríos, J.J.; Benito, I.; Pérez-Gálvez, A.; Roca, M. First-Pass Metabolism of Chlorophylls in Mice. *Mol. Nutr. Food Res.* **2018**, *62*, 1800562. [CrossRef] [PubMed]
38. Kondo, T.; Kishi, M.; Fushimi, T.; Kaga, T. Acetic Acid Upregulates the Expression of Genes for Fatty Acid Oxidation Enzymes in Liver to Suppress Body Fat Accumulation. *J. Agric. Food Chem.* **2009**, *57*, 5982–5986. [CrossRef]
39. Zhang, D.; Jian, Y.P.; Zhang, Y.N.; Li, Y.; Gu, L.T.; Sun, H.H.; Liu, M.D.; Zhou, H.L.; Wang, Y.S.; Xu, Z.X. Short-Chain Fatty Acids in Diseases. *Cell Commun. Signal.* **2023**, *21*, 212. [CrossRef]
40. Agus, A.; Clément, K.; Sokol, H. Gut Microbiota-Derived Metabolites as Central Regulators in Metabolic Disorders. *Gut* **2021**, *70*, 1174–1182. [CrossRef]
41. O'Riordan, K.J.; Collins, M.K.; Moloney, G.M.; Knox, E.G.; Aburto, M.R.; Fülling, C.; Morley, S.J.; Clarke, G.; Schellekens, H.; Cryan, J.F. Short Chain Fatty Acids: Microbial Metabolites for Gut-Brain Axis Signalling. *Mol. Cell. Endocrinol.* **2022**, *546*, 111572. [CrossRef]
42. Dai, Z.; Li, Z.; Shi, E.; Nie, M.; Feng, L.; Chen, G.; Gao, R.; Zeng, X.; Li, D. Study on the Interaction Between Four Typical Carotenoids and Human Gut Microflora Using an In Vitro Fermentation Model. *J. Agric. Food Chem.* **2022**, *70*, 13592–13601. [CrossRef] [PubMed]
43. Li, Z.; Dai, Z.; Shi, E.; Wan, P.; Chen, G.; Zhang, Z.; Xu, Y.; Gao, R.; Zeng, X.; Li, D. Study on the Interaction between β-Carotene and Gut Microflora Using an in Vitro Fermentation Model. *Food Sci. Hum. Wellness* **2023**, *12*, 1369–1378. [CrossRef]
44. Djuric, Z.; Bassis, C.M.; Plegue, M.A.; Ren, J.; Chan, R.; Sidahmed, E.K.; Turgeon, D.K.; Ruffin, M.T.; Kato, I.; Sen, A. Colonic Mucosal Bacteria Are Associated with Inter-Individual Variability in Serum Carotenoid Concentrations. *J. Acad. Nutr. Diet.* **2018**, *118*, 606–616.e3. [CrossRef]
45. Rajoka, M.S.R.; Thirumdas, R.; Mehwish, H.M.; Umair, M.; Khurshid, M.; Hayat, H.F.; Phimolsiripol, Y.; Pallarés, N.; Martí-Quijal, F.J.; Barba, F.J. Role of Food Antioxidants in Modulating Gut Microbial Communities: Novel Understandings in Intestinal Oxidative Stress Damage and Their Impact on Host Health. *Antioxidants* **2021**, *10*, 1563. [CrossRef]
46. Yin, R.; Kuo, H.C.; Hudlikar, R.; Sargsyan, D.; Li, S.; Wang, L.; Wu, R.; Kong, A.N. Gut Microbiota, Dietary Phytochemicals, and Benefits to Human Health. *Curr. Pharmacol. Rep.* **2019**, *5*, 332–344. [CrossRef] [PubMed]
47. Tan, K.M.L.; Chee, J.; Lim, K.L.M.; Ng, M.; Gong, M.; Xu, J.; Tin, F.; Natarajan, P.; Lee, B.L.; Ong, C.N.; et al. Safety, Tolerability, and Pharmacokinetics of β-Cryptoxanthin Supplementation in Healthy Women: A Double-Blind, Randomized, Placebo-Controlled Clinical Trial. *Nutrients* **2023**, *15*, 2325. [CrossRef]
48. Schmidt, K.M.; Haddad, E.N.; Sugino, K.Y.; Vevang, K.R.; Peterson, L.A.; Koratkar, R.; Gross, M.D.; Kerver, J.M.; Comstock, S.S. Dietary and Plasma Carotenoids Are Positively Associated with Alpha Diversity in the Fecal Microbiota of Pregnant Women. *J. Food Sci.* **2021**, *86*, 602–613. [CrossRef]
49. Li, Y.; Cui, Y.; Lu, F.; Wang, X.; Liao, X.; Hu, X.; Zhang, Y. Beneficial Effects of a Chlorophyll-Rich Spinach Extract Supplementation on Prevention of Obesity and Modulation of Gut Microbiota in High-Fat Diet-Fed Mice. *J. Funct. Foods* **2019**, *60*, 103436. [CrossRef]
50. Alves, J.L.d.B.; Costa, P.C.T.d.; Sales, L.C.S.d.; Silva Luis, C.C.; Bezerra, T.P.T.; Souza, M.L.A.; Costa, B.A.; de Souza, E.L. Shedding Light on the Impacts of Spirulina Platensis on Gut Microbiota and Related Health Benefits. *Crit. Rev. Food Sci. Nutr.* **2024**, *65*, 2062–2075. [CrossRef]
51. Böhm, F.; Edge, R.; Truscott, G. Interactions of Dietary Carotenoids with Activated (Singlet) Oxygen and Free Radicals: Potential Effects for Human Health. *Mol. Nutr. Food Res.* **2012**, *56*, 205–216. [CrossRef] [PubMed]

52. Núñez-Gómez, V.; Gómez-Gallego, C.; Kolehmainen, M.; González-Barrio, R.; Periago, M.J. In Vitro Colonic Fermentation of Orange Peel Fibres: Effect on Microbial Modulation, SCFAs Production and Carotenoid Degradation. *LWT* **2025**, *219*, 117536. [CrossRef]
53. Böhm, V.; Lietz, G.; Olmedilla-Alonso, B.; Phelan, D.; Reboul, E.; Bánati, D.; Borel, P.; Corte-Real, J.; De Lera, A.R.; Desmarchelier, C.; et al. From Carotenoid Intake to Carotenoid Blood and Tissue Concentrations-Implications for Dietary Intake Recommendations. *Nutr. Rev.* **2021**, *79*, 544–573. [CrossRef]

Disclaimer/Publisher's Note: The statements, opinions and data contained in all publications are solely those of the individual author(s) and contributor(s) and not of MDPI and/or the editor(s). MDPI and/or the editor(s) disclaim responsibility for any injury to people or property resulting from any ideas, methods, instructions or products referred to in the content.

Algal Research 85 (2025) 103886



Contents lists available at ScienceDirect

Algal Research

journal homepage: www.elsevier.com/locate/algal





Low-carbon microalgae manufacturing is possible: Here's how and where

Rosangela Rodrigues Dias, Mariany Costa Deprá, Leila Queiroz Zepka, Eduardo Jacob-Lopes *

Bioprocess Intensification Group, Federal University of Santa Maria, UFSM, Roraima Avenue 1000, 97105-900 Santa Maria, RS, Brazil

ARTICLE INFO

Keywords:
Microalgae
Raceway pond
Whole-cell dried biomass
Energy footprint
Energy matrix
Life cycle assessment

ABSTRACT

This paper presents an environmental assessment for whole-cell microalgae dried biomass production in raceway pond systems – focusing on the primary energy source from the phototrophic processes. Greenhouse gas emissions from the whole-cell dried biomass of *Arthrospira platensis* and *Chlorella vulgaris* were calculated for the 193 countries in the world according to each country's electrical mix. The functional unit was based on the recommended protein intake for adult individuals (kg/person/year). The results reveal how different the impact of the electrical mix can be on CO_2e emissions associated with whole-cell microalgae biomass. Countries with lower CO_2e emissions associated with the whole-cell dried biomass of *Arthrospira platensis* and *Chlorella vulgaris*, such as Bhutan and Ethiopia, record around 16 and 29 kg CO_2e, respectively. Countries with higher emissions, such as Poland and Botswana, have emissions between 2683 and 6092 kg CO_2e, respectively. South America, followed by Europe and North America, is the continent with the most efficient countries for resilient and eco-friendly microalgae installations. The end result of this assessment is a holistic overview of countries and regions whose electrical mix can favor the environmental performance of energy-intensive processes and products.

1. Introduction

Microalgae are a nature-based resource with high biomass yield and nutrient-rich chemical composition. They are recognized for containing various important components, including lipids, carbohydrates, proteins, and a range of bioactive compounds with potential health benefits [1]. Of all these components, proteins are the most abundant, sometimes reaching a concentration greater than 50 % of their dry weight [2,3]. This makes them comparable to or even better than other protein sources, such as soy (40 %), chicken (21.4 %), and egg (12.6 %) [4]. Whole-cell dried biomass of *Arthrospira platensis* and *Chlorella vulgaris* recognized by the FDA as GRAS and validated by the WHO as "superfoods" are some of the best sources of microbial protein and have great potential to complement diets deficient in proteins or as an alternative to animal-based proteins [5].

However, making microalgae a regular and sustainable source of proteins would require facing some challenges, of which intensive electricity consumption is a key point. The electricity-intensive demands of microalgae upstream and downstream processes have a high economic and environmental cost [6–11]. In that regard, strategies are being explored to face this challenge, such as developing more electricity-efficient upstream and downstream technologies and using environmentally friendly electricity sources [10,12–14].

The use of environmentally friendly electricity sources is an imperative of the energy transition [15]. The energy transition to clean and renewable sources has led to an increase in the number of studies evaluating the impact of electrical choices on the life cycle of electricity-intensive processes and products [16–22]. This is because the environmental footprint of a process or product is directly related to how the electricity used is produced. Microalgae-based processes have already been evaluated in terms of electrical energy consumption based on coal, nuclear, hydro, wind, biomass, photovoltaic, biogas, natural gas, and waste [13,14,16,23–25]. However, this approach has a fundamental gap because companies extract electricity from local grids and emissions correspond to the specific use of these sources. Another issue is that the electricity of a region or country is not normally based on a single source. It is common for there to be a shortage or temporary unavailability of the majority electricity source and, when this occurs, other available sources are used to ensure a stable supply. Electric grid interconnection is a reality in most – if not all – countries and regions. In this sense, instead of assuming specific electricity sources, it would be essential and more comprehensive to consider the impact of the electrical mix on the life cycle of the processes and products [26].

Most studies such as those conducted by Morales et al. [16], Depra et al. [23], Rapa et al. [27], de Paula Diniz et al. [21], Medeiros et al. [14], Dias et al. [24,25], and Moradiya et al. [13] have focused on assessing the impact of consuming a single electricity source, while

* Corresponding author.
E-mail address: ejacoblopes@gmail.com (E. Jacob-Lopes).

https://doi.org/10.1016/j.algal.2024.103886
Received 11 June 2024; Received in revised form 21 December 2024; Accepted 22 December 2024
Available online 26 December 2024
2211-9264/© 2024 Elsevier B.V. All rights are reserved, including those for text and data mining, AI training, and similar technologies.

Nomenclature

CO_2e	Carbon Dioxide Equivalent
FDA	U.S. Food and Drug Administration
GWP	Global Warming Potential
GRAS	Generally Recognized As Safe
GHG	Greenhouse Gases
ISO	International Organization for Standardization
LCA	Life Cycle Assessment
LCI	Life Cycle Inventory
LCIA	Life-Cycle Impact Assessment
kWh/d	Kilowatt-hours per day
WHO	World Health Organization

others focus on a limited number of electricity mix scenarios [19,28–30], which do not reflect the full totality and diversity of existing electric mixes in the world. Although some studies on the environmental footprint of microalgae have been carried out considering the local and, sometimes, regional, electric mix such as those presented by Taelman et al. [31], Thomassen et al. [32], Porcelli et al. [33], De Bortoli [34], and Pechsiri et al. [12], to our knowledge, no assessment considers the impact of each world's country electricity mix on the life cycle of microalgae-based processes and products. A global-level assessment can avoid simplistic generalizations and clarify whether and to what extent each country's electricity mix can help solve problems related to microalgae life cycle emissions. Furthermore, it can provide a north star for companies and stakeholders in identifying eco-sustainable sites for large-scale microalgae cultivation. Therefore, this study focused on the cradle-to-gate life cycle assessment of the most important commercial microalgae product – whole-cell dried biomass – and aims to present a carbon footprint analysis based on current scenarios of the electric mix of the world's 193 countries. This study – the first of its kind – could help identify countries best suited for inherently electricity-intensive facilities, processes, and products.

2. Material and methods

2.1. Life cycle assessment (LCA)

The LCA methodology standardized by ISO 14040 was adopted to quantify the greenhouse gas (GHG) emissions of whole-cell microalgae dried biomass production according to the electrical mix of each country in the world [35]. The LCA covered the goal and scope definition (I), inventory analysis (II), impact assessment (III), and results interpretation (IV).

2.1.1. Goal and scope definition

The study's objective was to evaluate the carbon footprint – a measure of greenhouse gas (GHG) emissions – of the two main commercial microalgae products under the electrical mix scenarios of each country in the world. The commercial products considered were the whole-cell dried biomass from *Chlorella vulgaris* and *Arthrospira platensis*. Data for analyzing the technological routes of the biological products were obtained from Depra et al. [23], Dias et al. [24], and Dias et al. [25]. Data relating to the electrical mix of each country were obtained from Our World in Data (OWID) [36]. The different sources of electricity that made up each country's electrical mix included coal, gas, oil, nuclear, biomass, waste, hydro, solar, wind, and other renewable energies (which include geothermal, tidal, and wave).

2.1.2. Functional unit and system boundaries

The study considered a functional unit of 20 kg/person/year of microalgae-based whole-cell dried biomass [37]. This functional unit was established based on the recommended protein intake for adult individuals (55 g of protein per day) [37–40]. System boundaries were defined using a cradle-to-gate approach, i.e., it is a partial assessment of the whole-cell microalgae-dried biomass life cycle that excludes product distribution, use, and disposal [41]. Only emissions associated with electricity consumption were accounted for because they represent the majority, if not almost the entire fraction of the environmental footprint of microalgae products [23]. The layout of system boundaries is shown in Fig. 1.

2.1.3. Life cycle inventory (LCI)

The microalgae species (*Chlorella vulgaris* and *Arthrospira platensis*), the cultivation system (raceway pond), and the final product (whole-cell dried biomass) were chosen to simulate the process and the most important commercial microalgae product [42]. The inventory data was obtained from biotechnological processes consolidated by classic literature references. The inputs and outputs of whole-cell dried biomass production from *Chlorella vulgaris* and *Arthrospira platensis* are shown in Table 1.

2.1.4. Life-cycle impact assessment (LCIA)

The carbon footprint in this study refers to the quantification of greenhouse gas (GHG) emissions generated from energy demand during the processes involved in whole-cell dried biomass production. Based on the life-cycle inventory data (Section 2.1.3), the carbon footprint of whole-cell dried biomass from *Chlorella vulgaris* and *Arthrospira platensis* was calculated according to the ReCiPe2016 method [43], using the Global Warming Potential for a time horizon of 100 years (GWP) as generically described in Eq. (1), expressed in kilograms of carbon dioxide equivalent (kg CO_2e). The ReCiPe2016 method for calculating the carbon footprint is particularly advantageous because it implements characterization factors that are representative of the global scale. The use of this method is appropriate once greenhouse gas (GHG) emissions impact the climate regardless of the location of their emissions. To calculate the carbon footprint, first, the specific contribution of each electricity source to the electricity mix of each country was defined. Then, based on this information, it was discovered proportionally how much of the energy consumption inventory of the whole-cell dried biomass life cycle corresponded to each of these electricity sources. These values multiplied by their specific characterization factors (kg CO_2e/kWh) and added together resulted in the CO_2e emissions from whole-cell dried biomass intended for per capita consumption per year per country. The Supplementary Material (Table S1) presents specific characterization factors by electricity source.

$$GWP = \Sigma\, GWP_i \times m_i \quad (1)$$

where GWP is the global warming potential, $_i$ is the time horizon of 100 years, GWP_i is the characterization factors for the substance $_i$ (kg e), and m_i is the emission mass of the substance $_i$ (kg), expressed in kg CO_2e.

2.1.5. LCA interpretation

LCI and LCIA data were considered together to extract insights that can contribute to a broader understanding of the role of each country's electrical mix in inherently energy-intensive processes, such as microalgae, identifying environmentally more efficient and inefficient countries. The characterized values for the environmental impact of whole-cell microalgae dried biomass production under the 193 electrical mix scenarios can be consulted through the link presented in Fig. 2 and Fig. 3.

3. Results and discussion

The carbon dioxide-equivalent (CO_2e) emissions for whole-cell dried biomass from *Arthrospira platensis* and *Chlorella vulgaris* based on a per capita functional unit per year of protein under the electricity mix

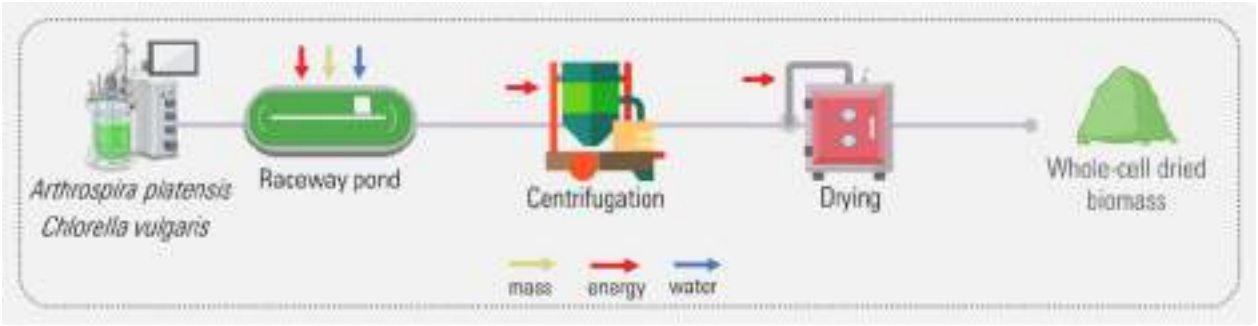


Fig. 1. Cradle-to-Gate limits for whole-cell microalgae dried biomass LCA.

Table 1
Inputs and outputs of the whole-cell dried biomass production from *Chlorella vulgaris* and *Arthrospira platensis*. Adapted from Ref. [23–25].

Process	Unit	Whole-cell dried biomass by		Reference
		Arthrospira platensis	*Chlorella vulgaris*	
Cultivation				
Input				
Raceway pond	m^3	113.62	212.75	[23]
Electric energy for paddle wheel	kWh/d	1472.5	2757.2	[23]
Electric energy for water pumping	kWh/d	272.6	510.6	[23]
Electric energy for CO_2 injection	kWh/d	900.96	1684.98	[23]
CO_2 consumption	kg	72.72	72.72	[23–25]
Water evaporation	m^3	14.77	27.65	[23]
Biomass productivity	kg/m^3/d	0.32	0.20	[23–25]
Output				
Algae liquid	kg	253.8	235.2	[23–25]
Harvest				
Input				
Power consumption centrifugation	kWh/d	142.0	265.9	[24,25]
Drying				
Input				
Wet biomass	kg	190.2	176.4	[23–25]
Spray-dryer	kWh/d	185.5	170.4	[24,25]
Output				
Whole-cell dried biomass	kg	20.0	20.0	[23–25]
Total energy	kWh/d	2973.56	5389.08	

scenarios by country are shown in Figs. 2 and 3. Firstly, considering the total energy consumption of 2973.56 kWh/d for *Arthrospira platensis* and 5389.08 kWh/d for *Chlorella vulgaris* (Table 1), it can be observed that the energy consumption for *Chlorella vulgaris* is approximately 1.8 times higher. Eventually, regardless of the country, as shown in Figs. 2 and 3, respectively, CO_2e emissions are higher for the consumption of whole-cell dried biomass of *Chlorella vulgaris*. This can be attributed to the following key points: (i) lower biomass productivity and (ii) lower protein content, which proportionally increases the amount of biomass required to meet the recommended protein intake. Therefore, under the assumptions of this study, in terms of microalgae species, there is a margin for a more eco-conscious choice. However, it is important to recognize that both the biomass productivity and the protein content of species such as *Chlorella vulgaris* and *Arthrospira platensis* can vary and be influenced by various factors, such as the cultivation conditions and the cultivation system. Nonetheless, there is a consistent scientific literature on the protein content of these microalgae, indicating that *Arthrospira platensis* has between 55 and 70 % and *Chlorella vulgaris* between 42 and 55 % protein based on dry weight [2,3,44–47].

Now, regarding the impact of the electrical mix, it is no surprise how different the results can be when considering each country's electrical mix. Countries with the lowest CO_2e emissions for whole-cell dried biomass from *Arthrospira platensis* and *Chlorella vulgaris* include Bhutan, the Democratic Republic of Congo, Ethiopia, Lesotho, and the Central African Republic with 16 and 29 kg of CO_2e, Paraguay with 21 and 38 kg CO_2e, Iceland with 38 and 68 kg CO_2e, Norway with 41 and 74 kg CO_2e, and Costa Rica with 78 and 141 kg CO_2e, respectively. These countries have some common characteristics that explain these results. Among them are: (i) a geography favorable to the production of renewable energy, (ii) a strong dependence on renewable energy sources, such as in Iceland (hydroelectric), Norway (hydroelectric), Paraguay (hydroelectric), and Costa Rica (hydroelectric), (iii) strict environmental policies, as in Norway and Iceland, which encourage investments in cleaner technologies, and/or (iv) a low industrialization level, observed in countries such as Bhutan, the Democratic Republic of Congo, Ethiopia, Lesotho, and the Central African Republic.

In contrast, among those with the highest CO_2e emissions for whole-cell dried biomass from *Arthrospira platensis* and *Chlorella vulgaris* are Indonesia with 2608 and 4726 kg CO_2e, Kazakhstan with 2648 and 4800 kg CO_2e, Poland with 2707 and 4906 kg CO_2e, India with 2732 and 4952 kg CO_2e, South Africa with 3066 and 5556 kg CO_2e, Kosovo with 3334 and 6043 kg CO_2e, and Botswana with 3361 and 6092 kg CO_2e, respectively. These countries, as well as others that share a high CO_2e metric, have in common (i) a dependence on fossil fuels, such as Poland, Kosovo, Botswana, and South Africa, (ii) an abundance of fossil resources, as seen in Indonesia and India, which have vast coal reserves, Kazakhstan, which has large oil and natural gas reserves, and South Africa, which is one of the largest coal producers in the world, and/or (iii) energy infrastructure developed based on fossil fuel technologies. Existing infrastructure and abundant fossil fuels make the transition to a cleaner electricity mix difficult.

Consequently, the transition to a low-carbon economy, especially in whole-cell dried biomass production from *Arthrospira platensis* and *Chlorella vulgaris*, involves a series of trade-offs that must be carefully considered. We can highlight three critical trade-offs. The first trade-off concerns renewable energy and existing infrastructure. Some countries stand out for their infrastructure and predominance of renewable energy sources, and others face the challenge of balancing the transition to cleaner energy sources with the limitations imposed by their already established infrastructures, built with fossil fuel-based technologies. The transition to renewable energy technologies requires significant investment and faces economic and political resistance. The second trade-off highlights the influence of geography and favorable climate in contrast to remote locations. Locating in a region or country with a climate favorable to renewable energy production, as in the case of Bhutan, can help to produce more sustainable whole-cell microalgae dried biomass; but, the limited logistics infrastructure can increase transportation costs and access to consumer markets. The third trade-off involves the relationship between the consumer market and carbon footprint. Proximity to robust consumer markets, such as North America and Europe, offers logistical and economic advantages. However,

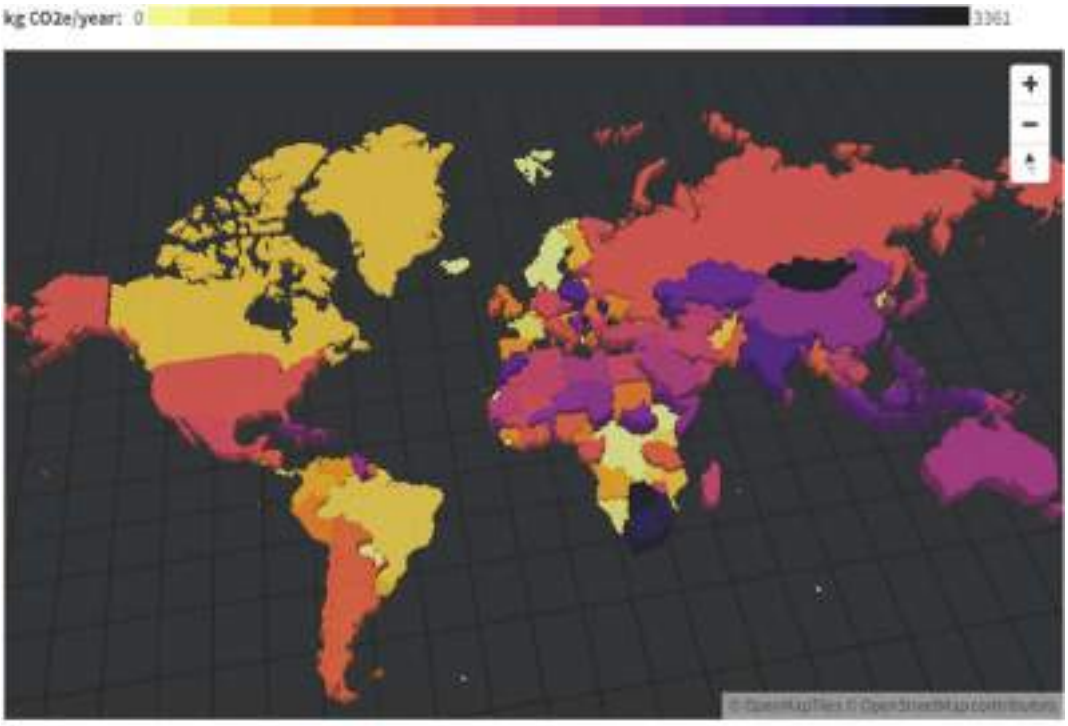


Fig. 2. CO_2e emissions for per capita consumption of whole-cell dried biomass from *Arthrospira platensis*. Link to interactive map: https://public.flourish.studio/visualisation/16425552/



Fig. 3. CO_2e emissions for per capita consumption of whole-cell dried biomass from *Chlorella vulgaris*. Link to interactive map: https://public.flourish.studio/visualisation/16427175/

producing biomass in energetically cleaner countries, distant from the main consumer markets, can result in significant additional emissions due to international transport. In sum, it is noteworthy that, managing trade-offs means strategic balance, that is, developing an integrated approach, which involves not only the country's electrical mix.

Thus, considering the trade-offs mentioned, some countries emerge

as promising options for producing whole-cell dried biomass with low carbon emissions. Norway and Iceland, for example, stand out for their predominantly renewable electrical mix, strict environmental policies, and transport infrastructure; however, the remote location concerning the main consumer markets is a shortcoming. This disadvantage is to some extent mitigated by favorable foreign trade policies. Likewise, Costa Rica appears as an option and presents the advantage of a predominantly renewable electrical mix and proximity to consumer markets in North America. However, the mountainous topography and less developed transport infrastructure are constraints that limit it. Other countries not discussed here, such as Paraguay and Sweden, also present a favorable combination for more sustainable whole-cell dried biomass production. However, it is crucial to recognize that each country has specific nuances and challenges that need to be considered in a more detailed analysis. Furthermore, not discussed in this work, but exhaustively investigated, it is noteworthy that the geographic position and local climate are crucial not only for renewable energy generation but also for microalgae cultivation. Microalgae production is commonly carried out outdoors, making climatic elements, such as solar irradiation, temperature, and photoperiod, determining factors that directly impact the productivity of photoautotrophic systems [48–51].

Now, from a continental perspective, bringing together the countries that make up each continent on Earth, South America, followed by Europe and North America, are strategic regions with a set of countries that are more eco-sustainable for energy-intensive facilities. The whole-cell dried biomass production from *Arthrospira platensis* and *Chlorella vulgaris* capable of meeting per capita protein consumption per year has CO_2e emissions in the order of 534 and 968 kg CO_2e for South America, 1119 and 2028 kg CO_2e for Europe, 1342 and 2432 kg CO_2e for North America, 1890 and 3425 kg CO_2e for Africa, 1982 and 3592 kg CO_2e for Oceania, and 2238 and 4057 kg CO_2e for Asia, respectively. The highest CO_2e emissions associated with the continent of Asia and Oceania are clearly because most of the electricity generated comes from fossil resources such as coal, oil, and natural gas. Throughout history, in Asia and Oceania, fossil resources have been an important source of energy due to their abundant availability and low cost, but in recent years, both have sought to diversify their sources in the face of environmental pressures.

Additionally, although it may seem intuitive that the number of countries included in each continent can influence the comparison of CO_2e emissions, this relationship is not always direct. Noteworthy, several factors can influence CO_2e emissions on each continent. An

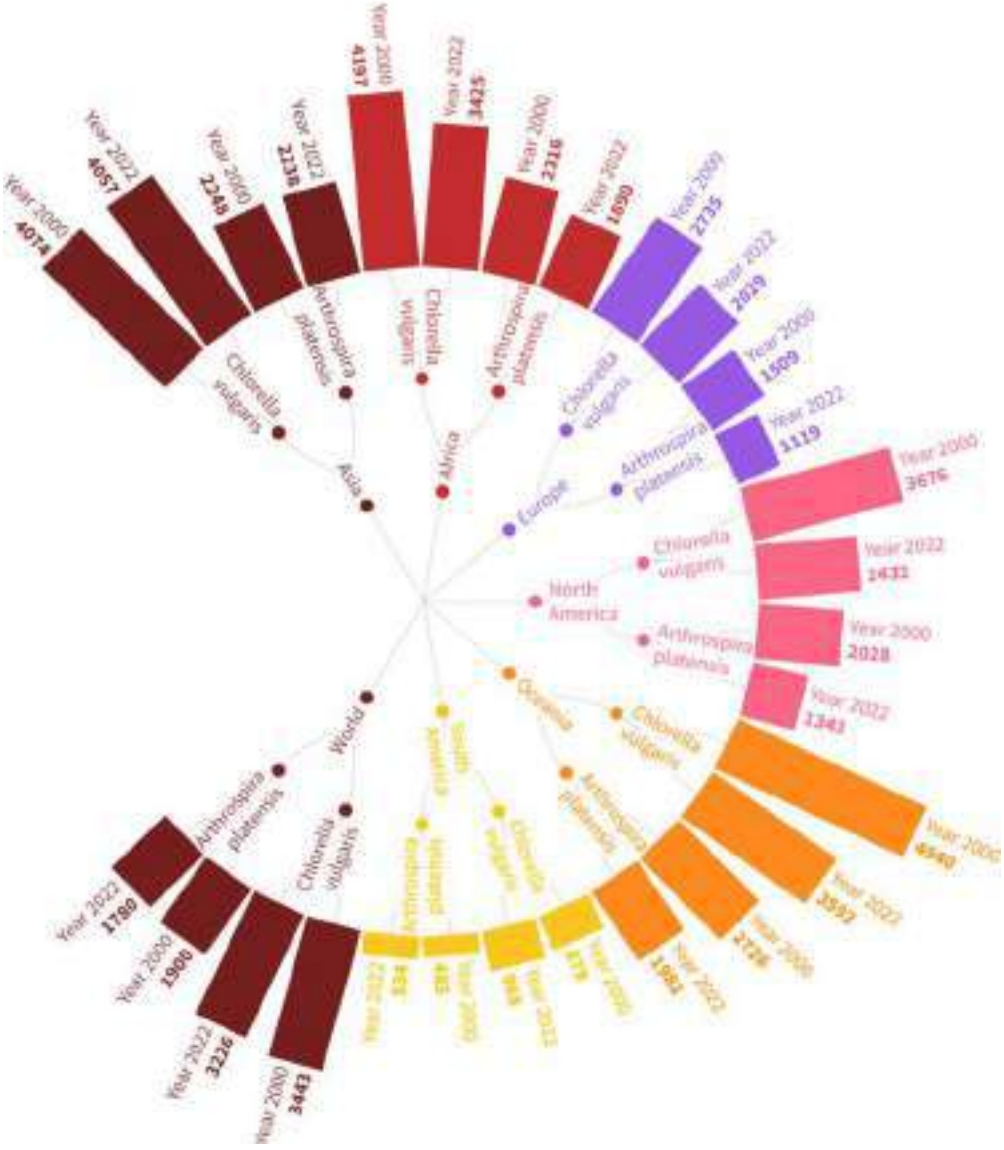


Fig. 4. kg CO_2e/year for whole-cell dried biomass under electrical mix scenarios in 2000 and 2022. Link to interactive map: https://public.flourish.studio/visualisation/16439509/

example of this is the size and population of countries. By way of example, even though Europe has a smaller geographical area but more countries than South America, a denser population and a more industrialized economy result in higher emissions. In this sense, the comparison between continents is valid; however, a clear understanding of the limitations and influences of the number of countries included in each continent on the calculated averages would only be possible in a more extensive and detailed analysis.

Still, from past to present, Fig. 4 shows the impact on CO_2e emissions of whole-cell microalgae dried biomass under the scenario of the electrical mix of the continents and the world in 2000 and 2022. In 2022, compared to 2000, there was a prominent increase in electricity generation through renewable energy sources [36]. As evidenced by our data, this progress was reflected in a reduction in CO_2e emissions and, consequently, in the emissions of the processes and products powered by them. This reduction in CO_2e emissions is particularly notable in the continents of North America (34 %), Oceania (27 %), Europe (26 %), and Africa (18 %). In contrast, although the electrical mix is predominantly renewable and clean in South America, there has been an increase in the consumption of fossil resources, especially natural gas. This resulted in an increase of around 10 % in CO_2e emissions from processes and products fed in this continental electrical mix scenario. This can be explained, in part, by the economic growth of some South American countries such as Brazil. Economic growth is often accompanied by an increase in demand for electricity, especially in the commercial and industrial sectors. As per capita income increases and living standards improve, companies expand their operations, invest in new facilities and equipment, and consequently, consume more electricity to power these production processes. Associated with this, when renewable electricity generation does not keep up with demand, the increase in electricity consumption from fossil fuels is notable. This occurs mainly as a way to complement the intermittent generation of renewable energy such as solar and wind.

Globally, considering the global electrical mix scenario, a reduction in CO_2e emissions of around 6 % is observed. Although this reduction may seem modest at first glance, considering the elapsed time, the scene is set for a transition to cleaner and renewable electrical matrices under a meteoric rise in all countries, especially those that have historically generated energy from fossil resources. Technological advances, government policies, and international commitments have encouraged countries to invest in sustainable infrastructure. The decline in CO_2e emissions under the global scenario shows that energy transition initiatives are starting to produce tangible results.

Finally, although the progressive elimination of fossil resources is globally clear, it is interesting to follow how currently the countries' electrical mix can influence the sustainability metrics of energy-intensive microalgae processes and products. To our knowledge, this is the only work in the literature to provide the impact of the electrical mix of each country in the world on the CO_2e metrics associated with a commercial microalgae-based product. However, this is just a primary assessment and the tip of the iceberg; many other issues must be carefully evaluated to make microalgae-based processes cleaner, as this is a multifaceted challenge that requires integrated approaches, involving not only the strategic location of facilities. Furthermore, although the results obtained in this study provide a north star on strategic location for energy-intensive companies, some limitations should be acknowledged. In particular, a detailed environmental life cycle costing analysis was not performed and represents an important part of this puzzle. A subsequent study on the economic life cycle in the world's electricity mix scenarios could deepen the understanding and validate the findings presented here.

4. Conclusions

This study evaluated CO_2e emissions associated with the whole-cell dried biomass of *Arthrospira platensis* and *Chlorella vulgaris* by country, according to the electricity mix, from a cradle-to-gate perspective, to provide a panorama of strategic locations for energy-intensive microalgae facilities. The difference between the lowest (16 kg CO_2e/year) and the highest (2683 kg CO_2e/year) CO_2e emission value for the whole-cell dried biomass of *Arthrospira platensis* is approximately 168 times. For *Chlorella vulgaris* it is approximately 210 times. The analysis also showed that, in continental terms, South America is the region with the lower average values of CO_2e emissions. A closer look at the countries with the highest CO_2e emissions for whole-cell dried biomass allows us to infer that most live in the shadow of infrastructures consistently established based on fossil resources. Finally, the study provides quick and valuable feedback from countries that can favor the environmental performance of microalgae-based processes and products. However, this is only a primary assessment; many other issues must be carefully considered to geolocate suitable locations for successfully implementing low-carbon microalgae facilities.

CRediT authorship contribution statement

Rosangela Rodrigues Dias: Writing – original draft, Methodology, Data curation, Conceptualization. **Mariany Costa Deprá:** Methodology, Data curation. **Leila Queiroz Zepka:** Supervision, Funding acquisition. **Eduardo Jacob-Lopes:** Writing – review & editing, Project administration, Conceptualization.

Statement of informed consent, human/animal rights

No conflicts, informed consent, or human or animal rights are applicable to this study.

Declaration of competing interest

The authors declare that they have no known competing financial interests or personal relationships that could have appeared to influence the work reported in this paper.

Acknowledgement

The authors would like to thank the National Council for Scientific and Technological Development (CNPq) – Brazil, and the Coordination of Improvement of Higher Education Personnel (CAPES), Finance Code 001.

Appendix A. Supplementary data

Supplementary data to this article can be found online at https://doi.org/10.1016/j.algal.2024.103886.

Data availability

Data will be made available on request.

References

[1] A. Kusmayadi, Y.K. Leong, H.W. Yen, C.Y. Huang, J.S. Chang, Microalgae as sustainable food and feed sources for animals and humans–biotechnological and environmental aspects, Chemosphere 271 (2021) 129800.
[2] Â.P. Matos, Microalgae as a potential source of proteins, in: Proteins: Sustainable Source, Processing and Applications, Academic Press, 2019, pp. 63–96.
[3] Y. Wang, S.M. Tibbetts, P.J. McGinn, Microalgae as sources of high-quality protein for human food and protein supplements, Foods 10 (12) (2021) 3002.
[4] R.R. Balandrán-Quintana, A.M. Mendoza-Wilson, G.R.C. Montfort, J.Á. Huerta-Ocampo, Plant-based proteins, in: Proteins: Sustainable Source, Processing and Applications, Academic Press, 2019, pp. 97–130.
[5] M. Verni, C. Demarinis, C.G. Rizzello, E. Pontonio, Bioprocessing to preserve and improve microalgae nutritional and functional potential: novel insight and perspectives, Foods 12 (5) (2023) 983.

[6] A.H. Shimako, L. Tiruta-Barna, Y. Pigné, E. Benetto, T.N. Gutiérrez, P. Guiraud, A. Ahmadi, Environmental assessment of bioenergy production from microalgae based systems, J. Clean. Prod. 139 (2016) 51–60.
[7] H. Alishah Aratboni, N. Rafiei, R. Garcia-Granados, A. Alemzadeh, J.R. Morones-Ramírez, Biomass and lipid induction strategies in microalgae for biofuel production and other applications, Microb. Cell Factories 18 (2019) 1–17.
[8] D.Y.Y. Tang, K.S. Khoo, K.W. Chew, Y. Tao, S.H. Ho, P.L. Show, Potential utilization of bioproducts from microalgae for the quality enhancement of natural products, Bioresour. Technol. 304 (2020) 122997.
[9] T.L.D. Silva, P. Moniz, C. Silva, A. Reis, The role of heterotrophic microalgae in waste conversion to biofuels and bioproducts, Processes 9 (7) (2021) 1090.
[10] L. Gurreri, M.C. Rindina, A. Luciano, S. Lima, F. Scargiali, D. Fino, G. Mancini, Environmental sustainability of microalgae-based production systems: roadmap and challenges towards the industrial implementation, Sustain. Chem. Pharm. 35 (2023) 101191.
[11] A. Herrera, G. D'Imporzano, F.G.A. Fernandez, F. Adani, Sustainable production of microalgae in raceways: nutrients and water management as key factors influencing environmental impacts, J. Clean. Prod. 287 (2021) 125005.
[12] J.S. Pechsiri, J.B.E. Thomas, N. El Bahraoui, F.G.A. Fernandez, J. Chaouki, S. Chidami, F. Gröndahl, Comparative life cycle assessment of conventional and novel microalgae production systems and environmental impact mitigation in urban-industrial symbiosis, Sci. Total Environ. 854 (2023) 158445.
[13] K.K. Moradiya, K.V. Marathe, Life cycle assessment (LCA) of marine microalgae cultivation and harvesting process for the Indian context, Sustain. Energy Technol. Assess. 56 (2023) 103063.
[14] D.L. Medeiros, Í.T.A. Moreira, Microalgae biomass production from cultivation in availability and limitation of nutrients: the technical, environmental and economic performance, J. Clean. Prod. 370 (2022) 133538.
[15] S. Wei, W. Jiandong, H. Saleem, The impact of renewable energy transition, green growth, green trade and green innovation on environmental quality: evidence from top 10 green future countries, Front. Environ. Sci. 10 (2023) 1076859.
[16] M. Morales, A. Hélias, O. Bernard, Optimal integration of microalgae production with photovoltaic panels: environmental impacts and energy balance, Biotechnol. Biofuels 12 (1) (2019) 1–17.
[17] M. van der Meide, C. Harpprecht, S. Northey, Y. Yang, B. Steubing, Effects of the energy transition on environmental impacts of cobalt supply: a prospective life cycle assessment study on future supply of cobalt, J. Ind. Ecol. 26 (5) (2022) 1631–1645.
[18] C. Reinert, S. Deutz, H. Minten, L. Dörpinghaus, S. von Pfingsten, N. Baumgärtner, A. Bardow, Environmental impacts of the future German energy system from integrated energy systems optimization and life cycle assessment, in: Computer Aided Chemical Engineering vol. 48, Elsevier, 2020, pp. 241–246.
[19] A.H. Tarighaleslami, S. Kambadur, J.R. Neale, M.J. Atkins, M.R. Walmsley, Sustainable Energy Transition toward Renewable Energies in the New Zealand Dairy Industry: An Environmental Life Cycle Assessment, 2019.
[20] Y. Man, J. Li, M. Hong, Y. Han, Energy transition for the low-carbon pulp and paper industry in China, Renew. Sust. Energ. Rev. 131 (2020) 109998.
[21] D. de Paula Diniz, M. Carvalho, R. Abrahao, Greenhouse gas accounting for the energy transition in a brewery, Environ. Prog. Sustain. Energy 40 (2) (2021) e13563.
[22] I.C. Gil-García, M.S. García-Cascales, H. Dagher, A. Molina-García, Electric vehicle and renewable energy sources: motor fusion in the energy transition from a multi-indicator perspective, Sustainability 13 (6) (2021) 3430.
[23] M.C. Depra, I.A. Severo, A.M. dos Santos, L.Q. Zepka, E. Jacob-Lopes, Environmental impacts on commercial microalgae-based products: sustainability metrics and indicators, Algal Res. 51 (2020) 102056.
[24] R.R. Dias, M.C. Deprá, L.Q. Zepka, E. Jacob-Lopes, Roadmap to net-zero carbon emissions in commercial microalgae-based products: environmental sustainability and carbon offset costs, J. Appl. Phycol. 34 (3) (2022) 1255–1268.
[25] R.R. Dias, M.C. Deprá, L.Q. Zepka, E. Jacob-Lopes, *In silico* study of hybrid renewable energy in microalgae facilities: a path towards net-zero emissions, Algal Res. 63 (2022) 102661.
[26] B. Alamri, M.A. Hossain, M.J. Asghar, Electric power network interconnection: a review on current status, future prospects and research direction, Electronics 10 (17) (2021) 2179.
[27] M. Rapa, L. Gobbi, R. Ruggieri, Environmental and economic sustainability of electric vehicles: life cycle assessment and life cycle costing evaluation of electricity sources, Energies 13 (23) (2020) 6292.
[28] Y. Wu, D. Su, LCA of an industrial luminaire using product environmental footprint method, J. Clean. Prod. 305 (2021) 127159.
[29] Q. Chen, X. Lai, H. Gu, X. Tang, F. Gao, X. Han, Y. Zheng, Investigating carbon footprint and carbon reduction potential using a cradle-to-cradle LCA approach on lithium-ion batteries for electric vehicles in China, J. Clean. Prod. 369 (2022) 133342.
[30] P. Ghisellini, R. Passaro, S. Ulgiati, Environmental assessment of multiple "cleaner electricity mix" scenarios within just energy and circular economy transitions, in Italy and Europe, J. Clean. Prod. 388 (2023) 135891.
[31] S.E. Taelman, S. De Meester, L. Roef, M. Michiels, J. Dewulf, The environmental sustainability of microalgae as feed for aquaculture: a life cycle perspective, Bioresour. Technol. 150 (2013) 513–522.
[32] G. Thomassen, M. Van Dael, S. Van Passel, The potential of microalgae biorefineries in Belgium and India: an environmental techno-economic assessment, Bioresour. Technol. 267 (2018) 271–280.
[33] R. Porcelli, F. Dotto, L. Pezzolesi, D. Marazza, N. Greggio, S. Righi, Comparative life cycle assessment of microalgae cultivation for non-energy purposes using different carbon dioxide sources, Sci. Total Environ. 721 (2020) 137714.
[34] A. De Bortoli, Environmental performance of shared micromobility and personal alternatives using integrated modal LCA, Transp. Res. Part D: Transp. Environ. 93 (2021) 102743.
[35] International Standard Organization, ISO-14040: Environmental Management–life Cycle Assessment–principles and Framework, 2006.
[36] H. Ritchie, P. Rosado, M. Roser, Electricity Mix, Our World in Data, 2023.
[37] D.A. Dutra, M.C. Deprá, R.R. Dias, L.Q. Zepka, E. Jacob-Lopes, Ensuring nutrition and food safety within planetary boundaries: the role of microalgae-based ingredients in sustainable food chain, J. Appl. Phycol. (2024) 1–20.
[38] FAO - Food and Agriculture Organization of the United Nations, Fats and oils in human nutrition, in: Report of an FAQ Expert Consultation, 1994 (ISBN 92-5-103621-7).
[39] FAO - Food and Agriculture Organization of the United Nations, Dietary protein quality evaluation in human nutrition, in: Report of an FAQ Expert Consultation. FAO Food Nutr Pap. 92, 2013, pp. 1–66 (PMID: 26369006).
[40] WHO - World Health Organization, Vitamin and Mineral Requirements in Human Nutrition, World Health Organization, 2004.
[41] E. Jacob-Lopes, L.Q. Zepka, M.C. Deprá, Sustainability Metrics and Indicators of Environmental Impact: Industrial and Agricultural Life Cycle Assessment, Elsevier, 2021.
[42] E. Jacob-Lopes, M.M. Maroneze, M.C. Deprá, R.B. Sartori, R.R. Dias, L.Q. Zepka, Bioactive food compounds from microalgae: an innovative framework on industrial biorefineries, Curr. Opin. Food Sci. 25 (2019) 1–7.
[43] M.A. Huijbregts, Z.J. Steinmann, P.M. Elshout, G. Stam, F. Verones, M. Vieira, R. Van Zelm, ReCiPe2016: a harmonised life cycle impact assessment method at midpoint and endpoint level, Int. J. Life Cycle Assess. 22 (2017) 138–147.
[44] P. Geada, C. Moreira, M. Silva, R. Nunes, L. Madureira, C.M. Rocha, J.A. Teixeira, Algal proteins: production strategies and nutritional and functional properties, Bioresour. Technol. 332 (2021) 125125.
[45] M.F. El Basuini, A.A. Khattab, S.H.A. Hafsa, I.I. Teiba, N.E. Elkassas, E.H. El-Bilawy, S.E.S. Atia, Impacts of algae supplements (*Arthrospira* & *Chlorella*) on growth, nutrient variables, intestinal efficacy, and antioxidants in New Zealand white rabbits, Sci. Rep. 13 (1) (2023) 7891.
[46] B. Prandi, F. Boukid, S. Van De Walle, S. Cutroneo, J. Comaposada, G. Van Royen, M. Castellari, Protein quality and protein digestibility of vegetable creams reformulated with microalgae inclusion, Foods 12 (12) (2023) 2395.
[47] S. Villaró, G. Acién, J. Alarcón, Á. Ruiz, L. Rodríguez-Chikri, E. Viviano, T. Lafarga, A zero-waste approach for the production and use of *Arthrospira platensis* as a protein source in foods and as a plant biostimulant in agriculture, J. Appl. Phycol. 35 (6) (2023) 2619–2630.
[48] B.J. Boruff, N.R. Moheimani, M.A. Borowitzka, Identifying locations for large-scale microalgae cultivation in Western Australia: a GIS approach, Appl. Energy 149 (2015) 379–391.
[49] S.F. Siqueira, M.M. Maroneze, R.R. Dias, R.G. Vendruscolo, R. Wagner, C.R. de Menezes, E. Jacob-Lopes, Mapping the performance of photobioreactors for microalgae cultivation: geographic position and local climate, J. Chem. Technol. Biotechnol. 95 (9) (2020) 2411–2420.
[50] R.R. Dias, P. Lasta, R.G. Vendruscolo, R. Wagner, L.Q. Zepka, E. Jacob-Lopes, Mapping the performance of photobioreactors for microalgae cultivation. Part II: equatorial and tropical climate zone, J. Chem. Technol. Biotechnol. 96 (3) (2021) 613–621.
[51] R.R. Dias, P.A. da Silva, M.C. Deprá, B. Deprá, R. Wagner, L.Q. Zepka, E. Jacob-Lopes, Mapping the performance of photobioreactors for microalgae cultivation. Part III: subtropical and mid-latitudes climate zone, J. Chem. Technol. Biotechnol. 98 (6) (2023) 1497–1519.

colorants

MDPI

Article

Trade-Off Between Growth Regimes in *Chlorella vulgaris*: Impact on Carotenoid Production

Patrícia Acosta Caetano, Pricila Pinheiro Nass, Mariany Costa Deprá, Tatiele Casagrande do Nascimento, Eduardo Jacob-Lopes and Leila Queiroz Zepka *

Food Science and Technology Department, Federal University of Santa Maria, UFSM, Roraima Avenue 1000, Santa Maria 97105-900, Brazil; pati.caetano98@gmail.com (P.A.C.); pricila.nass@gmail.com (P.P.N.); tatielecasagrande@gmail.com (T.C.d.N.)

* Correspondence: zepkaleila@yahoo.com.br; Tel.: +55-55-3220-8822

Abstract: With the increasing awareness of socio-environmental issues, a global trend has emerged emphasizing the valorization of natural ingredients that promote health and well-being within sustainable production systems, such as microalgae-based carotenoids. Currently, little is understood about the correlation between biomass productivity and carotenoid content, which is a fundamental parameter for facilitating the immediate expansion of microalgae bioprocesses and ensuring the availability and industrial viability of these compounds. In this context, this study aims to investigate the carotenoid profile of *Chlorella vulgaris* through growth curve experiments conducted under photoautotrophic and heterotrophic regimes. Additionally, a trade-off analysis was performed for the production of carotenoids from microalgae. Carotenoids were quantified using high-performance liquid chromatography coupled with diode array and mass spectrometry detectors (HPLC-PDA-MS/MS). The performance of kinetic phases and energy demands across growth regimes was assessed to provide insights into production trade-offs. The results indicated that a total of 22 different carotenoids were identified in all the extracts. The all-*trans*-lutein and all-*trans*-β-carotene were the majority compounds. The total carotenoid content of *Chlorella vulgaris* revealed significant differences in the kinetic phases of carotenoid production, indicating that carotenoid volumetric production is only viable if the cultures are conducted until the log and stationary phases, based on the function of the biomass volumetric production (weight.volume^{-1}). Therefore, the best trade-off for the process was to provide photoautotrophic growth until the exponential phase (log). Under this condition, the maximum carotenoid and lutein content was 2921.70 μg.L^{-1}, reaching a maximum cell biomass of 1.46 g.L^{-1}. From an environmental/economic point of view, the energy demand was 7.74 kWh.L^{-1}. Finally, the scientific advances achieved in this study provide a holistic view of the influence of the main cultivation methods on the production of microalgae carotenoids, suggesting a viable initial direction for different industrial applications.

Keywords: heterotrophic; microalgae; natural colorants; photoautotrophic

check for updates

Citation: Caetano, P.A.; Nass, P.P.; Deprá, M.C.; Nascimento, T.C.d.; Jacob-Lopes, E.; Zepka, L.Q. Trade-Off Between Growth Regimes in *Chlorella vulgaris*: Impact on Carotenoid Production. *Colorants* **2024**, *3*, 282–297. https://doi.org/10.3390/colorants3040020

Academic Editor: Dennis K.P Ng

Received: 31 July 2024
Revised: 18 October 2024
Accepted: 26 October 2024
Published: 4 November 2024

Copyright: © 2024 by the authors. Licensee MDPI, Basel, Switzerland. This article is an open access article distributed under the terms and conditions of the Creative Commons Attribution (CC BY) license (https://creativecommons.org/licenses/by/4.0/).

1. Introduction

Along with the growing global awareness of socio-environmental issues within the industrial sector, significant changes have also occurred in the preferences of the population [1,2]. These transformations are linked to a continuous increase in the popularity of natural ingredients that promote health, well-being, and quality of life within sustainable production systems. Consequently, the exploration of bioactive and functional biomolecules, such as natural carotenoids, paves the way for a new era of sustainable bioingredients and bioproducts [3,4]. These molecules play a notable role as antioxidants and precursors of vitamin A and in eye health. In addition, research has suggested their role as prebiotics, reducing cardiovascular diseases, obesity, diabetes, and cancer [5].

From this perspective, microalgae biotechnology assertively positions itself in the current global scenario, aligning with the principles of One Health. This is a consequence of

the metabolic versatility of algae biomass, which allows for a wide range of applications in the industrial sector, including human and animal nutrition, cosmetics, and medicine [4,6]. In addition, with biotechnology enhancement, the industrial production of fine chemical compounds has boosted the microalgae market. Estimates indicate that approximately 35.82 million tons per year of microalgae biomass is produced globally, totaling a value of 11.8 billion BRL. Modeling projects a market valued at 25.4 billion BRL by 2033 [7]. However, from these total numbers, it is estimated that 75% is directed toward the production of microalgae pigments, including carotenoids such as β-carotene, astaxanthin, and lutein [8].

Nevertheless, although carotenoids have reached consumers, the current biotechnological routes do not meet market demands. This occurs mainly due to the volumetric productivity of cultures. Also, another key aspect that directly influences this bottleneck is the understanding of the growth regimes and phases for the production of compounds of interest [9]. Therefore, investigating the carotenoid biosynthesis under the main growth regimes—autotrophic and heterotrophic—will help define substrate bioconversion patterns and direct the regimes and cultivation phases according to the intended interest.

Currently, little is known about the correlation between biomass productivity and carotenoid content, which is a fundamental parameter to facilitate the immediate expansion of microalgae bioprocesses and ensure the availability and industrial viability of these biocompounds. Most of the work available in the literature focuses only on specific carotenoids, disregarding the profile of carotenoids in their entirety. The reports available are limited to stoichiometric restrictions of cultures [10], different substrate sources [11], and surveys associated with bioaccessibilities and cellular uptakes [12,13].

In addition, although studies on carotenoid content under photoautotrophic and heterotrophic growth regimes with *Chlorella vulgaris* have been reported in the literature, most of these present only quantitative values of the total carotenoid profile or information from a photodiode array, without addressing characterization by mass spectrometry (MS) in detail [14,15]. In the carotenoid analysis, mass spectrometry is focused on identification, while other methods do not allow for the distinction between structures with the same UV–visible spectra and similar chromatographic behavior, or when the acquisition of high-quality UV–visible spectra is not possible in low-concentration samples. For this reason, the application of MS techniques to the analysis of carotenoids in phytoplankton has expanded the knowledge on the composition and metabolism of carotenoids [16].

These contributions are relevant to the literature and serve as building blocks for advancing to a new level in microalgae biotechnology. However, these previous approaches analyze one analytical stage or a dyad; when observing the evolutionary context of research, development, innovation, and industry, it is understood that this approach brought insufficient results to, on the whole, consolidate the future demands for microalgal-based pigment production.

Against this background, the rationale behind this study and the main objective of this research is to analyze, using HPLC-PDA-MS/MS, the qualitative and quantitative profile of carotenoids from *Chlorella vulgaris* under comparative growth regimes, photoautotrophic and heterotrophic, correlating with the growth phases and volumetric productivities. Also, to establish the industrial trade-off in the production of microalgae-based carotenoids, biosynthetic challenges including the promotion of viable pathways for the industrial consolidation of microalgae biotechnology, industrial viability, and market opportunities were discussed. Therefore, the discoveries found in this work will serve as the cornerstone to help overcome the current limitations and provide important reference data for studies on metabolic pathway effects, growth screening, and culture selection, opening pathways for full-fledged industrial exploration of microalgae carotenoids.

2. Material and Methods

2.1. Chemicals

The standards of all-*trans*-lutein, all-*trans*-β-cryptoxanthin, and all-*trans*-β-carotene (purity $\geq$ 98%, HPLC) were purchased from Sigma-Aldrich (Darmstadt, Germany). Methanol

(MeOH) and methyl tert-butyl ether (MTBE) (both of HPLC-grade) and the analytical-grade solvents, ethanol, acetone, ethyl acetate, petroleum ether, and diethyl ether, were purchased from Merck (Darmstadt, Germany).

2.2. Microalgae Culture and Biomass Production

Axenic cultures of *Chlorella vulgaris* (CPCC90) were used in the experiments. Stock cultures were propagated and maintained in synthetic BG-11 medium (Braun–Grunow medium) [17]. The incubation conditions were a temperature of 25 °C, a photon flux density of 30 µmol.m^{-2}.s^{-1}, and a photoperiod of 12/12 h light/dark.

The biomass productions were made under photoautotrophic and heterotrophic growth regimes. Photoautotrophic growth regimes were performed in a bubble column photobioreactor [18] operating under a batch regime, fed on 2.0 L of BG-11 medium. The experimental conditions were as follows: an initial cell concentration of 100 mg.L^{-1}, an isothermal reactor operating at a temperature of 25 °C, a photon flux density of 150 µmol.m^{-2}.s^{-1}, continuous aeration of 1 VVM (volume of air per volume of culture per minute), and continuous lighting conditions of 24:0 h light/dark.

For the heterotrophic growth regimes, the experiments were developed in a bioreactor operating in the batch system, fed with 2.0 L of culture medium. The experimental conditions were as follows: an initial inoculum concentration of 100 mg.L^{-1}, an isothermal reactor operating at a temperature of 25 °C, a pH adjusted to 7.6, aeration of 1 VVM, and the absence of light. The culture medium consisted of BG11 supplemented with an exogenous carbon source to obtain a fixed C/N ratio of 20. The monosaccharide concentration was adjusted stoichiometrically, using D-glucose (12.4 g.L^{-1}). The glucose was weighed and diluted in synthetic BG-11 medium, followed by autoclaving at 121 °C for 20 min [19].

In both growth regimes, the biomasses were separated from the culture medium by centrifugation (1500× *g*; 10 min; and 10 °C), the supernatants were discarded, and the wet biomasses (95% moisture) were stored immediately in closed containers protected from light, under refrigeration.

2.3. Experimental Setup and Kinetic Parameters

The monitoring of the kinetic growth phases was performed every 24 h. Beginning at the control zero time, there was a 24 h lag phase, 48–72–96 h log phase, and 120 h stationary phase for photoautotrophic cultivation. In the heterotrophic culture, the measurements were conducted in the periods at zero time, 04–08–16–20 and 24 h for the lag phase, 48–72–96 h for the log phase, and 120 h for the stationary phase. All the experiments were performed in duplicate; therefore, the kinetic data refer to the mean value of the replicates.

The biomass data were used to calculate the biomass productivity (g.L.d^{-1}), the maximum specific growth rate (d^{-1}), and the generation time (d) from Equations (1)–(3), respectively:

$$\mathrm{Px} = \frac{(X_i - \mathrm{X_{i-1}})}{(t_i - \mathrm{t_{i-1}})} \quad (1)$$

$$ln\left(\frac{Xi}{X0}\right) = \mu max \times t \quad (2)$$

$$Tg = \frac{0.693}{\mu max} \quad (3)$$

where X_i is the biomass concentration at time t_i (g.L^{-1}) and X_{i-1} is the biomass concentration at time t_{i-1} (g.L^{-1}), and t is the residence time (d). The residence time was defined as the elapsed time to reach maximum cell biomass.

2.4. Measurement of Biomass

The cell biomass was determined gravimetrically by filtering a known culture volume through a 0.45 µm membrane filter (Millex FG®, Billerica, MA, USA), and then drying was

conducted at 50 °C until constant weight (24 h). At each weighing, the filter containing the biomass was kept in a desiccator and subsequently weighed on an analytical balance.

2.5. Carotenoids Profile

The carotenoids were exhaustively extracted according to Rodrigues et al. (2015). They were analyzed by HPLC (Shimadzu, Kyoto, Japan) using a diode array detector (PDA) (model SPD-M20A) and a mass spectrometer with an ion-trap analyzer and atmospheric pressure chemical ionization (APCI) source (model Esquire 4000, Bruker Daltonics, Bremem, Germany). The carotenoid separation was performed on a C30 YMC column (5 µm, 250 × 4.6 mm) (Waters, Wilmington-DE, USA). Prior to the HPLC-PDA analysis, the carotenoid extract was solubilized in methanol (MeOH): methyl tert-butyl ether (MTBE) (70:30) and filtered through Millipore membranes (0.22 µm). The mobile phases were A (MeOH) and B (MTBE), using a linear gradient program as follows: from 0 to 30 min 5% B; from 30 to 40 min, 5 to 30% B; from 40 to 41 min, 30 to 50% B; and from 41 to 50 min, 50 to 5% B. The flow rate was set at 0.9 mL.min^{-1}, the injection volume was 20 µL, the column temperature was maintained at 22 °C, the UV/vis spectra were acquired between 300 and 700 nm, and the chromatograms were processed at 450 nm.

The MS/MS analysis was achieved according to [20] with adaptations, and the APCI interface operated in positive (+) mode with the following: detector voltage: 4.5 kV; interface temperature: 350 °C; DL temperature: 250 °C; heat block temperature: 200 °C; nebulizing gas flow (N_2): 3.0 L.min^{-1}; drying gas flow (N_2): 5.0 L.min^{-1}; collision-induced dissociation (CID) gas: 23 kPa (argon); and event time: 0.5 s. To improve the quality of identification, MS/MS was used simultaneously in the SIM (Select Ion Monitoring) and MRM (Multiple Reaction Monitoring) modes. The identification was performed according to the following combined information: elution order on a C30 HPLC column, co-chromatography with authentic standards, UV–visible spectrum, and mass spectral characteristics, which were compared with the data available in the literature. The carotenoids were also quantified by HPLC-PDA, using five-point analytical curves (all-*trans*-violaxanthin, all-*trans*-zeaxanthin, all-*trans*-lutein, all-*trans*-α-carotene, and all-*trans*-β-carotene).

2.6. Evaluation of Energy Requirements for an Industrial Trade-Off in Microalgal-Based Pigments Production

The energy demand of the microalgal process was established as the energy necessary for the full functioning of the cultivation systems during the hydraulic residence time and, subsequently, obtaining the final pigment. For the photoautotrophic regime, the energy required for aeration, carbon dioxide injection, and lighting of the photobioreactor was encompassed, as described by [18]. On the other hand, for the heterotrophic regime, agitation and sterilization of the bioreactor were considered [21]. Furthermore, for both regimes, the energy requirements for downstream steps, such as centrifugation, drying, and extraction of compounds, were considered, as described by [22]. The functional unit was considered kWh.L^{-1}.

2.7. Statistical Analysis

The analysis was performed using Statistica 7.0 software (Statsoft, Tulsa, OK, USA). The significance of the experimental data for the kinetic parameters was determined using Student's *t*-test ($p < 0.05$). For the remaining data, the significance was assessed through one-way ANOVA followed by Tukey's test ($p < 0.05$). The normality of the data was previously evaluated using the Shapiro–Wilk test.

3. Results

3.1. Identification of the Carotenoid Profile in All Growth Regimes

The chromatographic and spectrometric characteristics of the different carotenoids separated during phototrophic and heterotrophic growth are shown in Table 1. The carotenoids were identified based on the combined information obtained from chromatographic elution,

co-chromatography with standards, and UV–visible and mass spectra characteristics. A description of microalgae carotenoid identification using chromatographic information from HPLC-PDA-MS/MS (APCI positive mode) was previously described in detail in the literature [4,13,23–27].

In general, a total of twenty-two carotenoids were separated under the photoautotrophic or heterotrophic growth conditions, of which most were all-*trans*-α-carotene- or all-*trans*-β-carotene-derived structures, except 2′-dehydrodeoxymyxol, synthesized through cyclization, ketolation, *cis*-isomerization, hydroxylation, acetylation, epoxidation, and epoxide-furanoxide rearrangement reactions (Figure 1).

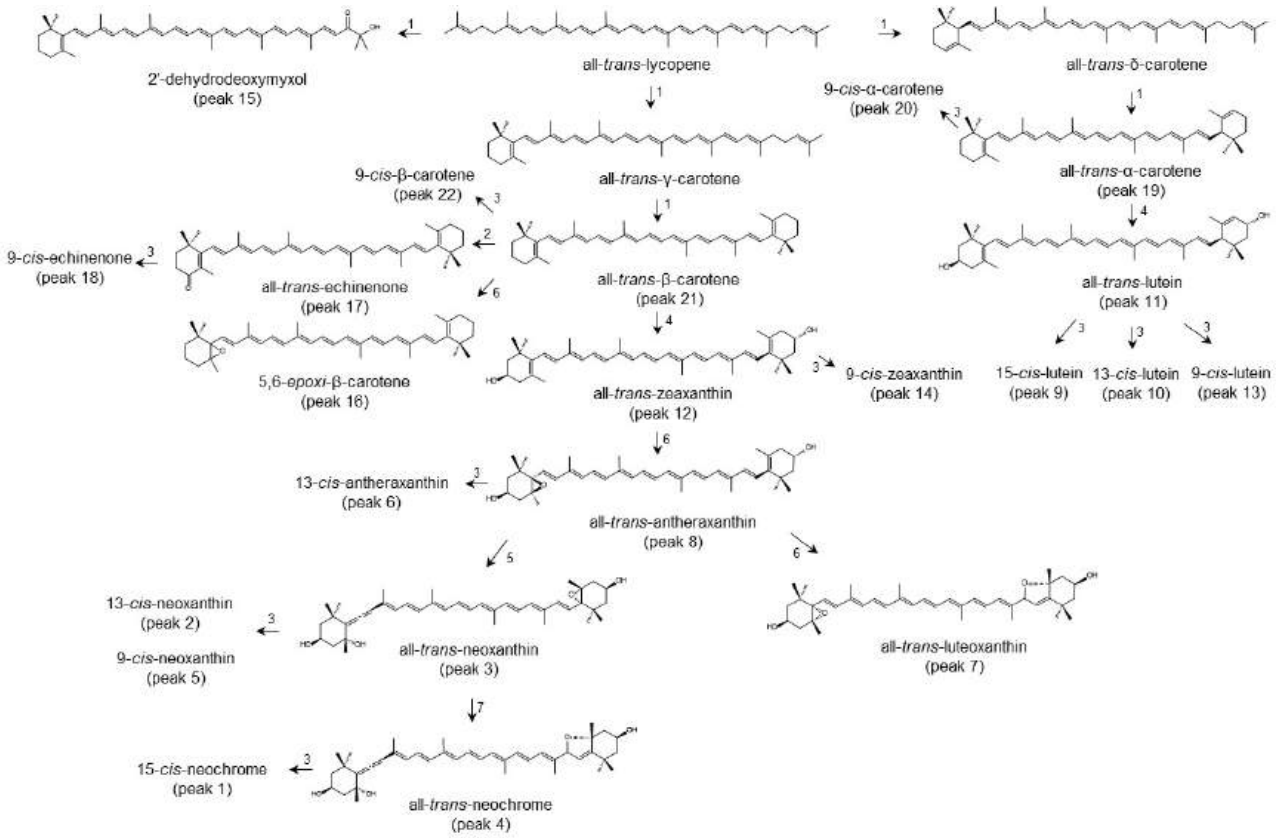


Figure 1. Chemistry mechanism for biotechnology production of carotenoids from *Chlorella vulgaris*. Description of the illustration: [1] cyclization; [2] ketolation; [3] *cis*-isomerization; [4] hydroxylation; [5] acetylation; [6] epoxidation; [7] epoxide-furanoxide rearrangement.

3.2. Determination of the Carotenoid Profile During Phototrophic Regime Growth

Table 2 presents the quantitative profiles of the carotenoids identified under the photoautotrophic growth conditions. Twelve carotenoids were identified at zero time from phototrophic conditions, including three epoxycarotenoids (peaks 3, 5, and 6), five hydroxycarotenoids (peaks 9, 10, 11, 12, and 13), and four carotenes (peaks 19, 20, 21, and 22). All-*trans*-lutein (1054.15 μg.g^{-1}, peak 11) and all-*trans*-β-carotene (214.22 μg.g^{-1}, peak 21) were the major ones, representing 68.03% of the total carotenoid content, followed by all-*trans*-neoxanthin (6.43%) and all-*trans*-α-carotene (5.55%) as the major carotenoids at zero time.

Table 1. Chromatographic, UV/Vis, and mass spectrometry characteristics of *Chlorella vulgaris* carotenoids, obtained by HPLC-PDA-MS/MS.

Peak [a]	Pigments	t_R (min) [b]	UV-Vis Characteristics			Fragment Ions (Positive Mode) (*m*/*z*)	
			$\lambda_{máx}$ (nm) [c]	III/II [d] (%)	A_B/II [e] (%)	$[M + H]^+$	MS/MS
1	15-*cis*-neochrome	6.2	327, 405, 428, 455	65	42	601	583 $[M + H - 18]^+$, 565 $[M + H - 18 - 18]^+$, 547 $[M + H - 18 - 18 - 18]^+$, 509 $[M + H - 92]^+$
2	13-*cis*-neoxanthin	6.7	337, 419, 443,471	81	17	601	583 $[M + H - 18f$, 547 $[M + H - 18 - 18 - 18]^+$, 221
3	all-*trans*-neoxanthin	7.5	415, 438, 468	78	0	601	583 $[M + H - 18]^+$, 565 $[M + H - 18 - 18]^+$, 547 $[M + H - 18 - 18 - 18]^+$, 509 $[M + H - 92]^+$
4	all-*trans*-neochrome	7.7	398,421, 447	80	0	601	583 $[M + H - 18]^+$, 547 $[M + H - 18 - 18 - 18]^+$, 221
5	9-*cis*- neoxanthin	8.0	325, 415, 438, 467	78	0	601	583 $[M + H - 18]^+$, 565 $[M + H - 18 - 18]^+$, 509 $[M + H - 92]^+$
6	13-*cis*-antheraxanthin	8.7	326, 415, 438, 467	72	13	585	583 $[M + H - 18]^+$, 565 $[M + H - 18 - 18]^+$, 509 $[M + H - 92]^+$
7	all-*trans*-luteoxanthin	8.8	400, 420, 447	100	0	601	583 $[M + H - 18]^+$
8	all-*trans*-antheraxanthin	9.3	416, 442, 473	50	0	585	567 $[M + H - 18]^+$, 549 $[M + H - 18 - 18]^+$, 531
9	15-*cis*-lutein	10.3	331, 415, 437, 465	37	31	569	551 $[M + H - 18]^+$, 533 $[M + H - 18 - 18]^+$
10	13-*cis*-lutein	11.2	328, 415, 438, 465	25	39	569	551 $[M + H - 18]^+$, 533 $[M + H - 18 - 18]^+$, 477 $[M + H - 92]^+$
11	all-*trans*-lutein	12.3	419, 443, 471	57	0	569	551 $[M + H - 18]^+$, 533 $[M + H - 18 - 18]^+$
12	all-*trans*-zeaxanthin	14.5	425, 449, 475	25	0	569	551 $[M + H - 18]^+$, 533 $[M + H - 18 - 18]^+$,495, 477 $[M + H - 92]^+$, 459
13	9-*cis*-lutein	15.2	326, 420, 440, 465	50	12	569	551 $[M + H - 18]^+$, 533 $[M + H - 18 - 18]^+$,495, 477 $[M + H - 92]^+$, 459
14	9-*cis*-zeaxanthin	17.6	338, 420, 445, 470	33	25	569	551 $[M + H - 18]^+$, 533 $[M + H - 18 - 18]^+$,495, 477 $[M + H - 92]^+$, 459
15	2′-dehydrodeoxymyxol	20.2	445, 473, 504	63	0	567	549 $[M + H - 18]^+$
16	5,6-epoxy-β-carotene	20.3	420, 446, 470	50	0	553	535 $[M + H - 18]^+$, 461 $[M + H - 92]^+$, 205
17	all-*trans*-echinenone	23.6	462	nc [f]	0	551	533 $[M + H - 18]^+$, 427, 203
18	9-*cis*-echinenone	25.6	342, 450	nc	20	551	533 $[M + H - 18]^+$, 427, 203
19	all-*trans*-α-carotene	27.8	420, 445, 473	62	0	537	444 $[M + H - 92]^+$, 399, 355
20	9-*cis*- α-carotene	28.9	330, 420, 444, 472	70	nc	537	444 $[M + H - 92]^+$, 399, 355
21	all-*trans*-β-carotene	31.0	425, 451, 476	25	0	537	444 $[M + H - 92]^+$, 399, 355
22	9-*cis*-β-carotene	33.7	341, 420, 446, 472	20	14	537	444 $[M + H - 92]^+$, 399, 355

[a] Numbered accordingly. [b] t_R: Retention time on the C30 column. [c] Linear gradient MeOH:MTBE. [d] Spectral fine structure: Ratio of the height of the longest wavelength absorption peak (III) and that of the middle absorption peak (II). [e] Ratio of the *cis* peak (A_B) and the middle absorption peak (II). [f] Not calculated.

Table 2. Quantitative characterization of carotenoids in kinetic growth phases (μg.g^{-1} dry weight).

Peak	Compounds	Phototrophic *				Heterotrophic *			
		Zero-Time	Lag	Log	Stacionary	Zero-Time	Lag	Log	Stacionary
1	15-*cis*-neochrome	nd [1]	nd	nd	nd	nd	36.31 ± 0.03 [a]	5.33 ± 0.02 [b]	nd
2	13-*cis*-neoxanthin	nd	nd	nd	nd	nd	22.41 ± 0.04 [a]	nd	nd
3	all-*trans*-neoxanthin	119.80 ± 0.82 [b]	170.89 ± 0.49 [a]	98.47 ± 0.10 [c]	99.07 ± 0.27 [c]	16.72 ± 0.07 [g]	61.50 ± 0.16 [d]	20.45 ± 0.02 [f]	28.31 ± 0.53 [e]
4	all-*trans*-neochrome	nd	nd	nd	nd	nd	nd	5.00 ± 0.00 [a]	nd
5	9-*cis*-neoxanthin	65.17 ± 0.09 [d]	103.11 ± 0.13 [a]	84.47 ± 0.07 [c]	98.47 ± 0.48 [b]	28.89 ± 0.00 [f]	52.74 ± 0.18 [e]	18.23 ± 0.15 [h]	22.50 ± 0.02 [g]
6	13-*cis*-antheraxanthin	72.44 ± 0.19 [b]	85.15 ± 0.21 [a]	nd	nd	nd	21.35 ± 0.13 [c]	12.69 ± 0.13 [e]	19.55 ± 0.17 [d]
7	all-*trans*-luteoxanthin	nd	nd	27.90 ± 0.46 [b]	81.60 ± 0.19 [a]	24.34 ± 0.09 [c]	24.28 ± 0.08 [c]	nd	nd
8	all-*trans*-antheraxanthin	nd	nd	nd	nd	nd	40.73 ± 0.18 [a]	5.35 ± 0.00 [c]	16.91 ± 0.01 [b]
9	15-*cis*-lutein	54.64 ± 0.14 [b]	44.79 ± 0.79 [c]	46.89 ± 0.60 [c]	59.31 ± 0.31 [a]	45.28 ± 0.08 [c]	30.42 ± 0.42 [d]	5.01 ± 0.13 [f]	11.51 ± 0.02 [e]
10	13-*cis*-lutein	27.08 ± 0.44 [a]	20.55 ± 0.31 [b]	15.03 ± 1.09 [d]	18.37 ± 0.13 [c]	21.78 ± 0.07 [b]	11.44 ± 0.15 [e]	3.27 ± 0.13 [f]	4.62 ± 0.12 [f]
11	all-*trans*-lutein	1054.15 ± 0.98 [a]	510.83 ± 1.25 [d]	654.05 ± 3.77 [c]	700.53 ± 1.81 [b]	96.68 ± 0.39 [h]	330.53 ± 2.94 [f]	236.46 ± 1.33 [g]	363.02 ± 0.69 [e]
12	all-*trans*-zeaxanthin	61.28 ± 0.10 [d]	85.88 ± 0.06 [c]	167.62 ± 1.17 [a]	161.04 ± 0.82 [b]	18.61 ± 0.02 [f]	50.53 ± 0.20 [e]	5.55 ± 0.01 [g]	nd
13	9-*cis*-lutein	14.53 ± 0.09 [b]	7.34 ± 0.19 [d]	8.26 ± 0.23 [c,d]	10.62 ± 0.31 [c]	64.19 ± 0.03 [a]	13.63 ± 0.24 [b]	6.89 ± 0.11 [d]	15.26 ± 0.17 [b]
14	9-*cis*-zeaxanthin	nd	nd	nd	nd	53.01 ± 0.60 [a]	41.62 ± 0.28 [b]	11.87 ± 0.07 [d]	18.32 ± 0.05 [c]
15	2′-dehydrodeoxymyxol	nd	nd	nd	nd	nd	16.21 ± 0.56 [a]	nd	nd
16	5,6-epoxy-β-carotene	nd	nd	nd	nd	nd	18.05 ± 0.35 [a]	nd	nd
17	all-*trans*-echinenone	nd	114.53 ± 0.36 [c]	266.67 ± 2.01 [a]	232.16 ± 2.41 [b]	nd	49.69 ± 0.16 [e]	nd	nd
18	9-*cis*-echinenone	nd	112.78 ± 0.52[c]	159.79 ± 1.64 [a]	137.44 ± 2.56 [b]	nd	45.61 ± 0.98 [e]	nd	nd
19	all-*trans*-α-carotene	103.42 ± 0.01 [a]	5.21 ± 0.20 [f]	27.87 ± 0.42 [d]	22.00 ± 0.24 [d]	72.23 ± 1.48 [b]	41.43 ± 0.68 [c]	13.93 ± 0.46 [e]	24.22 ± 0.18 [d]
20	9-*cis*-α-carotene	3.06 ± 0.12 [a]	nd	nd	nd	6.87 ± 0.40 [a]	nd	nd	nd
21	all-*trans*-β-carotene	214.22 ± 0.92 [c]	192.05 ± 0.49 [d]	311.64 ± 1.47 [a]	296.59 ± 1.08 [b]	92.82 ± 2.56 [f]	170.43 ± 1.05 [e]	31.81 ± 0.28 [h]	48.42 ± 0.02 [g]
22	9-*cis*-β-carotene	74.62 ± 0.70 [d]	87.63 ± 0.08 [c]	132.51 ± 0.83 [a]	117.79 ± 0.66 [b]	30.12 ± 0.43 [f]	48.81 ± 0.36 [e]	5.85 ± 0.03 [h]	17.86 ± 0.34 [g]
	Total	1849.88 ± 0.80 [c]	1540.74 ± 1.76 [d]	2001.17 ± 8.50 [b]	2034.99 ± 0.92 [a]	571.54 ± 5.07 [g]	1127.72 ± 7.25 [e]	387.69 ± 2.33 [h]	590.51 ± 1.91 [f]

[1] Not detected. * Values are average and standard deviation of triplicates. Values (rows) followed by different superscript letters indicate statistical differences ($p < 0.05$).

Among the 12 carotenoids identified at zero time from the phototrophic growth conditions, 11 compounds were common to the lag phase profile (peaks 3, 5, 6, 9, 10, 11, 12, 13, 19, 20, 21, and 22), and two compounds were characterized only after the lag phase (peaks 17 and 18).

Considering the quantitative profile, it was observed that the total amount of carotenoids decreased from zero time (1849.88 $\mu g.g^{-1}$) until the microalgae reached the lag phase (1540.74 $\mu g.g^{-1}$). This behavior is due to the response of the main carotenoids all-*trans*-lutein (510.83 $\mu g.g^{-1}$) and all-*trans*-β-carotene (192.05 $\mu g.g^{-1}$) to the continuous illumination.

In contrast, the log phase (2001.17 $\mu g.g^{-1}$) significantly increased the content of most carotenoids compared to the lag phase (1540.74 $\mu g.g^{-1}$) in the following order: all-*trans*-lutein (654.05 $\mu g.g^{-1}$) > all-*trans*-β-carotene (311.64 $\mu g.g^{-1}$) > all-*trans*-echinenone (266.67 $\mu g.g^{-1}$) > all-*trans*-zeaxanthin (167.62 $\mu g.g^{-1}$) > 9-*cis*-echinenone (159.79 $\mu g.g^{-1}$) > 9-*cis*-β-carotene (132.51 $\mu g.g^{-1}$) > all-*trans*-α-carotene (27.87 $\mu g.g^{-1}$). Meanwhile, all-*trans*-neoxanthin (98.47 $\mu g.g^{-1}$), 9-*cis*-neoxanthin (84.47 $\mu g.g^{-1}$), and 13-*cis*-antheraxanthin (not detected) showed a significant decrease concerning the lag phase. On the other hand, 15-*cis*-lutein (46.89 $\mu g.g^{-1}$) and 9-*cis*-lutein (8.26 $\mu g.g^{-1}$) showed no significant differences compared to the lag phase. Moreover, all-*trans*-luteoxanthin (27.90 $\mu g.g^{-1}$) was not detected at zero time and in the lag phase but was identified in the log phase.

Comparatively to the other growth stages (lag and log), the highest total carotenoid content in the dried biomass was determined in the stationary phase (2034.99 $\mu g.g^{-1}$) ($p < 0.05$).

As for the carotenoids detected in the stationary phase when compared to the lag phase, all-*trans*-lutein (700.53 $\mu g.g^{-1}$), all-*trans*-β-carotene (296.59 $\mu g.g^{-1}$), all-*trans*-echinenone (232.16 $\mu g.g^{-1}$), all-*trans*-zeaxanthin (161.04 $\mu g.g^{-1}$), 9-*cis*-echinenone (137.44 $\mu g.g^{-1}$), 9-*cis*-β-carotene (117.79 $\mu g.g^{-1}$), 15-*cis*-lutein (59.31 $\mu g.g^{-1}$), all-*trans*-α-carotene (22.00 $\mu g.g^{-1}$), and 9-*cis*-lutein (10.62 $\mu g.g^{-1}$) increased their contents in the *C. vulgaris* culture, even with the stationary growth. Nonetheless, the contents decreased for all-*trans*-neoxanthin (99.07 $\mu g.g^{-1}$), 9-*cis*-neoxanthin (98.47 $\mu g.g^{-1}$), and 13-*cis*-lutein (18.37 $\mu g.g^{-1}$) (compared to the lag phase). Moreover, all-*trans*-luteoxanthin (81.60 $\mu g.g^{-1}$) was not detected in the lag phase but was identified in the stationary phase.

3.3. Determination of the Carotenoid Profile During Heterotrophic Regime Growth

Thirteen carotenoids were identified at zero time from the heterotrophic conditions (see Table 2), presenting a total carotenoid content of 571.54 $\mu g.g^{-1}$. As in the photoautotrophic conditions, all-*trans*-lutein (96.68 $\mu g.g^{-1}$) and all-*trans*-β-carotene (92.82 $\mu g.g^{-1}$) were the largest carotenoids, followed by all-*trans*-α-carotene (72.23 $\mu g.g^{-1}$).

In this regime, the lag phase exhibited the most complete profile constituted by twenty carotenoids. The major carotenoids were the same ones detected at zero time, all-*trans*-lutein (330.53 $\mu g.g^{-1}$, peak 11) and all-*trans*-β-carotene (170.43 $\mu g.g^{-1}$, peak 21), which corresponds to 44.42% of the fraction of carotenoids in the extract. Unlike the results described at zero time, the lag phase presented three ketocarotenoids (peaks 15, 17, and 18), eight epoxycarotenoids (peaks 1, 2, 3, 5, 6, 7, 8, and 16), six hydroxycarotenoids (peaks 9, 10, 11, 12, 13, and 14), and three carotenes (peaks 19, 21, and 22).

Of particular interest, the lag phase of the heterotrophic growth promoted the production of unique carotenoids from the microalgae (peaks 15, 17, and 18) that can probably potentiate the antioxidant activity of the extract in the lag phase. In addition, the log phase led to a pronounced reduction in the total carotenoid contents (387.69 $\mu g\ g^{-1}$). Thus, all the carotenoids had a significant quantitative reduction. The concentration of all-*trans*-β-carotene decreased by 81%. This decrease was extended to a lower degree for all-*trans*-lutein (28%).

On the other hand, in the stationary phase, most carotenoids had a significant quantitative reduction, except all-*trans*-lutein and 9-*cis*-lutein. In addition, about the log phase, most carotenoids showed a higher concentration, except for peaks 1, 4, and 12, which were no longer detected in this growth phase.

3.4. Growth Curve Performance and Industrial Trade-Off in Microalgal-Based Pigment Production

Table 3 presents the kinetic growth parameters for *Chlorella vulgaris* under a photoautotrophic and heterotrophic growth regime.

Table 3. Growth kinetics for *Chlorella vulgaris* under photoautotrophic and heterotrophic growth regimes.

Parameter	Photoautotrophic	Heterotrophic
X_{max} (g/L)	1.90 ^{b} ± 0.01	2.20 ^{a} ± 0.02
μ_{max} (d^{-1})	0.51 ^{a} ± 0.00	0.45 ^{b} ± 0.00
Tg (d)	1.35 ^{b} ± 0.01	1.54 ^{a} ± 0.01
Px (average) (g/L/d)	0.23 ^{b} ± 0.02	0.24 ^{a} ± 0.02
Px (peak) (g/L/d)	0.36 ^{b} ± 0.01	0.42 ^{a} ± 0.01

X_{max}: maximum cell biomass; μ_{max}: maximum specific growth rate; Tg: cell generation time; and Px: cell productivity.

Under the autotrophic regime, the microalga *Chlorella vulgaris* did not present a latency phase, assuming exponential behavior immediately after inoculation. It obtained a maximum cell biomass of 1.9 $g.L^{-1}$, maximum specific growth rate of 0.51 d^{-1}, generation time of 1.35 d, and maximum biomass productivity of 0.36 $g.L.d^{-1}$.

Already under the heterotrophic regime, the microalgae showed a slight increase in the maximum cell concentration, reaching cell densities of 2.2 $g.L^{-1}$, as well as in the parameters of generation time (1.54 d) and maximum biomass productivity (0.42 $g.L.d^{-1}$), when compared to the photoautotrophic regime. In addition, the maximum specific growth rate parameter presented values lower than the autotrophic regime, around 0.45 d^{-1}.

To determine the optimal conditions for carotenoid production by microalgae, Figure 2 illustrates the interdependence between total carotenoid content and microalgae biomass productivity.

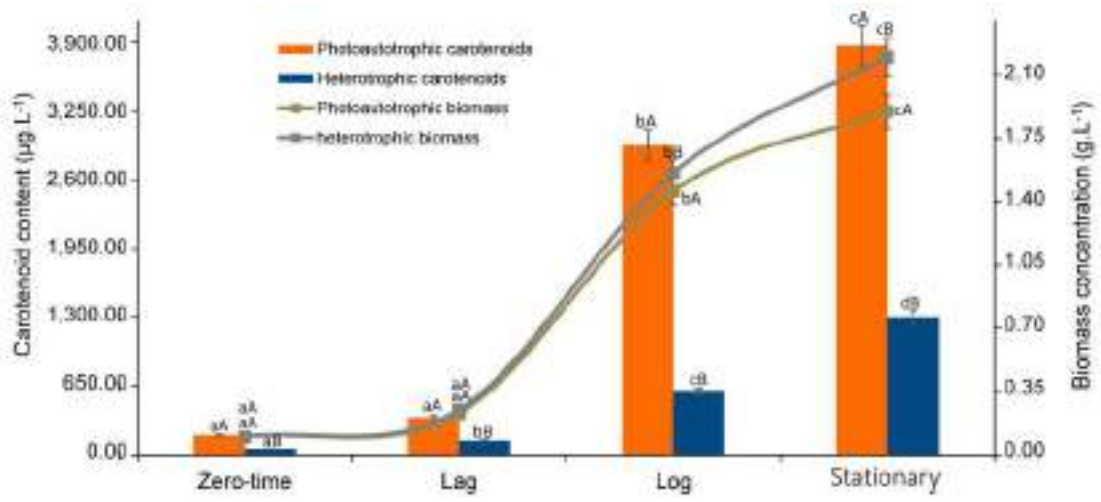


Figure 2. Dynamics of carotenoid concentration and biomass production under photoautotrophic and heterotrophic growth regimes for *Chlorella vulgaris*. Lowercase letters differ significantly in the same column. Uppercase letters differ significantly in the same row.

Lowercase letters indicate significant differences ($p < 0.05$) within the same column; uppercase letters indicate significant differences ($p < 0.05$) within the same column.

As observed in Figure 2, the general behavior of biomass production and carotenoid content presents a similar profile in both cultivation regimes, with carotenoid production being viable only if cultivation is carried out until the log and stationary phase due to biomass production. However, when the photoautotrophic cultivation regime is individually analyzed, it becomes clear that the trend in carotenoid content follows the exponential growth of biomass in all growth phases, with the final concentration of carotenoid content

reaching its peak in the stationary phase. The same slope is observed for time zero and the lag phase in the heterotrophic regime. However, it is noted that in the log phase, there is a certain containment of the production of carotenoid content compared to the production of microalgal biomass when compared to the photoautotrophic regime.

In the heterotrophic regime, it is clear that there is a priority in directing the energy generated toward the formation of biomass (1.56 $g.L^{-1}$), reaching values slightly higher than photoautotrophic cultivation (1.46 $g.L^{-1}$). The carotenoid content, as it is a secondary compound, tends to be substantially reduced for the heterotrophic regime (604.79 $\mu g.L^{-1}$) when compared to the autotrophic regime (2921.70 $\mu g.L^{-1}$). This premise can be reinforced with the similar behavior presented in the stationary phase, with a maximum biomass concentration of 2.2 $g.L^{-1}$ for the heterotrophic regime and 1.9 $g.L^{-1}$ for the autotrophic regime. Indeed, the concentrations of carotenoid content differ substantially, with values in the order of 3866.48 and 1299.12 $\mu g.L^{-1}$ being found for the photoautotrophic and heterotrophic regimes, respectively.

According to Figure 3, it is possible to observe that the carotenoid blends present in the photoautotrophic regimes have high energy demands, with the maximum value identified in the stationary phase (9.60 $kWh.L^{-1}$) when compared to the heterotrophic regimes in the same condition (0.06 $kWh.L^{-1}$).

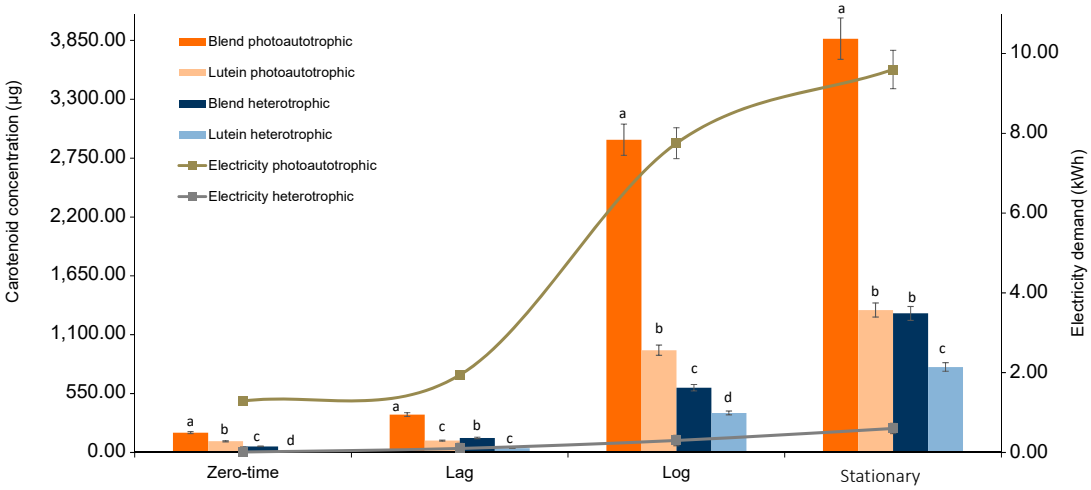


Figure 3. Dynamics of energy demands, carotenoid blend, and lutein production under photoautotrophic and heterotrophic growth regimes for *Chlorella vulgaris*. Lowercase letters differ significantly in the same column.

The disparity in the content and qualitative profile of carotenoids is notable since the photoautotrophic regime presents about 3 times greater quantity (~3866.48 $\mu g.L^{-1}$); this fraction is mostly composed of lutein (~30%) and β-carotene (~15%). Furthermore, in the adaptive (lag), exponential (log), and stationary phases, it is possible to identify the biosynthesis of unique carotenoids, such as all-*trans*-echinenone and 9-*cis*-echinenone, which have market prices estimated at up to 1250.00 USD/mg, resulting in a higher market value. On the other hand, when considering only the energy requirement, cultures in heterotrophic regimes, even with their lower productivity (1299.12 $\mu g.L^{-1}$), could be equivalent to the amount of carotenoids found in photoautotrophic regimes since three-batch cultures would consume about 0.18 $kWh.L^{-1}$, resulting in carotenoid content of up to 3897.36 $\mu g.L^{-1}$. Meanwhile, it is worth noting that around 20% of the costs of microalgae processing are related to the demand for nutrients and water, and, therefore, a more in-depth analysis must be established.

Similarly, when focusing on a specific carotenoid of interest, such as lutein, the scenario is viewed from a new perspective. In the photoautotrophic regime, the lutein concentration at time zero represents around 56% of the total content. However, as the biomass increases throughout the cultivation phases (lag, log, and stationary), its content decreases, reaching

around 30%. The opposite is observed in the heterotrophic regime, where at zero time and the adaptive (lag) phase the content is 16 and 29%, respectively. However, as the cultivation phases progress, the content doubles, reaching values of ~61% in the stationary phase.

4. Discussion

Chlorella vulgaris exhibited a typical carotenoid profile of the *Chlorophyta* taxon, which mainly contains all-*trans*-lutein and all-*trans*-β-carotene [28]. Under light conditions, the main differences observed between the zero time and lag phase extracts were in the keto carotenoids. Notably, unique microalgae carotenoids such as all-*trans*-echinenone and 9-*cis*-echinenone, which were not detected at zero time, were formed during the lag phase of growth, with contents ranging from 114.53 to 112.78 $\mu g.g^{-1}$ (Table 2). These microalgae carotenoids are highly valued for their antioxidant potential, attributed to the 12 conjugated double bonds in their structure [29–32].

Considering the quantitative profile, it was observed that the total amount of carotenoids decreased from zero time (1849.88 $\mu g.g^{-1}$) until the microalgae reached the lag phase (1540.74 $\mu g.g^{-1}$) (Table 2). This behavior is due to the response of the main carotenoids all-*trans*-lutein (510.83 $\mu g.g^{-1}$) and all-*trans*-β-carotene (192.05 $\mu g.g^{-1}$) (Table 2) to the continuous illumination. Taking as reference the green algae (*Chlorophyta*), all-*trans*-lutein and all-*trans*-β-carotene also exhibited a similar behavior in the lag phase of *Scenedesmus obliquus* [33].

Based on the results, it has been suggested to employ high lighting levels, which may result in photo-inhibition. The high light intensity in low-biomass concentrations can lead to photo-inhibition, while low light levels in high-biomass density result in photo-limitation. These conditions affect lutein productivity. Lutein reduces reactive oxygen species formed under excess light, but high light intensity at early growth stages can damage photosynthetic complexes. Low light intensity is preferable early on to enhance lutein synthesis [34]. *Chlorella vulgaris*, a versatile and valuable organism commonly used for bioresource studies that determine the stoichiometric regulation of commercial carotenoid production, stands out both for its total carotenoid yield and for the variety of carotenoids it produces [10]. The carotenogenic profile of *Chlorella* can vary significantly; with modifications in cultivation, it is possible to stimulate the biosynthesis of special carotenoids [35].

Moreover, these changes are also observed in the different growth phases. For example, all-*trans*-luteoxanthin (27.90 $\mu g.g^{-1}$) was not detected at zero time and in the lag phase but was identified in the log phase (see Table 2). This indicates the formation of an epoxy compound (Figure 1), and its mechanism is well known [23].

Compared to the log phase, in the stationary phase except for all-trans-neoxanthin and 9-*cis*-lutein, all showed a significant difference ($p < 0.05$) (Table 2). Likewise, except for all-*trans*-zeaxanthin, all-*trans*-echinenone, 9-*cis*-echinenone, all-*trans*-α-carotene, all-*trans*-β-carotene, and 9-*cis*-β-carotene, all the other compounds were significantly ($p < 0.05$) higher in the stationary phase compared to the log phase.

As for the carotenoid profile, the experimental conditions of photoautotrophic growth may have contributed to changes. Among all the carotenoids identified at zero time, 9-*cis*-α-carotene (peak 20) was not detected during the growth stages. In contrast, in the growth stages, all-*trans*-echinenone and 9-*cis*-echinenone (peaks 17 and 18) were observed, whereas all-*trans*-luteoxanthin (peak 7) was only detected in the log and stationary phases.

Considering the carotenoid structures identified during photoautotrophic growth that were not present at zero time, the main reactions observed were ketolation and epoxidation (Figure 1). Already, the production of ketocarotenoids from all-*trans*-β-carotene (peak 21) involves the introduction of keto moieties at the 4,4′ position of the β-rings. These conversions of all-*trans*-β-carotene into all-*trans*-echinenone (one keto group) are carried out by the β-carotene ketolase [36–39]. Finally, one epoxide derivative of zeaxanthin (all-*trans*-luteoxanthin) was formed [23].

Thus, the carotenoids identified in this regimen play a crucial role in the metabolism of the microalga *Chlorella vulgaris*, contributing both to growth and overall cellular health. Furthermore, determining the optimal pathway for the production of lutein, β-carotene, and echinenone advances biotechnological efforts toward the development of targeted nutraceutical and pharmaceutical applications.

In the heterotrophic regime, qualitatively and quantitatively, the total carotenoid content was notably higher in the lag phase (1127.72 $\mu g.g^{-1}$) (see Table 2). The increase in pigment concentration during a short period of darkness has also been observed in other microalgae [40,41]. In that regard, the lag phase presented a carotenoid profile with eight different compounds compared to zero time. Of these compounds, one was the *cis*-isomer of all-*trans*-neochrome (peak 1), the *cis*-isomer of all-*trans*-neoxanthin (peak 2), the *cis*-isomer of all-*trans*-antheraxanthin (peak 6), 2′-dehydrodeoxymyxol (peak 15), 5,6-epoxy-β-carotene (peak 16), all-*trans*-echinenone (peak 17), and 9-*cis*-echinenone (peak 18). In contrast, 9-*cis*-α-carotene (peak 20) was only detected in the carotenoid extract at zero time. Considering these aspects, the heterotrophic strategy induced cyclization, ketolation, *cis*-isomerization, epoxidation, and epoxide-furanoxide rearrangement reactions (Figure 1).

The most abundant fraction of carotenoids in this regime corresponded to all-trans-lutein and its cis-isomers at 68.87% (stationary phase). This fact suggests that (in dark conditions) this growth phase is a potential source of this xanthophyll. Also, according to our results, [42] showed that with distinct culture media, such as cultures in heterotrophic [43] or mixotrophic systems [44,45], the production of lutein is substantially significant and may be considered as a potential source of commercial output of this pigment.

Although unique carotenoids (peaks 15, 17, and 18) were produced (lag phase), in general, the reduction in both the qualitative and quantitative content of carotenoids in the heterotrophic regime can significantly impact the overall value of microalgal biomass, as various carotenoids may be diminished or absent, potentially compromising the economic viability of production and utilization pathways [46]. However, by addressing certain aspects and implementing appropriate production strategies, it can still remain useful (see Section 3.3).

Microalgae biomass is the chassis of almost all microalgae bioproducts. Like carotenoid content, most microalgae bioproducts are intracellular; therefore, the high biomass productivity reflects their proportionality to the high production of target bioproducts. As a result, the kinetic growth parameters for *Chlorella vulgaris* under a photoautotrophic and heterotrophic growth regime were determined (Table 3).

During the determination of these parameters, the absence of the lag phase observed in photoautotrophic cultivation may result from the microalga's rapid adaptation to the cultivation regime, as it is commonly maintained and propagated under similar conditions and can assimilate nutrients from the environment immediately [47].

In the heterotrophic regime, among all the kinetic parameters evaluated, the specific growth rate was the only one found to be lower compared to growth under light conditions. This is mainly due to the latency phase experienced in the first 24 h of hydraulic retention time. In addition, this behavior presented by the microalgae strain is associated with the adaptation of the photosynthetic apparatus to light deprivation conditions, as well as the disparity in time for the assimilation of the organic substrate. It is well known that species belonging to the phylum *Chlorophyta* have, as their main metabolic pathway, the assimilation of inorganic carbon (carbon dioxide). In this way, its photosynthetic apparatus relies on the presence of auxiliary enzymes, such as carbonic anhydrase, which promote greater access to inorganic carbon in the form of bicarbonate ions, accelerating the nutrient absorption process in the first hours of cultivation and, consequently, increasing the maximum growth rate and reducing the cell generation time [48].

Concurrently, expatiating on the kinetic results independently, considering only the final biomass density, is not enough to define the best scenario for the production of microalgae pigments. Thus, it was shown that the interdependence of total carotenoid content and microalgae productivity in both growth regimes (Figure 2) may be associated

with biochemical mechanisms intrinsically selected by microalgae depending on cultivation regimes. Since carotenoids help capture energy from light, contributing to the formation of adenosine triphosphate (ATP), a primordial compound for the formation of biomass, it is suggested that during cell growth, the carotenoid content will not be prejudiced, depending on the supply of light energy during the photoautotrophic regime.

Considering the substantial differences in carotenoid content between the photoautotrophic (3866.48 $\mu g.L^{-1}$) and heterotrophic (1299.12 $\mu g.L^{-1}$) regimes, it can be stated that in photoautotrophic conditions, the energy generated, when present in adequate amounts, is simultaneously used for the biosynthesis of both biomass and secondary compounds, such as carotenoids. In contrast, in the heterotrophic regime, due to light deprivation, energy is primarily allocated to the formation of structural compounds, such as carbohydrates and proteins. However, studies have reported that an increase in the carbon source, preferably glucose, can increase carotenogenesis in microalgae species and, consequently, increase the production of carotenoids [49–51].

Given the aspects presented, arguably the most successful technological route for the voluminous carotenoid production is the photoautotrophic regime. However, it must be considered that microalgae biotechnological processes present numerous bottlenecks to be overcome, the main hotspot being energy demand, which is responsible for more than 80% of the process costs. Therefore, when prioritizing the photoautotrophic regime, the demands of artificial lighting rates, associated with the downstream steps, can further leverage the unfeasibility of microalgae-based processes. In this sense, the energy demands (electricity) necessary for the production of the carotenoid blend, as well as the production of lutein, the majority compound found in all phases and cultivation regimes, to establish a trade-off in the biotechnological process needed to be considered (see Figure 3).

Considering the dynamics of energy demands to obtain the blend of pigments, the production of carotenoids with low processing demands and lower commercial value can be explored for high-volume, low-cost applications, such as ingredients for animal feed and food purposes (heterotrophic conditions). Conversely, cultures under a photoautotrophic regime could be directed to the cosmetic, medical, and chemical bioindustries, since these specific biocompounds of interest must have a high biological value, once the sales prices compensate for the onerous energy requirements.

In parallel, when a single carotenoid of interest, such as lutein, is evaluated, the scenario gains a new vision. Since photoautotrophic cultures have high energy expenditure and still have higher maximum rates of cell growth, the heterotrophic regime is suggested as the alternative that best provides viability in terms of lutein production.

Finally, from an overview of the process, the photoautotrophic regime conducted until the adaptive (lag) phase is what provides the best balance between the variables analyzed, as it allows for the use of both the carotenoid blends with high market value, as well as presenting a satisfactory lutein content, under a moderate energy demand.

5. Conclusions

The results in the present study demonstrated that, in general, carotenoid production is only viable if cultures are carried out until the log and stationary phase for both regimes (photoautotrophic and heterotrophic). Therefore, it is concluded that a high biomass yield is essential to ensure a high pigment yield. Additionally, the best condition for producing a blend of carotenoids and specific carotenoids, such as lutein, was observed under the photoautotrophic regime, carried out until the exponential (log) phase. On the other hand, when the focus is on singular lutein production, cultures carried out until the stationary phase under heterotrophic regimes showed the best performance. Thus, the scientific advances found in this study will assist in process control through decision-making about the best biochemical route for the particular production of compounds of interest, depending on the target industry and interest of the chosen bioproduct.

6. Future Perspectives

Future research could focus on consolidating processes at the industrial level, with more in-depth evaluations of process scalability and economic viability. The results of this study also highlight the need for further studies to obtain additional microalgae compounds, not just for carotenoid production. A key objective for future research is to analyze the applicability of microalgae-based carotenoids in food matrices, as well as the bioavailability and mechanisms of action of these compounds at the metabolic level.

Author Contributions: Conceptualization, P.A.C. and L.Q.Z.; methodology, P.P.N., P.A.C. and M.C.D.; software, P.P.N.; validation, P.P.N. and M.C.D.; formal analysis, P.A.C. and M.C.D.; investigation T.C.d.N.; resources, P.A.C. and T.C.d.N.; data curation, E.J.-L.; writing—original draft preparation, P.A.C.; writing—review and editing, T.C.d.N., P.P.N. and M.C.D.; visualization, E.J.-L. and L.Q.Z.; supervision, E.J.-L. and L.Q.Z.; project administration, E.J.-L. and L.Q.Z.; funding acquisition, L.Q.Z. All authors have read and agreed to the published version of the manuscript.

Funding: This study was financially supported by the CAPES (001), FAPERGS/CNPq (07/2022), FAPERGS (17/2551-0000930-4), and CNPq (306964/2017-1).

Informed Consent Statement: Not applicable.

Data Availability Statement: The data can be obtained in the paper.

Conflicts of Interest: The authors have no conflicts of interest to report.

References

1. Zhou, L.; Li, K.; Duan, X.; Hill, D.; Barrow, C.; Dunshea, F.; Suleria, H. Bioactive compounds in microalgae and their potential health benefits. *Food Biosci.* **2022**, *49*, 101932. [CrossRef]
2. Gebregziabher, B.S.; Gebremeskel, H.; Debesa, B.; Ayalneh, D.; Mitiku, T.; Wendwessen, T.; Habtemariam, E.; Nur, S.; Getachew, T. Carotenoids: Dietary sources, health functions, biofortification, marketing trend and affecting factors—A review. *J. Agric. Food Res.* **2023**, *14*, 100834. [CrossRef]
3. Pessoa JD, S.; de Oliveira CF, M.; Mena-Chalco, J.P.; de Carvalho JC, M.; Ferreira-Camargo, L.S. Trends on *Chlamydomonas reinhardtii* growth regimes and bioproducts. *Biotechnol. Appl. Biochem.* **2023**, *70*, 1830–1842. [CrossRef] [PubMed]
4. Fernandes, A.S.; Caetano, P.A.; Jacob-Lopes, E.; Zepka, L.Q.; de Rosso, V.V. Alternative green solvents associated with ultrasound-assisted extraction: A green chemistry approach for the extraction of carotenoids and chlorophylls from microalgae. *Food Chem.* **2024**, *455*, 139939. [CrossRef] [PubMed]
5. Bufka, J.; Lenka, V.; Josef, S.; Věra, K. Exploring carotenoids: Metabolism, antioxidants, and impacts on human health. *J. Funct. Foods* **2024**, *118*, 106284. [CrossRef]
6. Sun, H.; Wang, Y.; He, Y.; Liu, B.; Mou, H.; Chen, F.; Yang, S. Microalgae-derived pigments for the food industry. *Mar. Drugs* **2023**, *21*, 82. [CrossRef]
7. Market Research Reports. 2023. Available online: https://www.marketsandmarkets.com/Market-Reports/algae-product-market-250538721.html (accessed on 1 January 2023).
8. Gohara-Beirigo, A.K.; Matsudo, M.C.; Cezare-Gomes, E.A.; de Carvalho JC, M.; Danesi, E.D.G. Microalgae trends toward functional staple food incorporation: Sustainable alternative for human health improvement. *Trends Food Sci. Technol.* **2022**, *125*, 185–199. [CrossRef]
9. Thiviyanathan, V.A.; Ker, P.J.; Tang SG, H.; Amin, E.P.; Yee, W.; Hannan, M.A.; Jamaludin, Z.; Nghiem, L.D.; Mahlia, T.M.I. Microalgae biomass and biomolecule quantification: Optical techniques, challenges and prospects. *Renew. Sustain. Energy Rev.* **2024**, *189*, 113926. [CrossRef]
10. Jiang, M.; Nakano, S.I. New insights into the stoichiometric regulation of carotenoid production in *Chlorella vulgaris*. *Bioresour. Technol. Rep.* **2022**, *20*, 101227. [CrossRef]
11. Cai, Y.; Liu, Y.; Liu, T.; Gao, K.; Zhang, Q.; Cao, L.; Wang, Y.; Wu, X.; Zheng, H.; Ruan, R. Heterotrophic cultivation of *Chlorella vulgaris* using broken rice hydrolysate as carbon source for biomass and pigment production. *Bioresour. Technol.* **2021**, *323*, 124607. [CrossRef]
12. Akepach, P.; Ribeiro-Filho, N.; Wattanakul, J.; Darwish, R.; Gedi, M.A.; Gray, D.A. Bioaccessibility of carotenoids (β-carotene and lutein) from intact and disrupted microalgae (*Chlamydomonas reinhardtii*). *LWT* **2022**, *160*, 113292. [CrossRef]
13. Nass, P.P.; do Nascimento, T.C.; Fernandes, A.S.; Caetano, P.A.; de Rosso, V.V.; Jacob-Lopes, E.; Zepka, L.Q. Guidance for formulating ingredients/products from *Chlorella vulgaris* and *Arthrospira platensis* considering carotenoid and chlorophyll bioaccessibility and cellular uptake. *Food Res. Int.* **2022**, *157*, 111469. [CrossRef] [PubMed]
14. Masojídek, J.; Ranglová, K.; Rearte, T.A.; Plá, P.S.C.; Torzillo, G.; Benavides, A.M.S.; Neori, A.; Gómez, C.; Álvarez-Gómez, F.; Lukeš, M.; et al. Changes in photosynthesis, growth and biomass composition in outdoor *Chlorella* g120 culture during the metabolic shift from heterotrophic to phototrophic cultivation regime. *Algal Res.* **2021**, *56*, 102303. [CrossRef]

15. Cao, Y.; Yang, S.; Wang, J.; Kong, W.; Guo, B.; Xi, Y.; Zhang, A.; Yue, B. Metabolomic exploration of the physiological regulatory mechanism of the growth and metabolism characteristics of *Chlorella vulgaris* under photoautotrophic, mixotrophic, and heterotrophic cultivation conditions. *Biomass Bioenergy* **2023**, *173*, 106775. [CrossRef]
16. Pérez-Gálvez, A.; Fontecha, J. Analytical protocols in carotenoid analysis. In *Pigments from Microalgae Handbook*; Springer: Cham, Switzerland, 2020; pp. 151–178. [CrossRef]
17. Rippka, R.; Deruelles, J.; Waterbury, J.B.; Herdman, M.; Stanier, R.Y. Generic assignments, strain histories and properties of pure cultures of cyanobacteria. *Microbiology* **1979**, *111*, 1–61. [CrossRef]
18. Maroneze, M.M.; Deprá, M.C.; Zepka, L.Q.; Jacob-Lopes, E. Artificial lighting strategies in photobioreactors for bioenergy production by *Scenedesmus obliquus* CPCC05. *SN Appl. Sci.* **2019**, *1*, 1–12. [CrossRef]
19. Francisco, É.C.; Franco, T.T.; Wagner, R.; Jacob-Lopes, E. Assessment of different carbohydrates as exogenous carbon source in cultivation of cyanobacteria. *Bioprocess Biosyst. Eng.* **2014**, *37*, 1497–1505. [CrossRef]
20. Giuffrida, D.; Zoccali, M.; Giofre, S.V.; Dugo, P.; Mondello, L. Apocarotenoids determination in *Capsicum chinense* Jacq, cv. Habanero, by supercritical fluid chromatography-triple-quadrupole/mass spectrometry. *Food Chem.* **2017**, *231*, 316–323. [CrossRef]
21. Santos, A.M.; Deprá, M.C.; Santos, A.M.; Zepka, L.Q.; Jacob-Lopes, E. Aeration energy requirements in microalgal heterotrophic bioreactors applied to agroindustrial wastewater treatment. *Curr. Biotechnol.* **2016**, *5*, 249–254. [CrossRef]
22. Deprá, M.C.; Severo, I.A.; dos Santos, A.M.; Zepka, L.Q.; Jacob-Lopes, E. Environmental impacts on commercial microalgae-based products: Sustainability metrics and indicators. *Algal Res.* **2020**, *51*, 102056. [CrossRef]
23. Patias, L.D.; Fernandes, A.S.; Petry, F.C.; Mercadante, A.Z.; Jacob-Lopes, E.; Zepka, L.Q. Carotenoid profile of three microalgae/cyanobacteria species with peroxyl radical scavenger capacity. *Food Res. Int.* **2017**, *100*, 260–266. [CrossRef] [PubMed]
24. Maroneze, M.M.; Jacob-Lopes, E.; Zepka, L.Q.; Roca, M.; Pérez-Gálvez, A. Esterified carotenoids as new food components in cyanobacteria. *Food Chem.* **2019**, *287*, 295–302. [CrossRef] [PubMed]
25. Fernandes, A.S.; Petry, F.C.; Mercadante, A.Z.; Jacob-Lopes, E.; Zepka, L.Q. HPLC-PDA-MS/MS as a strategy to characterize and quantify natural pigments from microalgae. *Curr. Res. Food Sci.* **2020**, *3*, 100–112. [CrossRef]
26. Fernandes, A.S.; Nascimento, T.C.; Pinheiro, P.N.; Vendruscolo, R.G.; Wagner, R.; de Rosso, V.V.; Jacob-Lopes, E.; Zepka, L.Q. Bioaccessibility of microalgae-based carotenoids and their association with the lipid matrix. *Food Res. Int.* **2021**, *148*, 110596. [CrossRef]
27. Nascimento, T.C.D.; Pinheiro, P.N.; Fernandes, A.S.; Murador, D.C.; Neves, B.V.; de Menezes, C.R.; de Rosso, V.V.; Jacob-Lopes, E.; Zepka, L.Q. Bioaccessibility and intestinal uptake of carotenoids from microalgae *Scenedesmus obliquus*. *LWT* **2021**, *140*, 110780. [CrossRef]
28. Paliwal, C.; Ghosh, T.; George, B.; Pancha, I.; Maurya, R.; Chokshi, K.; Ghosh, A.; Mishra, S. Microalgal carotenoids: Potential nutraceutical compounds with chemotaxonomic importance. *Algal Res.* **2016**, *15*, 24–31. [CrossRef]
29. Rodrigues, E.; Mariutti, L.R.; Chisté, R.C.; Mercadante, A.Z. Development of a novel micro-assay for evaluation of peroxyl radical scavenger capacity: Application to carotenoids and structure–activity relationship. *Food Chem.* **2012**, *135*, 2103–2111. [CrossRef]
30. Chang, C.S.; Chang, C.L.; Lai, G.H. Reactive oxygen species scavenging activities in a chemiluminescence model and neuroprotection in rat pheochromocytoma cells by astaxanthin, beta-carotene, and canthaxanthin. *Kaohsiung J. Med. Sci.* **2013**, *29*, 412–421. [CrossRef]
31. Papp, T.; Csernetics, Á.; Nagy, G.; Bencsik, O.; Iturriaga, E.A.; Eslava, A.P.; Vágvölgyi, C. Canthaxanthin production with modified *Mucor circinelloides* strains. *Appl. Microbiol. Biotechnol.* **2013**, *97*, 4937–4950. [CrossRef]
32. El-Gawad, E.A.; Wang, H.P.; Yao, H. Diet supplemented with synthetic carotenoids: Effects on growth performance and biochemical and immunological parameters of yellow perch (*Perca flavescens*). *Front. Physiol.* **2019**, *10*, 1056. [CrossRef]
33. Maroneze, M.M.; Caballero-Guerrero, B.; Zepka, L.Q.; Jacob-Lopes, E.; Perez-Galvez, A.; Roca, M. Accomplished high-resolution metabolomic and molecular studies identify new carotenoid biosynthetic reactions in cyanobacteria. *J. Agric. Food Chem.* **2020**, *68*, 6212–6220. [CrossRef] [PubMed]
34. Dineshkumar, R.; Subramanian, G.; Dash, S.K.; Sen, R. Development of an optimal light-feeding strategy coupled with semi-continuous reactor operation for simultaneous improvement of microalgal photosynthetic efficiency, lutein production and CO2 sequestration. *Biochem. Eng. J.* **2016**, *113*, 47–56. [CrossRef]
35. Bazarnova, J.; Smyatskaya, Y.; Shlykova, A.; Balabaev, A.; Đurović, S. Obtaining fat-soluble pigments—Carotenoids from the biomass of Chlorella microalgae. *Appl. Sci.* **2022**, *12*, 3246. [CrossRef]
36. Misawa, N.; Satomi, Y.; Kondo, K.; Yokoyama, A.; Kajiwara, S.; Saito, T.; Ohtani, T.; Miki, W. Structure and functional analysis of a marine bacterial carotenoid biosynthesis gene cluster and astaxanthin biosynthetic pathway proposed at the gene level. *J. Bacteriol.* **1995**, *177*, 6575–6584. [CrossRef]
37. Armstrong, G.A. Genetics of eubacterial carotenoid biosynthesis: A colorful tale. *Annu. Rev. Microbiol.* **1997**, *51*, 629–659. [CrossRef]
38. Sun, Z.; Cunningham, F.X., Jr.; Gantt, E. Differential expression of two isopentenyl pyrophosphate isomerases and enhanced carotenoid accumulation in a unicellular chlorophyte. *Proc. Natl. Acad. Sci. USA* **1998**, *95*, 11482–11488. [CrossRef]
39. Grünewald, K.; Hagen, C. β-carotene is the intermediate exported from the chloroplast during accumulation of secondary carotenoids in *Haematococcus pluvialis*. *J. Appl. Phycol.* **2001**, *13*, 89–93. [CrossRef]
40. Hu, J.; Nagarajan, D.; Zhang, Q.; Chang, J.S.; Lee, D.J. Heterotrophic cultivation of microalgae for pigment production: A review. *Biotechnol. Adv.* **2018**, *36*, 54–67. [CrossRef]

41. Chua, E.T.; Dal'Molin, C.; Thomas-Hall, S.; Netzel, M.E.; Netzel, G.; Schenk, P.M. Cold and dark treatments induce omega-3 fatty acid and carotenoid production in *Nannochloropsis oceanica*. *Algal Res.* **2020**, *51*, 102059. [CrossRef]
42. Chen, J.H.; Nagarajan, D.; Huang, Y.; Zhu, X.; Liao, Q.; Chang, J.S. A novel and effective two-stage cultivation strategy for enhanced lutein production with *Chlorella sorokiniana*. *Biochem. Eng. J.* **2022**, *188*, 108688. [CrossRef]
43. Chen, C.Y.; Lu, I.C.; Nagarajan, D.; Chang, C.H.; Ng, I.S.; Lee, D.J.; Chang, J.S. A highly efficient two-stage cultivation strategy for lutein production using heterotrophic culture of *Chlorella sorokiniana* MB-1-M12. *Bioresour. Technol.* **2018**, *253*, 141–147. [CrossRef] [PubMed]
44. Chen, C.Y.; Liu, C.C. Optimization of lutein production with a two-stage mixotrophic cultivation system with *Chlorella sorokiniana* MB-1. *Bioresour. Technol.* **2018**, *262*, 74–79. [CrossRef] [PubMed]
45. Chen, W.C.; Hsu, Y.C.; Chang, J.S.; Ho, S.H.; Wang, L.F.; Wei, Y.H. Enhancing production of lutein by a mixotrophic cultivation system using microalga *Scenedesmus obliquus* CWL-1. *Bioresour. Technol.* **2019**, *291*, 121891. [CrossRef]
46. Ferreira, J.; Braga, M.Q.; Gama, R.C.N.; Magalhães, I.B.; Marangon, B.B.; Castro, J.S.; Lorentz, J.F.; Henriques, B.S.; Pereira, A.S.A.P.; Assemany, P.P.; et al. Carotenoids from wastewater-grown microalgae biomass: Life cycle assessment and techno-economical analysis. *J. Clean. Prod.* **2024**, *434*, 140526. [CrossRef]
47. Zhu, L.D.; Takala, J.; Hiltunen, E.; Wang, Z.M. Recycling harvest water to cultivate *Chlorella zofingiensis* under nutrient limitation for biodiesel production. *Bioresour. Technol.* **2013**, *144*, 14–20. [CrossRef] [PubMed]
48. Deprá, M.C.; Dias, R.R.; Severo, I.A.; de Menezes, C.R.; Zepka, L.Q.; Jacob-Lopes, E. Carbon dioxide capture and use in photobioreactors: The role of the carbon dioxide loads in the carbon footprint. *Bioresour. Technol.* **2020**, *314*, 123745. [CrossRef]
49. Shi, X.M.; Liu, H.J.; Zhang, X.W.; Chen, F. Production of biomass and lutein by *Chlorella protothecoides* at various glucose concentrations in heterotrophic cultures. *Process Biochem.* **1999**, *34*, 341–347. [CrossRef]
50. Ip, P.F.; Chen, F. Production of astaxanthin by the green microalga *Chlorella zofingiensis* in the dark. *Process Biochem.* **2005**, *40*, 733–738. [CrossRef]
51. Sun, N.; Wang, Y.; Li, Y.T.; Huang, J.C.; Chen, F. Sugar-based growth, astaxanthin accumulation and carotenogenic transcription of heterotrophic *Chlorella zofingiensis* (*Chlorophyta*). *Process Biochem.* **2008**, *43*, 1288–1292. [CrossRef]

Disclaimer/Publisher's Note: The statements, opinions and data contained in all publications are solely those of the individual author(s) and contributor(s) and not of MDPI and/or the editor(s). MDPI and/or the editor(s) disclaim responsibility for any injury to people or property resulting from any ideas, methods, instructions or products referred to in the content.

Journal of Applied Phycology
https://doi.org/10.1007/s10811-024-03313-y

RESEARCH

Ensuring nutrition and food safety within planetary boundaries: The role of microalgae-based ingredients in sustainable food chain

Darissa Alves Dutra[1] · Mariany Costa Deprá[1] · Rosangela Rodrigues Dias[1] · Leila Queiroz Zepka[1] · Eduardo Jacob-Lopes[1]

Received: 19 November 2023 / Revised: 1 July 2024 / Accepted: 2 July 2024
© The Author(s), under exclusive licence to Springer Nature B.V. 2024

Abstract
Although it is unanimous among scientists and researchers that the food production chain is a substantial contributor to environmental challenges, so far, no food ingredient has been evaluated for its environmental performance relative to planetary boundaries. Given this, this study conducts an analysis oriented to food key ingredients considered essential in human nutrition, namely: proteins, β-carotene as a precursor of vitamin A, and polyunsaturated fatty acids (docosahexaenoic and eicosapentaenoic acids), using life cycle assessment (LCA) linked to the planetary boundary structure, under nine indices: climate change, biosphere integrity, global biogeochemical fluxes, stratospheric ozone depletion, ocean acidification, global freshwater use, land use change, chemical pollution, and atmospheric aerosol loading. Protein sources from animals such as beef, pork, and poultry, β-carotene from palm oil and synthetic routes, and fatty acids from fish oil were also compared to alternative sources from microalgae-based ingredients. The results show that protein ingredients of animal origin and alternatives have largely contributed to the disruption of planetary boundaries. However, the worst environmental performance for protein ingredients studied was attributed to bovine protein, matching three risk indices (climate change, ecotoxicity, and photochemical ozone formation) out of the nine evaluated. On the other hand, among fine chemical food ingredients, only vitamin A from palm oil, which is mostly found in a risk and uncertainty zone, when compared to conventional synthetic processes and microalgae-based; these, in turn, operate fully within safe limits. In contrast, only one planetary index is assigned to the uncertainty zone for polyunsaturated fatty acids from fish oil, the others operate in safe zones equally for microalgae-based processes. Therefore, the conclusions highlight major challenges the food production chain faces to achieve safe and sustainable food. These results guide critical food groups and environmental indicators to prioritize in future efforts to reduce environmental impact.

Keywords Conventional/alternative protein · Environmental performance · Essential fatty acids · Planetary boundaries · Sustainable food chain · Vitamin A

Introduction

We live in the overshoot Era – The global boiling. The scourge of the climatic crisis imposed vertiginous changes on human life. And this is not just felt as heatwaves; climate change is also a crisis of reality disconnection. Acknowledging reality does not mean accepting it. However, to open the hand of reality is to commit a contract with chaos. Things are, regardless of how people feel or how we are fighting to make them different. Indeed, the reality is sovereign, and climatic changes cannot be denied (Deivanayagam and Osborne 2023).

Previously, we believed that the planet could always accommodate us. That the resilience of the Earth system meant that nature would always provide for us. But now we know that this is not necessarily the case. The latest scientific reports note the trajectory is grim. As big as the world may be, our impact is bigger. Therefore, understanding the interconnected environmental implications is crucial

✉ Mariany Costa Deprá
marianydepra@gmail.com

✉ Eduardo Jacob-Lopes
ejacoblopes@gmail.com

[1] Food Science and Technology Department, Federal University of Santa Maria, UFSM, Roraima Avenue 1000, Santa Maria, RS 97105-900, Brazil

Published online: 12 July 2024

if we, as humanity, want to deal with what is unequivocally a global crisis (IPCC 2022).

The global climate crisis, for the first time in decades, has been reflected in the food production chain. Extreme climatic events, from droughts to floods, have affected crop yields and their nutritional value, and some crops become inviable in certain areas (Hasegawa et al. 2021). Under thermal stress, animals will become less productive and more subject to plagues and diseases, which can become more frequent and spread (Sinel and Weis 2024). On the other hand, disclaiming the environmental impacts associated with the food production chain is equally reprehensible. Estimates suggest that agriculture and food production chains account for 24% of the total emissions of greenhouse gases (FAO 2022). This sector also appropriates one-third of ice-free land, and their use represents ~70% of groundwater extraction (Chen et al. 2018). Even so, this food system will have to supply 60% of the growing population's needs by 2050, and will still face enormous pressure from environmental changes (Raza et al. 2021). In this way, if simply feeding the current planet's population represents a critical challenge for our sustainable future, what could be our emergency solutions? Will we be condemned to tipping points that will plunge us into an unknown and nebulous territory, apart from planetary boundaries?

To try to solve these bottlenecks, several research fronts have investigated and modeled strategies to make food production chains more sustainable. Among them, research on resources use and emissions from conventional food production systems stands out, such as agricultural product segments (Lucas et al. 2023; Sajid et al. 2023), animal proteins (Kokemohr et al. 2022; Cheng et al. 2023; Goglio et al. 2023), grains, fruits and vegetables (Del Borghi et al. 2022; Nunez-Cardenas et al. 2022; Nabavi-Pelesaraei and Damgaard 2023; Vono et al. 2023), as well as food waste and loss management (Zhu et al. 2022; Zhen et al. 2023). However, although potential solutions have emerged from published scientific literature, there are gaps between the transfer of scientific knowledge to active agroindustrial practice, which makes it difficult to build cleaner production (Deprá et al. 2022a). This is because the sustainable transition is a complex and multidimensional long-term process, which should consider the technological and material resources applied, organizational and institutional structures, socio-cultural and economic aspects, and development policies (Verburg et al. 2022).

On the other hand, the next generation of alternative ingredients and foods such as plant-based proteins, cultured meat, and microbial ingredients have been touted as promising solutions to unburden many of the problems associated with conventional food production (Järviö et al. 2021; Allotey et al. 2023; Trinidad et al. 2023). Likewise, microalgal bioprocesses have been suggested as a jack-of-all-trades in the face of sustainable goals development, since photosynthesis-powered cells are expression chassis for multiple metabolites of nutritional interest. Among them, some primary and secondary metabolites, such as proteins (Janssen et al. 2022; Wang et al. 2023), essential fatty acids (Katayama et al. 2022; Vendruscolo et al. 2022), and pigments as vitamin A precursor, such as carotenoids (Fernandes et al. 2021; Sun et al. 2023), gain competitive space in the global market, due to their nutritional properties, bioaccessibility and cellular absorption (Nass et al. 2022). These biotechnological routes for alternative ingredients go beyond the scientific universe more easily than conventional systems, since there is greater investment from the private sector. Also, the race towards accelerating the technological readiness level is strengthened by this sector because the consumer market is concerned about acquiring sustainable ingredients and products that effectively provide nutritional and bioactive effects promised on the label, regardless high-ticket price to be paid (Cook et al. 2023).

However, taking the assumption that microalgae bioprocesses *per se* environmentally outperform conventional routes is not enough to make it sustainable. It is necessary to have a clear understanding of the project and the conditions of the process and submit it to the evaluation of its potential burdens. Faced with this, recent scientific discoveries suggest that the Achilles heel of microalgal biotechnology resides in the substantial energy footprint and natural resources high-demand in its industrial productions (Deprá et al. 2020a; Dias et al. 2023). In addition, identifying the sustainable pipeline of the food production chain, free from socio-political or economic inclinations, is essential to ensure nutritious and safe food for humanity. Given this narrative, becomes imperative to be alert to the vital signs of the Earth and recognize that the ecosystem is not unlimited. So, the starting point to begin a change in the environmental scenario is to account for its impacts. However, just stacking a pile of numbers is not enough to stop them. The scientific community must manage and provide immaculate environmental data and make it available to the public, to make the difference through actionable information so that more people can see the reality to which we situate ourselves; before all of our summers turn into smoke.

In this way, the concept and structure of planetary boundaries were developed to control anthropogenic pressure on the Earth system and define a safe operating space for humanity (Cernev 2022; Liao et al. 2023). This methodology assesses nine environmental indices, including climate change, biosphere integrity, global biogeochemical flows (nitrogen and phosphorus), stratospheric ozone layer depletion, ocean acidification, global use of freshwater, changes in land use, chemical pollution, and atmospheric aerosol load. Furthermore, it has been adopted on two main scales (i) absolute (global) and (ii) individual (per capita), which, with

the combined assistance of the life cycle assessment tool, allows the environmental impacts of the system considered to be quantified throughout its entire life cycle, from the extraction of the material, through the production, transport, and use phase until the end of its life (Bjørn and Hauschild 2015; Sala et al. 2020).

Nevertheless, even though studies have been published and the methodology has evolved, current approaches have not been able to avoid breaking safe operational limits, bringing deleterious and catastrophic consequences to humanity (Richardson et al. 2023; Stranddorf et al. 2023). This shows that science has not yet decided which emerging path to follow about sustainable food production. Furthermore, research generally evaluates the industrial aspects of the food production chain without an individual view of which points we are infringing. However, a quantitative description of the main inputs and outputs of the food system and their interdependencies is necessary to understand the effects of our food system on the multiple processes of the Earth system. In this way, our study hypothesis is that the description of the conventional and alternative system based on the individualization of key ingredients in the food chain will offer a new contribution by exploring potential transgressions of planetary boundaries on a downscaling per capita scale to satisfy the dietary demands associated with populations future. Besides, in the specific case of alternative microalgae-based ingredients, whose environmental issues and sustainability aspects have been put to the test in recent years, it is important to note that no research has focused on assessing the integrated environmental impact within planetary boundaries. Therefore, the core of the study aims to fill this knowledge gap and show that it is possible to alleviate future food demands, by operating in safe zones, through microalgae-based ingredients ingestion.

On the face of it, the main objective of this investigation is to bring a new look at microalgae-based key ingredients as a viable path towards sustainability practices for the food production chain. To this end, the research questions of this study consist of (i) quantifying the environmental impacts of key ingredients for human nutrition: proteins, vitamins, and essential fatty acids from the conventional food chain, (ii) measuring the environmental burdens of alternative microalgae-based ingredients, identifying their strong and blind spots to open research paths and perspectives to enhance their inclusion in the chain of more sustainable food production, and (iii) to compare approaches specific to the point where conventional or alternative systems depart or break planetary boundaries. Therefore, in this article, we take a step forward and create the first publication that draws a deeper understanding of the need to square environmental analyses of food production against planetary boundaries. Through this narrative, it is possible to present paths for future research on the sustainability assessment of the conventional and alternative food production chain, which interacts in a balanced way with the environment, society, and socioeconomic policies, seeking to reduce the negative impacts generated in recent decades. Thus, the novelty of this article is that it brings together for the first time the integrated sustainability approach to planetary boundaries under the evaluation of conventional and alternative ingredients, in order to provide a more complete framework of sustainable practices that both the production chain food can adopt in its industrial processes, as well as inform consumers about the environmental burdens associated with their food choices. This can help not only the conventional food chain on sustainability indicators but also researchers, consumers, decision-makers, and stakeholders who want to delve deeper into the nutrition and food safety sustainable and alternative approaches.

Material and methods

Life cycle assessment integrated to planetary boundaries

The life cycle assessment (LCA) methodology standardized by international standards ISO 14040 was adopted to identify and quantify the potential environmental impacts of production chains of proteins, vitamin A, and essential fatty acids for human consumption from conventional and alternative routes from microalgae-based processes (ISO 2006). This methodological tool included the definition of the objective and scope (I), inventory analysis (II), impact assessment (III), and interpretation of the results (IV).

Concomitantly, following the guidelines of Ryberg et al. (2018), changes were made in some specific aspects of the LCA methodology to allow the indicators of planetary boundaries to be used in the life cycle impact assessment phase. These changes are explained promptly when relevant. Therefore, in the following paragraphs, the four phases are described with reference to the processes evaluated in concern.

Goal and scope definition

The objective of the study was to evaluate the environmental impacts of three classes of key nutrients required by the human body and essentials to support the basis of food and nutritional safety, being: (i) proteins; (ii) vitamin A, and (iii) essential fatty acids, limited to eicosapentaenoic (EPA) and docosahexaenoic (DHA) acids, which are also frequently used as ingredients to formulate products with a healthy appeal. In this way, the first part of the study consisted of evaluating conventional proteins, originating from animal sources, such as bovine protein, pork, and poultry, in

comparison with an alternative protein source arising from the microalga *Arthrospira platensis*. Subsequently, the production scenarios of vitamin A were evaluated against the ingestion of β-carotene - the main precursor of this chemical compound, under the scenarios of obtaining it from its synthetic form, palm oil, and the microalga *Dunaliella salina*. Finally, the supplementation of essential fatty acids was investigated in the fish oil extraction scenario from anchovies and microalgae extraction for DHA by *Schizochytrium* sp. and EPA by *Nitzschia laevis*. It is worth noting that the data collection for theoretical and experimental analysis was based on process data consolidated by classical references from the literature and databases.

Functional unit and system boundaries

The main function of proteins, vitamins, and essential fatty acids is to provide macro- and micronutrients which serve as cellular building blocks for the good functioning of the human body. Therefore, the functional unit considered by this study was based on the recommended dietary allowance (RDA) for adult individuals. Namely, recommended dietary intake is the amount of a nutrient that must be ingested to meet your basic nutritional needs. Thus, protein intake was established at 20 kg person^{-1} year^{-1}, vitamin A at 0.6 g person^{-1} year^{-1}, and essential fatty acids at 73.0 and 36.5 g person^{-1} year^{-1} for DHA and EPA, respectively (FAO 1994; 2013; WHO 2004). This definition of functional unit allows a fair comparison between the raw materials under investigation, once it allows considering their respective performance rates. Furthermore, the expression of the functional unit in mass per unit of time is not common in LCA but would need to be established, because the LCIA method based on planetary limit requires that the function be continuously supplied (Ryberg et al. 2018).

System boundaries were defined from the cradle-to-gate approach, i.e., it is an assessment of a partial product life cycle, from resource extraction (cradle) to the factory gate (before being transported to the consumer). Additionally, it is essential to note that impacts on resource obtention of products such as electricity, nutrients, and chemicals were included in this analysis. However, the impacts associated with steps of construction, transport of inputs and materials, and end of life of equipment and infrastructure were not considered in any of the scenarios; just the requirements necessary for their operations. Therefore, the layout of all the technical features of the case studies analyzed for conventional food chains is presented in Fig. 1, and routes for alternative microalgae-based ingredients are s shown in Fig. 2.

Life-cycle inventory

The life cycle inventory data for the evaluated scenarios are derived from the literature and databases. The energy, chemical, and other nutrient requirements necessary for the production operations of conventional proteins are detailed in Table 1. The inputs/outputs of β-carotene production from the synthetic route and palm oil can be consulted in Table 2

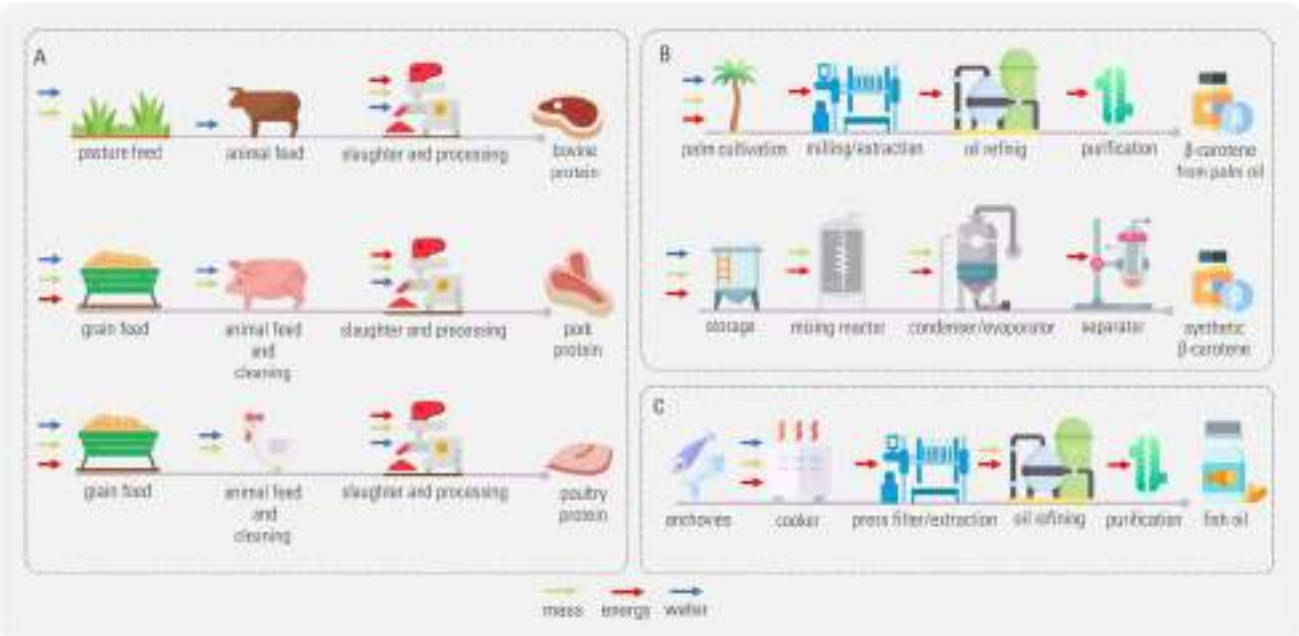


Fig. 1 The boundary systems of conventional ingredients for human nutrition. (**A**) Proteins from bovine, pork, and poultry; (**B**) β-carotene as an ingredient precursor for vitamin A from palm oil and synthetic process; (**C**) Polyunsaturated fatty acids from fish oil

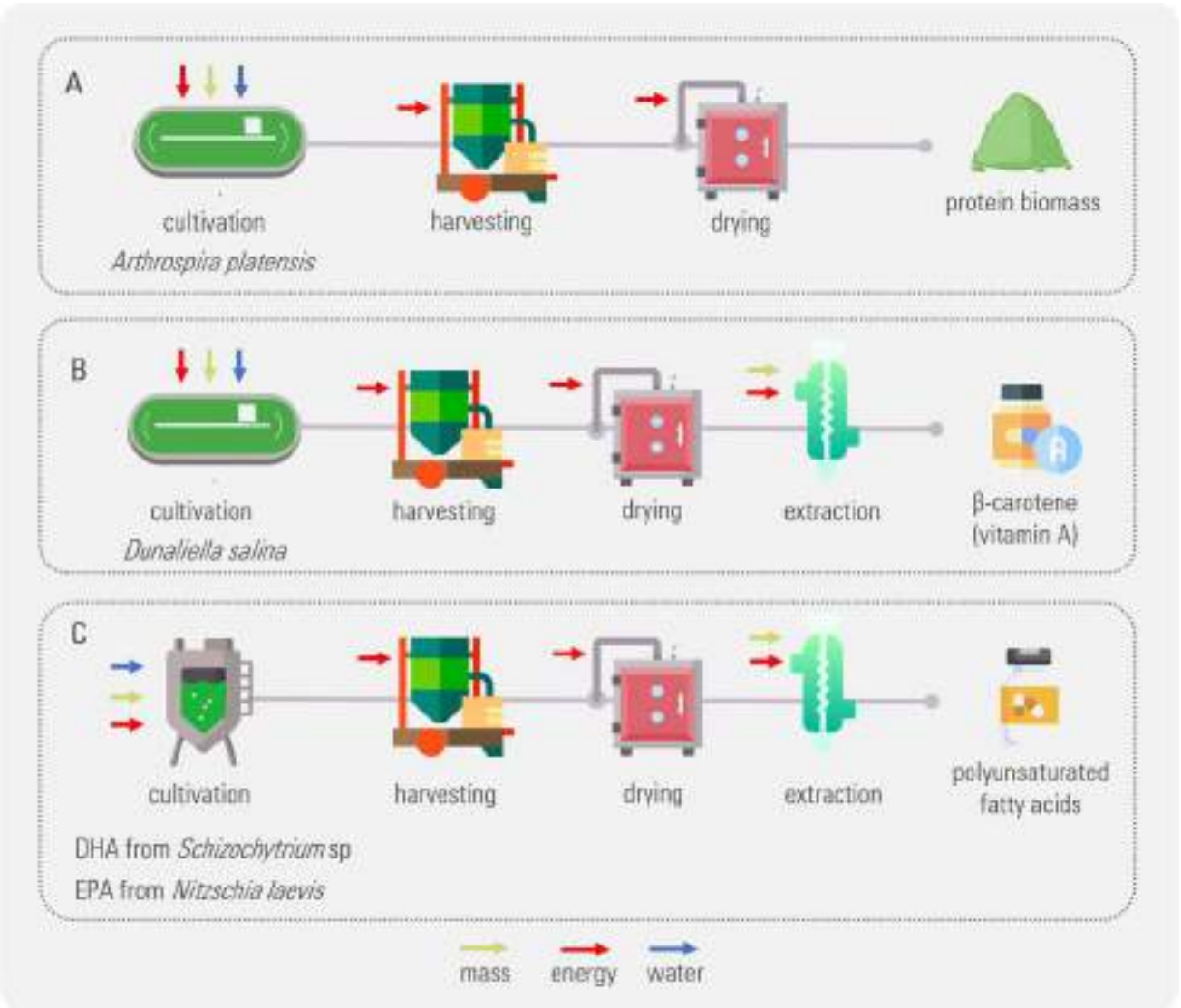


Fig. 2 The system boundaries for alternative ingredients production from microalgae-based processes. (**A**) Protein from *Arthrospira platensis*; (**B**) β-carotene as an ingredient precursor for vitamin A from *Dunaliella salina*; (**C**) Polyunsaturated fatty acids from *Schizochytrium* sp. and *Nitzschia laevis*. DHA: docosahexaenoic acid; EPA: eicosapentaenoic acid

and Table 3, respectively. Additionally, the inventories of the fatty acids production derived from fish oil are specified in Table 4. The inputs/outputs of alternative ingredients from microalgae-based processes are shown in Table 5.

Life-cycle impact assessment

The potential environmental impacts were determined by the *ReCiPe* method for traditional LCA (Midpoint, World – Hierachist version) according to Huijbregts et al. (2017). This method is particularly advantageous because it (1) contains the broadest set of midpoint impact categories; (2) enables impact categories to implement characterization factors at an international scale; and (3) does not include potential impacts from future extractions in the impact assessment and assumes that they have been included in the inventory analysis, which is different from other approaches. In this study, the nine impact categories were considered, being the global warming potential (GWP), fossil fuel depletion (FFD), photochemical ozone creation potential (SMOG), ozone depletion potential (ODP), ecotoxicity (ECO), water footprint as total water-scarcity (WF), eutrophication potential (EP), acidification potential (AP), and land use (LU) (Goedkoop et al. 2009; Jacob-Lopes et al. 2021). Using this method, research can capture a more holistic view of the environmental impacts associated with processes. The technical calculation was conducted by directly fitting the *Ecoinvent* database that are available as Microsoft Excel

Table 1 Materials, nutrients, and energy requirements for the production of protein from conventional sources. Values are referred to the functional unit of 20 kg protein person^{-1} year^{-1}. Adapted from Pelletier et al. (2010); González-García et al. (2015); Skunca et al. (2018); Pexas et al. (2021); Vibart et al. (2021); Deprá et al. (2022b)

Farm process	Unit	Bovine	Pork	Poultry
Input				
Pasture fertilizer				
Nitrogen	kg	36.15	-	-
Phosphate	kg	16.46	-	-
Potassium	kg	21.07	-	-
Herbicide	kg	0.32	-	-
Feed				
Maize grain	kg	-	174.99	90.36
Soybean grain	kg	-	-	71.84
Soybean meal	kg	-	49.99	-
Wheat grain	kg	-		17.77
Glucose	kg	-	12.50	-
Energy				
Diesel	L	1200.0	124.99	48.88
Water				
Water ingested	L	40.9	11.0	4.76
Cleaning				
Sodium hydroxide	kg	-	49.99	65.18
Sodium hypochlorite	kg	-	49.99	65.18
Processing and slaughter				
Water	L	1,307.64	499.98	274.05
Energy	MJ	923.04	579.97	325.90
Chemicals	g	296.14	119.16	199.24
Output				
Animal protein	kg	20.0	20.0	20.0

files (generally multiplying the data sets by a proportionality factor corresponding to the use case and then summing all data sets to be considered) as described generically in Eq. 1, which is expressed in mass released into the environment per functional unit. The characterization factors of the environmental impacts are presented in Supplementary Material (Table S1).

$$Ci = \sum CF \times Ei \quad (1)$$

where Ci is the environmental impact category, CF is the characterization factor, and Ei is the emission inventory, expressed in mass released into the environment per functional unit.

The integration between planetary boundaries and environmental impact metrics was performed by developing a specific impact assessment, according to Ryberg et al. (2018). This methodology assumes that the ecosystem can operate in natural boundaries, known as a safe operating zone (green), an uncertainty zone in increasing risk (yellow),

Table 2 Elementary flows of the process to produce synthetic β-carotene as an ingredient precursor vitamin A. Values are referred to the functional unit of 0.6 g β-carotene person^{-1} year $^{-1}$. Adapted from Herloff and Ferdinand 1954; Deprá et al. (2020b)

Process	Unit	Amount
Input		
Equipment's		
Storage tank	kWh	6.91×10^{-3}
Mixing reactor	kWh	3.6×10^{-5}
Metering pumps	kWh	2.0×10^{-2}
Condenser	kWh	2.55×10^{-3}
Evaporator	kWh	6.3×10^{-4}
Extractor	kWh	6.3×10^{-4}
Chemicals		
β-ionone	kg	6.36×10^{-4}
Phosphonium salt	kg	2.88×10^{-3}
Aldehyde	kg	2.04×10^{-4}
Acid acetic	m^3	5.4×10^{-7}
Ammonia acetate	m^3	1.8×10^{-5}
Water	m^3	2.28×10^{-4}
Output		
β-carotene – precursor vitamin A	kg	0.006

Table 3 Inputs and outputs energy and materials for palm oil production for extraction of β-carotene as an ingredient precursor of vitamin A. Values are referred to the functional unit of 0.6 g β-carotene person^{-1} year $^{-1}$. Adapted from Queiroz et al. (2012); Siregar et al. (2015); Saswattecha et al. (2016); Nasution et al. (2018)

Process	Unit	Amount
Agriculture stage		
Input		
Fertilizer		
Nitrogen	kg	25.09
Phosphorus	kg	15.05
Potassium	kg	60.22
Herbicide	kg	2.50
Output		
Fresh fruit bunch	tonne	5.01
Palm oil mill stage		
Steam	tonne	2.0
Electricity	MJ	405.81
Output		
Crude palm oil	tonne	1.62
Extraction stage		
sCO_2 extraction	kWh	1.29
Output		
β-carotene – precursor vitamin A	kg	0.006

Table 4 Inputs and outputs energy and materials of extraction fish oil for DHA and EPA ingredients. Values are referred to the functional units of 73.0 and 36.5 g person^{-1} year^{-1} for DHA and EPA, respectively, totaling a blend oil of 0.109 kg person^{-1} year^{-1}. Adapted from Laso et al. (2017); Monsiváis-Alonso et al. (2020); Bartek et al. (2021); Arfelli et al. (2023)

Process	Unit	Amount
Pre-treatment stage		
Input		
Fresh anchovies	kg	4.62
Preparation	kWh	0.40
Output		
Frames and heads fishes	kg	1.85
Extraction stage		
Cooker	kWh	20.9
Press filter	kWh	0.06
Decanter/Centrifuge	kWh	37.0
Oil refining stage		
Degumming	kWh	0.05
Neutralization	kWh	0.05
Deodorizer	kWh	0.91
Evaporation/Stripper	kWh	1.19
Winterization	kWh	0.01
Output		
Blend oil w/ DHA/EPA	kg	0.109

and a high-risk zone (red zone) (Fig. 3) (Rockström et al. 2009). However, in this study, the egalitarian approach and the downscaling to per capita levels were applied based on the method proposed by Moberg et al. (2020), by assuming an equal distribution across the global population in 2050 (10 billion) (United Nations 2022). The downscaling methodology was adopted because it elucidates information about how much each global citizen uses the globally allowed emissions and resource use of food systems, regardless of where the impacts are caused (Ryberg et al. 2020). The values considered as safe operational limits and the high-risk zone (red zone) are presented in Table S2. The results are presented on a 10-point scale, where 1 to 4 are the safe operational zones, 5 to 7 uncertainty zones and 8 to 10 are the risk zones.

Interpretation of results

The results of the LCI and LCIA from the life cycle assessment of nutritional key ingredients from conventional and alternative routes are considered together so that the information is interpreted and converged into conclusions and recommendations. To this end, the results were calculated according to the values characterized by the midpoint impact categories and compared against planetary boundaries to expand possible sustainability strategies and discussion with other studies found in the literature. In this case, the planetary boundaries established are the global perception of what environmental damage is acceptable and what risks and changes we are willing to assume in the face of this partial assessment. Therefore, in this case, our results are based on this principle for comparison purposes.

Results and discussion

Ingredients protein for human nutrition

Protein intake patterns are a strong feature of healthy diets, as these protein food sources contribute other nutrients that tend to cluster, resulting in important nutritional building blocks. However, protein sources have been linked to potentially irreversible environmental impacts on our ecosystem. Therefore, to be considered sustainable ingredients, these production systems must operate within a safe operating space (Perraud et al. 2023). Thus, the environmental impact of conventional (beef, pork, and poultry) and alternative (microalgae) sources of proteins as ingredients for human food are presented in Table 6, and their scores concerning the planetary boundaries in Fig. 4.

The results show that none of the conventional protein ingredients are sustainable across all planetary boundaries. In contrast, only one planetary limit was not exceeded for all scenarios, which is the index associated with land use. This is because the current level of the control variable is significantly below the portion occupied by the safe operating space.

When considering the number of limits that are exceeded, the performance of protein ingredients from beef production presents the worst environmental scenario, being one step away from breaking the planetary integrity indices for climate change, photochemical ozone formation potential, and ecotoxicity. In addition, indices related to acidification, eutrophication, demand for energy resources, and water footprint remain largely in uncertainty zones (yellow zone), which may be exceeded at any time. In comparison, conventional protein sources from swine and poultry production show a similar profile. However, these key ingredients show slight environmental improvement when referring to acidification, ecotoxicity, and water footprint indices. This can be attributed mainly to zootechnical practices and animal management, which directly influence the growth rates of the animals, as well as the feed conversion efficiencies, depending on the cultivation system (extensive or confined) and the formulation of the feed provided (Johnson et al. 2020; Schmid et al. 2024).

On the other hand, the alternative protein ingredient from microalgae-based processes showed a positive performance,

Table 5 Inventory inputs/outputs for alternative ingredients from microalgae-based processes. Values are referred to the functional units of 20 kg protein person^{-1} year^{-1}, 0.6 g β-carotene person^{-1} year^{-1}, and 73.0 and 36.5 g person^{-1} year^{-1} for DHA and EPA. Adapted from Huang et al. (2023); Deprá et al. (2020a), (2020b); Dias et al. (2023)

Process	Unit	Protein by *Arthrospira platensis*	β-carotene by *Dunaliella salina*	DHA by *Schizochytrium* sp.	EPA by *Nitzschia laevis*
Cultivation					
Input					
Nutrients enrichment					
Phosphate	kg	0.90	1.78×10^{-4}	2.05×10^{-3}	1.73×10^{-3}
Nitrate	kg	1.32	2.55×10^{-4}	0.04	3.46×10^{-2}
Glucose	kg	-	-	0.85	0.72
Open ponds	m^3	113.62	2.2×10^{-2}	-	-
Electric energy for paddle wheel	kWh	61.34		-	-
Electric energy for water pumping	kWh	11.36	0.52	-	-
Electric energy for CO_2 injection	kWh	37.54	1.75	-	-
CO_2 consumption	kg	72.72	2.0×10^{-2}	-	-
Water evaporation	m^3	14.77	2.86×10^{-3}	-	-
Fermenter	m^3	-	-	0.17	0.14
Sterilization	kWh	-	-	1.23	1.03
Agitation	kWh	-	-	0.03	0.02
Aeration	kWh	-	-	4.10	3.45
Biomass productivity	kg m^3	0.32	0.45	4.43	0.75
Output					
Algae liquid	kg	238.80	0.12	9.04	1.28
Harvest					
Input					
Power consumption centrifugation	kWh	-	-	0.17	0.14
Power consumption filtration	kWh	79.53	-	-	-
Power consumption pumping	kWh	-	1.46×10^{-1}	-	-
Flocculating - magnesium hydroxide	kg	-	1.60×10^{-4}	-	-
Flocculating – sodium hydroxide	kg	-	7.48×10^{-3}	-	-
Drying					
Input					
Wet biomass	kg	179.10	0.09	6.78	0.96
Spray-dryer	kWh	77.01	0.04	2.91	0.41
Extraction					
Input					
Dry biomass	kg	-	0.01	0.75	0.10
sCO_2	kWh	-	0.008	0.60	0.08
Output					
Alternative bioproduct	kg	20.0	0.006	0.073	0.036

operating in a safe zone for six of the nine planetary indices evaluated. However, this alternative ingredient also operates in risk zones for planetary indices associated with climate change and smog and uncertainty zones for eutrophication potential. These results are often attributed to the low cell yields found in industrial production systems, which drives the high energy demand associated with downstream steps, i.e., harvesting and drying of biomass (Valdovinos-García et al. 2021; Zhu et al. 2024). Likewise, the greater overcoming of environmental burdens for eutrophication occurs in the face of nitrogen and phosphorus flows, which are essential nutrients for microalgal metabolism (Medeiros and Moreira 2022; Dias et al. 2023).

Environmental burdens related to water footprint and water-scarcity are frequently questioned regarding key protein production. The water footprint for conventional proteins, even though they vary among species, presents expressive values, operating in uncertainty zones, and thresholds

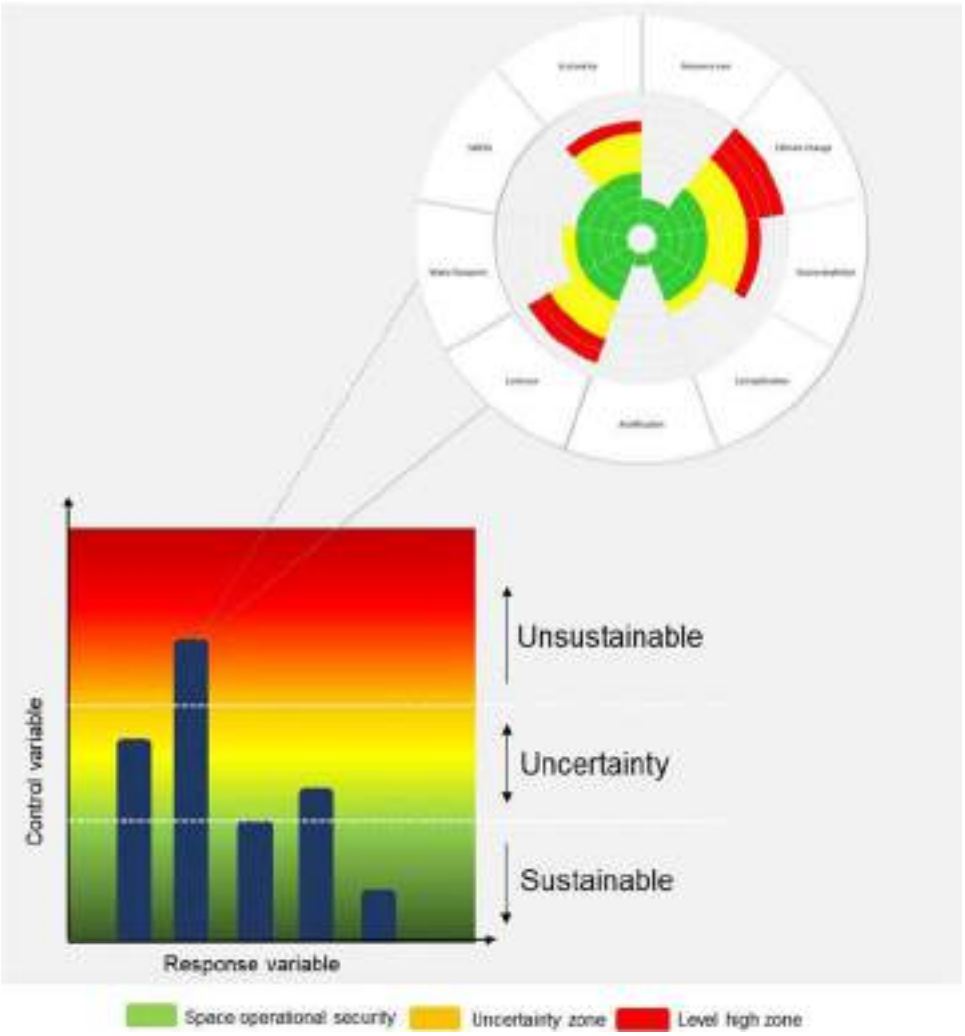


Fig. 3 The conceptual framework for the planetary boundary approach, showing the safe operating space, the zone of uncertainty, the position of the threshold (where one is likely to exist), and the area of high risk. Adapted from Steffen et al. (2015)

Table 6 Environmental impacts of the protein production from conventional sources (beef, pork, and poultry) and alternative source (microalgae *Arthrospira platensis*). The characterized values are referred to the functional unit of 20 kg protein person^{-1} year^{-1}

Impact categories	Unit	Protein			
		Conventional			Alternative
		Bovine	Pork	Poultry	Microalgae (*Artrhospira platensis*)
Ozone depletion	kg CFC-11 eq	4.00×10^{-4}	9.17×10^{-5}	2.04×10^{-7}	2.81×10^{-5}
Global warming	kg CO_2 eq	$3.91\times10^{+2}$	$1.77\times10^{+2}$	$1.49\times10^{+2}$	$1.60\times10^{+2}$
Photochemical ozone creation	kg NMVOC eq	$1.26\times10^{+1}$	$1.00\times10^{+1}$	4.10×10^{0}	$1.03\times10^{+1}$
Acidification	mole H^+ eq	2.07×10^{0}	7.94×10^{-1}	6.26×10^{-1}	4.67×10^{-1}
Eutrophication	kg N eq	1.36×10^{0}	1.62×10^{0}	1.87×10^{0}	3.14×10^{-1}
Ecotoxicity	CTUe	$2.34\times10^{+3}$	$9.32\times10^{+2}$	$6.51\times10^{+2}$	$9.56\times10^{+2}$
Fossil fuel depletion	MJ	$2.01\times10^{+3}$	$1.19\times10^{+3}$	$1.21\times10^{+3}$	$2.59\times10^{+2}$
Water footprint	m^3	$1.31\times10^{+3}$	$5.01\times10^{+2}$	$2.74\times10^{+2}$	$1.14\times10^{+2}$
Land use	kg soil loss	5.00×10^{0}	6.00×10^{-1}	3.00×10^{-1}	2.27×10^{0}

to breaking the planetary boundaries. This performance is associated with pasture irrigation, water consumption per animal, slaughtering, and processing of raw material (Cordeiro et al. 2022; Deprá et al. 2022b). Comparatively, microalgae-based ingredients operate in safe areas in this study, without presenting an imminent risk of breaking

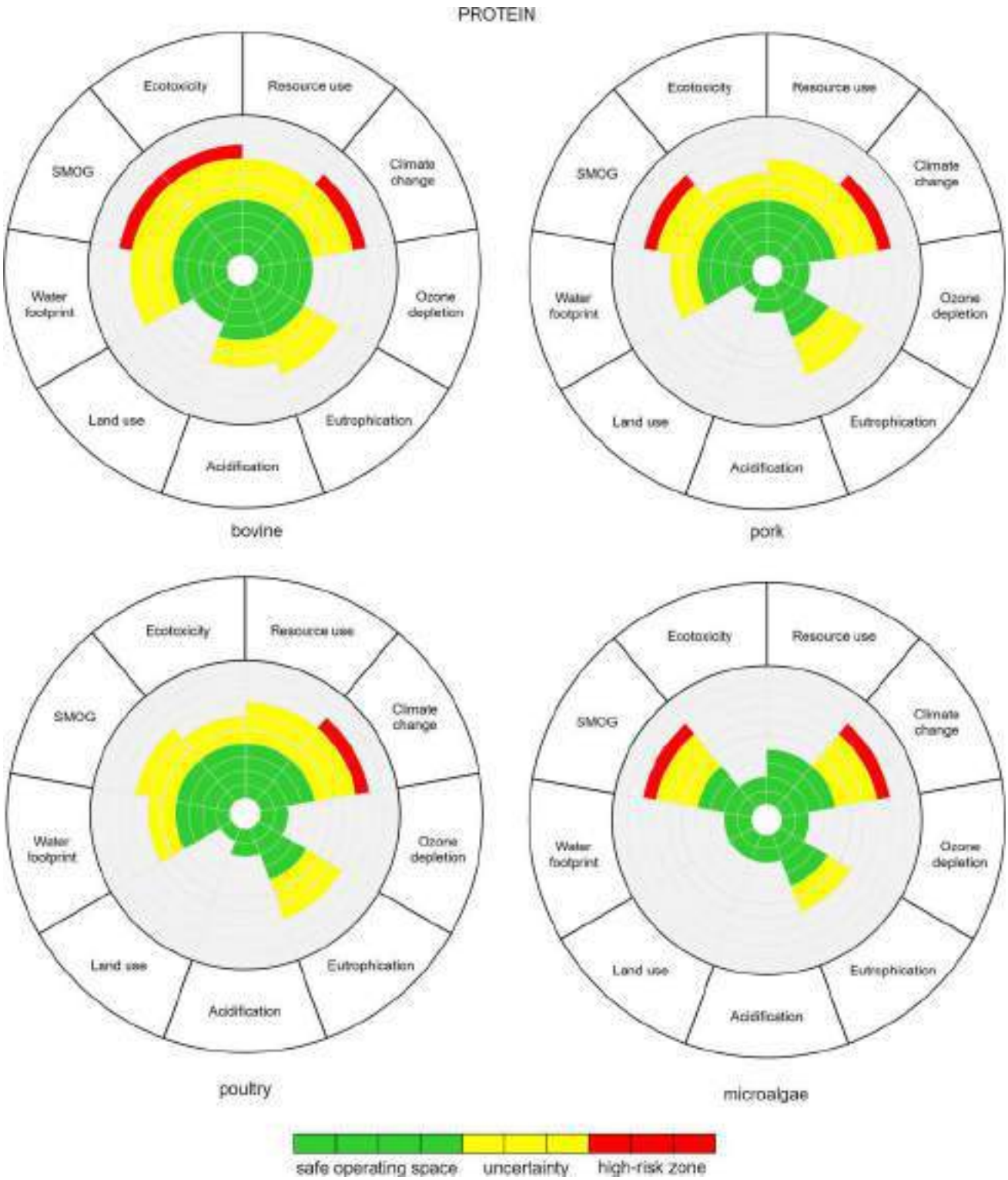


Fig. 4 Environmental performance of protein ingredients applied to planetary boundaries

planetary boundaries. There are many discussions about the environmental viability attributed to water use in microalgae bioprocesses. This is because water is indispensable for the survival of microalgae cells, once it acts as a thermal regulator, in addition to being the main nutrient supply mechanism. However, strains that present high cell density

and productivity can help reduce these demands. Also, lessening freshwater use through the water recovery from the cultures in the biomass harvesting stage can be reduced by up to 75% (Severo et al. 2020). Likewise, rainwater, seawater (in halotolerant/halophilic strains), or wastewater integration can also be a promising alternative to freshwater dependence in microalgae cultures (Ishika et al. 2019).

The impacts on land use change are an area of research commonly neglected in environmental assessment studies. However, the change in land use under the occupation approach is an equally important factor in this study, not only in conventional proteins but also in how microalgae cells are cultivated. As shown in Table 6, land use requirements for poultry and pork protein presented the best environmental scenarios. On the other hand, animal protein from bovine presented the worst scenario, since animal nutrition was defined by extensive pasture, which naturally results in greater land use (Nijdam et al. 2012). In contrast, when we highlight the results of the microalgae-based alternative protein, the evaluated scenario operates in a safe zone (Fig. 4). However, it must be considered that open cultivation system construction requires large structures, due to water depths at least 15 cm deep to have a surface/volume suitable for obtaining the maximum possible lighting for it to occur the photosynthetic reaction efficiently (Pruvost et al. 2016). This can be a problem when we scale impacts to functional units above those established in this study. However, it is important to highlight that microalgae-based systems can be deployed in non-arable land, that is, areas that are not suitable for traditional agriculture, such as deserts or coastal. This reduces pressure on agricultural land and can help conserve fertile soil for food production (Nagappan et al. 2021). Furthermore, microalgae cultivation in photobioreactors can be an alternative to the demand for land, since this equipment usually operates compactly, encompassing high-volumes of work; however, these photobioreactors operate under a high energy demand, which can overload other environmental indices (Deprá et al. 2021).

Against this background, in an environment as complex as the food chain, it becomes clear that the current model of producing proteins from microalgae will not solve the total problem. The barriers associated with the high energy demand with cultivation and harvesting systems, and productivity fluctuation rates, tend to be equally important factors for the sustainable certification of these alternative ingredients. Another latent factor that contributes to driving environmental inefficiency is associated with the selection of the energy matrix used to drive the units' operations. Electricity from coal-fired power plants has average emission values of ~0.602 $kgCO_2eq\ kWh^{-1}$, driving an increase in the environmental burden in these categories (Deprá et al. 2020a). Conversely, although microalgae-based processes are naturally adept at capturing and storing carbon, carbon dioxide fixation rates, depending on strains and cultivation conditions, are generally found in the range of 0.01-0.4. $kgCO_2\ m^3\ day^{-1}$, being insufficient to neutralize emissions generated by bioprocesses (Deprá et al. 2020c; Yao et al. 2023). Thus, recent studies have evaluated the possibility of alleviating the environmental burden related to climate change rates through renewable energy integration into microalgae platforms. These studies suggest reductions of up to 80% of total emissions (Dias et al. 2023). Therefore, in the race for sustainability, the integration of renewable energy and revenue generation from carbon credits are emerging as potential strategies that can be implemented to leverage these ingredients as promising opportunities for sustainable consolidation.

Additionally, we highlight the unanimous environmental pressure under climate change in all scenarios of protein ingredients evaluated here. As future concerns, we emphasize the difficulty in food diversity operating within the safe zone. In addition, climate change drives global phenomena such as reductions in agricultural production, supply instabilities, and increased food losses (Abbass et al. 2022). Consequently, the supply of protein has been highlighted as one of the main nutritional ingredients that will be lacking in the future, since animal proteins, specifically red and white meat, are not accessible to the food-insecure population. As a solution, the measures taken so far are moving towards the flexibility of a flexitarian diet based on vegetables. However, replacing protein sources with environmental factors can be a risky task. It is important to consider high-quality alternative strategies with well-proportioned amino acid profiles that meet WHO/FAO/UNO standards for human nutrition. From this perspective, microalgal proteins are presented as a new and accessible resource, equivalent to the usual sources. Siahbalaei et al. (2021), found that the essential, non-essential, non-protein, flavoring, hydrophobic, aromatic, bitter and sweet amino acids found in microalgae were equal to or greater than those found in animal proteins. Thus, proteins from species such as *A. platensis* and *Chlorella vulgaris* have been recognized by the World Health Organization for their potential to meet the needs of essential amino acids for humans. However, at the consumer level, greater health awareness and sustainability do not always translate into concrete actions. Therefore, measures to encourage flexibility and inclusion of alternative proteins must come from public policies to promote research, development, and the commercialization of potentially sustainable alternative ingredients. Some initial incentives include (i) research funding aimed at advancing technologies and filling knowledge gaps, (ii) industrial policy investments in infrastructure and processing facilities, (iii) incorporation of environmental considerations into approval processes regulations, and (iv) reinforced coordination between policies and interested parties (Smith et al. 2024). In addition, providing frameworks access to

facilitated knowledge, through harmonized regulatory and food standards across, which allows more transparency about risks about food safety and the allergenicity potential of these future ingredients, can help reduce complexity and become these more sustainable processes for society.

β-carotene as an ingredient precursor for vitamin A

Carotenoids, such as β-carotene, play vital roles in food and human health. For a long time, they captivated the interest of researchers around the world due to their pleasant orange-yellow tones, followed by their attribution in nutrition as precursors of vitamin A and retinoid. However, when embarking on the painstaking task of evaluating these food ingredients, food chemists were faced with the vast differences and discrepancies of these molecules; and most importantly, their actual effectiveness as vitamin A precursors, as well as their overall bioaccessibility and bioavailability (Nass et al. 2022; Meléndez-Martínez et al. 2023). Against this background, Table 7 and Fig. 5 direct the environmental performance and planetary boundaries integrity, respectively, for the main conventional routes of β-carotene marketed as vitamin A precursor ingredients and their respective microalgal countertype.

As can be seen in Fig. 5, the per capita supplementation of β-carotene as a precursor ingredient of vitamin A operates in a safe space for the conventional synthetic and alternative route based on microalgal processes. In contrast, the environmental performance attributed to the natural route derived from palm oil represents an imminent environmental risk to the ecosystem, infringing three (climate change, ecotoxicity, and energy resource) of the nine ecological dimensions evaluated here.

These estimates of potential environmental degradation caused by the processing of palm oil as a feedstock for obtaining β-carotene are driven by multiple factors, among which direct human pressures stand out, such as changes in land use during the seed plantation, palm tree cultivation, and fresh fruit bunches processing to obtain crude palm oil (Saswattecha et al. 2016). Moreover, flows from fertilizer use, and high energy load in steam and electricity form were identified as the main environmental stress factors, putting planetary biodiversity at risk (Pulingam et al. 2022).

In contrast, in a direct comparison between the synthetic and the microalgae-based alternative route, the more sustainable environmental profile is attributed to the synthetic route. In this process, the environmental charges are minimal, mainly derived from the demand for energy resources for the industrial plant operation. In addition, chemical streams depicted <1% and were therefore omitted from the system boundary of this study. However, the reason for synthetic β-carotene to operate smoothly in a safe operational space is that conventional routes are characterized by chemical methods that present high yields (>85%), such as the method used by Wittig condensation; which naturally makes these processes highly efficient in terms of material and energy use (Britton et al. 1996; Nielsen et al. 2022).

At the same time, the environmental performance of the microalgal countertype was also encouraging. The microalgae facilities for commodities require large energy resources and, currently, chemical resources are needed in large quantities, representing a technological, economic, and environmental challenge. However, when it comes to fine chemical compounds, the turning point of this biotechnological route presents itself as an advantageous solution for humanity and the environment. Science evolution and techniques' improvement allowed the benefits to reach an industrial scale. The first point is the high yield of the target compound, representing ~6-14% dry biomass weight (Xi et al. 2022). This unique characteristic identified in the species *Dunaliella salina* results in cells being negatively buoyant, allowing its harvest to be carried out through flocculation induced by the increase in pH of the culture sludge (Borowitzka 2018; Besson et al. 2019). Studies aimed at increasing the flocculation harvesting technique have demonstrated that flocculating agent combinations such as magnesium and sodium

Table 7 Environmental impacts of the β-carotene production from synthetic, palm oil and microalgae sources as an ingredient precursor for vitamin A. The characterized values are referred to the functional unit of 0.6 g β-carotene person^{-1} year^{-1}

Impact categories	Unit	β-carotene		
		Synthetic	Palm oil	Microalgae (*Dunaniella salina*)
Ozone depletion	kg CFC-11 eq	2.88×10^{-9}	3.78×10^{-4}	4.89×10^{-7}
Global warming	kg CO_2 eq	9.45×10^{-3}	$5.84\times10^{+2}$	1.63×10^{0}
Photochemical ozone creation	kg NMVOC eq	2.10×10^{-4}	$1.12\times10^{+1}$	3.78×10^{-2}
Acidification	mole H^+ eq	5.03×10^{-5}	2.81×10^{0}	8.62×10^{-3}
Eutrophication	kg N eq	1.80×10^{-5}	1.46×10^{0}	3.09×10^{-3}
Ecotoxicity	CTUe	6.69×10^{-2}	$2.37\times10^{+3}$	$1.39\times10^{+1}$
Fossil fuel depletion	MJ	2.04×10^{-2}	$5.12\times10^{+3}$	3.59×10^{0}
Water footprint	m^3	2.28×10^{-4}	$3.58\times10^{+1}$	2.20×10^{-2}
Land use	kg soil loss	1.00×10^{-2}	2.42×10^{-1}	4.40×10^{-2}

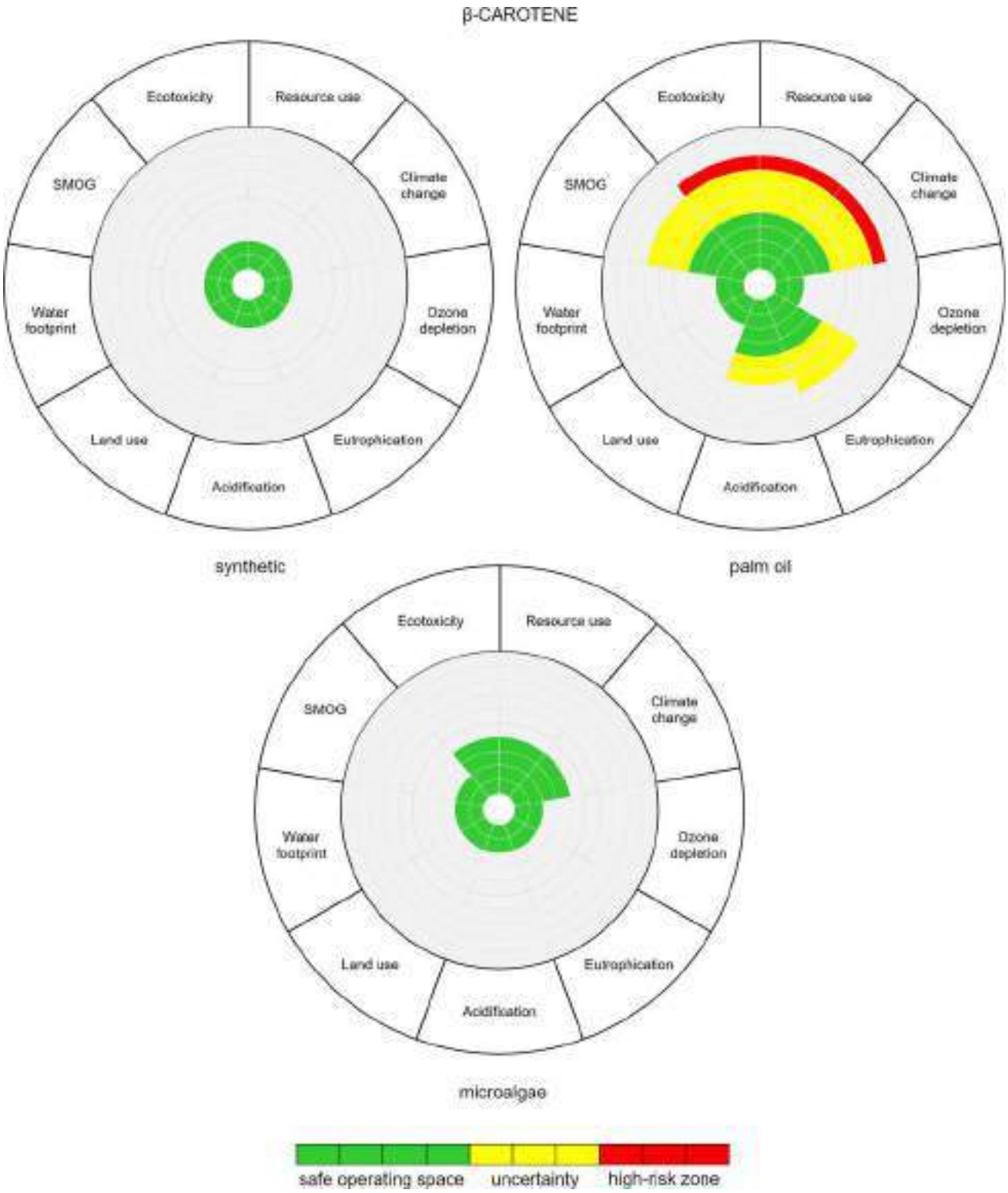


Fig. 5 Environmental performance of β-carotene as an ingredient precursor for vitamin A applied to planetary boundaries

hydroxide in the carotenogenic stage lead to a higher concentration of β-carotene in dried seaweed powder (Ben-Amotz and Mori 2014). Therefore, high pH flocculation application in industrial cultures is favorable in the β-carotene production process. This technique can reduce energy consumption by up to 30% when to compare the screen filtration techniques are applied to whole biomass by *Arthrospira platensis* (Belay 2013; Pirwitz et al. 2015; Chen et al. 2021).

Another factor that makes the industrial production of β-carotene *by Dunaliella salina* convenient is that it is grown in seawater at high salinity. This for freshwater to be reduced almost entirely. However, it is important to highlight that in this study the water footprint was considered total since water-scarcity is deemed a global resource use increase, given their limited availability (Liu et al. 2024). For example, a liter of green or blue water intended for consumption for one purpose is not available for a competing purpose, and a liter of green, blue, or gray water intended for human use is not available to nature. The green and blue water footprint thus subtracts from the remaining supply capacity. Therefore, given that water is a global resource, every liter of water consumption or pollution counts (Hoekstra 2016).

On the other hand, a forward-looking sustainable approach must also consider nutritional aspects. Scientific discoveries have increasingly deepened in investigating the effects of these molecules on human health. Among the results, studies show that chemical structures of the 9-*cis* isomer are more efficient in protecting against oxidative damage (Fernandes et al. 2021). Given this premise, the 9-*cis* content of synthetic molecules is around <2%, while palm oil and microalgae are approximately 24 and >40, respectively. It appears that the effects of natural molecules are innately superior to their synthetic counterparts. Therefore, designing sustainable ingredients goes beyond stacking environmental impacts. It is necessary to establish a trade-off considering nutritional, environmental, and economic factors. Thus, even though the synthetic profile is considered the best environmental scenario, the natural molecule based on microalgae stands out among the other evaluated feedstocks.

Polyunsaturated fatty acids

Dietary fatty acids are important in the development and metabolism of human tissues. The recommendation of daily intake of docosahexaenoic acid (DHA) and eicosapentaenoic acid (EPA) has been suggested as necessary supplements for brain development and other physiological activities, in addition to reducing potential metabolic changes, weight loss, and muscle loss (Yu et al. 2021). Given the above, the environmental impact categories and planetary integrity associated with the production of polyunsaturated fatty acids were examined and the results are shown in Table 8 and Fig. 5, respectively.

The results presented in Fig. 6 show that only one planetary dimension (climate changes) is in an uncertainty zone, referring to the conventional process of obtaining polyunsaturated fatty acids from fish oil; the others are completely in a safe operating space, both for fish oil and for the microalgal countertype.

As is known, most consumption of polyunsaturated fatty acids comes from fish oil. Furthermore, according to our results, this conventional process is partially in line with planetary boundaries. However, greater attention needs to be paid to its growing market demand. Conventional processes are currently unable to satisfy the population demands driving an increase in extractive activity and, consequently, pushing some dimensions into uncertain operating zones, alarming for the potential breaking of borders.

From this perspective, we must opt for processes that are less dependent on natural resources. Thus, in a closer comparison, the increased risk for potential depletion of marine resources seriously limits the use of polyunsaturated fatty acids from fish. In addition, most of the fatty acids currently commercialized are extracted from fish processing residues, which correspond to about 40% of body weight (Enascuta

Table 8 Environmental impacts of the blend oil extraction from fish oil and microalgae sources. The characterized values are referred to functional units of 73.0 and 36.5 g person^{-1} year^{-1} for DHA and EPA, respectively, totaling a blend oil of 0.109 kg person^{-1} year^{-1}

Impact categories	Unit	DHA/EPA blend oil	
		Fish oil	Microalgae (*Schizochytrium* sp. *and Nitzschia laevis)*
Ozone depletion	kg CFC-11 eq	5.57×10^{-6}	1.36×10^{-6}
Global warming	kg CO_2 eq	$1.83\times10^{+1}$	5.01×10^{0}
Photochemical ozone creation	kg NMVOC eq	4.06×10^{-1}	1.16×10^{-1}
Acidification	mole H^+ eq	9.73×10^{-2}	2.68×10^{-2}
Eutrophication	kg N eq	3.48×10^{-2}	1.19×10^{-2}
Ecotoxicity	CTUe	$1.29\times10^{+2}$	$3.35\times10^{+1}$
Fossil fuel depletion	MJ	$3.95\times10^{+1}$	$3.22\times10^{+1}$
Water footprint	m^3	1.50×10^{0}	3.15×10^{-1}
Land use	kg soil loss	1.00×10^{-2}	3.22×10^{-1}

DHA docosahexaenoic acid, *EPA* eicosapentaenoic acid

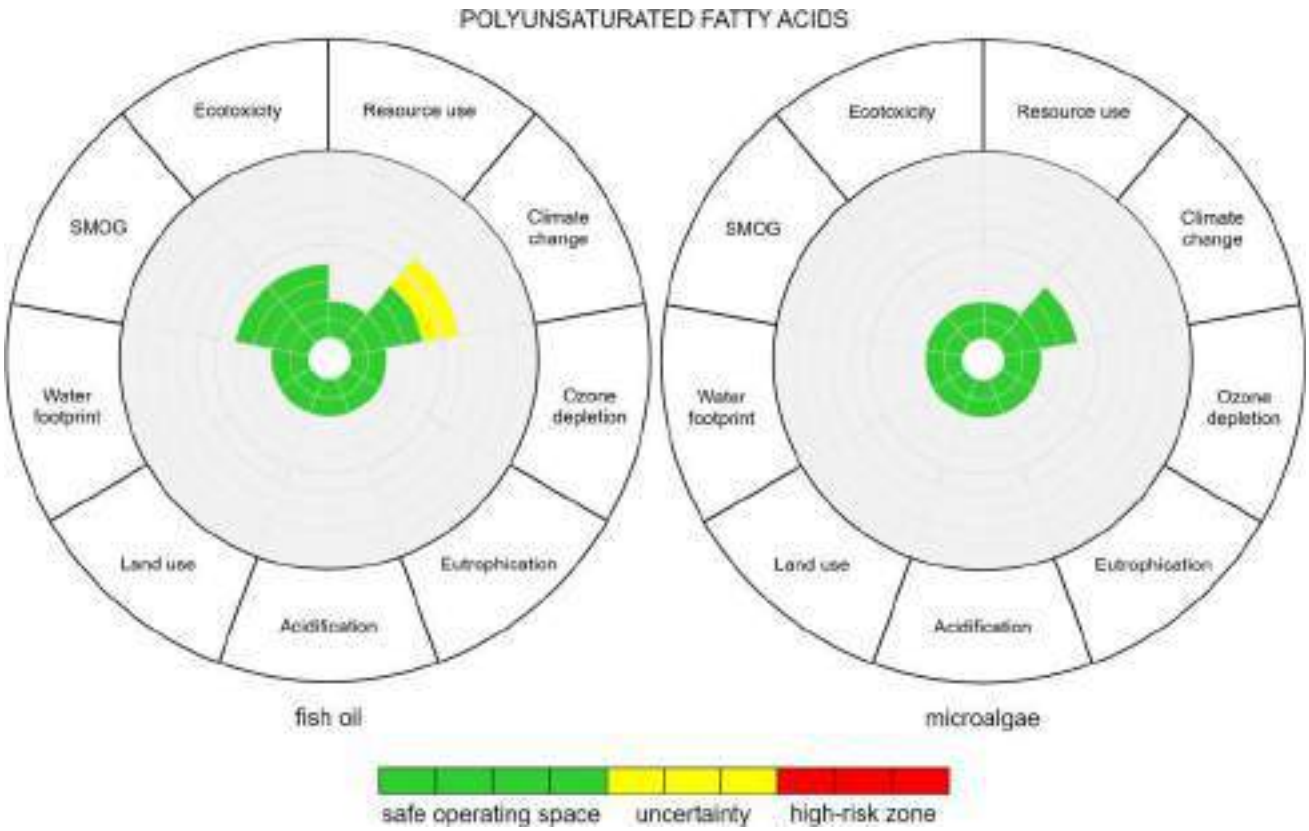


Fig. 6 Environmental performance of polyunsaturated fatty acids applied to planetary boundaries

et al. 2018). In this way, in addition to the intrinsic oxidative ease of these compounds, subjecting these raw materials to hot extractions, concomitantly with the various refinery operating units, puts the quality and stability of these ingredients to the test. Finally, it should consider the low or non-existent ability of fish to synthesize polyunsaturated fatty acids, since these compounds are obtained through food that, in turn, is based on microalgae. Therefore, the similar formulation of fish oils compared to microalgae oils aims to maintain the same concentrations of active principles to support market competition (Lu et al. 2021).

Limitations, uncertainties, and future recommendations

Of course, all scientific approaches have their weaknesses. In this study, the reliability and wider acceptance of the results depend mainly on four sources of uncertainty: (i) the modeling of sustainability assessment methods using planetary boundary indicators; (ii) the extension of life cycle inventories and system boundaries; (iii) coverage of key ingredients assessed under the planetary boundaries framework; and (iv) alternative approach to downscaling planetary boundaries for food key ingredients.

Sustainability assessment methods based on life cycle assessment have developed notably. However, there is no single commonly accepted methodology capable of integrating planetary boundaries. What happens is a translation of complex ecological mechanisms into specific metrics used by the life cycle assessment tool. This may result in uncertainties regarding the realistic determination of potential exceeding safe operational or risk planetary zones. However, this does not diminish the importance of considering reference values, based on science, as guiding principles to be adopted as parameters for evaluating processes and support tools to support the development of sustainable government policies. Regarding the selection of impact reference values to be compared with planetary boundaries, each approach suffers different pressure levels with their respective pros and cons. In this study, the main limitation may be associated with the choice of per capita approach. This methodology was defined in this way because most research that investigates the impacts of the food production chain does not direct the results at the individual level, making it difficult for the final decision-maker to understand the individual performance of ingredients that are consumed daily.

However, there are also principles addressed at a global level applied to the PB-LCIA methodology that more adequately address industrial processes (Hjalsted et al. 2021).

Another limiting factor is the cradle-to-gate assessment defined in this study. This partial evaluation of the process, considering only the extraction and production stages, undeniably delimits the scope of the data used to build the inventories. However, this study can serve as a basis for future investigations that enable the extension of assessments to include stages associated with transportation, consumption, and final disposal. Furthermore, the inventories presented here are based on the most recent publications presented in the scientific literature, but these estimates could be further refined. In particular, available data platforms on the chemical substances used must be consolidated, as well as greater transparency on the specific yields of agricultural stages, which contribute substantially to environmental impacts. Furthermore, as a suggestion for future work, efforts are needed to improve and monitor other relevant factors with greater scrutiny to reduce uncertainty in the results.

The scope of the key nutritional evaluated ingredients is the main point of this study. It is known that dietary diversity, advances in healthcare, and the ideological renewal of future generations have guided and influenced the basis of our daily food choices. However, evaluating a complete diet is a very complex task. This occurs because eating habits change depending on nutritional needs, personal preferences, environmental and social contexts, and other factors associated with behavioral aspects, resulting in untrustworthy data (Verdeau and Monnery-Patris 2024). Given this statement, we limited our study to ingredients like protein because it is at the discussion core about its implications and responsibilities for climate change. Furthermore, in this study, we considered fine chemical ingredients, such as β-carotene (precursor of vitamin A) and polyunsaturated fatty acids (DHA and EPA), which have been targeted in international markets, since their nutraceutical properties are scientifically recognized. Furthermore, the main study objective was to verify whether alternative microalgae-based ingredients could be a sustainable resource to alleviate environmental burdens. Therefore, the definition of three key ingredients that are found in microalgal biomass was also a relevant factor for delimiting this study. Besides, the growing demand for convenience and food security are some of the main reasons for this limitation. However, evaluating equally important key ingredients such as carbohydrates, other sources of vitamins and minerals, and/or alternative ingredient sources remains a priority for future research.

In the context of absolute sustainability, the approach selection to downscaling planetary boundary indices is a substantial source of uncertainty. In this study, we used an egalitarian reduction approach, where we adopted the population estimate of 10 billion people as a reference value. This approach places equal responsibility for consumption on each global citizen and allows for a clear and simple illustration of the contribution of individually assessed ingredients to different environmental problems. However, the main limitation of the status quo approach is that it does not take into account the current or future environmental performance (i.e., eco-efficiency) of a given product or service. Moreover, there is no way of knowing whether population projections will come to be achieved, which makes the data even more rigid if the population growth rate is lower than currently expected estimates. Besides, absolute sustainability approaches may penalize technologies that work (or have the potential to work) better than alternatives. This is particularly relevant for microalgae biotechnology, which may have real potential to improve performance as the level of technological maturity is expanded and consolidated. Likewise, the environmental burden associated with agricultural phases, as well as foods intended for animal feed, may receive a greater share, as they satisfy basic human needs, but there is still no approach that adequately captures this. Given these limitations, the results of our absolute assessments should be interpreted with caution.

In the last analysis, the multidimensional nature of sustainability cannot be neglected. In addition to environmental barriers, some segments recognize broader socioeconomic bottlenecks such as high production costs, financing problems, and lack of social acceptance. This brings to light the importance of promoting incentive policies for the inclusion of unconventional foods to broaden the visualization of the variability of alternative and potentially sustainable products, as is the case with alternative microalgae-based. Furthermore, the knowledge lacks or information disclosure fraught with conflicts of interest about benefits (environmental and/or nutritional) are some of the factors that hinder the global transition to a sustainable food production chain. For example, even though microalgae-based proteins present the best environmental scenario, in addition to safe nutritional characteristics and low allergenic potential, we cannot condemn animal protein options from poultry or pork. Likewise, we cannot eradicate bovine protein, since advances in animal science and adjustments in the food chain and industry can reduce the environmental impacts currently elucidated; after all, the food processing sector has many opportunities to generate value, while at the same time being able to operate within safe operational boundaries. However, this may require knowledge of new value attributes and multidisciplinary collaboration from different groups. Therefore, consumers must be encouraged to make conscious choices within their means. To this end, those responsible for government management must integrate existing evidence, establishing solid knowledge bases, to promote sustainability principles, free from biases. Many elements determine the sustainable performance of processes/products. The

sustainable results we seek depend on the choices of producers, intermediaries, and consumers. However, governments should guide these choices by creating incentive and regulatory policies. Therefore, policy changes should address key challenges and invest in opportunities. By doing this, the previously small efforts - together - will be able to correct and/or overcome vulnerable points, to achieve sustainability.

Conclusion

This study explored the environmental impacts associated with per capita consumption of food key ingredients from the perspective of planetary boundaries. The following conclusions were drawn from the comparative analysis of natural and non-renewable resource uses for conventional and alternative processes.

In general, protein ingredients of animal origin and the alternative have largely contributed to the warning of the disruption of planetary borders. However, the worst environmental performance for protein ingredients studied was attributed to bovine protein, matching three risk indices out of nine evaluated. The protein that presented the best overall performance was microalgae-based, falling within six safe operational indices. On the other hand, among fine chemical food ingredients, only vitamin A from palm oil, which is mostly found in a risk and uncertainty zone, when compared to conventional synthetic processes and microalgae-based; these, in turn, operate fully within safe limits. In contrast, only one planetary index is assigned to the uncertainty zone for polyunsaturated fatty acids from fish oil, the others operate in safe zones equally for microalgae-based processes.

Finally, the conclusions highlight major challenges faced by the food production chain to achieve safe and sustainable food. These results guide critical food groups and environmental indicators to prioritize in future efforts to reduce environmental impact. Therefore, it is important to integrate individual strategic needs with global ones to promote the integration of evaluation and management with the objectives of macro-sustainable development.

Supplementary Information The online version contains supplementary material available at https://doi.org/10.1007/s10811-024-03313-y.

Acknowledgment The authors would like to thank the Conselho Nacional de Desenvolvimento Científico e Tecnológico — Brasil (CNPq), and the Coordenação de Aperfeiçoamento de Pessoal de Nível Superior — Brasil (CAPES).

Author contribution **Darissa Alves Dutra**: Conceptualization, Methodology, Data curation, Writing – original draft. **Mariany Costa Deprá**: Conceptualization, Methodology, Data curation, Writing – review & editing. **Rosangela Rodrigues Dias**: Methodology, Data curation. **Leila Queiroz Zepka**: Supervision, Funding acquisition. **Eduardo Jacob-Lopes**: Conceptualization, Project administration, Writing – review & editing.

Funding This work was supported by the Conselho Nacional de Desenvolvimento Científico e Tecnológico — Brasil (CNPq), and the Coordenação de Aperfeiçoamento de Pessoal de Nível Superior — Brasil (CAPES) — Finance Code 001.

Data availability The authors declare that [the/all other] data supporting the findings of this study are available within the article [and its supplementary information files].

Declarations

Competing interests The authors declare no competing interests.

References

Abbass K, Qasim MZ, Song H, Murshed M, Mahmood H, Younis I (2022) A review of the global climate change impacts, adaptation, and sustainable mitigation measures. Environ Sci Pollut Res 29:42539–42559

Allotey DK, Kwofie EM, Adewale P, Lam E, Ngadi M (2023) Life cycle sustainability assessment outlook of plant-based protein processing and product formulations. Sustain Prod Consum 36:108–125

Arfelli F, Pizzone DM, Cespi D, Ciacci L, Ciriminna R, Calabrò PS, Pagliaro M, Mauriello F, Passarini F (2023) Prospective life cycle assessment for the full valorization of anchovy fillet leftovers: The LimoFish process. Waste Manag 168:156–166

Bartek L, Strid I, Henryson K, Junne S, Rasi S, Eriksson M (2021) Life cycle assessment of fish oil substitute produced by microalgae using food waste. Sustain Prod Consum 27:2002–2021

Belay A (2013) Biology and industrial production of *Arthrospira* (*Spirulina*). In: Richmond A, Hu Q (eds) Handbook of microalgal culture: Applied phycology and biotechnology. Blackwell, Oxford, pp 339–358

Ben-Amotz A, Mori N (2014) Method for producing β-carotene rich *Dunaliella* powder

Besson A, Formosa-Dague C, Guiraud P (2019) Flocculation-flotation harvesting mechanism of *Dunaliella salina*: From nanoscale interpretation to industrial optimization. Water Res 155:352–361

Bjørn A, Hauschild MZ (2015) Introducing carrying capacity-based normalisation in LCA: framework and development of references at midpoint level. Int J Life Cycle Assess 20:1005–1018

Borowitzka MA (2018) Commercial-Scale Production of Microalgae for Bioproducts. In: La Barre S, Bates SS (eds) Blue Biotechnology: Production and use of marine molecules, vol 1. Wiley-VCH, Weinheim, pp 33–65

Britton G, Liaaen-Jensen S, Pfander H (1996) Carotenoids, 2: Synthesis. Birkhaüser Verlag, Basel

Cernev T (2022) Global sustainability targets: Planetary boundary, global catastrophic risk, and disaster risk reduction considerations. Prog Disaster Sci 16:100264

Chen B, Han MY, Peng K, Zhou SL, Shao L, Wu XF, Chen GQ (2018) Global land-water nexus: Agricultural land and freshwater use embodied in worldwide supply chains. Sci Total Environ 613:931–943

Chen M, Chen Y, Zhang Q (2021) A Review of energy consumption in the acquisition of bio-feedstock for microalgae biofuel production. Sustainability 13:8873

Cheng Z, Jia Y, Bai Y, Zhang T, Ren K, Zhou X, Zhai Y, Shen X, Hong J (2023) Intensifying the environmental performance of chicken meat production in China: from perspective of life cycle assessment. J Clean Prod 384:135603

Cook B, Costa Leite J, Rayner M, Stoffel S, van Rijn E, Wollgast J (2023) Consumer interaction with sustainability labelling on food products: A narrative literature review. Nutrients 15:3837

Cordeiro MRC, Mengistu GF, Pogue SJ, Legesse G, Gunte KE, Taylor AM, McAllister TA (2022) Assessing feed security for beef production within livestock-intensive regions. Agric Syst 196:103348

Deivanayagam TA, Osborne RE (2023) Breaking free from tunnel vision for climate change and health. PLoS Glob Public Health 3:e0001684

Del Borghi A, Tacchino V, Moreschi L, Matarazzo A, Gallo M, Vazquez DA (2022) Environmental assessment of vegetable crops towards the water-energy-food nexus: A combination of precision agriculture and life cycle assessment. Ecol Indic 140:109015

Deprá MC, dos Santos AM, Jacob-Lopes E (2020) Sustainability metrics in the microalgae-based pigments production: a life cycle assessment approach. In: Jacob-Lopes E, Queiroz MI, Zepka LQ (eds) Pigments from Microalgae Handbook. Springer, Cham, pp 363–390

Deprá MC, Severo IA, dos Santos AM, Zepka LQ, Jacob-Lopes E (2020) Environmental impacts on commercial microalgae-based products: Sustainability metrics and indicators. Algal Res 51:102056

Deprá MC, Dias RR, Severo IA, de Menezes CR, Zepka LQ, Jacob-Lopes E (2020) Carbon dioxide capture and use in photobioreactors: The role of the carbon dioxide loads in the carbon footprint. Bioresour Technol 314:123745

Deprá MC, Severo IA, Dias RR, Zepka LQ, Jacob-Lopes E (2021) Photobioreactor design for microalgae culture. In: Galanakis CM (ed) Microalgae: Cultivation, Recovery of Compounds and Applications. Academic Press, London, pp 35–61

Deprá MC, Dias RR, Sartori RB, de Menezes CR, Zepka LQ, Jacob-Lopes E (2022) Nexus on animal proteins and the climate change: The plant-based proteins are part of the solution? Food Bioprod Process 133:119–131

Deprá MC, Dias RR, Zepka LQ, Jacob-Lopes E (2022) Building cleaner production: How to anchor sustainability in the food production chain? Environ Adv 9:100295

Dias RR, Deprá MC, Sartori RB, Schneider AT, Zepka LQ, Jacob-Lopes E (2023) Integrating solar cell technologies in microalgae facilities: Environmental sustainability metrics and indicators. Sustain Energy Technol Assess 58:103362

Enascuta CE, Stepan E, Bolocan I, Bombos D, Calin C, Oprescu EE, Lavric V (2018) Simultaneous production of oil enriched in ω-3 polyunsaturated fatty acids and biodiesel from fish wastes. Waste Manag. 75:205–214

FAO - Food and Agriculture Organization of the United Nations (1994) Fats and oils in human nutrition. Report of an FAQ Expert Consultation. FAO, Rome

FAO - Food and Agriculture Organization of the United Nations (2013) Dietary protein quality evaluation in human nutrition. Report of an FAQ Expert Consultation. FAO Food Nutr Pap. 92:1–66

FAO - Food and Agriculture Organization of the United Nations (2022) Greenhouse gas emissions from agrifood systems. Global, regional and country trends, 2000-2020. FAOSTAT Analytical Brief Series No. 50. FAO, Rome, pp 1–12

Fernandes AS, Nascimento TC, Pinheiro PN, Vendruscolo RG, Wagner R, de Rosso VV, Jacob-Lopes E, Zepka LQ (2021) Bioaccessibility of microalgae-based carotenoids and their association with the lipid matrix. Food Res Int 148:110596

Goedkoop M, Heijungs R, Huijbregts M, De Schryver A, Struijs JVZR, Van Zelm R (2009) ReCiPe: a life cycle impact assessment method which comprises harmonised category indicators at the midpoint and the endpoint level. Ruimte en Milieu, Ministerie van Volkshuisvesting, Ruimtelijke Ordening en Milieubeheer, The Netherlands

Goglio P, Knudsen MT, Van Mierlo K, Röhrig N, Fossey M, Maresca A, Hashemi F, Waqas MA, Yngvesson J, Nassy G, Broekema R, Moakes S, Pfeifer C, Borek R, Yanez-Ruiz D, Cascante MQ, Syp A, Zylowsky T, Romero-Huelva M, Smith LGLG (2023) Defining common criteria for harmonizing life cycle assessments of livestock systems. Clean Prod Lett 4:100035

González-García S, Belo S, Dias AC, Rodrigues JV, Da Costa RR, Ferreira A, de Antrade LP, Arroja L (2015) Life cycle assessment of pigmeat production: Portuguese case study and proposal of improvement options. J Clean Prod 100:126–139

Hasegawa T, Sakurai G, Fujimori S, Takahashi K, Hijioka Y, Masui T (2021) Extreme climate events increase risk of global food insecurity and adaptation needs. Nat Food 2:587–595

Herloff IH, Ferdinand B (1954) Process for the manufacture of beta-carotene

Hjalsted AW, Laurent A, Andersen MM, Olsen KH, Ryberg M, Hauschild M (2021) Sharing the safe operating space: Exploring ethical allocation principles to operationalize the planetary boundaries and assess absolute sustainability at individual and industrial sector levels. J Ind Ecol 25:6–19

Hoekstra AY (2016) A critique on the water-scarcity weighted water footprint in LCA. Ecol Indic 66:564–573

Huang PW, Yan CX, Sun XM, Huang H (2023) Economical downstream processing of microbial polyunsaturated fatty acids. Trends Biotechnol 41:857–859

Huijbregts MA, Steinmann ZJ, Elshout PM, Stam G, Verones F, Vieira M, Zijp M, Hollander A, Van Zelm R (2017) ReCiPe2016: a harmonised life cycle impact assessment method at midpoint and endpoint level. Int J Life Cycle Assess 22:138–147

IPCC - Intergovernmental Panel on Climate Change (2022) Impacts, Adaptation, and Vulnerability. Cambridge University Press, Cambridge

Ishika T, Moheimani NR, Laird DW, Bahri PA (2019) Stepwise culture approach optimizes the biomass productivity of microalgae cultivated using an incremental salinity increase strategy. Biomass Bioenergy 127:105274

ISO (2006) ISO-14040 Environmental management–life cycle assessment— principles and framework. International Organization for Standardization

Jacob-Lopes E, Zepka LQ, Deprá MC (2021) Sustainability Metrics and Indicators of Environmental Impact - Industrial and Agricultural Life Cycle Assessment. Elsevier, Amsterdam

Janssen M, Wijffels RH, Barbosa MJ (2022) Microalgae based production of single-cell protein. Curr Opin Biotechnol 75:102705

Järviö N, Maljanen NL, Kobayashi Y, Ryynänen T, Tuomisto HL (2021) An attributional life cycle assessment of microbial protein production: a case study on using hydrogen-oxidizing bacteria. Sci Total Environ 776:145764

Johnson CA, Duong T, Latham RE, Shirley RB, Lee JT (2020) Effects of amino acid and energy density on growth performance and processing yield of mixed-sex Cobb 700× MV broiler chickens. J Appl Poult Res 29:269–283

Katayama T, Rahman NA, Khatoon H, Kasan NA, Nagao N, Yamada Y, Takahashi K, Furuya K, Wahid MEA, Yussoff FM, Jusoh M (2022) Bioprospecting of tropical microalgae for high-value products: n-3 polyunsaturated fatty acids and carotenoids. Aquac Rep 27:101406

Kokemohr L, Escobar N, Mertens A, Mosnier C, Pirlo G, Veysset P, Kuhn T (2022) Life cycle sustainability assessment of

European beef production systems based on a farm-level optimization model. J Clean Prod 379:134552
Laso J, Margallo M, Fullana P, Bala A, Gazulla C, Irabien Á, Aldaco R (2017) When product diversification influences life cycle impact assessment: A case study of canned anchovy. Sci Total Environ 581:629–639
Liao X, Liu A, Chai L (2023) Global food trade alleviates transgressions of planetary boundaries at the national scale. iScience 26:107794
Liu J, Gao W, Zhang Y, Guo F, Peng W (2024) Overestimation of water pressure by traditional water footprint: Method revision and application. Ecol Indic 165:112225
Lu Q, Li H, Xiao Y, Liu H (2021) A state-of-the-art review on the synthetic mechanisms, production technologies, and practical application of polyunsaturated fatty acids from microalgae. Algal Res 55:102281
Lucas KR, Caldarelli CE, Ventura MU (2023) Agriculture and biodiversity damage: a prospective evaluation of the impact of Brazilian agriculture on its ecoregions through life cycle assessment methodology. Sci Total Environ 899:165762
Medeiros DL, Moreira ÍTA (2022) Microalgae biomass production from cultivation in availability and limitation of nutrients: The technical, environmental and economic performance. J Clean Prod 370:133538
Meléndez-Martínez AJ, Esquivel P, Rodriguez-Amaya DB (2023) Comprehensive review on carotenoid composition: Transformations during processing and storage of foods. Food Res Int 169:112773
Moberg E, Karlsson Potter H, Wood A, Hansson PA, Röös E (2020) Benchmarking the Swedish diet relative to global and national environmental targets—identification of indicator limitations and data gaps. Sustainability 12:1407
Monsiváis-Alonso R, Mansouri SS, Román-Martínez A (2020) Life cycle assessment of intensified processes towards circular economy: Omega-3 production from waste fish oil. Chem Eng Process: Process Intensif 158:108171
Nabavi-Pelesaraei A, Damgaard A (2023) Regionalized environmental damages and life cycle cost of chickpea production using LC-IMPACT assessment. Environ Impact Assess Rev 103:107259
Nagappan S, Das P, AbdulQuadir M, Thaher M, Khan S, Mahata C, Kumar G (2021) Potential of microalgae as a sustainable feed ingredient for aquaculture. J Biotechnol 341:1–20
Nass PP, do Nascimento TC, Fernandes AS, Caetano PA, de Rosso VV, Jacob-Lopes E, Zepka LQ (2022) Guidance for formulating ingredients/products from *Chlorella vulgaris* and *Arthrospira platensis* considering carotenoid and chlorophyll bioaccessibility and cellular uptake. Food Res Int 157:111469
Nasution MA, Wibawa DS, Ahamed T, Noguchi R (2018) Comparative environmental impact evaluation of palm oil mill effluent treatment using a life cycle assessment approach: A case study based on composting and a combination for biogas technologies in North Sumatera of Indonesia. J Clean Prod 184:1028–1040
Nielsen J, Tillegreen CB, Petranovic D (2022) Innovation trends in industrial biotechnology. Trends Biotech 40:1160–112
Nijdam D, Rood T, Westhoek H (2012) The price of protein: Review of land use and carbon footprints from life cycle assessments of animal food products and their substitutes. Food Policy 37:760–770
Nunez-Cardenas P, San Miguel G, Banales B, Álvarez S, Diezma B, Correa EC (2022) The carbon footprint of stone fruit production: Comparing process-based life cycle assessment and environmentally extended input-output analysis. J Clean Prod 381:135130
Pelletier N, Pirog R, Rasmussen R (2010) Comparative life cycle environmental impacts of three beef production strategies in the Upper Midwestern United States. Agric Syst 103:380–389
Perraud E, Wang J, Salomé M, Mariotti F, Kesse-Guyot E (2023) Dietary protein consumption profiles show contrasting impacts on environmental and health indicators. Sci Total Environ 856:159052
Pexas G, Mackenzie SG, Jeppsson KH, Olsson AC, Wallace M, Kyriazakis I (2021) Environmental and economic consequences of pig-cooling strategies implemented in a European pig-fattening unit. J Clean Prod 290:125784
Pirwitz K, Rihko-Struckmann L, Sundmacher K (2015) Comparison of flocculation methods for harvesting *Dunaliella*. Bioresour Technol 196:145–152
Pruvost J, Cornet JF, Pilon L (2016) Large-scale production of algal biomass: photobioreactors. In: Bux F, Chisti Y (eds) Algae biotechnology: products and processes. Springer, Cham, pp 41–66
Pulingam T, Lakshmanan M, Chuah JA, Surendran A, Zainab-L I, Foroozandeh P, Uke A, Kosugi A, Sudesh K (2022) Oil palm trunk waste: environmental impacts and management strategies. Ind Crops Prod 189:115827
Queiroz A, França L, Ponte MX (2012) The life cycle assessment of biodiesel from palm oil ("dendê") in the Amazon. Biomass bioenergy 36:50–59
Raza MY, Khan AN, Khan NA, Kakar A (2021) The role of food crop production, agriculture value added, electricity consumption, forest covered area, and forest production on CO_2 emissions: Insights from a developing economy. Environ Monit Assess 193:747
Richardson K, Steffen W, Lucht W, Bendtsen J, Cornell SE, Donges JF, Rockström J (2023) Earth beyond six of nine planetary boundaries. Sci Adv 9:2458
Rockström J, Steffen W, Noone K, Persson Å, Chapin FS, Lambin EF, Foley JA (2009) A safe operating space for humanity. Nature 461:472–475
Ryberg MW, Owsianiak M, Richardson K, Hauschild MZ (2018) Development of a life-cycle impact assessment methodology linked to the Planetary Boundaries framework. Ecol Indic 88:250–262
Ryberg MW, Andersen MM, Owsianiak M, Hauschild MZ (2020) Downscaling the planetary boundaries in absolute environmental sustainability assessments – A review. J Clean Prod 276:123287
Sajid MU, Khan SA, Koc M, Al-Ghamdi SG, Bicer Y (2023) Life cycle assessment of spectra-managed greenhouses for sustainable agriculture. Clean Environ Syst 9:100127
Sala S, Crenna E, Secchi M, Sanyé-Mengual E (2020) Environmental sustainability of European production and consumption assessed against planetary boundaries. J Environ Manage 269:110686
Saswattecha K, Kroeze C, Jawjit W, Hein L (2016) Options to reduce environmental impacts of palm oil production in Thailand. J Clean Prod 137:370–393
Schmid M, Weishaar R, Seifert J, Camarinha-Silva A, Rodehutscord M, Bennewitz J (2024) Genomic analyses of nitrogen utilization efficiency, its indicator trait blood urea nitrogen and the relationship to classical growth performance and feed efficiency traits in a Landrace× Piétrain crossbred population. J Anim Breed Genet
Severo IA, Deprá MC, Dias RR, Jacob-Lopes E (2020) Process integration applied to microalgae-based systems. In: Jacob-Lopes E, Maroneze MM, Zepka LQ (eds) Handbook of microalgae-based processes and products. Academic Press, London, pp 709–735
Siahbalaei R, Kavoosi G, Noroozi M (2021) Protein nutritional quality, amino acid profile, anti-amylase and anti-glucosidase properties of microalgae: Inhibition and mechanisms of action through *in vitro* and *in silico* studies. LWT 150:112023
Sinel M, Weis T (2024) Ventilation shutdown and the breath-taking violence of infectious disease emergency management in industrial livestock production. Environ Plan E: Nat Space
Siregar K, Tambunan AH, Irwanto AK, Wirawan SS, Araki T (2015) A comparison of life cycle assessment on oil palm (*Elaeis*

guineensis Jacq.) and physic nut (*Jatropha curcas* Linn.) as feedstock for biodiesel production in Indonesia. Energy Procedia 65:170–179

Skunca D, Tomasevic I, Nastasijevic I, Tomovic V, Djekic I (2018) Life cycle assessment of the chicken meat chain. J Clean Prod 184:440–450

Smith E, Etienne J, Montanari F (2024) Alternative protein sources for food and feed. EPRS | European Parliamentary Research Service Scientific Foresight Unit (STOA). European Union, Brussels

Steffen W, Richardson K, Rockström J, Cornell SE, Fetzer I, Bennett EM, Biggs R, Carpenter SR, De Vries W, De Wit CA, Folke C (2015) Planetary boundaries: Guiding human development on a changing planet. Science 347:736

Stranddorf LK, Clavreul J, Prieur-Vernat A, Ryberg MW (2023) Evaluation of life cycle impacts of European electricity generation in relation to the Planetary Boundaries. Sustain Prod Consum 39:414–424

Sun H, Wang Y, He Y, Liu B, Mou H, Chen F, Yang S (2023) Microalgae-derived pigments for the food industry. Mar Drugs 21:82

Trinidad K, Ashizawa R, Nikkhah A, Semper C, Casolaro C, Kaplan DL, Savchenko A, Blackstone NT (2023) Environmental life cycle assessment of recombinant growth factor production for cultivated meat applications. J Clean Prod 138153

United Nations (2022) Department of Economic and Social Affairs. World Population Prospects Revision 2022. UN, New York

Valdovinos-García EM, Petriz-Prieto MA, Olán-Acosta MDLÁ, Barajas-Fernández J, Guzmán-López A, Bravo-Sánchez MG (2021) Production of microalgal biomass in photobioreactors as feedstock for bioenergy and other uses: A techno-economic study of harvesting stage. Appl Sci 11:4386

Vendruscolo RG, Deprá MC, Pinheiro PN, Furlan VJM, Barin JS, Cichoski AJ, de Menenzes CR, Zepka LQ, Jacob-Lopes E, Wagner R (2022) Food potential of *Scenedesmus obliquus* biomasses obtained from photosynthetic cultivations associated with carbon dioxide mitigation. Food Res Int 160:111590

Verburg RW, Verberne E, Negro SO (2022) Accelerating the transition towards sustainable agriculture: The case of organic dairy farming in the Netherlands. Agric Syst 198:103368

Verdeau B, Monnery-Patris S (2024) When food is uncertain, how much does sustainability matter? A qualitative exploration of food values and behaviours among users of a social grocery store. Appetite 194:107175

Vibart R, de Klein C, Jonker A, van der Weerden T, Bannink A, Bayat AR, Crompton L, Durand A, Eugène M, Klumpp K, Kuhla B, Lanigan G, Lund P, Ramin M, Salazar F (2021) Challenges and opportunities to capture dietary effects in on-farm greenhouse gas emissions models of ruminant systems. Sci Total Environ 769:144989

Vono G, Falcone G, Mistretta M, Fazari A, Strano A (2023) Life Cycle Inventory of the Italian citrus fruit supply chain: Modelling the agricultural phase inventory through statistical data processing. Clean Environ Syst 10:100131

Wang M, Yin Z, Sun W, Zhong Q, Zhang Y, Zeng M (2023) Microalgae play a structuring role in food: Effect of *Spirulina platensis* on the rheological, gelling characteristics, and mechanical properties of soy protein isolate hydrogel. Food Hydrocoll 136:108244

WHO - World Health Organization (2004) Vitamin and mineral requirements in human nutrition. World Health Organization.

Xi Y, Bian J, Luo G, Kong F, Chi Z (2022) Enhanced β-carotene production in *Dunaliella salina* under relative high flashing light. Algal Res 67:102857

Yao S, Cao X, Wang Y, Li D, Wang W, Chen R, Li C (2023) Enhancing overall carbon fixation and energy conversion with formate in green microalga *Chlamydomonas reinhardtii*. Algal Res 72:103108

Yu J, Wen X, You C, Wang S, Chen C, Tocher DR, Li Y (2021) Comparison of the growth performance and long-chain polyunsaturated fatty acids (LC-PUFA) biosynthetic ability of red tilapia (Oreochromis mossambicus♀× O. niloticus♂) fed fish oil or vegetable oil diet at different salinities. Aquaculture 542:736899

Zhen H, Yuan K, Qiao Y, Li J, Waqas MA, Tian G, Dorca-Preda T, Knudsen MT (2023) Eco-compensation quantification of sustainable food waste management alternatives based on economic and environmental life cycle cost-benefit assessment. J Clean Prod 382:135289

Zhu J, Luo Z, Liu Y, Tong H, Yin K (2022) Environmental perspectives for food loss reduction via smart sensors: a global life cycle assessment. J Clean Prod 374:133852

Zhu J, Wakisaka M, Omura T, Yang Z, Yin Y, Fang W (2024) Advances in industrial harvesting techniques for edible microalgae: Recent insights into sustainable, efficient methods and future directions. J Clean Prod 430:140626

Publisher's Note Springer Nature remains neutral with regard to jurisdictional claims in published maps and institutional affiliations.

Springer Nature or its licensor (e.g. a society or other partner) holds exclusive rights to this article under a publishing agreement with the author(s) or other rightsholder(s); author self-archiving of the accepted manuscript version of this article is solely governed by the terms of such publishing agreement and applicable law.

Send Orders for Reprints to reprints@benthamscience.net

Recent Patents on Biotechnology, XXXX, *XX,* 000-000

RESEARCH ARTICLE

Decarbonizing the Transport of Microalgae-based Products — The Role of E-mobility

Rosangela Rodrigues Dias[1], Mariany Costa Deprá[1], Victor Cesar Rodrigues Carvalho[1], Cristiano Ragagnin de Menezes[1], Leila Queiroz Zepka[1] and Eduardo Jacob-Lopes[1,*]

[1]*Department of Food Science and Technology, Bioprocess Intensification Group, Federal University of Santa Maria, 97105-900, Santa Maria, RS, Brazil*

Abstract: ***Background:*** The decarbonization of road transport is a precondition for achieving carbon neutrality. Battery-electric vehicle technology can make this a reality. In this bias, the objective of the article is to shed light on the ongoing debate about the potentially important role of the adoption of electric vehicles in the transport of microalgae-based products to help them advance to a cleaner life cycle.

Methods: Five routes, including unimodal and multimodal conditions, were defined to assess the carbon emissions of the transport system and, more specifically, of road transport. The headquarters of market-leading microalgae manufacturers were selected as the origin of the routes and, as the destination, regions that sustain them.

Results: The results reveal the supremacy of road transport of microalgae-based products using electric vehicles powered by nuclear, hydroelectric, and wind, followed by biomass and photovoltaic energy. They also show that the positive impact of wind, water, and photovoltaic energy on the climate, added to the lower battery charging costs and the greater opportunity to generate revenue from the sale of carbon credits, make their trade-offs.

Conclusion: The exquisite results of this study convey key messages to decision-makers and stakeholders about the role of electromobility in building a zero-carbon delivery route.

ARTICLEHISTORY

Received: January 17, 2024
Revised: March 14, 2024
Accepted: March 20, 2024

DOI:
10.2174/0118722083305025240409071630

Keywords: Algae, algae-based products, road transport, electromobility, environmental impact assessment, decarbonization.

1. INTRODUCTION

Over time, as the potential of microalgae was unraveled, they moved from the petri dish to the commercial product, and today, the main players operating in the microalgae market are investing massive resources in the development of new and innovative cultivation technologies to capitalize on the promising capabilities of this unique feedstock [1, 2]. Many of the main microalgae companies are working tirelessly to reinforce their presence as the world's leading microalgae manufacturers. Involvement in R&D has helped, in part, to flourish the microalgae market in regions such as North America and Europe. The boom in the microalgae market in these regions is associated with the growing consumption of health supplements and aversion to synthetic dyes with increasingly stringent regulations against their use [3].

But regardless of these issues, when every business is competing to be the best, recognizing the relative maturity of technologies, evaluating their performance, and understanding their environmental footprint are key factors that will help them climb the ladder of success. When bench-

*Address correspondence to this author at the Department of Food Science and Technology, Bioprocess Intensification Group, Federal University of Santa Maria, 97105-900, Santa Maria, RS, Brazil; Tel: +55 55 3220 8822; E-mail: ejacoblopes@gmail.com

1872-2083/XX $65.00+.00 © XXXX Bentham Science Publishers

marking, many insights emerge, and bold actions for a low-carbon future seem to be the backbone to generate credibility and stay ahead of your peers [4].

However, building a low-carbon or even net-zero legacy for microalgae-based products will not be an easy task and requires a thorough analysis of each of the stages that make up the life cycle of these products [5, 6]. From a cradle-to-grave perspective, the life cycle of microalgae-based products includes primary energy and natural resource extraction, processing, manufacturing, transport, use, and end-of-life [7, 8]. Studies that assess the environmental burdens of microalgae-based products inform breaking points where it is possible to make the lifecycle cleaner. Unfortunately, most of these studies neglect the fact that transport has important environmental burdens that cannot be swept under the rug [9].

About this, looking exclusively at the transport sector – the sector that keeps the world moving – it is seen that it needs to evolve so that he can see the road ahead. This occurs because, as one of the three critical sources of carbon emissions and the only sector still increasing its greenhouse gas footprint, it will not be able to sustain strong future-proof fleets [10]. Within the transport sector, road transport, accounting for around 74.5% of all sector-related emissions, urgently needs to get rid of high tailpipe emissions. Not only to improve the sector's environmental metrics but also for those who depend on it [11, 12].

In that narrative, the good news is that battery electric vehicle technology is poised to lay the groundwork for a net-zero transition in road transport – and help meet the sustainability goals of those who depend on it to achieve low-carbon lifecycles. Furthermore, it cannot be belittled that, given the challenges of decarbonization in air and sea transport, achieving emission reduction targets will require completely eliminating carbon emissions from road modal. In light of this, leaders of nations, cities, and international organizations – and notably the private sector – are setting goals and launching strategies for the electrification of road transport, assuming the commitment to end the era of vehicles powered by diesel and gasoline [13].

However, despite current research indicating the overwhelming importance of vehicle electrification in the net-zero transition, it is uncertain that it will provide a green future. That is because, although battery electric vehicles do not emit carbon, the energy in their batteries does. Therefore, ignoring the emissions associated with electricity generation that fuels climate change would be problematic. Electricity generation technologies that are not low-carbon could be incompatible with carbon neutrality goals, as they do nothing to combat air pollution and greenhouse gas production [14].

When considering this, it can be argued that it is absolutely necessary to investigate whether, based on electricity generation technology, the adoption of electric vehicles would not result in a zero-sum game for the environment or, ultimately, an increase in carbon emissions in the life cycle of microalgae-based products. Therefore, to address this issue, the present study investigates the role of electromobility based on electricity generation technology in the potential to mitigate the global warming impacts of the transport of microalgae-based products. Five routes, including unimodal and multimodal conditions, are examined. As the origin of the routes, the headquarters of market-leading microalgae manufacturers were selected, and as the destination, regions that drive the demand for these products were selected. Economic drivers for decision-making processes are shown. To our knowledge, this article is the first to show the impact of adopting electric vehicles on the transport life cycle of microalgae-based products and the advantages that outweigh the costs of maintaining the status quo.

2. LITERATURE REVIEW

Electromobility, although considered a modern trend, has its roots in several innovations and developments throughout the 19th and 20th centuries. The first electric vehicles were introduced in the 19th century and preceded gasoline-powered vehicles [15, 16]. Inventors such as Thomas Davenport, who built an electric car in 1835, and Gustave Trouvé, who built an electric tricycle in 1881, were some of the first to explore the idea of electromobility. Other visionaries such as Robert Anderson, Sibrandus Stratingh, Ányos Jedlik, Gaston Planté, Charles Fritts, William Morrison, and

Ferdinand Porsche also left an indelible mark on the development of electric vehicles throughout history, and their works helped pave the way for the modern technology we see today [17-20].

During the 19th century, there was considerable interest in developing electric vehicles, which competed with steam and gasoline vehicles as viable transportation alternatives. At that time, electric vehicles had a great chance of winning the market dispute, as they were quieter, more practical, and cleaner. However, significant advances in internal combustion engine technology have given gasoline vehicles greater autonomy and performance, giving them greater popularity. The ascension of gasoline vehicles was also driven by the discovery of large oil reserves in the late 19th and early 20th centuries. This made petroleum a cheap and abundant fuel source for this technology, and as a result, electric vehicles were supplanted by gasoline vehicles and, later, diesel vehicles [21, 22].

However, in the 1970s to 1990s, growing awareness of the environmental impacts caused by burning fossil fuels led to a resurgence of interest in electric vehicles. Electric vehicles were considered one of the alternatives to reduce dependence on fossil fuels and mitigate associated environmental impacts. During this period, there was an increase in research and development of electric vehicles as a more sustainable mobility alternative. However, this progress has not translated into wide-scale adoption due to significant challenges, such as limited autonomy, high cost of batteries, and lack of charging infrastructure [23].

However, during the 1990s, there were continued efforts to improve electric vehicle technology. Batteries began to be improved, allowing greater autonomy. Hybrid vehicles were introduced, offering greater energy efficiency and lower pollutant emissions. Electric motors were designed to be more compact and powerful, and fast charging systems and networks of charging stations began to emerge [24]. This has spurred the development of more affordable electric vehicles. Later, in 2008, the launch of the Tesla Roadster marked the path towards mass adoption of electric vehicles. The Roadster was the first electric vehicle to have significant autonomy compared to other electric vehicles at the time. Although it was a limited and high-cost production, the Roadster helped show that battery electric vehicle technology could achieve high performance, challenging the perception that they were synonymous with low power and autonomy [25, 26].

From the early 2000s to the present day, electric mobility has experienced significant growth; several governments have implemented tax incentives, regulations, and charging infrastructure to promote the adoption of this technology and reduce greenhouse gas emissions [27, 28]. In numbers, the sale of electric light-duty vehicles from 2012 to 2017 grew from 100,000 to 1 million and, from 2017 to 2022, jumped from 1 to more than 10 million, representing 14% of all new cars sold. In 2022, the sale of electric heavy-duty vehicles and, more specifically, medium- and heavy-duty trucks represented around 1.2% of sales worldwide [29]. To date, although sales of electric heavy-duty vehicles are more modest compared to sales of electric light-duty vehicles, ambition for the electrification of heavy vehicles is growing, with several new models entering the market [30].

Undoubtedly, electric mobility is a catalyst for ongoing transformations in the transport sector and society as a whole, and the availability of charging infrastructure is a key factor in its widespread adoption [31]. Although still limited, charging infrastructure for electric vehicles has improved, with the number of public slow and fast charging points increasing. With 2.7 million public charging points worldwide by the end of 2022 and more than 33% of them installed in the same year, the vitality of the electric vehicle market is evident [29]. Improving charging infrastructure is essential for establishing electric mobility [32].

It is also absolutely necessary that the energy used to charge electric vehicle batteries comes from low-emission electricity sources [33, 34]. This is because although electric vehicles are known for their clean operation, because they do not emit exhaust gases while driving, emissions are not limited to their operation. It is necessary to consider the indirect emissions associated with the electricity production used to power the vehicle battery. In this sense, if the electricity used to charge these vehicles is generated from fossil fuel sources, such as coal and natural gas, the environmental gain related to reducing greenhouse gas emissions may be lost [35]. As a result, following some surveys, switching from an internal combus-

tion vehicle to an electric vehicle powered by fossil fuel energy would be like swapping six for half a dozen [36]. In this sense, it is part of the puzzle to put the environmental impact of electric vehicles based on the source of electricity at the tip of the pencil to clarify whether they are and will be the best option for sustainable mobility.

3 METHODOLOGY

3.1. Definition of Trade Routes

To assess and analyze the environmental sustainability in terms of carbon dioxide emissions from the microalgae-based product transport system, with emphasis on road transport, five routes were defined: one unimodal, using only road transport, and four multimodal, using a combination of the road/sea and road/air transport systems. Calipatria, located in the United States, and Pingtung, located in southern Taiwan, as the origin, were chosen because they are the headquarters of world-leading manufacturers in microalgae production, and Coral Gables, in the United States, and London, United Kingdom, as the destination, were chosen for two reasons, first, because they are headquarters to a supermarket chain known for commercialize natural products, and second, because the countries in question make a significant contribution to the revenue of the global microalgae market. The description of each route is given in Table **1** and illustrated in Fig. (**1**).

3.2. Life Cycle Assessment (LCA)

The carbon dioxide (CO_2) emissions from the transport system and, more specifically, from road

Table 1. Description of trade routes.

Route	Characteristics of the Route	Distances (km)			Origin	Destination
		Road	Sea	Air		
USA-USA (R)	USA-USA, road route	4167	-	-	Calipatria-USA	Coral Gables-USA
TWN-GBR (R+S+R)	TWN-GBR, road/sea route	242	24437	-	Pingtung-GBR	London-GBR
TWN-GBR (R+A+R)	TWN-GBR, road/air route	40	-	9989	Pingtung-GBR	London-GBR
TWN-USA (R+S+R)	TWN-USA, road/sea route	4484	11345	-	Pingtung-GBR	Coral Gables-USA
TWN-USA (R+A+R)	TWN-USA, road/air route	448	-	13872	Pingtung-GBR	Coral Gables-USA

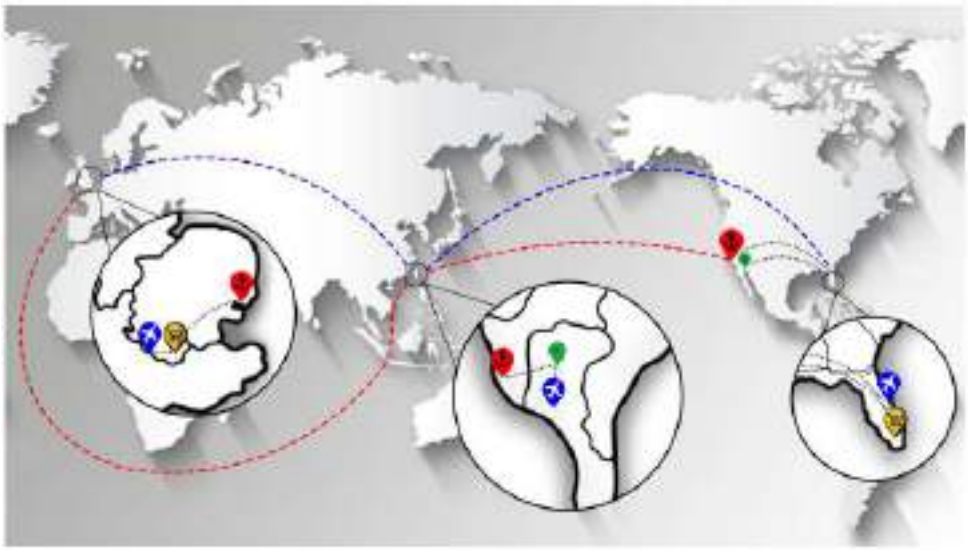


Fig. (1). The five investigated routes and the transport systems involved are represented by lines and icons of different colors: road (black line), sea (red line and icon), air (blue line and icon), microalgae manufacturer (green icon), natural products market (yellow icon). (*A higher resolution / colour version of this figure is available in the electronic copy of the article*).

transport using internal combustion and electric vehicles were quantified according to the methodological framework for life cycle assessment (LCA) of the International Organization for Standardization (ISO). This assessment comprises four main steps: (1) goal and scope definition, (2) inventory analysis, (3) impact assessment, and (4) interpretation of the result [37].

3.2.1. Goal and Scope Definition

The main objective of the study was to evaluate and compare CO_2 emissions from the phase of use of internal combustion and electric road vehicles powered by different sources of electricity (nuclear, hydro, wind, biomass, photovoltaic, biogas, natural gas, and coal), as well as of the transport system, including unimodal and multimodal conditions.

The functional unit was defined as the distance traveled (km). The scope of the analysis includes the life cycle assessment of the most critical phase in terms of CO_2 emissions from road transport, that is, the use phase. The use of vehicles with a combustion engine incorporates direct fuel emissions and battery electric vehicles; although they do not present direct emissions during the use phase, all emissions were accounted for by the electricity production process utilized to charge the battery. The assessment of sea and air transport emissions is also part of the scope. The description of the system boundaries is shown in Fig. (**2**).

3.2.2. Life Cycle Inventory

The life cycle inventory includes the characteristics and assumptions of the internal combustion and electric vehicles considered in the base case (Table **2**). It is assumed that the standard vehicle used for the delivery of microalgae-based products –whatever it may be – is a truck with a payload of 1 ton. The inventory includes data for vehicles with an internal combustion engine that uses diesel as an energy source. The sensitivity and uncertainty analysis section presents the results for internal combustion and electric vehicles with higher energy consumption.

3.2.3. Life Cycle Impact Analysis

The midpoint impact category used to quantify CO_2 emissions is global warming potential (GWP). The GWP was calculated using Eq. (1), being expressed in $kgCO_2eq$ [8]. CO_2 emissions from air and sea transport were also accounted for. The average emission factors for the transport of microalgae-based products by sea and air are shown in Supplementary Material (Table **S1**).

$$GWP = \Sigma\, GWP_i \times m_i \quad (1)$$

where GWP is the indicator ($kgCO_2eq$), GWP_i are the characterization factors for substance i, and m_i is the inventory of emissions for substance i.

3.3. Economic Assessment

The operating cost of internal combustion and electric road vehicles per distance traveled was cal-



Fig. (2). System boundaries for the evaluation of the transport of microalgae-based products. (*A higher resolution / colour version of this figure is available in the electronic copy of the article*).

Table 2. Characteristics and assumptions of internal combustion and electric vehicles.

-	Assumed Value	
	Combustion Engine	**Battery Electric**
Playload capacity (t)	1	1
Fuel consumption (l/km)	0.107	-
Electricity consumption (kWh/km)	-	0.20
Energy losses (%)	-	10%
Emissions ($kgCO_2/l$)	2.7	-
Emissions ($kgCO_2/kWh$)		
Nuclear		4.9×10^{-3}
Hydro		5.4×10^{-3}
Wind		8.9×10^{-3}
Biomass		3.2×10^{-2}
Photovoltaic		7.3×10^{-2}
Biogas		1.9×10^{-1}
Natural gas		5.9×10^{-1}
Coal		1.2

Note: Adapted from [5, 38-42].

culated according to Eq. (2). Average diesel fuel and electricity prices were obtained from the European Commission [38-43], Bhutada [44], IRENA [45], and Global Petrol Prices [46]. The composition of the electricity tariff was defined as 32%, corresponding to generation, 9%, 24%, and 35%, corresponding to transmission, distribution, and government, respectively. Other costs, such as vehicle maintenance and insurance, were not considered.

$$OC = \Sigma\, FC_{Total} \times FP \quad (2)$$

where OC is the operating cost, FC_{Total} is the total diesel fuel and electricity consumption, and FP is the price of diesel fuel per liter and electricity per kWh.

3.4. Estimation of Carbon Credits

The carbon credits were estimated based on the carbon footprint of the use phase of internal combustion and electric road vehicles (Eq. 3), following the methodology of Dias *et al.* [5]. The revenue generated by the sale of carbon credits was determined according to the carbon price recovered from the World Bank [47].

$$CO_{2avoided} = CO_{2conventional} - CO_{2emitted} \quad (3)$$

where conventional CO_2 and emitted CO_2 are the amounts of CO_2 released in the use phase of internal combustion and electric road vehicles, respectively.

4. RESULTS AND DISCUSSION

4.1. Electromobility – An Existing Lower Carbon Choice

It is necessary to close the curtain on the more than 100 years of history of vehicles with internal combustion engines. Climate change will not be interrupted without the decarbonization of transport that has fueled global warming for more than a century. Battery electric vehicle technology is one of the strongest bets for reducing CO_2 emissions. However, behind this captivating opportunity is the fierce debate about whether electric vehicles will mitigate the impact of climate change in different electric fuel consumption scenarios and whether their adoption will suit all countries.

In this context, the logic behind this study and the main objective of this article is to provide

comprehensive answers through the life cycle of road transport of microalgae-based products. In this regard, while the cradle-to-gate burdens for these products may represent most of the impacts, the contributions of transport from the production facility to the consumer – frequently ignored – may not be despicable. Therefore, in light of all this, the comparative lifecycle results of internal combustion road transport versus electric road transport of microalgae-based products, including unimodal and multimodal transport under one boundary - the use phase - are presented in Figs. (**3** and **4**). The Supplementary Material (Table **S2** and **S3**) presents the detailed numerical results.

As can be seen in Fig. (**3**), road transport using diesel-powered internal combustion vehicles has the greatest impact on climate change in terms of $kgCO_2eq$. Road transport using battery electric vehicles powered by coal-based electricity ranks second. When powered by coal-based electricity, electric vehicles reduce global warming potential by approximately 8.6% compared to internal combustion vehicles. In contrast, when powered by nuclear, hydro, wind, biomass, photovoltaic, biogas, and natural gas electricity, these values are around 99.6%, 99.5%, 99.3%, 97.5%, 94.4%, 85.5%, and 55.0 % smaller, respectively. This result confirms the supremacy over road transport routes using diesel-powered internal combustion vehicles and electric vehicles powered by coal.

With few negative consequences, electric road transport based on these seven sources of electricity – nuclear, hydro, wind, biomass, photovoltaic, biogas, and, ultimately, natural gas – represents a striking opportunity for all those who depend on the sector to transport their goods. However, despite this powerful impact on reducing CO_2 emissions, it is not sensible to reach an optimistic conclusion, ignoring that adopting electric vehicles is not suitable for all countries. In this sense, looking at the electricity mix of specific countries, such as China and South Africa, coal represents more than 62% and 87% of electricity production, respectively [48]. Consequently, establishing a fleet of electric vehicles for road transport in these countries may not lead to genuine progress in decarbonizing the product's life cycle. Besides that, despite relying on renewable and clean energy sources, it is reasonable to infer that it may be difficult or impossible to guarantee that the route runs on 100% low-carbon fuels.

Taking Taiwan, the United States, and the United Kingdom as examples – already that the

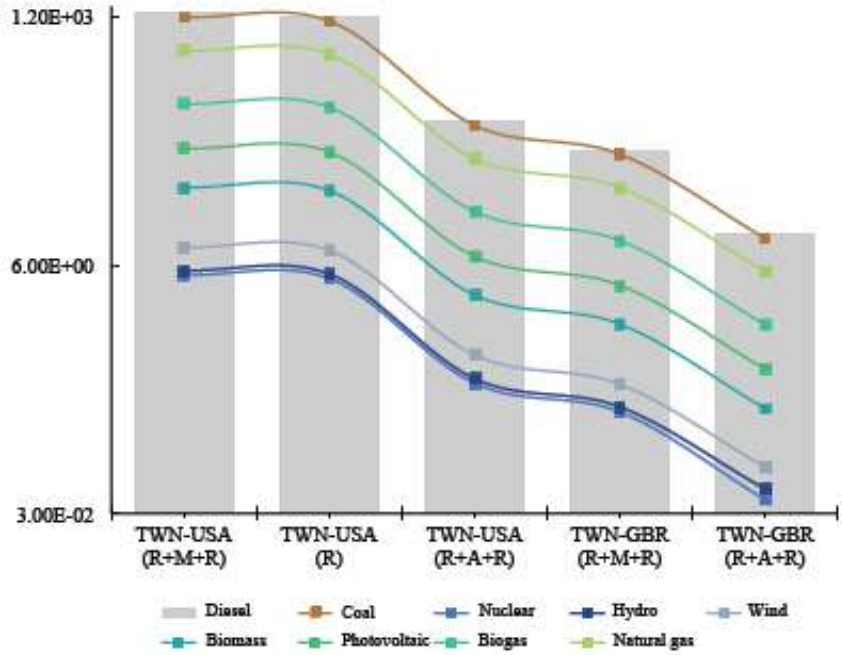


Fig. (3). Life cycle carbon footprint of electric and internal combustion road transport. Note: does not include emissions from maritime and air transport. TWN, Taiwan; USA, United States; GBR, United Kingdom. (*A higher resolution / colour version of this figure is available in the electronic copy of the article*).

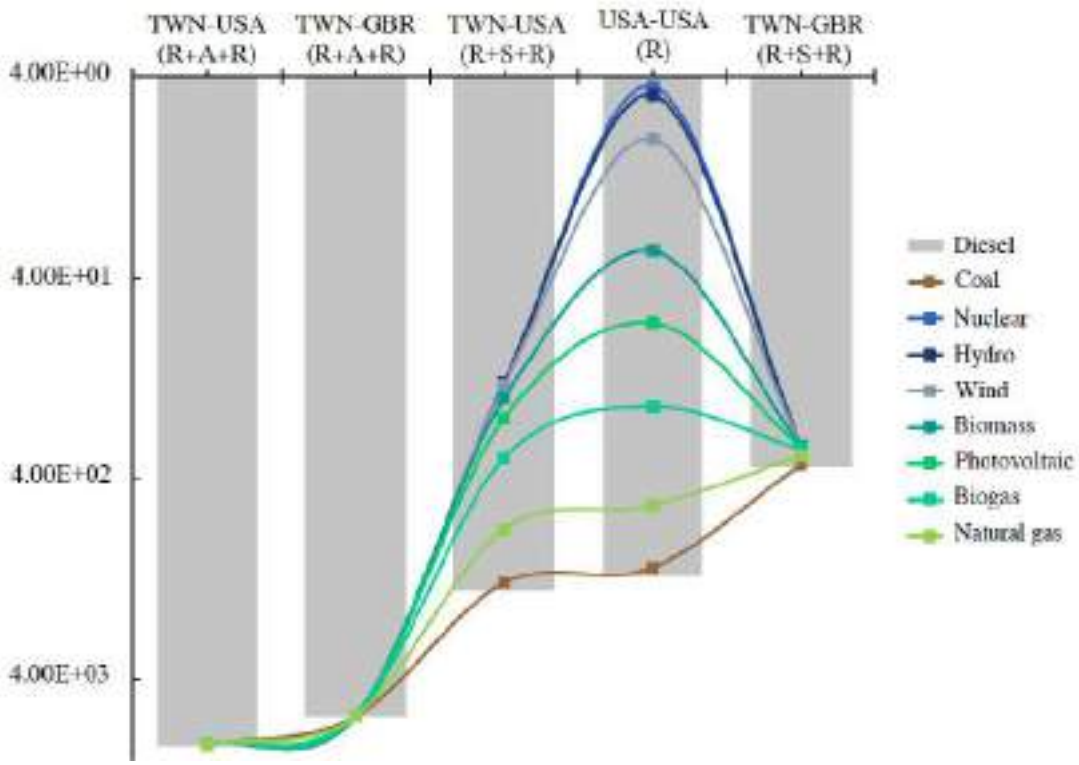


Fig. (4). Life cycle carbon footprint of uni-and multi-modality transport. Note: includes emissions from maritime and air transport. TWN, Taiwan; USA, United States; GBR, United Kingdom. (*A higher resolution / colour version of this figure is available in the electronic copy of the article*).

microalgae products run through these countries – coal represents about 44%, 22%, and 2% of electricity production. Fortunately, around 51%, 75%, and 84% of electricity production comes from the other sources considered here, with natural gas covering approximately half of this production [48, 49]. Of note, the hotspot here is that the axiomatic nature of the claim that electromobility enables more sustainable transport calls for caution.

As for the results shown in Fig. (**4**), it is worth mentioning that, different from Fig. (**3**), the distinctions between the impact of one route to another arise not only from differences in distances traveled (km) but also from multimodal transport. The results indicate that if the same destination is considered, the route that vehemently minimizes carbon emissions is road-sea instead of road-air. Furthermore, according to the premises considered in the base case, when there is a myriad of paths between the origin and the destination, opting for a route run through mostly by container ship would allow for a greater reduction in CO_2 emissions compared to routes operated entirely by diesel-powered trucks and electric trucks powered by coal, natural gas, and biogas as an energy source, respectively. On the other hand, routes entirely operated by electric vehicles powered by nuclear, hydro, wind, biomass, and photovoltaic energy would provide the best choice and, in light of the results, when operated together with ships (road-sea), can be considered the trade-offs.

Still, concerning the environmental sustainability of the transport service, it is also worth noting that all production chains – including microalgae – are exposed to new environmental regulations to reduce their CO_2 emissions. From a survival lens, it is important to consider electromobility as part of the puzzle to anchor sustainability in the chain of microalgae-based products. For transport operated entirely by truck, CO_2 emissions can be massively reduced. However, as can be seen from the example in Fig. (**5**), transport does not contribute significantly to the product's life cycle carbon footprint. And it does not contribute significantly independently to commercial microalgae-based products. But of course, it should not be ignored because, although at first sight, it is irrelevant, it hides a carbon footprint that is not small, and so little is the social cost of these emissions.

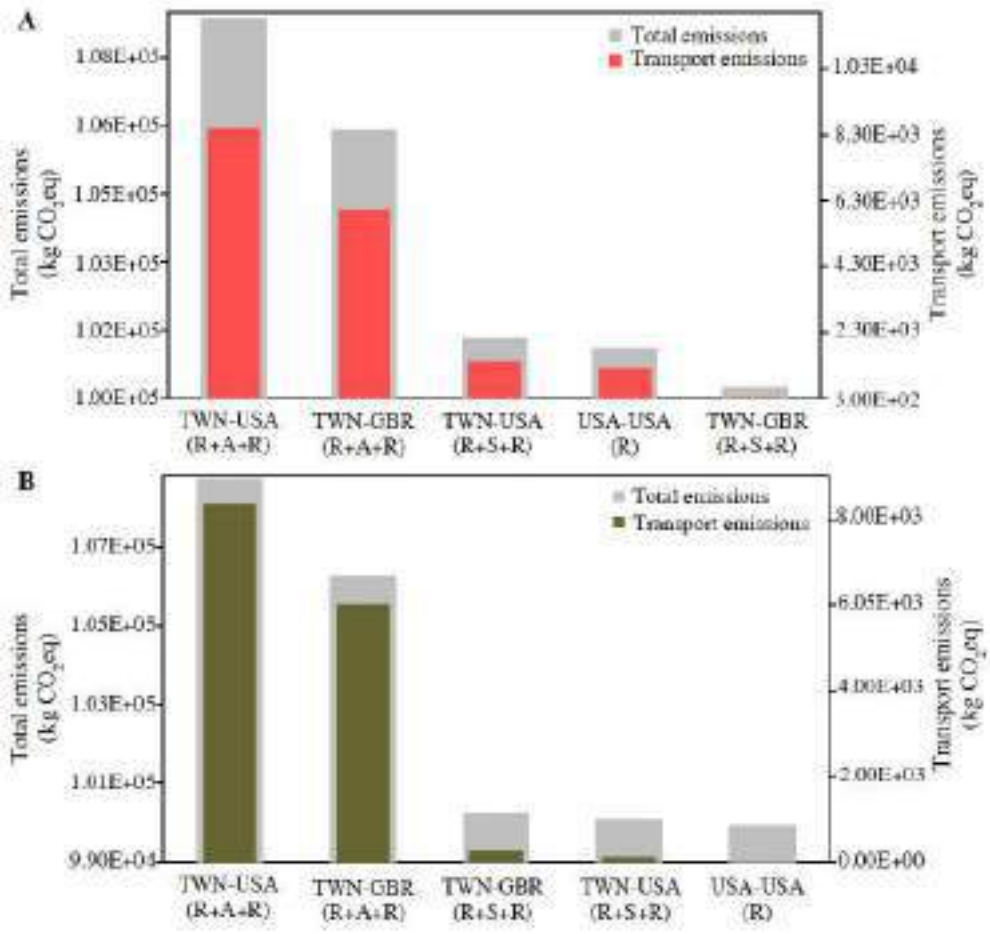


Fig. (5). Cradle-to-gate life cycle carbon footprint of 1 t month^{-1} of *Arthrospira platensis* dry biomass, including transport. (**A**) Diesel-powered road transport and (**B**) nuclear-powered road transport. The cradle-to-gate lifecycle carbon footprint data were obtained from Dias *et al*. [5, 6]. (*A higher resolution / colour version of this figure is available in the electronic copy of the article*).

From another perspective, considering that upstream and downstream processes are powered by photovoltaic and wind energy instead of fossil energy – the fastest growing electricity generation technologies in the world – and that road transport uses internal combustion vehicles, both unimodal transport and multimodal can respond to a significant part of CO_2 emissions from the microalgal products (Fig. **6**). If targeting the TWN-USA (R+S+R) route, for example, transport would account for around 18% (Fig. **6A**) and 66% (Fig. **6B**) of these emissions. Now, considering road-air transport (TWN-USA), it would account for about 58% and 92%, respectively. From this perspective, the results bring a new look at the potential impact of transport on the microalgae production chain.

4.1.1. Sensitivity Analysis and Uncertainty

Battery electric vehicles are an incipient technology under development, and it is difficult to fix values for parameters such as electric fuel consumption. In this sense, a sensitivity analysis was carried out to better understand the robustness of the results of CO_2 emission metrics. The analysis adopts the one-at-a-time (OAT) technique that shows the sensitivity of the electricity consumption parameter when all others are kept constant. The sensitivity of lifecycle CO_2 emissions from internal combustion road transport and electric transport is shown in Fig. (**7**).

As can be seen, a minimum increase of 0.02 kWh/km made the lifecycle emissions of coal-fired electric road transport 0.51% higher than that of internal combustion road transport (Fig. **7A**). Assuming a consumption of 0.50 kWh/km and 1.00 kWh/km, the lifecycle CO_2 emissions of coal-fired electric road transport are 56% and 78% higher, respectively. Besides that, before, when it was assumed that electric vehicles were charged

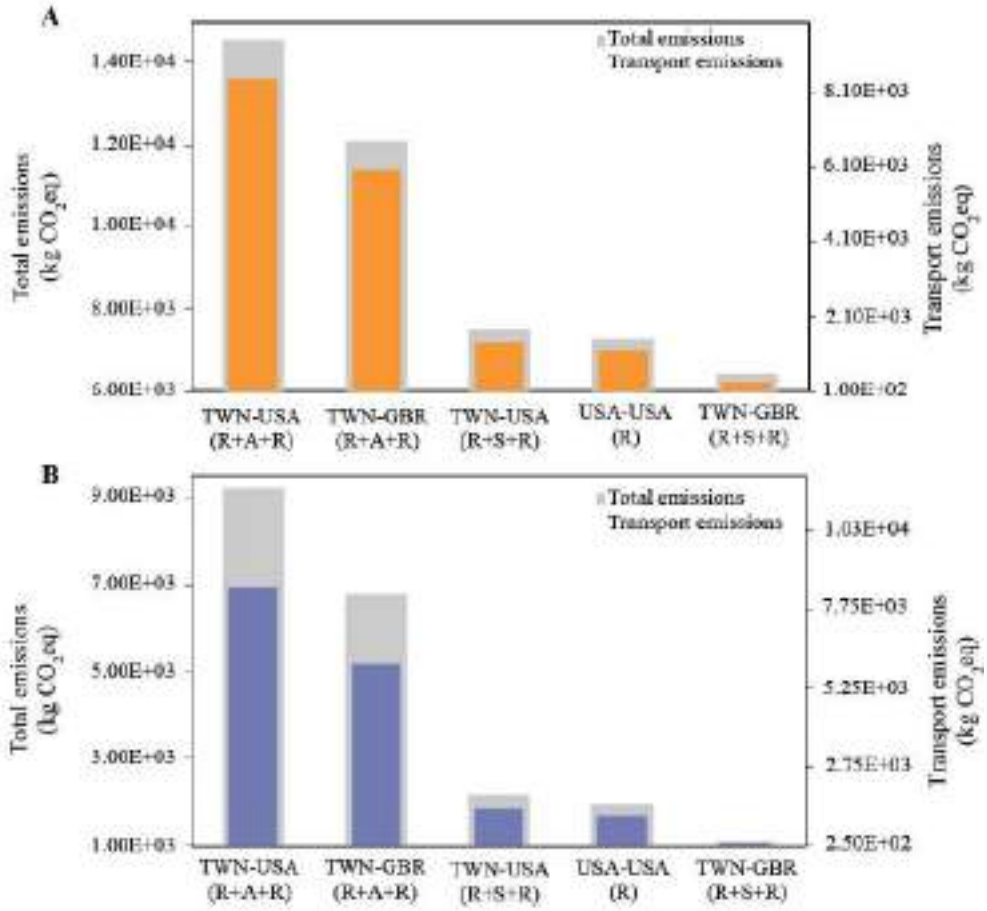


Fig. (6). Cradle-to-gate life cycle carbon footprint of 1 t month^{-1} of *Arthrospira platensis* dry biomass, including transport. (**A**) Upstream and downstream process powered by photovoltaic energy and (**B**) wind energy with diesel-powered road transport. The cradle-to-gate lifecycle carbon footprint data were obtained from Dias *et al*. [5, 6]. (*A higher resolution / colour version of this figure is available in the electronic copy of the article*).

with electricity based on natural gas, the carbon footprint was smaller compared to transport using internal combustion vehicles, but in this scenario, it is the opposite. Road transport using electric vehicles powered by electricity from natural gas showed a life cycle impact of 11% and 55% greater compared to using vehicles powered by diesel (Fig. **7B** and **7C**, respectively).

In synthesis, Fig. (**7**) shows that changing our assumption about electricity consumption can potentially alter the net benefits in terms of GWP for electric vehicles using electricity from coal and natural gas. This is problematic because coal and natural gas-based electricity account for around 60% of the global electricity mix. Furthermore, together, they more than double the share of some countries' electricity mix [48]. Consequently, these results send a signal that it may not be possible to reap local and, ultimately, global climate benefits from electric mobility. However, it is noteworthy that in some countries, renewable and nuclear sources can represent more than 90% of the electricity mix, and in these places, the adoption of electric vehicles would be adequate. Finally, according to Fig. (**7**), the supremacy of electric road transport powered by nuclear, hydro, wind, biomass, and photovoltaic energy remains.

4.2. Checking Economic Drivers for Decision-making Processes

While the international discussion on climate change remains mired in an ideological dialog of the deaf between the conflicting positions of developed versus developing countries, the planet slips into a radically different climate. The recent decision by the G7 to end the use of fossil fuels by the end of the century is not - for many climate scientists - a cause for celebration, just an example of climate procrastination. However, while the world's leaders present timid initiatives, many

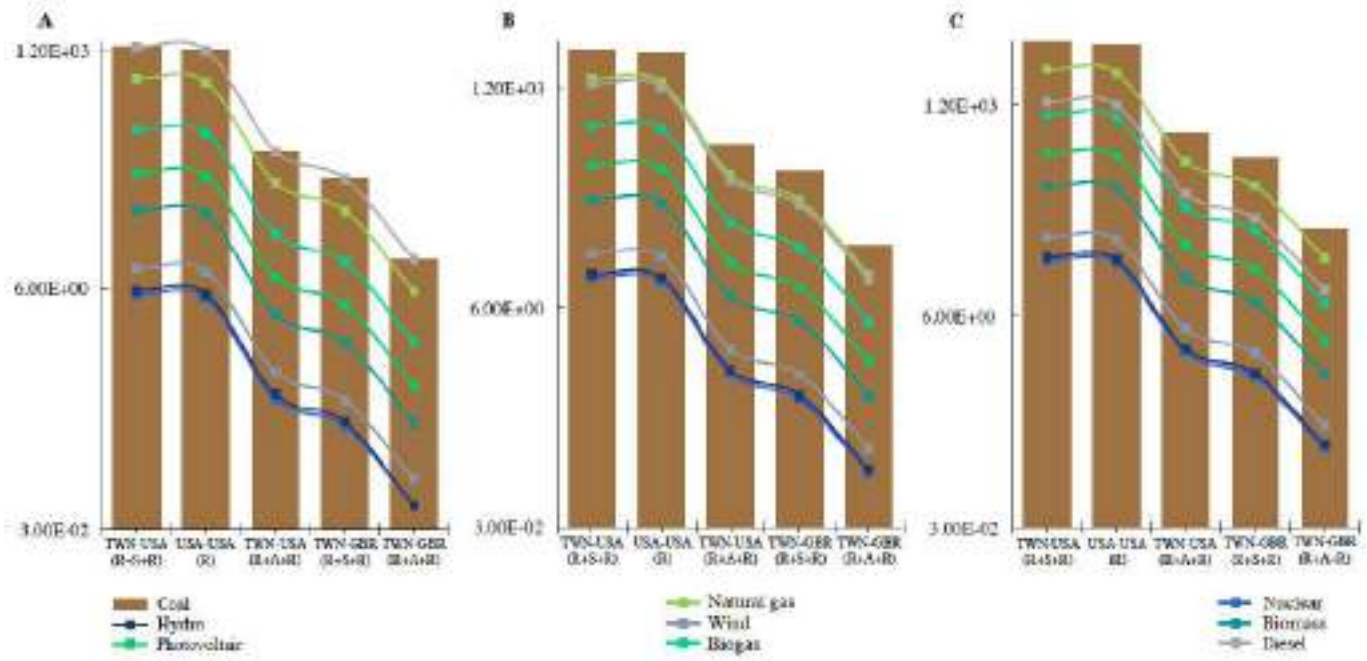


Fig. (7). Sensitivity analysis of the life cycle carbon footprint of electric and internal combustion road transport. (**A**) Taking into account an electricity consumption of 0.22 kWh/km, (**B**) 0.50 kWh/km, and (**C**) 1.00 kWh/km. TWN, Taiwan; USA, United States; GBR, United Kingdom. (*A higher resolution / colour version of this figure is available in the electronic copy of the article*).

companies are moving forward to reduce their environmental impact. Concerning road transport, the adoption of electric vehicles is set to skyrocket [50].

Even after considering manufacturing, battery electric vehicles are still a greener option if they are considered low-emission energy sources to charge their batteries [51]. Our results show that when vehicles leave the factory floor, the energy used to power their batteries makes them more or less carbon-intensive than diesel-powered ones. This provides insights for companies seeking to relentlessly reduce road transport carbon emissions from the lifecycle of their goods. Most importantly, they see in small positive contributions to the environment an opportunity to generate carbon credits that can be auctioned, generating revenue.

The opportunity to generate revenue from the sale of carbon credits extends to companies producing microalgae that can not only reduce the carbon footprint of road transport of their products but also claim credits for the adoption of electric vehicles. This is possible because it is a strategy that mitigates emissions from activities associated with the transport and mobility – sector covered by credit mechanisms [52]. That said, Fig. (**8**) shows, according to the route, the revenue potential generated by replacing internal combustion road transport with electric based on the source of electricity.

As Fig. (**8**) shows, the defossilization of road transport has both climate and economic benefits, as it can create a new revenue stream for companies as more land miles are driven on low-carbon electric fuel. Charging electric vehicles with nuclear, hydro, wind, biomass, and photovoltaic energy generates the best revenue opportunities from the sale of carbon credits. The use of energy from biogas followed by natural gas, in turn, presents the second best option. On the other hand, coal-based energy shows margins narrow of gain since, as previously shown, it does not significantly reduce the emissions of its counterpart based on fossil fuel (diesel).

In sum, companies that operate routes moved entirely or mostly by land vehicles such as USA-USA (R) and TWN-USA (R+S+R) can generate a greater balance of carbon credits that, reverted to economic advantage, contribute to leverage the company's growth. Besides that, those who change from a road-air route to a road-sea route can also generate carbon credits because this transition also

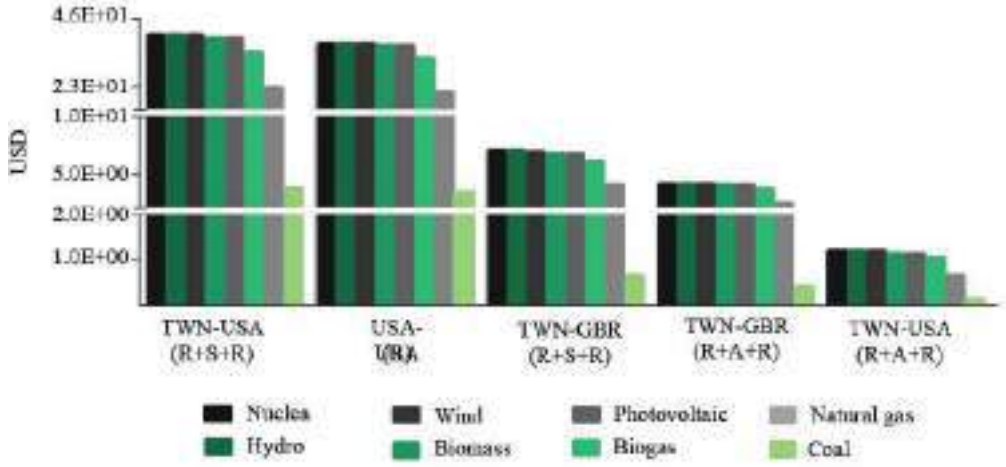


Fig. (8). Revenue generated for replacing internal combustion road transport with electric transport. The color of each bar represents the source of electrical energy. TWN, Taiwan; USA, United States; GBR, United Kingdom. For routes with a final destination in the USA and GBR, the carbon price of the California CaT and UK ETS programs for the year 2023 was considered, respectively. (*A higher resolution / colour version of this figure is available in the electronic copy of the article*).

massively reduces the emissions associated with transport and mobility (see Fig. **4**). Comparatively, if a company replaced the TWN-GBR (R+A+R) route with TWN-GBR (R+S+R) and TWN-USA (R+A+R) with TWN-USA (R+S+R) – with road transport powered by diesel or electric fuel – would raise about USD 568-562 and USD 253-218 in revenue from the sales of carbon credits per ton of transported product, considering the prices of carbon pricing initiatives in the UK and California, respectively.

Finally, when thought from the perspective of sustainable development, it is clear that the action of decarbonizing the distribution route is allied to the pillars of sustainability because, beyond the environmental criterion, it brings economic gains for companies and, in the social aspect, for people, relieves them from being disproportionately affected by climate disruption. Still, from an economic perspective, the costs associated with fuel in road transport are significantly higher for internal combustion vehicles fueled with diesel (Fig. **9**). Although less expensive, electric vehicles charged with nuclear energy, followed by biogas and coal, have a higher cost than those charged with energy from biomass and natural gas. According to our assumptions, the lowest fuel costs are for charging with wind energy, followed by hydro and photovoltaic, which, concomitantly, are the ones with the lowest energy generation costs [44].

Lastly, the positive impact of wind, hydro, and photovoltaic energy on the climate, added to the greater generation of revenue from the sale of carbon credits and lower cost of charging batteries, make them trade-offs. Also, it is important to say that although environmental awareness plays a key role in the adoption of electrified routes, adoption decisions are mainly economic motivations [53]. Today, the transition to an electric vehicle, despite having a higher initial cost, has cheaper fuel and maintenance costs, which, taking into account the useful life of vehicles, suggests that it is very worthwhile.

CONCLUSION

This work provides a new level of transparency to the ongoing discussion about the merits of electric road transport. Road transport that uses battery electric vehicles powered by coal-based electricity, natural gas, biogas, nuclear, hydro, wind, biomass, and photovoltaic reduces global warming potential by approximately 8.6%, 55.0%, 85.5%, 99.6%, 99.5%, 99.3%, 97.5%, and 94.4% compared to diesel-powered internal combustion vehicles. According to sensitivity analysis, road transport's electrification is counterproductive in regions where electricity is produced from coal and, ultimately, natural gas. The results confirm the supremacy of electric road transport powered by hydro, wind, and photovoltaic energy for three main reasons: firstly, due to the positive impact on the climate; secondly, due to the greater opportunity to generate carbon credits; and thirdly, due to the lower cost of recharging batteries. In this study,

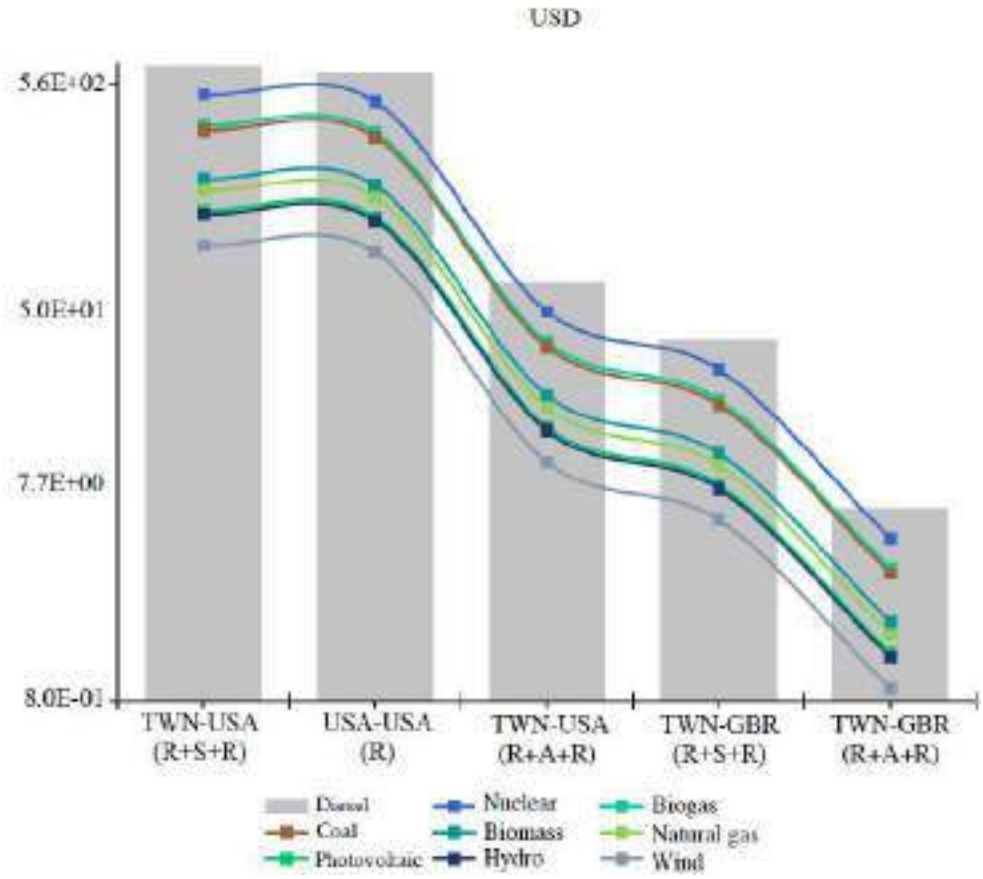


Fig. (9). Analysis of the cost associated with internal combustion road transport versus electric transport powered from different electricity sources. TWN, Taiwan; USA, United States; GBR, United Kingdom. (*A higher resolution / colour version of this figure is available in the electronic copy of the article*).

considering the origin of the energy that powers the battery of electric vehicles, the impact of indirect emissions from road transport on the products' life cycle was evaluated. Future works need to evaluate the impact of these emissions considering the world's electricity mix scenarios.

AUTHORS' CONTRIBUTIONS

Rosangela Rodrigues Dias: Conceptualization, Methodology, Data curation, Writing - original draft. Mariany Costa Deprá: Conceptualization, Methodology, Data curation. Victor Cesar Rodrigues Carvalho: Methodology. Cristiano Ragagnin de Menezes: Funding acquisition. Leila Queiroz Zepka: Supervision, Funding acquisition. Eduardo Jacob-Lopes: Conceptualization, Project administration, Writing - review & editing.

ETHICS APPROVAL AND CONSENT TO PARTICIPATE

Not applicable.

HUMAN AND ANIMAL RIGHTS

No animals/humans were used for studies that are basis of this research.

CONSENT FOR PUBLICATION

Not applicable.

AVAILABILITY OF DATA AND MATERIALS

The authors declare that [the/all other] data supporting the findings of this study are available within the article [and its supplementary information files].

FUNDING

The authors would like to thank the National Council for Scientific and Technological Development (CNPq) – Brazil and the Coordination of Improvement of Higher Education Personnel (CAPES), Finance Code 001.

CONFLICT OF INTEREST

Dr. Eduardo Jacob-Lopes is on the Editorial Advisory Board of the journal Recent Patents on Biotechnology.

ACKNOWLEDGEMENTS

Declared none.

SUPPLEMENTARY MATERIAL

Supplementary material is available on the publisher's website along with the published article.

REFERENCES

[1] Jacob-Lopes E, Maroneze MM, Deprá MC, Sartori RB, Dias RR, Zepka LQ. Bioactive food compounds from microalgae: an innovative framework on industrial biorefineries. Curr Opin Food Sci 2019; 25: 1-7. http://dx.doi.org/10.1016/j.cofs.2018.12.003

[2] Olabi AG, Shehata N, Sayed ET, *et al.* Role of microalgae in achieving sustainable development goals and circular economy. Sci Total Environ 2023; 854: 158689. http://dx.doi.org/10.1016/j.scitotenv.2022.158689 PMID: 36108848

[3] Polaris Market Research. In: Microalgae Market. Available from: https://www.polarismarketresearch.com/industry-analysis/microalgae-market

[4] Deprá MC, Dias RR, Zepka LQ, Jacob-Lopes E. Building cleaner production: How to anchor sustainability in the food production chain? Environ Adv 2022; 9: 100295. http://dx.doi.org/10.1016/j.envadv.2022.100295

[5] Dias RR, Deprá MC, Zepka LQ, Jacob-Lopes E. Roadmap to net-zero carbon emissions in commercial microalgae-based products: environmental sustainability and carbon offset costs. J Appl Phycol 2022; 34(3): 1255-68. http://dx.doi.org/10.1007/s10811-022-02725-y

[6] Dias RR, Deprá MC, Severo IA, Zepka LQ, Jacob-Lopes E. Smart override of the energy matrix in commercial microalgae facilities: A transition path to a low-carbon bioeconomy. Sustain Energy Technol Assess 2022; 52: 102073. http://dx.doi.org/10.1016/j.seta.2022.102073

[7] Reijnders L. Life cycle assessment of microalgae-based processes and products. In: Handbook of Microalgae-Based Processes and Products. Academic Press 2020; pp. 823-40. http://dx.doi.org/10.1016/B978-0-12-818536-0.00030-0

[8] Jacob-Lopes E, Zepka LQ, Deprá MC. Sustainability indicators and metrics of environmental impact: Industrial and agricultural life cycle assessment. 1st ed. Elsevier 2021.

[9] Ingrao C, Scrucca F, Matarazzo A, Arcidiacono C, Zabaniotou A. Freight transport in the context of industrial ecology and sustainability: evaluation of uni- and multi-modality scenarios *via* life cycle assessment. Int J Life Cycle Assess 2021; 26(1): 127-42. http://dx.doi.org/10.1007/s11367-020-01831-8

[10] Climate Watch. Historical GHG Emissions. https://www.climatewatchdata.org/ghg-emissions?breakBy=sector&end_year=2018&gases=co2&start_year=1990

[11] Zhang R, Fujimori S. The role of transport electrification in global climate change mitigation scenarios. Environ Res Lett 2020; 15(3): 034019. http://dx.doi.org/10.1088/1748-9326/ab6658

[12] Ritchie H. Cars, planes, trains: where do CO_2 emissions from transport come from. Our World in Data 2020.

[13] Ślusarczyk B. Electromobility for sustainable transport in Poland. In: Energy Transformation Towards Sustainability. Elsevier 2020; pp. 199-218. http://dx.doi.org/10.1016/B978-0-12-817688-7.00010-0

[14] Yigitcanlar T. Towards smart and sustainable urban electromobility: An editorial commentary. Sustainability 2022; 14(4): 2264. http://dx.doi.org/10.3390/su14042264

[15] Ajanovic A, Haas R, Schrödl M. On the historical development and future prospects of various types of electric mobility. Energies 2021; 14(4): 1070. http://dx.doi.org/10.3390/en14041070

[16] Chadha S, Jain V, Singh HR. A review on smart charging impacts of electric vehicles on grid. Mater Today Proc 2022; 63: 751-5. http://dx.doi.org/10.1016/j.matpr.2022.05.122

[17] Кириллова ОА, Виденеев АВ. Electric cars. Executive Editor 2015.

[18] Parthasarathy A. Electrical mobility: Gliding into the acceleration phase. 2022.

[19] Taylor J. Electric cars. Bloomsbury Publishing 2022.

[20] Patil DS, Patil Y, Kirange Y, Mahajan NS, Patil RS. Study on growth of electric vehicles in india: A review. In 2023 3rd Asian Conference on Innovation in Technology (ASIANCON) Ravet IN, India,. 1-7. http://dx.doi.org/10.1109/ASIANCON58793.2023.10270327

[21] Bordes A, Danilov DL, Desprez P, *et al.* A holistic contribution to fast innovation in electric vehicles: An overview of the DEMOBASE research project. eTransportation 2022; 11: 100144. http://dx.doi.org/10.1016/j.etran.2021.100144

[22] Shen F, Xie S, Teo CS, Lee CH. Recent Development of Electric and Hybrid Vehicles. In: Emerging Technologies for Electric and Hybrid Vehicles. Singapore: Springer Nature Singapore 2024; pp. 343-58. http://dx.doi.org/10.1007/978-981-99-3060-9_12

[23] Chandran M, Palanisamy K, Benson D, Sundaram S. A review on electric and fuel cell vehicle anatomy, technology evolution and policy drivers towards EVs

and FCEVs market propagation. Chem Rec 2022; 22(2): e202100235.
http://dx.doi.org/10.1002/tcr.202100235 PMID: 34796621

[24] Bejgam R, Sunkari S, Keshipeddi SB, Rangaraju MR, Dunde V. A brief study on hybrid electric vehicles. 2021 Third International Conference on Inventive Research in Computing Applications (ICIRCA). 54-9.

[25] Jose PS, Jose PSH, Wessley GJJ, Rajalakshmy P. Environmental impact of electric vehicles. In: E-Mobility: A New Era in Automotive Technology. SpringerLink 2022; pp. 31-42.
http://dx.doi.org/10.1007/978-3-030-85424-9_2

[26] Ekici YE, Dikmen İC, Nurmuhammed M, Karadağ T. A review on electric vehicle charging systems and current status in turkey. Int J Autom Sci TechnolL 2021; 5(4): 316-30.
http://dx.doi.org/10.30939/ijastech..958368

[27] Cansino J, Sánchez-Braza A, Sanz-Díaz T. Policy instruments to promote electro-mobility in the EU28: A comprehensive review. Sustainability 2018; 10(7): 2507.
http://dx.doi.org/10.3390/su10072507

[28] Agrawal M, Rajapatel MS. Global perspective on electric vehicle 2020. Int J Eng Res Technol 2020; 9(1): 8-11.

[29] Global EV. Global EV Outlook 2023: Catching up with climate ambitions. Paris, France: Energy Agency 2023.

[30] Martinez-Boggio S, Monsalve-Serrano J, García A, Curto-Risso P. High degree of electrification in heavy-duty vehicles. Energies 2023; 16(8): 3565.
http://dx.doi.org/10.3390/en16083565

[31] Lewicki W, Drożdż W. Electromobility and its development prospects in the context of industry 4.0: A comparative study of poland and the european union. Europ Res Stud J 2021.

[32] Bhardwaj R, Gupta S. Evolutionary progress of the electric car market with future directions. In: In Latest Trends in Renewable Energy Technologies: Select Proceedings of NCRESE 2020. Singapore: Springer 2021; pp. 315-21.
http://dx.doi.org/10.1007/978-981-16-1186-5_27

[33] Rapa M, Gobbi L, Ruggieri R. Environmental and economic sustainability of electric vehicles: Life cycle assessment and life cycle costing evaluation of electricity sources. Energies 2020; 13(23): 6292.
http://dx.doi.org/10.3390/en13236292

[34] Leal Filho W, Abubakar IR, Kotter R, *et al.* Framing electric mobility for urban sustainability in a circular economy context: An overview of the literature. Sustainability 2021; 13(14): 7786.
http://dx.doi.org/10.3390/su13147786

[35] Kurien C, Srivastava AK, Molere E. Indirect carbon emissions and energy consumption model for electric vehicles: Indian scenario. Integr Environ Assess Manag 2020; 16(6): 998-1007.
http://dx.doi.org/10.1002/ieam.4299 PMID: 32543043

[36] Kurien C, Srivastava AK. Impact of electric vehicles on indirect carbon emissions and the role of engine posttreatment emission control strategies. Integr Environ Assess Manag 2020; 16(2): 234-44.
http://dx.doi.org/10.1002/ieam.4206 PMID: 31403259

[37] ISO. ISO-14040 Environmental management–life cycle assessment–principles and framework. International Organization for Standardization 2006. Available from: https://www.iso.org/standard/37456.html

[38] SMMT. Heavy Commercial Vehicle Fuel Efficiency. https://www.smmt.co.uk/wp-content/uploads/sites/2/Heavy-CV-Fuel-Consumption-Fact-Sheet.pdf

[39] Prohaska R, Ragatz A, Simpson M, Kelly K. Medium-duty plug-in electric delivery truck fleet evaluation. In: 2016 IEEE Transportation Electrification Conference and Expo (ITEC),. Dearborn, MI, USA. 2016; pp. 2016; pp. 1-6.

[40] Sato S, Jiang YJ, Russell RL, *et al.* Experimental driving performance evaluation of battery-powered medium and heavy duty all-electric vehicles. Int J Electr Power Energy Syst 2022; 141: 108100.
http://dx.doi.org/10.1016/j.ijepes.2022.108100

[41] Faria R, Marques P, Moura P, Freire F, Delgado J, de Almeida AT. Impact of the electricity mix and use profile in the life-cycle assessment of electric vehicles. Renew Sustain Energy Rev 2013; 24: 271-87.
http://dx.doi.org/10.1016/j.rser.2013.03.063

[42] Masum MFH, Dwivedi P, De La Torre R. Assessing economic and environmental feasibility of wood-based electricity generation in South America: A case study from Colombia. For Policy Econ 2021; 124: 102381.
http://dx.doi.org/10.1016/j.forpol.2020.102381

[43] European Commission. Final Report – LCOE & LCOH: Energy costs, taxes and the impact of government interventions on investments. Available online: https://energy.ec.europa.eu/system/files/2020-10/final_report_levelised_costs_0.pdf (accessed on 15 December 2022).

[44] Bhutada G. Electricity from renewable energy sources is now cheaper than ever. Visual Capitalist 2021: Available from: https://www.visualcapitalist.com/electricity-from-renewable-energy-sources-is-now-cheaper-than-ever/.

[45] Renewable power generation costs in 2021. Abu Dhabi: International Renewable Energy Agency 2022: Available from: https://www.irena.org/publications/2022/Jul/Renewable-Power-Generation-Costs-in-2021.

[46] Global Petrol Prices. Diesel prices. Available online: https://www.globalpetrolprices.com/diesel_prices/ (accessed on 15 December 2022).

[47] World Bank. Carbon Pricing Dashboard. Available online:

https://carbonpricingdashboard.worldbank.org/map_data (accessed on 20 December 2022).

[48] Ritchie H, Roser M, Rosado P. Energy. Available online: https://ourworldindata.org/electricity-mix#citation (accessed on 15 December 2022).

[49] Ritchie H, Roser M, Rosado P. Taiwan: Energy Country Profile https://ourworldindata.org/energy/country/taiwan (accessed on 20 December 2022).

[50] Xia X, Li P, Xia Z, Wu R, Cheng Y. Life cycle carbon footprint of electric vehicles in different countries: A review. In: Sep Purif Technol. / Elsevier 2022; 301: p. 122063.

[51] Joshi A, Sharma R, Baral B. Comparative life cycle assessment of conventional combustion engine vehicle, battery electric vehicle and fuel cell electric vehicle in Nepal. J Clean Prod 2022; 379: 134407. http://dx.doi.org/10.1016/j.jclepro.2022.134407

[52] World Bank. State and Trends of Carbon Pricing 2022. Available online: https://openknowledge.worldbank.org/handle/10986/37455 (accessed on 10 December 2022).

[53] Li L, Wang Z, Xie X. From government to market? A discrete choice analysis of policy instruments for electric vehicle adoption. Transp Res Part A Policy Pract 2022; 160: 143-59. http://dx.doi.org/10.1016/j.tra.2022.04.004

DISCLAIMER: The above article has been published, as is, ahead-of-print, to provide early visibility but is not the final version. Major publication processes like copyediting, proofing, typesetting and further review are still to be done and may lead to changes in the final published version, if it is eventually published. All legal disclaimers that apply to the final published article also apply to this ahead-of-print version.

Send Orders for Reprints to reprints@benthamscience.net

Recent Patents on Biotechnology, XXXX, *XX,* 000-000

REVIEW ARTICLE

The Role of Light on the Microalgae Biotechnology: Fundamentals, Technological Approaches, and Sustainability Issues

Rafaela Basso Sartori[1], Mariany Costa Deprá[1], Rosangela Rodrigues Dias[1], Mariane Bittencourt Fagundes[1], Leila Queiroz Zepka[1] and Eduardo Jacob-Lopes[1,*]

[1]*Bioprocess Intensification Group, Federal University of Santa Maria, Roraima Avenue, 1000, 97105-900, Santa Maria, RS, Brazil*

ARTICLE HISTORY

Received: January 09, 2023
Revised: February 03, 2023
Accepted: February 14, 2023

DOI:
10.2174/1872208317666230504104051

Abstract: Light energy directly affects microalgae growth and productivity. Microalgae in natural environments receive light through solar fluxes, and their duration and distribution are highly variable over time. Consequently, microalgae must adjust their photosynthetic processes to avoid photo limitation and photoinhibition and maximize yield. Considering these circumstances, adjusting light capture through artificial lighting in the main culture systems benefits microalgae growth and induces the production of commercially important compounds. In this sense, this review provides a comprehensive study of the role of light in microalgae biotechnology. For this, we present the main fundamentals and reactions of metabolism and metabolic alternatives to regulate photosynthetic conversion in microalgae cells. Light conversions based on natural and artificial systems are compared, mainly demonstrating the impact of solar radiation on natural systems and lighting devices, spectral compositions, periodic modulations, and light fluxes when using artificial lighting systems. The most commonly used photobioreactor design and performance are shown herein, in addition to a more detailed discussion of light-dependent approaches in these photobioreactors. In addition, we present the principal advances in photobioreactor projects, focusing on lighting, through a patent-based analysis to map technological trends. Lastly, sustainability and economic issues in commercializing microalgae products were presented.

Keywords: Algae, photosynthesis, culture system, photoperiod, lighting devices, photobioreactors.

1. INTRODUCTION

Microalgae are considered a promising source of compounds of biological interest and have been widely explored due to their diverse and useful high-value applications. Microalgae growth and productivity are related to various factors, although metabolically speaking, light acts as a tool of paramount importance [1].

In the state of the art, photosynthesis rate under any set of conditions is mainly correlated with the function of absorbed light and the use of light energy to drive carbon assimilation, among other metabolic processes [2]. Thus, microalgae exposed to low irradiance tend to invest less in electron transport proteins and carbon assimilation enzymes and more in light capture in order to achieve the best photosynthetic performance given the imposed conditions. In contrast, when microalgae are exposed to excessive light intensities, transport and chain capacity electrons' supersaturation can result in photo-oxidative damage [3]. In this case, developing acclimatization involves protein content and composition changes, which affect different metabolic fluxes. These changes ensure the optimal use of resources under the new condition and provide the microalgae the neces-

*Address correspondence to this author at the Bioprocess Intensification Group, Federal University of Santa Maria, Roraima Avenue, 1000, 97105-900, Santa Maria, RS, Brazil; E-mail: ejacoblopes@gmail.com

1872-2083/XX $65.00+.00 © XXXX Bentham Science Publishers

sary plasticity to withstand environmental changes (*e.g.*, climatic change, different light cycles, and fluctuation in irradiance levels) [4].

The efficiency of converting light into biomass represents a major constraint to finally bridging the gap between theoretical and industrial productivity [5]. Microalgae have a light-collecting system responsible for improving the photosynthetic system. This system, for example, acts as a light energy collector and consequently transfers and regulates this energy to the photosystems [6]. Thus, these systems should be as sufficient as possible in the biotechnology and characterization of the photosynthetic system to achieve favorable biomass production on a large scale [7].

One of the crucial requirements for the satisfactory performance of this biotechnology segment is to provide sufficient light in an efficient form [8]. In microalgae cultures, the exploitation of sunlight as a light source is advantageous because it is free and abundant, although it also has some disadvantages, such as day/night cycles, weather conditions, seasonal changes, and site-specific factors [9]. These luminosity variations can be avoided when applied in culture systems controlled by artificial light. Artificial light sources typically have high efficiency in converting electricity into light with less waste of energy as heat; light intensity, period, and spectral range can be modified in these systems [10]. Thus, the ease of manipulating the optimal lighting conditions in closed photobioreactors (PBRs) can reduce the demand for light energy and, consequently, develop the microalgae systems and optimize bioenergy production through these processes [11, 12].

Unsurprisingly, lighting costs are currently the main challenge of microalgae-based processes [1]. In this regard, highly versatile LED (light-emitting diode) lighting technologies are gaining traction compared to conventional lighting technologies such as halogen and fluorescent lamps. In fact, the selection of electrics components and the intelligent control of the light units (for instance, the use of intermittent light and different photoperiods, colors, and spectral levels, control of the light fluxes absorbed inside the cultures, and the selection of the best culture system, as new closed photobioreactor configurations) can maximize light output and the system's energy efficiency [13].

Furthermore, adopting more sustainable practices has moved changes in commercial paradigms. Based on this premise, the technological routes of microalgae-based products have been the subject of debate regarding economic sustainability metrics and environmental indicators [14]. Although the commercialization of some products from microalgae is consolidated due to health and wellness trends and green principles, it is still worth mentioning that, it is highly recommended to submit them to especially sustainability assessments and examine the potential environmental impacts of the process, mainly when the subject is electricity associated with artificial lighting [15].

In this sense, this article brings necessary information on the role of light in microalgae biotechnology. Initially, we provide an overview of microalgae photosynthetic metabolism (light collection and transformation), valuing the significant role that lighting conditions play in these systems. We highlight the growth characteristics of microalgae in natural and artificial light and the efficiency of artificial light after providing light flux modulation strategies. The main projects of photobioreactors as one of the critical factors in the correlation with light performance is discussed, in addition to future advances in photobioreactors design and lighting projects. Lastly, we present the impact of artificial lighting on sustainability issues and the primary costs involved in microalgae systems. Overall, we aimed to gain a deeper understanding of the following questions: How microalgae adapt and develop from the varied fluctuations of light and irradiation received throughout the process and whether it is possible to state that microalgae systems with artificial lighting can be environmentally and economically acceptable at a commercial level in the near future.

2. FUNDAMENTALS OF PHOTOSYNTHETIC METABOLISM

The photosynthesis reaction is responsible for constructing molecules by metabolizing light. In chemical terms, light is electromagnetic energy, traveling at $3x10^8$ m/s^{-1}, where light is denoted as a wavelength. The wavelength used for the photosynthesis reaction varies between 380 and 750 nm, which is regarded as "visible light" [16]. Light is composed of matter (quanta), called photons, so in chemical terms, light has a duality characteristic

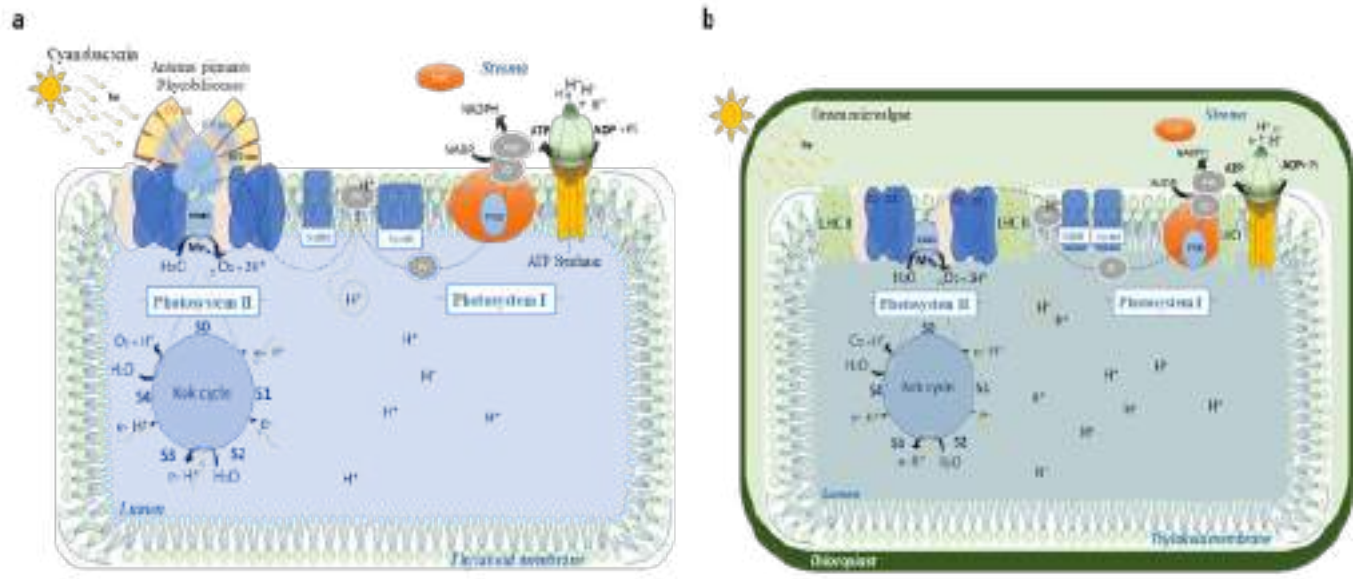


Fig. (1). Schematic representation of photosynthetic electron transport chain in cyanobacteria (**a**) and a green alga (**b**). Photosystem I (PSI), photosystem II (PSII), cytochrome b6f complex (Cyt b6f), plastocyanin (PC), ferredoxin (Fd), and ferredoxin-NADP reductase (FNR). Cytochrome c6 (Cyt c6) transfers electrons from the Cyt b6f, nicotinamide adenine dinucleotide phosphate (NAD), nicotinamide adenine dinucleotide phosphate reduced (NADH), adenosine diphosphate (ADP), adenosine triphosphate (ATP). The Sn states in the Kok diagram denote different discrete oxidation states where n this the number of oxidative equivalents. (*A higher resolution / colour version of this figure is available in the electronic copy of the article*).

(being called wave-particle duality) when in contact with cyanobacteria/microalgae cells, the first step of photosynthesis [17]. Structural differences and the photosynthetic pathway for both prokaryotic cells (represented by cyanobacteria) and eukaryotic cells (represented by green algae) can be seen in Fig. (**1**).

Numerous theories control photosynthetic metabolism. The first cells with photosynthetic capacity on Earth were cyanobacteria; however, more primitive cyanobacteria did not have a thylakoid system, only some molecules belonging to the photosynthetic system such as photoreceptor pigments, chlorophylls, phycocyanins, and phycoerythrins, distributed randomly in the cell cytoplasm, as well as proteins of the photosynthetic system [18]. It is important to note that over the years, through evolution, the photosynthetic system has adapted and become more complex [19]. Thus, it is necessary to comprise the photosystem and its metabolic pathways to understand the metabolism that controls the increase in photosynthetic efficiency. In this case, the steps of central carbon metabolism by the photosynthetic pathway are divided into two stages: (i) reactions of light, which absorbs energies at different wavelengths of 700 nm (photosystem I (PSI)) and 680 nm (photosystem II (PSII)), and (ii) the stage characterized by the Calvin cycle, also known as the dark phase [20, 21]. The reduction of carbon dioxide occurs at this stage, is fueled by adenosine triphosphate (ATP) and nicotinamide adenine dinucleotide phosphate reduced (NADPH), and is known to be an anabolic process [22].

2.1. Light Phase Reactions

The first step of photosynthesis is characterized by water splitting, which occurs in photosystem II. After energy acquisition through light absorption, the excitation energy is required to oxidize water molecules, which occurs through a manganese complex located in the protein active site, usually coordinated by the protein units of the photosystem called A (PsbA) and D (PsbD), the water molecule oxidation is known as Kok cycle [23]. The manganese complex is located at the entrance of the active site of the PSII protein complex and is composed of 4 manganese atoms, one calcium atom, and five O_2 atoms. The structure geometry is cubic, where three calcium molecules participate, and the fourth atom is outside the angle [24]. The amino acid residue of the PsbA protein structure, tyrosine, is responsible for communicating the manganese complex and the P680 nm photocenter

[25]. When light strikes microalgae cells, the photons are captured by photosynthetic pigments (chlorophylls, carotenoids, phycocyanins, and phycoerythrins) and transferred to this complex.

The photolysis process is based on a series of manganese redox reactions, the most reduced manganese state S0, which passes through the donation of 1 electron to the S1 state and consequently to the S2 and S3 states [26]. The electrons are acquired individually as a tyrosine amino acid residue and transferred directly to P680 nm. In the highest oxidation state (level four), the fourth manganese (Mn) atom involved in the reactions does not have an electron to donate, so the Mn atoms oxidate electrons from the water molecule (4 electrons), forming protons, and oxygen as a residue from this metabolic reaction, in short, water splitting is essential to restabilize manganese atoms [27]. After photolysis, the P680 photocenter is in a state of higher excitation level, transferring energy to pheophytin, initiating the process of the respiratory chain, and reaching the plastoquinone pool (PQ), which is responsible for performing the energy transport process within the membrane, as they are lipid-soluble and the main vectors of this respiratory chain. Plastoquinone carries the energy to the cytochrome complex b6f (Cyt b6f), which translocates the energy by mobile plastocyanin to photosystem I [17, 28].

Absorption of photons by the P700 photocenter occurs through the energy transported from PSII, and photons acquired from this protein complex are named light-harvesting complex I (LHCI) [29]. A second electron chain starts transferring electrons through an iron-sulfur enzyme complex at the stromal, where ferredoxin NADP+ reductase (FNR) transfers electrons from ferredoxin FSx, to reduce the energy transmitter NADP+ into NADPH [30]. Li *et al.* [31] reported that ferredoxin, or flavodoxin, performs various conformations between the PSI complex. A hydrogen gradient is formed within the lumen throughout this metabolic process, resulting in an ion gradient balanced across the ATP synthase protein generating ATP as a result.

2.2. Dark Phase Reactions

The real fixation of carbon dioxide is carried out through the Calvin-Benson-Bassham (C3) cycle discovered in 1950 [22]. This cycle occurs in the stroma, can be highlighted in three phases, and is expressed in Fig. (**2**). The first step is carbon fixation, performed by a carboxylase/oxygenase enzyme called Rubisco; this enzyme is responsible for capturing and fixing atmospheric carbon dioxide (CO_2). Fixation occurs on three molecules of rubisco-5-phosphate; the result of this fixation is a sugar molecule known as ribulose bisphosphate, a chemical structure of six carbons. The chemical instability of this structure provides the cleavage of this compound in 3-phosphoglycerate, forming six chemical structures [32].

Subsequently, the reduction of structures occurs, in which each of these molecules is phosphorylated by an ATP and reduced by an NADPH, forming the structure 1,3 bisphosphoglycerate, which in its final conformation it loses a phosphate, remaining as glyceraldehyde-3-phosphates (G3P) serves as a building block for other biomolecules of interest, such as carbohydrates, lipids, proteins, and nucleic acids, depending on cellular needs. The third stage, in turn, is characterized by the regeneration step, which involves a series of reactions, leading to three ATP molecules regenerating ribulose-phosphate [22].

2.3. Metabolic Alternatives to Regulate Photosynthetic Conversion in Microalgae Cells

The composition of each photosystem will vary according to the microalgae species, although they are segmented into core and antenna as structural characteristics. The nucleus is located in the active center complex, while the antenna is outside the structure of the protein complex, where all the light-accepting pigments are located [32]. Phycobiliproteins represent antenna in cyanobacteria, whereas in eukaryotic cells, throughout the evolution process, it was replaced by a complex of pigments interconnected named light-harvesting complex (LHC), represented by protein-bound chlorophylls and other pigments, mainly carotenoids [29]. Red algae, similar to cyanobacteria, have not lost their structure throughout evolution and have kept phycoerythrin as one of the main accessory pigments [33]. The antenna/LHC systems were formed to dissipate excess energy to protect PSII.

Photosystem II is represented by a structure that acts as a dimer. Each monomer composition is traditionally described as presenting 20 protein subu-

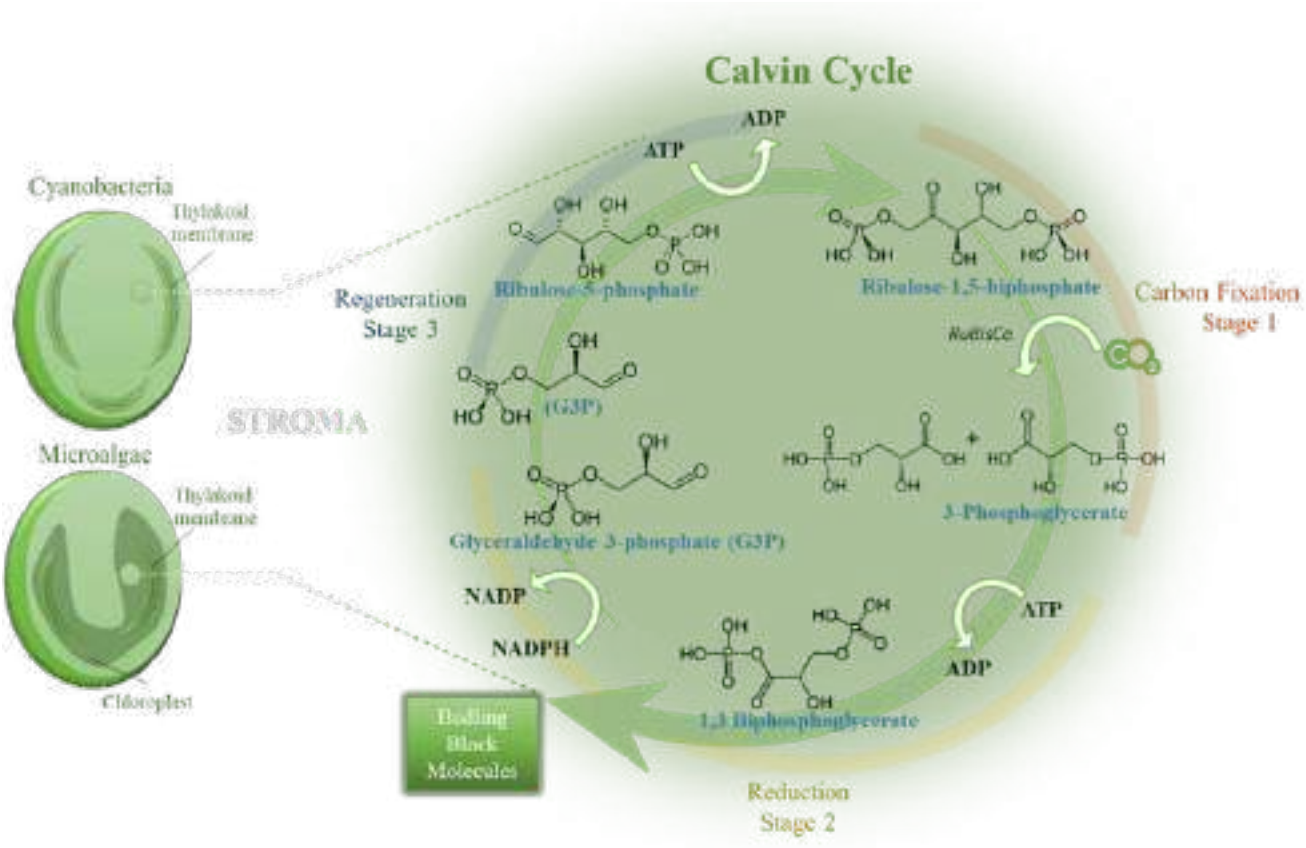


Fig. (2). The Calvin-Benson-Bassham cycle reactions. Presenting 3 stages, the first is associated with carbon fixation when Rubisco incorporates 3 CO_2 molecules into the 5-carbon sugar ribulose-1,5-bisphosphate, forming 6 molecules of 3-phosphoglycerate (3-PGA). Stage 2 is represented by the reduction phase, with 6 molecules of 3-PGA being converted into 6 molecules of Glyceraldehyde-3-P (G3P), using the number of 6 molecules of ATP and NADPH as reducing power. The last stage is characterized by RuBisCO regeneration. (*A higher resolution / colour version of this figure is available in the electronic copy of the article*).

nits, 4 calcium ions, 35 chlorophyll molecules, 3 chlorine ions, 20 to 25 lipid molecules, 12-beta carotenes, up to 3 plastoquinones, 2 pheophytins, 2 heme, non-heme iron, and the complex (Mn_4O_5Ca) [34], such pigments subunits can change according to microalgae strain. This information is important because photosystem II composition stands out among factors affecting the photosynthetic conversion rate. Mirkovic *et al.* [35] described that up to 80% of the solar energy captured by chlorophyll is dissipated by the accessory pigments from PSII, drastically reducing the photosynthetic rate. It is worth mentioning that, in this case, the presence of carotenoids and phycobiliproteins in several species increases the performance of light capture compared to species that have only chlorophylls. This is due to the light-capturing complexes in thylakoid membranes, which protect the photosynthetic apparatus from excess light through energy dissipation and the ability to deactivate oxygen (O_2) in microalgae [3].

In fact, for every 0.1 msec of light captured by chlorophyll, 1 msec is transported by the photosynthetic chain. Thus, to minimize these factors, researchers have focused on alternatives to reduce the size of antenna or LHC systems and the concentration of pigments to get a perfect balance for an optimal photosynthetic conversion rate [17]. Although great advances have been made in microalgae biotechnology and the characterization of the photosynthetic system, many improvements are still required. For instance, microalgae have an extensive antenna system or LCH complexes, which are responsible in this first step of photosynthesis for the low light absorption and distribution [6]; this phenomenon is explained in Fig. (**3**). Thus, the large size of the antenna does not allow homogeneous light dissipation, and when in high

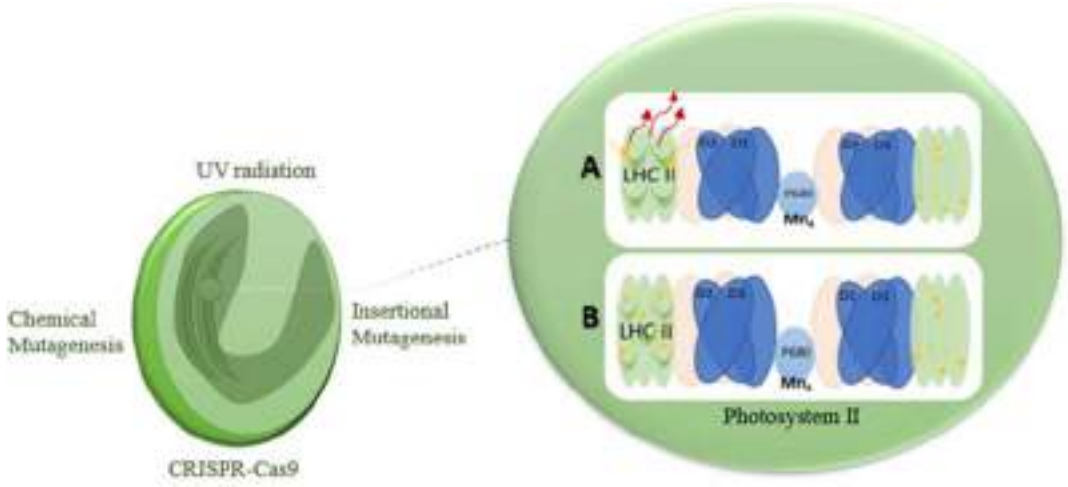


Fig. (3). Schematic representation of microalgae photosystem II response to different mutation agents, (**A**) wild microalgae antenna system (light-harvesting compounds), and (**B**) microalgae truncated antenna system. (*A higher resolution / colour version of this figure is available in the electronic copy of the article*).

cell density cultures, this problem increases dramatically.

Therefore, new alternatives are sought to reduce the loss of photosynthetic efficiency. As shown, reducing the antenna size is one of the possibilities. Currently, many research groups are studying genetic mutagenesis, also techniques known as genome editing, based on the introduction, deletion, or modification of DNA, target or not, generating new strains represented by different phenotypes. With this in mind, bioengineering has studied truncating the chlorophyll antenna to generate truncated light-harvesting antenna (TLA) mutants with a lower concentration of pigments, increasing the saturation photosynthetic irradiation capacity by 50% [36]. Truncated systems can be obtained by deleting the protein located in the chloroplast known as CrCpSRP43, which is responsible for assembling the peripheral components of the chlorophyll a/b light-gathering antenna and is also responsible for reducing the concentration of accessory pigments [37].

Nuclear genome modifications can also be acquired through chemical mutation or even modifying UV light. In fact, using different lengths of light radiation can reduce chlorophyll in the cell and consequently increase photosynthetic efficiency and biomass production in microalgae, probably due to changes in the entire photosynthetic system [10]. In general, antenna sizes are optimized by the ratio of chlorophyll a/b, with medium-sized antennas being the most prominent in increasing the photosynthetic capacity of microalgae [37].

Another alternative that has been used to increase the photosynthetic rate is to work with the key gene that encodes the catalysis of the large subunit of the Rubisco enzyme, an enzyme whose activity is modulated by light and the levels at which this light is distributed [38]. The overexpression of the rbcL gene leads to a higher maximum rate of carboxylation catalysis, consequently being an alternative to increase CO_2 fixation in the dark phase, thus optimizing photosynthetic efficiency (Fig. **4**).

Finally, regarding photosynthetic metabolism, much effort is needed to discover photosystems by elucidating structures and a complete genomic study to improve and correlate previously elucidated pathways. Furthermore, along the metabolic system, we can see that the importance of the potential changes in the capture system and the types of light distribution may be the necessary answer to circumvent the problems of photosynthetic efficiency and, in parallel, expand the cellular productivity in microalgae-based systems [4].

3. LIGHT CONVERSION IN MICROALGAE-BASED SYSTEMS

The availability of light is an essential factor for the cellular mechanism of microalgae, which has the power to limit the productivity and growth of these microorganisms [6]. In photoautotrophic growth modes, the light source can be provided

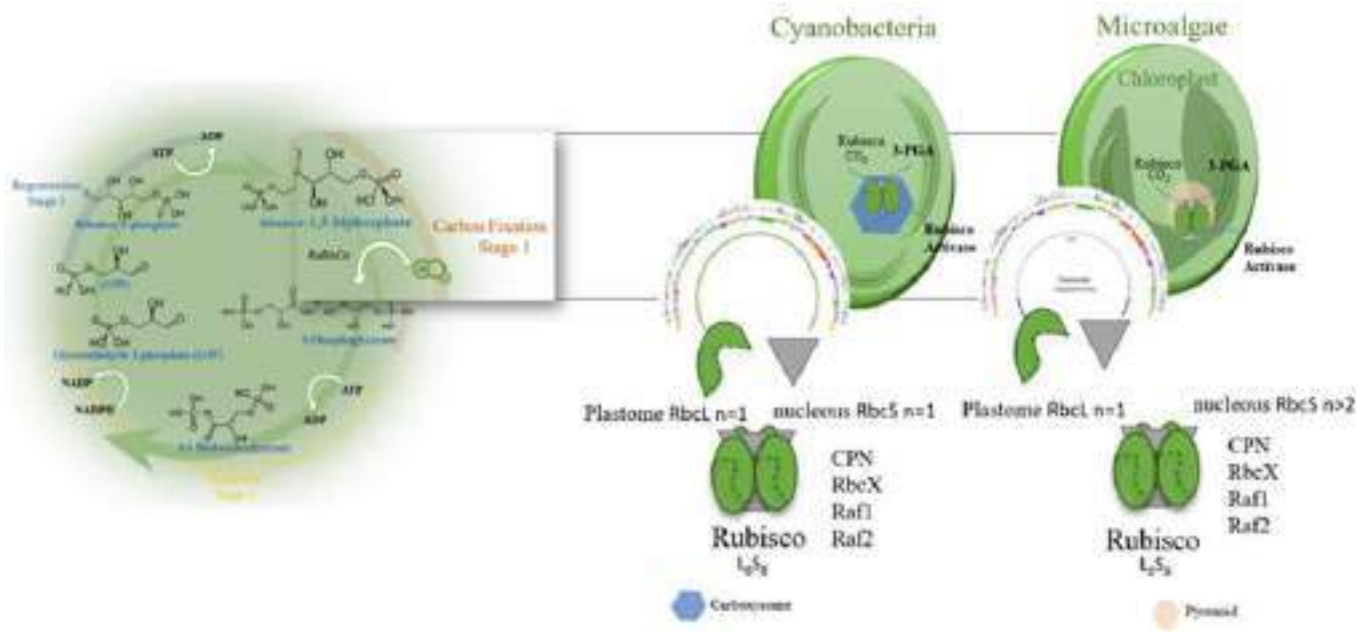


Fig. (4). A basic representation of rubisco biogenesis in cyanobacteria, and microalgae, CPN: chaperonin complexes, RbcX: ancient proteins to rubisco function, Raf1: rubisco accumulation factor 1, Raf2: rubisco accumulation factor 2. (*A higher resolution / colour version of this figure is available in the electronic copy of the article*).

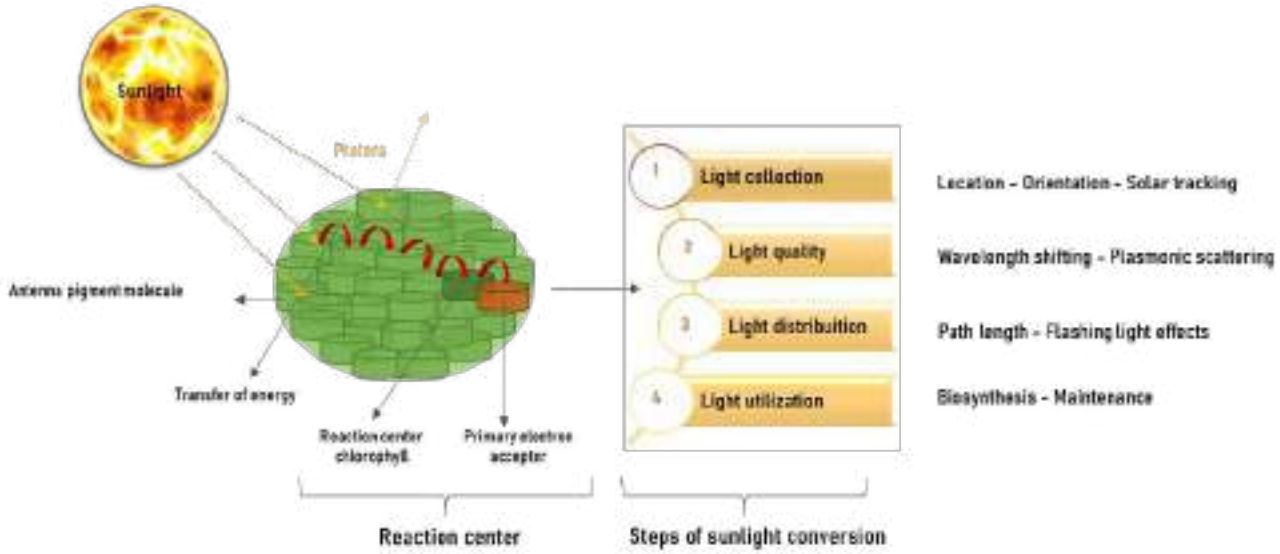


Fig. (5). Main steps in converting sunlight in microalgae systems. Adapted from Kumar *et al.* [6]. (*A higher resolution / colour version of this figure is available in the electronic copy of the article*).

naturally (sunlight) or artificially (lighting devices) [39].

3.1. Natural Light

Sunlight is the most economical energy source for microalgae cultivation. However, its exploitation has disadvantages that include changes in climate, day and night cycles, seasonal changes, and the geographic coordinates of the site, which affect the intensity of light and its spectrum [11].

So far, light conversion efficiency varies between 1-2% on a solar basis in microalgae production systems, far from the theoretical maximum of around 10% due to energy loss at all process steps such as capture, distribution, and use of light [40]. Some approaches have been suggested to overcome these losses to meet large-scale demand and achieve better production viability (Fig. **5**).

Solar resources vary according to geography and region and are determinants of the suitability

of a site for microalgae culture. In this case, the system's location can affect the capture of available solar energy [41]. In fact, scattering losses, measured in terms of direct beam plus diffuse radiation, increase with distance from the equator, incurring a factor that increases with latitude by up to 30%. Adverse weather conditions also result in an additional loss of over 60% since, at maximum sun intensity, 80% of absorbed solar energy is dissipated as fluorescence or heat [42]. Nonetheless, the physical orientation of the culture systems in relation to the sun can reduce the irradiation intensity by more than 50% for a horizontal surface compared to a surface oriented directly to the sun [43].

The impact of radiation on productivity is quite complex due to the interaction with other environmental variables. The average amount of photon energy received by each cell is a combination of several factors, including photon flux density, cell density, culture layer, light spectrum, and mixing rate, as well as the type of cultivation unit, light orientation, and which species and organisms are surveyed [8]. The cell irradiance suitable for photosynthesis can be estimated through the photosynthesis *versus* irradiance (P-I) curve. In any cultivation unit, we need to find an optimal biomass density (g DW L^{-1}) or optimal area density (g DW m^{-2}) at which productivity reaches a maximum value [32].

Microalgae can use only photosynthetically active radiation (PAR 400-700 nm) for photosynthesis among the various live organisms. The exact spectrum requirements of microalgae cells depend on the specific pigment composition of their light-harvesting antennae. Many photosynthetic organisms respond to changes in spectrum distribution through sophisticated sensory mechanisms to preferentially express desirable metabolites [10]. Therefore, based on PAR, only part of the solar spectrum of daylight available for microalgae growth is absorbed. This portion of the spectrum is responsible for approximately 41% of the solar energy incident on Earth and only about 20.4% of solar photons [44]. In microalgae, chlorophyll can be considered a semiconductor where the energy of a photon of wavelength 680 nm (PSII) is approximately 176 kJ/mol, while the energy for 700 nm (PSI) is 171 kJ/mol. If we assume that the average energy content of photons in the 400-700 nm range is about 218 kJ/mol, then the energy loss between absorption and charge separation in the two photosystems will be approximately {[218-(171+176)/2]/218}×100; This means that roughly 20.4% of the incident solar energy is irretrievably lost in the process, due to the relaxation of the higher chlorophyll excited states to the first singlet excited state [7, 40].

In this context, Dias *et al.* [9] mapped the biomass productivity of the microalgae *Scenedesmus obliquus* across the globe based on the Earth's climatic zones (*i.e*., equatorial, tropical, subtropical, and mid-latitudes), as shown in Fig. (**6**). According to our results, the central part of the globe (*i.e*., the equatorial and tropical climatic zones presented better productivity conditions, with a variation between 0.26 to 0.36 g L^{-1} d^{-1} in an annual average. These climatic zones have annual temperature and irradiance stability, which gives them greater stability against the biotechnological production of microalgae. In contrast, subtropical and mid-latitude zones show a greater degree of seasonal variation during the annual, which means it depends on a greater degree of adjustment between seasons. For example, in the summer, very high temperatures and irradiance can be lethal to microalgae, thus requiring cooling systems. In contrast, the low temperatures that occur mainly in subtropical zones in winter can lead to growth deterioration and loss of productivity, making it necessary to heat and artificially illuminate these cultures for part of the year. In this case, culture systems in these proportions can lead to a negative energy balance, even before considering other inputs (*e.g*., materials, mechanical operations, and necessary nutrients) [45]. The other climate zones on Earth (subantarctic, subarctic, antarctic, arctic, and polar) would only be able to support psychrophilic and psychrotolerant microalgae cultivation facilities that inhabit frigid environments. Therefore, daylighting is still a significant challenge for the overarching goal of natural production in environmentally sustainable, energy-efficient, and cost-effective microalgae systems.

Changing the quality or path length can transform low-utility photosynthetic light into high-efficiency light, controlling photosynthetically active radiation to make more energy available for photosynthesis and stimulate its growth. In this case, the introduction of artificial lighting gained

its space due to greater control, practicality, and flexibility [44]. In addition, the variation in the shape of this light distribution can also impact the final result, such as the effects of light intensity, saturation, and intermittence. Consequently, customizing the incident light spectrum transmitted to microalgae cultures through photobioreactors can ensure the efficient use of light to support microalgae-based processes.

3.2. Artificial Light

Artificial light sources are stable and easily controllable. Microalgal light utilization efficiencies and biomass productivities are higher under artificial light than in sunlight. This is because artificial lighting provides a constant source of lighting and still allows the installation of cultivation to take place in any location [1].

Light optimization is critical in microalgae biotechnology due to natural systems' low photosynthetic index and quantum efficiency [46]. As excess light is especially harmful to the photosynthetic apparatus, microalgae have developed different acclimation strategies to control and process the absorbed light in both photosystems. Improving biomass productivity through incident light manipulation can make the process economically viable. From this point of view, investigating methods to increase the use of light for biomass production is essential [32].

3.2.1. Lighting Devices

When trying to maintain an effective light distribution, using easily controlled lighting devices was sought, leading to the development of artificial lights in microalgae systems [10]. The evolution of technology in recent years has accompanied the advancement of lighting devices with different spectral characteristics, where the most commonly used ones are listed in Table **1**.

Among the most common, incandescent and halogen lamp applications have low cost, usability, and spectral range close to natural sunlight; conversely, they are technically not energy-saving and have low performance and durability. Therefore, fluorescent lamps and LEDs are the most promising artificial lights for growing microalgae, being LEDs generally preferred (Fig. **7**) [47].

LEDs are often preferred as light sources compared to the traditional ones used today, as they are more advantageous in terms of lifetime, compactness, and energy consumption. Although the

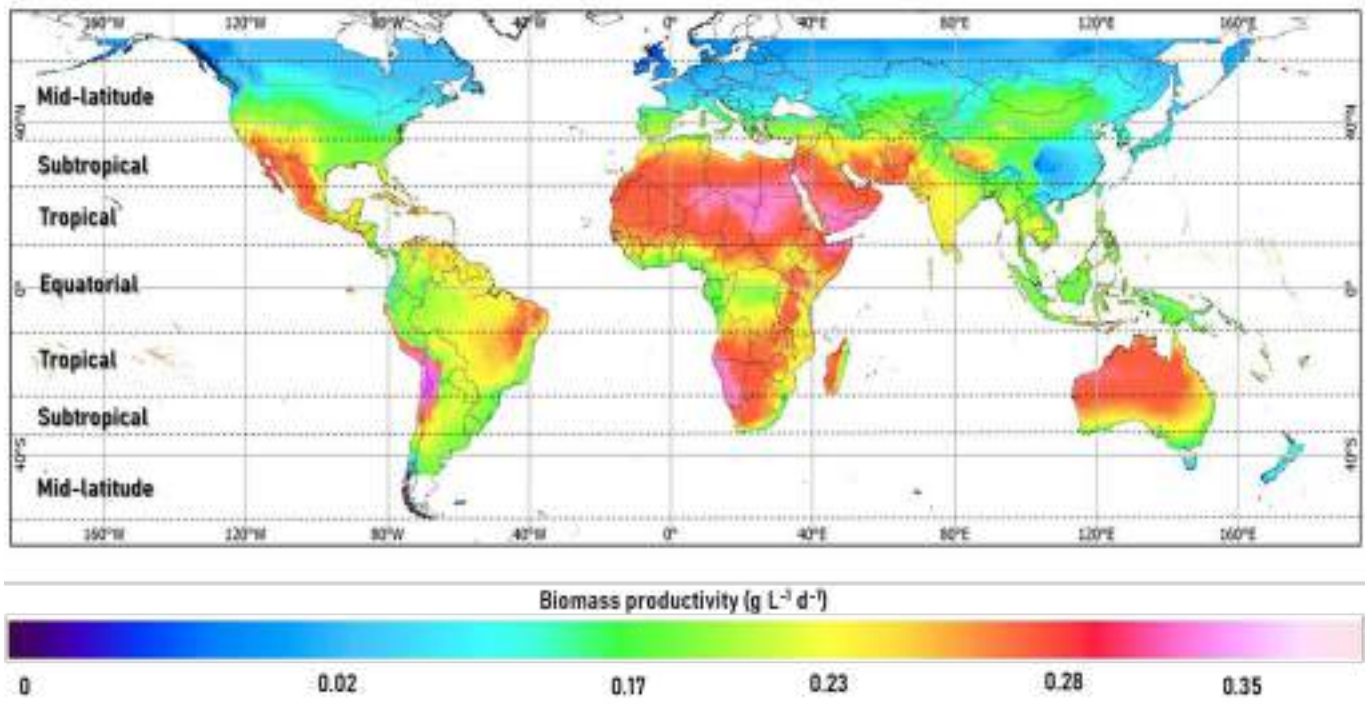


Fig. (6). World map of the average annual biomass productivity. Adapted from Dias *et al.* [9]. (*A higher resolution / colour version of this figure is available in the electronic copy of the article*).

Table 1. Main characteristics of artificial lights used in microalgae systems.

Light Sources	Wavelength (nm)	Intensity ($W \cdot m^{-2}$)	Energy Efficiency (400-500 nm) (%)	Energy Efficiency (600-700 nm) (%)	Duration (Hours)
Incandescent bulbs	300-1400	5.1	0.5	3.8	1440
Halogen lamps	650-950	1.6	0.3	3.3	3600
Fluorescent lamps	480-570	5.9	25	20.7	9984
Metal halide	200-2600	-	-	34	12000
LEDs	350-1100	14-55	0.08	87-98	40000

Note: Adapted from Nwoba *et al.* [10].

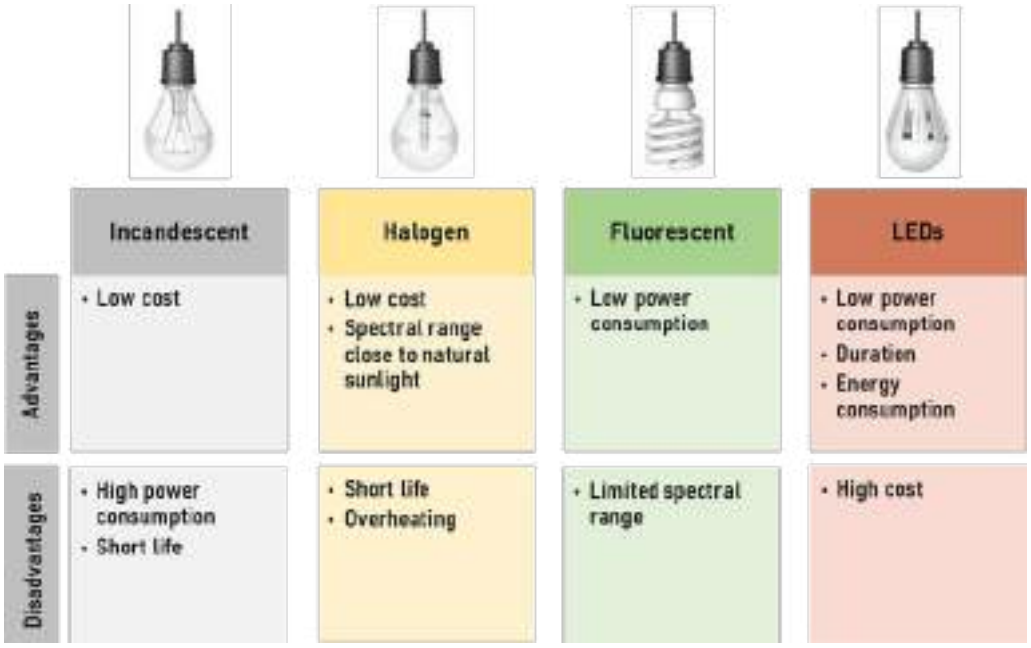


Fig. (7). Advantages and disadvantages of each type of lighting device. Adapted from Sero *et al.* [47]. (*A higher resolution / colour version of this figure is available in the electronic copy of the article*).

use of LED technology still presents some challenges to be overcome, mainly of its high initial cost and the regulation of its manufacture, it has greater advantages, such as quality and energy efficiency. In this case, only the spectrum necessary for the photosynthetic action of the microalgae is used, discarding the emission of ineffective frequencies in the form of heat, which results in lower costs and carbon emissions [10]. Another advantage can be cited about the environment, with less mercury emission at the time of disposal compared to fluorescent lamps. With all these characteristics, it can be said that lighting with LEDs is convenient and flexible, which makes the control of PBRs easily manageable [48].

3.2.2. Spectral Compositions

In general, microalgae pigment antennae undergo varied responses to different spectral compositions, which affects their photosynthetic machinery in parallel [1]. Therefore, lamps of different colors are used in microalgae cultures to provide the best conditions spectrally (Fig. **8**).

In microalgae, most photosynthesis occurs in the blue and red regions of the spectrum. In state-of-the-art, the PSII photosystem is enhanced by red light wavelengths, while PSI is enhanced by blue light wavelengths [39]. Blue light stimulates the up-regulation of phytoene synthase and phytoene desaturase, which are involved in carotenoid



Fig. (8). Main characteristics of lamps of differents colors and spectral levels. Adapted from Ramanna *et al.* [39]. (*A higher resolution / colour version of this figure is available in the electronic copy of the article*).

biosynthesis. Furthermore, cryptochrome photoreceptors respond to the blue and red wavelength, which triggers nitrogen metabolism, chlorophyll synthesis, and light-harvesting complexes [3].

Green fraction lamps also contribute to photosynthesis and the cell cycle by stimulating carotenoids, phycobiliproteins, and especially chlorophyll synthesis. The green and yellow light has been synonymous with stimulating photosynthetic efficiency and microalgal biomass productivity. This hypothesis relates to the fact that it is efficiently used since it is fully absorbed. Furthermore, cultures exposed to blank fall into a wavelength similar to the sunlight spectrum, ranging between 400 nm and 700 nm [49].

Although lamps with specific colors improve photosynthetic efficiency, the optimization of this process can best be attributed to when we combine two colors or more [1]. Some authors have reported that cell formation and cell growth are related to the red and blue colors of the spectrum, respectively. In this sense, microalgae cultivation conditions can be optimized using different colors of lamps in the process. In this case, instead of using various lamps in parallel, lamps in recent years have opted for bicolor lamps, where different colors are connected in a single contender to lower power consumption and maintain the efficiency of the process [3, 39]. A bidirectional current can produce mixed colours if the component is connected (through a suitable resistor) to a low-value, low-frequency alternating voltage, as seen in Fig. (**9**) [50].

3.2.3. Periodic Modulations

In general, using ideal light conditions increases the microalgae growth rate, which depends explicitly on the light flux's intensity, duration, and spectral composition [51]. A of the ways to achieve this objective is to guarantee the maximum light flux for all cells, meaning the activity of the photosynthetically active radiation (PAR) must be obtained in a range in which the most significant spectral activity is found, in this case, a wavelength between 400 and 700 nm is recommended. The quantitative energy characteristic of light radiation is the radiant energy flux, which arrives at the surface perpendicular to the rays per unit of time [1]. To determine the intensity of the photosynthetically active light flux, an estimate of the number of photons is widely used, expressing them in micro Einsteins ($\mu E\ m^{-2}s^{-1}$) or micromoles ($\mu mol\ m^{-2}\ s^{-1}$) per unit of energy area per second [52]. The light intensity can also be displayed in lux (1 l x = 1 lumen per square meter) or Watt per square Meter ($W\ m^{-2}$) [53].

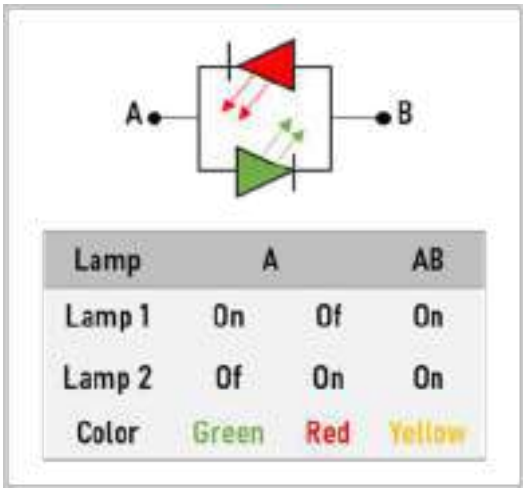


Fig. (9). A bidirectional current system in bicolor lamps. (*A higher resolution / colour version of this figure is available in the electronic copy of the article*).

In addition to determining the light source, it is necessary to understand how different lighting strategies (for example, flashing light and different light/dark cycles) affect microalgae development [54]. With a basic understanding of these factors, it is easy to manipulate cultures through lighting to meet one's needs, whether increasing yields or targeting certain specific compounds. By recognizing the role of these factors, it becomes easier to diagnose the problems and needs also caused by environmental stress related to lighting.

The basic concept of flashing light and using light/dark cycles is that, instead of continuous light, one can model or trigger changes in the light supply as the microalgae grow and adapt to being grown in the system [55]. This can usually be achieved by moving and cyclically exposing the microalgae cells within the PBR; However, today, artificial lighting devices already have fast electronic switches that cause this effect and make the efficiency of photosynthetic cultivation more balanced and uniform [50].

It can be said that three fundamental parameters are part of this process: (i) the intensity of the incident light that reaches the culture surface; (ii) the relationship between the photoperiods used in this culture, and (iii) the total time that these photoperiods are used [56]. It is also known that periodic modulations can be characterized according to the light frequencies used, meaning they can range from light/dark cycles of several hours, medium frequency band bursts (between 10 and 0.1 Hz), or even cycles above 10 Hz, better known as a pulsed light effect [57].

The three light band burst configurations mentioned above are best represented in Fig. (**10**), a result of studies by Maroneze *et al.* [11] and Sartori *et al.* [58]. For these authors, the best performance of maximum biomass productivity in *Scenedesmus obliquus* was achieved in long-term photoperiods of up to 2 h in the dark. Furthermore, when this 2 h in the dark was divided into 2 times/day (frequency photoperiods), an almost 20% gain in system performance was observed, demonstrating that the division of light/dark cycles can benefit the distribution of energy in the photosynthetic apparatus. Nevertheless, short photoperiods proved ideal when the objective was to produce specific compounds.

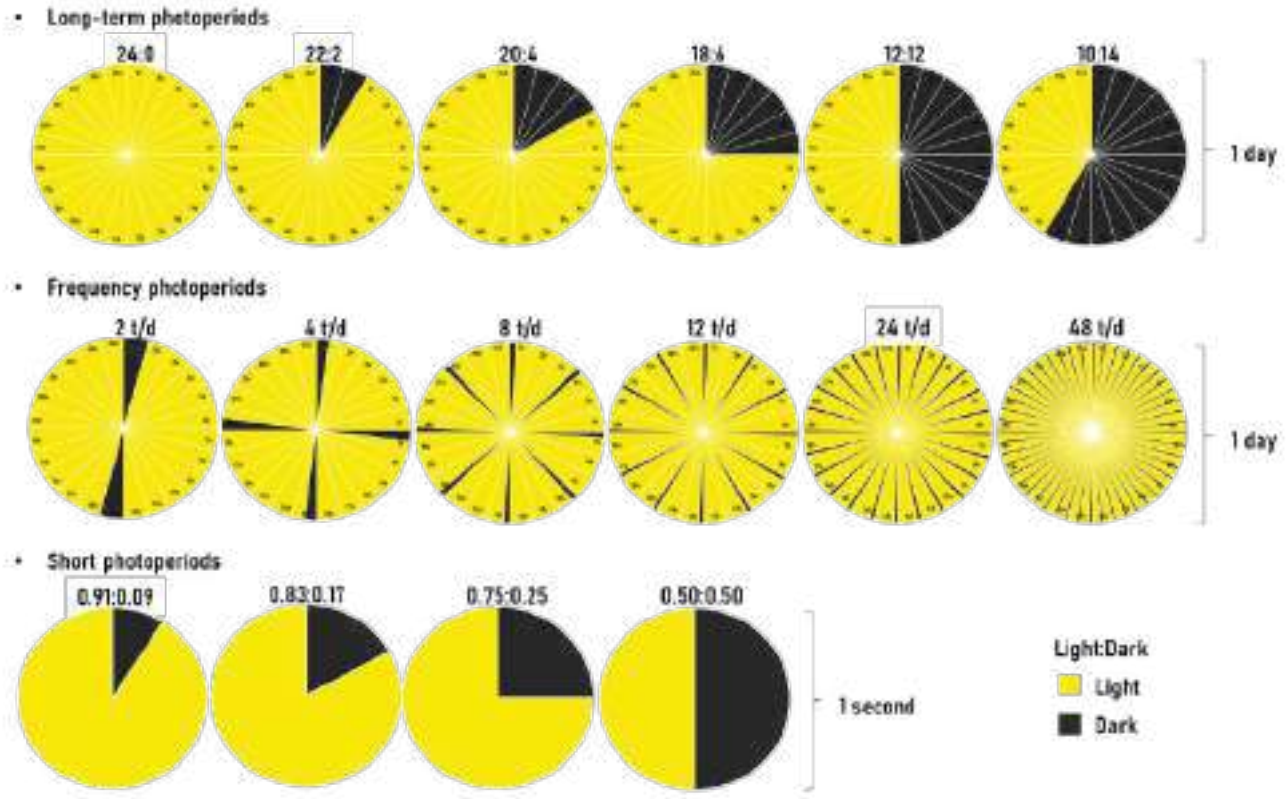


Fig. (10). Graphic representation of long-term, frequency, and short photoperiods. Adapted from Maroneze *et al.* [11]. (*A higher resolution / colour version of this figure is available in the electronic copy of the article*).

In this case, exposure of microalgae to universal stress factors, that is, very short and fast high-frequency cycles, tend to stimulate the synthesis of at least fatty acids and amino acids since higher yields of these compounds are not observed in contact with ideal growth conditions, as in the case of photoperiods of long-term (22:2 light: dark) and frequency of 2 times/day [59].

According to various studies, in photosynthetic systems, flashing light works as efficiently as, or slightly higher than, steady state under continuous light [60] because the light is less dissipated and used more efficiently [61]. In general, the dark intervals should be produced enough for adequate energy expansion and short enough to avoid triggering cellular respiration [62]. Fig. (**11**) represents these two types of systems generically. The best photosynthetic performance (in this case, occurred with intermittent light) promotes the best cell conversion, consequently producing greater productivity and generating microalgae biomass.

3.2.4. Light Fluxes in Photobioreactors

The efficiency of photosynthesis is directly related to the amount of light absorbed by the microalgae. At the cellular level, it is possible to know the amount of light needed to obtain the maximum performance of microalgae [6]. The photobioreactor system arises from the perception that the use of light by microalgae is closely related to the attenuation conditions of the light that exponentially penetrates the aqueous culture medium. Thus, it is easy to understand that if the microalgae absorb part of the light transmitted to it, the rest of the microalgae in this system will share the remaining flux. Consequently, the light energy is heterogeneous in the photobioreactor volume [63].

Given this, the calculation of light attenuation in the culture medium is given by the light intensity on the surface, the point of interest in the growth medium, and the result of the concentration of biomass formation [64]. Unless the culture exhibits a high area-to-volume ratio, the light becomes part of only a small area near the surface of the culture [65].

The light attenuation profile depends on several parameters, including each species' pigment content and radiative properties, biomass concentration, and microalgae's shape and cultivation parameters [6]. Theoretical studies identified three light attenuation regimes corresponding to different performances. In summary, these regimes are distinguished by the

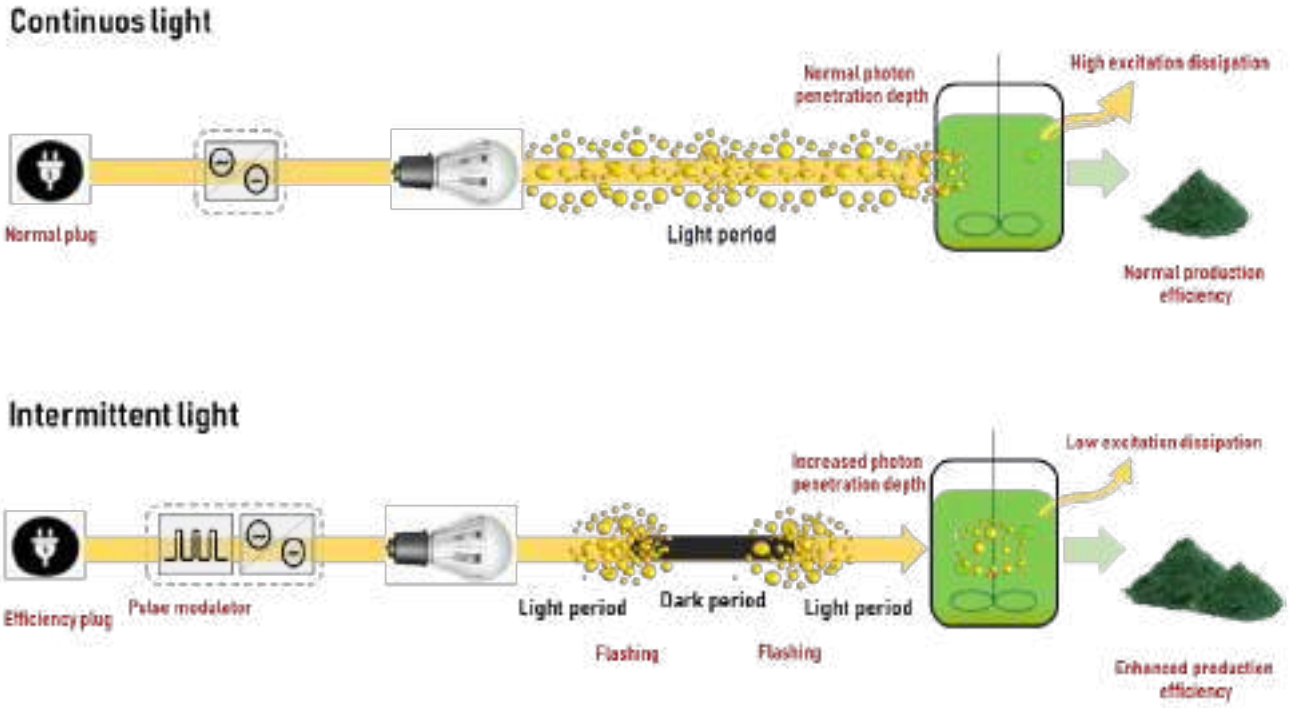


Fig. (11). Simplified diagram of continuous and flashing light in microalgae systems. Adapted from Schulze *et al.* [60]. (*A higher resolution / colour version of this figure is available in the electronic copy of the article*).

fraction of the volume illuminated in a PBR. This is defined by considering the ratio between the illuminated volume and the total volume of the PBR. The compensating irradiance then gives the boundary between these two zones. Thus, when the local irradiance is below this value, the zone is considered a dark volume in which the respiration phenomenon is predominant and negatively impacts biomass productivity [21]. The three light attenuation regimes are best exemplified in Fig. (**12**).

4. DESIGN AND PERFORMANCE OF PHOTOBIOREACTORS WITH EMPHASIS ON LIGHTING

Considering the significant and progressive advance in world interest in microalgae biotechnology, developing efficient production systems and a larger industrial scale is essential. Photobioreactors are most often categorized according to their size, mode of agitation (when available), culture depth, and structure type [63]. However, light is the most influential factor primarily because of the challenges associated with controlling it. It is hard to guarantee the stability of light over time and ensure its uniform distribution throughout the system. Biomass productivity in a PBR is therefore influenced by the ability of the design to provide sufficient photons of light for algal photosynthesis, highlighting the complexity and the non-universal nature of the microalgae cultivation bioprocess [21].

The choice of a specific technology will also depend on the application, the geographical area, the available resources, and the strain cultivated. Changing one of these parameters may favor different systems [66]. To date, two microalgae cultivation systems are categorized into open and closed systems, mainly distinguished by the natural or artificial light source.

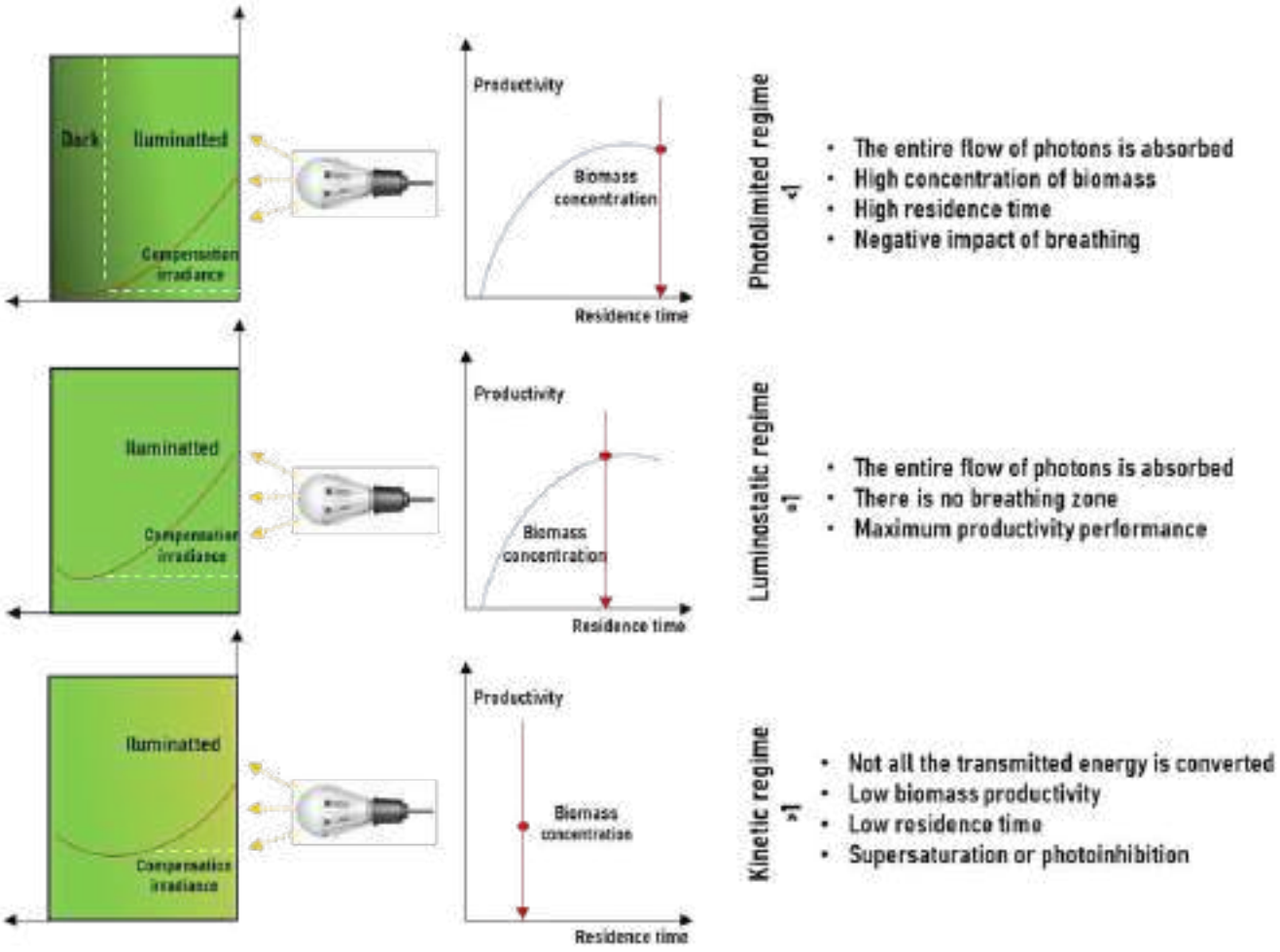


Fig. (12). Light attenuation regimes in microalgae photobioreactors. Adapted from Legrand *et al.* [21]. (*A higher resolution / colour version of this figure is available in the electronic copy of the article*).

4.1. Open Industrial Systems

Microalgae are usually grown in open pond systems based on sunlight due to low operating costs [67]. The main benefits of an open system are ease of operation and lower construction costs. Among the different projects are shallow ponds, inclined (cascade) systems, circular central-pivot ponds, mixed ponds, and raceway ponds. However, raceway ponds are the most used and economical for large-scale cultivation [45, 68].

Despite the development of the number of projects, only very few can effectively use solar energy for microalgae cultivation. Today's principal challenges are providing solar energy utilization and maximizing radiation and light exposure to all cells [69]. Structurally, open pond systems are based on constructions with a paddle wheel to allow greater flow and circulation in which microalgae can be brought closer to the surface for better CO_2 absorption and sunlight penetration [70].

The biggest problem in this type of system is the development of excessive irradiance on its surface, which can contribute to high photoinhibition in cultivation and consequently damage photosynthesis [8]. Another major disadvantage of open systems is the great need for land space for cultivation. Limitations due to evaporative losses, contamination, high temperature, high CO_2 desorption, low mass transfer efficiency, and inefficient mixing are also common. Thus, mass cultivation in open ponds results in a less photosynthetic effect and low microalgae performance [71].

4.2. Closed Industrial Systems

In order to overcome the problems related to open systems, the development of closed systems brought greater stability of control and operation [72]. A PBR is a closed container for phototrophic production, where energy is supplied through electric lights [69]. Furthermore, a typical PBR comprises growth nutrients and gaseous components (CO_2 and O_2).

PBR design must use light efficiently. Thus, it is necessary to understand the multiple interactions between biomass production and its operational parameters, which correspond, among others, to the transfer of light within the reactor [73]. In this sense, Table **2** presents the main lighting characteristics among the most conventionally known closed industrial systems.

Table 2. Lighting characteristics among the main industrial photobioreactors.

Cultivation Systems	Advantages	Limitations
Stirred tank	Very effective stirring mechanism. Therefore, the mass transfer and light scattering rates are very high, which leads to a lower incidence of dark zones inside the reactor and higher biomass productivity.	Low surface area/volume ratio, which in turn decreases light-gathering efficiency.
Bubble column	Light sources are distributed around the cylindrical bioreactor to obtain homogeneous illumination.	The intensity of incident light decreases from the surface to the middle of the cylindrical bubble column filled with the microalgae suspension, which can lead to microalgae growth with limited light in the center and photoinhibition effects near the surface.
Airlift	A circular mixing pattern in which the liquid culture continuously passes through the dark and light phases gives a flashing light effect to the microalgae cells.	Limited scale-up and high cost.
Horizontal tubular	Due to the geometric configuration of the receiving light, the incident light is diluted along the circumference. In the radial direction, it is focused on the tube axis, resulting in the mutual prevention of shading and increased radiation intensity.	Possibility of photoinhibition and capital and operating costs.
Flat panel	Large surface for light radiation and therefore the light use efficiency is high and dark zones can be avoided.	Short light penetration depth and not scalable.
Hybrid	They provide a high working volume while maintaining good lighting.	High capital expenditure and needs large infrastructure.

Based on the illuminated surface, tubular PBRs are the most common design industrially developed for these designs. Due to the high production cost usually achieved with this culture system, the leading R&D in closed PBR projects aims to achieve high light conversion efficiency, that is, to increase productivity far beyond what is currently achieved today, and this appears to be the best way to develop low-cost PBRs [74].

In summary, classic PBR configurations still have many limitations to overcome. Unfortunately, the associated costs can compromise the accessibility of the entire biotechnological process [67]. So far, a single system that meets all demands has not yet been found, making it necessary to rethink microalgae cultivation systems that reach the best commercial alternatives [55]. Faced with all these problems, Box 1 presents a discussion focused on the light and scaling of photobioreactors for a better choice of industrial production. Here, hydrodynamic characteristics, choice of materials, height/diameter, and surface/volume criteria are the main parameters related to light dependence in microalgae cultivation systems.

4.3. Box 1: Unlocking the Black Box of Photobioreactors: Light Dependency Approaches

Designing photobioreactor configurations is a titanic task [75]. Photobioreactors present tradeoffs that are difficult to balance due to the multitime and multi-scale coupling among physical, chemical, and biological phenomena. Furthermore, as they are strictly dependent on light, in order to achieve exceptional photosynthetic efficiencies, it is important to consider several simultaneous hydrodynamic factors, such as efficient mixing systems in reduced times, beyond correlating with the linearity of lighting, a high work volume and strict process control [15].

This way, the knowledge × know-how attributed to the hydrodynamic design of photobioreactors is one of the key factors in the correlation with the lighting efficiency of these types of equipment. Indeed, the intensity of light experienced by each microalgae cell during culture substantially influences metabolism and cell growth (as seen in detail in section 3). Still, light is attenuated along its path through the photobioreactor due to shielding, absorption, and scattering between cells. These factors result in light gradients within the photobioreactor itself [76]. Therefore, when considering the flow regime of a configuration, it is often assumed that turbulent flow regimes are ideal since there is a greater homogeneity of the culture and, consequently, a reduction in light gradients. However, high hydrodynamic forces can limit the cyclical movements of the liquid between the bottom (dark zone) and the surface (light zone) [77], which the need for exposure to light. According to Ugwu *et al*. [78], the Reynolds number is the main parameter to consider; more precisely, the transient flow regime is ideal in photobioreactor projections. This is because this regime ensures certain turbulence so that all cells are frequently exposed to light without shearing stress. Among the classic configurations of photobioreactors that fall into this regime are hybrid models (Re: 2500) [67] and thin-layer photobioreactors (Re: 2347) [79]. In contrast, bubble column and tubular photobioreactors have flow regimes characteristic of turbulent systems (Re: > 6368 and 25,000, respectively) [80], which, depending on cellular sensitivity, allows strong shear stress, resulting in cellular rupture. Meanwhile, for flat plate photobioreactors (Re: 1761), the flow regime is characterized by a laminar regime [81], which on the one hand, is satisfactory since the cells have a higher rate of exposure to light; however, the appearance of biofilms e/or photosaturation turns out to be a bottleneck still to be overcome [82].

On the other hand, the flow regime alone does not ensure the success of optimal light distribution in the photobioreactor industrial facilities. This is because these types of equipment must be able to reproduce the optimal conditions of cultivation in high volumes of work. Establishing a surface-to-volume relationship and choosing good materials must be prioritised as a basic requirement in expanding photobioreactors. To begin with, the choice of material must be highly transparent, allowing for no reduction in light transmittance after outdoor exposure. In addition, properties such as flexibility, durability, non-toxicity, resistance to chemicals and metabolites produced by microorganisms, as well as resistance to climatic conditions and low cost, should be interconnected in decision-making [83]. Under this bias, the main materials used are glass and some variations of polymers, such as polymethyl methacrylate (PMMA) and polycarbonate (PC). However, poly-

carbonate stands out from the other potentialities since it presents itself as a material with high light transmittance (~89%) and resistance and does not require cleaning efforts, offering intermediate-cost services. In contrast, glass is preferred for applications that require high quality (>90% light transmittance). However, its handling and cost expansion makes its use difficult [84].

Additionally, the scale-up of these types of equipment is the starting point to advance in the industrial consolidation of an ideal model of photobioreactors. For this, it is essential that the surface/volume (S/V) and height/diameter (H/D) ratio remains adequate. However, when the transition from benchtop photobioreactors to pilot and industrial scale occurs, the pre-established conventional performance does not follow the evolution, and, therefore, operational problems arise in the search for lighting and space. According to the literature, an adequate height/diameter ratio for the light path to reach the reactor core, without the interferences of cell density, is established at ~1.0-1.5 [85]. However, these industrial-scale configurations - today - generally present values in the order of 10. This reduces work volumes, increasing land demand, material costs, and operating energy. Otherwise, hybrid models can provide a high volume of work while maintaining an adequate height/diameter ratio (H/D = 1.5) since the largest reactor compartment is not light-dependent. For example, the lighting platform for hybrid photobioreactors requires only 0.22 m^2/m^3 [67, 86] when compared to tubular (14.28 m^2/m^3) and flat plate (14.42 m^2/m^3) photobioreactors. However, the disadvantages inherent to hybrid systems persist, given the possibility of contamination for more sensitive strains.

5. ADVANCES IN PHOTOBIOREACTORS DESIGN AND FRONTIERS OF THE LIGHTING

Mass production of microalgae requires suitable cultivation systems. Even today, many problems encountered in this type of system are related to design and implementation requirements [87]. In this case, problems involving efficient light distribution affect many of these projects, particularly the conventional PBRs. To resolve these adversities, carefully adapting settings using efficient lighting devices will offer a new opportunity to optimize microalgae-based processes [8, 10].

Notably, many light arrangement approaches have only focused on laboratory-scale designs. However, knowledge and understanding of light fluxes in photobioreactors seem instructive to advance in developing new designs more suitable for efficient and large-scale production in microalgae culture systems [6, 71].

5.1. Light Transfer Modeling

Radiation is widely accepted as the main limiting factor governing cell growth within a PBR, and light penetrating a culture medium can be absorbed or scattered [88]. As radiation depends on the spatial position and angular direction, many light transfer processes have been put to the test over the last few years to estimate the distribution of radiation within PBRs [89].

The average irradiance (I_{av}) allows calculating the average availability of light inside the cultures, from which a rate of photosynthesis occurs for the entire culture volume. The photosynthesis rate determines the growth rate, which in parallel defines how the average irradiance correlates within the culture, where the response curve is obtained in a hyperbolic fashion [90]. In this curve, the saturation irradiance (I_s) is the irradiance above which the growth is saturated, the constant irradiance (I_c) is the irradiance at which the growth is equal to half the maximum specific growth rate, and (I_i) above the inhibition irradiance, the photosynthesis rate decreases (Fig. **13**). Therefore, the response curve must be calculated from point to point, as the photosynthesis rate may vary according to light availability inside the photobioreactor [63]. The dependence of microalgae growth rate (μ) on mean irradiance has been presented in several models, although models that present the rate raised to a power greater than one can better fit the experimental observations in the literature, as observed in Eqs. (1 and 2).

$$\mu = \frac{\mu_{max} I_{av}^{n}}{I_c^{n} + I_{av}^{n}} \quad (1)$$

$$\mu = \frac{\mu_{max} I_{av}^{\left(b+\frac{c}{I_0}\right)}}{I_c\left(1+\left(\frac{I_0}{I_i}\right)^{a}\right)^{\left(b+\frac{c}{I_0}\right)} + I_{av}^{\left(b+\frac{c}{I_0}\right)}} \quad (2)$$

Researchers generally ignore studies on light scattering, so the simplified Beer-Lambert law is the one that has been most widely applied, as it provides a more accurate description of the effects

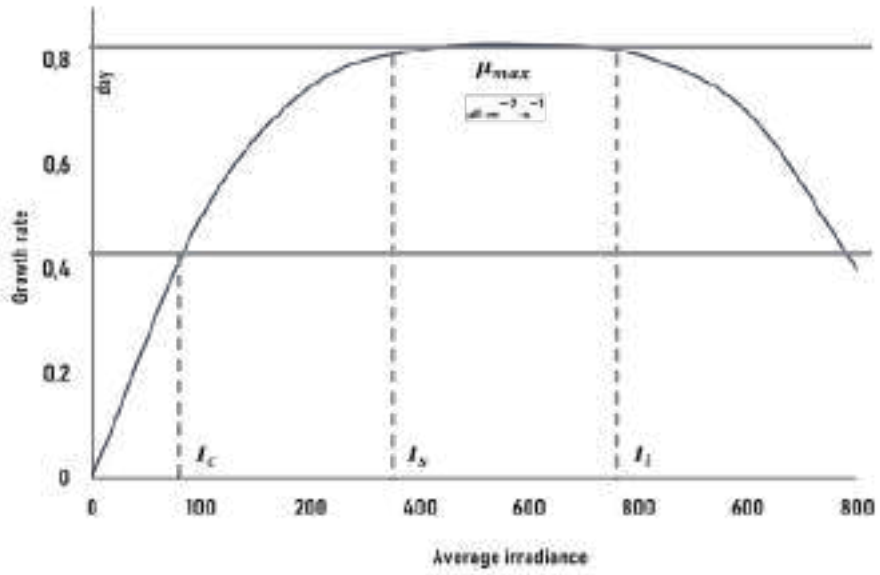


Fig. (13). Correlation of the growth rate with the average light irradiance. Adapted from Grima *et al.* [90]. (*A higher resolution / colour version of this figure is available in the electronic copy of the article*).

arising from the interaction between light and matter [89]. Classical mathematical modeling is complicated because the light is attenuated by absorption and scattering as it penetrates a culture containing medium and biomass. Thus, as the concentration of biomass increases in a growing culture, the attenuation of light becomes more and more pronounced with time [91]. In this case, the absorption of light by microalgae biomass according to the Beer-Lambert (Eq. 3) law results in an exponential decrease in light intensity as a function of light penetration distance, where the average in situ irradiance of the culture (E_{av}) is calculated as a function of the irradiance at the surface (E_{o}), the extinction coefficient of the biomass (K_{a}), the concentration of the biomass (C_{b}), and the incident light path in the reactor (p) [92, 93].

$$E_{\mathrm{av}} = \frac{E_{\mathrm{o}}}{K_{\mathrm{a}} \cdot p \cdot C_{\mathrm{b}}} \left(1 - \exp\left(-K_{\mathrm{a}} \cdot p \cdot C_{\mathrm{b}}\right)\right) \quad (3)$$

In addition, a light transport attenuation model using a two-flow (forward and backscattering) to model the transfer through a one-dimensional light was proposed by Cornet *et al.* [94-96], such as presented in Eq. (4), where: a_a is absorption, σ_s is scattering coefficients, a_1 is $(\sqrt{a_a/(a_a + \sigma_s)})$, and a_2 is $(a_1(a_a + \sigma_s)C_b L)$. This model emerged after the identification of general radiation problems related to the Beer-Lambert law, mainly involving: (i) limitation of light scattering; (ii); displacement of light in a single direction; (iii) limited wavelength; and (iv) semi-transparent homogeneous médium [97].

$$a = \frac{1}{L} \ln \frac{4a_1}{(1+a_1)^2 e^{a_2} - (1-a_1)^2 e^{-a_2}} \quad (4)$$

In recent decades, many simulation methods have been proposed to obtain a rigorous solution for radiative light transfer, including the Monte Carlo, ordinate, and finite volume methods [88]. Of these, the latter has become popular due to features such as the conservation of radiant energy and its easy incorporation into computational fluid dynamics (CFD) simulations [98]. The general radiation transport equation, which better explains light absorption, emission, and scattering, is given by the position ($\rightarrow_r$) and the direction ($\rightarrow_s$) in Eq. (5). Here, the wavelength-dependent absorption coefficient ($a_{a,\lambda}$), scattering coefficients ($\sigma_{s,\lambda}$), and phase function (θ_λ) can be calculated by Mie's method or light spectroscopy when the characteristics are known (*e.g.*, form, size, and cell concentration) or using the Rayleigh approximation.

$$\frac{dI_\lambda(\rightarrow_r, \rightarrow_s)}{ds} + \left(a_{a,\lambda} + \sigma_{s,\lambda}\right) I_\lambda(\rightarrow_r, \rightarrow_s) = \frac{a_{a,\lambda} n^2 \sigma T^4}{\pi} + \frac{\sigma_{s,\lambda}}{4\pi} \int_0^{4\pi} \emptyset_\lambda\left(\rightarrow_s, \rightarrow_s'\right) I_\lambda(\rightarrow_r, \rightarrow_s) d\Omega' \quad (5)$$

In fact, CFD has proven to be an effective tool for understanding the dynamic behaviors of complex fluids, which can help design and scale up the most varied types of photobioreactors [99]. A complete understanding of the underlying process-

es of photobioreactors through specified software is more challenging due to the multi-time and multi-scale coupling between physical, chemical, and biological phenomena [98]. Furthermore, these processes are interconnected by several subprocesses, such as fluid dynamics, light distribution, and, consequently, algae growth rate inside a photobioreactor [13].

Among the different processes studied is how the flashlight is highly efficient in CFDs. According to Ye *et al.* [100], air-lift loop photobioreactors with serial lantern-shaped suction tubes improved vortex flow and increased radial velocity and turbulent kinetic energy in the column; thus increasing biomass yield and CO_2 fixation rate (Fig. **14a**). The CFD modeling investigated in flat plane photobioreactors with inclined and horizontal baffles for light attenuation also showed better flux performance and light regime than in a conventional PBR. It was found that a reduced sloping angle and a reduced baffle opening rate increase the frequency of light cycles, generating greater radial velocity along the light direction (Fig. **14b**) [101].

New designs of CFD lighting devices for photobioreactors are being developed in varied geometries in the form of distribution in order to optimize light absorption. These new designs are based on a helical spiral and can be considered artificial photosynthetic trees, as they are based on the nature-inspired tree-style structure (Fig. **14c**) [98].

Numerical calculations and experimental studies were formed to understand these light fluxes better. The results showed that the fractural structure showed good flow performance, leading to better turbulence and light transfer. These new designs allow up to a 1.4-fold increase in intercepted light radiation compared to that received by light devices already in use [102]. In this case, the authors point out that the PBR-based fractal could be the process intensification so much sought after in recent years for phototrophic cultivation technology.

5.2. Patent-based Analysis to Map Technological Trends in Photobioreactors Illuminated Artificially

Based on the dilution and irradiance transfer within the culture volume, many PBR projects have been improved based on approaching the maximum thermodynamic limit of conversion of light energy into biomass [103]. Generally, these new designs aim to reduce the luminous flux sent to the culture to the same total amount of energy supplied to the system.

Although most literature articles provide valuable information about the results of a scientific process, patent documents, on the other hand, provide data with greater precision, especially when related to processes, devices, and applications [104]. To understand the bigger picture of PBRs with artificial lighting, a patent analysis was performed using the "google patents" database. It consists of a worldwide platform containing a database published by more than 100 patent authorities, providing a snapshot of the level of patenting activities over a given period. Through the search results, the tool uses several algorithms to cluster international documents into families based on the FamPat Collection and links between provisional and published applications. Moreover, this database allows access to publications (WO, US, EP, AT, BE, BR, CA, CH, CN, DE, ES, FR, GB, JP, RU, DK, FI, SE, IN, TW, TH, and KR), which assign codes and definitions based on International Patent Classification (IPC), CPC, EPO, US Patent and Trademark Office (USPTO), World Intellectual Property Organization (WIPO), and Japanese classifications. It also includes results from various sources of scientific literature.

The data scope was carried out through an advanced search of the last 3 years using keywords and their variants defined as (i) photobioreactor or bioreactor; (ii) algae or microalgae; (iii) photo or photosynthetic; (iv) design or projects; (v) light or lighting; and (vi) artificial. From this strategy, more than 400 documents were found. Subsequently, a new screening was carried out carefully in order to analyze each one in detail; of these, 45 patents were classified as the ones that most met the research requirements, as shown in Online Resource 1.

Major inventions include irradiated PBRs using optical fibers, fluorescent tubes, and LED lamps in different frame designs. Most lighting projects are based on outdoor lighting [13]. However, many projects currently focus on internal radiation and modular layout photobioreactors based on the principle of internal lighting by flat panels. These panels delimit harvest volumes whose repetition allows, in design mode, to extrapolate in volume,

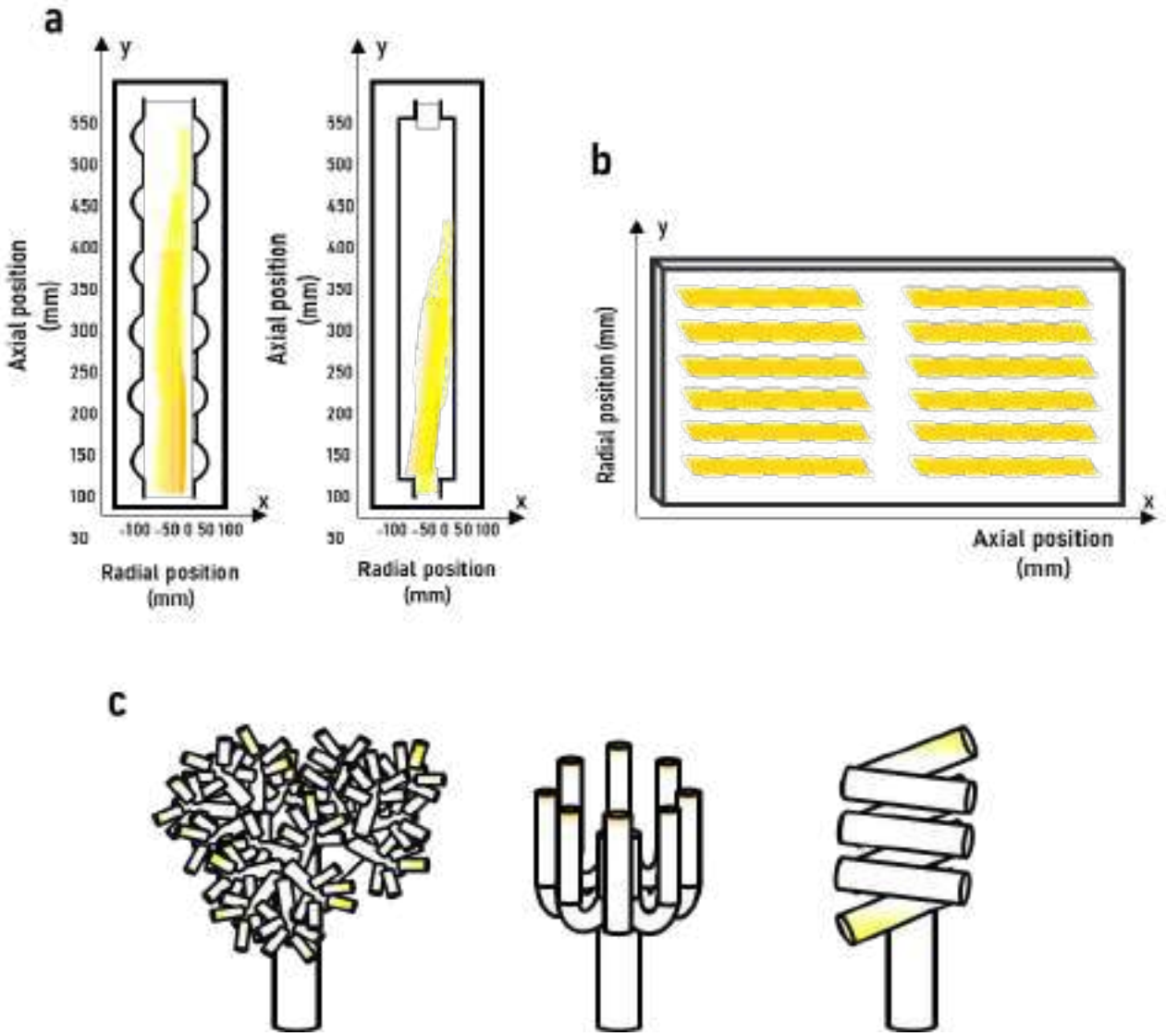


Fig. (14). CFD simulation in PBR with enhanced radiation. (**a**) Serial lantern-shaped draft tube; (**b**) Flat plane photobioreactors with inclined and horizontal baffles; (**c**) New designs of lighting devices. Adapted from Ranganathan *et al.* [98]. (*A higher resolution / colour version of this figure is available in the electronic copy of the article*).

simply increasing the number of panels. All these projects aim to beneficiation light transfer and improve microalgae's photosynthetic efficiency [21].

Optical fibers have gained prominence for their potential for efficient light redistribution, minimizing costs with lighting sources [21]. This type of design has been presented in many recent patents for different models of photobioreactors. Other inventions also comprise the adjustment and control of light intensity and photoperiods. For example, in document CN2021/113355211, when the light modulator receives the type of microalgae and the volume of the culture plate, it adjusts the luminous intensity of the set of fixed lamps respectively together with the luminous intensity of the set of supplementary lamps until the preset intensity light be obtained. The described process is similar to that presented in CN2021/113512489, in which a microalgae biofilm bioreactor consists of a photoperiod frequency controller. The LED lamp panels are arranged on two sides of the adsorption culture membrane assembly in parallel, and the flash frequency and lighting intensity are adjusted for the optimal process.

Collecting data and information on projects and configurations of all existing photobioreactors is still difficult to obtain. The latest lighting designs have varied their structures depending on modula-

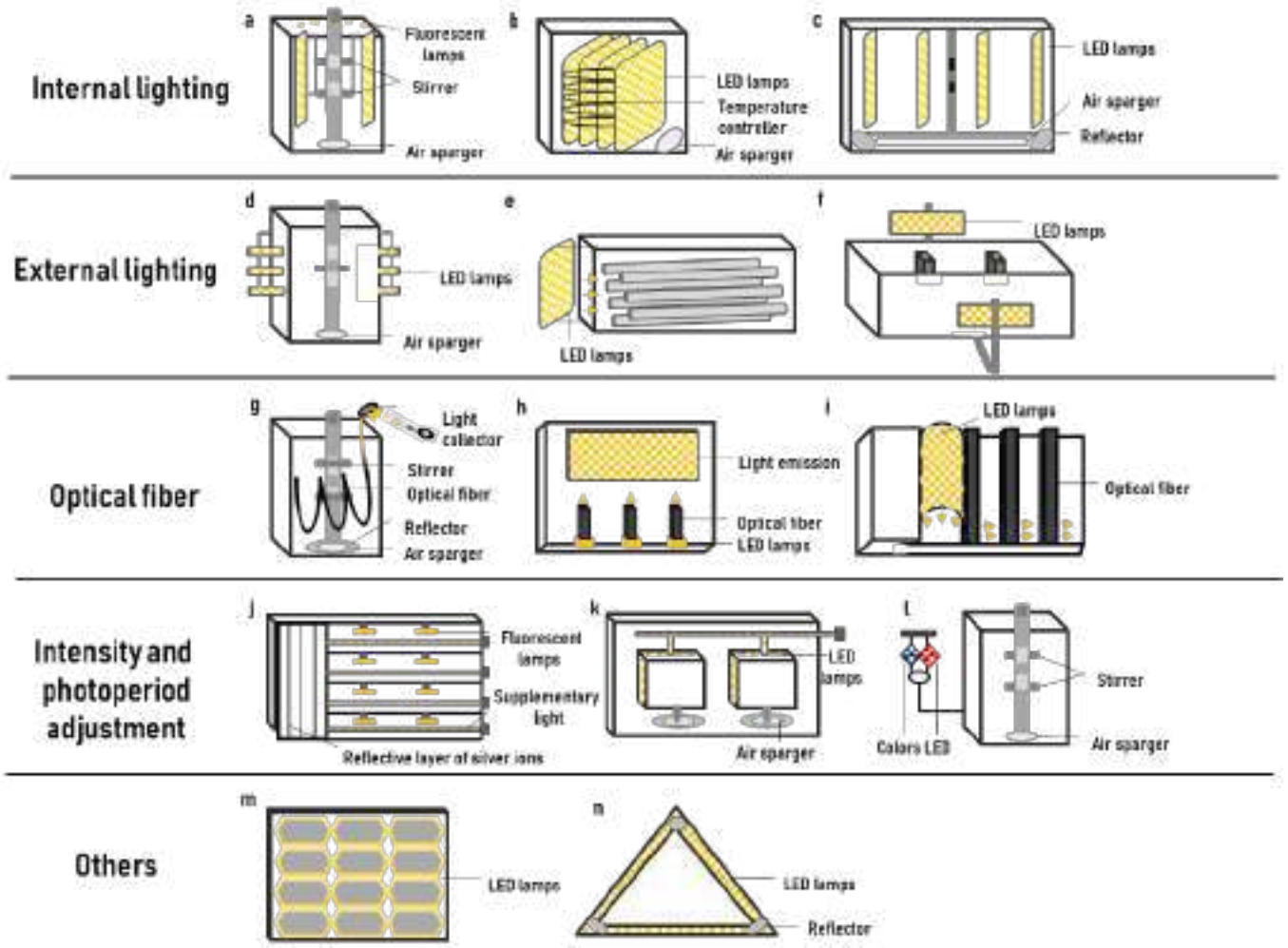


Fig. (15). PBR projects with indoor lighting based on recent patents. (**a**) US2009/7618813; (**b**) US2020/10808214; (**c**) WO2018/096107A1; (**d**) DE2022/10008769B4; (**e**) US2022/0213427; (**f**) CN2022/114921337ª; (**g**) 2010/102382754; (**h**) US2022/11402562; (**i**) US2022/82197; (**j**) CN2021/113355211; (**k**) CN2021/113512489; (**l**) CN2021/112680337; (**m**) EP2021/2734681; (**n**) WO2020/226481A2. (*A higher resolution / colour version of this figure is available in the electronic copy of the article*).

tions and devices combined with various strategies and alternatives for photobioreactors [46]. Other types of designs have specific characteristics. For instance, patents comprising various photobioreactor modules on building facades can be used for thermal regulation and insulation in industrial production. Advantageously, lighting means can be installed concentrically in the vessel to protect the internal lighting of the culture médium (EP2021/2734681). An illustrative image of the drawings of the majority of projects can be better visualized in Fig. (**15**).

6. SUSTAINABILITY METRICS AND COST EFFICIENCY ON ARTIFICIAL LIGHTING

Today, companies must adopt economic and sustainable practices instead of exploiting finite resources and protecting the planet and the remaining resources. Key stakeholders — investors, consumers, organizations, and governments — are moving in this direction. Moreover, if history is any indication, decision-makers will read the signals, anticipate market changes, and seek to adopt a paradigm shift to create long-term business value [105]. In this sense, knowledge of the environmental impacts associated with its production must be investigated (Box 2).

6.1. Box 2. Artificial Light: A Zero-sum Game for Sustainability?

The energy demand at the upstream and downstream stages is responsible for most, if not almost all, of the environmental impacts of commercial microalgae products [106]. The naturally energy-

intensive processes reveal an uncomfortable truth – PBRs with artificial lighting can push these processes into blind alleys, and this is because they will aggravate environmental sustainability metrics. By way of example, according to the literature, the production of 1 kg of whole dried biomass of the species *Chlorella vulgaris* in a tubular photobioreactor carries an impact of 1551.94 CTUe, 475.53 MJ, and 220.32 $kgCO_2eq$ in the midpoint categories of ecotoxicity, energy resource, and global warming, respectively. When considering the cultivation of *Chlorella vulgaris* in a tubular photobioreactor with artificial lighting, these values rise to approximately 1914.65 CTUe, 586.17 MJ, and 271.57 $kgCO_2eq$, representing an increase of roughly 23% in emissions in the ecotoxicity, energy resources, and global warming categories (Fig. **16a**). Furthermore, the energy demand required by closed and open systems is also quite explicit. By comparison, the production of 1 kg of whole dry biomass of *Chlorella vulgaris* grown in the raceway lagoon almost halved the level of global warming (141.30 $kgCO_2eq$) compared to tubular PBR with artificial lighting of current PAR efficiency of 2% (269.85 $kgCO_2eq$), although this impact value with artificial lighting in tubular PBR can decrease (by almost 10%) when PAR efficiency increases to 3%, in the not-too-distant future (Fig. **16b**).

Unfortunately, that is not all; the cost of investment and electricity associated with artificial lighting can double production costs, reinforcing that artificial light only compensates when applied to high-value products [107]. It is important to highlight that the focus of commercial applications of microalgae are these products that, over the years, have ensured the microalgae industry's survival as they can counterbalance the high operating costs of production. Additionally, it cannot be neglected that to circumvent the valley of death of microalgae biotechnology, most commercial microalgae production is still carried out today in an outdoor cultivation system [108, 109].

Evidently, in state of the art, it is possible to affirm that PBRs with artificial lighting are great in manufacturing products that add perceived value. However, we can say that they should be avoided frequently, as they did not contribute to amortizing the environmental and economic metrics. However, transitioning from high-emission fossil energy to low-emission renewable sources can provide a strong lever to reduce the environmental footprint of microalgae-based processes and products, con-

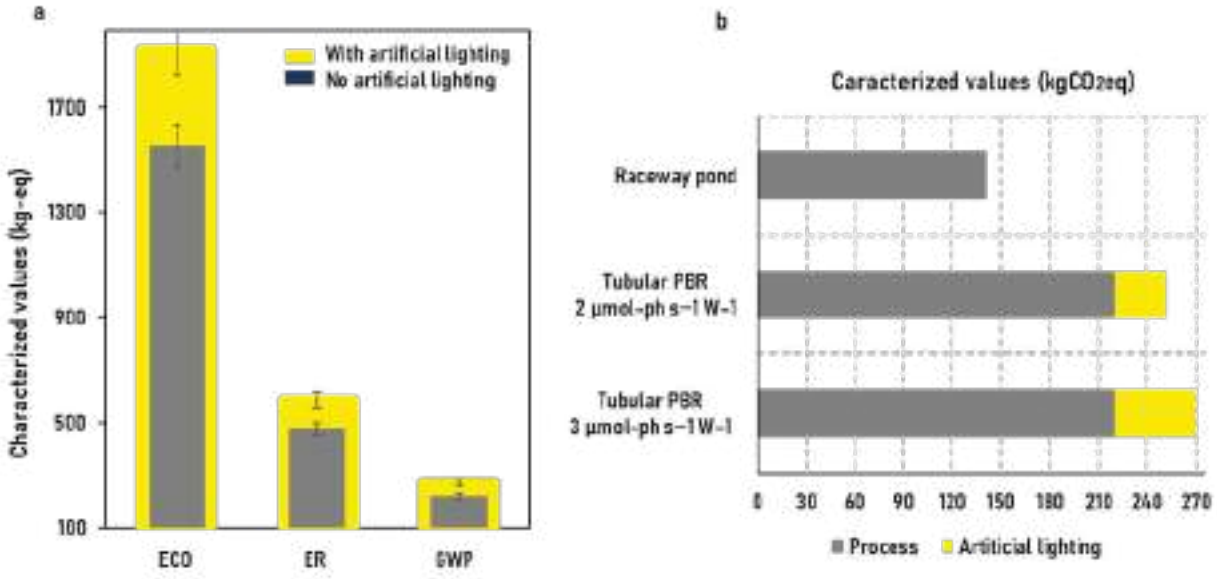


Fig. (16). Characterized values of environmental impact categories associated with producing 1 kg of whole dried biomass of the species *Chlorella vulgaris*. (**a**) in the tubular photobioreactor with artificial lighting and no artificial lighting; (**b**) differences between raceway ponds, tubular PBR with PAR efficiency of 2%, and tubular PBR with PAR efficiency of 3%. Adapted from Blanken *et al.* [107] and Deprá *et al.* [106]. **Abbreviations:** Global warming potential, GWP; Ecotoxicity, ECO; Energy resource, ER. (*A higher resolution / colour version of this figure is available in the electronic copy of the article*).

tributing to a future where we live well within planetary boundaries. Recently, Dias *et al.* [110] demonstrated that there could be a reduction in environmental impacts between 20 to 100% and 9 to 87% when fossil energy is replaced by onshore wind and solar photovoltaics in the midpoint categories of ozone depletion, global warming, photochemical ozone creation, acidification, eutrophication, ecotoxicity, fossil fuel depletion, and water footprint, respectively. Furthermore, according to the authors, implementing a renewable energy system would generate great economic gains, improving cost efficiency.

Finally, despite the impact of artificial lighting on biomass productivity, it is unwise to reach an optimistic conclusion by ignoring the increased production costs and emissions of microalgae cultivation with artificial light (Box 3). However, it is clear that in the future, with the increase in PAR efficiency of the light source and the development of technology, it may be possible to concentrate on using artificial light as the only energy source.

6.2. Box 3. Artificial Light: Cost Center or Value Generator?

The microalgae industry is known for its high electricity consumption in upstream and downstream processing (Fig. **17**) [111]. This electricity consumption differs between different types of cultures (Fig. **17a**). Careful examination of unit operations allows for a holistic understanding of the impact of costs related to electricity expended for optimal production and productivity. Notably, artificial lighting in photobioreactors has advanced dramatically in recent years due to the system's easy control and regular distribution of light [1]. In less than ten years, the electrical efficiency of LEDs has improved by more than 60% lumens per watts (lm/W), depending on product quality. Today, most commercial LEDs feature photosynthetically active radiation (PAR) measurements of 2 μmol-ph s^{-1} W^{-1}, which corresponds to approximately 160 (lm/W) [112]. Along with these benefits, the costs of LEDs have decreased to the point where they are competitive with conventional lighting products already in use. Despite these technological developments, there is still significant potential for efficiency, cost, and functionality advancement. Consequently, adoption rates have increased, which has resulted in considerable energy savings nationally and globally; as LED technologies continue to become efficient and more widely adopted, it is predicted that these energy savings will increase further. Estimates indicate that the PAR of LED lighting, when increased to 3 μmol-ph s^{-1} W^{-1}, will decrease costs by almost 7% when comparing the current world average electricity price of 0.135 $ kWh^{-1} [113] (Figs. **17b** and **17c**). It is worth mentioning that the average price of electricity can vary from place to place and can thus be optimized according to the choice of installation plant. For example, a plant installed in the United States would today have an electricity cost reduced by half compared to installation projects in European Union countries such as Spain, Germany, Denmark, and the Netherlands [110]. This huge difference in energy cost causes drastic variations in the economic analysis, particularly in annual net revenue and payback period. It is worth mentioning that the average productivity in tubular PBRs of more than 70% compared to raceway ponds would also compensate, in some way, for their high electricity consumption. However, considering current estimates of investment and operating costs (3-15$ kg-DW^{-1}), the exploitation of artificial light would still only be viable if optimized for the generation of high-value products (β-carotene, phycocyanin, astaxanthin, DHA, and EPA) to increase the profit margin of the photosynthetic process [114].

CONCLUSION

The supply and capture of light for efficient conversion into valuable bioproducts is an emerging challenge in the biotechnological production of microalgae. Natural light, despite being self-generated, accessible, and abundant on Earth, has control and performance inefficiencies, which makes artificial lights, on the contrary, excel in these aspects. The ideal settings of an artificial light regime need to correspond to a frequency high enough to obtain efficiencies superior to those obtained under natural light, in the shortest possible duty cycle, with a greater penetration depth of photons in the cell and above all, within the range of adequate energy consumption. LEDs, in this case, have an emission spectrum corresponding to the photosynthetic action of microalgae; it is convenient, flexible, and economical, which makes the control of the system easily manageable.

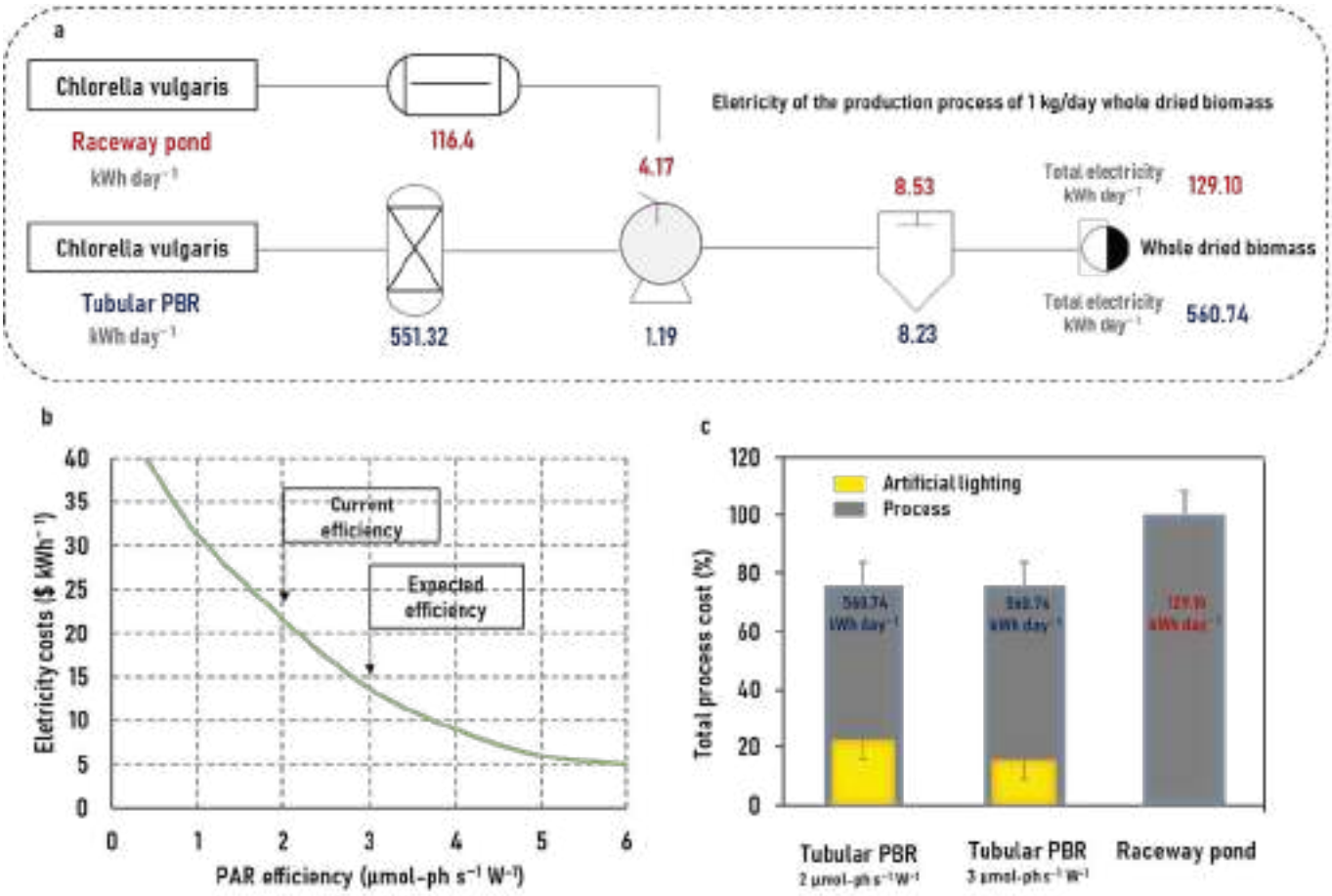


Fig. (17). Electricity consumption and costs between different types of microalgae cultures. (**a**) total electricity for raceway pond and tubular PBR system; (**b**) the cost of electricity measured on PAR efficiency; (**c**) the total process costs between raceway ponds, tubular PBR with PAR efficiency of 2%, and tubular PBR with PAR efficiency of 3%. Adapted from Blanken *et al.* [107] and Dias *et al.* [110]. (*A higher resolution / colour version of this figure is available in the electronic copy of the article*).

Manipulations in intensity and periodic modulations allow for increasing the productivity of microalgae as it considerably improves light capture. A characteristic of applying discontinuous light is the capacity to prevent light overexposure while at the same time regenerating energy vector stocks between one photoperiod and another. Furthermore, it is known that using different colors of LED lamps to reach maximum spectral absorption (*e.g.*, red and blue areas of the light spectrum) allows for more excellent photosynthetic performance of the system. So far, a single system that meets all necessary demands has not yet been found. Therefore, it is crucial to consider several factors simultaneously, such as successful lighting transfer in high workloads. Furthermore, highly transparent, flexible, durable, and low-cost materials are ideal for microalgae photobioreactor projections.

CURRENT AND FUTURE DEVELOPMENTS

Finally, it is worth noting that many gaps still need to be filled in approaches to studying the impact of artificial light, especially when we relate it to economic-environmental sustainability metrics. In this case, inflection points and action strategies are still poorly understood. Above all, we must remember that despite the high investment and electricity costs associated with artificial lighting, this still seems to be the best way to obtain high-added value compounds due to its high yield and more reliable cultivation techniques. In general, advances in research and development of new technologies in PBRs and lighting designs will undoubtedly allow

optimizing the performance of microalgae processes in a future industrial application scenario.

AUTHOR'S CONTRIBUTIONS

Rafaela Basso Sartori: conceptualization, data curation, writing — original draft. Mariany Costa Deprá: data curation, writing. Rosangela Rodrigues Dias: data curation, writing. Mariane Bittencourt Fagundes: data curation, writing. Leila Queiroz Zepka: supervision. Eduardo Jacob-Lopes: conceptualization, funding acquisition, project administration, writing — review and editing. All authors agreed to the submission of the manuscript.

LIST OF ABBREVIATIONS

ATP	=	Adenosine Triphosphate
CFD	=	Computational Fluid Dynamics
ECO	=	Ecotoxicity
GWP	=	Global Warming Potential
LHC	=	Light-harvesting Complex
NAD	=	Nicotinamide Adenine Dinucleotide Phosphate
NADPH	=	Nicotinamide Adenine Dinucleotide Phosphate Reduced
PAR	=	Photosynthetically Active Radiation
PC	=	Polycarbonate
PMMA	=	Polymethyl Methacrylate

CONSENT FOR PUBLICATION

Not applicable.

FUNDING

This study was supported by the National Council for Scientific and Technological Development (CNPq) - Brazil, and the Coordination of Improvement of Higher Education Personnel (CAPES), Funding No. 001.

CONFLICT OF INTEREST

The authors declare no conflict of interest, financial or otherwise.

ACKNOWLEDGEMENTS

The authors would like to thank the National Council for Scientific and Technological Development (CNPq) – Brazil, and the Coordination of Improvement of Higher Education Personnel (CAPES).

SUPPLEMENTARY MATERIAL

Patents for microalgae photobioreactors based on light devices from the last 3 years. (Online Resource).

REFERENCES

[1] Maltsev Y, Maltseva K, Kulikovskiy M, Maltseva S. Influence of light conditions on microalgae growth and content of lipids, carotenoids, and fatty acid composition. Biology 2021; 10(10): 1060. http://dx.doi.org/10.3390/biology10101060 PMID: 34681157

[2] Baslam M, Mitsui T, Hodges M, *et al.* Photosynthesis in a changing global climate: Scaling up and scaling down in crops. Front Plant Sci 2020; 11: 882. http://dx.doi.org/10.3389/fpls.2020.00882 PMID: 32733499

[3] Diaz-MacAdoo D, Mata MT, Riquelme C. Influence of irradiance and wavelength on the antioxidant activity and carotenoids accumulation in *Muriellopsis* sp. isolated from the antofagasta coastal desert. Molecules 2022; 27(8): 2412. http://dx.doi.org/10.3390/molecules27082412 PMID: 35458610

[4] Gjindali A, Herrmann HA, Schwartz JM, Johnson GN, Calzadilla PI. A holistic approach to study photosynthetic acclimation responses of plants to fluctuating light. Front Plant Sci 2021; 12: 668512. http://dx.doi.org/10.3389/fpls.2021.668512 PMID: 33936157

[5] Benedetti M, Vecchi V, Barera S, Dall'Osto L. Biomass from microalgae: The potential of domestication towards sustainable biofactories. Microb Cell Fact 2018; 17(1): 173. http://dx.doi.org/10.1186/s12934-018-1019-3 PMID: 30414618

[6] Kumar V, Sharma N, Jaiswal KK, *et al.* Microalgae with a truncated light-harvesting antenna to maximize photosynthetic efficiency and biomass productivity: Recent advances and current challenges. Process Biochem 2021; 104: 83-91. http://dx.doi.org/10.1016/j.procbio.2021.03.006

[7] Song Q, Van Rie J, Den Boer B, *et al.* Diurnal and seasonal variations of photosynthetic energy conversion efficiency of field grown wheat. Front Plant Sci 2022; 13: 817654. http://dx.doi.org/10.3389/fpls.2022.817654 PMID: 35283909

[8] Benner P, Meier L, Pfeffer A, Krüger K, Oropeza Vargas JE, Weuster-Botz D. Lab-scale photobioreactor systems: Principles, applications, and scalability. Bioproc Biosyst Eng 2022; 45(5): 791-813.

http://dx.doi.org/10.1007/s00449-022-02711-1 PMID: 35303143

[9] Dias RR, Lasta P, Vendruscolo RG, Wagner R, Zepka LQ, Jacob-Lopes E. Mapping the performance of photobioreactors for microalgae cultivation. Part II: Equatorial and tropical climate zone. J Chem Technol Biotechnol 2021; 96(3): 613-21. http://dx.doi.org/10.1002/jctb.6574

[10] Nwoba EG, Parlevliet DA, Laird DW, Alameh K, Moheimani NR. Light management technologies for increasing algal photobioreactor efficiency. Algal Res 2019; 39: 101433. http://dx.doi.org/10.1016/j.algal.2019.101433

[11] Maroneze MM, Siqueira SF, Vendruscolo RG, *et al*. The role of photoperiods on photobioreactors – A potential strategy to reduce costs. Bioresour Technol 2016; 219: 493-9. http://dx.doi.org/10.1016/j.biortech.2016.08.003 PMID: 27521786

[12] Maroneze MM, Deprá MC, Zepka LQ, Jacob-Lopes E. Artificial lighting strategies in photobioreactors for bioenergy production by Scenedesmus obliquus CPCC05. SN Applied Sci 2019; 1(12): 1695. http://dx.doi.org/10.1007/s42452-019-1761-0

[13] Singh V, Mishra V. A review on the current application of light-emitting diodes for microalgae cultivation and its fiscal analysis. Crit Rev Biotechnol 2022; 42: 1-15. http://dx.doi.org/10.1080/07388551.2022.2057274 PMID: 35658771

[14] Yadav G, Dubey BK, Sen R. A comparative life cycle assessment of microalgae production by CO_2 sequestration from flue gas in outdoor raceway ponds under batch and semi-continuous regime. J Clean Prod 2020; 258: 120703. http://dx.doi.org/10.1016/j.jclepro.2020.120703

[15] Deprá MC, Severo IA, Dias RR, Zepka LQ, Jacob-Lopes E. Photobioreactor design for microalgae culture. In: *Microalgae*. Massa Chusetts, US, Academic Press 2021; pp. 35-61. http://dx.doi.org/10.1016/B978-0-12-821218-9.00002-5

[16] Perrino JE, Ruez JDJ. Eastern Oyster (*Crassostrea virginica*) Filtration Efficiency of Chlorophyll-a under Dynamic Conditions in the Hudson-Raritan Estuary at Pier 40, New York City. In: *Photosynthesis in Algae*. Larkum AWD, Douglas SE, Raven JA (eds.). Kluwer Academic Publishers: Amsterdam, 2003. https://doi.org/10.1007/978-94-007-1038-2.

[17] Ali MF, Jayakody DNK, Li Y. Recent trends in underwater visible light communication (UVLC) systems. IEEE Access 2022; 10: 22169-225. http://dx.doi.org/10.1109/ACCESS.2022.3150093

[18] Rexroth S, Nowaczyk MN. Cyanobacterial Photosynthesis: The Light Reactions. Modern Topics in the Phototrophic Prokaryotes. Springer: Germany, 2007; pp. 163-91.

[19] Battchikova N, Aro EM. Proteomics in revealing the composition, acclimation and biogenesis of thylakoid membranes. In: *The Cell Biology of Cyanobacteria*. Flores E, Herrero A (eds.), pp. 89-120. Caister Academic press Massa Chusetls Us, 2014. ISBN: 978-1-908230-38-6.

[20] Raven J. Photosynthesis in watercolours. Nature 2007; 448(7152): 418. http://dx.doi.org/10.1038/448418a PMID: 17653178

[21] Legrand J, Artu A, Pruvost J. A review on photobioreactor design and modelling for microalgae production. React Chem Eng 2021; 6(7): 1134-51. http://dx.doi.org/10.1039/D0RE00450B

[22] Bassham JA, Benson AA, Calvin M. The path of carbon in photosynthesis. J Biol Chem 1950; 185(2): 781-7. http://dx.doi.org/10.1016/S0021-9258(18)56368-7 PMID: 14774424

[23] Kok B, Forbush B, McGloin Marion. Cooperation of charges in photosynthetic O_2 evolution-I. A linear four step mechanism. Photochem Photobiol 1970; 11(6): 457-75. http://dx.doi.org/10.1111/j.1751-1097.1970.tb06017.x PMID: 5456273

[24] Ono T, Noguchi T, Inoue Y, Kusunoki M, Matsushita T, Oyanagi H. X-ray detection of the period-four cycling of the manganese cluster in photosynthetic water oxidizing enzyme. Science 1992; 258(5086): 1335-7. http://dx.doi.org/10.1126/science.258.5086.1335 PMID: 17778358

[25] Avramov AV, Zhang M, Burnap RL. An amino residue that guides the correct photoassembly of the water-oxidation complex but is not required for high affinity Mn^{2+} binding. BioRxiv 2021; 2021: 470031. http://dx.doi.org/10.1101/2021.11.29.470031

[26] Najafpour MM, Heidari S, Balaghi SE, *et al*. Proposed mechanisms for water oxidation by Photosystem II and nanosized manganese oxides. Biochim Biophys Acta Bioenerg 2017; 1858(2): 156-74. http://dx.doi.org/10.1016/j.bbabio.2016.11.007 PMID: 27838231

[27] Liu Z, Chang W. Structure of the Light-Harvesting Complex II. In: *Photosynthetic protein complexes: A structural approach*. Fromme P (ed.), pp. 217-42. Wiley Onl. Lib 2008. http://dx.doi.org/10.1002/9783527623464.ch10

[28] Kern J, Renger G, Photosystem II. Photosystem II: Structure and mechanism of the water: Plastoquinone oxidoreductase. Photosynth Res 2007; 94(2-3): 183-202. http://dx.doi.org/10.1007/s11120-007-9201-1 PMID: 17634752

[29] Goldschmidt-Clermont M, Bassi R. Sharing light between two photosystems: Mechanism of state transitions. Curr Opin Plant Biol 2015; 25: 71-8. http://dx.doi.org/10.1016/j.pbi.2015.04.009 PMID: 26002067

[30] Masojıdek J, Koblızek M, Torzillo G. Photosynthesis in Microalgae. In: *Handbook of microalgal culture.*

Richmond A (ed.) Biotech. App. Phys, pp. 20-39. Blackwell: Hoboken New Jersey, 2004. http://dx.doi.org/10.1002/9780470995280

[31] Li J, Hamaoka N, Makino F, *et al.* Kurisu, G. Structure of cyanobacterial photosystem I complexed with cytochrome and ferredoxin at 1.97 Å resolution. BioRxiv 2022; 2022: 482405. http://dx.doi.org/10.1101/2022.03.01.482405

[32] Masojídek J, Ranglová K, Lakatos GE, Silva Benavides AM, Torzillo G. Variables governing photosynthesis and growth in microalgae mass cultures. Processes 2021; 9(5): 820. http://dx.doi.org/10.3390/pr9050820

[33] Enami I, Okumura A, Nagao R, Suzuki T, Iwai M, Shen JR. Structures and functions of the extrinsic proteins of photosystem II from different species. Photosynth Res 2008; 98(1-3): 349-63. http://dx.doi.org/10.1007/s11120-008-9343-9 PMID: 18716894

[34] Umena Y, Kawakami K, Shen JR, Kamiya N. Crystal structure of oxygen-evolving photosystem II at a resolution of 1.9 Å. Nature 2011; 473(7345): 55-60. http://dx.doi.org/10.1038/nature09913 PMID: 21499260

[35] Mirkovic T, Ostroumov EE, Anna JM, van Grondelle R, Govindjee , Scholes GD. Light absorption and energy transfer in the antenna complexes of photosynthetic organisms. Chem Rev 2017; 117(2): 249-93. http://dx.doi.org/10.1021/acs.chemrev.6b00002 PMID: 27428615

[36] Kirst H, García-Cerdán JG, Zurbriggen A, Melis A. Assembly of the light-harvesting chlorophyll antenna in the green alga *Chlamydomonas reinhardtii* requires expression of the TLA2-CpFTSY gene. Plant Physiol 2012; 158(2): 930-45. http://dx.doi.org/10.1104/pp.111.189910 PMID: 22114096

[37] Negi S, Perrine Z, Friedland N, *et al.* Light regulation of light-harvesting antenna size substantially enhances photosynthetic efficiency and biomass yield in green algae †. Plant J 2020; 103(2): 584-603. http://dx.doi.org/10.1111/tpj.14751 PMID: 32180283

[38] Martin-Avila E, Lim YL, Birch R, *et al.* Modifying plant photosynthesis and growth *via* simultaneous chloroplast transformation of rubisco large and small subunits. Plant Cell 2020; 32(9): 2898-916. http://dx.doi.org/10.1105/tpc.20.00288 PMID: 32647068

[39] Ramanna L, Rawat I, Bux F. Light enhancement strategies improve microalgal biomass productivity. Renew Sust Energ Rev 2017; 80: 765-73. http://dx.doi.org/10.1016/j.rser.2017.05.202

[40] Torzillo G. Photosynthesis basic principles to optimize growth of microalgae cultures outdoors. *Rev. Latin. Amb.* Algal 2021; 12(2): 30-4.

[41] Sartori RB, Siqueira SF, Maroneze MM, *et al.* Microalgal secondary metabolites: Effect of climatic variables, seasons, and photocycles on the biogeneration of volatile organic compounds (VOCs). J Appl Phycol 2021; 33(3): 1457-72. http://dx.doi.org/10.1007/s10811-021-02391-6

[42] Wang C, Dong W, Li A, Atinafu DG, Wang G, Lu Y. The reinforced photothermal effect of conjugated dye/graphene oxide-based phase change materials: Fluorescence resonance energy transfer and applications in solar-thermal energy storage. Chem Eng J 2022; 42: 130605. http://dx.doi.org/10.1016/j.cej.2021.130605

[43] Damergi E, Qin P, Sharma S, Nazeeruddin MK, Ludwig C. Enhancing algae biomass production by using dye-sensitized solar cells as filters. ACS Sust Chem Eng 2021; 9(43): 14353-64. http://dx.doi.org/10.1021/acssuschemeng.1c03780

[44] Ooms MD, Dinh CT, Sargent EH, Sinton D. Photon management for augmented photosynthesis. Nat Commun 2016; 7(1): 12699. http://dx.doi.org/10.1038/ncomms12699 PMID: 27581187

[45] Nwoba EG, Parlevliet DA, Laird DW, *et al.* Energy efficiency analysis of outdoor standalone photovoltaic-powered photobioreactors coproducing lipid-rich algal biomass and electricity. Appl Energy 2020; 275: 115403. http://dx.doi.org/10.1016/j.apenergy.2020.115403

[46] Assunção J, Malcata FX. Enclosed "non-conventional" photobioreactors for microalga production: A review. Algal Res 2020; 52: 102107. http://dx.doi.org/10.1016/j.algal.2020.102107

[47] Sero ET, Siziba N, Bunhu T, Shoko R, Jonathan E. Biophotonics for improving algal photobioreactor performance: A review. Int J Energy Res 2020; 44(7): 5071-92. http://dx.doi.org/10.1002/er.5059

[48] Esen V, Sağlam Ş, Oral B. Light sources of solar simulators for photovoltaic devices: A review. Renew Sust Energ Rev 2017; 77: 1240-50. http://dx.doi.org/10.1016/j.rser.2017.03.062

[49] Lv B, Liu Z, Chen Y, *et al.* Effect of different colored LED lighting on the growth and pigment content of *Isochrysis zhanjiangensis* under laboratory conditions. J Mar Sci Eng 2022; 10(11): 1752. http://dx.doi.org/10.3390/jmse10111752

[50] Porto B. Silva TFCV, Gonçalves AL, Esteves AF, *et al*. Tubular photobioreactors illuminated with LEDs to boost microalgal biomass production. Chem Eng J 2022; 435(1): 134747. http://dx.doi.org/10.1016/j.cej.2022.134747

[51] González-Camejo J, Viruela A, Ruano MV, Barat R, Seco A, Ferrer J. Effect of light intensity, light duration and photoperiods in the performance of an outdoor photobioreactor for urban wastewater treatment. Algal Res 2019; 40: 101511. http://dx.doi.org/10.1016/j.algal.2019.101511

[52] Kim S, Moon M, Kwak M, Lee B, Chang YK. Statistical optimization of light intensity and CO_2 concentration for lipid production derived from attached cul-

tivation of green microalga *Ettlia sp*. Sci Rep 2018; 8(1): 15390.
http://dx.doi.org/10.1038/s41598-018-33793-1 PMID: 30337595

[53] Hu X, Zhou J, Liu B. Effect of algal species and light intensity on the performance of an air-lift-type microbial carbon capture cell with an algae-assisted cathode. RSC Advances 2016; 6(30): 25094-100.
http://dx.doi.org/10.1039/C5RA26299B

[54] Chiarini A, Quadrio M. The light/dark cycle of microalgae in a thin-layer photobioreactor. J Appl Phycol 2021; 33(1): 183-95.
http://dx.doi.org/10.1007/s10811-020-02310-1

[55] Levasseur W, Pozzobon V, Perré P. Green microalgae in intermittent light: A meta-analysis assisted by machine learning. J Appl Phycol 2022; 34(1): 135-58.
http://dx.doi.org/10.1007/s10811-021-02603-z

[56] Jacob-Lopes E, Scoparo CHG, Lacerda LMCF, Franco TT. Effect of light cycles (night/day) on CO_2 fixation and biomass production by microalgae in photobioreactors. Chem Eng Process 2009; 48(1): 306-10.
http://dx.doi.org/10.1016/j.cep.2008.04.007

[57] Nedbal L, Lazár D. Photosynthesis dynamics and regulation sensed in the frequency domain. Plant Physiol 2021; 187(2): 646-61.
http://dx.doi.org/10.1093/plphys/kiab317 PMID: 34608969

[58] Sartori RB, Vendruscolo RG, Ribeiro SR, *et al.* The role of photo-cycles in the modulation of growth and biochemical profile of microalgae: Part I—food interest compounds. Life 2022; 12(3): 462.
http://dx.doi.org/10.3390/life12030462 PMID: 35330213

[59] Morales M, Aflalo C, Bernard O. Microalgal lipids: A review of lipids potential and quantification for 95 phytoplankton species. Biomass Bioenerg 2021; 150: 106108.
http://dx.doi.org/10.1016/j.biombioe.2021.106108

[60] Schulze PSC, Guerra R, Pereira H, Schüler LM, Varela JCS. Flashing LEDs for microalgal production. Trends Biotechnol 2017; 35(11): 1088-101.
http://dx.doi.org/10.1016/j.tibtech.2017.07.011 PMID: 28865804

[61] Liao Q, Li L, Chen R, Zhu X. A novel photobioreactor generating the light/dark cycle to improve microalgae cultivation. Bioresour Technol 2014; 161: 186-91.
http://dx.doi.org/10.1016/j.biortech.2014.02.119 PMID: 24704839

[62] Abu-Ghosh S, Fixler D, Dubinsky Z, Iluz D. Flashing light in microalgae biotechnology. Bioresour Technol 2016; 203: 357-63.
http://dx.doi.org/10.1016/j.biortech.2015.12.057 PMID: 26747205

[63] Chowdury KH, Nahar N, Deb UK. The growth factors involved in microalgae cultivation for biofuel production: A review. Comput Water Energ Environ Eng 2020; 9(4): 185-215.
http://dx.doi.org/10.4236/cweee.2020.94012

[64] Acién Fernández FG, Fernández Sevilla JM, Sánchez Pérez JA, Molina Grima E, Chisti Y. Airlift-driven external-loop tubular photobioreactors for outdoor production of microalgae: Assessment of design and performance. Chem Eng Sci 2001; 56(8): 2721-32.
http://dx.doi.org/10.1016/S0009-2509(00)00521-2

[65] Carvalho AP, Silva SO, Baptista JM, Malcata FX. Light requirements in microalgal photobioreactors: An overview of biophotonic aspects. Appl Microbiol Biotechnol 2011; 89(5): 1275-88.
http://dx.doi.org/10.1007/s00253-010-3047-8 PMID: 21181149

[66] Egbo MN, Okoani A. Photobioreactors for microalgae cultivation-An Overview. Int J Sci Eng Res 2018; 9: 11.

[67] Deprá MC, Mérida LGR, de Menezes CR, Zepka LQ, Jacob-Lopes E. A new hybrid photobioreactor design for microalgae culture. Chem Eng Res Des 2019; 144: 1-10.
http://dx.doi.org/10.1016/j.cherd.2019.01.023

[68] Vasumathi KK, Premalatha M, Subramanian P. Parameters influencing the design of photobioreactor for the growth of microalgae. Ren Sust Energy Ver 2012; 16(7): 5443-50.
http://dx.doi.org/10.1016/j.rser.2012.06.013

[69] Patwardhan SB, Pandit S, Ghosh D, *et al*. A concise review on the cultivation of microalgal biofilms for biofuel feedstock production. Biom. Conv. Bioref 2022.
http://dx.doi.org/10.1007/s13399-022-02783-9

[70] Severo IA, Deprá MC, Zepka LQ, Jacob-Lopes E. Carbon dioxide capture and use by microalgae in photobioreactors. Bioen Carb Capt Storage 2019; 8: 151-71.
http://dx.doi.org/10.1016/B978-0-12-816229-3.00008-9

[71] Tan JS, Lee SY, Chew KW, *et al.* A review on microalgae cultivation and harvesting, and their biomass extraction processing using ionic liquids. Bioengineered 2020; 11(1): 116-29.
http://dx.doi.org/10.1080/21655979.2020.1711626 PMID: 31909681

[72] Chisti Y. Biodiesel from microalgae. Biotechnol Adv 2007; 25(3): 294-306.
http://dx.doi.org/10.1016/j.biotechadv.2007.02.001 PMID: 17350212

[73] Sirohi R, Kumar Pandey A, Ranganathan P, *et al.* Design and applications of photobioreactors- A review. Bioresour Technol 2022; 349: 126858.
http://dx.doi.org/10.1016/j.biortech.2022.126858 PMID: 35183729

[74] Acién G, Grima ME, Torzillo G. Photobioreactors for the production of microalgae. In: *Microalgae-based*. Prokop A, *et al*. (eds.), Biofuels Biop, pp 1-44. Springer: Switzerland 2017.
http://dx.doi.org/10.1016/B978-0-08-101023-5.00001-7

[75] Merchuk, J. C. Photobioreactor design. In: *Handbook of Microalgae-Based Processes and Products: Fundamentals and Advances*. Borowitzka MA (ed.), En-

ergy, Food, Feed, Fertilizer, and Bioactive Compounds, pp. 101-126. Elsevier: Amsterdam, 2020. https://doi.org/10.1016/B978-0-12-818536-0.00005-1

[76] Pfaffinger CE, Severin TS, Apel AC, Göbel J, Sauter J, Weuster-Botz D. Light-dependent growth kinetics enable scale-up of well-mixed phototrophic bioprocesses in different types of photobioreactors. J Biotechnol 2019; 297: 41-8. http://dx.doi.org/10.1016/j.jbiotec.2019.03.003 PMID: 30898687

[77] Prussi M, Buffi M, Casini D, *et al.* Experimental and numerical investigations of mixing in raceway ponds for algae cultivation. Biomass Bioenerg 2014; 67(67): 390-400. http://dx.doi.org/10.1016/j.biombioe.2014.05.024

[78] Ugwu CU, Aoyagi H, Uchiyama H. Photobioreactors for mass cultivation of algae. Bioresour Technol 2008; 99(10): 4021-8. http://dx.doi.org/10.1016/j.biortech.2007.01.046 PMID: 17379512

[79] Apel AC, Pfaffinger CE, Basedahl N, *et al.* Open thin-layer cascade reactors for saline microalgae production evaluated in a physically simulated Mediterranean summer climate. Algal Res 2017; 25: 381-90. http://dx.doi.org/10.1016/j.algal.2017.06.004

[80] Kováts P, Thévenin D, Zähringer K. Characterizing fluid dynamics in a bubble column aimed for the determination of reactive mass transfer. Heat Mass Transf 2018; 54(2): 453-61. http://dx.doi.org/10.1007/s00231-017-2142-0

[81] Hernández-Melchor DJ, Cañizares-Villanueva RO, Terán-Toledo JR, López- Pérez PA, Cristiani-Urbina E. Hydrodynamic and mass transfer characterization of flat-panel airlift photobioreactors for the cultivation of a photosynthetic microbial consortium. Biochem Eng J 2017; 128: 141-8. http://dx.doi.org/10.1016/j.bej.2017.09.014

[82] Belohlav V, Zakova T, Jirout T, Kratky L. Effect of hydrodynamics on the formation and removal of microalgal biofilm in photobioreactors. Biosyst Eng 2020; 200: 315-27. http://dx.doi.org/10.1016/j.biosystemseng.2020.10.014

[83] Touloupakis E, Faraloni C, Carlozzi P. An outline of photosynthetic microorganism growth inside closed photobioreactor designs. Bioresour Technol Rep 2022; 18: 101066. http://dx.doi.org/10.1016/j.biteb.2022.101066

[84] Posten C. Design and performance parameters of photobioreactors. *TATuP-Zeitsc. Technik.* TATuP - Zeitschrift für Technikfolgenabschätzung in Theorie und Praxis 2012; 21(1): 38-45. http://dx.doi.org/10.14512/tatup.21.1.38

[85] Mérida RLG, Zepka LQ, Jacob-Lopes E. Current production of microalgae at industrial scale. Microalgae as a source of bioenergy: Products, process and economics. Rec Adv Renew Energ 2017; 278-92. http://dx.doi.org/10.2174/9781681085227117010013

[86] Jacob-Lopes E, Zepka LQ, Merida LGR, Maroneze MM, Neves C. Bioprocess of conversion of carbon dioxide from industrial emissions, bioproducts, their uses and hybrid photobioreactor. Patent WO 041028, 2014.

[87] Ramlee A, Rasdi AW, Effendy B, Jusoh M. Microalgae and the factors involved in successful propagation for mass production. J Sust Sci Manag 2021; 16(3): 21-42. http://dx.doi.org/10.46754/jssm.2021.04.003

[88] Huang Q, Jiang F, Wang L, Yang C. Design of photobioreactors for mass cultivation of photosynthetic organisms. Engineering 2017; 3(3): 318-29. http://dx.doi.org/10.1016/J.ENG.2017.03.020

[89] Laifa R, Morchain J, Barna L, Guiraud P. A numerical framework to predict the performances of a tubular photobioreactor from operating and sunlight conditions. Algal Res 2021; 60: 102550. http://dx.doi.org/10.1016/j.algal.2021.102550

[90] Grima EM, Camacho FG, Pérez JAS, Sevilla JMF, Fernández FGA, Gómez AC. A mathematical model of microalgal growth in light-limited chemostat culture. J Chem Technol Biotechnol 1994; 61(2): 167-73. http://dx.doi.org/10.1002/jctb.280610212

[91] Huesemann M, Crowe B, Waller P, *et al.* A validated model to predict microalgae growth in outdoor pond cultures subjected to fluctuating light intensities and water temperatures. Algal Res 2016; 13: 195-206. http://dx.doi.org/10.1016/j.algal.2015.11.008

[92] Grima E, Fernández JM, Sánchez JÁ, García F. A study on simultaneous photolimitation and photoinhibition in dense microalgal cultures taking into account incident and averaged irradiances. J Biotechnol 1996; 45(1): 59-69. http://dx.doi.org/10.1016/0168-1656(95)00144-1

[93] Acién Fernández FG, Fernández Sevilla JM, Molina Grima E. Photobioreactors for the production of microalgae. Rev Environ Sci Biotechnol 2013; 12(2): 131-51. http://dx.doi.org/10.1007/s11157-012-9307-6

[94] Cornet JF, Dussap CG, Gros JB. Conversion of radiant light energy in photobioreactors. AIChE J 1994; 40(6): 1055-66. http://dx.doi.org/10.1002/aic.690400616

[95] Cornet JF, Dussap CG, Gros JB, Binois C, Lasseur C. A simplified monodimensional approach for modeling coupling between radiant light transfer and growth kinetics in photobioreactors. Chem Eng Sci 1995; 50(9): 1489-500. http://dx.doi.org/10.1016/0009-2509(95)00022-W

[96] Cornet JF, Dussap CG, Gros JB. Kinetics and energetics of photosynthetic micro-organisms in photobioreactors. Adv Biochem Eng Biotechnol 1998; 59: 153-224. http://dx.doi.org/10.1007/BFb0102299

[97] Gao X, Kong B, Vigil RD. Simulation of algal photobioreactors: Recent developments and challenges. Biotechnol Lett 2018; 40(9-10): 1311-27.

http://dx.doi.org/10.1007/s10529-018-2595-3 PMID: 30051265

[98] Ranganathan P, Pandey AK, Sirohi R, Tuan Hoang A, Kim SH. Recent advances in computational fluid dynamics (CFD) modelling of photobioreactors: Design and applications. Bioresour Technol 2022; 350: 126920. http://dx.doi.org/10.1016/j.biortech.2022.126920 PMID: 35240273

[99] Luzi G, McHardy C. Modeling and simulation of photobioreactors with computational fluid dynamics—A comprehensive review. Energies 2022; 15(11): 3966. http://dx.doi.org/10.3390/en15113966

[100] Ye Q, Cheng J, Guo W, Xu J, Li H, Zhou J. Numerical simulation on promoting light/dark cycle frequency to improve microalgae growth in photobioreactor with serial lantern-shaped draft tube. Bioresour Technol 2018; 266: 89-96. http://dx.doi.org/10.1016/j.biortech.2018.06.055 PMID: 29957295

[101] Wang L, Wang Q, Zhao R, Tao Y, Ying K, Mao X. Novel flat-plate photobioreactor with inclined baffles and internal structure optimization to improve light regime performance. ACS Sust Chem Eng 2021; 9(4): 1550-8. http://dx.doi.org/10.1021/acssuschemeng.0c06109

[102] Díaz JP, Inostroza C, Acién Fernández FG. Fibonacci-type tubular photobioreactor for the production of microalgae. Proc Biochem 2019; 86: 1-8. http://dx.doi.org/10.1016/j.procbio.2019.08.008

[103] Capson-Tojo G, Batstone DJ, Grassino M, Hülsen T. Light attenuation in enriched purple phototrophic bacteria cultures: Implications for modelling and reactor design. Water Res 2022; 219: 118572. http://dx.doi.org/10.1016/j.watres.2022.118572 PMID: 35569276

[104] Severo IA, dos Santos AM, Deprá MC, Barin JS, Jacob-Lopes E. Microalgae photobioreactors integrated into combustion processes: A patent-based analysis to map technological trends. Algal Res 2021; 60: 102529. http://dx.doi.org/10.1016/j.algal.2021.102529

[105] Festus AF, Rufus AI, Janet TO. Janet, TO Sustainability reporting: Imperative for turnover growth. Asian. Asian J Econom Business Account 2020; 16(1): 8-18. http://dx.doi.org/10.9734/ajeba/2020/v16i130227

[106] Deprá MC, Severo IA, dos Santos AM, Zepka LQ, Jacob-Lopes E. Environmental impacts on commercial microalgae-based products: Sustainability metrics and indicators. Algal Res 2020; 51: 102056. http://dx.doi.org/10.1016/j.algal.2020.102056

[107] Blanken W, Cuaresma M, Wijffels RH, Janssen M. Cultivation of microalgae on artificial light comes at a cost. Algal Res 2013; 2(4): 333-40. http://dx.doi.org/10.1016/j.algal.2013.09.004

[108] Lane TW. Barriers to microalgal mass cultivation. Curr Opin Biotechnol 2022; 73: 323-8. http://dx.doi.org/10.1016/j.copbio.2021.09.013 PMID: 34710649

[109] Loke Show P. Global market and economic analysis of microalgae technology: Status and perspectives. Bioresour Technol 2022; 357: 127329. http://dx.doi.org/10.1016/j.biortech.2022.127329

[110] Dias RR, Deprá MC, Severo IA, Zepka LQ, Jacob-Lopes E. Smart override of the energy matrix in commercial microalgae facilities: A transition path to a low-carbon bioeconomy. Sust Energ Technol Assess 2022; 52: 102073. http://dx.doi.org/10.1016/j.seta.2022.102073

[111] Schade S, Meier T. Distinct microalgae species for food—part 1: A methodological (top-down) approach for the life cycle assessment of microalgae cultivation in tubular photobioreactors. J Appl Phycol 2020; 32(5): 2977-95. http://dx.doi.org/10.1007/s10811-020-02177-2

[112] Albatayneh A, Juaidi A, Abdallah R, Manzano-Agugliaro F. Influence of the Advancement in the LED lighting technologies on the optimum windows-to-wall ratio of Jordanians residential buildings. Energies 2021; 14(17): 5446. http://dx.doi.org/10.3390/en14175446

[113] Global Petrol Prices. Electricity prices. Available from: https://www.globalpetrolprices.com/electricity_prices

[114] Khor PY, Vearing RM, Charlton KE. The effectiveness of nutrition interventions in improving frailty and its associated constructs related to malnutrition and functional decline among community-dwelling older adults: A systematic review. J Hum Nutr Diet 2022; 35(3): 566-82. http://dx.doi.org/10.1111/jhn.12943 PMID: 34494314

DISCLAIMER: The above article has been published, as is, ahead-of-print, to provide early visibility but is not the final version. Major publication processes like copyediting, proofing, typesetting and further review are still to be done and may lead to changes in the final published version, if it is eventually published. All legal disclaimers that apply to the final published article also apply to this ahead-of-print version.

sustainability

MDPI

Article

The High-Value Product, Bio-Waste, and Eco-Friendly Energy as the Tripod of the Microalgae Biorefinery: Connecting the Dots

Rosangela Rodrigues Dias, Mariany Costa Deprá, Cristiano Ragagnin de Menezes, Leila Queiroz Zepka and Eduardo Jacob-Lopes *

Bioprocess Intensification Group, Federal University of Santa Maria (UFSM), Roraima Avenue 1000, Santa Maria 97105-900, RS, Brazil; ro.rosangelard@gmail.com (R.R.D.); marianydepra@gmail.com (M.C.D.); cristiano.ufsm@gmail.com (C.R.d.M.); zepkaleila@yahoo.com.br (L.Q.Z.)

* Correspondence: ejacoblopes@gmail.com; Tel.: +55-55-3220-8822

Abstract: A bio-based circular economy is fundamental to catalyzing the transition to a new economic model that thrives well within the planet's ecological limits. The microalgae biorefinery, which consists of converting biomass into multiple products, operates in light of the principles of a circular economy. Therefore, as the pivot of a new economic paradigm that aims to promote ecological robustness, the main scope and motivation of this article are to use life cycle assessment to scrutinize the environmental sustainability of a microalgae-based biorefinery system. We assume β-carotene as the flagship of the microalgae industry and evaluate the sustainability metrics and indicators of two residual products: bulk oil and defatted biomass. The role of the use of renewable energy in the unit operations of the biorefinery was also evaluated. The results of this study show that waste products contribute an almost insignificant fraction of the ecological footprint and the cost and energy demand of the microalgae-based biorefinery. It is also confirmed from the results that the transition from coal-based energy to renewable is the most realistic path to production with significantly lower emissions. In sum, the consolidation of the microalgae biorefinery seems to be just around the corner, and our highlights can help make this a successful route.

Keywords: algae; circular bioeconomy; environmental sustainability; green electricity; waste valorization

check for updates

Citation: Rodrigues Dias, R.; Deprá, M.C.; Ragagnin de Menezes, C.; Queiroz Zepka, L.; Jacob-Lopes, E. The High-Value Product, Bio-Waste, and Eco-Friendly Energy as the Tripod of the Microalgae Biorefinery: Connecting the Dots. *Sustainability* **2023**, *15*, 11494. https://doi.org/10.3390/su151511494

Academic Editor: G. Venkatesh

Received: 2 June 2023
Revised: 15 July 2023
Accepted: 21 July 2023
Published: 25 July 2023

Copyright: © 2023 by the authors. Licensee MDPI, Basel, Switzerland. This article is an open access article distributed under the terms and conditions of the Creative Commons Attribution (CC BY) license (https://creativecommons.org/licenses/by/4.0/).

1. Introduction

Our current economic system has surpassed many of the earth's capacity limits [1,2]. It failed to value nature and, now, lives under the threat of increasing losses. The prognosis is that there is no future for business as usual. And turning the tide requires connecting the dots between investors, companies, governmental and non-governmental organizations, and local communities to promote a new paradigm of producing goods and services—putting nature back at the center of our economy [3].

With this bias, with the fossil and linear economy approaching its expiration date, the biobased circular economy has gained prominence and could be the catalyst for a prosperous future. In a circular bioeconomy, natural capital is renewable, recovered, and reused as much as possible, creating new products and replacing conventional high-carbon materials. Biowaste is not discarded; they create secondary products that, after use, can flow back into the biosphere, closing biogeochemical cycles. The value is maximized and waste is minimized in this conceptual framework [4].

From this perspective, microalgae biotechnology—under a biorefinery model—emerges as a promising approach to achieving a cost-effective, bio-based circular economy that thrives well within the confines of the planet [5]. In a historical context, since the dawn of humanity, species such as *Arthrospira platensis* and *Chlorella vulgaris* have been used by society as a food bioresource—a priori, due to their high protein content. Later, in the face of the energy crisis, species such as *Crypthecodinium cohnii*, *Ankistrodesmus* sp, *Botrycoccus braunii*, *Nitzschia laevis*, and *Nannochloropsis oculata* became pioneers in prospecting the production of fatty acids as

feedstock for bioenergy production and also food supplementation. Subsequently, with the increase in awareness and health promotion, research focused on natural product exploitation, with the spotlight being directed to pigments such as beta-carotene and astaxanthin biosynthesized by the microalgae *Dunaliella salina* and *Haematococcus pluvialis*, respectively [6,7].

However, although scientific advances have invested in and reinforced promising findings, commercial microalgae cultivation is technically recent, less than 70 years old. The challenges of manipulating and producing microorganisms with such versatile and complex metabolisms result in a universe of bottlenecks to be overcome. Indeed, microalgae are most commonly cultivated commercially in open systems such as raceway ponds under photoautotrophic and/or mixotrophic regimes. However, these systems are susceptible to contamination and low cell productivity, putting the mass production of microalgal bioproducts to the test. The use of closed systems, such as photobioreactors, or biofermenters—under heterotrophic culture regimes—even if they benefit from the technological subsystems of microbial biosynthesis already developed, require high energy for processing, beyond the intrinsic requirements of the strains of microalgae, making it difficult to obtain a large-scale sustainable standard project to work with [8,9].

Thereby, in view of the highlights of the scientific journey for the commercialization of microalgae, it was possible to learn that, despite the path full of bumps and twists, new insights and important opportunities to improve this technology have emerged [10]. The experiences on laboratory and commercial scales have shown that the biorefinery concept applied to microalgae is a hopeful route to more economically and environmentally sustainable productions. In the state of the art, as is known, a world reference of sustainable microalgae-based biorefinery has not been established. This is because the research and development of biotechnological routes related to algal biorefineries has focused on the use of low-value commodities (biomass and biofuels) as the biorefinery core. However, this primary use of microalgae has not shown successful results unless the yield of high-value compounds is addressed together [11]. In this vein, following the cascade principle, that is, giving priority to the production of a high-value product before a low-value one, it may be possible to successfully move towards a microalgae-based circular bioeconomy using the biorefinery approach. This can make microalgae-based biological processes less dystopian. Furthermore, it is important to highlight that the use of ecologically correct energy in unit operations seems to be, at the same time, the definitive key to overcoming the environmental deficit of microalgae processes and products [12].

In light of this, our paradigm shift proposes high-value fine chemicals use, such as β-carotene, as the value center of a microalgae biorefinery, emphasizing biowaste recovery and integration with eco-friendly energy. Like this, a microalgae-based biorefinery realigned with nature was assembled and used as a robust justification to be replicated on an industrial scale by microalgae producers. The research questions addressed in this article provide a holistic assessment of the environmental profile of a microalgae-based biorefinery system that, following the cascade principle with the use of renewable energy and the circular economy approach, seeks to overcome environmental and economic restrictions of the current linear economic model that struggles to create revenue. The role of this article for sustainability is to promote a bio-based circular economy that takes off and consolidates in what appears to be the beginning of a new age—the Age of Sustainability.

2. Material and Methods

2.1. Life Cycle Assessment (LCA)

The life cycle assessment (LCA) was performed according to the ISO 14040 series [13]. The LCA, as detailed below, is composed of four phases: goal and scope definition (i), inventory analysis (ii), impact assessment (iii), and interpretation of results (iv).

2.1.1. Goal and Scope Definition

The objective of applying the LCA was to evaluate the metrics and indicators of environmental sustainability of a biorefinery system based on *Dunaliella salina* with a main focus on β-carotene and valorization waste biomass. The species *Dunaliella salina* was considered in this study because it is considered one of the best candidates for β-carotene production (~14% dry weight), beyond being the main strain used in the commercial production of natural carotene. In addition, its biomass composition also shows high content values of protein, lipid, and glycerol. Thus, the centesimal composition as the basis of this study considered the values on a dry basis found in the literature, being the fraction of β-carotene of 10%, proteins of 35%, fatty acids of 20%, and glycerol of 15%, disregarding other potential bioproducts such as the fraction of carbohydrates, vitamins, and minerals also present in the residual biomass [14,15]. In addition, bio-waste was selected due to its high potential for application in the microalgae global market, with bulk oil being the main feedstock for bioenergy segments such as biodiesel, as well as a food supplement considering the fatty acids polyunsaturated fraction. Likewise, defatted biomass has been required as a bioresource of protein supplementation for animal and human feed, beyond the application in bioenergy, such as bioethanol production (see Supplementary Material Table S1).

The LCA was also applied to assess the environmental footprint of the biorefinery from *Dunaliella salina* powered by coal-based energy versus photovoltaic energy from amorphous silicon solar cells (a-Si) and onshore wind energy. The study uses theoretical and experimental data collected from the scientific literature [6,16–18].

The system boundaries were defined from the cradle-to-gate life cycle and comprise a microalgae plant with a production of 9.38 tons/year of dry biomass, fractionated into 1 ton/year of β-carotene pigment (main product), 1.51 tons/year of bulk oil (secondary product), and 2.34 tons/year of defatted biomass (tertiary product). Only the environmental impacts of electricity consumption were included in the analysis because they represent the majority, if not almost the entire fraction of the ecological footprint of microalgae products [6].

Step 1: *β*-Carotene Production

The unit operations proposed in Step 1 are in accordance with the production process consolidated by classic references in the literature (Figure 1) [6,19]. The growth conditions considered in raceway ponds were a pH of 7.5, an average temperature of 26 °C, a light intensity of 50 μmol/m^2/s^{-1}, and a photoperiod of 12:12 h [20]. Also, it is important to mention that the culture medium of *Dunaliella salina* is predominantly hypersaline; therefore, the contamination risk rates are low.

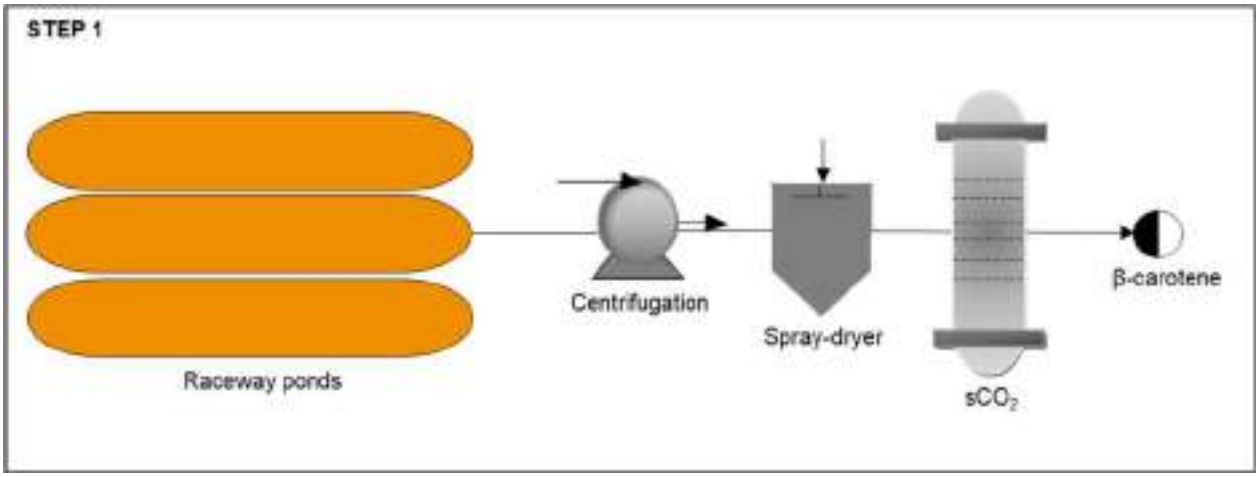


Figure 1. Process flow diagram of the commercial production of β-carotene from *Dunaliella salina*.

Step 2: Bulk Oil Production

The unit operations proposed in Step 2 are in accordance with dos Santos et al. [17] (Figure 2). The residual biomass from the β-carotene extraction process is then submitted to the lipid extraction process. This lipid extraction, based on hexane, was defined as the method for large-scale applications [21]. Subsequently, the biomass blend with the extractor solvent is centrifuged, going through the solvent recovery and evaporation/stripper step. The evaporation/stripper is the most economical method on an industrial scale for reducing volatiles in heat-sensitive materials and viscous products. Finally, the oil-rich extract is directed to the desolventizer, obtaining the bulk oil.

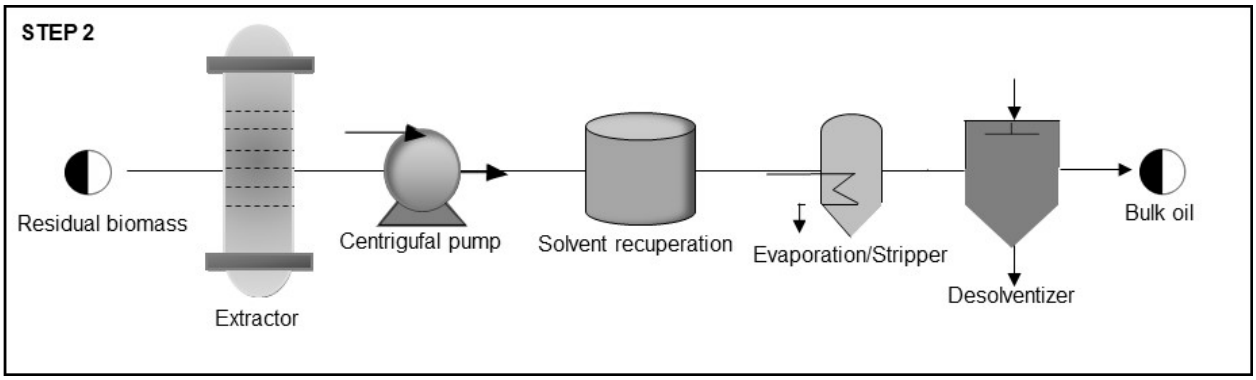


Figure 2. Flow diagram of the bulk oil production process from *Dunaliella salina*.

Step 3: Defatted Biomass Production

The unit operation for defatted biomass production is proposed in Step 3, according to dos Santos et al. [17] (Figure 3). This unique step consists of removing the residual solvent, in this case, the hexane, from the flours produced in the oil extraction process. Along with solvent removal, the solid protein flour obtained also goes through a roasting process that improves its nutritional characteristics. The industrial equipment is called a desolventizer-toaster-dryer-cooler (DTDC).

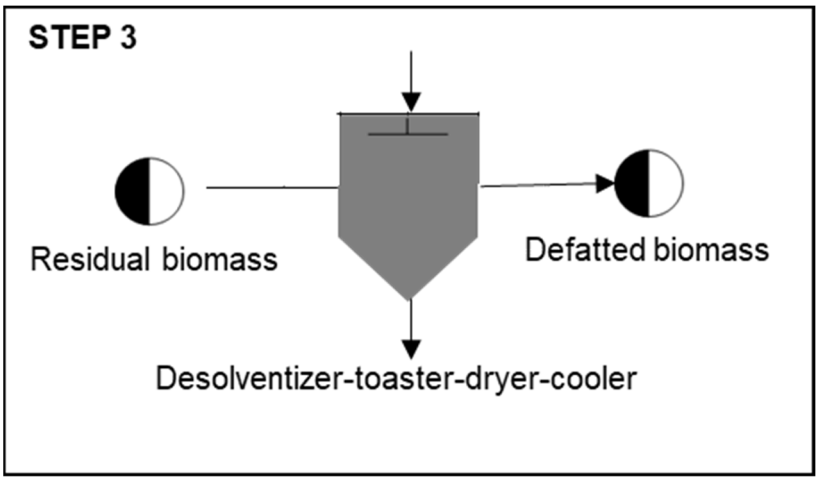


Figure 3. Flow diagram of the defatted biomass production process from *Dunaliella salina*.

2.1.2. Life Cycle Inventory (LCI)

Life cycle inventory (LCI) data were obtained from the literature [22–27]. The input and output flow for each step of the process scope are shown in Table 1.

Table 1. Elementary flows for each step of the process scope.

Process	Unit	Base Case
Cultivation		
Raceway pond	m^3	63.16
Electric energy for paddle wheel	kWh	270,122.68
Electric energy for water pumping	kWh	50,022.72
Electric energy for CO_2 injection	kWh	165,074.97
Water evaporation	m^3	8.21
Biomass productivity	ton/m^3/year	0.15
Output		
Algae liquid	ton	50.03
Harvest		
Input		
Energy consumption centrifugation	kWh	1894.80
Drying		
Input		
Wet biomass	ton	12.50
Spray-dryer	kWh	13,632.25
Output		
Dry biomass	ton	9.38
Pigment extraction		
Input		
Dry biomass	ton	9.38
sCO_2	kWh	7504.0
Output		
β-carotene pigment	ton	1.0
Bulk oil production		
Input		
Residual biomass	ton	8.38
Extractor	kWh	594.51
Energy consumption centrifugation	kWh	875.24
Solvent recuperation	kWh	1037.72
Evaporation/Stripper	kWh	194.13
Desolventizer	kWh	328.21
Output		
Bulk oil	ton	1.51
Defatted biomass production		
Residual biomass	ton	6.71
Desolventizer-toaster-dryer-cooler	kWh	922.73
Defatted biomass	ton	2.34
Total electric energy requirement	kWh/year	512,203.96

Acronyms: sCO_2, Supercritical CO_2 extraction.

2.1.3. Life Cycle Impact Analysis (LCIA)

Potential environmental impacts were calculated according to the ReCiPe midpoint method (hierarchical approach) [28] and consistently applied accordingly with Jacob-Lopes et al. [29]. The midpoint impact categories considered were global warming (GWP), stratospheric ozone depletion (SOD), ionizing radiation (IR), ozone formation–human health (OFHH), fine particulate matter formation (FPMF), ozone formation–terrestrial ecosystems (OFTE), terrestrial acidification (TA), freshwater eutrophication (FEU), terrestrial ecotoxicity (TE), freshwater ecotoxicity (FEC), marine ecotoxicity (ME), human carcinogenic toxicity (HCT), human non-carcinogenic toxicity (HNCT), mineral resource scarcity (MRS), fossil resource scarcity (FRS), land use (LU), and water consumption (WC). The characterization factors are shown in the Supplementary Material (Table S2).

Global Warming (GWP)

The determination of global warming potential was evaluated by greenhouse gas emissions, according to Equation (1):

$$GWP = \sum GWP_i \times m_i \quad (1)$$

where GWP is the global warming potential, i is the time horizon (year), GWP_i is the characterization factor for the substance i (CO_2-eq), and m_i is the mass of the emission substance i (kg), expressed in kg CO_2-eq.

Stratospheric Ozone Depletion (SOD)

The quantification of stratospheric ozone depletion potential that corresponds to stratospheric ozone degradation due to emissions of substances that deplete the ozone layer, such as long-lasting gases containing chlorine and bromine, was estimated using Equation (2):

$$SOD = \sum SOD_i \times m_i \quad (2)$$

where SOD is the stratospheric ozone depletion potential, SOD_i is the characterization factor for the substance i (CFC-11-eq), and m_i is the mass of the emission substance i (kg), expressed in kg CFC-11-eq.

Ionizing Radiation (IR)

The ionizing radiation potential was calculated based on radioactive discharges using Equation (3):

$$IR = \sum IR_i \times m_i \quad (3)$$

where IR is the ionizing radiation potential, IR_i is the characterization factor for the substance i (Co-60-eq), and m_i is the mass of the emission substance i (kBq), expressed in kBq Co-60-eq.

Ozone Formation–Human Health (OFHH)

The ozone formation–human health potential was estimated using Equation (4):

$$OFHH = \sum OFHH_i \times m_i \quad (4)$$

where $OFHH$ is the ozone formation–terrestrial ecosystems potential, $OFHH_i$ is the characterization factor for the substance i (NOx-eq), and m_i is the mass of the emission substance i (kg), expressed in kg NOx-eq.

Fine Particulate Matter Formation (FPMF)

The fine particulate matter formation potential was calculated according to Equation (5):

$$FPMF = \sum FPMF_i \times m_i \quad (5)$$

where *FPMF* is the fine particulate matter formation potential, $FPMF_i$ is the characterization factor for the substance *i* ($PM_{2.5}$-eq), and m_i is the mass of the emission substance *i* (kg), expressed in kg $PM_{2.5}$-eq.

Ozone Formation–Terrestrial Ecosystems (OFTE)

The ozone formation–terrestrial ecosystems potential was estimated using Equation (6):

$$OFTE = \sum OFTE_i \times m_i \quad (6)$$

where *OFTE* is the ozone formation–terrestrial ecosystems potential, $OFTE_i$ is the characterization factor for the substance *i* (NOx-eq), and m_i is the mass of the emission substance *i* (kg), expressed in kg NOx-eq.

Terrestrial Acidification (TA)

The terrestrial acidification potential which refers to the presence of acidifying substances such as NOx, NH_3, and SOx on the terrestrial surface was calculated using Equation (7):

$$TA = \sum TA_i \times m_i \quad (7)$$

where *TA* is the terrestrial acidification potential, TA_i is the characterization factor for the substance *i* (SO_2-eq), and m_i is the mass of the emission substance *i* (kg), expressed in kg SO_2-eq.

Freshwater Eutrophication (FEU)

The freshwater eutrophication potential was calculated using Equation (8):

$$FEU = \sum FEU_i \times m_i \quad (8)$$

where *FEU* is the terrestrial acidification potential, FEU_i is the characterization factor for the substance *i* (P-eq), and m_i is the mass of the emission substance *i* (kg), expressed in kg P-eq.

Terrestrial Ecotoxicity (TE)

Toxic impacts affecting the terrestrial surface that are harmful to different species and that alter ecosystem structure and function were calculated using Equation (9):

$$TE = \sum TE_i \times m_i \quad (9)$$

where *TE* is the terrestrial acidification potential, TE_i is the characterization factor for the substance *i* (1,4-DCB-eq), and m_i is the mass of the emission substance *i* (kg), expressed in kg 1,4-DCB-eq.

Freshwater Ecotoxicity (FEC)

Toxic impacts affecting freshwater that are harmful to different species and that alter ecosystem structure and function were calculated according to Equation (10):

$$FEC = \sum FEC_i \times m_i \quad (10)$$

where *FEC* is the freshwater ecotoxicity potential, FEC_i is the characterization factor for the substance *i* (1,4-DCB-eq), and m_i is the mass of the emission substance *i* (kg), expressed in kg 1,4-DCB-eq.

Marine Ecotoxicity (ME)

Toxic impacts affecting marine waters that are harmful to different species and that alter ecosystem structure and function were calculated using Equation (11):

$$ME = \sum ME_i \times m_i \quad (11)$$

where ME is the marine ecotoxicity potential, ME_i is the characterization factor for the substance i (1,4-DCB-eq), and m_i is the mass of the emission substance i (kg), expressed in kg 1,4-DCB-eq.

Human Carcinogenic Toxicity (HCT)

Toxic impacts affecting human health by absorption of toxic substances by inhalation of air, ingestion of food or water, or penetration through the skin insofar as they are related to cancer were measured using Equation (12):

$$HCT = \sum HCT_i \times m_i \quad (12)$$

where HCT is the human carcinogenic toxicity potential, HCT_i is the characterization factor for the substance i (1,4-DCB-eq), and m_i is the mass of the emission substance i (kg), expressed in kg 1,4-DCB-eq.

Human Non-Carcinogenic Toxicity (HNCT)

Toxic impacts affecting human health by absorption of toxic substances by inhalation of air, ingestion of food or water, or penetration through the skin unrelated to cancer were measured using Equation (13):

$$HNCT = \sum HNCT_i \times m_i \quad (13)$$

where $HNCT$ is the human non-carcinogenic toxicity potential, $HNCT_i$ is the characterization factor for the substance i (1,4-DCB-eq), and m_i is the mass of the emission substance i (kg), expressed in kg 1,4-DCB-eq.

Mineral Resource Scarcity (MRS)

The mineral resource scarcity potential that references the consumption of materials extracted from nature, such as metals and rocks, was calculated using Equation (14):

$$MRS = \sum MRS_i \times m_i \quad (14)$$

where MRS is the mineral resource scarcity potential, MRS_i is the characterization factor for the substance i (Cu-eq), and m_i is the mass of the emission substance i (kg), expressed in kg Cu-eq.

Fossil Resource Scarcity (FRS)

The fossil resource scarcity potential that refers to the use of fuels from petroleum, coal or non-renewable natural gas was calculated according to Equation (15):

$$FRS = \sum FRS_i \times m_i \quad (15)$$

where FRS is the fossil resource scarcity potential, FRS_i is the characterization factor for the substance i (oil-eq), and m_i is the mass of the emission substance i (kg), expressed in kg oil-eq.

Land Use (LU)

The land use impact that considers the effects of land use, the extent of the surface involved and the duration of its occupation was estimated using Equation (16):

$$LU = \sum CF \times E_i \quad (16)$$

where LU is the land use impact, CF is the characterization factor, and E_i is the emission inventory, being expressed in m^2a crop-eq.

Water Consumption (WC)

Water consumption was used to measure the amount of water resources consumed. The detailed calculation model is provided by Equation (17):

$$WC = \sum CF \times E_i \quad (17)$$

where WC is the water consumption, CF is the characterization factor, and E_i is the emission inventory, being expressed in m^3.

2.1.4. Interpretation of Results

The LCI and LCIA results of the life cycle assessment of the products from the *Dunaliella salina* biorefinery are considered together so that the information is interpreted and converged in the form of conclusions and recommendations. The results are discussed according to the values characterized by midpoint impact categories, in order to enhance possible comparisons with other studies found in the literature. The values characterized for the environmental impacts of each microalgae bioproduct considered in this study can be consulted in the Supplementary Material (Table S3).

3. Results and Discussion

3.1. Environmental Sustainability Analysis of the Microalgae Biorefinery

Biorefinery is a strategy that facilitates the circular bioeconomy, which assumes great relevance by maximizing revenue and minimizing waste. This biorefinery concept applied to microalgae biomass is an opportunity to improve the use of biomass that, following the cascade principle, has prioritized the production of high-value products before low-value ones. In the state of the art, although many studies have reported the use of microalgae biomass within a biorefinery structure, few have pored over the holistic assessment of the environmental profile. Therefore, here, we evaluate the metrics of seventeen environmental sustainability indicators for the biorefinery of *Dunaliella salina* (Figure 4). The characterized values of the environmental impacts can also be consulted in Supplementary Material (Table S2).

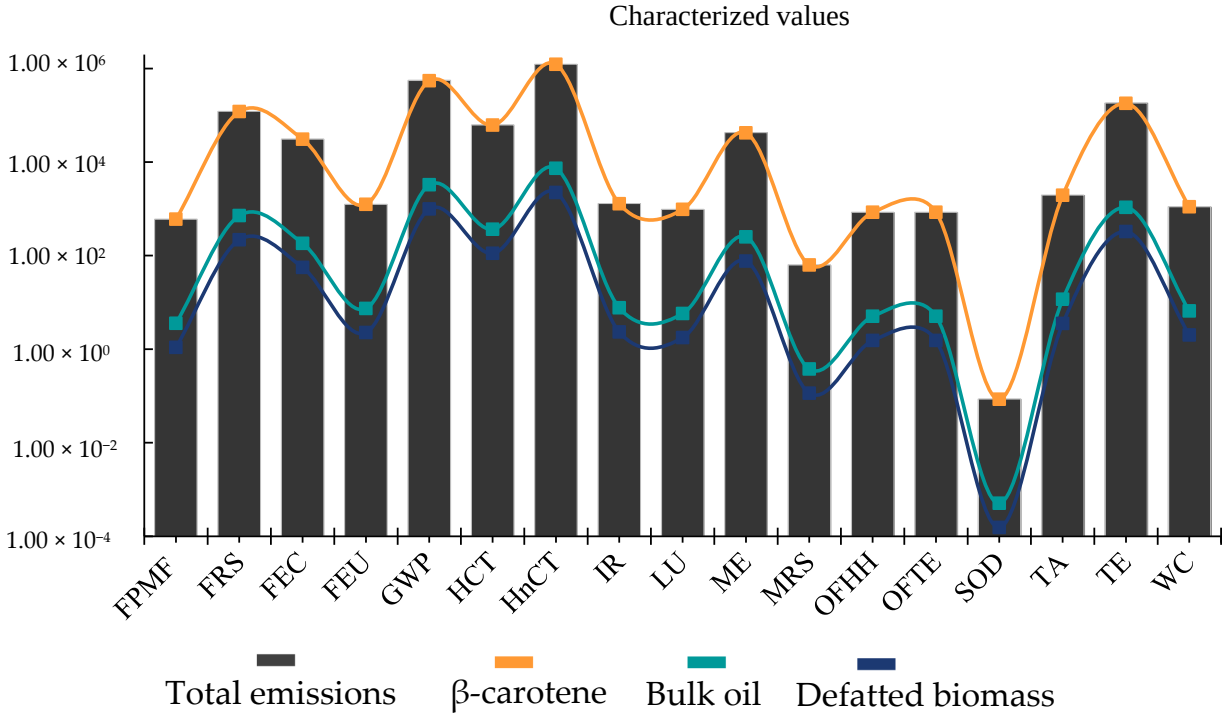


Figure 4. Characterized values of the environmental impact associated with the biorefinery from *Dunaliella salina*. Note: Bioprocesses powered by coal-based energy.

The production of 1 ton of β-carotene, 1.51 tons of bulk oil, and 2.34 tons of defatted biomass of the *Dunaliella salina* species in the raceway pond showed total emissions of around 6.04×10^2 kg $PM_{2.5}$-eq for FPMF, 1.21×10^5 kg oil-eq for FRS, 3.09×10^4 kg 1,4-DCB-eq for FEC, 1.25×10^3 kg P-eq for FEU, 5.53×10^5 kg CO_2-eq for GWP, 6.20×10^4 kg 1,4-DBC-eq for HCT, 1.24×10^6 kg 1,4-DBC-eq for HnCT, 1.30×10^3 kBq Co-60-eq for IR, 9.78×10^2 m^2a crop-eq for LU, 4.25×10^4 kg 1,4-DBC-eq for ME, 6.35×10^1 kg Cu-eq for MRS, 8.50×10^2 kg NO_x-eq for OFHH, 8.50×10^2 kg NOx-eq for OFTE, 8.55×10^{-2} kg CFC11-eq for SOD, 1.97×10^3 kg SO_2-eq for TA, 1.82×10^5 kg 1,4-DCB-eq for TE, 1.11×10^3 m^3 for WC. As can be seen, the midpoint impact categories of HnCT, followed by the category of FRS, TE, and GWP are the most influential midpoints. SOD followed by the MRS category exhibited, in contrast, the lowest impact among all midpoints in the lifecycle of the biorefinery of *Dunaliella salina*. Also, as can be seen, the environmental profile of the biorefinery of *Dunaliella salina* showed significant variations in impact magnitude, which ranged from 6.35×10^1 kg Cu-eq for MRS to 1.24×10^6 kg 1,4-DBC-eq for HnCT.

According to the results, the contributions of the cultivation step, harvesting, drying, pigment extraction, bulk oil, and defatted biomass to the midpoint impact categories were about 94.73%, 0.37%, 2.66%, 1.47%, 0.59%, and 0.18%, respectively. As for the cultivation step, which contributes most of the environmental impact in the life cycle of the biorefinery of *Dunaliella salina*, when comparing the inventory of the energy demand of cultivation in raceway pond and tubular photobioreactor, it should be noted that cultivation in raceway pond consumes much less energy, thus contributing to the mitigation of pollutant emissions [8].

Comparatively, studies evaluating the environmental profile of producing 1 ton of *Arthrospira platensis* tablets showed impacts of 7.71×10^5 kg CO_2-eq for GWP, 1.32×10^{-3} kg CFC11-eq for SOD, 9.63×10^1 kg SO2-eq for TA and 2.16×10^1 kg P-eq for FEU [30]. When verifying these results, it is possible to state that in terms of GWP, our study presented a 30% reduction in emissions; however, the other categories had higher emissions. In contrast, when analyzing a scenario of trade-offs, the revenue value of biomass presents just 8000 USD/ton, while β-carotene is valued at 790,000 USD/ton. Considering the environmental impacts and revenues of a single product, biomass represents only 1% of return and, therefore, to balance the viability of the process, it would be necessary to produce 99 process cycles to break even the profits. In this way, the impacts of this biotechnological route and the process costs would increase, making the process unfeasible.

When assessing the environmental profile of a high-added-value product such as photosynthetic pigments, studies report that for the GWP, SOD, TA, and FEU categories the environmental burdens were 2.8×10^6 and 1.17×10^6, 6.28×10^4 and 2.64×10^4, 1.49×10^4 and 6.23×10^3, and 5.34×10^3 and 2.24×10^3 for astaxanthin and phycocyanin from *Haematococcus pluvialis* and *Arthrospira platensis*, respectively [6]. These values are higher for the GWP and SOD impact categories, but the TA and FEU categories are slightly similar to the results found in this study. This difference can be attributed to a greater requirement of process steps required for pigment production, such as astaxanthin, which requires the system to present two cultivation stages: tubular photobioreactors and raceway ponds, making the process more emissive. However, even if astaxanthin sales prices (~2500 USD/kg) are higher than β-carotene, the environmental pillar balance should be achieved to make the process sustainable.

In addition, as shown, the residual products: bulk oil and defatted biomass do not contribute significantly to emissions in the life cycle of the biorefinery of *Dunaliella salina*. It is also to be inferred that they do not contribute significantly to the cost and energy demand, thus confirming the paradigm of doing more with less, both in environmental and economic terms. Furthermore, it is worth emphasizing that if these products were produced individually without valorization of waste biomass, they would generate a greater environmental and economic impact.

Additionally, when compared to conventional sources, it is worth mentioning that the oil recovery step of *Dunaliella salina* is about 10 times more electricity intensive than

the soybean oil recovery. Evidently, this represents a huge environmental burden when it comes to overcoming the death valley of the production of bulk oil for fuel purposes, for example. The electricity footprint of microalgae-based processes nearly dooms the mission; but, if considering the expense with fuel in the soy oil recovery, the magnitude of the environmental impact is equivalent. This assertion is legitimized by the data presented by Chen et al. [31].

Furthermore, it is interesting to note that soybean oil recovery is not electricity-intensive but is fuel intensive. Fuel consumption in the oil recovery process from *Dunaliella salina* is, in turn, null. In this sense, when considering the soybean oil recovery inventory, we see that it is not better in pollutant emissions. And when we include the energy expenditure of soybean farming in the oil recovery inventory, the lifecycle emissions are about 1.5 times more significant compared to oil recovery from *Dunaliella salina*. This excludes the energy demand of the unit operations proposed in step 1 (β-carotene production).

Finally, although the microalgae biorefinery concept is powerful, it can be concluded that, despite the microalgae are a unique feedstock, there are technological knots that need to be untied to create a "utopian" system, and not trying to improve the degree of environmental sustainability will make the biorefinery concept applied to microalgae more and more dystopian. The eco-smart substitution of coal-based electricity in microalgae biorefineries can help overcome the environmental deficit presented by projects that are not satisfactory with the environmental impact objectives. Furthermore, it is not news that the ongoing energy transition takes center stage, and not adhering to it could mean falling into a dead end.

3.2. Transposing the Environmental Deficit in Microalgae Biorefinery

The transition from coal-based electricity to clean and renewable sources is not a zero-sum game for the environment. It is actually the "golden thread" that can allow climate conditions to remain hospitable. Therefore, measuring the impact of the transition from high-emission electricity to low-emission sources in biorefineries based on microalgae is part of the puzzle to make them environmentally benign. Figures 5 and 6 show the values characterized for the environmental impact associated with the biorefinery of *Dunaliella salina*, which has its unit operations powered by photovoltaic and wind energy, respectively. Figure 7 is a comparison of the total environmental impact of the biorefinery of *Dunaliella salina* when powered by coal-based, photovoltaic, and wind electricity.

As can be seen in Figures 5 and 7, the replacement from coal-based electricity to photovoltaics contributes to reducing lifecycle emissions from the biorefinery of *Dunaliella salina* in 14 of the 17 midpoint impact categories. In the categories of FPMF, FRS, FEC, FEU, GWP, HCT, HnCT, OFHH, OFTE, SOsD, TA, ME, and WC the environmental impacts are one to two orders of magnitude smaller. The environmental impact associated with LU, TE, and IR, in turn, are in the same order of magnitude, and only for MRS the magnitude of the impact is greater, and, therefore, their differences are not within the uncertainty of the predicted impact.

In contrast, the use of wind electricity in the unit operations of the microalgae biorefinery when compared to the use of coal-based and photovoltaic electricity carries the lowest environmental impact in 16 and 15 of the 17 midpoint categories, respectively. Considering the use of wind energy, the impacts associated with HCT and LU are of the same magnitude as for the use of fossil energy; however, the impact in the HCT category is an order of magnitude greater than for the use of photovoltaic energy. And in the MRS category, although it is within the same order of magnitude as the use of photovoltaic energy, it is an order of magnitude greater than the use of fossil energy. In sum, as can be seen in Figure 7, under an overview of the results, the electricity source that most contribute to reducing the environmental burden in microalgae-based biorefineries is wind, followed by photovoltaics. Additionally, from these results, it is clear that replacing the electrical matrix in a microalgae biorefinery is a sure-shot target. It also cannot be neglected that renewable

energy is becoming as cheap as fossil energy and it is possible that they will take control of electricity generation in the world [32].

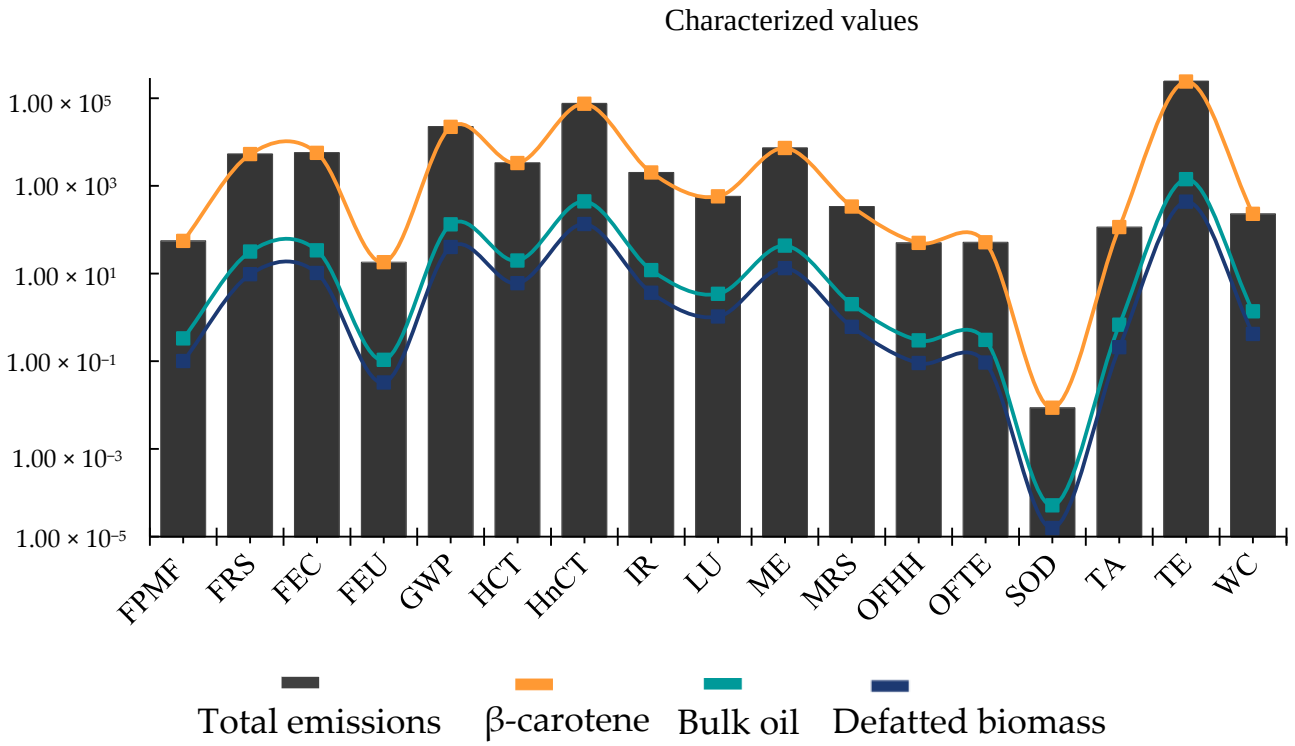


Figure 5. Characterized values of the environmental impact associated with the biorefinery from *Dunaliella salina*. Note: Bioprocesses powered by photovoltaic energy from amorphous silicon solar cells (a-Si).

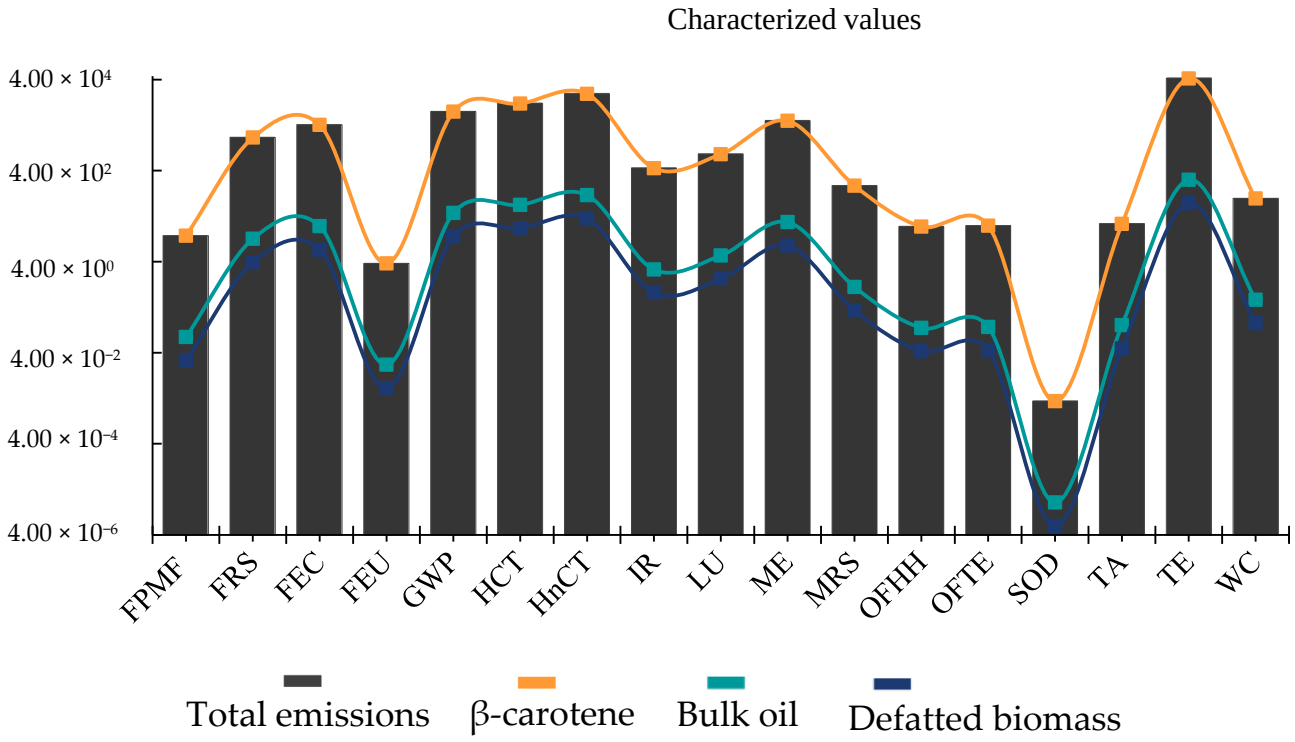


Figure 6. Characterized values of the environmental impact associated with the biorefinery from *Dunaliella salina*. Note: Bioprocesses powered by onshore wind energy.

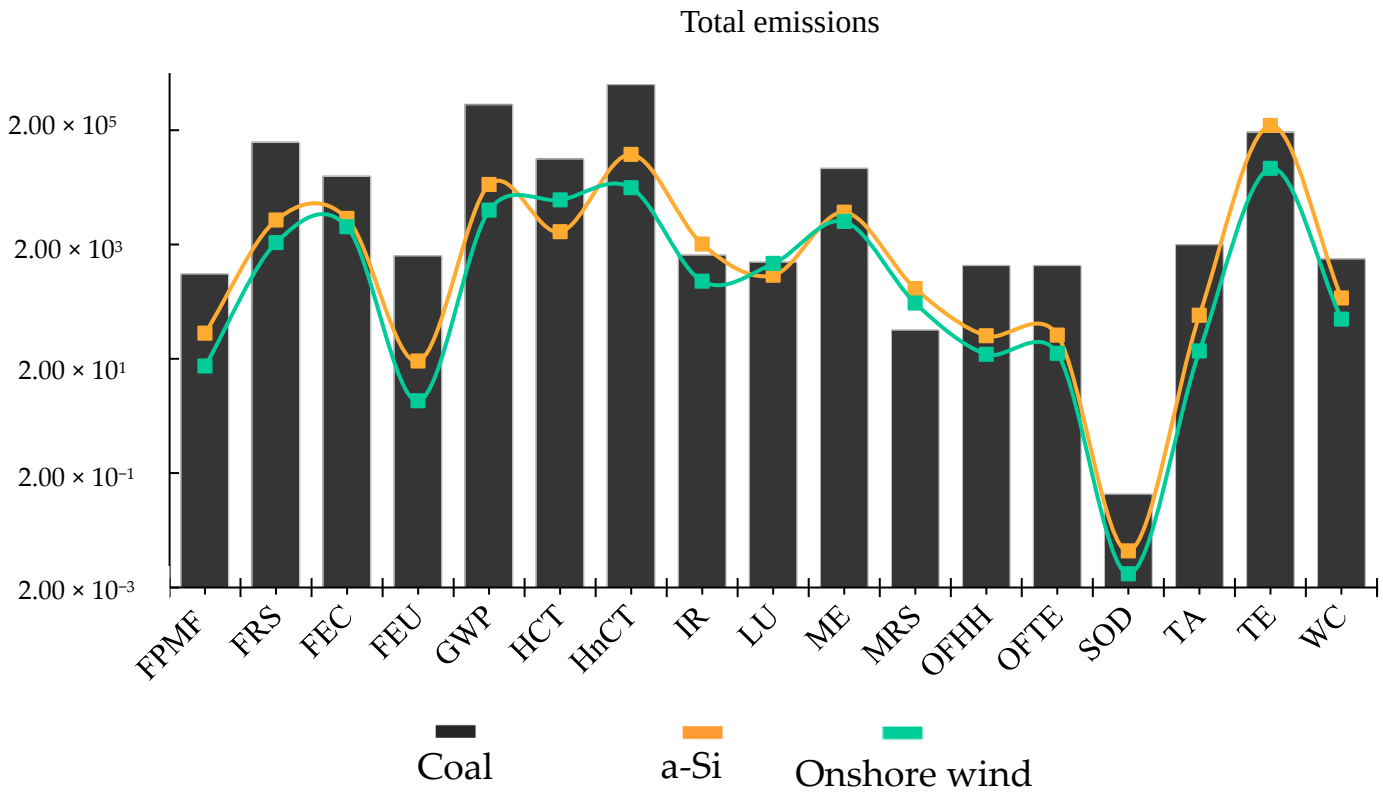


Figure 7. Characterized values of the total environmental impact associated with the biorefinery from *Dunaliella salina*. Note: Bioprocesses driven by different sources of electrical energy.

Finally, it is important to mention that many microalgae-based products languish in the research and development phase because there is a path full of problematic obstacles. However, even with their early potential weakened after setbacks, many microalgae products remain a tempting biobased solution, with some stakeholders still chasing them. The biorefinery following the principles of a circular bioeconomy has supported the long road ahead of low-value microalgae products. But, unless companies, researchers, industry, and government demonstrate their ingenuity and collaboration, microalgae biotechnology will continue to be a game played by those who can afford it and tolerate the high risks.

4. Conclusions

Our study highlighted that the valorization of bio-wastes from a biotechnological high-value route, such as the production of β-carotene, resulted in secondary bioproducts with a small if not almost negligible, collection of ecological footprint, cost, and energy demand, under the guise of a microalgae-based biorefinery. In addition, among our findings, the switching from coal-based electricity to renewable energy contributed to reducing lifecycle emissions from the biorefinery from *Dunaliella salina*. In addition, it was possible to verify that the source of electricity that most contribute to reducing the environmental load in microalgae-based biorefineries is wind power. Thus, we underscore that the transition from coal-based to renewable electricity is the backbone for conducting climate-neutral operations. The answers found in this study allow us to understand that the concept of biorefinery applied to microalgae capacitate circular production systems, and that the use of eco-friendly energy makes them more emission-efficient.

Supplementary Materials: The following supporting information can be downloaded at: https://www.mdpi.com/article/10.3390/su151511494/s1, Table S1: Overview of potential applications and market estimation of microalgae-based bioproducts [33]; Table S2: Characterization factors of the environmental impacts for onshore wind, photovoltaic from amorphous silicon solar cells (a-Si),

and coal-based fossil energy [16,18]; Table S3: Characterized values of the environmental impact associated with the biorefinery from *Dunaliella salina*.

Author Contributions: R.R.D.: Conceptualization, Methodology, Data curation, Writing—original draft. M.C.D.: Methodology, Data curation. C.R.d.M.: Funding acquisition. L.Q.Z.: Supervision, Funding acquisition. E.J.-L.: Conceptualization, Project administration, Writing—review and editing. All authors have read and agreed to the published version of the manuscript.

Funding: This research was supported by the National Council for Scientific and Technological Development—Brazil (CNPq), and the Coordination for the Improvement of Higher Education Personnel—Brazil (CAPES)—Finance Code 001.

Institutional Review Board Statement: Not applicable.

Informed Consent Statement: Not applicable.

Data Availability Statement: The datasets used and analyzed during the current study are available from the corresponding author upon reasonable request.

Acknowledgments: The authors would like to thank the National Council for Scientific and Technological Development—Brazil (CNPq), and the Coordination for the Improvement of Higher Education Personnel—Brazil (CAPES).

Conflicts of Interest: The authors declare that they have no known competing financial interests or personal relationships that could have appeared to influence the work reported in this paper.

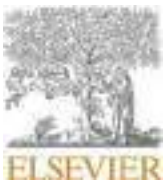
References

1. Steffen, W.; Richardson, K.; Rockström, J.; Cornell, S.E.; Fetzer, I.; Bennett, E.M.; Biggs, R.; Carpenter, S.R.; De Vries, W.; De Wit, C.A.; et al. Planetary boundaries: Guiding human development on a changing planet. *Science* **2015**, *347*, 1259855. [CrossRef] [PubMed]
2. Persson, L.; Carney Almroth, B.M.; Collins, C.D.; Cornell, S.; de Wit, C.A.; Diamond, M.L.; Fantke, P.; Hassellöv, M.; MacLeod, M.; Ryberg, M.W.; et al. Outside the safe operating space of the planetary boundary for novel entities. *Environ. Sci. Technol.* **2022**, *56*, 1510–1521. [CrossRef] [PubMed]
3. Palahi, M.; Adams, J. Why the world needs a 'circular bioeconomy'—For jobs, biodiversity and prosperity. In *World Economic Forum*; World Economic Forum: Cologny, Switzerland, 2020.
4. Tan, E.C.; Lamers, P. Circular bioeconomy concepts—A perspective. *Front. Sustain.* **2021**, *2*, 701509. [CrossRef]
5. Premaratne, M.; Nishshanka, G.K.S.H.; Anthonio, R.A.D.P.; Liyanaarachchi, V.C.; Thevarajah, B.; Nimarshana, P.H.V.; Malik, A.; Ariyadasa, T.U. Resource recovery from waste streams for production of microalgae biomass: A sustainable approach towards high-value biorefineries. *Bioresour. Technol. Rep.* **2022**, *18*, 101070. [CrossRef]
6. Deprá, M.C.; Severo, I.A.; dos Santos, A.M.; Zepka, L.Q.; Jacob-Lopes, E. Environmental impacts on commercial microalgae-based products: Sustainability metrics and indicators. *Algal Res.* **2020**, *51*, 102056. [CrossRef]
7. Calijuri, M.L.; Silva, T.A.; Magalhães, I.B.; de Paula Pereira, A.S.A.; Marangon, B.B.; de Assis, L.R.; Lorentz, J.F. Bioproducts from microalgae biomass: Technology, sustainability, challenges and opportunities. *Chemosphere* **2022**, *305*, 135508. [CrossRef]
8. Liyanaarachchi, V.C.; Premaratne, M.; Ariyadasa, T.U.; Nimarshana, P.H.V.; Malik, A. Two-stage cultivation of microalgae for production of high-value compounds and biofuels: A review. *Algal Res.* **2021**, *57*, 102353. [CrossRef]
9. Ruiz, J.; Wijffels, R.H.; Dominguez, M.; Barbosa, M.J. Heterotrophic vs. autotrophic production of microalgae: Bringing some light into the everlasting cost controversy. *Algal Res.* **2022**, *64*, 102698. [CrossRef]
10. Borowitzka, M.A. Energy from microalgae: A short history. In *Algae for Biofuels and Energy*; Springer: Berlin/Heidelberg, Germany, 2012; pp. 1–15.
11. Ubando, A.T.; Felix, C.B.; Chen, W.H. Biorefineries in circular bioeconomy: A comprehensive review. *Bioresour. Technol.* **2020**, *299*, 122585. [CrossRef]
12. Dias, R.R.; Deprá, M.C.; Zepka, L.Q.; Jacob-Lopes, E. Roadmap to net-zero carbon emissions in commercial microalgae-based products: Environmental sustainability and carbon offset costs. *J. Appl. Phycol.* **2022**, *34*, 1255–1268. [CrossRef]
13. *ISO-14040*; Environmental Management–Life Cycle Assessment–Principles and Framework. International Organization for Standardization: Geneva, Switzerland, 2006.
14. Xi, Y.; Bian, J.; Luo, G.; Kong, F.; Chi, Z. Enhanced β-carotene production in *Dunaliella salina* under relative high flashing light. *Algal Res.* **2022**, *67*, 102857. [CrossRef]
15. de Souza Celente, G.; Rizzetti, T.M.; Sui, Y.; de Souza Schneider, R.D.C. Potential use of microalga *Dunaliella salina* for bioproducts with industrial relevance. *Biomass Bioenergy* **2022**, *167*, 106647. [CrossRef]
16. Milousi, M.; Souliotis, M.; Arampatzis, G.; Papaefthimiou, S. Evaluating the environmental performance of solar energy systems through a combined life cycle assessment and cost analysis. *Sustainability* **2019**, *11*, 2539. [CrossRef]

17. dos Santos, A.M.; Deprá, M.C.; dos Santos, A.M.; Cichoski, A.J.; Zepka, L.Q.; Jacob-Lopes, E. Sustainability metrics on microalgae-based wastewater treatment system. *Desalin. Water Treat.* **2020**, *185*, 51–61. [CrossRef]
18. Hosseini, S.M.; Kanagaraj, N.; Sadeghi, S.; Yousefi, H. Midpoint and endpoint impacts of electricity generation by renewable and nonrenewable technologies: A case study of Alberta, Canada. *Renew. Energy* **2022**, *197*, 22–39. [CrossRef]
19. Maroneze, M.M.; Dias, R.R.; Severo, I.A.; Queiroz, M.I. Microalgae-Based Processes for Pigments Production. In *Pigments from Microalgae Handbook*; Springer: Berlin/Heidelberg, Germany, 2020; pp. 241–264.
20. Deprá, M.C.; dos Santos, A.M.; Jacob-Lopes, E. Sustainability metrics in the microalgae-based pigments production: A life cycle assessment approach. In *Pigments from Microalgae Handbook*; Springer: Berlin/Heidelberg, Germany, 2020; pp. 363–390.
21. Peralta-Ruiz, Y.; González-Delgado, A.D.; Kafarov, V. Evaluation of alternatives for microalgae oil extraction based on exergy analysis. *Appl. Energy* **2013**, *101*, 226–236. [CrossRef]
22. Lardon, L.; Hélias, A.; Sialve, B.; Steyer, J.P.; Bernard, O. Life-cycle assessment of biodiesel production from microalgae. *Environ. Sci. Technol.* **2009**, *43*, 6475–6481. [CrossRef]
23. Martinez-Guerra, E.; Gude, V.G. Energy aspects of microalgal biodiesel production. *Aims Energy* **2016**, *4*, 347–362. [CrossRef]
24. Corrêa, P.S.; Morais Júnior, W.G.; Martins, A.A.; Caetano, N.S.; Mata, T.M. Microalgae biomolecules: Extraction, separation and purification methods. *Processes* **2020**, *9*, 10. [CrossRef]
25. Patel, S.; Kannan, D.C. A method of wet algal lipid recovery for biofuel production. *Algal Res.* **2021**, *55*, 102237. [CrossRef]
26. Valdovinos-García, E.M.; Bravo-Sánchez, M.G.; Olán-Acosta, M.D.L.Á.; Barajas-Fernández, J.; Guzmán-López, A.; Petriz-Prieto, M.A. Technoeconomic Evaluation of Microalgae Oil Production: Effect of Cell Disruption Method. *Fermentation* **2022**, *8*, 301. [CrossRef]
27. Chalermthai, B.; Giwa, A.; Moheimani, N.; Taher, H. Techno-economic strategies for improving economic viability of β-carotene extraction using natural oil and supercritical solvent: A comparative assessment. *Algal Res.* **2022**, *68*, 102875. [CrossRef]
28. Huijbregts, M.A.; Steinmann, Z.J.; Elshout, P.M.; Stam, G.; Verones, F.; Vieira, M.; Zijp, M.; Hollander, A.; Van Zelm, R. ReCiPe2016: A harmonised life cycle impact assessment method at midpoint and endpoint level. *Int. J. Life Cycle Assess.* **2017**, *22*, 138–147. [CrossRef]
29. Jacob-Lopes, E.; Zepka, L.Q.; Deprá, M.C. *Sustainability Indicators and Metrics of Environmental Impact: Industrial and Agricultural Life Cycle Assessment*, 1st ed.; Elsevier: Amsterdam, The Netherlands, 2021.
30. Ye, C.; Mu, D.; Horowitz, N.; Xue, Z.; Chen, J.; Xue, M.; Zhou, W. Life cycle assessment of industrial scale production of spirulina tablets. *Algal Res.* **2018**, *34*, 154–163. [CrossRef]
31. Chen, R.; Qin, Z.; Han, J.; Wang, M.; Taheripour, F.; Tyner, W.; O'Connor, D.; Duffield, J. Life cycle energy and greenhouse gas emission effects of biodiesel in the United States with induced land use change impacts. *Bioresour. Technol.* **2018**, *251*, 249–258. [CrossRef]
32. Roser, M. *Why Did Renewables Become So Cheap So Fast? and What Can We Do to Use This Global Opportunity for Green Growth*; Our World in Data: Oxford, UK, 2020.
33. Mordor Intelligence. Algae Products Market Size & Share Analysis—Growth Trends & Forecasts (2023–2028). 2023. Available online: https://www.mordorintelligence.com/ (accessed on 1 July 2023).

Disclaimer/Publisher's Note: The statements, opinions and data contained in all publications are solely those of the individual author(s) and contributor(s) and not of MDPI and/or the editor(s). MDPI and/or the editor(s) disclaim responsibility for any injury to people or property resulting from any ideas, methods, instructions or products referred to in the content.

Sustainable Energy Technologies and Assessments 58 (2023) 103362



Contents lists available at ScienceDirect

Sustainable Energy Technologies and Assessments

journal homepage: www.elsevier.com/locate/seta



Integrating solar cell technologies in microalgae facilities: Environmental sustainability metrics and indicators

Rosangela Rodrigues Dias, Mariany Costa Deprá, Rafaela Basso Sartori, Adriane Terezinha Schneider, Leila Queiroz Zepka, Eduardo Jacob-Lopes *

Bioprocess Intensification Group, Federal University of Santa Maria (UFSM), Roraima Avenue, 1000, 97105-900 Santa Maria, RS, Brazil

ARTICLE INFO

Keywords:
Algae-based products
Carbon credit
Environmental impact
Life-cycle assessment
Photovoltaics

ABSTRACT

All solar cell technologies have an impact on the environment. So, it is important to consider that the choice of solar cell technology can have a significant influence on the environmental sustainability metrics of microalgae-based processes and products. That's why this article is concerned with scrutinizing the environmental sustainability of integrating solar cell technologies in microalgae facilities. One of the focal aspects of this research is to provide insights to stakeholders in incorporating photovoltaics into their facilities. Four solar cell technologies, namely, single-crystalline silicon, multi-crystalline silicon, copper-indium-diselenide, and amorphous silicon were investigated. The results of the study confirm that the choice of solar cell technology can further reduce the metrics of environmental sustainability indicators of microalgae-based processes and products. The energy use from the lowest emitting technology versus the highest emitting technology can lead to a reduction in sustainability metrics of 1.13 to 9.04 times. It was also revealed, from weighting the results, that integrating microalgae production with amorphous silicon solar cell technology has a lower overall environmental impact, followed sequentially by copper-indium-diselenide, multi-crystalline silicon, and monocrystalline silicon. These results provide guidance for the environmentally conscious integration of photovoltaics in microalgae facilities.

Introduction

Sustainability metrics and indicators studies show that most if not almost all the environmental impact of commercial microalgae-based products is attributed to electricity-intensive demand in upstream and downstream processes [1–6]. The good news is that the microalgae industry can radically reduce emissions from its operations by transitioning from high-emission energy sources like coal and natural gas to low-emission sources like solar photovoltaics [7–9]. However, while transitioning from fossil-based energy to solar photovoltaics is better for the environmental sustainability metrics of microalgae products, no form of energy – renewable or not – is impact free [10]. Therefore, it's helpful to know that, despite solar cell technologies being a shining symbol of environmental virtue, they leave a trail of pollution often overlooked in studies on photovoltaic technologies integration [11,12].

In fact, there are several studies that describe the different technologies for photovoltaic energy generation, but few comparatively analyze the contribution of each one to the emissions of processes and products powered by these technologies [13–16]. Thus, although the integration of solar energy into manufacturing has become an icon of all that is green, there are no clear directions for choosing photovoltaic technology. Furthermore, the few studies that report the eco-profile of these technologies present metrics for a limited number of environmental impact indicators, making it difficult to holistically understand their inherent environmental peculiarities [10,12,17,18].

Against this background, the rationale of this study and the main objective of the article is to provide a holistic assessment of the environmental profile of the integration of solar cell technologies in powering microalgae facilities, which could be a baseline for microalgae producers and non-specialists in the solar energy field. The present study compares the metrics of seventeen environmental impact indicators of microalgae-based products powered by photovoltaic energy from solar cell technologies with the highest levels of technology readiness [18]. The impact on microalgae product metrics when using energy from one technology over another is shown individually by midpoint impact category and weighted to show among solar cell technologies the one with the lowest overall environmental impact by endpoint category and global — that includes all midpoint categories.

So far, the research found in the literature does not point to the use of

* Corresponding author.
E-mail address: ejacoblopes@gmail.com (E. Jacob-Lopes).

https://doi.org/10.1016/j.seta.2023.103362
Received 29 September 2022; Received in revised form 22 June 2023; Accepted 30 June 2023
2213-1388/© 2023 Elsevier Ltd. All rights reserved.

Nomenclature

Abbreviations

a-Si	Amorphous Silicon
CdTe	Cadmium Telluride
CIS	Copper-Indium-diSelenide
CO_2	Carbon Dioxide
DHA	Docosahexaenoic Acid
EPA	Eicosapentaenoic Acid
EU ETS	European Union Emissions Trading System
FE	Freshwater Eutrophication
FET	Freshwater Ecotoxicity
FPMF	Fine Particulate Matter Formation
FRS	Fossil Resource Scarcity
GW	Global Warming
HCT	Human Carcinogenic Toxicity
HNCT	Human Non-Carcinogenic Toxicity
IR	Ionizing Radiation
ISO	International Organization for Standardization
kW	Kilowatt
LCA	Life Cycle Assessment
LCI	Life Cycle Inventory
LCIA	Life Cycle Impact Assessment
LU	Land Use
mc-Si	Multi-Crystalline Silicon
ME	Marine Ecotoxicity
MRS	Mineral Resource Scarcity
OFHH	Ozone Formation–Human Health
OFTE	Ozone Formation–Terrestrial Ecosystems
sCO_2	Supercritical Carbon Dioxide
sc-Si	Single-Crystalline Silicon
SOD	Stratospheric Ozone Depletion
TA	Terrestrial Acidification
TE	Terrestrial Ecotoxicity
USD	United States Dollar
WC	Water Consumption

a specific solar cell technology to generate photovoltaic energy to meet energy demand, whether from the microalgae industry or not. Therefore, in this article, we give a step ahead to provide valuable guidance in terms of choosing solar cell technology to further reduce emissions from commercial processes and products. To this end, the research questions in this article aim to (1) assess the environmental profile of integrating solar cell technologies into microalgae facilities through a cradle-to-gate life cycle assessment of microalgae-based products, (2) identify the metrics for seventeen environmental impact indicators, (3) weight life cycle assessment results to support decision-making, and (4) estimate carbon credit revenues by replacing coal-based energy consumption with photovoltaics in microalgae facilities. This study provides insights that can help not only the microalgae industry but also decision-makers and stakeholders who wish to integrate photovoltaics into their manufacturing facilities.

Methodology

The methodological steps of the study are shown in Fig. 1. The assumptions and procedures for each step are described in detail below.

Life cycle assessment (LCA)

The life cycle assessment (LCA) methodology standardized by ISO

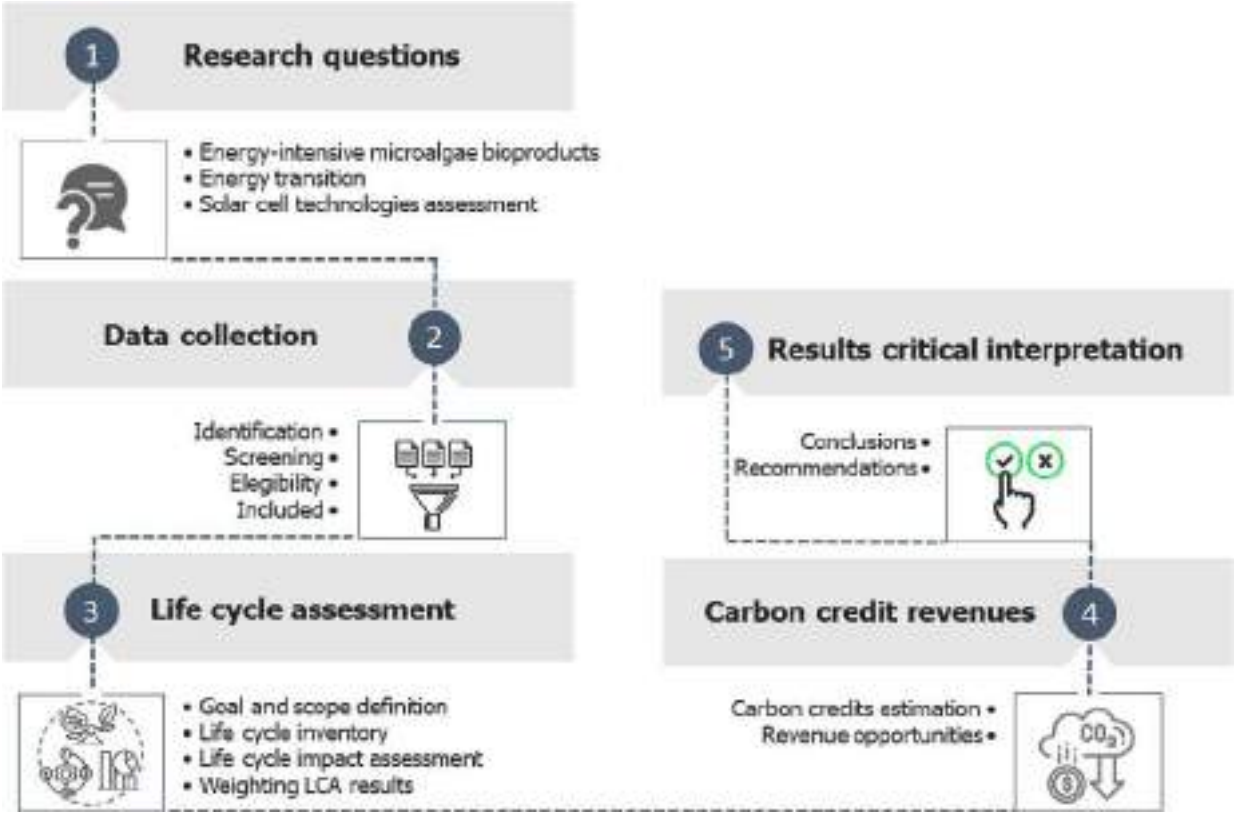


Fig. 1. Methodological steps of the study.

14040 was adopted to quantify the potential environmental impacts of processes and products based on microalgae powered by photovoltaic energy from different solar cell technologies [19]. The LCA, as detailed below, included the goal and scope definition (I), inventory analysis (II), impact assessment (III), and interpretation of results (IV).

Goal and scope definition of the LCA

The main objective of the application of the LCA was to evaluate the environmental footprint of microalgae-based commercial products powered by photovoltaic energy from single-crystalline silicon solar cells (sc-Si), multi-crystalline silicon (mc-Si), copper-indium-diselenide (CIS), and amorphous silicon (a-Si). The environmental footprint of microalgae products powered by coal-based energy was also evaluated. The commercial products considered were whole dried biomass from *Chlorella vulgaris* and *Arthrospira platensis*, β-carotene from *Dunaliella salina*, astaxanthin from *Haematococcus pluvialis*, phycocyanin from *Arthrospira platensis*, docosahexaenoic acid (DHA) from *Crypthecodinium cohnii*, and eicosapentaenoic acid (EPA) from *Nitzschia laevis*. The data for analysis are based on biotechnological routes consolidated obtained from Deprá et al. [4].

The study considered a functional unit of 1 t month^{-1} of product. The boundaries of the study system were defined from the life cycle of the cradle-to-gate. Only emissions associated with electricity consumption were accounted for. The layout of the system boundaries defined from the cradle to the gate with the technical characteristics is shown in Fig. S1 (Supplementary Material).

Life cycle inventory (LCI)

The species of microalgae (*Chlorella vulgaris*, *Arthrospira platensis*, *Dunaliella salina*, *Haematococcus pluvialis*, *Crypthecodinium cohnii*, and *Nitzschia laevis*), the production systems (raceway ponds, tubular photobioreactors, and fermenters) and the final products (whole dried biomass, pigments, and polyunsaturated fatty acids) were chosen for analysis aiming to simulate the industrial production processes. The productivity data was estimated according to values reported by Deprá et al. [4]. The physical method of drying by spray-dryer and the extraction using supercritical carbon dioxide (sCO_2) was assumed as the methods of downstream processing. The electricity requirement for the production of 1 t month^{-1} of microalgae-based products was estimated according to Deprá et al. [4] and Dias et al. [7]. The electricity demand needed to operate the microalgae production systems is shown in Table S1 (Supplementary Material). The input and output conditions of the microalgae-based product production processes are shown in Table 1.

Life cycle impact assessment (LCIA)

The potential environmental impacts of microalgae-based processes and products powered by photovoltaic energy from different solar cell technologies were calculated according to the ReCiPe midpoint method (hierarchical approach) [20] and consistently applied accordingly with Maroneze et al. [21] and Jacob-Lopes et al. [22]. The calculation model is given in Eq. (1). The characterization phase was performed considering the following midpoint impact categories: global warming (i), stratospheric ozone depletion (ii), ionizing radiation (iii), ozone formation–human health (iv), fine particulate matter formation (v), ozone formation–terrestrial ecosystems (vi), terrestrial acidification (vii), freshwater eutrophication (viii), terrestrial ecotoxicity (ix), freshwater ecotoxicity (x), marine ecotoxicity (xi), human carcinogenic toxicity (xii), human non-carcinogenic toxicity (xiii), mineral resource scarcity (xiv), fossil resource scarcity (xv), land use (xvi), and water consumption (xvii). The characterization factors are presented in the Supplementary Material (Table S2). Details of the calculation model for each of the seventeen impact categories are also shown in the Supplementary Material.

$$IC = \Sigma CF \times EI \quad (1)$$

where IC is the environmental impact category, CF is the characterization factor, and EI is the emission inventory.

LCA interpretation

The LCI and LCIA results from the life cycle assessment of microalgae-based products are considered together so that the information is interpreted and converged in the form of conclusions and recommendations. The midpoint impact categories are discussed within their respective endpoint categories. The results are representatively discussed from the whole dried biomass of *Arthrospira platensis*. The characterized values of the environmental impacts of each microalgae product considered in this study can be consulted in the Supplementary Material (Table S3).

Weighting LCA results

The weighting process in this study consists of applying a specific weight to each of the solar cell technologies that express their degree of importance within each midpoint impact category. To create a single score and arrive at an intensity scale for the overall environmental impact of each technology on emissions from microalgae processes and products a weight for each solar cell technology, namely 1, 2, 3, and 4 was applied. Simply put, within each midpoint impact category, weight 1 corresponds to the solar cell technology that contributes less to the impact of the microalgae products, and so on, with weight 4 corresponding to the technology that contributes most to the environmental impact. Adding up the weights of the respective midpoint categories of the damage areas: human health, ecosystem quality, resource consumption, and climate change, an endpoint intensity scale was arrived at for the overall environmental impact of each technology on emissions from microalgae processes and products. A global intensity scale was also obtained by summing the weights of the seventeen midpoint categories.

Estimating carbon credit revenues

The carbon credits were estimated according to the carbon footprint of microalgae-based processes and products, and the current carbon prices suggested by the European Union Emissions Trading Scheme (EU ETS) [23]. The avoided carbon dioxide emissions were quantified according to Eq. (2), following the methodology of Dias et al. [7].

$$CO_{2avoided} = CO_{2conventional} - CO_{2emitted} \quad (2)$$

where $CO_{2avoided}$ is the amount of CO_2 that is no longer emitted (kg CO_2-eq), $CO_{2conventional}$ is the amount of CO_2 released in the conventional production process powered by coal-based electricity (kg CO_2-eq), and the $CO_{2emitted}$ is the amount of CO_2 released in the production process powered by photovoltaic electricity (kg CO_2-eq).

Results and discussion

While integrating solar cell technologies into microalgae facilities mitigate significant amounts of emissions due to the avoided use of coal-based electricity [7–9], they also leave a trail of environmental pollution and may not be as green as they appear [10–12]. Indeed, despite the overall track record of integrating solar cell technologies into manufacturing facilities is good, the technology used to generate photovoltaic energy to power microalgae-based processes can make a difference in the lifecycle emissions balance of these products. Therefore, operating in light of the recognition that the environmental sustainability metrics of microalgae products can be improved, it is useful

Table 1
Energy requirement for the production of 1 t month^{-1} of whole dried biomass, pigment, and polyunsaturated fatty acid. Adapted from Deprá et al. [4] and Dias et al. [7].

Process	Unit	*Chlorella vulgaris* biomass in RP	*Chlorella vulgaris* biomass in TPBR	*Arthrospira platensis* biomass in RP	Phycocyanin from *Arthrospira platensis*	β-carotene from *Dunaliella salina*	Astaxanthin from *Haematococcus pluvialis*	DHA from *Crypthecodinium cohnii*	EPA from *Nitzschia laevis*
Cultivation									
Input									
Tubular photobioreactor	m^3	–	47.62	–	–	–	100.27	–	–
Chemical sterilization (sodium hypochlorite)	kg month^{-1}	–	7.14	–	–	–	15.04	–	–
Energy consumption for cooling	kWh month^{-1}	–	514,285.71	–	–	–	1,082,891.70	–	–
Aeration energy	kWh month^{-1}	–	4,457.14	–	–	–	9,385.06	–	–
Pumping (riser and degasser)	kWh month^{-1}	–	32,571.43	–	–	–	68,583.14	–	–
CO_2 consumption	kg	–	1,500.00	–	–	–	1,804.82	–	–
Water evaporation	m^3	–	0.10	–	–	–	0.20	–	–
Fermenter	m^3	–	–	–	–	–	–	27.77	133.33
Physical sterilization	kWh month^{-1}	–	–	–	–	–	–	200.48	962.67
Agitation	kWh month^{-1}	–	–	–	–	–	–	145.94	700.80
Aeration	kWh month^{-1}	–	–	–	–	–	–	19,992.00	96,000.00
Raceway pond	m^3	166.67	–	104.17	1,388.54	925.93	2,677.23	–	–
Electric energy for paddle wheel	kWh month^{-1}	64,800.00	–	40,500.00	539,865.00	360,000.00	1,040,907.90	–	–
Electric energy for water pumping	kWh month^{-1}	12,000.00	–	7,500.00	99,975.00	66,666.67	192,760.72	–	–
Electric energy for CO_2 injection	kWh month^{-1}	39,600.00	–	24,750.00	329,917.50	220,000.00	636,110.38	–	–
CO_2 consumption	kg	2,000.00	–	2,000.00	26,660.00	25,000.00	64,253.57		
Water evaporation	m^3	21.67	–	13.54	180.51	120.37	348.04	–	–
Biomass productivity	kg m^3 month^{-1}	6.00	21.00	9.60	9.60	13.50	12.00	300.00	22.50
Output									
Algae liquid	kg	11,760.00	11,420.00	12,690.00	71,090.00	83,300.00	222,200.00	44,420.00	16,000.00
Harvest									
Input									
Energy consumption centrifugation	kWh month^{-1}	416.67	119.05	260.42	3,471.35	2,314.81	6,943.75	69.42	333.33
Drying									
Input									
Wet biomass	kg	8,820.00	8,550.00	9,510.00	53,310.00	49,980.00	133,320.00	33,300.00	12,000.00
Spray-dryer	kWh month^{-1}	8,523.80	8,229.50	9,275.90	43,578.20	40,853.20	108,989.10	27,217.30	9,810.00
Output									
Whole dried biomass	t	1	1	1	–	–	–	–	–
Extraction									
Input									
Dry biomass	kg	–	–	–	13,330.00	12,500.00	33,330.00	8,330.00	3,000.00
sCO_2	kWh month^{-1}	–	–	–	10,664.00	10,000.00	26,664.00	6,664.00	2,400.0
Output									
Oil-rich pigments	t	–	–	–	1	1	1	–	–
Oil	t	–	–	–		–	–	1	1
Energy	kWh month^{-1}	125,340.47	559,662.83	82,286.32	1,027,471.05	699,834.68	3,173,250.80	54,289.13	110,206.80

Tubular photobioreactor, TPBR; Raceway pond, RP; Docosahexaenoic, DHA; Eicosapentaenoic, EPA; Supercritical CO_2 extraction, sCO_2.

to know the impact of each solar cell technology on the lifecycle of microalgae-based products. Figs. 2-5 shows the potential impact of integrating four solar cell technologies, as well as coal-based energy, on the metrics of environmental sustainability indicators of the whole dried biomass of *Arthrospira platensis*. The values characterized for the potential impacts of the other microalgae-based products considered in this study can be consulted in the Supplementary Material (Table S3).

As can be seen in Fig. 2, in the midpoint categories related to the ecosystem quality damage category, the integration of *Arthrospira platensis* production with CIS solar cell technology, when compared to the other solar cell technologies, contributes to the lower environmental impact attributed to the whole dried biomass in the midpoint categories of ozone formation, terrestrial acidification, and terrestrial ecotoxicity. In the midpoint categories of freshwater eutrophication, freshwater ecotoxicity, and marine ecotoxicity, integration with a-Si solar cell technology carries the least impact. It is observed from these results that the choice of the lowest emission versus the highest emission solar cell technology can lead to a reduction of the environmental impact in the life cycle of microalgae-based products from 1.17 to 2.53 times. The terrestrial ecotoxicity midpoint category is the only one related to the ecosystem quality damage category where the integration of solar cell technologies to power microalgae-based processes does not contribute to reducing the environmental impact of the products when compared to coal-based electricity consumption.

Figs. 3 and 4, in turn, present the metrics for environmental impact indicators related to the damage category: resource consumption and human health, respectively. The integration of *Arthrospira platensis* production with CIS and a-Si solar cell technologies contributes to the lowest environmental impact attributed to whole dried biomass in eight of the ten midpoint categories. In Fig. 3 and in Fig. 4, respectively, the integration with the lowest emission versus the highest emission solar cell technology can lead to a reduction in the environmental sustainability metrics of the whole dried biomass of *Arthrospira platensis* from 1.28 to 9.04 times and from 1.13 to 1.56 times. The integration of solar cell technologies to power microalgae production processes when compared to coal-based electricity consumption is discouraging only for the metrics of the indicators of ionizing radiation and fossil resource scarcity. However, the impact on sustainability metrics of microalgae-based products when consuming coal-based electricity or solar cell technologies for these categories — including the terrestrial ecotoxicity midpoint category — are of the same order of magnitude and, therefore, it can be inferred that their differences are within the uncertainty of the predicted impacts.

In contrast, as shown in Fig. 5, the impact associated with coal-based electricity consumption compared to the consumption of electricity generated by photovoltaic technologies for the global warming midpoint category is an order of magnitude higher and, therefore, is not within the uncertainty of the predicted impacts. As can be seen in Fig. 5, among solar cell technologies, integration with CIS technology followed by the a-Si is the one that most contribute to reducing the impact of the whole dried biomass of *Arthrospira platensis* and other commercial microalgae products (See Table S3). Integrating lowest-emission versus highest-emission solar cell technology achieved a 1.33 times reduction in environmental impact.

In light of these results, it is possible to conclude that the transition from the use of coal-based energy, as well as the choice of solar cell technology to power the microalgae-based product production processes, can result in ecological consequences that can be more or less

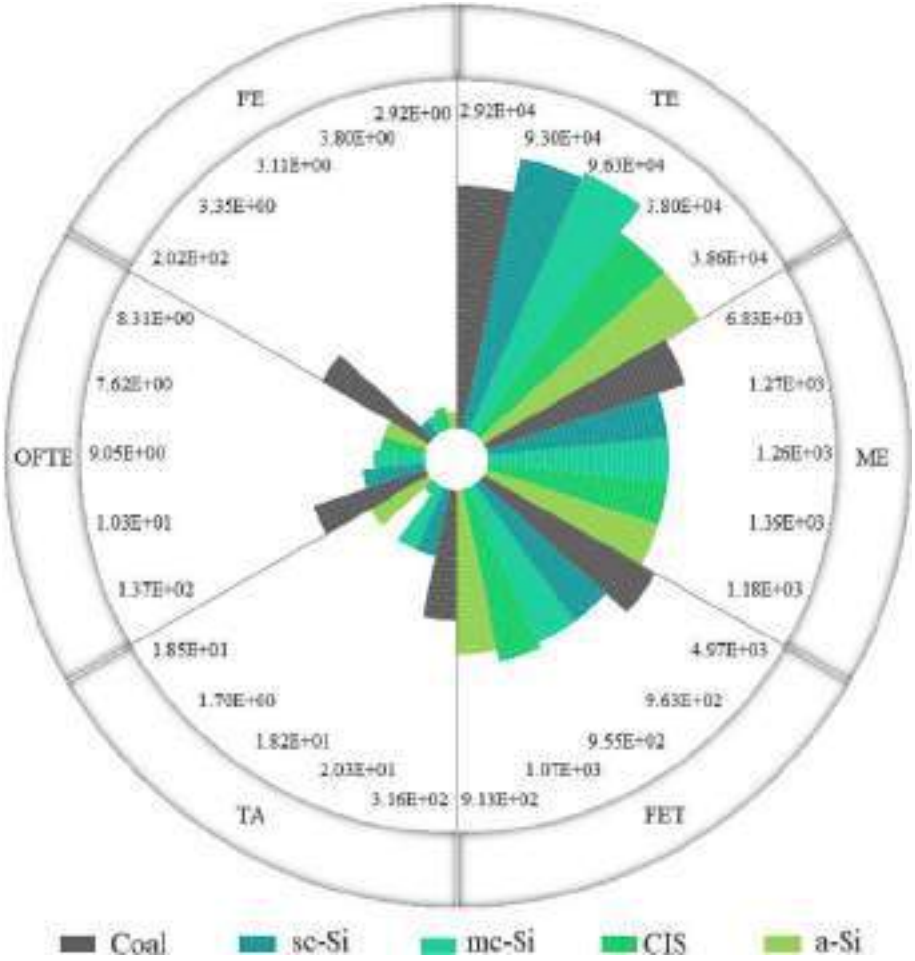


Fig. 2. Impacts associated with coal-based versus solar photovoltaic energy consumption by solar cell technology per 1 t month^{-1} of whole dried biomass of *Arthrospira platensis*. Amorphous silicon, a-Si; Copper-indium-diselenide, CIS; Multi-crystalline silicon, mc-Si; Single-crystalline silicon, sc-Si; Terrestrial ecotoxicity, TE (kg 1,4-DCB-eq); Freshwater eutrophication, FE (kg P-eq); Freshwater ecotoxicity, FET (kg 1,4-DCB-eq); Marine ecotoxicity, ME (kg 1,4-DCB-eq); Terrestrial acidification, TA (kg SO_2-eq); Ozone formation–terrestrial ecosystems, OFTE (kg NOx-eq).

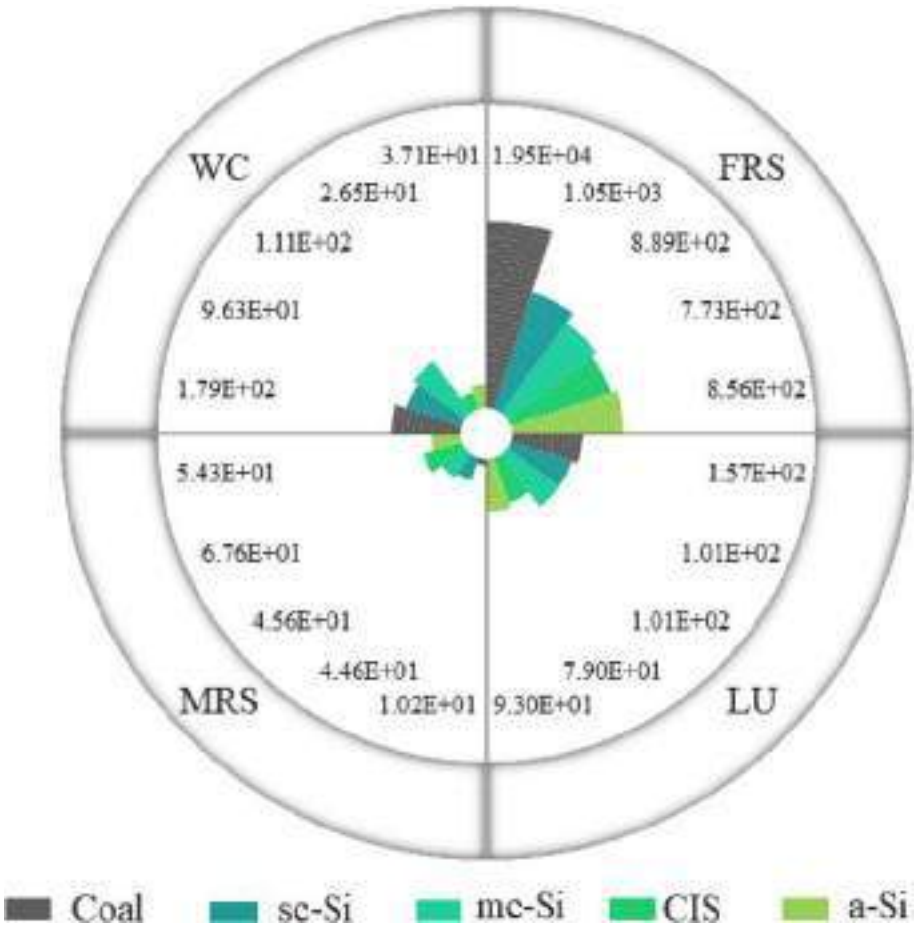


Fig. 3. Impacts associated with coal-based versus solar photovoltaic energy consumption by solar cell technology per 1 t month^{-1} of whole dried biomass of *Arthrospira platensis*. Amorphous silicon, a-Si; Copper-indium-diselenide, CIS; Multi-crystalline silicon, mc-Si; Single-crystalline silicon, sc-Si; Fossil resource scarcity, FRS (kg oil-eq); Land use, LU (m^{2}a crop-eq); Mineral resource scarcity, MRS (kg Cu-eq); Water consumption, WC (m^3).

significant. There are differences in the impact of the products for all midpoint categories, and, most importantly, they can be mitigated depending on the energy source and solar cell technology used. Evidently, the better or worse environmental performance of the microalgae products powered by photovoltaic energy from a-Si, CIS, mc-Si, and sc-Si solar cell technologies are related to the life cycle of these technologies. The environmental issues associated with the use of materials and energy for the manufacture, installation, and disposal of each solar cell technology, which are taken into account, affect the environmental profile of the processes and products powered by these systems [18,24].

In this sense, the article is concerned with shedding light on how the particularities of solar cell technologies influence the environmental burdens of microalgae-based processes and products. The results presented above provide insights into the influence of solar cell technologies on each one of the seventeen environmental impact categories. However, at first glance, it is difficult to say which solar cell technology carries the lower overall environmental impact in the lifecycle of microalgae-based products. Therefore, in this study, weighting the results of the life cycle assessment, we give a step ahead in the sense of guiding decision-making. Many microalgae producers and non-specialists in the solar energy field when investing in integration with solar energy are really concerned about the environment. Thus, showing the best solar cell technology for integration in the manufacturing facilities, through the weighting of the LCA results, is a great way to help them make assertive choices in favor of the environment. The weighting results are shown in Fig. 6.

As can be seen in Fig. 6, the integration of microalgae production with a-Si solar cell technology contributes to the lower overall environmental impact of microalgae-based products in the ecosystem quality damage category and human health damage category. Integration with CIS solar cell technology, in turn, contributes to lower overall environmental impact in the resource consumption damage category and climate change damage category. In sum, the integration of microalgae production with a-Si and CIS solar cell technologies seem to be the best choice, as they are between the first- and second-best option on the endpoint intensity scale. The least preferred choice due to its greater contribution to the overall environmental impact of microalgae-based products in three of the four endpoint categories is intended for integration with sc-Si solar cell technology.

On the other hand, from a global perspective, i.e., considering the seventeen midpoint impact categories, the integration of microalgae production with a-Si solar cell technology is the best option. CIS solar cell technology is the second-best option, leaving for the integration with mc-Si technology and, more specifically, sc-Si, the higher overall impact on the environmental sustainability metrics of microalgae-based products.

As mentioned earlier, it is worth emphasizing that the environmental performance of the microalgae products powered by these solar cell technologies is intrinsically linked to how they are made, ie, the life cycle. Crystalline silicon solar cells like sc-Si and mc-Si compared to thin film solar cells like a-Si and CIS need a greater amount of semiconductor material due to the lower absorption coefficient [18]. Besides that, crystalline silicon solar cells not only use more materials but also more energy and problematic chemicals at the production stage, and as a result, this is reflected in the greater cumulative emissions of the life

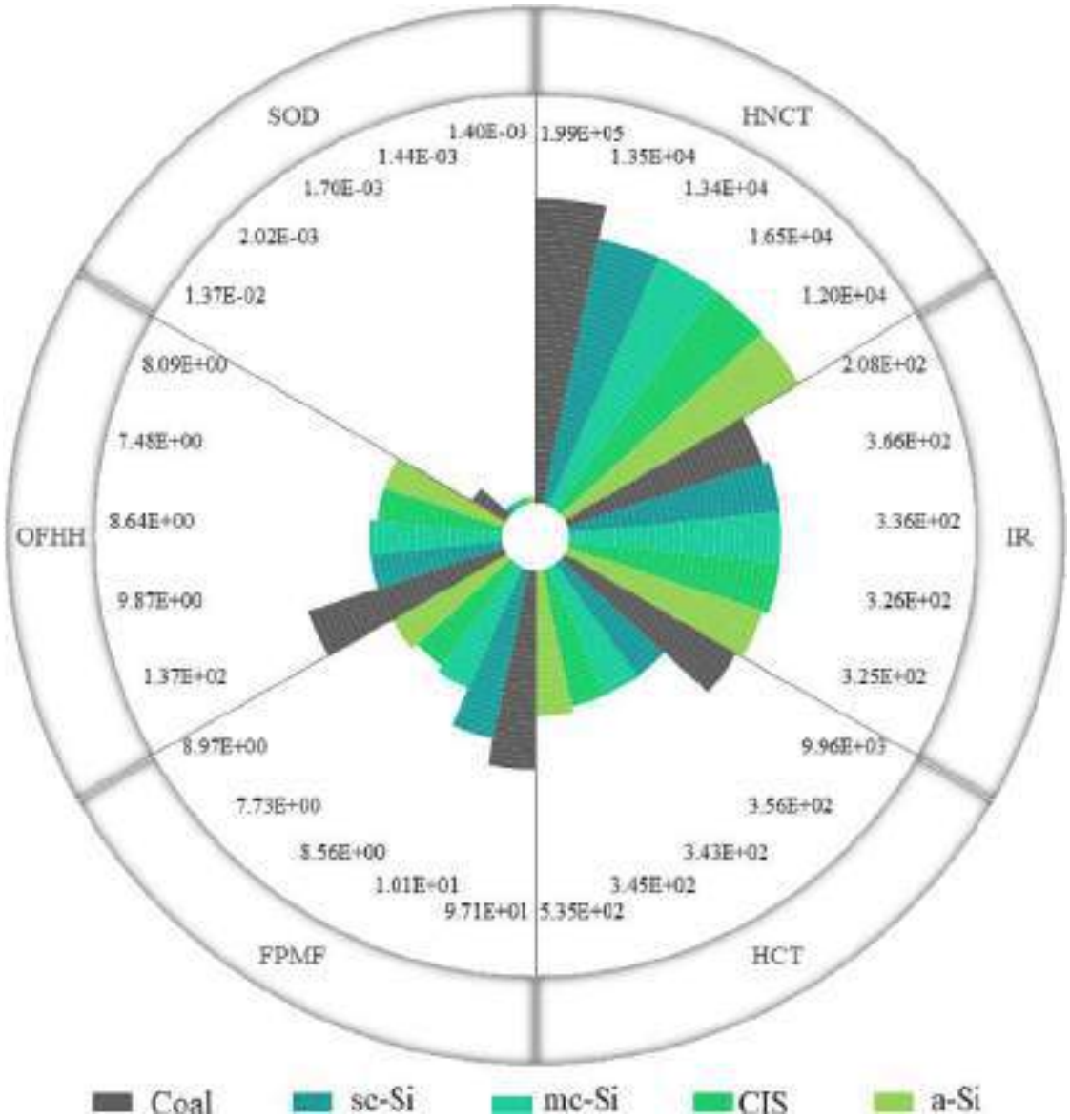


Fig. 4. Impacts associated with coal-based versus solar photovoltaic energy consumption by solar cell technology per 1 t month^{-1} of whole dried biomass of *Arthrospira platensis*. Amorphous silicon, a-Si; Copper-indium-diselenide, CIS; Multi-crystalline silicon, mc-Si; Single-crystalline silicon, sc-Si; Human non-carcinogenic toxicity, HNCT (kg 1,4-DCB-eq); Ionizing radiation, IR (kBq Co-60-eq); Human carcinogenic toxicity, HCT (kg 1,4-DCB-eq); Fine particulate matter formation, FPMF (kg $PM_{2.5}$-eq); Ozone formation–human health, OFHH (kg NOx-eq); Stratospheric ozone depletion, SOD (kg CFC-11-eq).

cycle of these two technologies and their impact on emissions of the life cycle of microalgae-based products [18]. Studies such as those by Ahmadi et al. [13], Ludin et al. [14], and Rabaia et al. [16] describe in more detail the particularities of photovoltaic technologies for energy generation.

In synthesis, the characterized and weighted results presented here are a transparent approach that leaves less room for bias and provides microalgae producers with guidance on the impact of solar cell technology used to generate photovoltaics for microalgae-based processes and products. Naturally, this is only a primary assessment, and weighting the LCA results is a highly debated step, as applied weights can influence outcomes and conclusions; however, it has many benefits, as it provides a north for decision-making.

Lastly, it is worth discussing how a company's ability to see and predict where the world is going increases the chances of long-term success. In this sense, what is expected in the light of an increasingly narrow window for climate action is that microalgae-producing companies will take seriously the transition to energy sources with lower emissions of pollutants [25–28].

Besides that, replacing the use of energy with high CO_2 emissions with renewable energy sources, such as solar photovoltaics, is a great business opportunity, as it can ensure that climate opportunities be captured. Of note, for commercial purposes, the representation of a ton of CO_2 that has ceased to be emitted into the atmosphere corresponds to a carbon credit that can be traded on the international market [23]. Thus, as shown in Table 2, replacing coal-based energy consumption with solar photovoltaic at the process level would generate revenue opportunities. Furthermore, the solar cell technology utilized implies a higher or lower revenue opportunity.

Still, the implementation of a photovoltaic energy project with its own resources, besides generating revenue opportunities, can generate great savings in fossil energy for the company [29]. The most encouragingly is that the technology needed to electrify microalgae-based processes using photovoltaic energy is already, or close to being, cheaper than fossil fuels worldwide. In just one decade, the levelized cost of photovoltaic electricity has dropped by 89%, making it cheaper

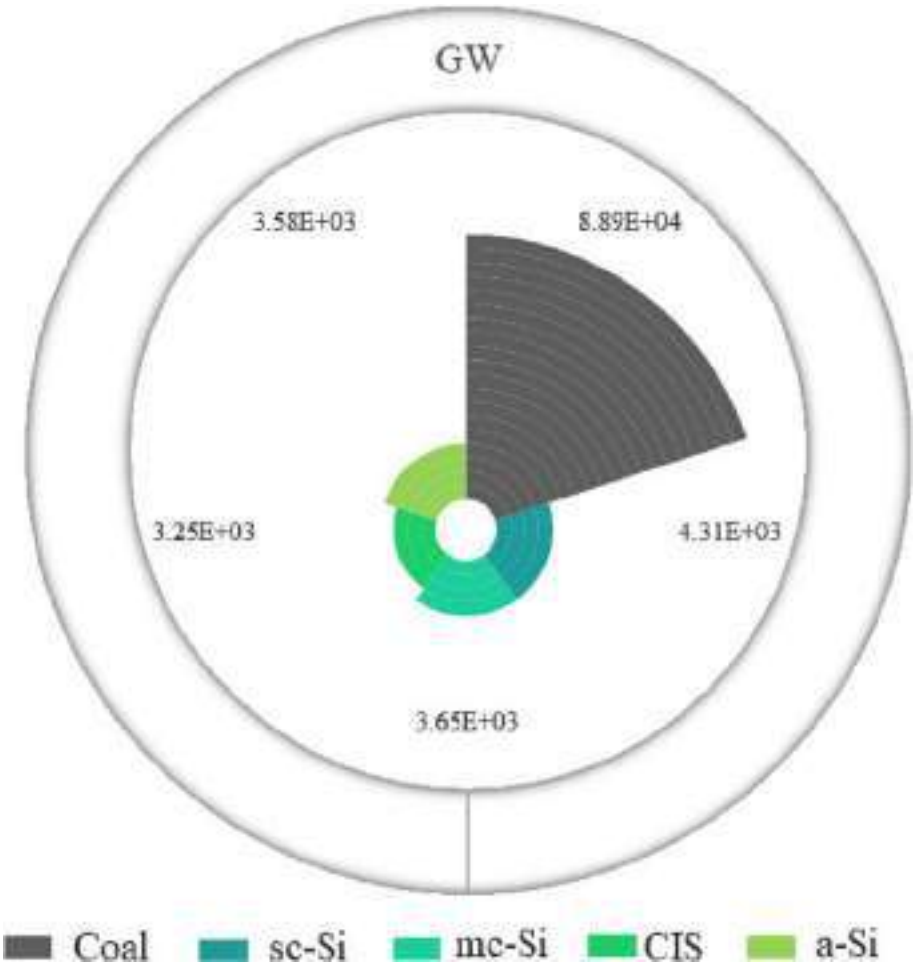


Fig. 5. Global warming potential associated with coal-based versus solar photovoltaic energy consumption by solar cell technology per 1 t month^{-1} of whole dried biomass of *Arthrospira platensis*. Amorphous silicon, a-Si; Copper-indium-diselenide, CIS; Multi-crystalline silicon, mc-Si; Single-crystalline silicon, sc-Si; Global warming, GW (kg CO_2-eq).

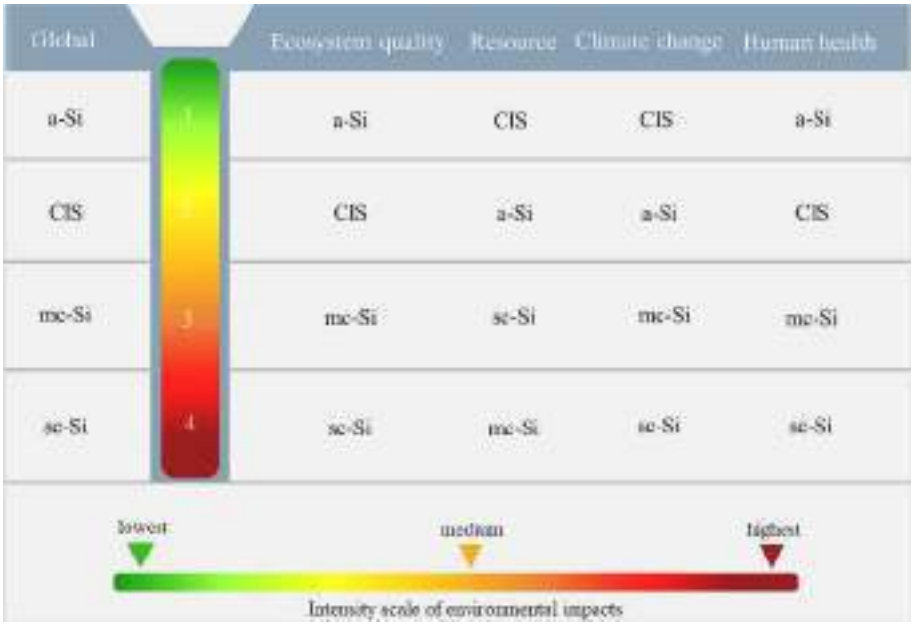


Fig. 6. Impacts weighting of the producing microalgae-based products using different solar cell technologies. Note that the global scale considers all impact categories and the endpoints only consider their respective impact categories. Amorphous silicon, a-Si; Copper-indium-diselenide, CIS; Multi-crystalline silicon, mc-Si; Single-crystalline silicon, sc-Si.

Table 2
Estimation of carbon credits according to solar cell technology.

	USD/year			
	CIS	a-Si	mc-Si	Sc-Si
Chlorella vulgaris biomass in raceway pond	35,134.7	34,611.3	34,506.6	33,446.7
Chlorella vulgaris biomass in tubular photobioreactor	156,881.3	154,544.2	154,076.7	149,344.0
Arthrospira platensis biomass in raceway pond	23,066.0	22,722.4	22,653.7	21,957.8
Phycocyanin from *Arthrospira platensis*	288,014.5	283,723.8	282,865.7	274,177.0
β-carotene from *Dunaliella salina*	196,173.5	193,250.9	192,666.4	186,748.4
Astaxanthin from *Haematococcus pluvialis*	889,506.6	876,255.1	873,604.8	846,770.6
DHA from *Crypthecodinium cohnii* in fermenter	15,218.0	14,991.3	14,945.9	14,486.9
EPA from *Nitzschia laevis* in fermenter	30,892.5	30,432.3	30,340.2	29,408.3

Docosahexaenoic, DHA; Eicosapentaenoic, EPA; Amorphous silicon, a-Si; Copper-indium-diselenide, CIS; Multi-crystalline silicon, mc-Si; Single-crystalline silicon, sc-Si. *Considering the carbon price in the EU ETS of USD 87/tCO_2e for the year 2022.

than fossil fuels, as shown in the data from Ritchie and Roser [30].

As for the different solar cell technologies, Milousi et al. [24] present a complete technical–economic assessment of the photovoltaic-based technologies studied here. According to the author's analysis, the energy production and the investment cost for a system with a nominal capacity of 3 kW are approximately the same. This is because all the technical advantages between the technologies are harmonized when considering the same nominal capacity.

Conclusively, if companies adhere to the energy transition, they will have an incredible opportunity ahead, which is not just the direct benefit of low carbon but also the reduction of the plant's operating costs. Furthermore, ultimately, to make the microalgae-based processes and products carbon neutral, if produced with coal-based energy, the values in Table 2 represent, from another perspective, part of the expenses with carbon offsets. The carbon offset is part of the strategy to achieve net zero, once there are emissions that cannot be avoided. But what should have in mind is that carbon offsetting needs to be just part of the strategy to get to net zero and not an excuse to delay cutting emissions that can actually be reduced [8].

And finally, it is worth emphasizing that in this study we only considered commercial solar cell technologies with the highest levels of technological readiness [18]. However, there are other technologies that, despite having lower levels of technological readiness, are becoming an interesting option for the energy transition already underway in many countries and industries [31].

Conclusions

Weighting the life cycle assessment results, it was possible to easily compare the environmental impact of a-Si, CIS, mc-Si, and sc-Si solar cell technologies on emissions from microalgae-based products. It was uncovered from the global intensity scale that the integration of a-Si solar cell technology to power microalgae facilities, followed by CIS technology, carries a smaller impact on the lifecycle of microalgae-based products. Furthermore, these two technologies, provide a greater carbon credit revenue opportunity for microalgae producers. What can be concluded from the results is that the choice of solar cell technology can contribute to further reducing the environmental impact of microalgae-based processes and products. However, of course, this is only a primary assessment, new solar cell technologies are emerging and need to be investigated in future studies on integrating photovoltaic technologies into manufacturing facilities, as they may be even greener than that of the old generation.

Statement of informed consent, human/animal rights

No conflicts, informed consent, or human or animal rights apply to this study.

CRediT authorship contribution statement

Rosangela Rodrigues Dias: Conceptualization, Methodology, Data curation, Writing – original draft. **Mariany Costa Deprá:** Methodology, Data curation. **Rafaela Basso Sartori:** Methodology, Data curation. **Adriane Terezinha Schneider:** Methodology, Data curation. **Leila Queiroz Zepka:** Supervision, Funding acquisition. **Eduardo Jacob-Lopes:** Conceptualization, Project administration, Writing – review & editing.

Declaration of Competing Interest

The authors declare that they have no known competing financial interests or personal relationships that could have appeared to influence the work reported in this paper.

Data availability

Data will be made available on request.

Acknowledgment

The authors would like to thank the Coordination for the Improvement of Higher Education Personnel (CAPES) (Finance Code 001) and the National Council for Scientific and Technological Development (CNPq) for financial support.

Appendix A. Supplementary data

Supplementary data to this article can be found online at https://doi.org/10.1016/j.seta.2023.103362.

References

[1] Chew KW, Yap JY, Show PL, Suan NH, Juan JC, Ling TC, et al. Microalgae biorefinery: high value products perspectives. Bioresour Technol 2017;229:53–62.
[2] Mata TM, Cameira M, Marques F, Santos E, Badenes S, Costa L, et al. Carbon footprint of microalgae production in photobioreactor. Energy Procedia 2018;2018 (153):432–7.
[3] Porcelli R, Dotto F, Pezzolesi L, Marazza D, Greggio N, Righi S. Comparative life cycle assessment of microalgae cultivation for non-energy purposes using different carbon dioxide sources. Sci Total Environ 2020;721:137714.
[4] Deprá MC, Severo IA, dos Santos AM, Zepka LQ, Jacob-Lopes E. Environmental impacts on commercial microalgae-based products: Sustainability metrics and indicators. Algal Res 2020;51:102056.
[5] Qin Z-H, Hu X, Mou J-H, He G-H, Ye G-B, Li H-Y, et al. Environmental profiling microalgae-based eicosapentaenoic acid production along the technical advancement via life cycle assessment. J Clean Prod 2023;397:136477.
[6] Pechsiri JS, Thomas J-B, Bahraoui NE, Fernandez FGA, Chaouki J, Chidami S, et al. Comparative life cycle assessment of conventional and novel microalgae production systems and environmental impact mitigation in urban-industrial symbiosis. Sci Total Environ 2023;854:158445.
[7] Dias RR, Deprá MC, Severo IA, Zepka LQ, Jacob-Lopes E. Smart override of the energy matrix in commercial microalgae facilities: a transition path to a low-carbon bioeconomy. Sustain Energy Technol Assess 2022;52:102073.
[8] Dias RR, Deprá MC, Zepka LQ, Jacob-Lopes E. Roadmap to net-zero carbon emissions in commercial microalgae-based products: environmental sustainability and carbon offset costs. J Appl Psychol 2022;34(3):1255–68.
[9] Dias RR, Deprá MC, Zepka LQ, Jacob-Lopes E. *In silico* study of hybrid renewable energy in microalgae facilities: A path towards net-zero emissions. Algal Res 2022; 63:102661.
[10] Tawalbeh M, Al-Othman A, Kafiah F, Abdelsalam E, Almomani F, Alkasrawi M. Environmental impacts of solar photovoltaic systems: A critical review of recent progress and future outlook. Sci Total Environ 2021;759:143528.
[11] Adeyeye K, Ntagwirumugara E, Colton J, Ijumba N. Integrating Photovoltaic Technologies in Smart Homes. In: In 2018 International Conference on Advances in

Big Data, Computing and Data Communication Systems (icABCD). IEEE; 2018. p. 1–6.
[12] Kanz O, Reinders A, May J, Ding K. Environmental impacts of integrated photovoltaic modules in light utility electric vehicles. Energies 2020;13(19):5120.
[13] Ahmadi MH, Ghazvini M, Sadeghzadeh M, Alhuyi Nazari M, Kumar R, Naeimi A, et al. Solar power technology for electricity generation: A critical review. Energy Sci Eng 2018;6(5):340–61.
[14] Ludin NA, Mustafa NI, Hanafiah MM, Ibrahim MA, Asri Mat Teridi M, Sepeai S, et al. Prospects of life cycle assessment of renewable energy from solar photovoltaic technologies: A review. Renew Sust Energ Rev 2018;96:11–28.
[15] Morales M, Hélias A, Bernard O. Optimal integration of microalgae production with photovoltaic panels: environmental impacts and energy balance. Biotechnol biofuels 2019;12(1):1–17.
[16] Rabaia MKH, Abdelkareem MA, Sayed ET, Elsaid K, Chae K-J, Wilberforce T, et al. Environmental impacts of solar energy systems: A review. Sci Total Environ 2021; 754:141989.
[17] Pimentel Da Silva GD, Branco DAC. Is floating photovoltaic better than conventional photovoltaic? Assessing environmental impacts. Impact Assess Proj Apprais 2018;36(5):390–400.
[18] Settino J, Sant T, Micallef C, Farrugia M, Spiteri Staines C, Licari J, et al. Overview of solar technologies for electricity, heating and cooling production. Renew Sust Energ Rev 2018;90:892–909.
[19] International Standard Organization. ISO-14040: Environmental management–life cycle assessment–principles and framework. 2006.
[20] Huijbregts MAJ, Steinmann ZJN, Elshout PMF, Stam G, Verones F, Vieira M, et al. ReCiPe2016: a harmonised life cycle impact assessment method at midpoint and endpoint level. Int J LCA 2017;22(2):138–47.
[21] Maroneze MM, Deprá MC, Zepka LQ, Jacob-Lopes E. Artificial lighting strategies in photobioreactors for bioenergy production by *Scenedesmus obliquus* CPCC05. SN Appl Sci 2019;1(12):1–12.
[22] Jacob-Lopes E, Zepka LQ, Deprá MC. Sustainability indicators and metrics of environmental impact: industrial and agricultural life cycle assessment. 1th ed. Elsevier; 2021.
[23] World Bank. Carbon Pricing Dashboard, https://carbonpricingdashboard.worldbank.org/map_data; 2022 [accessed 10 August 2022].
[24] Milousi M, Souliotis M, Arampatzis G, Papaefthimiou S. Evaluating the environmental performance of solar energy systems through a combined life cycle assessment and cost analysis. Sustainability 2019;11(9):2539.
[25] Overpeck JT, Conde C. A call to climate action. Sci 2019;364(6443):807-807.
[26] Matthews HD, Wynes S. Current global efforts are insufficient to limit warming to 1.5° C. Sci 2022;376(6600):1404–9.
[27] Lee H, Birol F. Energy is at the heart of the solution to the climate challenge. Intergov Panel Clim Chang 2020.
[28] Nurdiawati A, Urban F. Towards deep decarbonisation of energy-intensive industries: a review of current status, technologies and policies. Energies 2021;14 (9):2408.
[29] Cyanotech. Our History, https://www.cyanotech.com/our-history/; 2022 [accessed 20 August 2022].
[30] Ritchie H, Roser M. Why did renewables become so cheap so fast?, https://ourworldindata.org/cheap-renewables-growth; 2022 [accessed 21 August 2022].
[31] Akinoglu BG, Tuncel B, Badescu V. Beyond 3rd generation solar cells and the full spectrum project. Recent advances and new emerging solar cells. Sustain Energy Technol Assess 2021;46:101287.

Research Article

Received: 26 April 2022 Revised: 6 February 2023 Accepted article published: 11 March 2023 Published online in Wiley Online Library:

(wileyonlinelibrary.com) DOI 10.1002/jctb.7369

Mapping the performance of photobioreactors for microalgae cultivation. Part III: subtropical and mid-latitudes climate zone

Rosangela R. Dias,[a] Patricia A. da Silva,[a] Mariany C. Deprá,[a] Bruno Deprá,[b] Roger Wagner,[a] Leila Q. Zepka[a] and Eduardo Jacob-Lopes[a]*

Abstract

BACKGROUND: Identifying geographic locations with favorable climates for large-scale openwork microalgae cultivation is a trend. In light of that, what we propose in this study is to map the performance of photobioreactors for microalgae culture in the subtropical (25° to 35° N and S) and mid-latitudes (35° to 55° N and S) climate zones. Twenty geographic locations were chosen to represent 14 types of climates in the four seasons of the year. The study is a latitudinal, climatological and seasonal assessment.

RESULTS: The results showed that the subtropical climatic zone presents better conditions for microalgae growth with higher levels of biomass productivity and lipid productivity. The highest annual average biomass productivity (0.210 g L^{-1} d^{-1}) and annual average lipid productivity (0.025 g L^{-1} d^{-1}) were recorded in a simulation of hot desert climate (BWh). The winter season presents a minor potential for microalgae cultivation.

CONCLUSION: The results of this study shed light on the impact of subtropical and mid-latitudes climate zone and seasons of the year on the performance of photoautotrophic microalgae-based processes.
© 2023 Society of Chemical Industry (SCI).

Supporting information may be found in the online version of this article.

Keywords: *Scenedesmus obliquus*; thermal zones; geographic position; energy cost; environmental impact

INTRODUCTION

Microalgae comprise a diverse group of microscopic organisms that can provide, beyond basic nutrition, additional health benefits, as they are a source of a variety of compounds that have biological activity. These microorganisms are, in the state of the art, a last-generation resource with the potential to meet diverse demands and mitigate the environmental tensions of today's world.[1]

Currently, some microalgae, such as species of *Arthrospira platensis*, *Dunaliella salina* and *Crypthecodinium cohnii*, are cultivated commercially, and products such as whole-dried biomass, pigments and polyunsaturated fatty acids are available. Other particularly commercially attractive microalgae species, such as *Scenedesmus obliquus*, are being investigated for their biochemical characteristics.[2]

The global microalgae market, although modest, is a growth market primarily as a result of the health and wellness trends. However, it is assumed that the complex production chain may hamper, to some extent, the growth of this market. In reality, what has particularly hamperedthe growth of the microalgae market is the high cost of operating the cultivation facilities. This has been a significant barrier to expanding the production and marketing of more competitive products.[3]

Despite microalgae productivity being comparatively higher than that of terrestrial crops, the high fixed costs make production very sensitive to high biomass productivity without an off-season. Of note, as most microalgae products are intracellular, biomass productivity is a crucial part of the puzzle to achieving economic viability of these products. Despite numerous researchers having focused on improving this parameter, there is no universal system of highly productive cultivation. This is because it involves the intrinsic characteristics of each microalgae strain as well as factors

* *Correspondence to: E Jacob-Lopes, Bioprocess Intensification Group, Federal University of Santa Maria, 97105-900, Santa Maria, RS, Brazil. E-mail: ejacoblopes@gmail.com*

a *Bioprocess Intensification Group, Federal University of Santa Maria, Santa Maria, Brazil*

b *Department of Geoprocessing, University of Santa Cruz do Sul, Santa Cruz do Sul, Brazil*

related to the geospatial location of the facilities, such as supply availability and climate.[4]

Climate, in particular, is a key element for outdoor cultivation of photoautotrophic microalgae. And it is known that today most commercial microalgae production is carried out outdoors with little or no control over the climate. In this sense, the need to highlight the parameters that influence the efficiency of microalgae growth such as light and temperature is evident, considering that they can undergo daily and seasonal fluctuations, causing more or less favorable conditions.[5,6] The diversity of the spatial manifestation of sunlight and temperature modifies the photosynthetic apparatus of microalgae and, consequently, can affect the physiological and biochemical properties of the biomass.[7] Therefore, because location-dependent light and temperature dynamics can play an important role in trends in microalgae productivity, it is crucial to map the performance of cultivation systems for large-scale production.[8,9]

Proof-of-concept experiments investigating the influence of geographic position and local climate on the performance of photobioreactors for large-scale microalgae cultivation taking *S. obliquus* as the model microorganism are demonstrated in Part I of this study.[2] The results confirm their decisive role in the performance of these processes. The lack of a semi-empirical estimate of microalgae productivity on the globe led us to map the performance of photobioreactors in the Earth's climate zones. In Part II of the study, the performance of photobioreactors in the equatorial and tropical climate zone is mapped.[10] From an annual perspective, 14 types of climates distributed in 33 geographic positions were simulated. In Part III, we map the performance of photobioreactors in the subtropical and mid-latitudes climate zones.

It is noteworthy that the subtropical and mid-latitudes climate zones show a greater degree of variation between seasons and, therefore, we focused on simulating the climate as well as the four seasons of the year. Fourteen types of climates distributed in twenty geographic positions representative of the subtropical and mid-latitudes zones were simulated. Posteriorly, the effects of climate and seasonality on biomass and lipid production and the quantitative and qualitative fatty acid composition of the model microorganism are evaluated. The impact of climate on environmental and economic sustainability metrics also is assessed. Parts II and III provide the first semi-empirical study of microalgae productivity around the globe based on cultivation that simulates climate in photobioreactors.

MATERIAL AND METHODS

Microorganism, culture conditions and photobioreactor design

Scenedesmus obliquus CPCC05 was used as model microorganism. Axenic cultures of *S. obliquus* originally obtained from the Canadian Psychological Culture Centre were propagated and conditioned in synthetic medium BG-11, with the following composition (g L^{-1}): K_2HPO_4 (0.03), $MgSO_4.7H_2O$ (0.075), $CaCl_2.2H_2O$ (0.036), ammonium iron citrate (0.006), Na_2EDTA (0.001), NaCl (0.072), $NaNO_3$ (1.5), citric acid (0.0006), Na_2CO_3 (0.002), 1 mL L^{-1} of trace metals (H_3BO_3 [2.86], $MnCl_2.4H_2O$ [1.81], $ZnSO_4.7H_2O$ [0.22], $Na_2MoO_4.2H_2O$ [0.39], $CuSO_4.5H_2O$ [0.079], $CoCl_2.6H_2O$ [0.04]), pH 7.6.[11] Incubation conditions were 25 °C, 15 µmol m^{-2} s^{-1} and 12 h:12 h, light:dark photoperiod.[12]

Measurements were carried out in a closed bubble-column photobioreactor with a total and nominal working volume of

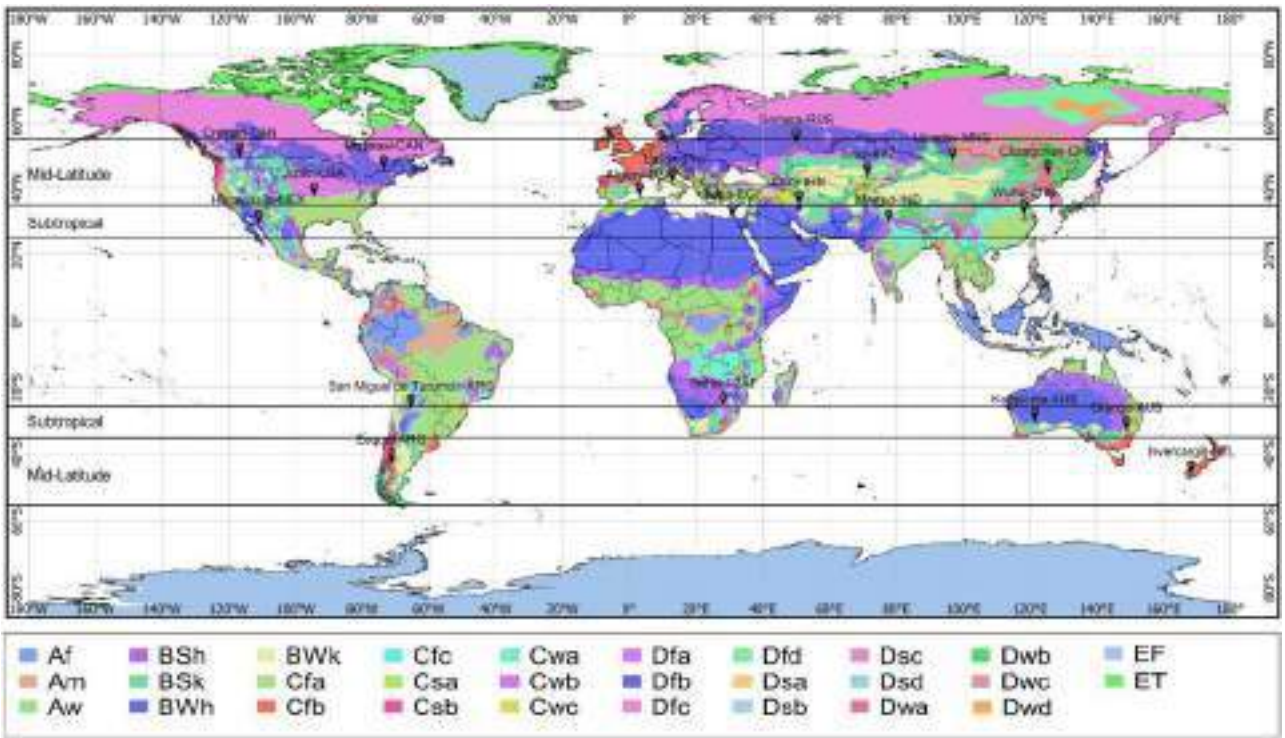


Figure 1. World map of the Köppen–Geiger climate classification with the geographicgeographic positions of the study. MEX, Mexico; IRN, Iran; EGY, Egypt; AUS, Australia; ARG, Argentina; IND, India; ZAF, South Africa; CHN, China; USA, United States; NZL, New Zealand; DZA, Algeria; ITA, Italy; RUS, Russia; CAN, Canada; KAZ, Kazakhstan; MNG, Mongolia.

 © 2023 Society of Chemical Industry (SCI).

10974660, 0, Downloaded from https://onlinelibrary.wiley.com/doi/10.1002/jctb.7369 by IFSC - Instituto Federal de Santa Catarina, Wiley Online Library on [28/03/2023]. See the Terms and Conditions (https://onlinelibrary.wiley.com/terms-and-conditions) on Wiley Online Library for rules of use; OA articles are governed by the applicable Creative Commons License

Table 1. Köppen–Geiger climate classification and experimental conditions for each geographic position

Geographic Positions	Classification	Köppen–Geiger	Elevation (m)	Latitude	Longitude	Light intensity (μmol.m^{-2} s^{-1})	Day length (hr)	Temperature (°C)
Subtropical (25 to 35° N and S)								
Hermosillo–MEX	(B) Dry	BWh	200	29° 04′ N	110° 57′ W			
Summer	(W) desert					2214.9^{i}	14.03^{bcdefghijk}	21.57^{jklmn}
Autumn	(h) hot					1891.0^{x}	11.87^{opqrstu}	25.73^{cdef}
Winter						1611.8^{O}	11.13^{stuvwx}	16.76^{stuv}
Spring						2402.4^{b}	13.26^{hijklmno}	23.07^{ghijk}
Qom–IRN			935	34° 38′ N	50° 53′ E			
Summer						2208.3^{j}	14.46^{bcdefghij}	30.00^{ab}
Autumn						1659.8^{M}	11.77^{pqrstu}	19.37^{nopq}
Winter						1305.2^{EE}	10.58^{uvwxyz}	5.76^{J}
Spring						1948.6^{t}	13.10^{jklmnopq}	17.00^{rstu}
Tanta–EGY			16	30° 47′ N	31° 00′ E			
Summer						2332.9^{c}	14.20^{bcdefghijk}	26.00^{cde}
Autumn						1731.7^{l}	11.83^{opqrstu}	22.00^{ijklm}
Winter						1380.7^{AA}	11.00^{stuvwx}	13.36^{yzAB}
Spring						2120.9^{n}	13.00^{klmnopqr}	19.30^{nopqr}
Kalgoorlie–AUS	(B) Dry	BSh	359	30° 47′ S	121° 28′ E			
Summer	(S) steppe					2445.7^{a}	14.16^{bcdefghijk}	25.00^{defg}
Autumn	(h) hot					1688.6^{K}	11.18^{stuvwx}	18.00^{pqrst}
Winter						1414.2^{Z}	11.00^{stuvwx}	11.00^{BCDEF}
Spring						2247.6^{h}	13.13^{jklmnop}	18.00^{pqrst}
San Miguel de Tucumán–ARG	(C) Humid subtropical	Cfa	431	26° 82′ S	65° 22′ W			
Summer	(f) fully humid					2031.8^{p}	13.93^{cdefghijk}	24.46^{defgh}
Autumn	(a) hot summer					1821.7^{E}	12.10^{mnopqrst}	21.57^{jklmn}
Winter						1681.2^{L}	11.13^{stuvwx}	16.60^{stuvw}
Spring						2182.4^{l}	13.13^{jklmnop}	21.40^{jklmn}
Orange–AUS	(C) Humid subtropical	Cfb	15	27° 34′ S	153° 00′ E			
Summer	(f) fully humid					2253.8^{g}	13.93^{cdefghijk}	24.33^{efgh}
Autumn	(b) warm summer					1556.8^{R}	11.86^{opqrstu}	20.00^{mnop}
Winter						1121.9^{KK}	11.16^{stuvwx}	14.00^{xyz}
Spring						1936.0^{u}	13.13^{jklmnop}	20.00^{mnop}
Meerut–IND	(C) Humid subtropical	Cwa	226	28° 58′ N	77° 43′ E			
Summer	(w) winter dry					1849.5^{B}	14.06^{bcdefghijk}	31.37^{a}
Autumn	(a) hot summer					1830.7^{D}	11.90^{nopqrstu}	25.17^{defg}
Winter						1582.6^{Q}	11.13^{stuvwx}	12.83^{yzAB}
Spring						2263.0^{f}	13.23^{ijklmno}	27.70^{bc}
Benoni–ZAF	(C) Humid subtropical	Cwb	1641	26° 18′ S	28° 32′ E			
Summer	(w) winter dry					2116.6^{o}	13.86^{cdefghijk}	20.36^{lmno}
Autumn	(b) warm summer					1832.2^{C}	12.13^{lmnopqrs}	16.00^{tuvwx}
Winter						1802.3^{F}	11.20^{stuvwx}	10.73^{BCDEF}
Spring						2132.9^{m}	13.07^{jklmnopq}	17.63^{qrst}

© 2023 Society of Chemical Industry (SCI).

10974660, 0, Downloaded from https://onlinelibrary.wiley.com/doi/10.1002/jctb.7369 by IFSC - Instituto Federal de Santa Catarina, Wiley Online Library on [28/03/2023]. See the Terms and Conditions (https://onlinelibrary.wiley.com/terms-and-conditions) on Wiley Online Library for rules of use; OA articles are governed by the applicable Creative Commons License

Table 1. Continued

Geographic Positions	Classification	Köppen–Geiger	Elevation (m)	Latitude	Longitude	Light intensity (μmol.m^{-2} s^{-1})	Day length (hr)	Temperature (°C)
Wuhu–CHN	(D) Wet continental	Dwb	15	31° 20′ N	118° 21′ E			
Summer	(W) dry winter					1523.6^{U}	14.23^{bcdefghijk}	26.67^{cd}
Autumn	(b) cool summer					1285.5^{GG}	11.83^{opqrstu}	17.33^{qrst}
Winter						1151.2^{JJ}	11.00^{stuvwx}	5.00^{J}
Spring						1353.0^{CC}	13.33^{hijklmn}	15.00^{uvwxy}
Mid-latitudes (35 to 55° N and S)								
Joplin–USA	(C) Humid subtropical	Cfa	298	37° 08′ N	94° 29′ W			
Summer	(f) fully humid					1856.9^{z}	14.70^{abcdefgh}	25.33^{defg}
Autumn	(a) hot summer					1371.4^{BB}	11.67^{qrstuvw}	14.67^{vwxy}
Winter						1013.8^{OO}	10.60^{uvwxyz}	2.33^{K}
Spring						1630.9^{N}	13.56^{fghijkl}	13.00^{yzAB}
Invercargill-NZL	(C) Humid subtropical	Cfb	6	46° 40′ S	168° 35′ E			
Summer	(f) fully humid					1854.9^{A}	15.00^{abcdef}	13.66^{yzA}
Autumn	(b) warm summer					1064.2^{NN}	10.80^{stuvwxy}	11.00^{BCDEF}
Winter						728.4^{UU}	9.27^{zA}	6.33^{IJ}
Spring						1555.3^{S}	13.43^{hijklm}	10.00^{CDEFG}
Algiers–DZA	(C) Humid subtropical	Csa	24	36° 43′ N	03° 15′ E			
Summer	(s) summer dry					2279.2^{e}	14.66^{abcdefghi}	23.67^{fghij}
Autumn	(a) hot summer					1529.3^{T}	11.73^{pqrstuv}	20.00^{mnop}
Winter						1175.2^{II}	10.66^{tuvwxyz}	11.66^{ABCD}
Spring						1992.6^{r}	13.53^{ghijklm}	14.33^{wxy}
Latina–ITA			21	41° 32′ N	12° 54′ E			
Summer						2206.2^{k}	15.13^{abcde}	22.60^{hijkl}
Autumn						1345.7^{DD}	11.57^{rstuvwx}	17.10^{qrstu}
Winter						951.9^{PP}	10.30^{vwxyz}	8.93^{FGH}
Spring						1800.5^{G}	14.00^{bcdefghijk}	14.00^{xyz}
Esquel–ARG	(C) Humid subtropical	Csb	815	42° 56′ S	71° 09′ W			
Summer	(s) summer					2326.6^{d}	15.16^{abcde}	14.00^{xyz}
Autumn	(b) warm summer					1346.2^{DD}	11.43^{stuvwx}	9.40^{DEFG}
Winter						864.1^{RR}	10.16^{xyz}	2.33^{K}
Spring						1871.0^{y}	13.77^{defghijk}	9.61^{DEFG}
Samara-RUS	(D) Wet continental	Dfa	117	53° 20′ N	50° 15′ E			
Summer	(f) fully humid					1741.9^{H}	15.97^{a}	20.67^{lmno}
Autumn	(a) hot summer					902.4^{QQ}	10.57^{uvwxyz}	6.00^{J}
Winter						548.9^{WW}	8.57^{A}	−9.33^{N}

© 2023 Society of Chemical Industry (SCI).

10974660, 0, Downloaded from https://onlinelibrary.wiley.com/doi/10.1002/jctb.7369 by IFSC - Instituto Federal de Santa Catarina, Wiley Online Library on [28/03/2023]. See the Terms and Conditions (https://onlinelibrary.wiley.com/terms-and-conditions) on Wiley Online Library for rules of use; OA articles are governed by the applicable Creative Commons License

Table 1. Continued

Geographic Positions	Classification	Köppen–Geiger	Elevation (m)	Latitude	Longitude	Light intensity (μmol.m^{-2} s^{-1})	Day length (hr)	Temperature (°C)
Spring						1468.2^{X}	$14.00^{bcdefghijk}$	6.67^{HIJ}
Montreal-CAN	(D) Wet continental	Dfb	201	45° 50′ N	73° 58′ W			
Summer	(f) fully humid					1906.9^{w}	$14.93^{abcdefg}$	20.33^{lmno}
Autumn	(b) warm summer					1199.9^{HH}	10.97^{stuvwx}	9.33^{EFG}
Winter						856.0^{SS}	9.47^{yzA}	-7.00^{M}
Spring						1606.3^{P}	$13.53^{ghijklm}$	6.67^{HIJ}
Taraz–KAZ	(D) Wet continental	Dsa	626	42° 54′ N	71° 22′ E			
Summer	(s) dry summer					1923.6^{v}	15.26^{abc}	24.00^{efghi}
Autumn	(a) Hot summer					1285.5^{GG}	11.53^{stuvwx}	11.53^{ABCDE}
Winter						786.2^{TT}	10.23^{wxyz}	1.90^{K}
Spring						1470.5^{W}	$13.33^{hijklmn}$	12.00^{zABC}
Creston-CAN	(D) Wet continental	Dsb	641	49° 10′ N	116° 50′ W			
Summer	(s) dry summer					1988.8^{s}	15.40^{ab}	18.67^{opqrs}
Autumn	(b) warm summer					1150.2^{JJ}	$10.77^{stuvwxy}$	8.33^{GHI}
Winter						719.7^{VV}	9.10^{zA}	-1.66^{N}
Spring						1610.4^{O}	$13.73^{efghijk}$	8.33^{GHI}
Changchun–CHN	(D) Wet continental	Dwa	238	43° 54′ N	125° 13′ E			
Summer	(w) dry winter					1516.9^{V}	15.40^{ab}	21.33^{klmn}
Autumn	(a) Hot summer					1291.9^{FF}	$11.57^{rstuvwx}$	6.33^{IJ}
Winter						1095.5^{LL}	10.13^{xyz}	-12.33^{O}
Spring						1703.9^{J}	$13.90^{cdefghijk}$	6.67^{HIJ}
Uliastay-MNG	(D) Wet continental	Dwb	1755	47° 74′ N	96° 84′ E			
Summer	(w) dry winter					2021.7^{q}	15.20^{abcd}	14.33^{wxy}
Autumn	(b) warm summer					1432.6^{Y}	$10.87^{stuvwxy}$	-2.67^{N}
Winter						1070.3^{MM}	9.23^{zA}	-20.33^{P}
Spring						1949.6^{t}	13.63^{fghijk}	-1.00^{L}

Note: Different lowercase letters followed by different capital letters within the same column express significant differences between the averages ($P \leq 0.05$).

© 2023 Society of Chemical Industry (SCI).

10974660, 0, Downloaded from https://onlinelibrary.wiley.com/doi/10.1002/jctb.7369 by IFSC - Instituto Federal de Santa Catarina, Wiley Online Library on [28/03/2023]. See the Terms and Conditions (https://onlinelibrary.wiley.com/terms-and-conditions) on Wiley Online Library for rules of use; OA articles are governed by the applicable Creative Commons License

© 2023 Society of Chemical Industry (SCI).

Table 2. Kinetic parameters for *Scenedesmus obliquus* in different geographic locations of the subtropical and mid-latitudes climate zone

Köppen-Geiger	Geographic positions	X_{max} (g L^{-1})	μ_{max} (d^{-1})	HRT(d)	t_g (d)	P_X (g L^{-1} d^{-1})	P_X annual average (g L^{-1} d^{-1})
Subtropical (25 to 35° N and S)							
BWh	**Hermosillo–MEX**						$0.210^{a} \pm 0.01$
	Summer	$2.20^{f} \pm 0.02$	$0.68^{cd} \pm 0.02$	$9^{ab} \pm 0.00$	$1.02^{xy} \pm 0.01$	$0.233^{ef} \pm 0.02$	
	Autumn	$2.18^{f} \pm 0.01$	$0.50^{hij} \pm 0.01$	$7^{abc} \pm 0.00$	$1.38^{s} \pm 0.02$	$0.297^{a} \pm 0.01$	
	Winter	$0.40^{no} \pm 0.00$	$0.21^{tu} \pm 0.00$	$6^{abc} \pm 0.00$	$3.33^{c} \pm 0.00$	$0.050^{stuv} \pm 0.00$	
	Spring	$2.70^{a} \pm 0.01$	$0.78^{b} \pm 0.00$	$10^{a} \pm 0.00$	$0.88^{z} \pm 0.01$	$0.260^{d} \pm 0.0.02$	
	Qom–IRN						$0.130^{e} \pm 0.01$
	Summer	$2.56^{bc} \pm 0.02$	$1.09^{a} \pm 0.00$	$8^{abc} \pm 0.00$	$0.64^{A} \pm 0.04$	$0.307^{a} \pm 0.00$	
	Autumn	$1.88^{j} \pm 0.02$	$0.41^{lmnop} \pm 0.00$	$11^{a} \pm 0.00$	$1.69^{n} \pm 0.02$	$0.161^{n} \pm 0.1$	
	Winter	-	-	-	-	-	
	Spring	$0.46^{m} \pm 0.00$	$0.24st \pm 0.00$	$7^{abc} \pm 0.00$	$2.88^{g} \pm 0.00$	$0.051^{stu} \pm 0.00$	
	Tanta–EGY						$0.184^{bc} \pm 0.00$
	Summer	$2.70^{a} \pm 0.02$	$0.78^{b} \pm 0.01$	$10^{a} \pm 0.00$	$0.88^{z} \pm 0.03$	$0.260^{d} \pm 0.01$	
	Autumn	$2.44^{d} \pm 0.01$	$0.62^{defg} \pm 0.00$	$10^{a} \pm 0.00$	$1.11^{vw} \pm 0.02$	$0.234^{ef} \pm 0.00$	
	Winter	$0.24^{rst} \pm 0.00$	$0.39^{mnopq} \pm 0.00$	$3^{bc} \pm 0.00$	$1.77^{m} \pm 0.01$	$0.046^{tuv} \pm 0.00$	
	Spring	$2.26^{e} \pm 0.01$	$0.42^{klmno} \pm 0.00$	$11^{a} \pm 0.00$	$1.65^{no} \pm 0.02$	$0.196^{j} \pm 0.00$	
BSh	**Kalgoorlie–AUS**						$0.085^{j} \pm 0.01$
	Summer	$1.66^{l} \pm 0.02$	$0.43^{klmn} \pm 0.00$	$10^{a} \pm 0.00$	$1.61^{o} \pm 0.00$	$0.156^{no} \pm 0.01$	
	Autumn	$1.62^{l} \pm 0.01$	$0.34^{qr} \pm 0.00$	$10^{a} \pm 0.00$	$2.03^{i} \pm 0.01$	$0.152^{nop} \pm 0.00$	
	Winter	-	-	-	-	-	
	Spring	$0.20^{tuv} \pm 0.00$	$0.34^{qr} \pm 0.00$	$3^{bc} \pm 0.00$	$2.03^{i} \pm 0.02$	$0.033^{w} \pm 0.00$	
Cfa	**San Miguel de Tucumán–ARG**						$0.187^{b} \pm 0.00$
	Summer	$1.94^{i} \pm 0.01$	$0.60^{fg} \pm 0.01$	$8^{abc} \pm 0.00$	$1.15^{v} \pm 0.02$	$0.230^{fg} \pm 0.01$	
	Autumn	$1.72^{k} \pm 0.02$	$0.37^{nopq} \pm 0.00$	$10^{a} \pm 0.00$	$1.87^{kl} \pm 0.01$	$0.162^{mn} \pm 0.00$	
	Winter	$1.56^{m} \pm 0.01$	$0.35^{pqr} \pm 0.00$	$10^{a} \pm 0.00$	$1.98^{ij} \pm 0.01$	$0.146^{op} \pm 0.00$	
	Spring	$2.00^{h} \pm 0.01$	$0.66^{cdef} \pm 0.00$	$9^{ab} \pm 0.00$	$1.05^{wx} \pm 0.01$	$0.211^{i} \pm 0.01$	
Cfb	**Orange–AUS**						$0.146^{d} \pm 0.01$
	Summer	$2.54^{c} \pm 0.01$	$0.66^{cdef} \pm 0.01$	$9^{ab} \pm 0.00$	$1.05^{wx} \pm 0.02$	$0.271^{c} \pm 0.01$	
	Autumn	$0.46^{m} \pm 0.00$	$0.23st \pm 0.00$	$6^{abc} \pm 0.00$	$3.01^{e} \pm 0.01$	$0.060^{rs} \pm 0.00$	
	Winter	$0.32^{pq} \pm 0.00$	$0.35^{pqr} \pm 0.00$	$3^{bc} \pm 0.00$	$1.98^{ij} \pm 0.02$	$0.073^{q} \pm 0.00$	
	Spring	$2.08^{g} \pm 0.02$	$0.45^{jklm} \pm 0.01$	$11^{a} \pm 0.00$	$1.54^{pq} \pm 0.01$	$0.180^{kl} \pm 0.00$	
Cwa	**Meerut–IND**						$0.180^{c} \pm 0.01$
	Summer	$2.60^{b} \pm 0.01$	$0.84^{b} \pm 0.00$	$9^{ab} \pm 0.00$	$0.82^{z} \pm 0.00$	$0.277^{bc} \pm 0.00$	
	Autumn	$1.86^{j} \pm 0.02$	$0.53^{hi} \pm 0.00$	$8^{abc} \pm 0.00$	$1.30^{t} \pm 0.01$	$0.220^{ghi} \pm 0.01$	
	Winter	$0.20^{tuv} \pm 0.00$	$0.34^{qr} \pm 0.00$	$2^{c} \pm 0.00$	$2.00^{i} \pm 0.01$	$0.050^{stuv} \pm 0.0$	
	Spring	$2.00^{h} \pm 0.01$	$0.36^{opq} \pm 0.01$	$11^{a} \pm 0.00$	$1.92^{jk} \pm 0.02$	$0.172^{lm} \pm 0.02$	

10974660, 0, Downloaded from https://onlinelibrary.wiley.com/doi/10.1002/jctb.7369 by IFSC - Instituto Federal de Santa Catarina, Wiley Online Library on [28/03/2023]. See the Terms and Conditions (https://onlinelibrary.wiley.com/terms-and-conditions) on Wiley Online Library for rules of use; OA articles are governed by the applicable Creative Commons License

Table 2. Continued

Köppen-Geiger	Geographic positions	X_{max} (g L^{-1})	μ_{max} (d^{-1})	HRT(d)	t_g (d)	P_X (g L^{-1} d^{-1})	P_X annual average (g L^{-1} d^{-1})
Cwb	**Benoni–ZAF**						$0.115^{g} \pm 0.00$
	Summer	$1.86^{j} \pm 0.02$	$0.34^{qr} \pm 0.00$	$10^{a} \pm 0.00$	$2.04^{i} \pm 0.02$	$0.176^{l} \pm 0.01$	
	Autumn	$0.26^{rs} \pm 0.01$	0.23st ± 0.00	$5^{abc} \pm 0.00$	$3.01^{e} \pm 0.01$	$0.032^{w} \pm 0.00$	
	Winter	-	-	-	-	-	
	Spring	$1.88^{j} \pm 0.002$	$0.48^{ijk} \pm 0.01$	$7^{abc} \pm 0.00$	$1.44^{rs} \pm 0.02$	$0.254^{d} \pm 0.01$	
Dwb	**Wuhu–CHN**						$0.090^{i} \pm 0.00$
	Summer	$2.28^{e} \pm 0.02$	$0.36^{opq} \pm 0.00$	$9^{ab} \pm 0.00$	$1.92^{jk} \pm 0.02$	$0.242^{e} \pm 0.02$	
	Autumn	$0.36^{op} \pm 0.00$	$0.15^{u} \pm 0.00$	$5^{abc} \pm 0.00$	$4.62^{a} \pm 0.00$	0.053st ± 0.00	
	Winter	-	-	-	-	-	
	Spring	$0.28^{qr} \pm 0.00$	$0.37^{nopq} \pm 0.00$	$3^{bc} \pm 0.00$	$1.87^{kl} \pm 0.01$	$0.060^{rs} \pm 0.00$	
Mid-latitudes (35 to 55° N and S)							
Cfa	**Joplin–USA**						$0.097^{h} \pm 0.00$
	Summer	$2.06^{g} \pm 0.02$	$0.71^{c} \pm 0.00$	$7^{abc} \pm 0.00$	$0.97^{y} \pm 0.03$	$0.280^{bc} \pm 0.02$	
	Autumn	$0.18^{uv} \pm 0.01$	$0.29^{rs} \pm 0.00$	$2^{c} \pm 0.00$	$2.38^{h} \pm 0.01$	$0.040^{vw} \pm 0.00$	
	Winter	-	-	-	-	-	
	Spring	$0.24^{rst} \pm 0.0$	$0.43^{klmn} \pm 0.00$	$2^{c} \pm 0.00$	$1.59^{op} \pm 0.00$	$0.070^{qr} \pm 0.00$	
Cfb	**Invercargill-NZL**						$0.005^{o} \pm 0.00$
	Summer	$0.16^{v} \pm 0.02$	0.23st ± 0.00	$3^{bc} \pm 0.00$	$2.94^{fg} \pm 0.01$	$0.020^{x} \pm 0.00$	
	Autumn	-	-	-	-	-	
	Winter	-	-	-	-	-	
	Spring	-	-	-	-	-	
Csa	**Algiers–DZA**						$0.122^{f} \pm 0.00$
	Summer	$2.68^{a} \pm 0.01$	$0.67^{cde} \pm 0.01$	$9^{ab} \pm 0.00$	$1.03^{xy} \pm 0.02$	$0.286^{b} \pm 0.01$	
	Autumn	$1.86^{j} \pm 0.01$	$0.46^{jkl} \pm 0.00$	$2^{c} \pm 0.00$	$1.50^{qr} \pm 0.01$	$0.160^{n} \pm 0.00$	
	Winter	-	-	-	-	-	
	Spring	$0.40^{no} \pm 0.00$	$0.22^{t} \pm 0.00$	$2^{c} \pm 0.00$	$3.15^{d} \pm 0.00$	$0.042^{uvw} \pm 0.00$	
	Latina–ITA						$0.113^{g} \pm 0.00$
	Summer	$2.20^{f} \pm 0.02$	$0.33^{qr} \pm 0.01$	$11^{a} \pm 0.00$	$2.04^{i} \pm 0.04$	$0.190^{jk} \pm 0.02$	
	Autumn	$1.88^{j} \pm 0.02$	$0.61^{efg} \pm 0.01$	$8^{abc} \pm 0.00$	$1.13^{v} \pm 0.02$	$0.222^{gh} \pm 0.01$	
	Winter	-	-	-	-	-	
	Spring	$0.22^{stu} \pm 0.00$	$0.39^{mnopq} \pm 0.00$	$3^{bc} \pm 0.00$	$1.77^{m} \pm 0.02$	$0.040^{vw} \pm 0.00$	
Csb	**Esquel–ARG**						$0.015^{n} \pm 0.00$
	Summer	$0.22^{stu} \pm 0.00$	$0.39^{mnopq} \pm 0.00$	$2^{c} \pm 0.00$	$1.77^{m} \pm 0.02$	$0.060^{rs} \pm 0.01$	
	Autumn	-	-	-	-	-	
	Winter	-	-	-	-	-	
	Spring	-	-	-	-	-	

© 2023 Society of Chemical Industry (SCI).

10974660, 0, Downloaded from https://onlinelibrary.wiley.com/doi/10.1002/jctb.7369 by IFSC - Instituto Federal de Santa Catarina, Wiley Online Library on [28/03/2023]. See the Terms and Conditions (https://onlinelibrary.wiley.com/terms-and-conditions) on Wiley Online Library for rules of use; OA articles are governed by the applicable Creative Commons License

Table 2. Continued

Köppen-Geiger	Geographic positions	X_{max} (g L^{-1})	μ_{max} (d^{-1})	HRT(d)	t_g (d)	P_X (g L^{-1} d^{-1})	P_X annual average (g L^{-1} d^{-1})
Dfa	**Samara-RUS**						$0.040^{lm} \pm 0.00$
	Summer	$1.72^{k} \pm 0.02$	$0.38^{nopq} \pm 0.00$	$10^{a} \pm 0.00$	$1.82^{lm} \pm 0.01$	$0.162^{mn} \pm 0.01$	
	Autumn	-	-	-	-	-	
	Winter	-	-	-	-	-	
	Spring	-	-	-	-	-	
Dfb	**Montreal-CAN**						$0.036^{m} \pm 0.00$
	Summer	$1.54^{m} \pm 0.01$	$0.35^{pqr} \pm 0.00$	$10^{a} \pm 0.00$	$1.98^{ij} \pm 0.03$	$0.144^{p} \pm 0.00$	
	Autumn	-	-	-	-	-	
	Winter	-	-	-	-	-	
	Spring	-	-	-	-	-	
Dsa	**Taraz–KAZ**						$0.054^{k} \pm 0.00$
	Summer	$2.06^{g} \pm 0.00$	$0.56^{gh} \pm 0.02$	$9^{ab} \pm 0.00$	$1.23^{u} \pm 0.03$	$0.217^{hi} \pm 0.00$	
	Autumn	-	-	-	-	-	
	Winter	-	-	-	-	-	
	Spring	-	-	-	-	-	
Dsb	**Creston-CAN**						$0.012^{n} \pm 0.00$
	Summer	$0.46^{m} \pm 0.01$	$0.23st \pm 0.00$	$7^{abc} \pm 0.00$	$2.97^{ef} \pm 0.02$	$0.051^{stu} \pm 0.00$	
	Autumn	-	-	-	-	-	
	Winter	-	-	-	-	-	
	Spring	-	-	-	-	-	
Dwa	**Changchun–CHN**						$0.044^{l} \pm 0.00$
	Summer	$2.04^{gh} \pm 0.01$	$0.20^{tu} \pm 0.01$	$11^{a} \pm 0.00$	$3.46^{b} \pm 0.00$	$0.176^{l} \pm 0.1$	
	Autumn	-	-	-	-	-	
	Winter	-	-	-	-	-	
	Spring	-	-	-	-	-	
Dwb	**Uliastay-MNG**						$0.011^{n} \pm 0.00$
	Summer	$0.42^{mn} \pm 0.00$	$0.21^{tu} \pm 0.00$	$7 \pm {}^{abc}0.00$	$3.30^{c} \pm 0.03$	$0.045^{tuv} \pm 0.00$	
	Autumn	-	-	-	-	-	
	Winter	-	-	-	-	-	
	Spring	-	-	-	-	-	

Note: Different lowercase letters followed by different capital letters within the same column express significant differences between the averages ($P \leq 0.05$). X_{max}, maximum biomass density (g L^{-1}); μ_{max}, maximum specific growth rate (d^{-1}); HRT, hydraulic retention time (d); t_g, generation time (d); P_X, biomass productivity (g L^{-1} d^{-1}).

© 2023 Society of Chemical Industry (SCI).

10974660, 0, Downloaded from https://onlinelibrary.wiley.com/doi/10.1002/jctb.7369 by IFSC - Instituto Federal de Santa Catarina, Wiley Online Library on [28/03/2023]. See the Terms and Conditions (https://onlinelibrary.wiley.com/terms-and-conditions) on Wiley Online Library for rules of use; OA articles are governed by the applicable Creative Commons License

Table 3. Total lipid content and lipid productivity of *Scenedesmus obliquus* CPCC05

Köppen-Geiger	Geographic position	*L* (%)	P_L (g L^{-1} d^{-1})	P_L annual average (g L^{-1} d^{-1})
Subtropical (25 to 35° N and S)				
BWh	**Hermosillo–MEX**			$0.025^{a} \pm 0.00$
	Summer	$13.54^{def} \pm 0.12$	$0.031^{bcd} \pm 0.00$	
	Autumn	$11.79^{ijk} \pm 0.05$	$0.035^{ab} \pm 0.00$	
	Winter	$10.41^{nop} \pm 0.21$	$0.005^{mno} \pm 0.00$	
	Spring	$11.58^{jkl} \pm 0.37$	$0.030^{cde} \pm 0.00$	
	Qom–IRN			$0.011^{ef} \pm 0.00$
	Summer	$6.76^{vw} \pm 0.08$	$0.020^{f} \pm 0.00$	
	Autumn	$11.10^{klmn} \pm 0.22$	$0.018^{fgh} \pm 0.00$	
	Winter	-	-	
	Spring	$13.95^{cd} \pm 0.36$	$0.007^{klm} \pm 0.00$	
	Tanta–EGY			$0.019^{bc} \pm 0.00$
	Summer	$10.74^{lmno} \pm 0.12$	$0.028^{de} \pm 0.00$	
	Autumn	$13.18^{defg} \pm 0.09$	$0.031^{bcd} \pm 0.00$	
	Winter	8.43st ± 0.08	$0.004^{mno} \pm 0.00$	
	Spring	$7.80^{tu} \pm 0.06$	$0.015^{ghi} \pm 0.00$	
BSh	**Kalgoorlie–AUS**			$0.009^{fg} \pm 0.00$
	Summer	$9.44^{qr} \pm 0.03$	$0.015^{ghi} \pm 0.00$	
	Autumn	$13.74^{de} \pm 0.11$	$0.020^{f} \pm 0.00$	
	Winter	-	-	
	Spring	$8.05^{stu} \pm 0.04$	$0.002^{no} \pm 0.00$	
Cfa	**San Miguel de Tucumán–ARG**			$0.018^{bc} \pm 0.00$
	Summer	$13.32^{defg} \pm 0.10$	$0.031^{bcd} \pm 0.00$	
	Autumn	$10.60^{mnop} \pm 0.13$	$0.017^{fgh} \pm 0.00$	
	Winter	$13.76^{de} \pm 0.21$	$0.015^{ghi} \pm 0.00$	
	Spring	$5.21^{x} \pm 0.09$	$0.011^{ijk} \pm 0.00$	
Cfb	**Orange–AUS**			$0.017^{bcd} \pm 0.00$
	Summer	$12.06^{hij} \pm 0.04$	$0.033^{abc} \pm 0.00$	
	Autumn	$10.47^{nop} \pm 0.07$	$0.006^{lmn} \pm 0.00$	
	Winter	$13.00^{efg} \pm 0.10$	$0.010^{jkl} \pm 0.00$	
	Spring	$11.79^{ijk} \pm 0.33$	$0.021^{f} \pm 0.00$	
Cwa	**Meerut–IND**			$0.020^{b} \pm 0.00$
	Summer	$12.56^{ghi} \pm 0.36$	$0.035^{ab} \pm 0.00$	
	Autumn	$8.04^{stu} \pm 0.02$	$0.018^{fgh} \pm 0.00$	
	Winter	$4.32^{y} \pm 0.08$	$0.002^{no} \pm 0.00$	
	Spring	$15.52^{ab} \pm 0.42$	$0.026^{e} \pm 0.00$	

© 2023 Society of Chemical Industry (SCI).

10974660, 0, Downloaded from https://onlinelibrary.wiley.com/doi/10.1002/jctb.7369 by IFSC - Instituto Federal de Santa Catarina, Wiley Online Library on [28/03/2023]. See the Terms and Conditions (https://onlinelibrary.wiley.com/terms-and-conditions) on Wiley Online Library for rules of use; OA articles are governed by the applicable Creative Commons License

Table 3. Continued

Köppen-Geiger	Geographic position	L (%)	P_L (g L^{-1} d^{-1})	P_L annual average (g L^{-1} $d-^{1}$)
Cwb	**Benoni–ZAF**			$0.001^{hi} \pm 0.00$
	Summer	$11.12^{klmn} \pm 0.09$	$0.019^{fg} \pm 0.00$	
	Autumn	$10.68^{mno} \pm 0.06$	$0.003^{mno} \pm 0.00$	
	Winter	-	-	
	Spring	$12.80^{fgh} \pm 0.45$	$0.032^{abcd} \pm 0.00$	
Dwb	**Wuhu–CHN**			$0.012^{ef} \pm 0.00$
	Summer	$14.75^{bc} \pm 0.41$	$0.036^{a} \pm 0.00$	
	Autumn	$13.18^{defg} \pm 0.29$	$0.007^{klm} \pm 0.00$	
	Winter	-	-	
	Spring	$8.58^{rst} \pm 0.22$	$0.005^{mno} \pm 0.00$	
Mid-latitudes (35 to 55° N and S)				
Cfa	**Joplin–USA**			$0.009^{fg} \pm 0.00$
	Summer	$11.37^{jklm} \pm 0.13$	$0.032^{abcd} \pm 0.00$	
	Autumn	8.20st ± 0.05	$0.003^{mno} \pm 0.00$	
	Winter	-	-	
	Spring	$4.28^{y} \pm 0.02$	$0.003^{mno} \pm 0.00$	
Cfb	**Invercargill-NZL**			$0.0003^{i} \pm 0.00$
	Summer	$6.00^{wx} \pm 0.06$	$0.001^{o} \pm 0.00$	
	Autumn	-	-	
	Winter	-	-	
	Spring	-	-	
Csa	**Algiers–DZA**			$0.015^{cde} \pm 0.00$
	Summer	$12.62^{ghi} \pm 0.04$	$0.036^{a} \pm 0.00$	
	Autumn	$10.80^{lmno} \pm 0.09$	$0.017^{fgh} \pm 0.00$	
	Winter	-	-	
	Spring	$13.95^{cd} \pm 0.56$	$0.006^{lmn} \pm 0.00$	
	Latina–ITA			$0.013^{def} \pm 0.00$
	Summer	$7.20^{uv} \pm 0.08$	$0.014^{hij} \pm 0.00$	
	Autumn	$16.27^{a} \pm 0.23$	$0.036^{a} \pm 0.00$	
	Winter	-	-	
	Spring	$5.81^{x} \pm 0.15$	$0.002^{no} \pm 0.00$	
Csb	**Esquel–ARG**			$0.0007^{hi} \pm 0.00$
	Summer	$5.61^{x} \pm 0.07$	$0.003^{mno} \pm 0.00$	
	Autumn	-	-	
	Winter	-	-	
	Spring	-	-	

© 2023 Society of Chemical Industry (SCI).

10974660, 0, Downloaded from https://onlinelibrary.wiley.com/doi/10.1002/jctb.7369 by IFSC - Instituto Federal de Santa Catarina, Wiley Online Library on [28/03/2023]. See the Terms and Conditions (https://onlinelibrary.wiley.com/terms-and-conditions) on Wiley Online Library for rules of use; OA articles are governed by the applicable Creative Commons License

Table 3. Continued

Köppen-Geiger	Geographic position	L (%)	P_L (g L^{-1} d^{-1})	P_L annual average (g L^{-1} $d-^{1}$)
Dfa	**Samara-RUS**			$0.004^{hi} \pm 0.00$
	Summer	$10.60^{mnop} \pm 0.17$	$0.017^{fgh} \pm 0.00$	
	Autumn	-	-	
	Winter	-	-	
	Spring	-	-	
Dfb	**Montreal-CAN**			$0.004^{hi} \pm 0.00$
	Summer	$10.18^{opq} \pm 0.30$	$0.015^{ghi} \pm 0.00$	
	Autumn	-	-	
	Winter	-	-	
	Spring	-	-	
Dsa	**Taraz–KAZ**			$0.005^{gh} \pm 0.00$
	Summer	$9.80^{pq} \pm 0.09$	$0.021^{f} \pm 0.00$	
	Autumn	-	-	
	Winter	-	-	
	Spring	-	-	
Dsb	**Creston-CAN**			$0.002^{hi} \pm 0.00$
	Summer	$14.00^{cd} \pm 0.38$	$0.007^{klm} \pm 0.00$	
	Autumn	-	-	
	Winter	-	-	
	Spring	-	-	
Dwa	**Changchun–CHN**			$0.004^{hi} \pm 0.00$
	Summer	$8.73^{rs} \pm 0.10$	$0.015^{ghi} \pm 0.00$	
	Autumn	-	-	
	Winter	-	-	
	Spring	-	-	
Dwb	**Uliastay-MNG**			$0.002^{hi} \pm 0.00$
	Summer	$13.00^{efg} \pm 0.18$	$0.006^{lmn} \pm 0.00$	
	Autumn	-	-	
	Winter	-	-	
	Spring	-	-	

Note: Different letters within the same column express significant differences between the means ($P \leq 0.05$). L, total lipid content (%); P_L, lipid productivity (g L^{-1} d^{-1}).

© 2023 Society of Chemical Industry (SCI).

10974660, 0, Downloaded from https://onlinelibrary.wiley.com/doi/10.1002/jctb.7369 by IFSC - Instituto Federal de Santa Catarina, Wiley Online Library on [28/03/2023]. See the Terms and Conditions (https://onlinelibrary.wiley.com/terms-and-conditions) on Wiley Online Library for rules of use; OA articles are governed by the applicable Creative Commons License

Table 4. Fatty acid profile of *Scenedesmus obliquus* under different climatic conditions

Fatty acids (%)

Köppen–Geiger	Geographic Geographic Positions	C11:0	C12:0	C13:0	C16:0	C16:1	C17:1	C18:0	C18:1n9c	C18:2n6c	C18:3n3	C20:2	C21:0	Minorities	∑SFA	∑MUFA	∑PUFA
Subtropical (25 to 35° N and S)																	
BWh	Hermosillo-MEX																
	Summer	$1.05^{e} \pm 0.08$	ND	ND	$26.80^{J} \pm 0.37$	$0.32^{zAB} \pm 0.00$	$3.59^{e} \pm 0.01$	$4.50^{I} \pm 0.00$	$19.55^{I} \pm 0.63$	$10.53^{h} \pm 0.5$	$31.19^{u} \pm 0.31$	ND	ND	$2.47^{pq} \pm 0.00$	33.38^{L}	23.76^{f}	42.86^{v}
	Autumn	ND	$0.51^{s} \pm 0.04$	$2.07^{c} \pm 0.14$	$33.02^{w} \pm 1.48$	$3.05^{I} \pm 0.32$	ND	$1.49^{A} \pm 0.10$	$14.75^{s} \pm 0.28$	$9.71^{m} \pm 0.37$	$30.63^{v} \pm 0.86$	ND	$2.99^{h} \pm 0.24$	$1.78^{z} \pm 0.09$	41.12^{u}	17.95^{r}	40.93^{y}
	Winter	ND	$1.25^{o} \pm 0.07$	$0.47^{r} \pm 0.03$	$25.73^{O} \pm 1.18$	$0.35^{yz} \pm 0.03$	$0.18^{kl} \pm 0.01$	$1.52^{A} \pm 0.16$	$18.18^{J} \pm 0.76$	$9.14^{o} \pm 0.29$	$35.25^{o} \pm 1.66$	ND	$5.10^{c} \pm 0.37$	$2.84^{n} \pm 0.15$	35.34^{F}	19.83^{n}	44.84^{r}
	Spring	ND	ND	ND	$40.69^{J} \pm 0.01$	$0.25^{B} \pm 0.01$	ND	$2.51^{s} \pm 0.19$	$27.48^{a} \pm 0.09$	$8.43^{r} \pm 0.16$	$18.55^{J} \pm 0.56$	$0.16^{i} \pm 0.00$	$0.10^{m} \pm 0.00$	$1.84^{yz} \pm 0.00$	44.05^{q}	27.87^{b}	28.09^{O}
	Qom-IRN																
	Summer	ND	ND	ND	$39.18^{n} \pm 0.47$	$4.05^{c} \pm 0.22$	ND	$2.99^{n} \pm 0.05$	$23.27^{d} \pm 0.05$	$7.01^{y} \pm 0.15$	$17.41^{K} \pm 0.25$	$4.06^{f} \pm 0.31$	ND	$2.04^{w} \pm 0.07$	43.45^{r}	27.39^{c}	29.17^{l}
	Autumn	ND	$1.65^{kl} \pm 0.07$	$0.86^{q} \pm 0.03$	$29.23^{C} \pm 1.18$	$0.35^{zA} \pm 0.03$	$0.05^{n} \pm 0.01$	$1.86^{w} \pm 0.16$	$10.78^{A} \pm 0.76$	$13.94^{c} \pm 0.29$	$33.56^{r} \pm 0.37$	ND	$5.35^{b} \pm 0.37$	$2.37^{r} \pm 0.15$	39.87^{y}	12.47^{C}	47.66^{m}
	Winter	-	-	-	-	-	-	-	-	-	-	-	-	-	-	-	-
	Spring	ND	$2.02^{h} \pm 0.22$	$1.23^{I} \pm 0.12$	$27.80^{F} \pm 0.16$	$0.56^{v} \pm 0.04$	ND	$1.32^{E} \pm 0.06$	$6.79^{L} \pm 0.38$	$5.80^{E} \pm 0.24$	$52.36^{b} \pm 1.65$	ND	ND	$2.12^{v} \pm 0.10$	33.62^{K}	7.91^{O}	58.47^{a}
	Tanta-EGY																
	Summer	ND	ND	ND	$40.71^{J} \pm 0.47$	$0.27^{B} \pm 0.02$	ND	$2.49^{s} \pm 0.19$	$27.46^{a} \pm 0.09$	$8.46^{r} \pm 0.16$	$18.50^{J} \pm 0.56$	$0.18^{i} \pm 0.00$	$0.13^{m} \pm 0.13$	$1.81^{yz} \pm 0.01$	44.07^{q}	27.84^{b}	28.10^{O}
	Autumn	$0.94^{g} \pm 0.04$	ND	ND	$28.91^{D} \pm 0.33$	$0.31^{zAB} \pm 0.01$	$3.21^{f} \pm 0.11$	$8.78^{c} \pm 0.83$	$17.33^{n} \pm 0.85$	$9.47^{n} \pm 0.33$	$28.90^{z} \pm 0.20$	ND	ND	$2.15^{uv} \pm 0.13$	39.73^{z}	21.15^{I}	39.12^{A}
	Winter	ND	$1.49^{m} \pm 0.12$	$0.94^{op} \pm 0.03$	$26.57^{L} \pm 0.09$	$0.59^{uv} \pm 0.09$	$0.09^{m} \pm 0.00$	$1.51^{A} \pm 0.08$	$9.54^{F} \pm 0.17$	$3.54^{I} \pm 0.18$	$49.48^{e} \pm 0.92$	ND	$3.58^{f} \pm 0.17$	$2.66^{o} \pm 0.19$	35.35^{F}	11.43^{F}	53.21^{g}
	Spring	ND	ND	ND	$40.24^{I} \pm 0.73$	$3.19^{h} \pm 0.11$	ND	$3.46^{k} \pm 0.13$	$24.05^{c} \pm 0.38$	$7.74^{v} \pm 0.43$	$14.82^{O} \pm 0.39$	$4.64^{e} \pm 0.04$	ND	$1.85^{y} \pm 0.08$	44.82^{n}	27.36^{c}	27.81^{P}
BSh	Kalgoorlie-AUS																
	Summer	ND	$2.69^{b} \pm 0.04$	$1.81^{d} \pm 0.02$	$41.28^{g} \pm 0.01$	$0.75^{s} \pm 0.01$	ND	$2.14^{u} \pm 0.03$	$13.31^{t} \pm 0.26$	$10.10^{I} \pm 0.04$	$24.57^{C} \pm 0.18$	ND	ND	$3.36^{j} \pm 0.00$	49.10^{I}	15.50^{u}	35.41^{D}
	Autumn	ND	ND	ND	$39.17^{n} \pm 0.26$	$1.13^{p} \pm 0.07$	ND	$2.60^{q} \pm 0.03$	$21.23^{h} \pm 0.43$	$8.04^{t} \pm 0.38$	$18.67^{I} \pm 0.43$	$5.34^{c} \pm 0.45$	ND	$3.82^{h} \pm 0.03$	44.43^{p}	22.84^{I}	32.73^{F}
	Winter	-	-	-	-	-	-	-	-	-	-	-	-	-	-	-	-
	Spring	ND	$1.80^{J} \pm 0.15$	$1.18^{I} \pm 0.08$	$54.31^{d} \pm 0.75$	$5.20^{b} \pm 0.26$	ND	$1.38^{BCD} \pm 0.01$	$4.11^{R} \pm 0.40$	$5.93^{D} \pm 0.33$	$14.21^{P} \pm 0.29$	ND	ND	$11.88^{b} \pm 0.01$	60.42^{d}	10.13^{H}	29.46^{H}
Cfa	San Miguel de Tucumán-ARG																
	Summer	ND	$0.44^{t} \pm 0.03$	$1.70^{e} \pm 0.14$	$31.07^{x} \pm 0.40$	$2.99^{J} \pm 0.15$	ND	$2.56^{qr} \pm 0.22$	$15.39^{q} \pm 1.14$	$11.79^{e} \pm 0.25$	$29.04^{y} \pm 1.14$	ND	$3.11^{g} \pm 0.11$	$1.91^{x} \pm 0.05$	40.01^{x}	18.57^{o}	41.42^{x}
	Autumn	ND	$0.19^{u} \pm 0.01$	ND	$29.56^{B} \pm 0.68$	$2.88^{k} \pm 0.19$	ND	$0.78^{H} \pm 0.04$	$10.09^{C} \pm 0.49$	$10.17^{k} \pm 0.64$	$38.31^{i} \pm 1.29$	$6.62^{a} \pm 0.49$	ND	$1.40^{B} \pm 0.02$	31.39^{O}	13.07^{A}	55.54^{e}
	Winter	$0.74^{h} \pm 0.06$	ND	ND	$30.07^{z} \pm 0.40$	$0.48^{w} \pm 0.02$	$2.71^{h} \pm 0.22$	$4.93^{h} \pm 0.39$	$18.07^{K} \pm 0.43$	$10.41^{I} \pm 0.38$	$29.10^{x} \pm 0.43$	ND	ND	$3.49^{I} \pm 0.09$	36.88^{D}	21.58^{k}	41.54^{w}
	Spring	ND	$0.98^{p} \pm 0.04$	$3.43^{a} \pm 0.14$	$56.11^{c} \pm 1.48$	$0.42^{x} \pm 0.32$	ND	$1.78^{x} \pm 0.10$	$6.11^{P} \pm 0.28$	$5.58^{F} \pm 0.37$	$19.41^{F} \pm 0.86$	ND	$1.85^{J} \pm 0.24$	$4.33^{f} \pm 0.09$	65.68^{c}	8.83^{K}	25.49^{Q}
Cfb	Orange-AUS																
	Summer	ND	ND	ND	$40.30^{k} \pm 2.67$	$2.06^{I} \pm 0.20$	ND	$2.77^{o} \pm 0.26$	$22.95^{e} \pm 0.62$	$9.13^{o} \pm 0.89$	$19.24^{G} \pm 1.20$	$0.03^{j} \pm 0.00$	$0.04^{n} \pm 0.00$	$3.48^{I} \pm 0.12$	46.03^{m}	25.10^{d}	28.87^{K}
	Autumn	ND	$1.22^{o} \pm 0.07$	$0.50^{r} \pm 0.03$	$25.76^{O} \pm 1.18$	$0.36^{yz} \pm 0.03$	$0.15^{kl} \pm 0.01$	$1.49^{A} \pm 0.16$	$18.20^{J} \pm 0.76$	$9.16^{o} \pm 0.00$	$35.23^{o} \pm 0.37$	ND	$5.13^{c} \pm 0.37$	$2.80^{n} \pm 0.15$	35.34^{F}	19.83^{n}	44.83^{r}
	Winter	ND	$2.13^{g} \pm 0.14$	$1.70^{e} \pm 0.06$	$52.36^{e} \pm 1.05$	$6.62^{a} \pm 0.23$	ND	$1.35^{CDE} \pm 0.10$	$5.10^{Q} \pm 0.06$	$12.15^{d} \pm 0.48$	$4.00^{O} \pm 0.02$	ND	ND	$14.59^{a} \pm 0.02$	58.92^{e}	12.92^{B}	28.16^{N}
	Spring	ND	ND	ND	$29.99^{A} \pm 0.18$	$3.82^{d} \pm 0.23$	ND	$1.08^{F} \pm 0.02$	$15.97^{o} \pm 0.22$	$11.20^{f} \pm 0.52$	$30.66^{v} \pm 00.39$	$5.92^{b} \pm 00.25$	ND	$1.35^{B} \pm 0.06$	31.84^{M}	19.86^{n}	48.29^{k}
Cwa	Meerut-IND																
	Summer	$1.24^{c} \pm 0.03$	ND	ND	$26.01^{M} \pm 0.039$	$0.35^{zA} \pm 0.01$	$4.70^{a} \pm 0.12$	$5.40^{g} \pm 0.00$	$14.88^{r} \pm 0.76$	$10.40^{ij} \pm 0.04$	$34.82^{p} \pm 0.58$	ND	ND	$2.20^{tu} \pm 0.04$	33.60^{K}	20.15^{m}	46.25^{o}
	Autumn	ND	ND	ND	$41.07^{h} \pm 0.52$	$1.71^{o} \pm 00.04$	ND	$2.66^{p} \pm 0.09$	$22.31^{f} \pm 0.32$	$7.62^{w} \pm 00.10$	$16.64^{M} \pm 0.36$	$3.90^{g} \pm 0.03$	ND	$4.09^{g} \pm 0.07$	46.46^{I}	24.55^{e}	28.99^{J}
	Winter	ND	$0.67^{q} \pm 0.04$	$0.44^{s} \pm 0.02$	$62.76^{a} \pm 1.20$	$1.84^{n} \pm 0.08$	$0.12^{lm} \pm 0.02$	$3.24^{m} \pm 0.24$	$7.14^{I} \pm 0.07$	$2.65^{J} \pm 0.12$	$16.85^{L} \pm 0.40$	ND	$1.79^{k} \pm 0.12$	$2.49^{pq} \pm 0.18$	70.5^{a}	9.78^{J}	19.71^{S}
	Spring	ND	$2.15^{g} \pm 0.05$	$1.39^{h} \pm 0.01$	$40.84^{i} \pm 0.41$	$0.60^{tuv} \pm 0.00$	ND	$2.54^{rs} \pm 0.03$	$15.90^{p} \pm 0.09$	$10.35^{j} \pm 0.12$	$23.41^{D} \pm 0.23$	ND	ND	$2.82^{n} \pm 0.12$	48.09^{j}	17.66^{t}	34.25^{E}
Cw	Benoni-ZAF																
	Summer	ND	$2.37^{e} \pm 0.06$	$1.44^{g} \pm 0.07$	$29.52^{B} \pm 0.74$	$0.41^{xy} \pm 0.02$	$0.21^{j} \pm 0.01$	$2.08^{v} \pm 0.18$	$13.25^{u} \pm 1.22$	$15.16^{a} \pm 1.28$	$33.04^{s} \pm 1.91$	ND	ND	$2.52^{p} \pm 0.10$	37.22^{C}	14.29^{w}	48.49^{j}
	Autumn	ND	$1.84^{J} \pm 0.00$	$1.05^{I} \pm 0.01$	$35.16^{r} \pm 0.23$	$1.79^{n} \pm 0.03$	ND	$2.04^{v} \pm 0.17$	$11.43^{y} \pm 0.24$	$6.16^{B} \pm 0.03$	$37.82^{I} \pm 0.12$	ND	ND	$2.71^{o} \pm 0.06$	41.67^{t}	13.26^{z}	45.07^{q}
	Winter	-	-	-	-	-	-	-	-	-	-	-	-	-	-	-	-
	Spring	$1.10^{d} \pm 0.02$	ND	ND	$25.90^{N} \pm 0.21$	$0.55^{v} \pm 0.01$	$3.05^{g} \pm 0.05$	$6.49^{f} \pm 0.38$	$6.18^{O} \pm 0.06$	$8.52^{q} \pm 0.14$	$45.99^{g} \pm 03$	ND	ND	$2.22^{t} \pm 0.06$	34.42^{H}	9.85^{I}	55.73^{d}
Dwb	Wuhu-CHN																
	Summer	$0.56^{i} \pm 0.02$	ND	ND	$26.74^{K} \pm 0.21$	$0.31^{zAB} \pm 0.01$	$4.53^{b} \pm 0.05$	$6.74^{e} \pm 0.36$	$12.98^{v} \pm 0.05$	$10.49^{h} \pm 0.14$	$35.34^{n} \pm 0.29$	ND	ND	$2.31^{s} \pm 0.06$	34.92^{G}	18.04^{q}	47.04^{n}
	Autumn	$2.51^{a\pm}0.00$	ND	ND	$25.95^{N} \pm 0.00$	$3.83^{d} \pm 0.00$	$1.26^{i} \pm 0.01$	$7.62^{d} \pm 0.00$	$17.54^{m} \pm 0.00$	$6.14^{B} \pm 0.00$	$29.63^{w} \pm 0.00$	ND	ND	$5.52^{e} \pm 0.00$	38.55^{B}	23.39^{g}	38.06^{B}
	Winter	-	-	-	-	-	-	-	-	-	-	-	-	-	-	-	-
	Spring	ND	$1.67^{k} \pm 0.12$	$0.98^{no} \pm 0.03$	$26.69^{K} \pm 0.09$	$0.65^{t} \pm 0.04$	$0.10^{m} \pm 0.00$	$1.40^{BC} \pm 0.08$	$9.78^{E} \pm 0.17$	$3.79^{H} \pm 0.18$	$48.18^{f} \pm 0.92$	ND	$3.82^{e} \pm 0.17$	$2.94^{m} \pm 0.19$	35.65^{E}	11.67^{E}	52.68^{h}

wileyonlinelibrary.com/jctb © 2023 Society of Chemical Industry (SCI). J Chem Technol Biotechnol 2023

10974660, 0, Downloaded from https://onlinelibrary.wiley.com/doi/10.1002/jctb.7369 by IFSC - Instituto Federal de Santa Catarina, Wiley Online Library on [28/03/2023]. See the Terms and Conditions (https://onlinelibrary.wiley.com/terms-and-conditions) on Wiley Online Library for rules of use; OA articles are governed by the applicable Creative Commons License

© 2023 Society of Chemical Industry (SCI).

Table 4. Continued

Fatty acids (%)

Köppen–Geiger	Geographic Geographic Positions	C11:0	C12:0	C13:0	C16:0	C16:1	C17:1	C18:0	C18:1n9c	C18:2n6c	C18:3n3	C20:2	C21:0	Minorities	∑SFA	∑MUFA	∑PUFA
Mid-latitudes (35 to 55° N and S)																	
Cfa	Joplin-USA																
	Summer	ND	$0.54^{rs} \pm 0.04$	$2.04^{c} \pm 0.14$	$30.30^{y} \pm 1.48$	$3.32^{f} \pm 0.32$	ND	$1.62^{z} \pm 0.10$	$14.71^{s} \pm 0.28$	$10.40^{ij} \pm 0.37$	$32.34^{t} \pm 0.86$	ND	$3.11^{g} \pm 3.18$	$1.63^{A} \pm 0.09$	38.54^{B}	18.17^{P}	43.30^{u}
	Autumn	ND	$1.42^{n} \pm 0.06$	$1.12^{k} \pm 0.04$	$34.20^{v} \pm 0.56$	$3.60^{e} \pm 0.28$	$0.16^{k} \pm 0.01$	$1.80^{x} \pm 0.20$	$6.42^{M} \pm 0.08$	$10.12^{kl} \pm 0.40$	$26.26^{B} \pm 0.28$	$0.04^{J} \pm 0.01$	$4.20^{d} \pm 0.20$	$10.66^{c} \pm 0.10$	52.34^{f}	11.05^{G}	36.61^{C}
	Winter	-	-	-	-	-	-	-	-	-	-	-	-	-	-	-	-
	Spring	ND	$0.56^{r} \pm 0.01$	$0.40^{s} \pm 0.00$	$58.76^{b} \pm 0.40$	$1.92^{m} \pm 0.03$	$0.16^{k} \pm 0.00$	$3.26^{m} \pm 0.30$	$8.14^{H} \pm 0.62$	$2.62^{J} \pm 0.02$	$16.80^{L} \pm 0.04$	ND	$1.74^{I} \pm 0.02$	$5.64^{d} \pm 0.12$	66.10^{b}	9.78^{J}	24.12^{R}
Cfb	**Invercargill-NZL**																
	Summer	ND	$1.90^{j} \pm 0.02$	$0.99^{mn} \pm 0.01$	$35.00^{s} \pm 0.32$	$1.80^{n} \pm 0.04$	ND	$1.87^{w} \pm 0.08$	$11.74^{x} \pm 0.21$	$6.33^{z} \pm 0.18$	$38.23^{j} \pm 0.63$	ND	ND	$2.14^{v} \pm 0.07$	40.90^{v}	14.54^{v}	44.56^{s}
	Autumn	-	-	-	-	-	-	-	-	-	-	-	-	-	-	-	-
	Winter	-	-	-	-	-	-	-	-	-	-	-	-	-	-	-	-
	Spring	-	-	-	-	-	-	-	-	-	-	-	-	-	-	-	-
Csa	Algiers-DZA																
	Summer	$1.43^{b} \pm 0.10$	ND	ND	$34.50^{u} \pm 0.71$	$0.30^{AB} \pm 0.02$	$3.87^{d} \pm 0.17$	$12.30^{a} \pm 1.0$	$17.63^{I} \pm 0.19$	$8.74^{P} \pm 0.30$	$17.46^{K} \pm 1.04$	ND	ND	$3.77^{h} \pm 0.13$	49.60^{g}	22.10^{j}	28.30^{M}
	Autumn	ND	$1.61^{I} \pm 0.08$	$0.91^{p} \pm 0.05$	$28.14^{E} \pm 0.69$	$0.33^{zA} \pm 0.01$	$0.05^{n} \pm 0.00$	$1.58^{z} \pm 0.16$	$10.66^{B} \pm 0.13$	$14.21^{b} \pm 0.17$	$34.60^{q} \pm 0.53$	ND	$5.45^{a} \pm 0.12$	$2.46^{q} \pm 0.01$	38.60^{B}	12.40^{D}	48.99^{i}
	Winter	-	-	-	-	-	-	-	-	-	-	-	-	-	-	-	-
	Spring	ND	$2.43^{d} \pm 0.22$	$1.47^{g} \pm 0.12$	$27.66^{G} \pm 0.16$	$0.63^{tu} \pm 0.04$	ND	$1.41^{B} \pm 0.06$	$6.94^{K} \pm 0.38$	$6.15^{B} \pm 0.24$	$51.05^{d} \pm 0.85$	ND	ND	$2.25^{t} \pm 0.10$	34.30^{I}	8.19^{M}	57.50^{c}
	Latina-ITA																
	Summer	ND	ND	ND	$38.79^{o} \pm 0.73$	$3.26^{g} \pm 0.11$	ND	$3.33^{I} \pm 0.13$	$24.82^{b} \pm 0.38$	$8.26^{s} \pm 0.43$	$14.99^{N} \pm 0.39$	$4.64^{e} \pm 0.04$	ND	$1.91^{x} \pm 0.08$	43.27^{s}	28.22^{a}	28.51^{L}
	Autumn	$0.99^{f} \pm 0.04$	ND	ND	$26.86^{I} \pm 1.77$	$0.44^{wx} \pm 0.00$	$4.21^{c} \pm 0.30$	$9.89^{b} \pm 0.09$	$8.21^{G} \pm 0.55$	$8.25^{s} \pm 0.39$	$38.03^{k} \pm 2.05$	ND	ND	$3.12^{k} \pm 0.02$	38.94^{A}	13.03^{A}	48.02^{I}
	Winter	-	-	-	-	-	-	-	-	-	-	-	-	-	-	-	-
	Spring	ND	$1.84^{j} \pm 0.00$	$1.03^{lm} \pm 0.01$	$34.69^{t} \pm 0.23$	$1.72^{o} \pm 0.03$	ND	$1.70^{y} \pm 0.17$	$11.91^{w} \pm 0.24$	$6.23^{A} \pm 0.03$	$38.06^{k} \pm 0.12$	ND	ND	$2.82^{n} \pm 0.06$	40.48^{w}	14.08^{x}	45.44^{p}
Csb	Esquel-ARG																
	Summer	ND	$1.46^{mn} \pm 0.06$	$0.92^{p} \pm 0.06$	$37.45^{p} \pm 0.05$	$0.36^{yz} \pm 0.03$	$0.04^{n} \pm 0.00$	$3.63^{J} \pm 0.36$	$6.29^{N} \pm 0.00$	$7.13^{x} \pm 0.53$	$36.76^{m} \pm 1.22$	ND	$2.95^{I} \pm 0.27$	$3.01^{I} \pm 0.00$	48.01^{J}	7.93^{O}	44.06^{t}
	Autumn	-	-	-	-	-	-	-	-	-	-	-	-	-	-	-	-
	Winter	-	-	-	-	-	-	-	-	-	-	-	-	-	-	-	-
	Spring	-	-	-	-	-	-	-	-	-	-	-	-	-	-	-	-
Dfa	**Samara-RUS**																
	Summer	ND	$0.22^{u} \pm 0.01$	ND	$29.98^{A} \pm 0.68$	$3.08^{I} \pm 0.19$	ND	$0.98^{G} \pm 0.04$	$10.00^{D} \pm 0.49$	$11.17^{f} \pm 0.64$	$39.51^{h} \pm 1.29$	$3.66^{h} \pm 0.49$	ND	$1.40^{B} \pm 0.05$	31.58^{N}	14.08^{x}	54.34^{f}
	Autumn	-	-	-	-	-	-	-	-	-	-	-	-	-	-	-	-
	Winter	-	-	-	-	-	-	-	-	-	-	-	-	-	-	-	-
	Spring	-	-	-	-	-	-	-	-	-	-	-	-	-	-	-	-
Dfb	**Montreal-CAN**																
	Summer	ND	ND	ND	$39.36^{m} \pm 0.26$	$1.08^{p} \pm 0.07$	ND	$2.57^{qr} \pm 0.03$	$21.34^{g} \pm 0.43$	$7.88^{u} \pm 0.38$	$18.75^{H} \pm 0.43$	$5.25^{d} \pm 0.45$	ND	$3.77^{h} \pm 0.03$	44.55^{o}	22.90^{h}	32.55^{G}
	Autumn	-	-	-	-	-	-	-	-	-	-	-	-	-	-	-	-
	Winter	-	-	-	-	-	-	-	-	-	-	-	-	-	-	-	-
	Spring	-	-	-	-	-	-	-	-	-	-	-	-	-	-	-	-
Dsa	Taraz-KAZ																
	Summer	ND	$3.35^{a} \pm 0.27$	$2.45^{b} \pm 0.10$	$37.26^{q} \pm 0.75$	$0.82^{r} \pm 0.02$	ND	$2.38^{t} \pm 0.21$	$10.90^{z} \pm 0.48$	$9.67^{m} \pm 0.16$	$28.80^{A} \pm 0.02$	ND	ND	$4.36^{f} \pm 0.00$	46.71^{k}	13.65^{y}	39.63^{z}
	Autumn	-	-	-	-	-	-	-	-	-	-	-	-	-	-	-	-
	Winter	-	-	-	-	-	-	-	-	-	-	-	-	-	-	-	-
	Spring	-	-	-	-	-	-	-	-	-	-	-	-	-	-	-	-
Dsb	**Creston-CAN**																
	Summer	ND	$2.27^{f} \pm 0.22$	$1.36^{h} \pm 0.12$	$27.65^{G} \pm 0.16$	$0.60^{tuv} \pm 0.04$	ND	$1.34^{DE} \pm 0.06$	$7.08^{J} \pm 0.38$	$6.07^{C} \pm 0.24$	$51.39^{c} \pm 0.85$	ND	ND	$2.24^{t} \pm 0.10$	33.92^{J}	8.28^{L}	57.79^{b}
	Autumn	-	-	-	-	-	-	-	-	-	-	-	-	-	-	-	-
	Winter	-	-	-	-	-	-	-	-	-	-	-	-	-	-	-	-
	Spring	-	-	-	-	-	-	-	-	-	-	-	-	-	-	-	-
Dwa	Changchun-CHN																
	Summer	ND	$2.62^{c} \pm 0.26$	$1.73^{e} \pm 0.02$	$41.59^{f} \pm 1.52$	$0.97^{q} \pm 0.02$	ND	$2.36^{t} \pm 0.11$	$15.40^{q} \pm 0.36$	$10.76^{g} \pm 0.42$	$20.23^{E} \pm 0.94$	ND	ND	$4.34^{f} \pm 0.00$	49.48^{h}	17.82^{s}	32.70^{F}
	Autumn	-	-	-	-	-	-	-	-	-	-	-	-	-	-	-	-
	Winter	-	-	-	-	-	-	-	-	-	-	-	-	-	-	-	-
	Spring	-	-	-	-	-	-	-	-	-	-	-	-	-	-	-	-

10974660, 0, Downloaded from https://onlinelibrary.wiley.com/doi/10.1002/jctb.7369 by IFSC - Instituto Federal de Santa Catarina, Wiley Online Library on [28/03/2023]. See the Terms and Conditions (https://onlinelibrary.wiley.com/terms-and-conditions) on Wiley Online Library for rules of use; OA articles are governed by the applicable Creative Commons License

Table 4. Continued

Köppen–Geiger	Geographic Positions	Fatty acids (%) C11:0	C12:0	C13:0	C16:0	C16:1	C17:1	C18:0	C18:1n9c	C18:2n6c	C18:3n3	C20:2	C21:0	Minorities	∑SFA	∑MUFA	∑PUFA
Dwb	**Uliastay-MNG**																
	Summer	ND	$2.30^{f} \pm 0.12$	$1.60^{f} \pm 0.05$	$27.00^{H} \pm 0.17$	$0.73^{s} \pm 0.02$	ND	$1.50^{A} \pm 0.09$	$7.15^{I} \pm 0.22$	$5.50^{G} \pm 0.16$	$53.00^{a} \pm 0.85$	ND	ND	$1.22^{C} \pm 0.06$	33.40^{L}	8.10^{N}	58.50^{a}
	Autumn	-	-	-	-	-	-	-	-	-	-	-	-	-	-	-	-
	Winter	-	-	-	-	-	-	-	-	-	-	-	-	-	-	-	-
	Spring	-	-	-	-	-	-	-	-	-	-	-	-	-	-	-	-

Note: Different lowercase letters followed by different capital letters within the same column express significant differences between the averages ($P \leq 0.05$). Values are the average ± SD of three replicates. ND, not detected; SFA, saturated fatty acid; MUFA, monounsaturated fatty acid; PUFA, polyunsaturated fatty acid.

3.0 L and 2.0 L, respectively (Tecnal, Piracicaba-SP, Brazil). Besides a temperature sensor and a temperature control loop through a thermostat-controlled bath, the photobioreactor had a photoperiod system. Through this system, it was possible to simulate the duration and intensity of sunlight. The minimum light intensity (0 μmol m^{-2} s^{-1}) was increased linearly to the maximum intensity which remained for 3 h and then linearly returned to the minimum intensity. The mixture of gases, that is, air and CO_2, was controlled through rotameters. For more details on the technical characteristics of the photobioreactor, consult Siqueira *et al.*[2]

Experimental conditions

The cultivations of *S. obliquus* CPCC05 were carried out in a single-batch regimen with an initial cell density of 0.1 g L^{-1} and permanent aeration of 1 VVM (volume of air per volume of medium per minute) with air injection containing 15% industrial grade commercial CO_2 (99.8% purity; Praxair, Inc., Danbury, CT, USA). The evaporation rate was verified experimentally using labels on the photobioreactor and distilled water was added to eliminate the effect of water evaporation during cultivation. In the section below are given the conditions for temperature, light intensity and photoperiod.

The cell density of all cultivation was monitored every 24 h until the stationary phase of growth. Cell density was evaluated gravimetrically by filtering a known volume of culture medium through a 0.45-μm filter (Millex FG, Billerica, MA, USA) and drying it at 60 °C for 24 h.[13]

At the end of the experiments, the biomasses were harvested by centrifugation, the supernatant was discarded and the remaining biomass was freeze-drying in a lyophilizer (L101, Liotop; Liobras, Sao Paolo, BR) for 24 h with 0.200–0.300 μHg of vacuum and a condenser temperature of −37 °C. Posteriorly, the freeze-dried biomasses were stored under refrigeration at −18 °C without the presence of light until the quantitative and qualitative analysis of the composition of the microalgae. The cultivations were carried out in duplicate and the kinetic parameters are the average of four replicates.

Simulation of climatic elements

The day length, solar irradiance and temperature of 20 geographic positions of the subtropical (25° to 35° N and S) and mid-latitudes (35° to 55° N and S) climate zones were simulated: Creston–CAN, Montreal–CAN, Samara–RUS, Invercargill-NZL, Uliastay–MNG, Algiers–DZA, Benoni–ZAF, Changchun–CHN, Esquel–ARG, Hermosillo–MEX, Joplin–USA, Kalgoorlie–AUS, Latina–ITA, Meerut–IND, Orange–AUS, Qom–IRN, San Miguel de Tucumán–ARG, Tanta–EGY, Taraz–KAZ and Wuhu–CHN. The choice of geographic positions was based on the availability of normal climatological data of the climatic elements that were obtained from the Solar Electricity Handbook[14] and Weatherbase[15] websites. Besides that, they were representatively selected to cover the most diverse types of climate in the study area. Figure 1 illustrates the geographic positions of the study. The Köppen–Geiger climate classification and experimental conditions for each location are given in Table 1.

Kinetic parameters

Biomass data were used to calculate biomass productivity [$P_X = (X_i - X_{i-1})/(t_i - t_{i-1})$, g L^{-1} d^{-1}], lipid productivity [$P_L = P_X \times L_C$, g L^{-1} d^{-1}], maximum specific growth rate [$\ln\left(\frac{X_i}{X_0}\right) = \mu_{max} \times t$, d^{-1}] and generation time [$tg = \frac{\ln(2)}{\mu_{max}}$, d], where X_i is the biomass density

© 2023 Society of Chemical Industry (SCI).

10974660, 0, Downloaded from https://onlinelibrary.wiley.com/doi/10.1002/jctb.7369 by IFSC - Instituto Federal de Santa Catarina, Wiley Online Library on [28/03/2023]. See the Terms and Conditions (https://onlinelibrary.wiley.com/terms-and-conditions) on Wiley Online Library for rules of use; OA articles are governed by the applicable Creative Commons License

Table 5. Energy cost and environmental impacts associated with coal-based fossil energy demand to produce 1 t month^{-1} of whole-dried biomass in closed systems

Geographic positions	Production cost (US$)	AP (kg SO_2-eq)	EP (kg Phosphate-eq)	FAETP (kg DCB-eq)	GWP (kg CO_2-eq)	HTP (kg DCB-eq)	POCP (kg Ethene-eq)
Subtropical (25 to 35° N and S)							
Hermosillo–MEX	251 102.32	4800.49	535.44	923.17	2 215 608.73	51 697.54	295.41
Qom–IRN	404 938.08	7741.46	863.47	1488.74	3 572 983.09	83 369.61	476.40
Tanta–EGY	286 426.02	5475.79	610.76	1053.04	2 527 288.44	58 970.06	336.97
Kalgoorlie–AUS	618 724.55	11 828.56	1319.34	2274.72	5 459 334.22	127 384.47	727.91
San Miguel de Tucumán–ARG	281 848.91	5388.29	601.00	1036.21	2 486 902.14	58 027.72	331.59
Orange–AUS	360 683.96	6895.43	769.11	1326.04	3 182 505.54	74 258.46	424.33
Meerut–IND	292 766.17	5597.00	624.28	1076.35	2 583 230.96	60 275.39	344.43
Benoni–ZAF	457 610.11	8748.43	975.79	1682.39	4 037 736.27	94 213.85	538.36
Wuhu–CHN	584 413.14	11 172.60	1246.18	2148.58	5 156 586.51	120 320.35	687.54
Mid-latitudes (35 to 55° N and S)							
Joplin–USA	542 319.76	10 367.88	1156.42	1993.82	4 785 174.37	111 654.07	638.02
Invercargill-NZL	10 500 409.88	200 743.13	22 390.58	38 604.45	92 650 675.40	2 161 849.09	12 353.42
Algiers–DZA	431 418.01	8247.70	919.94	1586.10	3 806 629.50	88 821.35	507.55
Latina–ITA	465 689.59	8902.89	993.01	1712.09	4 109 025.84	95 877.27	547.87
Esquel–ARG	3 500 882.76	66 928.64	7465.12	12 870.89	30 890 142.07	720 769.98	4118.69
Samara-RUS	1 313 530.54	25 111.61	2800.91	4829.16	11 589 975.40	270 432.76	1545.33
Montreal-CAN	1 459 354.02	27 899.42	3111.86	5365.27	12 876 653.18	300 455.24	1716.89
Taraz–KAZ	973 275.75	18 606.74	2075.37	3578.22	8 587 727.25	200 380.30	1145.03
Creston-CAN	4 375 823.65	83 655.45	9330.80	16 087.59	38 610 208.73	900 904.87	5148.03
Changchun–CHN	1 194 220.42	22 830.68	2546.50	4390.52	10 537 239.04	245 868.91	1404.97
Uliastay-MNG	4 773 524.06	91 258.55	10 178.84	17 549.72	42 119 329.95	982 784.37	5615.91

Abbreviation: GWP, global warming potential; AP, acidification potential; FAETP, freshwater ecotoxicity potential; HTP, human toxicity potential; EP, eutrophication potential; POCP, photochemical ozone creation potential.

© 2023 Society of Chemical Industry (SCI).

10974660, 0, Downloaded from https://onlinelibrary.wiley.com/doi/10.1002/jctb.7369 by IFSC - Instituto Federal de Santa Catarina, Wiley Online Library on [28/03/2023]. See the Terms and Conditions (https://onlinelibrary.wiley.com/terms-and-conditions) on Wiley Online Library for rules of use; OA articles are governed by the applicable Creative Commons License

© 2023 Society of Chemical Industry (SCI).

Table 6. Energy cost and environmental impacts associated with coal-based fossil energy demand to produce 1 t month-1 of whole-dried biomass in open systems

Geographic positions	Production cost (US$)	AP (kg SO_2-eq)	EP (kg Phosphate-eq)	FAETP (kg DCB-eq)	GWP (kg CO_2-eq)	HTP (kg DCB-eq)	POCP (kg Ethene-eq)
Subtropical (25 to 35° N and S)							
Hermosillo–MEX	46 550.86	889.94	99.26	171.14	410 742.85	9584.00	54.77
Qom–IRN	74 484.16	1423.96	158.83	273.84	657 213.18	15 334.97	87.63
Tanta–EGY	52 964.89	1012.56	112.94	194.72	467 337.26	10 904.54	62.31
Kalgoorlie–AUS	113 303.24	2166.09	241.60	416.56	999 734.44	23 327.14	133.30
San Miguel de Tucumán–ARG	52 133.78	996.68	111.17	191.67	460 003.96	10 733.43	61.33
Orange–AUS	66 448.55	1270.34	141.69	244.30	586 310.75	13 680.58	78.17
Meerut–IND	54 116.13	1034.57	115.39	198.96	477 495.23	11 141.56	63.67
Benoni–ZAF	84 048.28	1606.81	179.22	309.00	741 602.47	17 304.06	98.88
Wuhu–CHN	107 073.01	2046.98	228.32	393.65	944 761.89	22 044.44	125.97
Mid-latitudes (35 to 55° N and S)							
Joplin–USA	99 429.75	1900.86	212.02	365.55	877 321.34	20 470.83	116.98
Invercargill-NZL	1 907 607.24	36 468.96	4067.69	7013.26	16 831 828.56	392 742.67	2244.24
Algiers–DZA	79 292.35	1515.88	169.08	291.52	699 638.40	16 324.90	93.29
Latina–ITA	85 515.34	1634.85	182.35	314.39	754 547.14	17 606.10	100.61
Esquel–ARG	636 641.90	12 171.10	1357.55	2340.60	5 617 428.56	131 073.33	748.99
Samara-RUS	239 465.24	4578.01	510.62	880.39	2 112 928.56	49 301.67	281.72
Montreal-CAN	265 943.68	5084.22	567.09	977.73	2 346 561.89	54 753.11	312.87
Taraz–KAZ	177 682.20	3396.87	378.88	653.24	1 567 784.12	36 581.63	209.04
Creston-CAN	795 512.57	15 208.33	1696.31	2924.68	7 019 228.56	163 782.00	935.90
Changchun–CHN	217 801.05	4163.84	464.43	800.74	1 921 774.01	44 841.39	256.24
Uliastay-MNG	867 726.51	16 588.89	1850.30	3190.17	7 656 410.38	178 649.58	1020.85

Abbreviation: GWP, global warming potential; AP, acidification potential; FAETP, freshwater ecotoxicity potential; HTP, human toxicity potential; EP, eutrophication potential; POCP, photochemical ozone creation potential.

10974660, 0, Downloaded from https://onlinelibrary.wiley.com/doi/10.1002/jctb.7369 by IFSC - Instituto Federal de Santa Catarina, Wiley Online Library on [28/03/2023]. See the Terms and Conditions (https://onlinelibrary.wiley.com/terms-and-conditions) on Wiley Online Library for rules of use; OA articles are governed by the applicable Creative Commons License

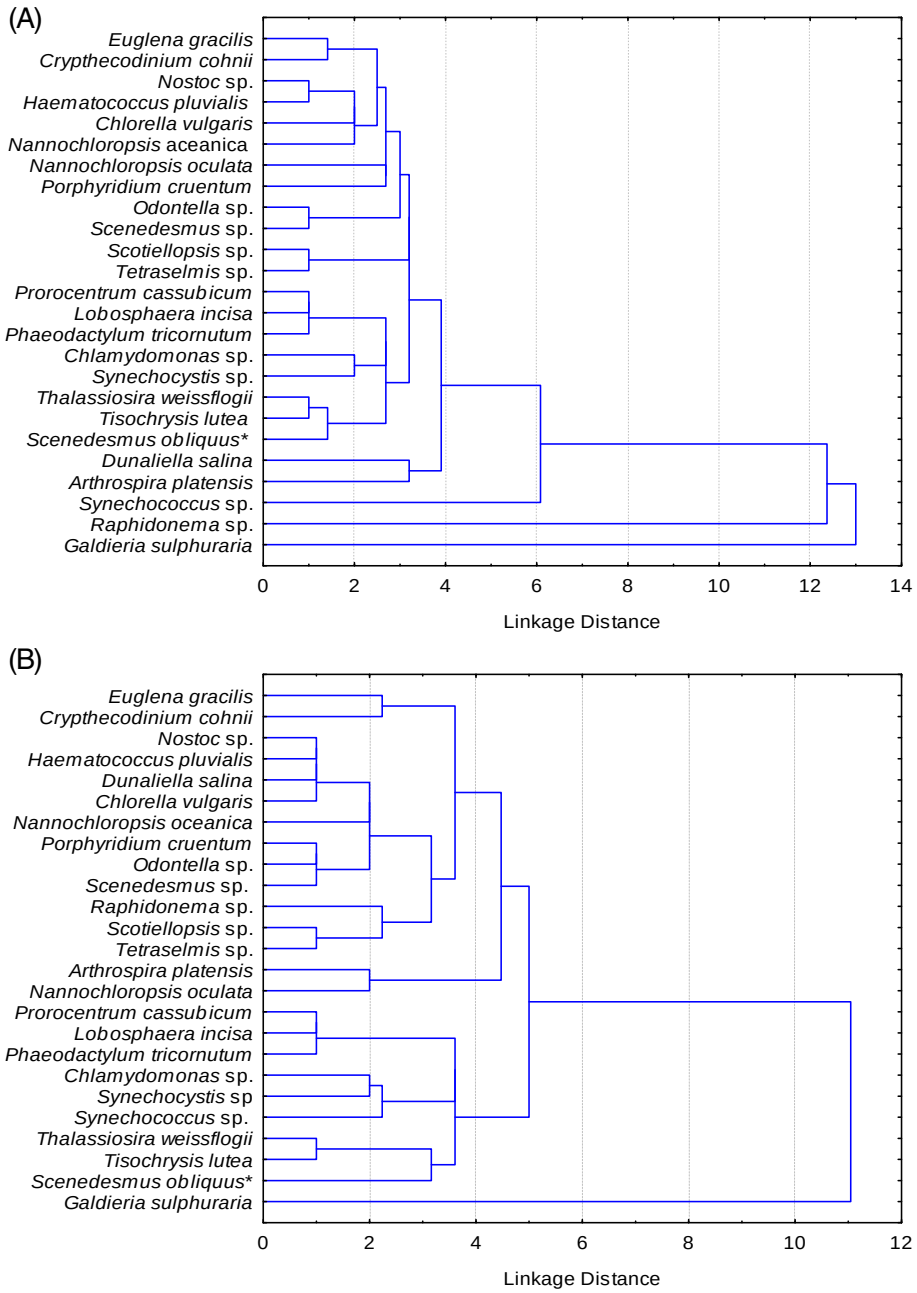


Figure 2. Cluster dendrograms (A) for the average temperature ranges and (B) for the suitable temperature amplitudes to support growth with biotechnological potential. *Model microorganism used in this study. The average temperature ranges and temperature amplitudes were obtained from Malakootian *et al.*[46] Safdar *et al.*[47] Tiwari and Sharma,[48] Rehman *et al.*[49] and A4F.[50]

at the time t_i (g L^{-1}), X_{i-1} is the biomass density at the time t_{i-1} (g L^{-1}), L_C is the lipid content of the biomass (%), X_0 is the biomass concentration at time t_0 (g L^{-1}) and t is the residence time (d). The hydraulic retention time (d) corresponds to the time elapsed until the maximum biomass density (g L^{-1}).

Quantitative and qualitative analysis of fatty acids

The total concentration of lipids and the obtained fatty acid methyl esters (FAME) was determined through the modified method of Bligh and Dyer[16] and Hartman and Lago,[17] described by Vendruscolo *et al.*[18] respectively. The determination of the fatty acid profile followed the method described by Vendruscolo *et al.*[19]

Life cycle assessment

The life cycle assessment (LCA) tool was used to assess potential environmental impacts according to the midpoint categories of global warming potential (GWP), acidification potential (AP), freshwater ecotoxicity potential (FAETP), human toxicity potential (HTP), eutrophication potential (EP) and photochemical ozone creation potential (POCP). The objective and scope of the application of the LCA were to evaluate the environmental burdens of coal-based fossil energy demand from the processes upstream

© 2023 Society of Chemical Industry (SCI).

10974660, 0, Downloaded from https://onlinelibrary.wiley.com/doi/10.1002/jctb.7369 by IFSC - Instituto Federal de Santa Catarina, Wiley Online Library on [28/03/2023]. See the Terms and Conditions (https://onlinelibrary.wiley.com/terms-and-conditions) on Wiley Online Library for rules of use; OA articles are governed by the applicable Creative Commons License

and downstream of the model microorganism. The functional unit covers the production of 1 t month^{-1} of whole-dried biomass in a closed system. The energy demand data, as well as the input and output conditions to obtain 1 t month^{-1} of the product, was based on process data consolidated by classic references in the literature.[20] Potential environmental impacts were calculated using mathematical modeling (Ci = $\sum CF$ X Ei), where Ci is the impact category, *CF* is the characterization factor and Ei is the emissions inventory, expressed in mass released into the environment per functional unit. Characterization factors were obtained from Dias *et al.*[21]

Energy cost

The cost associated with coal-based fossil energy demand from the upstream and downstream processes of *S. obliquus* at the geographic positions of the study was calculated using the life cycle inventory data. The energy demand values (i.e. electricity) were multiplied by the global average electricity price for business users.[22] The analysis included only the cost of the electricity demand needed to operate the system.

Sensitivity analysis

A sensitivity analysis was performed to determine the effect of open-system cultivation of the model microorganism on production cost and life-cycle emissions of whole-dried biomass. Biomass productivities three times lower than those achieved in closed systems were considered for analysis in open systems.[23,24] The analysis followed the methodology described in the two sections above.

Statistical analyses

Analysis of variance (one-way ANOVA) and Tukey's honestly significant difference (HSD) test ($P \leq 0.05$) were used to test differences between geographic positions. Multivariate cluster analysis was used to determine the similarity between the average temperature ranges and suitable temperature amplitudes to support growth with biotechnological potential. The analysis compares the data from this study with consolidated data in the literature for 24 microalgae of commercial and biotechnological importance. Single linkage as an amalgamation rule and Euclidean linkage distances as a measure of similarity were used in the multivariate cluster analysis. The analyses were performed with the software Statistica 7.0 (StatSoft, Tulsa, OK, USA).

RESULTS AND DISCUSSION

Effects of the climate on the kinetic performance of the system

There are numerous laboratory studies on important aspects of microalgae growth kinetics under a range of environmental conditions. The data from these studies can be used to design a highly productive process. However, microalgae cultivation commonly is carried out outdoors with little or no control over physical parameters. In this sense, it is imperative to identify, considering the climate diversification of the globe, climates that are more suitable for microalgae cultivation in openwork production systems. The physical simulation of external environmental conditions can support the reliable determination of the growth kinetics of these microorganisms for real outdoor processes.[4]

Some studies have dedicated themselves to the physical simulation of climate programmed in photobioreactors for a semi-empirical estimate of microalgae productivity.[9,25,26] However, given the absence of a comprehensive assessment of the continental surface covered by the subtropical (25° to 35° N and S) and mid-latitudes (35° to 55° N and S) climate zones, we propose to evaluate the performance of microalgae culture in photobioreactors in the four seasons of the year within these two climatic zones. Geographic locations for estimating biomass and lipid productivity were chosen to cover a wide range of solar irradiance, day length and temperature (Table 1; Fig. 1). The choice also includes the climatic diversity of the subtropical and mid-latitudes zones. Table 2 presents the kinetic parameters for *S. obliquus* microalgae used as model microorganism.

As can be seen in Table 2, the simulated climate in photobioreactors to estimate the biomass productivity of *S. obliquus* to openwork at different geographic locations of the subtropical and mid-latitudes zones resulted in statistically different productivities. The biomass productivities considering the four growing seasons in 1 year varied from 0.307 to 0.020 g L^{-1} d^{-1}. The highest biomass productivity (0.307 g L^{-1} d^{-1}) was obtained in the summer simulation of the BWh climate, with a maximum biomass density of 2.56 g L^{-1}, and a maximum specific growth rate of 1.09 d^{-1}, a generation time of 0.64 d and a hydraulic retention time of 8 d. However, the summer simulation of the Cfb climate located in the mid-latitudes zone resulted in the lowest biomass productivity (0.020 g L^{-1} d^{-1}), with a maximum biomass density of 0.16 g L^{-1}, a maximum specific growth rate of 0.23 d^{-1}, a generation time of 2.94 d and a hydraulic retention time of 3 d.

In general, summer simulations exhibiting relatively high solar irradiance and temperature produced the highest biomass productivities. However, the summer for most climates located in the mid-latitudes zone was the only season with temperatures capable of supporting the growth of *S. obliquus* microalgae. The simulation of Dwb, Csb and Cfb climates with average summer temperatures of 14 °C does not provide satisfactory growth rates. Notably, the temperature of these climates is very cold, which prevents the microalgae from absorbing solar energy and transforming it into organic matter.

The climates of the dry group (B) and humid subtropical (C) mostly presented four growing seasons, and the climates of the wet continental group (D), in turn, presented only one season. Of importance, the latitude in which these climates are found affects the light conditions and temperature and, consequently, all growth kinetics of photoautotrophic microalgae. By way of example, as can be seen, the Cfa and Cfb climates present in the subtropical and mid-latitudes zones show statistically different growth kinetics. In theory, the closer a location is to 0° latitude, the higher the solar irradiance and temperature.[27] This explains the difference found in the kinetic parameters of the microalgae *S. obliquus* for the same climate but located latitudinally in different climatic zones.

In synthesis, geographic factors such as latitude and altitude alone provide a good indication of potential locations for large-scale microalgae cultivation. These factors directly influence the climatic elements and, therefore, the local climate. The climate typology also can help target appropriate locations, yet does not provide the best indicator; for example, group C presents a temperature discrepancy that can lead to climates with four growing seasons or only one or none as observed for the Cfb climate.[28] Therefore, the selection of sites based solely on their climate classification proves to be unfeasible without a more in-depth geographic examination.

The geographic examination of suitable locations for microalgae cultivation should consider, among other parameters, the

© 2023 Society of Chemical Industry (SCI).

10974660, 0, Downloaded from https://onlinelibrary.wiley.com/doi/10.1002/jctb.7369 by IFSC - Instituto Federal de Santa Catarina, Wiley Online Library on [28/03/2023]. See the Terms and Conditions (https://onlinelibrary.wiley.com/terms-and-conditions) on Wiley Online Library for rules of use; OA articles are governed by the applicable Creative Commons License

potential for microalgae productivity throughout the year.[5] It is known that the greater the latitude, the greater the variation between the seasons of the year. This variation can represent a major limitation for the high average annual productivity of biomass and, consequently, low production cost. In this sense, Table 2 also presents the average annual biomass productivity of the microalgae *S. obliquus*.

According to the results, the average annual biomass productivity considering the different types of climate varied from 0.210 to 0.005 g L^{-1} d^{-1}. The highest average annual biomass productivities were recorded in the simulation of BWh, Cfa, Cfb and Cwa climates. All are present in the subtropical zone. By contrast, the lowest average annual biomass productivities were obtained in the simulation of climates present in the mid-latitudes zone. The average annual biomass productivity in the subtropical and mid-latitudes zone was 0.144 g L^{-1} d^{-1} and 0.049 g L^{-1} d^{-1}, respectively. The variation is about three-fold greater and reaches 42-fold between the highest and lowest observed productivity.

Based on these results, it can be said that the mid-latitudes zone does not have the potential for microalgae cultivation without an off-season. The exception may be locations of lower latitude and altitude, as is the case of Algiers–DZA, Latina–ITA and Joplin–USA which, although not having four growing seasons, can have up to three seasons in a year. Besides that, in the nonproduction season, there is the option of interrupting photoproduction so that there are no operating costs, as proposed by Spruijt *et al.*[29]

The subtropical zone, in turn, has a greater potential for microalgae cultivation facilities without an off-season. This is because the lower latitudes of this zone provide better conditions of light and temperature, giving higher productivity. In corroboration, Speranza *et al.*[30] when making a coarse observation about the possible global area for microalgae cultivation, delimit the best latitude areas as up to 37° N and S.

Finally, it is notable that as most products are intracellular, biomass productivity is the main parameter of microalgae-based processes. Furthermore, it is crucial for determining the economic and environmental sustainability of these processes. Higher biomass productivity results in lower energy demand and, consequently, provides a lower production cost and lower environmental footprint.[21] In this regard, it also is worth mentioning that one of the great challenges related to the downstream phase of large-scale microalgae biomass processing is harvesting. The low final biomass productivity in large-scale systems results in the centrifugation of large volumes of culture media, which is a significant concern to be addressed properly for the greater sustainability of microalgae-based processes and products.[20]

Effects of the climate on lipids and fatty acids profile

Light and temperature are climatic elements that most affect the metabolic processes of photoautotrophic microalgae.[31] That said, the choice of geographic positions for the cultivation of microalgae outdoors must be a consequence of environmental conditions – the local climate. In other words, the choice must consider the needs of the species and the cultivation finality. Besides that, it is interesting that the environmental conditions are stable throughout the year for better stability, reproducibility and predictability. However, this is a predominant condition of equatorial and tropical latitudes and not of those in the study. In the latitudes of the study, the degree of variation between the growing seasons is more pronounced and this affects not only the biomass productivity, but also the synthesis and composition of lipids. Table 3 shows the content and seasonal lipid productivity, as well as the average annual lipid productivity of the microalga *S. obliquus*.

The total lipid content (%) of *S. obliquus* microalgae in the four growing seasons varied from 16.27% to 4.28%. The highest and lowest total lipid content was recorded in the autumn simulation of the Csa climate and spring of the Cfa climate, both located in the mid-latitudes zone. In these climates and seasons, the culture was exposed to a light intensity of 1345.7 and 1630.9 μmol m^{-2} s^{-1}, day length of 11.57 and 13.56 h, and temperature of 17.10 and 13 °C, respectively.

To date, there have been few reports on the combined assessment of light intensity, day length and temperature in microalgae-based processes. The combined variation of these climatic elements in our study may, therefore, support a database on their effect on total lipid content. In general, it is observed that low light intensity and temperature favored lipid accumulation in cells. This behavior fits with the identified by other researchers, regardless of the strain used and cultivation system.[32-35] However, this is not a dominant trend and the reasons for discrepancies are complex, but related to the dynamics simulation of the climate, which also is reported by Siqueira *et al.*[2]

As for lipid productivity, it is noteworthy that this is the main parameter of the process to evaluate the production of unicellular oil. This is because it takes into consideration the biomass productivity multiplied by the total lipid content. The highest lipid productivities were recorded in growing seasons with light intensity between 1345.7 and 2402.4 μmol m^{-2} s^{-1}, day length between 11.57 and 14.70 h, and temperature between 17 and 31 °C. Simultaneously, these environmental conditions provided the highest biomass productivities which, associated with a high total lipid content, resulted in the best conditions for oil production. The highest average annual productivities of lipids, as well as biomass (see Table 2), were recorded in the subtropical zone in the simulation of BWh, Cfa, Cfb and Cwa climates. The average annual lipid productivity in the subtropical zone was 0.015 g L^{-1} d^{-1} and in the mid-latitudes zone it was 0.005 g L^{-1} d^{-1}. This result reaffirms the potential of the subtropical zone for the cultivation of microalgae, being able to increase the biomass and lipid productivity by up to three-fold.

In our study, the lipids consisted of four main fatty acids: palmitic, oleic, linoleic and alpha-linolenic acid (Table 4). This majority profile is typical of most microalgae that commonly synthesize fatty acids with chain lengths in the range of C16–C18. The concentrations of saturated, monounsaturated and polyunsaturated fatty acids were in the ranges 70.5–31.39%, 28.22–7.91% and 58.50–19.71%, respectively. Of the 49 profiles, 25 presented higher content of polyunsaturated and 24 of saturated. As some fatty acid profiles showed more than half the content of polyunsaturated or saturated, it is conjectured that, based on the cultivation finality, specific local climates can be chosen.

In general, it is observed that at low temperatures the concentration of unsaturated fatty acids increases.[36] Besides that, there is a tendency that at low light intensities, the content of polyunsaturated fatty acids is higher.[34] However, from the results presented in Table 4, this propensity was not verified, which contrasts with previous reports in which an effective pattern is observed. However, it is noted that they are generally based on a single variable – temperature or light – despising the combined and dynamic effect of these variables in time and space and the composition of the microalgae biomass.

However, although there are contrasting reports about the temperature being more influential than light intensity on the growth

© 2023 Society of Chemical Industry (SCI).

10974660, 0, Downloaded from https://onlinelibrary.wiley.com/doi/10.1002/jctb.7369 by IFSC - Instituto Federal de Santa Catarina, Wiley Online Library on [28/03/2023]. See the Terms and Conditions (https://onlinelibrary.wiley.com/terms-and-conditions) on Wiley Online Library for rules of use; OA articles are governed by the applicable Creative Commons License

and chemical composition of microalgae biomass and *vice versa*, both parameters are indisputably the driving force of photoautotrophic microalgae-based processes. And it is of note that each microalgae species has a range of light intensity and temperature that, if exceeded, affects all metabolic processes. Choosing geographic positions with climates that do not go beyond this single range is crucial for the more economical and sustainable production of microalgae. In our study, the simulation of growing seasons with light intensities between 1345.7 and 2402.4 μmol m^{-2} s^{-1} and temperatures between 17 and 31 °C provided the highest biomass and lipid productivities of *S. obliquus* microalgae. It is imperative from this result that the best option is to choose geographic positions with seasonal light and temperature variations in this range for high annual microalgae productivity, without an off-season.

Finally, the mapping of the performance of photobioreactors for microalgae cultivation in the climate zones of the earth shows that the equatorial and tropical regions, followed by the subtropics, harbor the most suitable climates for microalgae productivity throughout the year. This is a result of the geoid shape of the earth and how the sun's rays strike its surface. Regions located in the mid-latitudes zone generally have only one growing season and this is not favorable for the implementation of outdoor microalgae cultivation facilities. As for the sub-Antarctic (55° to 60° N and S), Antarctic (60° to 75° S), subarctic (55° to 60° N), arctic (60° to 75° N) and polar (75° to 90° N and S) zones, it is clear that they would be able to support only psychrophilic and psychrotolerant microalgae cultivation facilities that inhabit extremely cold environments.[37] Lastly, holistically, the geographic examination of potential sites for microalgae cultivation involves, beyond climate, parameters such as the physical suitability of the site, the availability of land and inputs, access to transport infrastructure and viable manpower.[38] Therefore, this study is a primary assessment of geographic restrictions to consider for microalgae cultivation facilities.

Environmental and economic sustainability issues

The loss and damage of climate change can no longer be viewed with any degree of scepticism. The sustainability imperative puts everyone on an unprecedented journey for which there seems to be no roadmap. But, regardless of that, sustainability is a megatrend, and disheartening and even cynical tactics such as greenwashing – which is already at the top of the regulatory agenda – will quickly be condemned. And what all this means for microalgae-producing companies is that they will have to review their timely allegations of environmentally conscious and often sustainable products. This is because this statement has become questionable given the growing recognition of the sustainability metrics which, if we look, do not trustworthy correspond to this presupposed.[39]

The truth is that successful microalgae applications face several challenges . The high operational cost and low productivity of commercial cultivations are unanimously the most significant challenges to be overcome to improve the metrics of environmental and economic sustainability indicators.[40] And on this, it is appropriate to mention that the true success of any microalgae-based process is conditioned to these indicators. And of course, for openwork cultivation, one cannot ignore the important role of geographic location in the sustainability of these processes.[41] In light of all this, Table 5 shows the impact of geographic location on the sustainability metrics of whole-dried biomass of *S. obliquus* cultivated in closed outdoor system.

As can be seen in Table 5, the production costs and the environmental footprint associated with the coal-based fossil energy demand of the upstream and downstream processes of *S. obliquus* to obtain 1 t $month^{-1}$ of whole-dried biomass can vary abruptly from one geographic location to another. This was expected considering that the indicators are sensitive to variations in biomass productivity, which change locally as a function of climate. In sum, the values shown in Table 5 are surprisingly high and add, undoubtedly, a prohibitive barrier to large-scale commercial production. However, if we look at the data of the geographic positions of the equatorial and tropical zone, from Part II of this study, we will see that most of the evaluated locations have a production cost and an environmental footprint associated with energy lower than that presented in the locations of the subtropical and mid-latitudes zone (see Supporting Information Table S1). This is attributed to higher biomass productivities.

Even so, these are values that endorse the idea that closed systems, beyond immature technologies, are limited to some microalgae species. This is due to the high cost of building and maintainance. It is important to highlight here that in large-scale systems the costs associated with electricity followed by capital goods define most of the system costs.[29] Comparatively, based on the data presented, it is impossible to reach an optimistic conclusion ignoring that in closed systems the productivity of commercial strains such as *Chlorella vulgaris* is about two- to three-fold times higher and, consequently, the impact on costs and emissions are proportionately smaller.[21] However, if we analyze the sensitivity of production cost and life cycle emissions of *S. obliquus* whole-dried biomass in open cultivation systems, the values drop dramatically (Table 6).

As can be seen in Table 6, the production costs and environmental footprint of open system cultivation – although presenting lower productivities – are relatively minor, which makes it foolish to justify the use of closed systems *versus* open systems for the production of *S. obliquus*. It is notablealso that most of commercial production of microalgae – if not almost all – is carried out in open systems.[2] This just goes to show that mapping locations with a favorable climate for microalgae cultivation are of critical importance. Besides that, our findings are in line with values presented by Deprá *et al.*[20] when comparing the performance of closed and open culture systems considering the same strain of microalgae (*C. vulgaris*). But despite that, even presenting supremacy over closed culture systems, it is of note that the cultivation in geographic positions such as Invercargill-NZL and Creston-CAN, for example, remains unsustainable given the low productivity. However, for most locations, especially in equatorial and tropical zones (see Table S2), the production cost indicates that the whole-dried biomass of *S. obliquus* could compete with the selling price of the biomass of *C. vulgaris* and *Arthrospira platensis*.[42]

Besides that, it is noteworthy that production cost is not solely associated with the biomass productivity of geographic location. It also is associated with the energy local tariff. For example, if we consider the average electricity price of Egypt of US$0.034 kWh^{-1} and India of US$0.074 kWh^{-1} – instead of the global average price used for analysis (US$0.136 kWh^{-1}) – the production cost for Tanta-EGY and Meerut-IND would fall from US $52 964 t^{-1} to 13 241 t^{-1} and from US$54 116 t^{-1} to US$29 445 t^{-1} of product, respectively. These values send a signal that the energy local price also is an important factor in locating suitable sites for large-scale microalgae cultivation. Evidently, although it

© 2023 Society of Chemical Industry (SCI).

10974660, 0, Downloaded from https://onlinelibrary.wiley.com/doi/10.1002/jctb.7369 by IFSC - Instituto Federal de Santa Catarina, Wiley Online Library on [28/03/2023]. See the Terms and Conditions (https://onlinelibrary.wiley.com/terms-and-conditions) on Wiley Online Library for rules of use; OA articles are governed by the applicable Creative Commons License

does not improve environmental indicators, it does improve economic indicators.

However, a further cause for delays in the replacement and decarbonization of energy-intensive industries is the outdated perception that renewable energy is not competitive with fossil energy.[43] Replacing fossil energy with renewables such as solar photovoltaics, wind and hydro in commercial microalgae facilities is the backbone for carrying out climate-neutral operations. It also is already economically competitive in most places in the world. Some studies have demonstratedthat the implementation of a photovoltaic solar system in the production facility can, beyond massively reducing the environmental footprint, amortize the costs of the energy demand of the products, becoming beneficial for the company and the environment.[44] However, it also is worth highlighting that, even if the replacement of the fossil matrix for a renewable one does not represent an improvement in economic indicators, it can be considered as a socio-environmental trade-off to be achieved. Not all profit should be considered genuine if it is positive through a greater social cost generated by pollutant emissions.[45]

In light of this discussion, it is difficult to anticipate the sustainability of geographic locations for large-scale cultivation of *S. obliquus* – and physiologically similar strains – without a detailed geographic examination of all these issues. However, it is not difficult to predict that locations with favorable climatic conditions for microalgae cultivation without off-season and with an abundance of renewable energy resources would provide the best choice. And, finally, the results presented here are just a valuable first step in identifying suitable locations for large-scale cultivation of microalgae worldwide.

Comparisons: multivariate cluster analysis

When analyzing a database, one of the main challenges facing researchers in many areas is how to summarize the data into meaningful structures. Cluster analysis is an effective generic method for examining information to reveal groups according to their degree of similarity. Thus, considering the relevance of this analysis, we sought to demonstrate the similarity between the average temperature ranges and suitable temperature amplitudes to support growth with the biotechnological potential of *S. obliquus* and 24 important microalgae regarding biotechnological exploitation and use (Fig. 2).

Figure 2(a) is a dendrogram, for the average temperature ranges, showing three distinct sets of clusters: Cluster 1 (*Galdieria sulphuraria*), Cluster 2 (*Raphidonema* sp.) and Cluster 3 (*Euglena gracilis*, *Crypthecodinium cohnii*, *Nostoc* sp., *Haematococcus pluvialis*, *Dunaliella salina*, *C. vulgaris*, *Arthrospira platensis*, *Nannochloropsis oceanica*, *Nannochloropsis oculata*, *Porphyridium cruentum*, *Odontella* sp., *Scenedesmus* sp., *S. obliquus*, *Scotiellopsis* sp., *Tetraselmis* sp., *Prorocentrum cassubicum*, *Lobosphaera incisa*, *Phaeodactylum tricornutum*, *Chlamydomonas* sp., *Synechococcus* sp., *Synechocystis* sp., *Thalassiosira weissflogii* and *Tisochrysis lutea*). By contrast, Fig. 2(B) is a dendrogram, for temperature amplitudes, showing two sets of clusters: Cluster 1 (*Galdieria sulphuraria*) and Cluster 2 (*Raphidonema* sp., *Euglena gracilis*, *Crypthecodinium cohnii*, *Nostoc* sp., *Haematococcus pluvialis*, *Dunaliella salina*, *C. vulgaris*, *Arthrospira platensis*, *Nannochloropsis oceanica*, *Nannochloropsis oculata*, *Porphyridium cruentum*, *Odontella* sp., *Scenedesmus* sp., *S. obliquus*, *Scotiellopsis* sp., *Tetraselmis* sp., *Prorocentrum cassubicum*, *Lobosphaera incisa*, *Phaeodactylum tricornutum*, *Chlamydomonas* sp., *Synechococcus* sp., *Synechocystis* sp., *Thalassiosira weissflogii* and *Tisochrysis lutea*).

Of note, with regard to temperature, we highlight two important points: the first, temperature, according to a previous study,[2] has a greater influence on the kinetic performance of the microalgae when compared to the day length and the light intensity; and second, the average temperature range supporting growth of *S. obliquus* growth with biotechnological potential is the same as that for other microalgae of commercial and biotechnological importance, as can be seen in Fig. 2(A). Thus, based on this analysis, it is possible to amplify the data presented in this study in the direction not only of mapping locations for the large-scale cultivation of *S. obliquus*, but also of all other microalgae shown in Cluster 3 of Fig. 2(A). Additionally, considering the temperature amplitudes [Fig. 2(B)], the possibility of extrapolating the data obtained for the model microorganism to Cluster 2 (except *Galdieria sulphuraria*) is confirmed Cluster 2. In summary, our results can serve as a starting point to identify locations for the cultivation of mesophilic microalgae significant regarding biotechnological exploitation and use.

CONCLUSION

Proof-of-concept experiments show that geographic position and local climate are decisive criteria in the performance of photobioreactors for outdoor microalgae cultivation (Part I). Based on the results of Part I of this study, in parts II and III identify regions most suitable for commercial microalgae cultivation, taking *S. obliquus* as the model microorganism via mapping the Earth's climate zones to. The data reported in parts II and III provide a semi-empirical estimate of microalgae productivity around the globe. This work also provides an assessment of the impact of the local climate on environmental and economic sustainability metrics. This is the first study to provide an in-depth latitudinal, climatological and seasonal assessment of the performance of photobioreactors for microalgae culture. As final considerations, the results support the high potential of equatorial, tropical and subtropical regions for highly productive mesophilic microalgae-based systems.

ACKNOWLEDGEMENTS

Funding for this research has been provided by the Coordination for the Improvement of Higher Education Personnel (CAPES) (grant no. 001) and the National Council for Scientific and Technological Development (CNPq) for financial support.

CONFLICT OF INTEREST

The authors declare that there is no conflict of interest regarding the publication of the manuscript.

SUPPORTING INFORMATION

Supporting information may be found in the online version of this article.

REFERENCES

1 Markou G, Chentir I and Tzovenis I, Microalgae and cyanobacteria as food: legislative and safety aspects, in *Cultured Microalgae for the Food Industry*. Academic Press, New York, pp. 249–264 (2021).
2 Siqueira SF, Maroneze MM, Dias RR, Vendruscolo RG, Wagner R, de Menezes CR *et al.*, Mapping the performance of photobioreactors

 © 2023 Society of Chemical Industry (SCI).

10974660, 0, Downloaded from https://onlinelibrary.wiley.com/doi/10.1002/jctb.7369 by IFSC - Instituto Federal de Santa Catarina, Wiley Online Library on [28/03/2023]. See the Terms and Conditions (https://onlinelibrary.wiley.com/terms-and-conditions) on Wiley Online Library for rules of use; OA articles are governed by the applicable Creative Commons License

for microalgae cultivation: geographic position and local climate. *J Chem Technol Biotechnol* **95**:2411–2420 (2020).
3 Meticulous Research, [Online] Available: https://www.meticulousresearch.com/product/microalgae-market-5197 [20 March 2022].
4 Jesus CS, da Silva UL, Costa SS, Miranda AL, de Morais EG, de Morais MG *et al*., Outdoor pilot-scale cultivation of *Spirulina* sp. LEB-18 in different geographic locations for evaluating its growth and chemical composition. *Bioresour Technol* **256**:86–94 (2018).
5 Boruff BJ, Moheimani NR and Borowitzka MA, Identifying locations for large-scale microalgae cultivation in Western Australia: a GIS approach. *Appl Energy* **149**:379–391 (2015).
6 De-Luca R, Trabuio M, Barolo M and Bezzo F, Microalgae growth optimization in open ponds with uncertain weather data. *Comput Chem Eng* **117**:410–419 (2018).
7 Ras M, Steyer JP and Bernard O, Temperature effect on microalgae: a crucial factor for outdoor production. *Rev Environ Sci Biotechnol* **12**:153–164 (2013).
8 Malek A, Zullo LC and Daoutidis P, Modeling and dynamic optimization of microalgae cultivation in outdoor open ponds. *Ind Eng Chem Res* **55**:3327–3337 (2016).
9 Coronel CD and Curatti L, Climate-simulated culturing suggests high microalgal biomass and oil productivities in most of the south American continent. *Biotechnol J* **16**:2100067 (2021).
10 Dias RR, Lasta P, Vendruscolo RG, Wagner R, Zepka LQ and Jacob-Lopes E, Mapping the performance of photobioreactors for microalgae cultivation. Part II: equatorial and tropical climate zone. *J Chem Technol Biotechnol* **96**:613–621 (2021).
11 Rippka R, Derulles J, Watrerbury JB, Herdman M and Stainer RY, Generic assignments, strain histories and properties of pure cultures of cyanobacteria. *J Gen Microbiol* **111**:1–61 (1979).
12 Francisco EC, Neves DB, Jacob-Lopes E and Franco TT, Microalgae as feedstock for biodiesel production: carbon dioxide sequestration, lipid production and biofuel quality. *J Chem Technol Biotechnol* **85**:395–403 (2010).
13 Deprá MC, Mérida LG, de Menezes CR, Zepka LQ and Jacob-Lopes E, A new hybrid photobioreactor design for microalgae culture. *Chem Eng Res Des* **144**:1–10 (2019).
14 Solar Electricity Handbook, [Online] Available: http://www.solarelectricityhandbook.com [20 August 2021].
15 Weatherbase, Travel Weather Averages, Great Falls, Virginia. [Online] Available: https://www.weatherbase.com [20 August 2021].
16 Bligh EG and Dyer JW, A rapid method of total lipid extraction and purification. *Can J Biochem Physiol* **37**:911–917 (1959).
17 Hartman L and Lago RCA, Rapid preparation of fatty acids methyl esters. *Lab Pract* **22**:475–476 (1973).
18 Vendruscolo RG, Facchi MMX, Maroneze MM, Fagundes MB, Cichoski AJ, Zepka LQ *et al*., Polar and non-polar intracellular compounds from microalgae: methods of simultaneous extraction, gas chromatography determination and comparative analysis. *Food Res Int* **109**:204–212 (2018).
19 Vendruscolo RG, Deprá MC, Pinheiro PN, Furlan VJM, Barin JS, Cichoski AJ *et al*., Food potential of *scenedesmus obliquus* biomasses obtained from photosynthetic cultivations associated with carbon dioxide mitigation. *Food Res Int* **160**:111590 (2022).
20 Deprá MC, Severo IA, dos Santos AM, Zepka LQ and Jacob-Lopes E, Environmental impacts on commercial microalgae-based products: sustainability metrics and indicators. *Algal Res* **51**:102056 (2020).
21 Dias RR, Deprá MC, Zepka LQ and Jacob-Lopes E, Roadmap to net-zero carbon emissions in commercial microalgae-based products: environmental sustainability and carbon offset costs. *J Appl Phycol* **34**:1255–1268 (2022).
22 Global Petrol Prices, [Online] Available: https://www.globalpetrolprices.com [10 November 2022].
23 Shen Y, Yuan W, Pei ZJ, Wu Q and Mao E, Microalgae mass production methods. *Trans ASABE* **52**:1275–1287 (2009).
24 Eustance E, Badvipour S, Wray JT and Sommerfeld MR, Biomass productivity of two Scenedesmus strains cultivated semi-continuously in outdoor raceway ponds and flat-panel photobioreactors. *J Appl Phycol* **28**:1471–1483 (2016).
25 Roles J, Yarnold J, Hussey K and Hankamer B, Techno-economic evaluation of microalgae high-density liquid fuel production at 12 international locations. *Biotechnol Biofuels* **14**:1–19 (2021).
26 Cheregi O, Engelbrektsson J, Andersson MX, Strömberg N, Ekendahl S, Godhe A *et al*., Marine microalgae for outdoor biomass production—a laboratory study simulating seasonal light and temperature for the west coast of Sweden. *Physiol Plant* **173**:543–554 (2021).
27 Rohli RV and Vega AJ, *Climatology*. Jones & Bartlett Learning, Burlington, USA (2017).
28 Kottek M, Grieser J, Beck C, Rudolf B and Rubel F, World map of the Köppen-Geiger climate classification updated. *Meteorol Z* **15**:259–263 (2006).
29 Spruijt J, Schipperus R, Kootstra AMJ, Visser C and Parker B, AlgaEconomics: bio-economic production models of micro-algae and downstream processing to produce bioenergy carriers, in *EnAlgae Report WP2A7.10*. Swansea University, Swansea, UK (2015).
30 Speranza LG, Ingram A and Leeke GA, Assessment of algae biodiesel viability based on the area requirement in the European Union, United States, and Brazil. *Renewable Energy* **78**:406–417 (2015).
31 López-Muñoz I and Bernard O, Modeling the influence of temperature, light intensity, and oxygen concentration on microalgal growth rate. *Processes* **9**:496 (2021).
32 Cheirsilp B and Torpee S, Enhanced growth and lipid production of microalgae under mixotrophic culture condition: effect of light intensity, glucose concentration, and fed-batch cultivation. *Bioresour Technol* **110**:510–516 (2012).
33 Chaisutyakorn P, Praiboon J and Kaewsuralikhit C, The effect of temperature on growth and lipid and fatty acid composition on marine microalgae used for biodiesel production. *J Appl Phycol* **30**:37–45 (2018).
34 Nzayisenga JC, Farge X, Groll SL and Sellstedt A, Effects of light intensity on growth and lipid production in microalgae grown in wastewater. *Biotechnol Biofuels* **13**:1–8 (2020).
35 Rehman M, Kesharvani S, Dwivedi G and Suneja KG, Impact of cultivation conditions on microalgae biomass productivity and lipid content. *Mater Today: Proc* **56**:282–290 (2022).
36 El-Sheekh M, Abomohra AEF, Abd El-Azim M and Abou-Shanab R, Effect of temperature on growth and fatty acids profile of the biodiesel producing microalga *Scenedesmus acutus*. *Biotechnol Agron Soc Environ* **21**:233–239 (2017).
37 Dasauni K and Nailwal TK, Cyanobacteria in cold ecosystem: tolerance and adaptation, in *Survival Strategies in Cold-Adapted Microorganisms*. Springer, Singapore, pp. 1–29 (2022).
38 Katooli MH, Aslani A, Razi Astaraee F, Mazzuca Sobczuk T and Bakhtiar A, Multi-criteria analysis of microalgae production in Iran. *Biofuels* **12**:789–795 (2021).
39 Gills B and Morgan J, Global climate emergency: after COP24, climate science, urgency, and the threat to humanity. *Globalizations* **17**:885–902 (2020).
40 Schade S and Meier T, Distinct microalgae species for food—part 1: a methodological (top-down) approach for the life cycle assessment of microalgae cultivation in tubular photobioreactors. *J Appl Phycol* **32**:2977–2995 (2020).
41 Banerjee S and Ramaswamy S, Process model and techno-economic analysis of natural astaxanthin production from microalgae incorporating geospatial variabilities. *Bioresour Technol Rep* **20**:101260 (2022).
42 Alibaba, [Online] Available: https://www.alibaba.com/ [10 November 2022].
43 Ritchie H and Roser M, [Online] Available: https://ourworldindata.org/cheap-renewables-growth [10 November 2022].
44 Dias RR, Deprá MC, Severo IA, Zepka LQ and Jacob-Lopes E, Smart override of the energy matrix in commercial microalgae facilities: a transition path to a low-carbon bioeconomy. *Sustainable Energy Technol Assess* **52**:102073 (2022).
45 Deprá MC, Dias RR, Zepka LQ and Jacob-Lopes E, Building cleaner production: how to anchor sustainability in the food production chain? *Environ Adv* **9**:100295 (2022).
46 Malakootian M, Hatami B, Dowlatshahi S and Rajabizadeh A, Growth and lipid accumulation in response to different cultivation temperatures in *Nannochloropsis oculata* for biodiesel production. *Environ Health Eng Manage J* **3**:29–34 (2016).
47 Safdar W, Zan X and Song Y, Synergistic effects of pH, temperature and agitation on growth kinetics and docosahexaenoic acid production of *C. cohnii* cultured on different carbon sources. *Int J Res Agric Sci* **4**:2348–3997 (2017).

© 2023 Society of Chemical Industry (SCI).

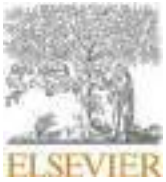
10974660, 0, Downloaded from https://onlinelibrary.wiley.com/doi/10.1002/jctb.7369 by IFSC - Instituto Federal de Santa Catarina, Wiley Online Library on [28/03/2023]. See the Terms and Conditions (https://onlinelibrary.wiley.com/terms-and-conditions) on Wiley Online Library for rules of use; OA articles are governed by the applicable Creative Commons License

48 Tiwari P and Sharma PK, Effect of temperature on fatty acid profile of *Nostoc spongiaeforme* (freshwater) and marine water *Nostoc calcicola* (marine water): a comparative study. *J Stress Physiol Biochem* **17**:119–125 (2021).
49 Rehman M, Kesharvani S, Dwivedi G and Suneja KG, Impact of cultivation conditions on microalgae biomass productivity and lipid content. *Mater Today Proc* **56**:282–290 (2022).
50 A4F, [Online] Available: https://a4f.pt/pt/historico-microalgas [31 January 2023].

10974660, 0, Downloaded from https://onlinelibrary.wiley.com/doi/10.1002/jctb.7369 by IFSC - Instituto Federal de Santa Catarina, Wiley Online Library on [28/03/2023]. See the Terms and Conditions (https://onlinelibrary.wiley.com/terms-and-conditions) on Wiley Online Library for rules of use; OA articles are governed by the applicable Creative Commons License

 © 2023 Society of Chemical Industry (SCI).

Food Research International 160 (2022) 111590



Contents lists available at ScienceDirect

Food Research International

journal homepage: www.elsevier.com/locate/foodres





Food potential of *Scenedesmus obliquus* biomasses obtained from photosynthetic cultivations associated with carbon dioxide mitigation

Raquel Guidetti Vendruscolo [a], Mariany Costa Deprá [a], Pricila Nass Pinheiro [a], Valcenir Junior Mendes Furlan [b], Juliano Smanioto Barin [a], Alexandre José Cichoski [a], Cristiano Ragagnin de Menezes [a], Leila Queiroz Zepka [a], Eduardo Jacob-Lopes [a], Roger Wagner [a,*]

[a] Department of Food Science and Technology, Federal University of Santa Maria (UFSM), 97105-900 Santa Maria, RS, Brazil
[b] Federal University of Pampa (Unipampa), 97650-000 Itaqui, RS, Brazil

ARTICLE INFO

Keywords:
Free polar compounds
Proteins
Amino acids
Chlorophylls
Carotenoids
Lipids
Fatty acids

ABSTRACT

Microalgae are photosynthetic microorganisms that stand out from conventional food sources and ingredients due to their high growth rate and adaptability. In addition to being highly sustainable, significant concentrations of proteins, lipids, and pigments accumulate in their cell structures from photosynthesis. Hence, this study sought to evaluate the food potential of *Scenedesmus obliquus* biomasses obtained from photosynthetic cultures enriched with 3, 5, 10, 15, 20, and 25% carbon dioxide (CO_2) (v/v). Cultivations with 3, 5, and 10% CO_2 showed greater amino acids and proteins synthesis; the protein content reached values above 56% of the dry biomass and high protein quality, due to the presence of most essential amino acids at recommended levels for the human diet. The highest concentrations of chlorophylls were found in cultures with 15, 20, and 25% CO_2 (24.2, 23.1 and 30.8 mg g^{-1}, respectively), although the profiles showed higher percentages of degradation compounds. Carotenoid concentrations were three times higher in cultures with 3, 5, and 10% CO_2 (25.3, 22.7 and 18.1 mg g^{-1}, respectively) and all-*trans*-β-carotene was the major compound. Lipid synthesis was intensified at higher CO_2 enrichment; the percentages obtained were 14.8% of lipids in the culture with 15% CO_2, 15.0% with 20% CO_2, and 13.7% with 25% CO_2. In addition, greater polyunsaturated fatty acids accumulation and a significant reduction in the n6/n3 ratio were also observed at the highest CO_2 concentrations. Our findings showed that CO_2 treatments significantly altered all compounds concentrations in *S. obliquus* biomasses, which presented satisfactory composition for application in foods and as ingredients.

1. Introduction

Microalgae are widely recognized in biotechnology due to their vast diversity, development in various habitats, photosynthetic capacity, and high biomass productivity (Hachicha et al., 2022). Their ubiquitous nature and ability to synthesize compounds with applicability in human and animal food, chemical feed, pharmaceuticals, and bioenergy has stimulated biotechnological research on microalgae species, which are estimated at 200,000–800,000 in total (Goswami, Mehariya, Karthikeyan, Gupta, & Verma, 2022). Given the countless morphological, physiological, and genetic differences, there is a considerable variation between microalgae in terms of growth rate, productivity, biomass composition, and nutrient and light requirements (Sonmez et al., 2022), thereby making research limited to species with rapid growth and considerable accumulation of compounds of interest.

In this sense, diatoms (*Bacillariophyceae*) and green algae (*Chlorophyceae*), both eukaryotic, and cyanobacteria (*Cyanophyceae*), with prokaryotic cell structures, are more popular themes in biotechnological research (Jacob-Lopes et al., 2019). *Chlorophyceae* is among the phyla with the highest number of species and geographic distribution (Kumar, Prasanthkumar, & Ray, 2017; Patel & Sahoo, 2021). These microalgae are characterized by having significant concentrations of chlorophylls, mainly chlorophyll *a*, in their chloroplasts and are commonly found in places with abundant light, including shallow water (Morais et al., 2020; Tunay, Yildirim, Ozkaya, & Demir, 2022). The intrinsic characteristics of *Chlorophyceae* make them possess a high photosynthetic capacity and carbon dioxide (CO_2) assimilation (Chauhan, Sahoo, & Mohanty, 2022).

CO_2 generation in energy production and other industrial processes

* Corresponding author.
E-mail address: rogerwagner@gmail.com (R. Wagner).

https://doi.org/10.1016/j.foodres.2022.111590
Received 29 April 2022; Received in revised form 22 June 2022; Accepted 27 June 2022
Available online 8 July 2022
0963-9969/© 2022 Elsevier Ltd. All rights reserved.

significantly contributes to greenhouse gas emissions. Carbon capture and use, as well as alternative and renewable energies, are strategies for reducing CO_2 emissions (Daneshvar, Wicker, Show, & Bhatnagar, 2022; Dias, Deprá, Zepka, & Jacob-Lopes, 2022). Biologically capturing and using CO_2 by microalgae such as *Chlorophyceae* have demonstrated potential and provide various advantages, including using solar energy (reducing costs through chemical and physical methods), high photosynthetic efficiency (10–50 times higher than plants), rapid growth rate (multiplication in a few hours), adaptability to different environments, and biomass and compounds obtained with food applicability (Demarco et al., 2022; Quiroz-Arita et al., 2022).

Research with Chlorophyceae *S. obliquus* have shown that it can mitigate CO_2, including photosynthetic cultivations enriched with values of up to 50 and 70% (v/v of air) (Tang, Han, Li, Miao, & Zhong, 2011; Ho, Chen, & Chang, 2010). These studies verified the biomass and lipid productivity and fatty acid profiles, despite concluding that the best performance of *S. obliquus* in the evaluated parameters was with 10% CO_2 enrichment, the authors reported that the strain performed well with values in the 20% CO_2 range. More recently, researchers evaluated the biomass productivity of *S. obliquus* photosynthetically cultivated with 1–25% CO_2 (v/v air), and the values obtained in the cultivations with 20 and 25% were significantly higher than those with lower CO_2 values (Deprá et al., 2020). The highest CO_2 percentages were favorable for biomass accumulation, albeit further studies on the chemical composition are required.

External conditions (e.g., CO_2 percentages) directly imply biomass productivity and the production of various metabolites by microalgae (Li, Li, & Ho, 2022). Thus, this study aimed to evaluate the effects of CO_2 concentrations (3, 5, 10, 15, 20, and 25%) on free polar compounds, total protein and protein amino acid profile, total lipid and fatty acid profile, total chlorophylls and carotenoids, and their profiles, thereby combining the possibility of CO_2 mitigation by *S. obliquus* and biomass obtaining for applications as food or ingredients.

2. Material and methods

2.1. Microorganism and culture medium

Axenic cultures of *S. obliquus* (CPCC05) from Canadian Phycological Culture Center were maintained and propagated in synthetic BG-11 medium (Rippka, Deruelles, Waterbury, Herdman, & Stanier, 1979) with the following conditions: initial pH 8.0, 25 °C, continuous aeration of 1 VVM (volume of air per volume of culture per minute) without CO_2 enrichment, the incident light intensity of 30 μmol m^{-2} s^{-1}.

2.2. Bioreactor design and experimental conditions

The microalgal cultivations were carried out in a bubble column photobioreactor with a nominal working volume of 2.0 L (Tecnal, BR) as described by Maroneze et al. (2016). The photobioreactor was operated in batch mode with synthetic BG-11 medium, initial cell concentration 100 mg L^{-1}, isothermal temperature 28 °C, incident light intensity 150 μmol m^{-2} s^{-1} and continuous aeration of 1 VVM. The injected air was enriched with 3, 5, 10, 15, 20, and 25% of industrial grade commercial CO_2 (purity > 99.8%; White Martins, BR). Cell concentration was monitored every 24 h during the microalgae growth. All experiments were conducted until the decline phase was reached, where the cellular concentration began to reduce, according to Deprá et al. 2020. At the end of the experiments, the *S. obliquus* biomasses were freeze-drying in lyophilizer (L101, Liotop, BR) for 24 h with 0.200–0.300 μHg of vacuum and condenser temperature at −37 °C.

2.3. Extraction of free polar compounds and total lipids

The free polar compounds and the total lipids were extracted with methanol:chloroform mixture according to the method described by Vendruscolo et al. 2018. 80 mg of freeze-dried biomass were added 3 mL of methanol, 1.5 mL of chloroform and 1.2 mL of distilled water. The extraction occurred by homogenization on an orbital shaking table (Q225M, Quimis, BR) for 30 min. Afterwards, another 1.5 mL of chloroform and 1.5 mL of distilled water were added and centrifuged (80-2B, Centrilab, BR) for 2 min (1006*g*), where the separation of the aqueous phase with the free polar compounds and organic phase with de total lipids occurred. Extractions were performed in triplicate.

2.4. Free polar compounds determination

The solvents from the aqueous fraction (100 μL) and the norleucine (P/N N1398, Supelco, USA) internal standard (100 μL, at 20 μg mL^{-1}) were evaporated at 60 °C in a heating block (CE-350/25, Cienlab, BR) with nitrogen flow. To the residue were added 40 μL of pyridine and kept at 38 °C for 90 min, then 60 μL of MTBSTFA (N-Methyl-N-*tert*-butyldimethylsilyltrifluoroacetamide) were added, and maintained for another 30 min at 38 °C to occur the silylation reaction. After derivatization, 1 μL of the samples was injected in splitless mode (1 min split-valve off, then split 20:1) in a gas chromatograph (3400, Varian, USA) equipped with a flame ionization detector (GC-FID) and an autosampler (8100, Varian, USA). The free polar compounds were separated in RTX-5MS capillary column (Restek, USA; 30 m × 0.25 mm; 0.25 μm of thickness film). The initial column temperature was 100 °C for 2 min, increasing to 165 °C at a rate of 2 °C min^{-1}, then increased to 200 °C at a rate of 5 °C min^{-1} and then at a rate of 3 °C min^{-1} reached 300 °C, where it remained for 5 min. Injector and detector were kept at 320 °C. The compounds were identified by comparing the retention times with the authentic standards of 22 amino acids (P/N LAA21, Supelco, USA), citric acid (P/N 251275, Sigma Aldrich, USA), malic acid (P/N 02300, Sigma Aldrich, USA) and tartaric acid (P/N 251380, Sigma Aldrich, USA). Quantification was performed by external calibration (0.1–80 μg mL^{-1}) with areas previously normalized by the internal standard. Results were expressed as μg g^{-1} of dry biomass. The determinations were carried out in triplicate.

2.5. Total lipids determination and fatty acids profile

Part of the organic fraction containing the lipids was placed in a beaker previously tared, and the content of total lipids was determined by gravimetry on an analytical balance with 0.01 mg minimum display (AUW220D, Shimadzu, JP) after solvent evaporation in air circulation oven (B5AFD, DeLeo, BR) at 105 °C. The rest of the organic fraction was derivatized with 1 mL of methanolic KOH (0.4 M) followed by 3 mL of methanolic H_2SO_4 (1 M), after each addition, the samples were kept for 10 min in a heating block (CE-350/25, Cienlab, BR) at 100 °C (Hartman & Lago, 1973) to obtain fatty acid methyl esters (FAME). The FAME were recovered hexane and analyzed using a Varian 3600 gas chromatograph equipped with a flame ionization detector (GC-FID) (USA) and Varian 8200 autosampler (USA). 1 μL was injected in splitless mode (0.8 min split-valve off, then split 20:1), and the FAME were separated in an HP-88 capillary column (Agilent Technologies, USA) (100 m × 0.25 mm; 0.20 μm of thickness film). The column temperature was held at 50 °C for 1 min; then it was increased to 185 °C at a rate of 15 °C min^{-1}, followed by an increase at 0.5 °C min^{-1} to 190 °C and finally at a rate of 15 °C min^{-1} until reaching 230 °C, remaining for 10 min. Injector and detector temperature was 250 °C. FAME were identified by comparison with authentic standard FAME Mix 37 (P/N 47885-U, Supelco, USA). Results were expressed as a percentage of the total area of the chromatograms, considering the correction factors of the flame ionization detector and conversion of the ester to acid (Visentainer, 2012). The determinations were carried out in triplicate.

2.6. Total protein determination and protein amino acids profile

Crude protein was analyzed by the Kjeldahl method (981.10) according to the Association of Official Analytical Chemists (AOAC)

guidelines (Horowitz & Latimer, 2000), using a conversion factor of 5.8 as proposed by da Silva, Leal, Resende, Martins, and Coimbra (2021). To determine the protein amino acid profile, 50 mg of biomass were weighed into vacuum hydrolysis tube, added 2 mL of 6 M hydrochloric acid (HCl) and kept at 110 °C for 24 h in a heating block (CE-350/25, Cienlab, BR) (Do Nascimento et al., 2019). After hydrolysis, the samples were derivatized and analyzed in GC-FID as previously described in item 2.4. The determinations were carried out in triplicate.

2.7. Chlorophylls and carotenoids determination

Chlorophylls and carotenoids were extracted according to the method described by Vendruscolo et al. (2021), using the solvents chloroform and ethanol. The total chlorophylls concentration was determined by UV–Vis diode array spectrophotometer (8453, Agilent Technologies, USA) and calculated according to Porra, Thompson and Kriedemann (1989). To determine total carotenoids, extracts were submitted to saponification procedure with 10% (w/v) KOH methanolic solution for 16 h at room temperature (do Nascimento et al., 2020). After removing the alkali by washing with distilled water, the total carotenoids concentration was determined by UV–Vis spectrophotometer and calculated according to Davies (1976). Afterwards, pigments were analyzed by high performance liquid chromatography HPLC (Shimadzu, JP) equipped with binary pumps (LC-20AD), online degasser, and automatic injector (SIL-20A HT). The equipment was connected in series to a Diode Array Detector (PDA) (SPD-M20A) and a mass spectrometry was performed with a Shimadzu 8040 triple quadrupole mass spectrometer and atmospheric pressure chemical ionization (APCI) source (Shimadzu America, USA). The pigments separation was performed on a C30 YMC column (5 μm, 250 × 4.6 mm) (Waters, USA). HPLC-PDA-APCI (+)QqQ analysis was performed according to De Rosso and Mercadante (2007) and Murillo et al. (2013), with adaptations. Prior to HPLC-PDA-APCI(+)QqQ analysis, the pigments extracts were solubilized in methanol (MeOH): methyl-tercbutyl-ether (MTBE) (70:30) and filtered through Millipore membranes (0.22 μm). The mobile phases A (MeOH) and phase B (MTBE), using a linear gradient program as follows: from 0 to 30 min 5% B; from 30 to 40 min, 5 to 30% B; from 40 to 41 min, 30 to 50% B, from 41 to 50 min, 50 to 5% B. The flow rate was set at 0.9 mL min^{-1}, the injection volume was 20 μL, the column temperature was maintained at 29 °C, the UV/vis spectra were acquired between 220 and 700 nm, and the chromatograms were processed at 450 nm for carotenoids and 660 nm for chlorophylls. The MS/MS detection was achieved through an APCI interface operated in positive (+) mode; detector voltage: 4.5 kV; interface temperature: 350 °C; desolvation line (DL) temperature: 200 °C; heat block temperature: 200 °C; nebulizing gas flow (N_2): 3.0 L min^{-1}; drying gas flow (N_2): 5.0 L min^{-1}; collision induced dissociation (CID) gas: 23 kPa (argon); event time: 0.5 s. The identification was performed according to the following combined information: elution order on C30 HPLC column, co-chromatography with authentic standards, UV–visible spectrum (λ max, spectral fine structure, peak cis intensity), and mass spectra characteristics (protonated molecule ([M+H]+) and MS/MS fragments), compared with data available in the literature (Rodrigues et al., 2014; Rodrigues, Menezes, Mercadante, Jacob-Lopes, & Zepka, 2015; Chen, Ríos, Pérez-Gálvez, & Roca, 2015; Patias et al., 2017; Fernandes et al., 2017; Maroneze, Jacob-Lopes, Zepka, Roca, & Pérez-Gálvez, 2019; Maroneze et al., 2020; Fernandes, Petry, Mercadante, Jacob-Lopes, & Zepka, 2020). Results were expressed as a percentage of the total area of the chromatograms.

2.8. Statistical analysis

Data normality was checked using the Shapiro-Wilk test and differences between treatments were evaluated by Student's *t*-test ($p < 0.05$) and analysis of variance (ANOVA), followed by Tukey's test ($p < 0.05$), all performed using STATISTICA 7.0 (Statsoft Inc., USA). In addition, all data were submitted to Principal Component Analysis (PCA) using Pirouette 3.11 software (Infometrix Co., USA). Before this multivariate analysis, the data matrix was autoscaled for each variable so that each assumed the same weight during analysis.

Table 1
Free polar compounds (μg g^{-1}) from *Scenedesmus obliquus* biomass obtained with enrichment of CO_2 (%).

	3%	5%	10%	15%	20%	25%
Amino Acids						
Alanine	33.7 ^{cd} ± 2.7	48.1^{b} ± 4.5	149.6^{a} ± 0.6	28.0^{d} ± 0.8	35.6^{c} ± 2.24	34. 6 ^{cd} ± 1.8
Glycine	27.1^{ab} ± 0.7	19.3^{c} ± 0.6	28.3^{a} ± 1.7	15.4^{d} ± 1.3	23. 9^{b} ± 1.79	15.6^{d} ± 0.5
Valine	–	–	42.1^{a} ± 0.6	12.7^{b} ± 0.9	9.7^{c} ± 0.49	9.3^{c} ± 0.5
Leucine	–	–	47.1^{a} ± 0.0	21.4^{b} ± 1.6	16.1^{c} ± 0.93	18.2^{c} ± 0.9
Isoleucine	–	–	32.2^{a} ± 1.2	9.7^{c} ± 0.4	–	28.8^{b} ± 2.2
Proline	–	–	69.2^{a} ± 2.2	–	–	–
Methionine	119.0^{b} ± 5.3	127.9^{a} ± 6.2	–	–	–	–
Threonine	21.6^{b} ± 1.7	24.5^{b} ± 1.6	29.8^{a} ± 1.0	11.4 ^{cd} ± 0.3	14. 6^{c} ± 0.64	9.9^{d} ± 0.8
Phenylalanine	–	–	29.3^{a} ± 2.6	12.0^{d} ± 1.1	19.1^{c} ± 1.10	23.3^{b} ± 0.6
Aspartic Acid	54.2^{a} ± 3.4	16.5^{b} ± 1.0	7.3^{c} ± 0.7	–	5.1^{c} ± 0.34	6. 7^{c} ± 0.4
Cysteine	–	25.1^{a} ± 1.6	–	–	–	–
Glutamic Acid	426.0^{a} ± 31.6	471.8^{a} ± 10.8	246.1^{b} ± 18.2	55.5^{c} ± 1.7	93.6^{c} ± 5.78	52.9^{c} ± 2.2
Tyrosine	168.2^{a} ± 16.8	156.1^{a} ± 7.6	19.3^{b} ± 0.8	11.1^{b} ± 0.2	13.9^{b} ± 0.32	11.8^{b} ± 0.3
Total FAA	849.7^{a} ± 31.7	889.3^{a} ± 27.9	700.1^{b} ± 22.6	177.1^{c} ± 5.1	231.5^{c} ± 11.2	211.1^{c} ± 6.1
Organic Acids						
Malic Acid	–	–	25.3^{a} ± 0.8	–	18.6^{b} ± 0.1	–
Citric Acid	108.1^{a} ± 5.8	84.1^{b} ± 6.0	6.2^{c} ± 0.4	–	8.4^{c} ± 0.4	1.5^{c} ± 0.1
Total OA	108.1^{a} ± 5.8	84.1^{b} ± 6.0	31.5^{c} ± 1.1	–	27.0^{c} ± 0.5	1.5^{d} ± 0.1

*Results expressed in Mean ± Standard Deviation.
* Different letters on the same line indicate difference by Tukey test ($p > 0.05$).

3. Results and discussion

Microalgae can absorb inorganic carbon in different ways, direct assimilation of CO_2 by the plasma membrane, convert bicarbonates into CO_2 through extracellular carbonic anhydrase, or direct capture bicarbonates by active membrane transporters. These mechanisms are intrinsic to each strain; the microalgae *S. obliquus*, for instance, can perform the three forms of assimilation (Prasad et al., 2021). After absorption, inorganic carbon fixation can occur through autotrophic (inorganic carbon only) or mixotrophic (presence of inorganic and organic carbon) metabolism (Vuppaladadiyam et al., 2018). *S. obliquus* cultivation was conducted exclusively with inorganic carbon (CO_2), and briefly, in autotrophic metabolism through the Calvin-Benson cycle (CBC), two 3-phosphoglycerate (3PG) molecules are formed from a ribulose 1,5-bisphosphate (RuBP) molecule, CO_2 and water. When six 3PG molecules are formed, five are directed to restore RuBP, and one is used to create the most diverse metabolites necessary for the cellular activity (Xu et al., 2019). The results showing the influence of the CO_2 concentration in forming *S. obliquus* metabolites are presented and discussed below.

3.1. Free polar compounds

Free polar metabolites are precursors to microalgal compounds,

Table 2
Protein amino acids (mg g^{-1}) and total protein (%) *Scenedesmus obliquus* cultivated photosynthetically with different percentages of CO_2.

	3%	5%	10%	15%	20%	25%
Alanine	53.3^{a} ± 2.5	47.1^{b} ± 1.3	46.4^{b} ± 3.6	23.3^{c} ± 0.6	21.3^{c} ± 1.9	26.3^{c} ± 1.6
Glycine	40.0^{a} ± 3.4	35.1^{b} ± 0.8	34.7^{b} ± 2.4	22.4^{b} ± 2.0	21.8^{bc} ± 0.5	18.2^{c} ± 0.4
Valine	43.6^{a} ± 1.3	39.1^{b} ± 2.7	37.5^{b} ± 0.2	19.6^{c} ± 0.5	17.1^{c} ± 0.6	18.4^{c} ± 0.2
Leucine	60.4^{a} ± 0.6	56.1^{b} ± 3.6	52.6^{c} ± 1.2	28.6^{d} ± 0.3	25.3^{e} ± 0.5	29.8^{d} ± 0.2
Isoleucine	41.6^{a} ± 0.7	37.4^{b} ± 1. 7	35.4^{c} ± 0.4	15.8^{d} ± 0.2	13.7^{e} ± 4.4	15.2^{de} ± 4.4
Proline	21.1^{a} ± 2.0	19.8^{a} ± 1.0	19.1^{a} ± 1.8	12.6^{b} ± 0.3	10.8^{b} ± 0.6	11.3^{b} ± 0.8
Methionine	19.2^{a} ± 1.9	16.9^{ab} ± 0.6	14.7^{b} ± 0.9	10.3^{c} ± 0.4	9.3^{c} ± 0.6	9.4^{c} ± 0.6
Serine	15.7^{a} ± 0.3	14.3^{b} ± 0.4	14.3^{b} ± 0.8	7.8^{c} ± 0.2	6.2^{d} ± 0.5	7.8^{c} ± 0.6
Threonine	36.5^{a} ± 1.4	33.1^{a} ± 1.3	19.5^{b} ± 1.7	16.0^{c} ± 0.6	14.4^{c} ± 0.6	9.9^{d} ± 0.2
Phenylalanine	46.9^{a} ± 3.3	48.9^{a} ± 2.3	50.1^{a} ± 2.0	36.9^{b} ± 1.3	37.2^{b} ± 0.4	39.2^{b} ± 0.9
Aspartic Acid	–	3.1^{a} ± 0.3	3.1^{a} ± 0.3	1.4d ± 0.1	2.0^{c} ± 0.1	2.5^{b} ± 0.1
Glutamic Acid	52.5^{a} ± 2.7	55.1^{a} ± 3.3	52.4^{a} ± 4.6	24.7^{b} ± 0.5	25.1^{b} ± 0.4	28.4^{b} ± 1.8
Lysine	–	65.6^{a} ± 1.5	–	31.1^{b} ± 1.3	–	–
Histidine	–	–	10.1^{a} ± 0.7	–	–	–
Tyrosine	20.9^{a} ± 0.6	–	21.7^{a} ± 2.1	11.1^{b} ± 0.4	10.3^{b} ± 0.4	10.5^{b} ± 0.8
Tryptophan	12.8^{a} ± 0.7	8.9^{b} ± 0.8	9.5^{b} ± 0.9	6.0^{c} ± 0.4	8.0^{b} ± 0.2	5.8^{c} ± 0.4
∑Essential AA	280.0^{b} ± 6.6	322.8^{a} ± 9.4	233. 9^{c} ± 5.0	174.4^{d} ± 2.6	134.2^{e} ± 2.3	137.2^{e} ± 3.2
∑Non-essential AA	203.3^{a} ± 3.5	174.5^{b} ± 5.4	201.7^{a} ± 15.1	103.2^{c} ± 2.3	97.4^{c} ± 3.1	104.9^{c} ± 5.1
Total Protein	57.8^{a} ± 2.3	57.2^{a} ± 0.2	56.4^{a} ± 0.9	31.0^{b} ± 0.2	27.0^{c} ± 1.2	28.9^{bc} ± 0.05

*Results expressed in Mean ± Standard Deviation.
*Essential AA- essential amino acids; Non-essential AA- non-essential amino acids.
* Different letters on the same line indicate difference by Tukey test ($p > 0.05$).

formed from the CBC and tricarboxylic acid (TCA) cycle and can be used as markers of the cellular activity of these microorganisms; we detected several free amino acids and the organic acids malic and citric, important TCA intermediates, were detected (Table 1). The detected amino acids can be synthesized from 3PG, intermediates between CBC and TCA, such as phosphoenolpyruvate and pyruvate, and TCA intermediates, α-ketoglutarate and oxalate. The presence of these compounds indicates that all routes were being performed regardless of CO_2 enrichment in *S. obliquus* cultivations, although at different intensities, as significant differences were detected in the concentrations of organic and free amino acids (Table 1).

Higher concentrations of free polar metabolites were found in cells in cultivations with 3, 5, and 10% CO_2; it is possible that the polymer formation routes had their activities reduced at the time of obtaining the biomass, leading to this accumulation. The values decreased significantly with CO_2 enrichment (15, 20 and 25%) (Table 1), and despite the reduction, glutamic acid remained the free amino acid with the highest concentration, possibly because it is also a precursor to chlorophylls, the main photosynthetic pigment, through the C5 route (Kang, Wang, Wang, & Qi, 2011; Nehmé et al., 2017).

Cultivations with 3, 5, and 10% CO_2 that showed the highest accumulation of free amino acids inside *S. obliquus* cells were also the ones with the highest proteins concentrations (Table 2). The cells continued synthesizing high amino acid amounts even with high protein content. In these cultivations, the 3PG was directed, preferably, to the routes of amino acid and protein formation. In addition, in cases of low CO_2, oxygen can compete in the CBC for RuBP, 3PG and 2-phosphoglycolate (2PG) are obtained as products, and 2PG is metabolized directly to amino acids. Photorespiration, as this process is called, occurs mainly in the presence of light, such as in these *S. obliquus* cultivations that are performed with constant lighting. (Zeng, Danquah, Chen, & Lu, 2011).

Glutamic acid, a protein component, and chlorophyll precursor was the major free amino acid in the evaluated biomasses. The highest concentrations of this amino acid were found in the cultures with the lowest CO_2 enrichment levels (3, 5, and 10%) (Table 1). The most significant synthesis of chlorophyll compounds occurred in cultures with 15, 20, and 25% CO_2 (Table 3), in which greater photosynthetic efficiency was required for gas assimilation and absorption, and possibly glutamic acid was directed to the C5 route to obtain chlorophylls. The results regarding the pigments will be presented and discussed later.

3.2. Protein and protein amino acids

Protein synthesis in microalgae is the most important and complex process; it begins with synthesizing amino acids that condense into peptides and then into primary proteins (Zeng et al., 2011). In the *S. obliquus* biomasses cultured with 3, 5, and 10% CO_2, a high synthesis of free amino acids was observed (Table 1), as well as protein synthesis, with values of 57.8, 57.2, and 56.4% of total proteins being found, respectively (Table 2). The higher CO_2 levels in cultivation inversely affected the protein content in the culture with 15% CO_2, which was 31.0%, 27.0% with 20% CO_2 and 28.9% with 25% CO_2 (Table 2). Previous studies have also reported this relationship for *S. obliquus*, reduced total protein levels in cultivation with an increase in CO_2 from 0.03 to 13.8% and for *Chlorella pyrenoidosa* cultivated with 3, 5, and 10% of CO_2 (Basu, Roy, Mohanty, & Ghoshal, 2013; Huang et al., 2017). In these cases, it is suggested that in cultivation with less CO_2 enrichment, 3PG is directed at the production routes of free amino acids and these in turn in proteins, in addition to photorespiration as mentioned herein.

Besides total protein levels, the protein amino acid profiles were also modified significantly by the CO_2 enrichment percentages. In the 3% CO_2 cultivation, the major protein amino acids were leucine (60.4 mg g^{-1}), alanine (53.3 mg g^{-1}), and glutamic acid (52.5 mg g^{-1}). With 5% CO_2, they were lysine (65.6 mg g^{-1}), leucine (56.1 mg g^{-1}), and glutamic acid (55.1 mg g^{-1}), and with 10% CO_2, they were leucine (52.6 mg g^{-1}), glutamic acid (52.4 mg g^{-1}), and phenylalanine (50.1 mg g^{-1}). By increasing to 15% of CO_2, the concentrations of major amino acids significantly decreased: phenylalanine (36.9 mg g^{-1}), lysine (31.1 mg g^{-1}), and leucine (28.6 mg g^{-1}). In the cultivation of *S. obliquus* with 20% CO_2, the highest concentrations were found for phenylalanine (37.2 mg g^{-1}), leucine (25.3 mg g^{-1}), and glutamic acid (25.1 mg g^{-1}). Cultivation with 25% CO_2 showed the same major compounds as cultivation with 20% CO_2, although at different concentrations: phenylalanine (39.2 mg g^{-1}), leucine (29.8 mg g^{-1}), and glutamic acid (28.4 mg g^{-1}) (Table 2).

S. obliquus biomass has a high protein content, although values above 56% were obtained for the lower CO_2 percentages applied in the cultivation. In addition, what attracts attention for applications in food and supplements is also related to the microalgal protein quality (Ejike et al., 2017). The essential amino acids for human nutrition, including valine, leucine, isoleucine, methionine, threonine, phenylalanine, lysine, histidine and tryptophan, represent oven 53% of the amino acid profile, regardless of the treatment. In order to combine protein quantity and quality, *S. obliquus* biomass cultivated with 5% CO_2 stands out, with 57.2% of total proteins, the highest essential amino acid concentration (322.8 mg g^{-1} of dry biomass), and over 32% of the biomass content (Table 2).

The essential amino acid histidine was not found in most treatments, it was only present in the composition of the treatment with 10% CO_2, being the main limiting amino acid. Regarding the other essential amino acids, treatment with 5% CO_2 presented adequate concentrations for

Table 3
Total pigments (mg g^{-1}) and chlorophylls and carotenoids profiles (%) from *Scenedesmus obliquus* cultivated with different levels of CO_2 enrichment.

Compounds	3% CO_2	5% CO_2	10% CO_2	15% CO_2	20% CO_2	25% CO_2
Chlorophylls						
13^2-hydroxy-chlorophyll-*b*	–	–	–	$6.7^{a} \pm 0.0$	$3.4^{b} \pm 0.6$	$3.5^{b} \pm 0.2$
15^1-hydroxy-lactone-chlorophyll-*a*	$3.3^{e} \pm 0.3$	$4.1^{de} \pm 0.1$	$5.4^{d} \pm 0.2$	$53.4^{a} \pm 1.1$	$14.0^{c} \pm 0.2$	$23.2^{b} \pm 0.5$
chlorophyll-*b*	–	–	–	$3.2^{c} \pm 1.1$	$12.0^{a} \pm 0.1$	$9.0^{b} \pm 0.6$
chlorophyll-*b*′	–	–	–	–	–	$4.6^{a} \pm 0.0$
13^2-hydroxy-chlorophyll-*a*	$3.7^{a} \pm 0.4$	$4.2^{a} \pm 0.1$	$4.5^{a} \pm 0.3$	$1.6^{b} \pm 0.0$	$4.4^{a} \pm 0.5$	–
Chlorophyll-*a*	$88.1^{a} \pm 0.8$	$85.0^{b} \pm 0.!$	$86.5^{ab} \pm 0.5$	$26.9^{e} \pm 0.0$	$59.0^{c} \pm 1.3$	$45.7^{d} \pm 0.4$
Chlorophyll-*a*′	$4.9^{e} \pm 0.2$	$6.7^{c} \pm 0.1$	$3.6^{f} \pm 0.0$	$7.2^{b} \pm 0.0$	$5.9^{d} \pm 0.1$	$9.9^{a} \pm 0.0$
Pheophytin-*a*	–	–	–	$1.0^{b} \pm 0.0$	$1.3^{b} \pm 0.2$	$4.0^{a} \pm 0.5$
Total Chlorophylls (mg g^{-1})	$19.5^{d} \pm 0.2$	$18.\ 5^{e} \pm 0.2$	$18.0^{e} \pm 0.1$	$24.2^{b} \pm 0.5$	$23.1^{c} \pm 0.5$	$30.8^{a} \pm 0.4$
Carotenoids						
all-*trans*-loroxanthin	–	–	–	$0.9^{c} \pm 0.0$	$3.4^{b} \pm 0.0$	$4.1^{a} \pm 0.0$
all-*trans*-neoxanthin	$0.1^{e} \pm 0.0$		$0.2^{d} \pm 0.0$	$4.8^{b} \pm 0.0$	$5.4^{a} \pm 0.0$	$4.4^{c} \pm 0.0$
9-*cis*-neoxanthin	–	–	–	$1.7^{b} \pm 0.0$	$1.6^{c} \pm 0.0$	$2.7^{a} \pm 0.1$
all-*trans*-luteoxanthin	–	–	–	$2.0^{c} \pm 0.0$	$2.2^{b} \pm 0.0$	$2.5^{a} \pm 0.1$
15-*cis*-lutein	–	–	–	$4.3^{b} \pm 0.1$	$3.6^{c} \pm 0.1$	$5.3^{a} \pm 0.0$
13-*cis*-lutein	–	–	–	$2.0^{b} \pm 0.0$	$1.6^{c} \pm 0.0$	$2.6^{a} \pm 0.1$
all-*trans*-lutein	$0.8^{f} \pm 0.0$	$2.0^{e} \pm 0.0$	$4.0^{d} \pm 0.0$	$73.0^{b} \pm 0.3$	$76.8^{a} \pm 0.3$	$67.9^{c} \pm 0.2$
all-*trans*-zeaxanthin	$9.3^{c} \pm 0.0$	$10.5^{a} \pm 0.3$	$10.0^{b} \pm 0.0$	$1.1^{d} \pm 0.0$	$0.4^{e} \pm 0.0$	$0.3^{e} \pm 0.0$
9-*cis*-lutein	–	–	–	$2.0^{b} \pm 0.1$	$0.8^{c} \pm 0.1$	$2.7^{a} \pm 0.1$
9-*cis*-zeaxanthin	$1.\ 7^{b} \pm 0.0$	$1.6^{c} \pm 0.0$	$1.1^{d} \pm 0.0$	$1.6^{bc} \pm 0.0$	$0.7^{e} \pm 0.0$	$2.0^{a} \pm 0.1$
13-*cis*-cantaxanthin	$4.7^{a} \pm 0.0$	$3.9^{b} \pm 0.4$	$3.4^{b} \pm 0.0$	–	–	–
2′-dehydrodeoxymyxol	$3.7^{c} \pm 0.0$	$4.3^{b} \pm 0.1$	$4.6^{a} \pm 0.0$	–	–	–
all-*trans*-zeinoxanthin	$0.5^{b} \pm 0.0$	$0.3^{c} \pm 0.0$	$0.6^{a} \pm 0.0$	–	–	–
all-*trans*-β-cryptoxanthin	$1.5^{c} \pm 0.0$	$1.8^{b} \pm 0.0$	$2.0^{a} \pm 0.0$	–	–	–
all-*trans*-echinenone	$13.5^{a} \pm 0.0$	$12.0^{b} \pm 0.1$	$10.7^{c} \pm 0.0$	–	–	–
9-*cis*-echinenone	$17.0^{b} \pm 1.1$	$18.1^{a} \pm 0.9$	$15.4^{c} \pm 0.0$	–	–	–
all-*trans*-β-carotene	$44.2^{a} \pm 1.1$	$40.2^{b} \pm 1.1$	$44.5^{a} \pm 0.0$	$6.4^{c} \pm 0.1$	$3.7^{d} \pm 0.2$	$5.5^{c} \pm 0.1$
9-*cis*-β-carotene	$3.2^{c} \pm 0.0$	$5.4^{a} \pm 0.1$	$3.5^{b} \pm 0.0$	–	–	–
Total Carotenoids (mg g^{-1})	$25.3^{a} \pm 0.5$	$22.7^{b} \pm 0.1$	$18.1^{c} \pm 1.0$	$7.3^{d} \pm 0.4$	$5.7^{e} \pm 0.3$	$7.7^{d} \pm 0.4$

*Results expressed in Mean ± Standard Deviation.
* Different letters on the same line indicate difference by Tukey test ($p > 0.05$).

valine, isoleucine, methionine, threonine, phenylalanine, lysine, histidine and tryptophan according to the latest recommendation of the World Health Organization (WHO 2007), that is, greater than 100% (mg of essential amino acid/g of protein) for the protein to be considered of high biological value, with the exception of the essential amino acid leucine which presented 95% of the recommended value.

Treatment with 5% CO_2 enrichment proved to be a viable alternative for food supplementation in protein terms since the value of 57.2% on a dry basis is higher than animal foods such as eggs, milk, cheese, and even soy, which is a reference protein food of plant origin. Despite some limitations, regarding the amount of histidine and leucine, the essential amino acid composition of this treatment provides adequate concentrations of the amino acids lysine, methionine, and cysteine, which are the main limiting amino acids in vegetarian and vegan diets (Mariotti & Gardner, 2019). Thus, enrichment with 5% CO_2 enabled us to obtain microalgal biomass suitable to enrich plant-based foods.

3.3. Total pigments and profiles of chlorophylls and carotenoids

Total chlorophyll concentrations in the *S. obliquus* biomasses were more significant at the highest CO_2 percentages (Table 3), being 19.5 mg g^{-1} (3% CO_2), 18.5 mg g^{-1} (5% CO_2), 18.0 mg g^{-1} (10% CO_2), 24.2 mg g^{-1} (15% CO_2), 23.1 mg g^{-1} (20% CO_2) and 30.8 mg g^{-1} (25% CO_2). Previous studies have also reported increased chlorophyll concentrations in *S. obliquus* by increasing CO_2 from 0.03 to 13.8% and in *Scenedesmus* sp. in cultivations with 0 to 15% CO_2 (Basu et al., 2013; Tripathi, Singh, & Thakur, 2015). Swarnalatha, Hegde, Chauhan, and Sarada (2015) evaluated the total chlorophyll content of different microalgae strains grown with 0, 10, 20 and 30% CO_2 and found that, *Desmodesmus* sp. and *Acutodesmus* sp. increased chlorophyll synthesis up to 20% CO_2 and showed a reduction with 30% CO_2. In contrast, *Kirchneriella commuta* had higher concentrations of up to 30% CO_2.

Chlorophylls are composed of a phytol tail and a macrocycle with four pyrrole rings joined by a magnesium molecule (D'Alessandro & Antoniosi Filho, 2016). In microalgal cells, the phytol tail is found next to the chloroplast membrane lipids. At the same time, the double bonds of the pyrrole rings act as antennas for capturing light and the magnesium atom charges the electrons for photosynthesis reactions to occur. Chlorophyll-*a* is the most important and found in the reaction center. However, other pigments act as accessories, such as other chlorophylls compounds absorbing light at other wavelengths and passing energy to chlorophyll-*a* and carotenoids absorbing the excess (Carvalho, Silva, Baptista, & Malcata, 2011). As in the *S. obliquus* cultivation constant lighting was used, and there was an increase in the CO_2 present in the medium, the cells synthesized higher chlorophyll concentrations to intensify the photosynthetic process.

The chlorophyll profiles in cultures with 3, 5 and 10% CO_2 showed over 80% chlorophyll-*a* (88.1, 85.0, and 86.5%, respectively). The other minority compounds are derived from chlorophyll-*a*, 15^1-hydroxy-lactone-chlorophyll-*a*, 13^2-hydroxy-chlorophyll-*a*, and chlorophyll-*a*′. In cultivations with 20 and 25% CO_2, the compound with the highest concentration was also chlorophyll-*a* (59.0 and 45.7%, respectively). In addition to the derivatives already mentioned, pheophytin-*a*, the accessory pigment chlorophyll-*b* and its derivative 13^2-hydroxy-chlorophyll-*b* were also detected. Cultivation with 15% CO_2 showed the same compounds in those with 20 and 25% CO_2 enrichment, although the compound with the highest concentration was 15^1-hydroxy-lactone-chlorophyll-*a*. All derivatives are products of chemical reactions; 15^1-hydroxy-lactone-chlorophyll-*a* is an extreme oxidation product of chlorophyll-*a* by peroxidase enzyme and not from synthesis by *S. obliquus* (Kao, Chen, & Chen, 2011). Hence, the chlorophylls from *S. obliquus* biomasses grown at 3, 5, and 10% CO_2, despite the lower concentration, are more viable for functional applications as bioactive compounds due to the higher proportion of chlorophyll-*a* in relation to derivatives that are degradation products (Table 3).

The carotenoids, in turn, showed a behavior inversely proportional to the increased CO_2 percentages. The cultivations at the highest concentration were those with 3, 5, and 10% CO_2 (25.3, 22.7, and 18.1 mg

Table 4
Fatty acids composition and total lipids (%) from *Scenedesmus obliquus* cultivated with different CO_2 concentrations.

Compounds	3%	5%	10%	15%	20%	25%
C12:0	$1.3^{b} \pm 0.1$	$1.2^{bc} \pm 0.1$	$1.2^{b} \pm 0.0$	$0.9^{d} \pm 0.0$	$1.1^{c} \pm 0.0$	$1.8^{a} \pm 0.0$
C13:0	$1.6^{bc} \pm 0.1$	$1.4^{cd} \pm 0.1$	$1.7^{b} \pm 0.0$	$1.1^{e} \pm 0.1$	$1.3^{de} \pm 0.1$	$2.0^{a} \pm 0.0$
C14:0	$0.2^{d} \pm 0.0$	$0.3^{cd} \pm 0.0$	$0.3^{bc} \pm 0.0$	$0.5^{a} \pm 0.0$	$0.4^{b} \pm 0.0$	$0.4^{b} \pm 0.0$
C14:1	$0.6^{b} \pm 0.1$	$0.9^{a} \pm 0.1$	$0.8^{a} \pm 0.1$	$0.6^{b} \pm 0.0$	$0.6^{b} \pm 0.0$	$0.8^{a} \pm 0.0$
C16:0	$59.0^{b} \pm 0.1$	$62.1^{a} \pm 1.0$	$56.9^{c} \pm 0.7$	$43.3^{d} \pm 0.8$	$38.8^{e} \pm 0.5$	$36.9^{f} \pm 0.3$
C16:1	$1.4^{b} \pm 0.0$	$1.2^{c} \pm 0.1$	$1.6^{a} \pm 0.0$	$0.3^{d} \pm 0.0$	$0.2^{d} \pm 0.0$	$0.3^{d} \pm 0.0$
C17:0	$0.8^{b} \pm 0.1$	$1.0^{a} \pm 0.1$	$1.0^{a} \pm 0.1$	$0.4^{c} \pm 0.0$	$0.3^{c} \pm 0.0$	$0.4^{c} \pm 0.0$
C17:1	$0.5^{b} \pm 0.0$	$0.5^{b} \pm 0.0$	$0.8^{a} \pm 0.0$	$0.2^{c} \pm 0.0$	$0.2^{c} \pm 0.0$	$0.2^{c} \pm 0.0$
C18:0	$2.6^{f} \pm 0.1$	$2.9^{e} \pm 0.1$	$3.9^{d} \pm 0.0$	$7.9^{a} \pm 0.2$	$7.3^{b} \pm 0.2$	$5.3^{c} \pm 0.0$
C18:1n9c	$6.5^{e} \pm 0.1$	$7.2^{de} \pm 0.3$	$7.6^{d} \pm 0.1$	$21.2^{b} \pm 0.7$	$22.8^{a} \pm 0.1$	$16.3^{c} \pm 0.2$
C18:2n6c	$10.1^{b} \pm 0.1$	$7.6^{d} \pm 0.4$	$9.0^{c} \pm 0.3$	$10.2^{b} \pm 0.1$	$10.3^{b} \pm 0.3$	$12.4^{a} \pm 0.1$
C18:3n6	$10.9^{a} \pm 0.3$	$8.7^{b} \pm 0.7$	$8.5^{b} \pm 0.2$	$1.!^{c} \pm 0.0$	$1.0^{c} \pm 0.1$	$1.1^{c} \pm 0.0$
C18:3n3	$0.8^{e} \pm 0.0$	$0.9^{e} \pm 0.0$	$1.9^{d} \pm 0.1$	$9.0^{c} \pm 0.3$	$11.9^{b} \pm 0.5$	$17.9^{a} \pm 0.2$
C20:1n9	$1.3^{bc} \pm 0.1$	$1.5^{ab} \pm 0.1$	$1.3^{bc} \pm 0.1$	$1.2^{c} \pm 0.1$	$1.3^{abc} \pm 0.1$	$1.6^{a} \pm 0.1$
C21:0	$1.3^{d} \pm 0.0$	$1.3^{d} \pm 0.1$	$1.7^{c} \pm 0.1$	$1.6^{c} \pm 0.0$	$2.0^{b} \pm 0.1$	$2.4^{a} \pm 0.0$
C22:0	$0.2^{c} \pm 0.0$	$0.4^{b} \pm 0.0$	$0.9^{a} \pm 0.1$	$0.1^{cd} \pm 0.0$	$0.1^{d} \pm 0.0$	$0.1^{d} \pm 0.0$
C20:4n6	$0.1^{b} \pm 0.0$	$0.2^{a} \pm 0.0$	$0.1^{a} \pm 0.0$	–	–	–
C24:0	–	–	–	$0.2^{b} \pm 0.0$	$0.3^{a} \pm 0.0$	$0.3^{a} \pm 0.0$
C22:5n3	$0.8^{b} \pm 0.1$	$0.9^{a} \pm 0.1$	$0.8^{b} \pm 0.0$	$0.2^{c} \pm 0.0$	$0.1^{c} \pm 0.0$	$0.1^{c} \pm 0.0$
C22:6n3	–	–	–	$0.2^{a} \pm 0.0$	$0.1^{b} \pm 0.0$	$0.1^{c} \pm 0.0$
∑SFA	$66.9^{b} \pm 0.2$	$70.6^{a} \pm 0.9$	$67.7^{b} \pm 0.6$	$56.0^{c} \pm 0.9$	$51.5^{d} \pm 0.6$	$49.4^{e} \pm 0.3$
∑MUFA	$10.4^{f} \pm 0.2$	$11.2^{e} \pm 0.2$	$12.0^{d} \pm 0.1$	$23.\ 5^{b} \pm 0.6$	$25.1^{a} \pm 0.2$	$19.1^{c} \pm 0.2$
∑PUFA	$22.7^{b} \pm 0.3$	$18.3^{d} \pm 1.1$	$20.3^{c} \pm 0.5$	$20.6^{c} \pm 0.4$	$23.4^{b} \pm 0.7$	$31.5^{a} \pm 0.3$
n6/n3	$13.6^{a} \pm 0.6$	$8.8^{b} \pm 0.9$	$6.7^{c} \pm 0.2$	$1.2^{d} \pm 0.0$	$0.9^{d} \pm 0.0$	$0.8^{d} \pm 0.0$
Total Lipids	$12.3^{c} \pm 0.0$	$11.5^{d} \pm 0.3$	$12.5^{c} \pm 0.2$	$14.8^{a} \pm 0.4$	$15.0^{a} \pm 0.2$	$13.7^{b} \pm 0.1$

* Results expressed in Mean ± Standard Deviation.
* SFA- saturated fatty acids; MUFA- monounsaturated fatty acids; PUFA- polyunsaturated fatty acids; n6/n3- omega 6 and omega 3 ratio.
* Different letters on the same line indicate difference by Tukey test ($p > 0.05$).

g^{-1}, respectively). In the other cultures, there was a significant reduction in carotenoids: 7.3 mg g^{-1} (15% CO_2), 5.7 mg g^{-1} (20% CO_2), and 7.7 mg g^{-1} (25% CO_2). Carotenoids are accessory pigments that absorb excess light so that chlorophyll degradation does not occur. There was a high chlorophyll synthesis in treatments with 12, 20, and 25% CO_2 and that they are mainly responsible for absorbing light for the photosynthetic process, so there was low carotenoids production. Nonetheless, the proportion of carotenoids to chlorophylls in these biomasses was low, causing oxidative damage and the formation of more derivatives in greater proportions.

CO_2 treatments also changed the carotenoid profiles; in cultures with 3, 5, and 10% CO_2 the significant compounds were all-*trans*-β-carotene with over 40% of the total chromatogram area, 9-*cis*-echinenone above 15%, all-*trans*-echinenone with over 10% and all-*trans*-zeaxanthin in the range of 10%. The *S. obliquus* biomass cultivated with 15% CO_2 showed the major compounds all-*trans*-lutein (73.0%), all-*trans*-β-carotene (6.4%), and all-*trans*-neoxanthin (4.8%); with 20% CO_2, the major compounds were all-*trans*-lutein (76. 8%), all-*trans*-neoxanthin (5.4%), and all-*trans*-β-carotene (3.7%). In the 25% CO_2 cultivation, the compounds with the highest percentage were all-*trans*-lutein, all-*trans*-β-carotene, and 15-*cis*-lutein (67.9, 5.5, and 5.3%, respectively). UV–vis characteristics and fragment ions used to identify chlorophyll and carotenoid compounds are presented in Supplementary Material 1.

The glyceraldehyde 3-phosphate formed in the CBC from the 3PG is conducted through the methylerythritol phosphate pathway for carotenoids synthesis. The synthesis begins with the condensation of two molecules of geranylgeranyl pyrophosphate, giving rise to the phytoene that is converted into lycopene. α-Carotene and γ-carotene are formed from lycopene (Igreja, Maia, Lopes, & Chisté, 2021); the α conformation gives rise to lutein, a major compound in cultivations with 15, 20, and 25% CO_2. γ-Carotene originates β-carotene, and from it, echinenone and zeaxanthin are formed, compounds in greater concentration in cultures with 3, 5, and 10% CO_2. The highest CO_2 percentages intensified the formation of the derivative from α-carotene. While in the lowest gas concentrations, a greater proportion of compounds formed from γ-carotene was observed (Mander & Liu, 2010; Zhang, Selão, Selstam, & Norling, 2015).

However, all carotenoid profiles obtained have market potential, due to the significant β-carotene and lutein concentrations, which have high added value (Novoveská et al., 2019), in addition to their application in functional foods and nutraceuticals, antioxidant properties, reduction of chronic disease incidence, type 2 diabetes, and some types of cancer (Fernandes et al., 2021).

3.4. Total lipids and fatty acids profiles

The different CO_2 levels significantly influenced the total lipid content of the biomasses (Table 4). The highest values were 14.8 and 15.0% in treatments with 15 and 20% CO_2, respectively, followed by cultivation with 25% CO_2 with 13.7% lipids. The other values were 12.3% of lipids in the cultivation with 3% CO_2, 11.5% with 5% CO_2, and 12.5% with 10% CO_2. This same behavior has been observed in previous research on CO_2 mitigation with *S. obliquus* (Ho et al., 2010; Tang et al., 2011; Basu et al., 2013), *Scenedesmus dimorphus* (Vidyashankar, Deviprasad, Chauhan, Ravishankar, & Sarada, 2013), and *Scenedesmus bajacalifornicus* (Patil & Kaliwal, 2017). Higher lipids levels in microalgal cells are related to stress conditions, and the studies cited found that enrichment above 15% CO_2 could be considered one of these conditions.

The fatty acid (FA) profiles were also modified by the different levels of CO_2 enrichment (Table 4) and the total lipid content; the results obtained for treatments with a lower percentage of enrichment (3, 5, and 10% CO_2) showed similarities. Changes in FA concentrations were observed, although the major compounds were palmitic acid (C16:0), oleic acid (C18:1n9c), linoleic acid (C18:2n6c), and γ-linolenic acid (C18:3n6) in these treatments. In the cultivation with 3% of CO_2 the concentrations of the majority FA were 59.0% (C16:0), 10.9% (C18:3n6), 10.1% (C18:2n6), and 6.5% (C18:1n9c); in the sample that was grown with 5% CO_2, 62.1% (C16:0), 8.7% (C18:3n6), 7.6% (C18:2n6c), and 7.2% (C18:1n9c); and in cultivation with 10% CO_2, C16:0 showed a concentration of 56.9%, C18:2n6 of 9.0%, C18:3n6 of 8.5%, and C18:1n9c of 7.6%.

The biomasses obtained with 15, 20, and 25% CO_2 also showed C16:0, C18:1n9c, and C18:2n6 as major FA; nevertheless, instead of C18:3n6, one of the compounds with the highest concentration was α-linolenic acid (C18:3n3), which is also called ALA and known extensively for its health benefits. In the 15% CO_2 cultivation the highest concentrations were 43.3% (C16:0), 21.2% (C18:1n9c), 10.2% (C18:2n6c), and 9.0% (C18:3n3); with 20% CO_2, they were 38.8% (C16:0), 22.8% (C18:1n9c), 11.9% (C18:3n3), and 10.3% (C18:2n6); and with 25% CO_2 they were 36.9% (C16:0), 17.9% (C18:3n3), 16.3%

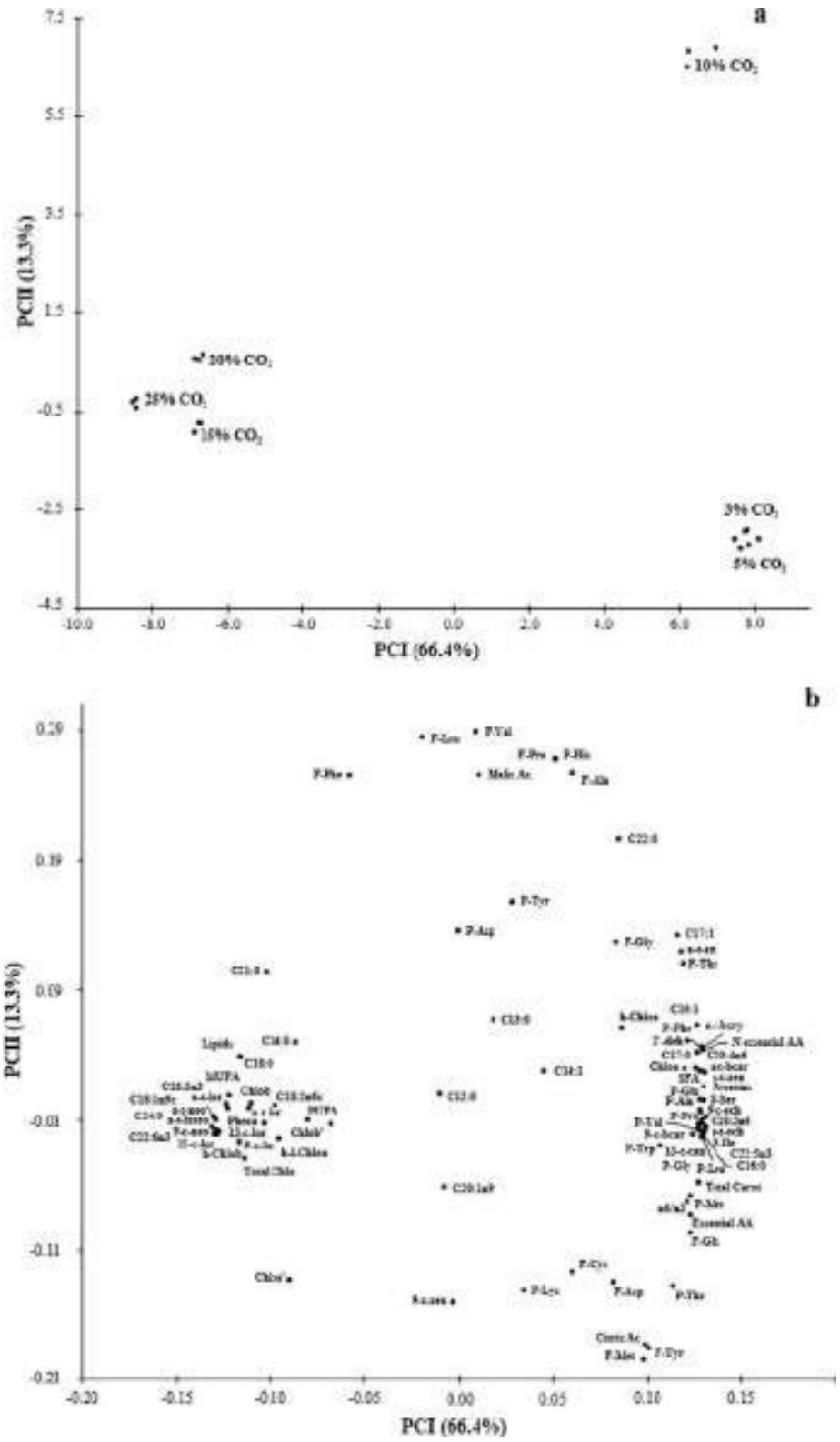


Fig. 1. a, b Plots of scores (samples) and loadings (variables) showing the principal component 1 (PCI) and 2 (PCII) from *Scenedesmus obliquus* cultivated with different percentages of CO_2. Figure Abbreviations. h-Chlob- 13^2-hydroxy-chlorophyll-*b*; h-l-Chloa- 15^1-hydroxy-lactone-chlorophyll-*a*; Chlob- chlorophyll-*b*; Chlob′- chlorophyll-*b*′; h-Chloa- 13^2-hydroxy-chlorophyll-*a*; Chloa- chlorophyll-*a*; Chloa′- chlorophyll-*a*′; Pheoa- pheophytin-*a*; a-t-lor- all-*trans*-loroxanthin; a-t-neo- all-*trans*-neoxanthin; 9-c-neo- 9-*cis*-neoxanthin; a-t-luteo- all-*trans*-luteoxanthin; 15-c-lut- 15-*cis*-lutein; 13-c-lut- 13-*cis*-lutein; a-t-lut- all-*trans*-lutein; a-t-zea- all-*trans*-zeaxanthin; 9-c-lut- 9-*cis*-lutein; 9-c-zea- 9-*cis*-zeaxanthin; 13-c-can- 13-*cis*-cantaxanthin; 2′-deh- 2′-dehydrodeoxymyxol; a-t-zei- all-*trans*-zeinoxanthin; a-t-bcry- all-*trans*-β-cryptoxanthin; a-t-ech- all-*trans*-echinenone; 9-c-ech- 9-*cis*-echinenone; a-t-bcar- all-*trans*-β-carotene; 9-c-bcar- 9-*cis*-β-carotene.

(C18:1n9c), and 12.4% (C18:2n6c). The greatest enrichment with CO_2 showed a clear tendency to reduce saturated FA C16:0 and increase the synthesis of the FA omega-3 C18:3n3.

In addition to the differences observed in the majority FA, stearic acid (C18:0), which was present at concentrations of 2.6–3.9% in cultivations with 3, 5, and 10% CO_2, ranged from 5.3 to 7.9% in the other treatments (15, 20, and 25% CO_2). Arachidonic acid (C20:4n6) was only detected in the three cultures with the lowest CO_2 content, and docosapentaenoic acid (DPA) (C22:5n3) showed concentrations five to ten times higher (0.8–0.9%) in these cultures. Nonetheless, lignoceric (C24:0) and docosahexaenoic (DHA) acids (C22:6n3) were only detected in cultivations with higher CO_2 levels (15, 20, and 25% CO_2). Through these compounds, there was a proportional increase in the percentage of higher carbon chain compounds caused by the increase in CO_2.

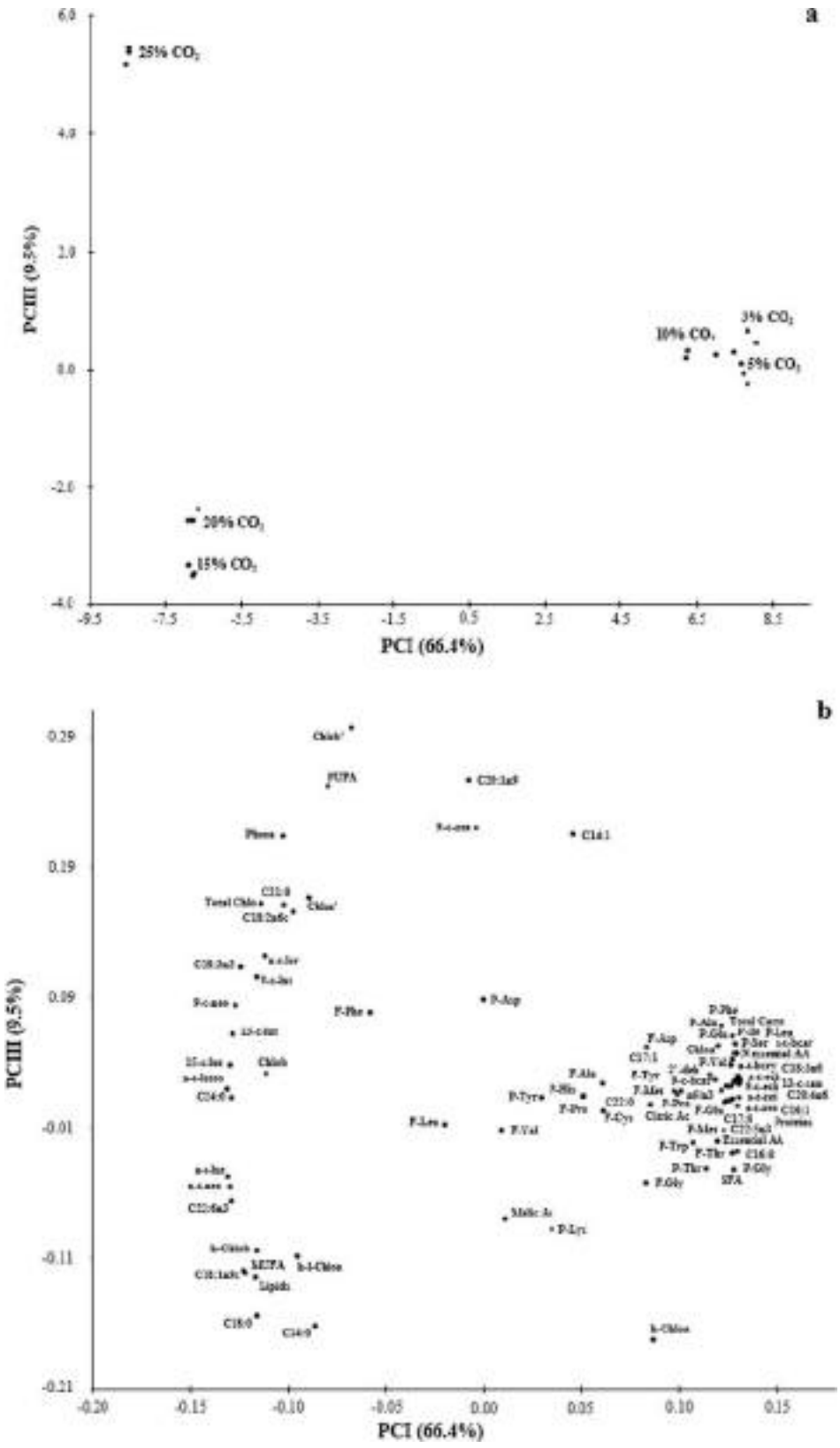


Fig. 2. a, b Plots of scores (samples) and loadings (variables) showing the principal component 1 (PCI) and 3 (PCIII) from *Scenedesmus obliquus* cultivated with enrichment levels of CO_2. Figure Abbreviations. h-Chlob- 13^2-hydroxy-chlorophyll-*b*; h-l-Chloa- 15^1-hydroxy-lactone-chlorophyll-*a*; Chlob- chlorophyll-*b*; Chlob′- chlorophyll-*b*′; h-Chloa- 13^2-hydroxy-chlorophyll-*a*; Chloa- chlorophyll-*a*; Chloa′- chlorophyll-*a*′; Pheoa- pheophytin-*a*; a-t-lor- all-*trans*-loroxanthin; a-t-neo- all-*trans*-neoxanthin; 9-c-neo- 9-*cis*-neoxanthin; a-t-luteo- all-*trans*-luteoxanthin; 15-c-lut- 15-*cis*-lutein; 13-c-lut- 13-*cis*-lutein; a-t-lut- all-*trans*-lutein; a-t-zea- all-*trans*-zeaxanthin; 9-c-lut- 9-*cis*-lutein; 9-c-zea- 9-*cis*-zeaxanthin; 13-c-can- 13-*cis*-cantaxanthin; 2′-deh- 2′-dehydrodeoxymyxol; a-t-zei- all-*trans*-zeinoxanthin; a-t-bcry- all-*trans*-β-cryptoxanthin; a-t-ech- all-*trans*-echinenone; 9-c-ech- 9-*cis*-echinenone; a-t-bcar- all-*trans*-β-carotene; 9-c-bcar- 9-*cis*-β-carotene.

The CBC forms the 3PG, the first stable molecule of photosynthesis; phosphoenolpyruvate is formed from it by enzymatic reactions, followed by pyruvate and acetyl coenzyme A (acetyl-CoA). For FA synthesis, specifically, acetyl-CoA and bicarbonate give rise to malonyl-CoA, a reaction catalyzed by acetyl-CoA carboxylase. Afterwards, malonyl-CoA ACP (acyl carrier protein) transacylase catalyzes the reaction of malonyl-CoA to malonyl-ACP (carbon donor molecule for elongation reactions). Saturated FAs are formed from malonyl-ACP, mainly C16:0 and C18:0-ACP, precursors of the other compounds due to carbon chain elongation and desaturation reactions (Rismani-Yazdi,

Haznedaroglu, Bibby, & Peccia, 2011; Blatti, Michaud, & Burkart, 2013). The increased CO_2 percentages in *S. obliquus* cultivation intensified the FA elongation and desaturation reactions, especially in the C18:3n3 pathway. In this case, C18:0 (also C16:0), through Δ9 and Δ12 (or ω6) desaturases originate C18:2n6, which is desaturated by Δ15 (or ω3) desaturase, originating C18:3n3 (Monroig, Tocher, & Navarro, 2013).

By altering the metabolism of *S. obliquus*, the FA profiles and their applicability were modified (Sun, Ren, Zhao, Ji, & Huang, 2019). In the lowest CO_2 enrichment percentages, mostly saturated profiles were found, reaching up to 70.6% saturated fatty acids (SFA) in the 5% CO_2 treatment, 11.2% monounsaturated fatty acids (MUFA) and 18.3% polyunsaturated fatty acids (PUFA), profile suitable for biodiesel production. As the CO_2 levels increased, the profiles changed and proved more attractive for applications in food and supplementation, and we found 49.4% SFA, 19.1% MUFA, and 31.5% PUFA with 25% CO_2. Additionally, the n6/n3 ratio was used to check the oil healthiness level, and the lower the ratio, the greater the benefit provided; in the cultivation with 3% CO_2 the n6/n3 ratio was 13. 6, and in the cultivation with 25% CO_2, it reduced to 0.8 (Table 4).

3.5. Exploratory multivariate analysis

Principal component analysis (PCA) was used to better visualize the effect of different CO_2 treatments on *S. obliquus* biomass composition. The three main components (PC) explained 89.2% of the general variance of the results obtained, and the scores (samples) and loadings (compounds) of PC1 and PC2 are shown in Fig. 1a and 1b. In PC1, the samples were separated into two groups, those obtained with a lower CO_2 enrichment (3, 5 and 10%) and those with the highest percentages (15, 20 and 25%). Samples with 3, 5, and 10% CO_2 were located in the right quadrant, mainly due to the higher concentrations of free amino acids, protein amino acids, total proteins, SFA, chlorophyll-*a*, total carotenoids, and all-*trans*-β-carotene. In the lowest percentages of CO_2 enrichment, the metabolic pathways of *S. obliquus* were directed to the greater synthesis of amino acids and these, preferably, to protein formation. Even with the high availability of glutamic acid, there was less chlorophyll synthesis, while there was, greater carotenoid production, which are accessory pigments in the photosynthetic process (Amaral, de Melo, & dos Santos, 2021).

Samples grown with 15, 20, and 25% CO_2 were placed on the left quadrant, with higher levels of total lipids, MUFA, PUFA, C18:3n3, total chlorophylls, hydroxylated chlorophyll derivatives, chlorophyll-*b*, and derivatives and all-*trans*-lutein. Our findings show that CO_2 levels significantly altered the metabolic routes of all compounds evaluated, and the superior availability of inorganic carbon in the medium increased chlorophyll synthesis to increase the photosynthetic capacity due to the greater substrate availability. In these cultivations, higher lipids percentages were also observed, which are associated with stress conditions; this change may represent an adaptive mechanism to ensure effective photosynthesis of microalgae in environments with different CO_2 levels. Furthermore, the increased PUFA levels, which are functional membrane elements, stand out (Ren et al., 2022).

In PC2, we noted a difference in the sample grown with 10% CO_2 in the upper quadrant compared to those grown with 3 and 5% CO_2. The distinction of cultivation with 10% CO_2 is related to high alanine concentrations in the free form and C22:0 and compounds that only appeared in this treatment, such as proline in the free form and histidine in the protein form. The separation of the 10% CO_2 treatment also appears as the beginning of the microalgal metabolism transition that was performed in the 15, 20, and 25% CO_2 treatments, and compounds such as valine, leucine and phenylalanine (all in free form) and malic acid were detected with this CO_2 concentration.

The scores and loadings of PC1 and PC3 are presented in Fig. 2a and 2b; PC3 allowed us to differentiate between treatments with higher CO_2 enrichment. The samples obtained in cultures with 15 and 20% CO_2 are in the lower quadrant, while the treatment with 25% CO_2 enrichment is in the upper quadrant. The biomass of the cultivation with 25% CO_2 showed the highest significant concentrations of PUFA, C18:3n3, total chlorophylls, chlorophyll-*a*′, pheophytin-*a*, and the chlorophyll-*b*′ was only detected in this treatment.

4. Conclusion

Enrichment with 3, 5, 10, 15, 20, and 25% of CO_2 in the photosynthetic cultures of *S. obliquus* modified or intensified the metabolic routes, causing alterations in the compounds evaluated herein. In general, treatments with lower CO_2 percentages (3, 5, and 10%) showed a total composition of proteins, chlorophylls and carotenoids, as well as their respective profiles, with a high potential for applications in the area of food and supplementation. However, there was less lipid synthesis and the FA profiles, mostly saturated, proved to be more suitable for biofuel production. What is more, the higher CO_2 percentages, led to increased lipid production by *S. obliquus*, and significant changes in the FA profile, with high concentrations of C18:3n3 and PUFA, as well as low n6/n3 ratios, which are ideal modifications for application in the food sector. These changes in relation to the lipid fraction, peaked in the culture enriched with 25% CO_2.

CRediT authorship contribution statement

Raquel Guidetti Vendruscolo: Conceptualization, Data curation, Formal analysis, Investigation, Methodology, Writing – original draft. **Mariany Costa Deprá:** Investigation, Methodology, Writing – review & editing. **Pricila Nass Pinheiro:** Data curation, Formal analysis, Investigation, Methodology. **Valcenir Junior Mendes Furlan:** Data curation, Formal analysis, Investigation, Methodology. **Juliano Smanioto Barin:** Funding acquisition, Resources, Writing – review & editing. **Alexandre José Cichoski:** Funding acquisition, Resources, Writing – review & editing. **Cristiano Ragagnin de Menezes:** Funding acquisition, Resources, Writing – review & editing. **Leila Queiroz Zepka:** Funding acquisition, Resources, Supervision, Visualization, Writing – review & editing. **Eduardo Jacob-Lopes:** Funding acquisition, Resources, Supervision, Visualization, Writing – review & editing. **Roger Wagner:** Conceptualization, Funding acquisition, Project administration, Resources, Supervision, Visualization, Writing – review & editing.

Declaration of Competing Interest

The authors declare that they have no known competing financial interests or personal relationships that could have appeared to influence the work reported in this paper.

Acknowledgement

To the Coordenação de Aperfeiçoamento de Pessoal de Nível Superior (CAPES) - Finance Code 001 and Edital 11/2014 - Pró-Equipamentos. To Conselho Nacional de Desenvolvimento Científico e Tecnológico (CNPq) PQ-2018, Process: 311125/2018-2.

Appendix A. Supplementary material

Supplementary data to this article can be found online at https://doi.org/10.1016/j.foodres.2022.111590.

References

Amaral, R., de Melo, J., & dos Santos, L. M. A. (2021). Pigments from *Eustigmatophyceae*: An interesting class of microalgae for carotenoid production. *Journal of Applied Phycology, 33*(1), 371–384.

Basu, S., Roy, A. S., Mohanty, K., & Ghoshal, A. K. (2013). Enhanced CO2 sequestration by a novel microalga: *Scenedesmus obliquus* SA1 isolated from bio-diversity hotspot region of Assam, India. *Bioresource Technology, 143*, 369–377.

Blatti, J. L., Michaud, J., & Burkart, M. D. (2013). Engineering fatty acid biosynthesis in microalgae for sustainable biodiesel. *Current Opinion in Chemical Biology, 17*(3), 496–505.

Carvalho, A. P., Silva, S. O., Baptista, J. M., & Malcata, F. X. (2011). Light requirements in microalgal photobioreactors: An overview of biophotonic aspects. *Applied Microbiology and Biotechnology, 89*(5), 1275–1288.

Chauhan, D. S., Sahoo, L., & Mohanty, K. (2022). Maximize microalgal carbon dioxide utilization and lipid productivity by using toxic flue gas compounds as nutrient source. *Bioresource Technology, 348*, Article 126784.

Chen, K., Ríos, J. J., Pérez-Gálvez, A., & Roca, M. (2015). Development of an accurate and high-throughput methodology for structural comprehension of chlorophylls derivatives. (I) Phytylated derivatives. *Journal of Chromatography A, 1406*, 99–108.

D'Alessandro, E. B., & Antoniosi Filho, N. R. (2016). Concepts and studies on lipid and pigments of microalgae: A review. *Renewable and Sustainable Energy Reviews, 58*, 832–841.

da Silva, M. E. T., Leal, M. A., de Oliveira Resende, M., Martins, M. A., & dos Reis Coimbra, J. S. (2021). *Scenedesmus obliquus* protein concentrate: A sustainable alternative emulsifier for the food industry. *Algal Research, 59*, Article 102468.

Daneshvar, E., Wicker, R. J., Show, P. L., & Bhatnagar, A. (2022). Biologically-mediated carbon capture and utilization by microalgae towards sustainable CO_2 biofixation and biomass valorization–A review. *Chemical Engineering Journal, 427*, Article 130884.

Davies, B. H. (1976). Chemistry and biochemistry of plant pigments. *Carotenoids, 2*, 38–165.

de Rosso, V. V., & Mercadante, A. Z. (2007). HPLC–PDA–MS/MS of anthocyanins and carotenoids from dovyalis and tamarillo fruits. *Journal of Agricultural and Food Chemistry, 55*(22), 9135–9141.

Demarco, M., de Moraes, J. O., Matos, Â. P., Derner, R. B., de Farias Neves, F., & Tribuzi, G. (2022). Digestibility, bioaccessibility and bioactivity of compounds from algae. *Trends in Food Science & Technology, 121*, 114–128.

Deprá, M. C., Dias, R. R., Severo, I. A., de Menezes, C. R., Zepka, L. Q., & Jacob-Lopes, E. (2020). Carbon dioxide capture and use in photobioreactors: The role of the carbon dioxide loads in the carbon footprint. *Bioresource Technology, 314*, Article 123745.

Dias, R. R., Deprá, M. C., Zepka, L. Q., & Jacob-Lopes, E. (2022). Roadmap to net-zero carbon emissions in commercial microalgae-based products: Environmental sustainability and carbon offset costs. *Journal of Applied Phycology*, 1–14.

do Nascimento, T. C., Cazarin, C. B., Marostica Jr, M. R., Risso, É. M., Amaya-Farfan, J., Grimaldi, R., …, & Zepka, L. Q. (2019). Microalgae biomass intake positively modulates serum lipid profile and antioxidant status. *Journal of Functional Foods, 58*, 11-20.

do Nascimento, T. C., Nass, P. P., Fernandes, A. S., Vieira, K. R., Wagner, R., Jacob-Lopes, E., & Zepka, L. Q. (2020). Exploratory data of the microalgae compounds for food purposes. *Data in Brief, 29*, 105182.

Ejike, C. E., Collins, S. A., Balasuriya, N., Swanson, A. K., Mason, B., & Udenigwe, C. C. (2017). Prospects of microalgae proteins in producing peptide-based functional foods for promoting cardiovascular health. *Trends in Food Science & Technology, 59*, 30–36.

Fernandes, A. S., Nogara, G. P., Menezes, C. R., Cichoski, A. J., Mercadante, A. Z., Jacob-Lopes, E., & Zepka, L. Q. (2017). Identification of chlorophyll molecules with peroxyl radical scavenger capacity in microalgae *Phormidium autumnale* using ultrasound-assisted extraction. *Food Research International, 99*, 1036–1041.

Fernandes, A. S., Petry, F. C., Mercadante, A. Z., Jacob-Lopes, E., & Zepka, L. Q. (2020). HPLC-PDA-MS/MS as a strategy to characterize and quantify natural pigments from microalgae. *Current Research in Food Science, 3*, 100–112.

Fernandes, A. S., Nascimento, T. C., Pinheiro, P. N., Vendruscolo, R. G., Wagner, R., de Rosso, V. V., … Zepka, L. Q. (2021). Bioaccessibility of microalgae-based carotenoids and their association with the lipid matrix. *Food Research International, 148*, Article 110596.

Goswami, R. K., Mehariya, S., Karthikeyan, O. P., Gupta, V. K., & Verma, P. (2022). Multifaceted application of microalgal biomass integrated with carbon dioxide reduction and wastewater remediation: A flexible concept for sustainable environment. *Journal of Cleaner Production, 130654*.

Hachicha, R., Elleuch, F., Ben Hlima, H., Dubessay, P., de Baynast, H., Delattre, C., … Fendri, I. (2022). Biomolecules from microalgae and cyanobacteria: Applications and market survey. *Applied Sciences, 12*(4), 1924.

Hartman, L., & Lago, R. C. (1973). Rapid preparation of fatty acid methyl esters from lipids. *Laboratory Practices, 22*, 475–476.

Ho, S. H., Chen, W. M., & Chang, J. S. (2010). *Scenedesmus obliquus* CNW-N as a potential candidate for CO_2 mitigation and biodiesel production. *Bioresource Technology, 101*(22), 8725–8730.

Horowitz, W., & Latimer, G. W. (2000). AOAC official methods of analysis. *Association of Official Analytical Chemists International, Gaithersburg, 50*(21), 992–1005.

Huang, Y., Zhao, S., Ding, Y. D., Liao, Q., Huang, Y., & Zhu, X. (2017). Optimizing the gas distributor based on CO_2 bubble dynamic behaviors to improve microalgal biomass production in an air-lift photo-bioreactor. *Bioresource Technology, 233*, 84–91.

Igreja, W. S., Maia, F. D. A., Lopes, A. S., & Chisté, R. C. (2021). Biotechnological production of carotenoids using low cost-substrates is influenced by cultivation parameters: A review. *International Journal of Molecular Sciences, 22*(16), 8819.

Jacob-Lopes, E., Maroneze, M. M., Deprá, M. C., Sartori, R. B., Dias, R. R., & Zepka, L. Q. (2019). Bioactive food compounds from microalgae: An innovative framework on industrial biorefineries. *Current Opinion in Food Science, 25*, 1–7.

Kang, Z., Wang, Y., Wang, Q., & Qi, Q. (2011). Metabolic engineering to improve 5-aminolevulinic acid production. *Bioengineered Bugs, 2*(6), 342–345.

Kao, T. H., Chen, C. J., & Chen, B. H. (2011). An improved high performance liquid chromatography–photodiode array detection–atmospheric pressure chemical ionization–mass spectrometry method for determination of chlorophylls and their derivatives in freeze-dried and hot-air-dried *Rhinacanthus nasutus* (L.) Kurz. *Talanta, 86*, 349–355.

Kumar, K. S., Prasanthkumar, S., & Ray, J. G. (2017). Biomass yield, oil productivity and fatty acid profile of *Chlorella lobophora* cultivated in diverse eutrophic wastewaters. *Biocatalysis and Agricultural Biotechnology, 11*, 338–344.

Li, S., Li, X., & Ho, S. H. (2022). How to enhance carbon capture by evolution of microalgal photosynthesis? *Separation and Purification Technology, 291*, Article 120951.

Mander, L., & Liu, H. W. (2010). *Comprehensive natural products II: chemistry and biology*. Elsevier.

Mariotti, F., & Gardner, C. D. (2019). Dietary protein and amino acids in vegetarian diets—A review. *Nutrients, 11*(11), 2661.

Maroneze, M. M., Jacob-Lopes, E., Zepka, L. Q., Roca, M., & Pérez-Gálvez, A. (2019). Esterified carotenoids as new food components in cyanobacteria. *Food Chemistry, 287*, 295–302.

Maroneze, M. M., Siqueira, S. F., Vendruscolo, R. G., Wagner, R., de Menezes, C. R., Zepka, L. Q., & Jacob-Lopes, E. (2016). The role of photoperiods on photobiorectors - A potential strategy to reduce costs. Bioresource Technology. *Bioresource International, 219*, 493–499.

Maroneze, M. M., Caballero-Guerrero, B., Zepka, L. Q., Jacob-Lopes, E., Perez-Galvez, A., & Roca, M. (2020). Accomplished high-resolution metabolomic and molecular studies identify new carotenoid biosynthetic reactions in Cyanobacteria. *Journal of Agricultural and Food Chemistry, 68*(22), 6212–6220.

Monroig, Ó., Tocher, D. R., & Navarro, J. C. (2013). Biosynthesis of polyunsaturated fatty acids in marine invertebrates: Recent advances in molecular mechanisms. *Marine Drugs, 11*(10), 3998–4018.

Morais, T., Inácio, A., Coutinho, T., Ministro, M., Cotas, J., Pereira, L., & Bahcevandziev, K. (2020). Seaweed potential in the animal feed: A review. *Journal of Marine Science and Engineering, 8*(8), 559.

Murillo, E., Giuffrida, D., Menchaca, D., Dugo, P., Torre, G., Meléndez-Martinez, A. J., & Mondello, L. (2013). Native carotenoids composition of some tropical fruits. *Food Chemistry, 140*(4), 825–836.

Nehmé, R., Atieh, C., Fayad, S., Claude, B., Chartier, A., Tannoury, M., … Morin, P. (2017). Microalgae amino acid extraction and analysis at nanomolar level using electroporation and capillary electrophoresis with laser-induced fluorescence detection. *Journal of Separation Science, 40*(2), 558–566.

Novoveská, L., Ross, M. E., Stanley, M. S., Pradelles, R., Wasiolek, V., & Sassi, J. F. (2019). Microalgal carotenoids: A review of production, current markets, regulations, and future direction. *Marine Drugs, 17*(11), 640.

Patel, S. S., & Sahoo, S. (2021). Biodiversity and Abundance of Phytoplankton from Auranga Estuary, Valsad District, Gujarat, India. *Çanakkale Onsekiz Mart University Journal of Marine Sciences and Fisheries, 4*(2), 86–98.

Patias, L. D., Fernandes, A. S., Petry, F. C., Mercadante, A. Z., Jacob-Lopes, E., & Zepka, L. Q. (2017). Carotenoid profile of three microalgae/cyanobacteria species with peroxyl radical scavenger capacity. *Food Research International, 100*, 260–266.

Patil, L., & Kaliwal, B. (2017). Effect of CO_2 concentration on growth and biochemical composition of newly isolated indigenous microalga *Scenedesmus bajacalifornicus* BBKLP-07. *Applied Biochemistry and Biotechnology, 182*(1), 335–348.

Porra, R. J., Thompson, W. A., & Kriedemann, P. E. (1989). Determination of accurate extinction coefficients and simultaneous equations for assaying chlorophylls a and b extracted with four different solvents: Verification of the concentration of chlorophyll standards by atomic absorption spectroscopy. *Biochimica et Biophysica Acta (BBA) - Bioenergetics, 975*(3), 384–394.

Prasad, R., Gupta, S. K., Shabnam, N., Oliveira, C. Y. B., Nema, A. K., Ansari, F. A., & Bux, F. (2021). Role of microalgae in global CO_2 sequestration: Physiological mechanism, recent development, challenges, and future prospective. *Sustainability, 13*(23), 13061.

Quiroz-Arita, C., Shinde, S., Kim, S., Monroe, E., George, A., Quinn, J. C., … Davis, R. W. (2022). Bioproducts from high-protein algal biomass: An economic and environmental sustainability review and risk analysis. *Sustainable Energy & Fuels*.

Ren, X., Liu, Y., Fan, C., Hong, H., Wu, W., Zhang, W., & Wang, Y. (2022). Production, Processing, and Protection of Microalgal n-3 PUFA-Rich Oil. *Foods, 11*(9), 1215.

Rippka, R., Deruelles, J., Waterbury, J. B., Herdman, M., & Stanier, R. Y. (1979). Generic assignments, strain histories and properties of pure cultures of cyanobacteria. *Microbiology, 111*(1), 1–61.

Rismani-Yazdi, H., Haznedaroglu, B. Z., Bibby, K., & Peccia, J. (2011). Transcriptome sequencing and annotation of the microalgae *Dunaliella tertiolecta*: Pathway description and gene discovery for production of next-generation biofuels. *BMC Genomics, 12*(1), 1–17.

Rodrigues, D. B., Flores, É. M., Barin, J. S., Mercadante, A. Z., Jacob-Lopes, E., & Zepka, L. Q. (2014). Production of carotenoids from microalgae cultivated using agroindustrial wastes. *Food Research International, 65*, 144–148.

Rodrigues, D. B., Menezes, C. R., Mercadante, A. Z., Jacob-Lopes, E., & Zepka, L. Q. (2015). Bioactive pigments from microalgae *Phormidium autumnale*. *Food Research International, 77*, 273–279.

Sonmez, M. E., Eczacıoglu, N., Gumuş, N. E., Aslan, M. F., Sabanci, K., & Aşikkutlu, B. (2022). Convolutional neural network-Support vector machine based approach for classification of cyanobacteria and chlorophyta microalgae groups. *Algal Research, 61*, Article 102568.

Sun, X. M., Ren, L. J., Zhao, Q. Y., Ji, X. J., & Huang, H. (2019). Enhancement of lipid accumulation in microalgae by metabolic engineering. *Biochimica et Biophysica Acta (BBA)-Molecular and Cell Biology of Lipids, 1864*(4), 552–566.

Swarnalatha, G. V., Hegde, N. S., Chauhan, V. S., & Sarada, R. (2015). The effect of carbon dioxide rich environment on carbonic anhydrase activity, growth and metabolite production in indigenous freshwater microalgae. *Algal Research, 9*, 151–159.

Tang, D., Han, W., Li, P., Miao, X., & Zhong, J. (2011). CO_2 biofixation and fatty acid composition of *Scenedesmus obliquus* and *Chlorella pyrenoidosa* in response to different CO_2 levels. *Bioresource Technology, 102*(3), 3071–3076.

Tripathi, R., Singh, J., & Thakur, I. S. (2015). Characterization of microalga *Scenedesmus* sp. ISTGA1 for potential CO_2 sequestration and biodiesel production. *Renewable Energy, 74*, 774–781.

Tunay, D., Yildirim, O., Ozkaya, B., & Demir, A. (2022). Determination of photoautotrophic growth and inhibition kinetics by the Monod and the Aiba models and bioenergetics of local microalgae strain. *Chemosphere, 292*, Article 133330.

Vendruscolo, R. G., Facchi, M. M. X., Maroneze, M. M., Fagundes, M. B., Cichoski, A. J., Zepka, L. Q., … Wagner, R. (2018). Polar and non–polar intracellular compounds from microalgae: Methods of simultaneous extraction, gas chromatography determination and comparative analysis. *Food Research International, 109*, 204–212.

Vendruscolo, R. G., Fernandes, A. S., Fagundes, M. B., Zepka, L. Q., de Menezes, C. R., Jacob-Lopes, E., & Wagner, R. (2021). Development of a new method for simultaneous extraction of chlorophylls and carotenoids from microalgal biomass. *Journal of Applied Phycology, 33*(4), 1987–1997.

Vidyashankar, S., Deviprasad, K., Chauhan, V. S., Ravishankar, G. A., & Sarada, R. (2013). Selection and evaluation of CO_2 tolerant indigenous microalga *Scenedesmus dimorphus* for unsaturated fatty acid rich lipid production under different culture conditions. *Bioresource Technology, 144*, 28–37.

Visentainer, J. V. (2012). Aspectos analíticos da resposta do detector de ionização em chama para ésteres de ácidos graxos em biodiesel e alimentos. *Química Nova, 35*(2), 274–279.

Vuppaladadiyam, A. K., Yao, J. G., Florin, N., George, A., Wang, X., Labeeuw, L., … Zhao, M. (2018). Impact of flue gas compounds on microalgae and mechanisms for carbon assimilation and utilization. *ChemSusChem, 11*(2), 334–355.

WHO, J. (2007). Protein and amino acid requirements in human nutrition. *World Health Organization technical report series*, (935), 1.

Xu, X., Gu, X., Wang, Z., Shatner, W., & Wang, Z. (2019). Progress, challenges and solutions of research on photosynthetic carbon sequestration efficiency of microalgae. *Renewable and Sustainable Energy Reviews, 110*, 65–82.

Zeng, X., Danquah, M. K., Chen, X. D., & Lu, Y. (2011). Microalgae bioengineering: From CO_2 fixation to biofuel production. *Renewable and Sustainable Energy Reviews, 15*(6), 3252–3260.

Zhang, L., Selão, T. T., Selstam, E., & Norling, B. (2015). Subcellular localization of carotenoid biosynthesis in *Synechocystis* sp. PCC 6803. *PLoS ONE, 10*(6), Article e0130904.

BMS-BIOT-2022-14
Arshad 26-Aug-2022

Send Orders for Reprints to reprints@benthamscience.net

Recent Patents on Biotechnology, XXXX, *XX*, 000-000

MINI-REVIEW ARTICLE

Bioactive Polysaccharides from Microalgae: A Close Look at the Biomedical Applications

Mariany C. Deprá[1], Rosangela R. Dias[1], Mariana M. Maroneze[1], Tatiele C. Nascimento[1], Ihana A. Severo[1], Leila Q. Zepka[1] and Eduardo Jacob-Lopes[1,*]

[1]*Bioprocess Intensification Group, Federal University of Santa Maria, 97105-900, Santa Maria, RS, Brazil*

ARTICLE HISTORY

Received: April 18, 2022
Revised: June 14, 2022
Accepted: June 28, 2022

DOI:
10.2174/1872208316666220820092643

Abstract: There is a current tendency towards bioactive natural products that can be used in different areas such as food, pharmaceutical, and biomedical. In the last decades, polysaccharides have attracted increasing interest because of their potent nontoxic effects, therapeutic properties, and diversified range of applications. Polysaccharides are complex and heterogeneous macromolecules constituted of different monosaccharides and, in some cases, of glucuronic acid and sulphate groups. Polysaccharides with biological activity can be derived from plants, animals and microorganisms, especially microalgae. Microalgae are considered one of the most promising sources of these compounds that have already proved to have several important biological properties. In this sense, our objective is to elucidate the use of bioactive polysaccharides from microalgae in biomedical applications, emphasizing the biological activity of these compounds. Furthermore, the microalgal biomass production systems and polysaccharides extraction methods were presented and discussed.

Keywords: Algae, natural products, bioactive compounds, biological activity, sulphated polysaccharides, exopolysaccharides.

1. INTRODUCTION

In the last decades, natural compounds have been directed to promote improvements in human health, aiming to prevent and treat chronic diseases. There is a strong appeal for natural medicines, but their production has declined due to the low availability of the resources from which they are extracted. In this way, there are innumerable classes of compounds that can be extracted from nature, and one of them is represented by polysaccharides [1].

The polysaccharides are carbohydrates of polymeric molecules with a diverse structure, composed of long chains of different monosaccharides (hexoses and pentoses), including many complex sugars, bound together by glycosidic linkages. Various substituents, such as sulfates, phosphates, acyl groups, amino acids, or selenium, may be attached to such structures, which may be linear or highly branched. In any case, the basic formula of polysaccharide is $C_x(H_2O)_y$, where *x* is usually a large number between 200 and 2500 [2]. Firstly, polysaccharides were exploited by the industry for their rheological properties as a thickening or gelling agents and more recently received attention due to the detection of biological activities [3].

At present, thousands of polysaccharides have been isolated from different sources and, according to this, can be classified into animal polysaccharides, plant polysaccharides, and microbial polysaccharides [4]. Researchers around the world have shown that microbial polysaccharides are a

*Address correspondence to this author at the Bioprocess Intensification Group, Federal University of Santa Maria, 97105-900, Santa Maria, RS, Brazil; Tel: +55 55 3220 8822; E-mail: ejacoblopes@gmail.com

1872-2083/XX $65.00+.00 © XXXX Bentham Science Publishers

better choice because of their biological properties, high production rates, and ease of control of production parameters [5]. These polymers play several roles in microorganisms, depending on their structure and molecular arrangement. However, they provide carbon and energy reserves for the cells; generally, some of them are excreted (exopolysaccharides), both under normal conditions and under physiological stress. Among the microorganisms that produce bioactive polysaccharides, microalgae have gained space in the last years [6].

Microalgae are a group of unicellular prokaryotic and eukaryotic microorganisms, and although they have different biological characteristics, the fundamentals of production are the same, as are the bioproducts generated and their technological application. The annual production of microalgal biomass dry is about 19,000 tons, generating an estimated USD 5.7 billion [7]. The current demand for microalgae concentrates mainly on the production of single-cell protein, polyunsaturated fatty acids, and carotenoids [8]. However, in the last decade, several other compounds have been investigated, such as polysaccharides, which present high exploration potential. These compounds have been linked to various bioactive activities, such as antiviral, antibacterial, antifungal, anti-inflammatory, immunomodulatory, antitumor proliferation, tumor suppressants, apoptotic and cytotoxic agents, anticoagulant, antithrombotic, antilipidemic, hypoglycemic, hypotensive, antioxidant, and anti-aging [9,10].

On the other hand, there are still technical-economic hurdles to the production of bioactive polysaccharides from microalgae, among which stand out: (i) the selection of the microalgal species; (ii) the definition of the biomass production system and harvesting techniques, which should enable the highest yield of the compound of interest at a suitable cost; (iii) the choice of extraction and purification methods for polysaccharides, which must be efficient, as well as economically feasible and scalable, and (iv) proving the biological activity through clinical tests, finally to obtain the approval by the regulatory agencies [11].

In this sense, the objective of this review was to elucidate the potential of the use of bioactive polysaccharides from microalgae in biomedical applications. The review focused on the microalgal biomass production systems, the biological activities of these compounds, and the extraction and purification methods.

2. MICROALGAE-BASED PROCESSES AND PRODUCTS

Microalgae are primarily oxygen-releasing photosynthetic microorganisms found in both marine and freshwater environments. It comprises a diverse group of about 72,500 species of microorganisms already identified. The current taxonomic classification divides these organisms into 16 classes. Between these classes, the most abundant in nature are the diatoms (*Bacillariophyceae*), the green algae (*Crysophyceae*), and the golden algae (*Chrysophyceae*). Conversely, the green algae, the cyanobacteria (*Cyanophyceae*), and the diatoms are the most significant in terms of biotechnological exploitation and use [12].

Commercial microalgae-based processes were started in the early 1960s with cultures of *Chlorella and Spirulina*, mainly targeting the production of proteins, with applications directed to food and prophylactic use. Later, the exploration of these microorganisms for production in the carotenoid market, mainly β-carotene and astaxanthin, and of polyunsaturated fatty acids, especially EPA and DHA, was started [13]. Currently, the major focus of research involving microalgae is to produce biofuels. In terms of microalgae polysaccharides, many advances have been made in the last decade, but it is still in their first stages, without a forecast for commercial production [14].

Benefits of using microalgae for sustainable production of bioactive compounds, including polysaccharides, are numerous. These microorganisms do not compete with food crops since they do not require arable land, present fast growth rates and several species can tolerate a wide range of temperatures, salinities, pH values, light intensities, and photoperiods; and can grow alone or in symbiosis with other organisms [15]. Additionally, the different microalgae species contain multiple compounds with commercial value, which makes a potential bioresource for use in biorefineries [16].

However, any microalgae-based process success depends on two key factors: high productivity

in biomass and the target bioproduct, with a low production cost [17].

2.1. Potential Species for Polysaccharides Production

Since there is a wide variety of microalgae species available and the composition of the biomasses are highly variable according to the species, knowledge of the biochemical composition is a requisite for the selection of suitable microalgae towards specific bioproduct. However, even for particular microalgae specie, variable biomass profiles can be found, which is attributed to the differences in cultivation conditions, such as light supply, temperature, salinity, nutrient availability, and the geometry of the culture system. At the same time, this variation allows the optimization of cultivation conditions to maximize the production of target biomolecules [18].

The microalgae polysaccharides are usually classified as polysaccharides (PS), corresponding to those of the cell wall, sulphated polysaccharides (SPs) and exopolysaccharides (EPS). Unlike macroalgae, microalgae do not have proper names for their polysaccharides, except spirulan, produced by *Arthrospira platensis* [19]. The species with the highest polysaccharide generation potential reported in the literature are presented in Table **1**, as well as their respective polysaccharides of commercial interest and proven biological activities.

The majority of microalgae polysaccharides are heteropolymers, as shown early, where only the exopolysaccharide produced by *Dunaliella tertiolecta* is a homopolymer formed by galactose units. Heteropolymers produced by microalgae are mainly composed of arabinose, fucose, fructose, galactose, galacturonic acid, glucose, mannose, rhamnose, ribose, xylose, and methylated sugars. Although there is already a considerable number of studies on microalgae polysaccharides, there is not much information on the content of these polymers in biomass. Regarding exopolysaccharides, it is estimated that there is a production ranging from 0.50 to 20 g/L, but very few studies have investigated their production in quantitative terms [3,36].

2.2. Microalgae Biomass Production

Regardless of the potential that microalgae can offer, the largest and most critical barrier to the implementation of economically viable microalgae-based products remains the high cost of microalgal biomass cultivation and harvesting [37]. Thus, the first criterion to be considered for the choice of the cultural system is the type and quality of the desired product, which will reflect in its selling price [38].

Microalgae cultivations can be categorized based on carbon supply. These microorganisms are preferentially photosynthetic, but some species have metabolic versatility. In this sense, microalgae can be cultivated in three ways: (i) photoautotrophically, using light as an energy source and CO_2 or bicarbonates as an inorganic source of carbon; (ii) heterotrophically, in the dark, supported by an organic exogenous carbon source; or (iii) mixotrophically, where microalgae perform photosynthesis as the principal energy source, but both organic and inorganic compounds are used [39].

Photoautotrophic cultivations are still the most traditional method to obtain microalgae-based products. These cultivations, on a commercial scale, generally occur in open systems, such as raceways or closed systems, mainly tubular photobioreactors. Open systems are much cheaper and simpler to operate than closed systems but are more susceptible to contamination and variations in biomass composition due to weather changes. In contrast, closed systems can eliminate these limitations; however, with a high capital cost, therefore, they are more recommended for high-value products [40].

Raceway ponds are the most widely used systems for commercial production of microalgal biomass owing to their flexibility and ease of scale-up. It is estimated that 95% of all algae production around the world is performed in raceway ponds [17]. These systems consist of a closed loop recirculation channel with a culture depth of about 0.25-0.30 m, where the cells and the culture medium circulate continuously on a racetrack through paddlewheels. In contrast, climatic conditions and contamination problems may greatly affect their performance. In addition, the practicality of using microalgae ponds to convert CO_2 is limited. Chisti [41] and Norsker *et al*. [42] estimated the cost of producing microalgal biomass between US$ 4.63

Table 1. Main species of microalgae producing polysaccharides, their composition and bioactivities. Ara: arabinose; Fuc: fucose; Fru: fructose; Gal: galactose; GalA: galacturonic acid; GlcA: glucuronic acid; Glc: glucose; Mann: mannose; 3-O-Methyl-Rham: 3-O-methyl rhamnose (acofriose); Rham: rhamnose; Rib: ribose; Xyl: xylose.

Algal Class	Specie	Polyssacharide	Main Sugars	Biological Activity	Refs.
Chlorophyta	*Chlorella ellipsoidea*	PS	Rham, Mann, Gal	Immunomodulatory	Qi and Kim [20]
	Chlorella stigmatophora	PS	Glc, Xyl, Fuc	Anti-inflammatory, immunomodulatory	Guzmán *et al*. [21]
	Dunaliella salina	SPs	Glc, Gal, Ara, Xyl, Mann, Rham, Fuc, Rib, GalA, GlcA	Antioxidant, antiviral	Dai *et al*. [22]
	Dunaliella tertiolecta	EPS	Glc	-	Goo *et al*. [23]
	Chlamydomonas reinhardtii	EPS	Ara, Rham, Rib, Xyl, Gal, Glc, GalA	Antioxidant	Bafana [24]
	Graesiella sp.	EPS	Glc, Gal, Mann, Fuc, Rham, Xyl, Ara, Rib	Antioxidant, antitumor	Trabelsi *et al*. [25]
	Chlorella vulgaris	PS	Glc	Antiaging	Mourelle *et al*. [26]
	Haematococcus pluvialis	PS	Glc, Gal, Fuc, Ara, Mann, Xyl, Rham	Antiviral	Santoyo *et al*. [27]
Cyanophyta	*Arthrospira platensis*	EPS	Gal, Xyl, Glc, Fru	Antiviral, antibacterial, antitumor	Raposo *et al*. [28]
	Arthrospira platensis	SPs (Spirulan)	Rham, Fuc, Glc, 3-O-Methyl-Rham	Antiproliferative, antiadhesive, antiviral	Raposo *et al*. [29]
	Arthrospira maxima	SPs (Spirulan)	Rham, Fuc, Glc, 3-O-Methyl-Rham	Antiviral	Hernandez-Corona *et al*. [30]
	Nostoc flagelliforme	PS	Glc, Gal, Mann, GalA	Antioxidant	Shen *et al*. [31]
	Nostoc commune	PS	Rib, Ara, Xyl, Mann, Glc	Antioxidant, antibacterial	Quan *et al*. [32]
Rhodophyta	*Gyrodinium impudicum* strain KG03	EPS	Gal	Immunomodulatory, antiviral	Yim *et al*. [33]
	Gracilariopsis lemaneiformis	SPs	Gal, Glc, Mann, Xyl, Ara, Rham, Fuc	Antitumor	Kang *et al*. [34]
	Porphyridium sp.	SPs	Xyl	Antiviral	Ginzberg *et al*. [35]

and US$ 6.34 per kg (dry weight). These values have been adjusted for inflation and correspond to a 2018 estimate like all other monetary values presented in this review [43]. However, raceway ponds have many disadvantages, among which are the high land area requirement, low efficiency in light utilization, poor CO_2 diffusivity, and difficulty in control of the cultural conditions [44].

Recently, closed photobioreactors (PBRs), especially tubular photobioreactors, have been successfully used for microalgal biomass production on a large-scale. Despite the relative success of raceway ponds, tubular PBRs permit proper control of culture conditions, efficient natural or artificial light penetration, and, consequently, high biomass productivity. Tubular photobioreactors are a set of transparent tubes, usually constructed

with either glass or plastic, that can be arranged in different orientations (vertical, horizontal, or inclined) and patterns (straight, bent, or spiral). In these systems, mechanical pumps circulate microalgae cells, nutrients, and water through the light trap tubes. Despite the potential advantages, tubular photobioreactors still face challenges regarding scaling and the cost of construction and operation. The production cost is quite variable since it is a function of biomass productivity, system size, and growing conditions. The values found in the literature range from US$ 5 to US$ 29.42 per kg (dry weight) [14].

Already heterotrophic bioreactors are a feasible alternative to overcome the light energy dependency that is the major limitation in photobioreactors, both open and closed. Although restricted to a few microalgal species, heterotrophic cultivations can be conducted in conventional fermenters. The significant bottlenecks of these systems are the limited number of microalgal species that can grow heterotrophically, susceptibility to contamination, inability to produce light-induced metabolites, and the dependence of exogenous sources of organic carbon. It is estimated that this carbon source accounts for 80% of the total costs of the culture medium. On the other hand, microalgae can assimilate various organic carbon sources, making it possible to use cheaper sources than the usual glucose, such as starch and wastewater [45, 46]. Tabernero, del Valle and Galán [47] estimated the production cost of *Chlorella* biomass in a heterotrophic bioreactor following the biorefinery system and concluded that the cost to produce 1 kg of dry biomass is around US$ 1.33.

3. BIOLOGICAL ACTIVITIES OF MICROALGAL POLYSACCHARIDES

The immense chemical diversity of the microalgae biomass provides numerous applications in different areas, especially in biological activities. Usually, the bioactivity of microalgae polysaccharides is attributed to the degree of sulfation, molecular size, types, and proportions of monosaccharides, as well as glycosidic bonds [48]. Given these aspects, the polysaccharides present a wide range of biological properties, being they antiviral, antibacterial, anti-inflammatory, immunomodulatory, antitumor, anticoagulant, antihyperlipidemic, antihepatotoxic, hypoglycemic, and antioxidant [49].

The antiviral activity of microalgae polysaccharides is based on the biochemical mechanism of complexation of the virus-polysaccharide, which blocks access to the virus in the cell [50]. Among the studies reported, the main microalgal sulfated polysaccharides that present this biological activity are the fucoidans, synthesized by *Phaeophyceae*, ramnhams of the *Chlorophyta* and galactans of the *Rhodophyta* [51,52]. These polysaccharides act to inhibit a wide range of viruses, including human pathogens such as human immunodeficiency virus (HIV), herpes simplex virus (HSV), human cytomegalovirus, and dengue virus and also the respiratory syncytial virus [53].

Antibacterial activities from microalgae polysaccharides have also been gaining prominence in biological applications [54]. In short, the mechanism of action of antibacterial agents occurs as a function of the glycoprotein receptors found in the cell wall of polysaccharides, whose compounds bind to the surface of bacterial cells, DNA, and cytoplasmic membrane [55]. Some examples of polysaccharides, such as fucoidan and laminarin, are exploited in the management of pharmaceuticals, such as antibiotics, to prevent adhesion of *Helicobacter pylori* biofilms and to inhibit the growth of *Escherichia coli* and *Staphylococcus aureus* [56].

Additionally, polymer molecules synthesized by microalgae are known to have promising anti-inflammatory activities [57,58]. Conversely, to date, research on anti-inflammatory mechanisms is limited. However, some studies report that *Rhodophyta* derived polysaccharides, such as *Porphyridium* sp, induce anti-inflammatory agents in coronary endothelial cells. As known, vascular endothelial dysfunction is directly related to hypertension and atherosclerosis [59]. Thus, polysaccharides act directly as inhibitors of the signaling pathway of angiotensin II (Ag-II), the hormone peptide responsible for the system that increases inflammation and oxidative stress, causing endothelial dysfunction [60].

The immunomodulatory activity of microalgal polysaccharides is associated with the modulation of immunological cells, such as macrophages [61].

These cells are capable of absorbing deformed cells, attacking invaders and reacting to infections, tumors, and inflammation [62]. Thus, the mechanism of action occurs through the binding of polysaccharides to groups of transmembrane type I proteins, known as Toll-like receptors (TLRs). These receptors stimulate signaling pathways in order to activate macrophages [63]. Therefore, macrophages act by damaging pathogens by phagocytosis, triggering the release of antigens responsible for immunological responses [64]. Some studies report that the polysaccharides of the *Chlorella* microalgae are the most effective for this biological activity [20].

In contrast, the antitumor activity has recently attracted significant importance among biological activities [65]. This is because studies attributed antiproliferative activities to cancer cells *in vivo* and showed inhibitory activity in growing tumors *in vivo* [66]. More precisely, the mechanism of action of these polysaccharides results from inhibition of angiogenesis by the interference of vascular endothelial growth factor binding. Similarly, the basic growth factor of fibroblasts (bFGF) also undergoes such interference to their respective receptors. In addition, the ability to block interactions between cancer cells and basement membranes makes microalgal polysaccharides a potential source of application to antimetastatic activity. Thus, by way of exemplification, studies with *Saccharin japonicum* and *Undaria pinnatifida* were able to inhibit the proliferation and formation of new cellular colonies of breast cancer and melanomas [67].

As in antitumor activity, apoptotic and cytotoxicity activity are biologically induced traits by microalgal polymers. In the past, apoptotic was described as a form of cell death that had distinct characteristics, followed by low inflammatory response. Apoptosis is believed to be the result of a sequential and ordered series of cellular events [68]. Concurrently, cytotoxicity activity differs from apoptotic since it is known as the active mechanism of cell death by necrosis. In other words, cytotoxicity is the ability to be harmful to cells. In view of these aspects, cancer cell lines can be inhibited by necrosis, *i.e*., by the loss of membrane integrity and cell lysis. Also, the inactivation of growth and the cell division and the activation of the program of controlled cell death may be routes of action in front of the cancerogenic cells by microalgal polysaccharides [69].

Conversely, it is presumed that bioactivity is widely researched and recognized by sulfated polymers of microalgae as anticoagulant activity. To date, the scientific basis for this biological activity is not fully understood. However, it is suggested that there is more than one active mechanism, being it the direct and indirect inhibition of thrombin through the activation of thrombin inhibitors [70]. Thus, there would be one pathway for antithrombin and one as a heparin cofactor II. Furthermore, it is known that the strengthened effect of anticoagulant activity is associated with a greater number of carboxyl compounds, thus increasing the load and interactions with the proteins enveloped in the coagulation cascade. Some studies with *Ulothrix flacca* showed significant anticoagulant activity since it increased activated partial thromboplastin time (APTT) and thrombin time (TT) [71].

Also, in recent years, research has shown that sulfated exopolysaccharides exert antihyperlipidemic and antihepatotoxic activities [54,72]. These properties may reduce body weight gain, plasma triglycerols (TGs) and total cholesterol (TC). In addition, attributes such as decreased hepatic triglycerides and liver weight may also be seen. In parallel, as cholesterol levels decrease, some authors suggest that it promotes the decreasing blood levels of insulin and glucose, thus conferring the microalgae polysaccharides the potential hypoglycemic activity [28, 73]. Studies such as Wang *et al*. [74] reported a strong *in vivo* hypoglycemic effect, as well as a slight effect on normal glucose tolerance with *Saccharina japonica* microalgae.

Finally, natural antioxidant activity has been considered the most potent compound for the prevention of pathologies [75]. Microalgae polysaccharides, such as SPs, meet these requirements and their mechanism of action is based on the reduction reaction providing H^+, which will combine with a free radical (formed in living organisms and causing oxidative effects) stabilized in its final reaction. In the scientific literature, carrageenans and ulvanos are reported as polysaccharides, which are synthesized from *Rhodophyta*, such as *Gracilaria*

fisheri [76]. Therefore, the various algal groups have the potential for biotechnological exploitation as natural antioxidants, where synthetic chemical routes are often inefficient regarding efficiency and safety [77]. Similarly, anti-aging activity is related to antioxidant activity. SPs can also protect against oxidative stress and free radical agents [78]. The β-1,3-glucan, for example, is considered a good free radical scavenger, which benefits its applicability in skin care cosmetics, especially those related to protection and regeneration in the combat against external agents. According to Mourelle *et al*. [26], extracts of the species *Chlorella vulgaris*, *Porphyridium* sp., and *Rhodella reticulata* showed positive effects related to the use of cosmetic and skin supplements reinforcing collagen.

4. BIOMEDICAL APPLICATIONS

Microalgal polysaccharides are considered promising biomaterials for biomedical uses [79]. This application is mainly related to the content of sulfated exopolysaccharides. The exploration of polysaccharides for tissue engineering purposes (biological signaling, cell adhesion, cell proliferation, cell differentiation, responsive cellular degradation and remodeling) has attracted great interest in promoting the regeneration of new tissues or in the definition of the structure of cell growth [1, 80]. For this reason, they include microalgal biomass as an attractive alternative to this type of application since they allow the use of biomass as natural biomaterials, nanofibers or scaffolds that can be implanted to replace or repair tissue.

In the concept of tissue engineering, the principles of engineering are applied to treat or replace damaged tissues and organs. The model employs the use of 3D scaffolds to culture cells to produce living tissues that mimic the morphology and function of what occurs naturally *in vivo* [81]. However, new substitutes must meet the requirements of biocompatibility and non-toxicity, biodegradability with controllable degradation rate, adequate porosity and structural integrity [15].

The development of new tissue substitutes is based on the construction of a scaffold in the form of films, hydrogels, plates, sheets, nanofibers, and sponges, most of which come from naturally occurring polymers. There are several products derived from polysaccharides of marine origin that are used for this purpose, traditionally, the dominant focus of research has been on organisms such as macroalgae; however biotechnological advances and molecular techniques are allowing opportunities to exploit the biological resources of microalgae, including cyanobacteria [82].

In particular, sulphated polysaccharides that are abundantly found in different species of microalgae have no equivalent in terrestrial plants and resemble the chemical and biological properties of mammalian glycosaminoglycans [23, 28, 29, 83, 84]. This allows their application in the development of innovative systems for tissue engineering [85]. This application is made possible by its ability to bind to proteins at various levels of specificity, its involvement in cell development, cell differentiation, cell adhesion, cell signaling and cell-matrix interactions [86].

Some research has confirmed the potential of sulfated polysaccharides of *Chlorella vulgaris*, *Phorfiridium cruentum* and *Artrosphira platensis* to obtain nanofibers and scaffolds for tissue regeneration or joint lubricants [87]. Besides another promising application in regenerative medicine is the use of biomaterials based on biomass as a whole [88].

Also aiming to develop a scaffold to cultivate stem cells for tissue engineering Belini *et al*. [89] developed non-toxic biomaterials from cyanobacteria biomass (*Trichormus variabilis*). The success of these studies was associated with significant amounts of biocompounds present in the biomass, with an emphasis on polysaccharides. Although it is an attractive alternative for regenerative medicine, the use of microalgal polysaccharides for this purpose is still little explored, possibly, due to the difficulties encountered in elucidating its real structure [90]. Considering that the structural characteristic of microalgae polysaccharides is responsible for their biomedical applications, knowledge of their structure is fundamental, and knowledge of appropriate extraction/purification methods and determination methods are essential.

5. EXTRACTION, PURIFICATION AND STRUCTURAL DETERMINATION METHODS

The extraction of polysaccharides usually occurs through mechanisms involving thermal reflux and alcoholic precipitation. However, these methods require high extraction times, high-energy costs and the use of toxic solvents, making them expensive and harmful to human health and the environment. Also, prolonged extraction times and high temperatures can cause structural degradation of the polysaccharide, reducing its bioactivity. In this context, green technologies were developed to aid the extraction of these biocompounds: (i) membrane microfiltration; (ii) enzyme-assisted processes; (iii) ultrasound; (iv) microwave; and (v) ultra-high-pressure homogenization (UHPH) [91].

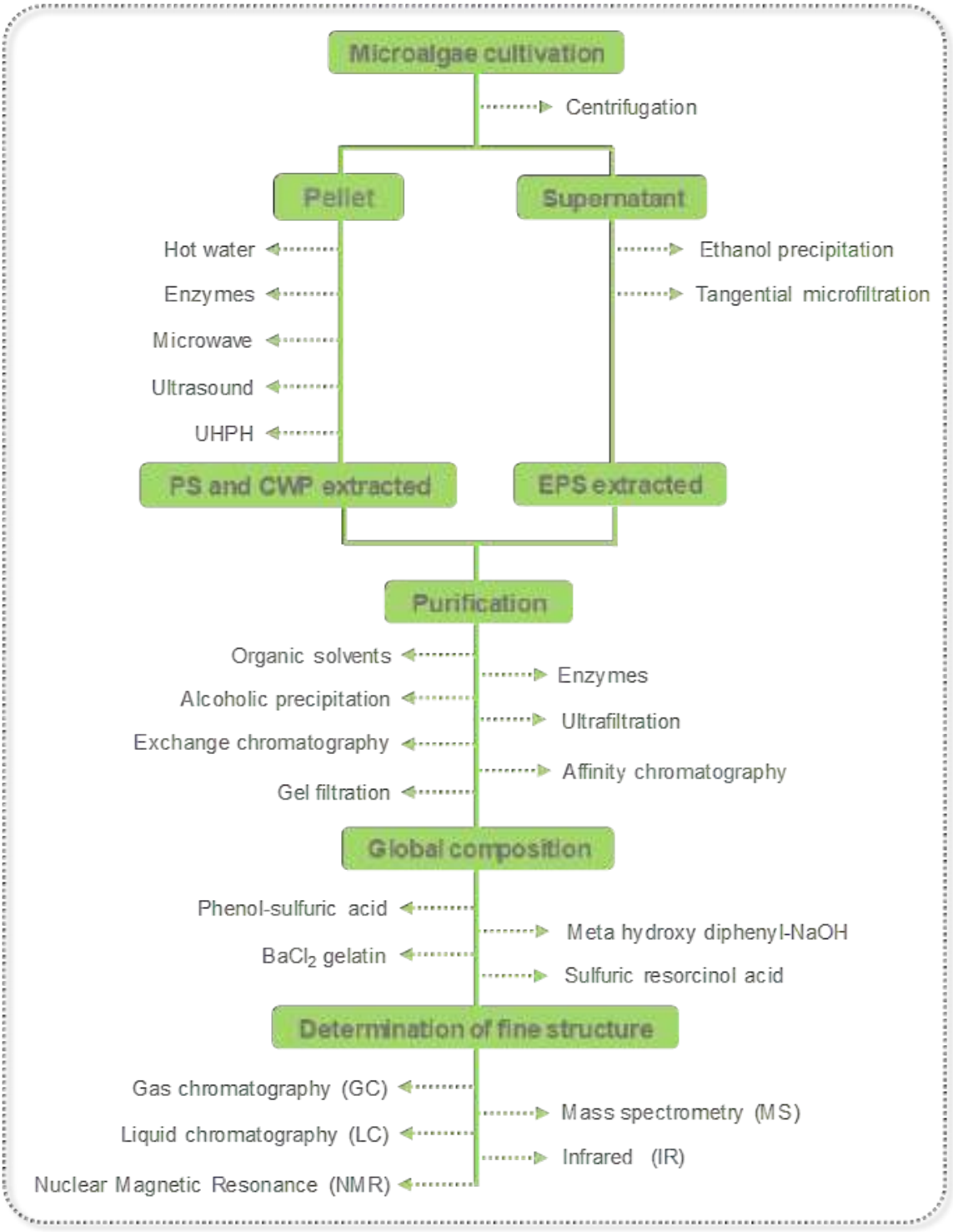


Fig. (1). Strategies for a systematic analysis for determination of microalgae polysaccharides. PS: Storage polysaccharide; CWP: Cell wall polysaccharide; EPS: Exopolysaccharide; UHPH: Ultra High Pressure Homogenization.

Fig. (**1**) shows the main techniques of extraction, purification, and methods for the determination of polysaccharides of microalgae. Where the extraction methods are organized according to the polysaccharide of interest: storage (SP), related to the cell wall (CWP) and those secreted in the culture medium (EPS).

Among existing conventional methods, the use of hot water reflux is the most commonly used method. Generally, the yield of this method depends on a large part on the extraction time and the temperature used [11]. Although it is the most popular method to extract CWP polysaccharides [92], it has also been used to extract EPS from *Spirulina* sp. and *Chlorella* sp., respectively [93,94]. In this process, the long extraction time (30 min to 24 hours) as well as the requirement of high temperatures (around 100ºC) add costs to the process and may affect the bioactivity of the compound [95].

Alcoholic precipitation, another conventional method, can be considered both as a method of extraction (when the focus is only EPS) or a preliminary purification method (in SP and CWP extraction). The use of 70% ethanol is the most recurrent in the literature. Referring to the selective extraction of EPS, most available studies include one or two steps of centrifugation and filtration to remove the microalgae biomass from the rich extracts in the compound of interest. According to Delattre [3], the most efficient precipitation technique is using alcohols such as methanol: isopropanol or ethanol in the ratio of 3:1 (v/v). Recently, Bernaerts *et al*. [96] made use of ethanolic precipitation followed by dialyzed filtration to extract EPS from different microalgae species (*Chlorella vulgaris, Porphyridium cruentum, Odontella aurita, Arthrospira platensis*).

As alcoholic precipitation is not applicable to microalgae due to the high salt concentration that co-precipitates with the polysaccharide, the ideal is the application of emerging technologies based on the use of membranes [97]. The method of tangential microfiltration is an attractive alternative because the extraction takes place without the use of chemical solvents and at low-pressure temperature. It is used in ultrafiltration modules with polymer membranes with cuts ranging from 1kDa - 500kDa [3]. This technology was successfully used in the extraction of polysaccharides from *Porphyridium cruentum, Chaetoceros muelleri, Chlorella pyrenoidosa, Spirulina platensis, Haematococcus pluvialis, Nostoc commune*, and *Nostoc spheroid* [98,99].

Among the existing green technologies, enzyme-assisted extraction is based on its hydrolytic action, which weakens the cell wall structure, destroys complex internal storage compounds and thus releases intracellular polysaccharides. It is a widely used technique for this purpose in studies with seaweed, but for microalgae, its use is recent, cellulose, being the most used [94]. In addition, Bernaerts *et al*. [96] explored the use of enzymes such as endo-β-1,3-glucanase, α-amylase amyloglucosidase and subtilisin A protease to assist in the isolation (elimination of interferences) of CWP of various microalgae (*Arthrospira platensis, Chlorella vulgaris, Diacronema lutheri, Tisochrysis lutea, Nannochloropsis* sp., *Odontella aurita, Phaeodactylum tricornutum, Porphyridium cruentum, Schizochytrium* sp., *Tetraselmis chuii*).

Another attractive green alternative is the ultrasound-assisted polysaccharide extraction, based on the breakdown of the cell wall of the microalgae by the propagation of the ultrasonic waves in the extraction solvent [95]. Its efficiency is associated with the cavitation effect, which is responsible for the increase in mass transfer rate, where bubbles in the liquid/solid extraction can collapse explosively, generating a localized pressure that causes cell rupture and the release of intracellular substances in the solvent demonstrated the effectiveness of this technology for the extraction of polysaccharides from *Dunaliella salina, Spirulina platensis* [95,100-102], respectively, while Yang *et al*. [92] and Sheng *et al*. [103] tested the use for the biomass of *Chlorella pyrenoidosa*. According to Tang *et al*. [104] and the above mentioned studies, ultrasonic assisted extraction reduces extraction time and does not affect the structure of the polysaccharides.

The microwave-assisted extraction is another method that has attracted interest due to its high efficiency and its main mechanisms, such as the rapid increase in temperature (responsible for the reduction of the emulsion viscosity) and molecular rotation (accountable for the breakage of the external film of the cellular structure and greater ionic movement) [105]. This technique was demonstrated to be efficient in the extraction of polysaccharides from various substrates of *Arthrospira platensis*. Compared to conventional extraction, it was very advantageous due to the energy savings of 99.7% and being a high-speed method since it promoted extraction in only 1 min of microwave exposure [91].

Recently, Bernaerts *et al*. [18] and Bernaerts *et al*. [96] demonstrated that UHPH can also be exploited as an alternative for the extraction of polysaccharides from microalgae. According to Carullo *et al*. [106], UHPH is a promising and scalable cell-breaking technology for microalgae cells. This technique has a similar mechanism to conventional homogenization, differing in the fact that it uses significantly higher pressures, reaching up to 400 MPa [107]. Cavitation, turbulence, impact and shear forces are the physical phenomena that occur during this treatment and cause the rupture of the cellular structure [108].

In general, the use of these emerging technologies for extracting polysaccharides from microalgae has been combined with at least one stage involving hot water or alcohol precipitation as a strategy to aid in the isolation of the compound [91, 101, 102, 104, 109].

Regardless of the method of extraction adopted, the extract purification step is primordial because these compounds in their crude form are together with several other components, such as proteins, nucleotides, lipids, lignin and some inorganic mineral substances that can alter their activities in biology and cause antagonistic effects or undesirable toxicity [3, 93]. This step ensures an understanding of the relationship between structures and the safety of biomedical or food applications of the polysaccharide. One purification strategy has been single use or combination of techniques based on: the use of organic solvents, enzymes, ethanol precipitation, ultrafiltration, ion exchange chromatography, gel filtration and affinity chromatography, taking advantage of particular properties of the desired compound, such as acidity, polarity and molecular size [110].

After obtaining the purified extract, the polysaccharide content is sequentially determined by chemical methods (global composition) and instrumental (detailed structure). Frequently, in the microalgae, the global composition is determined by colorimetric assays such as the phenol-sulfuric acid (total carbohydrates), and $BaCl_2$ gelatin (sulphate groups) [23, 109], meta hydroxy diphenyl-NaOH [87], and sulfuric-resorcinol acid methods (neutral sugars) [3].

However, these overall determination methods are not entirely satisfactory because they do not provide specific structural information and may overestimate or suppress the total polysaccharide content in the function of possible spectral interferences. Thus, for advanced biotechnological development, it is necessary to have access to detailed structural information and thus establish the relationships between structures and biological properties of polysaccharides [3]. In this sense, the exploration of instrumental analytical methods based on chromatography, mass spectrometry, infrared, NMR and hyphenation of these techniques are fundamental in the search for a complete mapping of the polysaccharide structure [111]. This can be seen in the works of Sadovskaya *et al*. [112] and Goo *et al*. [23] in the determination of homopolysaccharides of *Isochrysis galbana* and *Dunaliella tertiolecta*, respectively.

According to Yang and Zhang [113], the establishment of a systematic methodology can contribute to advances in the complete elucidation structural of the polysaccharides in general. Due to the complexity of these polymers associated with the structural diversity of microalgae, it is difficult to establish a universal methodology [90]; however, this section presents the main strategies that can be used.

CONCLUSION

Historically, it is evident that several discoveries have been made towards natural bioactive products, yet there are still many resources that can be investigated in modern cutting-edge research in the biomedical sector. Polysaccharides with specific biological properties have been wide-

ly accepted for this purpose due to their various beneficial characteristics. As an alternative technological route, microalgae are highlighted as a promising bioresource for use as bioactive molecules. However, despite its notorious success, the field of microalgae research is limited, which somehow prevents the final destination of applicability. Probably, the vast majority of microalgae species have not yet been systematically investigated for this knowledge area and needs better future exploration.

CONSENT FOR PUBLICATION:

Not applicable.

FUNDING

None.

CONFLICT OF INTEREST

Dr. Eduardo Jacob-Lopes is the Editorial Advisory Board Member of the journal BIOT.

ACKNOWLEDGEMENTS

The authors would like to thank the National Council for Scientific and Technological Development (CNPq) – Brazil and the Coordination of Improvement of Higher Education Personnel (CAPES), Finance Code 001.

REFERENCES

[1] Sathasivam R, Radhakrishnan R, Hashem A, Abd Allah EF. Microalgae metabolites: A rich source for food and medicine. Saudi J Biol Sci 2019; 26(4): 709-22. http://dx.doi.org/10.1016/j.sjbs.2017.11.003 PMID: 31048995

[2] Zheng Y, Bai L, Zhou Y, *et al.* Polysaccharides from Chinese herbal medicine for anti-diabetes recent advances. Int J Biol Macromol 2019; 121: 1240-53. http://dx.doi.org/10.1016/j.ijbiomac.2018.10.072 PMID: 30342938

[3] Delattre C, Pierre G, Laroche C, Michaud P. Production, extraction and characterization of microalgal and cyanobacterial exopolysaccharides. Biotechnol Adv 2016; 34(7): 1159-79. http://dx.doi.org/10.1016/j.biotechadv.2016.08.001 PMID: 27530696

[4] Chen L, Huang G. The antiviral activity of polysaccharides and their derivatives. Int J Biol Macromol 2018; 115: 77-82. http://dx.doi.org/10.1016/j.ijbiomac.2018.04.056 PMID: 29654857

[5] Yildiz H, Karatas N. Microbial exopolysaccharides: Resources and bioactive properties. Process Biochem 2018; 72: 41-6. http://dx.doi.org/10.1016/j.procbio.2018.06.009

[6] Michaud P. Polysaccharides from microalgae, what's future? Adv Biotechnol Microbiol 2018; 8(2): 1-2.

[7] Ramírez MLG, Zepka LQ, Jacob-Lopes E. Current production of microalgae at industrial scale. In: Pires JCM, Ed. Recent Advances in Renewable Energy Microalgae as a Source of Bioenergy: Products, Processes and Economics. Sharjah: Bentham Science Publishers 2017; pp. 278-96. http://dx.doi.org/10.2174/9781681085227117010013

[8] Jacob-Lopes E, Maroneze MM, Deprá MC, Sartori RB, Dias RR, Zepka LQ. Bioactive food compounds from microalgae: An innovative framework on industrial biorefineries. Curr Opin Food Sci 2019; 25: 1-7. http://dx.doi.org/10.1016/j.cofs.2018.12.003

[9] Levine I, Fleurence J. Microalgae in Health and Disease Prevention. 1st ed. London: Academic Press 2018.

[10] Saide A, Martínez KA, Ianora A, Lauritano C. Unlocking the health potential of microalgae as sustainable sources of bioactive compounds. Int J Mol Sci 2021; 22(9): 4383. http://dx.doi.org/10.3390/ijms22094383 PMID: 33922258

[11] Khanra S, Mondal M, Halder G, Tiwari ON, Gayen K, Bhowmick TK. Downstream processing of microalgae for pigments, protein and carbohydrate in industrial application: A review. Food Bioprod Process 2018; 110: 60-84. http://dx.doi.org/10.1016/j.fbp.2018.02.002

[12] Guiry MD. How many species of algae are there? J Phycol 2012; 48(5): 1057-63. http://dx.doi.org/10.1111/j.1529-8817.2012.01222.x PMID: 27011267

[13] Ogbonna JC, Uzochukwu S, Nwoba EG, *et al.* Fermentation and Algal Biotechnologies for the Food, Beverage and Other Bioproduct Industries. 1st ed. Boca Raton: CRC Press 2022. [Epub Ahead of Print] http://dx.doi.org/10.1201/9781003178378

[14] Maroneze MM, Queiroz MI. Microalgal production systems with highlights of bioenergy production. In: Jacob-Lopes E, Zepka LQ, Queiroz MI, Eds. Energy from Microalgae. Switzerland: Springer 2018; pp. 5-34. http://dx.doi.org/10.1007/978-3-319-69093-3_2

[15] Khan F, Ahmad SR. Polysaccharides and their derivatives for versatile tissue engineering application. Macromol Biosci 2013; 13(4): 395-421. http://dx.doi.org/10.1002/mabi.201200409 PMID: 23512290

[16] Cheng P, Li Y, Wang C, *et al.* Integrated marine microalgae biorefineries for improved bioactive com-

pounds: A review. Sci Total Environ 2022; 817: 152895. http://dx.doi.org/10.1016/j.scitotenv.2021.152895 PMID: 34998757

[17] Siqueira SF, Maroneze MM, Dias RR, *et al.* Mapping the performance of photobioreactors for microalgae cultivation: Geographic position and local climate. J Chem Technol Biotechnol 2020; 95(9): 2411-20. http://dx.doi.org/10.1002/jctb.6423

[18] Bernaerts TMM, Gheysen L, Kyomugasho C, *et al.* Comparison of microalgal biomasses as functional food ingredients: Focus on the composition of cell wall related polysaccharides. Algal Res 2018; 32: 150-61. http://dx.doi.org/10.1016/j.algal.2018.03.017

[19] Raposo MFJ, De Morais AMMB. Microalgae for the prevention of cardiovascular disease and stroke. Life Sci 2015; 125: 32-41. http://dx.doi.org/10.1016/j.lfs.2014.09.018 PMID: 25277945

[20] Qi J, Kim SM. Characterization and immunomodulatory activities of polysaccharides extracted from green alga *Chlorella ellipsoidea.* Int J Biol Macromol 2017; 95: 106-14. http://dx.doi.org/10.1016/j.ijbiomac.2016.11.039 PMID: 27856321

[21] Guzmán S, Gato A, Lamela M, Freire-Garabal M, Calleja JM. Anti-inflammatory and immunomodulatory activities of polysaccharide from *Chlorella stigmatophora* and *Phaeodactylum tricornutum*. Phytother Res 2003; 17(6): 665-70. http://dx.doi.org/10.1002/ptr.1227 PMID: 12820237

[22] Dai J, Wu Y, Chen S, *et al.* Sugar compositional determination of polysaccharides from *Dunaliella salina* by modified RP-HPLC method of precolumn derivatization with 1-phenyl-3-methyl-5-pyrazolone. Carbohydr Polym 2010; 82(3): 629-35. http://dx.doi.org/10.1016/j.carbpol.2010.05.029

[23] Geun GB, Baek G, Jin Choi D, *et al.* Characterization of a renewable extracellular polysaccharide from defatted microalgae *Dunaliella tertiolecta.* Bioresour Technol 2013; 129: 343-50. http://dx.doi.org/10.1016/j.biortech.2012.11.077 PMID: 23262010

[24] Bafana A. Characterization and optimization of production of exopolysaccharide from *Chlamydomonas reinhardtii.* Carbohydr Polym 2013; 95(2): 746-52. http://dx.doi.org/10.1016/j.carbpol.2013.02.016 PMID: 23648037

[25] Trabelsi L, Chaieb O, Mnari A, Abid ES, Aleya L. Partial characterization and antioxidant and antiproliferative activities of the aqueous extracellular polysaccharides from the thermophilic microalgae *Graesiella* sp. BMC Complement Altern Med 2016; 16(1): 210. http://dx.doi.org/10.1186/s12906-016-1198-6 PMID: 27405739

[26] Mourelle M, Gómez C, Legido J. The potential use of marine microalgae and cyanobacteria in cosmetics and thalassotherapy. Cosmetics 2017; 4(4): 46. http://dx.doi.org/10.3390/cosmetics4040046

[27] Santoyo S, Jaime L, Plaza M, *et al.* Antiviral compounds obtained from microalgae commonly used as carotenoid sources. J Appl Phycol 2012; 24(4): 731-41. http://dx.doi.org/10.1007/s10811-011-9692-1

[28] De Jesus RM, De Morais A, De Morais R. Marine polysaccharides from algae with potential biomedical aplications. Mar Drugs 2015; 13(5): 2967-3028. http://dx.doi.org/10.3390/md13052967 PMID: 25988519

[29] Raposo M, De Morais R, De Morais BA. Bioactivity and applications of sulphated polysaccharides from marine microalgae. Mar Drugs 2013; 11(1): 233-52. http://dx.doi.org/10.3390/md11010233 PMID: 23344113

[30] Hernándezcorona A, Nieves I, Meckes M, Chamorro G, Barron B. Antiviral activity of *Spirulina maxima* against herpes simplex virus type 2. Antiviral Res 2002; 56(3): 279-85. http://dx.doi.org/10.1016/S0166-3542(02)00132-8 PMID: 12406511

[31] Shen S, Jia S, Wu Y, *et al.* Effect of culture conditions on the physicochemical properties and antioxidant activities of polysaccharides from *Nostoc flagelliforme.* Carbohydr Polym 2018; 198: 426-33. http://dx.doi.org/10.1016/j.carbpol.2018.06.111 PMID: 30093019

[32] Quan Y, Yang S, Wan J, Su T, Zhang J, Wang Z. Optimization for the extraction of polysaccharides from *Nostoc commune* and its antioxidant and antibacterial activities. J Taiwan Inst Chem Eng 2015; 52: 14-21. http://dx.doi.org/10.1016/j.jtice.2015.02.004

[33] Yim JH, Kim SJ, Ahn SH, Lee CK, Rhie KT, Lee HK. Antiviral effects of sulfated exopolysaccharide from the marine microalga *Gyrodinium impudicum* strain KG03. Mar Biotechnol 2004; 6(1): 17-25. http://dx.doi.org/10.1007/s10126-003-0002-z PMID: 14508657

[34] Kang Y, Wang ZJ, Xie D, *et al.* Characterization and potential antitumor activity of polysaccharide from *Gracilariopsis lemaneiformis.* Mar Drugs 2017; 15(4): 100. http://dx.doi.org/10.3390/md15040100 PMID: 28353631

[35] Ginzberg A, Korin E, Arad SM. Effect of drying on the biological activities of a red microalgal polysaccharide. Biotechnol Bioeng 2008; 99(2): 411-20. http://dx.doi.org/10.1002/bit.21573 PMID: 17625787

[36] Markou G, Nerantzis E. Microalgae for high-value compounds and biofuels production: A review with focus on cultivation under stress conditions. Biotechnol Adv 2013; 31(8): 1532-42.

http://dx.doi.org/10.1016/j.biotechadv.2013.07.011 PMID: 23928208

[37] Udayan A, Sirohi R, Sreekumar N, Sang BI, Sim SJ. Mass cultivation and harvesting of microalgal biomass: Current trends and future perspectives. Bioresour Technol 2022; 344(Pt B): 126406. http://dx.doi.org/10.1016/j.biortech.2021.126406 PMID: 34826565

[38] Larroche C, Sanromán MA, Du G, Pandey A. Current Developments in Biotechnology and Bioengineering: Bioprocesses, Bioreactors and Controls. 3rd ed. Atlanta: Elsevier 2017, pp.785-821.

[39] Dragone G. Challenges and opportunities to increase economic feasibility and sustainability of mixotrophic cultivation of green microalgae of the genus *Chlorella*. Renew Sustain Energy Rev 2022; 160: 112284. http://dx.doi.org/10.1016/j.rser.2022.112284

[40] Jacob-Lopes E, Zepka LQ, Queiroz MI. Energy from Microalgae. 1st ed. Switzerland: Springer 2018. http://dx.doi.org/10.1007/978-3-319-69093-3

[41] Chisti Y. Biodiesel from microalgae. Biotechnol Adv 2007; 25(3): 294-306. http://dx.doi.org/10.1016/j.biotechadv.2007.02.001 PMID: 17350212

[42] Norsker NH, Barbosa MJ, Vermuë MH, Wijffels RH. Microalgal production — A close look at the economics. Biotechnol Adv 2011; 29(1): 24-7. http://dx.doi.org/10.1016/j.biotechadv.2010.08.005 PMID: 20728528

[43] Chisti Y. Raceways-based production of algal crude oil. Green 2013; 3(3-4):195-216.

[44] Zheng H, Wang Y, Li S, *et al.* Recent advances in lutein production from microalgae. Renew Sustain Energy Rev 2022; 153: 111795. http://dx.doi.org/10.1016/j.rser.2021.111795

[45] Francisco ÉC, Teixeira Franco T, Queiroz Zepka L, Jacob-Lopes E. From waste-to-energy: The process integration and intensification for bulk oil and biodiesel production by microalgae. J Environ Chem Eng 2015; 3(1): 482-7. http://dx.doi.org/10.1016/j.jece.2014.12.017

[46] Maurya R, Zhu X, Valverde-Pérez B, *et al.* Advances in microalgal research for valorization of industrial wastewater. Bioresour Technol 2022; 343: 126128. http://dx.doi.org/10.1016/j.biortech.2021.126128 PMID: 34655786

[47] Tabernero A, Del Valle MEM, Galán MA. Evaluating the industrial potential of biodiesel from a microalgae heterotrophic culture: Scale-up and economics. Biochem Eng J 2012; 63: 104-15. http://dx.doi.org/10.1016/j.bej.2011.11.006

[48] Hu D, Cheong K, Zhao J, Li S. Chromatography in characterization of polysaccharides from medicinal plants and fungi. J Sep Sci 2013; 36(1): 1-19. http://dx.doi.org/10.1002/jssc.201200874 PMID: 23225747

[49] Patel AK, Vadrale AP, Singhania RR, *et al.* Algal polysaccharides: Current status and future prospects. Phytochem Rev 2022; 1-30. http://dx.doi.org/10.1007/s11101-021-09799-5

[50] Damonte E, Matulewicz M, Cerezo A. Sulfated seaweed polysaccharides as antiviral agents. Curr Med Chem 2004; 11(18): 2399-419. http://dx.doi.org/10.2174/0929867043364504 PMID: 15379705

[51] Montanha JA, Bourgougnon N, Boustie J, Amoros M. Antiviral activity of carrageenans from marine red algae. Lat Am J Pharm 2009; 28(3): 443-8.

[52] Trinchero J, Ponce NMA, Córdoba OL, *et al.* Antiretroviral activity of fucoidans extracted from the brown seaweed *Adenocystis utricularis*. Phytother Res 2009; 23(5): 707-12. http://dx.doi.org/10.1002/ptr.2723 PMID: 19107862

[53] Pérez RM, Carlucci MJ, Noseda MD, Matulewicz MC. Chemical modifications of algal mannans and xylomannans: Effects on antiviral activity. Phytochemistry 2012; 73(1): 57-64. http://dx.doi.org/10.1016/j.phytochem.2011.10.002 PMID: 22071136

[54] Morais A M, Alves A, Kumla D, Morais R M. Pharmaceutical and biomedical potential of sulphated polysaccharides from algae. In: Polysaccharides of Microbial Origin. New York: Springer, 2022; pp. 1-28. [ePub Ahead of print]

[55] Pierre G, Sopena V, Juin C, Mastouri A, Graber M, Maugard T. Antibacterial activity of a sulfated galactan extracted from the marine alga *Chaetomorpha aerea* against *Staphylococcus aureus.* Biotechnol Bioprocess Eng; BBE 2011; 16(5): 937-45. http://dx.doi.org/10.1007/s12257-011-0224-2

[56] Shannon E, Abu-Ghannam N. Antibacterial derivatives of marine algae: An overview of pharmacological mechanisms and applications. Mar Drugs 2016; 14(4): 81. http://dx.doi.org/10.3390/md14040081 PMID: 27110798

[57] Abad M, Bedoya L, Bermejo P. Natural marine anti-inflammatory products. Mini Rev Med Chem 2008; 8(8): 740-54. http://dx.doi.org/10.2174/138955708784912148 PMID: 18673130

[58] Naqvi SAR, Sherazi TA, Hassan SU, Shahzad SA, Faheem Z. Anti-inflammatory, anti-infectious and anti-cancer potential of marine algae and sponge: A review. Eur J Inflamm 2022; 20 http://dx.doi.org/10.1177/20587392221075514

[59] Hamias R, Wolak T, Huleihel M, Paran E, Levy OO. Red alga polysaccharides attenuate angiotensin II-induced inflammation in coronary endothelial cells. Biochem Biophys Res Commun 2018; 500(4): 944-51. http://dx.doi.org/10.1016/j.bbrc.2018.04.206 PMID: 29705698

[60] Cameron AC, Lang NN, Touyz RM. Drug treatment of hypertension: Focus on vascular health. Drugs 2016; 76(16): 1529-50. http://dx.doi.org/10.1007/s40265-016-0642-8 PMID: 27667708

[61] Hwang J, Yadav D, Lee PCW, Jin JO. Immunomodulatory effects of polysaccharides from marine algae for treating cancer, infectious disease, and inflammation. Phytother Res 2022; 36(2): 761-77. http://dx.doi.org/10.1002/ptr.7348 PMID: 34962325

[62] Levy OO, Huleihel M, Hamias R, Wolak T, Paran E. An anti-inflammatory effect of red microalga polysaccharides in coronary artery endothelial cells. Atherosclerosis 2017; 264: 11-8. http://dx.doi.org/10.1016/j.atherosclerosis.2017.07.017 PMID: 28738269

[63] Gupta PK, Rajan MGR, Kulkarni S. Activation of murine macrophages by G1-4A, a polysaccharide from *Tinospora cordifolia*, in TLR4/MyD88 dependent manner. Int Immunopharmacol 2017; 50: 168-77. http://dx.doi.org/10.1016/j.intimp.2017.06.025 PMID: 28667885

[64] Azevedo MLV, Bonan NB, Dias G, *et al.* p-Cresyl sulfate affects the oxidative burst, phagocytosis process, and antigen presentation of monocyte-derived macrophages. Toxicol Lett 2016; 263: 1-5. http://dx.doi.org/10.1016/j.toxlet.2016.10.006 PMID: 27760375

[65] Wang J, Bao A, Wang Q, *et al.* Sulfation can enhance antitumor activities of *Artemisia sphaerocephala* polysaccharide *in vitro* and *vivo*. Int J Biol Macromol 2018; 107(Pt A): 502-11. http://dx.doi.org/10.1016/j.ijbiomac.2017.09.018 PMID: 28893683

[66] Ye H, Wang K, Zhou C, Liu J, Zeng X. Purification, antitumor and antioxidant activities *in vitro* of polysaccharides from the brown seaweed *Sargassum pallidum*. Food Chem 2008; 111(2): 428-32. http://dx.doi.org/10.1016/j.foodchem.2008.04.012 PMID: 26047446

[67] Vishchuk OS, Ermakova SP, Zvyagintseva TN. Sulfated polysaccharides from brown seaweeds *Saccharina japonica* and *Undaria pinnatifida*: Isolation, structural characteristics, and antitumor activity. Carbohydr Res 2011; 346(17): 2769-76. http://dx.doi.org/10.1016/j.carres.2011.09.034 PMID: 22024567

[68] Perrotta PL, Perrotta CL, Snyder EL. Apoptotic activity in stored human platelets. Transfusion 2003; 43(4): 526-35. http://dx.doi.org/10.1046/j.1537-2995.2003.00349.x PMID: 12662287

[69] Queiroz KCS, Assis CF, Medeiros VP, *et al.* Cytotoxicity effect of algal polysaccharides on HL60 cells. Biochemistry 2006; 71(12): 1312-5. http://dx.doi.org/10.1134/S0006297906120042 PMID: 17223782

[70] Jiao G, Yu G, Zhang J, Ewart H. Chemical structures and bioactivities of sulfated polysaccharides from marine algae. Mar Drugs 2011; 9(2): 196-223. http://dx.doi.org/10.3390/md9020196 PMID: 21566795

[71] Li P, Wen S, Sun K, Zhao Y, Chen Y. Structure and bioactivity screening of a low molecular weight ulvan from the green alga *Ulothrix flacca*. Mar Drugs 2018; 16(8): 281. http://dx.doi.org/10.3390/md16080281 PMID: 30111709

[72] Wang L, Wang X, Wu H, Liu R. Overview on biological activities and molecular characteristics of sulfated polysaccharides from marine green algae in recent years. Mar Drugs 2014; 12(9): 4984-5020. http://dx.doi.org/10.3390/md12094984 PMID: 25257786

[73] Sun Z, Dai Z, Zhang W, *et al.* Antiobesity, Antidiabetic, Antioxidative, and Antihyperlipidemic Activities of Bioactive Seaweed Substances. Bioactive Seaweeds for Food Applications. USA: Academic Press 2018; pp. 239-53. http://dx.doi.org/10.1016/B978-0-12-813312-5.00012-1

[74] Wang J, Jin W, Zhang W, Hou Y, Zhang H, Zhang Q. Hypoglycemic property of acidic polysaccharide extracted from *Saccharina japonica* and its potential mechanism. Carbohydr Polym 2013; 95(1): 143-7. http://dx.doi.org/10.1016/j.carbpol.2013.02.076 PMID: 23618250

[75] Patias LD, Fernandes AS, Petry FC, Mercadante AZ, Jacob-Lopes E, Zepka LQ. Carotenoid profile of three microalgae/cyanobacteria species with peroxyl radical scavenger capacity. Food Res Int 2017; 100(Pt 1): 260-6. http://dx.doi.org/10.1016/j.foodres.2017.06.069 PMID: 28873686

[76] Imjongjairak S, Ratanakhanokchai K, Laohakunjit N, Tachaapaikoon C, Pason P, Waeonukul R. Biochemical characteristics and antioxidant activity of crude and purified sulfated polysaccharides from *Gracilaria fisheri*. Biosci Biotechnol Biochem 2016; 80(3): 524-32. http://dx.doi.org/10.1080/09168451.2015.1101334 PMID: 26507584

[77] Sun Y, Wang H, Guo G, Pu Y, Yan B. The isolation and antioxidant activity of polysaccharides from the marine microalgae *Isochrysis galbana*. Carbohydr Polym 2014; 113: 22-31. http://dx.doi.org/10.1016/j.carbpol.2014.06.058 PMID: 25256454

[78] Liu X, Zhang M, Liu H, Zhou A, Cao Y, Liu X. Preliminary characterization of the structure and immunostimulatory and anti-aging properties of the polysaccharide fraction of *Haematococcus pluvialis*. RSC Advances 2018; 8(17): 9243-52. http://dx.doi.org/10.1039/C7RA11153C PMID: 35541856

[79] Morais MG, Rosa GM, Moraes L, Alvarenga AGP, Da Silva JLV, Costa JAV. Microalgae polysaccharides with potential biomedical application. In: Oliveira JM, Radhouani H, Reis RL, Eds. Polysaccharides of Microbial Origin. New York: Springer 2022. [ePub Ahead of Print] http://dx.doi.org/10.1007/978-3-030-42215-8_20

[80] Symonette CJ, Kaur Mann A, Tan XC, *et al.* Hyaluronan-phosphatidylethanolamine polymers form pericellular coats on keratinocytes and promote basal keratinocyte proliferation. BioMed Res Int 2014; 2014: 1-14. http://dx.doi.org/10.1155/2014/727459 PMID: 25276814

[81] Jensen G, Morrill C, Huang Y. 3D tissue engineering, an emerging technique for pharmaceutical research. Acta Pharm Sin B 2018; 8(5): 756-66. http://dx.doi.org/10.1016/j.apsb.2018.03.006 PMID: 30258764

[82] Colliec-Jouault S. Skin tissue engineering using functional marine biomaterials. In: Kim SK, Ed. Functional Marine Biomaterials: Properties and Applications. USA: Elsevier 2015; pp. 69-86. http://dx.doi.org/10.1016/B978-1-78242-086-6.00005-4

[83] Roussel M, Villay A, Delbac F, *et al.* Antimicrosporidian activity of sulphated polysaccharides from algae and their potential to control honeybee nosemosis. Carbohydr Polym 2015; 133: 213-20. http://dx.doi.org/10.1016/j.carbpol.2015.07.022 PMID: 26344274

[84] Mohamed ZA. Polysaccharides as a protective response against microcystin-induced oxidative stress in *Chlorella vulgaris* and *Scenedesmus quadricauda* and their possible significance in the aquatic ecosystem. Ecotoxicology 2008; 17(6): 504-16. http://dx.doi.org/10.1007/s10646-008-0204-2 PMID: 18389369

[85] Silva TH, Alves A, Popa EG, *et al.* Marine algae sulfated polysaccharides for tissue engineering and drug delivery approaches. Biomatter 2012; 2(4): 278-89. http://dx.doi.org/10.4161/biom.22947 PMID: 23507892

[86] Senni K, Pereira J, Gueniche F, *et al.* Marine polysaccharides: A source of bioactive molecules for cell therapy and tissue engineering. Mar Drugs 2011; 9(9): 1664-81. http://dx.doi.org/10.3390/md9091664 PMID: 22131964

[87] Raposo MFJ, De Morais AMMB, De Morais RMSC. Influence of sulphate on the composition and antibacterial and antiviral properties of the exopolysaccharide from *Porphyridium cruentum.* Life Sci 2014; 101(1-2): 56-63. http://dx.doi.org/10.1016/j.lfs.2014.02.013 PMID: 24582595

[88] Furmaniak MA, Misztak AE, Franczuk MD, Wilmotte A, Waleron M, Waleron KF. Edible cyanobacterial genus *Arthrospira*: Actual state of the art in cultivation methods, genetics, and application in medicine. Front Microbiol 2017; 8: 2541. http://dx.doi.org/10.3389/fmicb.2017.02541 PMID: 29326676

[89] Bellini E, Ciocci M, Savio S, *et al. Trichormus variabilis* (Cyanobacteria) biomass: From the nutraceutical products to novel EPS-cell/protein carrier systems. Mar Drugs 2018; 16(9): 298. http://dx.doi.org/10.3390/md16090298 PMID: 30150548

[90] Domozych DS, Ciancia M, Fangel JU, Mikkelsen MD, Ulvskov P, Willats WGT. The cell walls of green algae: A journey through evolution and diversity. Front Plant Sci 2012; 3: 82. http://dx.doi.org/10.3389/fpls.2012.00082 PMID: 22639667

[91] Silva AS, De Magalhães WT, Moreira LM, Rocha MVP, Bastos AKP. Microwave-assisted extraction of polysaccharides from *Arthrospira (Spirulina) platensis* using the concept of green chemistry. Algal Res 2018; 35: 178-84. http://dx.doi.org/10.1016/j.algal.2018.08.015

[92] Yang F, Shi Y, Sheng J, Hu Q. *In vivo* immunomodulatory activity of polysaccharides derived from *Chlorella pyrenoidosa.* Eur Food Res Technol 2006; 224(2): 225-8. http://dx.doi.org/10.1007/s00217-006-0315-z

[93] Chaiklahan R, Chirasuwan N, Triratana P, Loha V, Tia S, Bunnag B. Polysaccharide extraction from *Spirulina* sp. and its antioxidant capacity. Int J Biol Macromol 2013; 58: 73-8. http://dx.doi.org/10.1016/j.ijbiomac.2013.03.046 PMID: 23541559

[94] Zhao C, Yang C, Liu B, *et al.* Bioactive compounds from marine macroalgae and their hypoglycemic benefits. Trends Food Sci Technol 2018; 72: 1-12. http://dx.doi.org/10.1016/j.tifs.2017.12.001

[95] Xu SY, Huang X, Cheong KL. Recent advances in marine algae polysaccharides: Isolation, structure, and activities. Mar Drugs 2017; 15(12): 388. http://dx.doi.org/10.3390/md15120388 PMID: 29236064

[96] Bernaerts TMM, Kyomugasho C, Van Looveren N, *et al.* Molecular and rheological characterization of different cell wall fractions of *Porphyridium cruentum.* Carbohydr Polym 2018; 195: 542-50. http://dx.doi.org/10.1016/j.carbpol.2018.05.001 PMID: 29805010

[97] Patel AK, Laroche C, Marcati A, *et al.* Separation and fractionation of exopolysaccharides from *Porphyridium cruentum.* Bioresour Technol 2013; 145: 345-50. http://dx.doi.org/10.1016/j.biortech.2012.12.038 PMID: 23313179

[98] Marcati A, Ursu AV, Laroche C, *et al.* Extraction and fractionation of polysaccharides and B-phycoerythrin from the microalga *Porphyridium cruentum* by membrane technology. Algal Res 2014; 5: 258-63.

http://dx.doi.org/10.1016/j.algal.2014.03.006

[99] Li H, Li Z, Xiong S, *et al.* Pilot-scale isolation of bioactive extracellular polymeric substances from cell-free media of mass microalgal cultures using tangential-flow ultrafiltration. Process Biochem 2011; 46(5): 1104-9.
http://dx.doi.org/10.1016/j.procbio.2011.01.028

[100] Knorr D, Zenker M, Heinz V, Lee DU. Applications and potential of ultrasonics in food processing. Trends Food Sci Technol 2004; 15(5): 261-6.
http://dx.doi.org/10.1016/j.tifs.2003.12.001

[101] Kurd F, Samavati V. Water soluble polysaccharides from *Spirulina platensis*: Extraction and *in vitro* anticancer activity. Int J Biol Macromol 2015; 74: 498-506.
http://dx.doi.org/10.1016/j.ijbiomac.2015.01.005
PMID: 25583023

[102] Mishra A, Jha B. Isolation and characterization of extracellular polymeric substances from micro-algae *Dunaliella salina* under salt stress. Bioresour Technol 2009; 100(13): 3382-6.
http://dx.doi.org/10.1016/j.biortech.2009.02.006
PMID: 19272770

[103] Sheng J, Yu F, Xin Z, Zhao L, Zhu X, Hu Q. Preparation, identification and their antitumor activities *in vitro* of polysaccharides from *Chlorella pyrenoidosa*. Food Chem 2007; 105(2): 533-9.
http://dx.doi.org/10.1016/j.foodchem.2007.04.018

[104] Tang W, Lin L, Xie J, *et al.* Effect of ultrasonic treatment on the physicochemical properties and antioxidant activities of polysaccharide from *Cyclocarya paliurus*. Carbohydr Polym 2016; 151: 305-12.
http://dx.doi.org/10.1016/j.carbpol.2016.05.078
PMID: 27474571

[105] Thirugnanasambandham K, Sivakumar V, Maran JP. Microwave-assisted extraction of polysaccharides from mulberry leaves. Int J Biol Macromol 2015; 72: 1-5.
http://dx.doi.org/10.1016/j.ijbiomac.2014.07.031
PMID: 25064558

[106] Carullo D, Abera BD, Casazza AA, *et al.* Effect of pulsed electric fields and high pressure homogenization on the aqueous extraction of intracellular compounds from the microalgae *Chlorella vulgaris*. Algal Res 2018; 31: 60-9.
http://dx.doi.org/10.1016/j.algal.2018.01.017

[107] Yap BHJ, Dumsday GJ, Scales PJ, Martin GJO. Energy evaluation of algal cell disruption by high pressure homogenisation. Bioresour Technol 2015; 184: 280-5.
http://dx.doi.org/10.1016/j.biortech.2014.11.049
PMID: 25435068

[108] Floury J, Legrand J, Desrumaux A. Analysis of a new type of high pressure homogeniser. Part B. study of droplet break-up and recoalescence phenomena. Chem Eng Sci 2004; 59(6): 1285-94.
http://dx.doi.org/10.1016/j.ces.2003.11.025

[109] Zhao W, Duan M, Zhang X, Tan T. A mild extraction and separation procedure of polysaccharide, lipid, chlorophyll and protein from *Chlorella* sp. Renew Energy 2018; 118: 701-8.
http://dx.doi.org/10.1016/j.renene.2017.11.046

[110] Jin M, Huang Q, Zhao K, Shang P. Biological activities and potential health benefit effects of polysaccharides isolated from *Lycium barbarum* L. Int J Biol Macromol 2013; 54: 16-23.
http://dx.doi.org/10.1016/j.ijbiomac.2012.11.023
PMID: 23200976

[111] Zhang A, Sun H, Wang P, Han Y, Wang X, Wang X. Modern analytical techniques in metabolomics analysis. Analyst 2012; 137(2): 293-300.
http://dx.doi.org/10.1039/C1AN15605E PMID: 22102985

[112] Sadovskaya I, Souissi A, Souissi S, *et al.* Chemical structure and biological activity of a highly branched (1→3,1→6)-β-d-glucan from *Isochrysis galbana*. Carbohydr Polym 2014; 111: 139-48.
http://dx.doi.org/10.1016/j.carbpol.2014.04.077
PMID: 25037339

[113] Yang L, Zhang LM. Chemical structural and chain conformational characterization of some bioactive polysaccharides isolated from natural sources. Carbohydr Polym 2009; 76(3): 349-61.
http://dx.doi.org/10.1016/j.carbpol.2008.12.015

Journal of Applied Phycology
https://doi.org/10.1007/s10811-022-02725-y

Roadmap to net-zero carbon emissions in commercial microalgae-based products: environmental sustainability and carbon offset costs

Rosangela Rodrigues Dias[1] · Mariany Costa Deprá[1] · Leila Queiroz Zepka[1] · Eduardo Jacob-Lopes[1]

Received: 25 November 2021 / Revised and accepted: 7 March 2022
© The Author(s), under exclusive licence to Springer Nature B.V. 2022

Abstract
The global ecological awakening has made carbon–neutral production an imperative. Ignoring the call of the mermaid to protect the environment does not seem to be an option. In this study, given the fundamental role of sustainability for stakeholders, we propose actions to reduce the carbon emissions from the most important commercial microalgae-based products. Beyond that, we calculate the offset costs of the remaining emissions. The life cycle assessment tool was used to estimate total carbon emissions from the production of whole dry biomass by *Chlorella vulgaris* and *Arthrospira platensis*, as well as astaxanthin, phycocyanin, β-carotene, eicosapentaenoic acid, and docosahexaenoic acid by *Haematococcus pluvialis*, *Arthrospira platensis*, *Dunaliella salina*, *Nitzschia laevis*, and *Crypthecodinium cohnii*, respectively. The steps of the CarbonNeutral Protocol methodology were followed to achieve a final result of net-zero carbon emissions for the microalgal products. Our findings indicate that the electrical matrix replacement is the backbone for accomplishing carbon neutral operations in commercial microalgal facilities. The replacement of coal electricity by nuclear, followed by hydro, wind, biomass, and photovoltaic are the main forces to achieve low carbon emissions and lower environmental offset costs. The study results are the first step found in the literature to achieve carbon neutrality in consolidated biotechnological production routes of microalgae-based products.

Keywords Algae · Bioproducts · Life cycle assessment · Carbon neutrality · Sustainability · Climate change mitigation

Introduction

The relevance of microalgae as a rich source of feedstocks for high-value natural products is clearly increasing. The global market for microalgae-based products estimated at US$ 3.4 billion in 2020 should reach around US$ 4.6 billion by 2027 (GlobeNewswire 2021). The single-cell protein (whole biomass of *Spirulina* and *Chlorella*), natural pigments (β-carotene, astaxanthin, and phycocyanin), and polyunsaturated fatty acids (EPA and DHA) are yet the most important commercial products (Jacob-Lopes et al. 2019). The next generation of microalgae-based products will include lutein, fucoxanthin, phycoerythrin, beta-glucans, exopolysaccharides, arachidonic acid, and recombinant proteins (Dias et al. 2020).

In the current conjuncture, microalgal products are well established in the market. However, they may have difficulties in the next decade. The current products lifecycle assessments point to an impact on the environment that can and needs to be improved for business resilience. The ecological footprint calculations show that the production of microalgae-based products involves processes with high carbon emissions (Vuppaladadiyam et al. 2018; Guieysse and Plouviez 2021). And, about this, the facts do not lie and tell a convincing story that, sooner or later, the industry will be forced to respond to increasing market pressure, which moves in favor of the environment (Cai et al. 2019; Gills and Morgan 2020).

Globally, while most industries, independent of the sector, are taking a risky "wait-and-see" approach, there are those that are taking a proactive approach to meet the demand of the consumers and regulators concerned about climate change. These industries are basically measuring their carbon footprint and implementing the principle of carbon neutrality. The state of being carbon

✉ Eduardo Jacob-Lopes
ejacoblopes@gmail.com

[1] Bioprocess Intensification Group, Federal University of Santa Maria (UFSM), Roraima Avenue, 1000, Santa Maria, RS 97105-900, Brazil

neutral does not mean that the entity, product, or activity does not emit the pollutant, it simply indicates that the overall production is neutral, i.e., equal to zero (Becker et al. 2020).

The growing interest in implementing the state of being carbon–neutral and the advantages that can outweigh the costs of maintaining the status quo has recently reached a global prominent position. More than 100 countries, together with companies, cities, and financial institutions, have established or are considering the goal of reducing emissions to net zero by 2050 (ECIU 2022; Motive Power 2022). At the center of several carbon neutrality studies are today the transport sector (Choi and Ritchie 2014; Cui and Li 2017), energy (Gils and Simon 2017), and agriculture (Fantozzi et al. 2015; Birkenberg and Birner 2018; Chiriaco et al. 2019).

In the case of the microalgae-based industry, whose environmental issues were neglected for years, it is important to note that little research has focused on assessing the environmental impact of the processes and products and, in general, very little is known about solutions to become carbon–neutral. Therefore, this study aims to fill the knowledge gap about the implementation of the principle of carbon neutrality in microalgal facilities. The core of the study is to show that it is possible to achieve low carbon emissions and low environmental impact by adopting cleaner production approaches. This is the first article to calculate the carbon footprint of commercial microalgae-based products to propose an action plan to reduce greenhouse gas emissions and assess the costs of offsetting the remaining emissions.

Methodology

Life cycle assessment (LCA)

The methodological framework for life-cycle assessment (LCA) established by the International Organization for Standardization (ISO) series 14,040 was adopted to quantify carbon dioxide emissions from commercial microalgae-based products (ISO 2006). The procedures considered in each step of the LCA methodology are detailed below.

Goal and scope definition

The objective and scope of the application of the LCA were to quantify the carbon footprint of the most important microalgae-based commercial products, which are (i) whole dried biomass, (ii) β-carotene, (iii) phycocyanin, (iv) astaxanthin, (v) docosahexaenoic acid (DHA), and (vi) eicosapentaenoic acid (EPA). It should be noted that the collection of data for analysis was based on fundamentally consolidated technological processes and routes (Deprá et al. 2020a).

Functional unit and system boundaries

The study considered a functional unit of 1 t month^{-1} of whole dried biomass, pigments, and polyunsaturated fatty acids. The system boundaries were defined using the cradle-to-gate approach. Only emissions related to the demand for electricity and materials were accounted for. Emissions associated with infrastructure and equipment maintenance were not included in the analysis. The layout of the system boundaries with the technical characteristics of the study is shown in Fig. 1.

Life cycle inventory (LCI)

The LCI includes material and electricity requirement data for the production of 1 t month^{-1} of whole dried biomass by *Chlorella vulgaris* and *Arthrospira platensis*, besides phycocyanin, astaxanthin, β-carotene, eicosapentaenoic acid (EPA), and docosahexaenoic acid (DHA), by *Arthrospira platensis*, *Haematococcus pluvialis*, *Dunaliella salina*, *Nitzschia laevis*, and *Crypthecodinium cohnii*, respectively (Table 1). The Supplementary Material presents a sensitivity analysis that includes the LCI for biomass productivities lower than that considered in the base case.

Life cycle impact assessment (LCIA)

The global warming potential (GWP) is the indicator used to quantify carbon dioxide (CO_2) emissions. The GWP was calculated as described in Eq. (1), being expressed in tCO_2e (Jacob-Lopes et al. 2021). Material and electricity characterization factors are presented in Supplementary Material (Table S1).

$$GWP = \sum GWP_i \times m_i \quad (1)$$

where GWP is the indicator (tCO_2e), GWP_i are the characterization factors for substance *i*, and m_i is the inventory of emissions for substance *i* (t).

Emission assessment: reduce and offset

Practical implementation actions to reduce carbon dioxide emissions were established following the framework of the CarbonNeutral Protocol (Natural Capital Partners 2021). The action plan exposed encompasses reductions based on the establishment of a climate action project that includes three carbon credit-generating trends, which are (i) renewable and/or clean electricity, (ii) carbon capture and use, and (iii) mitigation of wastewater treatment.

The present study considered the replacement of coal electricity by nuclear, hydro, wind, biomass, photovoltaic, biogas, natural gas, and waste. The carbon dioxide capture and use

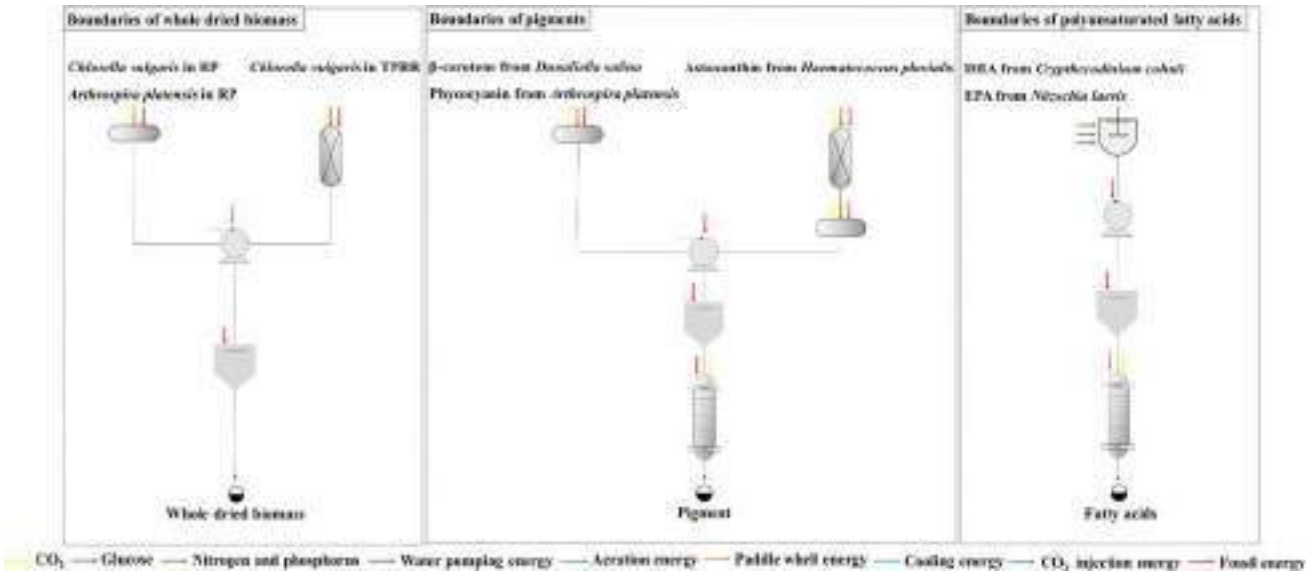


Fig. 1 Cradle-to-gate limits for LCA of microalgae-based products. *DHA* docosahexaenoic, *EPA* eicosapentaenoic. Adapted from Deprá et al. (2020a)

potential in open and closed photobioreactors were estimated under the parameter of elimination capacity, according to Basu et al. (2014) and Deprá et al. (2020b), respectively. The elimination capacity is the mass of carbon dioxide removed per unit volume of reactor per unit time (kg m^{-3} day^{-1}). Regarding the mitigation of wastewater treatment, it is noteworthy that it was considered to reuse the cultivation water a single time, and the carbon footprint of the water unit was estimated at 0.18 kg CO_2e m^{-3} (Hu et al. 2012).

Finally, according to the remaining emissions and the carbon price, the offset cost was calculated through Eq. (2). The global average carbon price and the European Union Emissions Trading System (EU ETS) carbon price were used to calculate the offsetting cost and its impact on the selling price of microalgae-based products (World Bank 2021). Sales prices of microalgae-based products were obtained from Fernández et al. (2021) and Schade and Meier (2021).

$$OC = RE \times CP \quad (2)$$

where OC is the offset cost per tonne of bioproduct (USD t^{-1}), RE is the remaining carbon dioxide emissions (tCO_2), and CP is the carbon price (USD t^{-1}).

Results and discussion

Reaching net-zero emissions: the role of prevention, removal, and compensation

The microalgal industry is known for its high consumption of electricity in upstream and downstream processing (Schade and Meier 2020). The careful examination of unitary operations allows for a holistic understanding of the impact of switching to CO_2-neutral production. Noteworthy, emissions in the microalgal sector have been researched. Previous studies discuss the environmental hotspots of microalgae-based processes and products and emphasize the importance of ecologically sound practices to improve the carbon footprint (Pérez-López et al. 2014; Papadaki et al. 2017; Yadav et al. 2020). However, the means to reduce or offset CO_2 emissions remain unexplored. In this sense, the importance of the present study is in providing a comprehensive climate protection solution that combines CO_2 prevention, removal, and compensation for carbon–neutral microalga industrial operations. Table 2 shows the carbon footprint, the action plan to reduce emissions, and the remaining emissions from the 1t $month^{-1}$ lifecycle of microalgae-based products.

By examining the net CO_2 emissions from the life cycle of microalgae-based products, it is possible to identify that the main contributor to the emissions are electricity inputs, while the requirement for materials has limited consequences (see Supplementary Material, Fig. S1). Through the calculation of sustainability metrics, it was possible to attribute that 97 to 99% of the carbon footprint came from electricity demand in the upstream and downstream stages. The second-largest contributor, despite having insignificant emissions compared to the electricity demand, is the nutrient requirement, especially CO_2, followed by the water demand and the use of sanitizers for bioreactor sterilization. This result corroborates the studies carried out by Deprá et al. (2020a), who, when evaluating the environmental impact

Table 1 Inventory inputs/outputs for the base case of the production process inventory of 1 t month^{-1} of whole dried biomass, phycocyanin, β-carotene, astaxanthin, docosahexaenoic acid, and eicosapentaenoic acid

Process		Whole dried biomass			Pigment			Polyunsaturated fatty acid	
		Chlorella vulgaris	*Chlorella vulgaris*	*Arthrospira platensis*	*Arthrospira platensis*	*Dunaliella salina*	*Haematococcus pluvialis*	*Crypthecodinium cohnii*	*Nitzschia laevis*
Cultivation system		*RP*	*TPBR*	*RP*	*RP*	*RP*	*TPBR and RP*	*Fermenter*	*Fermenter*
Cultivation									
Input									
Nutrient enrichment									
Phosphate	t month^{-1}	0.004	0.001	0.002	0.033	0.022	0.066	0.001	0.005
Nitrate	t month^{-1}	0.006	0.002	0.004	0.050	0.033	0.099	0.020	0.096
Glucose	t month^{-1}	-	-	-	-	-	-	0.417	1.99
Tubular photobioreactor	m^3	-	47.62	-	-	-	100.27	-	-
Chemical sterilization (sodium hypochlorite)	t month^{-1}	-	0.007	-	-	-	0.015	-	-
Energy consumption for cooling	kWh month^{-1}	-	514,296.0	-	-	-	1,082,916.0	-	-
Aeration energy	kWh month^{-1}	-	4457.23	-	-	-	9385.27	-	-
Pumping (riser and degasser)	kWh month^{-1}	-	32,572.08	-	-	-	68,584.68	-	-
CO_2 consumption	T	-	1.5	-	-	-	1.80	-	-
Water evaporation	m^3	-	0.095	-	-	-	0.20	-	-
Fermenter	m^3	-	-	-	-	-	-	27.77	133.33
Physical sterilization	kWh month^{-1}	-	-	-	-	-	-	200.49	962.64
Agitation	kWh month^{-1}	-	-	-	-	-	-	145.96	700.78
Aeration	kWh month^{-1}	-	-	-	-	-	-	19,994.4	95,997.6
Raceway pond	m^3	166.66	-	104.16	1388.55	925.9	2677.23	-	-
Electric energy for paddle wheel	kWh month^{-1}	64,797.40	-	40,497.41	539,868.24	359,989.92	1,040,907.02	-	-
Electric energy for water pumping	kWh month^{-1}	11,999.52	-	7499.52	99,975.6	66,664.8	192,760.56	-	-

Table 1 (continued)

Process		Whole dried biomass			Pigment			Polyunsaturated fatty acid	
		Chlorella vulgaris	*Chlorella vulgaris*	*Arthrospira platensis*	*Arthrospira platensis*	*Dunaliella salina*	*Haematococcus pluvialis*	*Crypthecodinium cohnii*	*Nitzschia laevis*
Electric energy for CO_2 injection	kWh month^{-1}	39,598.42	-	24,748.42	329,919.48	219,993.84	636,109.85	-	-
CO_2 consumption	T	2.0	-	2.0	26.66	25.0	64.25		
Water evaporation	m^3	21.67	-	13.54	180.51	120.37	348.04	-	-
Biomass productivity	t m^3 month^{-1}	0.006	0.021	0.0096	0.0096	0.0135	0.012	0.3	0.0225
Output									
Algae liquid	T	11.76	11.42	12.69	71.09	83.3	222.2	44.42	16.0
Harvest									
Input									
Energy consumption centrifugation	kWh month^{-1}	416.65	119.05	260.4	3471.38	2314.75	6943.75	69.43	333.33
Drying									
Input									
Wet biomass	T	8.82	8.55	9.51	53.31	49.98	133.32	33.3	12.0
Spray-dryer	kWh month^{-1}	8523.8	8229.5	9275.9	43,578.2	40,853.2	108,989.1	27,217.3	9810.0
Output									
Whole dried biomass	T	1	1	1	-	-	-	-	-
Extraction									
Input									
Dry biomass	T	-	-	-	13.33	12.5	33.33	8.33	3.0
sCO_2	kWh month^{-1}	-	-	-	10,664.0	10,000.0	26,664.0	6664.0	2400.0
Output									
Oil rich pigments	T	-	-	-	1	1	1	-	-
Oil	T	-	-	-		-	-	1	1
Electricity	kWh month^{-1}	125,335.8	559,673.86	82,281.65	1,027,476.9	699,816.51	3,173,260.23	54,291.58	110,204.35

Adapted from Deprá et al. (2020a), Dias et al. (2022), Fasaei et al. (2018), and Sobczuk et al. (2000)

TPBR tubular photobioreactor, *RP* raceway pond, *sCO_2* supercritical CO_2 extraction

of the portfolio of commercial microalgae-based products, identified that around 98% of the environmental impacts were also due to the electricity requirement and that the remaining were related to the demand for materials.

Table 2 Carbon footprint, action plan to reduce emissions, and remaining emissions from the life cycle of microalgae-based products

	Chlorella vulgaris biomass in RP	*Chlorella vulgaris* biomass in TPBR	*Arthrospira platensis* biomass in RP	Phycocyanin from *Arthrospira platensis*	β-carotene from *Dunaliella salina*	Astaxanthin from *Haematococcus pluvialis*	DHA from *Crypthecodinium cohnii*	EPA from *Nitzschia laevis*
Total emissions (tCO_2e)	152.38	673.07	100.69	1258.96	864.00	3872.07	65.32	133.07
Emission reductions (tCO_2e)								
Renewable/clean electricity								
Nuclear	149.79	668.87	98.33	1227.94	836.35	3792.36	64.88	131.70
Hydro	149.73	668.59	98.29	1227.42	836.00	3790.78	64.86	131.65
Wind	149.29	666.63	98.01	1223.83	833.55	3779.67	64.67	131.26
Biomass	146.39	653.70	96.10	1200.09	817.39	3706.37	63.41	128.72
Photovoltaic	145.45	649.50	95.49	1192.39	812.14	3682.57	63.00	127.89
Biogas	126.59	565.27	83.10	1037.75	706.81	3204.99	54.83	111.31
Natural gas	76.45	341.40	50.19	626.76	426.89	1935.69	33.12	67.22
Waste	68.93	307.82	45.25	565.11	384.90	1745.29	29.86	60.61
Wastewater treatment mitigation	0.03	0.008	0.018	0.249	0.166	0.499	0.005	0.024
Biological carbon capture and use	0.343	0.628	0.214	2.86	1.91	6.84	-	-
Emissions that need to be offset (tCO_2e)								
Renewable/clean electricity								
Nuclear	2.22	3.56	2.12	27.92	25.58	72.36	0.433	1.34
Hydro	2.28	3.84	2.16	28.43	25.93	73.95	0.460	1.40
Wind	2.72	5.80	2.45	32.03	28.38	85.06	0.650	1.78
Biomass	5.61	18.73	4.35	55.76	44.54	158.36	1.90	4.33
Photovoltaic	6.55	22.93	4.97	63.47	49.79	182.16	2.31	5.16
Biogas	25.42	107.16	17.35	218.10	155.11	659.73	10.48	21.74
Natural gas	75.55	331.03	50.26	629.09	435.04	1929.04	32.20	65.82
Waste	83.07	364.61	55.20	690.74	477.03	2119.43	35.46	72.44

DHA docosahexaenoic, *EPA* eicosapentaenoic, *TPBR* tubular photobioreactor, *RP* raceway pond

It is evident, given the contribution of the electricity demand to the carbon footprint, that integrating renewable and clean sources of electricity into microalgal facilities is the key element for carrying out zero-carbon operations. The results in Table 2 confirm the potential to rigorously reduce CO_2 emissions by replacing coal-fired electricity with nuclear, hydro, wind, biomass, photovoltaic, biogas, natural gas, and waste. Replacing the high-carbon fossil electrical matrix with nuclear, hydro, wind, biomass, and photovoltaic saves around 94 to 99% of the CO_2 emissions generated in the bioproduct production, while for biogas, natural gas, and waste it saves in the order of 82 to 84%, 49 to 51%, and 45 to 46% of emissions, respectively.

Nuclear electricity, in terms of carbon emissions, has among the sources assessed the lowest net impact on climate change. Emissions per kWh of electricity for nuclear technology, as well as hydro and wind, are about three orders of magnitude lower than for coal. The emissions for photovoltaic and biomass technologies, in turn, are about two orders of magnitude smaller, while for the others about an order of magnitude smaller (Environmental 2021). By way of addition, the emissions per kWh of electricity for other environmental indicators, besides the global warming potential, can be consulted in the Supplementary Material (Table S2).

About nuclear electricity, despite being the best option in terms of carbon emissions, is not a long-term option worth pursuing. The potential for devastating accidents and the difficulty of nuclear waste management provide evidence that this electricity source is as bad, if not worse, than that of fossil fuels (McCombie and Jefferson 2016). Hydroelectric power is a better option. However, it is must be aware that the construction of hydroelectric facilities deeply affects the surrounding environments due to their large infrastructure. Furthermore, the impact of climate change has unleashed

an irregular climate, casting doubt on its future as a reliable and economical electricity source (Bagher et al. 2015). Electricity from biomass and waste, in turn, present problems of transformation into electricity that are beginning to outweigh the benefits, and electricity from biogas and natural gas, compared to other sources, is not the best choice for the environment, since they contribute more effectively with the increase in the greenhouse effect (Nunes et al. 2017).

Comparatively, although photovoltaic technology presents itself as the fifth-best option to reduce CO_2 emissions, photovoltaic systems, as well as wind systems, are practical to install and present the potential to be implemented for individual use in commercial microalgal facilities. By way of example, Cyanotech Corporation, one of the main companies producing microalgae-based products, installed its own photovoltaic system. By not using the equivalent of 1,147,000 kWh of standard petroleum-based electricity, the company not only reduces greenhouse gas emissions by 791 metric tons of CO_2 per year as but also saves about US$ 123,000 per year in fossil electricity (Cyanotech 2021). About the fossil electricity economy, recent studies have shown relatively short investment return period values for the case of the implementation of photovoltaic and wind systems. Besides that, although there are local variations in the total installed cost and operating and maintenance of these systems, the gains, considering their useful life, outweigh the total implementation costs (Dias et al. 2022).

As for the availability of solar and wind resources, it is well known that they are inherently variable in space. In this regard, it should be noted that, since renewable and clean electricity is the backbone for accomplishing carbon–neutral operations, the local availability of these resources must be taken into account when identifying suitable locations for large-scale microalgal cultivation. About this, when making a geographic examination of microalgal cultivation potential considering specific parameters such as productivity per unit area, availability of low agricultural value land, access to the necessary infrastructure, and the availability of solar and/or wind resources for electricity generation it is possible to identify that North and East Africa, the Middle East, western South America, the Caribbean, and Oceania have the most promising areas for the microalgal culture (Correa et al. 2021; Kapica et al. 2021; Dias et al. 2022). Notoriously, it would be pertinent that the proper locations for the development of microalgal biotechnology were also promising for the establishment of photovoltaic and wind systems or, ultimately, that they were strategically located near renewable and/or clean electricity generation plants.

Simultaneously, besides replacing the electrical matrix, another way to reduce CO_2 emissions through prevention is wastewater treatment mitigation. Unsurprisingly, the clean water supply and distribution systems contain embedded carbons. Nevertheless, with the reuse of cultivation water, the carbon footprint of the water unit (m^3) can be reduced (Hu et al. 2012). As can be seen in Table 2, the wastewater treatment mitigation of microalgae does not have an expressive contribution to reducing the CO_2 metric of the microalgae-based products (<0.1%). However, considering the large volumes of water needed for cultivation, its reuse contributes not only to the mitigation of emissions from the wastewater treatment but also to the reduction of the water footprint and expenditure on nutrients, improving the overall sustainability of the microalgal production systems (Fret et al. 2017).

It is important to highlight that, as for environmental sustainability, despite the carbon footprint being the great villain of the ecological footprint, there are other indicators related to ecosystem quality, human health, and natural resources, including the water footprint, which is also important and will require the same commitment with mitigation in the near future (Jacob-Lopes et al. 2021). The water footprint, particularly from a political perspective, is becoming as important as the carbon footprint. That is because unprecedented pressure on renewable water resources, but finite, is leading to water scarcity and water stress in many regions of the world. And, for this reason, companies committed to the environment have been looking for ways to optimize their production processes. Among the most representative actions in this field is water reuse in its cycles (Hogeboom 2020).

In this narrative, it is also important to highlight that some studies have shown that the reuse of microalgal cultivation water one or even three times has a neutral or sometimes increased effect on cell growth. However, it should be observed that most carried out experiments on a laboratory scale (Morocho-Jácome et al. 2016a, 2016b; Loftus and Johnson 2019; Fret et al. 2020; Lu et al. 2020). In this sense, although life cycle analyses have calculated savings in the nutrient use as well as water and carbon footprint, a question that remains is the effect of water reused on large-scale and long-term microalgal growth, and how many times it can be reused to make the process is cheap and still maintain the productivity and quality of the microalgal biomass.

With regard to so-called CO_2 removal techniques, which are intentional efforts to remove carbon from the atmosphere, biological carbon capture and utilization (BCCU) mediated by microalgae-based processes is an innovative technology with potential applicability for this end (Severo et al. 2020a). Previous studies have evaluated the capture and utilization of CO_2 by photoautotrophic microalgae in photobioreactors and confirmed their potential to convert CO_2 from different sources, including the atmosphere, industrial exhaust gases, and soluble carbonate salts (Jacob-Lopes et al. 2009; Severo et al. 2019; Ayatollahi et al. 2021).

However, although this is true, the photosynthetic capacity of microalgae is relatively low to satisfy practical demands. As can be seen in Table 2, CO_2 capture and use really do not play a significant role in the emission mitigation process. And on this, it is noteworthy that the CO_2 sequestered by microalgae during cultivation only influences the short-term carbon cycle where it is hardly transferred to the long-term cycle. In other words, it can be said that the commercial cultivation of microalgae offers temporary carbon sinks because the only real carbon sinks are part of a long-term cycle. But regardless, these microorganisms act as natural buffers against climate change, capturing and using CO_2 (Hilton and West 2020).

As for the published CO_2 conversion values, unfortunately, these generally refer to bench-scale experiments. In light of that, larger scale experiments are needed to fully explore the actual rates of biological CO_2 conversion. While this continues to be a remaining question, the state of the art of regulation of the Calvin cycle with the purpose of improving the biological conversion of CO_2 in microalgae advances. There is solid evidence that the manipulation of key genes involved in the photosynthetic pathway can increase CO_2 conversion capacity and cell growth (Yang et al. 2017; Cheng et al. 2019). This provides important insights on the potential to enhance biological CO_2 conversion and reduce the proportion of bioreactor volumes, which, consequently, reduces the carbon footprint of electricity consumption of the engineering elements needed in the different cultures.

Finally, in relation to the need for environmental compensation (Table 2), the emission analysis reveals that, for microalgae-based products to become carbon neutral, it would be necessary to offset about 1 to 6% of emissions if considering the use of nuclear electricity, hydroelectric, wind, photovoltaic, and/or biomass in the bioprocesses. In contrast, it would be necessary to offset approximately 16 to 18%, 49 to 55%, and 54 to 55% if considered the use of electricity from biogas, natural gas, and waste, respectively. As can be seen, again nuclear, hydro, and wind electricity, followed by biomass and photovoltaic are indisputably the best options.

Noteworthy, although not contemplated in this study, the redesign of the operational processes through process integration and intensification could provide additional reductions and a lower offset value. Process integration and intensification have emerged as one of the timeliest topics in chemical and process engineering that can actually face the processes enhancement challenges with a reduced environmental footprint (Walmsley et al. 2018). Many integrations and enhancement possibilities applied to microalgae-based systems have been proposed. However, due to the complexity of the integrations and intensification approaches, there are still bottlenecks that need to be elucidated, and these can only be well explained by the application of environmental and economic performance tools (Severo et al. 2020b).

Getting to net-zero is feasible and affordable?

By adhering to a carbon–neutral label, microalga-producing companies can benefit from an enhanced image that gives them a competitive edge. However, the question at hand is not just whether it is worth being carbon neutral, but also how much does it cost to be carbon neutral. According to the International Monetary Fund, the global average price of a ton of carbon is US$ 2. Therefore, considering the different sources of electricity, it would cost around US$ 4–729, US$ 51–4239, and US$ 1–145 in carbon credits to offset the remaining emissions from the one-ton production of whole dried biomass, pigments, and polyunsaturated fatty acids, respectively (Fig. 2). These values represent an increase in sales prices of approximately 0.02–4% (whole dried biomass), 0.01–0.25% (pigments), and 0.001–0.15% (polyunsaturated fatty acids).

As can be seen in Fig. 2, the electricity sources that have the lowest compensation cost and, consequently, the lowest impact on the sales price of the products are the same ones that have the best carbon footprints, that is, nuclear, followed by hydro, wind, biomass, and photovoltaic. In contrast, replacing coal electricity with waste, followed by natural gas and biogas, provides the highest offsetting costs. However, it should be noted that these costs are not significant and that their impact on the selling price remains relatively low. This has given the low global average price of carbon (US$ $t^{-1}CO_2e$).

About this, although about half of carbon emissions are covered with prices below US$ 10 $t^{-1}CO_2e$, and the global average price is calculated at only US$ 2 $t^{-1}CO_2e$, these are values substantially lower than those needed to be consistent with the global treaties, which aim to contain the rise of global warming. In view of this, the jurisdictions are progressively raising the internal carbon price to cost-effectively reduce emissions (Deprá et al. 2021). This is really the case with the European Union (EU), which has increased the internal carbon price by approximately 188% since 2010. The European Union represents a central pillar of climate change policy. Furthermore, besides being the oldest emission trading system for greenhouse gases operating in the world, it has been currently one of the highest carbon prices in the global market (World Bank 2021).

That said, in an attempt to make the analysis of the cost of purchasing carbon credits more sensible, the cost of environmental compensation and its impact on the selling price of microalgae-based products was also calculated using the carbon price of the EU emission trading system. As can be seen in Fig. 3, transforming the carbon footprint of microalgae-based products into a neutral value becomes

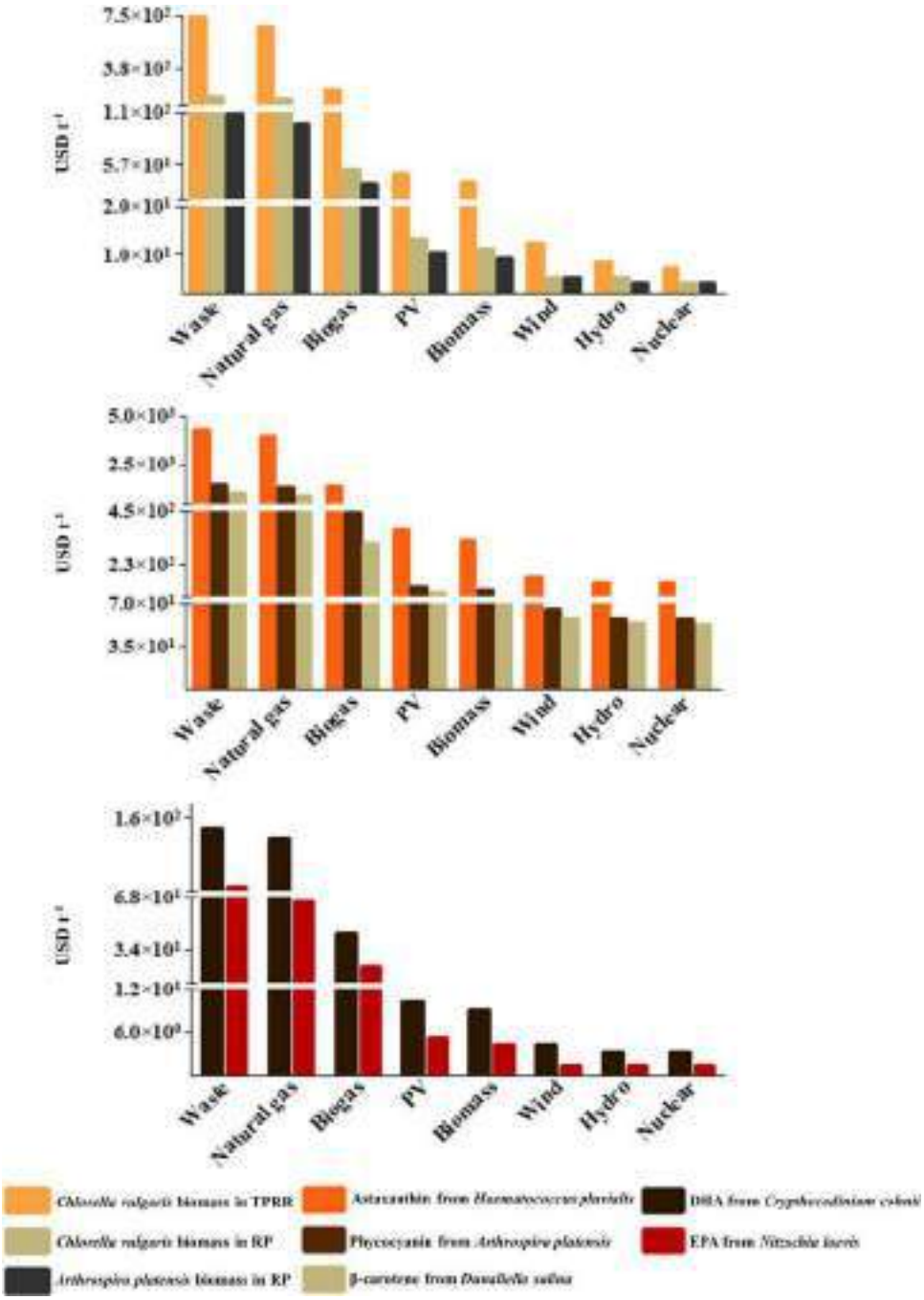


Fig. 2 Environmental offset cost per tonne of bioproduct. Note that the bar graphs consider the global average carbon price of USD 2 t^{-1} CO_2e. *PV* photovoltaic, *DHA* docosahexaenoic, *EP* eicosapentaenoic, *TPBR* tubular photobioreactor, *RP* raceway pond

more expensive. The acquiring carbon credits to offset the unavoidable emissions from the one-ton production of whole dried biomass, pigments, and polyunsaturated fatty acids would cost around US$ 106–18,150, US$ 1273–105,505, and US$ 22–3606, respectively. This corresponds, considering the different sources of electricity, to an increase in the sale price of approximately 0.6 to 95% for whole dried biomass, 0.1 to 6% for pigments, and 0.02 to 4% for polyunsaturated fatty acids.

The role of low-emission electricity sources becomes even more notorious with a high cost of purchasing carbon credits. The replacement of coal electricity with waste and natural gas provides the biggest increases in the sales price of the products. This increase for the case of *Chlorella vulgaris* biomass in TPBR, for example, is equivalent to more than 85%. Undoubtedly, passing this cost on to consumers is unfeasible. In general, the best electricity options that provide the most acceptable costs to be passed on are nuclear, hydro, wind, biomass, and photovoltaic.

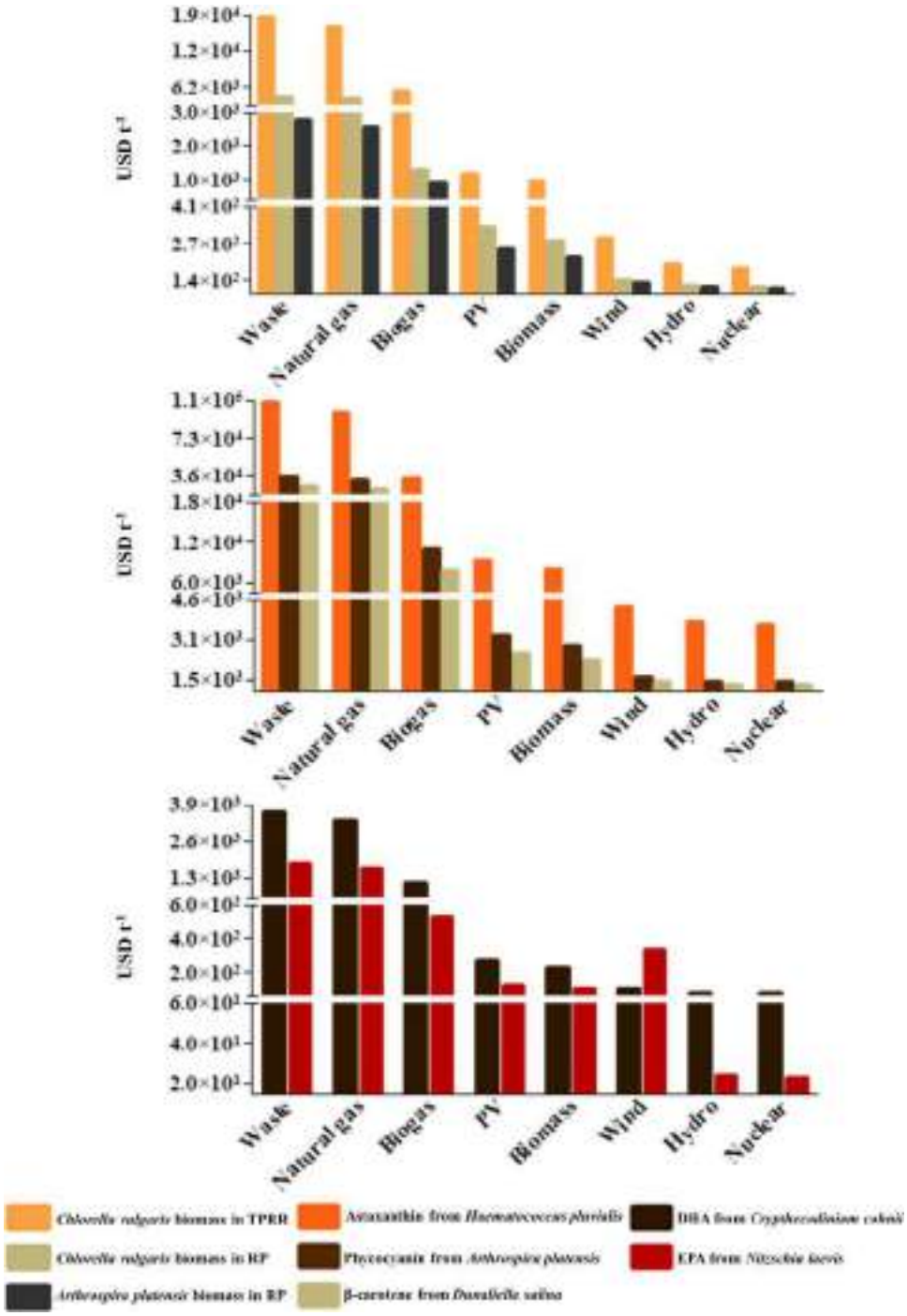


Fig. 3 Environmental offset cost per tonne of bioproduct. Note that the bar graphs consider the carbon price of USD 49.78 t^{-1} CO_2e. *PV* photovoltaic, *DHA* docosahexaenoic, *EPA* eicosapentaenoic, *TPBR* tubular photobioreactor, *RP* raceway pond

Noteworthy, when considering biomass productivities 25, 50, and 75% lower than that considered in the base case, the replacement of coal electricity by nuclear and hydroelectric, followed by wind, biomass, and photovoltaic would continue to provide the most acceptable carbon offset costs to be passed on. According to the sensitivity analysis presented in the Supplementary Material (Table S5A-S6C), this cost would be equivalent to an increase in the selling price of 0.02 to 1.6% for pigments and polyunsaturated fatty acids and 0.6 to 23% for whole dried biomass. On the other hand, the use of electricity from waste, biogas, and natural gas would reach an increase in the selling price of up to 23% for pigments and polyunsaturated fatty acids and up to 377% for whole dried biomass. Given these values, it is indisputable that biomass productivity plays a crucial role in the material and energy requirement of microalgal processes which also directly reflects on the environmental offset cost. But even considering relatively lower biomass productivities than the

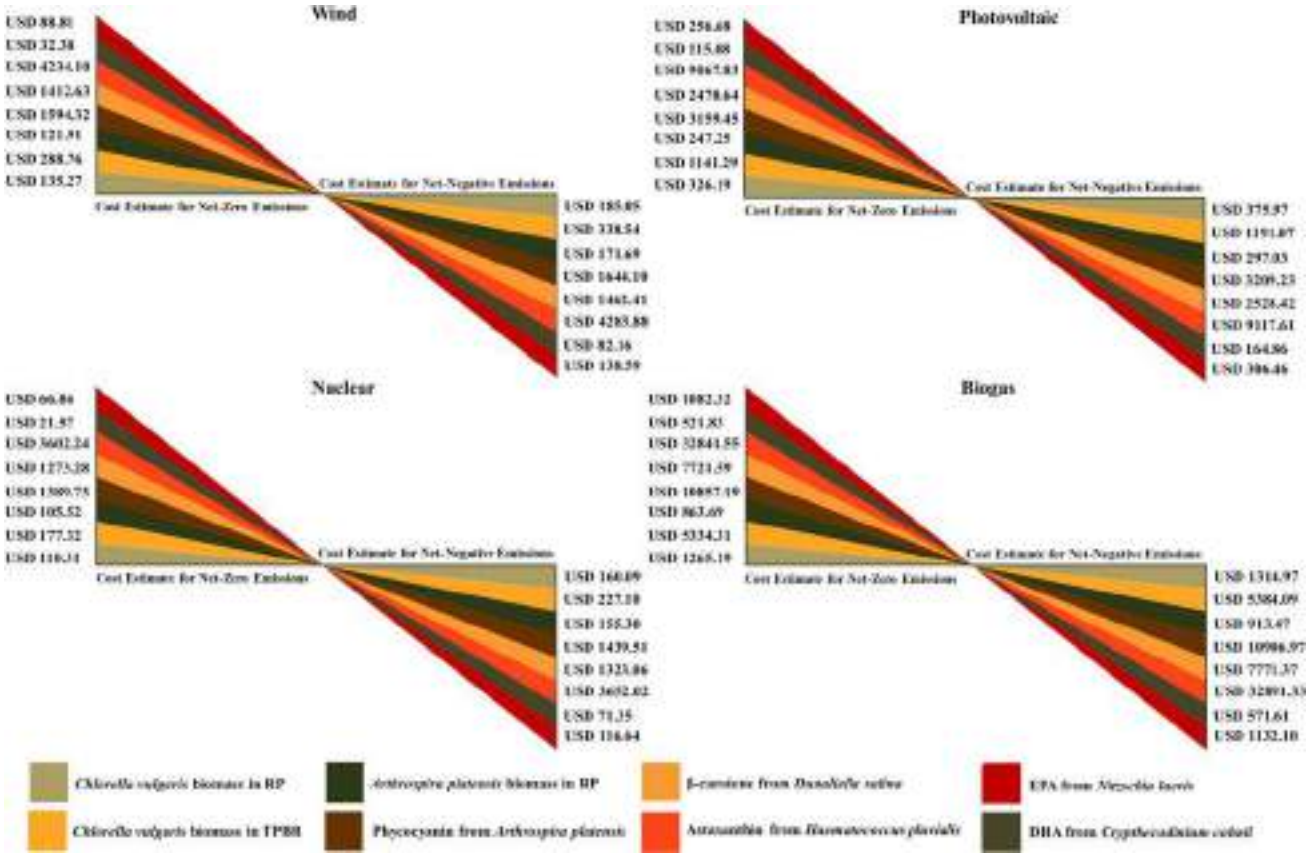


Fig. 4 Estimated cost per tonne of microalgae-based product for net-zero emissions and net-negative emissions. *Note*: considering the replacement of coal electricity by wind, photovoltaic, nuclear, and biogas. *DHA* docosahexaenoic, *EPA* eicosapentaenoic, *TPBR* tubular photobioreactor, *RP* raceway pond

base case, it is notorious that nuclear, hydroelectric, wind, biomass, and photovoltaic electricity sources are the best options for replacing coal electricity.

Furthermore, these five sources of electricity can be seen as enablers of the highest level of climate protection, that is, negative CO_2 emissions. At a minimum addition of US$ 0.05 kg^{-1}, taking into account the base case and the carbon price of the EU emission trading system, the carbon footprint of microalgae-based products could be turned into a negative value. The cost of offset to achieve negative emissions added to that to achieve neutrality is feasible to be passed on to the consumer given its low value. Figures 4 and 5 show the estimated cost per ton of microalgae-based product for net-zero emissions and the cost for net-negative emissions.

As can be seen in Figs. 4 and 5, the estimated cost of achieving negative emissions represents an increase in the selling price of whole dried biomass, pigments, and polyunsaturated fatty acids of 0.26–0.62%, 0.002–0.009%, and 0.04–0.05%, respectively. This value can be low enough to adhere to the label of products with net-negative emissions of CO_2. Nevertheless, it is important to note that it could be higher according to the company's climate ambition.

As for the replacing cost of the electrical matrix in the sale price of microalgae-based products, it is worth mentioning that we do not consider it in this study. However, renewable electricity, in particular, has entered a virtuous cycle of falling costs (US$ kWh^{-1}). A significant and unnecessary barrier to its implementation is, actually, the outdated perception that renewable electricity is not competitive. It is competitive and it is possible that it becomes the cheapest form of electricity in the world. This is particularly true with regard to photovoltaic and wind electricity (IRENA 2021).

Finally, although there is an upward trend in carbon prices, in some jurisdictions the emissions are currently covered at a price of US$ 1–5 $t^{-1}CO_2e$. In these jurisdictions, it may be less expensive to invest in sinks (purchase of carbon credits) than to reduce emissions by adopting cleaner production approaches. However, it seems clear that, sooner or later, just compensating will not be economically viable. In the long term, it will be, ultimately, cheaper to commence the process of solutions implementing than delaying what

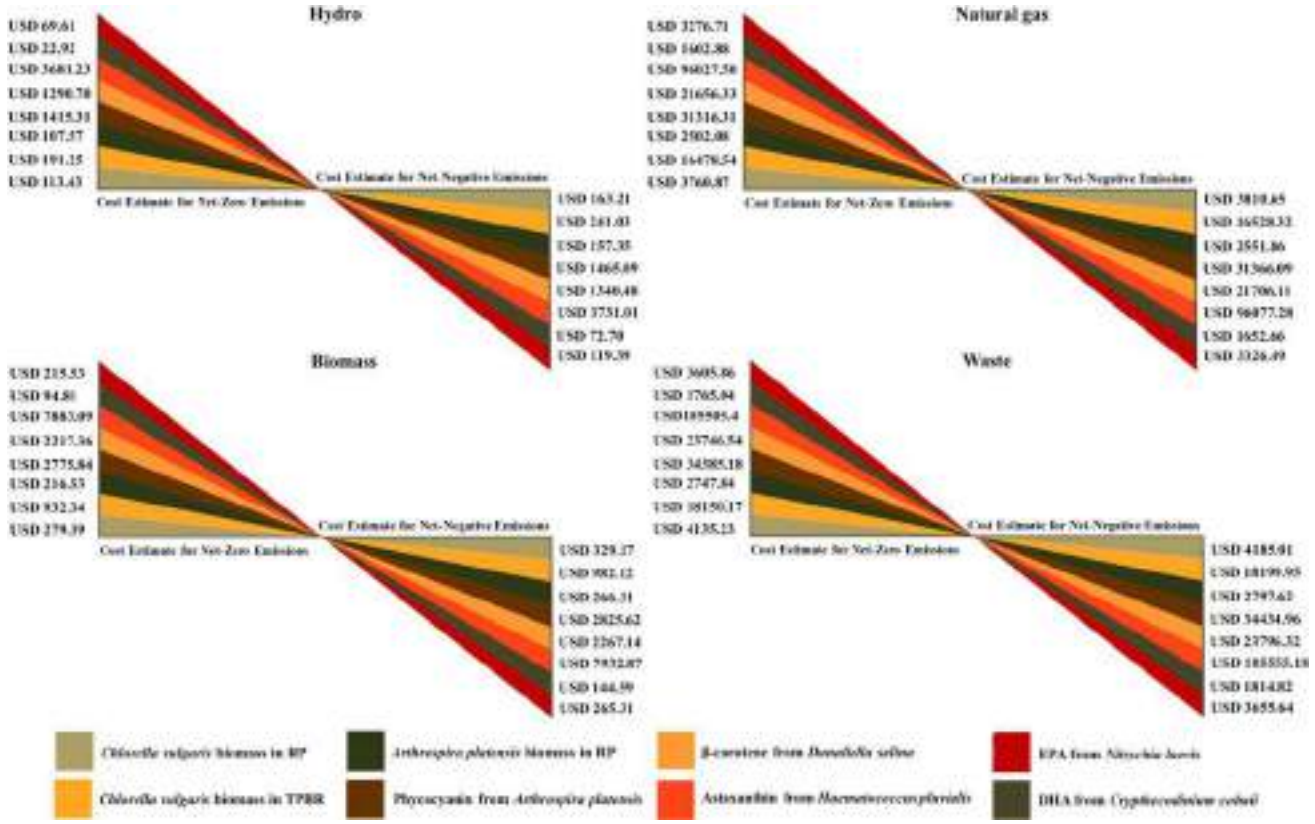


Fig. 5 Estimated cost per tonne of microalgae-based product for net-zero emissions and net-negative emissions. *Note*: considering the replacement of coal electricity by hydro, natural gas, biomass, and waste. *DHA* docosahexaenoic, *EPA* eicosapentaenoic, *TPBR* tubular photobioreactor, *RP* raceway pond

will ultimately unlock a greener future for the microalgal industry.

Conclusion

The main objective of this study was to show that microalgal production can achieve low carbon emissions and, consequently, a low net impact on climate change. The potential for implementing the principle of carbon neutrality in microalgal facilities has been confirmed. Our study highlighted that the replacement of the electrical matrix in microalgal installations is the definitive key to carrying out carbon–neutral operations. Furthermore, the end result of rigorously reducing CO_2 emissions and offsetting remaining emissions is a zero-emission microalgae-based product that, as a whole, stands for climate action. The "carbon–neutral" label shows that the process of reducing carbon emissions has already started. Under this horizon, from a business point of view, welcoming net-zero emission labels is a great step in the right direction, as prioritizing environmental sustainability outweighs the cost of doing nothing.

Supplementary Information The online version contains supplementary material available at https://doi.org/10.1007/s10811-022-02725-y.

Acknowledgements The authors would like to thank the National Council for Scientific and Technological Development (CNPq) – Brazil, and the Coordination of Improvement of Higher Education Personnel (CAPES), Finance Code 001.

Author contribution Rosangela Rodrigues Dias: conceptualization, methodology, data curation, writing — original draft. Mariany Costa Deprá: methodology, data curation. Leila Queiroz Zepka: supervision, funding acquisition. Eduardo Jacob-Lopes: conceptualization, project administration, writing — review and editing.

Availability of data and materials The authors declare that (the/all other) data supporting the findings of this study are available within the article (and its supplementary information files).

Declarations

Competing interests The authors declare no competing interests.

References

Ayatollahi SZ, Esmaeilzadeh F, Mowla D (2021) Integrated CO_2 capture, nutrients removal and biodiesel production using *Chlorella vulgaris*. J Environ Chem Eng 9:104763

Bagher AM, Vahid M, Mohsen M, Parvin D (2015) Hydroelectric energy advantages and disadvantages. Am J Energy Sci 2:17

Basu S, Roy AS, Mohanty K, Ghoshal AK (2014) CO_2 biofixation and carbonic anhydrase activity in *Scenedesmus obliquus* SA1 cultivated in large scale open system. Bioresour Technol 164:323–330

Becker S, Bouzdine-Chameeva T, Jaegler A (2020) The carbon neutrality principle: a case study in the French spirits sector. J Clean Prod 274:122739

Birkenberg A, Birner R (2018) The world's first carbon neutral coffee: lessons on certification and innovation from a pioneer case in Costa Rica. J Clean Prod 189:485–501

Cai W, Lai KH, Liu C, Wei F, Ma M, Jia S, Jiang Z, Lv L (2019) Promoting sustainability of manufacturing industry through the lean energy-saving and emission-reduction strategy. Sci Total Environ 665:23–32

Cheng J, Zhu Y, Zhang Z, Yang W (2019) Modification and improvement of microalgae strains for strengthening CO_2 fixation from coal-fired flue gas in power plants. Bioresour Technol 291:121850

Chiriaco MV, Belli C, Chiti T, Trotta C, Sabbatini S (2019) The potential carbon neutrality of sustainable viticulture showed through a comprehensive assessment of the greenhouse gas (GHG) budget of wine production. J Clean Prod 225:435–450

Choi AS, Ritchie BW (2014) Willingness to pay for flying carbon neutral in Australia: an exploratory study of offsetter profiles. J Sustain Tour 22:1236–1256

Correa DF, Beyer HL, Possingham HP, Fargione JE, Hill JD, Schenk PM (2021) Microalgal biofuel production at national scales: reducing conflicts with agricultural lands and biodiversity within countries. Energy 215:119033

Cui Q, Li Y (2017) Will airline efficiency be affected by "Carbon neutral growth from 2020" strategy? Evidences from 29 international airlines. J Clean Prod 164:1289–1300

Cyanotech (2021) Our history. https://www.cyanotech.com/our-history/. Accessed 13 July 2021

Deprá MC, Dias RR, Sartori RB, da Silva PA, de Oliveira AS, Zepka LQ, Jacob-Lopes E (2021) Carbon footprint on microalgae-based processes. In: Justin AD (ed) Advances in environmental research. Nova Science Publishers, New York, pp 203–222

Deprá MC, Dias RR, Severo IA, de Menezes CR, Zepka LQ, Jacob-Lopes E (2020) Carbon dioxide capture and use in photobioreactors: the role of the carbon dioxide loads in the carbon footprint. Bioresour Technol 314:123745

Deprá MC, Severo IA, dos Santos AM, Zepka LQ, Jacob-Lopes E (2020) Environmental impacts on commercial microalgae-based products: sustainability metrics and indicators. Algal Res 51:102056

Dias RR, Deprá MC, Severo IA, Zepka LQ, Jacob-Lopes E (2022) Smart override of the energy matrix in commercial microalgae facilities: a transition path to a low-carbon bioeconomy. Sustain Energy Technol Assess 52:102073

Dias RR, Severo IA, Deprá MC, Maroneze MM, Zepka LQ, Jacob-Lopes E (2020) The next-generation of microalgae-based products. In: Shukla P (ed) Microbial enzymes and biotechniques. Springer, Singapore, pp 15–42

ECIU (2022) Net zero scorecard. https://eciu.net/netzerotracker. Accessed 14 Feb 2022

Environmental (2021) Environmental impacts of electricity production technologies in Slovenia. http://lab.fs.uni-lj.si/kes/erasmus/LCA%20report%20for%20Slovenian%20electricity%20generation%20technologies.pdf. Accessed 13 July 2021

Fantozzi F, Bartocci P, D'Alessandro B, Testarmata F, Fantozzi P (2015) Carbon footprint of truffle sauce in central Italy by direct measurement of energy consumption of different olive harvesting techniques. J Clean Prod 87:188–196

Fasaei F, Bitter JH, Slegers PM, Van Boxtel AJB (2018) Techno-economic evaluation of microalgae harvesting and dewatering systems. Algal Res 31:347–362

Fernández FGA, Reis A, Wijffels RH, Barbosa M, Verdelho V, Llamas B (2021) The role of microalgae in the bioeconomy. N Biotechnol 61:99–107

Fret J, Roef L, Blust R, Diels L, Tavernier S, Vyverman W, Michiels M (2017) Reuse of rejuvenated media during laboratory and pilot scale cultivation of *Nannochloropsis* sp. Algal Res 27:265–273

Fret J, Roef L, Diels L, Tavernier S, Vyverman W, Michiels M (2020) Combining medium recirculation with alternating the microalga production strain: a laboratory and pilot scale cultivation test. Algal Res 46:101763

Gills B, Morgan J (2020) Global climate emergency: after COP24, climate science, urgency, and the threat to humanity. Globalizations 17:885–902

Gils HC, Simon S (2017) Carbon neutral archipelago—100% renewable energy supply for the Canary Islands. Appl Energy 188:342–355

GlobeNewswire (2021) $4.6 billion worldwide microalgae industry to 2027 — impact of COVID-19 on the market. https://www.globenewswire.com/en/news-release/2020/09/18/2095854/28124/en/4-6-Billion-Worldwide-Microalgae-Industry-to-2027-Impact-of-COVID-19-on-the-Market.html. Accessed 13 July 2021

Guieysse B, Plouviez M (2021) Sustainability of microalgae cultivation. In: Lafarga T, Acien G (eds) cultured microalgae for the food industry: current and potential applications. Academic Press, NY, pp 343–365

Hilton RG, West AJ (2020) Mountains, erosion and the carbon cycle. Nat Rev Earth Environ 1:284–299

Hogeboom RJ (2020) The water footprint concept and water's grand environmental challenges. One Earth 2:218–222

Hu AH, Wang LH, Fan CW, Lin YZ, Lin JH, Yao KF, Nien P-F, Feng Y-T, Kuo W-M (2012) Carbon footprint assessment of water supply systems in Taiwan. In: Matsumoto M, Umeda Y, Masui K, Fukushige S (eds) Design for innovative value towards a sustainable society. Springer, Dordrecht, pp 318–322

IRENA (2021) Costs. https://www.irena.org/costs. Accessed 13 July 2021

ISO (2006) ISO-14040 Environmental management–life cycle assessment—principles and framework. International Organization for Standardization

Jacob-Lopes E, Maroneze MM, Deprá MC, Sartori RB, Dias R, Zepka LQ (2019) Bioactive food compounds from microalgae: an innovative framework on industrial biorefineries. Curr Opin Food Sci 25:1–7

Jacob-Lopes E, Revah S, Hernández S, Shirai K, Franco TT (2009) Development of operational strategies to remove carbon dioxide in photobioreactors. Chem Eng J 153:120–126

Jacob-Lopes E, Zepka LQ, Deprá MC (2021) Sustainability indicators and metrics of environmental impact: industrial and agricultural life cycle assessment. Elsevier, Amsterdam

Kapica J, Canales FA, Jurasz J (2021) Global atlas of solar and wind resources temporal complementarity. Energy Convers Manag 246:114692

Loftus SE, Johnson ZI (2019) Reused cultivation water accumulates dissolved organic carbon and uniquely influences different marine microalgae. Front Bioeng Biotechnol 7:101

Lu Z, Loftus S, Sha J, Wang W, Park MS, Zhang X, Johnson ZI, Hu Q (2020) Water reuse for sustainable microalgae cultivation: current knowledge and future directions. Resour Conserv Recycl 161:104975

McCombie C, Jefferson M (2016) Renewable and nuclear electricity: comparison of environmental impacts. Energy Policy 96:758–769

Morocho-Jácome AL, Mascioli GF, Sato S, de Carvalho JCM (2016a) Evaluation of physicochemical treatment conditions for the reuse of a spent growth medium in *Arthrospira platensis* cultivation. Algal Res 13:159–166

Morocho-Jácome AL, Sato S, de Carvalho JCM (2016b) Ferric sulfate coagulation and powdered activated carbon adsorption as simultaneous treatment to reuse the medium in *Arthrospira platensis* cultivation. J Chem Technol Biotechnol 91:901–910

Motive Power (2022) Carbon neutral goals by country. https://www.motive-power.com/npuc-resource/carbon-neutral-goals-by-country/#:~:text=As%20far%20as%20early%20achievers,more%20carbon%20than%20they%20emit. Accessed 14 Feb 2022

Natural Capital Partners (2021) The carbonneutral protocol: the global standard for carbon neutral programmes. https://www.carbonneutral.com/pdfs/The_CarbonNeutral_Protocol_Jan_2021.pdf. Accessed 13 July 2021

Nunes LJR, Matias JCO, Catalão JPS (2017) Biomass in the generation of electricity in Portugal: a review. Renew Sust Energ Rev 71:373–378

Papadaki S, Kyriakopoulou K, Tzovenis I, Krokida M (2017) Environmental impact of phycocyanin recovery from *Spirulina platensis* cyanobacterium. Innov Food Sci Emerg Technol 44:217–223

Pérez-López P, González-García S, Jeffryes C, Agathos SN, McHugh E, Walsh D, Murray P, Moane S, Feijoo G, Moreira MT (2014) Life cycle assessment of the production of the red antioxidant carotenoid astaxanthin by microalgae: from lab to pilot scale. J Clean Prod 64:332–344

Schade S, Meier T (2020) Distinct microalgae species for food—part 1: a methodological (top-down) approach for the life cycle assessment of microalgae cultivation in tubular photobioreactors. J Appl Phycol 32:2977–2995

Schade S, Meier T (2021) Techno-economic assessment of microalgae cultivation in a tubular photobioreactor for food in a humid continental climate. Clean Technol Environ Policy 23:1475–1492

Severo IA, Deprá MC, Dias RR (2020a) Process integration applied to microalgae-based systems. In: Jacob-Lopes E, Maroneze MM, Queiroz MI, Zepka LQ (eds) Handbook of microalgae-based processes and products. Academic Press, NY, pp 709–735

Severo IA, Depra MC, Dias RR, Barin JS, de Menezes CR, Wagner R, Zepka LQ, Jacob-Lopes E (2020a) Bio-combustion of petroleum coke: the process integration with photobioreactors. Part II—sustainability metrics and bioeconomy. Chem Eng Sci 213:115412

Severo IA, Deprá MC, Jacob-Lopes E (2019) Carbon dioxide capture and use by microalgae in photobioreactors. In: Pires JCM, Goncalves ALC (eds) Bioenergy with carbon capture and storage. Academic Press, NY, pp 151–171

Sobczuk TM, Camacho FG, Rubio FC, Fernández FA, Grima EM (2000) Carbon dioxide uptake efficiency by outdoor microalgal cultures in tubular airlift photobioreactors. Biotechnol Bioeng 67:465–475

Vuppaladadiyam AK, Prinsen P, Raheem A, Luque R, Zhao M (2018) Sustainability analysis of microalgae production systems: a review on resource with unexploited high-value reserves. Environ Sci Technol 52:14031–14049

Walmsley TG, Varbanov PS, Su R, Ong B, Lal N (2018) Frontiers in process development, integration and intensification for circular life cycles and reduced emissions. J Clean Prod 201:178–191

World Bank (2021) Carbon Pricing Dashboard. https://carbonpricingdashboard.worldbank.org/map_data. Accessed 13 July 2021

Yadav G, Dubey BK, Sen R (2020) A comparative life cycle assessment of microalgae production by CO_2 sequestration from flue gas in outdoor raceway ponds under batch and semi-continuous regime. J Clean Prod 258:120703

Yang B, Liu J, Ma X, Guo B, Liu B, Wu T, Jiang Y, Chen F (2017) Genetic engineering of the Calvin cycle toward enhanced photosynthetic CO_2 fixation in microalgae. Biotechnol Biofuels 10:229

Publisher's note Springer Nature remains neutral with regard to jurisdictional claims in published maps and institutional affiliations.

World Journal of Microbiology and Biotechnology (2022) 38:150
https://doi.org/10.1007/s11274-022-03342-0

REVIEW

Microalgae-derived polysaccharides: Potential building blocks for biomedical applications

Ihana A. Severo[1] · Rosangela R. Dias[2] · Tatiele C. do Nascimento[2] · Mariany C. Deprá[2] · Mariana M. Maroneze[2] · Leila Q. Zepka[2] · Eduardo Jacob-Lopes[2]

Received: 21 January 2022 / Accepted: 20 June 2022
© The Author(s), under exclusive licence to Springer Nature B.V. 2022

Abstract

In recent years, the increasing concern about human health well-being has strongly boosted the search for natural alternatives that can be used in different fields, especially in biomedicine. This has put microalgae-based products in evidence since they contain many bioactive compounds, of which polysaccharides are attractive due to the diverse physicochemical properties and new or improved biological roles they play. Polysaccharides from microalgae, specially exopolysaccharides, are critically important for market purposes because they can be used as anti-inflammatory, immunomodulatory, anti-glycemic, antitumor, antioxidant, anticoagulant, antilipidemic, antiviral, antibacterial, and antifungal agents. Therefore, to obtain higher productivity and competitiveness of these naturally available compounds, the cultivation parameters and the extraction/purification processes must be better optimized in order to bring perspectives for the exploitation of products in commercial and clinical practice. In this sense, the objective of the present review is to elucidate the potential biomedical applications of microalgae-derived polysaccharides. A closer look is taken at the main polysaccharides produced by microalgae, methods of extraction, purification and structural determination, biological activities and their applications, and current status.

Keywords Microalgae · Bioactive substances · Biological activities · Exopolysaccharides · Extraction techniques

Introduction

Over the last few years, the interest of researchers, developers, and industrialists has increased significantly in natural products directed to promote improvements in human health from aquatic organisms, such as microalgae and cyanobacteria. These two photosynthetic microorganisms, eukaryotic and prokaryotic, respectively, have been extensively studied because of their versatility in producing many valuable compounds for commercial purposes (Russell et al. 2022).

The term "microalgae" is commonly assigned to cyanobacteria because, although they have different biological attributes, the principles of microorganism maintenance and cultivation, products formed and applications are equal. They represent a very distinct group, including more than 72,500 species already identified in marine environments, freshwater, lakes, and even desert areas. In taxonomic terms, these organisms are divided into 16 classes, of which the most plentiful in nature are the diatoms (*Bacillariophyceae*), the green algae (*Crysophyceae*), and the golden algae (*Chrysophyceae*). Conversely, the green algae, the cyanobacteria (*Cyanophyceae*), and the diatoms are the most expressive in the biotechnology field (Jacob-Lopes et al. 2019). These microorganisms use solar energy, water, organic and inorganic nutrients, and fix CO_2 with great efficiency for cell growth. They can be cultivated in open systems, such as raceway ponds, or in closed systems, such as photobioreactors, which have various configurations and are more suitable for biomass propagation (Assunção and Malcata 2020).

This vast diversity makes microalgae very attractive for prospecting countless products that can be extracted from its biomass, which is rich in proteins, lipids, and carbohydrates, in addition to many small molecules (Rempel et al. 2019). Biomolecules derived from these compounds include natural pigments (e.g. carotenoids, chlorophylls, phycobiliproteins)

✉ Ihana A. Severo
ihana.aguiar@gmail.com; ihanasevero@ufpr.br

[1] Sustainable Energy Research and Development Center (NPDEAS), Federal University of Paraná (UFPR), P.O. Box 19011, Curitiba, PR 81531-980, Brazil

[2] Department of Food Science and Technology, Federal University of Santa Maria (UFSM), Roraima Avenue, 1000, Santa Maria, RS 97105-900, Brazil

(Santos and Bicas 2021), polyunsaturated fatty acids, vitamins, and especially bioactive polysaccharides, whose benefits are numerous (Fernandes et al. 2021; Silvello et al. 2022; Chandrasekhar et al. 2022). When refined, these compounds are unique raw materials for several industries, allowing successful applications in areas such as human nutrition (Jacob-Lopes et al., 2019), animal feed, agricultural (Chanda et al. 2019), biofuels (El-Sheekh et al. 2013), pharmaceuticals, cosmetics, biomedical products, as well as uses in environmental bioremediation (e.g. wastewater treatment and CO_2 capture) (Deprá et al. 2018; Nisar et al. 2021). However, the development and competitiveness of these products are still premature and only a few specific niches are available on the market (Severo et al. 2019, 2021).

Among the many biocompounds from microalgae, polysaccharides are very promising because of their ability to form hydrogels, rheology modifiers, texturizing, and emulsifying agents, whose uses are already established. Nonetheless, many polysaccharides are emerging as suitable materials for various biomedical applications. Today, there is a strong appeal for natural medicines but only a few types of polysaccharides, extracted from a handful of microalgae, are explored (Beaumont et al. 2021).

Polysaccharides are high molecular weight carbohydrates present in all living organisms, presenting a great diversity of novel or improved biochemical properties compared with synthetic polysaccharides, as well as those obtained from other natural sources. Microalgae contain considerable amounts of polysaccharides as the main constituent of the cell wall, which gives them strength and flexibility to support the aquatic environment and maintain ionic balance (Morais et al. 2022a). They are classified into homopolysaccharides, which are composed of only one type of repeating monosaccharide (e.g., starch, glycogen, and cellulose), and heteropolysaccharides, which are composed of two or more types of monosaccharide units. Based on this, they can be divided into three different categories: 1) structural cell wall polysaccharides; 2) storage polysaccharides, which are intracellular (they are not completely released into the medium and remain attached to the cell); and 3) matrix polysaccharides released into the environment, called exopolysaccharides (EPS) or extracellular polymeric substances (Mohammed et al. 2021; Laroche 2022). EPSs are of particular interest because they are easily synthesized and excreted by microalgae as a function of the adaptation mechanism of these microorganisms to certain stress factors such as luminosity, temperature, pH, depletion of nutrients, and toxic substances (Costa et al. 2021).

The evaluation of structures, compositions, functions, and characteristics of polysaccharides is crucial for understanding their production mechanism and attributes for biomedical applications. In this field, polysaccharides have appeared as highly useful materials for drug delivery, wound healing, and tissue engineering systems (Bilal and Iqbal 2020). Also, due to their various physicochemical properties and biological activities, EPS exhibits important biomedical uses, including mainly anti-inflammatory, immunomodulatory, anti-glycemic, antitumor, antioxidant, anticoagulant, antilipidemic, antiviral, antibacterial, and antifungal activities (Levine and Fleurence 2018; Kang et al. 2020; Dias et al. 2020; do Nascimento et al. 2021).

The plethora of research being conducted to further elucidate the full potential of polysaccharides is part of the realization that this substance is capable of putting microalgae under the scientific spotlight as producers of a key bioactive compound in biomedicine, according to previous reviews (Raposo et al. 2015; Venkatesan et al. 2015, 2017; Zhong et al. 2021; Beaumont et al. 2021; Arlov et al. 2021; Morais et al. 2021). To further push these issues, several paths are possible and different points of view are discussed in this work. One of them is to present the possible activities and uses of polysaccharides in human health. This demands a deep comprehension of their physicochemical characteristics, which can be modified to acquire specific functions in the biomedicine field. In parallel, these aspects can be improved through knowledge of current and emerging extraction and purification techniques. In view of the above, the objective of this study is to elucidate the potential biomedical applications of microalgae-derived polysaccharides. This review critically discusses (i) the main polysaccharides produced by microalgae, (ii) the methods of extraction, purification, and structural determination, (iii) biological activities and potential biomedical applications of microalgal polysaccharides, as well as (iv) current status.

Polysaccharides produced by microalgae

Polysaccharides have been exploited by the industry for several decades because of their properties as thickening or gelling agents. Nowadays, they have attracted attention due to the detection of biological activities for biomedical purposes. It is known that hundreds of polysaccharides have been isolated from different sources (e.g. animal, plant, microbes and algae). However, those obtained from microalgae have superior advantages over other sources because these microorganisms can be cultivated using liquid or gaseous effluents as a nutrients source, without the demand for arable land, relatively high productivity rates, and uncomplicated control of operating parameters (Laroche 2022). These biomolecules are necessary for the life of microalgae as they are responsible for energy reserves in cells. In general, a fraction of them is released into the medium under both normal and adverse conditions, the so-called exopolysaccharides (Marcati et al. 2014).

Most microalgae polysaccharides are heteropolymers, that is, they are macromolecules with a chain composed of a mixture of two or more different monomeric units, consisting mainly of galactose, xylose, and glucose. Other sugars such as arabinose, fucose, mannose, rhamnose, and glucuronic and galacturonic acid residues can also be constituents of these macromolecules (Dias et al. 2020). There are data for polysaccharides produced by the most different classes of microalgae. Among these classes, green algae (*Chlorophyta*), cyanobacteria (*Cyanophyta*), and red algae (*Rhodophyta*) seem to be the most significant in terms of exploitation of bioactive polysaccharides. *Porphyridium* sp., *Chlorella* sp., and *Arthrospira* sp. have been extensively studied to produce these biologically active macromolecules (Jacob-Lopes et al. 2019; Costa et al. 2021). An overview of species with the potential to generate polysaccharides, as well as their respective polysaccharides of commercial interest, main sugars, and biological activities proved in vitro and/or in vivo is shown in Table 1.

The microalgae, with some exceptions, do not have proper names for their polysaccharides (Raposo and Morais 2015). Few studies have investigated in detail the polysaccharides from these microorganisms, and it can be said that none of them led to a complete and well-defined structure. Obviously, the polysaccharide structures of microalgae are complex structures that differ from species to species and by cultivation conditions. However, it is worth highlighting that detailed structural information is necessary to establish

Table 1 Microalgae species that produce polysaccharides, main sugars, and biological activity in vitro and/or in vivo. Data are not exhaustive

Specie	Polysaccharide	Main sugars	Biological activity	in vitro/in vivo	Reference
Chlorella ellipsoidea	PS	Rham, Mann, Gal	Immunomodulatory	in vitro	Qi and Kim (2017)
Chlorella stigmatophora	PS	Glc, Xyl, Fuc	Anti-inflammatory, immunomodulatory	in vitro/in vivo	Guzmán et al. (2003)
Chlorella zofingiensis	EPS	Mann, Glc, Gal; Glu	Antioxidant, antitumor	in vitro	Zhang et al. (2019b)
Chlorella pyrenoidosa	PS	Fuc, Rha, Ara, Glc, GlcA, Xyl, Man	Hypolipidemic	in vivo	Wan et al. (2019)
Dunaliella salina	SPs	Glc, Gal, Ara, Xyl, Mann, Rham, Fuc, Rib, GalA, GlcA	Antioxidant, antiviral	–	Dai et al. (2010)
Tetraselmis sp.	PS	–	Antioxidant, antifungal	in vitro	Kashif et al. (2018)
Chlamydomonas reinhardtii	EPS	Ara, Rham, Rib, Xyl, Gal, Glc, GalA	Antioxidant	in vitro	Bafana (2013)
Graesiella sp.	EPS	Glc, Gal, Mann, Fuc, Rham, Xyl, Ara, Rib	Antiproliferative	in vitro	Trabelsi et al. (2016)
Chlorella vulgaris	EPS	Gal, Ara, Rham,, Mann, Glc, Xyl	Anti-asthmatic, anti-inflammatory, antitussive	in vivo	Barboríková et al. (2019)
Chlorella vulgaris	EPS	Mann, Glc, Gal, Ara, Glu	Antioxidant, antitumor	in vitro	Zhang et al. (2019b)
Haematococcus pluvialis	PS	Glc, Gal, Fuc, Ara, Mann, Xyl, Rham	Antiviral	in vitro	Santoyo et al. (2012)
Arthrospira platensis	SPs	Rham, Fuc, Glc, 3-O-Methyl-Rham	Antiproliferative, antiadhesive, antiviral	–	Raposo et al. (2013)
Arthrospira platensis	SPs	Rham, Xyl, Mann, Glc, Gal, GalA, GlcA	Anticoagulant	in vitro	Majdoub et al. (2009)
Arthrospira maxima	SPs	Rham, Fuc, Glc, 3-O-Methyl-Rham	Antiviral	in vitro	Hernández-Corona et al. (2002)
Nostoc flagelliforme	PS	Glc, Gal, Mann, GalA	Antioxidant	in vitro	Shen et al. (2018)
Nostoc commune	PS	Rib, Ara, Xyl, Mann, Glc	Antioxidant, antibacterial	in vitro	Quan et al. (2015)
Gyrodinium impudicum strain KG03	EPS	Gal	Immunomodulatory, antiviral	in vitro	Yim et al. (2004)
Gracilariopsis lemaneiformis	SPs	Gal, Glc, Mann, Xyl, Ara, Rham, Fuc	Antitumor	in vitro	Kang et al. (2017)
Porphyridium cruentum	EPS	–	Anti-glycemic	in vivo	Setyaningsih et al. (2020)
Porphyridium sp.	SPs	–	Antilipidemic; hypocholesterolemic; Antitumor	in vivo	Ginzberg et al. (2000); Dvir et al. (2009); Gardeva et al. (2014)
Porphyridium sp.	SPs	Xyl	Antiviral	in vitro	Ginzberg et al. (2008)

relationships between biological structures and activities and, thus, develop future-oriented technologies (Delattre et al. 2016).

A closer look at the production of microalgae polysaccharides is also crucial to leading the technology to market. This is because, besides having an impact on the chemical structure of polysaccharides, it affects productivity. Regarding the culture parameters for polysaccharide production, the effects of cultivation conditions on production are species-dependent, but polysaccharide synthesis is related to normal physiological processes or stressful conditions applied to the producing microorganism (Costa et al. 2021). The nutrient limitation is commonly used to increase polysaccharide accumulation. However, since biomass productivity is generally reduced under these conditions, the two-stage cultivation can be applied to obtain a high yield of polysaccharides associated with high biomass productivity. The strategy is based on a growth phase with ideal culture conditions, followed by a production phase with nutrient deprivation. Alternative strategies include exposure to the high luminous intensity and optimal temperature conditions. Notably, the development of customized microalgae cultivation strategies can lead to efficient production of biomass and polysaccharides in terms of both quality and quantity; however, this is a real challenge. Furthermore, considering the particularities of each microalgae species, it is difficult to reach a global approach, which is regrettable (Pierre et al. 2019). Figure 1 outlines a general summary of the process of obtaining microalgae polysaccharides, the most common species, and their biological properties.

Extraction, purification, and structural determination methods

After the microalgae cultivation stage under favorable conditions for the production of the polysaccharide content, it is important that the exploration procedure for the target product is as efficient, green, and economical as possible. Thus, the scientific community worldwide should look more closely at systematic and robust methodologies that can contribute to the improvement of extraction performance. Furthermore, to obtain these compounds with maximum biomedical activities, purification and structural determination approaches must be well established (Yang and Zhang 2009).

Given these aspects, microalgal polysaccharide extraction procedures involve a series of steps that include the preparation and pretreatment of the biomass before extraction, followed by conventional and advanced extraction techniques, purification methods, and structural characterization to obtain the desired compound (Wassie et al. 2021), as shown in Fig. 2. It is worth mentioning that the extraction methods can be organized according to polysaccharides of interest: storage (SP), related to the cell wall (CWP), and those secreted in the culture medium (EPS).

Biomass preparation begins when the cultivation stage ceases, whose process consists of harvesting cells, generally by centrifugation, separating the pellet from the supernatant and drying in air, lyophilization, or in an oven. The biomass can also be subjected to the milling procedure to generate even finer particles and increase the contact surface, thus allowing better interaction with the solvent (Nigam et al. 2021).

Subsequently, several pre-treatments can be applied to the biomass, including many types of solvents and their mixtures with different polarities that do not affect the polysaccharide structure. These procedures are used to remove low molecular weight compounds that are attached to the carbohydrate. As reviewed by Nigam et al. (2021), solvents such as formaldehyde, acetone, methanol, petroleum ether or mixtures with methanol, chloroform and water can be efficiently used to extract different types of polysaccharides. Evidently, solvents have demerits in terms of toxicity and environmental impact, so new methods have been researched and developed (Costa et al. 2021).

Extraction is the key step in polysaccharide isolation. Conventional, well-known techniques are employed for this purpose, such as hydrothermal methods, solvent extraction (alcohol precipitation), and/or tangential ultrafiltration. These procedures subject the pre-treated biomass to different solvents for a given time and temperature to ensure polysaccharides with low impurities (Prybylski et al. 2020).

Hot water reflux is the most widely used hydrothermal method, due to its low cost and simple requirements for experimental equipment. Although the yield depends on factors such as extraction time and the temperature used, it generally has a low yield (< 7%) which leads to the waste of experimental raw materials (Khanra et al. 2018; Li et al. 2022). However, it is considered the most popular method to extract CWP polysaccharides (Yang et al. 2006), even though it has also been applied to extract EPS from *Spirulina* sp. and *Chlorella* sp. (Chaiklahan et al. 2013; Zhao et al. 2018a, b). By way of exemplification, in the study by Malagoli et al. (2014), about 7% yield under hot water extraction for 2 h at 60 °C was obtained, with the predominant recovery of galactose, glucose, xylose, mannose, rhamnose, and arabinose structures. Nevertheless, it is noteworthy that the extraction time is a determining parameter regarding the structure integrity and bioactivity of the extracted compound. This is because, in long extraction times and high temperatures (time: 30 min to 24 h; temperature: 60-100ºC), the exopolysaccharides extracted can suffer losses of bioactivity due to structural degradation of the compound (Xu et al. 2017).

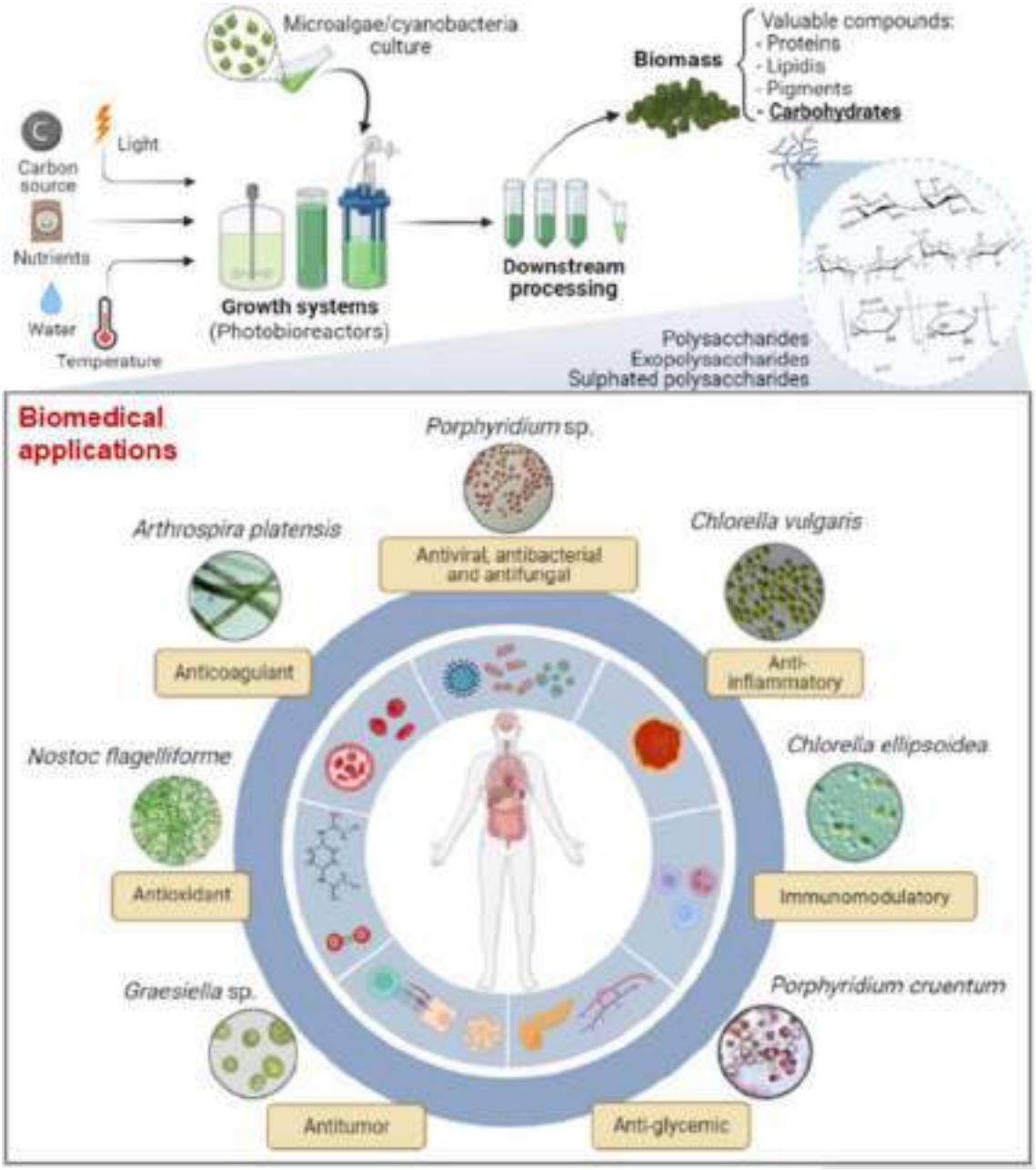


Fig. 1 Overview of obtaining microalgae-based polysaccharides for biomedical applications, with the associated biological property and the most common species

Otherwise, alcoholic precipitation method has dual purposes: when applied to EPS, it is considered an extraction method; however, in SP and CWP extraction, it has been applied as a preliminary purification method. In agreement with Delattre et al. (2016), the traditional alcoholic precipitation and, also, the most efficient technique uses alcohols such as methanol, isopropanol, or ethanol in a 3:1 (v/v) ratio. Furthermore, it is essential to note that alcohol polarity, concentration, and precipitation temperature (between -20 °C and 20 °C) have an impact on polysaccharide yield (~ 70–80% yield) and also on co-precipitation of impurities. Studies carried out by Xu et al. (2014) suggest that molecular size is the main parameter that influences yield. For example, at the most commonly used ethanol concentration (80%), the dextrans precipitate yield increased from 10 to 100% as the molecular size increased from 1 to 270 kDa. However, although the yields are satisfactory, these well-known strategies are not efficient for microalgae, as they led to lead low purified polymers with high salt content and poor solubility, resulting in co-precipitates; incompatible with an

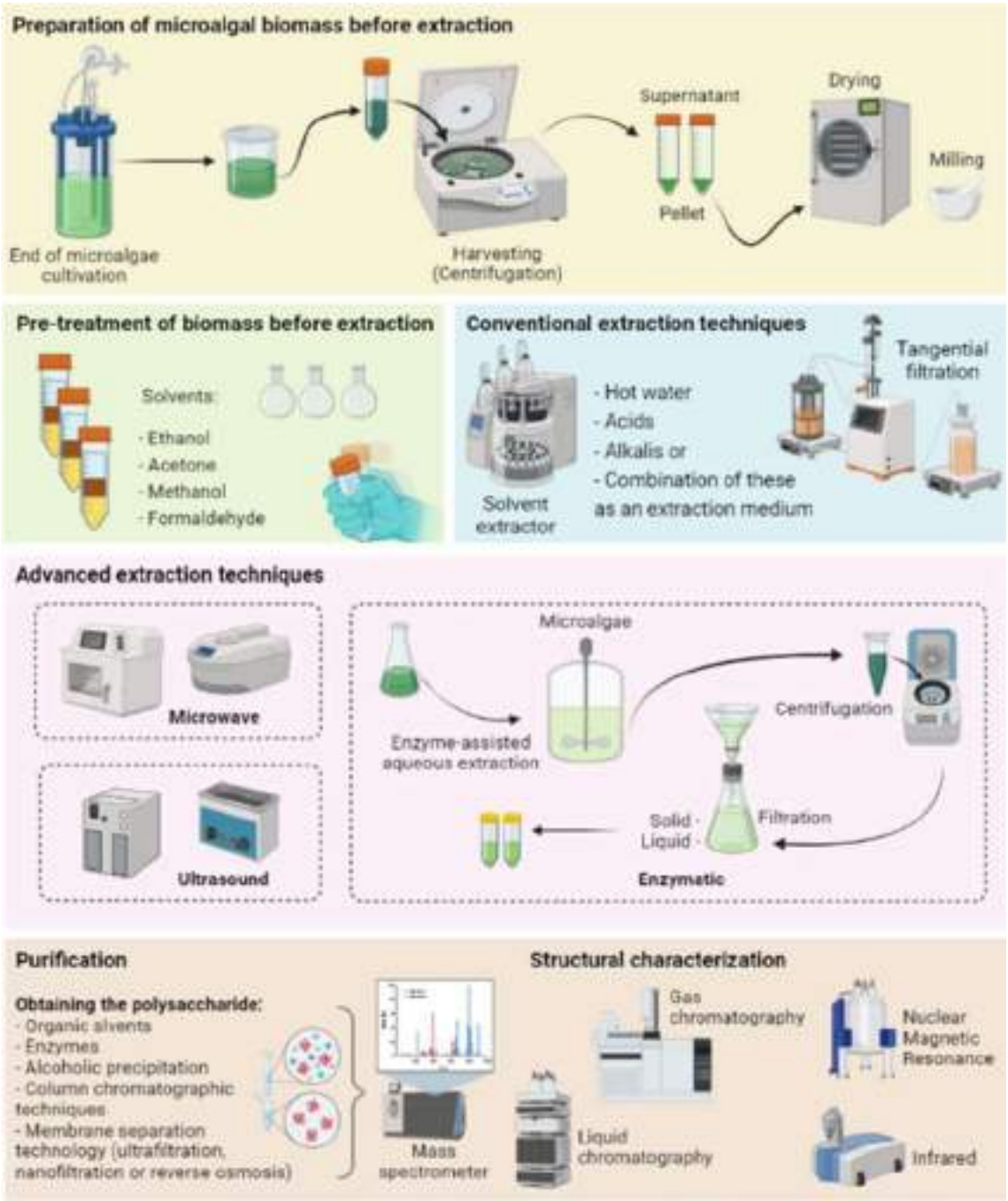


Fig. 2 Summary of the steps, techniques, and methods involved in the extraction, purification, and structural characterization of microalgae polysaccharides

industrial application. Therefore, the ideal is the application of emerging technologies, such as those based on membrane use (Patel et al. 2013).

To circumvent this technical bottleneck, tangential microfiltration is a potential membrane technology, once it indicates the filtration principle based on the passage of the analyte that is parallel to the membrane flow, where the permeate will be collected with the filtrate and retentate is returned back to the feed tank. This technique presents a high performance and exhibits an increasing selectivity, in addition to occurring without the presence of chemical solvents and at low temperatures. Ultrafiltration modules with polymeric membranes with cuts ranging from 1 kDa – to 500 kDa are used. When comparing the three conventional methods of extraction, the results showed that the filtration techniques were the most effective to isolate EPS from

culture media with high saline concentration (Delattre et al. 2016).

At the same time, in view of the difficulties in defining an exceptional method for all variations of the compounds and algae matrices to be explored, alternative technologies for extracting polysaccharides have been studied to increase the extraction yield, reduce the volume of solvents and, consequently, make the most environmentally friendly processes. Existing advanced techniques include ultrasound-assisted extraction, microwave extraction, and enzymatic extraction.

In brief, ultrasound applications have as their basic principle the cell rupture by cavitation, and mechanical and thermal effects, which result in favoring the extraction of EPS, depending on the permeability of the cell membrane (Morais et al. 2022b). Studies conducted by Mishra & Jha (2009) and Kurd & Samavati (2015) proved the technological efficiency of the polysaccharides extraction from *Dunaliella salina* and *Spirulina platensis*, respectively. In addition, this technique has a short extraction time, less use of solvents, cheaper, easy handling, and yields above 8% dry biomass. However, the methods must be optimized as they can lead to degradation and change in the composition of polysaccharides (Lin et al. 2018).

On the other hand, the microwave-assisted extraction (MAE) technique is another technology that has been investigated, as it increases the porosity of membranes, allowing greater permeation of the solvent into the cells (Rostami and Gharibzahedi 2016; Zhou et al. 2022). Among the advantages of this technique, beyond yields above 15%, the low temperature, as well as the short extraction time are factors that make this technique one of the most promising (Li and Huang 2021). Furthermore, this method was revealed to be efficient in the extraction of microalgae polysaccharides from different genres such as *Chlorella*, *Chlamydomonas*, *Scenedesmus*, and *Arthrospira platensis*. When compared to conventional extraction, this technique is very advantageous, since in a short time (less than 1 min), microwave irradiation deeply breaks the cell wall, improving the extraction yield. In addition, this rapid extraction promotes an energy reduction of up to 99%, making the process more sustainable (Silva et al. 2018).

Additionally, enzyme-assisted extraction has as basic principle the disruption of the microorganism cell wall by hydrolyzing it using enzyme as a catalyst under optimum experimental conditions, in order to release the intracellular components, the polysaccharides (Wijesinghe and Jeon 2012). Recently, it has been a technique applied to microalgae, with cellulase being the most used enzyme (Zhao et al. 2018a, b). Investigated by Bernaerts et al. (2018), studies have demonstrated the use of enzymes such as endo-β-1,3-glucanase, α-amylase amyloglucosidase, and subtilisin A protease to aid in the isolation (interferences elimination) of CWP from microalgal genres such as *Chlorella*, *Schizochytrium*, and *Arthrospira*. However, the yields found are less than 2%. Besides, the costs involved in acquiring the enzymes make the technique inaccessible.

In general, the techniques with the most significant potential for application—until then investigated—consist of tangential microfiltration (conventional method) and microwave (advanced method). However, it is essential to consider specific factors of interest, such as the species to be studied, target compounds, and available resources (Nigam et al. 2021).

Regardless of the extraction method chosen, the purification step is essential to enable the isolation of polysaccharides with high yield and purity. This is because these compounds, in their raw form, are interlinked with other elements such as proteins, nucleotides, lipids, lignin, and some inorganic mineral substances that can change their biological activity properties and cause antagonistic effects or undesirable toxicity (Chaiklahan et al. 2013; Delattre et al. 2016). Besides, it is a crucial step in the face of biosafety regulations due to biomedical and food applications.

There are many available techniques for purification step, and choosing the best one will depend on the target molecule (for example, polarity and molecular size). Amidst the techniques, we can highlight the use of organic solvents, enzymes, ethanol precipitation, ultrafiltration, ion-exchange chromatography, gel filtration, and affinity chromatography (Jin et al. 2013).

After obtaining the purified extract, it is necessary to identify and characterize the polysaccharides. Overall, four main levels can be defined, namely (i) primary composition, (ii) global composition, (iii) first structural analysis, and (iv) complete structure investigation. Currently, the primary structure is the target for determining the structure of polysaccharides, mainly analyzing the molecular weight range of polysaccharides, type, proportion, and order of connection of monosaccharides, and configuration of glycosidic bonds. In microalgae, it is determined by colorimetric assays such as phenol sulfuric acid (total carbohydrates), and $BaCl_2$ gelatin (sulfate groups) (Goo et al. 2013), meta-hydroxydiphenyl-NaOH (Raposo et al. 2016), and sulfuric acid-resorcinol methods (neutral sugars) (Delattre et al. 2016). Unfortunately, these global determination methods are not entirely satisfactory, as they do not provide specific structural information, and may overestimate or suppress the total polysaccharide content due to possible spectral interference.

Therefore, for advanced biotechnological development, it is necessary to have access to a variety of innovative methods that provide detailed structural information and thus establish relationships between structures and biological properties of polysaccharides (Delattre et al. 2016). In this sense, the exploration of instrumental analytical methods based on chromatography, mass spectrometry, infrared and nuclear magnetic resonance (NMR), as well as the hyphenation of these techniques are fundamental in the search for a

complete mapping of the polysaccharide structure (Zhang et al. 2012). In general, the main advances among these complex researches use the identification of binding and specific substitution patterns by methylation analysis and NMR scope. However, monosaccharide sequence determination is often facilitated by partial depolymerization (either enzymatic) or Smith degradation. This can be seen in the works by Sadovskaya et al. (2014) and Goo et al. (2013) in the determination of homopolysaccharides from *Isochrysis galbana* and *Dunaliella tertiolecta*, respectively. Through these advanced methodologies, it was possible to observe that the main polysaccharide structures already identified in these microorganisms are glycogen, agar, fucoidan, laminarin, alginate, and cellulose, among others (Table 2) (Hamed et al. 2015; Becker and Hehemann 2018; Lafarga et al. 2020). However, the main chemical composition of these structures is formed from galactose, xylose, glucose, rhamnose, fucose, arabinose, mannose, orthomethyl sugar, and acid residues of glucuronic acid and galacturonic acid (Kumar et al. 2018).

Biological activities and potential biomedical applications of microalgal polysaccharides

The chemical composition of microalgae biomass provides a myriad of applications in various industries, such as cosmetic, pharmaceutical, and biomedical. The polysaccharides in particular are one of the compounds of interest that have already been shown to have a wide range of biological properties such as antiviral, anti-inflammatory, immunomodulatory, antitumor, antioxidant, anticoagulant, antilipidemic, anti-glycemic, among others (Colusse et al. 2021). These properties are commonly attributed to its structure and physicochemical characteristics, which depend on the organism that produces it (Hu et al. 2013).

Antiviral activity

Many studies have already highlighted that the polysaccharides released by some microalgae show antiviral activity against different types of viruses. Calcium-spirulan, a sulfated polysaccharide produced by *Arthrospira platensis*, demonstrated the ability to inhibit viral virus replication. Radonić et al. (2011) showed that this polysaccharide released into the medium by the aforementioned microalgae exhibited in vitro and in vivo activity against vaccinia and ectromelia viruses. This compound has also been identified as having a high selectivity index for herpes simplex virus type 1, human cytomegalovirus, measles virus, mumps virus, influenza A virus, and human immunodeficiency virus 1 (Hayashi et al. 1996). The antiviral activity of the microalgae *Porphyridium* sp. has also been extensively investigated and shown in vitro and in vivo antiviral activity against herpes simplex virus types 1 and 2. The polysaccharide of this microalgae, depending on the concentration (as high as 250 µg/ml), inhibited or delayed the development of the cytopathic effect in cells infected with the herpes virus (Huheihel et al. 2002). In sum, there are many others in vitro and in vivo studies that show the antiviral potential of polysaccharides from different microalgae species against the most diverse types of viruses; however, both still seek to elucidate the step or steps during the viral replication cycle that are affected by these polysaccharides.

Anti-inflammatory activity

Polysaccharide molecules synthesized by microalgae are known so far to have promising anti-inflammatory activities (Abad et al. 2008; Dias et al. 2020). An example is a sulfated polysaccharide derived from the red microalgae *Porphyridium* sp. which inhibited in vitro the migration of polymorphonuclear leukocytes towards a standard chemoattractant molecule and also partially blocked the adhesion of polymorphonuclear leukocytes to endothelial cells (Matsui et al. 2003). Crude polysaccharide extracts obtained from the microalgae *Chlorella stigmatophora* and *Phaeodactylum tricornutum* were also evaluated for their anti-inflammatory activity. Both showed an anti-inflammatory effect in the carrageenan-induced paw edema test (Guzmán et al. 2003). The polysaccharide *Coccomyxa gloeobotrydiformis* extracted from the alga of the same name is able to significantly inhibit lipopolysaccharide-induced inflammation in RAW 264.7 macrophages. This effect resides in its regulatory effects on inflammatory and anti-inflammatory signaling pathways (Dai et al. 2018). Another example is the exopolysaccharide from *Crypthecodinium cohnii*, which also exhibited significant anti-inflammatory activity by regulating the expression of toll-like receptor 4, mitogen-activated protein kinases, and nuclear factor-κB protein (Ma et al. 2017).

Immunomodulatory activity

Immunomodulatory activity of microalgae polysaccharides is also reported to be potentially promising. *Chlorella* belonging to the phylum *Chlorophyta* is a genus of unicellular green microalgae that have been extensively studied in vitro and in vivo. Yang et al. (2006), for example, studied the immunomodulatory effect of the *Chlorella pyrenoidosa* polysaccharides and the results showed that oral administration of this compound potentiated the immune response of mice, significantly increasing the phagocytic rate and phagocytic index compared to the control. In another study, polysaccharides from *Chlorella pyrenoidosa* induced IL-1β secretion in macrophages, stimulated cell surface expression

Table 2 Algal polysaccharides: composition and chemical structure

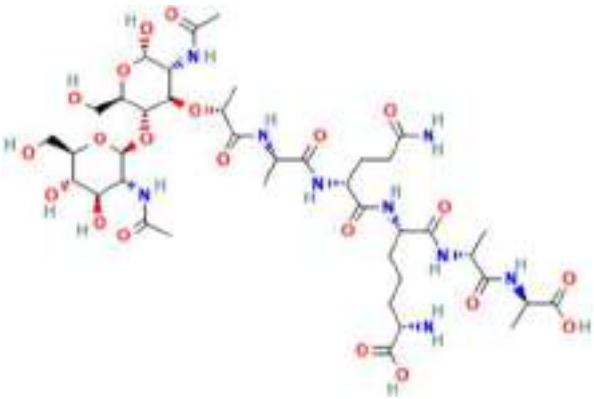
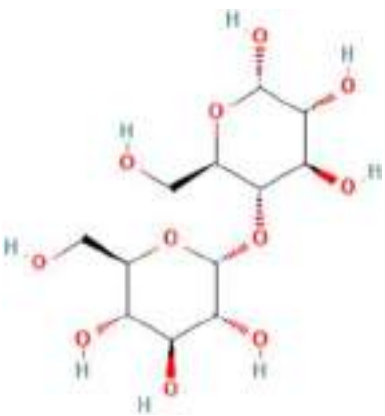
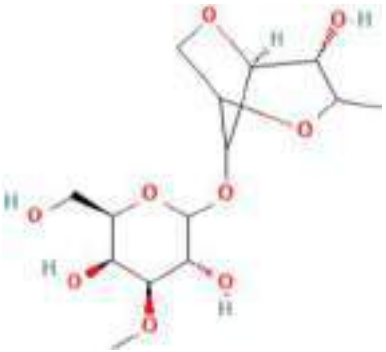
Polysaccharides	Microalgal division	Glycosidic bonds	Chemical structure
Peptidoglycan	*Cyanophyta*	β (1→4)	
Cellulose	All microalgal groups (except diatoms)	β (1→4)	
Glycogen	*Cyanophyta*	α-(1→4) α-(1→6)	
Starch	*Chlorophyta* *Cryptophyta* *Glaucocystophyta*	α-(1→4) α-(1→6)	

Table 2 (continued)

Polysaccharides	Microalgal division	Glycosidic bonds	Chemical structure
Laminarin	*Chrysophyta*	β-(1 → 3) β-(1 → 6)	
Paramylon	*Euglenophyta*	β-(1 → 3)	
Agar	*Rhodophyta*	β-(1 → 3) α-(1 → 4)	
Fucoidan	Brown seaweed	-	

of HLA-DA/DB/DC, HLA-DR/DP/DQ, and expression of co-stimulatory family molecules, revealing itself thus a modulating agent of immune response in humans and some animal species. The main monosaccharides of the polysaccharide of *Chlorella pyrenoidosa* identified were rhamnose (31.8%), glucose (20.42%), galactose (10.28%), mannose (5.23%), and xylose (1.27%) (Hsu et al. 2010). This same microalga was studied regarding the structure–activity relationship and it is noteworthy that the polysaccharide bioactivity was correlated with the molecular weight. Suárez et al. (2006) showed in their study that the galactofuran and arabinogalactans of 27 and 50 kDa showed no bioactivity while arabinogalactans of 188 and 1020 kDa increased the production of nitric oxide, which indicates their biological activity. Corroboratively, Qi and Kim (2017) reported that the strongest immunomodulatory activity was associated with *Chlorella ellipsoidea* polysaccharide with higher molecular weight and protein content. According to the authors, polysaccharides from *Chlorella ellipsoidea* exhibited immunomodulatory activities through activation of the NF-κB and MAPK pathways in RAW264.7 cells.

Antitumor activity

Antitumor action has also attracted significant importance among biological activities (Wang et al. 2018). This is because studies have shown inhibitory activity on growing tumors in vitro and in vivo. By way of example, the exopolysaccharide p-KG03 produced by the microalgae *Gyrodinium impudicum* strain KG03, which has immunostimulating activity, increased the tumoricidal activities of macrophages and natural killer cells in vivo (Yim et al. 2005). The calcium-spirulan from *Arhrospira platensis*, in turn, has been reported to inhibit tumor invasion of B16-BL6 melanoma cells, colon 26 carcinoma, and HT-1080 fibrosarcoma cells across the Matrigel basement membrane (Saiki et al. 2004; Morais et al. 2010). In contrast, Gardeva et al. (2009) reported the strong antitumor activity of the sulfated polysaccharide from the cell wall of the microalgae *Porphyridium cruentum* against the Graffi myeloid tumor both in vitro and in vivo. When tested in vivo, tumor growth was retarded and survival time was prolonged by 10–16 days. The results of the study suggest that sulfated polysaccharide from *Porphyridium cruentum* is a promising candidate as an antitumor agent. However, the mechanisms of biological action remain unclear and more studies are needed to evidence them. Besides, the *Chlorella zofingiensis* polysaccharides were also evaluated for their antitumor activity and the results point to positive effects against HCT116 and HCT8 human colon cancer cells. However, although in vitro antitumor activities have been demonstrated, a detailed analysis of in vivo activities and antitumor mechanisms of action is lacking (Yuan et al. 2020).

Antioxidant activity

The antioxidant's ability to protect the organism against free radicals and reactive oxygen species can delay the pathogenesis of numerous diseases, including cancer, diabetes mellitus, and disorders associated with aging. Notably, the antioxidant potential of microalgae polysaccharides with unique biological properties has not gone unnoticed. Chen et al. (2016) reported that all polysaccharides extracted from the microalgae *Chlorella pyrenoidosa* using different concentrations of ethanol had antioxidant activity in vivo. However, microalgae polysaccharides precipitated by a final ethanol concentration of 70% exhibited greater sequestering activity against superoxide radicals, 2,2-diphenyl-1-picrylhydrazyl radicals, and hydroxyl radicals than those with a final concentration of 60% and 85%. More recently, Zhang et al. (2019a) reported the antioxidant and antitumor activities of the exopolysaccharides produced by *Chlorella pyrenoidosa*, *Chlorococcum* sp., and *Scenedesmus* sp. The polysaccharides obtained from these microalgae showed in vitro hydroxyl radicals and 1,1-Diphenyl-2-picrylhydrayl elimination abilities and inhibitory effect on the cell viability of HCT116 and HCT8 human colon cancer cells. The partially purified exopolysaccharides of *Chlorella zofingiensis* and *Chlorella vulgaris* were also evaluated for the same purpose. In this study by Zhang et al. (2019b) the exopolysaccharides of the two strains exhibited hydroxyl radical and α radical elimination activity, α-diphenyl-β-picrylhydrazyl, and antitumor effect, considering their inhibitory activity on cell viability of HCT-8 in vitro.

In short, with regard to antioxidant activity, the various strains of microalgae have potential for biotechnological exploration as natural antioxidants, being able to replace the synthetic chemical pathways (Yingying et al. 2014). Likewise, it is worth noting that anti-aging activity is related to antioxidant activity. And, about this, since the bioactive polysaccharides of microalgae can eliminate free radicals, they can find applicability in skin cosmetics. Mourelle et al. (2017) showed in their study the potential use of marine microalgae and cyanobacteria in cosmetics and thalassotherapy. Bayona et al. (2012), in turn, proved the potential of sulfated polysaccharides from the microalgae *Porphyridium cruentum* to inhibit hyaluronidase and elastase, suggesting that, given their anti-aging properties, they can be used as active ingredients in formulations to maintain good health and skin appearance.

Anticoagulant activity

Regarding anticoagulant activity, there are few references about microalgae polysaccharides with these properties, unlike macroalgae polysaccharides, which have been extensively studied for this purpose in recent decades. The

scientific basis for this biological activity is therefore not fully understood for microalgae (Jiao et al. 2011). Furthermore, it is of note that only calcium-spirulan is known to have anticoagulant activity. Some studies have shown that calcium-spirulan exhibited anticoagulant activity mediated by heparin cofactor II, which is a member of the serine protease inhibitor family known to reduce clotting by inhibiting thrombin in the presence of dermatan sulfate or heparin (Majdoub et al. 2009; Prybylski et al. 2020).

Antilipidemic and anti-glycemic activities

Interestingly, in recent years, research has also shown that sulfated polysaccharides exert antilipidemic and anti-glycemic activities (Wang et al. 2013). However, it is worth mentioning that sulfated polysaccharides produced by macroalgae have been extensively studied for this purpose, unlike those produced by microalgae. But, regardless of that, some studies have advanced in this field of research. Wan et al. (2019) evaluated in vivo the hypolipidemic activity of the bioactive polysaccharide from the microalgae *Chlorella pyrenoidosa* and reported that the compound significantly improved serum and liver lipid parameters, as well as levels of total bile acid and short-chain fatty acids. The findings of this study indicate that the identified *Chlorella pyrenoidosa* polysaccharide may be a natural lipid-lowering drug, given its eminent hypolipidemic effect. In parallel, in vivo studies with the microalgae *Porphyridium* sp., whose biomass constitutes a unique combination of functional sulfated polysaccharides, have shown to significantly improve serum cholesterol and triglycerides, hepatic cholesterol levels, and the relationship between HDL and LDL levels if showing, thus, a potent hypocholesterolemic agent (Dvir et al. 2000, 2009). Chickens fed with *Porphyridium* sp. also showed increased levels of linoleic acid and arachidonic acid in egg yolk (Ginzberg et al. 2000). On the other hand, Setyaningsih et al. (2020) evaluated in vivo the antihyperglycemic potential of extracellular polysaccharides from *Porphyridium cruentum* and showed that the red microalgae polysaccharide was as effective as glibenclamide in reducing blood glucose levels in streptozotocin-induced diabetic rats, thus having the potential to solve hyperglycemic problems. Navarro et al. (2020), in turn, evaluated in vivo the protective antihyperglycemic and antihyperlipidemic effects of the microalgae *Coccomyxa onubensis* and found a significant reduction in serum levels of glucose (38.47%), total cholesterol (22.65%) and LDL-cholesterol (26.70%). Of note, the antihyperlipidemic effects of the microalgae were analogous to those of 10 mg/kg body weight per day of atorvastatin, which is a drug used to lower blood cholesterol levels.

Other biological activities and uses

In addition to the above biological activities, microalgae polysaccharides also play health benefits in other aspects, including antibacterial, antifungal, antiasthmatic, antitussive, and anticancer effects. By way of exemplification, it was reported that *Nostoc commune* and *Nostoc flagelliforme*, besides the antioxidant effect, have antibacterial activity against *Staphylococcus aureus* and *Escherichia coli* (Quan et al. 2015; Shen et al. 2018). The polysaccharides obtained from *Tetraselmis* sp. showed a potent antifungal effect against *Candida albicans* and *Penicillium italicum* (Kashif et al. 2018). On the other hand, the administration of extracellular polysaccharides produced by *Chlorella vulgaris* showed a significant bronchodilator and antitussive effect in guinea pigs with experimentally induced allergic airway inflammation (Barboríková et al. 2019). Already, the sulfated polysaccharides of *Phaeodactylum tricornutum* and *Tribonema* sp. showed significant dose-dependent anticancer activity on human liver cancer cells (HepG2) (Chen et al. 2019; Yang et al. 2019). The extracellular polysaccharides of the microalgae *Graesiella* sp. also showed anticancer properties in a dose-dependent manner in HepG2 cells and human colorectal adenocarcinoma cells (Caco-2) (Trabelsi et al. 2016).

Noteworthy, some research has confirmed the biomaterials development from microalgae such as *Artrosphira platensis* and *Chlamydomonas reinhardtii* for use in tissue engineering (Furmaniak et al. 2017; Hopfner et al. 2014). Bellini et al. (2018) in their preliminary study reported good results when combining the production of exopolymeric substances from cyanobacteria with that of photopolymerizable hydrogels for enzyme- and stem cell-carrier systems. However, although has been observed potential for microalgal biomaterials for use in tissue engineering, there are numerous technological knots that need to be untied before they can be applied in clinical settings. Still, it should be noted that the use of polymeric substances such as microalgae polysaccharides for use as a biomaterial is still little explored, possibly, due to the difficulties encountered in elucidating their real structure (Domozych et al. 2012).

Current status

The polysaccharides from different microalgae species are complex and heterogeneous macromolecules that often do not have their chemical structure elucidated; consequently, their bioactivity is not fully understood. In truth, so far, few were those who leaned over the challenging task of exploring the possible chemical structure-bioactivity relationship of microalgae polysaccharides. In the scientific literature, chemical structure-bioactivity relationships are generally

based on inferences from studies with macroalgae and invertebrate polysaccharides. Unraveling this enigmatic relationship requires an in-depth understanding of the complex interplay of several structural peculiarities, including the level of sulfation, distribution of sulfate groups, molecular weight, and sugar residue composition (Raposo et al. 2015).

As discussed, the biological activities of these macromolecules are authentic and varied; however, it is important to note that today the market is practically closed for these macromolecules as their structures and action mechanisms remain unclear. The biological activities of microalgae polysaccharides have been studied in vitro, in vivo, and ex vivo, but a detailed investigation of these activities in clinical studies is lacking. In the literature, it is also not clear whether some genera or species of microalgae are more promising for a specific biological activity, but it is notable that the polysaccharides produced by a certain strain usually show more than one pharmacological/biomedical activity (Dias et al. 2020). Importantly, some polysaccharides extracted from certain microalgae such as calcium-spirulan from the microalgae *Arthrospira platensis* are named because they are already well characterized. It is worth highlighting that *Porphyridium cruentum* exopolysaccharides are the only active ingredient to achieve commercial success, but exclusively in the cosmetic industry. Today, although the production costs of bioactive polysaccharides from microalgae are prohibitive compared to conventional sources such as plants and macroalgae, they must be able to compete with some polysaccharides of animal origin, such as glycosaminoglycans, as therapeutic agents (Prybylski et al. 2020). It is hoped that the development of modern structural characterization tools will help pave the way for the development of these macromolecules in the therapeutic field.

Conclusions and way forward

Microalgae are potential alternatives to produce polysaccharides with countless biological activities, which have applications in many sectors, especially biomedical, as reviewed here. However, microalgae-based technologies are emerging and still under development with many co-existing barriers, of which three are prominent: (i) productivity rate, (ii) production costs, and (iii) little knowledge about these compounds. Regarding the first obstacle, although there is a high yield of polysaccharides, the amount of biomass, commonly generated in photobioreactors, is insufficient for competitiveness compared to those carbohydrates from other sources. It is necessary to better study the algal species, design new cropping systems and optimize existing ones in terms of highly robust operational parameters, and improve extraction processes to maximize production. Secondly, minimizing downstream processing costs, i.e., harvesting, is also a critical point for implementation on the scale. Finally, as it is very challenging to purify the components that constitute the polysaccharides, it is required better elucidation of the properties and configurations of their structures in order to direct the synthesis toward biomolecules with desired functionalities. Therefore, solving these hot spots will pave the way to heat the microalgae products market and make them commercially competitive since they have been constantly in the searchlight of researchers, industries, and all stakeholders.

Acknowledgements The authors would like to thank the National Council for Scientific and Technological Development (CNPq) – Brazil, and the Coordination of Improvement of Higher Education Personnel (CAPES), Finance Code 001.

Author contributions IAS: involved in the writing, edition, review, and final approval of the version to be published. RRD: participated in the writing, review and final approval of the version to be published. TCdN: participated in the conception and design of the work. MCD: information collection, information analysis. MMM: drafting the article and edition. LQZ: supervision of the entire work. EJ-L: performed the interpretation, critical revision and supervision. All authors have read and approved the final manuscript.

Declarations

Competing interests The authors have no competing interests to declare that are relevant to the content of this article.

Ethical approval Not applicable.

Consent to participate Not applicable.

Consent for Publication All authors declare consent for publication of this article, being represented by the author for correspondence.

References

Abad MJ, Bedoya LM, Bermejo P (2008) Natural marine anti-inflammatory products. Mini Rev Med Chem 8(8):740–754. https://doi.org/10.2174/138955708784912148

Arlov O, Rütsche D, Korayem MA, Öztürk E, Zenobi-Wong M (2021) Engineered Sulfated Polysaccharides for Biomedical Applications. Adv Funct Mater 31(19):2010732. https://doi.org/10.1002/adfm.202010732

Assunção J, Malcata FX (2020) Enclosed "non-conventional" photobioreactors for microalga production: a review. Algal Res 52:102107. https://doi.org/10.1016/j.algal.2020.102107

Bafana A (2013) Characterization and optimization of production of exopolysaccharide from *Chlamydomonas reinhardtii*. Carbohydr Polym 95(2):746–752. https://doi.org/10.1016/j.carbpol.2013.02.016

Barboríková J, Šutovská M, Kazimierová I, Jošková M, Fraňová S, Kopecký J, Capek P (2019) Extracellular polysaccharide produced by *Chlorella vulgaris*–chemical characterization and anti-asthmatic profile. Int J Biol Macromol 135:1–11. https://doi.org/10.1016/j.ijbiomac.2019.05.104

Bayona KD, Navarro SM, Lara AD, Colorado JR, Atehortúa LG, Martínez M (2012) Activity of sulfated polysaccharides from

microalgae *Porphyridium cruentum* over degenerative mechanisms of the skin. Int J Sci Adv Technol 2(8):85–92

Beaumont M, Tran R, Vera G et al (2021) Hydrogel-forming algae polysaccharides: from seaweed to biomedical applications. Biomacromolecules 22(3):1027–1052. https://doi.org/10.1021/acs.biomac.0c01406

Bellini E, Ciocci M, Savio S, Antonaroli S, Seliktar D, Melino S, Congestri R (2018) *Trichormus variabilis* (Cyanobacteria) biomass: from the nutraceutical products to novel EPS-cell/protein carrier systems. mar Drugs 16(9):298. https://doi.org/10.3390/md16090298

Bernaerts TMM, Kyomugasho C, Looveren NV, Gheysen L, Foubert I, Hendrickx ME, Van Loey AM (2018) Molecular and rheological characterization of different cell wall fractions of *Porphyridium cruentum*. Carbohydr Polym 195:542–550. https://doi.org/10.1016/j.carbpol.2018.05.001

Bilal M, Iqbal HMN (2020) Marine seaweed polysaccharides-based engineered cues for the modern biomedical sector. Mar Drugs 18(1):7. https://doi.org/10.3390/md18010007

Chaiklahan R, Chirasuwan N, Triratana P, Loha V, Tia S, Bunnag B (2013) Polysaccharide extraction from *Spirulina* sp. and its antioxidant capacity. Int J Biol Macromol 58:73–78. https://doi.org/10.1016/j.ijbiomac.2013.03.046

Chanda M-J, Merghoub N, EL Arroussi H (2019) Microalgae polysaccharides: the new sustainable bioactive products for the development of plant bio-stimulants? World J Microbiol Biotechnol 35:177. https://doi.org/10.1007/s11274-019-2745-3

Chandrasekhar K, Raj T, Ramanaiah SV et al (2022) Algae biorefinery: a promising approach to promote microalgae industry and waste utilization. J Biotechnol 345:1–16. https://doi.org/10.1016/j.jbiotec.2021.12.008

Chen YX, Liu XY, Xiao Z, Huang YF, Liu B (2016) Antioxidant activities of polysaccharides obtained from *Chlorella pyrenoidosa* via different ethanol concentrations. Int J Biol Macromol 91:505–509. https://doi.org/10.1016/j.ijbiomac.2016.05.086

Chen X, Song L, Wang H, Liu S, Yu H, Wang X et al (2019) Partial characterization, the immune modulation and anticancer activities of sulfated polysaccharides from filamentous microalgae *Tribonema* sp. Molecules 24(2):322. https://doi.org/10.3390/molecules24020322

Colusse GA, Carneiro J, Duarte MER, de Carvalho JC, Noseda MD (2021) Advances in microalgal cell wall polysaccharides: a review focused on structure, production, and biological application. Crit Rev Biotechnol 28:1–16. https://doi.org/10.1080/07388551.2021.1941750

Costa JAV, Lucas BF, Alvarenga AGP, Moreira JB, de Morais MG (2021) Microalgae polysaccharides: an overview of production, characterization, and potential applications. Polysaccharides 2(4):759–772. https://doi.org/10.3390/polysaccharides2040046

Dai J, Wu Y, Chen S, Zhu S, Yin H, Wang M, Tang J (2010) Sugar compositional determination of polysaccharides from *Dunaliella salina* by modified RP-HPLC method of precolumn derivatization with 1-phenyl-3-methyl-5-pyrazolone. Carbohydr Polym 82(3):629–635. https://doi.org/10.1016/j.carbpol.2010.05.029

Dai B, Wei D, Zheng NN, Chi ZH, Xin N, Ma TX et al (2018) *Coccomyxa gloeobotrydiformis* polysaccharide inhibits lipopolysaccharide-induced inflammation in RAW 264.7 macrophages. Cell Physiol Biochem 51(6):2523–2535. https://doi.org/10.1159/000495922

Delattre C, Pierre G, Laroche C, Michaud P (2016) Production, extraction and characterization of microalgal and cyanobacterial exopolysaccharides. Biotechnol Adv 34(7):1159–1179. https://doi.org/10.1016/j.biotechadv.2016.08.001

Do Nascimento TC, Pinheiro PN, Fernandes AS, Murador DC, Neves BV, de Menezes CR, de Roso VV, Jacob-Lopes E, Zepka LQ (2021) Bioaccessibility and intestinal uptake of carotenoids from microalgae *Scenedesmus obliquus*. LWT 140:110780. https://doi.org/10.1016/j.lwt.2020.110780

Domozych DS, Ciancia M, Fangel JU, Mikkelsen MD, Ulvskov P, Willats WG (2012) The cell walls of green algae: a journey through evolution and diversity. Front Plant Sci 3:82. https://doi.org/10.3389/fpls.2012.00082

dos Santos MC, Bicas JL (2021) Natural blue pigments and bikaverin. Microbiol Res 244:126653. https://doi.org/10.1016/j.micres.2020.126653

Dvir I, Chayoth R, Sod-Moriah U, Shany S, Nyska A, Stark AH et al (2000) Soluble polysaccharide and biomass of red microalga *Porphyridium* sp. alter intestinal morphology and reduce serum cholesterol in rats. Br J Nutr 84(4):469–476. https://doi.org/10.1017/S000711450000177X

Dvir I, Stark AH, Chayoth R, Madar Z, Arad SM (2009) Hypocholesterolemic effects of nutraceuticals produced from the red microalga *Porphyridium* sp. in rats. Nutrients 1(2):156–167. https://doi.org/10.3390/nu1020156

El-Sheekh M, Abomohra AEF, Hanelt D (2013) Optimization of biomass and fatty acid productivity of *Scenedesmus obliquus* as a promising microalga for biodiesel production. World J Microbiol Biotechnol 29:915–922. https://doi.org/10.1007/s11274-012-1248-2

Fernandes AS, Nascimento TC, Pinheiro PN, Vendruscolo RG, Wagner R, de Rosso VV, Jacob-Lopes E, Zepka LQ (2021) Bioaccessibility of microalgae-based carotenoids and their association with the lipid matrix. Food Res Int 148:110596. https://doi.org/10.1016/j.foodres.2021.110596

Furmaniak MA, Misztak AE, Franczuk MD, Wilmotte A, Waleron M, Waleron KF (2017) Edible cyanobacterial genus *Arthrospira*: actual state of the art in cultivation methods, genetics, and application in medicine. Front Microbiol 8:25–41. https://doi.org/10.3389/fmicb.2017.02541

Gardeva E, Toshkova R, Minkova K, Gigova L (2009) Cancer protective action of polysaccharide, derived from red microalga *Porphyridium cruentum*—a biological background. Biotechnol Biotechnol Equip 23:783–787. https://doi.org/10.1080/13102818.2009.10818540

Ginzberg A, Cohen M, Sod-Moriah UA, Shany S, Rosenshtrauch A, Arad SM (2000) Chickens fed with biomass of the red microalga *Porphyridium* sp. have reduced blood cholesterol level and modified fatty acid composition in egg yolk. J Appl Phycol 12(3):325–330. https://doi.org/10.1023/A:1008102622276

Ginzberg A, Korin E, Arad SM (2008) Effect of drying on the biological activities of a red microalgal polysaccharide. Biotechnol Eng 99:411–420. https://doi.org/10.1002/bit.21573

Goo BG, Baek G, Choi DJ, Park Y, Synytsya A, Bleha R, Seong DH, Lee CG, Park JK (2013) Characterization of a renewable extracellular polysaccharide from defatted microalgae *Dunaliella tertiolecta*. Bioresour Technol 129:343–350. https://doi.org/10.1016/j.biortech.2012.11.077

Guzmán S, Gato A, Lamela M, Freire-Garabal M, Calleja JM (2003) Anti-inflammatory and immunomodulatory activities of polysaccharide from *Chlorella stigmatophora* and *Phaeodactylum tricornutum*. Phytother Res 17(6):665–670. https://doi.org/10.1002/ptr.1227

Hamed I, Özogul F, Özogul Y, Regenstein JM (2015) Marine bioactive compounds and their health benefits: a review. Compr Rev Food Sci Food Saf 14(4):446–465. https://doi.org/10.1111/1541-4337.12136

Hayashi T, Hayashi K, Maeda M, Kojima I (1996) Calcium spirulan, an inhibitor of enveloped virus replication, from a blue-green alga *Spirulina platensis*. J Nat Prod 59(1):83–87. https://doi.org/10.1021/np960017o

Hernández-Corona A, Nieves I, Meckes M, Chamorro G, Barron BL (2002) Antiviral activity of *Spirulina maxima* against herpes

simplex virus type 2. Antivir Res 56:279–285. https://doi.org/10.1016/S0166-3542(02)00132-8
Hopfner U, Schenck TL, Chávez MN, Machens HG, Bohne AV, Nickelsen J et al (2014) Development of photosynthetic biomaterials for in vitro tissue engineering. Acta biomater 10(6):2712–2717. https://doi.org/10.1016/j.actbio.2013.12.055
Hsu HY, Jeyashoke N, Yeh CH, Song YJ, Hua KF, Chao LK (2010) Immunostimulatory bioactivity of algal polysaccharides from *Chlorella pyrenoidosa* activates macrophages via Toll-like receptor 4. J Agric Food Chem 58(2):927–936. https://doi.org/10.1021/jf902952z
Hu D-J, Cheong KI, Zhao J, Li S-P (2013) Chromatography in characterization of polysaccharides from medicinal plants and fungi. J Sep Sci 36:1–19. https://doi.org/10.1002/jssc.201200874
Huheihel M, Ishanu V, Tal J, Arad SM (2002) Activity of *Porphyridium* sp. polysaccharide against herpes simplex viruses in vitro and in vivo. J Biochem Biophys Methods 50(2–3):189–200. https://doi.org/10.1016/S0165-022X(01)00186-5
Jacob-Lopes E, Maroneze MM, Deprá MC, Sartori RB, Dias RR, Zepka LQ (2019) Bioactive food compounds from microalgae: an innovative framework on industrial biorefineries. Curr Opin Food Sci 25:1–7. https://doi.org/10.1016/j.cofs.2018.12.003
Jin M, Huang Q, Zhao K, Shang P (2013) Biological activities and potential health benefit effects of polysaccharides isolated from *Lycium barbarum* L. Int J Biol Macromol 54:16–23. https://doi.org/10.1016/j.ijbiomac.2012.11.023
Kang Y, Zhi-Jiang W, Xie D, Sun X, Yang W, Zhao X, Xu N (2017) Characterization and potential antitumor activity of polysaccharide from *Gracilariopsis lemaneiformis*. Mar Drugs 15:1–14. https://doi.org/10.3390/md15040100
Kang J, Jia X, Wang N, Xiao M, Song S, Wu S, Li Z, Wang S, Cui SW, Guo Q (2020) Insights into the structure-bioactivity relationships of marine sulfated polysaccharides: a review. Food Hydrocoll 123:107049. https://doi.org/10.1016/j.foodhyd.2021.107049
Kashif SA, Hwang YJ, Park JK (2018) Potent biomedical applications of isolated polysaccharides from marine microalgae *Tetraselmis* species. Bioprocess Biosyst Eng 41(11):1611–1620. https://doi.org/10.1007/s00449-018-1987-z
Khanra S, Mondal M, Halder G, Tiwari ON, Gayen K, Bhowmick TK (2018) Downstream processing of microalgae for pigments, protein and carbohydrate in industrial application: a review. Food Bioprod Process 110:60–84. https://doi.org/10.1016/j.fbp.2018.02.002
Kumar D, Kaštánek P, Adhikary SP (2018) Exopolysaccharides from cyanobacteria and microalgae and their commercial application. Curr Sci 115(2):234–241
Kurd F, Samavati V (2015) Water soluble polysaccharides from *Spirulina platensis*: extraction and in vitro anti-cancer activity. Int J Biol Macromol 74:498–506. https://doi.org/10.1016/j.ijbiomac.2015.01.005
Lafarga T, Acién-Fernández FG, Garcia-Vaquero M (2020) Bioactive peptides and carbohydrates from seaweed for food applications: natural occurrence, isolation, purification, and identification. Algal Res 48:101909. https://doi.org/10.1016/j.algal.2020.101909
Laroche C (2022) Exopolysaccharides from microalgae and cyanobacteria: diversity of strains, production strategies, and applications. Mar Drugs 20(5):336. https://doi.org/10.3390/md20050336
Levine I, Fleurence J (2018) Microalgae in health and disease prevention. Academic Press, Cambridge
Li J, Huang G (2021) Extraction, purification, separation, structure, derivatization and activities of polysaccharide from Chinese date. Process Biochem 110:231–242. https://doi.org/10.1016/j.procbio.2021.08.018
Li J, Fan Y, Huang G, Huang H (2022) Extraction, structural characteristics and activities of *Zizylphus vulgaris* polysaccharides. Ind Crops Prod 178:114675. https://doi.org/10.1016/j.indcrop.2022.114675
Ma X, Xie B, Du J, Zhang A, Hao J, Wang S et al (2017) The Anti-Inflammatory Effect and Structure of EPCP1-2 from *Crypthecodinium cohnii* via Modulation of TLR4-NF-κB Pathways in LPS-Induced RAW 264.7 Cells. Mar drugs 15(12):376. https://doi.org/10.3390/md15120376
Majdoub H, Mansour MB, Chaubet F, Roudesli MS, Maaroufi RM (2009) Anticoagulant activity of a sulfated polysaccharide from the green alga *Arthrospira platensis*. Biochim Biophys Acta Gen Subj 1790(10):1377–1381. https://doi.org/10.1016/j.bbagen.2009.07.013
Malagoli BG, Cardozo FT, Gomes JHS, Ferraz VP, Simões CM, Braga FC (2014) Chemical characterization and antiherpes activity of sulfated polysaccharides from *Lithothamnion muelleri*. Int J Biol Macromol 66:332–337. https://doi.org/10.1016/j.ijbiomac.2014.02.053
Marcati A, Ursu AV, Laroche C, Soanen N, Marchal L, Jubeau S, Djelveh G, Michaud P (2014) Extraction and fractionation of polysaccharides and B-phycoerythrin from the microalga *Porphyridium cruentum* by membrane technology. Algal Res 5:258–263. https://doi.org/10.1016/j.algal.2014.03.006
Matsui MS, Muizzuddin N, Arad S, Marenus K (2003) Sulfated polysaccharides from red microalgae have antiinflammatory properties in vitro and in vivo. Appl Biochem Biotechnol 104(1):13–22. https://doi.org/10.1385/ABAB:104:1:13
Mishra A, Jha B (2009) Isolation and characterization of extracellular polymeric substances from micro-algae *Dunaliella salina* under salt stress. Bioresour Technol 100:3382–3386. https://doi.org/10.1016/j.biortech.2009.02.006
Mohammed ASA, Naveed M, Jost N (2021) Polysaccharides; classification, chemical properties, and future perspective applications in fields of pharmacology and biological medicine (a review of current applications and upcoming potentialities). J Polym Environ 29:2359–2371. https://doi.org/10.1007/s10924-021-02052-2
Morais AMMB, Alves A, Kumla D, Morais RMSC (2021) Pharmaceutical and biomedical potential of sulphated polysaccharides from algae. In: Oliveira J, Radhouani H, Reis R (eds) Polysaccharides of microbial origin. Springer, Cham, pp 1–28. https://doi.org/10.1007/978-3-030-35734-4_49-1
Morais MG, Rosa GM, Moraes L, Alvarenga AGP, da Silva JLV, Costa JAV (2022a) Microalgae polysaccharides with potential biomedical application. In: Oliveira JM, Radhouani H, Reis RL (eds) Polysaccharides of microbial origin. Springer, Cham, pp 363–380. https://doi.org/10.1007/978-3-030-42215-8_20
Mourelle ML, Gómez CP, Legido JL (2017) The potential use of marine microalgae and cyanobacteria in cosmetics and thalassotherapy. Cosmetics 4(4):46. https://doi.org/10.3390/cosmetics4040046
Navarro F, Toimil A, Ramírez S, Montero Y, Fuentes JL, Perona JS et al (2020) The acidophilic microalga *Coccomyxa onubensis* and atorvastatin equally improve antihyperglycemic and antihyperlipidemic protective effects on rats fed on high-fat diets. J Appl Phycol 32(6):3923–3931. https://doi.org/10.1007/s10811-020-02280-4
Nigam S, Singh R, Bhardwaj SK, Sami R, Nikolova MP, Chavali M, Sinha S (2021) Perspective on the therapeutic applications of algal polysaccharides. J Polym Environ 30:785–809. https://doi.org/10.1007/s10924-021-02231-1
Nisar A, Khan S, Hameed M, Nisar A, Ahmad H, Mehmood SA (2021) Bio-conversion of CO_2 into biofuels and other value-added chemicals via metabolic engineering. Microbiol Res 251:126813. https://doi.org/10.1016/j.micres.2021.126813
Patel AK, Laroche C, Marcati A, Ursu AV, Jubeau S, Marchal L, Petit E, Djelveh G, Michaud P (2013) Separation and fractionation of exopolysaccharides from *Porphyridium cruentum*. Bioresour

Technol 145:345–350. https://doi.org/10.1016/j.biortech.2012.12.038
Pierre G, Delattre C, Dubessay P, Jubeau S, Vialleix C, Cadoret JP et al (2019) What is in store for EPS microalgae in the next decade? Molecules 24(23):4296. https://doi.org/10.3390/molecules24234296
Qi J, Kim SM (2017) Characterization and immunomodulatory activities of polysaccharides extracted from green alga *Chlorella ellipsoidea*. Int J Biol Macromol 95:106–114. https://doi.org/10.1016/j.ijbiomac.2016.11.039
Quan Y, Yang S, Wan J, Su T, Zhang J, Wang Z (2015) Optimization for the extraction of polysaccharides from *Nostoc commune* and its antioxidant and antibacterial activities. J Taiwan Inst Chem Eng 52:14–21. https://doi.org/10.1016/j.jtice.2015.02.004
Radonić A, Thulke S, Achenbach J, Kurth A, Vreemann A, König T et al (2011) Anionic polysaccharides from phototrophic microorganisms exhibit antiviral activities to Vaccinia virus. J Antivir Antiretrovir 2:051–055. https://doi.org/10.4172/ jaa.1000023
Raposo MFJ, Morais AMMB (2015) Microalgae for the prevention of cardiovascular disease and stroke. Life Sci 125:32–41. https://doi.org/10.1016/j.lfs.2014.09.018
Raposo MFJ, Morais RMSC, Morais AMMB (2013) Bioactivity and applications of sulphated polysaccharides from marine microalgae. Mar Drugs 11(12):233–252. https://doi.org/10.3390/md11010233
Raposo MFJ, Morais AMMB, Morais RMSC (2015) Marine polysaccharides from algae with potential biomedical applications. Mar Drugs 13(5):2967–3028. https://doi.org/10.3390/md13052967
Raposo MFJ, Morais AMMB, Morais RMSC (2016) Emergent sources of prebiotics: seaweeds and microalgae. Mar Drugs 14(2):2–27. https://doi.org/10.3390/md14020027
Rostami H, Gharibzahedi SMT (2016) Microwave-assisted extraction of jujube polysaccharide: optimization, purification and functional characterization. Carbohydr Polym 143:100–107. https://doi.org/10.1016/j.carbpol.2016.01.075
Russell C, Rodriguez C, Yaseen M (2022) High-value biochemical products & applications of freshwater eukaryotic microalgae. Sci Total Environ 809:151111. https://doi.org/10.1016/j.scitotenv.2021.151111
Sadovskaya I, Souissi A, Souissi S, Grard T, Lencel P, Greene CM, Duin S, Dmitrenok PS, Chizhove AO, Shashkove AS, Usove AI (2014) Chemical structure and biological activity of a highly branched (1 → 3,1 → 6)-β-d-glucan from *Isochrysis galbana*. Carbohydr Polym 111:139–148. https://doi.org/10.1016/j.carbpol.2014.04.077
Saiki I, Murata J, Fujii H, Kato T (2004) Inhibition of tumor invasion and metastasis by calcium spirulan (Ca-SP), a novel sulfated polysaccharide derived from a blue-green alga *Spirulina platensis*. Nutr Sci 7(3):144–150
Santoyo S, Jaime L, Plaza M, Herrero M, Rodriguez-Meizoso I, Ibañez E, Reglero G (2012) Antiviral compounds obtained from microalgae commonly used as carotenoid sources. J Appl Phycol 24:731–741. https://doi.org/10.1007/s10811-011-9692-1
Setyaningsih I, Prasetyo H, Agungpriyono DR, Tarman K (2020) Antihyperglycemic activity of *Porphyridium cruentum* biomass and extra-cellular polysaccharide in streptozotocin-induced diabetic rats. Int J Biol Macromol 156:1381–1386. https://doi.org/10.1016/j.ijbiomac.2019.11.178
Severo IA, Siqueira SF, Deprá MC, Maroneze MM, Zepka LQ, Jacob-Lopes E (2019) Biodiesel facilities: What can we address to make biorefineries commercially competitive? Renew Sustain Energy Rev 112:686–705. https://doi.org/10.1016/j.rser.2019.06.020
Shen S, Jia S, Wu Y, Yan R, Lin Y-H, Zhao D, Han P (2018) Effect of culture conditions on the physicochemical properties and antioxidant activities of polysaccharides from *Nostoc flagelliforme*. Carbohydr Polym 198:426–433. https://doi.org/10.1016/j.carbpol.2018.06.111
Silvello MAC, Gonçalves IS, Azambuja SPH, Costa SS, Silva PGP, Santos LO, Goldbeck R (2022) Microalgae-based carbohydrates: a green innovative source of bioenergy. Bioresour Technol 344:126304. https://doi.org/10.1016/j.biortech.2021.126304
Suárez ER, Syvitski R, Kralovec JA, Noseda MD, Barrow CJ, Ewart HS et al (2006) Immunostimulatory polysaccharides from *Chlorella pyrenoidosa*. A new galactofuranan. Measurement of molecular weight and molecular weight dispersion by DOSY NMR. Biomacromolecules 7(8):2368–2376. https://doi.org/10.1021/bm060365x
Trabelsi L, Chaieb O, Mnari A, Abid-Essaf S, Aleya L (2016) Partial characterization and antioxidant and antiproliferative activities of the aqueous extracellular polysaccharides from the thermophilic microalgae *Graesiella* sp. BMC Complement Altern Med 16:210. https://doi.org/10.1186/s12906-016-1198-6
Venkatesan J, Lowe B, Anil S et al (2015) Seaweed polysaccharides and their potential biomedical applications. Starch 67(5–6):381–390. https://doi.org/10.1002/star.201400127
Venkatesan J, Anil S, Kim S-K (2017) Seaweed polysaccharides. isolation, biological and biomedical applications. Elsevier, Amsterdam
Wan XZ, Ai C, Chen YH, Gao XX, Zhong RT, Liu B et al (2019) Physicochemical characterization of a polysaccharide from green microalga *Chlorella pyrenoidosa* and its hypolipidemic activity via gut microbiota regulation in rats. J Agric Food Chem 68(5):1186–1197. https://doi.org/10.1021/acs.jafc.9b06282
Wang J, Jin W, Zhang W, Hou Y, Zhang H, Zhang Q (2013) Hypoglycemic property of acidic polysaccharide extracted from *Saccharina japonica* and its potential mechanism. Carbohydr Polym 95(1):143–147. https://doi.org/10.1016/j.carbpol.2013.02.076
Wang J, Bao A, Wang Q, Guo H, Zhang Y, Liang J, Kong W, Yao J, Zhang J (2018) Sulfation can enhance antitumor activities of *Artemisia sphaerocephala* polysaccharide in vitro and vivo. Int J Biol Macromol 107:502–511. https://doi.org/10.1016/j.ijbiomac.2017.09.018
Wassie T, Niu K, Xie C, Wang H, Xin W (2021) Extraction techniques, biological activities and health benefits of marine algae *Enteromorpha prolifera* polysaccharide. Front Nutr 8:747928. https://doi.org/10.3389/fnut.2021.747928
Wijesinghe WAJP, Jeon Y-J (2012) Enzyme-assistant extraction (EAE) of bioactive components: a useful approach for recovery of industrially important metabolites from seaweeds: a review. Fitoterapia 83(1):6–12. https://doi.org/10.1016/j.fitote.2011.10.016
Xu J, Yue RQ, Liu J, Ho HM, Yi T, Chen HB, Han QB (2014) Structural diversity requires individual optimization of ethanol concentration in polysaccharide precipitation. Int J Biol Macromol 67:205–209. https://doi.org/10.1016/j.ijbiomac.2014.03.036
Yang L, Zhang LM (2009) Chemical structural and chain conformational characterization of some bioactive polysaccharides isolated from natural sources. Carbohydr Polym 76(3):349–361. https://doi.org/10.1016/j.carbpol.2008.12.015
Yang F, Shi Y, Sheng J, Hu Q (2006) *In vivo* immunomodulatory activity of polysaccharides derived from *Chlorella pyrenoidosa*. Eur Food Res Tech 224(2):225–228. https://doi.org/10.1007/s00217-006-0315-z
Yang S, Wan H, Wang R, Hao D (2019) Sulfated polysaccharides from *Phaeodactylum tricornutum*: isolation, structural characteristics, and inhibiting HepG2 growth activity in vitro. PeerJ 7:e6409. https://doi.org/10.7717/peerj.6409
Yim JH, Kim SJ, Ahn SH, Lee CK, Rhie KT, Lee HK (2004) Antiviral Effects of Sulfated Exopolysaccharide from the Marine Microalga *Gyrodinium impudicum* Strain KG03. Mar Biotechnol 6:17–25. https://doi.org/10.1007/s10126-003-0002-z

Yim JH, Son E, Pyo S, Lee HK (2005) Novel sulfated polysaccharide derived from red-tide microalga *Gyrodinium impudicum* strain KG03 with immunostimulating activity in vivo. Mar Biotechnol 7(4):331–338. https://doi.org/10.1007/s10126-004-0404-6

Yingying S, Hui W, Ganlina G, Yinfanga P, Binluna Y (2014) The isolation and antioxidant activity of polysaccharide from the marine microalgae *Isochrysis galbana*. Carbohydr Polym 113:22–31. https://doi.org/10.1016/j.carbpol.2014.06.058

Yuan Q, Li H, Wei Z, Lv K, Gao C, Liu Y, Zhao L (2020) Isolation, structures and biological activities of polysaccharides from *Chlorella*: a review. Int J Biol Macromol 163:2199–2209. https://doi.org/10.1016/j.ijbiomac.2020.09.080

Zhang A, Sun H, Wang P, Hui Sun Han Y, Wang X (2012) Modern analytical techniques in metabolomics analysis. Analyst 137:293–300. https://doi.org/10.1039/c1an15605e

Zhang J, Liu L, Ren Y, Chen F (2019a) Characterization of exopolysaccharides produced by microalgae with antitumor activity on human colon cancer cells. Int J Biol Macromol 128:761–767. https://doi.org/10.1016/j.ijbiomac.2019.02.009

Zhang J, Liu L, Chen F (2019b) Production and characterization of exopolysaccharides from *Chlorella zofingiensis* and *Chlorella vulgaris* with anti-colorectal cancer activity. Int J Biol Macromol 134:976–983. https://doi.org/10.1016/j.ijbiomac.2019.05.117

Zhao C, Yang C, Liu B, Sarker SD, Nahar L, Yu H, Cao H, Xiau J (2018) Bioactive compounds from marine macroalgae and their hypoglycemic benefits. Trends Food Sci Technol 72:1–12. https://doi.org/10.1016/j.tifs.2017.12.001

Zhao W, Duan M, Zhang X, Tan T (2018) A mild extraction and separation procedure of polysaccharide, lipid, chlorophyll and protein from *Chlorella* spp. Renew Energy 18:701–708. https://doi.org/10.1016/j.renene.2017.11.046

Zhong D, Du Z, Zhou M (2021) Algae: a natural active material for biomedical applications. View 2(4):20200189. https://doi.org/10.1002/VIW.20200189

Zhou J, Wang M, Saraiva JA, Martins AP, Pinto CA, Prieto MA, Barba FJ (2022) Extraction of lipids from microalgae using classical and innovative approaches. Food Chem 384:132236. https://doi.org/10.1016/j.foodchem.2022.132236

Becker S, Hehemann JH (2018) Laminarin quantification in microalgae with enzymes from marine microbes. Bio-protocol. https://doi.org/10.21769/BioProtoc.2666

Deprá MC, Santos AM, Severo IA, Santos AB, Zepka LQ, Jacob-Lopes E (2018) Microalgal biorefineries for bioenergy production: can we move from concept to industrial reality? BioEnergy Res 11(4):727–747. https://doi.org/10.1007/s12155-018-9934-z

Dias RR, Severo IA, Deprá MC, Maroneze MM, Zepka LQ, Jacob-Lopes E (2020) The next-generation of microalgae-based products. in: Shukla P (ed) Microbial enzymes and biotechniques. Springer Singapore, pp 15–42. https://doi.org/10.1007/978-981-15-6895-4_2

Jiao G, Yu G, Zhang J, Ewart H (2011) Chemical structures and bioactivities of sulfated polysaccharides from marine algae. Mar Drugs 9(2):196–223. https://doi.org/10.3390/md9020196

Lin T, Liu Y, Lai C, Yang T, Xie J, Zhang Y (2018) The effect of ultrasound assisted extraction on structural composition, antioxidant activity and immunoregulation of polysaccharides from *Ziziphus jujuba* Mill var. *spinosa* seeds. Ind Crops Prod 125:150–159. https://doi.org/10.1016/j.indcrop.2018.08.078

Maity S, Mallick N (2022) Trends and advances in sustainable bioethanol production by marine microalgae: a critical review. J Clean Prod. https://doi.org/10.1016/j.jclepro.2022.131153

Morais MG, Santos TD, Moraes L, Vaz BS, Morais EG, Costa JAV (2022b) Exopolysaccharides from microalgae: Production in a biorefinery framework and potential applications. Bioresour Technol Rep. https://doi.org/10.1016/j.biteb.2022.101006

Morais MG, Stillings C, Dersch R, Rudisile M, Pranke P, Costa JAV, Wendorff J (2010) Preparation of nanofibers containing the microalga *Spirulina* (*Arthrospira*). Bioresour Technol 101(8):2872–2876. https://doi.org/10.1016/j.biortech.2009.11.059

Prybylski N, Toucheteau C, El Alaoui H, Bridiau N, Maugard T, Abdelkafi S, Michaud P (2020) Bioactive polysaccharides from microalgae. In: Jacob-Lopes E, Maroneze MM, Queiroz MI, Zepka LQ (eds) Handbook of Microalgae-Based Processes and Products. Fundamentals and Advances in Energy, Food, Feed, Fertilizer, and Bioactive Compounds, Academic Press, pp 533–571. https://doi.org/10.1016/B978-0-12-818536-0.00020-8

Rempel A, de Souza Sossella F, Margarites AC, Astolfi AL, Steinmetz RL, Kunz A, Treichel H, Colla LM (2019) Bioethanol from Spirulina platensis biomass and the use of residuals to produce biomethane: an energy efficient approach. Bioresour Technol 288:121588. https://doi.org/10.1016/j.biortech.2019.121588

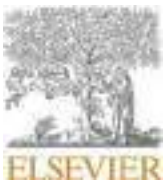
Severo IA, Dias RR, Sartori RB, Maroneze MM, Zepka LQ, Jacob-Lopes E (2021) Technological Bottlenecks in Establishing Microalgal Biorefineries. In: Shekh A, Schenk P, Sarada R (eds) Microalgal Biotechnology: Recent Advances, Market Potential, and Sustainability. Royal Society of Chemistry, pp 118–134. https://doi.org/10.1039/9781839162473-00118

Silva AS, Magalhães WT, Moreira LM, Rocha MVP, Bastos AKP (2018) Microwave-assisted extraction of polysaccharides from *Arthrospira* (*Spirulina*) *platensis* using the concept of green chemistry. Algal Res 35:178–184. https://doi.org/10.1016/j.algal.2018.08.015

Xu SY, Huang X, Cheong KL (2017) Recent advances in marine algae polysaccharides: isolation, structure, and activities. Mar Drugs 15:2–16. https://doi.org/10,3390/md15120388

Publisher's Note Springer Nature remains neutral with regard to jurisdictional claims in published maps and institutional affiliations.

Sustainable Energy Technologies and Assessments 52 (2022) 102073



Contents lists available at ScienceDirect

Sustainable Energy Technologies and Assessments

journal homepage: www.elsevier.com/locate/seta



Smart override of the energy matrix in commercial microalgae facilities: A transition path to a low-carbon bioeconomy

Rosangela Rodrigues Dias, Mariany Costa Deprá, Ihana Aguiar Severo, Leila Queiroz Zepka, Eduardo Jacob-Lopes *

Bioprocess Intensification Group, Federal University of Santa Maria (UFSM), Roraima Avenue, 1000, 97105-900, Santa Maria, RS, Brazil

ARTICLE INFO

Keywords:
Algae
Geospatial location
Onshore wind energy
Photovoltaic solar energy
Sustainability metrics

ABSTRACT

The sustainability and economic viability of the microalgae-based processes and products remain questionable by requiring high fossil energy demands. Therefore, herein, we seek to evaluate from an environmental and economic point of view the integration potential of green electricity into microalgae production facilities. Ten geographic positions with commercial microalgae cultivation plants were investigated as to the potential to generate photovoltaic solar and onshore wind energy and as to the economic feasibility of the implementation of these systems. The results reveal that for the production of 1 ton/month of whole dried biomass, pigments, and polyunsaturated fatty acids, the greatest impact, with the exception of the land use category, was for fossil energy consumption. In this line, replacing fossil energy with onshore wind and photovoltaic solar energy, these impacts were reduced in the order of 20–100% and 9–87%, respectively. The investment return period for the renewable energy systems was found to be within a range of 0.85–4.86 years. The solar and wind potential, and the investment return period are highly dependent on geospatial location. The results of this study demonstrate that the implementation of a renewable energy system can supply part of the plant's energy demand, reducing electricity costs, and its environmental footprints.

Introduction

Humanity lives in a pathological system that damages all the earth's ecosystems. We are exceeding the regenerative capacity of the ecological resources and services and dumping tons of carbon dioxide into the atmosphere. The consequences are already being felt and, unfortunately, there has not yet been a satisfactory performance to avoid changes that will be irreversible [13]. However, the race to overcome the climate emergency is underway, and many countries are committed to achieving carbon neutrality up until 2050 [11,30].

Currently, the largest emitter of CO_2 related to energy is coal. Coal is responsible for most of the electricity generated and, as the global demand for electricity continues to grow, the decarbonization of its offer becomes urgent [2]. Besides that, the impacts of energy generated from coal are not limited to CO_2 emissions, there are other environmental charges related to its generation that affect the ecosystem quality and the use of natural resources. Ending the coal age and embracing a new energy paradigm is undoubtedly a necessary action, and the pressure on nations to end their dependence is increasing [39,17].

In particular, in the business ambit, the concern with sustainability has become a differentiator and one of the reasons that have motivated companies to adhere to the use of renewable energy in their stores and production lines is commercial visibility. Besides that, many companies have sought to adapt to a low-carbon economy. Noteworthy, it is likely that those that do not adapt to more sustainable business opportunities will lose space in the domestic and foreign markets [23].

Moreover, meeting the needs of a crescent population requires the exploration of renewable feedstocks, such as microalgae. Microalgae biotechnology can help overcome concerns related to food, feed, energy, materials, and the environment. In the last years, the number of companies that are betting on the biotechnological potential of the microalgae for biofuel production, biological mitigation of greenhouse gases, and meeting future demands for food and feed has grown exponentially. Naturally, if exploited under a synergistic approach, the microalgae can be used to overcome these concerns in an integrated manner [26,5].

At the moment, the microalgae have been exploited especially to obtain single-cell protein and chemical specialties, such as pigments and polyunsaturated fatty acids [21]. These products are a business opportunity quite ecological. In particular, single-cell protein offer new food

* Corresponding author.
E-mail address: ejacoblopes@gmail.com (E. Jacob-Lopes).

https://doi.org/10.1016/j.seta.2022.102073
Received 20 July 2021; Received in revised form 24 January 2022; Accepted 2 February 2022
2213-1388/© 2022 Elsevier Ltd. All rights reserved.

Nomenclature

CO_2	Carbon dioxide
LCA	Life cycle assessment
DHA	Docosahexaenoic acid
EPA	Eicosapentaenoic acid
LCI	Life cycle inventory
LCIA	Life cycle impact assessment
ILCD	International Reference Life Cycle Data System
ODP	Ozone depletion potential
GWP	Global warming potential
SMOG	Photochemical ozone creation potential
AP	Acidification potential
EP	Eutrophication potential
ECO	Ecotoxicity
FFD	Fossil fuel depletion
WF	Water footprint
LU	Land use
TWN	Taiwan
IND	India
ISR	Israel
USA	United States of America
ESP	Spain
DEU	Germany
AUS	Australia
CIGS	Copper-Indium-Gallium-Selenium
O&M	Operation and maintenance
TIC	Total installed cost
IRP	Investment return period
ROI	Return on investment
MW	Megawatt
TPBR	Tubular photobioreactor
RP	Raceway Pond
sCO_2	Supercritical CO_2 extraction

and feed platform, more efficient and sustainable [36]. As microalgae are now highlighted in the global market, the environmental impact of the current portfolio of commercial products underwent a rigorous assessment. The findings make it clear that the main environmental critical point of microalgae-based processes and products is the energy footprint. The energy demand in the stages upstream and downstream of the production chain are responsible for approximately 98% of environmental impacts. The hotspots identified in these stages are attributed to the equipments, which are of energy-intensive use [6].

From the point of view of energy consumption, besides the problems related to pollutant emissions, the energy invoice is excessive, which affects the viability of the products to use as commodities. Thus, having as the main motivation the reduction of fossil energy consumption and its impacts, this study assessed, from an environmental and economic point of view, the integration potential of renewable energies in microalgae-based processes and products. Ten geographical positions, with relevant commercial microalgae cultivation plants worldwide, were selected to assess the potential for photovoltaic solar and onshore wind electricity generation, besides the economic feasibility of implementation of these systems in these geospatial locations. According to the best of our knowledge, this is the first report that assesses the influence of the energy source on the environmental impacts of microalgae consolidated production chains.

Methods

The flowchart in Fig. 1 shows the methodological steps used in this study. The assumptions and procedures for each step are described in detail below.

Life cycle assessment (LCA)

Goal and scope definition

The framework for LCA described by ISO 14040 was selected for environmental assessment [20]. The commercial microalgae products considered were whole dried biomass, pigments, and polyunsaturated fatty acids. The biotechnological route of these products and the data for the theoretical–experimental analysis were based on consolidated processes.

Functional unit and system boundaries

The scope of the system covers the production and energy demand of 1 ton/month of whole dried biomass, β-carotene, phycocyanin, astaxanthin, docosahexaenoic acid (DHA), and eicosapentaenoic acid (EPA). Fig. 2 illustrates the limits of the system, microalgae species, and cultivation systems considered in the analyzed case study. System boundaries were defined from the cradle-to-gate life cycle according to Deprá et al. [6]. The analysis included the impact of the fossil, onshore wind, and photovoltaic solar energy requirements, and only the energy demand needed to operate the system was accounted for. Physical sterilization was established only for fermenters and for closed photobioreactors, chemical sterilization was considered.



Fig. 1. Methodological steps were used in this study.

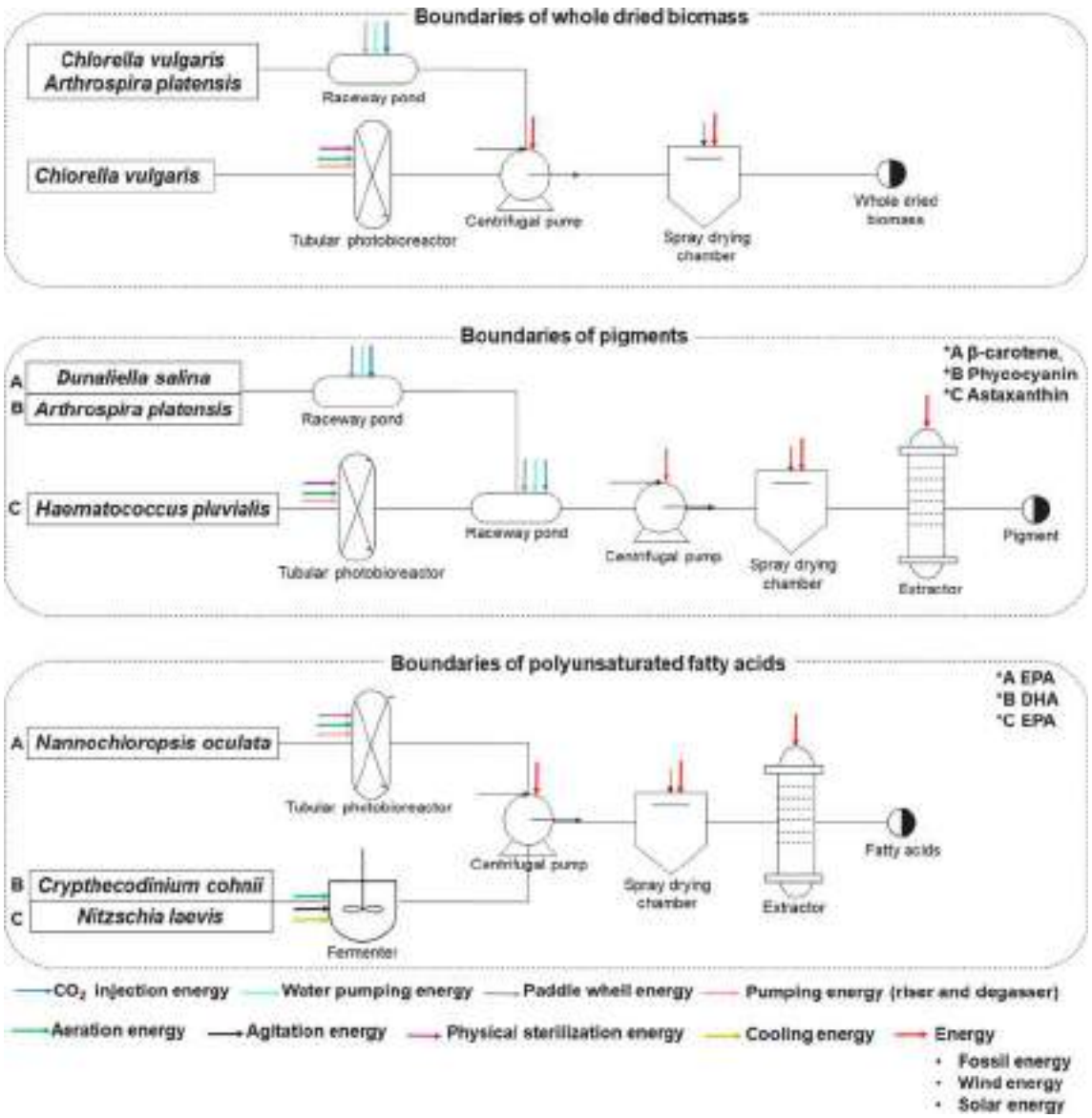


Fig. 2. System boundaries for the evaluation of commercial microalgae products. Docosahexaenoic, DHA; Eicosapentaenoic; EPA. Adapted from Deprá et al. [6].

Table 1
Energy requirement for the operation in raceway pond, tubular photobioreactor and fermenter. Adapted from Sobczuk et al. [33], Acién et al. [1], Spruijt et al. (2015), Deprá et al. [6].

Process	Unit	Raceway Pond (RP)	Tubular photobioreactor (TPBR)	Fermenter
Cultivation				
Energy consumption for cooling	kWh/m^3	–	15	–
Aeration energy	kWh/m^3	–	0.13	1
Agitation energy	kWh/m^3	–	–	0.0073
Physical sterilization	kWh/m^3	–	–	7.22
Water evaporation	m^3	1.3×10^{-1}	2×10^{-3}	–
Electric energy for paddle wheel	kWh/m^3	0.54	–	–
Electric energy for water pumping	kWh/m^3	0.1	–	–
Pumping energy (riser and degasser)	kWh/m^3	–	0.95	–
Electric energy for CO_2 injection	kWh/m^3	0.33	–	–
Harvest				
Energy consumption centrifugation	kWh/m^3	1.25	1.25	1.25
Drying				
Spray-dryer	kWh/kg evaporated water	1.09	1.09	1.09
Extraction				
sCO_2	kWh/kg	0.8	0.8	0.8

Supercritical CO_2 extraction, sCO_2.

Life cycle inventory (LCI)

The LCI data were obtained from the literature. The energy specifications required for operation are based on the main industrial-scale configurations, i.e., raceway ponds, tubular photobioreactors, and fermenters (Table 1). Noteworthy, raceway ponds are the most widely used culture systems for commercial microalgae production because of their flexibility, low cost, and ease of expansion. On the other hand, closed photobioreactors, especially tubular photobioreactors, have been used for their good control of cultivation conditions and high productivity. Fermenters, in turn, are a viable alternative that, although restricted to a few species, overcomes the light dependence of photoautotrophic systems. For more information on microalgae production systems, see Maroneze and Queiroz [25] and Deprá et al. [7]. The input and output conditions of the bioprocesses for obtaining 1 ton/month of whole dried biomass, β-carotene, phycocyanin, astaxanthin, DHA, and EPA, as well as the energy demand, are shown in Table 2.

Life cycle impact assessment (LCIA)

The characterized values of the environmental impact categories were estimated according to Deprá et al. [6] and Maroneze et al. [24]. The normalization of data followed the methodology described by the International Reference Life Cycle Data System (ILCD) Handbook [15]. The impact categories considered were: ozone depletion potential (ODP), global warming potential (GWP), photochemical ozone creation potential (SMOG), acidification potential (AP), eutrophication potential (EP), ecotoxicity (ECO), fossil fuel depletion (FFD), water footprint (WF), and land use (LU). The respective characterization and normalization factors are shown in the Supplementary Material (Table S1 and S2). The main objective of the application of LCA was to assess the environmental footprint of the energy sources, that is, the conventional process powered fossil energy versus onshore wind and photovoltaic solar energy.

Geographic positions

Ten geographical positions were selected to assess the availability of photovoltaic solar and onshore wind energy for electricity generation, and the economic feasibility of installing a renewable energy system. The selected geographical positions were: Pingtung-TWN, Unaiyur-IND, Ketura-ISR, Kona-USA, Calipatria-USA, Moses Lake-USA, Arcos de La Frontera-ESP, Roquette Klötze-DEU, Las Palmas-ESP, Hutt Lagoon-AUS (Fig. 3). These geographical positions were selected because they have commercially established microalgae production units. The data of average solar irradiance and the average wind speed of the geographical positions were retrieved from the Solar Electricity Handbook (http://www.solarelectricityhandbook.com) and Weather Spark (https://weatherspark.com) websites. From these data, the energy produced monthly by photovoltaic module and wind turbine in each geographic position was obtained, as described in Eq. 1–5. This study considered CIGS photovoltaic modules (copper-indium-gallium-selenium) with an efficiency of 18%, an area of 0.94 m^2, and a useful life of 25 years for the photovoltaic solar energy system and for the onshore wind energy system horizontal wind turbines with an efficiency of 35%, a blade length of 54 m, a rotor diameter of 110 m, and a service life of 20 years. The real efficiency of the wind turbine was found discounting possible mechanical losses, electrical losses of the turbine, electrical transmission losses, and losses due to downtime due to failure or maintenance. The information on the blade length and rotor diameter of the onshore wind energy system was used to calculate land use (LU). To calculate the number of wind turbines needed to meet the energy demand of 1 ton/month of bioproduct was considered the specifications of the model VERNE 555 wind turbine. The number of photovoltaic modules and wind turbines needed to meet the energy demand of 1 ton/month of bioproduct was determined through Eq. (6). The total area required for the installation of the photovoltaic modules and wind turbines was determined using Eqs. (7) and (8), respectively. The considerations for the economic analysis of the feasibility of installing a renewable energy system are provided in Section 2.3.1.

$$ES_{output} = (Es \times Ap \times \grave{E}\ p \times\ ) \times 30d \quad (1)$$

where ES_{output} is the energy produced by the module monthly (kWh), Es is the solar irradiance (kWh/m^2/day), Ap is the panel surface area (m^2), and Ηp is the panel efficiency.

$$A_{HAWT} = \pi \times L^2 \quad (2)$$

$$P_{wind} = 0.5 \times \rho \times V^3 \times A_{HAWT} \quad (3)$$

$$\hat{I}¼ = (1 - K_m) \times (1 - K_e) \times (1 - K_{e,t}) \times (1 - K_t) \times C_p \quad (4)$$

$$EW_{output} = (\hat{I}¼ \times P_{wind}) \times 720h \quad (5)$$

where A_{HAWT} is the swept area of the horizontal-axis wind turbine, L is the blade length, P_{wind} is the available wind power, ρ is the air density (assumed to be 1.225 kg/m^3 by default), V is the wind speed, C_p is the turbine efficiency (assumed to be 35%), K_m are the mechanical losses of the blades and gearbox (assumed to be 0.15%), K_e are the electrical losses of the turbine (assumed to be 1.25%), $K_{e,t}$ are the electrical losses of transmission to the grid (assumed to be 5%), K_t is the percentage of time out of order due to failure or maintenance (assumed to be 2.5%), and μ is the real efficiency, and EW_{output} is the energy produced (kWh/month).

$$N\hat{A}° = \frac{Er}{EP} \quad (6)$$

where N° is the number of photovoltaic modules and wind turbines to meet energy demand, Er is the required energy (kWh/month), EP is the energy produced by a photovoltaic module and wind turbine (kWh/month).

$$Ar = N\hat{A}° \times Am \quad (7)$$

where Ar is the area required for installation of photovoltaic modules, N° is the number of photovoltaic modules, and Am is the area of each photovoltaic module.

$$Ar = (10 \times RD) \times (5 \times RD) \quad (8)$$

where the distance considered safe for the installation of wind turbines is 10 times the rotor diameter (RD), if installed downstream, and 5 times the RD, if installed at the side, in relation to the wind direction.

Bioeconomy

Cost analysis

The total installed cost (TIC) of grid-connected photovoltaic solar energy and grid-connected onshore wind energy was obtained from the International Renewable Energy Agency [19]. The annual cost of operation and maintenance (O&M) was estimated at 2% of TIC. To calculate the investment return period (IRP), the TIC plus the O&M was divided by the expected monetary savings over the period of one month. The fossil energy savings expected have been converted into monetary savings according to the electricity price of each country (USD/kWh for business users). It should be noted that, although the energy requirement for 1 ton/month of bioproduct is the same for all geographic positions, the electricity price is not. The electricity price by country was obtained from the Global Petrol Prices website [14]. To calculate the return on investment (ROI) was subtracted the TIC plus the O&M from the revenue generated during the useful life of the renewable energy system and the result was divided again by the TIC plus the O&M.

Table 2
Inputs/outputs of the production process of 1 ton/month whole dried biomass, β-carotene, phycocyanin, astaxanthin, DHA and EPA.

Process	Unit	*C. vulgaris* (RP)	*C. vulgaris* (TPBR)	*A. platensis* (RP)	*A. platensis* (RP)	*D. salina* (RP)	*H. pluvialis* (TPBR and RP)	*C. cohnii* (Fermenter)	*N. laevis* (Fermenter)	*N. oculata* (TPBR)
Cultivation										
Tubular photobioreactor	m^3	–	47.62	–	–	–	100.27	–	–	1,587.1
Energy consumption for cooling	kWh	–	514,296.0	–	–	–	1,082,916.0	–	–	17,140,680.0
Aeration energy	kWh	–	4,457.23	–	–	–	9,385.27	–	–	148,552.56
Pumping (riser and degasser)	kWh	–	32,572.08	–	–	–	68,584.68	–	–	1,085,576.4
Water evaporation	m^3	–	0.095	–	–	–	0.201	–	–	3.17
Fermenter	m^3	–	–	–	–	–	–	27.77	133.33	–
Physical sterilization	kWh	–	–	–	–	–	–	200.49	962.64	–
Agitation energy	kWh	–	–	–	–	–	–	145.96	700.78	–
Aeration energy	kWh	–	–	–	–	–	–	19,994.4	95,997.6	–
Raceway pond	m^3	166.66	–	104.17	1,388.54	925.93	2,677.23	–	–	–
Electric energy for paddle wheel	kWh	64,797.41	–	40,501.3	539,864.35	360,001.58	1,040,907.02	–	–	–
Electric energy for water pumping	kWh	11,995.2	–	7,500.24	99,974.88	66,666.96	192,760.56	–	–	–
Electric energy for CO_2 injection	kWh	39,592.8	–	24,750.8	329,917.10	220,000.97	636,109.85	–	–	–
Water evaporation	m^3	21.67	–	13.54	180.51	120.4	348.04	–	–	–
Biomass productivity	ton/m^3/ month	0.006	0.021	0.0096	0.0096	0.0135	0.012	0.300	0.023	0.045
Output										
Algae liquid	ton	11.76	11.42	12.69	71.09	83.3	222.2	44.42	16.0	380.9
Harvest										
Input										
Energy consumption centrifugation	kWh	208.33	59.53	130.21	1,735.68	1,157.41	3,471.88	34.71	166.66	1,983.88
Drying										
Input										
Wet biomass	ton	8.82	8.55	9.51	53.31	49.98	133.32	33.3	12.0	285.66
Spray-dryer	kWh	9,613.8	9,319.5	10,365.9	58,107.9	54,478.2	145,318.8	36,297.0	13,080.0	311,369.4
Output										
Whole dried biomass	ton	1	1	1	–	–	–	–	–	–
Extraction										
Input										
Dry biomass	ton	–	–	–	13.33	12.5	33.33	8.33	3.0	71.42
sCO_2	kWh	–	–	–	10,664.0	10,000.0	26,664.0	6,664.0	2,400.0	57,136.0
Output										
Oil rich pigments	Ton	–	–	–	1	1	1	–	–	–
Oil	Ton	–	–	–		–	–	1	1	1
Electricity	kWh/month	126,207.54	560,704.34	83,248.45	1,040,263.91	712,305.12	3,206,200.06	63,336.56	113,307.68	18,745,298.24

Docosahexaenoic, DHA; Eicosapentaenoic, EPA; Raceway pond, RP; Tubular photobioreactor, TPBR; Supercritical CO_2 extraction, sCO_2.

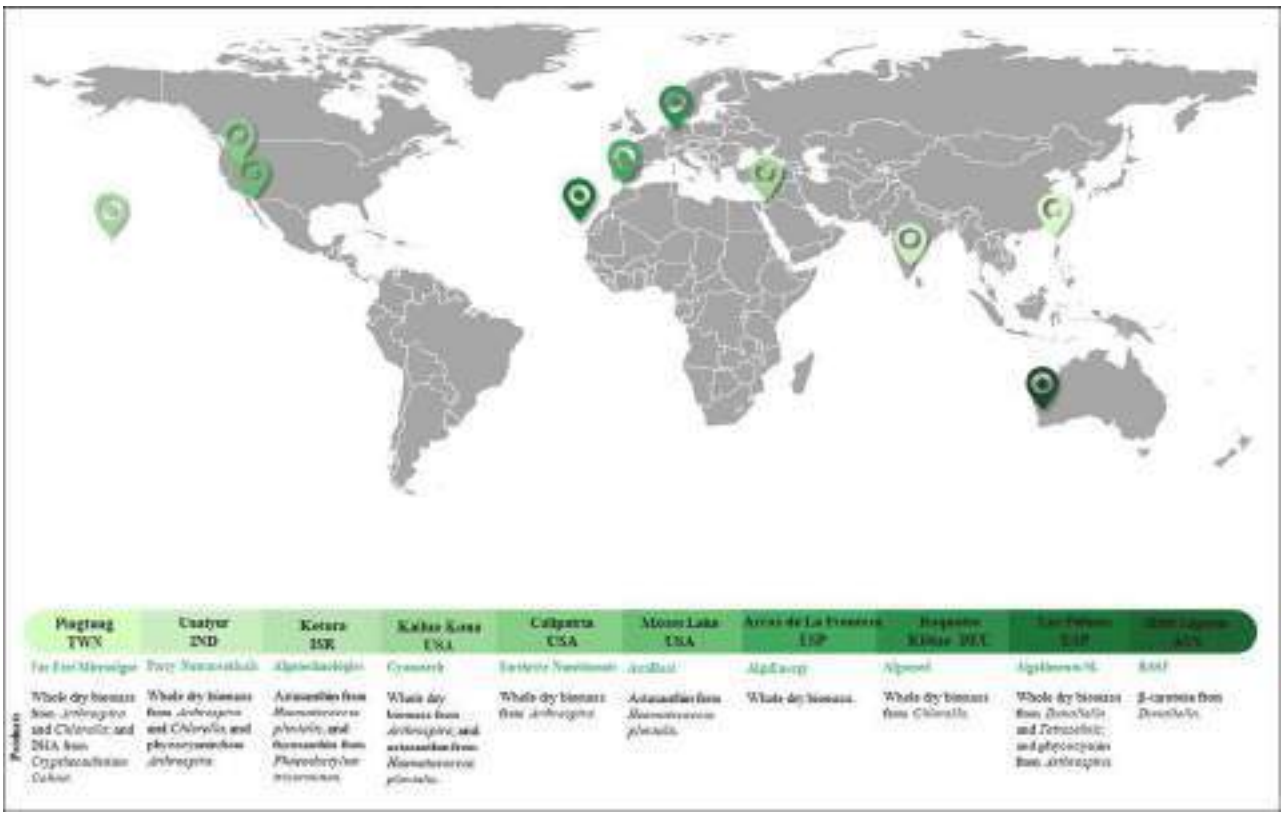


Fig. 3. World Map with the geographical positions of the study. Docosahexaenoic, DHA; India, IND; Australia, AUS; Taiwan, TWN; Israel, ISR; United States of America, USA; Spain, ESP; Germany, DEU.

Table 3 shows the electricity price, the TIC, and O&M of photovoltaic solar and onshore wind energy by country/region.

Estimation of carbon credits

Carbon credits were estimated according to the carbon footprint of the renewable energy system integrated into the production process for commercial microalgae products. The carbon price was recovered from the World Bank [38]. The potential benefit of installing a renewable energy system was quantified according to Eqs. (9) and (10), following the methodology of Severo et al. [31] and Pérez-Fortes et al. [29].

$$CO_{2not\text{-}produced} = CO_{2conventional} - CO_{2emitted} \quad (9)$$

$$CO_{2avoided} = CO_{2not\text{-}produced} + CO_{2captured} \quad (10)$$

where conventional CO_2 is the amount of CO_2 released in the conventional process, while CO_2 emitted and CO_2 captured refer to the renewable energy system integrated into the production process for microalgae products.

Results and discussion

Influence of geospatial location on the potential for renewable energy generation

The production of electric energy from renewable sources, such as solar and wind, plays a noble role in the supply of sustainable energy. Unlike traditional sources of energy, the availability of solar and wind energy depends on the climate, which temporally and spatially is very variable. Choosing locations that are unfavorable to energy generation can result in an investment loss. Notoriously, the economic viability of such an enterprise is conditioned especially to solar irradiation and the wind speed of the geographical positions [9]. In this sense, Fig. 4 shows the annual average of solar irradiance and wind speed of the different geographical positions considered in this study. The values of average solar irradiance and average wind speed from month to month are provided in the Supplementary Material (Table S3).

According to Fig. 4, Roquette Klötze-DEU has the lowest potential for generating photovoltaic solar energy, with an annual average solar irradiance of 3.3 kWh/m^2/d. In summer, the average monthly solar irradiance reaches 6.2 kWh/m^2/d, but in autumn and winter, it reaches monthly averages of up to 0.6 kWh/m^2/d. In the other geographical positions, the annual average values of 4.99 to 6.4 kWh/m^2/d suggest a good potential for the installation of solar panels throughout the year. The positions that presented the greatest potential for generating photovoltaic solar energy are Hutt Lagoon-AUS, Ketura-ISR, and Calipatria-USA. In these geographical positions, the average monthly solar irradiance reaches 8.5 kWh/m^2/d in summer.

Concerning wind potential, only Roquette Klötze-DEU, Las Palmas-ESP, and Hutt Lagoon-AUS showed potential for onshore wind energy generation. In theory, small on-grid power systems, normally used in rural residences and farms, require an average speed of at least 3.5–4.5 m/s to be economically viable. As can be seen in Fig. 3, the other geographic positions of the study present winds with a speed equal to or less than 4.5 m/s, i.e., insufficient the viability of such an enterprise. It is worth mentioning that viability would not be achieved for any of the geographical positions if considering the application of large machines, with a nominal power greater than 1 MW. This is because these systems require an average speed of at least 6.5–7.5 m/s to be economically viable and profitable [3].

In general, depending on the local wind speed, it is possible to install large machines and, the higher the wind speed, the smaller the number of wind turbines to be installed to meet the determined energy demand and, by consequence, the smaller the area required for installation. The same goes for solar irradiation (Fig. 5). Taking as an example the Fig. 5,

Table 3
Electricity price, the total installed cost, and operation and maintenance cost of the photovoltaic solar and onshore wind energy by country/region.

Geographic Position	Renewable Energy	Electricity Price (USD/kWh)	O&M (USD/kW/year)	TIC (USD/kW)
Pingtung-TWN	Photovoltaic Solar	0.13	15.20	760
	Onshore Wind		32.66	1633
Unaiyur-IND	Photovoltaic Solar	0.11	16.34	817
	Onshore Wind		21.10	1055
Ketura-ISR	Photovoltaic Solar	0.11	19.92	996
	Onshore Wind		32.66	1633
Kona-USA	Photovoltaic Solar	0.11	49.60	2480
	Onshore Wind		32.72	1636
Calipatria-USA	Photovoltaic Solar	0.11	49.60	2480
	Onshore Wind		32.72	1636
Moses Lake-USA	Photovoltaic Solar	0.11	61.62	3081
	Onshore Wind		32.72	1636
Arcos de La Frontera-ESP	Photovoltaic Solar	0.15	21.60	1080
	Onshore Wind		36.00	1800
Roquette Klötze-DEU	Photovoltaic Solar	0.23	22.60	1130
	Onshore Wind		36.00	1800
Las Palmas-ESP	Photovoltaic Solar	0.15	21.60	1080
	Onshore Wind		36.00	1800
Hutt Lagoon-AUS	Photovoltaic Solar	0.20	29.28	1464
	Onshore Wind		31.10	1555

India, IND; Australia, AUS; Taiwan, TWN; Israel, ISR; United States of America, USA; Spain, ESP; Germany, DEU; Total installed cost, TIC; Operation and maintenance, O&M.

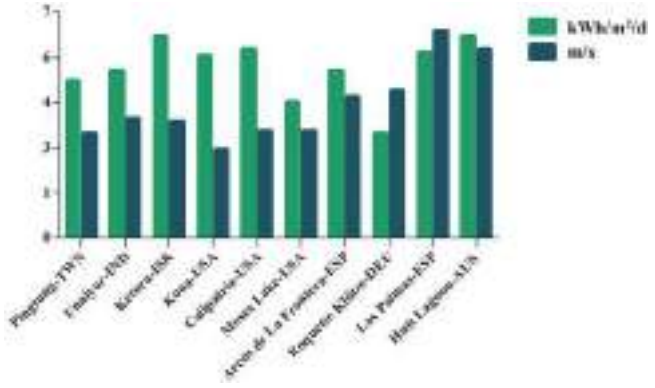


Fig. 4. Annual average solar irradiance and wind speed by geographic position. India, IND; Australia, AUS; Taiwan, TWN; Israel, ISR; United States of America, USA; Spain, ESP; Germany, DEU.

what is observed is that less sunny locations and with low wind speeds require larger systems to generate the same amount of energy that a smaller system can produce in a sunny location and with high wind speeds. In this sense, it is notable that the geographical position influences the generation potential of onshore wind and photovoltaic solar energy and the economic viability of these systems.

Noteworthy, the geographical position is also strongly related to the

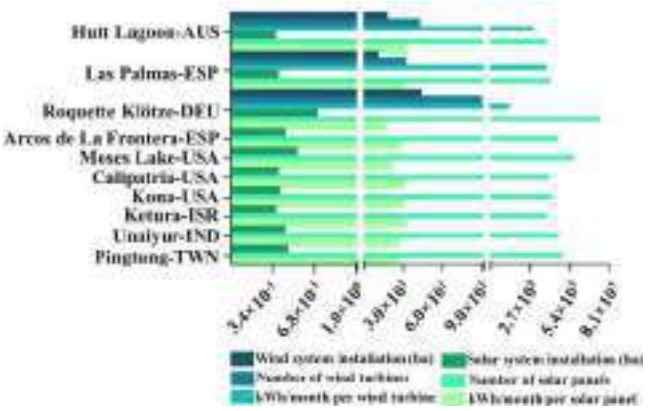


Fig. 5. Number of solar panels/wind turbines and area required for installation of the photovoltaic solar and onshore wind system to meet the energy demand for production of 1 ton/month of *Chlorella vulgaris* biomass in RP. Raceway Pond, RP; India, IND; Australia, AUS; Taiwan, TWN; Israel, ISR; United States of America, USA; Spain, ESP; Germany, DEU.

bioprocesses performance that occurs predominantly outdoors [32]. Dias et al. [8] when mapping the photobioreactors' performance for microalgae culture indicated the equatorial and tropical zone as favorable to the cultivation and harvesting of microalgae without an off-season. This is because these zones present favorable light and temperature conditions. At the same time, these zones also present great potential for generating photovoltaic solar energy, greater than the other zones. This is because the solar irradiation reaches these two climatic zones more intensely and the seasonal variations are more stable.

Comparatively, onshore wind systems are more efficient than photovoltaic solar systems by have a smaller carbon footprint and produce more energy, considering that they operate during the day and night. Besides that, a single wind turbine can generate the same amount of electricity that hundreds of solar panels. However, the installation of such systems generally has a higher total installed cost and requires a larger area for installation (Table 3 and Fig. 5). Therefore, in economic terms, when the availability of resources allows choosing between solar and wind, solar can have advantages. Besides that, wind resource, unlike solar, seems to be available in specific regions. Finally, it is noteworthy that, it would be pertinent that suitable sites for the development of microalgae biotechnology were also promising for the establishment of wind and/or photovoltaic solar systems or, ultimately, that they were strategically located close to renewable power generation plants.

Environmental impact of microalgae-based products

The environmental impacts of the production of 1 ton/month of whole dried biomass, β-carotene, phycocyanin, astaxanthin, DHA, and EPA in consolidated cultivation systems using fossil, onshore wind, and photovoltaic solar energy are shown in Fig. 6.

The environmental impacts of the cradle-to-gate for the production of 1 ton/month of bioproduct for most categories are not in the same order of magnitude. For 8 of the 9 impact categories considered, the consumption of fossil energy in the bioprocesses has, by far, the highest emissions. Besides that, independent of the microalgae species, product, technological route, and cultivation system, it has the greatest environmental footprint. Land use (LU) is the only category in which fossil energy has an equal and/or lesser impact than that of renewable energies. This is because the installation of an on-grid renewable energy system to feed a microalgae plant requires an extra land area.

In this study, based on the requirement of photovoltaic solar and onshore wind energy, for almost all bioproducts, the implementation of a photovoltaic solar energy system next to the microalgae installation presented a greater impact associated with LU. The exceptions were for

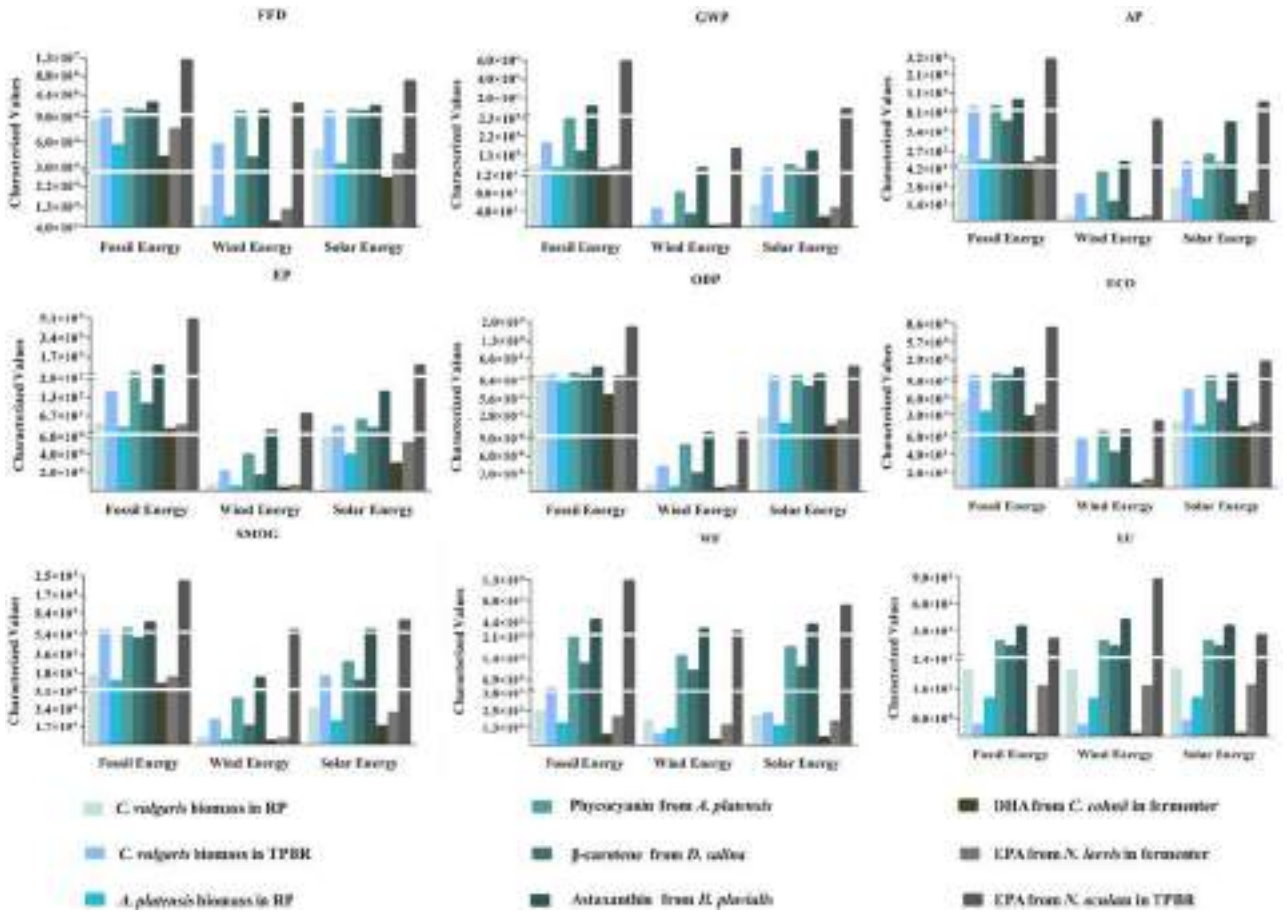


Fig. 6. Characterized values of the environmental impact categories associated with microalgae-based products based on the energy source. Docosahexaenoic, DHA; Eicosapentaenoic, EPA; Tubular photobioreactor, TPBR; Raceway pond, RP; Global warming potential, GWP; Fossil fuel depletion, FFD; Acidification potential, AP; Eutrophication potential, EP; Ecotoxicity, ECO; Photochemical oxidant creation potential, SMOG; Water footprint, WF; Ozone depletion potential, ODP; Land use, LU.

the production of astaxanthin by *H. pluvialis* and EPA by *N. oculata*. These bioproducts are the most energy-intensive and the area occupied for installing wind turbines has exceeded the area required for installing solar panels. The reason for this is that the installation of more than one wind turbine requires a spacing in the order of 5 and 10 times the diameter of the rotor, when installed laterally and downstream, respectively. Due to the spacing between one turbine and another, the portion of the total area of the onshore wind installation was larger than it gives photovoltaic solar. However, it is worth mentioning that the area occupied for installing wind turbines does not prevent the soil from fulfilling other functions. Likewise, it is possible to allocate the solar panels on the roof of the industrial unit, which would provide a smaller or null footprint. In short, the results of this study show that, regardless of the energy source and bioproduct, the impact related to LU remained in the same order of magnitude and, therefore, their differences are within the uncertainty of the foreseen impacts.

However, it is important to highlight that the impact associated with the LU for installing a renewable energy system can vary considerably and basically depends on the characteristics of the wind turbine and/or solar panel and the geospatial location. The characteristics of the product to be installed, as well as the average wind speed and average solar irradiation of a given location, determine the number of wind turbines and solar panels to be installed to meet the energy demand, as well as the area required for installation and consequently, its environmental impact. Besides that, although the impact of cloud cover on the efficiency of solar panels was not considered in the study, it is emphasized that cloud cover can lead to the lowest or taller output power under certain conditions [27,22]. About that, the detailed analysis of the region and of the climatic interferences allows program yourself so that the energy production goals are reached.

Regarding water consumption, the generation of onshore wind energy followed by photovoltaic solar has the lowest consumption. It is worth mentioning here that water consumption occurs mainly in the production step of solar panels and wind turbines, and this step dominates the life cycle, being responsible for a large part of all environmental impacts [10,12,28]. As expected, for all bioproducts evaluated, the WF was lower for powered processes to onshore wind energy, followed by photovoltaic solar and fossil, respectively. Our results show that the impact of WF cannot be measured only based on the operating volume of the bioreactors. This is because the energy demand and the electricity source also have an influence. By way of example, Deprá et al. [6] when disregarding the consumption of water to generate fossil electricity, necessary for the production of 1 ton/month of *C. vulgaris* biomass in RP and *C. vulgaris* biomass in TPBR, found values of 166.6 and 47.62 m^3, respectively. In contrast, we found slightly higher values in the order of 242 m^3 for *C. vulgaris* biomass in RP and 384 m^3 for *C. vulgaris* biomass in TPBR. Comparatively, under the same functional unit, values of 207 and 228 m^3 were found for the photovoltaic solar-powered process. What is observed is that for *C. vulgaris* biomass in TPBR the impact of WF was lower when associated only with the operational volume of the bioreactor, however, it was greater when considering the energy demand and the energy source. These results show that the impact associated with WF is enlarged not only in proportion to the operating volume of the bioreactor but mainly to the energy demand and the source of electrical energy.

The impacts associated with the categories of ECO, FFD, AP, EP,

GWP, ODP, and SMOG are also intimately related to energy demand and the energy source. For all these categories including WF, the environmental impact of the production of 1 ton/month of *C. vulgaris* biomass in TPBR, phycocyanin, astaxanthin, and EPA by *N. oculata* are higher, and for the other bioproducts they are lower. This can be attributed to the energy demand in the upstream and downstream steps of each product. In parallel, the emissions vary according to the energy source. In general, onshore wind-powered processes have the lowest emissions for both categories. The emissions for photovoltaic solar-powered processes are also low, however, depending on the bioproduct, the impacts are in the same magnitude as those using coal as an energy source.

Concerning the carbon neutrality and decarbonization goals of the electric sector, the environmental impact category of particular interest is related to the global warming potential (GWP). Our results demonstrate that there is a net potential for the reduction of CO_2 emissions. The consumption of onshore wind and photovoltaic solar energy in the bioprocesses produced about 97 and 87% less CO_2 compared to fossil energy consumption. The findings corroborate the results found in previous studies [16]. Less energy-intensive products, such as *A. platensis* biomass in RP and EPA from *N. laevis*, the emissions with the consumption of onshore wind energy are reduced by 300 and 408 tCO_2/year. For energy-intensive products, such as astaxanthin and EPA from *N. oculata*, are reduced by 11,556 and 67,548 tCO_2/year. These values are slightly lower for photovoltaic solar energy consumption.

What is significant about this issue is that the microalgae-based products could become 100% carbon neutral if there were an environmental compensation of the gases that cannot be avoided. This compensation could be made through the purchase of carbon credits or complementary actions such as wastewater treatment and biological carbon capture and utilization. Notoriously, the implementation of environmental compensation actions can be prohibitively expensive and, therefore, the viability of such actions would need to be better evaluated.

Finally, the magnitude of the CO_2 net emission savings with the consumption of photovoltaic solar and onshore wind energy is undoubtedly an opportunity to leverage the bioeconomy of the microalgae-based products, once it enables the generation of additional revenues from the sale of carbon credits. Feeding the bioprocesses with renewable energy would be in alignment with the sustainability objective.

Normalization

The characterized values of the environmental impact categories were related to a global reference value to better understand the relative magnitude of the emissions associated with the production of 1 ton/month of whole dried biomass, pigments, and polyunsaturated fatty acids using fossil energy, onshore wind energy, and photovoltaic solar energy. The normalized data for the impact categories are shown in Fig. 7.

The analysis shows that powered bioprocesses the onshore wind energy, followed by photovoltaic solar, have a smaller impact for 8 of the 9 evaluated categories. The exception is the LU category where the impact associated with the production of astaxanthin by *H. pluvialis* and EPA by *N. oculata* is greater for the use of onshore wind energy, and for

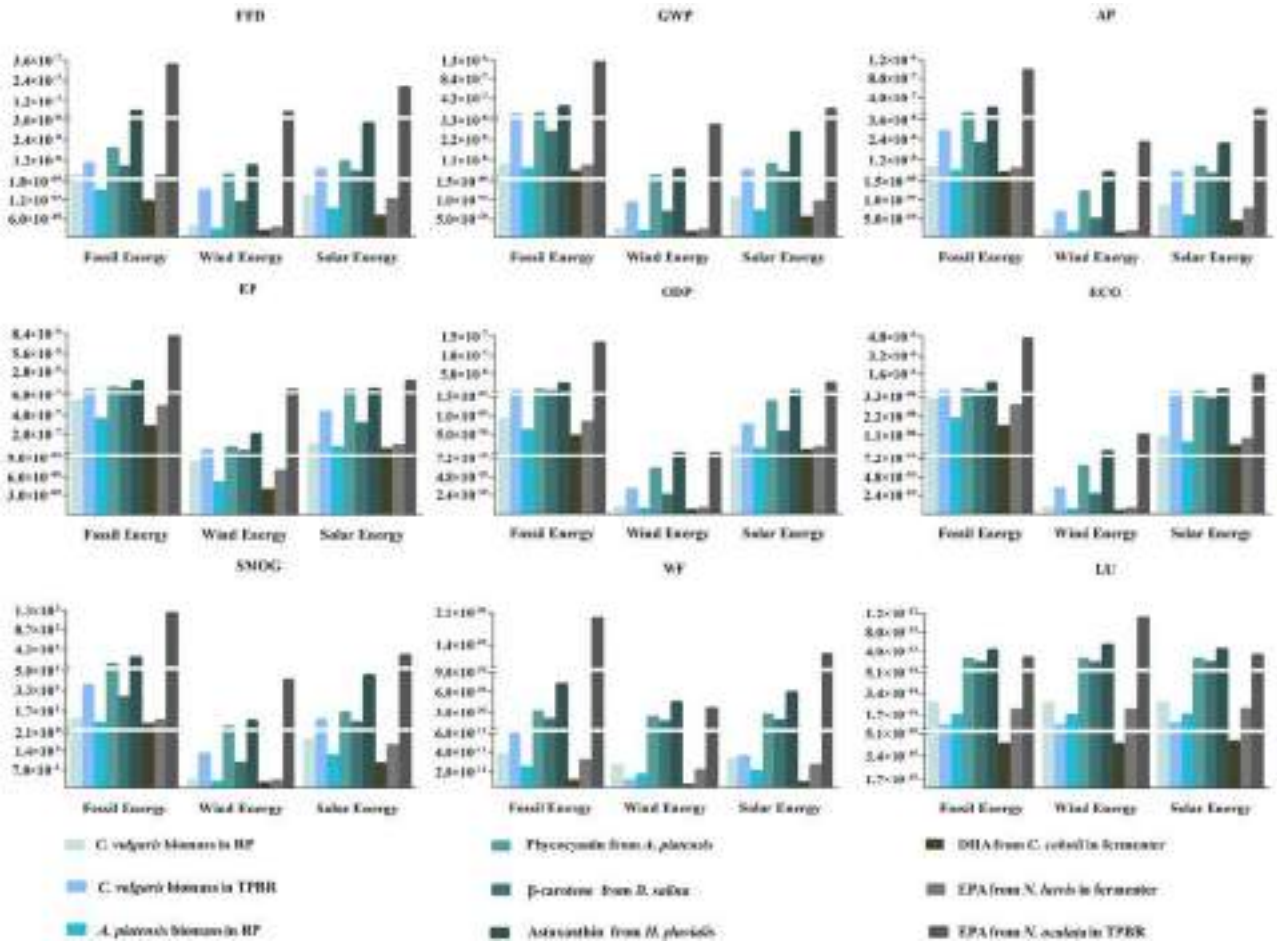


Fig. 7. Impact categories normalized data for microalgae-based products based on the energy source. Docosahexaenoic, DHA; Eicosapentaenoic, EPA; Tubular photobioreactor, TPBR; Raceway pond, RP; Global warming potential, GWP; Fossil fuel depletion, FFD; Acidification potential, AP; Eutrophication potential, EP; Ecotoxicity, ECO; Photochemical oxidant creation potential, SMOG; Water footprint, WF; Ozone depletion potential, ODP; Land use, LU.

the other products, it is greater for the use of photovoltaic solar energy. The environmental impacts for the categories WF and LU (except for the production of EPA by *N. oculata*) and FFD for the production of *C. vulgaris* biomass in TPBR, for onshore wind energy, are within the same order of magnitude that the other energy sources. Therefore, it can be inferred that for these categories and bioproducts, the energy source does not contribute to an expressive environmental impact, since their differences are within the uncertainty of the foreseen impacts.

Concerning the use of photovoltaic solar energy, the analysis shows that for all bioproducts, the impact associated with WF and LU had the same magnitude as for the use of fossil energy. On the other hand, for the categories AP, EP, and ECO only the production of EPA by *N. oculata* remained at the same magnitude; for GWP it was the production of *C. vulgaris* biomass in RP; for ODP and SMOG it was the biomass production of *A. platensis* and *C. vulgaris* in RP, phycocyanin and EPA from *N. laevis*; and, finally, the environmental impact associated with FFD wasn't in the same order of magnitude only for the production of DHA from *C. cohnii* and *A. platensis* biomass in RP. With regard to the environmental impact of bioproducts, for all categories evaluated and regardless of the energy source used to feed the bioprocess, the production of phycocyanin, astaxanthin, and EPA from *N. oculata* presented the highest emissions. This because these products are the most energy-intensive.

Conclusively, the normalization of the data indicates that the categories that probably can contribute to the significant environmental impact are SMOG and EP, followed by FFD, GWP, AP, and ECO. The ODP, WF, and LU categories had low impacts and it can be inferred that they do not contribute significantly. In short, the use of onshore wind energy to feed the production of 1 ton/month of bioproduct has the best environmental performance, followed by photovoltaic solar energy. The exceptions for which the environmental performance of the use of renewable energy is within the forecast uncertainty in relation to the use of fossil energy are specific of the impact category and energy footprint of the bioproduct.

Bioeconomy

Cost analysis

The cost analysis is very important for decision-makers to assess the feasibility of installing a standalone renewable energy system. Therefore, in this study, the economic indicators of the investment return period (IRP) and return on investment (ROI) were used to demonstrate the economic viability of installing a photovoltaic solar and onshore wind energy system capable of meeting the energy demand of 1 ton/month of bioproduct. Noteworthy, the analysis considered the impact of geographic location. Notoriously, the expenses incurred with the installation cost are summarized in different components of the systems and there is a variation in the total cost of installation from one location to another due to local differences in the cost of these components. The same applies to the cost of operation and maintenance (O&M), and the electricity price also varies with the location. In this sense, for the calculation of the IRP and ROI, were considered the electricity price, the total installed cost (TIC), and O&M cost of renewable energy of the country/region of the locations considered (Table 3). Table 4 shows the IRP and ROI for the different locations.

As expected, the results show that IRP and ROI are highly dependent on location. The economic return on capital invested in the different locations can be achieved in the period of 0.85–4.86 years. Pingtung-TWN, Unaiyur-IND, Arcos de La Frontera-ESP, Roquette Klötze-DEU, Las Palmas-ESP, and Hutt Lagoon-AUS present the lowest IRP for photovoltaic solar energy with an attractive ROI. In these locations, the IRP is less than three years and the lowest ROI is 7.9 times greater than the investment. In particular, Pingtung-TWN and Unaiyur-IND presented a return of 23.63 and 21.91 times greater than the investment made to install a photovoltaic solar energy system, respectively. On the other hand, Kona-USA, Calipatria-USA, and Moses Lake-USA presented the highest IRP and the lowest ROI. More specifically, Moses Lake-USA was the location that presented the highest IRP (4.86 years) and the lowest ROI (5.08). The results obtained for the three USA locations can be attributed to the largest TIC and O&M of photovoltaic solar energy in the region.

Table 4
IRP and ROI for the different locations.

Geographic Position	Renewable Energy	IRP (year)	ROI
Pingtung-TWN	Photovoltaic Solar	1.01	23.63
	Onshore Wind	2.04	8.83
Unaiyur-IND	Photovoltaic Solar	1.29	21.91
	Onshore Wind	1.55	14.21
Ketura-ISR	Photovoltaic Solar	1.57	17.80
	Onshore Wind	2.41	8.83
Kona-USA	Photovoltaic Solar	3.91	6.55
	Onshore Wind	2.41	8.81
Calipatria-USA	Photovoltaic Solar	3.91	6.55
	Onshore Wind	2.41	8.81
Moses Lake-USA	Photovoltaic Solar	4.86	5.08
	Onshore Wind	2.41	8.81
Arcos de La Frontera-ESP	Photovoltaic Solar	1.25	16.33
	Onshore Wind	1.94	7.91
Roquette Klötze-DEU	Photovoltaic Solar	0.85	15.57
	Onshore Wind	1.27	7.91
Las Palmas-ESP	Photovoltaic Solar	1.25	16.33
	Onshore Wind	1.94	7.91
Hutt Lagoon-AUS	Photovoltaic Solar	1.27	11.79
	Onshore Wind	1.26	9.32

India, IND; Australia, AUS; Taiwan, TWN; Israel, ISR; United States of America, USA; Spain, ESP; Germany, DEU; Investment return period, IRP; Return on investment, ROI.

In sum, considering the useful life of 25 and 20 years of photovoltaic solar and onshore wind systems, respectively, it is possible to conclude from the economic indicators that their installation would bring great economic gains. The analysis showed that the investment in renewable energy to meet the electricity demand of 1 ton/month of bioproduct, in all the considered locations, brings a return in the short term. However, it is important to highlight that the greater the installed energy capacity higher may be the IRP and the lower the ROI, and this can make the investment unattractive or economically unviable. In this sense, a trade-off must be achieved. The best trade-off will depend on the production capacity, the total electricity demand, and the location of each microalgae producing company.

Companies with a low production capacity and, consequently, lower electricity demand can economically meet 100% of the demand by renewable sources. Notoriously, as mentioned earlier, the economic viability of the systems will depend especially on the cost of installation, operation, and maintenance of the region. By way of example, when considering the costs of a photovoltaic solar system in the locations of Roquette Klötze-DEU and Moses Lake-USA, two distinct scenarios present themselves. In Roquette Klötze-DEU, assuming that the commercial plant has a monthly production of only 10 tons, it would be possible to meet 100% of the energy demand, since the IRP and ROI would still be viable. On the other hand, in Moses Lake-USA it would be unfeasible because would operate with a negative ROI and the economic return would take almost twice the system's lifetime to be achieved. The good news is that globally the costs of low-carbon technologies, such as green electricity generation, are falling and energy tariffs are already very competitive with fossil energy and may become cheaper in the near future [19].

Lastly, assuming that the investment in a renewable energy system pays yourself over the years with a zero ROI, it would be worth it? This is a pertinent question and the answer may not be easy. However, in a

hypothetical scenario, according to this study, the production of 10 tons/month of EPA from *N. oculata* in TPBR using photovoltaic solar energy, for example, would generate a carbon credit revenue of 6,039,720.0 USD/year. Here, it is worth mentioning that if the investment in clean energy creates carbon credits equal to the emissions reduced in tCO_2, it can, under this condition, generate significant profit for the company.

Carbon credits

The use of green electricity in biotechnological processes through the implementation of a renewable energy system can help companies of the sector to enter a low-carbon economy. Besides that, it can leverage the bioeconomy of the processes through the sale of carbon credits. The non-emission of carbon dioxide generates credits that can be negotiated on the international market. Often overlooked, this economic aspect can reduce the operating costs of the installation. Table 5 shows the carbon credits generated by the use of renewable energy and the associated to biological carbon capture and utilization.

Table 5
Carbon credits generated by the use of renewable energy and the associated to biological carbon capture and utilization.

		$CO_{2not\text{-}produced}$		$CO_{2avoided}$	
		Carbon Credits (month)	USD/ year	Carbon Credits (month)	USD/ year
Onshore Wind Energy	*C. vulgaris* biomass in RP	37.9	4,548	38.2	4,584
	C. vulgaris biomass in TPBR	168.4	20,208	169	20,280
	A. platensis biomass in RP	25.0	3,000	25.2	3,024
	Phycocyanin from *A. platensis*	312.4	37,488	315.3	37,836
	β-carotene from *D. salina*	213.9	25,668	215.8	25,896
	Astaxanthin from *H. pluvialis*	962.8	115,536	969.7	116,364
	DHA from *C. cohnii* in fermenter	19.02	2,282.4	19.02	2,282.4
	EPA from *N. laevis* in fermenter	34.03	4,083.6	34.03	4,083.6
	EPA from *N. oculata* in TPBR	5629.2	675,504	5650.2	678,024
Photovoltaic Solar Energy	*C. vulgaris* biomass in RP	33.9	4,068	34.2	4,104
	C. vulgaris biomass in TPBR	150.6	18,072	151.2	18,144
	A. platensis biomass in RP	22.4	2,688	22.6	2,712
	Phycocyanin from *A. platensis*	279.3	33,516	282.2	33,864
	β-carotene from *D. salina*	191.3	22,956	193.2	23,184
	Astaxanthin from *H. pluvialis*	860.9	103,308	867.7	104,124
	DHA from *C. cohnii* in fermenter	17.01	2,041.2	17.01	2,041.2
	EPA from *N. laevis* in fermenter	30.4	3,648	30.4	3,648
	EPA from *N. oculata* in TPBR	5033.1	603,972	5054.1	606,492

Docosahexaenoic, DHA; Eicosapentaenoic, EPA; Raceway pond, RP; Tubular photobioreactor, TPBR.
*Considering the carbon price of USD 10/tCO_2e.

According to Table 5, the use of onshore wind energy in the biotechnological processes compared to the use of photovoltaic solar energy present a gain of around 11% in terms of carbon credits. The greatest revenues, regardless of the renewable energy source, were for the production of phycocyanin, astaxanthin, and EPA from *N. oculata*. The bioeconomic analysis of these bioprocesses showed that the use of onshore wind and photovoltaic solar energy could generate revenues of USD 37,488 and 33,516/year, USD 115,536, and 103,308/year, and USD 675,504 and 603,972/year, respectively. Taking into account the ability of microalgae to capture carbon, slightly higher revenues could be generated, in the order of USD 37,836 and 33,864/year, USD 116,364 and 104,124/year, and USD 678,024 and 606,492/year, respectively.

The additional revenue generated by the potential of CO_2 avoided using onshore wind and photovoltaic solar energy, would subsidize about 2.3 and 2.1% of the fossil electricity cost of 1 ton/month of bioproduct, considering the world average price of USD 0.13/kWh. Here, it is important to highlight that currently in many jurisdictions the carbon prices are low, with emissions covered at prices below USD 10/tCO_2 [38]. However, as nations take on more ambitious promises to confront climate change, the carbon price will rise to maintain a trajectory consistent with the goals. In a scenario consistent with the goals of the Paris Agreement, for example, the IEA affirms that is needed a carbon price ranging between USD 75–100/tCO_2 up until 2030 and USD 125–140/tCO_2 up until 2040 [18]. This sends a signal that investments in renewable energy are valuable today and will be even more valuable in the future. In a hypothetical scenario, considering the price of USD 0.13/kWh and a carbon price of USD 125/tCO_2, the revenue generated by the potential of CO_2 avoided using onshore wind and photovoltaic solar energy, would subsidize about 29 and 26% of the fossil electricity cost of 1 ton/month of bioproduct, respectively.

Noteworthy, Cyanotech Corporation, a world leader in the production of products derived from microalgae, is one of the few branch companies that have a renewable energy system to supply part of the farm's production. The system produces 1,147,000 kWh of electricity per year, which translates to a reduction of 791 tCO_2/year. Besides the carbon credits generated, the company has a fossil fuel-based electricity savings of USD 123,000/year [4]. Corroboratively, our results show that the implementation of a renewable energy system, besides reducing the carbon footprint of microalgae-based products and generating additional revenue from the sale of carbon credits, can reduce fossil electricity costs.

Conclusion

By replacing fossil energy with onshore wind and photovoltaic solar energy, environmental impacts, with the exception of the land use category, are reduced by 20 to 100% and 9 to 87%, respectively. As for the transition to a low-carbon bioeconomy, the consumption of wind and solar photovoltaic energy produces 97% and 87% less CO_2, thus there is a net potential to rigorously reduce emissions of this pollutant. The study results also indicate that the investment return period for renewable energy systems is relatively short. Migrating to a renewable energy matrix can promote the production and consumption of more sustainable microalgae-based products. The potential of using renewable energy to power microalgae-based facilities refers to the opportunity to severely reduce your environmental footprint, especially the carbon footprint, and also save costs. Finally, the results of this study may allow microalgae producers to make better decisions about their environmental and economic costs and the choice of suitable sites for the development of microalgae biotechnology.

CRediT authorship contribution statement

Rosangela Rodrigues Dias: Conceptualization, Methodology, Data curation, Writing – original draft. **Mariany Costa Deprá:** Methodology, Data curation. **Ihana Aguiar Severo:** Methodology. **Leila Queiroz Zepka:** Supervision, Funding acquisition. **Eduardo Jacob-Lopes:** Conceptualization, Project administration, Writing – review & editing.

Declaration of Competing Interest

The authors declare that they have no known competing financial interests or personal relationships that could have appeared to influence the work reported in this paper.

Acknowledgments

Funding for this research has been provided by the Coordination for the Improvement of Higher Education Personnel (CAPES) (grant number 001) and the National Council for Scientific and Technological Development (CNPq) for financial support.

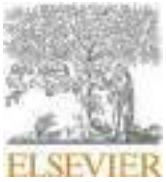
Appendix A. Supplementary data

Supplementary data to this article can be found online at https://doi.org/10.1016/j.seta.2022.102073.

References

[1] Acién FG, Fernández JM, Magán JJ, Molina E. Production cost of a real microalgae production plant and strategies to reduce it. Biotechnol Adv 2012;30(6):1344–53.
[2] Berrill P, Arvesen A, Scholz Y, Gils HC, Hertwich EG. Environmental impacts of high penetration renewable energy scenarios for Europe. Environ Res Lett 2016;11 (1):014012. https://doi.org/10.1088/1748-9326/11/1/014012.
[3] CRESESB, 2020. CRESESB-Reference Center for Solar and Wind Energy. http://www.cresesb.cepel.br/ (accessed 10 october 2020).
[4] Cyanotech, 2020. Our history. https://www.cyanotech.com/our-history/ (accessed 20 august 2020).
[5] de Mendonça HV, et al. Microalgae in a global world: new solutions for old problems? Renew Energy 2020.
[6] Deprá MC, Severo IA, dos Santos AM, Zepka LQ, Jacob-Lopes E. Environmental impacts on commercial microalgae-based products: Sustainability metrics and indicators. Algal Res 2020;51:102056. https://doi.org/10.1016/j.algal.2020.102056.
[7] Deprá MC, Severo IA, Dias RR, Zepka LQ, Jacob-Lopes E. In: Microalgae. Elsevier; 2021. p. 35–61. https://doi.org/10.1016/B978-0-12-821218-9.00002-5.
[8] Dias RR, Lasta P, Vendruscolo RG, Wagner R, Zepka LQ, Jacob-Lopes E. Mapping the performance of photobioreactors for microalgae cultivation. Part II: equatorial and tropical climate zone. J Chem Tech Biotechnol 2021;96(3):613–21.
[9] Drücke J, Borsche M, James P, Kaspar F, Pfeifroth U, Ahrens B, et al. Climatological analysis of solar and wind energy in Germany using the Grosswetterlagen classification. Renew Energy 2021;164:1254–66.
[10] Evans A, Strezov V, Evans TJ. Assessment of sustainability indicators for renewable energy technologies. Renew Sust Energ Rev 2009;13(5):1082–8.
[11] Fuhrman, J., et al., 2020. China's 2060 carbon neutrality goal will require up to 2.5 $GtCO_2$/year of negative emissions technology deployment. arXiv preprint arXiv: 2010.06723.
[12] Garrett P, Rønde K. Life cycle assessment of wind power: comprehensive results from a state-of-the-art approach. Int J Life Cycle Assess 2013;18(1):37–48.
[13] Gills, B., Morgan, J., 2020. Global Climate Emergency: after COP24, climate science, urgency, and the threat to humanity.
[14] Global Petrol Prices, 2019. https://www.globalpetrolprices.com/electricity_prices (accessed 20 august 2020).
[15] Heinrich AB. International reference life cycle data system handbook. Int J Life Cycle Assess 2010;15(5):524–5.
[16] Hung, C., 2010. Environmental Impacts of Renewable Energy: An Overview of Life Cycle Results (Master's thesis, Institutt for energi-og prosessteknikk).
[17] IEA, 2020a. Renewables 2020: Analysis and forecast to 2025. https://www.iea.org/reports/renewables-2020 (accessed 20 august 2020).
[18] IEA, 2020b. The importance of real-world policy packages to drive energy transitions. https://www.iea.org/commentaries/the-importance-of-real-world-policy-packages-to-drive-energy-transitions (accessed 20 august 2020).
[19] IRENA. Renewable power generation costs in 2019. Abu Dhabi: International Renewable Energy Agency; 2020.
[20] ISO, 2006. ISO-14040 Environmental management–life cycle assessment–principles and framework: International Organization for Standardization.
[21] Jacob-Lopes E, Maroneze MM, Deprá MC, Sartori RB, Dias RR, Zepka LQ. Bioactive food compounds from microalgae: an innovative framework on industrial biorefineries. Curr Opin Food Sci 2019;25:1–7.
[22] Kreuwel FPM, Knap WH, Visser LR, van Sark WGJHM, Vilà-Guerau de Arellano J, van Heerwaarden CC. Analysis of high frequency photovoltaic solar energy fluctuations. Sol Energy 2020;206:381–9.
[23] Linnenluecke MK, Han J, Pan Z, Smith T. How markets will drive the transition to a low carbon economy. Econ Model 2019;77:42–54.
[24] Maroneze MM, Deprá MC, Zepka LQ, Jacob-Lopes E. Artificial lighting strategies in photobioreactors for bioenergy production by *Scenedesmus obliquus* CPCC05. SN Appl Sci 2019;1(12). https://doi.org/10.1007/s42452-019-1761-0.
[25] Maroneze MM, Queiroz MI. Microalgal production systems with highlights of bioenergy production. In: Energy from Microalgae. Cham: Springer; 2018. p. 5–34.
[26] Mattiasson B. Conquering climate change: The vital role of industrial biotechnology to meet Paris Agreement's ambitious goals. Biotechnol Rep 2016;11: 1. https://doi.org/10.1016/j.btre.2016.02.003.
[27] Matuszko D. Influence of the extent and genera of cloud cover on solar radiation intensity. Int J Climatol 2012;32(15):2403–14.
[28] Milousi M, Souliotis M, Arampatzis G, Papaefthimiou S. Evaluating the environmental performance of solar energy systems through a combined life cycle assessment and cost analysis. Sustainability 2019;11(9):2539. https://doi.org/10.3390/su11092539.
[29] Pérez-Fortes M, Schöneberger JC, Boulamanti A, Tzimas E. Methanol synthesis using captured CO_2 as raw material: techno-economic and environmental assessment. Appl Energy 2016;161:718–32.
[30] Salvia M, Reckien D, Pietrapertosa F, Eckersley P, Spyridaki N-A, Krook-Riekkola A, et al. Will climate mitigation ambitions lead to carbon neutrality? An analysis of the local-level plans of 327 cities in the EU. Renew Sust Energy Rev 2021;135:110253. https://doi.org/10.1016/j.rser.2020.110253.
[31] Severo IA, Deprá MC, Dias RR, Barin JS, de Menezes CR, Wagner R, et al. Biocombustion of petroleum coke: The process integration with photobioreactors. Part II–Sustainability metrics and bioeconomy. Chem Eng Sci 2020;213:115412. https://doi.org/10.1016/j.ces.2019.115412.
[32] Siqueira SF, Maroneze MM, Dias RR, Vendruscolo RG, Wagner R, Menezes CR, et al. Mapping the performance of photobioreactors for microalgae cultivation: geographic position and local climate. J Chem Technol Biotechnol 2020;95(9): 2411–20.
[33] Sobczuk TM, et al. Carbon dioxide uptake efficiency by outdoor microalgal cultures in tubular airlift photobioreactors. Biotechnol Bioeng 2000;67(4):465–75.
[36] Torres-Tiji Y, Fields FJ, Mayfield SP. Microalgae as a future food source. Biotechnol Adv 2020;41:107536. https://doi.org/10.1016/j.biotechadv.2020.107536.
[38] World Bank, 2020. State and Trends of Carbon Pricing 2020. Washington, DC: World Bank. © World Bank. https://openknowledge.worldbank.org/handle/10986/33809 (accessed 20 august 2020).
[39] York R, Bell SE. Energy transitions or additions?: Why a transition from fossil fuels requires more than the growth of renewable energy. Energy Res Soc Sci 2019;51: 40–3.

Algal Research 63 (2022) 102661



Contents lists available at ScienceDirect

Algal Research

journal homepage: www.elsevier.com/locate/algal





In silico study of hybrid renewable energy in microalgae facilities: A path towards net-zero emissions

Rosangela R. Dias, Mariany C. Deprá, Leila Q. Zepka, Eduardo Jacob-Lopes *

Bioprocess Intensification Group, Federal University of Santa Maria (UFSM), Roraima Avenue, 1000, 97105-900 Santa Maria, RS, Brazil

ARTICLE INFO

Keywords:
Algae
Green electricity
Resource mapping
Life-cycle assessment
Bioeconomy
Sustainability metrics

ABSTRACT

The decarbonization of electricity use has become indispensable in the fight against climate change and can be seen as a business opportunity. Investing in green electricity is becoming a trend and, in the microalgae industry, the initiative can improve the sustainability of the processes and products. In this sense, we seek to assess the environmental and economic sustainability of the commercial microalgae-based products by the solar–wind hybrid renewable electricity integration into manufacturing processes. Besides that, geospatial variability and availability of hybrid renewable electricity resources have been mapped. The results indicate that the production of 1 ton/month of the main commercial microalgae-based products (whole dry biomass, β-carotene, phycocyanin, astaxanthin, docosahexaenoic acid, and eicosapentaenoic acid), using solar-wind electricity saves on the order of 70 to 89% of the environmental impacts in the categories of ozone depletion potential, global warming potential, photochemical ozone creation potential, acidification potential, eutrophication potential, and ecotoxicity. Also indicate that the implementation of an on-grid solar-wind electrical system can reduce the plant's electricity invoice by more than 80% per year. The greatest theoretical potential for implementing solar-wind systems is experienced in West and North Africa, Australasia, and the Middle East. The results found in this study provide substantial evidence that investing in renewable electricity can bring environmental and economic benefits.

1. Introduction

Guaranteeing a sustainable future will undoubtedly be one of the most prodigious challenges of the 21st century and thereunto it will be necessary not only to improve land management but also to drastically reduce pollutant gas emissions. The global emissions are at an alarming level, approaching values for which the probability of keeping global warming below 2 °C, if not 1.5 °C, drops abruptly. Energy, in particular, represents almost 75% of global emissions and, within this sector, the largest emitter of greenhouse gases (GHG) is the electricity/heat subsector [1,2].

Fortunately, in recent years, rich economies, as a starting point to meet key climate goals, have been abandoning the use of coal to generate electricity [3,4]. Besides that, the business community, attentive to the demands of combating climate change, that has as the villain is the massive emissions of polluting gases, is also replacing, principally, in a way voluntary the electric energy generated in coal-fired power plants with green electricity [5,6].

Companies and industries in electricity-intensive sectors are, in fact, emerging as great drivers of renewable energy expansion. They are not only consuming, but also building clean electricity projects to feed their operations. Microalgae-producing companies that are of special interest in the present study can benefit from using the same strategy. Since the environmental and economic sustainability of microalgae-based products remains questionable by the high electricity demand in all stages of upstream and downstream processing [7].

The electricity footprint represents approximately 98% of the environmental impacts on commercial microalgae-based products. More than three-quarters of these environmental impacts for the production of whole dried biomass by *Chlorella vulgaris* and *Arthrospira platensis*, beyond eicosapentaenoic acid by *Nitzschia laevis* and *Nannochloropsis oculata*, are associated with the upstream processing stage. This is also attributed to the production of β-carotene, astaxanthin, and phycocyanin by *Dunaliella salina*, *Haematococcus pluvialis*, and *Arthrospira platensis*, respectively. Conversely, with regard to docosahexaenoic acid from *Crypthecodinium cohnii*, most of these impacts are attributed to the downstream phase. This taking into account one same basis of functional unit [8]. In sum, regardless of the processing phase, the environmental

* Corresponding author.
E-mail address: ejacoblopes@gmail.com (E. Jacob-Lopes).

https://doi.org/10.1016/j.algal.2022.102661
Received 14 June 2021; Received in revised form 28 September 2021; Accepted 9 March 2022
Available online 18 March 2022
2211-9264/© 2022 Elsevier B.V. All rights reserved.

impacts of electricity consumption in the different cultures considering the same base of functional unit and biotechnological route are expanded in proportion to the operational volumes of the bioreactor. Besides that, it is essential to mention that the hotspot identified in all processes for obtaining products based on microalgae are attributed to the equipments, which is electricity intensive use [9–11].

Notoriously, recognizing the protagonism of the electric footprint not only in environmental sustainability but also in economic sustainability is the first step towards achieving important improvements, which can be achieved by replacing the electrical power matrix [12]. In this narrative, omnipresent and environmentally friendly sources of renewable electricity, such as solar and wind, have been investigated to play a significant role not only in reducing environmental pollutants, but also in reducing the costs of producing industrial products, as shown by the studies by Bazen et al. [13], Mostafaeipour et al. [14], Mukisa et al. [15], and Amo-Aidoo et al. [16].

However, there is very limited information for the case of solar-wind hybrid renewable electricity. Solar-wind hybrid renewable electricity has recently gained significant importance because it satisfactorily exploiting the complementarity of solar and wind resources in space and time, mitigating the impact of the intermittent of resources [17,18]. And, with regard to its integration in microalgae industries, according to the best of our knowledge, there are no concrete reports that assess the impact of the transition from fossil electricity to solar-wind hybrid renewable on the economic-environmental nexus.

Against this background, this is the first article that assesses the environmental and economic sustainability of commercial microalgae-based products (whole dried biomass, phycocyanin, β-carotene, astaxanthin, eicosapentaenoic acid, and docosahexaenoic acid) by the migration of the fossil electric matrix to the solar–wind hybrid renewable. In this study, we also mapped geospatial variability and the availability of hybrid renewable electricity resources with a focus on integration with microalgae-based facilities.

2. Methods

2.1. Life cycle assessment (LCA)

The framework for LCA established by ISO 14040 was used to assess environmental aspects and potential impacts of the electricity consumption of microalgae-based processes and products. The methodological structure of the LCA included the goal and scope definition (I), inventory analysis (II), impact assessment (III), and interpretation of results (IV) [19]. The procedures considered in each phase are detailed below.

2.1.1. Goal and scope definition

The main objective of the application of LCA in this study was to assess the environmental footprint of the bioprocesses powered by solar-wind renewable electricity, which consists of the electricity generated from two sources, the solar photovoltaic and onshore wind. The commercial microalgae products considered were whole dried biomass, β-carotene, phycocyanin, astaxanthin, docosahexaenoic acid (DHA), and eicosapentaenoic acid (EPA). The biotechnological route of the products and the data for theoretical-experimental analysis were based on consolidated processes [8].

2.1.2. Functional unit and system boundaries

The functional unit covers the production of 1 ton/month of microalgae-based products. The functional unit of 1 ton/month of product was selected to be an approximate value of large-scale production capacity. Besides that, it is important to mention that the evaluation of the products was carried out individually.

The system boundaries were defined employing a Cradle-to-Gate framework. The analysis included the impact of the electricity requirement, and only the electricity demand needed to operate the system was accounted for. Fig. 1 shows all the technical characteristics of the study. Noteworthy, physical sterilization was established for fermenters, and for closed photobioreactors, chemical sterilization.

2.1.3. Life cycle inventory (LCI)

The electric power required for the operation in each cultivation system considered, as well as the input and output conditions of the bioprocesses to obtain 1 ton/month of product are presented in Tables 1 and 2, respectively.

2.1.4. Life cycle impact assessment (LCIA)

The potential environmental impacts were calculated as described in Eq. (1), which is expressed in mass released into the environment per functional unit [23,24]. The impact categories considered were: global warming potential (GWP), fossil fuel depletion (FFD), photochemical ozone creation potential (SMOG), ozone depletion potential (ODP), ecotoxicity (ECO), water footprint (WF), eutrophication potential (EP), acidification potential (AP), and land use (LU). The normalization followed the methodology of the International Reference Life Cycle Data System (ILCD) Handbook [25]. The characterization factors of the environmental impacts of electricity and the normalization factors are presented in Tables 3 and 4, respectively.

$$Ci = \Sigma CF \times Ei \quad (1)$$

where Ci is the environmental impact category, *CF* is the characterization factor, and Ei is the emission inventory.

2.2. Global theoretical potential for solar-wind electricity generation

The present study sought to find the best areas of the globe for the establishment of solar-wind electric power systems using QGIS software version 3.10 'A Coruña' (open-source software). Combining information from locations with minimum solar irradiation of 5 kWh/m^2/d and minimum wind speed of 6 m/s, the areas with potential for electricity generation were obtained. It is important to mention that the minimum values of solar irradiation and wind speed were selected because they have sufficient potential for generating economically viable solar and wind electricity [32–34]. The climatic information used to generate the map of suitable locations for the installation of solar-wind electricity systems was obtained from the Global Solar Atlas [35] and Global Wind Atlas [36].

It is noteworthy that based on the monthly electricity demand of each bioproduct, as well as the efficiency of land use and occupation, and considering one solar irradiation of 5 kWh/m^2/d and wind speed of 6 m/s, the area occupied for the installation of the solar-wind electricity system and the electricity generated by the solar resource and by the wind resource, respectively, were determined. The environmental impact of the consumption of electricity generated by the solar resource summed to the consumption of electricity generated by the wind resource resulted in the environmental impact of each bioproduct. The electricity produced monthly by the photovoltaic module and wind turbine, as well as the installation area of the solar-wind system was determined according to Dias et al. [37]. The detailed specifications for the photovoltaic module and wind turbine considered are presented in the Supplementary Material (Table S1).

2.3. Evaluation of investments in solar-wind systems

The feasibility of implementing a solar-wind power system capable of meeting the electricity demand of a microalgae cultivation plant was investigated. Ten sites from the portion of geographical locations with sufficient potential to generate economically viable solar-wind electricity were selected for the brief case study. They were selected for their solar-wind potential considered sufficient both in terms of technical and economic feasibility [32–34].

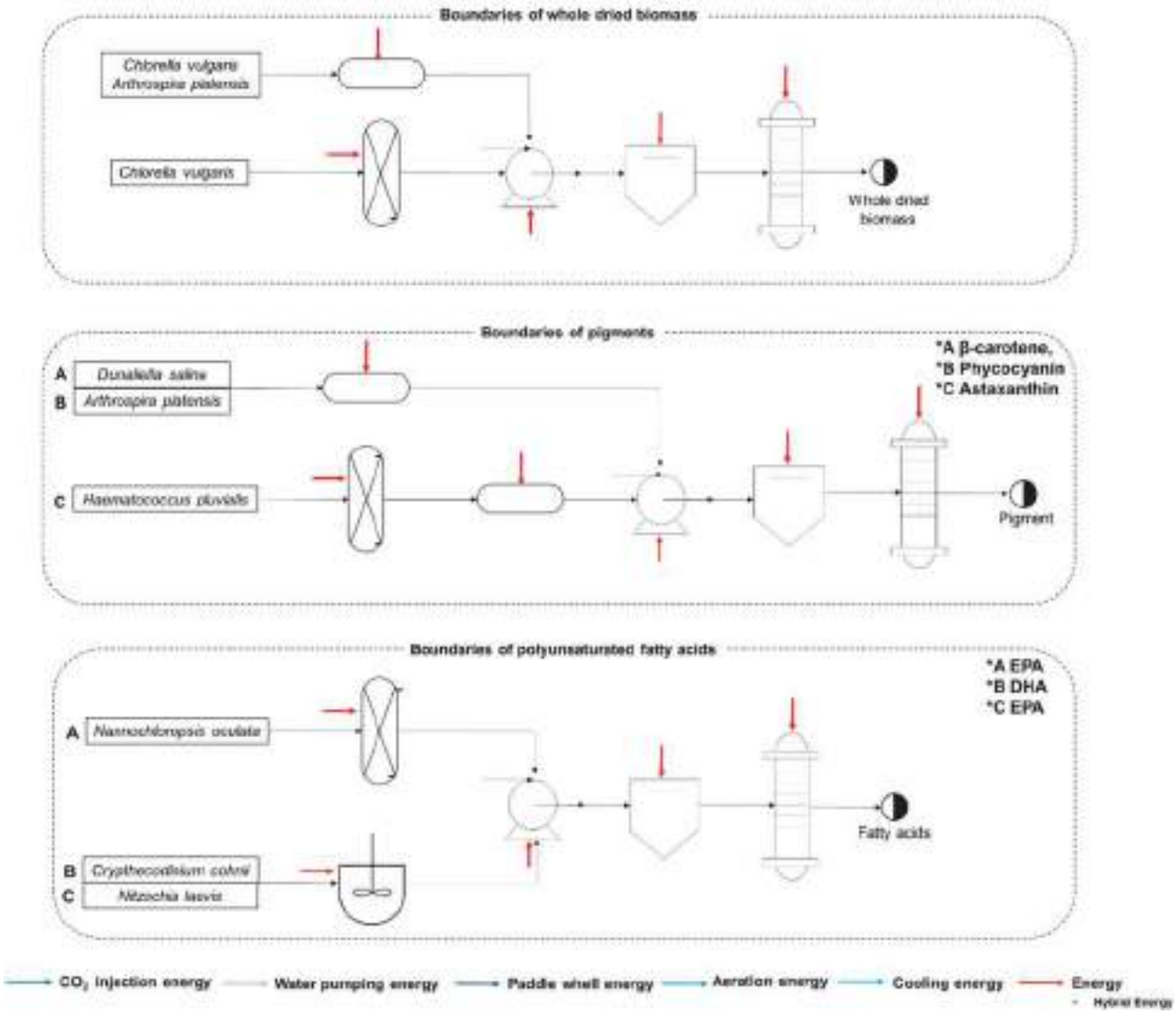


Fig. 1. System boundaries for the assessment of commercial microalgae products. Acronyms: DHA, Docosahexaenoic; EPA, Eicosapentaenoic. Adapted from Ref. [8].

2.3.1. Feasibility analysis

The total installed cost of the solar-wind electricity system was obtained from the International Renewable Energy Agency [38]. The cost of operation and maintenance was estimated at 2% per year of the total installed cost [39]. The investment return period (IRP) and return on investment (ROI) were calculated using Eqs. (1) and (2), respectively. The expected electric power saving was converted into monetary saving according to the electricity price of countries. The electricity price for commercial users was obtained from the Global Petrol Prices [40] website. Table 5 shown the electricity price, the total installed cost, and operation and maintenance cost for photovoltaic solar and onshore wind systems by country/region.

$$\mathrm{IRP} = \frac{\mathrm{TIC} + \mathrm{O\&M}}{\mathrm{ME}} \tag{2}$$

$$\mathrm{ROI} = \frac{Re - (\mathrm{TIC} + \mathrm{O\&M})}{(\mathrm{TIC} + \mathrm{O\&M})} \tag{3}$$

where IRP is the investment return period (year), ROI is the return on investment, TIC is the total installed cost (USD/kW), O&M is the operation and maintenance cost (USD/kW/year), ME is the monetary saving (USD/month), and Re is the revenue generated during the lifespan of the system.

2.3.2. Estimation of carbon credits

The carbon credits were estimated based on the carbon footprint of the solar-wind power system (Eq. (4)–(5)), following the methodology of Severo et al. [41]. The additional revenue generated by the sale of carbon credits was determined according to the current carbon price of the country of the locations considered in the case study [42]. It is noteworthy that for those located in jurisdictions without implemented carbon pricing initiatives was considered the global average carbon price.

$$\mathrm{CO_{2not-produced}} = \mathrm{CO_{2conventional}} - \mathrm{CO_{2emitted}} \tag{4}$$

$$\mathrm{CO_{2avoided}} = \mathrm{CO_{2not-produced}} + \mathrm{CO_{2captured}} \tag{5}$$

where conventional CO_2 is the amount of CO_2 released in the conventional process, while CO_2 emitted and CO_2 captured refer to the renewable electricity system integrated into the microalgae-based processes.

Table 1
Electricity requirement for the operation in tubular photobioreactor, raceway pond, and fermenter.

	Unit	Tubular photobioreactor (TPBR)	Raceway pond (RP)	Fermenter
Cultivation				
Energy consumption for cooling	kWh/m^3	15	–	–
Aeration energy	kWh/m^3	0.13	–	1
Agitation	kWh/m^3	–	–	0.0073
Physical sterilization	kWh/m^3	–	–	7.22
Water evaporation	m^3	2×10^{-3}	1.3×10^{-1}	–
Electric energy for paddle wheel	kWh/m^3	–	0.54	–
Electric energy for water pumping	kWh/m^3	–	0.1	–
Pumping (riser and degasser)	kWh/m^3	0.95	–	–
Electric energy for CO_2 injection	kWh/m^3	–	0.33	–
Harvest				
Energy consumption centrifugation	kWh/m^3	1.25	1.25	1.25
Drying				
Spray-dryer	kWh/kg evaporated water	1.09	1.09	1.09
Extraction				
sCO_2	kWh/kg	0.8	0.8	0.8

CO_2, carbon dioxide; sCO_2, Supercritical CO_2 extraction.
Adapted from Refs. [8,20–22].

3. Results and discussion

3.1. Mapping of suitable areas for integration of solar-wind systems in microalgae production facilities

There are several studies aimed at finding suitable locations for the establishment of solar and wind electricity installations [39]. However, there is a lack of complementarity studies covering the whole globe to find the best regions for the utilization of solar-wind hybrid renewable electricity potential, as well as for integration in microalgae production facilities. Thus, seeking to increase knowledge about the availability of resources for solar-wind technologies, the best areas for hybrid electricity generation from the perspective of countries and regions were mapped.

In terms of solar-wind resource availability, West and North Africa, Australasia, and the Middle East are the regions of the globe that present the highest proportion of areas suitable to accommodate hybrid solar-wind electricity systems (see Supplementary Material, Fig. S1). On the other hand, beyond these regions, southern Africa, Chile and Mexico are highly qualified for the establishment of solar systems and Central Asia, the Midwest of the United States, Patagonia, Greenland, New Zealand, and part of Canada for the establishment of wind systems (see Supplementary Material, Fig. S2, and S3).

Noteworthy, for the production of low-carbon microalgae-based products and with a good cost-effective relation, a location with high availability of renewable electricity resources is extremely important. However, holistically, it also needs to present inputs availability (water and nutrients), lands of low agricultural value, relatively flat topography with workable soils, a suitable climate for the cultivation, and access to infrastructure including an available viable workforce. These factors to be considered when identifying locations for microalgae cultivation facilities affect capital and operational expenditures [43].

In this regard, when evaluating the best areas for microalgae production considering all countries, Correa et al. [44] concluded that the most promising countries are precisely located in North Africa, Australasia, and the Middle East. According to the authors, the countries located in these regions, besides presenting high microalgae productivity, cover areas of low agricultural value and less biodiversity. Simultaneously, Prasad et al. [45] and Boruff et al. [46] when mapping resources to identify locations for microalgae cultivation in Australia, concluded that many regions of Western Australia and Queensland present several key advantages including a suitable climate for microalgae growth year-round, an extensive land area unsuitable for agriculture, high soil workability, access to abundant seawater and the infrastructure necessary, and political stability.

In sum, based on the information presented in the spatial analyzes of the potential of microalgae cultivation; it is possible to emphasize that the areas highly suitable for the establishment of solar-wind systems are also promising for the development of microalgae biotechnology.

3.2. Environmental impact of commercial microalgae-based products

The majority if not almost all environmental impacts of commercial microalgae-based products result from electricity entry in the upstream and downstream steps of the manufacturing [8]. The transition from fossil electricity consumption to renewable can positively influence the environmental burdens of the obtainment processes, making them more sustainable. In light of this, Fig. 2 illustrates the values characterized of the environmental impact categories associated with the production of 1 ton/month of whole dried biomass, β-carotene, phycocyanin, astaxanthin, DHA, and EPA using solar-wind electric power.

The results of the environmental assessment indicate that the replacement of the fossil electric matrix by solar-wind can substantially improve the sustainability of bioproducts. The consumption of solar-wind electric power per ton of bioproduct saves more than 80% of the impacts in the categories of GWP, AP, EP, and ODP and more than 70% and 41% in the categories of SMOG and ECO and FFD and WF, respectively. Comparatively, the consumption of wind electricity presents higher values, and the consumption of solar electricity, slightly lower values [37]. About this, it is worth mentioning that when dimensioning the area occupied for the implementation of the solar-wind system, with a focus on electric power demand and the perspective of optimizing the use and occupation of the land, a great part of the electric power generated and consumed would come from the solar resource (Fig. S4 and S5). For this reason, our results are closer to the environmental performance obtained for the transition of solar electric power consumption. However, if the wind resource provided most of the electricity of the hybrid system, the environmental impacts would be smaller and reduced proportionally.

At this point, it is also important to highlight that for analysis was considered one solar irradiation of 5 kWh/m^2/d and a wind speed of 6 m/s. If were considered one solar irradiation lower and a wind speed higher, the electric power generated by the wind resource would be superior and the environmental performance of microalgae-based products even better. In this context, we emphasize the important role of the geographic position and the intensity of its resources in environmental impacts. Furthermore, it is up to mention that the bigger part of the environmental burdens of the solar and wind systems are associated with the stage of manufacture of solar panels and wind turbines and not the operation of the systems. The systems are almost environmentally neutral in their operation phase and the use of fossil electricity during manufacture is responsible for the great part of the environmental burdens in the impact categories assessed [26,47].

Table 2
Inputs/outputs of the production process of 1 ton/month whole dried biomass (*C. vulgaris* and *A. platensis*), phycocyanin (*A. platensis*), β-carotene (*D. salina*), astaxanthin (*H. pluvialis*), EPA (*N. oculata* and *N. laevis*) and DHA (*C. cohnii*). Acronyms: TPBR, Tubular photobioreactor; RP, Raceway pond; DHA, Docosahexaenoic; EPA, Eicosapentaenoic; CO_2, Carbon dioxide; sCO_2, Supercritical CO_2 extraction.

Cultivation system		Unit	*C. vulgaris*	*C. vulgaris*	*A. platensis*	*A. platensis*	*D. salina*	*H. pluvialis*	*N. oculata*	*N. laevis*	*C. cohnii*
			TPBR	RP	RP	RP	RP	TPBR and RP	TPBR	Fermenter	Fermenter
Cultivation											
Tubular photobioreactor		m^3	47.62	–	–	–	–	100.27	1587.1	–	–
Energy consumption for cooling		kWh/month	514,296.0	–	–	–	–	1,082,916.0	17,140,680.0	–	–
Aeration energy		kWh/month	4457.23	–	–	–	–	9385.27	148,552.56	–	–
Pumping (riser and degasser)		kWh/month	32,572.08	–	–	–	–	68,584.68	1,085,576.4	–	–
Water evaporation		m^3	0.095	–	–	–	–	0.201	3.17	–	–
Fermenter		m^3	–	–	–	–	–	–	–	133.33	27.77
Physical sterilization		kWh/month	–	–	–	–	–	–	–	962.64	200.49
Agitation		kWh/month	–	–	–	–	–	–	–	700.78	145.96
Aeration		kWh/month	–	–	–	–	–	–	–	95,997.6	19,994.4
Raceway pond		m^3	–	166.66	104.17	1388.54	925.93	2677.23	–	–	–
Electric energy for paddle wheel		kWh/month	–	64,797.41	40,501.3	539,864.35	360,001.58	1,040,907.02	–	–	–
Electric energy for water pumping		kWh/month	–	11,995.2	7500.24	99,974.88	66,666.96	192,760.56	–	–	–
Electric energy for CO_2 injection		kWh/month	–	39,592.8	24,750.8	329,917.10	220,000.97	636,109.85	–	–	–
Water evaporation		m^3	–	21.67	13.54	180.51	120.4	348.04	–	–	–
Biomass productivity		Ton/m^3/month	0.021	0.006	0.0096	0.0096	0.0135	0.012	0.045	0.023	0.300
Output	Algae liquid	Ton	11.42	11.76	12.69	71.09	83.3	222.2	380.9	16.0	44.42
Harvest											
Input	Energy consumption centrifugation	kWh/month	59.53	208.33	130.21	1735.68	1157.41	3471.88	1983.88	166.66	34.71
Harvest											
Input	Wet biomass	Ton	8.55	8.82	9.51	53.31	49.98	133.32	285.66	12.0	33.3
	Spray-dryer	kWh/month	9319.5	9613.8	10,365.9	58,107.9	54,478.2	145,318.8	311,369.4	13,080.0	36,297.0
Output	Whole dried biomass	ton	1	1	1	–	–	–	–	–	–
Extraction											
Input	Dry biomass	Ton	–	–	–	13.33	12.5	33.33	71.42	3.0	8.33
sCO_2		kWh/month	–	–	–	10,664.0	10,000.0	26,664.0	57,136.0	2400.0	6664.0
Output	Oil rich pigments	Ton	–	–	–	1	1	1	–	–	–
Oil		Ton	–	–	–		–	–	1	1	1
		kWh/month	560,704.34	126,207.54	83,248.45	1,040,263.91	712,305.12	3,206,200.06	18,745,298.24	113,307.68	63,336.56

Adapted from Ref. [8].

Table 3
Factors of characterization of environmental impacts of electricity in processes. Acronyms: Photovoltaic, PV; Copper-indium-diselenide, CIS.

	Units	Global warming	Terrestrial acidification	Freshwater eutrophication	Ozone depletion	Freshwater ecotoxicity	Fossil fuel depletion	Water consumption	Photochemical ozone creation
		(kg CO_2 eq)	(kg SO_2 eq)	(kg P eq)	(kg CFC-11 eq)	(Kg DCB eq)	(MJ)	m^3	(kg C_2H_4 eq)
Onshore wind	kWh	7.7×10^{-3}	3.7×10^{-5}	3.7×10^{-6}	7.3×10^{-14}	1×10^{-4}	0.10	3.9×10^{-5}	4.1×10^{-6}
PV (CIS)	kWh	3.95×10^{-2}	2.07×10^{-4}	4.62×10^{-5}	1.75×10^{-8}	1.30×10^{-2}	0.394	3.22×10^{-4}	2.6×10^{-5}

Adapted from Refs. [26,27].

Table 4
Global normalization factors for emissions and resource extraction.

Impact categories	Unit	Reference value
Fossil fuel depletion	MJ	$4.50 \times 10^{+14}$
Global warming	kg CO_2 eq	$5.79 \times 10^{+13}$
Terrestrial acidification	kg SO_2 eq	$3.83 \times 10^{+11}$
Freshwater eutrophication	kg P eq	$7.41 \times 10^{+8}$
Photochemical ozone creation	kg C_2H_4 eq	22
Ozone depletion	kg CFC-11 eq	$1.61 \times 10^{+8}$
Freshwater ecotoxicity	kg DCB eq	$2.07 \times 10^{+12}$
Land use	ha	$9.64 \times 10^{+15}$
Water footprint	m^3	$7.91 \times 10^{+13}$

Adapted from Refs. [8,28–31].

Table 5
Electricity price, the total installed cost, and operation and maintenance cost of photovoltaic solar and onshore wind systems by country. Acronyms: Australia, AUS; Spain, ESP; BRA; Brazil, MAR; Morocco, CHN; China, IND; India, JPN; Japan, USA; United States, MEX; Mexico, SAU; Saudi Arabia, Total installed cost, TIC; Operation and maintenance, O&M.

	Renewable electricity	Electricity price (USD/kWh)	O&M (USD/kW/year)	TIC (USD/kW)
Geraldton-AUS	Photovoltaic solar	0.13	29.3	1464
	Onshore wind		31.1	1555
Cádis-ESP	Photovoltaic solar	0.12	21.6	1080
	Onshore wind		36.0	1800
Trairi-BRA	Photovoltaic solar	0.12	20.8	1040
	Onshore wind		31.2	1559
Laayoune-MAR	Photovoltaic solar	0.13	36.9	1843
	Onshore wind		39.0	1952
Xagmakajor-CHN	Photovoltaic solar	0.09	15.2	760
	Onshore wind		24.5	1223
Jaffna-IND	Photovoltaic solar	0.08	16.3	817
	Onshore wind		21.1	1055
Okinawa-JPN	Photovoltaic solar	0.26	39.6	1980
	Onshore wind		47.4	2368
Laramie-USA	Photovoltaic solar	0.15	73.0	3652
	Onshore wind		32.7	1636
Salina Cruz-MEX	Photovoltaic solar	0.08	24.8	1238
	Onshore wind		32.7	1636
Az Zulfi-SAU	Photovoltaic solar	0.05	19.9	996
	Onshore wind		47.4	2368

In terms of product, the greatest environmental impact in the categories of GWP, AP, EP, ODP, SMOG, ECO, FFD, and WF is for the production of phycocyanin, astaxanthin, and EPA from *N. oculata*. The electricity demand of these products is 1 to 3 order of magnitude higher than that of the other products and, consequently, the proportion of emissions is also in this range. Moreover, the cultivation system and the biotechnological route used have a strong influence on the environmental burdens. For example, when analyzing the environmental impacts associated with the production of *C. vulgaris* biomass in RP and TPBR, two consolidated but distinct cultivation systems, there are strong discrepancies of values. The hotspot of this disparity of values is associated with electricity demand during the cultivation phase in these systems (see Table 2). On the other hand, as for the biotechnological route, the disparity of values can be observed when comparing the electricity demand in autotrophic and heterotrophic regimes. When analyzing the extent of these impacts to obtain the same product, it is observed a path of choice in favor of environmental protection.

With regard to the LU, calculated based on the area occupied for the implementation of the solar-wind system, values were obtained in the order of 0.12 to 42.12 PDF/ha. The lowest values were for DHA from *C. cohnii* (0.12 PDF/ha), *A. platensis* biomass (0.17 PDF/ha), EPA from *N. laevis* (0.24 PDF/ha), and *C. vulgaris* biomass in RP (0.27 PDF/ha). The *C. vulgaris* biomass in TPBR, β-carotene, phycocyanin, astaxanthin, and EPA from *N. oculata* presented values in the order of 1.23, 1.57, 2.30, 7.14, and 42.12 PDF/ha, respectively. These values are strongly related to solar irradiation and wind speed. Notoriously, the higher the wind speed and solar irradiation, the less the impact associated with the LU category. In this study, the impact on land use for fossil electricity was not considered since the electricity consumed would come from the distribution network.

Finally, seeking to better understand the relative significance of the results, the values characterized of the categories of environmental impact associated with the production of 1 ton/month of whole dried biomass, β-carotene, phycocyanin, astaxanthin, DHA, and EPA using solar-wind electricity were related to a global reference value. The normalized data are shown in Fig. 3. The general analysis of the normalized data shows a significant reduction in the impacts associated with the categories of GWP, AP, EP and ODP, followed by the SMOG and ECO categories. Already in the categories of FFD and WF is observed an intermediate reduction. The normalization of the data reflects the importance of the electric power transition especially for the ecosystem quality and the maintenance of global warming below 2 °C. Besides that, the findings indicate that the transition to renewable electricity is undoubtedly part of the puzzle to achieve net-zero emissions in electricity-intensive microalgae facilities.

3.3. Evaluation of investments in solar-wind systems

The feasibility analysis is very important for those decision-makers to know the costs and consequences of implementing renewable electricity projects. The objective of the analysis is to ensure that the benefits outweigh the cost. The light of this, in this study, ten locations were selected for a case study. The investment return period (IRP) and return on investment (ROI) were used as indicators of the feasibility of investments in solar-wind systems. Table 6 shows the IRP, ROI and savings on the electricity invoice per year for the different locations.

The evaluation results revealed that the return of the capital invested in the implementation of an on-grid solar-wind system in the different locations can be achieved in a period of 1 to 4 years. This result points to savings in the electricity invoices of the commercial microalgae facility of 81 to 94% per year. More specifically, as seen in Table 6, Geraldton-AUS, Cádis-ESP, Trairi-BRA, Xagmakajor-CHN, Jaffna-IND, and Okinawa-JPN present a smaller IRP with an attractive return on investment. In these locations, the IRP is less than 2 years and the smallest ROI is 10 times the investment made to install and operate the hybrid system. In contrast, Laayoune-MAR, Laramie-USA, Salina Cruz-MEX, and Az Zulfi-SAU presented the highest IRP and lowest ROI. In particular, Az Zulfi-SAU presented an IRP of 3.5 years and an ROI of 4, and Laramie-USA an IRP of 3.8 years and an ROI of 5. Although they have a higher IRP and a lower ROI, the gains, considering the useful life of the system, outweigh the total implementation costs.

Comparatively, Xiong and Nour [48] when investigating the feasibility of grid-connected photovoltaic systems obtained a return period of 11.1 years for systems without the application of renewable energy adoption incentives and 7 years for the case of systems with the incentives application. For autonomous photovoltaic solar systems, the authors report a return period of 16.6 and 9 years for the cases without and with incentive. It is important to mention that in this study the incentives application was considered in the total installed cost of the hybrid renewable electricity system. The details of the items considered in the total installed cost applied to the study can be consulted in IRENA [38].

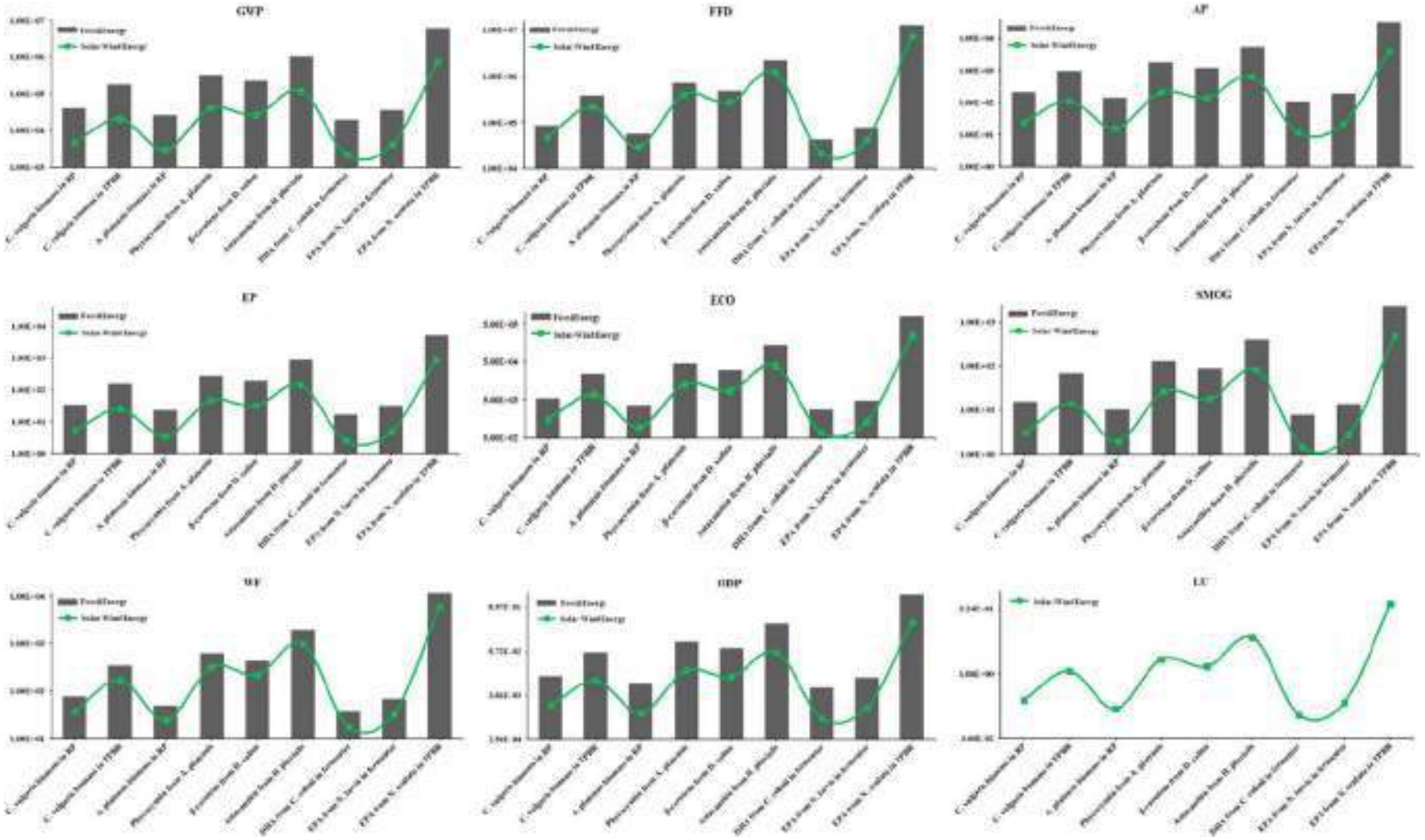


Fig. 2. Characterized values of environmental impact categories associated with the production of 1 ton/month of microalgae-based products using solar-wind electricity. The fossil electricity data used for comparison were obtained from [14]. Acronyms: Docosahexaenoic, DHA; Eicosapentaenoic, EPA; Tubular photobioreactor, TPBR; Raceway pond, RP; Global warming potential, GWP; Fossil fuel depletion, FFD; Acidification potential, AP; Eutrophication potential, EP; Ecotoxicity, ECO; Photochemical oxidant creation potential, SMOG; Water footprint, WF; Ozone depletion potential, ODP; Land use, LU.

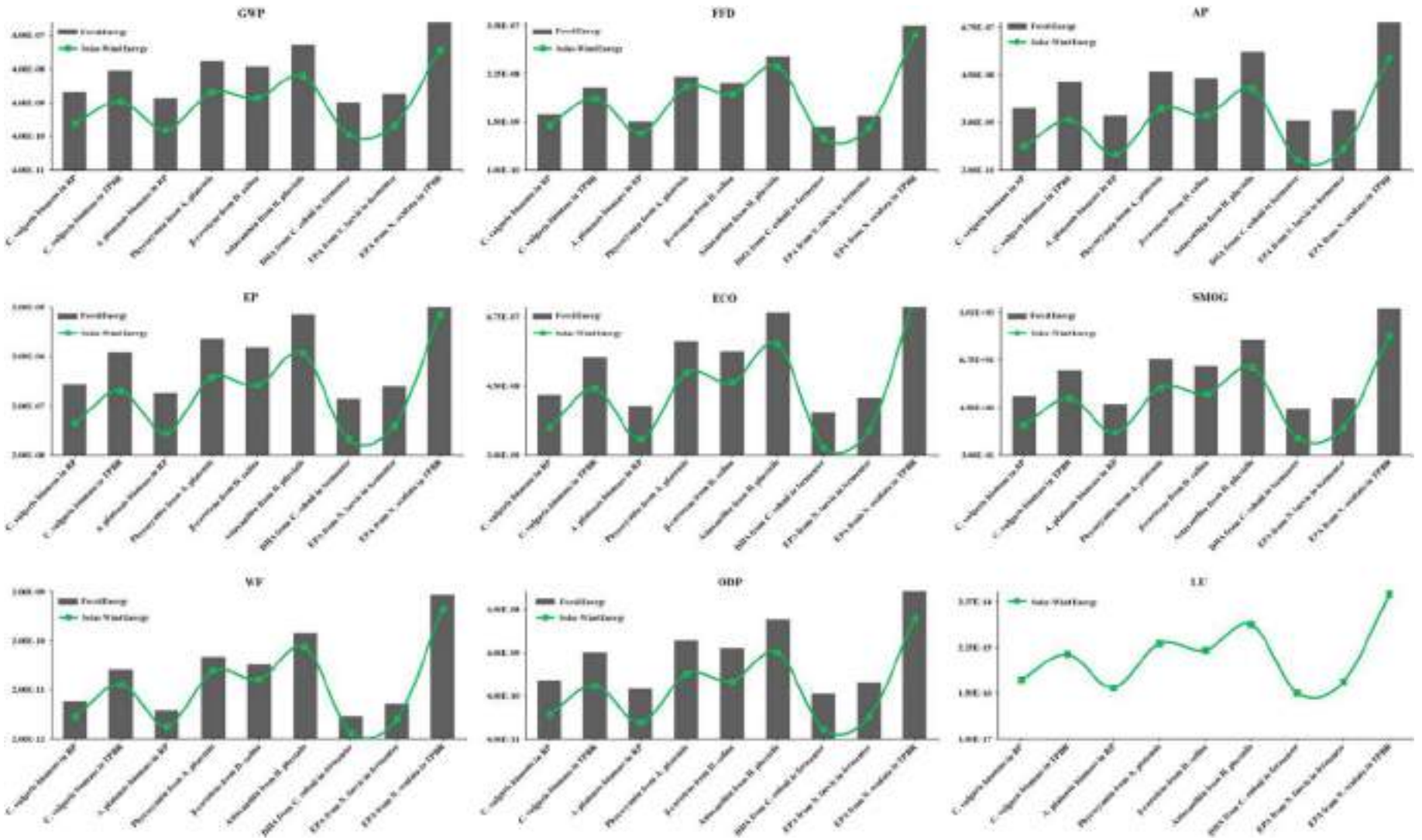


Fig. 3. Impact categories normalized data associated with the production of 1 ton/month of microalgae-based products using solar-wind electricity. The fossil electricity data used for comparison were obtained from [14]. Acronyms: Docosahexaenoic, DHA; Eicosapentaenoic, EPA; Tubular photobioreactor, TPBR; Raceway pond, RP; Global warming potential, GWP; Fossil fuel depletion, FFD; Acidification potential, AP; Eutrophication potential, EP; Ecotoxicity, ECO; Photochemical oxidant creation potential, SMOG; Water footprint, WF; Ozone depletion potential, ODP; Land use, LU.

Table 6
IRP, ROI and savings on the electricity invoice per year for the different locations. Acronyms: Investment return period, IRP; Return on investment, ROI.

	IRP (year)	ROI	Savings (%/year)
Geraldton-AUS	1.8	10	91
Cádis-ESP	1.5	12	92
Trairi-BRA	1.4	13	93
Laayoune-MAR	2.3	8	88
Xagmakajor-CHN	1.4	13	93
Jaffna-IND	1.7	11	92
Okinawa-JPN	1.2	15	94
Laramie-USA	3.8	4	81
Salina Cruz-MEX	2.6	7	87
Az Zulfi-SAU	3.5	5	82

Currently, there is a series of works in the literature that investigate the viability of the most diverse electrical systems and it is important to note that each study presents distinct values for the same feasibility indicators [39,49,50]. This is because each study considers specific values of total installed cost, operation and maintenance cost, and electricity tariffs. Notoriously, the assessment of the feasibility of implementing the systems is conducted on a case-by-case basis and generally involves particularities of the region in question.

Consistently, the results of the study's feasibility analysis provide some important insights into local differences in the cost of implementing solar-wind systems. The expenses incurred with the installation of the systems are summarized in different components and their cost, as well as the operation and maintenance cost and the electricity price, varies locally. This variation can, ultimately, be understood as a driver that enables the implementation of these systems in certain locations. However, in general, as the results show, the investment return period in solar-wind systems, regardless of location, is relatively short. In this regard, it should be noted that in the last years solar and wind technologies have had aggressive cost decreases. The declining costs of these technologies, coupled with high electricity prices, have increased investments in solar and wind energy. However, although this is true, the outdated perception that they are not competitive continues to be a significant and unnecessary barrier to their deployment [51].

Based on the results and a reasonable estimate of the selling prices of the commercial microalgae-based products [52], it is presumed that viewed from another perspective, the investment in the implementation of an on-grid solar-wind system is paid in the short term for biomass in RP, pigments and fatty acids polyunsaturated, with the exception of EPA from *N. oculata* (Fig. 4). For the *C. vulgaris* biomass in TPBR it is liquidated in the medium term, except for the location of Laramie-USA, and for EPA from *N. oculata* it is liquidated in the long term. The unit quantity of product (ton) needed to pay off the investment is intrinsically related to electricity demand and the selling price of the products. Although the electricity demand for the production of 1 ton/month of astaxanthin is one of the higher, for example, this product has an elevated selling price (2500 USD/kg) which results in a faster return on investment.

Meantime, without considering this perspective, it is highlighted that geographic location can be identified as having a key role in the economic viability of solar-wind systems and in the environmental sustainability of the microalgae-based processes and products. Concerning the costs of implementing the systems, as mentioned earlier, there are local differences and in relation to environmental sustainability, it is essential that it have the potential to generate hybrid electricity and thus integrate it with microalgae installations. This integration is a key component of pathways to achieve a life cycle with net-zero emissions.

Finally, at the current juncture, an important fact to be observed is that many companies have found in combating pollution is an alternative source of generating additional revenues. The replacement of the fossil electric matrix with renewables is a measure of energy efficiency eligible for obtaining carbon credits that can be negotiated at attractive prices. In this context, Table 7 shows the revenue generated estimate by the use of solar-wind electricity and that associated with biological carbon capture and utilization.

The results presented in Table 7 indicate, in general, opportunities to generate relevant revenues. The greatest revenues were for EPA from *N. oculata*, astaxanthin, and phycocyanin, while the lowest was for less electricity-intensive products. When considering carbon capture by microalgae, slightly higher revenues can be generated. As for the locations, the disparities in revenue for the same product can be attributed to the carbon pricing initiative of the jurisdiction in question. In sum, it can be inferred, given the revenue values, there is a great potential for reducing other costs of the commercial microalgae facility by the replacement of the electric matrix or to contribute to a shorter IRP in the case of implementation of a solar-wind system.

4. Conclusion

The consumption of solar-wind electricity is less environmentally impactful compared to fossil electric power, and the implementation of an on-grid system can reduce the electric power invoice by more than 80% per year. Our highlights indicate that the choice of a geographical location for the production of low-carbon microalgae-based products

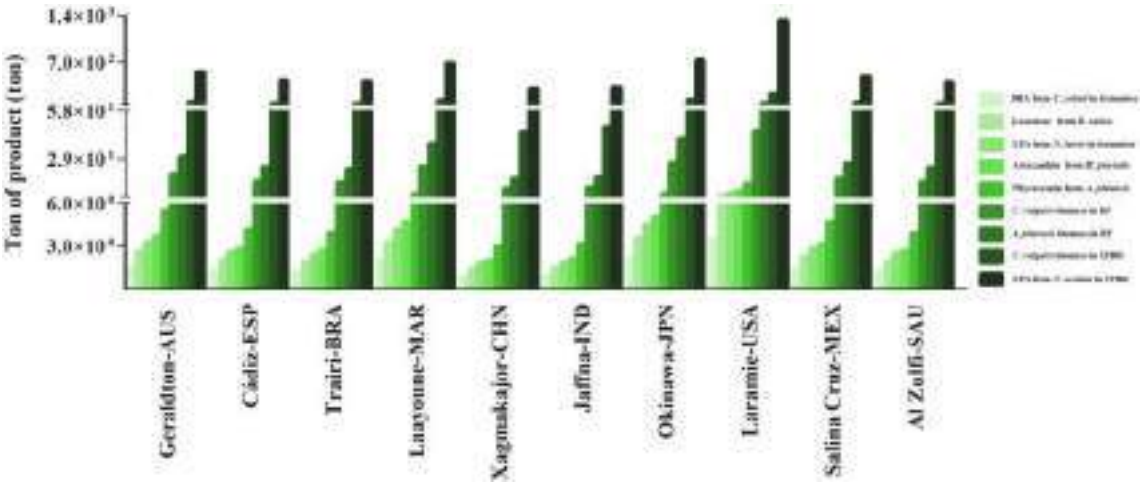


Fig. 4. Tonnes of product to be sold to offset the cost of implementing a solar-wind system. The selling prices of the commercial microalgae-based products were obtained from [52]. Acronyms: Docosahexaenoic, DHA; Eicosapentaenoic, EPA; Tubular photobioreactor, TPBR; Raceway pond, RP; Australia, AUS; Spain, ESP; BRA; Brazil, MAR; Morocco, CHN; China, IND; India, JPN; Japan, USA; United States, MEX; Mexico, SAU; Saudi Arabia.

Table 7
Revenue generated by the use of solar-wind electricity and the associated with biological carbon capture and utilization. Acronyms: Docosahexaenoic, DHA; Eicosapentaenoic, EPA; Tubular photobioreactor, TPBR; Raceway pond, RP; Australia, AUS; Spain, ESP; BRA; Brazil, MAR; Morocco, CHN; China, IND; India, JPN; Japan, USA; United States, MEX; Mexico, SAU; Saudi Arabia.

	Geraldton-AUS[a]	Cádis-ESP[b]	Trairi-BRA[c]	Laayoune-MAR[c]	Xagmakajor-CHN[d]	Jaffna-IND[c]	Okinawa-JPN[e]	Laramie-USA[f]	Salina Cruz-MEX[c]	Az Zulfi-SAU[c]
$CO_{2not\text{-}produced}$ (USD/year)										
C. vulgaris biomass in RP	4547.60	12,359.30	820.13	820.13	2456.28	820.13	2349.66	6925.96	820.13	820.13
C. vulgaris biomass in TPBR	20,134.60	54,721.08	3631.13	3631.13	10,875.22	3631.13	10,403.18	30,664.86	3631.13	3631.13
A. platensis biomass in RP	3012.02	8185.96	543.20	543.20	1626.87	543.20	1556.26	4587.29	543.20	543.20
Phycocyanin from *A. platensis*	37,320.24	101,427.61	6730.43	6730.43	20,157.64	6730.43	19,282.69	56,838.50	6730.43	6730.43
β-Carotene from *D. salina*	25,576.70	69,511.43	4612.57	4612.57	13,814.65	4612.57	13,215.01	38,953.15	4612.57	4612.57
Astaxanthin from *H. pluvialis*	114,962.69	312,441.44	20,732.68	20,732.68	62,094.37	20,732.68	59,399.12	175,087.46	20,732.68	20,732.68
DHA from *C. cohnii* in fermenter	2300.53	6252.30	414.88	414.88	1242.58	414.88	1188.64	3503.69	414.88	414.88
EPA from *N. laevis* in fermenter	4086.10	11,105.05	736.90	736.90	2207.01	736.90	2111.21	6223.10	736.90	736.90
EPA from *N. oculata* in TPBR	671,401.89	1,824,711.7	121,082.40	121,082.40	362,641.78	121,082.40	346,901.06	1,022,540.83	121,082.40	121,082.40
$CO_{2avoided}$ (USD/year)										
C. vulgaris biomass in RP	4593.36	12,483.68	828.38	828.38	2481.00	828.38	2373.31	6995.66	828.38	828.38
C. vulgaris biomass in TPBR	20,218.25	54,948.42	3646.21	3646.21	10,920.41	3646.21	10,446.40	30,792.27	3646.21	3646.21
A. platensis biomass in RP	3040.63	8263.70	548.35	548.35	1642.32	548.35	1571.04	4630.85	548.35	548.35
Phycocyanin from *A. platensis*	37,701.53	102,463.86	6799.19	6799.19	20,363.59	6799.19	19,479.69	57,419.20	6799.19	6799.19
β-carotene from *D. salina*	25,830.96	70,202.44	4658.42	4658.42	13,951.98	4658.42	13,346.38	39,340.39	4658.42	4658.42
Astaxanthin from *H. pluvialis*	115,873.99	314,918.14	20,897.02	20,897.02	62,586.58	20,897.02	59,869.97	176,475.36	20,897.02	20,897.02
DHA from *C. cohnii* in fermenter	2300.53	6252.30	414.88	414.88	1242.58	414.88	1188.64	3503.69	414.88	414.88
EPA from *N. laevis* in fermenter	4086.10	11,105.05	736.90	736.90	2207.01	736.90	2111.21	6223.10	736.90	736.90
EPA from *N. oculata* in TPBR	674,189.87	1,832,288.8	121,585.19	121,585.19	364,147.64	121,585.19	348,341.57	1,026,786.92	121,585.19	121,585.19

[a] Considering the carbon price in the Australia ERF Safeguard Mechanism of USD 11.09/tCO_2e for the year 2020.
[b] Considering the carbon price in the EU ETS of USD 30.14/tCO_2e for the year 2020.
[c] Considering the global average carbon price of USD 2/tCO_2e for the year 2020.
[d] Considering the Shanghai Cap-and-Trade program carbon price of USD 5.99/tCO_2e for the year 2020.
[e] Considering the Tokyo Cap-and-Trade program carbon price of USD 5.73/tCO_2e for the year 2020.
[f] Considering the California Cap-and-Trade program carbon price of USD 16.89/tCO_2e for the year 2020.

does not only fall over a place with favorable climatic conditions for cultivation, with access to water and nutrients, transport infrastructure, and flat topography, but also with the availability of renewable energy resources. This study provides evidence that the transition to green electricity is a prominent part of the puzzle to eliminating the carbon legacy of the microalgae industry towards net-zero emissions. Furthermore, it is noteworthy that the carbon capture and utilization by microalgae is not a key component of pathways to zero the emissions, but relevant if they aiming net-negative emissions.

Statement of informed consent, human/animal rights

No conflicts, informed consent, or human or animal rights are applicable to this study.

CRediT authorship contribution statement

Rosangela R. Dias: Conceptualization, Methodology, Data curation, Writing – original draft. **Mariany C. Deprá:** Methodology, Data curation. **Leila Q. Zepka:** Supervision, Funding acquisition. **Eduardo Jacob-**

Lopes: Conceptualization, Project administration, Writing – review & editing.

Declaration of competing interest

The authors declare that they have no known competing financial interests or personal relationships that could have appeared to influence the work reported in this paper.

Acknowledgement

The authors would like to thank the National Council for Scientific and Technological Development (CNPq) – Brazil, and the Coordination for the Improvement of Higher Education Personnel (CAPES), Finance Code 001.

Appendix A. Supplementary data

Supplementary data to this article can be found online at https://doi.org/10.1016/j.algal.2022.102661.

References

[1] Climate Watch. https://www.climatewatchdata.org/ghg-emissions?breakBy=sector&end_year=2018&gases=co2&start_year=1990, 2021.
[2] IEA. https://www.iea.org/data-and-statistics/charts/global-energy-related-co2-emissions-1990-2021, 2021.
[3] L.E.V. Contreras, K.M. Perkins, M. Ellenbecker, R. Moure-Eraso, N.E.M. Vega, COVID-19 pandemic lessons to facilitate future engagement in the global climate crisis, J. Clean. Prod. 125178 (2020).
[4] IEA. https://www.iea.org/reports/renewables-2020, 2020.
[5] J.N. Kang, Y.M. Wei, L.C. Liu, R. Han, B.Y. Yu, J.W. Wang, Energy systems for climate change mitigation: a systematic review, Appl. Energy 263 (2020), 114602.
[6] A. Birkenberg, M.E. Narjes, B. Weinmann, R. Birner, The potential of carbon neutral labeling to engage coffee consumers in climate change mitigation, J. Clean. Prod. 278 (2021), 123621.
[7] I.A. Severo, M.C. Deprá, R.R. Dias, E. Jacob-Lopes, Process integration applied to microalgae-based systems, in: Handbook of Microalgae-based Processes and Products, Academic Press, 2020, pp. 709–735.
[8] M.C. Deprá, I.A. Severo, A.M. dos Santos, L.Q. Zepka, E. Jacob-Lopes, Environmental impacts on commercial microalgae-based products: sustainability metrics and indicators, Algal Res. 51 (2020), 102056.
[9] P. Pérez-López, S. González-García, C. Jeffryes, S.N. Agathos, E. McHugh, D. Walsh, M.T. Moreira, Life cycle assessment of the production of the red antioxidant carotenoid astaxanthin by microalgae: from lab to pilot scale, J. Clean. Prod. 64 (2014) 332–344.
[10] S. Papadaki, K. Kyriakopoulou, I. Tzovenis, M. Krokida, Environmental impact of phycocyanin recovery from Spirulina platensis cyanobacterium, Innov. Food Sci. Emerg. Technol. 44 (2017) 217–223.
[11] G. Yadav, B.K. Dubey, R. Sen, A comparative life cycle assessment of microalgae production by CO2 sequestration from flue gas in outdoor raceway ponds under batch and semi-continuous regime, J. Clean.Prod. 258 (2020), 120703.
[12] C. Wang, R. Dargaville, M. Jeppesen, Power system decarbonisation with global energy Interconnection–a case study on the economic viability of international transmission network in Australasia, Glob. Energy Interconnect. 1 (4) (2018) 507–519.
[13] E.F. Bazen, M.A. Brown, Feasibility of solar technology (photovoltaic) adoption: a case study on Tennessee's poultry industry, Renew. Energy 34 (3) (2009) 748–754.
[14] A. Mostafaeipour, M. Rezaei, A. Moftakharzadeh, M. Qolipour, M. Salimi, Evaluation of hydrogen production by wind energy for agricultural and industrial sectors, Int. J. Hydrog. Energy 44 (16) (2019) 7983–7995.
[15] N. Mukisa, R. Zamora, T.T. Lie, Store-on grid scheme model for grid-tied solar photovoltaic systems for industrial sector application: costs analysis, Sustain. Energy Technol. Assess. 41 (2020), 100797.
[16] A. Amo-Aidoo, O. Hensel, J.K. Korese, F.A. Neba, B. Sturm, A framework for optimization of energy efficiency and integration of hybridized-solar energy in agro-industrial plants: bioethanol production from cassava in Ghana, Energy Rep. 7 (2021) 1501–1519.
[17] GVR. https://www.grandviewresearch.com/industry-analysis/hybrid-solar-wind-systems-market, 2020.
[18] M. Guezgouz, J. Jurasz, M. Chouai, H. Bloomfield, B. Bekkouche, Assessment of solar and wind energy complementarity in Algeria, Energy Convers. Manag. 238 (2021), 114170.
[19] ISO, ISO-14040 Environmental Management–Life Cycle Assessment–Principles and Framework, International Organization for Standardization, 2006.
[20] T.M. Sobczuk, F.G. Camacho, F.C. Rubio, F.A. Fernández, E.M. Grima, Carbon dioxide uptake efficiency by outdoor microalgal cultures in tubular airlift photobioreactors, Biotechnol. Bioeng. 67 (4) (2000) 465–475.
[21] F.G. Acién, J.M. Fernández, J.J. Magán, E. Molina, Production cost of a real microalgae production plant and strategies to reduce it, Biotechnol. Adv. 30 (6) (2012) 1344–1353.
[22] J. Spruijt, R. Schipperus, A.M.J. Kootstra, C.L.M. de Visser, AlgaeEconomics: Bio-economic Production Models of Micro-algae and Downstream Processing to Produce Bio Energy Carriers, EnAlgae Swansea University, 2015.
[23] E. Jacob-Lopes, L.Q. Zepka, M.C. Deprá, in: Sustainability Indicators and Metrics of Environmental Impact: Industrial and Agricultural Life Cycle Assessment, Elsevier, 2021, p. 250. ISBN 9780128234112.
[24] M.M. Maroneze, M.C. Deprá, L.Q. Zepka, E. Jacob-Lopes, Artificial lighting strategies in photobioreactors for bioenergy production by Scenedesmus obliquus CPCC05, SN Appl. Sci. 1 (12) (2019) 1–12.
[25] A.B. Heinrich, International reference life cycle data system handbook, Int. J. LCA 15 (5) (2010) 524–525.
[26] P. Garrett, K. Rønde, Life cycle assessment of wind power: comprehensive results from a state-of-the-art approach, Int. J. Life Cycle Assess. 18 (1) (2013) 37–48.
[27] M. Milousi, M. Souliotis, G. Arampatzis, S. Papaefthimiou, Evaluating the environmental performance of solar energy systems through a combined life cycle assessment and cost analysis, Sustainability 11 (9) (2019) 2539.
[28] R. Frischknecht, N. Jungbluth, H.J. Althaus, C. Bauer, G. Doka, R. Dones, Y. Loerincik, Implementation of Life Cycle Impact Assessment Methods, 2007.
[29] S. Sala, L. Benini, L. Mancini, R. Pant, Integrated assessment of environmental impact of Europe in 2010: data sources and extrapolation strategies for calculating normalisation factors, Int. J. Life Cycl. Assess. 20 (11) (2015) 1568–1585.
[30] S. Sala, E. Crenna, M. Secchi, R. Pant, Global Normalisation Factors for the Environmental Footprint and Life Cycle Assessment, Publications Office of the European Union, Luxembourg, 2017.
[31] H. Stranddorf, L. Hoffmann, A. Schmidt, Impact categories, normalisation and weighting in LCA (Påvirkningskategories, normalisering og vægtning i LCA–in Danish), Environmental News No. 77, in: The Danish Ministry of the Environment, Environmental Protection Agency, Copenhagen, 2004.
[32] N.Y. Aydin, E. Kentel, H.S. Duzgun, GIS-based site selection methodology for hybrid renewable energy systems: a case study from western Turkey, Energy Convers. Manag. 70 (2013) 90–106.
[33] M. Jahangiri, R. Ghaderi, A. Haghani, O. Nematollahi, Finding the best locations for establishment of solar-wind power stations in middle-east using GIS: a review, Renew. Sust. Energ. Rev. 66 (2016) 38–52.
[34] CRESESB, Reference Center for Solar and Wind Energy Sérgio de Salvo Brito. http://www.cresesb.cepel.br, 2021.
[35] Global Solar Atlas. https://globalsolaratlas.info/download/world, 2021.
[36] Global Wind Atlas. https://globalwindatlas.info/, 2021.
[37] R.R. Dias, M.C. Deprá, I.A. Severo, L.Q. Zepka, E. Jacob-Lopes, Smart override of the energy matrix in commercial microalgae facilities: a transition path to a low-carbon bioeconomy, Sustain. Energy Technol. Assess. 52 (2022) 102073.
[38] IRENA, Renewable Power Generation Costs in 2019, International Renewable Energy Agency, Abu Dhabi, 2020.
[39] B. Chang, K. Starcher, Evaluation of wind and solar energy investments in Texas, Renew. Energy 132 (2019) 1348–1359.
[40] Global Petrol Prices. https://www.globalpetrolprices.com, 2020.
[41] I.A. Severo, M.C. Deprá, R.R. Dias, J.S. Barin, C.R. de Menezes, R. Wagner, E. Jacob-Lopes, Bio-combustion of petroleum coke: the process integration with photobioreactors. Part II–Sustainability metrics and bioeconomy, Chem. Eng. Sci. 213 (2020), 115412.
[42] World Bank, Carbon pricing dashboard. https://carbonpricingdashboard.worldbank.org/map_data, 2021.
[43] S.F. Siqueira, M.M. Maroneze, R.R. Dias, R.G. Vendruscolo, R. Wagner, C.R. de Menezes, L.Q. Zepka, E. Jacob-Lopes, Mapping the performance of photobioreactors for microalgae cultivation: geographic position and local climate, J. Chem. Technol. Biotechnol. 95 (9) (2020) 2411–2420.
[44] D.F. Correa, H.L. Beyer, H.P. Possingham, J.E. Fargione, J.D. Hill, P.M. Schenk, Microalgal biofuel production at national scales: reducing conflicts with agricultural lands and biodiversity within countries, Energy 215 (2021), 119033.
[45] P. Prasad, D. Pullar, S. Pratt, Facilitating access to the algal economy: mapping waste resources to identify suitable locations for algal farms in Queensland, Resour. Conserv. Recycl. 86 (2014) 47–52.
[46] B.J. Boruff, N.R. Moheimani, M.A. Borowitzka, Identifying locations for large-scale microalgae cultivation in Western Australia: a GIS approach, Appl. Energy 149 (2015) 379–391.
[47] A. Evans, V. Strezov, T.J. Evans, Assessment of sustainability indicators for renewable energy technologies, Renew. Sust. Energ. Rev. 13 (5) (2009) 1082–1088.
[48] L. Xiong, M. Nour, Techno-economic analysis of a residential PV-storage model in a distribution network, Energies 12 (16) (2019) 3062.
[49] F. Dawood, G.M. Shafiullah, M. Anda, Stand-alone microgrid with 100% renewable energy: a case study with hybrid solar PV-battery-hydrogen, Sustainability 12 (5) (2020) 2047.
[50] M. Gonzalez-Salazar, W.R. Poganietz, Evaluating the complementarity of solar, wind and hydropower to mitigate the impact of El Niño southern oscillation in Latin America, Renew. Energy 174 (2021) 453–467.
[51] IRENA. https://www.irena.org/, 2021.
[52] E. Jacob-Lopes, M.M. Maroneze, M.C. Deprá, R.B. Sartori, R.R. Dias, L.Q. Zepka, Bioactive food compounds from microalgae: an innovative framework on industrial biorefineries, Curr. Opin. Food Sci. 25 (2019) 1–7.

Environmental performance for microalgae cultivation commercial systems: sustainability metrics and indicators

Desempenho ambiental para sistemas comerciais de cultivo de microalgas: métricas e indicadores de sustentabilidade

DOI:10.34117/bjdv7n3-354

Recebimento dos originais: 08/02/2021
Aceitação para publicação: 12/03/2021

Mariany Costa Deprá
Mestre em Ciência e Tecnologia de Alimentos pela Universidade Federal de Santa Maria
Instituição: Universidade Federal de Santa Maria –UFSM
Endereço: Avenida Roraima, 1000, 97105-900 –Camobi, Santa Maria –RS, Brasil
E-mail: marianydepra@gmail.com

Patrícia Arrojo da Silva
Graduada em Tecnologia em Alimentos pela Universidade Federal de Santa Maria
Instituição: Universidade Federal de Santa Maria –UFSM
Endereço: Avenida Roraima, 1000, 97105-900 –Camobi, Santa Maria –RS, Brasil
E-mail: pati.arrojo@hotmail.com

Rosangela Rodrigues Dias
Mestre em Ciência e Tecnologia de Alimentos pela Universidade Federal de Santa Maria
Instituição: Universidade Federal de Santa Maria –UFSM
Endereço: Avenida Roraima, 1000, 97105-900 –Camobi, Santa Maria –RS, Brasil
E-mail: ro.rosangleard@gmail.com

Rafaela Basso Sartori
Mestre em Ciência e Tecnologia de Alimentos pela Universidade Federal de Santa Maria
Instituição: Universidade Federal de Santa Maria –UFSM
Endereço: Avenida Roraima, 1000, 97105-900 –Camobi, Santa Maria –RS, Brasil
E-mail: rafaa.sartori@hotmail.com

Paola Lasta
Graduada em Tecnologia em Alimentos pela Universidade Federal de Santa Maria
Instituição: Universidade Federal de Santa Maria –UFSM
Endereço: Avenida Roraima, 1000, 97105-900 –Camobi, Santa Maria –RS, Brasil
E-mail: paolalasta@outlook.com

Leila Queiroz Zepka
Doutora em Ciência de Alimentos pela Faculdade de Engenharia de Alimentos da Universidade Estadual de Campinas
Instituição: Universidade Federal de Santa Maria –UFSM
Endereço: Avenida Roraima, 1000, 97105-900 -Camobi, Santa Maria –RS, Brasil
E-mail: zepkaleila@yahoo.com.br

Eduardo Jacob-Lopes
Doutor em Engenharia Química pela Universidade Estadual de Campinas
Instituição: Universidade Federal de Santa Maria –UFSM
Endereço: Avenida Roraima, 1000, 97105-900 –Camobi, Santa Maria –RS, Brasil
E-mail: ejacoblopes@gmail.com

ABSTRACT
In this study, we evaluated metrics and sustainability indicators for cultivation commercial systems based on microalgae. Cultivation systems as a raceway pond, tubular photobioreactor, flat plate photobioreactor, and fermenter were evaluated under a standard functional unit of 1 m^3. These cultivation systems were estimated by midpoint indicators through the nine impact categories and later submitted to the normalization phase. Among the results found, three impact categories were shown to be more expressive to contribute to environmental impacts for the four cultivation systems, which are ecotoxicity potential, energy resource, and global warming potential. The best environmental performance was identified for raceway pond, although the worst-case scenario for the water footprint category was identified. Besides, in a comparative analysis between closed systems, fermenters showed better environmental indicators, followed by tubular and flat plate photobioreactors. In this way, the life cycle assessment allowed to highlight the hot points of the process, identifying the energy requirements as the critical points of the whole performance of the cultivation systems. Finally, regardless of the impacts associated with different cultivation configurations, it is important to note that the choice of the system will be directly associated with the target product to be produced. Therefore, the results found about the environmental performance of cultivation systems can serve as basic information to reduce the global environmental impacts of microalgae-based processes and bioproducts.

Keywords: biomass, raceway pond, tubular photobioreactor, flat plate photobioreactor, fermenter, life-cycle assessment.

RESUMO
Neste estudo, avaliamos métricas e indicadores de sustentabilidade para sistemas comerciais de cultivo baseados em microalgas. Sistemas de cultivo como lagoa aberta, fotobiorreator tubular e placa plana, e fermentador foram avaliados sob uma unidade funcional padrão de 1 m^3. Esses sistemas de cultivo foram estimados por indicadores de ponto médio através das nove categorias de impacto e posteriormente submetidos à fase de normalização. Dentre os resultados encontrados, três categorias de impacto mostraram-se mais expressivas para contribuir com os impactos ambientais para os quatro sistemas de cultivo, que são potenciais de ecotoxicidade, recurso energético e potencial de aquecimento global. O melhor desempenho ambiental foi identificado para a lagoa do canal adutor, embora o pior cenário para a categoria de pegada hídrica tenha sido identificado. Além disso, em uma análise comparativa entre sistemas fechados, os fermentadores apresentaram melhores indicadores ambientais, seguidos pelos fotobiorreatores tubulares e de placa plana. Desta forma, a avaliação do ciclo de vida permitiu destacar os pontos quentes do processo, identificando as necessidades energéticas como os pontos críticos de todo o desempenho dos sistemas de cultivo. Finalmente, independentemente dos impactos associados às diferentes configurações de cultivo, é importante notar que a escolha do sistema estará diretamente associada ao produto alvo a ser produzido. Portanto, os resultados encontrados sobre o desempenho ambiental dos sistemas de cultivo podem servir como informações básicas para reduzir os impactos ambientais globais de processos e bioprodutos baseados em microalgas.

Palavras-chave: biomassa, lagoa aberta, fotobiorreator tubular, fotobiorreator de placa plana, fermentador, avaliação do ciclo de vida.

1 INTRODUCTION

Environmental and energy challenges currently arise from industrialization associated with the growing demand for services, where it has negatively impacted the environment, leading to the need to discover promising alternatives (Bhattacharya and Goswami, 2020; Hussain et al., 2021). Based on this understanding, emerge microalgae as a potential source of biotechnological transformation molecules and can lead to a portfolio of alternative resources for today's world. In addition, it presents great market possibilities such as the production of food, fuel, and pharmaceutical products (Rahman, 2020; Erbland et al., 2020). According to market look, seaweed products in various segments is expected to expand at a compound annual growth rate of approximately 4.2% from 2018 to 2025 and will have a total market value of over 3,4 billion dollars (Markets and Markets, 2021). Associated with this, statistics show that the seaweed industry is becoming increasingly popular and can be used in different branches of the industrial sector (Tang et al., 2020).

As consequence, algae cultivation has become a growing area of research in recent years. However, the success in large-scale commercial production of microalgae depends on several factors, mainly the microalgae cultivation system used, which becomes the core for this purpose. In this sense, continuous efforts are deliberated in the construction of models with low energy consumption to ensure the economic viability of microalgae bioprocesses (Qin and Wu, 2019).

Many configurations of cultivation systems have been developed over the years to increase the productivity of microalgae biomass (Deprá et al., 2019). However, regardless of the target product, algae-based products at an industrial scale are produced exclusively in open systems (Ramírez-Mérida et al., 2017). These, in turn, consist of simple external lagoons, where the commercial operation of microalgae because they are more economical and relatively easy to expand. However, these systems are widely known for having low cell productivity, high contamination rates, cell selectivity, beyond demanding intensive for energy and nutrients. On other hand, closed systems provide controlled conditions and weathering, maximum cell productivity, automated maintenance of environmental parameters (Kirnev et al., 2020).

Notwithstanding, beyond cultivation systems meeting the intrinsic demands of microorganisms, these processes need to adapt to the demands for sustainability indicators

imposed by society and regulatory bodies (Deprá et al., 2021). To do this, environmental performance must be examined to predict and model what the future impacts will be and, consequently, how industry stakeholders can align with this. It is worth mentioning that, as microalgae production systems are on the rise, it is highly recommended to subject them to sustainability assessments to support their implementation. In short, these tools become a powerful way to quantify and examine the potential environmental impacts of the process based on the principles of life cycle assessment (LCA), the application of sustainability metrics (Corona et al., 2019).

Recently, some studies have focused on environmental assessments associated with microalgae processes and their potential in the treatment of waste, such as the research by Tua et al. (2021) and Santos et al. (2020). On the other hand, other research lines have suggested the assessment of the environmental scenario of energy potential (Cruce et al., 2021) and microalgae bioproducts (Deprá et al., 2020). However, although these studies have shown and it is now widely disseminated that downstream processes are the hotspot of the environmental impacts of microalgae-based processes, to date, no article has attempted to review the environmental impact of processes core – the cultivation systems. Therefore, the present work aims to explore the potential impact through indicators and metrics of sustainability generated by the use of the main systems of marketable cultivation based on microalgae. In this study, once the values of the potential environmental impacts characterized were identified, the LCA methodology allowed the results to be normalized to a global reference value, in order to assess the magnitude of the impacts aiming to optimize their environmental performance in the scenario industrial application.

2 MATERIAL AND METHODS

The general framework for LCA was determined according to the International Organization for Standardization (ISO) 14000 series (ISO, 2006). The implementation methodology of LCA was determined according to four phases: (I) goal and scope definition, (II) inventory analysis, (III) impact assessment, and (IV) interpretation. Further, the procedures considered in each step are detailed below.

2.1 GOALS AND SCOPE DEFINITION

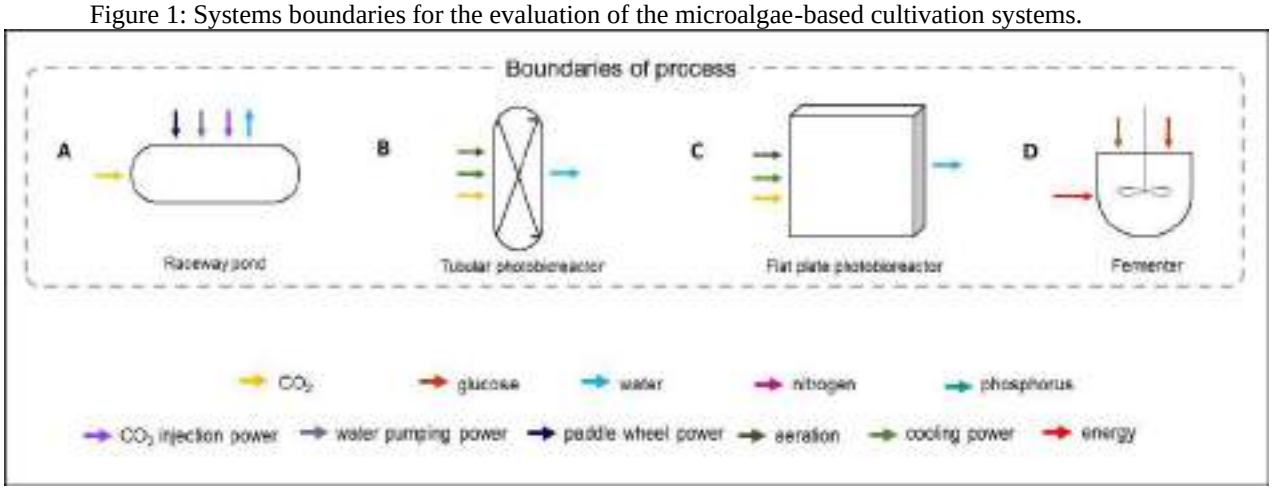
The study aim was to evaluate the main cultivation systems based on microalgae, which consist of (i) raceway ponds, (ii) tubular photobioreactor, (iii) flat plate photobioreactor, and (iv) fermenter. The cultivation systems evaluated involve

biotechnological equipment commercially consolidated. Besides, data collection for theoretical-experimental analysis was based on process data consolidated by classic references in the literature.

2.2 FUNCTIONAL UNIT AND SYSTEM BOUNDARIES

The present study considered the functional unit indicated the comparison of microalgae cultivation systems under the 1 m³ operating mode. In addition, system boundaries have been set from the gate-to-gate life cycle, according to Deprá et al. (2020). The general layout of all the technical features of the case studies analyzed is presented in Figure 1.

Figure 1: Systems boundaries for the evaluation of the microalgae-based cultivation systems.



2.3 LIFE CYCLE INVENTORY (LCI)

Life cycle inventory data were obtained from the literature. For microalgal culture systems, the energy and nutrient specifications required for operation are based on the main industrial-scale configurations (Table 1).

Table 1: Energy requirements for the operation volume of 1 m³ the different operating cultivation systems.

Process	**Unit**	**Raceway pond**	**Tubular photobioreactor**	**Flat-panel**	**Fermenter**
Cultivation					
Power consumption for cooling	kWh	-	15	3.5	-
Aeration power	kWh	-	0.1	0.9	1.0
Agitation	kWh	-	-	-	0.0073
Sterilization	kWh	-	-	-	7.22
Water evaporation	m³	1.3×10^{1}	1×10^{-4}	5×10^{-5}	1×10^{-4}
Electric power for paddle wheel	kW	0.54	-	-	-
Electric power for water pumping	kW	0.5	-	-	-
Electric power for CO_2 injection	kW	0.33	-	-	-
CO_2 consumption	kg	2.0	1.5	2.5	-
Glucose	kg	-	-	-	5.0

Adapted from Lee and Low (1992); Marsullo et al. (2015); Albarelli et al. (2018); Kumar et al. (2019

2.4 LIFE CYCLE IMPACT ASSESSMENT (LCIA)

Potential environmental impacts were calculated according to a hierarchical approach (Goedkoop et al., 2009). The assessment was based on a wide spectrum of environmental indicators, divided between midpoint indicators, the energy indicator, the water demand indicator, and an indicator associated with land occupation and transformation.

In the midpoints, the global warming potential (GWP) was determined according to Laratte et al. (2014). Besides, photochemical ozone creation potential (POCP), ozone depletion potential (ODP), acidification potential (AP), eutrophication potential (EP), and ecotoxicity (ECO) were quantified according to Hauschild and Wenzel, H. (1998). While, the energy resource (ER), water footprint (WF), and land use (LU) were evaluated according to Maroneze et al. (2019), Hoekstra (2016), and Lathuillière et al. (2017), respectively. More details about the characterization factors are shown in Table 2

Table 2: Factors of characterization of environmental impacts of materials and energy in processes.

		Ozone Depletion	**Global Warming**	**Smog**	**Acidification**	**Eutrophication**	**Ecotoxicity**	**Fossil Fuel Depletion**
	Units	(kg CFC-11 eq)	(kg CO_2 eq)	(kg O_3 eq)	(kg SO_2 eq)	(kg N eq)	(CTUe)	(MJ Surplus)
Sodium hypochlorite	1 kg	1.2×10^{-6}	9.3×10^{-1}	1.0×10^{-2}	3.16×10^{-3}	2.29×10^{-2}	-	16.7
Glucose	1 kg	-	1.60×10^{-1}	-	1.21×10^{-3}	1.23×10^{-3}	-	14.23
Food grade CO_2	1 kg	3.28×10^{-8}	9.54×10^{-1}	1.12×10^{-1}	2.75×10^{-3}	1.65×10^{-3}	4.13	1.02
Electricity	1 kWh	9.39×10^{-8}	3.08×10^{-1}	6.84×10^{-3}	1.64×10^{-3}	5.86×10^{-4}	2.18	0.665

2.5 NORMALIZATION

The normalization step was established according to ILDC (2010), and the reference value corresponding to the world environmental impact normalization factor was provided by the European Commission (Table 3).

Table 3: Global normalization factors for emissions and resource extraction.

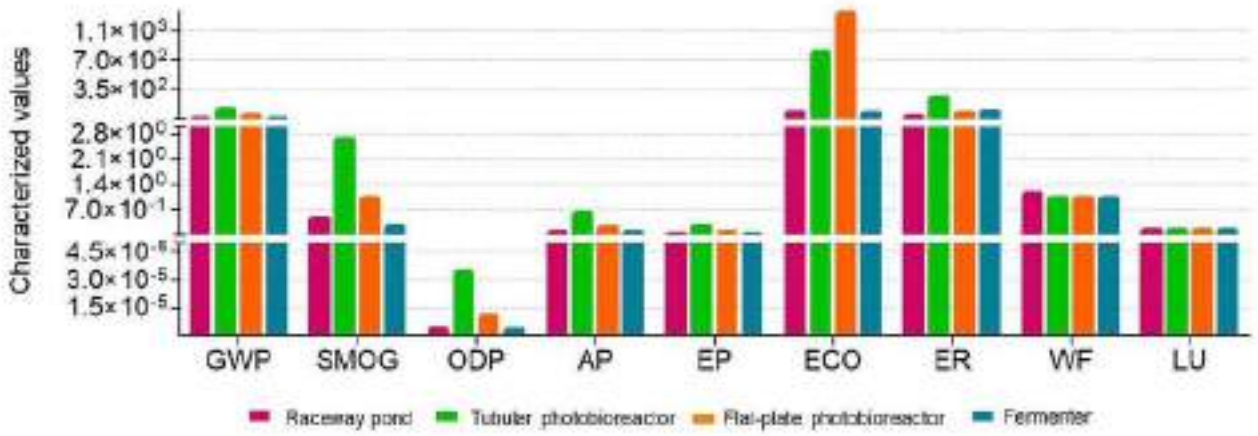
Impact categories	Unit	Reference value
Energy resource	MJ	$4.50\times10^{+14}$
Global warming potential	kg CO_2 eq	$5.79\times10^{+13}$
Water footprint	m^3	$7.91\times10^{+13}$
Acidification potential	kg SO_2 eq	$3.83\times10^{+11}$
Eutrophication potential	kg N eq	$1.95\times10^{+11}$
Ozone depletion potential	kg CFC-11 eq	$1.61\times10^{+08}$
Ecotoxicity	CTUe	$8.15\times10^{+13}$
Land use	ha	$9.64\times10^{+15}$
Photochemical ozone formation	kg O_3 eq	$2.80\times10^{+11}$

3 RESULTS AND DISCUSSION

3.1 CULTURE SYSTEMS

The main hardware of any microalgae-based process is the bioreactor, whose operation is part of the upstream processing stage. Today, raceway ponds, tubular and flat-panel photobioreactors, and fermenters are the most widely accepted existing designs for large-scale work. Although open systems require fewer consumables than closed systems, it is known that productivity is also lower. In contrast, photobioreactors overcome these yield issues, but with higher capital and operational expenses (Deprá et al., 2019). In view of this, the environmental performance of microalgae cultivation systems should be compared, since the selection of the reactor strongly influences it. Thus, the Figure 2 shows the environmental impact categories evaluated (GWP, SMOG, ODP, AP, EP, ECO, ER, WF, and LU), associated with the elements demanded the operation of the different microalgae cultivation systems.

Figure 2: Characterized values of environmental impact categories associated with cultivation systems.



Based on Figure 2, the raceway pond had a potential impact in the order of 79.93 CTUe, 23.90 MJ, 12.02 $kgCO_2eq$, and 1.13 m^3/d for the ECO, ER, GWP and WF categories, respectively. In this system, the electricity consumption considered was of the order of 0.54, 0.50, and 0.33 kW/m^3 for the culture mixture, water pumping, and CO_2 injection, respectively. These three demands depend on each other to improve the performance of the track. In addition, technically, these devices are part of crucial procedures for gas-liquid mixing. In this way, the identification of this hottest point reveals that the engineering element contributes to the scenario of environmental emissions, beyond the high energy in the operations of the primary unit of processes based on microalgae as a fundamental economic prerequisite for commercialization (Quin et al., 2012).

However, whether, on the one hand, the paddlewheel impacts the categories supported by fossil energy, on the other, it influences the WF category. For hydrodynamic reasons, the raceway pond has a considerable demand for freshwater, whose value obtained here was 1.13 $m^3/m^3/d$. This is precisely due to the movement of the paddle wheels, blade configuration, and geometry, which leads to an increase in total water losses through evaporation. According to the study by Kumar et al., (2015), propeller, centrifugal pump, and micro-channel paddlewheels could replace conventional paddle wheels, which have been tested to increase efficiency. This approach allows the operation of raceway ponds with shallow levels of WF and higher efficiency of water circulation, with a parallel reduction in energy consumption. These issues depend, of course, on factors that affect productivity in the raceway pond, such as depth and length (Chiaramonti et al., 2013).

In terms of a tubular photobioreactor, the most expressive potentials of the impact categories were 796.22 CTUe (ECO), 242.52 MJ (ER), 113.04 $kgCO_2eq$ (GWP), and 2.63 kgO_3eq (SMOG). The hotspot identified in the environmental load is due to the energy

consumption for refrigeration, which in this study is 15 kWh/m³. Due to the arrangement of the tubes, the light penetration is high enough to cause the system to overheat and, consequently, photo-oxidative damage to the culture. Therefore, in addition to the mixture for efficient energy and mass transfer (CO_2/O_2 exchange), it is essential to balance the temperature throughout the system. Heat exchange devices generally assist cooling at regular intervals. However, this consumable severely increases the demand for energy (Molina et al., 2001). The use of heat exchangers requires the analysis of the global heat transfer coefficients between the tubes of the photobioreactor with the microalgae broth and the surrounding air and between the culture and the liquid medium that circulates within the internal heat exchanger (Sierra et al., 2008). To get around these problems, the most obvious solution would be to cool the system with freshwater or seawater for thermoregulation. However, this demand has an unsustainable effect because it would impact the WF category (Nowoba et al., 2019).

In addition, the analysis of the impact categories attributed to the flat plate photobioreactor indicated potential values of 1262.20 CTUe (ECO), 72.77 MJ (ER), 34.9 kgCO_2eq (GWP), and 1.0 kgO_3eq (SMOG). The hotspot recognized in these bioreactors is due to the aeration power of the culture mixture. This is due to the design of the system, which consists of a rectangular and narrow vertical reaction vessel. Its structure is individually designed, but for commercial operation, it is necessary to expand the number of plate units instead of increasing the volume of the reactor. Therefore, according to hydrodynamic principles, as the plates have a larger lateral area for a unit compared to a tubular photobioreactor, for example, aeration occurs mainly on the vertical axis, disadvantaging mixing on the horizontal axis. In this zone, the fluid flow pattern is lower, and the aeration is insufficient (Sierra et al., 2008). This results in increased shear force (can cause cell damage) and intense energy demand from the aerator source to maintain flow and a more homogeneous mixture. Generally, mixing is induced by high electrical capacity consumables, such as blowers, mechanical agitation using an impeller, static mixer or bubble aeration, or pumping of CO_2-enriched gas (Huang et al., 2017). Thus, adequate aeration strategies on the hardware are needed to minimize the effects of this engineering demand on the environmental impact.

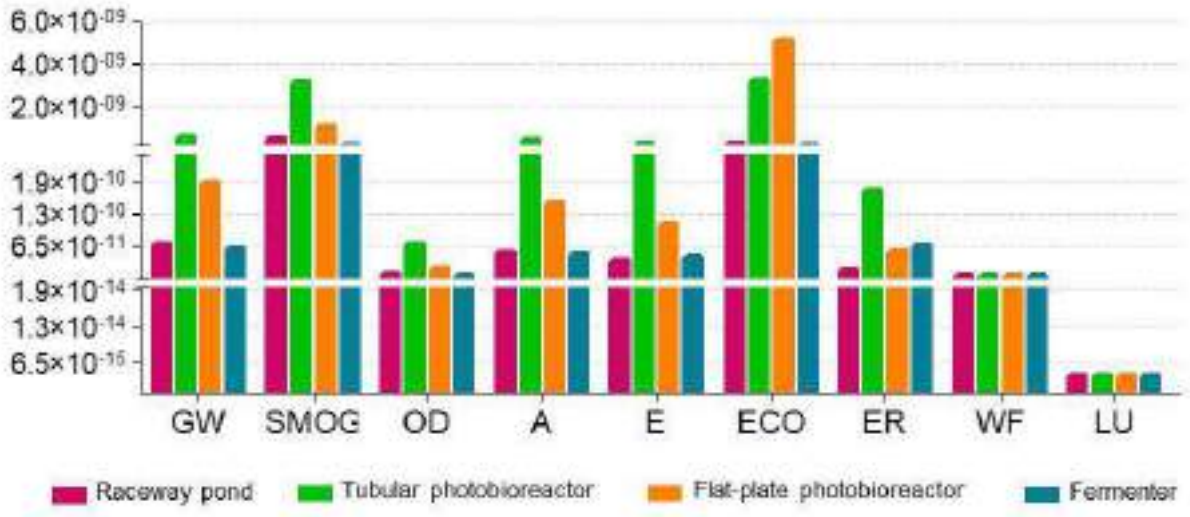
The use of the fermenter for the cultivation of microalgae contributes to the following impacts: 68.43 CTUe (ECO), 92.02 MJ (ER), 10.48 kgCO_2eq (GWP), and 0.21 kgO_3eq (SMOG). Although this type of agitated tank bioreactor requires fewer elements throughout the process compared to a photobioreactor, the hottest point identified is that of

sterilization, with an energy consumption of 7.22 kWh/m³. Second, aeration also contributes to the environmental load (1.0 kWh/m³). Under non-sterile conditions, the cultivation of heterotrophic microalgae is susceptible to contamination and competition with other microorganisms. Therefore, sterilization becomes essential at this stage of the process. This implies the implementation of a heat exchanger in the facility to obtain sufficient sterility and ensure productivity. However, in addition to being a lengthy operation, this additional equipment consumes a lot of energy due to the high heat demand. On a small scale, sterilization is possible because the volume of the bioreactor rarely exceeds 200 L. Still, it would be difficult for large quantities, as the equipment available for this purpose does not reflect a level of technological readiness for large-scale operations (Walls et al., 2019). At the same time, the energy associated with the aeration system, including the expense of the compressor with the additional expense of the airflow supply agitator, may even improve mass transfer, but contribute to the carbon footprint. The energy reduction of these demands can be achieved; however, careful selection of the impeller type, geometry, and size of the fermenter should be taken into account (Fitzpatrick et al., 2017).

3.2 NORMALIZATION

To facilitate the comparison and interpretation of results, and to understand the magnitude of environmental impacts, from uncertainties assessment perspectives, the normalization step was applied to our results, as shown in Figure 3.

Figure 3: Impact categories normalized data for the microalgae-based cultivation systems.



As can be seen in Figure 3, considering the integrity of the reference data sources used, among the nine categories evaluated for the cultivation system, four are considered to be the majority: ECO, SMOG, GWP, and ER. In contrast, the categories of AP, EP, and ODP have an impact that varies from intermediate to low, followed by the categories WF and LU. In this way, it can be inferred that these five minority categories are unlikely to contribute to the significant environmental impact.

The data normalization procedure indicates that the majority categories have a marked impact on the damage of the midpoint, linked to the deterioration of the resource base, that is, the high indirect demand for non-renewable primary energy resources. Second, the normalization of the other categories also indicates an impact associated with the extraction and consumption of energy resources, such as water and land, human health, and quality of the ecosystem. Under this assessment, among the evaluated cultivation systems, environmental charges were included in groups, with the major determining aspects being considered: (i) electricity consumption, (ii) nutrient production, (iii) water consumption, and (iv) demand land use and transformation.

From this, it is suggested that assessing the pros and cons of the cultivation system choice is crucial to introducing the technology and comparing it with a baseline option to verify whether there is a gap for future improvement. This is because the cultivation phase associated with the harvesting process is always the most impactful in microalgae cultivation processes (Sills et al., 2020). Therefore, to develop environmentally sustainable products, the algae industry needs to be aware of the environmental performance in order to obtain a holistic view of the critical points of the process, so that it can then apply optimization in the face of technical and economic challenges, and these, at last, will are overcome.

4 CONCLUSIONS

The strategy proposed in this study allowed the evaluation of metrics and sustainability indicators for microalgae-based cultivation systems. The results found indicated that the system with the greatest environmental impact prevails in the tubular photobioreactor, whereas the raceway pond presented the best environmental performance among the evaluated configurations. While we believe that these results provide an indication of the magnitude of the impacts caused by emissions from cultivation systems, we are aware that they are estimates based on experimental theoretical values, and consequently, it not perfect and cannot replace reliable statistics compiled in industrial

practice. In this way, both the characterized results and the normalized data found in this study suggest visualizing the environmental impacts under the global context of sustainability indicators, in order to bring numerically values that can fill gaps for the implementation of processes based on microalgae.

ACKNOWLEDGEMENT

The authors would like to thank the National Council for Scientific and Technological Development (CNPq) – Brazil, and the Coordination of Improvement of Higher Education Personnel (CAPES), Finance Code 001.

REFERENCES

Albarelli, J. Q., Santos, D. T., Ensinas, A. V., Marechal, F., Cocero, M. J., & Meireles, M. A. A. (2018). Product diversification in the sugarcane biorefinery through algae growth and supercritical CO2 extraction: Thermal and economic analysis. Renewable energy, 129, 776-785. DOI: 10.1016/j.renene.2017.05.022

Bhattacharya, M., & Goswami, S. (2020). Microalgae–A green multi-product biorefinery for future industrial prospects. Biocatalysis and Agricultural Biotechnology, 101580. DOI: 10.1016/j.bcab.2020.101580

Chiaramonti, D., Prussi, M., Casini, D., Tredici, M. R., Rodolfi, L., Bassi, N., ... & Bondioli, P. (2013). Review of energy balance in raceway ponds for microalgae cultivation: re-thinking a traditional system is possible. Applied Energy, 102, 101-111. DOI: 10.1016/j.apenergy.2012.07.040

Corona, B., Shen, L., Reike, D., Carreón, J. R., & Worrell, E. (2019). Towards sustainable development through the circular economy—A review and critical assessment on current circularity metrics. Resources, Conservation and Recycling, 151, 104498.DOI: 10.1016/j.resconrec.2019.104498.

Cruce, J. R., Beattie, A., Chen, P., Quiroz, D., Somers, M., Compton, S., ... & Quinn, J. C. (2021). Driving toward sustainable algal fuels: A harmonization of techno-economic and life cycle assessments. Algal Research, 54, 102169. DOI: 10.1016/j.algal.2020.102169

Deprá, M. C., Mérida, L. G., de Menezes, C. R., Zepka, L. Q., & Jacob-Lopes, E. (2019). A new hybrid photobioreactor design for microalgae culture. Chemical Engineering Research and Design, 144, 1-10. DOI:10.1016/j.cherd.2019.01.023

Deprá, M. C., Severo, I. A., Dias, R. R., Zepka, L. Q., & Jacob-Lopes, E. (2021). Photobioreactor design for microalgae culture. In *Microalgae* (pp. 35-61). Academic Press. DOI: 10.1016/B978-0-12-821218-9.00002-5

Deprá, M. C., Severo, I. A., dos Santos, A. M., Zepka, L. Q., & Jacob-Lopes, E. (2020). Environmental impacts on commercial microalgae-based products: Sustainability metrics and indicators. Algal Research, 51, 102056. DOI: 10.1016/j.algal.2020.102056

Erbland, P., Caron, S., Peterson, M., & Alyokhin, A. (2020). Design and performance of a low-cost, automated, large-scale photobioreactor for microalgae production. Aquacultural Engineering, 90, 102103. DOI:10.1016/j.aquaeng.2020.102103

Fitzpatrick, J. J., de Lima, K. G., & Keller, E. (2017). Application of mathematical modelling for investigating oxygen transfer energy requirement and process design of an aerobic continuous stirred tank fermenter. Food and bioproducts processing, 103, 39-48. DOI: 10.1016/j.fbp.2017.02.009

Goedkoop, M., Heijungs, R., Huijbregts, M., De Schryver, A., Struijs, J., & Van Zelm, R. (2009). ReCiPe 2008. A life cycle impact assessment method which comprises harmonised category indicators at the midpoint and the endpoint level, 1, 1-126.

Hauschild, M. Z., Wenzel, H. (1998). Environmental Assessment of Products. Volume 2: Scientific Background. 1st edition, Springer US, 566p.

Heinrich, A. B. (2010). International reference life cycle data system handbook. The International Journal of Life Cycle Assessment, 15(5), 524-525.

Hoekstra, A. Y. (2016). A critique on the water-scarcity weighted water footprint in LCA. Ecological indicators, 66, 564-573. DOI: 10.1016/j.ecolind.2016.02.026

Huang, Q., Jiang, F., Wang, L., & Yang, C. (2017). Design of photobioreactors for mass cultivation of photosynthetic organisms. Engineering, 3(3), 318-329.DOI: 10.1016/J.ENG.2017.03.020

Hussain, F., Shah, S. Z., Ahmad, H., Abubshait, S. A., Abubshait, H. A., Laref, A., & Iqbal, M. (2021). Microalgae an ecofriendly and sustainable wastewater treatment option: Biomass application in biofuel and bio-fertilizer production. A review. *Renewable and Sustainable Energy Reviews*, *137*, 110603. DOI: 10.1016/j.rser.2020.110603

ISO (International Organization for Standardization), 2006. ISO 14040:2006(E) Environmental Management – Life Cycle Assessment – Principles and Framework.

Kirnev, P. C. S., Carvalho, J. C., Vandenberghe, L. P. S., Karp, S. G., & Soccol, C. R. (2020). Technological mapping and trends in photobioreactors for the production of microalgae. World Journal of Microbiology and Biotechnology, 36(3), 1-9.DOI: 10.1007/s11274-020-02819-0

Kumar, K., Mishra, S. K., Shrivastav, A., Park, M. S., & Yang, J. W. (2015). Recent trends in the mass cultivation of algae in raceway ponds. Renewable and Sustainable Energy Reviews, 51, 875-885. DOI: 10.1016/j.rser.2015.06.033

Kumar, L. R., Yellapu, S. K., Zhang, X., Tyagi, R. D. (2019). Energy balance for biodiesel production processes using microbial oil and scum. Bioresource technology, 272, 379-388. DOI: 10.1016/j.biortech.2018.10.071

Laratte, B., Guillaume, B., Kim, J., Birregah, B. (2014). Modeling cumulative effects in life cycle assessment: The case of fertilizer in wheat production contributing to the global warming potential. Science of The Total Environment, 481, 588-595. DOI: 10.1016/j.scitotenv.2014.02.020

Lathuillière, M. J., Miranda, E. J., Bulle, C., Couto, E. G., & Johnson, M. S. (2017). Land occupation and transformation impacts of soybean production in Southern Amazonia, Brazil. Journal of cleaner production, 149, 680-689. DOI: 10.1016/j.jclepro.2017.02.120

Lee, Y. K., Low, C. S. (1992). Productivity of outdoor algal cultures in enclosed tubular photobioreactor. Biotechnology and bioengineering, 40(9), 1119-1122. DOI: 10.1002/bit.260400917

Market Research Reports (2021). Algae Products Market by Type (Spirulina, Chlorella, Astaxanthin, Beta Carotene, and Hydrocolloids), Source (Brown Algae, Blue-Green Algae, Red Algae, and Green Algae), Form (Solid and Liquid), and Application (Food &

Beverages, Nutraceuticals & Dietary Supplements, Personal Care, Feed, Pharmaceuticals, Chemicals, and Fuel): Global Opportunity Analysis and Industry Forecast, 2018 – 2025. Accessed in January, 10th, 2021 <https://www.alliedmarketresearch.com/algae-products-market>

Maroneze, M. M., Deprá, M. C., Zepka, L. Q., & Jacob-Lopes, E. (2019). Artificial lighting strategies in photobioreactors for bioenergy production by Scenedesmus obliquus CPCC05. SN Applied Sciences, 1(12), 1-12. DOI: 10.1007/s42452-019-1761-0

Marsullo, M., Mian, A., Ensinas, A. V., Manente, G., Lazzaretto, A., & Marechal, F. (2015). Dynamic modeling of the microalgae cultivation phase for energy production in open raceway ponds and flat panel photobioreactors. Frontiers in Energy Research, 3, 41. DOI: 10.3389/fenrg.2015.00041

Molina, E., Fernández, J., Acién, F. G., & Chisti, Y. (2001). Tubular photobioreactor design for algal cultures. Journal of biotechnology, 92(2), 113-131.DOI: 10.1016/S0168-1656(01)00353-4

Nwoba, E. G., Parlevliet, D. A., Laird, D. W., Alameh, K., & Moheimani, N. R. (2019). Light management technologies for increasing algal photobioreactor efficiency. Algal research, 39, 101433. DOI: 10.1016/j.algal.2019.101433

Qin, C., & Wu, J. (2019). Influence of successive and independent arrangement of Kenics mixer units on light/dark cycle and energy consumption in a tubular microalgae photobioreactor. *Algal Research*, *37*, 17-29. DOI: 10.1016/j.algal.2018.09.020

Quinn, J. C., Yates, T., Douglas, N., Weyer, K., Butler, J., Bradley, T. H., & Lammers, P. J. (2012). Nannochloropsis production metrics in a scalable outdoor photobioreactor for commercial applications. Bioresource Technology, 117, 164-171. DOI: 10.1016/j.biortech.2012.04.073

Rahman, K. M. (2020). Food and High Value Products from Microalgae: Market Opportunities and Challenges. In Microalgae Biotechnology for Food, Health and High Value Products (pp. 3-27). Springer, Singapore. DOI: 10.1007/978-981-15-0169-2_1

Ramírez-Mérida, L. G. R., Zepka, L. Q., & Jacob-Lopes, E. (2017). Current production of microalgae at industrial scale. Recent advances in renewable energy, 242-260.

Santos, A. M., Deprá, M. C., Cichoski, A. J., Zepka, L. Q., & Jacob-Lopes, E. (2020). Sustainability metrics on microalgae-based wastewater treatment system. Desalin. Water Treat., 185, 51-61. DOI: 10.5004/dwt.2020.25397

Sierra, E., Acién, F. G., Fernández, J. M., García, J. L., González, C., & Molina, E. (2008). Characterization of a flat plate photobioreactor for the production of microalgae. Chemical Engineering Journal, 138(1-3), 136-147. DOI: 10.1016/j.cej.2007.06.004

Sills, D. L., Van Doren, L. G., Beal, C., & Raynor, E. (2020). The effect of functional unit and co-product handling methods on life cycle assessment of an algal biorefinery. Algal Research, 46, 101770. DOI: 10.1016/j.algal.2019.101770

Tang, D. Y. Y., Khoo, K. S., Chew, K. W., Tao, Y., Ho, S. H., & Show, P. L. (2020). Potential utilization of bioproducts from microalgae for the quality enhancement of natural products. Bioresource Technology, 304, 122997. DOI: 1016/j.biortech.2020.122997

Tua, C., Ficara, E., Mezzanotte, V., & Rigamonti, L. (2021). Integration of a side-stream microalgae process into a municipal wastewater treatment plant: A life cycle analysis. Journal of Environmental Management, 279, 111605. DOI: 10.1016/j.jenvman.2020.111605

Walls, L. E., Velasquez-Orta, S. B., Romero-Frasca, E., Leary, P., Noguez, I. Y., & Ledesma, M. T. O. (2019). Non-sterile heterotrophic cultivation of native wastewater yeast and microalgae for integrated municipal wastewater treatment and bioethanol production. Biochemical Engineering Journal, 151, 107319. DOI: 10.1016/j.bej.2019.107319

Algal Research 60 (2021) 102529

Contents lists available at ScienceDirect

Algal Research

journal homepage: www.elsevier.com/locate/algal

Microalgae photobioreactors integrated into combustion processes: A patent-based analysis to map technological trends

Ihana Aguiar Severo [a,*], Aline Meireles dos Santos [b], Mariany Costa Deprá [b], Juliano Smanioto Barin [b], Eduardo Jacob-Lopes [b]

[a] Sustainable Energy Research & Development Center (NPDEAS), Federal University of Paraná (UFPR), P.O. Box 19011, 81531-980 Curitiba, PR, Brazil
[b] Department of Food Science and Technology, Federal University of Santa Maria (UFSM), 97105-900 Santa Maria, RS, Brazil

ARTICLE INFO

Keywords:
Combustion
Biological carbon capture and use (BCCU)
Microalgae
CO_2 mitigation
Patent database
Innovation

ABSTRACT

Combustion processes contribute to the deleterious products emission in the environment. This has stimulated the development of disruptive technologies with mitigation potential, which race with climate change in real-time, such as those based on microalgae. Many works are often published on this subject, but evaluation of technological trends involving patents is poorly investigated. The aim of work is to analyze the state-of-the-art of microalgae photobioreactors integrated into combustion processes through a technological mapping based on a patent survey. The Cooperative Patent Classification (CPC) criteria were considered. More than 700 patent families were mapped. The results indicated an increase in the applications since 2007–2013 and reduction in the contributions of new documents in recent years. The leading countries in patents are represented by USA and China, responsible for 20 and 12%, respectively. This analysis suggests that it is possible to inform investment strategies of decision-makers and help researchers identify technical barriers and potential research.

1. Introduction

As the world enters the third decade of the 21st century, changes in energy supply and use patterns are urgently needed. Combustion processes are among the biggest energy consumers due to the burning of fossil fuels. This results in negative effects on the environment — particularly greenhouse gas (GHG) emissions [1]. Among them, CO_2 represents more than 50% of emissions and has increased at an average rate of 2% since the last decade [2]. These issues have been addressed by the United Nations, with the Sustainable Development Goals (SDGs). Particularly, SDG 13 encourages action to tackle climate change and its impacts and is aligned with the politics to contain this global problem [3].

Thus, properly manage combustion processes and improve energy efficiency are the leading strategies to reduce the CO_2 atmospheric burden [4]. For this, it is essential to consider all opportunities for mitigation or adaptation against emissions, which will require a multi-faceted approach, such as the development of new and renewable processes, flexible and robust combustion designs that can be easily operated with low-carbon fuels (e.g. biofuels and biomass), and implementation of innovative, ecologically correct, and cost-effective technologies [5].

Short-term partial solutions to these issues are carbon capture and storage (CCS) or utilization (CCU), which are intended to sequester CO_2 from flue gases. Both procedures can be applied in different combustion processes [6]. However, once captured, CO_2 requires additional purification steps through processes of absorption, adsorption, cryogenic, or membrane separation [7]. In most industrial applications, the hottest spot for CCS and CCU is the need for a substantial redesign of traditional processes with the expansion of facilities, incurring high capital and operating costs [8].

Alternatively, microalgae-based processes have been highlighted as one of the most promising long-term approaches for biological carbon capture and use (BCCU). Many studies have proven that microalgae thrive and grow satisfactorily in high concentrations of CO_2 [9–13]. Besides, they assimilate other pollutants of industrial flue gases, such as NO_X, SO_X, CO, particulate matter, and heavy metals [14]. This kind of process was previously evidenced in the sequential study of the research group led by the authors [15,16] and is considered an innovation [17].

Microalgae are unicellular microorganisms that, through photosynthesis, convert CO_2 into organic carbon using light energy. They have fast growth rates, being 10–50 times more efficient in fixing carbon than

* Corresponding author.
E-mail address: ihana.aguiar@gmail.com (I.A. Severo).

https://doi.org/10.1016/j.algal.2021.102529
Received 7 March 2021; Received in revised form 31 August 2021; Accepted 5 October 2021
2211-9264/© 2021 Elsevier B.V. All rights reserved.

terrestrial plants. About 1.8 kg of CO_2 can be biofixed for every 1 kg of biomass produced [18] [19]. This route is viable not only for the environmental aspect but also for the technical-economic one because they use CO_2 as precursors of many metabolites, such as carbohydrates, lipids, and proteins, which are of great commercial relevance and value-added in several industrial sectors [20–22].

Microalgae cultivation is the critical factor in CO_2 capture. It is generally performed in open systems, such as raceway ponds. Nonetheless, closed systems, such as photobioreactors, are highly desirable because they have a precisely controlled medium, ensuring high photosynthetic efficiency and productivity per unit area [23,24]. Photobioreactors are illuminated three-phase reaction equipment: culture medium (liquid phase), cells (solid phase), and CO_2-enriched air (gas phase), which can have many configurations, including tubular, flat plates, air-lift, bubble column, and hybrids systems. Engineering aspects, such as design and operation, are the main elements that influence CO_2 bioconversion and microalgal growth [25].

In recent years, many disruptive projects have been created, selling entire processes or key units, such as photobioreactors. Advances in research and development (R&D) to explore the photobioreactors as an approach to be retrofitted into existing conventional combustion systems with minimal infrastructure change are increasingly boost this market niche. This will pave the way for new businesses and profits from microalgae trade [26]. According to the recent announcement by the US Department of Energy (Office of Fossil Energy and Carbon Management) [27], millionaire investments have been attributed to microalgae technology development to capture CO_2 from power plants and create valuable products and services.

Considering these aspects, surveys on this subject show its progress, trends, problems that require solution, and technology readiness level. Currently, this information is often found in a myriad of scientific articles and textbooks that provide insights regarding the application of photobioreactors in CO_2 mitigation. However, the analysis and landscape of patents are rarely discussed. By way of exemplification, in the papers by Míguez et al. [28], Norhasyima et al. [29], Sharifzadeh et al. [30], and Hussin et al. [31], carbon capture technologies are presented under a patents overview. These authors emphasize conventional methods, with some information on the use of microalgal photobioreactors for CO_2 capture. In contrast, Miguez et al. [32] reviewed capture systems based on bacteria, enzymes, and algae, highlighting an innovation indicator. In the research by Kirnev et al. [33], they focused on specific issues such as improvements in photobioreactor geometry and industry trends. Furthermore, Tabernero et al. [34] described general microalgae patents.

Patents provide an unparalleled wealth of information to identify technological innovation opportunities and support investor decision-making. These documents are essential to map the level of development of innovative technologies in a particular domain. Besides, the patent analysis helps to determine the novelty and its inventions, in intellectual property and competitor's technological competitiveness and estimating its evolution or decline in a given period [35].

Given the above, this work goes beyond publications currently available in the literature, whose objective was to present the state-of-the-art of microalgae photobioreactors integrated into combustion processes through technological mapping based on patent analysis. The novelty of the current study lies in investigating the following: 1) historical evolution in the patenting activity to understand how technologies have prospered over time in search of sustainable solutions; 2) geographic distribution to reflect the location that most invests in innovation in the world; 3) analysis of patent families by assignee, focusing on the value index and its impacts; and 4) technological domain by assignee and area of knowledge. In addition, a detailed evaluation of the key inventions patented within the scope of this study was performed and discussed, as well as the process feasibility.

2. Methodology and data

2.1. Patent analysis

In order to understand the intellectual property landscape in the research scope of this study, a patent analysis was performed using the software developed by Orbit Intelligence Questel (version 1.9.8) [36]. It consists of a worldwide platform containing a database published by more than 100 patent authorities, providing a snapshot of the level of patenting activities over a given period. Through the search results, the tool uses several algorithms to cluster international documents into families based on the FamPat Collection, which incorporates the strict rules of the European Patent Office (EPO) with that supplementary publication of the EP and/or Patent Cooperation Treaty (PCT) and links between provisional and published US applications. Moreover, this database allows access to publications from 22 offices (WO, US, EP, AT, BE, BR, CA, CH, CN, DE, ES, FR, GB, JP, RU, DK, FI, SE, IN, TW, TH, and KR), which assign codes and definitions based on International Patent Classification (IPC), CPC, EPO, US Patent and Trademark Office (USPTO), World Intellectual Property Organization (WIPO), and Japanese classifications, and also includes results from various sources of scientific literature.

2.2. Search strategy

The patents search was done on September 20, 2020, selecting in the software the advanced research option. The quest method comprised a three-step procedure: (1) search using the CPC classification codes, which are organized by section, and in them, the classes, subclasses, groups, and subgroups are embedded (https://www.cooperativepatentclassification.org/index). The fields selected are presented in Table 1. These codes are standardized to classify patents according to the different technological areas to which they belong, providing a high level of detail in searches with more accurate results. Based on this strategy, more than 700 patent families were found, resulting in approximately 3580 individual patents.

After that, (2) the screening of data was taken to withdraw documents not belonging to the scope of the present study by searching with keywords and their variants using the syntax: [(“photobioreactor”+, “photo-bioreactor”+, “photo bioreactor”+, “bioreactor”+, “cultur”+, “cultiv”+, “grow”+, “microalg”+, “alg”+, or “cyanobacteri”+) and (“combust”+ and “heat”+, “burn”+, or “fuel”+)], among others combinations, reducing the data set to about 260 patent families. The truncation “+”replaces one or more characters and allows to retrieve different relevant variations linked to a term (plural, synonym, and

Table 1
Cooperative Patent Classification (CPC) codes.

Section	Code	Description
B	B01D 53/00	Separation; separation of gases or vapors; recovering vapors of volatile solvents from gases; chemical or biological purification of waste gases, e.g. engine exhaust gases, smoke, fumes, flue gases, aerosols.
C	C12M 1/002	Apparatus for enzymology or microbiology; apparatus for culturing microorganisms for producing biomass, for growing cells or for obtaining fermentation or metabolic products, i.e. bioreactors or fermenters; • {photo bio reactors}
	C12M 21/02	{Bioreactors or fermenters specially adapted for specific uses}; • {Photobioreactors (culturing algae)}
	C12N 1/12	Microorganisms or enzymes; compositions thereof; propagating, preserving, or maintaining microorganisms; mutation or genetic engineering; culture media; • unicellular algae; culture media therefor.
F	F23N	Combustion apparatus; combustion processes. Regulating or controlling combustion.
Y	Y02E	Reduction of greenhouse gas [GHG] emissions, related to energy generation, transmission or distribution

genres) plus the Boolean operators "AND" (used to find all terms in the search) and "OR" (refers to any one of the search terms) were inserted among those keywords. The use of CPC codes combined with the words for every family serves to refine further the results obtained. The fields considered for the search query were: Title, Abstract, and Claims.

Subsequently, (3) a new screening was carried out to filter documents related to microalgae photobioreactors combined with combustion, heating, or other types of thermal systems, resulting in more than 100 patent families. Finally, they were carefully tabulated and analyzed in detail.

Fig. 1 outlines a map of the main concepts related to the fields of the invention search. The word "algae" and its derivations should be noted because it shows the wide use of these microorganisms in areas of CO_2 capture, energy, biofuels, GHG emissions, combustion, gas stream, among others, justifying the portfolio analyzed in this study.

The principal subgroups of the CPC classification codes in which the innovations are identified comprise Y02E-050 (Reduction of greenhouse gas [GHG] emissions, related to energy generation, transmission or distribution; technologies for the production of fuel of non-fossil origin), C12M-021 (Bioreactors or fermenters specially adapted for specific uses […]), C12N-001 (Microorganisms, e.g. protozoa; compositions thereof […]), and Y02P-020 (Technologies for climate change mitigation technologies in the production or processing of goods related to chemical industry), representing more than 52% of patents. To a lesser proportion, it was found that significant subgroups like Y02C-020 (Capture, storage, sequestration or disposal of greenhouse gases [GHG]), and Y02A-050 (Technologies for adaptation to climate change related to human health protection, e.g. against extreme weather), accounting about 27% of the patents identified.

Regarding the data interpretation, it is worth noting that there is no single method of searching and analyzing patents. The efficiency of research depends, among other factors, on the object under study and the intended objective. Besides, only documents that have already been published can be mapped during the search. The time between the submission of the patent application and its publication modifies substantially between different offices worldwide; thus, it can cause a certain margin of error when carrying out the search queries.

3. Results and discussion

3.1. Historical evolution in patenting activity

The first patents in the field of microalgae in the EPO database emerged in the 1960s and refer to food products. This fact coincided with the first commercial developments for large-scale cultivations in Japan, as well documented in the book of Borowitzka and Moheimani [37]. This initiative was quickly expanding in the area of climate change.

Thus, to seek as much patent information as possible, the word "microalgae" or "algae" was searched. It was initially described in the mid-1980s in a few documents addressing environmental issues. Later, between 1960 and 1990, patent applications in this field of research were scarce, on average one each year. This trend remained until the 2000s when patent applications were really boosted.

According to the mapped documents, Fig. 2 illustrates the evolution of patent applications submitted and published overtime on microalgae photobioreactors integrated into combustion systems. The timeline dynamics shows that in the early years (2000–2006), there were 6 patent families. Since then, a new trend arose. There has been a sharp increase until 2013, with a slight decline in 2012, showing a production activity of approximately 10–12 patent families per year. This jump in the number of patents may be related to the consolidation of intergovernmental agreements on global climate change, such as the Kyoto Protocol, which came into force in 2005 and expired in 2012. This treaty postulated strict guidelines for reducing GHG emissions for member countries, especially developed ones. In the same context, the Nations Framework Convention on Climate Change (UNFCCC) was a treaty signed by almost all countries worldwide in an attempt to stabilize the GHG concentration in the atmosphere [19].

This growth pattern of patenting activity on microalgae-based processes for the CO_2 mitigation from flue gases associated with climate agreements demonstrates two important scenarios: (i) an intense commitment on the part of financial investors to commercialize the field of microalgal biotechnology, and (ii) the technological advance. Undoubtedly, the instability in the oil market in the 2000s, which caused an energy crisis, further prompted its progress. This is because it was indispensable to industrialize these technological routes to produce biofuels as an alternative energy source in an economical and renewable way for competition in the market. This profile of patenting is indisputable and corroborates with the data available in several scientific

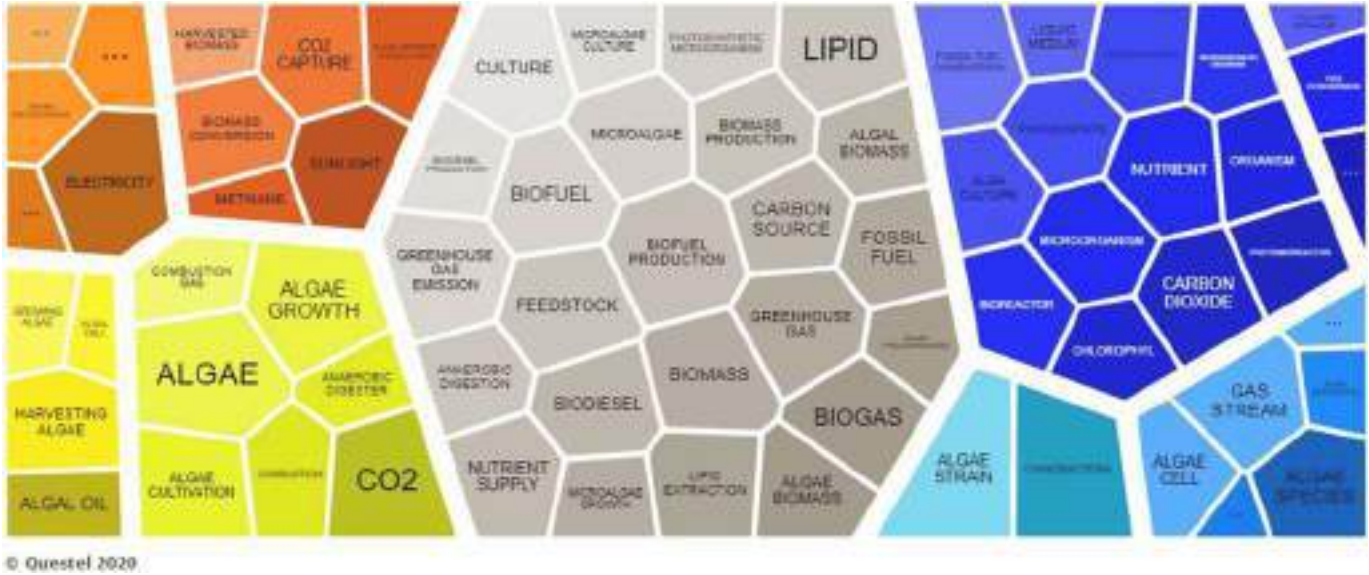


Fig. 1. Concept clusters of the analyzed portfolio.

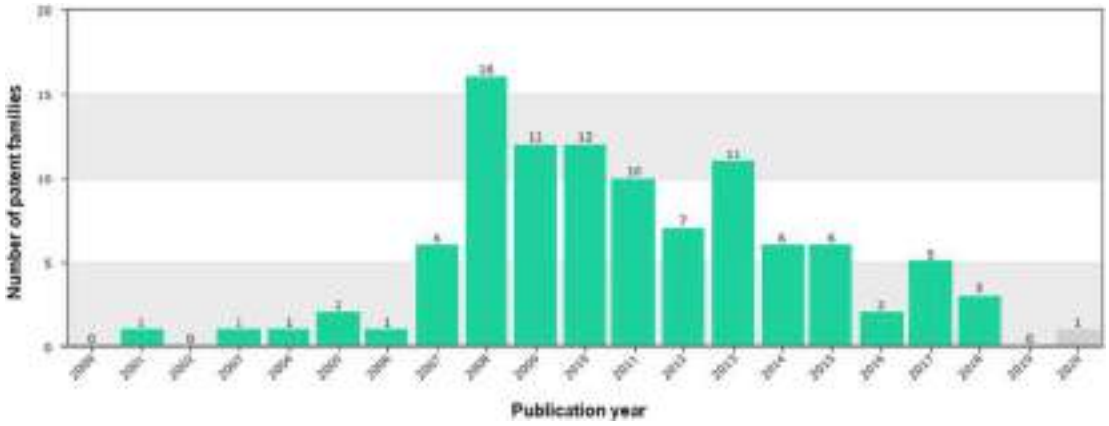


Fig. 2. Timeline of technology investment trend over last 20 years (2000–2020).

publications [38,39].

After this period, there was a drop in the number of patents filed, which is usually symptomatic of a substantial decline in R&D or intellectual property contingency. In this case, this can be attributed to the consolidation of microalgae processes, mainly in terms of photobioreactors. This represents relatively low investments in the design of these equipment's, probably because additional costs are expected concerning to the models currently available, among others factors, which despite being technically feasible, force changes in R&D budgets. Importantly, the low number of patents does not necessarily represent a low degree of inventiveness. This means that other points in these systems require further improvements. It is also worth mentioning that there is a backwardness of approximately 18-month between the filing of an application and its publication; that is, the number of patents would be incomplete from 2019 to the current year.

Finally, the market for microalgae-based processes has benefited enormously from the vast amount of information available in articles and patent documents over the past 20 years on the advantages of these bioprocesses for sustainable industrial and technological development [28].

3.2. Global geographical distribution of patents

The priority country is the location of the first patent filing or where the invented technology originates. This represents the number of priority registries in a given region and the R&D scope within that jurisdiction. Therefore, the origin of the technologies in the several assignee international offices can be seen in Fig. 3. It is observed that North America, China, India, and EPO are the leaders in the ranking of innovations in microalgae processes combined with energy-based systems,

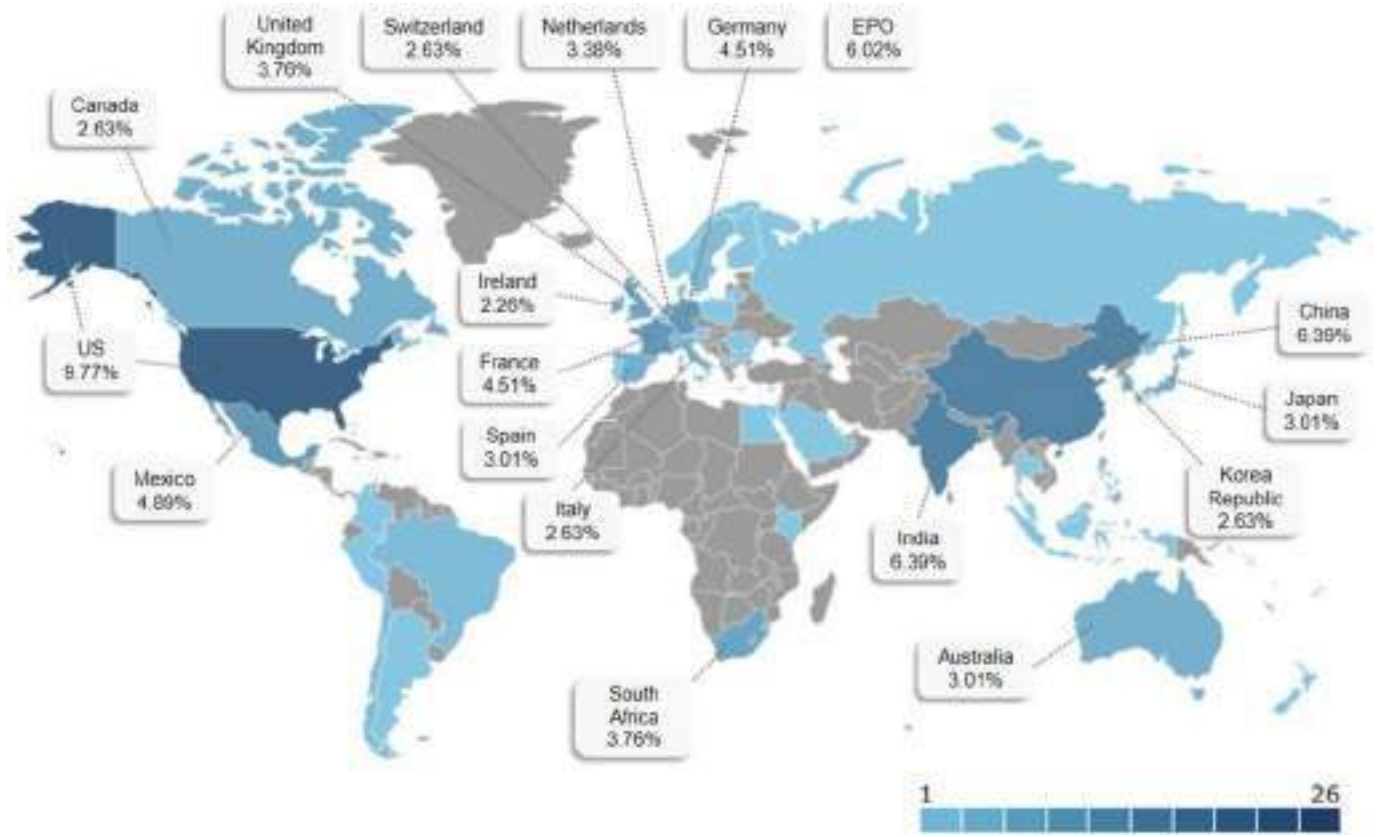


Fig. 3. Geographic origin of technologies based on alive patents protected.

including combustion or heating, contributing 26, 17, 17 and 16 patents families (~28.6%), respectively, in the last two decades.

This fact is linked to the engagement and participation of each country in mitigating GHG emissions from its different sectors of industrial manufacturing, especially in energy ones. This, in turn, emitted 6% more in 2013 than in 2010, that is, more than 18 Gt CO_2eq. According to Intergovernmental Panel on Climate Change (IPCC), the final report ("*Climate Change 2014: Mitigation of Climate Change. Contribution of Working Group III to the Fifth Assessment Report of the Intergovernmental Panel on Climate Change*") was conclusive in pointing out that the cement production industries, which use almost all fossil fuels, with coal predominating, contributed about 43% of CO_2 emissions in countries like China, USA, and India. These countries are considered the top 3 annual CO_2 emitters, accounting for 10.06, 5.41, and 2.65 Gt, respectively, in 2018 [40]. Despite this, the two major world powers, the USA and China, are at the forefront of technological progress and innovations. They use this argument to accelerate commercialization, competitiveness and maintain a high market share on emerging microalgae-based processes.

For example, the USA concentrates most companies producing microalgae due to high public funding for their development. From a private point of view, there are also many industrial and commercial efforts on the rise compared to other countries in the world. The USA remains the major driving force to boost R&D in this field, in addition to being involved in major cooperation with other countries, such as Australia, which has propitious environmental conditions for microalgae production [41].

In contrast, in China, the microalgae area was stimulated by the Medium and Long Term Development Plan for Renewable Energy promulgated by The National Development and Reform Commission of the People's Republic of China (NDRC) in 2007 [33]. In 2010, strategies for capturing and using CO_2 by photobioreactors were included in the

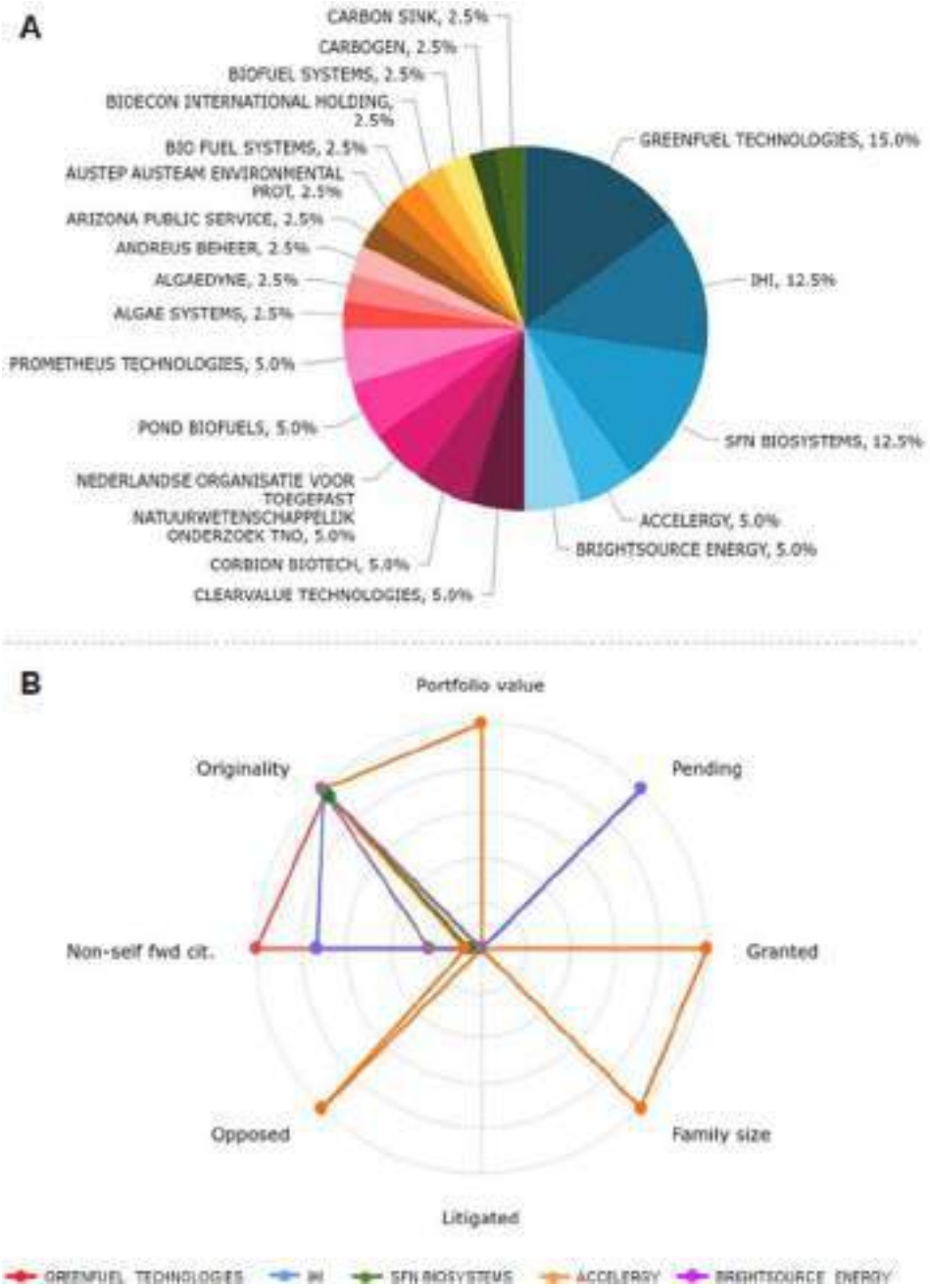


Fig. 4. Portfolio of main active assignees. (A) Top 20 players from the patent families; (B) impact indicators of the top 5 players.

country's objectives to deal with severe environmental degradation, in addition to efforts to produce cleaner energy, biofuels (biodiesel), green manufacturing, and sustainable services [41].

3.3. Analysis of patent families by assignee

The assignee, developer, or creator refers to the entity that holds the exclusive legal right to protect intellectual property over a certain period of time. Besides, applicants may include companies, public or private agencies, including universities, research centers, and institutes, or individual inventors [42]. For this reason, the assignee analysis is conducted to comprise which are the active players in the research field as well as their areas of technical expertise. Fig. 4 shows the main active assignees in the patent pool analyzed in this study and their impact indicators.

According to Fig. 4(A), the 20 company names presented lead the patents on disruptive technologies involving microalgae photobioreactors combined with combustion processes, indicating the level of inventiveness. The development of these technological routes is dominated by three companies: GreenFuel Technologies Corporation, IHI Corporation, and SFN Biosystems Inc., with 6, 5, and 5 published patent families, respectively. The GreenFuel Technologies Corporation has two important patents on its credit that deal with processes for microalgae cultivation integrated with fossil fuel emissions to produce biofuel. They correspond to publications US20080009055A1 and WO2003094598A1, with great relevance in terms of citation. In this sense, through this analysis, it is possible to demonstrate the applicant's propensity to collaborate and identify their preferred partners. Additionally, private companies are the most representative in filing patent applications. However, they are generally in collaboration with research institutes and universities, which have been researching more actively in this sector in recent years.

Fig. 4(B) shows the portfolio value index by assignees with impact indicators. Because it is considered the top 1, GreenFuel Technologies Corporation's patents show originality scores close to 0.93, 496 non-self-citations, and 0 opposition or annulment procedures. On the other hand, the Accelergy Corporation patents had an impact on the categories of originality (0.95), portfolio value (11.5), granted (2), family size (13), litigated (0), and opposed (1); however, it had a relatively low impact on non-self-citations (35). In general, these quality indicators suggest that these patents are particularly valuable because they obtained the highest originality scores, considering the scale of 0 to 1 [43]. The other categories indicate that patents are positively correlated to the value of rights.

Additionally, patent families by assignees can also be analyzed by the technological domain in which they are contained, which is based on classification codes, and can appear in different categories. Fig. 5 provides an overview of the main technology areas covered by the top

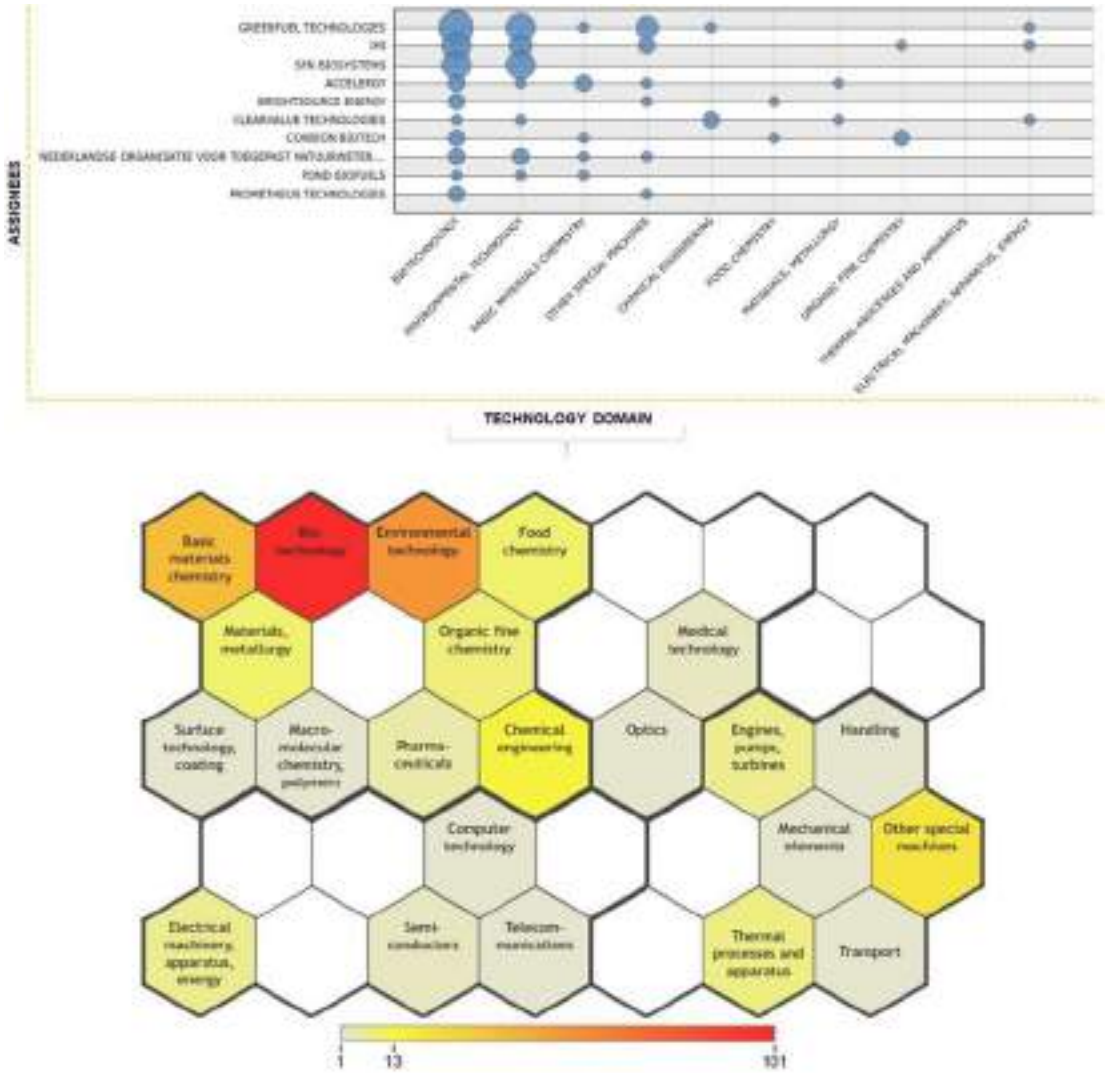


Fig. 5. Technology domain by assignee.

players.

Through this thematic concept map, it is possible to identify that the companies' patents are mainly concentrated in the areas of biotechnology and environmental technology. Evidently, these areas are the pillars that support the microalgae-based processes, which are currently considered extremely relevant to the industry in the search for innovation and new knowledge. These disruptive approaches show the strong relationship between scientific research in the area, emphasizing the important role of science in the generation of some technologies and inventions in the sector. Thus, it is possible to quickly identify the main business of a specific company and the potential partners in the market [44].

3.4. Analysis of key patented inventions

Microalgae technologies integrated into combustion processes and with the potential to mitigate climate change have been extensively studied. The papers generally report efforts to improve the photobioreactors design, studies on the parameters that affect culture performance when integrated to capture CO_2, and renewable energy generation. Although the articles provide valuable information on the results of a scientific process, whether experimental or not, and the inferences established, the patent documents offer technical reports that describe the processes, methods, and devices along with their intended industrial applications [35].

The patent families that meet the quality requirements (as discussed in Section 3.3) were ranked as the top 30 and are presented in Table 2. They were analyzed and ordered according to the percentage of the relevance score obtained on the search platform. According to the first patent shown (ranking #1), the leading company GreenFuel Technologies has several patents to capture and use CO_2 and produce energy-based products in parallel. By way of exemplification, the patent number WO2008008262A2, entitled "*Photobioreactor systems and methods for treating CO_2-enriched gas and producing biomass*", claims a microalgal photobioreactor fed with high concentrations of CO_2 as part of a fuel generation system. In certain embodiments, the invention uses the biomass generated as biofuel in an integrated combustion device, such as a power plant. The described process is similar to that presented in documents WO2003/094598 "*Photobioreactor and process for biomass production and mitigation of pollutants in flue gases*" (ranking #3), WO2008/008263 "*Integrated photobioreactor-based pollution mitigation and oil extraction processes and systems*" (ranking #24), and WO2007/011343 "*Photobioreactor and process for biomass production and mitigation of pollutants in flue gases*" (ranking #30).

On the other hand, in the second score (ranking #2), the patent WO2012/024758 "Extraction of CO_2 gas" comprises a photobioreactor used to remove CO_2 from the exhaust gases of a combustion engine and recover heat (energy integration technique) as a kind of heat exchanger device for cooling the exhaust gas and heating the liquid container using heat.

Other patents such as WO2014/110668 "*Process for managing photobioreactor exhaust*" (ranking #14), BRPI0720662A2 "*Closed system photobioreactors and biofuel production method*" (ranking #18), and US20130224841 "*Method for establishing synergism between renewable energy production and fossil energy production*" (ranking #25) also present relevant processes, both as an individual inventor and as well-known companies in the microalgae industry.

Regarding applications from university, the patent WO2017112984A1 "*Process and system for re-using carbon dioxide transformed by photosynthesis into oxygen and hydrocarbons used in an integrated manner to increase the thermal efficiency of combustion systems*" (ranking #4), from the Federal University of Santa Maria, Brazil, in collaboration with the company InterCement S/A, is the most representative document. The invention deals with the partial or total replacement of the air used in combustion processes by oxygen as an oxidizer, volatile and/or semi-volatile organic compounds as gaseous fuels, and carbon dioxide as nitrogen diluent, originating from biological GHG conversion through photosynthesis in a photobioreactor. More specifically, this document claims the treatment and conversion of said gases, the recovery of the photobioreactor gaseous phase, the integration of O_2, volatile organic compounds, and unconverted-CO_2 for use as an adjuvant in a petroleum coke combustion furnace, and the total or partial regeneration of the furnace exhaust gases for use in the photobioreactor. The present invention finds its field of application among the processes and systems for increasing thermal efficiency in industrial furnaces through the "bio-combustion" technique, as also reported in the two-part works by Severo et al. [15,16].

The most technologically impacting patent documents analyzed above, in general, present many unit operations for the treatment of microalgal biomass and conversion into biofuels or bioenergy. Some, on the other hand, address integrated processes with more simplified steps. The point is that these documents do not anticipate the direct use of photobioreactor exhaust gases to increase the energy efficiency of industrial combustion furnaces compared to the bio-combustion technique, as described in the patent WO2017112984A1. That is, no records were found of a process with claims as peculiar as this one. This process was also subjected to strict metrics and sustainability indicators and bioeconomy analysis, foreseeing to be a highly disruptive technology with environmental, economic, and social influence. The findings show that the process integration approach provided an improved performance on these issues. This is particularly important when dealing with impactful and traditional industrial combustion facilities.

3.5. Process feasibility

The processes claimed in the patents have certain limitations in terms of i) productivity and system yield; ii) the implementation remains very costly; and iii) several engineering issues need to be addressed, including the proper photobioreactor design for the CO_2 capture and conversion, the difficulties in sustaining the long-term continuous and stable production rate of metabolites, scale-up, and a better understanding of the photobioreactor hydrodynamic. This must be carefully considered before they can be engineered to operate in the open market [25].

In terms of technology readiness level, few of these technological routes undertook development during the commercial installation, reaching level 9, referred to as actual systems "flight-proven" through successful operations. In contrast, others remained in the proof-of-concept stage, with a lower TRL, from 3 to 5.

Considering these aspects, the industrial production of microalgae-based processes and products are often held back by the lack of conception of an ideal photobioreactor. This equipment is the core of the process and must be designed in order to efficiently obtain biomass and other metabolic products. For example, closed photobioreactors are essential to manufacturing valuable compounds. Several authors have investigated techniques to increase productivity in large-scale plants.

Despite advances in reactor engineering, overcoming the culture yield deficit has been challenging. Associated with this, the problems encountered so far have generated many mistaken dimensioning attempts. Many companies with large-scale commercial systems have sought the support of researchers to try to solve these shortcomings. However, as far as is known, there is practically no photobioreactor design to operate with large production volumes and meet the actual demand of the industry. Depending on its configuration, the scale-up is done by increasing the height, diameter, length, or number of modules for better lighting and space usage.

In the meantime, attempts to find an ideal photobioreactor have paved the way for technological innovation systems (TIS), which have been used as a *proxy* to direct continuous developments and identify potential technologies [45]. In addition, as costs are high, technical-economic analyzes need to be continuously updated to guarantee the viability at all phases of technology development, from its conception,

Table 2
Main innovations according to relevance score.

#	Publication number	Title	Applicant/assignee	Claims	Families	Citations	Year	Valid till or legal status
#1	WO2008008262A2	Photobioreactor systems and methods for treating CO_2-enriched gas and producing biomass	GreenFuel Technologies (original); Tron Group LLC, IHI Inc., and Algae Systems (acquisition)	14	6	195	2006	Adjusted expiration (2030)
#2	WO2012/024758	Extraction of CO_2 gas	SFN Biosystems	43	–	3	2010	Lapsed
#3	WO2003/094598	Photobioreactor and process for biomass production and mitigation of pollutants in flue gases	GreenFuel Technologies; IHI Inc.,	108	10	80	2003	Lapsed
#4	WO2017112984A1	Process and system for re-using carbon dioxide transformed by photosynthesis into oxygen and hydrocarbons used in an integrated manner to increase the thermal efficiency of combustion systems	InterCement Brazil, Federal University of Santa Maria	15	4	4	2017	2035
#5	WO2010068288A2	Solar biofactory, photobioreactors, passive thermal regulation systems and methods for producing products	Joule Biotechnologies, Inc.	46	10	62	2010	Lapsed
#6	WO2009/112624	Liquid-phase gas collection	Endesa Generación	10	5	8	2008	2028
#7	EP3150697	Method for treating liquid effluent and producing microalgae, comprising a pyrolysis step	CEA - Commissariat al Energie Atomique & Aux Energies Alternatives	15	2	4	2015	2035
#8	WO2008/042919	Method and apparatus for extracting carbon dioxide from air	Kilimanjaro Energy (original); Carbon Sink (acquisition)	16	14	327	2007	2027
#9	CA2630297	Extraction of CO_2 gas from engine exhaust	SFN Biosystems	25	–	2	2008	Lapsed
#10	CN104962476	Coal-mine-goaf-based carbon dioxide underground sealing method and system	China Shenhua Energy	14	–	1	2015	2035
#11	WO2007/101172	Process for the production of ethanol from algae	Propulsion Logic	4	–	6	2006	Lapsed
#12	WO2011/163111	Process for the selective production of hydrocarbon based fuels from algae utilizing water at subcritical conditions	Old Dominion University Research Foundation	20	20	10	2011	2032
#13	WO2013/106932	Integrated process for dual biocatalytic conversion of CO_2 gas into bio-products by enzyme enhanced hydration	CO_2 Solutions (original); Saipem (acquisition)	74	4	4	2013	Pending
#14	WO2014/110668	Process for managing photobioreactor exhaust	Pond Biofuels (original); Pond Technologies (acquisition)	16	5	17	2013	2034
#15	EP2159195	Accelerated method for converting carbon dioxide into energy	Stroiazzo-Mougin, Bernard A. J.	14	20	15	2007	2027
#16	BRPI0806678	Process sped up for the conversion of energy of carbon dioxide	Stroiazzo-Mougin, Bernard A. J.	14	20	15	2007	2027
#17	CA2780103	Growing microorganisms using exhaust gas as a nutrient supply	SFN Biosystems	16	–	2	2012	Lapsed
#18	BRPI0720662A2	Closed system photobioreators and biofuel production method	Solix Biosystems; Colorado State University	50	11	88	2007	2035
#19	DE4212334C1	Burning fuel oil or natural gas with pure oxygen to obtain heat with high efficiency without harmful emissions, with photosynthetic conversion using bioreactor	Henry Schwetzingen De Tischmacher	67	–	1	1992	Lapsed
#20	WO2013/089814	Integrated bioprocessing for fuel production	ExxonMobil Research & Engineering	36	4	22	2011	2033
#21	WO2010/116611	Micro-alga belonging to genus navicula, process for production of oil by culture of the micro-alga, and oil collected from the micro-alga	Electric Power Development	–	11	11	2010	2030
#22	CN107899375	Carbon dioxide mixed capturing and microalgae carbon fixation coupling technology for coal-fired power plant flue gas	Yang Zhengshan	3	–	4	2017	Pending
#23	US20050064577	Hydrogen production with photosynthetic organisms and from biomass derived therefrom	GreenFuel Technologies; IHI Inc.	89	7	46	2005	Lapsed
#24	WO2008/008263	Integrated photobioreactor-based pollution mitigation and oil extraction processes and systems	GreenFuel Technologies	42	2	29	2007	Lapsed
#25	US20130224841	Method for establishing synergism between renewable energy production and fossil energy production	Charles Bliss	23	2	5	2012	Lapsed
#26	US20110283618	Supplying bioreactor gaseous effluent to combustion process	Pond Biofuels	11	12	3	2010	Lapsed
#27	EP2582783	System for supporting algae growth with adsorbed carbon dioxide	General Atomics	–	9	7	2010	2032
#28	US8877488B2	Photobioreactor systems and methods for treating CO_2-enriched gas and producing biomass	Algae System; GreenFuel Technologies	14	6	195	2007	Adjusted expiration (2026)
#29	US20140011263	Photobioreactor cell culture systems, methods for pre-conditioning photosynthetic organisms, and cultures of photosynthetic organisms produced thereby	IHI Inc.	28	7	185	2013	Lapsed

(*continued on next page*)

Table 2 (*continued*)

#	Publication number	Title	Applicant/assignee	Claims	Families	Citations	Year	Valid till or legal status
#30	WO2007/011343	Photobioreactor and process for biomass production and mitigation of pollutants in flue gases	GreenFuel Technologies	77	108	7	2005	Lapsed

(–): not presented.

prototyping, demonstration to full commercialization. In practical terms, implementation is not an easy task. There is a real and strong demand for systems, methods, techniques, and apparatus to produce high capacity microalgae for commercial competitiveness.

4. Conclusions

The use of disruptive technologies with the potential to mitigate against climate change will be increasingly necessary, considering the current patterns of energy consumption and generation, world population growth, public policy trends, which subsidize stimulus for innovation. Technological prospecting involving patent analysis in this field of knowledge contributes to the considerable advance to be optimized by other industries. Certainly, these approaches could be implemented in a way that complements the traditional industrial combustion facilities. Besides, the process integration would allow for more sustainable development and contribute to the circular bioeconomy of the current industry portfolio.

Statement of informed consent, human/animal rights

No conflicts, informed consent, or human or animal rights are applicable to this study.

CRediT authorship contribution statement

Ihana Aguiar Severo: Conceptualization, Software, Data curation, Validation, Writing – original draft, Writing – review & editing, Supervision. **Aline Meireles dos Santos:** Formal analysis, Methodology. **Mariany Costa Deprá:** Investigation, Methodology. **Juliano Smanioto Barin:** Resources, Visualization. **Eduardo Jacob-Lopes:** Conceptualization, Funding acquisition.

Declaration of competing interest

The authors declare that they have no known competing financial interests or personal relationships that could have appeared to influence the work reported in this paper.

Acknowledgements

The authors would like to thank the National Council for Scientific and Technological Development (CNPq) – Brazil, and the Coordination of Improvement of Higher Education Personnel (CAPES), Finance Code 001. This work was also supported by the Agency for Innovation and Technology Transfer (AGITTEC) at Federal University of Santa Maria (UFSM).

References

[1] EPA, Environmental Protection Agency of United States, Available from: https://www.epa.gov/ghgemissions, 2021. Accessed in: August 21, 2021.
[2] IEA, International Energy Agency. Global Energy & CO_2 status report 2019. The latest trends in energy and emissions in 2018, Available from: https://www.iea.org/reports/global-energy-co2-status-report-2019, 2021. Accessed in: August 22, 2021.
[3] UN, United Nations sustainable development goals, Available from: https://www.un.org/sustainabledevelopment/sustainable-development-goals/, 2021. Accessed in: August 22, 2021.
[4] T.F. Wall, Combustion processes for carbon capture, Proc. Combust. Inst. 31 (2007) 31–47, https://doi.org/10.1016/j.proci.2006.08.123.
[5] U.S. Department of Energy, Office of Energy Efficiency and Renewable Energy, Advanced Manufacturing Office, Industrial Technologies Program (ITP), and Industrial Heating Equipment Association (IHEA), Improving Process Heating System Performance: A Sourcebook for Industry, Third edition, 2015. Available from: https://www.energy.gov/eere/amo/downloads/improving-process-heating-system-performance-sourcebook-industry-third-edition. Accessed in: August 22, 2021.
[6] R.M. Cuéllar-Franca, A. Azapagic, Carbon capture, storage and utilisation technologies: a critical analysis and comparison of their life cycle environmental impacts, J. CO_2 Util. 9 (2015) 82–102, https://doi.org/10.1016/j.jcou.2014.12.001.
[7] J.C.M. Pires, M.C.M. Alvim-Ferraz, F.G. Martins, M. Simões, Carbon dioxide capture from flue gases using microalgae: engineering aspects and biorefinery concept, Renew. Sust. Energ. Rev. 16 (2012) 3043–3053, https://doi.org/10.1016/j.rser.2012.02.055.
[8] IEA, International Energy Agency. Carbon capture, utilisation and storage, Available from: https://www.iea.org/fuels-and-technologies/carbon-capture-utilisation-and-storage, 2021. Accessed in: August 24, 2021.
[9] F.-F. Li, Z.-H. Yang, R. Zeng, G. Yang, X. Chang, J.-B. Yan, Y.-L. Hou, Microalgae capture of CO_2 from actual flue gas discharged from a combustion chamber, Ind. Eng. Chem. Res. 50 (2011) 6496–6502, https://doi.org/10.1021/ie200040q.
[10] A. Concas, G.A. Lutzu, M. Pisu, G. Cao, Experimental analysis and novel modeling of semi-batch photobioreactors operated with *Chlorella vulgaris* and fed with 100% (v/v) CO_2, Chem. Eng. J. 213 (2012) 203–213, https://doi.org/10.1016/j.cej.2012.09.119.
[11] B. Zhao, Y. Su, Y. Zhang, Carbon dioxide fixation and biomass production from combustion flue gas using energy microalgae, Energy, 89 (2015) 347–357, doi: https://doi.org/10.1016/j.energy.2015.05.123.
[12] J.A. Lara-Gil, C. Senés-Guerrero, A. Pacheco, Cement flue gas as a potential source of nutrients during CO_2 mitigation by microalgae, Algal Res. 17 (2016) 285–292, https://doi.org/10.1016/j.algal.2016.05.017.
[13] A.M. Miranda, A.A. Sáez, B.S. Hoyos, D.A. Gómez, G.J. Vargas, Improving microalgal biomass production with industrial CO_2 for bio-oil obtention by hydrothermal liquefaction, Fuel 302 (2021), 121236, https://doi.org/10.1016/j.fuel.2021.121236.
[14] S. Van Den Hende, H. Vervaeren, N. Boon, Flue gas compounds and microalgae: (bio-)chemical interactions leading to biotechnological opportunities, Biotechnol. Adv. 30 (2012) 1405–1424, https://doi.org/10.1016/j.biotechadv.2012.02.015.
[15] I.A. Severo, M.C. Deprá, J.S. Barin, R. Wagner, C.R. de Menezes, L.Q. Zepka, E. Jacob-Lopes, Bio-combustion of petroleum coke: the process integration with photobioreactors, Chem. Eng. Sci. 177 (2018) 422–430, https://doi.org/10.1016/j.ces.2017.12.001.
[16] I.A. Severo, M.C. Deprá, R.R. Dias, J.S. Barin, R. Wagner, C.R. de Menezes, L. Q. Zepka, E. Jacob-Lopes, Bio-combustion of petroleum coke: The process integration with photobioreactors. Part II — sustainability metrics and bioeconomy, Chem. Eng. Sci. 213 (2020), 115412, https://doi.org/10.1016/j.ces.2019.115412.
[17] E. Jacob-Lopes, Severo, I. A., Bizello, R. S., J. S. Barin, C. R. de Menezes, A. J. Cichoski, Process and System for Re-using Carbon Dioxide Transformed by Photosynthesis into Oxygen and Hydrocarbons Used in an Integrated Manner to Increase the Thermal Efficiency of Combustion Systems, Patent WO2017/112984 A1, 2017.
[18] R.H. Wijffels, M.J. Barbosa, An outlook on microalgal biofuels, Science 329 (2010) 796–799, https://doi.org/10.1126/science.1189003.
[19] E. Daneshvar, R.J. Wicker, P.-L. Show, A. Bhatnagar, Biologically-mediated carbon capture and utilization by microalgae towards sustainable CO_2 biofixation and biomass valorization — a review, Chem. Eng. J. 427 (2022), 130884, https://doi.org/10.1016/j.cej.2021.130884.
[20] I.A. Severo, S.F. Siqueira, M.C. Deprá, M.M. Maroneze, L.Q. Zepka, E. Jacob-Lopes, Biodiesel facilities: What can we address to make biorefineries commercially competitive? Renew. Sust. Energ. Rev. 112 (2019) 686–705, https://doi.org/10.1016/j.rser.2019.06.020.
[21] M.C. Deprá, I.A. Severo, A.M. dos Santos, L.Q. Zepka, E. Jacob-Lopes, Environmental impacts on commercial microalgae-based products: sustainability metrics and indicators, Algal Res. 51 (2020), 102056, https://doi.org/10.1016/j.algal.2020.102056.
[22] M. Wiatrowski, B.C. Klein, R.W. Davis, C. Quiroz-Arita, E.C.D. Tan, R.W. Hunt, R. E. Davis, Techno-economic assessment for the production of algal fuels and value-

added products: opportunities for high-protein microalgae conversion, Biotechnol. Biofuels (2021), https://doi.org/10.21203/rs.3.rs-565656/v1. In Review.
[23] M.G. de Morais, J.A.V. Costa, Biofixation of carbon dioxide by *Spirulina* sp. and *Scenedesmus obliquus* cultivated in a three-stage serial tubular photobioreactor, J. Biotechnol. 129 (2007) 439–445, https://doi.org/10.1016/j.jbiotec.2007.01.009.
[24] L. Moraes, G.M. Rosa, A. Morillas España, L.O. Santos, M.G. Morais, E. Molina Grima, J.A.V. Costa, G. Acién Fernández, Engineering strategies for the enhancement of *Nannochloropsis gaditana* outdoor production: Influence of the CO_2 flow rate on the culture performance in tubular photobioreactors, Process Biochem. 76 (2019) 171–177, https://doi.org/10.1016/j.procbio.2018.10.010.
[25] J. Assunção, F.X. Malcata, Enclosed "non-conventional" photobioreactors for microalga production: a review, Algal Res. 52 (2020), 102107, https://doi.org/10.1016/j.algal.2020.102107.
[26] F.G.A. Fernández, A. Reis, R.H. Wijffels, M. Barbosa, V. Verdelho, B. Llamas, The role of microalgae in the bioeconomy, New Biotechnol. 61 (2021) 99–107, https://doi.org/10.1016/j.nbt.2020.11.011.
[27] U.S. Department of Energy, Office of Fossil Energy and Carbon Management, Available from: https://www.energy.gov/fe/articles/department-energy-invests-8-million-projects-develop-algae-based-technologies-capture. Accessed in: August 27, 2021.
[28] J.L. Míguez, P. Porteiro, R. Pérez-Orozco, D. Patiño, S. Rodríguez, Evolution of CO_2 capture technology between 2007 and 2017 through the study of patent activity, Appl. Energy 211 (2018) 1282–1296, https://doi.org/10.1016/j.apenergy.2017.11.107.
[29] R.S. Norhasyima, T.M.I. Mahlia, Advances in CO_2 utilization technology: a patent landscape review, J. CO_2 Util. 26 (2018) 323–335, https://doi.org/10.1016/j.jcou.2018.05.022.
[30] M. Sharifzadeh, G. Triulzi, C.L. Magee, Quantification of technological progress in greenhouse gas (GHG) capture and mitigation using patent data, Energy Environ. Sci. 12 (2019) 2789, https://doi.org/10.1039/C9EE01526D.
[31] F. Hussin, M.K. Aroua, Recent trends in the development of adsorption technologies for carbon dioxide capture: a brief literature and patent reviews (2014–2018), J. Clean. Prod. 253 (2020), 119707, https://doi.org/10.1016/j.jclepro.2019.119707.
[32] J.L. Míguez, P. Porteiro, R. Pérez-Orozco, D. Patiño, M.A. Gómez, Biological systems for CCS: patent review as a criterion for technological development, Appl. Energy 257 (2020), 114032, https://doi.org/10.1016/j.apenergy.2019.114032.
[33] P.C.S. Kirnev, J.C. Carvalho, L.P.S. Vandenberghe, S.G. Karp, C.R. Soccol, Technological mapping and trends in photobioreactors for the production of microalgae, World J. Microbiol. Biotechnol. (2020) 36–42, https://doi.org/10.1007/s11274-020-02819-0.
[34] A. Tabernero, E.M.M. del Valle, M.A. Galan, Microalgae technology: a patent survey, Int. J. Chem. React. Eng. 11 (2013) 2, https://doi.org/10.1515/ijcre-2012-0043.
[35] Abbas, L. Zhang, S.U. Khan, A literature review on the state-of-the-art in patent analysis, World Pat. Inf. 37 (2014) 3–13, https://doi.org/10.1016/j.wpi.2013.12.006.
[36] Questel, Questel intelligence software, Available from: https://www.questel.com/business-intelligence-software/orbit-intelligence/, 2020. Accessed in: October 25, 2020.
[37] M.A. Borowitzka, N.R. Moheimani, Algae for Biofuels and Energy, Springer, Dordrecht, 2013, https://doi.org/10.1007/978-94-007-5479-9.
[38] T.M.I. Mahlia, Z.A.H.S. Syazmi, M. Mofijur, A.E. Pg Abas, M.R. Bilad, H.C. Ong, A. S. Silitonga, Patent landscape review on biodiesel production: technology updates, Renew. Sust. Energ. Rev. 118 (2020), 109526, https://doi.org/10.1016/j.rser.2019.109526.
[39] J.-N. Kang, Y.-M. Wei, L.-C. Liu, J.-W. Wang, Observing technology reserves of carbon capture and storage via patent data: paving the way for carbon neutral, Technol. Forecast. Soc. Change 171 (2021), 120933, https://doi.org/10.1016/j.techfore.2021.120933.
[40] IEA. International Energy Agency, Global energy & CO_2 status report 2019. The latest trends in energy and emissions in 2018, Available from: https://www.iea.org/reports/global-energy-co2-status-report-2019, 2020. Accessed in: October 6, 2020.
[41] IEA Bioenergy, State of technology review — algae bioenergy an IEA Bioenergy inter-task strategic project, Available from: https://www.ieabioenergy.com/wp-content/uploads/2017/02/IEA-Bioenergy-Algae-report-update-Final-template-20,170,131.pdf, 2017. Accessed in: October 6, 2020.
[42] G.A.V. Norman, R. Eisenkot, Technology transfer: from the research bench to commercialization: part 1: intellectual property rights—basics of patents and copyrights, JACC: Basic Transl. Sci. 2 (2017) 85–97, https://doi.org/10.1016/j.jacbts.2017.01.003.
[43] D. Harhoff, F.M. Scherer, K. Vopel, Citations, family size, opposition and the value of patent rights, Res. Policy 32 (2003) 1343–1363, https://doi.org/10.1016/S0048-7333(02)00124-5.
[44] WIPO. World Intellectual Property Organization, Patent landscape report: microalgae-related technologies, Available from: https://www.wipo.int/edocs/pubdocs/en/wipo_pub_947_5.pdf, 2016. Accessed in: October 10, 2020.
[45] S. Berg, M. Wustmans, S. Bröring, Identifying first signals of emerging dominance in a technological innovation system: a novel approach based on patents, Technol. Forecast. Soc. Change 146 (2019) 706–722, https://doi.org/10.1016/j.techfore.2018.07.046.

Biomass and Bioenergy 142 (2020) 105756

Contents lists available at ScienceDirect

Biomass and Bioenergy

journal homepage: http://www.elsevier.com/locate/biombioe

Dual production of bioenergy in heterotrophic cultures of cyanobacteria: Process performance, carbon balance, biofuel quality and sustainability metrics

Eduardo Jacob-Lopes *, Andriéli B. Santos, Ihana A. Severo, Mariany C. Deprá, Mariana M. Maroneze, Leila Q. Zepka

Bioprocess Intensification Group, Federal University of Santa Maria, UFSM, Roraima Avenue 1000, Santa Maria, RS, 97105-900, Brazil

ARTICLE INFO

Keywords:
Microalgae
Bioreactor
Carbon bioconversion
Mass balance
Biofuels
Environmental impact

ABSTRACT

This research evaluated the dual production of bioenergy in heterotrophic cultures of cyanobacteria. Process performance parameters, carbon balance, single-cell oil production, biofuel quality, volatile organic compounds (VOCs) generation, and sustainability metrics and impact indicators were assessed. The results showed biomass productivity of 1.03 kg/m^3/d. Biomass (63.9%) and VOCs (8.56%) were the main products formed from the conversion of the substrate in the bioreactor. For single-cell-oil production, it is possible to obtain 0.18 kg/m^3/d of lipid with this bioprocess. It was determined the fatty acid profile and the quality of biodiesel properties, meeting the requirements established by national and international standards. Besides, the 22 volatile compounds identified presented the energy potential of 122,205.00 kJ/kg and a power generation rate of 10,580.5 kg/m^3/d. From an environmental point of view, the net energy ratio was 0.13, while the eight mid-points impact categories resulted in an ecotoxicity potential of 430.86 CTUe, energy resources of 230.04 MJ, global warming of 171.05 kg CO_2 eq, photochemical oxidation of 1.33 kg O_3 eq, water footprint of 1.08 m^3, acidification of 0.44 kg SO_2 eq, eutrophication of 0.13 kg N eq, and ozone depletion of kg 1.83×10^{-5} CFC-11 eq, per functional unit of 1 m^3 of the bioreactor, operating for 5 days. Finally, the proposed process can be considered as a promising strategy for renewable energy production from microalgae.

1. Introduction

Due to the unprecedented growth of the global population, and excessive use of fossil energy, a resource of exhausting nature, dependence on fuels has long been increasing the burden on the environment. It is crucial to realize that worldwide needs to change its energy matrix for a more sustainable source in the future. Based on this, renewable energy production systems have progressed. Although there are several sources of them, aquatic feedstock's, including a wide variety of prokaryotic and eukaryotic microorganisms, such as cyanobacteria and microalgae, seems to be a promising option for fulfilling this need [1]. Microalgae and cyanobacteria are potential to generate energy products due to the following reasons: (i) they have elevated calorific value; (ii) higher growth rate; (iii) non-requirement of arable land for cultivation; and (iv) adaptive capacity to sudden fluctuations in light, salinity, temperature, and nutrient composition [2].

Despite these potentialities, the success of microalgae-based processes depends on high biomass productivity. This parameter is related to the optimal light supply to the culture. Microalgae and cyanobacteria are usually cultivated under photoautotrophic conditions, using sunlight and atmospheric carbon dioxide (CO_2) for growth. However, depending on the cultivation system, light is not available for whole periods, affecting CO_2 assimilation. In terms of artificial lighting, high energy demand makes the process more expensive and complicated [3].

In contrast, some microalgae strains also can grow heterotrophically in the dark, supported by an exogenous carbon source [4]. In this case, much higher biomass productivities and lipid accumulation are common under optimized culture conditions. It was demonstrated that the biomass concentration in fed-batch cultivation reaches values of 15.5 and 14.2 g/L in a laboratory and industrial-scale bioreactors, respectively. These values may exceed the volumetric productivity of photoautotrophic mode [5]. In addition to eliminating light dependence, the heterotrophic route is considered more straightforward to build and less

* Corresponding author.
E-mail address: ejacoblopes@gmail.com (E. Jacob-Lopes).

https://doi.org/10.1016/j.biombioe.2020.105756
Received 2 April 2020; Received in revised form 18 August 2020; Accepted 24 August 2020
Available online 14 September 2020
0961-9534/© 2020 Elsevier Ltd. All rights reserved.

onerous to maintain on a large-scale [6]. However, the critical point is the culture medium cost, which can represent up to 50% of bioprocess operational expenses. Glucose has been the most common substrate to support the growth of microalgae. But it is estimated that about 80% of total cultivation costs are associated with this carbon source. Thus, using cheap raw materials is fundamental to make the process economically viable [7]. Cassava starch, a substrate widely available in tropical and subtropical regions, with relatively low processing cost and selling price, has been a good alternative. The use of cassava starch has already been tested in some studies under heterotrophy conditions, and its assimilation efficiency for the potential production of biomass and biofuel was evidenced [8,9].

Regarding products, the biomass of microalgae and cyanobacteria has considerable oil content, which can be converted into biodiesel. This single-cell-oil is one of the most popular biofuels, being biodegradable, non-toxic, with high flash point, and lower emissions compared to diesel fuel. Its environmental advantages, the parameters affecting the process of extraction, transesterification, and lipid yield, have been extensively studied [10–13]. Yet, it is known that only some microalgae products have a consolidated market share, such as specialty chemicals. Bulk products, such as biofuels and bioenergies, are not yet competitive. Demand for these commodities is high, and, at the current technology readiness level, the scale production needs to be expanded at reasonable costs.

Considering the above fact, producing stand-alone microalgae biodiesel is not yet economically viable, however it could very well be a preferable and profitable path [14–16]. Thus, the co-production of other energy materials could be a turning point. Studies have shown that, in addition to liquid biofuels, gaseous ones can also be generated simultaneously by microalgae. This energy source comes from a broad spectrum of volatile organic compounds (VOCs) released by the algal cells into the culture medium, which can be recovered in the form of exhaust gases. Besides, VOCs production occurs without the intermediate step commonly followed for biomass processing and conversion. Some research has evaluated the formation and use of microalgae volatiles in different technological domains [17–21]. But the highlight is the VOCs application as an additional bioenergy source in thermal systems [22,23].

Given these aspects, managing the path of the carbon source used in cultivation is an essential operational factor [24]. Knowing that the key to designing and optimizing microalgae processes is in the high productivity rates, the mass balance is vital for balancing the reactions in the heterotrophic bioreactors [25]. The quantitative elucidation of carbon in the three-phase system, that is, solid, liquid, and gaseous, can contribute to the consolidation of the metabolic routes, which will contribute to the targeting commercial production of a product of interest.

At the same time, the improvement of these studies directs the development of microalgae-based processes on a large scale. For this to happen, environmental performance must be analyzed to anticipate what the impacts will be and how the industries and all interested parties can adjust to this. It is imperative to point out that as microalgae production systems are on the rise, it is strongly recommended to submit them to sustainability assessments to support their implementation. This is because, although they have a sustainable appeal, the hottest point remains in high energy demand. Moreover, this energy comes mainly from coal transformed into electricity, which further aggravates the environmental framework. Thereby, based on the precepts of life cycle assessment, the application of sustainability metrics is a powerful way to quantify and examine the potential environmental impacts of processes. They comprise indicators related to the energy and material intensity, emissions, and demand for resources throughout the useful life cycle [26].

In this sense, the objective of the present work was to assess the dual production of bioenergy in heterotrophic cultures of cyanobacteria *P. autumnale*. The study focused on the evaluation of process performance, carbon balance, biofuel quality, and sustainability metrics. To the best of our knowledge, we have not found any research that brings together the topics covered here. Therefore, we understand that this investigation could contribute to the advancement of knowledge concerning the currently available literature on 3rd generation biofuels.

2. Material and methods

2.1. Microorganism and culture conditions

Axenic cultures of *Phormidium autumnale* were originally isolated from the Cuatro Cienegas desert (26°59′N, 102°03′W-Mexico). Stock cultures were propagated and maintained in solidified agar–agar (20 g/L) containing sterile synthetic BG11 medium [27]. The cultures were illuminated with 20-W fluorescent daylight-type tubes (Osram Sylvania, Brazil) located in a photoperiod chamber. The incubation conditions used were as follows: photon flux density of 15 μmol/m^2/s, photoperiod of 12 h, and temperature of 25 °C. The photon flux density was adjusted and controlled by using a digital photometer (Spectronics, model XRP3000).

To obtain the inoculums in liquid form, 1 mL of sterile synthetic medium was transferred to slants, the colonies were scraped and then homogenized with the aid of mixer tubes. The entire procedure was performed aseptically.

2.2. Cultivation in heterotrophic bioreactor

Measurements were made in a bubble column bioreactor [8]. The system was built of borosilicate glass and had an external diameter of 12.5 cm and a height of 16 cm, resulting in a height/diameter (h/D) ratio equal to 1.28, with a nominal working volume of 2.0 L. The dispersion system of the reactor consisted of a 2.5-cm diameter air diffuser located inside the bioreactor. The air flow was monitored by flow meter (KI-Key Instruments®, Trevose-PA, USA) and the inlet of air and outlet of gases were filtered through filtering units made up of polypropylene membrane with a pore diameter of 0.22 μm and total diameter of 50 mm (Millex FG®, Billerica-MA, USA). The bioreactor, including filtering units, was previously sterilized by autoclaving at 121 °C for 40 min and then for 30 min.

2.3. Obtaining kinetic data in the bioreactor

The experiments were conducted in the heterotrophic bioreactor operating under batch regime, fed on 2.0 L of culture medium. The experimental conditions were: initial inoculum concentration of 0.1 g/L, temperature of 26 °C, pH adjusted to 7.6, aeration of 0.1 VVM (volume of air per volume of culture per minute), and privation light [18]. The culture consisted of a synthetic BG11 medium complemented with cassava starch as an exogenous carbon source. The concentration of cassava starch (7 g/L) was adjusted using a calibration curve based on dilutions of a known amount of dry substrate.

2.4. Sampling and analytical methods

Samplings were as follows: liquid phase (culture medium), where collections were performed aseptically in a previously sterilized laminar flow hood; gaseous phase (headspace of the bioreactor); and solid phase (biomass). Cell biomass, pH dynamics, carbon concentrations, and VOCs were monitored. These procedures were performed every 24 h during the microorganism growth phases. The tests were performed in duplicate, and the kinetic data refer to the mean value of four repetitions.

Cell biomass concentration was evaluated gravimetrically, filtering a known volume of culture medium through a 0.45 μm filter (Millex FG®, Billerica-MA, USA) and drying it at 60 °C for 24 h. The biomass was separated from the culture medium by centrifugation, followed by lyophilization (Lyophilizer Liotop L101), to evaluate the carbon content.

The elemental composition of the *Phormidium autumnale* biomass was determined using a PerkinElmer 2400 CHNS/O element analyzer (PerkinElmer®, Waltham, USA). The chemical composition of biomass was performed based on the method described in AOAC [28], except to total lipid concentration. The calorific value of the biomass was calculated by the Atwater System, using factors of 17 kJ/g for protein, 38 kJ/g for lipid, and 17 kJ/g for total carbohydrate content [29]. The pH values were determined by a potentiometer (Mettler-Toledo, São Paulo-SP, Brazil).

2.5. Analysis of total carbon

Measurements of total carbon (TC) in the liquid and gaseous phases were conducted in a carbon analyzer TOC-VCSN model (Shimadzu, Kyoto, Japan) with a normal sensitivity catalyst (platinum on 1/800 Alumina Pellets) [9]. The organic carbon (OC) was calculated by the difference between TC and inorganic carbon (IC). When determining TC, 27 μL samples were injected into the combustion tube at 680 °C, where the catalytic oxidation to CO_2 occurs. For the determination of IC, samples injected of 27 μL reacted with hydrochloric acid 2 mol/L to convert all the inorganic carbon into CO_2. The CO_2 produced in both catalytic oxidations from IC and TC is quantified by non-dispersive infrared absorption. The TC and IC concentrations are obtained by interpolation using calibration curves (peak area as a function of standard concentration) previously constructed by injection of standards.

2.6. Isolation of the volatile organic compounds

The volatile compounds were isolated using headspace solid-phase micro-extraction (HS-SPME) with a 50/30 μm divinylbenzene/carboxen/polydimethylsiloxane (DVB/CAR/PDMS) fiber (Supelco, Bellefonte, USA). Sample preparation was performed using 20 mL of culture medium, equally separated into two portions. These two portions were analyzed by HS-SPME coupled with GC/MS for the quantitative determination of the volatile compounds. The aliquot was placed in a headspace septum vial containing 3 g of NaCl and 10 μL of 3-octanol standard solution (82.2 μg/mL). The SPME fiber was inserted into the headspace of the vial containing the sample for 45 min at 40 °C, with agitation provided by a magnetic stir bar. After this period, the fiber was removed from the vial and immediately desorbed into the injector of the GC [18].

2.7. GC/MS analysis

The volatile compounds were separated on a DB-Wax fused silica capillary column, 60 m in length, 0.25 mm id, and 0.25 μm film thickness (Chrompack Wax 52-CB) in a Shimadzu QP 2010 Plus gas chromatograph-mass spectrometer. The initial oven temperature for the DB-Wax column was set at 35 °C for 5 min, followed by a linear increase at 5 °C.min^{-1} to 220 °C, and this temperature was held for 5 min. For identification, an electron-impact ionization voltage of 70 eV was applied, with a scan ranges of *m/z* 35–350, and helium was used as the carrier gas. The volatile compounds were identified by a comparison of their MS spectra with those provided by the computerized library (NIST MS Search). Besides, to assist with identification, each volatile linear retention index (LRI) was calculated using the retention times of a standard mixture of paraffin homologs prepared in hexane and compared with the LRI values published in the literature for columns with the same polarity [30]. Co-injection of the sample and the standard mixture provided experimental LRIs for the compounds, which were compared with those of standards analyzed under similar conditions.

2.8. Extraction and determination of total lipids, preparation of the fatty acid methyl esters, and determination of the fatty acid composition

At the end of the analytical process, total lipid concentration of the biomass was determined gravimetrically by the modified Bligh and Dyer method [31], using the ratio between methanol, chloroform, and distilled water of 2:1:0.8 (v/v/v). The methodology of Hartman and Lago [32] was used to saponify and esterify the dried lipid extract and, then, to obtain the fatty acid methyl esters (FAME) (biodiesel). The fatty acid composition was determined by using a VARIAN 3400CX gas chromatograph (Varian, Palo Alto-CA, USA). FAMEs were identified by comparison of the retention times with the authentic standards from FAME Mix-37 (P/N 47885-U, Sigma-Aldrich, St. Louis, USA) and quantified through area normalization by software T2100p Chromatography Station (Plus Edition) v9.04.

2.9. Quality evaluation of biodiesel

The fuel properties were determined through the software BiodieselAnalyzer© 1.1, which estimates biodiesel properties based on the fatty acid profile of the parent oil, through an empirical equations system [33]. The biodiesel properties are determined by ester content (EC), cetane number (CN), iodine value (IV), degree of unsaturation (DU), saponification value (SV), long-chain saturated factor (LCSF), cold filter plugging point (CFPP), cloud point (CP), allylic position equivalents (APE), bis-allylic position equivalents (BAPE), oxidation stability (OS), higher heating value (HHV), kinematic viscosity (μ), and kinematic density (ρ).

2.10. Process performance indicators

Biomass data were used to calculate the biomass productivity (kg/m^3/d), the maximum specific growth rate (d^{-1}), and the generation time (d) from Eqs. (1)–(3), respectively:

$$P_X = \frac{(X_i - X_{i-1})}{(t_i - t_{i-1})} \quad (1)$$

$$\ln\left(\frac{X_i}{X_0}\right) = \mu_{max} \times t \quad (2)$$

$$Gt = \frac{0.693}{\mu_{max}} \quad (3)$$

where X_i is biomass concentration at time t_i (kg/m^3) and X_{i-1} is biomass concentration at time t_{i-1} (kg/m^3), t is residence time (d), and μ_{max} is the maximum specific growth rate.

The total carbon concentration was used to calculate the substrate consumption rate (kg/m^3/d) were calculated according to Eq. (4):

$$r_S = \frac{ds}{dt} \quad (4)$$

where S is the organic carbon concentration (kg/m^3), and t is the time (d).

Conversion efficiency (%) and the biomass yield coefficient ($kg_{biomass}/kg_{substrate}$), were calculated from Eqs. (5) and (6):

$$CE = \frac{S_0 - S}{S_0} \times 100 \quad (5)$$

$$Y_{X/S} = \frac{dx}{ds} \quad (6)$$

where S_0 and S are the initial and final organic carbon concentrations, respectively.

Carbon mass balance was calculated from Eq. (7) according to the inputs and outputs in the system [24]:

$$C_{in} - C_{out} = V_L M_C \left(\frac{d[C_{biomass}]}{dt} + \frac{d[DIC]}{dt}\right) + V_g M_C \left(\frac{d[C_{headspace}]}{dt}\right) \quad (7)$$

where C_{in} and C_{out} correspond to the carbon mass flow rate at the inlet and outlet of bioreactor, respectively (kg/d), V_L and V_g are the medium

and headspace volumes, respectively (m^3), M_C is the atomic weight of carbon (kg), ($d[C_{biomass}]$)/dt is the rate of change in carbon concentration converted into biomass ($kg/m^3/d$), (d[DIC])/dt is the rate of change in dissolved inorganic carbon concentration ($kg/m^3/d$), and ($d[C_{headspace}]$)/dt is the rate of change in carbon concentration in headspace ($kg/m^3/d$).

The VOCs production rate ($kg/m^3/d$) was estimated corroborating the total organic carbon data measured in the bioreactor gaseous phase with the total compounds identified and quantified in the GC/MS using Eq. (8) [23]:

$$r_{VOCs} = \frac{\left(\frac{(OC_i - OC_O)\times C_C}{100}\right) \times Q}{V_R} \quad (8)$$

where OC_i and OC_O corresponds to the inlet and outlet carbon organic concentration, respectively, and C_C is the concentration of the volatile organic compound. Additionally, the power generation rate was estimated based on the calorific power of the carbon (34,000 kJ/kg) and hydrogen (120,000 kJ/kg) atoms of organic molecule.

The net energy ratio (NER) (Eq. (9)) was defined as the ratio of the total energy produced (calorific potential of all products generated) over the total energy consumed in the process (see energy requirements values in Table 1) [34].

$$NER = \frac{E_{out}}{E_{in}} \quad (9)$$

where E_{out} is the output energy (kJ) and E_{in} is the required input energy (kJ).

2.11. Sustainability metrics

The sustainability metrics were applied in consensus with the guidelines of the International Organization for Standardization (ISO) 14040 series, to evaluate the potential environmental impacts of all process steps, following four stages: (i) goal and scope definition, (ii) inventory analysis, (iii) life cycle impact assessment, and (iv) interpretation of life cycle results [35].

The objective and scope of the application of this process were to assess the environmental footprint of all energy and nutrient requirements for the heterotrophic cultivation proposed here. In addition, issues regarding the operational steps for extraction and lipid conversion to biodiesel, as well as the chemical reagents used were included in the analysis. The scope and boundaries of the system for this process (gate-to-gate assessment) are illustrated and summarized in Fig. 1. The study considered the functional unit of the bioreactor system under the operation mode of 1 m^3 for 5 days. At the end of the operation, the final biomass of approximately 5 kg and the lipid content of about 1 kg of biodiesel can be obtained.

Table 1
Data inventory of energy requirements for biodiesel production.

Processing step	Process items	Unit	Requirement
1. Cultivation	Cassava starch	kg/m^3	7.0
	Sodium nitrate	kg/m^3	0.011
	Phosphate	kg/m^3	0.008
	Sterilization	kJ/kg	26.60
	Agitation	W/m^3	0.1752
	Aeration	kW/m^3	0.0240
2. Harvesting	Centrifugation	kWh/m^3	1.0
3. Drying	Lyophilization	kWh/kg	0.134
4. Lipid extraction	Chloroform	m^3	0.005
	Methanol	m^3	0.010
	Solvent recovery	kWh/kg	0.019
	Centrifugation	kWh/m^3	1.0
5. Transesterification	Potassium hydroxide	kg/m^3	0.05
	Mixing	kWh/kg biodiesel	0.3

The life cycle impact assessment stage translates the impact of the inventory analysis into the results of mid-point environmental indicators. These indicators consider the following categories: energy resource (ER), global warming potential (GWP), water footprint (WF), acidification potential (AP), eutrophication potential (EP), ozone depletion potential (ODP), photochemical ozone formation potential (SMOG), and ecotoxicity (ECO). Still at this stage, the characterization of the results of each category was quantified through mathematical modeling, according to Eq. (10).

$$C_i = \sum C_F \times E_I \quad (10)$$

The compilation of data inventory was developed from the relevant energy attributes during the upstream and downstream processing phases for the biodiesel production. The inventoried steps and the main unit operations considered are shown in Table 1.where C_i is impact category, C_F is the characterization factor, and E_I is emission inventory, expressed in mass released into the environment per functional unit. Table 2 shows the respective categories with theirs characterized values.

3. Results and discussion

3.1. Growth kinetics

The use of cassava starch as an exogenous organic carbon source is considered a promising alternative to replace more expensive substrates. Therefore, assessing heterotrophic cultures performance against the assimilation of this carbohydrate is essential to consolidate cyanobacteria-based processes and products. In this sense, kinetic parameters for *Phormidium autumnale* cultivated with cassava starch are presented in Table 3.

The kinetic data showed a rapid growth rate ($\mu_{max} = 1.1\ d^{-1}$) and low generation time (0.6 d), resulting in maximum cell biomass of 5.28 kg/m^3 and average biomass productivity of 1.03 $kg/m^3/d$. Besides, a substrate conversion efficiency of 81.0% and a biomass yield coefficient of 0.60 $kg_{biomass}/kg_{substrate}$ were verified. Similar results were found in the study by Francisco et al. [36] for the heterotrophic cultivation of *Phormidium* sp. in cassava wastewater. They reported the biomass productivity of 1.27 $kg/m^3/d$, biomass yield coefficient of 5.2×10^{-4} kg/kg, and carbon conversion of 66.1%. Additionally, Santos et al. [9] evaluated the growth of cyanobacteria *Aphanothece microscopica Nägeli* supported by different starch sources, and the cassava starch resulted in a better performance for the analyzed kinetic parameters. Wang et al. [7] developed a heterotrophic co-culture system, where the microalgae *Chlorella pyrenoidosa* efficiently assimilated soluble starch for its kinetic growth. Furthermore, Tan et al. [37], using the same strain, but with the mixture of different stages of starch wastewater, demonstrated that the proposed strategy improved the microalgal biomass concentration by more than 78%.

In chemical terms, the adequate assimilation of cassava starch as an exogenous carbon source by cyanobacteria is related to the characteristics of the molecule, which is composed of high amylopectin (76–83%) and low amylose content (17–24%) [38]. This is because, metabolically, the endogenous reserves of oxidizable substrates in cyanobacteria are mainly glycogen and cyanophycean starch, which is composed of α-1, 4-glucan. That is, in the absence of exogenous carbon source, these reserves are used to maintain the level of ATP in the cell in a process coupled to anaerobic respiratory phosphorylating electron transport chain. As the chemical structure of cyanophycean starch is very similar to amylopectin e, consequently to cassava starch, the cells are fully adapted to this substrate. Then, its use as an exogenous carbon source is suitable for cyanobacterial heterotrophic growth [8,9].

3.2. Carbon balance

Mass balances in biological processes have been conducted to investigate carbon assimilation routes. Here, we use the technique to indicate its location (solid, liquid, and gaseous phase) and subsequently

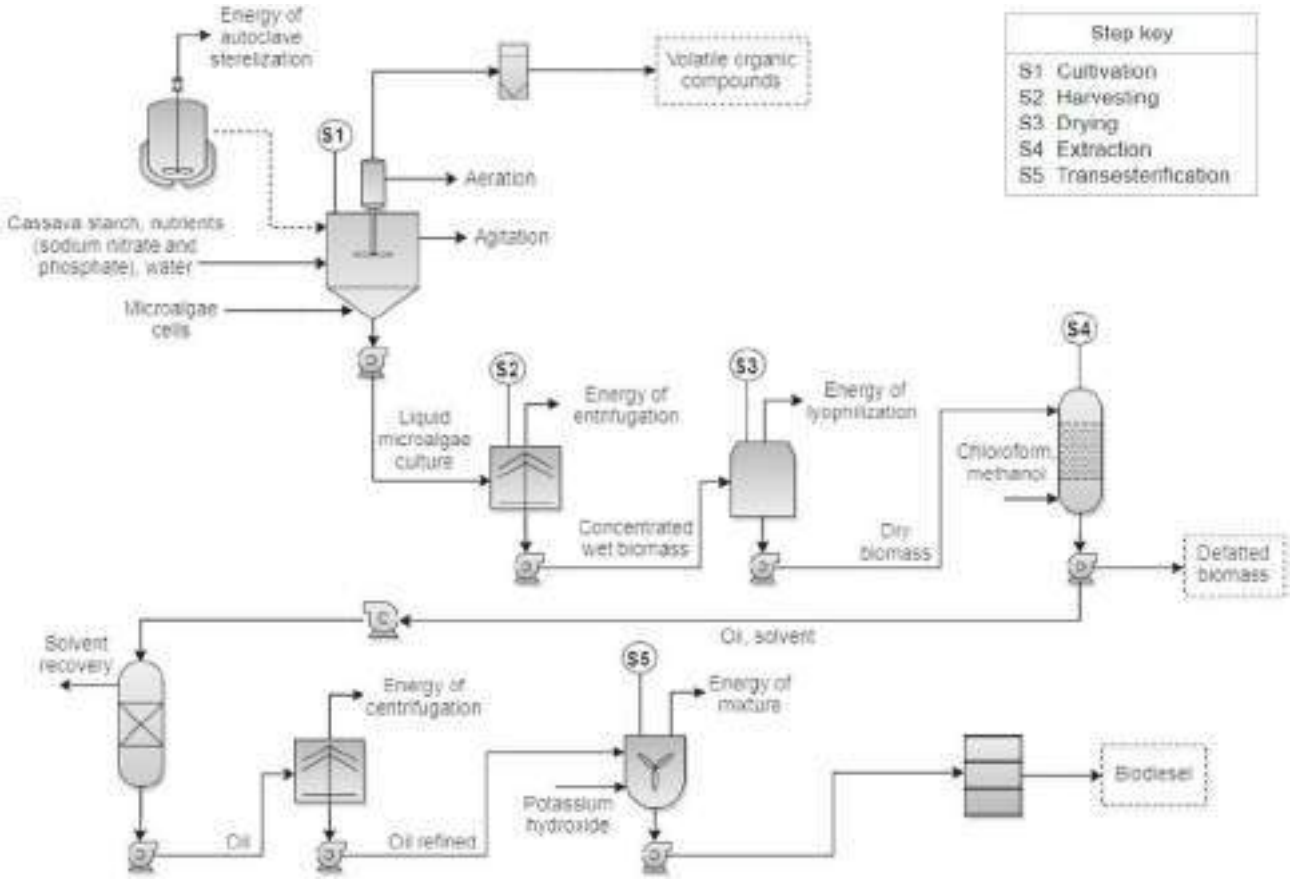


Fig. 1. Process flow diagram showing material and energy streams for heterotrophic cultivation of *P. autumnale* and the several downstream processing steps from the microalgal slurry to products.

Table 2
Characterization factors of environmental impacts.

		Ozone Depletion	Global Warming	Smog	Acidification	Eutrophication	Ecotoxicity	Fossil Fuel Depletion
	Units	(kg CFC-11 eq)	(kg CO_2 eq)	(kg O_3 eq)	(kg SO_2 eq)	(kg N eq)	(CTUe)	(MJ Surplus)
Sodium nitrate	1 kg	3.62×10^{-7}	4.94	2.34×10^{-1}	1.98×10^{-2}	2.08×10^{-2}	$3.08 \times 10^{+1}$	4.12
Potassium hydroxide	1 kg	–	1.94	–	1.50×10^{-2}	3.62×10^{-3}	7.31×10^{-1}	–
Methanol	1 kg	–	2.97	–	6.49×10^{-3}	5.48×10^{-4}	1.63×10^{-1}	2.04×10^{-2}
Chloroform	1 kg	–	16.0	–	1.35×10^{-2}	3.13×10^{-3}	6.71×10^{-1}	7.81×10^{-3}
Phosphate	1 kg	2.99×10^{-7}	1.88	1.45×10^{-1}	2.06×10^{-2}	1.91×10^{-2}	$4.07 \times 10^{+1}$	2.92
Cassava starch	1 kg	–	1.60×10^{-1}	–	1.21×10^{-3}	1.23×10^{-3}	–	14.23
Electricity	1 kWh	9.39×10^{-8}	3.08×10^{-1}	6.84×10^{-3}	1.64×10^{-3}	5.86×10^{-4}	2.18	0.665

Note: The values are based on the consumption of 1 kWh of electricity in the process, which is calculated from primary energy (100% coal fuel).

Table 3
Kinetic parameters of the process using cassava starch as a carbon source.

Kinetic parameters	Values
μ_{max} (d^{-1})	1.10 ± 0.00
tg (d)	0.60 ± 0.00
X_{max} (kg/m^3)	5.28 ± 99.7
P_X ($kg/m^3/d$)	1.03 ± 17.4
r_s ($kg/m^3/d$)	1.71 ± 42.7
CE (%)	81.0 ± 2.10
$Y_{X/S}$ (kg/kg)	0.60 ± 0.00
HRT (d)	5.00 ± 0.00

μ_{max}: maximum specific growth rate; tg: generation time; X_{max}: maximum cell biomass; P_X: biomass productivity; r_s: average rate of substrate conversion; CE: conversion efficiency; $Y_{X/S}$: substrate yield coefficient; HRT: hydraulic retention time.

to determine its composition. Table 4 shows the representation of carbon mass balance in the heterotrophic bioreactor at a hydraulic retention time (HRT) of 5 days.

Most of the carbon available to the cells (63.9%) was used for biomass production, which is considered as the primary product of the process. In cyanobacterial biomass, carbon is distributed in carbohydrates (mono- and oligosaccharides, starch, cellulose, and other polysaccharides), lipids (free fatty acids, triacylglycerides, and sterols), proteins (including amino acids and peptides), and other minor compounds (chlorophyll, carotenoids, phycobiliproteins, nucleic acids, and inorganic material) [40]. However, the lipid fraction has been more impressive in energy terms due to the physicochemical characteristics of biodiesel obtained from single-cell oils.

In addition to the intracellular compounds of interest, cyanobacteria can also excrete various extracellular polymeric substances into the medium. As shown in Table 4, the cyanobacteria *Phormidium autumnale* converted 0.03% of the organic carbon into these polymers. According

Table 4
Carbon mass balance in the bioreactor.

Carbon balance	Mass (kg)	Percent (%)
Input carbon	$5.60 \times 10^{-3} \pm 0.00$	100.00
Converted carbon	$4.53 \times 10^{-3} \pm 0.01$	81.00
Biomass	$3.58 \times 10^{-3} \pm 3.30$	63.94
VOCs	$4.80 \times 10^{-4} \pm 0.70$	8.56
CO_2	$3.71 \times 10^{-4} \pm 0.20$	6.74
Extracellular polymeric substances	$2.09 \times 10^{-6} \pm 0.00$	0.03
Minerals substrates	$5 \times 10^{-7} \pm 0.00$	0.008
Not identified	$9.59 \times 10^{-5} \pm 0.01$	1.70

As seen previously, the cyanobacteria *P. autumnale* was able to convert 81% (4.53×10^{-3} kg) of the available carbon and, approximately 19% (1.06×10^{-3} kg) remained in the culture medium. The organic carbon (5.60×10^{-3} kg) bioconverted in the system was distributed in biomass (3.58×10^{-3} kg), VOCs (4.80×10^{-4} kg), CO_2 (3.71×10^{-4} kg), extracellular polymeric substances (2.09×10^{-6} kg), and minerals substrates (5×10^{-7} kg). About 1.7% (9.59×10^{-5} kg) of the converted carbon was not identified, which was probably used for cell maintenance, that has been defined as the additional consumption of energy and carbon for functions other than the production of biomass [39].

to Liu et al. [41], among the extracellular polymeric substances produced by microalgae and cyanobacteria can be the exopolysaccharides, extracellular protein, organic acids, extracellular lipids, and extracellular phytohormones.

Although the commercial cultivation of microalgae became increasingly popular, only microalgal biomass is processed to current products, while large amounts of VOCs are unexploited. Considering these aspects, it is known that during respiration in heterotrophic cultures, oxygen is consumed, and CO_2 is produced, and according to the HRT of 5 days, about 3.71×10^{-4} kg of CO_2 was generated (Table 4). This means that 6.74% of the organic carbon was converted to CO_2, which represents the 8.56% bioconversion into VOCs.

In this sense, the carbon mass balance indicates two potential technological routes for the simultaneous production of biofuel/bioenergy in this heterotrophic culture strategy. The first pathway refers to biodiesel production from solid fraction, represented by cyanobacteria biomass. Because they have substantial energetic content, the second pathway refers to the gaseous fraction, where metabolically generated VOCs were exploited.

3.3. Single-cell oil production

For the successful commercial microalgae biodiesel production, quantitative and qualitative aspects of lipid production need to be considered. In this way, the viability of this biofuel from the biomass obtained in the experiments in terms of lipid production and fatty acid profile was evaluated (Table 5).

According to Table 5, biomass presented a lipid content of 17.85%, which resulted in lipid productivity of 0.18 kg/m^3/d. For economic biodiesel production, volumetric lipid productivity is considered as a crucial indicator for the selection of bioreactor engineering operating parameters and, therefore, to take a step forward towards the bioenergy industry from a bioresource [42]. The achieved lipid productivity in this study was substantially higher than the average of 55 microalgae species of 0.05 kg/m^3/d reported by Griffiths and Harrison [43], where in the same review, the higher lipid productivity was 0.164 kg/m^3/d, found in *Neochloris oleoabundans*. In terms of heterotrophic cultivation for lipid/biodiesel production, most studies found on search platforms refers to the use the green microalgae of the genus *Chlorella*, whose productivities varies greatly [44–46]. It is important to note that these researches are based on the use of purified monosaccharides and disaccharides, such as glucose, sucrose, and lactose, or some types of carbohydrates isolated from agricultural materials, which inevitably need additional processing steps, such as hydrolysis and saccharification, impacting process costs. Additionally, the manipulation of cyanobacterial culture conditions can be optimized to enhance lipid biosynthesis.

Table 5
Lipid and fatty acids production in the heterotrophic bioreactor.

Parameter	Values
Lipid content (%)	17.85 ± 0.49
Lipid productivity (kg/m^3/d)	0.18 ± 2.86
Fatty acids (%)	
C11:0	7.20 ± 0.09
C12:0	5.90 ± 0.07
C16:0	16.40 ± 0.16
C16:1	19.80 ± 0.28
C18:1n9c	21.80 ± 0.31
C18:2n6c	3.10 ± 0.05
C18:3n6t	6.50 ± 0.08
C22:0	4.40 ± 0.01
C22:2	7.02 ± 0.11
Minority	8.60 ± 0.13
Saturated (SFA)	37.00 ± 0.61
Monounsaturated (MUFA)	41.90 ± 0.40
Polyunsaturated (PUFA)	21.10 ± 0.09

The single-cell oil composition indicated nine different fatty acids between 11 and 22 carbon chain lengths. The oleic acid was the dominant fatty acid occupying 21.8% in the overall fatty acid pool followed by palmitoleic acid (19.8%), and palmitic acid (16.4%). The oil presented a predominantly monounsaturated profile (41.9%), followed by saturated (37.0%) and polyunsaturated (21.1%) fatty acids (Table 5). These algal fatty acid fractions are decisive in the properties and, consequently, the quality of the biodiesel obtained [47].

3.4. Production and quality of biodiesel

To be considered a complement or substitute traditional petroleum diesel in combustion engines, all biodiesel fuels must fulfill the properties defined in biodiesel standards. A comparison of these properties from cyanobacteria biodiesel, soybean oil, and Brazilian [48], American [49], and European [50] biodiesel standards is shown in Table 6.

The oils with predominantly monounsaturated profiles are the most suitable for biodiesel synthesis [51], such as that obtained from the heterotrophic cultivation of *Phormidium autumnale*. In this sense,

Table 6
Biodiesel properties produced in the heterotrophic bioreactor and its comparison with soybean and international standards.

Properties	*Phormidium autumnale*	Soybean[a]	ANP 255	ASTM 6751	EN 14214
EC (%)	97.0	96.9	–	–	min. 96.5
CN	52.86	49.0	min. 45	min. 47	min. 51
IV (gI_2/100 g)	82.12	128	–	–	max. 120
DU (%)	81.44	143.8	–	–	–
SV	218.01	–	–	–	–
LCSF (%)	8.58	1.6	–	–	–
CFPP (°C)	10.48	−5.0	max. 19	–	–
CP (°C)	5.42	–	–	–	–
APE	52.02	–	–	–	–
BAPE	22.10	–	–	–	–
OS (h)	11.95	1.3	–	min. 3	min. 6
HHV	38.93	–	–	–	–
μ (mm^2/s)	1.22	4.2	–	1.9-6.0	3.5–5.0
ρ (g/cm^3)	0.87	–	–	–	–

EC: ester content; CN: cetane number; IV: iodine value; DU: degree of unsaturation; SV: saponification value; LCSF: long-chain saturated factor; CFPP: cold filter plugging point; CP: cloud point; APE: allylic position equivalents; BAPE: bis-allylic position equivalents; OS: oxidation stability; HHV: higher heating value; μ: kinematic viscosity; ρ: kinematic density.

[a] Knothe (2005); (–) not specified.

according to Table 6, biodiesel produced from cyanobacterial oil has similar characteristics to soybean biodiesel. Besides, it also presented parameters that comply with the requirements established by the American, European, and Brazilian standards. The exception reported here is concerning to kinematic viscosity ($\mu = 1.22$ mm^2/s), which can be increased by using additives or by blending with biodiesel from oilseeds, which are characterized by high viscosity [42]. Blending has been considered as a technically viable method to upgrade the biodiesel quality [52]. These results indicate that this type of aquatic feedstock is conceptually attractive for biodiesel exploration.

3.5. Volatile organic compounds generation

The VOCs from microalgae have long been neglected in the development of production, detection, and recovery methods for valuable secondary metabolites. With the advances in the last years, uncountable structures of these compounds have been identified, and the potential use in many fields is attracting attention [53]. Given these aspects, we evaluate the VOCs generated in heterotrophic cultivation. Fig. 2 shows the VOCs concentration and the cell growth curve as a function of the hydraulic retention time.

According to Fig. 2, the impact is notorious between VOCs concentration and metabolic changes as a function of hydraulic retention time in the heterotrophic bioreactor supplemented with cassava starch. At 5 days of cultivation, the maximum biomass concentration (5.28 kg/m^3) reflected in a maximum VOCs concentration (1.88 kg/m^3). According to Jacob-Lopes et al. [54], VOCs production by microalgae/cyanobacteria increases proportionally during the exponential growth phase and decreases during senescence, representing a classic bell-shaped standard curve. Carbon is the energy source from primary metabolism, considered as the basic building block for VOCs biosynthesis. The availability and type of chemical structure of this substrate directly reflect in the VOCs concentration formed in the bioprocess. This is because the volatile fraction represents most of the carbon converted into microalgae cultures, as suggested by Deprá et al. [21].

Additionally, Table 7 and Fig. 3 show the generated VOCs in 5 days of the experiment. Despite the selective character of HS-SPME, a total of 22 different compounds were identified in the gaseous phase of the bioreactor, which are alcohols (12), aldehydes (5), ketones (4), and hydrocarbon (1). Among the identified chemical classes, (E,E)-2,4-decadienal (0.503 kg/m^3), (E,Z)-2,4-decadienal (0.385 kg/m^3), hexanol (0.166 kg/m^3), and 2-ethyl-1-hexanol (0.150 kg/m^3) were identified as the majority. The different groups of VOCs generated in the experiment have already been found in previous studies and are commonly identified in microalgae and cyanobacteria. Considering the biosynthetic origin, these molecules found in the *Phormidium autumnale* cultivation are derived from different classes, such as terpenoids, fatty acid derivatives, and 2-keto acid pathway products [55,56].

Regarding application, some studies are already being carried out by companies that wish to produce VOCs from biological origin. The VOCs of microalgae and cyanobacteria have been identified as potential advanced biofuels. In general, it is known that some of these microorganisms are capable of producing compounds that are precursors of various fossil fuels, which contain high energy density. Some cyanobacteria are recognized by the biosynthesis of short-chain alcohols or

Table 7
Production and power generation rate of volatile organic compounds produced in the heterotrophic bioreactor.

Peak	LRI[a]	Compound	Production rate[b] (kg/m^3/d)	Energy potential (kJ/kg)	Power generation rate (kJ/m^3/d)
1	1015	4,7-dimethylundecane	0.043	8664	372.5
2	1084	hexanal	0.015	3888	58.3
3	1178	2-heptanone	0.007	4536	31.7
4	1229	3,3-dimethylhexane	0.008	5424	43.3
5	1255	1-pentanol	0.055	3480	191.4
6	1336	2-heptenal	0.018	4296	77.3
7	1346	6-methyl-5-hepten-2-one	0.032	4944	158.2
8	1360	hexanol	0.166	4128	685.2
9	1438	2-octenal	0.059	4944	291.6
10	1451	1-octen-5-ol	0.129	5184	668.7
11	1467	1-heptanol	0.032	4776	152.8
12	1487	2-ethyl-1-hexanol	0.150	5424	813.6
13	1535	2-nonanol	0.004	6072	24.2
14	1553	1-octanol	0.039	5424	211.5
15	1610	2-octen-1-ol	0.046	5184	238.4
16	1612	1-nonanol	0.014	6072	85.0
17	1632	(E,E)-2,4-decadienal	0.503	6000	3018.0
18	1710	(Z)-4-decen-1-ol	0.041	6480	265.7
19	1768	(E,Z)-2,4-decadienal	0.385	6000	2310.0
20	1953	β-ionone	0.019	7704	146.3
21	1976	1-undecanol	0.006	7368	44.2
22	1987	2,4-decadien-1-ol	0.111	6240	692.6
TOTAL			1.880	122.205.00	10,580.50

[a] Linear retention indices in the DB-Wax column.
[b] Mean values based on the VOCs concentration (HRT = 5 days).

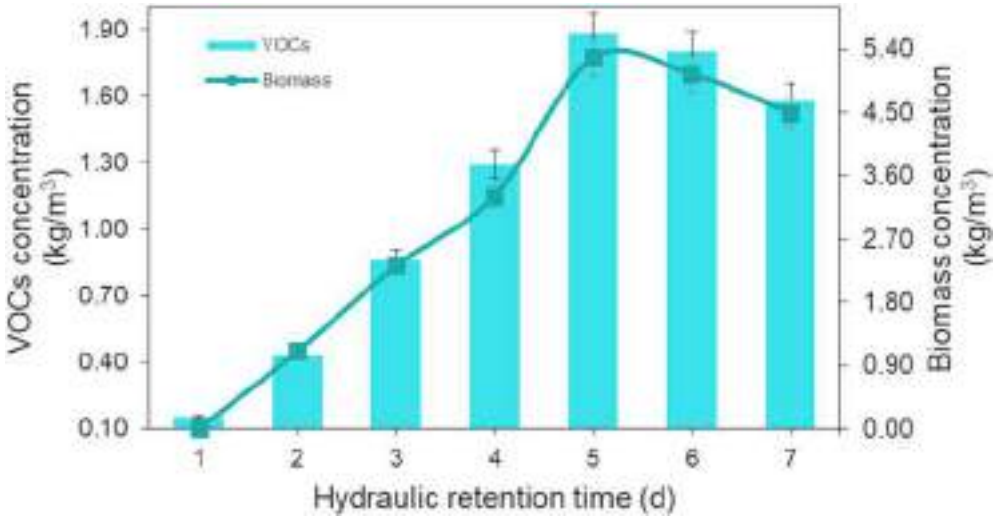


Fig. 2. Concentration of VOCs and biomass in the heterotrophic bioreactor.

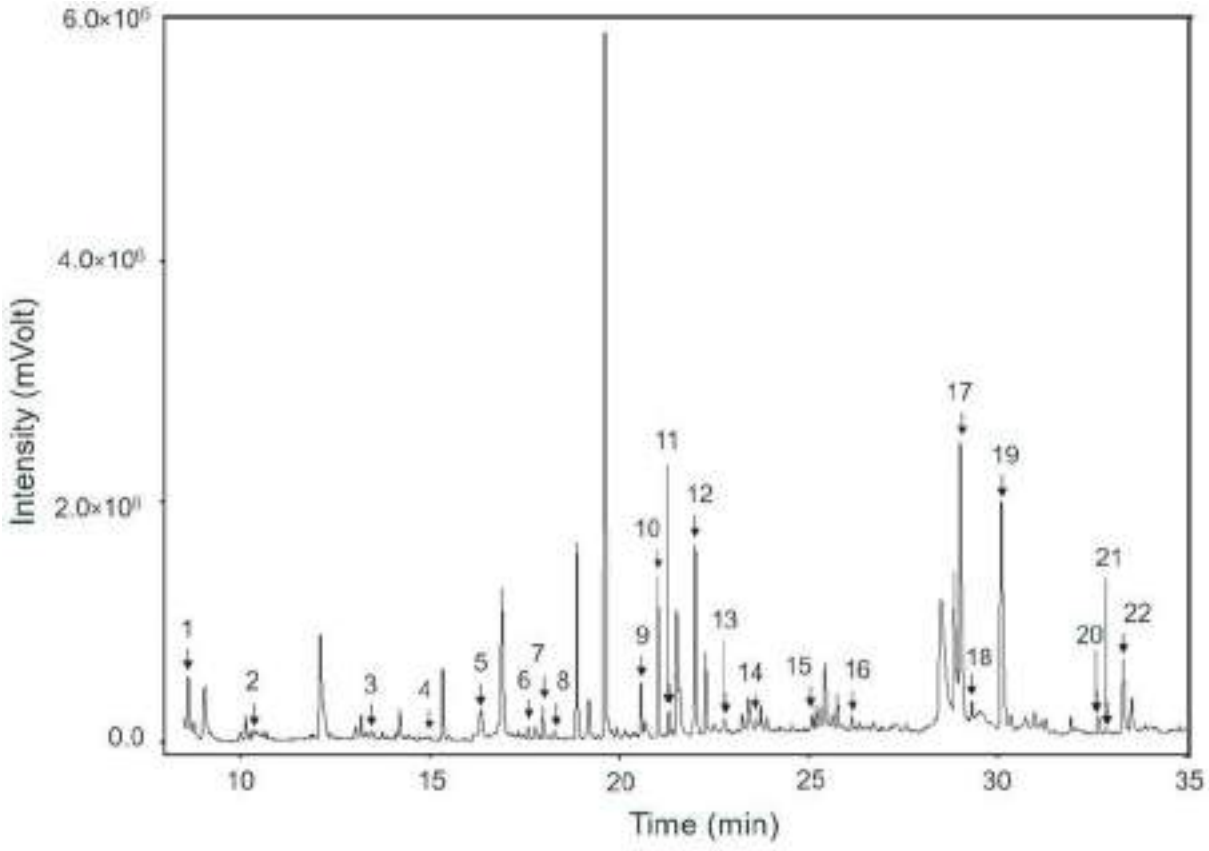


Fig. 3. Chromatogram obtained at the hydraulic retention time of 5 days in the heterotrophic bioreactor. Note: Constituent compounds are listed in Table 7.

higher alcohols, alkanes, alkenes, and aliphatic hydrocarbons, which have desirable combustion properties [57].

Therefore, we estimate the energy potential of the VOCs produced in the heterotrophic bioreactor. The values ranged from 3480 to 8664 kJ/kg, totaling an energy content of 122,205.00 kJ/kg. Besides, the estimated power generation rate was 10,580.50 kJ/m^3/d under these cultivation conditions (Table 7). Comparatively, in the study by Severo et al. [1], in photoautotrophic cultivation, the VOCs produced in the photobioreactor presented energetic potential and volumetric power generation rate of 86.320 and 15,247.78 kJ/m^3/d, respectively. According to these same authors, these energetic values stand out from those of fossil inputs. As an example, the energy potentials of gasoline, liquefied petroleum gas, diesel fuel, and natural gas are estimated to be close to 47,300, 46,100, 44,800 and 39,360 kJ/kg, respectively. Thus, it can be inferred that VOCs produced in microalgae and cyanobacterial cultivations could be an essential renewable energy source if properly separated and collected [19].

3.6. Sustainability metrics and impact indicators

3.6.1. Net energy ration analysis

One of the main bottlenecks for the development of a bioprocess on a commercial scale is related to the difficulty of achieving a positive net energy relationship. This is because the energy demands of bioenergy production systems are much less favorable than that of petroleum fuels. Therefore, higher energy efficiency is a crucial factor when microalgae systems are designed to produce biofuels. In general, the net energy ratio (NER) is applied to estimate the sustainability and efficiency of the system, indicating whether the production process results in energy loss or gain [58]. Thus, the higher the NER, the more efficient the energy system will be. Also, some authors suggest that NER should be greater than 1 [59,60]. However, most scaling processes do not meet this theoretically established condition, indicating that the NER metric should be improved via optimization. Table 8 presents the input/output energies and their respective NER values obtained for all energy vectors in the process.

Indeed, the starting point is to obtain NER >1 in microalgae-based processes. However, in realistic cases, where drying, dewatering, lipid extraction, and esterification steps are considered, the system assessments result in a NER <1, and, therefore, the values changes from 0.05 to 0.1 to 0.5–0.75 [61]. In view of this, it can be observed in this study that, considering the integration of all energy vectors, it is possible to achieve a NER of 0.13, indicating improvements of more than 60% in the energy balance. First, this means that the energy incorporated (total energy demanded together with the limit system) is superior to energy from renewable (renewable) production [62]. Second, it must be taken into account that, although the NER of microalgae processes is still

Table 8
Input/output energies and net energy ratio of the heterotrophic cyanobacteria process.

Vector	Input energy (kJ)	Output energy (kJ)	NER
Defatted biomass	116,710	8720	0.08
Volatile organic compounds	109,080	160	1.4×10^{-3}
Biodiesel	116,730	6630	0.06
Integrated energy vectors	116,730	15,510	0.13

Based on the data reported in Table 8, each vector (represented by the end-products of the process) is characterized by an amount of input and output energy, reflecting in the NER. When analyzing the vectors individually, the defatted biomass represents the majority energy source (61.5%), followed by biodiesel (37%), and then with a slight energetic contribution from VOCs fraction (1.7%).

disadvantageous compared to fossil energy options, it can be substantially improved by increasing the output energy or decreasing the input energy. Non-renewable energies, those understood as long-term technologies with no potential for improvement, generally perform slightly better than microalgae systems in energy. These, in turn, have enormous potential for additional updates, as they are constantly developing.

This can be proven from the data of many studies of integrated processes that envisions to achieve this purpose, as reported by Severo et al. [20], with a NER of 0.71. Besides, research shows wide variability in results for analogous microalgal processes. Values of NER can range from less than 0.0016 to greater than 0.15, in the biodiesel case, and the optimization of the deficit of renewable energy output has been suggested [63,64]. It is worth mentioning that when comparing with other traditional bioenergy sources, such as soybean biodiesel, the values are generally higher. Evidently, the NER obtained in this study is not ideal. But this comparison shows that there is a possibility that microalgae/cyanobacteria bioenergies may be something viable in the future. This if some joint considerations are made. In this case, for biomass, the productivity upgrading, while for biodiesel, the gain per unit of land area concerning traditional land crops and higher lipid yields; and then, in the case of VOCs, design of robust recovery techniques for bioreactors exhaust gases. It is also worth noting that the high NER values found in the literature are probably the result of far less conservative estimates due to the biomass productivity, exclusion of significant inputs, as well as the disregard for the energy losses of the input conversion in the systems. Therefore, we believe that our more conservative values of lipid and biomass production, as well as the derivation of energy expenditures from the system, result in a more realistic NER for the study under evaluation.

3.6.2. Environmental impact assessment

Beyond energy balance criterion, the process proposed here has subjected to assessment of environmental performance. Fig. 4 illustrates the scores obtained for the eight mid-points impact categories.

According to Fig. 4, under the assessment of the characterized environmental results corresponding to the demands for nutrients, chemical substances as well as the energy required for the process, the categories of ecotoxicity (ECO), energy resource (ER), and global warming potential (GWP) presented values in the order of 430.86 CTUe, 230.04 MJ, and 171.05 kg CO_2 eq. After that, the impacts of the other categories were: photochemical oxidation potential (SMOG) of 1.33 kg O_3 eq, water footprint (WF) of 1.08 m^3, acidification potential (AP) of 0.44 kg SO_2 eq and eutrophication potential (EP) of 0.13 kg N eq. The ozone depletion potential (ODP) of 1.83×10^{-5} kg CFC-11 eq almost not impacts the environment.

Still, under more detailed investigation, the results indicate that 98% (425.23 CTUe) of the impacts associated with ECO category are attributed to the emission of toxic substances resulting from electricity and steam that will affect humans, terrestrial, freshwater and marine toxicity. On the other hand, chemical substances represent values below 2% (4.98 CTUe). Similarly, the electricity demand depicted about 56% (129.71 MJ) of the total impacts referring to the ER category. However, the need for nutrients proved to be an expressive result among the complete impacts of this category, resulting in values in the order of 100.29 MJ (~43%). Moreover, under the same logic of discussion, the values reported for GWP express that about 64% (109.79 kg CO_2 eq) of the impacts are related to the activities of obtaining chemical substances, that is, methanol, chloroform and potassium hydroxide, used for obtaining microalgal biodiesel. Thus, it is estimated that approximately 35% (~60 kg CO_2 eq) of the burdens are attributed to energy generation, and only a portion less than 1% is attributed to the nutrients required by the microorganism's cultivation stage.

Comparatively, the results obtained here are consistent with those of other microalgae energetic processes [65]. Studies conducted by Santos et al. [66] presented environmental impacts for the production of 1 kg of microalgal biodiesel in an integrated system for the wastewater treatment of 14.28×10^3 CO_2 eq for GWP and 44×10^3 MJ for ER. In contrast, according to Hou et al. [67], the microalgae biodiesel production may have a lower environmental impact for the GWP and ODP categories, for example, when compared to soybean, jatropha, and fossil diesel. Still, the scenarios shown by these same authors corroborate the question mentioned above about the optimization of microalgal technologies. It is possible to improve further the performance of specific categories, such as WF, by recycling the harvesting water, for example. The integration of surplus heat and mass are also options that would have a positive influence on other sustainability metrics.

At this point, additional criteria need to be adopted. In this particular study, the hottest point of all the sustainability metrics analyzed comes from the consumption of fossil energy in the form of electricity from the operational steps, as well as the chemical substances used. An alternative to this key driver needs further investigation concerning the change in the world energy matrix, which is still dominated by coal. Its displacement by cleaner sources would bring reduced environmental impacts on several levels.

4. Conclusion

The study evaluated the dual production of bioenergy in a heterotrophic bioreactor, where the process performance parameters, carbon mass balance, biofuel quality, and sustainability metrics and impact indicators were established. The strategy proposed in this research demonstrates that the microalgae-based energy processes and products can contribute to the advancement of technological and scientific knowledge towards the projection, optimization, and management of

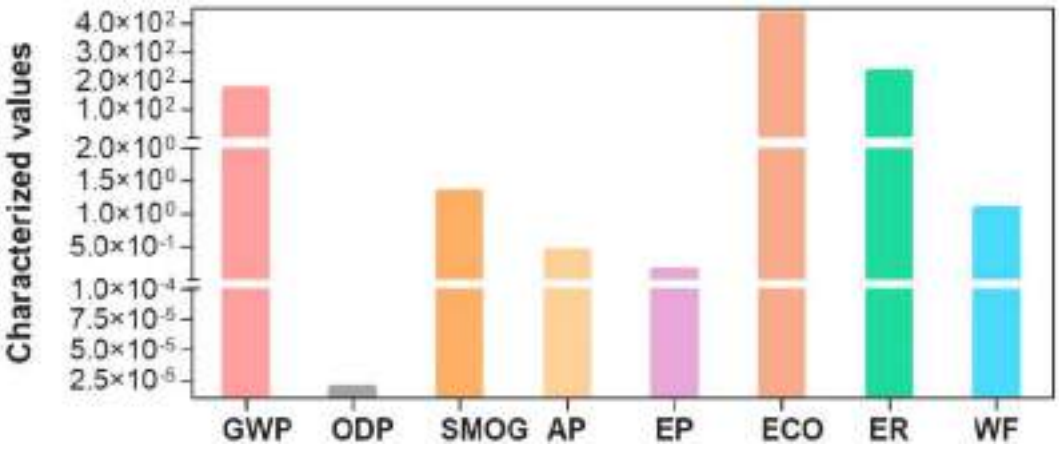


Fig. 4. Environmental impact categories of the heterotrophic cyanobacteria cultivation per functional unit of 1 m^3 of the bioreactor, operating for 5 days.

systems on a commercial scale in the future, meeting environmental needs.

Acknowledgement

The authors are grateful to the Coordination for the Improvement of Higher Education Personnel (CAPES) for the financial support.

References

[1] M.C. Deprá, A.M. dos Santos, I.A. Severo, A.B. Santos, L.Q. Zepka, Q. Jacob-Lopes, Microalgal biorefineries for bioenergy production: can we move from concept to industrial reality? Bioen. Res. 11 (2018) 727–747.
[2] I.A. Severo, S.F. Siqueira, M.C. Deprá, M.M. Maroneze, L.Q. Zepka, E. Jacob-Lopes, Biodiesel facilities: what can we address to make biorefineries commercially competitive? Renew. Sustain. Energy Rev. 112 (2019) 686–705.
[3] M.M. Maroneze, S. F Siqueira, R.G. Vendruscolo, R. Wagner, C.R. de Menezes, L. Q. Zepka, E. Jacob-Lopes, The role of photoperiods on photobioreactors – a potential strategy to reduce costs, Biores. Technol. 219 (2016) 493–499.
[4] M.B. Fagundes, R.B. Falk, M.M.X. Facchi, R.G. Vendruscolo, M.M. Maroneze, L. Q. Zepka, E. Jacob-Lopes, R. Wagner, Insights in cyanobacteria lipidomics: a sterols characterization from Phormidium autumnale biomass in heterotrophic cultivation, Food Res. Int. 119 (2019) 777–784.
[5] Z. Jia, Y. Liu, M. Daroch, S. Geng, J.J. Cheng, Screening, growth medium optimisation and heterotrophic cultivation of microalgae for biodiesel production, Appl. Biochem. Biotechnol. 173 (2014) 1667–1679.
[6] L. Soto-Sierra, P. Stoykova, Z.L. Nikolov, Extraction and fractionation of microalgae-based protein products, Algal Res. 36 (2018) 175–192.
[7] S.-K. Wang, X. Wang, Y.-T. Tian, H.-H. Tao, X.-S. Sun, Direct utilization of starch for heterotrophic cultivation of Chlorella pyrenoidosa by co-culture with immobilized Saccharomycopsis fibuligera, Algal Res. 33 (2018) 406–411.
[8] E.C. Francisco, T.T. Franco, R. Wagner, E. Jacob-Lopes, Assessment of different carbohydrates as exogenous carbon source in cultivation of cyanobacteria, Bioproc. Biosyst. Eng. 37 (2014) 1497–1505.
[9] A.M. Santos, A. M Santos, R.B. Sartori, K.R. Vieira, L.Q. Zepka, M.I. Queiroz, E. Jacob-Lopes, Heterotrophic cultivation of cyanobacteria: study of effect of exogenous sources of organic carbon, absolute amount of nutrients and stirring speed on biomass and lipid productivity, Front. Bioeng. Biotech. 5 (2017) 1–7.
[10] R. Katiyar, B.R. Gurjar, R. K Bharti, A. Kumar, S. Biswas, V. Pruthi, Heterotrophic cultivation of microalgae in photobioreactor using low cost crude glycerol for enhanced biodiesel production, Renew. Energy 113 (2017) 1359–1365.
[11] M.A. Islam, K. Heimann, R.J. Brown, Microalgae biodiesel: current status and future needs for engine performance and emissions, Renew. Sustain. Energy Rev. 79 (2017) 1160–1170.
[12] M. Song, H. Pei, The growth and lipid accumulation of Scenedesmus quadricauda during batch mixotrophic/heterotrophic cultivation using xylose as a carbon source, Bioresour. Technol. 263 (2018) 525–531.
[13] E. Jacob-Lopes, M.M. Maroneze, M.I. Queiroz, L.Q. Zepka, Handbook of Microalgae-Based Processes and Products, Fundamentals and Advances in Energy, Food, Feed, Fertilizer, and Bioactive Compounds, first ed., Academic Press, Elsevier, Massachusetts, 2020.
[14] E. Stephens, I.L. Ross, J.H. Mussgnug, L.D. Wagner, M.A. Borowitzka, C. Posten, O. Kruse, B. Hankamer, Future prospects of microalgal biofuel production systems, Trends Plant Sci. 15 (2010) 554–564.
[15] E. Stephens, I.L. Ross, Z. King, J.H. Mussgnug, O. Kruse, C. Posten, M. A. Borowitzka, B. Hankamer, An economic and technical evaluation of microalgal biofuels, Nat. Biotechnol. 28 (2010) 126–128.
[16] IEA, International Energy Agency, State of technology review – algae bioenergy, an IEA bioenergy inter-task strategic project. Published by IEA bioenergy: task 39: January 2017, Available at: http://www.ieabioenergy.com/wp-content/uploads/2017/01/IEA-Bioenergy-Algae-report-update-20170114.pdf.
[17] E. Jacob-Lopes, T.T. Franco, From oil refinery to microalgal biorefinery, J. CO2 Util. 2 (2013) 1–7.
[18] A.B. Santos, A.F. Fernandes, R. Wagner, E. Jacob-Lopes, L.Q. Zepka, Biogeneration of volatile organic compounds produced by Phormidium autumnale in heterotrophic bioreactor, J. Appl. Phycol. 28 (2016) 1561.
[19] K.R. Vieira, P.N. Pinheiro, A.B. Santos, A.J. Cichoski, C.R. de Menezes, R. Wagner, L.Q. Zepka, E. Jacob-Lopes, The role of microalgae-based systems in the dynamics of odors compounds in the meat processing industry, Desalin. Water Treat. 150 (2019) 282–292.
[20] I.A. Severo, M.C. Deprá, R.R. Dias, J.S. Barin, C. R de Menezes, R. Wagner, L. Q. Zepka, E. Jacob-Lopes, Bio-combustion of petroleum coke: the process integration with photobioreactors. Part II – sustainability metrics and bioeconomy, Chem. Eng. Sci. 213 (2020), 115412.
[21] M. C Deprá, R.R. Dias, I.A. Severo, C.R. de Menezes, L.Q. Zepka, E. Jacob-Lopes, Carbon dioxide capture and use in photobioreactors: the role of the carbon dioxide loads in the carbon footprint, Bioresour. Technol. 314 (2020) 123745.
[22] E. Jacob-Lopes, I.A. Severo, R.S. Bizello, J.S. Barin, C.R. de Menezes, A.J. Cichoski, Process and System for Re-using Carbon Dioxide Transformed by Photosynthesis into Oxygen and Hydrocarbons Used in an Integrated Manner to Increase the Thermal Efficiency of Combustion Systems, Patent, 2017. WO2017/112984 A1.
[23] I.A. Severo, M.C. Deprá, J.S. Barin, R. Wagner, C.R. de Menezes, L.Q. Zepka, E. Jacob-Lopes, Bio-combustion of petroleum coke: the process integration with photobioreactors, Chem. Eng. Sci. 177 (2018) 422.
[24] M.C. Deprá, L.G. Mérida, C.R. de Menezes, L.Q. Zepka, E. Jacob-Lopes, A new hybrid photobioreactor design for microalgae culture, Chem. Eng. Res. Des. 144 (2019) 1–10.
[25] J. Buchholz, M. Graf, B. Blombach, R. Takors, Improving the carbon balance of fermentations by total carbon analyses, Biochem. Eng. J. 90 (2014) 162–169.
[26] B. Corona, L. Shen, D. Reike, J.R. Carreón, E. Worrell, Towards sustainable development through the circular economy—a review and critical assessment on current circularity metrics, Resour. Conserv. Recycl. 151 (2019), 104498.
[27] R. Rippka, J. Deruelles, J.B. Waterbury, M. Herdman, R.Y. Stanier, Generic assignments, strain histories and properties of pure cultures of cyanobacteria, J. Gen. Microbiol. 111 (1979) 1–61.
[28] AOAC. Official, Methods of Analysis of AOAC International, AOAC International, Gaithersburg, 2000.
[29] B.K. Watt, A.L. Merrill, Composition of foods. Agriculture Handbook No 8, Dept. of Agriculture, Washington, 1963.
[30] T. Acree, H. Arn, H, Flavornet and human odor space, Available at: http://www.flavornet.org, 2020. (Accessed 30 January 2020).
[31] E.G. Bligh, J.W. Dyer, A rapid method of total lipid extraction and purification, Can. J. Biochem. Physiol. 37 (1959) 911–917.
[32] L. Hartman, R.C.A. Lago, Rapid preparation of fatty acids methyl esters, Lab. Pract. 22 (1973) 475–476.
[33] A.F. Talebi, M. Tabatabaei, Y. Chisti, Biodiesel Analyzer: a user-friendly software for predicting the properties of prospective biodiesel, Biofuel Res. J. 5 (2014) 55–57.
[34] O. Jorquera, A. Kiperstok, E.A. Sales, M. Embirucu, M.L. Ghirardi, Comparative energy life-cycle analyses of microalgal biomass production in open ponds and photobioreactors, Bioresour. Technol. 101 (2010) 1406–1413.
[35] ISO. International Organization for Standardization, ISO 14040:2006(E) Environmental Management – Life Cycle Assessment – Principles and Framework, 2016.
[36] E.C. Francisco, T.T. Franco, L.Q. Zepka, E. Jacob-Lopes, From waste-to-energy: the process integration and intensification for bulk oil and biodiesel production by microalgae, J. Environ. Chem. Eng. 3 (2015) 482–487.
[37] X.-B. Tan, X.-C. Zhao, L.-B. Yang, Strategies for enhanced biomass and lipid production by Chlorella pyrenoidosa culture in starch processing wastewater, J. Clean. Prod. 236 (2019), 117671.
[38] A.M. Peres, R.R. Pires, R.L. Oréfice, Evaluation of the effect of reprocessing on the structure and properties of low density polyethylene/thermoplastic starch blends, Carbohydr. Polym. 136 (2016) 210–215.
[39] S.J. Pirt, The maintenance energy of bacteria in growing cultures, Proc. Roy. Soc. Lond. B. 163 (1965) 224–231.
[40] M.I. Queiroz, J.G. Vieira, M.M. Maroneze, E. Jacob-Lopes, M.M. Maroneze, M. I. Queiroz, L.Q. Zepka (Eds.), Morphophysiological, Structural, and Metabolic Aspects of Microalgae, Academic Press, 2020, p. 25.
[41] L. Liu, G. Pohnert, D. Wei, Extracellular metabolites from industrial microalgae and their biotechnological potential, Mar. Drugs 14 (2016) 191.
[42] M.M. Maroneze, M.C. Deprá, L.Q. Zepka, E. Jacob-Lopes, Artificial lighting strategies in photobioreactors for bioenergy production by Scenedesmus obliquus CPCC05, SN Appl. Sci. 1 (2019) 1695.
[43] M.J. Griffiths, S.R.L. Harrison, Lipid productivity as a key characteristic for choosing algal species for biodiesel production, J. Appl. Phycol. 21 (2009) 493–507.
[44] C. Gao, Y. Zhai, Y. Ding, Q. Wu, Application of sweet sorghum for biodiesel production by heterotrophic microalga Chlorella protothecoides, Appl. Energy 87 (2010) 756–761.
[45] H. Rismani-Yazdi, K.H. Hampel, C.D. Lane, B.A. Kessler, N.M. White, K.M. Moats, F.C. Thomas Allnutt, High-productivity lipid production using mixed trophic state cultivation of Auxenochlorella (Chlorella) protothecoides, Bioproc. Biosyst. Eng. 38 (2015) 639–650.
[46] M.H. Morowvat, Y. Ghasemi, Maximizing biomass and lipid production in heterotrophic culture of Chlorella vulgaris: techno-economic assessment, Recent Pat. Food, Nutr. Agric. 10 (2018) 115–123.
[47] G. Knothe, L.F. Razon, Biodiesel fuels, Prog. Energy Combust. Sci. 58 (2017) 36–59.
[48] ANP. National Petroleum Agency, ANP 255 - Provisional Brazilian Biodiesel Standard, ANP, Brasília, DF, Brazil, 2003.
[49] ASTM. American Society for Testing and Materials, ASTM 6751 - Standard Specification for Biodiesel Fuel (B100) Blend Stock for Distillate Fuels, ASTM, West Conshohocken, PA, USA, 2002.
[50] EN 14214. European Standard, Automotive Fuels – Fatty Acid Methyl Esters (FAME) for Diesel Engine - Requirements and Test Methods, Pilsen, Czech Republic, 2003.
[51] G. Knothe, Dependence of biodiesel fuel properties on the structure of fatty acid alkyl esters, Fuel Process. Technol. 86 (2005) 1059–1070.
[52] U. Rajak, P. Nashine, T.N. Verma, Effect of spirulina microalgae biodiesel enriched with diesel fuel on performance and emission characteristics of CI engine, Fuel 268 (2020), 117305.
[53] I.A. Severo, P.N. Pinheiro, K.V. Veira, L.Q. Zepka, E. Jacob-Lopes, in: A. Inamuddin, M. Abdullah, E. Lichtfouse (Eds.), Biological Conversion of Carbon Dioxide into Volatile Organic Compounds, Springer International Publishing, Switzerland, 2020, p. 45.
[54] E. Jacob-Lopes, C.H.G. Scoparo, M.I. Queiroz, T.T. Franco, Biotransformations of carbon dioxide in photobioreactors, Energy Convers. Manag. 51 (2010) 894–900.

[55] E. Eroglu, A. Melis, Extracellular terpenoid hydrocarbon extraction and quantitation from the green microalgae Botryococcus braunii var, Showa, Biores. Technol. 101 (2010) 2359–2366.
[56] I. Milovanović, A. Misan, J. Simeunovic, D. Kovac, D. Jambrec, A. Mandic, Determination of volatile organic compounds in selected strains of cyanobacteria, J. Chem. (2015), 969542.
[57] N.S. Lau, M. Matsui, A.A.A. Abdullah, Cyanobacteria: photoautotrophic microbial factories for the sustainable synthesis of industrial products, BioMed Res. Int. (2015), 754934.
[58] M.A.A. Farid, A.M. Roslan, M.A. Hassan, M.Y. Hasan, M.R. Othman, Y. Shirai, Net energy and techno-economic assessment of biodiesel production from waste cooking oil using a semi-industrial plant: a Malaysia perspective, Renew. Sustain. Energy Rev. 39 (2020), 100700.
[59] C.H. Sun, Q. Fu, Q. Liao, A. Xia, Y. Huang, X. Zhu, H.X. Chang, Life-cycle assessment of biofuel production from microalgae via various bioenergy conversion systems, Energy 171 (2019) 1033–1045.
[60] F. D Mayer, M. Brondani, M.C.V. Carrillo, R. Hoffmann, E.E.S. Lora, Revisiting energy efficiency, renewability, and sustainability indicators in biofuels life cycle: analysis and standardization proposal, J. Clean. Prod. 252 (2020), 119850.
[61] A. Yousuf, in: A. Yousuf (Ed.), Microalgae Cultivation for Biofuels Production. Chapter 1: Fundamentals of Microalgae Cultivation, Academic Press, Elsevier, 2020, pp. 1–9.
[62] R. Slade, A. Bauen, Micro-algae cultivation for biofuels: cost, energy balance, environmental impacts and future prospects, Biomass Bioenergy 53 (2013) 29–38.
[63] K. Sander, G.S. Murthy, Life cycle analysis of algae biodiesel, Int. J. Life Cycle Assess. 15 (2010) 704–714.
[64] S. Nagappan, S. Devendran, P.C. Tsai, S. Dinakaran, H.U. Dahms, V.K. Ponnusamy, Passive cell disruption lipid extraction methods of microalgae for biofuel production–A review, Fuel 252 (2019) 699–709.
[65] S.C. Togarcheti, M.K. Mediboyina, V.S. Chauhan, S. Mukherji, S. Ravi, S. N. Mudliar, Life cycle assessment of microalgae based biodiesel production to evaluate the impact of biomass productivity and energy source, Resour. Conserv. Recycl. 122 (2017) 286–294.
[66] J. Hou, P. Zhang, X. Yuan, Y. Zheng, Life cycle assessment of biodiesel from soybean, jatropha and microalgae in China conditions, Renew. Sustain. Energy Rev. 15 (2011) 5081–5091.
[67] A.M. dos Santos, M.C. Deprá, A.J. Cichoski, L.Q. Zepka, E. Jacob-Lopes, Sustainability metrics on microalgae-based wastewater treatment system, Desalin. Water Treat. 185 (2020) 51–61.

Algal Research 51 (2020) 102056

Contents lists available at ScienceDirect

Algal Research

journal homepage: www.elsevier.com/locate/algal

Environmental impacts on commercial microalgae-based products: Sustainability metrics and indicators

Mariany C. Deprá, Ihana A. Severo, Aline M. dos Santos, Leila Q. Zepka, Eduardo Jacob-Lopes*

Bioprocess Intensification Group, Federal University of Santa Maria, UFSM, Roraima Avenue 1000, 97105-900 Santo Maria, RS, Brazil

ARTICLE INFO

Keywords:
Algae
Single-cell protein
Single-cell oil
Pigments
Life-cycle assessment
Beyond sustainability

ABSTRACT

Herein, the environmental impact of commercial microalgae-based products was assessed. The whole dried biomass production by *Chlorella vulgaris* and *Arthrospira platensis* were evaluated under different cultivation configurations. Besides, pigments such as β-carotene, astaxanthin, and phycocyanin, by *Dunaliella salina*, *Haematococcus pluvialis*, and *Arthrospira platensis*, respectively, were also subjected to environmental analysis, as well as docosahexaenoic (DHA) and eicosapentaenoic (EPA) acids by *Crypthecodinium cohnii*, *Nitzschia laevis*, and *Nannochloropsis oculata*. These products were estimated by midpoint indicators through the nine impact categories and subsequently submitted to the normalization stage. Also, environmental critical points of the process were identified and discussed, focusing on the combined operations of dehydration and drying of biomass, as well as the central role of the energy footprint and the challenges of the transition from fossil energy to renewable matrices. Among the results found for whole dried biomass, the parameters that most influence the burdens are directly related to the energy requirements of the downstream processes. In intracellular microalgal products, the extraction stage and yield of the compounds are factors that most affect environmental performance. Additionally, this work provides quantitative numbers of sustainability indicators for microalgae projects considering the current stage of the technology. Therefore, the results found in this study are the first step found in the literature to identify environmental improvements in the consolidated biotechnological routes of microalgae.

1. Introduction

Industrial manufacturing is the core of the world economy. However, the significance of a strong industry has become responsible for major environmental damage and growing social rejection [1]. In this context, visions of sustainable strategies emerge through biotechnological transformation to represent a process of change that applies to the entire industrial chain. This global trend adopts strategies that aim to reduce dependence on fossil fuel resources beyond designing safe foods, significantly reducing the environmental effects on the ecosystem. Generally, these objectives are designed to be achieved by substantially increasing the use of biomass [2].

Based on this understanding, microalgal products can be considered one of the biobased economy frontiers [3]. It is estimated that the industrial relevance of microalgae as production systems for non-food raw materials, as well as a wide range of valuable food bioproducts, is constantly increasing [4]. In recent years, the global cultivation of microalgae has been characterized by being a very dynamic sector, with exponential entrepreneurial growth, corresponding to around 150 new companies each year. As a result, this market represents an annual global expansion of over 3% per year [5]. However, despite projections of significant growth in the coming decades, the market today is still modest [6]. These barriers are attributed to current technological limitations since they appear not to be sufficient to achieve the goals of economic viability and present questionable sustainable resources [7].

Despite the refutable character and the numerous challenges to be overcome, microalgae products are undeniably well established in the market. Historically, given the increased demand for energy resources and an energy crisis potential, microalgae have become pioneers in prospecting for fatty acids production as a feedstock for the biofuels generation [8,9]. Yet, aware of the richness of polyunsaturated fatty acids (PUFAs), the exploitation of essential fatty acids such as docosahexaenoic acid (DHA) and eicosapentaenoic acid (EPA), commonly found in species such as *Crypthecodinium cohnii*, *Nitzschia laevis*, and *Nannochloropsis oculata*, received the attention of manufacturers as a food supplement [10]. In parallel, the increased awareness of the harmful effects of synthetic or chemical dyes and preference for the use of natural products, microalgae such as *Dunaliella salina* and

* Corresponding author.
E-mail address: ejacoblopes@gmail.com (E. Jacob-Lopes).

https://doi.org/10.1016/j.algal.2020.102056
Received 1 May 2020; Received in revised form 11 August 2020; Accepted 12 August 2020
2211-9264/ © 2020 Elsevier B.V. All rights reserved.

Haematococcus pluvialis have gained prominence in the microalgal market [11]. This is because these microorganisms produce carotenoids such as β-carotene and astaxanthin, which have been explored as dietary supplements in the food industry, applications in nutraceuticals and pharmaceuticals, as well as a source of pigmentation in aquaculture. Likewise, natural protein dyes as phycocyanin from the cyanobacterium *Arthrospira platensis*, have been used as a food color and in cosmetic segments. Besides, its application also covers the techniques of immunofluorescence and the labeling of antibodies [12]. Moreover, *Chlorella vulgaris* received prominence recently for its high protein functionality, being recognized by a promising niche as an ingredient to innovate future foods.

However, although it is an apparent attractive advantage, only a limited number of species have been successfully found on the market. In view of this, the uncertainties of microalgae-based processes and products need to be overcome to stimulate investments in these segments [13]. Besides, the real success of any devised technology must be able to answer questions such as: is technology really feasible? Or even, if the new process proposal is qualified to emit lower environmental impacts than conventional processes? Therefore, beyond being possible, achieve to techno-economic requirements, any future technology should undergo a rigorous assessment of its environmental potential in order to anticipate commercial viability [14].

Associated with these aspects, it is necessary to constantly search to develop optimization research and increase the efficiency of processes and products based on microalgae. This is because robust production on an industrial scale usually involves some downstream processing that accounts for about 60% of the total cost [15]. Besides, the determination of optimal parameters is essential to expand the process and promote the efficient integration of large-scale steps upstream and downstream [16,17]. Thus, if sustainable and economic technologies based on microalgae can be developed, their prospective advantages can be confirmed and will support the development of policies for investments in research and development in the near future [13,18].

At the same time, as microalgae processes require a lot of energy, the need for clean, sustainable, economically effective and efficient energy production systems has become a significant concern in the past century. And, nowadays, it remains a challenging global goal [19]. Therefore, to properly align strategic and scientific initiatives, government incentives and industrial managers need a more detailed environmental analysis of the real potential of renewable energy matrices, in order to identify the demands and fill research gaps, to assist the strengthening the biotechnological industrial transition on a sustainable path [20].

Given these numerous barriers, life cycle assessment (LCA) emerges as a projective analysis tool on a systematic scale to assess the overall sustainability of a process [21]. Its methodology allows us to evaluate the possible impacts associated with a process or product, compile inventories of relevant inputs, and convert the demands into reasonable environmental charges related to sustainable metrics [22]. Recent applications of LCA in microalgae generally address the environmental aspects of products mainly for energy purposes [23] as is the case with the study by Severo et al. [24], where an integrated bio-combustion process of petroleum coke with photobioreactors and the energy valuation of volatile organic compounds was evaluated. Other authors have used the tool to assess predictive routes for potential production techniques or microalgae extraction lipid recovery for biofuel production [25]. Still, studies by Santos et al. [26] evaluated a large-scale simulated and integrated process for agro-industrial wastewater treatment using microalgae heterotrophic bioreactors. However, many of these efforts fail to assess the possible impacts related to the exploitation of microalgae products from technological routes already commercially consolidated [27]. Besides, all of these studies present hypothetical scenarios, none of which is commercially viable to date.

Against this background, since microalgae are at the spotlight of attention in global market, the novelty of this study resides in the in-depth assessment of the sustainability indicators and metrics of the main sale microalgae products (whole dried biomass, β-carotene, astaxanthin, phycocyanin, docosahexaenoic acid, and eicosapentaenoic acid). In this study, once the limitation points of the processes and products were identified, four different scenarios of the combined methods of dehydration and drying were compared to test energy consumption. Besides, a critical assessment of the effect of the energy matrix was carried out to investigate the impacts on environmental performance. In the last part of the article, aspects were explored beyond sustainability and how the high revenue from the main microalgae products can offset the operational and capital costs of the process. Through this approach, guidelines and recommendations of the current environmental scenario of the microalgae products industry can be provided a knowledge trade-off to assist engineers and decision-makers in the development and improvement of existing technologies and production processes. Therefore, this is the first article that uses theoretical and experimental data to evaluate the sustainable indicators of technological routes already microalgae products consolidated.

2. Material and methods

The general framework for LCA was determined according to the International Organization for Standardization (ISO) 14000 series [28]. The applied methodology of LCA was defined based on four phases: (I) goal and scope definition, (II) inventory analysis, (III) impact assessment, and (IV) interpretation. The procedures considered in each step are detailed below.

2.1. Goals and scope definition

The objective of the study was to evaluate the main commercial products based on microalgae, which are (i) whole dried biomass, (ii) pigments, and (iii) polyunsaturated fatty acids. The scenarios evaluated consist of commercially consolidated biotechnological routes. It should be noted that the inclusion of more than one route for the same product was considered, in order to recognize its wide biotechnological versatility. Also, data collection for theoretical-experimental analysis was based on process data consolidated by classic references in the literature.

2.2. Functional unit and system boundaries

The present study considered three main functional units. The first functional unit covers the production of 1 kg whole dried biomass for *Chlorella vulgaris* in the raceway pond and a tubular photobioreactor, and *Arthrospira platensis* in the raceway pond. The second functional unit considered 1 kg of β-carotene, astaxanthin, and phycocyanin by *Dunaliella salina*, *Haematococcus pluvialis*, and *Arthrospira platensis*, respectively. And, finally, the third functional unit was established of 1 kg of DHA by *Cryptthecodinium cohnii* in heterotrophic cultivation, 1 kg of EPA by *Nitzschia laevis* in heterotrophic cultivation, and 1 kg of EPA by *Nannochloropsis oculata* in autotrophic cultivation.

System boundaries were defined from the cradle-to-gate life cycle, i.e., it is an assessment of a partial product life cycle, from resource extraction (cradle) to the factory gate (before being transported to the consumer). Additionally, it is essential to note that impacts about resource obtention of products such as electricity and nutrients were included in this analysis. On the other hand, the impacts associated with the results related to infrastructure and maintenance of equipment were disregarded, being only accounted for resources into their operations.

Moreover, physical sterilization was established for fermenters. In contrast, chemical sterilization (sodium hypochlorite solution) was considered for closed photobioreactors, on account of the difficulty of obtaining sterile physical conditions in the high workloads. Thus, the general layout of all the technical features of the case studies analyzed is presented in Fig. 1.

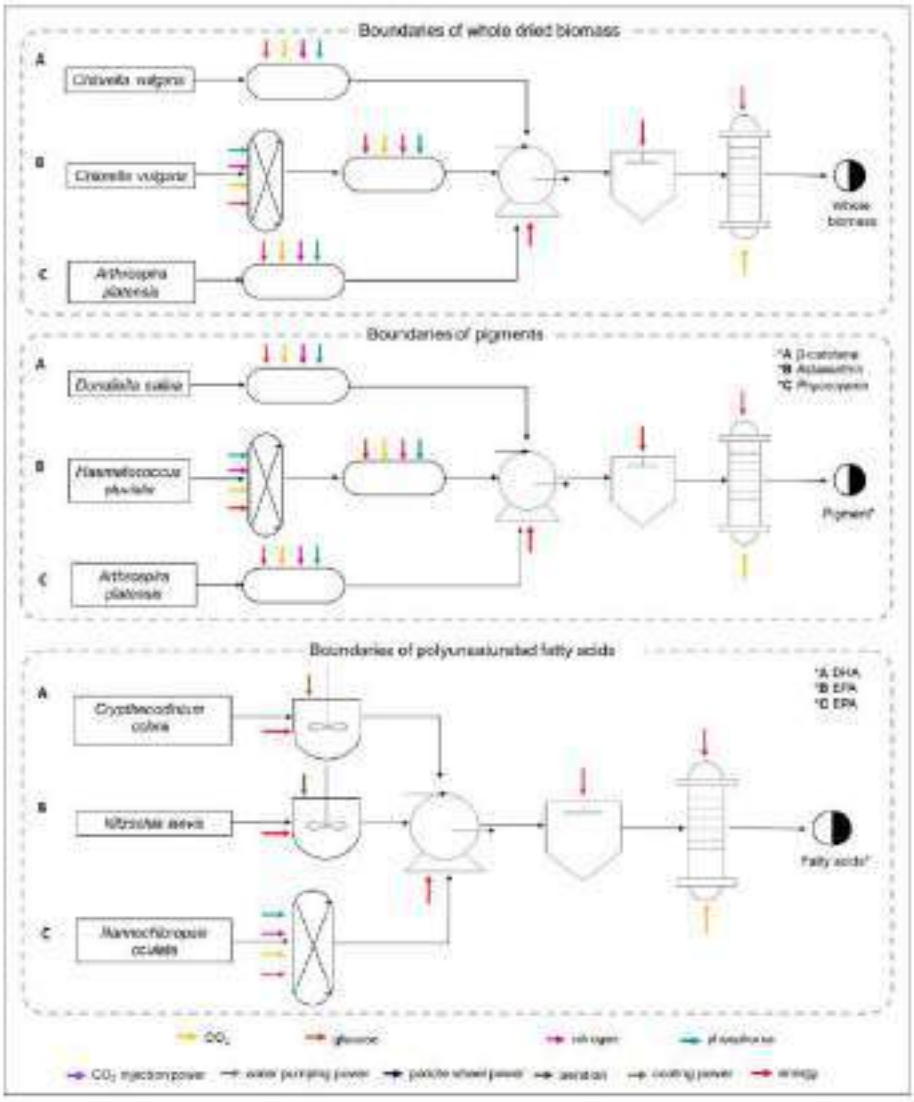


Fig. 1. Systems boundaries for the evaluation of the microalgae-based products. DHA: Docosahexaenoic; Eicosapentaenoic, EPA.

2.3. Life cycle inventory (LCI)

Life cycle inventory data were obtained from the literature. The input and output conditions of the processes for obtaining whole dried biomass, pigments, and polyunsaturated fatty acids are shown directly in Tables 1, 2, and 3, respectively.

2.4. Life cycle impact assessment (LCIA)

Potential environmental impacts were calculated according to a hierarchical approach (midpoint method) [44]. The characterization phase was performed considering the following impact categories: global warming potential, photochemical ozone creation potential, ozone depletion potential, acidification potential, eutrophication potential, ecotoxicity, energy resource, water footprint and land use, and their respective characterization factors are shown in Supporting Information (Table S1).

2.4.1. Global warming potential (GWP)

The determination of global warming potential was evaluated by greenhouse gas emissions (CO_2, N_2O, and CH_4) released by the processes. The gas values were combined with their respective characterization factors, in the period 100 years timeframe, expressed in $kgCO_{2eq}$, as described in Eq. (1) [45]:

$$GWP = \sum GWP_i \times m_i \quad (1)$$

where *GWP* is the global warming potential ($kgCO_{2eq}$), *i* is the time horizon of 100 years, GWP_i is the characterization factors for the substance i and, m_i is the emission mass of the substance *i* (kg).

2.4.2. Photochemical oxidant creation potential (SMOG)

Photochemical smog was calculated based on the volatile organic compounds and nitrogen releases, according to Hauschild and Wenzel [46], being expressed in kgO_{3eq} (Eq. (2)):

$$POCP = \frac{OI_{VOC}}{OI_{ethene}} \quad (2)$$

where *POCP* is photochemical ozone creation potential (kgO_{3eq}), OI_{VOC} is ozone increment with VOC (kg), and OI_{ethene} is ozone increment with ethene (kg).

2.4.3. Ozone depletion potential (ODP)

The quantification of ozone depletion potential was estimated through Eq. (3). Whose refer to emissions of chlorofluorocarbons and other halogenated hydrocarbons in the ozone layer. Values were expressed in $kgCFC\text{-}11_{eq}$ [46]:

$$ODP = \sum ODP_i \times m_i \quad (3)$$

Table 1
Materials and energy requirements for the production of 1 kg whole dried biomass for *Chlorella vulgaris* in raceway pond, *Chlorella vulgaris* in a tubular photobioreactor, and *Arthrospira platensis* in raceway pond.
Adapted from [29–33].

Process	Unit	Chlorella vulgaris in raceway pond	Chlorella vulgaris in tubular photobioreactor	Arthrospira platensis in raceway pond
Cultivation				
Input				
Nutrients enrichment				
Phosphate	kg	0.040	0.011	0.025
Nitrate	kg	0.058	0.017	0.036
Tubular photobioreactor	m^3	–	1.45	–
Chemical sterilization (sodium hypochlorite)	kg	–	0.21	–
Energy consumption for cooling	kWh	–	21.45	–
Aeration energy	kWh	–	1.45	–
Pumping (riser and degasser)	kWh	–	1.35	–
CO_2 consumption	kg	–	1.5	–
Water evaporation	m^3	–	0.002	–
Raceway pond	m^3	5.0	–	3.12
Electric energy for paddle wheel	kWh	2.7	–	1.68
Electric energy for water pumping	kWh	0.6	–	0.31
Electric energy for CO_2 injection	kWh	1.66	–	1.03
CO_2 consumption	kg	2.0	–	2.0
Water evaporation	m^3	0.65	–	0.40
Biomass productivity	kg/m^3/d	0.20	0.76	0.32
Output				
Algae liquid	kg	11.76	11.42	12.69
Harvest				
Input				
Energy consumption centrifugation	kWh	10.15	2.88	6.33
Drying				
Input				
Wet biomass	kg	8.82	8.55	9.51
Spray dryer	kWh	3.80	3.67	4.08
Output				
Whole dried biomass	kg	1	1	1

where *ODP* is the ozone depletion potential ($kgCFC\text{-}11_{eq}$), ODP_i is the characterization factors for the substance i and, m_i is the emission mass substance i (kg).

2.4.4. Acidification potential (AP)

The acidification potential was quantified by acids such as SO_x, NOx, HCl, NH_3, and HF, emitted into the atmosphere and then deposited in soils and surface waters, expressed in $kgSO_{2eq}$, as described in Eq. (5) [46]:

$$AP = \sum AP_i \times m_i \tag{4}$$

where *AP* is the acidification potential ($kgSO_{2eq}$), AP_i is the characterization factors for the substance i, and m_i is the emission mass substance i (kg).

2.4.5. Eutrophication potential (EP)

The eutrophication potential is calculated using Eq. (5), considering the weighted sum of the emission of nitrogen and phosphorus derivatives, such as N_2, NO_x, NH_4^+, PO_4^{3-}, P and chemical oxygen demand, being expressed in kgN_{eq} [46]:

$$EP = \sum EP_i \times m_i \tag{5}$$

where *EP* is the eutrophication potential ($kgPO_{4eq}$), EP_i is the characterization factors for the substance i and, m_i is the emission mass substance i (kg).

2.4.6. Ecotoxicity (ECO)

The impact of ecological toxicity of freshwater was quantified by toxic substances (CTUe), represented by Eq. (7):

$$ETP_{(FAEP)} = \sum ETP_i \times m_i \tag{7}$$

where *ETP* is the ecotoxicity potential corresponding to the score of *freshwater aquatic ecotoxicity potential* (*FAEP*) (CTUe), ETP_i is the characterization factor for the substance i emitted to the environmental freshwater, and m_i is the amount emitted to a given environmental compartment (kg).

2.4.7. Energy resource (ER)

Energy resource was used to calculate the non-renewable energy (coal) demand required for the different scenarios, expressed in megajoules (MJ) (Eq. (8)):

$$ER = EED \times RTI \tag{8}$$

where *ER* is energy resource (MJ), *EED* is electrical energy required to the system (kWh), *RTI* is the residence time in operation (h).

2.4.8. Water footprint (WF)

Water footprint was used to measure the among of renewable water resources consumed, being expressed in m^3. The detailed calculation model, described by Hoekstra [47], is given through Eq. 9:

$$WF = WF_{blue} + WF_{green} + WF_{grey} \tag{9}$$

where *WF* is the total water footprint, WF_{blue} is the blue water footprint (m^3), WF_{green} is the green water footprint (m^3) and WF_{grey} is the grey water footprint (m^3).

2.4.9. Land use (LU)

The determination of the impacts of land transformation and occupation was calculated for assessing the effects of land use on biodiversity, expressed in ha, following Lathuillière et al. [48], according to Eq. (10):

$$LU = CF_{transf} \times CF_{occup} \times A \tag{10}$$

Table 2
Inputs/outputs inventory the process producing 1 kg of β-carotene, astaxanthin and phycocyanin by *Dunaliella salina*, *Haematococcus pluvialis* and *Arthrospira platensis*, respectively.
Adapted from [29–39].

Process	Unit	β-carotene	Astaxanthin	Phycocyanin
Cultivation				
Input				
Nutrients enrichment				
Phosphate	kg	0.22	0.66	0.33
Nitrate	kg	0.32	0.96	0.48
Tubular photobioreactor	m^3	–	3.0	–
Chemical sterilization (sodium hypochlorite)	kg	–	0.45	–
Energy consumption for cooling	kWh	–	45	–
Aeration energy	kWh	–	3.0	–
Pumping (riser and degasser)	kWh	–	2.85	–
CO_2 consumption	kg	–	1.5	–
Water evaporation	m^3	–	0.006	–
Raceway pond	m^3	27.77	80.0	41.66
Electric energy for paddle wheel	kW	15.0	43.2	22.50
Electric energy for water pumping	kW	2.77	8.0	4.16
Electric energy for CO_2 injection	kW	9.21	26.56	13.83
CO_2 consumption	kg	2.0	2.0	2.0
Water evaporation	m^3	5.61	10.40	5.41
Biomass productivity	$kg/m^3/d$	0.45	0.40	0.32
Output				
Algae liquid	kg	83.3	222.2	71.09
Harvest				
Input				
Energy consumption centrifugation	kWh	56.33	168.40	84.52
Drying				
Input				
Wet biomass	kg	49.98	133.32	53.31
Spray-dryer	kWh	21.49	57.32	22.92
Extraction				
Input				
Dry biomass	kg	12.5	33.33	13.33
sCO_2	kWh	10.0	26.66	10.66
Output				
Oil rich pigments	kg	1	1	1

Supercritical CO_2 extraction, sCO_2.

where LU is the land use (ha), CF_{trans} is the characterization factor for land transformation, CF_{occ} is the characterization factor defined for land occupation, A is the area (ha).

2.5. Normalization

The normalization was determined according to Eq. (11), described by the International Reference Life Cycle Data System (ILDC) handbook [49]. During this step, each of the environmental impact potentials was divided by reference value, corresponding the world environmental impact normalization factor provided by the European Commission (Table S2):

$$N_k = \frac{S_k}{R_k} \tag{11}$$

where k denotes the impact category, N is the normalized indicator, S is the category indicator from the characterization phase, and R is the reference value or the normalization factor.

Table 3
Inputs/outputs inventory the process producing 1 kg of the DHA by *Crypthecodinium cohnii* in heterotrophic cultivation, EPA by *Nitzschia laevis* in heterotrophic cultivation, and EPA by *Nannochloropsis oculata* in autotrophic cultivation.
Adapted from [29–32,40–43].

Process	Unit	DHA heterotrophic	EPA Heterotrophic	EPA autotrophic
Cultivation				
Input				
Nutrients enrichment				
Phosphate	kg	0.01	0.03	0.37
Nitrate	kg	0.20	1.0	0.55
Glucose	kg	4.15	20.0	–
Fermenter	m^3	0.83	4.0	–
Physical sterilization	kWh	5.99	28.88	–
Agitation	kWh	0.14	0.70	–
Aeration	kWh	0.83	4.0	–
Tubular photobioreactor	m^3	–	–	47.61
Chemical sterilization (sodium hypochlorite)	kg	–	–	7.14
Energy consumption for cooling	kWh	–	–	707.25
Aeration energy	kWh	–	–	47.61
Pumping (riser and degasser)	kWh	–	–	45.22
CO_2 consumption	kg	–	–	1.5
Water evaporation	m^3	–	–	0.004
Biomass productivity	kg/m^3	10	0.75	1.5
Output				
Algae liquid	kg	44.42	16.0	380.90
Harvest				
Input				
Energy consumption centrifugation	kWh	1.68	8.15	96.6
Drying				
Input				
Wet biomass	kg	33.3	12.0	285.66
Spray-dryer	kWh	14.32	5.16	122.83
Extraction				
Input				
Dry biomass	kg	8.33	3.0	71.42
sCO_2	kWh	6.66	2.4	57.13
Output				
Oil	kg	1	1	1

Docosahexaenoic, DHA; Eicosapentaenoic, EPA; Supercritical CO_2 extraction, sCO_2.

3. Results and discussion

3.1. Whole dried biomass

The whole dried biomass is the first product commercialized. In this sense, knowledge of the environmental impacts associated with its production should be investigated (Fig. 2).

Fig. 2 shows the values characterized by the production of 1 kg of whole dried biomass in consolidated cultivation systems. The biomass production of the species *Chlorella vulgaris* in the tubular photobioreactor and on the raceway pond presented impacts of 1551.94 and 995.79 CTUe for ECO, 475.53 and 302.59 MJ for ER, 220.32 and 141.30 $kgCO_2eq$ for GWP and 5.05 and 3.31 kgO_3eq for SMOG, respectively. The biomass production of the species *Arthrospira platensis* in the raceway pond had an impact of 710.95 CTUe (ECO), 216.09 MJ (ER), 100.92 $kgCO_2eq$ (GWP), and 2.38 kgO_3eq (SMOG). Comparatively, studies by Porcelli et al. [7] evaluated the environmental

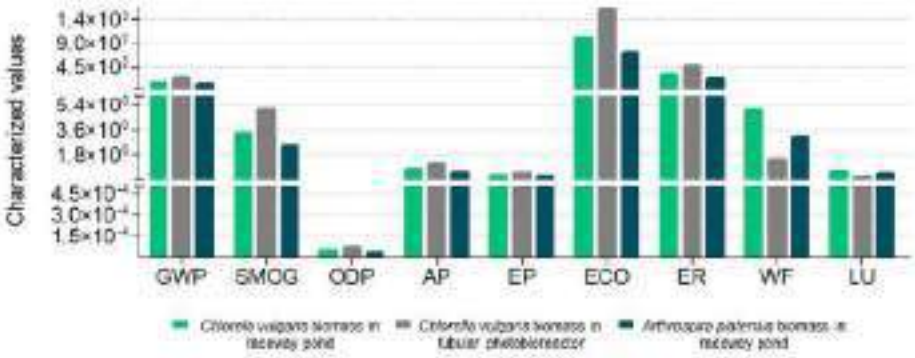


Fig. 2. Characterized values of environmental impact categories associated with whole dried biomass. Global warming potential, GWP; Photochemical oxidant creation potential, SMOG; Ozone depletion potential, ODP; Acidification potential, AP; Eutrophication potential, EP; Ecotoxicity, ECO; Energy resource, ER; Water footprint, WF; Land use, LU.

indicators for whole biomass processes by *Phaeodactylum tricornutum* in a column photobioreactor. The scenario assessed presented GWP values of 2.57×10^{2} kg CO_2 eq, ECO of 2.70×10^{1} CTUe, AP of 8.15×10^{-1} kg SO_2 eq, EP of 1.69×10^{-1} kg N eq, and ODP of 1.69×10^{-7} kg CFC-11 eq, using residual CO_2. In contrast, results from the pilot-scale operation for simulating a large-scale plant-based in raceway ponds by *Chlorella vulgaris* showed values in order to 1014.8 kg CO_2 eq for GWP, 274.5 kg oil eq for ER, 0.529 kg PO_4^{-3} for EP, and 211.6 kg 1,4-DB eq for ECO [50].

Evidently, part of these environmental impacts for all biomass production is also related to the upstream phase. However, it should be noted now that, to compare the functional base of 1 kg of dry biomass, operational volumes have been increased to allow for the high workload for the bioproduct production. Thus, the operational volumes of the assumed bioreactors were 5.0, 3.12, and 1.43 m^3 for *Chlorella vulgaris* in the raceway pond, *Arthrospira platensis* in the raceway pond, and *Chlorella vulgaris* in the tubular photobioreactor, respectively. Therefore, the environmental impacts of the energy consumption of the engineering elements required in the different cultures are expanded in proportion to the bioreactor volumes.

In addition, the environmental impacts attributed exclusively to the downstream phase of biomass processing must be considered. Consequently, the hot point identified in the harvesting phase is attributed to the centrifugation, which is energy-intensive equipment used to obtain concentrated microalgae sludge. In short, centrifugation is highly dependent on many factors, including characteristics of microalgae species (i.e., size, morphology, and specific gravity), cell sedimentation, sludge retention time in the centrifuge and sedimentation depth [51]. All of this is also linked to the type of cultivation systems, which affects the typical final concentration of biomass in large-scale systems [52].

By way of comparison, the production of 1 kg of whole dried biomass from *Chlorella vulgaris* and *Arthrospira platensis* grown in the raceway pond had an energy consumption during the centrifugation of 10.15 and 6.33 kWh/kg, respectively. On the other hand, the energy consumption for the production of 1 kg of whole dried biomass from *Chlorella vulgaris* in a tubular photobioreactor was 2.88 kWh/kg, up to 5 times less compared to the raceway pond. This demand is related to several factors, such as the high dilution of the culture broth, as well as the diameter of cells. As can be seen, the average cell diameter of the *Chlorella vulgaris* microalgae are around 5.7 μm [53]. In contrast, *Arthrospira platensis* cells can reach up to 12 μm [54]. This information corroborates the energy data required by the centrifugation step. In the same way that the energy demand required by closed systems is substantially lower when compared to open systems. Consequently, to recover the diluted biomass, large volumes of broth need to be centrifuged [52].

After harvesting, the subsequent process is dehydration of the biomass. The specific post-harvest processing required depends on the desired target product. Among the many existing methods, the most used on a commercial scale is the spray-dryer. Thus, the hotspot identified in the drying step is attributed to this equipment, which is expensive in electricity. In general, the energy consumption for the biomass production was similar in the two cultivation systems, whose values are in the order of 4.08 kWh/kg (*Arthrospira platensis* in the raceway pond), 3.80 kWh/kg (*Chlorella vulgaris* in the raceway pond) and 3.67 kWh/kg (*Chlorella vulgaris* in the tubular photobioreactor). However, slightly higher for production in the raceway pond. This is due to the higher moisture content of the biomasses and the high dilution cell rate in this type of bioreactor. Consequently, as biomass density is low, longer drying time is required.

In this sense, the considerations made about the upstream and downstream phases present their pros and cons. Each cultivation mode does not follow a logic that indicates the best option for processing whole dried biomass with minimal environmental impact. Regardless, the basic metric for its production in different cultivation systems is fundamentally supported by productivity. Cellular concentrations of the cultures are usually in the range 0.1 to 4 g/L (DW), considered extremely low, which corroborates the values obtained in this study. Therefore, the microalgae biomass concentration must be expanded about 25–500 times, to generate either concentrated sludge, paste, or dry solid. But while a consistent technological route did not develop that achieves biomass yields of around 50–100 g/L, its commercialization both as a whole as the refined form will still impact the resource use.

Finally, the level of comparison between species, although the microalgae *Arthrospira platensis* shows a lower environmental performance when compared to *Chlorella vulgaris*, the industrial production of this microalgae persists due to the different purposes of consumers. Consumers of *Arthrospira platensis*, opt for this product, given its very high recognition for its unique composition, comprising not only up to 70% of proteins containing all essential amino acids, but also polysaccharides, one of the best sources of gamma-linoleic acid, and source of vitamins B12, C, E [55,56]. Also, increased consumption of alternative proteins has led consumers to explore the biomass of *Arthrospira platensis*, as a pioneering protein source [57]. On the other hand, the target audience related to the consumption of *Chlorella vulgaris*, uses food supplementation, not only for its high protein content but mainly for the bioaccessibility properties attributed to the lipid fraction contained in the biomass. Besides, they are recognized for their high concentration of peroxisome proliferator-activated receptors, which regulate metabolism and strengthen the immune system [58,59].

3.2. Pigments

β-carotene from *Dunaliella salina*, astaxanthin from *Haematococcus pluvialis*, and phycocyanin from *Arthrospira platensis* are commercially produced pigments with regulatory approval as food ingredients [60–63]. These natural molecules present effects on human health innately superior to your synthetic counterparts, due to the presence of 9-*cis* isomer, more efficient in protecting against oxidative damage [37]. Despite the perceived advantages, the environmental footprint of the

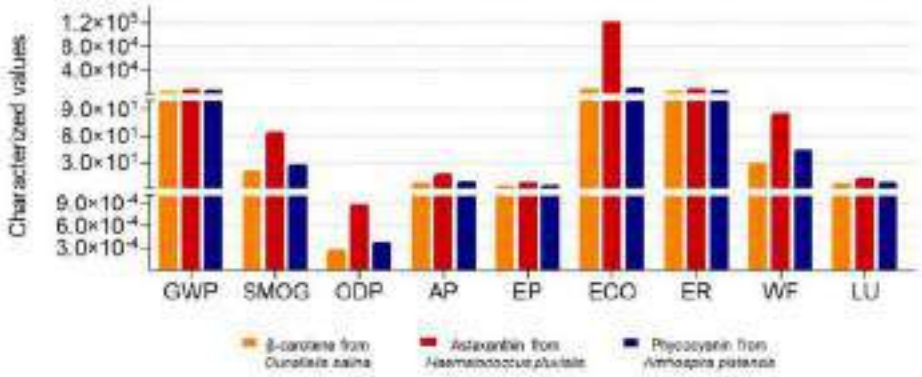


Fig. 3. Characterized values of environmental impact categories associated with microalgae-based pigments. Global warming potential, GWP; Photochemical oxidant creation potential, SMOG; Ozone depletion potential, ODP; Acidification potential, AP; Eutrophication potential, EP; Ecotoxicity, ECO; Energy resource, ER; Water footprint, WF; Land use, LU.

current production processes of natural pigments has not been extensively explored. In this sense, the environmental impacts associated with microalgae-based pigments production were examined, and the results are presented in Fig. 3.

As shown in Fig. 3, the characterized results indicate the ECO potentials of 6033.39, 119,861.36, and 8333.89 CTUe, ER of 1836.20, 6054.04, and 2336.0 MJ, GWP of 852.5, 2805.78 and 1177.2 $kgCO_2eq$, SMOG of 19.15, 62.81 and 26.40 kgO_3eq, such as the most relevant impact categories in the production of 1 kg of β-carotene, astaxanthin, and phycocyanin, respectively. Comparatively, the literature lacks studies that evaluate the production of pigments by microalgae-based processes. However, studies by Kyriakopoulou et al. [64] assessed the production of β-carotene by microalgae *Dunaliella salina*, in raceway pond systems. It is estimated that the impacts associated with the categories of AP, EP, GWP, ODP, and SMOG were of 4.63 kg SO_2 eq, 1.37×10^{-1} kg PO_4^{-3}, 4.87×10^{2} $kgCO_2$ eq, 7.32×10^{-5} mg CFC-11 eq, and 2.22×10^{-1} g C_2H_4 eq. In addition, Pérez-López et al. [65] evaluated the production of astaxanthin by *Haematococcus pluvialis* in a tubular photobioreactor under pilot-scale operation. Among the results found, for each 1 kg of pigment approximately 447.00 kg SO_2 eq for AP, 150.0 kg PO_4^{-3} for EP, 87×10^{2} $kgCO_2$ eq for GWP, 5.0×10^{6} mg CFC-11 eq for ODP, and 15.0×10^{3} g C_2H_4 eq for SMOG were emitted. Likewise, to obtain 1 kg of phycocyanin under wet biomass recovery by *Arthrospira platensis*, studies by Papadaki et al. [66] resulted in impacts in the categories: AP of 4.27×10^{1} kg SO_2 eq, EP of 1.51 kg PO_4^{-3} eq, GWP of 6.72×10^{3} $kgCO_2$ eq, and ODP of 4.68×10^{-4} kg CFC-11 eq. Through the environmental tool, it was possible to attribute that approximately 98% of these environmental impacts are attributed to the demand for energy in the upstream and downstream stages.

As for the energy demands related to the upstream stages, it is important to highlight specific morphological characteristics of each species. Currently, most microalgae species that have reached the commercial level grow in highly selective environments, capable of overcoming other contaminating microorganisms in open systems [67]. However, *Haematococcus pluvialis* does not have this selective advantage and requires cultivation in two-stage systems, involving the growth phase ideally carried out in batches by tubular photobioreactors, followed by the phase of carotenogenesis induced under nutrient deprivation conditions and high irradiance in the raceway pond [68]. This results in higher consumption of energy in the astaxanthin production from *Haematococcus pluvialis* (127.26 kWh/kg) when compared to the β-carotene production from *Dunaliella salina* (26.98 kWh/kg) and phycocyanin from *Arthrospira platensis* (40.49 kWh/kg).

At the same time, attributed to the specific cultivation requirements, the greater environmental footprint of the production of astaxanthin by *Haematococcus pluvialis* is not restricted only to the indirect effects of energy requirements. Associated with these aspects, this operation also strongly influences the environmental impacts associated with WF and LU. In terms of comparison, the cultivation systems that integrate photobioreactor models and raceway pond presented values in the order of 83 m^3 for WF and 9.9 PDF/ha for LU. On the other hand, cultures with only one-unit stage showed values of 27.77 m^3 WF and 3.41 PDF/ha for *Dunaliella salina*, and 41.66 m^3 for WF and 4.95 PDF/ha for *Arthrospira platensis*.

Subsequently, the centrifugation and spray dryer methods were the most energy-intensive, consuming fossil energy of approximately 77.82 kWh/kg for β-carotene, 225.72 kWh/kg for astaxanthin, and 107.44 kWh/kg for phycocyanin. It is worth mentioning that the energy-intensive requirements are consistent with the low cell density of *Dunaliella salina* (0.45 $kg/m^3/d$), *Haematococcus pluvialis* (0.40 $kg/m^3/d$) and *Arthrospira platensis* (0.32 $kg/m^3/d$). Attributed to these factors, the collection and dehydration of diluted systems represent the most significant barrier to the expansion of the microalgae-based pigments market [69].

As for the extraction methods, SC-CO_2 is the best method under optimized conditions, leading to an ideal yield with the highest purity, and without using environmentally toxic solvents, without the need for further purification steps [70]. However, the firm association between intracellular pigments and other macromolecules makes it difficult to transfer mass during extraction, resulting in considerable energy consumption. Energetically, in the extraction stage, the required energy values for β-carotene and phycocyanin presented similar demands, with values of approximately 10 kWh/kg. However, the extraction of astaxanthin showed about 26 kWh/kg. This significant increase is closely related to the morphology and biochemical routes of pigment production by *Haematococcus pluvialis*. First, the robust three-layer cell wall structure in *Haematococcus pluvialis* generally requires intense methods for efficient disruption, featuring an outer layer of hard silica (frustule) [71]. In addition, a higher volume of biomass is necessary, as astaxanthin is a secondary carotenoid, that results in lower yields (~3–5%) when compared to a primary carotenoid as β-carotene (~14%).

Finally, the results of the life-cycle assessment showed that less than 3% of the emissions generated in the industrial production of β-carotene, astaxanthin, and phycocyanin are related to the demand for CO_2 and fertilizers. The environmental impacts generated by the addition of nutrients are related to the insertion of nutrients during the cultivation phase, as well as a slight demand for CO_2 in the extraction process. However, these requirements can be reduced by process integration approaches as nutrient recycling, seawater use, and exploitation of gaseous effluents [67].

3.3. Polyunsaturated fatty acids

Microalgae are considered an important and sustainable alternative as a source of polyunsaturated fatty acids (PUFAs) pool, as the majority of the EPA and DHA. Due to their health benefits, there is a growing interest in the commercial application of these fatty acids in health, dietary products, and food for aquaculture [72]. In this sense, the environmental impacts associated with the production of fatty acids based on microalgae were examined, and the results are shown in Fig. 4.

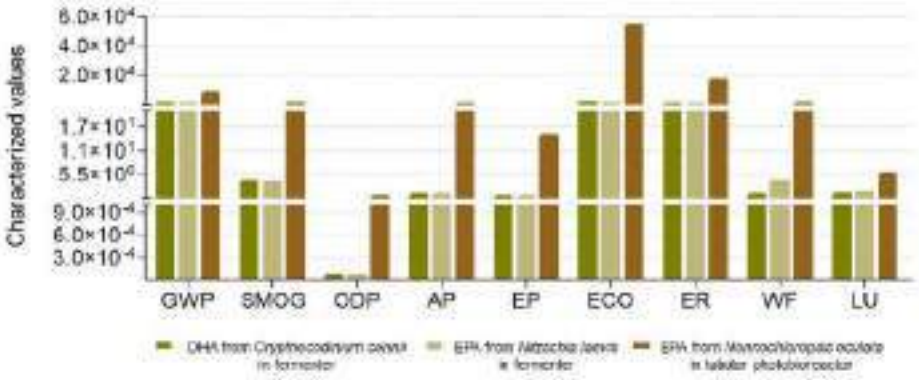


Fig. 4. Characterized values of environmental impact categories associated with microalgae polyunsaturated fatty acids. Docosahexaenoic, DHA; Eicosapentaenoic, EPA; Global warming potential, GWP; Photochemical oxidant creation potential, SMOG; Ozone depletion potential, ODP; Acidification potential, AP; Eutrophication potential, EP; Ecotoxicity, ECO; Energy resource, ER; Water footprint, WF; Land use, LU.

The characterized results presented in Fig. 4 indicate that, in general, the heterotrophic cultivation and autotrophic systems contribute to a relevant impact in the categories of ECO, ER, GWP, and SMOG. These four major categories are mainly related to the indirect effects of fossil energy consumption.

When analyzing the obtaining of the same product, by two consolidated but distinct technological routes, the environmental impacts present discrepant values for the evaluated categories. In summary, when submitted to environmental analysis, the process of obtaining EPA by the microalgae *Nannochloropsis oculata*. Under autotrophic regime in photobioreactors presented values in the order of 54,107.97 CTUe (ECO), 16,615.63 MJ (ER), 7649.64 $kgCO_2eq$ (GWP), and 170.37 kgO_3eq (SMOG). In comparison, obtaining EPA by microalgal *Nitzschia laevis* in the heterotrophic regime in fermenters, it presented potential impact values of 1143.10 CTUe (ECO), 633.74 MJ (ER), 167.95 $kgCO_2eq$ (GWP), and 3.54 kgO_3eq (SMOG). The hotspot for this disparity in data is associated with the energy demand required in autotrophic regimes compared to heterotrophic production. In addition, EPA yields by autotrophic cultivation (0.0021 $kg/m^3/d$) are lower compared to EPA yields by heterotrophic cultivation (0.25 $kg/m^3/d$). This is due to two unresolved problems, the limitation of light and the accumulation of oxygen in the photoautotrophic culture. The heterotrophic growth of microalgae eliminates the need for light and therefore offers the possibility to increase the density and productivity of algae cells on a large scale [73].

On the other hand, the environmental charges related to these technological routes go further and also impact on the category of water footprint and land use. Since autotrophic processes require larger volumes of water than heterotrophic regimes, the production of EPA in photobioreactors showed values of 47.61 m^3 of WF. In comparison, the production of EPA in fermenters resulted in water requirements of 4.0 m^3 of WF. Likewise, autotrophic and heterotrophic production showed land requirement values of 5.57 and 0.50 PDF/ha. Given the technological aspect, the use of the fermenter for the cultivation of microalgae involves more compact and optimized equipment, reflected in a processing plant with less occupation of physical space and with less water consumption when compared to the use of the tubular photobioreactor for the cultivation of microalgae [74].

Concurrently, in terms of the heterotrophic culture of microalgae in fermenters to obtain DHA by *Crypthecodinium cohnii*, the most significant impact categories were 1250.38 CTUe (ECO), 441.0 MJ (ER), 178.15 $kgCO_2eq$ (GWP), and 3.93 kgO_3eq (SMOG). Under the environmental burden aspect, the use of fermenters to obtain fatty acids is more sustainable for commercial production. This is associated with the fossil energy requirements for the system that are absurdly lower than those required by other technologies. Reasons for this include the combination with mature microbial fermentation techniques, which allow relatively complete control of culture conditions, resulting in appropriate growth and production of bioproducts. Besides, the available capacity of installed fermenters that are accessible worldwide [40].

However, heterotrophic production has some process bottlenecks that need to be overcome. In short, the biochemical synthesis of polyenoic fatty acids is essential and requires the presence of molecular oxygen for the stretching and desaturation of polyunsaturated fatty acids [40,75]. For this, technologically, the aeration and agitation methods found in the fermenters are necessary to increase the oxygenation rate, and thus to increase the species bioconversion rates. As a consequence, energy consumption can increase up to 22% of the total process consumption. Likewise, the growth of filamentous species, such as the microalgae *Nitzschia laevis*, results in high viscosity of the fermentation broth, which dramatically increases the energy requirements for mixing [40].

Commonly to bioproducts extracted from microalgae, the steps that anticipate the extraction, that is, the centrifugation and drying, also presented energy-intensive values. The centrifugation method required about 1.68, 8.15, and 96.6 kWh/kg for DHA, heterotrophic EPA, and autotrophic EPA, respectively. Likewise, approximate values of 14.32, 5.16, and 122.83 kWh/kg were observed for the spray dryer drying process. Notably, these values are attributed to the variability of cell density since the species varied in cell productivity from 0.75–10 $kg/m^3/d$ (see Table 3).

In addition, the extraction process also influences energy demands. According to analyzes, the energy demands of the extractor with supercritical fluid showed values of 6.66, 2.4, and 57.13 kWh/kg for DHA, heterotrophic EPA, and autotrophic EPA, respectively. These fluctuations between conditions are related to the productivity of the compound, as well as the dependence of the increase in the interface area of the cell-matrix for cell disruption [76]. However, this method has advantages, since it reduces the extraction time from 8 to 2 h, when compared to conventional methods, in addition to increasing the degree of purity and quality of the final product [77]. Still, no further purification step is necessary after the application of SFE, since CO_2 is gaseous at ambient pressure, which allows easy recovery of the extractor, resulting in a mix of resin oil with the predominance of the desired oil [78].

3.4. Normalization

Normalization aims to understand better the relative significance of the results of the impact category. The normalization references used are the results characterized by a reference system, generally a global economy. Besides, it is widely practiced in LCA-based decision support and policy analysis (for example, LCA cases in renewable energy technologies and environmentally preferable purchasing programs). Based on this understanding, the values of the characterized impacts associated with whole dried biomass, pigments, and polyunsaturated fatty acids were subjected to a comparison with a selected global reference to obtain information on the results of the most significant contribution LCIA, as shown Fig. 5.

The general analysis shows that of the nine categories evaluated for

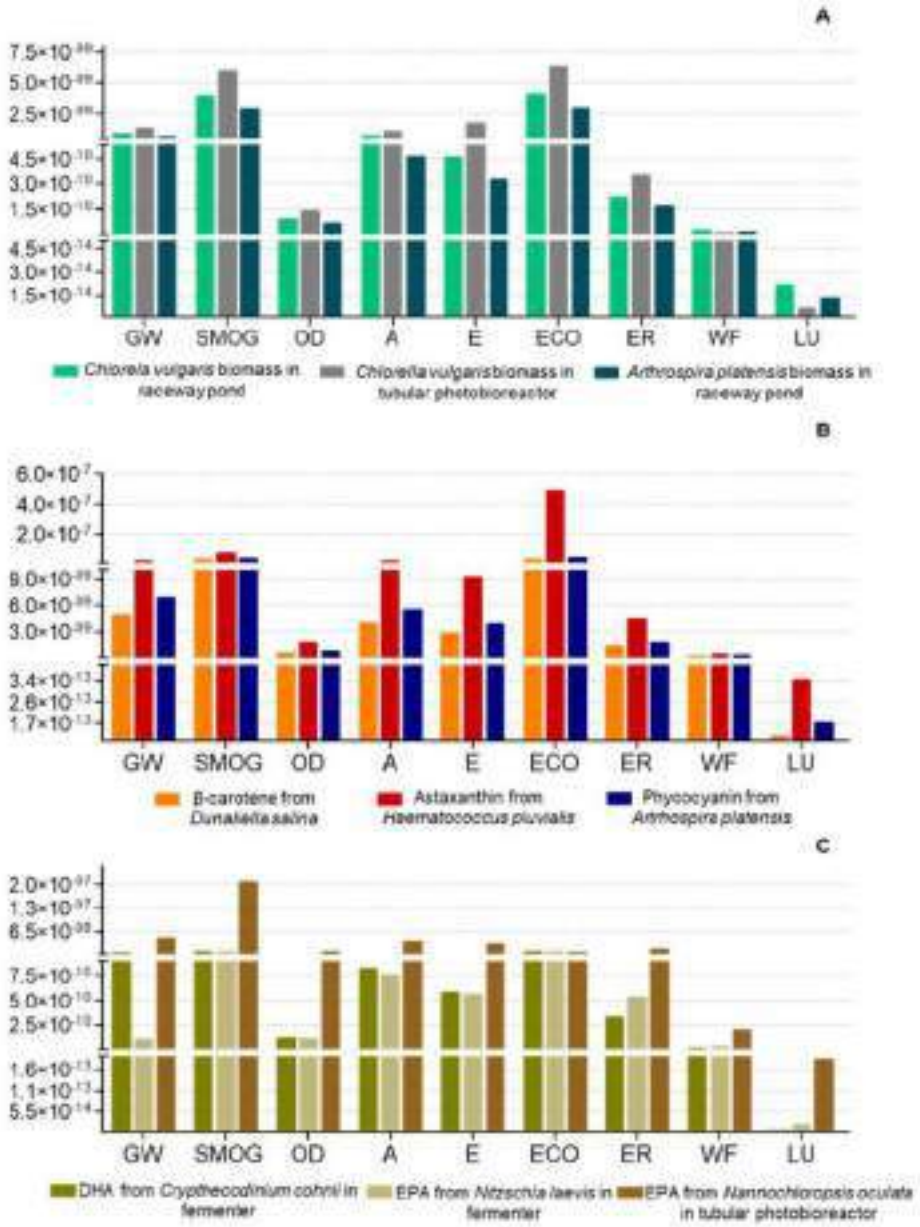


Fig. 5. Impact categories normalized data for the microalgae-based process. (A) Whole dried biomass. (B) Pigments microalgae. (C) Polyunsaturated fatty acids microalgae. Docosahexaenoic, DHA; Eicosapentaenoic, EPA; Global warming, GW; Photochemical oxidant creation, SMOG; Ozone depletion, OD; Acidification, A; Eutrophication, E; Ecotoxicity, ECO; Energy resource, ER; Water footprint, WF; Land use, LU.

all processes, four are considered to be the majority: ECO, SMOG, GWP, and ER. The categories of AP, EP, and ODP, on the other hand, have an impact that varies from intermediate to low, followed by the categories WF and LU. It can be inferred that these five minority categories are unlikely to contribute to the significant environmental impact.

The data normalization procedure indicates that the majority categories have a marked impact on the damage of the midpoint, linked to the deterioration of the resource base, that is, the high indirect demand for non-renewable primary energy resources. In short, all standardized systems consume more energy than they produce (Fig. 5). Second, the normalization of the other categories also indicates an impact associated with the extraction and consumption of energy resources, such as water and land, human health, and quality of the ecosystem.

Likewise, a similar trend is attributed to the impacts generated by the upstream and downstream stages, which is essential to obtain the whole dried biomass, as well as the intracellular products (pigments and fatty acids). This behavior is related to the energy requirements, previously mentioned, arising from three main activities: (i) consumables necessary for cultivation, (ii) centrifugation, and (iii) drying. In a less expressive category of energy demand, intracellular compounds still need robust equipment to extract the molecules of interest and, therefore, contribute to energy consumption and the consequent increase in environmental impacts.

Finally, it is important to emphasize that microalgae-based technologies, despite having a positive influence in certain aspects, can impose negative impacts on others, making full engagement difficult. Thus, assessing the pros and cons of the processing steps is crucial to introducing the technology and comparing it with a baseline option to verify whether there is a gap for future improvement. Therefore, systematically identifying the accurate points of energy-intensive stages is necessary to obtain a holistic view of the environmental hotspots of the technology in question.

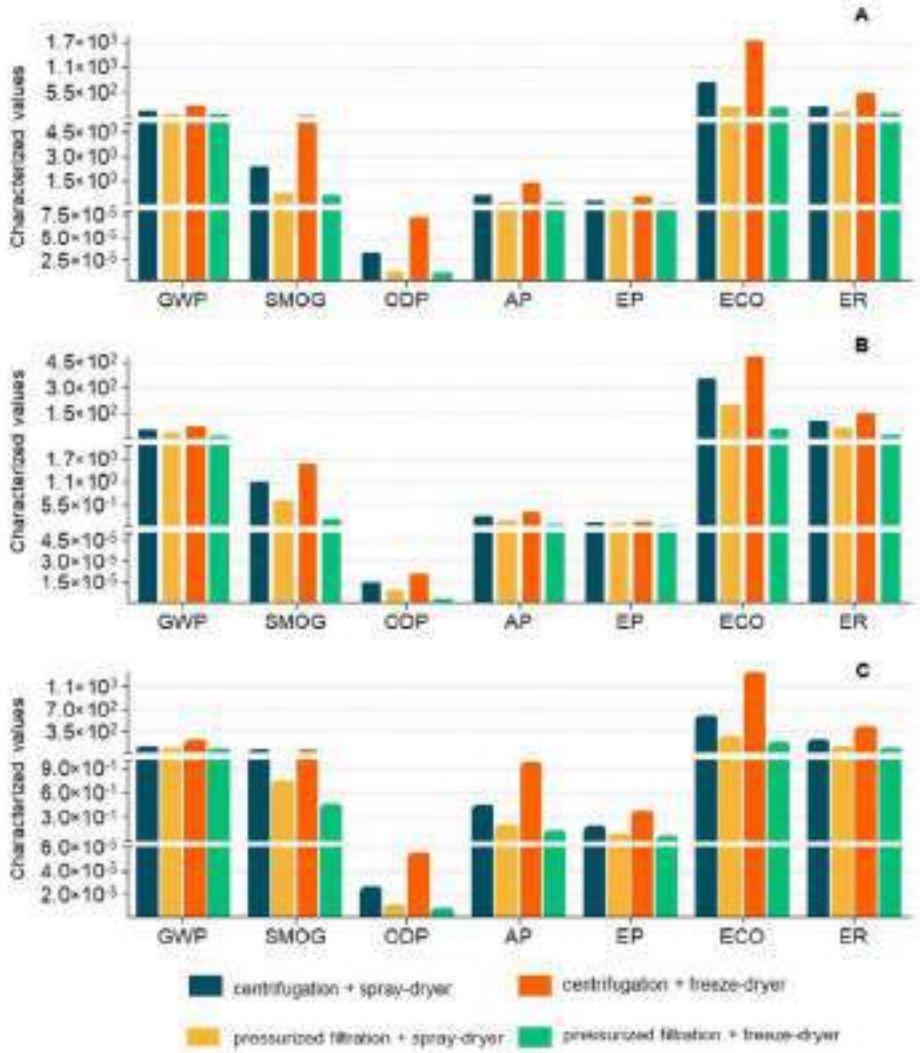


Fig. 6. Values characterized by the different combined dewatering and drying operations for microalgae biomass: (A) Energy requirements for whole dried biomass from *Chlorella vulgaris* in raceway pond, (B) Energy requirements for whole dried biomass from *Chlorella vulgaris* in tubular photobioreactor, and (C) Energy requirements for whole dried biomass from *Arthrospira platensis* in raceway pond. Global warming potential, GWP; Photochemical oxidant creation potential, SMOG; Ozone depletion potential, ODP; Acidification potential, AP; Eutrophication potential, EP; Ecotoxicity, ECO; Energy resource, ER; Water footprint, WF.

3.5. Environmental hotspots of the microalgae-based processes and products

3.5.1. Dewatering and drying combined operations

As seen in the previous sections, microalgae-based processes present energy-intensive demands, resulting mainly from cultivation, dewatering, and drying operations [79]. Some authors suggest that harvesting stages alone can represent about 20–30% of the total cultivation cost [25]. On the other hand, it is estimated that the energy demands of downstream processes can represent up to 60% of the costs [15]. Hence, the technologies applied in downstream processing are considered to be the most substantial effects on environmental charges and can be regarded as among the main bottlenecks for the development of commercial products. Therefore, in the following section, the influence of different combined methods of downstream about their respective environmental impacts for the microalgal biomass production was investigated through case studies (Fig. 6). Among the most diverse technologies in use, the choice of dewatering and drying methods as determined concerning their effective biomass harvesting efficiency, including the combination of only two methods. Therefore, methods with a high recovery rate and effective as centrifugation and filtration were chosen as representatives of dewatering. Likewise, the selection of drying methods such as freeze-dryer and spray-dryer was determined, given its high applicability in microalgae processes, as well as its ability to ensure the integrity of intracellular compounds. In short, four different scenarios were alternated with the combination of the dewatering and drying methods. The basic operating conditions and the requirements for the dehydration and drying methods were presented in Table S3.

Currently, microalgae-based processes use the combined centrifugation and spray dryer methods as the main methodology for their industrial processes. In raceway ponds, when applied for the cultivation of *Chlorella vulgaris*, this combination represented about 334.8 kWh (74.16%) of the total energy required, while cultivation corresponds to approximately 116.64 kWh (26%) of the process (Fig. 6A). Also, the same behavior for *Arthrospira platensis* in raceway pond production can be observed, as about 249.84 kWh (77.51%) of the required energy was attributed to the dewatering and drying operation (Fig. 6C). In contrast, for closed systems such as tubular photobioreactors, the energy requirements for drying were in the order of 157.2 kWh (30%), while the cultivation system comprised approximately 549.12 (80%) of the total energy (Fig. 6B).

Attractive strategies for reducing energy requirements propose the use of pressurized filtration. Thus, another possibility, such as pressurized filtration combined with spray dryer, was evaluated. For the

drying of *Chlorella vulgaris* in the raceway pond, the energy demand was about 98.88 kWh, representing approximately 21.90% of the total process energy. Similarly, for *Arthrospira platensis* was found in the order of 102.72 kWh. On the other hand, in whole dried biomass tubular photobioreactors from *Chlorella vulgaris*, values below 15% were required for this step (90.24kWh). However, although dewatering processes using pressurized filtration require only 0.08 kWh/m^3 compared to conventional centrifugation methods, which can reach up to 8 kWh/m^3, centrifugation methods continue to be used as they can adjust their speed and consequently decrease energy input [80]. Besides, the development and consolidation of equipment with high centrifugal working capacities provide the predominance of this method.

Another reduction proposal is regarding the biomass drying method. Thus, the centrifugation and freeze dryer method were considered. However, for both *Chlorella vulgaris* and *Arthrospira platensis* in the raceway pond, the values were substantially increased, corresponding to about 768.38 and 565.87 kWh, respectively of the total process energy. In contrast, for the tubular photobioreactor, although the energy demand was not as expensive, the values nevertheless showed slight increases, representing about 31.14% of the total process energy. Furthermore, it is noteworthy that the viability of the freeze-drying method is only applicable to industrial processes where the workload is lower. In addition, pretreatment before drying requires that wet biomass present about 80% of total soluble solids.

Yet, in order to comparative purposes, the combined method of pressurized filtration and lyophilization were evaluated to establish the best scenario. Thus, both whole dried biomass processes for *Chlorella vulgaris* and *Arthrospira platensis*, the energy requirements were 84.86 and 62.83 kWh, respectively, resulting in values below 20% of the total required energy. By comparison, *Chlorella vulgaris* in tubular photobioreactor values needed in the order of 24.36 kWh, representing approximately 4% of the total process energy required. Thus, given the profiles of the combined methods evaluated, it is worth mentioning that the combination of pressurized filtration and lyophilization represents the best method in terms of energy requirements. However, technological improvements in the development of this equipment are necessary, since the freeze-dries and pressurized filtrations have low workloads operation and highly unstable and slow processes. Also, problems with the maintenance of auxiliary equipment such as vacuum pumps, as well as the ensure of sterilization of the freeze-dryer chambers, are some factors that increase the investment costs of these processes [81].

3.5.2. *The key role of the energy footprint on the microalgae-based processes and products*

The findings above make it clear that regardless of the method of dewatering and drying, microalgae-based processes continue to require high energy demands and to influence indirect environmental burdens. Therefore, from the point of view of energy consumption, a more in-depth analysis of the transition of energy from fossil matrices to the sustainable renewable perspective must be strengthened.

Given this context, the centralized coal-fired power generation system has brought more significant environmental concerns in recent years [82]. This is because, globally, it is estimated that the share of coal in electricity production represents approximately 41% of total demand [83]. As a result, the increase in greenhouse gases, resulting from this process, urged nations to take protective measures. In this way, specific technologies and political infrastructures to promote the energy transition from electricity generation from renewable energy sources, have become crucial.

Under the environmental aspect, the main indicators related to electric energy can be pointed out by the categories of global warming potential and the water footprint of the systems. It is known that electricity from fossil resources, such as coal, has average emission values of the order of 0.604 $kgCO_2eq$/kWh, while natural gas has values of 0.543 $kgCO_2eq$/kWh. Comparatively, renewable energies, such as hydroelectric, wind, and photovoltaic solar panels, have values of 0.041, 0.025, and 0.09 $kgCO_2eq$, respectively [84]. Likewise, in terms of water footprint, fossil resources have average values of 78 L/kWh. At the same time, the photovoltaic, wind, and hydroelectric systems indicate water consumption around 10, 1, and 36 L/kWh, respectively [85]. Therefore, it is clear that renewable resources stand out from the environmental point of view.

Nonetheless, the availability and technological limitations of renewable energy matrices become the main parameters for choosing industrial processes. Indeed, the lowest environmental charges can be seen in wind power installations. However, the location of these plants requires geographical positions with constant wind speed rates. Thus, the intermittency of the winds makes this technology a variable source of energy and not a safe supplier [86]. Besides, although solar radiation and temperature have proved to be the crucial factors under the influence of microalgae cultivation. It should be noted that places with high winds can be obstructive in open systems due to contamination, beyond influencing biomass productivity in regarding the cooling effects of cultures [87,88].

Subsequently, electricity from hydroelectric plants shows efficient responses to environmental indicators. According to Álvarez et al. [89], it is estimated that the potential of hydropower represents up to 70% of the world supply. However, to date, only 18% of the world's energy is produced by hydroelectric plants, since most countries do not have the natural conditions necessary for the construction of these plants. Also, even if the locations do not have high water volumes, favorable measures such as the installation of small hydroelectric plants (SHPs) can be established, since they present advantages such as the local energy generation in relation to oil products [90]. Yet, depending on the location of the plant, large hydroelectric complexes may not be environmentally friendly. Thus, environmental licenses, as well as governmental public policies, must focus on meeting minimum requirements in view of engineering feasibility, costs, and spillway adaptations with run-of-river generators [91].

Otherwise, the integration of microalgae bioreactors with photovoltaic panels seems to be the most promising alternative. This is because this configuration can increase the overall efficiency of photoconversion of the entire culture system, producing electrical energy directly available together with microalgae biomass [92]. In addition, if the photovoltaic cells are placed with a suitable geometry, it can be beneficial to avoid or reduce photoinhibition phenomena, in addition to the notable reduction in environmental impacts [93]. Therefore, it is clear that decision-making to replace the energy matrix with clean sources can bring immediate results to reduce environmental impacts [94]. For instance, the reduction of environmental charges in relation to GWP could be reduced by up to 95% considering wind and hydroelectric matrices, while the photovoltaic energy matrix can achieve a decrease of up to 85% in greenhouse gas emissions.

Conversely, if the intensive planning of adequate geographical location is essential in the implementation policies of renewable energies, the economic aspect defines the choice of the energy source. Thus, economic evidence reveals that the preference for fossil resources. This is because the energy from coal and natural gas have lower values, around 0.042 and 0.048 USD/kWh, respectively. In contrast, renewable sources represent an investment of 0.085 USD/kWh for photovoltaic, 0.056 USD/kWh for wind, and 0.047 USD/kWh for hydroelectric [95].

Finally, beyond the financial issues, there are still some environmental problems to be analyzed, since only these two categories do not verify the total efficiency and superiority of renewable energies. And, therefore, to resolve these problems, more detailed data about the environmental burdens related to the other impact categories must be elucidated, in order to bring more assertive conclusions under the proposed models for the implementation of renewable energies to processes and products based on microalgae.

3.6. Beyond the environmental indicators

As widespread discussed, countless decision-makers incorporate the term sustainability as part of aggregation value to their processes and products. But, can microalgae-based processes and products be considered sustainable?

Indeed, since the delineation of the term sustainability, many theories have been generated regarding the veracity of the criteria for considering a sustainable process. However, many problems remain unsolved. Thus, the most widespread theory among managers indicates compensation criteria. In short, environmental performance is directly related to the capacity for economic growth. That is, if economic growth is equal to or greater than the cost of compensating for deteriorated environmental performance, this process can be considered sustainable [96].

In view of this argument, in which return capital presupposes natural capital, the most important point for the consolidation of any bioprocess is the economy [97]. In this sense, the hotspot of microalgae-based processes and products is characterized by the excessive demand for energy. Therefore, these processes need reforms based on the intensification and integration of processes. Among some measures, the increase in biomass productivity, such as net return energy in cultivations, is the first factor to be circumvented [98]. In addition, improvements and technological advances in the downstream stages can be overwhelming. This is because the combination of effective lipid harvesting and extraction methods should increase production efficiency, resulting in decreased energy requirements. In parallel, as long as this is possible, microalgae-based products can also contribute to improving the availability of fossil fuel resources, replacing some use of non-renewable resources, and adding to a reliable and decentralized energy supply.

Additionally, the exploration of microalgal intracellular bioproducts cannot continue to be the main focus of exploration. Biorefinery approach measures are crucial. This is because this concept aims to achieve multiple spectra of valuable products through the transformation of biomass [99]. In this context, the current market trend and the growing consumer demand for healthy products have strengthened microalgae as an emerging source of natural nutrient-rich food supplements.

It is estimated that more than the global production of microalgal supplements, such as *Chlorella vulgaris* biomass powder, represents about 5279.53 Mton/year, representing an average growth rate of > 6.1%. Likewise, the whole dried biomass of *Arthrospira platensis* for human use exceeds 3000 tons/year [100]. Considering the production price and average selling price, these processes together represent a net return of approximately USD 1.5 billion for whole dried biomass [101,102]. This can be explained due to supply and demand, as so far, there is no substitute product of the same level to microalgal products [103].

The market price related to microalgal pigments behaves similarly. The global pigment market is expected to grow with a compound annual growth rate of around 5.1% over the next decade, reaching approximately USD 2.0 billion by 2022 [104]. Unlike whole dried biomass, microalgal pigments have more affordable substitutes. However, competition for synthetic pigments is selective, since the improved deposition of natural microalgal pigments associated with consumer demand and regulatory requirements, as well as the appeal to health are relevant in the final choice of the product [105].

Likewise, polyunsaturated fatty acids have been recognized for playing an important role in human health and nutrition. In view of this aspect, the global EPA/DHA market showed a notable rise. In the last few years, about 124 thousand tons have been consumed, representing approximately USD 2.17 billion. In addition, the current market predicts that 241 thousand tons will be valued at USD 4.0 billion until 2024 [82,106]. Although it presents a positive scenario, oils based on microalgae have an analogous competitor, fish oil. This is because, through research, it was possible to identify that fish are not able to synthesize compounds such as DHA and EPA, are then obtained through food, in this case, based on microalgae. Thus, the similar formulation of fish oils compared to microalgal oils seeks to maintain the same concentrations of active ingredients in order to support competition in the market [107].

Notoriously, the net return values of microalgae products show undeniable compensations in the market. For this reason, sustainability, as it is currently employed, verifies processes based on microalgae with high sustainable potential. However, given the environmental scenario of the processes, are the most expensive products really the most sustainable? Furthermore, are consumers willing to pay the high price related to environmental quality?

Actually, from the acquisition of raw materials to the shipment of the final product, almost all stages of the manufacturing process and production of sustainable products cost more than traditional products [108]. Consequently, this trend reflects consumer behavior when buying sustainable products at a higher price. Therefore, to extract the willingness of consumers to pay for environmental quality, companies rely on eco-labeling programs to verify that their products comply with the standards determined by government incentive programs. However, most consumers are not willing to pay more or invest in sustainable products for long-term environmental benefits. Thus, an effective measure is based on supply and demand models. So, only an increase in demand can result in a reduction in the price of the product [109].

It is known that price is, therefore, a barrier to buying behavior. However, when consumers are fully convinced that the product meets the environmental criteria and recognizes the potential benefits of the product, consumers do not consider it to be the determining factor [110]. This usually happens in natural products, as is the case with polyunsaturated fatty acids and pigments. For example, changes in legislation on the use of synthetic dyes and consumer awareness of the health benefits associated with natural food colors have increased demand for natural products, making synthetic routes less desirable even with cleaner environmental performance, which justifies the considerable efforts that are being paid in the promotion and optimization of microalgae-based processes [111]. Likewise, essential fatty acids such as EPA can be produced by two separate consolidated routes, and even with lower environmental performance (autotrophic EPA), there is still demand this product. The same purchase profile is observed for products such as whole dried biomass (See Section 3.1). Since there is no similar alternative available on the market, consumers will initially assess their purchase purposes, then assess the amount to be paid and only then consider the environmental character.

Therefore, it is worth mentioning that the technical and scientific notion of sustainable development, so far, does not cover the core of the environmental crisis. Thus, it is prospective that a political-governmental reorientation is necessary so that, in fact, there are ways to develop technologies that use fewer natural resources and that provide products with the same quality, without substantially impacting ecosystems.

Finally, there is a strong emerging convergence between the transfer guidelines for clean technologies. To move forward in this transition, companies must face great uncertainty about the expected return generated by innovation. Therefore, in the near future, current technologies will have to be abandoned, and industrial managers will have to pay the price, so that in the medium to long term, industrial technologies will evolve.

4. Conclusions

The ad hoc detailing of environmental impacts provided in this study allowed significantly contribute to filling the research gaps in view of the bottlenecks of the development and optimization of the operational parameters of the microalgae-based processes and products. Besides, the outcomes founded indicated that the main immediate

measure to be taken is the simplification of the energy inputs of all the processing stages. However, although many of the strategies discussed have been demonstrated as a valuable and powerful way to design technologies, it is worth noting that only the rational vision of systematic integration into a strategic biorefinery model can play increasing roles to achieve, in the future perspectives, the desired economically viable and environmentally sustainable seal of microalgae-based processes and products.

CRediT authorship contribution statement

Mariany C. Deprá:Conceptualization, Methodology, Data curation, Writing - original draft.**Ihana A. Severo**:Methodology, Validation.**Aline M. dos Santos**:Methodology, Validation.**Leila Q. Zepka**:Supervision, Funding acquisition.**Eduardo Jacob-Lopes**:Conceptualization, Project administration, Writing - review & editing.

Declaration of competing interest

The authors declare that there is no conflict of interest regarding the publication of the manuscript.

Acknowledgement

The authors would like to thank the National Council for Scientific and Technological Development (CNPq) – Brazil, and the Coordination of Improvement of Higher Education Personnel (CAPES), Finance Code 001.

Statement of informed consent, human/animal rights

No conflicts, informed consent, or human or animal rights are applicable to this study.

Appendix A. Supplementary data

Supplementary data to this article can be found online at https://doi.org/10.1016/j.algal.2020.102056.

References

[1] R. Miehe, T. Bauernhansl, M. Beckett, C. Brecher, A. Demmer, W.G. Drossel, J. Herbelt, The biological transformation of industrial manufacturing-technologies, status and scenarios for a sustainable future of the German manufacturing industry, J. Manuf. Syst. 54 (2020) 50–61, https://doi.org/10.1016/j.jmsy.2019.11.006.

[2] M. Rodrigues, J.A. Camacho, The development of trade of biomass in Spain: a raw material equivalent approach, Biomass Bioenergy 133 (2020) 105450, , https://doi.org/10.1016/j.biombioe.2019.105450.

[3] J.G. de Carvalho, A.I. Magalhães Jr., G.V. de Melo Pereira, A.B.P. Medeiros, E.B. Sydney, C. Rodrigues, C.R. Soccol, Microalgal biomass pretreatment for integrated processing into biofuels, food, and feed, Bioresour. Technol. (2020) 122719, , https://doi.org/10.1016/j.biortech.2019.122719.

[4] C.A.S. Rais, S.Z. Baca, L.A. van den Broek, C. van den Berg, R.H. Wijffels, M.H. Eppink, Selective fractionation of free glucose and starch from microalgae using aqueous two-phase systems, Algal Res. 46 (2020) 101801, , https://doi.org/10.1016/j.algal.2020.101801.

[5] FAO, Food and Agriculture Organization of the United Nations, The Global Status of Seaweed Production, Trade and Utilization, Rome, Italy, (2018) (ISBN: 978-92-5-130870-7).

[6] M.P. Caporgno, L. Böcker, C. Mösner, E. Stirnemann, T. Haberkorn, H. Adelmann, A. Mathys, Extruded meat analogues based on yellow, heterotrophically cultivated *Auxenochlorella protothecoides* microalgae, Innovative Food Sci. Emerg. Technol. 59 (2020) 102275, , https://doi.org/10.1016/j.ifset.2019.102275.

[7] R. Purcell, F. Dotto, L. Pezzolesi, D. Maracza, N. Greggio, S. Righi, Comparative life cycle assessment of microalgae cultivation for non-energy purposes using different carbon dioxide sources, Sci. Total Environ. (2020) 137714, , https://doi.org/10.1016/j.scitotenv.2020.137714.

[8] A. Banerjee, C. Banerjee, S. Negi, J.S. Chang, P. Shukla, Improvements in algal lipid production: a systems biology and gene editing approach, Crit. Rev. Biotechnol. 38 (3) (2018) 369–385, https://doi.org/10.1080/07388551.2017.1356803.

[9] S. Jagadevan, A. Banerjee, C. Banerjee, C. Guria, R. Tiwari, M. Baweja, P. Shukla, Recent developments in synthetic biology and metabolic engineering in microalgae towards biofuel production, Biotechnology for biofuels 11 (1) (2018) 185, https://doi.org/10.1186/s13068-018-1181-1.

[10] A. Banerjee, N. Kumar, S.J. Varjani, C. Guria, R. Bandopadhyay, P. Shukla, C. Banerjee, Computational modelling and prediction of microalgae growth focused towards improved lipid production, Energy, Environment, and Sustainability (2017) 223–232, https://doi.org/10.1007/978-981-10-7434-9_13.

[11] D.K. Saini, S. Pabbi, P. Shukla, Cyanobacterial pigments: perspectives and biotechnological approaches, Food Chem. Toxicol. 120 (2018) 616–624, https://doi.org/10.1016/j.fct.2018.08.052.

[12] D.K. Saini, D. Yadav, S. Pabbi, D. Chhabra, P. Shukla, Phycobiliproteins from *Anabaena variabilis* CCC821 and its production enhancement strategies using combinatory evolutionary algorithm approach, Bioresour. Technol. (2020) 123347, , https://doi.org/10.1016/j.biortech.2020.123347.

[13] A.K. Kumar, S. Sharma, G. Dixit, E. Shah, A. Patel, Techno-economic analysis of microalgae production with simultaneous dairy effluent treatment using a pilot-scale high volume V-shape pond system, Renew. Energy 145 (2020) 1620–1632, https://doi.org/10.1016/j.renene.2019.07.087.

[14] S.B. Unmalynna, D. Sahoo, A. Pandey, Microalgal biorefineries for industrial products, Microalgae Cultivation for Biofuels Production, 2020, pp. 187–195, , https://doi.org/10.1016/b978-0-12-817536-1.00013-6.

[15] O. Paladino, M. Neviani, Scale-up of photo-bioreactors for microalgae cultivation by π-theorem, Biochem. Eng. J. (2020) 107398, , https://doi.org/10.1016/j.bej.2019.107398.

[16] X.B. Tan, M.K. Lam, Y. Uemura, J.W. Lim, C.Y. Wong, K.T. Lee, Cultivation of microalgae for biodiesel production: a review on upstream and downstream processing, Chin. J. Chem. Eng. 26 (1) (2018) 17–30, https://doi.org/10.1016/j.cjche.2017.08.010.

[17] L. de Souza Leite, P.R. dos Santos, L.A. Daniel, Microalgae harvesting from wastewater by pH modulation and flotation: assessing and optimizing operational parameters, J. Environ. Manag. 254 (2020) 109825, , https://doi.org/10.1016/j.jenvman.2019.109825.

[18] M. Bussa, C. Zollfrank, H. Röder, Life-cycle assessment and geospatial analysis of integrating microalgae cultivation into a regional economy, J. Clean. Prod. 243 (2020) 118630, , https://doi.org/10.1016/j.jclepro.2019.118630.

[19] C. Ghenai, M. Albawab, M. Bettayeb, Sustainability indicators for renewable energy systems using multi-criteria decision-making model and extended SWARA/ARAS hybrid method, Renew. Energy 146 (2020) 580–597, https://doi.org/10.1016/j.renene.2019.06.157.

[20] U. Uzar, Is income inequality a driver for renewable energy consumption? J. Clean. Prod. 255 (2020) 120287, , https://doi.org/10.1016/j.jclepro.2020.120287.

[21] M.C. Deprá, A.M. dos Santos, I.A. Severo, A.B. Santos, L.Q. Zepka, E. Jacob-Lopes, Microalgal biorefineries for bioenergy production: can we move from concept to industrial reality? BioEnergy Research 11 (4) (2018) 727–747, https://doi.org/10.1007/s12155-018-9934-z.

[22] M.C. Deprá, R.R. Dias, I.A. Severo, C.R. de Menezes, L.Q. Zepka, E. Jacob-Lopes, Carbon dioxide capture and use in photobioreactors: the role of the carbon dioxide loads in the carbon footprint, Bioresour. Technol. (2020) 123745, , https://doi.org/10.1016/j.biortech.2020.123745.

[23] C. Quiroz-Arita, M.L. Blaylock, P.E. Ghamgosha, T.H. Bradley, T. Dempster, J. McGowen, R. Davis, A dynamic thermal algal growth model for pilot-scale open-channel raceways, Bioresource Technology Reports (2020) 100405, , https://doi.org/10.1016/j.biteb.2020.100405.

[24] I.A. Severo, M.C. Deprá, R.R. Dias, J.S. Barin, C.R. de Menezes, R. Wagner, L.Q. Zepka, E. Jacob-Lopes, Bio-combustion of petroleum coke: the process integration with photobioreactors. Part II-sustainability metrics and biseconomy, Chem. Eng. Sci. 213 (2020) 115412, , https://doi.org/10.1016/j.ces.2019.115412.

[25] K.S. Khoo, K.W. Chew, G.Y. Yew, W.H. Leong, Y.H. Chai, P.L. Show, W.H. Chen, Recent advances in downstream processing of microalgae lipid recovery for biofuel production, Bioresour. Technol. (2020) 122996, , https://doi.org/10.1016/j.biortech.2020.122996.

[26] A.M. dos Santos, M.C. Deprá, A.J. Cichoski, L.Q. Zepka, E. Jacob-Lopes, Sustainability metrics on microalgae-based wastewater treatment system, Desalin. Water Treat. 185 (2020) 51–61, https://doi.org/10.5004/dwt.2020.25397.

[27] S. Kavitha, M. Gunasekaran, Microalgae based biorefinery promoting circular bioeconomy techno economic and life cycle analysis, Bioresour. Technol. (2020) 122822, , https://doi.org/10.1016/j.biortech.2020.122822.

[28] ISO (International Organization for Standardization), ISO 14040:2006(E) Environmental Management–Life Cycle Assessment – Principles and Framework, (2006).

[29] Y.K. Lee, C.S. Low, Productivity of outdoor algal cultures in enclosed tubular photobioreactor, Biotechnol. Bioeng. 40 (9) (1992) 1119–1122, https://doi.org/10.1002/bit.260400917.

[30] M. Marsullo, A. Mian, A.V. Ensinas, G. Manente, A. Lazzaretto, F. Marechal, Dynamic modeling of the microalgae cultivation phase for energy production in open raceway ponds and flat panel photobioreactors, Frontiers in Energy Research 3 (2015) 41, https://doi.org/10.3389/fenrg.2015.00041.

[31] J.Q. Albarelli, D.T. Santos, A.V. Ensinas, F. Marechal, M.J. Cocero, M.A.A. Meireles, Product diversification in the sugarcane biorefinery through algae growth and supercritical CO_2 extraction: thermal and economic analysis, Renew. Energy 129 (2018) 776–785, https://doi.org/10.1016/j.renene.2017.05.022.

[32] L.R. Kumar, S.K. Yellapu, X. Zhang, R.D. Tyagi, Energy balance for biodiesel production processes using microbial oil and scum, Bioresour. Technol. 272 (2019) 379–388, https://doi.org/10.1016/j.biortech.2018.10.071.

[33] S. Li, S. Luo, R. Guo, Efficiency of CO_2 fixation by microalgae in a closed raceway pond, Bioresour. Technol. 136 (2013) 367–372, https://doi.org/10.1016/j.biortech.2013.03.025.

[34] M.A. Borowitzka, L.J. Borowitzka, D. Kessly, Effects of salinity increase on carotenoid accumulation in the green alga *Dunaliella salina*, J. Appl. Phycol. 2 (2) (1990) 111–119, https://doi.org/10.1007/BF00023372.

[35] Boussiba, S., Vonshak, A., Cohen, Z., Richmond, A. (2000). Procedure for large-scale production of astaxanthin from *Haematococcus*. U.S. Patent No. 6, 022, 701. Washington, DC: U.S. Patent and Trademark Office.

[36] S.T. Eriksen, Production of phycocyanin—a pigment with applications in biology, biotechnology, foods and medicine, Appl. Microbiol. Biotechnol. 80 (1) (2008) 1–14, https://doi.org/10.1007/s00253-008-1542-y.

[37] G. Britton, S. Liaaen-Jensen, H. Pfander, Carotenoids: a colourful history, CarotoNature, 1st ed., 2017 (236p).

[38] L. Begejc-Rzekonska, J. Baranym, β-Carotene—properties and production methods, Food Quality and Safety 2 (2) (2018) 69–74, https://doi.org/10.1093/fqsafe/fyy004.

[39] F. Pagels, A.C. Guedes, H.M. Amaro, A. Kijjoa, V. Vasconcelos, Phycobiliproteins from cyanobacteria: chemistry and biotechnological applications, Biotechnol. Adv. 37 (3) (2019) 422–443, https://doi.org/10.1016/j.biotechadv.2019.02.010.

[40] W. Barclay, E. Apt, X.D. Dong, Commercial production of microalgae via fermentation, Handbook of Microalgal Culture: Applied Phycology and Biotechnology, Blackwell, Chichester, 2013, pp. 134–145, , https://doi.org/10.1002/9781118567166.ch9.

[41] G.C. Zittelli, F. Lavista, A. Bastianini, L. Rodolfi, M. Vincenzini, M.R. Tredici, Production of eicosapentaenoic acid by *Nannochloropsis* sp. cultures in outdoor tubular photobioreactors, J. Biotechnol. 70 (1–3) (1999) 299–312, https://doi.org/10.1016/S0168-1656(99)00082-6.

[42] A. Mendes, A. Reis, R. Vasconcelos, P. Guerra, T.L. da Silva, *Crypthecodinium cohnii* with emphasis on DHA production: a review, J. Appl. Phycol. 21 (2) (2009) 199–214, https://doi.org/10.1007/s10811-008-9351-3.

[43] Y. Ouanaz, G.C. Izbil, Effect of light path length of tubes on growth rate of *Nannochloropsis oculata* using industrial scale tubular photobioreactor in the marine hatchery, Feb Fresenius Environmental Bulletin 4783 (2017).

[44] M. Goedkoop, R. Heijungs, M. Huijbregts, A. De Schryver, J. Struijs, R. Van Zelm, ReCiPe 2008, A life cycle impact assessment method which comprises harmonised category indicators at the midpoint and the endpoint level, 1 (2009) 1–126.

[45] B. Liratte, B. Guillaume, J. Kim, B. Birregah, Modeling cumulative effects in life cycle assessment: the case of fertilizer in wheat production contributing to the global warming potential, Sci. Total Environ. 481 (2014) 588–595, https://doi.org/10.1016/j.scitotenv.2014.02.020.

[46] M.Z. Hauschild, R. Wenzel, Environmental assessment of products, Scientific Background, 1st edition, vol. Volume 2, Springer, US, 1998(566p).

[47] A.Y. Hoekstra, A critique on the water-scarcity weighted water footprint in LCA, Ecol. Indic. 66 (2016) 564–573, https://doi.org/10.1016/j.ecolind.2016.02.026.

[48] M.J. Lathuillière, E.J. Miranda, C. Bulle, E.G. Gouin, M.S. Johnson, Land occupation and transformation impacts of soybean production in southern Amazonia, Brazil, J. Clean. Prod. 149 (2017) 680–689, https://doi.org/10.1016/j.jclepro.2017.02.120.

[49] ILCD, International Reference Life Cycle Data System Handbook: General Guide for Life Cycle Assessment – Detailed Guidance, 1st edition, Institute for Environment and Sustainability, Joint Research Centre, European Commission, Luxembourg, 2010.

[50] G. Yadav, B.K. Dubey, R. Sen, A comparative life cycle assessment of microalgae production by CO_2 sequestration from flue gas in outdoor raceway ponds under batch and semi-continuous regime, J. Clean. Prod. (2020) 120703, , https://doi.org/10.1016/j.jclepro.2020.120703.

[51] S.L. Pahl, A.K. Lee, T. Kalaitzidis, P.J. Ashman, S. Sathe, D.M. Lewis, Harvesting, thickening and dewatering microalgae biomass, Algae for biofuels and energy, Springer, Dordrecht, 2013, pp. 165–185, , https://doi.org/10.1007/978-94-007-5479-9_10.

[52] E.M. Grima, E.H. Belarbi, F.A. Fernández, A.R. Medina, Y. Chisti, Recovery of microalgal biomass and metabolites: process options and economics, Biotechnol. Adv. 20 (7–8) (2003) 491–515, https://doi.org/10.1016/S0734-9750(02)00050-2.

[53] E.E. Powell, M.L. Mapiour, R.W. Evitts, G.A. Hill, Growth kinetics of *Chlorella vulgaris* and its use as a cathodic half cell, Bioresour. Technol. 100 (1) (2009) 269–274, https://doi.org/10.1016/j.biortech.2008.05.022.

[54] P.G. Nieto, E. García-Gonzalo, J.A. Fernández, C.D. Muñiz, A hybrid PSO optimized SVM-based model for predicting a successful growth cycle of the *Spirulina platensis* from raceway experiments data, J. Comput. Appl. Math. 291 (2016) 293–303, https://doi.org/10.1016/j.cam.2015.01.009.

[55] I. Michalak, M. Mironiuk, K. Godlewska, J. Tuhodz, K. Muryn, Arthrospira (Spirulina) platensis an effective biosorbent for nutrients, Process Biochem. 88 (2020) 129–137.

[56] M.V. Vieira, S.M. Oliveira, I.R. Amado, L.H. Fasolin, A.A. Vicente, L.M. Pastrana, P. Fuciños, 3D printed functional cookies fortified with *Arthrospira platensis*: evaluation of its antioxidant potential and physical-chemical characterization, Food Hydrocoll. (2020) 105893, , https://doi.org/10.1016/j.foodhyd.2020.105893.

[57] S. Grahl, M. Strack, A. Mensching, D. Mörlein, Alternative protein sources in Western diets: food product development and consumer acceptance of spirulina-filled pasta, Food Qual. Prefer. (2020) 103933, , https://doi.org/10.1016/j.foodqual.2020.103933.

[58] G. Carelli, L. Neutsch, R. Carpine, S. Tevere, F. Giuffrida, Z. Rohfritsch, A. Mathys, *Chlorella vulgaris* in a heterotrophic bioprocess: study of the lipid bioaccessibility and oxidative stability, Algal Res. 45 (2020) 101754, , https://doi.org/10.1016/j.algal.2019.101754.

[59] Q. Yu, H. Wang, X. Li, Y. Yin, S. Qin, R. Ge, Enhanced biomass and CO_2 sequestration of *Chlorella vulgaris* using a new mixotrophic cultivation method, Process Biochem. 90 (2020) 168–176, https://doi.org/10.1016/j.procbio.2019.11.022.

[60] MHLW, Ministry of Health, Labor and Welfare of Japan List of Existing Food Additives: Notification N. 120 of the Ministry of Health and Welfare, (1996).

[61] EC-Regulation, Regulation N. 258/97 of the European Parliament and of the Council Concerning Novel Foods and Novel Food Ingredients, (1997).

[62] ANVISA-Brazilian Health Regulatory Agency, Normative Instruction No. 28 of Ministry of Health, (2018).

[63] FDA-Food and Drug Administration, USA, Substances generally recognized as safe, viewed 21 June, https://www.federalregister.gov/d/2016-19164/p-1, (2019).

[64] K. Kyriakopoulou, S. Papadaki, M. Krokida, Life cycle analysis of β-carotene extraction techniques, J. Food Eng. 167 (2015) 51–58, https://doi.org/10.1016/j.jfoodeng.2015.03.008.

[65] P. Pérez-López, S. González-García, C. Jeffryes, S.N. Agathos, E. McHugh, D. Walsh, M.T. Moreira, Life cycle assessment of the production of the red antioxidant carotenoid astaxanthin by microalgae: from lab to pilot scale, J. Clean. Prod. 64 (2014) 332–344, https://doi.org/10.1016/j.jclepro.2013.07.011.

[66] S. Papadaki, K. Kyriakopoulou, I. Tzovenis, M. Krokida, Environmental impact of phycocyanin recovery from *Spirulina platensis* cyanobacterium, Innovative Food Sci. Emerg. Technol. 44 (2017) 217–223, https://doi.org/10.1016/j.ifset.2017.02.014.

[67] M. Borowitzka, Commercial-scale production of microalgae for bioproducts, Blue Biotechnology: Production and Use of Marine Molecules, vol. 1, 2018, pp. 33–65, , https://doi.org/10.1002/9783527801718.ch2.

[68] E.A. Cezare-Gomes, L. del Carmen Mejia-da-Silva, L.S. Pérez-Mora, M.C. Matsudo, L.S. Ferreira-Camargo, A.K. Singh, J.C.M. de Carvalho, Potential of microalgae carotenoids for industrial application, Appl. Biochem. Biotechnol. 188 (3) (2019) 602–634, https://doi.org/10.1007/s12010-018-02945-4.

[69] M.N. Ranmuni, T.U. Aryadasa, P.H.V. Nimarshana, R.A. Attalage, Comparative assessment on the extraction of carotenoids from microalgal sources: Astaxanthin from *H. pluvialis* and β-carotene from *D. salina*, Food Chem. 277 (2019) 128–134, https://doi.org/10.1016/j.foodchem.2018.10.066.

[70] A. Molino, S. Mehariya, G. Di Sanzo, V. Larocca, M. Martino, G.P. Leone, D. Musmarra, Recent developments in supercritical fluid extraction of bioactive compounds from microalgae: role of key parameters, technological achievements and challenges, Journal of CO_2 Utilization 36 (2020) 196–209, https://doi.org/10.1016/j.jcou.2019.11.014.

[71] R.K. Saini, Y.S. Keum, Carotenoid extraction methods: a review of recent developments, Food Chem. 240 (2018) 90–103, https://doi.org/10.1016/j.foodchem.2017.07.099.

[72] X. Li, J. Liu, G. Chen, J. Zhang, C. Wang, B. Liu, Extraction and purification of eicosapentaenoic acid and docosahexaenoic acid from microalgae: a critical review, Algal Res. 43 (2019) 101619, , https://doi.org/10.1016/j.algal.2019.101619.

[73] Y. Jiang, F. Chen, S.Z. Liang, Production potential of docosahexaenoic acid by the heterotrophic marine dinoflagellate *Cryptheodinium cohnii*, Process Biochem. 34 (6–7) (1999) 633–637, https://doi.org/10.1016/S0032-9592(98)00134-4.

[74] H.W. Yen, I.C. Hu, C.Y. Chen, D. Nagarajan, J.S. Chang, Design of photobioreactors for algal cultivation, Biofuels from Algae, Elsevier, 2019, pp. 225–256, , https://doi.org/10.1016/B978-0-444-64192-2.00010-X.

[75] Bailey, R. B., DiMasi, D., Hansen, J. M., Mirzoeva, P. J., Brecker, C. M., Veeder III, G. T., Barclay, W. R. (2003). Enhanced production of lipids containing polyenoic fatty acid by very high density cultures of eukaryotic microbes in fermenters. U.S. Patent No. 6, 607, 900. Washington, DC: U.S. Patent and Trademark Office.

[76] Y. Zhang, V. Ward, D. Dennis, N.V. Plechkova, R. Armenta, L. Rehmann, Efficient extraction of a docosahexaenoic acid (DHA)-rich lipid fraction from *Thraustochytrium* sp. using ionic liquids, Materials 11 (10) (2018) 1986, https://doi.org/10.3390/ma11101986.

[77] S. Yang, C. Qin, H. Wang, R. Li, S. Tian, Study on supercritical extraction of lipids and enrichment of DHA from oil-rich microalgae, J. Supercrit. Fluids 57 (1) (2011) 44–49, https://doi.org/10.1016/j.supflu.2011.01.010.

[78] H.W. Yen, S.C. Yang, C.H. Chen, J.S. Chang, Supercritical fluid extraction of valuable compounds from microalgal biomass, Bioresour. Technol. 184 (2015) 291–296, https://doi.org/10.1016/j.biortech.2014.10.030.

[79] Q. Emparan, Y.S. Jye, M.R. Danquah, R. Harun, Cultivation of *Nannochloropsis* sp. microalgae in palm oil mill effluent (POME) media for phycoremediation and biomass production: effect of microalgae cells with and without beads, Journal of Water Process Engineering 33 (2020) 101043, , https://doi.org/10.1016/j.jwpe.2019.101043.

[80] N. Uduman, Y. Qi, M.K. Danquah, G.M. Forde, A. Hoadley, Dewatering of microalgal cultures: a major bottleneck to algae-based fuels, Journal of Renewable and Sustainable Energy 2 (1) (2010) 012701, , https://doi.org/10.1063/1.3294480.

[81] G. Assegehegn, E. Brito-de la Fuente, J.M. Franco, C. Gallegos, An experimental-based approach to construct the process design space of a freeze-drying process: an effective tool to design an optimum and robust freeze-drying process for pharmaceuticals, J. Pharm. Sci. 109 (1) (2020) 785–796, https://doi.org/10.1016/j.xphs.2019.07.001.

[82] A. Wang, K. Yan, B. Chu, M. Noor, N.T. Lin, D. Samarasinghe, J. Chang, Microalgae as a Mainstream Food Ingredient: Demand and Supply Perspective, In Microalgae Biotechnology for Food, Health and High Value Products, Springer,

Singapore, 2020, pp. 29–79 (ISBN 978-981-15-0169-2).
[83] F. Liu, Y. Lei, J. Shi, L. Zhou, Z. Wu, Y. Dong, W. Bi, Effect of microbial nutrients supply on coal bio-desulfurization, J. Hazard. Mater. 384 (2020) 121324, , https://doi.org/10.1016/j.jhazmat.2019.121324.
[84] A. Evans, V. Strezov, T.J. Evans, Assessment of sustainability indicators for renewable energy technologies, Renew. Sust. Energ. Rev. 13 (5) (2009) 1082–1088, https://doi.org/10.1016/j.rser.2008.03.008.
[85] H. Schaber, Water use in renewable and conventional electricity production, Energy Sources 26 (3) (2004) 309–322 (ISSN 1556-7036).
[86] X. Castroa, M. de Castro, D. Carvalho, M. Gómez-Gesteira, On the suitability of offshore wind energy resource in the United States of America for the 21st century, Appl. Energy 262 (2020) 114537, , https://doi.org/10.1016/j.apenergy.2020.114537.
[87] S. Schade, T. Meier, A comparative analysis of the environmental impacts of cultivating microalgae in different production systems and climatic zones: a systematic review and meta-analysis, Algal Res. 40 (2019) 101485, , https://doi.org/10.1016/j.algal.2019.101485.
[88] S.F. Siqueira, M.M. Maroneze, R.R. Dias, E.G. Vendruscolo, R. Wagner, C.R. Menezes, L.Q. Zepka, E. Jacob-Lopes, Mapping the performance of photobioreactors for microalgae cultivation: geographic position and local climate, J. Chem. Technol. Biotechnol. (2020), https://doi.org/10.1002/jctb.6423.
[89] E. Álvarez, E. Valero, N. de la Torre-Rodríguez, C. Acuña-Alonso, Influence of small hydroelectric power stations on river water quality, Water 12 (2) (2020) 312, https://doi.org/10.3390/w12020312.
[90] L. Gnatyshyna, V. Khoma, O. Mishchuk, V. Martinyuk, G. Springe, O. Stolfar, Multi-marker study of the responses of the Unio tumidus from the areas of small and micro hydropower plants at the Dniester River basin, Ukraine, Environ. Sci. Pollut. Res. (2020) 1–12, https://doi.org/10.1007/s11356-020-07698-6.
[91] J. Opgrand, P.V. Preckel, P.T. Sparrow, G. Thomas, D.P. Loucks, Restoring the natural flow regime of a large hydroelectric complex: costs and considerations, Energy 190 (2020) 116260, , https://doi.org/10.1016/j.energy.2019.116260.
[92] J. Reles, J. Yarnold, J. Wolf, E. Stephens, K. Hussey, B. Hankamer, Charting a development path to deliver cost competitive microalgae-based fuels, Algal Res. 45 (2020) 101721, , https://doi.org/10.1016/j.algal.2019.101721.
[93] E.G. Nwoba, D.A. Parlevliet, D.W. Laird, K. Alameh, N.R. Moheimani, Pilot-scale self-cooling microalgal closed photobioreactor for biomass production and electricity generation, Algal Res. 45 (2020) 101731, , https://doi.org/10.1016/j.algal.2019.101731.
[94] J. Lelieveld, K. Klingmüller, A. Pozzer, R.T. Burnett, A. Haines, V. Ramanathan, Effects of fossil fuel and total anthropogenic emission removal on public health and climate, Proc. Natl. Acad. Sci. 116 (15) (2019) 7192–7197, https://doi.org/10.1073/pnas.1819989116.
[95] IRENA, Renewable Power Generation Costs in 2018, International Renewable Energy Agency, Abu Dhabi, 2019 (ISBN 978-92-9260-126-3).
[96] D. Jamieson, Sustainability and beyond, Ecol. Econ. 24 (2–3) (1998) 183–192, https://doi.org/10.1016/S0921-8009(97)00142-0.
[97] A.K. Patel, Y.Y. Choi, S.J. Sim, Emerging prospects of mixotrophic microalgae: way forward to sustainable bioprocess for environmental remediation and cost-effective biofuels, Bioresour. Technol. (2020) 122741, , https://doi.org/10.1016/j.biortech.2020.122741.
[98] L.A. Severo, M.C. Deprá, J.S. Barin, R. Wagner, C.R. de Menezes, L.Q. Zepka, E. Jacob-Lopes, Bio-combustion of petroleum coke: the process integration with photobioreactors, Chem. Eng. Sci. 177 (2018) 433–438.
[99] L.A. Severo, S.F. Siqueira, M.C. Deprá, M.M. Maroneze, L.Q. Zepka, E. Jacob-Lopes, Biodiesel facilities: what can we address to make biorefineries commercially competitive? Renew. Sust. Energ. Rev. 112 (2019) 686–705, https://doi.org/10.1016/j.rser.2019.06.020.
[100] Y. Torres-Tiji, F.J. Fields, S.P. Mayfield, Microalgae as a future food source, Biotechnol. Adv. (2020) 107536, , https://doi.org/10.1016/j.biotechadv.2020.107536.
[101] W. Levasseur, P. Perré, V. Pozzobon, A review of high value-added molecules production by microalgae in light of the classification, Biotechnol. Adv. (2020) 107545, , https://doi.org/10.1016/j.biotechadv.2020.107545.
[102] S. Parsons, M.J. Allen, C.J. Chuck, Coproducts of algae and yeast-derived single cell oils: a critical review of their role in improving biorefinery sustainability, Bioresour. Technol. (2020) 122862, , https://doi.org/10.1016/j.biortech.2020.122862.
[103] E. Jacob-Lopes, M.M. Maroneze, M.C. Deprá, R.B. Sartori, R.R. Dias, L.Q. Zepka, Bioactive food compounds from microalgae: an innovative framework on industrial biorefineries, Curr. Opin. Food Sci. 25 (2019) 1–7, https://doi.org/10.1016/j.cofs.2018.12.003.
[104] T. Butler, Y. Golan, Astaxanthin production from microalgae, Microalgae Biotechnology for Food, Health and High Value Products, Springer, Singapore, 2020, pp. 175–242 (DOI:ISBN 978-981-15-0169-2).
[105] M.M. Maroneze, E. Jacob-Lopes, L.Q. Zepka, M. Roca, A. Pérez-Gálvez, Esterified carotenoids as new food components in cyanobacteria, Food Chem. 287 (2019) 295–302, https://doi.org/10.1016/j.foodchem.2019.02.102.
[106] T.S. Lopes, P. Muniz, C. Silva, A. Reis, The dark side of microalgae biotechnology: a heterotrophic biorefinery platform directed to ω-3 rich lipid production, Microorganisms 7 (12) (2019) 670, https://doi.org/10.3390/microorganisms7120670.
[107] R. Katiyar, A. Arora, Health promoting functional lipids from microalgae post: a review, Algal Res. 46 (2020) 101800, , https://doi.org/10.1016/j.algal.2020.101800.
[108] K.J. Chen, T.L. Marsh, P.R. Toaer, S.P. Galitzato, Biotechnology to sustainability: consumer preferences for food products grown on biodegradable mulches, Food Res. Int. 116 (2019) 200–210, https://doi.org/10.1016/j.foodres.2018.08.013.
[109] Y. Li, Competing eco-labels and product market competition, Resour. Energy Econ. 60 (2020) 101149. , https://doi.org/10.1016/j.reseneeco.2020.101149.
[110] A.T. Nguyen, L. Parker, L. Brennan, S. Lockrey, A consumer definition of eco-friendly packaging, J. Clean. Prod. 252 (2020) 119792, , https://doi.org/10.1016/j.jclepro.2019.119792.
[111] A.M. Santos, M.C. Deprá, L.Q. Zepka, E. Jacob-Lopes, Sustainability metrics in the microalgae-based pigments production: a life cycle assessment approach, Pigments from Microalgae Handbook, Springer Nature Switzerland AG, 2020.

Desalination and Water Treatment
www.deswater.com

doi: 10.5004/dwt.2020.25397

185 (2020) 51–61
May

Sustainability metrics on microalgae-based wastewater treatment system

Aline Meireles dos Santos, Mariany Costa Deprá, Alberto Meireles dos Santos, Alexandre José Cichoski, Leila Queiroz Zepka, Eduardo Jacob-Lopes*

Food Science and Technology Department, Federal University of Santa Maria, UFSM, Roraima Avenue 1000, 97105-900, Santa Maria, RS, Brazil, Tel. +555532208822; emails: jacoblopes@pq.cnpq.br (E. Jacob-Lopes), alinemeirelessm@hotmail.com (Aline Meireles dos Santos), marianydepra@gmail.com (M.C. Deprá), albertomsrs@gmail.com (Alberto Meireles dos Santos), ajcichoski@gmail.com (A.J. Cichoski), lqz@pq.cnpq.br (L.Q. Zepka)

Received 10 July 2019; Accepted 22 December 2019

ABSTRACT

This paper presents a life cycle assessment of a simulated large-scale process of agroindustrial wastewater treatment through microalgal heterotrophic bioreactors. The study focuses on establishing sustainability metrics for recovering energy and nutrients from wastewater to produce bulk oil and lipid extracted algae (LEA) in an integrated process. The experimental data, obtained from a bench-scale facility, were used to estimate the life cycle impacts of a wastewater treatment plant with a capacity of 16,000 m^3/d, with a production of 4.32 ton/d of biomass, fractioned in 0.84 ton/d of bulk oil and 3.45 ton/d of LEA. The sustainability metrics of the integrated process indicate a net energy ratio of 0.41, reduction of 98% of the water footprint, global warming potential of 47×10^6 kgCO_{2eq}/y, eutrophication potential of 5×10^4 kg eq PO_4/y, acidification potential of 7×10^4 kg SO_2-eq/y and ozone depletion potential of 3.33 kg CFC-11-eq/y. The assessment of the life cycle demonstrated that this technological route presents itself as a new sustainable approach for wastewater treatment plants and their implementation and dissemination can help to support a change towards resource recovery and a sustainable circular economy.

Keywords: Microalgae/cyanobacteria; Nutrient cycling; Biodiesel; Animal feed; Process integration; Impact categories

1. Introduction

Sustainability is one of the main concerns in many industrial areas, which is particularly true when concerning indispensable commodities such as food, feed, clean water, and energy. With the increasing populations as well as industrial activities, countries face global water stress, both in the aspect of water scarcity and deteriorated quality given the large electricity costs and greenhouse gas emissions associated with water delivery and wastewater treatment [1].

Historically, wastewater treatment plants have been designed and operated to minimize the environmental effects focusing only on treatment efficiency and final effluent quality. Economic and technical aspects are still today the major concerns of environmental projects. Though will economic criteria continue to lead the way for industrial development, this is not well enough in the near future. Sustainability metrics will be inserted in the projects and will be a determinant criterion in decision-making [2]. Thus, the full quantification of adverse environmental effects in addition to the establishment of recovery indices of energy and nutrients will be fundamental to consolidate sustainable technological routes [3,4].

Microalgae-based systems play a central role in this process by incorporating and redistributing dissolved organic matter and inorganic nutrients in the environment. These microorganisms show wide potential for use as

* Corresponding author.

1944-3994/1944-3986 © 2020 Desalination Publications. All rights reserved.

biocatalysts in environmental biotechnology processes due to their toughness and simple nutritional requirements. Also, microalgae can manufacture a wide range of commercially attractive biobased chemicals [5]. However, sustainability metrics of microalgae-based processes need to be studied before the large-scale implementation of these strategies [6].

Given these aspects, the life cycle assessment (LCA) of processes and products is the most consistent tool to the transition of the theory to the practice in the development of technologies to sustainable development, once that assists evaluation of inputs and outputs of the system, demonstrating the environmental performances throughout the entire life cycle of the process [7–9].

Therefore, this article is a sequence of proof-of-principle experimental and theoretical studies investigating the nutrient cycling of poultry and swine slaughterhouse wastewater, through a microalgal heterotrophic bioreactor [10–12]. The results previously published showed that the microalgal heterotrophic bioreactor is capable of simultaneously converting organic matter, nitrogen, and phosphorus of the wastewater into biomass with great potential to be applied as biofuel and animal feed, being able to support the oscillations of organic matter typical of agroindustrial processes. Besides that, it presents a competitive cost. Building on these promising results, an LCA was performed to establish sustainability metrics on microalgae-based wastewater treatment systems. The study focuses on establishing energy resources, water footprint, global warming potential (GWP), eutrophication potential, acidification potential, and ozone depletion potential (ODP) for recovering energy and nutrients from wastewater to produce bulk oil and lipid extracted algae (LEA) in an integrated process.

2. Material and methods

2.1. Microorganism and culture conditions

Axenic cultures of *Phormidium autumnale* were used in the experiments. Stock cultures were propagated and maintained in solidified agar-agar (20 g/L) containing synthetic BG11 medium [13]. The incubation requirements used were 25°C, a photon flux density of 15 μmol/m^2/s, and a photoperiod of 12:12 h (light:dark).

2.2. Wastewater

The wastewater was collected from the discharge point of an equalization tank over one year in an industry located in Santa Catarina, Brazil (27°14′02″S, 52°01′40″W), whose activity covers the slaughter and processing of poultry and swine. Standard Methods for the Examination of Water and Wastewater [14] were utilized to measure pH, chemical oxygen demand (COD), total nitrogen (N–TKN), total phosphorus (P–PO_4^{-3}), total solids (TS), suspended solids (SS), volatile solids (VS), and fixed solids (FS). The average composition of the wastewater has the following composition (mg/L): pH of 5.90 ± 0.05, COD of 4,100.00 ± 874.00, N–TKN of 128.50 ± 12.10, P–PO_4^{-3} of 2.84 ± 0.02, TS of 3.80 ± 2.70, SS of 1.90 ± 0.81, VS of 2.90 ± 1.42, and FS of 0.90 ± 0.31, carbon/nitrogen (C/N) ratio of 31.90 ± 0.30 and nitrogen/phosphorous (N/P) ratio of 45.24 ± 0.54. The C/N and N/P were calculated through COD, N–TKN, and P–PO_4^{-3}.

2.3. Bioreactor configuration

Measurements were made in a bubble column bioreactor. The system was built of borosilicate glass and it had an external diameter of 12.5 cm and a height of 16 cm, resulting in a height/diameter (h/d) ratio equal to 1.28 and a nominal working volume of 2.0 L. The dispersion system of the reactor consisted of a 2.5 cm diameter air diffuser located inside the bioreactor. The airflow was monitored by a flow meter (KI-Key Instruments®, Trevose, PA, USA).

The experiments were performed in bioreactors, operating in a batch system, fed to 2.0 L of the poultry and swine slaughterhouse wastewater. The operational conditions were an initial cell concentration of 100 mg/L, constant aeration of 1.0 volume of air per volume of culture per minute (VVM), pH adjusted to 7.6, temperature 25°C, and the absence of light [10–12].

2.4. Life cycle assessment

2.4.1. Goal and scope definition

The LCA was performed according to the ISO standards [15]. The experimental data were obtained from laboratory experiments, where the elementary flows of the process were selected. Subsequently, the data were extrapolated for an industrial scale where system boundaries comprised a wastewater treatment plant with a capacity of 16,000 m^3/d, with a production of 4.32 ton/d of biomass, fractioned in 0.84 ton/d of bulk oil and 3.45 ton/d of LEA, for a period one year. The theoretical scale-up of the process was performed, as described by Santos et al. [10].

Since there is an absence of data on large-scale microalgae wastewater treatment, laboratory remarks combined with published data of known industrial procedures have been employed and extrapolated [10,16–18,]. Besides, promising technologies that can be commercialized shortly were employed as the basis for the experimental calculation to determine the sustainability metrics of the proposed process. Fig. 1 shows the scope of the proposed process.

2.4.1.1. Step 1: agroindustrial wastewater treatment

The unit operations proposed in step 1 was based on a patent application developed by Jacob-Lopes et al. [19]. A primary treatment composed by a fine screen, Parshall flume, rotary sieve, and equalization tank was used. The core of this step was the biological treatment in a bench-scale heterotrophic microalgal bioreactor, as described in item 2.3. The performance parameters are described in Table 1 [10]. After the biological treatment, the microalgal sludge was processed by a decanter and a belt filter to obtain biomass.

Furthermore, the bench-scale facility had all the necessary equipment to convert the pollutants of the agroindustrial wastewater into dried microalgal biomass and the fractionation of biomass into bioproducts.

2.4.1.2. Step 2: biodiesel production

In a bench-scale, the modified Bligh and Dyer method [20] was applied to extract the lipid content of the biomass. Based on laboratory experiments, an industrial process was

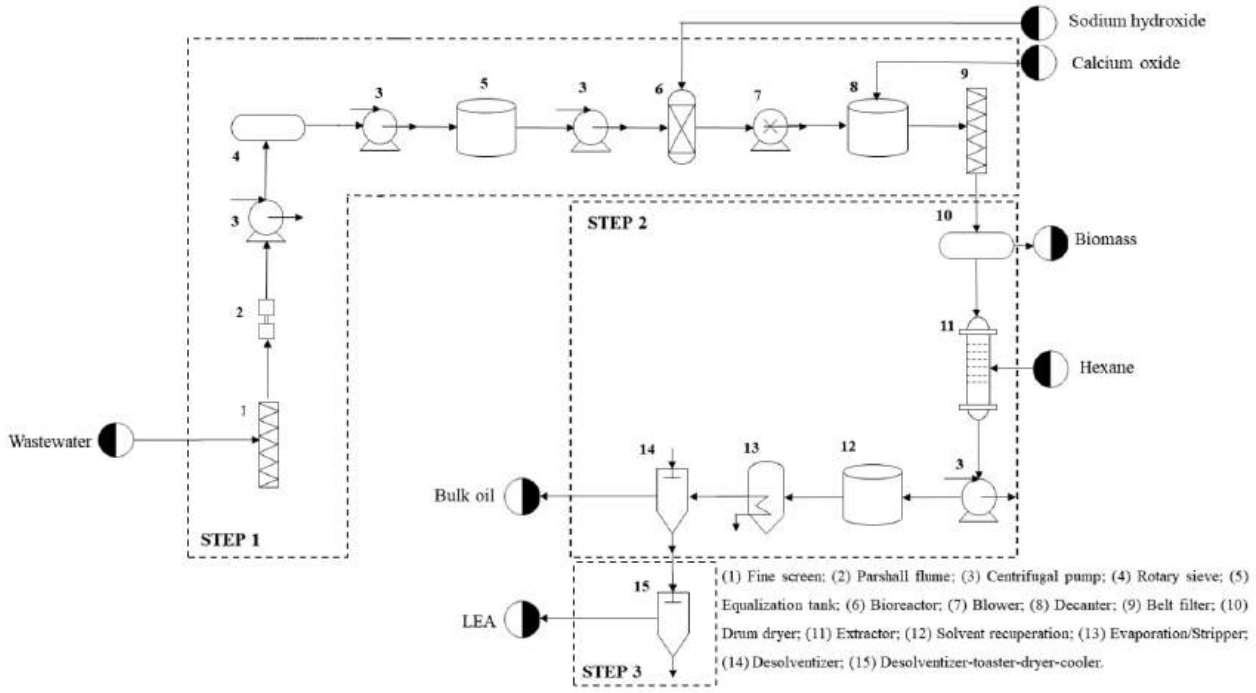


Fig. 1. Process flow diagram of the agroindustrial wastewater treatment in an integrated process. Adapted from Santos et al. [10].

Table 1
Performance parameters of the heterotrophic microalgal bioreactor. Adapted from Santos et al. [10]

Parameter	Value
$RE_{(COD)}$ (%)	97.6 ± 1.64
$RE_{(N-TKN)}$ (%)	85.5 ± 2.37
$RE_{(P-PO4^{-3})}$ (%)	92.4 ± 0.22
P_X (kg/m³/d)	0.27 ± 0.01
HDT (d)	1.67 ± 0.00

$RE_{(COD)}$: COD removal efficiency; $RE_{(N-TKN)}$: N–TKN removal efficiency; $RE_{(P-PO_4^{-3})}$: $P–PO_4^{-3}$ removal efficiency; P_X: average biomass productivity; HDT: hydraulic retention time.

proposed for oil extraction of the dried biomass (Fig. 1). The hexane extraction was defined as the method for large-scale applications [21].

2.4.1.3. Step 3: animal feed production

Drying in a vacuum oven at 60°C simulating an industrial process was used for hexane separation and drying of the LEA on a laboratory scale. On industrial scale, it was proposed the desolventizer-toaster-dryer-cooler (DTDC) [22].

2.4.2. Life cycle inventory (LCI)

A summary of elementary flows of the process is presented in Table 2. These data were analytically evaluated to quantify and compile all the input and output flows for each step within the process scope. The impacts of production were based on the Ecoinvent database, and are shown in Supplementary Material (Table S1).

2.4.3. Life cycle impact assessment (LCIA)

2.4.3.1. Net energy ratio

The characterization of the net energy ratio (NER) was performed as described by Jorqueira et al. [23] in Eq. (1).

$$\mathrm{NER} = \frac{\sum E_{\mathrm{out}}}{\sum E_{\mathrm{in}}} \tag{1}$$

where NER is net energy ratio, E_{out} is the energy produced, and E_{in} is the total input energy required, expressed in Joule/Joule (dimensionless).

2.4.3.2. Water footprint

The water footprint is a metric that counts the direct and indirect use of water as well as pollution. The characterization of the total water footprint was performed as described by Hoekstra and Mekonnen [24] in Eq. (2).

$$\mathrm{WF} = \sum \mathrm{WF}_{\mathrm{blue}} + \mathrm{WF}_{\mathrm{green}} + \mathrm{WF}_{\mathrm{grey}} \tag{2}$$

where WF is the total water footprint, WF_{blue} is the blue water footprint, WF_{green} is the green water footprint, and WF_{gray} is the gray water footprint, expressed in m³/y.

The blue water footprint is an indicator of consumptive use of so-called water fresh or groundwater, evaporated or incorporated into the products, and it was quantified according to Eq. (3):

$$\mathrm{WF}_{\mathrm{blue}} = \mathrm{BW}_e + \mathrm{BW}_i + L_{\mathrm{rf}} \tag{3}$$

Table 2
Elementary flows for the different steps of process scope

Steps	In/Out	Utilities/materials	Base case
Wastewater treatment	Input	Wastewater, m³/h	666.66
		Fine screen, kWh	4.80
		Parshall flume, kWh	32.05
		Centrifugal pump, kWh	617.27
		Rotary sieve, kWh	0.72
		Centrifugal pump, kWh	617.27
		Equalization tank, kWh	1,799.80
		Centrifugal pump, kWh	617.27
		Sodium hydroxide, kWh	4,000.00
		Heterotrophic microalgal bioreactor, kWh	6.45
		Blower, kWh	9.43
		Decanter, kWh	599.90
		Calcium oxide, kWh	266.66
		Belt filter, kWh	183.30
	Output	Biomass, kg/h	180.00
Biodiesel production	Input	Drum dryer, kWh	1,249.98
		Extractor, kWh	12.77
		Hexane, kg/h	1,310.00
		Centrifugal, kWh	18.80
		Solvent recuperation, kWh	22.29
		Evaporation/Stripper, kWh	4.17
		Desolventizer, kWh	7.05
	Output	Bulk oil, kg/h	36.00
Animal feed production	Input	Residual biomass, kg/h	144.00
		DTDC, kWh	19.82
	Output	LEA, kg/h	144.00

where WF_{blue} is blue water footprint, BW_e is blue water evaporation, BW_i is blue water incorporation, and L_{rf} is the lost return flow, expressed in m³/y.

The green water footprint is the consumed of water, evaporated or absorbed during the production of biomass, and it was quantified according to Eq. (4):

$$WF_{green} = GW_e + GW_i \quad (4)$$

where WF_{Green} is green water footprint, GW_e is green water evaporation, GW_i is green water incorporation, expressed in m³/y.

The grey water footprint is the volume of water needed to dilute the pollution generated in the production process to the levels established by current environmental standards [25,26] and it was quantified according to Eq. (5):

$$WF_{grey} = \frac{L}{c_{max} - c_{nat}} \quad (5)$$

where WF_{grey} is the grey water footprint, L is the pollutant load, in mass/time, c_{max} is the ambient water quality standard for that pollutant and c_{nat} is the natural concentration in the receiving water body. c_{max} and c_{nat} are based on the values established by current legislation, expressed in m³/y.

Nitrogen and phosphorus were the pollutants chosen to calculate the gray water footprint of the process, considering their concentrations in the raw wastewater, quality standards according to Brazilian and European laws (both 75% removal efficiency) and concentrations in the waterbody in their natural state, according to Brazilian law (N = 3.7 mg/L and P = 0.1 mg/L) [25,26].

2.4.3.3. Global warming potential

The GWP is the sum of direct and indirect greenhouse gas emissions. Direct emissions are greenhouse gases generated during the wastewater biological treatment process, and they were calculated by the stoichiometry of the biochemical oxidation of organic compounds. The indirect emissions are those attributable to carbon footprints associated with the operation of the proposed process due to the inputs of power and chemicals. The characterization of the GWP was performed as described by Laratte et al. [27] in Eq. (6).

$$GWP = \sum i GWP_i \times m_i \quad (6)$$

where GWP is the global warming potential, i is the time horizon of 100 years, GWP_i is the equivalence factor for a

substance *i* and, m_i is the emission of substance *i*, expressed in kgCO_2eq/y.

2.4.3.4. Eutrophication potential (EP)

The characterization of the eutrophication potential was performed as described by Hauschild et al. [28] in Eq. (7), and their specific characterization factors are shown in Supplementary Material (Table S2).

$$EP = \sum iEP_i \times m_i \quad (7)$$

where EP is the eutrophication potential, EP_i is the equivalence factor for a substance *i* and, m_i is the emission of substance *i*, expressed in kg eq PO_4/y.

2.4.3.5. Acidification potential (AP)

The characterization of the acidification potential was performed as described by Hauschild et al. [28] in Eq. (8).

$$AP = \sum iAP_i \times m_i \quad (8)$$

where AP is the acidification potential, AP_i is the equivalence factor for substance *i*, and m_i is the emission of substance *i*, expressed in kg SO_2-eq.

2.4.3.6. Ozone depletion potential

The characterization of the ODP was performed as described by Hauschild and Wenzel [29] in Eq. (9).

$$ODP = \sum ODP_i \times m_i \quad (9)$$

where ODP is the ozone depletion potential, ODP_i is the equivalency factor for a substance *i* and, m_i is the mass of the emission substance *i*, expressed in kg CFC-11-eq.

2.4.4. Normalization

The impact categories were normalized as described by International Reference Life Cycle Data System (ILCD) [30,31] in Eq. (10). During this step, each of the environmental impact potentials was divided by reference value, corresponding to the global normalization factors from European Commission (Table S3).

$$N_k = \frac{S_k}{R_k} \quad (10)$$

where *k* is the impact category, N_k is the normalized results, S_k is the characterized impact of the impact category *k* of the system under study, and R_k is the characterized impact of the impact category *k* of the reference system.

3. Results and discussion

3.1. Resource use

3.1.1. Net energy ratio

The NER is a basic relation that helps with understanding the energy effectiveness of a particular system. The correlation between the renewable energy produced and the fossil energy required in the production process implies ideally in an NER higher than 1.0 [32]. In this sense, the energy balances of the process were examined, and the results are presented in Fig. 2.

According to the results, inputs of 127 × 10^6 MJ/y, 37 × 10^6 MJ/y and 0.5 × 10^6 MJ/y of fossil energy is required to generate 32 × 10^6 MJ/y, 11 × 10^6 MJ/y, and 23 × 10^6 MJ/y of renewable energy in the steps of wastewater treatment, biodiesel production and animal feed production resulting in NERs of 0.25, 0.31 and 42.00, respectively. In addition, the agroindustrial wastewater treatment in microalgal heterotrophic bioreactor and the production of bulk oil and LEA in an integrated process require an input of 164 × 10^6 MJ/y of fossil energy to generate 66 × 10^6 MJ/y of renewable energy, resulting in a NER of 0.41. Microalgae-based processes potential for bioproducts production such as biofuels has been proven in some studies. However, it is associated with an NER of less than one. Many authors highlight the indirect effects of fossil energy consumption in reducing the NER [33–35].

Under the aspect of fossil energy consumption, there are a few stages that make up a large proportion of primary energy consumption. Unit operations for agroindustrial wastewater treatment (step 1) consume approximately 77% of the fossil energy of the proposed process, being the primary wastewater treatment responsible for most of this consumption (3,689.16 kWh). The unit operations for biomass harvesting are responsible for 21% of fossil energy consumption in step 1 (792.62 kWh). The dilute nature of microalgal cultures (0.27 kg/m^3/d) creates a huge energetic cost during harvest, which results in a low net energy rate for microalgae-based products [36]. There is no superior method of dewatering microalgae, and this is a bottleneck of the process [37]. Unit operations for biodiesel production (step 2) consume approximately 23% of the fossil energy in the process, being the biomass drying responsible for most of this consumption (1,249.95 kWh). The drying of microalgae sludge for large-scale hexane extraction may not be economically viable in terms of absorbed energy for biofuels. However, for being a developed technology and with well-established economics for practice on a large scale for oilseeds, this unit operation is steadily used in the economic assessments of microalgal biofuel production [9,38,39]. The animal feed production (step 3) from the residual biomass consumed only 0.33% (19.79 kWh) of the total fossil energy process. This step presents a potential solution towards reducing the energy demand of this process once the renewable energy produced is greater than the required fossil energy.

In this context, wastewater treatment in microalgal heterotrophic bioreactor represents an interesting alternative for conventional activated sludge treatment plants once that they require significantly lower energy consumption (0.00968 kW/m^3) than conventional activated sludge systems (0.0132 kW/m^3) [40]. In addition, the conventional system shows a high biomass yield coefficient ($Y_{X/S}$), usually in the order of 0.3 kg_{sludge}/kg_{BOD} resulting in massive production of sludge with low use potential that will require adequate treatment and disposal, further burdening the process [41].

3.1.2. Water footprint

The use of nutrient-rich wastewater in the microalgae-based processes can contribute to energy recovery and significantly reduce the water footprint [42]. In this sense, Fig. 3 presents a flow diagram of the water footprint of the integrated process.

From the data analysis, it is possible to verify that in the integrated process, the water footprint is composed only of the blue and green fractions. The blue water footprint considered in this study refers to the volume of water consumed in the lipid extraction stage of the biomass (1.11 m^3/y). In addition, the green water footprint is directly related to the water volume incorporated into the biomass (1,056,000 m^3/y), representing about 20% of the wastewater. The rate evaporated during the process represents about 528,000 m^3/y. Thus, the total water footprint of the integrated process results in values in the order of 1,584,001.11 m^3/y.

The gray water footprint is generally not accounted for in the water footprint calculation of industrial processes due to the unavailability and/or poor quality of data on a global scale [43,44]. However, considering the gray footprint before the wastewater treatment, as a theoretical reference for assimilation of the body of water, this would result in values in the order of 1,07,713,204.76 m^3/y.

Given these volumes, the process proposed in this study presents itself as a potential technology, since the total water footprint (1,584,001.11 m^3/y) represents close to 2% when compared to the gray water footprint, which corresponds to 100%. Therefore, this technology could represent the prevention of more than 98% of the total water demand, if the gray footprint was considered usually as an alternative for nutrient assimilation.

Moreover, from the economic point of view, considering that the average water price in the world show values of approximately 1.50 USD/m^3 [45], the total water footprint of the integrated treatment wastewater process costs around USD 276001.66.

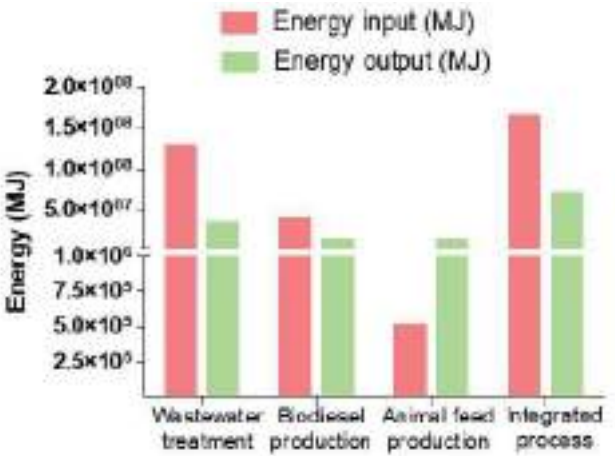


Fig. 2. Energy balances for the different steps and integrated process over one year.

3.2. Climate change

3.2.1. Global warming potential

GWP is related to emissions of greenhouse gases, including CO_2, CH_4, and N_2O. This impact category being among the aspect that has become key-factors concerning the overall performance of the wastewater treatment plants, once

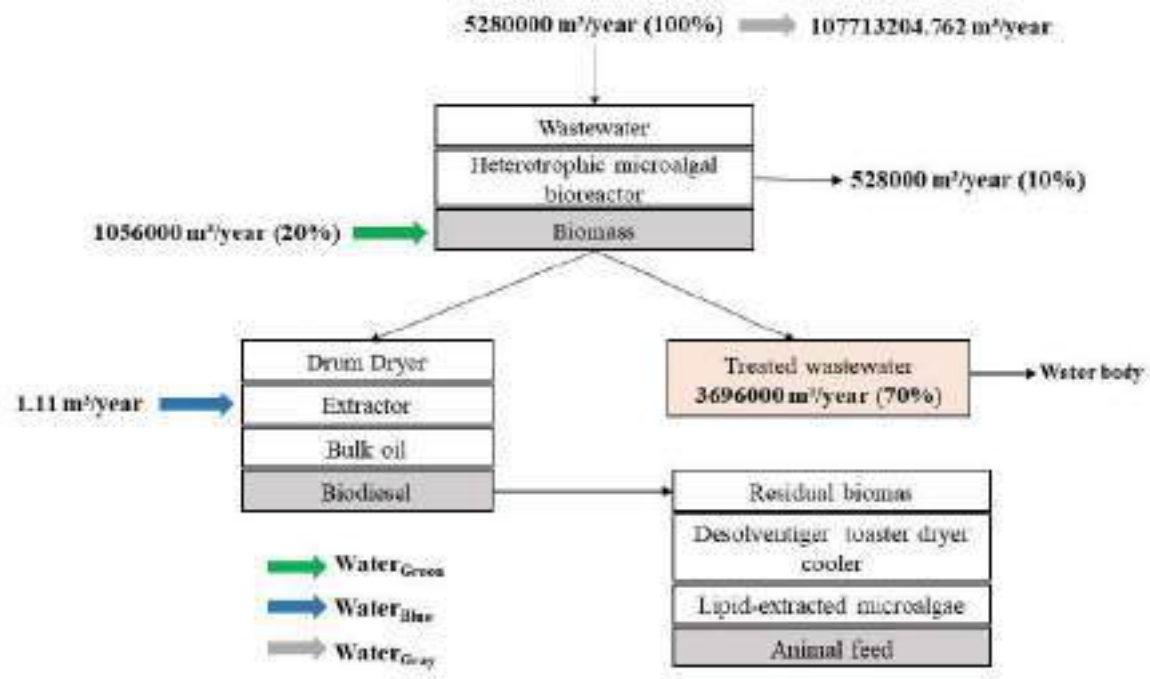


Fig. 3. Flow diagram of the water footprint of the process.

sustainability metrics are under consideration to ensure the viability of this type of process [2]. In this sense, Table 3 presents the results of GWP for the agroindustrial wastewater treatment in the integrated process.

From the data analysis, it is possible to verify that the sum of the direct and indirect emissions results in GWPs of 34×10^6, 12×10^6 and 0.08×10^6 $kgCO_{2eq}$/y in the steps of wastewater treatment, biodiesel production, and animal feed production, respectively. The agroindustrial wastewater treatment in microalgal heterotrophic bioreactor and production of bulk oil and LEA in the integrated process resulted in a GWP of 47×10^6 $kgCO_{2eq}$/y, being the biochemical oxidation, use of chemical reagents, and demand for fossil energy responsible for 1%, 46% and 53% of total emissions, respectively. Understanding the dynamics of greenhouse gas emissions in microalgae-based processes is of the utmost importance to improve strategic investments in the areas of climate change. Although these estimates are uncertain, due to the lack of large-scale applications, they sustain a case for improving mechanistic understanding of pathways and main inducements for this type of process [46].

Given the aspect of emissions generated by the employed of chemical reagents, the use of 31,680 ton/y of sodium hydroxide to control the culture pH and 2,112 ton/y of calcium oxide to separate the extracellular water from the microalgae suspension are responsible for 14×10^6 $kgCO_{2eq}$/y of the indirect emissions of greenhouse gases related to the use of chemical reagents in step 1. The use of 10,375 ton/y of hexane for biodiesel extraction is responsible for 7×10^6 $kgCO_{2eq}$/y of the indirect emissions of greenhouse gases related to the use of chemical reagents in step 2. Greenhouse gas emissions released due to the use of chemical reagents are inevitable in wastewater treatment plants. However, they can be reduced by enhancing the energy efficiency of the wastewater treatment plant and reducing the use of chemicals [2].

Additionally, considering the initial concentrations of nitrogen (678,480 kg/y) and phosphorus (14,982 kg/y) in the composition of poultry and swine slaughterhouse wastewater (Table 1) and their removal efficiencies of approximately 86% and 93% (Table 2), respectively, it is estimated a biorecovery of 583,492.8 $kg_{nitrogen}$/y and 13,933.26 $kg_{phosphorus}$/y. If these nutrients were reusing for fertilizer production could be avoid close to 3 million $kgCO_{2eq}$ [47].

In terms of emissions generated by the demand for fossil energy, coal, and oil-fired plants represent 29% and 31% of the world total primary energy supply, being responsible for approximately 46 %and 34% of global CO_2 emissions, respectively [48]. Due to heavy carbon content per unit of energy released, approximately 0.34 and 0.26 $kgCO_2$ are emitted to generate 1 kWh of energy from coal and oil, respectively [49].

The GWP of the integrated process (47×10^6 $kgCO_{2eq}$/y) is 1.4 times greater than the value emitted just in the wastewater treatment step (34×10^6 $kgCO_{2eq}$/y). However, with the integration of the steps, there will be the possibility of valorization of agroindustrial wastewater from the recovery of energy and nutrients through the production of biodiesel and animal feed. The nutrient cycling from microalgae integrated to the wastewater treatment plant has long been proposed as a means to reduce the environmental impact of commodities output such as biofuels [50,51].

3.3. Ecosystem quality

3.3.1. Eutrophication potential, acidification potential, and ODP

Rupture of natural nitrogen and phosphorus cycles causes an excess of nutrients of anthropic origin on aquatic ecosystems resulting in loss of ecosystem services and species extinctions. Therefore, it is important to quantify the eutrophication potential of production processes and minimize their impacts on ecosystem quality [52]. Thus, the result obtained for the eutrophication potential of the integrated process is presented in Table 4.

The microalgal heterotrophic bioreactor is attractive for organic matter and nutrients recovery due to its great removal efficiency of the COD (97.6%), total nitrogen (85.5%) and total phosphorus (92.4%) present in agroindustrial wastewater. From these removal efficiencies, it is possible to verify a reduction of 80×10^4 kg eq PO_4/y for 5×10^4 kg eq PO_4/y on the eutrophication potential of the integrated process (Table S4). Nutrient recovery reduces the consumption of bioresources, and it saves costs related to N and P removal, thus minimizing the environmental impact of wastewater treatment [53]. Additionally, it also saves the costs of fertilizing once that the prices of ammonium nitrate and superphosphates are approximately USD/ton 550 and 300, respectively [54]. Studies conducted by Zhang and Kendall [55] report the requirements of ammonium nitrate 0.15 kg/kg of biomass and superphosphate in the order of 0.10 kg/kg of biomass. Therefore, in an estimated production of 1 ton of microalgal biomass, the required costs involving nutrient demand would be around 82.5 USD for nitrates and USD 30.00 for phosphates.

Additionally, the acidification potential and ODP are impact categories related to emissions of air pollutants that result in environmental problems such as global warming,

Table 3
Global warming potential for the individual steps and integrated process

GWP ($kgCO_{2eq}$/y)		Step 1 ($kgCO_{2eq}$/y)	Step 2 ($kgCO_{2eq}$/y)	Step 3 ($kgCO_{2eq}$/y)	Integrated process ($kgCO_{2eq}$/y)
Direct	Biochemical oxidation	0.05×10^6	NA	NA	0.05×10^6
Indirect	Fossil energy	19×10^6	5×10^6	0.08×10^6	25×10^6
	Chemicals	14×10^6	7×10^6	NA	22×10^6
Total		34×10^6	12×10^6	0.08×10^6	47×10^6

NA: not applicable.

Table 4
Impact categories that damage ecosystem quality

Impact category	Integrated process
Eutrophication potential	5×10^4 kg eq PO_4/y
Acidification potential	7×10^4 kg SO_2-eq/y
Ozone depletion potential	3.33 kg CFC-11-eq/y

acid rain, and ozone layer depletion [56,57]. Thus, sustainability metrics that predict the environmental impacts associated with emissions of air pollutants is indispensable to minimize negative environmental effects. In this sense, the results obtained for the acidification potential and ODP (Table 4) indicate values of 7×10^4 kg SO_2-eq/y and 3.33 kg CFC-11-eq/y, respectively. The results are related to the input of fossil energy resources to operate the integrated process, and agroindustrial wastewater treatment and biodiesel production steps are the main responsible for these impacts. Fossil fuels consumption to operate wastewater treatment plant is the largest contributing parameter for pollutant emissions, once only 20%–30% of the chemical energy of the fuel burned is typically transformed into useful work or heating, the rest is dissipated into the atmosphere as polluting gases [58].

The elementary input flows for sodium hydroxide, calcium oxide, and hexane were disregarded in the characterization of the acidification potential and ODP since these chemical reagents contribute lightly to these impact categories.

The comparison of the sustainability metrics obtained in this study with other technologies for wastewater treatment is limited by the fundamentals of the methodology used. The LCAs are usually performed using similar methodologies; however, there are variabilities in tool application, in terms of choice of allocation, system boundary and procedures followed to data collection. In addition, the comparative LCA applied to wastewater treatment systems is severely hampered by the choice of characterization factors, which vary in function of the database and reports considered in the life cycle impact assessment phase [59]. In this sense, considering these aspects, it's possible to reference other studies as the work of Pasqualino et al. [60] that shows sustainability metrics of 0.5214 kgCO_{2eq}/m^3, 3.36×10^{-4} kg eq PO_4/m^3, 4.61×10^{-3} kg SO_2-eq/m^3 and 4.2×10^{-8} CFC-11-eq/m^3 for a system of aerobic digestion applied to urban wastewater treatment. Additionally, the sustainability metrics showed by Buonocore et al. [61], Garfí et al. [62], and Li et al. [63] can be used as the comparison referential.

3.4. Normalization

Normalization is a step in LCIA that helps decision-makers interpret LCA results and determine where to prioritize efforts aimed at reducing a products environmental impact. This step serves to calculate the relevance of the results of the impact category indicators related to reference information [64]. Thus, for a better understanding between the scores and to compare the magnitude of the emissions of the integrated process, the gate-to-gate impact categories were normalized. Fig. 4 illustrates the results after normalizing the impact categories.

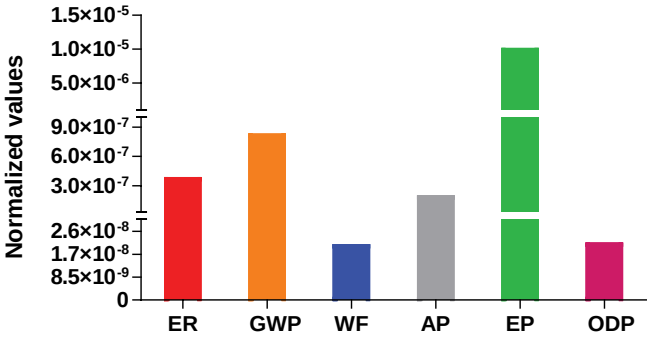


Fig. 4. Normalized values of the impact categories for the integrated process. ER: Energy resource; GWP: Global warming potential; WF: Water footprint; AP: Acidification potential; EP: Eutrophication potential; ODP: Ozone depletion potential.

As shown in Fig. 4, once normalized, the integrated process presented EP as the most significant impact (9.88×10^{-7}), followed by GWP (8.11×10^{-7}), AP (1.82×10^{-7}), ER (3.68×10^{-7}), ODP (2.06×10^{-8}) and WF (2×10^{-8}). Most of the emissions of the integrated process are related to the indirect effects of fossil energy consumption. According to Gao et al. [65], the total of pollutants emitted per unit of energy produced by fossil fuels is typically two orders of magnitude bigger than those emitted by non-fossil energy.

In this sense, the transition from fossil energy matrix to non-fossil energy has become an urgent issue for all wastewater facilities, once that these energies can supply two-thirds of the total global energy demand, and they contribute to the greenhouse gas emissions reduction. Furthermore, the development of renewable energy technologies would greatly promote the realization of a circular economy [66]. Policies and incentives of governments improve the prospects for clean energy. The total generation from renewable resources increases by 2.8% annually [48]. Although it is reasonable to expect that renewables will come to provide a growing share of the global energy supply, it should be noted that replacing fossil energy with non-fossil fuels remains challenging, especially for future global policy [67].

4. Conclusion

The LCA results demonstrate that the process integration mediated by microalgae is an appropriate and innovative approach to comply with green engineering requirements, through nutrient cycling. However, the biggest challenge will be implementing these heterotrophic systems in process chains operating across wastewater management already existing.

In this sense, new approaches to process engineering must be oriented towards promoting the exploitation and development of a commercially viable and integrated microalgae-based wastewater treatment in the future. Process integration, process intensification, and the implementation of the biorefinery concept have been considered as the main process engineering strategies that, in the medium term, will consolidate.

References

[1] A. Pyka, Transformation of Economic Systems: The Bioeconomy Case, In: Knowledge-Driven Developments in the Bioeconomy, Springer, Cham, 2017, pp. 3–16.

[2] J.L. Campos, D. Valenzuela-Heredia, A. Pedrouso, A. Val del Rio, M. Belmonte, A. Mosquera-Corral, Greenhouse gases emissions from wastewater treatment plants: minimization, treatment, and prevention, J. Chem., 2016 (2016) 12p.

[3] UNFCCC, Synthesis Report on the Aggregate Effect of the Intended Nationally Determined Contributions, Conference of the Parties, United Nations, 2015.

[4] H. Awad, M.G. Alalm, H.K. El-Etriby, Environmental and cost life cycle assessment of different alternatives for improvement of wastewater treatment plants in developing countries, Sci. Total Environ., 660 (2019) 57–68.

[5] A.M. Santos, A.M. Santos, I.A. Severo, M.I. Queiroz, L.Q. Zepka, E. Jacob-Lopes, Nutrient Cycling in Wastewater Treatment Plants by Microalgae-Based Processes, S.N. Barton, Ed., Industrial Waste: Management, Assessment, and Environmental Issues, Nova Science Publishers, Inc., New York, 2016, pp. 41–63.

[6] L.M. González-González, D.F. Correa, S. Ryan, P.D. Jensen, S. Pratt, P.M. Schenk, Integrated biodiesel and biogas production from microalgae: towards a sustainable closed-loop through nutrient recycling, Renewable Sustainable Energy Rev., 82 (2018) 1137–1148.

[7] A. Padilla-Rivera, L.P. Güereca, A proposal metric for sustainability evaluations of wastewater treatment systems (SEWATS), Ecol. Indic., 103 (2019) 22–33.

[8] B. Agarski, I. Budak, D. Vukelic, J. Hodolic, Fuzzy multi-criteria-based impact category weighting in life cycle assessment, J. Cleaner Prod., 112 (2016) 3256–3266.

[9] M.C. Deprá, E. Jacob-Lopes, L.Q. Zepka, Life Cycle Assessment of Biofuels from Microalgae, E. Jacob-Lopes, L.Q. Zepka, M.I. Queiroz, Eds., Energy from Microalgae, 1st ed., Springer, Switzerland, 2018, pp. 141–155.

[10] A.M. Santos, G.R. Roso, C.R. Menezes, M.I. Queiroz, L.Q. Zepka, E. Jacob-Lopes, The bioeconomy of microalgal heterotrophic bioreactors applied to agroindustrial wastewater treatment, Desal. Wat. Treat, 64 (2017) 12–20.

[11] A.M. Santos, A.M. Santos, R.B. Sartori, L.Z. Queiroz, J.S. Barin, E. Jacob-Lopes, Nutrient cycling in meat processing industry by microalgae-based processes, Desal. Wat. Treat., 100 (2017b) 91–99.

[12] A.M. Santos, A.M. Santos, R.B. Sartori, L.Z. Queiroz, E. Jacob-Lopes, Influence of poultry and swine blood shocks on the performance of microalgal heterotrophic bioreactor, Desal. Wat. Treat., 114 (2018) 128–134.

[13] R. Rippka, J. Deruelles, J.B. Waterbury, M. Herdman, R.Y. Stanier, Generic assignments, strain histories and properties of pure cultures of cyanobacteria, Microbiology, 111 (1979) 1–61.

[14] APHA, Standard Methods for the Examination of Water and Wastewater, American Public Health Association, Washington, D.C., 2005.

[15] ISO 14040, International Standard, Environmental Management–Life Cycle Assessment – Principles and Framework, International Organisation for Standardization, Geneva, Switzerland, 2006.

[16] L. Xu, D.W.F. Brilman, J.A.M. Withag, G. Brem, S. Kersten, Assessment of a dry and a wet route for the production of biofuels from microalgae: energy balance analysis, Bioresour. Technol., 8 (2011) 5113–5122.

[17] N. Pragya, K. Panved, Life cycle assessment of green diesel production from microalgae, Renewable Energy, 86 (2016) 623–632.

[18] V.O. Adesanya, E. Cadena, S.A. Scott, A.G. Smit, Life cycle assessment on microalgal biodiesel production using a hybrid cultivation system, Bioresour. Technol., 163 (2014) 343–355.

[19] E. Jacob-Lopes, A.M. Santos, D.B. Rodrigues, M.C.Y. Lui, C. Souza, D. Prudente, L.Q. Zepka, Bioprocess of Conversion of Hybrid Wastewaters, Heterotrophic Bioreactor, Bioproducts, and Their Uses, Brazilian Patent Application BR 10 2013 020490-0 A2, 2013.

[20] E.G. Bligh, W.J. Dyer, A rapid method of total lipid extraction and purification, Can. J. Biochem. Phys., 37 (1959) 911–917.

[21] Y. Peralta-Ruiz, A.D. González-Delgado, V. Kafarov, Evaluation of alternatives for microalgae oil extraction based on exergy analysis, Appl. Energy, 101 (2013) 226–236.

[22] G.R. Roso, A.M. Santos, M.I. Queiroz, J.S. Barin, L.Q. Zepka, E. Jacob-Lopes, The econometrics of production of bulk oil and lipid extracted algae in an agroindustrial biorefinery, Curr. Biotechnol., 4 (2015) 547–553.

[23] O. Jorqueira, A. Kiperstok, E.A. Sales, M. Embirucu, M.L. Ghirardi, Comparative energy life-cycle analyses of microalgal biomass production in open ponds and photobioreactors, Bioresour. Technol., 101 (2010) 1406–1413.

[24] A.Y. Hoekstra, M.M. Mekonnen, The water footprint of humanity, Proc. Nat. Acad. Sci., 109 (2012) 3232–3237.

[25] CONAMA, Resolução n° 357/2005, Dispõe sobre a classificação dos corpos de água e diretrizes ambientais para o seu enquadramento, bem como estabelece as condições e padrões de lançamento de efluentes, in: Conselho Nacional do Meio Ambiente, Ed., Brasília, BR, 2005.

[26] Council Directive, Council Directive 91/271/EEC of 21 May 1991 Concerning Urban Waste-water Treatment, Official Journal L 135, European Union, 1991, pp. 40–52.

[27] B. Laratte, B. Guillaume, J. Kim, B. Birregah, Modeling cumulative effects in life cycle assessment: the case of fertilizer in wheat production contributing to the global warming potential, Sci. Total Environ., 481 (2014) 588–595.

[28] M.Z. Hauschild, H. Wenzel, M. Hauschild, Environmental Assessment of Products: Scientific Background, Vol. 2, Springer Science & Business Media, London, 1997.

[29] M.Z. Hauschild, H. Wenzel, Environmental Assessment of Products, Vol. 2, Kluwer Academic Publishers, Chapman & Hall, Hingham, United Kingdom, 1998.

[30] European Commission - Joint Research Centre - Institute for Environment and Sustainability: International Reference Life Cycle Data System (ILCD) Handbook – General guide for Life Cycle Assessment - Detailed guidance, First edition March 2010, EUR 24708 EN, Publications Office of the European Union, Luxembourg, 2010.

[31] S. Sala, E. Crenna, M. Secchi, R. Pant, Global Normalisation Factors for the Environmental Footprint and Life Cycle Assessment, EUR (28984), Publications Office of the European Union, Publications Office of the European Union, Luxembourg, 2017, ISBN 978-92-79-77213-9, doi:10.2760/88930, JRC109878.

[32] M.R. Tredici, N. Bassi, M. Prussi, N. Biondi, L. Rodolfi, G.C. Zittelli, G. Sampietro, Energy balance of algal biomass production in a 1-ha "Green Wall Panel" plant: how to produce algal biomass in a closed reactor achieving a high net energy ratio, Appl. Energy, 154 (2015) 1103–1111.

[33] L. Lardon, A. Helias, B. Sialve, J.P. Steyer, O. Bernard, Life-cycle assessment of biodiesel production from microalgae, Environ. Sci. Technol., 43 (2009) 6475–6481.

[34] M.O.P. Fortier, G.W. Roberts, S.M. Stagg-Williams, B.S. Sturm, Life cycle assessment of bio-jet fuel from hydrothermal liquefaction of microalgae, Appl. Energy, 122 (2014) 73–82.

[35] M. Morales, P. Collet, L. Lardon, A. Hélias, J.-P. Steyer, O. Bernard, Chapter 20 - Life-cycle assessment of microalgal-based biofuel, In: Biofuels from Algae Sustainable Platform for Fuels, Chemicals and Remediation Biomass, Biofuels, Biochemicals, 2019, pp. 507–550.

[36] C. Zamalloa, E. Vulsteke, J. Albrecht, W. Verstraete, The techno-economic potential of renewable energy through the anaerobic digestion of microalgae, Bioresour. Technol., 102 (2011) 1149–1158.

[37] A.M. Santos, A.M. Santos, L.Q. Zepka, E. Jacob-Lopes, Downstream Recovery of Microalgal Bioproducts with Highlights on Biorefineries, In: Biorefineries: Concepts, Advancements, and Research, Nova Science Publishers, Inc., New York, 2017, pp. 1–38.

[38] P.D. Patil, V.G. Gude, A. Mannarswamy, S. Deng, P. Cooke, S. Munson-McGee, I. Rhodes, P. Lammers, N. Nirmalakhandan, Optimization of direct conversion of wet algae to biodiesel under supercritical methanol conditions, Bioresour. Technol., 102 (2011) 118–122.

[39] A. Sathish, R.C. Sims, Biodiesel from mixed culture algae via a wet lipid extraction procedure, Bioresour. Technol., 118 (2012) 643–647.
[40] A.M. Santos, M.C. Deprá, A.M. Santos, L.Q. Zepka, E. Jacob-Lopes, Aeration energy requirements in microalgal heterotrophic bioreactors applied to agroindustrial wastewater treatment, Curr. Biotechnol., 5 (2015) 249–254.
[41] M. Von Sperling, R.F. Gonçalves, Lodo de esgotos: características e produção. In: C.V. Andreoli, M. Von Sperling, F. Fernandes, Lodo de esgotos: tratamento e disposição final, Belo Horizonte: Departamento de Engenharia Sanitária e Ambiental, UFMG, Curitiba: SANEPAR, 6 (2001) 17–67.
[42] B.G. Subhadra, M. Edwards, Coproduct market analysis and water footprint of simulated commercial algal biorefineries, Appl. Energy, 88 (2011) 3515–3523.
[43] A.Y. Hoekstra, The global dimension of water governance: why the river basin approach is no longer sufficient and why cooperative action at global level is needed, Water, 3 (2011) 21–46.
[44] P.R. Van Oel, A.Y. Hoekstra, Towards quantification of the water footprint of paper: a first estimate of its consumptive component, Water Resour. Manage., 26 (2012) 733–749.
[45] J. Clere, True Cost of Water: Monetization of Water Risks, Shared Value Creation, and Local Acceptability of Extractive Projects, J. Field Actions: Field Actions Science Reports, (Special Issue 14), (2016), http://journals.openedition.org/factsreports/4069.
[46] M. Plouviez, A. Shilton, M.A. Packer, B. Guieysse, Nitrous oxide emissions from microalgae: potential pathways and significance, J. Appl. Phycol., 31 (2019) 1–8.
[47] EC, European Commission Environment, 2019. https://ec.europa.eu/ [accessed June 2019].
[48] IEA International Energy Agency, CO_2 Emissions from Fuel Combustion Highlights 2018, International Energy Agency, 2018. http://www.indiaenvironmentportal.org.in/files/file/CO2_Emissions_from_Fuel_Combustion_2018_Highlights.pdf [accessed June 2019].
[49] US Energy Information Administration, Ed., Annual Energy Outlook 2019 with Projections to 2050, Government Printing Office, 2019.
[50] C.Q. Arita, J.J. Sheehan, T.H. Bradley, Life cycle net energy and greenhouse gas emissions of photosynthetic cyanobacterial biorefineries: challenges for industrial production of biofuels, Algal Res., 26 (2017) 445–452.
[51] C.Q. Arita, C. Peebles, T.H. Bradley, Scalability of combining microalgae-based biofuels with wastewater facilities: a review, Algal Res., 9 (2015) 160–169.
[52] F. Gao, Y.-Y. Peng, C. Li, W. Cui, Z.-H. Yang, G.-M. Zeng, Coupled nutrient removal from secondary effluent and algal biomass production in membrane photobioreactor (MPBR): effect of HRT and long-term operation, Chem. Eng. J., 335 (2018) 169–175.
[53] T. Yan, Y. Ye, H. Ma, Y. Zhang, W. Guo, B. Du, Q. Wei, D. Wei, H. H. Ngo, A critical review on membrane hybrid system for nutrient recovery from wastewater, Chem. Eng. J., 348 (2018) 143–156.
[54] USDA, U.S. Department of Agriculture, 2019. https://www.usda.gov/ [accessed June 2019].
[55] Y. Zhang, A. Kendall, Effects of system design and co-product treatment strategies on the life cycle performance of biofuels from microalgae, J. Cleaner Prod., 230 (2019) 536–546.
[56] J.O. Reuss, D.W. Johnson, Acid Deposition and the Acidification of Soils and Waters, Vol. 59, Springer Science & Business Media, New York, 2012.
[57] M. Z. Hauschild, M. Goedkoop, J. Guinée, R. Heijungs, M. Huijbregts, O. Jolliet, S. Sala, Identifying best existing practice for characterization modeling in life cycle impact assessment, Int. J. Life Cycle Assess., 18 (2013) 683–697.
[58] S. Bilgen, Structure and environmental impact of global energy consumption, Renewable Sustainable Energy Rev., 38 (2014) 890–902.
[59] S. Fazio, V. Castellani, S. Sala, E.M. Schau, M. Secchi, L. Zampori, Supporting Information to the Characterisation Factors of Recommended EF Life Cycle Impact Assessment Methods, EUR 28888 EN, European Commission, Ispra, 2018.
[60] J.C. Pasqualino, M. Meneses, F. Castells, Life cycle assessment of urban wastewater reclamation and reuse alternatives, J. Ind. Ecol., 15 (2011) 49–63.
[61] E. Buonocore, S. Mellino, G. De Angelis, G. Liu, S. Ulgiati, Life cycle assessment indicators of urban wastewater and sewage sludge treatment, Ecol. Indic., 94 (2018) 13–23.
[62] M. Garfí, L. Flores, I. Ferrer, Life cycle assessment of wastewater treatment systems for small communities: activated sludge, constructed wetlands and high rate algal ponds, J. Cleaner Prod., 161 (2017) 211–219.
[63] Y. Li, X. Luo, X. Huang, D. Wang, W. Zhang, Life cycle assessment of a municipal wastewater treatment plant: a case study in Suzhou, China, J. Cleaner Prod., 57 (2013) 221–227.
[64] ISO 14044 International Standard, In: Environmental Management – Life Cycle Assessment – Requirements and Guidelines, International Organisation for Standardisation, Geneva, Switzerland, 2006.
[65] C.K. Gao, H.M. Na, K.H. Song, N. Dyer, F. Tian, Q.J. Xu, Y.H. Xing, Environmental impact analysis of power generation from biomass and wind farms in different locations, Renewable Sustainable Energy Rev., 102 (2019) 307–317.
[66] D. Gielen, F. Boshell, D. Saygin, M.D. Bazilian, N. Wagner, R. Gorini, The role of renewable energy in the global energy transformation, Energy Strategy Rev., 24 (2019) 38–50.
[67] J. Chen, Y. Wu, C. Xu, M. Song, X. Liu, Global non-fossil fuel consumption: driving factors, disparities, and trends, Manage. Decis., 57 (2019) 791–810.

Supplementary information

Table S1
Factors of characterization of environmental impacts of energy in process

Impact category	Electricity
Global warming potential (kg CO_2 eq)	5.45×10^{-1}
Acidification potential (kg SO_2 eq)	1.64×10^{-3}
Ozone depletion potential (kg CFC-11 eq)	9.39×10^{-8}

Ecoinvent 2.2 database

Table S2
Characterization factors referring the eutrophication category [47]

Nutrient	PO_4 equivalence factor
1 kg Total nitrogen (water)	0.420 kg eq PO_4
1 kg Total phosphorous (water)	3.070 kg eq PO_4
1 kg Chemical oxygen demand (COD)	0.022 kg eq PO_4

Table S3
Global normalization factors for emissions and resource extraction (Sala et al. [31])

Impact categories	Unit	Reference value
Energy resource	MJ	4.50×10^{14}
Global warming potential	kg CO_2 eq	5.79×10^{13}
Water footprint	m^3	7.91×10^{13}
Acidification potential	kg SO_2 eq	3.83×10^{11}
Eutrophication potential	kg PO_4 eq	1.22×10^{12}
Ozone depletion potential	kg CFC11 eq	1.61×10^{8}

Table S4
Eutrophication potential reduction behavior on wastewater treatment in a heterotrophic microalgal bioreactor [25,26]

Parameter	Wastewater	Treated wastewater
COD (kg PO_4 eq)	476,256	11,430
N–TKN (kg PO_4 eq)	284,961	41,319
$P–PO_4^{-3}$ (kg PO_4 eq)	46,034	3,493
EP (kg PO_4 eq)	807,252	56,242

Bioresource Technology 314 (2020) 123745

Contents lists available at ScienceDirect

Bioresource Technology

journal homepage: www.elsevier.com/locate/biortech

Carbon dioxide capture and use in photobioreactors: The role of the carbon dioxide loads in the carbon footprint

Mariany C. Deprá, Rosangela R. Dias, Ihana A. Severo, Cristiano R. de Menezes, Leila Q. Zepka, Eduardo Jacob-Lopes*

Bioprocess Intensification Group, Federal University of Santa Maria, UFSM, Roraima Avenue 1000, 97105-900 Santa Maria, RS, Brazil

ARTICLE INFO

Keywords:
Algae/chlorophyceae
Mass balance
Bioconversion routes
Carbon loads
Carbon credits
Life cycle assessment

ABSTRACT

This research evaluated the carbon dioxide capture and use by *Scenedesmus obliquus* in a photobioreactor under different CO_2 loads. Performance indicators, carbon and energy balances, sustainability indicators, and carbon credits on the photobioreactor were assessed. The results expressed that the CO_2 loads of 384.9 kg/m^3/d (15% CO_2) provide the best trade-off for the process. For this condition, maximum biomass productivities of 0.36 kg/m^3/d, carbon dioxide conversion rates of 0.44 kgCO_2/m^3/d, and oxygen release rates of 0.33 kgO_2/m^3/d were observed, reaching maximum CO_2 removal efficiencies of 30.76%. Volatile organic compounds were the major products generated (> 80%). However, only < 3% was fixed in biomass. From the environmental and economic point of view, the net energy ratio was 3.44, while the potential carbon credit was of 0.04 USD per m^3 of culture. Finally, the use of adequate CO_2 loads was also proven to be determinant to improve the global performance of the system.

1. Introduction

Carbon dioxide (CO_2) is the major pollutant among greenhouse gases. In 2018, global energy-associated CO_2 emissions grew by an average of 1.7%, achieving a landmark high of 33.1 Gt CO_2 (IEA, 2019). The alarming status of CO_2 concentration rates in the ecosystem has contributed substantially to climate change and loss of natural resources – key elements of sustainable development (Ahmed et al., 2020).

Knowing the magnitude of this problem, reductions on this scale require urgent and sustained commitment at all levels of society. Notoriously, these restrictions strongly need support from government policies, including fiscal policies, as well as hard work in research, development, and innovation (RD&I). In this way, the basis of these developments has boosted the implementation of the bioprocess engineering fundamentals to solve the drawbacks related to the operational controls. As a result, to meet the demands of society and, concomitantly, contributing to industrial economic progress has become the priority in these systems (Gani et al., 2020).

Simultaneously, global efforts focus on carbon reduction and control alternatives. Associated with this, the microalgae-based biological carbon capture and utilization has become a mitigation and bioconversion strategy (Severo et al., 2020). This is because the versatile metabolism of microalgae allows the assimilation of inorganic nutrients and energy to result in biomass with profitable potential. Besides, the vast biodiversity and consequent variability in the biochemical composition of biomass, combined with genetic enhancement, has enabled the exploitation of an expansive range of high-value bioproducts in the world market (Patel et al., 2020).

Regardless of cutting-edge microalgae research initiatives, which promoted several research organizations and produced patents, the propagation of this knowledge to companies seems limited and restricted to only a few locations (Andrade et al., 2020). Over the past 30 years of research and development, the technological and market barriers of microalgae-based processes and products have yet to be overcome for this consolidation to become a reality.

Among the numerous bottlenecks to be circumvented, attempts to integrate and intensify the processes associated with microalgae biorefinery concepts, as well as carbon capture and storage processes, have not yet left the table (Choi et al., 2019). This is because most microalgae-based processes are still in in their infancy and have specific problems, such as the massive consumption of resources, including nutrients and energy. Moreover, biomass productivity rates are still unsatisfactory lower than the recommended value for commercial production, making it limited to the feasibility of the process (Anwar et al., 2020).

* Corresponding author.
E-mail addresses: marianydepra@gmail.com (M.C. Deprá), ejacoblopes@gmail.com (E. Jacob-Lopes).

https://doi.org/10.1016/j.biortech.2020.123745
Received 18 May 2020; Received in revised form 22 June 2020; Accepted 23 June 2020
Available online 26 June 2020
0960-8524/ © 2020 Elsevier Ltd. All rights reserved.

Nomenclature

C_i	inlet CO_2 concentration (kg/m^3/d)
C_{ci}	carbon mass flow rate at the inlet (kg/d)
C_o	outlet CO_2 concentration (kg/m^3/d)
C_{co}	carbon mass flow rate at the outlet (kg/d)
$d[C_{biomass}]/dt$	rate of change in concentration of carbon in the biomass (kg/m^3/d)
$d[C_{headspace}]/dt$	rate of change in carbon concentration in headspace (kg/m^3/d)
$d[DIC]/dt$	rate of change in dissolved inorganic carbon concentration (kg/m^3/d)
dCO_2/dt	variation of the concentration CO_2 over time (kg/m^3/d)
dO_2/dt	variation concentration O_2 over time (kg/m^3/d)
E_{inp}	required input energy (MJ)
E_{out}	output energy (MJ)
Mc	atomic weight of carbon (kg)
Px	biomass productivity (kg/m^3/d)
Q	gas flow (m^3/min)
t	residence time (d).
V_g	volume of the headspace (m^3)
V_L	liquid volume (m^3).
V_R	reactor volume (m^3)
X_i	biomass concentration at time t_i (kg/m^3)
X_{i-1}	biomass concentration at time t_{i-1} (kg/m^3)

Abbreviations

LCA	life cycle assessment
GWP	global warming potential (kg CO_{2eq})
AP	acidification potential (kg SO_{2eq})
EP	eutrophication potential (kg N_{eq})
ODP	ozone depletion potencial (kg $CFC11_{eq}$)
WF	water footprint (m^3)
LU	land use (PDF/ha)
ECO	ecotoxicity (CTU_e)
ER	energy resource (MJ)
EC	elimination capacity (kg/m^3/d)
HRT	hydraulic retention time VR/Q (d)
NER	net energy ratio (dimensionless)
PC	production capacity (kg/m^3/d)
PQ	photosynthetic quotient (dimensionless)

Greek letters

μ_{max}	maximum specific growth rate (d^{-1})

Over time, many scientists have formulated hypotheses to explain these numerous failed attempts on a large scale. To this end, substantial interest was spent on elucidating the basic principles of science, related mainly in terms of dynamics and carbon footprint. Hence, researches have referenced that microalgae cells have around 50% carbon, in which 1.8 kg of CO_2 are biofixed on 1 kg of microalgae biomass (Lam et al., 2012). However, based on the current scientific maturity and anchored by the advance of analytical techniques and instrumental improvement, although theoretical evaluations have shown plausible results, unfortunately, in practice, this premise does not match reality.

Associated with these aspects, carbon management is a critical operational factor. Since the triumph of microalgae-based processes is straightly associated with the high rates of biomass productivity, carbon loads play a crucial role in balancing the reaction in photobioreactors. Thereby, the carbon balance characterization under the three-phase system (solid, liquid, and gas) may contribute to substrate bioconversion routes setting and directing the reaction according to the intended interest. In this sense, conducting scientific and quantitative control research on the carbon bioconversion process will elucidate the biochemical pathways, assisting in bioprospecting studies, enabling the channeling of the process for a specific commercial application (Barros et al., 2017).

Concurrently, the successful improvement of these research and development (R&D) will drive future progression on a large scale. To do this, sustainability must be examined to model and predict its consequent impacts and to identify ways in which industries and governments can better prepare for these impending transformations (Bussa et al., 2020). It is worth mentioning that, although the microalgal processes seem to be environmentally friendly, generally, the most critical point of the process is its extensive energy consumption. And, to make matters worse, it is often overlooked that energy input is generally in the form of electricity generated by burning coal and natural gas, which contributes to a substantial share in the global CO_2 emission (IEA, 2018). Therefore, life cycle assessment and carbon footprint appear as one of the most promising methodologies for quantifying metrics and sustainability indicators. In short, these crucial tools assist in the recognition and discovery of possible solutions for minimizing greenhouse gas emissions, as well as measuring the environmental burden of a product or process over its useful life (Deprá et al., 2018, Patel et al., 2020).

In this sense, this research aimed to analyze the CO_2 utilization in a photobioreactor. The study focused on the role of the CO_2 loads in the kinetic, environmental, and economic performance of the system. As far as we know, no article combines all of the fields above and, so, could fill a gap in the scientific literature.

2. Material and methods

2.1. Microorganism and photobioreactor design

The strains of the *Scenedesmus obliquus* CPCC05 from the Canadian Phycological Culture Centre were used to evaluate the conversion capacity of carbon dioxide in photobioreactors. The incubation conditions and details of the procedures were described by Deprá et al. (2019).

The bubble column photobioreactor was operated in batch mode, fed with 2.0 l. of synthetic BG-11 medium (Braun-Grunow medium) used as a culture system (Rippka et al., 1979). The configuration and design details of the system were defined by Maroneze et al. (2016).

2.2. Experimental conditions, sampling, and analytical methods

The photobioreactor experimental conditions were as follows: initial

Table 1
System flows and their respective mass loads for different experimental conditions.

Parameter	Unit	1% (v/v)	5% (v/v)	10% (v/v)	15% (v/v)	20% (v/v)	25% (v/v)
CO_2 loads	kg/m^3/d	25.6	128.3	256.6	384.9	513.2	641.5
Carbon loads	kg/m^3/d	7.0	35.0	70.0	104.9	139.9	174.9
Air volume	L/min	1.42	0.95	0.90	0.85	0.80	0.75
CO_2 volume	L/min	0.01	0.05	0.10	0.15	0.20	0.25

cell concentration of 100 mg/L, isothermal reactor operating at 28 °C, the photon flux density of 150 μmol/m²/s and continuous aeration of 1 VVM (volume of air per volume of culture per minute).

The air injections were continuously enriched and tested with 1, 5, 10, 15, 20, and 25% (v/v) carbon dioxide. The CO_2 loads and their respective carbon loads were established according to Table 1.

Samplings were as follows: liquid phase (culture medium), gaseous phase (headspace of the bioreactor), and solid phase (biomass). Cell biomass, pH dynamics, carbon concentrations, and volatile organic compounds (VOCs) were monitored under different experimental conditions. These procedures were performed every 24 h during the microorganism growth phases. The samples were carried out in duplicate, and the kinetic data indicate the mean value of four replicates.

Cell biomass concentration was assessed gravimetrically, filtering the 10 mL of culture medium through a 0.45 μm filter (Millex FG, Billerica-MA, USA) and drying it at 60 °C until a constant weight was reached.

The pH values were determined by a potentiometer (Mettler-Toledo, São Paulo-SP, Brazil).

To determine the CO_2/O_2 concentrations of photobioreactor exhaust gases, the equipment used was a GC-Greenhouse (Shimadzu, Kyoto, Japan), according to the methodology previously described by Severo et al. (2018).

Measurements of the total, organic, and inorganic carbon in the liquid and gaseous phases of the system were arranged in a carbon analyzer TOC-VCSN (Shimadzu, Kyoto, Japan), according to procedures described by Santos et al. (2017).

2.3. Performance indicators

Biomass data were used to evaluate the biomass productivity (kg/m²/d), the maximum specific growth rate (d^{-1}), and generation time (d) from Eq. 1–3, respectively:

$$PX = \frac{(X_i - X_{i-1})}{(t_i - t_{i-1})} \quad (1)$$

$$ln\left(\frac{XI}{X0}\right) = \mu max \times t \quad (2)$$

$$G_T = \frac{0.693}{\mu\,max} \quad (3)$$

where X_i is the biomass concentration at time t_i (kg/m³) and X_{i-1} is the biomass concentration at time t_{i-1} (kg/m³), X_o is the biomass concentration at time t_o (kg/m³), t is the residence time (d), and μ_{max} is the maximum specific growth rate (d^{-1}).

The photobioreactor performance was also evaluated under parameters of elimination capacity (EC, kg/m³/d) and removal efficiency (RE, %), according to Eqs. (4) and (5):

$$EC = \frac{(S_{Cin} - S_{Cout}) \times Q}{V_R} \quad (4)$$

$$RE = \frac{(S_{Cin} - S_{Cout})}{S_{Cin}} \times 100 \quad (5)$$

where V_R is the reactor volume (m³), Q corresponds to gas flow (m³/min), Sc_{in} and S_{Cout} are the inlet and outlet carbon substrate concentrations (kg), respectively.

Oxygen concentration data were used to assess the production capacity (PC, kg/m³/d), and the photosynthetic quotient (PQ) (Eq. 6–7):

$$PC = \frac{(OC_0 - OC_i) \times Q}{V_R} \quad (6)$$

$$PQ = \frac{\frac{d(O_2)}{dt}}{\frac{-d(CO_2)}{dt}} \quad (7)$$

where OC_0 and OC_i match the inlet and outlet O_2 concentration (kg), respectively, dO_2/dt and $-dCO_2/dt$ match the variation of the concentration of O_2 and CO_2 over time, respectively, and V_R is the reactor volume (m³).

2.4. Mass balances

The carbon mass balance (kg) was calculate from Eq. (8) according to Deprá et al. (2019):

$$Fin - Fout = VLMC\left(\frac{d\,[Cbiomass]}{dt} + \frac{d\,[DIC]}{dt}\right) + V_GMC\left(\frac{d\,[Cheadspace]}{dt}\right) \quad (8)$$

where F_{in} (kg/d): the carbon mass flow rate; F_{out} (kg/d): the carbon mass flow rate out of the photobioreactor; V_L (m³): culture volume; V_g (m³): headspace volume; Mc (kg): carbon concentration; $(d[C_{biomass}])/dt$ (kg/m³/d): change rate in the carbon concentration in biomass; $(d\,[DIC])/dt$ (kg/m³/d): change rate in dissolved inorganic carbon concentration; $(d[C_{headspace}])/dt$ (kg/m³/d): change rate in carbon concentration in the headspace.

2.5. Sustainability metrics and indicators

The life cycle assessment tool (LCA) assessed sustainability metrics and indicators (ISO, 2006). The purpose and scope of the implementation of this LCA were to evaluate, through the cradle to gate approach, the environmental footprint of energy and emission gas requirements for cultures under different carbon loads. Since the focus of the analysis was to determine the carbon and energy footprint, parameters such as other nutrients required by the cultivation system and post-cultivation stages, such as harvesting and drying biomass, were disregarded. Besides, the functional unit (FU) was established for a photobioreactor with a capacity of 1 m³ per period in operation of 7 days, i.e., a culture batch mode. The impact categories selected were global warming potential (GWP), energy resource (ER), ecotoxicity (ECO), acidification potential (AP), photochemical oxidant creation potential (SMOG), eutrophication potential (EP), ozone depletion potential (ODP). Additionally, the impact assessments referring to the categories of water footprint (WF) and land use (LU) were quantified in a unique evaluation, since their impact would be the same for all conditions.

The GWP was assessed according to Laratte et al. (2014), expressed in $kgCO_{2eq}$, as shown in Eq.9:

$$GWP = \sum_i GWP_i \times m_i \quad (9)$$

where GWP is the global warming potential ($kgCO_{2eq}$), i is the time horizon, GWP_i is the equivalence factor for the substance i and, m_i is the emission of the substance i (kg), both in a period of 100 years.

The ER measured the non-renewable energy demand required for the system operation expressed in kilojoules (kJ) (Eq. (10)):

$$ER = EED \times RTI \quad (10)$$

where ER is the energy resource (kJ), EED is the electrical energy required to the system (kWh), RTI is the residence time in operation (h).

The ECO was determined by toxic substances (CTUe), described by Eq. (11):

$$ETP_{(FAEP)} = \sum_i ETP_i \times m_i \quad (11)$$

where ETP is the ecotoxicity potential corresponding to the score of *freshwater aquatic ecotoxicity potential (FAEP)* (CTUe), $ETPi$ is the characterization factor for the substance i emitted to the environmental freshwater, and m_i is the amount emitted to a given environmental compartment (kg).

The AP was measured following Hauschild and Wenzel (1998),

expressed in $kgSO_{2eq}$, as presented in Eq. (12):

$$AP = \sum_i API_i \times m_i \quad (12)$$

where *AP* is the acidification potential ($kgSO_{2eq}$), *API* is the equivalence factor for the substance i, and m_i is the emission of substance *i* (kg).

The SMOG was calculated according to Hauschild and Wenzel (1998), being expressed in kgO_{3eq} (Eq. (13)):

$$POCP = \frac{OI_{VOC}}{OI_{ethene}} \quad (13)$$

where *POCP* is photochemical ozone creation potential (kgO_{3eq}), OI_{VOC} is ozone increment with VOC (kg), and OI_{ethene} is ozone increment with ethene (kg).

The EP was calculated using Eq. (14), according to Hauschild and Wenzel (1998), being expressed in kgN_{eq}:

$$EP = \sum_i EP_i \times m_i \quad (14)$$

where *EP* is the eutrophication potential ($kgPO_{4eq}$), *EPi* is the equivalence factor for the substance *i* and, m_i is the emission of the substance *i* (kg).

The ODP was determined according to Hauschild and Wenzel (1998), through Eq. (15), being expressed in kg CFC-11 $_{eq}$:

$$ODP = \sum_i ODP_i \times m_i \quad (15)$$

where *ODP* is the ozone depletion potential (kgCFC-11 $_{eq}$), ODP_i is the equivalency factor for the substance *i* and, m_i is the mass of the emission substance *i* (kg).

The WF was used to measure water resources consumed for the photobioreactor, being expressed in m^3. The detailed calculation model, described by Hoekstra (2016), is given through Eq. (16):

$$WF = WF_{blue} + WF_{green} + WF_{gray} \quad (16)$$

where *WF* is the total water footprint, WF_{blue} is the blue water footprint (m^3), WF_{green} is the green water footprint (m^3) and WF_{grey} is the grey water footprint (m^3).

The LU was calculated for assessing the efforts of transformation and occupation on biodiversity, expressed in ha, following Lathuillière et al (2017) (Eq. (17)):

$$LU = CF_{transf} \times CF_{occup} \times A \quad (17)$$

where LU is the land use (ha), CF_{trans} is the characterization factor for land transformation, CF_{occ} is the characterization factor defined for land occupation, *A* is the area (ha).

The net energy ratio (NER) (Eq. (18)) was measured following Jorquera et al. (2010). The biomass chemical composition was determined according to the methodology described in Nascimento et al. (2020). The Atwater System determined calorific values, through factors as an of 17 kJ/g for protein and carbohydrate and 37 kJ/g for lipid content (Watt and Merrill, 1963):

$$NER = \frac{\Sigma Eout}{\Sigma Einp} \quad (18)$$

where E_{out} is the output energy (kJ) and E_{inp} is the required input energy (kJ).

2.6. Potential production and power generation from VOCs

The VOCs production rate ($kg/m^3/d$) was evaluated according to Severo et al. (2018) (Eq. (19)):

$$P_{VOCs} = \frac{\left(\frac{(OC_i - OC_o)\times C_t}{100}\right) \times Q}{V_R} \quad (19)$$

where OC_i and OC_o match the inlet and outlet carbon organic concentration, respectively, and C_t is the VOC concentration. According to Hanby (2012), the power generation rate was estimated based on the calorific power of the carbon and hydrogen, 34,000 and 120,000 kJ/kg, respectively.

2.7. Carbon credits

The carbon credits were estimated according to Pérez-Fortes et al. (2016) (Eq. 20–21). The carbon prices used were proposed by the World Bank Group (World Bank and Ecofys, 2019):

$$CO_{2_{net\ produced}} = CO_{2\ conventional} - CO_{2\ emitted} \quad (20)$$

$$CO_{2_{emitted}} = CO_{2\ net\ produced} - CO_{2\ captured} \quad (21)$$

where $CO_{2\ conventional}$ is the quantity of CO_2 released in the conventional process, while $CO_{2\ emitted}$ and $CO_{2\ captured}$ refer to the microalgal system.

2.8. Statistical analyses

Analysis of variance (one-way ANOVA) and Tukey's test ($p < 0.05$) was used to test differences between carbon loads conditions. The report was carried with the Statistica 7.0 software (StatSoft, Tulsa OK, USA).

3. Results and discussion

3.1. Growth performance

The main aim of microalgae biomass large-scale production is to enhance productivity. Studies report that high concentrations of CO_2 play an essential role in the high biomass recovery of microalgae. Thus, the optimization of growth conditions remains vital to establish the kinetic behavior of microorganisms. Therefore, Table 2 presents the kinetic growth parameters for *Scenedesmus obliquus* microalgae in a photobioreactor, under different carbon dioxide load regimes.

As provided in Table 2, cultures under different carbon dioxide loads showed a significant difference in biomass productivity. The conditions with CO_2 loads of 641.5 and 513.2 $kg/m^3/d$ (25% and 20% CO_2) showed the highest rates of biomass productivity, around 0.46 and

Table 2
Growth kinetics for *Scenedesmus obliquus*.

Parameter	1% (v/v)	5% (v/v)	10% (v/v)	15% (v/v)	20% (v/v)	25% (v/v)
pH_{max}	$8.10^{c} \pm 0.02$	$8.08^{c} \pm 0.06$	$7.90^{c} \pm 0.05$	$8.20^{c} \pm 0.03$	$8.0^{d} \pm 0.01$	$8.30^{b} \pm 0.02$
X_{max} (kg/m^3)	$2.30^{fg} \pm 0.01$	$2.24^{g} \pm 0.03$	$1.70^{h} \pm 0.05$	$2.44^{fg} \pm 0.08$	$2.58^{ab} \pm 0.02$	$2.85^{a} \pm 0.07$
μ_{max} (d^{-1})	$0.40^{c} \pm 0.00$	$0.34^{d} \pm 0.00$	$0.33^{d} \pm 0.00$	$0.34^{d} \pm 0.00$	$0.80^{a} \pm 0.00$	$0.55^{b} \pm 0.00$
G_T (d)	$1.73^{c} \pm 0.01$	$2.03^{b} \pm 0.01$	$2.10^{a} \pm 0.03$	$2.03^{b} \pm 0.05$	$0.86^{e} \pm 0.03$	$1.26^{d} \pm 0.02$
Px (average) ($kg/m^3/d$)	$0.32^{fg} \pm 0.02$	$0.35^{b} \pm 0.02$	$0.23^{e} \pm 0.05$	$0.31^{fg} \pm 0.03$	$0.34^{bc} \pm 0.02$	$0.41^{a} \pm 0.04$
Px (peak) ($kg/m^3/d$)	$0.34^{c} \pm 0.01$	$0.36^{bc} \pm 0.04$	$0.29^{d} \pm 0.08$	$0.36^{bc} \pm 0.09$	$0.41^{ab} \pm 0.02$	$0.46^{a} \pm 0.03$

Within the same line, means with different superscripts are significantly different ($p < 0.05$) by Tukey's test.
pH_{max}: maximum pH value, X_{max}: maximum cell biomass, μ_{max}: maximum specific growth rate, G_T: cell generation time, Px: biomass productivity.

0.41 kg/m^3/d, respectively, without statistical difference (Tukey's test $P < 0.05$). In contrast, the lowest values were found for conditions corresponding to CO_2 loads of 25.6, 128.3, and 256.6 kg/m^3/d (1, 5, and 10% CO_2). Comparatively, Derakhshandeh and Un (2019) obtained biomass productivity values from *Scenedesmus* sp. of 0.37 kg/m^3/d and 0.23 kg/m^3/d, both under CO_2 loads of 190.0 and 380.0 kg/m^3/d, respectively. In contrast, using CO_2 loads of 30.0, 60.0, and 100.0 kg/m^3/d, the *Scenedesmus dimorphus* showed biomass productivities of 0.05, 0.06, and 0.08 kg/m^3/d, respectively (Vidyashankar et al., 2013). Besides, when evaluating the behavior of the microalgae *Scenedesmus obliquus* SJTU-3, Tang et al. (2011) reported values of 0.16 kg/m^3/d for CO_2 loads of 30.0 kg/m^3/d, 0.15 kg/m^3/d for CO_2 loads of 60.0 kg/m^3/d, and 0.13 kg/m^3/d for CO_2 loads of 130 kg/m^3/d. Also, Ramos-Ibarra et al. (2019), by providing CO_2 loads of 3.0 kg/m^3/d for *Scenedesmus* sp., found values of 0.35 kg/m^3/d. Notably, the photochemical metabolic properties of microalgae are influenced by CO_2 loads. Since CO_2 is the mainline source of carbon, its restricted supply will inhibit biomass productivity. In contrast, the literature reports that high CO_2 loads hinder algae growth. Lower tolerance to CO_2 is due to acidification of the medium. This occurs because the aqueous CO_2 forms carbonic acid in the water, being that some deprotonate to bicarbonate and H^+, resulting in a decrease in the pH of the solution. However, as in previous studies, the empty bed residence time (EBRT) of the gas mixture in the photobioreactor was maintained constant at 1 min with the flow per unit volume of 1 VVM, the microalgae can correct the pH of culture medium and increase the same, resulting in non-inhibition of the microorganism. Furthermore, morphologically, the presence of the bifunctional enzyme ribulose biphosphate carboxylase/oxygenase (RuBisCO), catalyzes the photosynthetic carbon fixation mechanism (Liu et al., 2019). Thus, the injection of an appropriate amount of CO_2 increases the competition of the RuBisCO binding sites and correspondingly increase the carboxylation speed in the pentose phosphate (C3) reducing pathway, allowing greater ease of conversion and, consequently, higher biomass productivity.

3.2. Carbon dioxide conversion and oxygen production

The dynamics of CO_2 conversion and O_2 release for *Scenedesmus obliquus* in the photobioreactor is shown in Fig. 1. The behavior of the microorganism is similar throughout the experiments (bell-shaped curves pattern), indicating low values in the early and late growing and achieving maximum rates at 4 d of culture. This behavior is attributed to the depletion of nutrients present in the culture media, related to the formation of cell clusters in the later stages of the process (Jacob-Lopes et al., 2009).

The highest rates of carbon conversion and removal efficiency can be observed in cultures with CO_2 loads of 25.6, 128.3, and 256.6 kg/m^3/d (1, 5 and 10% CO_2), with maximum values, found of 0.98, 0.77 and 0.62 kgCO_2/m^3/d and 68.65, 54.02 and 43.02%, respectively. Likewise, oxygen production reached maximum rates of 0.74, 0.58, and 0.46 kgO_2/m^3/d. Conversely, the experimental condition with CO_2 loads of 641.5 kg/m^3/d (25% CO_2), presented the lowest rates, assimilating and generating values of 0.08 kgCO_2/m^3/d and 0.06 kgO_2/m^3/d, presenting removal efficiencies lower to 6%. Comparatively, Severo et al. (2018), using the microalgae *Scenedesmus obliquus*, showed maximum rates of 0.44 kgCO_2/m^3/d and 0.38 kgO_2/m^3/d, for CO_2 conversion and O_2 release, respectively. Similar behavior was found for our condition with CO_2 loads of 384.9 kg/m^3/d (15% CO_2), where values were observed in the order of 0.44 kgCO_2/m^3/d for CO_2 conversion and 0.33 kgO_2/m^3/d for O_2 release, reaching maximum removal efficiency values of 30%. Additionally, Chandra et al. (2016) evaluated the CO_2 conversion dynamics of the *Scenedesmus abundans* microalgae, where conversion values of 0.08 kgCO_2/m^3/d (5% CO_2), 0.09 kgCO_2/m^3/d (10% CO_2), 0.11 kgCO_2/m^3/d (15% CO_2), and 0.09 kgCO_2/m^3/d (20% CO_2) were observed. Still, studies by Chaudhary et al. (2018), reported average conversion values of 0.13 kgCO_2/m^3/d under CO_2 loads of 20.0 kg/m^3/d (5% CO_2) for *Scenedesmus obliquus*. The higher rates of carbon conversion are associated with carbonic anhydrase activity since, in cells cultivated with low CO_2 content air, their activity is more significant than in cells cultivated with high CO_2 consent air (Aizawa and Miyachi, 1986).

Simultaneously, the photosynthetic quotient (PQ) of the microalgae *Scenedesmus obliquus*, obtained under different CO_2 loads, reached average values of 0.75 (data not shown). This outcome is coherent with the theoretical value projected from the photosynthetic equation, which affirms that each 1 kg of CO_2 consumed matches a 0.73 kg O_2 released (Jacob-Lopes et al., 2010). Also, the results found in the present study corroborate the studies carried out by Deprá et al. (2019), who using *Scenedesmus obliquus*, observed a photosynthetic quotient value of 0.75. In terms of comparison, the characterization of the photosynthetic quotient was determined for microalgae *Muriellopsis* sp. by Fernández-Sevilla et al. (2018), who the authors found values of 0.56. Similarly, photorespiration was observed at a low photosynthetic quotient value (0.50) for co-cultivation of the predominant microalgae of *Scenedesmus*

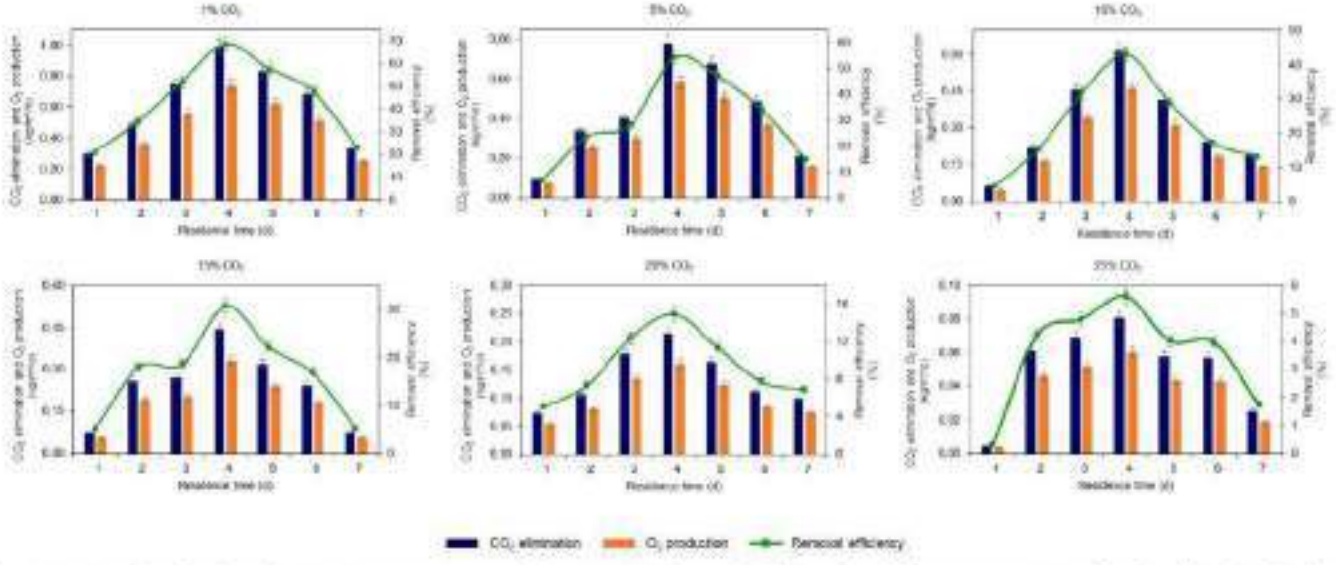


Fig. 1. Dynamics of carbon dioxide conversion rates, oxygen release rates, and removal efficiency for different concentrations of carbon dioxide in the photobioreactor.

sp. (Toro-Huertas et al., 2019). Moreover, studies showed values of 1.26 for *Scenedesmus obliquus* (Undurraga et al., 2016). Evidently, the efficiency of photorespiration is associated with the metabolic versatility of carbon assimilation (Chen et al., 2020). This is because the distinct microalgae species present different preferential pathways for carbon acquisition, mainly in the types and plenty of dissolved inorganic carbon transporters and carbonic anhydrases. Besides, it is essential to note that environmental specifications such as light frequency and intensity, temperature, available nutrients, and other stressors substantially influence the performance of the photosynthetic apparatus of these microorganisms.

3.3. Carbon footprint

Accurate carbon balance is essential for the successful development of microalgae-based processes. Thus, Table 3 presents the determination of the mass carbon balance for the microalgae *Scenedesmus obliquus* under different carbon loads.

As seen in Table 3, the photosynthetic mechanism of microalgae is responsible for a large proportion of the global carbon conversion. Under conditions of low carbon concentration (loads of 7.0 $kgC/m^3/d$, i.e., 1% CO_2), microalgae tend to convert slightly higher rates of carbon into biomass (1.28 $kgC/m^3/d$), representing a total of 8.90%. Likewise, the intermediate availability of carbon (loads 70.0 and 104.9 $kgC/m^3/d$, i.e., 10 and 15% CO_2) did not show the significant statistical difference (Tukey's test $P < 0.05$) in the conversion of carbon into biomass. The values were observed in the order of 1.30 $kgC/m^3/d$ (10% CO_2) and 1.28 $kgC/m^3/d$ (15% CO_2), representing an estimate of 1.44 and 1.32%, respectively.

On the other hand, cultures with higher carbon availability achieved the best conversions in biomass, resulting in values in the range of 1.80 $kgC/m^3/d$ (25% CO_2) and 1.66 $kgC/m^3/d$ (20% CO_2), corresponding to total proportion of 6.12 and 2.64%, respectively. Comparatively, the studies by Jacob-Lopes et al. (2010) report that about 3% of the converted fraction is directed to biomass. Likewise, Deprá et al. (2019) it reached carbon values for the biomass of 1.28%. Indicators show that the carbon conversion into biomass is associated with the action of the enzyme carbonic anhydrase. Thus, the biomass values have become constant since the performance of the catalyst has increased in comparison with cultures treated with CO_2 (Basu et al., 2014). This is because its activity favors the diffusion of dissolved inorganic carbon from outside the cells to the sites of the carboxylation reactions.

Notoriously, the ratio between carbon consumption and biomass generation does not match its global biotransformation (Deprá et al., 2019). Since the conversion to biomass resulted in maximum values below 10%, it is evident that the microalgae were using carbon as building blocks for other metabolites. In this sense, not only the measurement of the liquid fractions of the culture but also the volatile fraction becomes crucial for the total determination of the overall mass carbon balance (Fig. 2).

The mineralization process is the result of a delicate set of chemical reactions. As the carbon dioxide is in continuous contact with the oxygen produced by the microalgae, the oxidation reactions become permanent. Besides, mineralization can occur when the inserted CO_2 dissolves in an aqueous medium forming the carbonic acid. Hence, the microalgae absorb this through the ionic balance established by bicarbonate ion. Thus, when assessing the mineralization potential at different carbon concentrations, the highest point reached was the carbon loads of 174.9 $kgC/m^3/d$ (25% CO_2), resulting in a conversion of 2.06×10^{-2} $kgC/m^3/d$ (0.10%). In opposition, the lowest mineralization rates, about 1.12×10^{-2} $kgC/m^3/d$, were observed under the carbon loads of 7.0 $kgC/m^3/d$ (1% CO_2), representing about 0.07% of the overall conversion. In comparison, Kishi et al. (2020), when establishing the carbon balance for *Arthrospira platensis*, presented higher mineralization rates, reaching maximum values between 2.60×10^{-1} and 3.60×10^{-1} $kgC/m^3/d$.

At the same time, microalgae are acknowledged for their potential to excrete species-specific viscous substances, known as exopolymers. As can be seen in Fig. 2, the behavior of the *Scenedesmus obliquus* microalgae was similar for all conditions. In fact, the microorganism tends to excrete these substances exponentially, reaching a stationary character in the 4 d. Under these aspects, the conditions that showed the highest rates of conversion of carbon to exopolymers were 3.67×10^{-1} (1.25%), 3.16×10^{-1} (0.50%), and 2.64×10^{-1} (0.27%) $kgC/m^3/d$, referring to cultures with carbon loads of 174.9 (25% CO_2), 139.9 (20% CO_2), and 104.9 $kgC/m^3/d$ (15% CO_2), respectively. Comparatively, for *Scenedesmus* sp., the excreted values of exopolymers under traditional cultivation were 5.10×10^{-2} $kg/m^3/d$, whereas, after a stress condition, the content was increased to 1.22×10^{-1} $kg/m^3/d$ (Sivaramakrishnan et al., 2020). Still, studies by Qian et al. (2020) showed exopolymeric concentrations for *Microcoleus vaginatus* in the order of 1.80×10^{-1} kg/m3/d. This behavior can be attributed to a normal part of the microorganism's physiological processes. However, this behavior is usually reported under conditions of stress caused by the imbalance of the C/N ratio. Also, the occurrence of critical concentrations of CO_2 shows the beginning of a short-term stress stimulus. Therefore, the longer a microorganism remains in an area with critical concentration, the more severe the internal changes to the cell will be.

Finally, the volatile fraction represents the majority of carbon conversion. Among the different conditions tested, the condition with carbon loads of 7.0 $kgC/m^3/d$ (1% CO_2), presented values of 11.38 $kgC/m^3/d$ (79%), which is the lowest volatile carbon conversion. In contrast, the condition with carbon loads of 70.0 and 104.9 $kgC/m^3/d$ (10 and 15% CO_2) proved to be the state of the highest volatile carbon conversion, being a total of 86.48 and 95.19 kgC/m^3, resulting in an overall transformation of 98%. Likewise, the intermediate carbon loads (35.0 and 139.9 kg/d, i. e., 5 and 20% CO_2), represented average values of total volatile conversion of 95%. However, under the condition of 174.9 $kg/m^3/d$ (25% CO_2), the microalgae are prone to show a slight decline in the generation of volatiles, resulting in conversion values in

Table 3
Carbon mass balance in the photobioreactor (HRT = 4 d).

Carbon balance	1% (v/v)	5% (v/v)	10% (v/v)	15% (v/v)	20% (v/v)	25% (v/v)
Input carbon (kg/m^3)	$21.0^{f} \pm 0.01$	$104.0^{e} \pm 0.01$	$210.0^{d} \pm 0.02$	$314.0^{c} \pm 0.03$	$420.0^{b} \pm 0.02$	$524.0^{a} \pm 0.01$
Lost carbon (kg/m^3)	$6.0^{f} \pm 0.01$	$48.0^{e} \pm 0.01$	$120.0^{d} \pm 0.01$	$218.0^{c} \pm 0.01$	$357.0^{b} \pm 0.01$	$495.0^{a} \pm 0.01$
Converted carbon (kg/m^3)	$14.34^{f} \pm 0.02$	$56.0^{e} \pm 0.03$	$90.30^{b} \pm 0.01$	$96.80^{a} \pm 0.02$	$62.60^{c} \pm 0.04$	$29.38^{d} \pm 0.04$
Biomass (kg/m^3)	$1.28^{d} \pm 0.01$	$1.38^{c} \pm 0.03$	$1.30^{d} \pm 0.05$	$1.28^{d} \pm 0.08$	$1.66^{b} \pm 0.02$	$1.80^{a} \pm 0.07$
Exopolymers (kg/m^3)	$2.32 \times 10^{-1} \pm 0.04$	$1.80 \times 10^{-1} \pm 0.02$	$1.21 \times 10^{-1} \pm 0.03$	$2.64 \times 10^{-1} \pm 0.02$	$3.16 \times 10^{-1} \pm 0.01$	$3.67 \times 10^{-1} \pm 0.01$
Mineralization (kg/m^3)	$1.12 \times 10^{-2a} \pm 0.02$	$1.53 \times 10^{-2a} \pm 0.01$	$1.37 \times 10^{-2d} \pm 0.01$	$1.72 \times 10^{-2b} \pm 0.04$	$1.73 \times 10^{-2b} \pm 0.01$	$2.06 \times 10^{-2a} \pm 0.02$
VOCs (kg/m^3)	$11.38^{f} \pm 0.01$	$50.78^{d} \pm 0.06$	$86.48^{b} \pm 0.01$	$95.19^{a} \pm 0.02$	$59.92^{c} \pm 0.02$	$26.55^{e} \pm 0.01$

Within the same line, means with different superscripts are significantly different ($p < 0.05$) by Tukey's test.

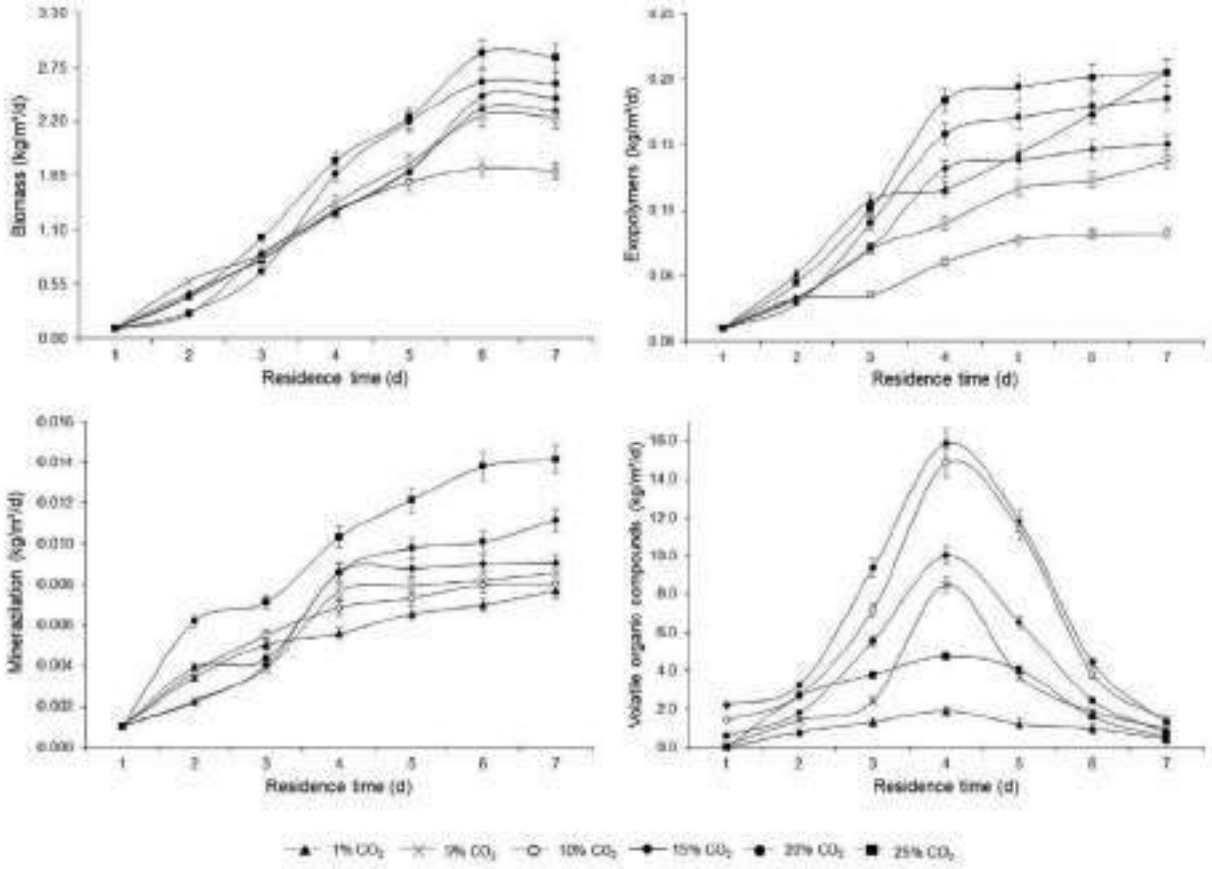


Fig. 2. Carbon footprint dynamics in the photobioreactor.

the order of 26.55 kgC/m^3 (90%), following the behavior of bell-shaped curves pattern. In terms of comparison, the values of 92% were presented by Jacob-Lopes and Franco (2013). This high carbon conversion into volatile compounds is directly associated with the availability of inserted carbon. After the conversion stability of carbon into biomass, inorganic carbon bioconversion simultaneously metabolizes, glyceraldehyde-3-phosphate, pyruvate, or acetyl-CoA. Consequently, several routes enzymatic by a reaction degradation can convert these metabolites into VOCs. As a result, these compounds can be generated into distinct various chemical classes as terpenes, alcohols, ketones, aldehydes, esters, hydrocarbons, carboxylic acids, and sulfurized compounds. However, despite its metabolic production potential, the recovery of these compounds represents a bottleneck to be overcome in industrial systems. This because of the techniques explored for the separation and recovery of VOCs in bioreactors whose systems utilized are adapted to the principles of adsorption, condensation, absorption, and membrane-based methods, which assist microalgae-based process (Vieira et al., 2019).

3.4. Sustainability metrics and indicators

The evaluation of sustainability metrics and indicators of potential process paths is a necessary step to guide future developments. Although several *ad hoc* criteria are proposed in the literature to guide the sustainable design systems, the leading indicators focus on the environmental and economical approach.

Among these approaches, energy demands are the hottest point in a microalgae-based process. This is because the starting point for developing a sustainable system is the consolidation of a favorable energy balance. For this reason, the NER is considered the primary quantification model, since its application is to demonstrate the difference between the amount of energy available and the amount of energy used in systems. Thus, for processes to be considered technically feasible, it was theoretically established that the NER must be greater than 1. However, most industrial processes in operation do not meet energetic requirements, enforcing their optimization to achieve this theoretical value. In this sense, Table 4 presents the consumed energy requirements for the cultivation step, the produced energy potentials of the biomass and volatile compounds, as well as the energy balance of the culture system under different carbon loads for FU of 1 m^3 of photobioreactor per operation of 7 days.

In terms of the energy potential of biomass, the best conditions identified were with CO_2 loads of 384.9, 513.2, and 641.4 kg/m^3/d (15, 20, and 25% CO_2), resulting in values in the order of 44.47, 47.02, and

Table 4
Input and output energy values and their respective net energy ratio on the photobioreactor.

Parameter[a]	1% (v/v)	5% (v/v)	10% (v/v)	15% (v/v)	20% (v/v)	25% (v/v)
Biomass energy produced (kJ)	41.92	40.83	30.98	44.47	47.02	51.96
VOCs energy produced (kJ)	569,297.66	1,642,013.57	3,688,004.74	4,162,833.79	2,382,846.34	1,466,338.62
Cultivation energy consumed (kJ)	1,209,600.0	1,209,600.0	1,209,600.0	1,209,600.0	1,209,600.0	1,209,600.0
Net energy ratio (NER)	0.47	1.35	3.04	3.44	1.96	1.23

[a] The period considered was 7 days per 1 m^3 of the photobioreactor, or more precisely, 1 batch mode of culture.

51.96 kJ, respectively. Likewise, these conditions resulted in the best volatile energy potentials. These results are associated with greater availability of free carbon for cell conversion in both biomass and volatile compounds. However, under the aspects of the NER, all conditions had a positive energy balance, except for the condition with CO_2 loads of 25.6 kg/m^3/d (1% CO_2), which had a NER of 0.47. This energy imbalance can be attributed to the energetic potential of volatile organic compounds since this condition has the lowest production potential. On the other hand, among all conditions tested, the best values for NER (3.44) were found in CO_2 loads of 384.9 kg/m^3/d (15% CO_2), followed by CO_2 loads of 256.6 kg/m^3/d (10% CO_2) with a NER of 3.04.

Moreover, when assessing the environmental impacts related to cultures under different carbon concentrations, the condition with CO_2 loads of 25.6 kg/m^3/d (1% CO_2) had the best environmental profile, resulting in estimated the GWP values of 99.33 kg CO_2 eq, the ER of 219.00 MJ, the ECO of 714.48 CTUe, the AP of 0.53 kg SO_2 eq, the SMOG of 1.80 kg O_3 eq, the EP of 0.18 kg N eq, the ODP of 3.13×10^{-6} kg CFC11 eq (Fig. 3). Regarding the impacts related to the WF and LU, values in the order of 1.02 m^3 and 0.13 PDF/ha, respectively, were evaluated for all conditions since the standardized FU of 1 m^3 was established. However, conditions with higher CO_2 loads showed a slightly higher environmental burden, resulting in impacts without significant differences. In contrast, the most environmental impacts were found for the highest concentrations of carbon dioxide (CO_2 loads of 641.5 kg/m^3/d). Comparatively, studies by Porcelli et al. (2020) evaluated the environmental indicators for microalgal processes by comparing CO_2 sources. The scenarios being assessed presented GWP values of 3.00×10^2 and 2.57×10^2 kg CO_2 eq, the ECO of 2.83×10^1 and 2.70×10^1 CTUe, the AP of 8.52×10^{-1} and 8.15×10^{-1} kg SO_2 eq, the EP de 1.81×10^{-1} and 1.69×10^{-1} kg N eq, and the ODP of 1.73×10^{-7} and 1.69×10^{-7} kg CFC11 eq, for synthetic and residual CO_2, respectively. Although the microalgae have converted a large part of the carbon inserted in the photobioreactor, it is important to note that photobioreactors have conversion efficiency below 30%. Because of this premise, high charges of carbon dioxide inserted in the system are lost through exhausting gases (Jacob-Lopes et al., 2009). Thus, most of the environmental impacts associated with this system are the result of high energy demand and low conversion efficiency.

Besides, as seen previously, energy demand also influences these categories. In this respect, Fig. 4 shows the environmental impacts related to the global warming potential under different energy matrices for FU of 1 m^3 of photobioreactor per operation of 7 days. It is possible to observe that, for all conditions evaluated, when using the energy matrix of hydroelectric plants, the impacts can be reduced by up to 80%. In contrast, in the use of wind energy, the reduction can reach 95%, and the photovoltaic panels achieved a 33% reduction in

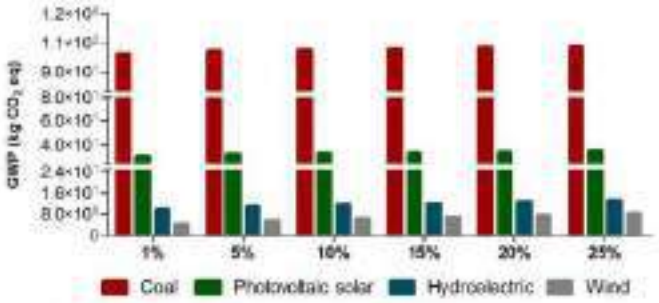


Fig. 4. Global warming potential under different energy resources, considering UF of 1 m^3 of the photobioreactor per 7 days of operation.

environmental impacts. However, despite being a clean source of energy, only 18% of the world's energy is produced by hydroelectric plants, once most countries do not have the natural conditions necessary for the construction of these plants. Likewise, the intermittency of the winds and the geographic location of the wind plants, make this technology a variable source of energy, and not a safe supplier.

On the other hand, the integration of microalgae bioreactors to photovoltaic panels seems to be the most promising alternative. This is because this configuration can increase the overall efficiency of photoconversion of the entire cultivation system, producing electrical energy directly available together with microalgae biomass. In addition, if the photovoltaic cells are placed with a suitable geometry, it can be beneficial to avoid or reduce photoinhibition phenomena, beyond to the notable reduction in environmental impacts (Nwoba et al., 2020). Therefore, it is evident that decision-making to replace the energy matrix with clean sources can bring immediate results to reduce environmental impacts.

3.5. Estimation of carbon credits

Simultaneously, elucidating insights of environmental and economic sustainability through the benefits of environmental bioremediation and carbon credits seems to be by far the most influential parameter for the successful acquisition of microalgae on a commercial scale. In this sense, Table 5 presents the estimates of the carbon emitted and sequestered, beyond the hypothetical scenario of the carbon credits generated.

According to Table 5, the best conditions of the mass of relative carbon captured were the cultures under injection with CO_2 loads of 25.6, 128.3, and 256.6 kg/m^3/d (1, 5 and 10% CO_2), presenting values in the order of 4.36, 3.0 and 2.20 kg/m^3, respectively. In contrast, the condition with CO_2 loads of 641.5 kg/m^3/d (25% CO_2) that had the

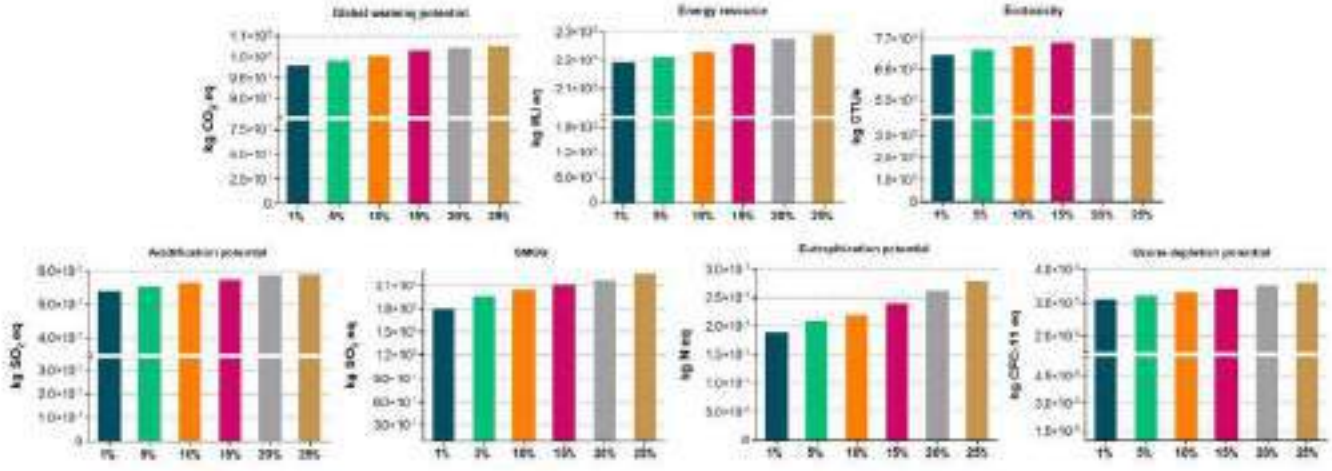


Fig. 5. Sustainability metrics and indicators in the photobioreactor under different CO_2 loads, considering UF of 1 m^3 of the photobioreactor per 7 days of operation.

Table 5
Carbon credit estimates in the photobioreactor.

Parameter	1% (v/v)	5% (v/v)	10% (v/v)	15% (v/v)	20% (v/v)	25%(v/v)
Carbon captured (kg/m^3)	4.36	3.0	2.20	1.68	0.94	0.35
Carbon emitted (kg/m^3)	103.48	103.48	103.48	103.48	103.48	103.48
Carbon credits (USD/m^3)	0.12	0.08	0.06	0.04	0.02	0.01

The period considered was 7 days per 1 m^3 of the photobioreactor, or more precisely, 1 batch mode of culture.

worst carbon capture performance (0.35 kg/m^3). On the other hand, the bioeconomic of the process of carbon capture by microalgae in photobioreactors showed that the condition with CO_2 loads of 25.6 kg/m^3/d (1% CO_2) could gain in terms of carbon credits around USD 0.12/m^3. Obviously, this revenue does not represent obtaining economic profits, since the microalgae processes present more significant expenses. However, these values could be considered as auxiliary revenues in the costs of the processes related to these facilities.

Evidently, as carbon loads in cultures are increased, there is a significant reduction in carbon capture. As a consequence, the exhaust gases raise the potential environmental impacts. In this sense, a trade-off must be achieved, considering beyond the environmental impacts, the energy balance, the potentials of the generated bioproducts, as well as the overall performance of the process. Thus, from a process control management point of view, for demands where economic viability allows the use of food-grade CO_2, experiments with lesser CO_2 loads (25.6 and 128.3 kg/m^3/d, 1 and 5% CO_2 respectively) are the best scenarios for exploring microalgal biomass. This is because it allows, in a safe way, the bio-exploration of intracellular products for applications in products for food purposes.

However, the injection condition with 10% CO_2, i.e., CO_2 loads of 256.6 kg/m^3/d, can be potentially explored under the aspect of an integrated system for bioenergy. In view of the fact that industrial gaseous waste can be utilized beyond providing satisfactory biomass productivity with the prospective applicants for the production of biofuels. In addition, this experimental condition provides an imminent application of volatile compounds as energy enhancers. Likewise, the conditions of 20 and 25% of CO_2 (loads of 513.2 and 641.5 kg/m^3/d, respectively), presented the best conditions for the exploitation of microalgal biomass. However, if we start from the principle of applying an integrated process with the use of greenhouse gases, this biomass can be exploited for the application of animal feeds or biofertilization.

Finally, under an integrated system view, the condition with the injection of 15% CO_2 (CO_2 loads of 384.9 kg/m^3/d), provides the best balance between the process variables analyzed, since it allows the reuse of most of the exhaust gases released from the industrial units. Besides, it presents satisfactory values of biomass productivity and carbon capture, beyond offering the optimal conditions for the production of volatile compounds, where its exploration in an integrated manner results in a positive energy balance.

4. Conclusions

Study established the carbon footprint in a photobioreactor under different CO_2 loads. The best condition for microalgae biomass production was observed under CO_2 loads of 641.5 kg/m^3/d, while that for bioconversion into VOCs was determined by CO_2 loads of 256.6 and 384.9 kg/m^3/d. From an integrated perspective, the culture with CO_2 loads of 384.9 kg/m^3/d allowed to capture and use the CO_2 on the photobioreactor, resulting in bioproducts for commercial exploitation. Thus, scientific advances found will enable us to assist in process control through the decision-making about the carbon loads used, depending on the target industry and interest chosen bioproduct.

CRediT authorship contribution statement

Mariany C. Deprá: Conceptualization, Methodology, Data curation, Writing - original draft. **Rosangela R. Dias:** Methodology, Validation. **Ihana A. Severo:** Methodology, Validation. **Cristiano R. de Menezes:** Supervision, Funding acquisition. **Leila Q. Zepka:** Supervision, Funding acquisition. **Eduardo Jacob-Lopes:** Conceptualization, Project administration, Writing - review & editing.

Declaration of Competing Interest

The authors declare that they have no known competing financial interests or personal relationships that could have appeared to influence the work reported in this paper.

Acknowledgement

Funding for this research has been provided by the National Council for Scientific and Technological Development (CNPq), Coordination of Improvement of Higher Education Personnel (CAPES), Finance Code 001 (Brazil).

Appendix A. Supplementary data

Supplementary data to this article can be found online at https://doi.org/10.1016/j.biortech.2020.123745.

References

Ahmed, E., Lu, G., Yousaf, S., Abbas, Q., Ullah, H., Ali, M.U., 2020. Recent advances in carbon-based renewable adsorbent for selective carbon dioxide capture and separation – a review. J. Cleaner Prod. https://doi.org/10.1016/j.jclepro.2019.118409. 118409.

Aizawa, K., Miyachi, S., 1986. Carbonic anhydrase and CO_2 concentrating mechanisms in microalgae and cyanobacteria. FEMS Microbiol. Rev. 2 (3), 215–233. https://doi.org/10.1016/0378-1097(86)90447-7.

Andrade, D.S., Telles, T.S., de Castro, G.H.L., 2020. The Brazilian microalgae production chain and alternatives for its consolidation. J. Cleaner Prod. https://doi.org/10.1016/j.jclepro.2019.119526.

Anwar, M.N., Fayyaz, A., Sohail, N.F., Khokhar, M.F., Baqar, M., Yasar, A., Aghbashlo, M., 2020. CO_2 utilization: Turning greenhouse gas into fuels and valuable products. J. Environ. Manage. 260, 110059. https://doi.org/10.1016/j.jenvman.2019.110059.

Barros, A., Guerra, L.T., Simões, M., Santos, E., Fonseca, D., Silva, J., Costa, L., Navalho, J., 2017. Mass balance analysis of carbon and nitrogen in industrial scale mixotrophic microalgae cultures. Algal research 21, 35–41. https://doi.org/10.1016/j.algal.2016.10.014.

Basu, S., Roy, A.S., Mohanty, K., Ghoshal, A.K., 2014. CO_2 biofixation and carbonic anhydrase activity in *Scenedesmus obliquus* SA1 cultivated in large scale open system. Bioresour. Technol. 164, 323–330. https://doi.org/10.1016/j.biortech.2014.05.017.

Busse, M., Zollfrank, C., Röder, H., 2020. Life-cycle assessment and geospatial analysis of integrating microalgae cultivation into a regional economy. J. Cleaner Prod. 243, 118630. https://doi.org/10.1016/j.jclepro.2019.118630.

Chandra, T.S., Deepak, R.S., Kumar, M.M., Mukherji, S., Chauhan, V.S., Sarada, R., Mudliar, S.N., 2016. Evaluation of indigenous fresh water microalga *Scenedesmus obtusus* for food and fuel applications: effect of carbon dioxide, light and nutrient sources on growth and biochemical characteristics. Bioresour. Technol. 207, 430–439. https://doi.org/10.1016/j.biortech.2016.01.044.

Chaudhary, R., Dikshit, A.K., Tong, Y.W., 2018. Carbon-dioxide biofixation and phycoremediation of municipal wastewater using *Chlorella vulgaris* and *Scenedesmus obliquus*. Environ. Sci. Pollut. Res. 25 (21), 20399–20406. https://doi.org/10.1007/s11356-017-9575-3.

Chen, Y., Xu, C., Vaidyanathan, S., 2020. Influence of gas management on biochemical conversion of CO_2 by microalgae for biofuel production. Appl. Energy 261, 114420. https://doi.org/10.1016/j.apenergy.2019.114420.

Choi, Y.Y., Patel, A.K., Hong, M.E., Chang, W.S., Sim, S.J., 2019. Microalgae Bioenergy with Carbon Capture and Storage (BECCS): An emerging sustainable bioprocess for reduced CO_2 emission and biofuel production. Bioresource Technology Reports 100270. https://doi.org/10.1016/j.biteb.2019.100270.

Deprá, M.C., Jacob-Lopes, E., Zepka, L.Q., 2018. Life Cycle Assessment of Biofuels from Microalgae. In: Energy from Microalgae. Springer, Cham, pp. 141–155. https://doi.org/10.1007/978-3-319-69093-3_6.

Deprá, M.C., Mérida, L.G., de Menezes, C.R., Zepka, L.Q., Jacob-Lopes, E., 2019. A new hybrid photobioreactor design for microalgae culture. Chem. Eng. Res. Des. 144, 1–10. https://doi.org/10.1016/j.cherd.2019.01.023.

Derakhshandeh, M., Un, U.T., 2019. Optimization of microalgae Scenedesmus sp. growth rate using a central composite design statistical approach. Biomass Bioenergy 122, 213–220. https://doi.org/10.1016/j.biombioe.2019.01.022.

Fernández-Sevilla, J.M., Brindley, C., Jiménez-Ruiz, N., Acién, F.G., 2018. A simple equation to quantify the effect of frequency of light/dark cycles on the photosynthetic response of microalgae under intermittent light. Algal Res. 35, 479–487. https://doi.org/10.1016/j.algal.2018.06.026.

Gani, R., Boldyga, J., Biscans, B., Brunazzi, E., Charpentier, J.C., Drioli, E., Feise, H., Furlong, A., Geen, R.M.V., Hamptiaux, J.-C., ten Kate, A.J., Kontogeorgis, G.M., Manenti, F., Marin, G.B., Manousiri, S.S., Piccinono, P.M., Povoa, A., Rodrigo, M.A., Woodley, J.M., 2020. A multi-layered view of chemical and biochemical engineering. Chem. Eng. Res. Des. https://doi.org/10.1016/j.cherd.2020.01.008.

Hanby, V.I., 2012. Combustion and Pollution Control in Heating Systems. Springer Science & Business Media 10.1007/978-3-4471-2071-1.

Hauschild, M. Z., Wenzel, H., 1998. Environmental Assessment of Products. Volume 2: Scientific Background. 1st edition, Springer US, 566p.

Hoekstra, A.Y., 2016. A critique on the water-scarcity weighted water footprint in LCA. Ecol. Ind. 66, 564–573. https://doi.org/10.1016/j.ecolind.2016.02.026.

IEA. International Energy Agency (2018). Key World Energy Statistics 2018, IEA, Paris, https://doi.org/10.1787/key_energ_stat-2018-en.

IEA. International Energy Agency. Energy, G. (2019). CO2 Status Report—The Latest Trends in Energy and Emissions in 2018.

ISO (International Organization for Standardization), 2006. ISO 14040:2006(E) Environmental Management – Life Cycle Assessment – Principles and Framework.

Jacob-Lopes, E., Franco, T.T., 2013. From oil refinery to microalgal biorefinery. J. CO_2 Utiliz. 2, 1–7. https://doi.org/10.1016/j.jcou.2013.06.001.

Jacob-Lopes, E., Revah, S., Hernández, S., Shirai, K., Franco, T.T., 2009. Development of operational strategies to remove carbon dioxide in photobioreactors. Chem. Eng. J. 153 (1–3), 120–126. https://doi.org/10.1016/j.cej.2009.06.025.

Jacob-Lopes, E., Scoparo, C.H.G., Queiroz, M.I., Franco, T.T., 2010. Biotransformations of carbon dioxide in photobioreactors. Energy Convers. Manage. 51, 894–900. https://doi.org/10.1016/j.enconman.2009.11.027.

Jorquera, O., Kiperstok, A., Sales, E.A., Embirucu, M., Ghirardi, M.L., 2010. Comparative energy life-cycle analyses of microalgal biomass production in open ponds and photobioreactors. Bioresour. Technol. 101, 1406–1413. https://doi.org/10.1016/j.biortech.2009.09.038.

Kishi, M., Yamada, Y., Katayama, T., Matsuyama, T., Toda, T., 2020. Carbon mass balance in *Arthrospira platensis* culture with medium recycle and high CO_2 supply. Appl. Sci. 10 (1), 220. https://doi.org/10.3390/app10010220.

Lam, M.K., Lee, K.T., Mohamed, A.R., 2012. Current status and challenges on microalgae-based carbon capture. Int. J. Greenhouse Gas Control 10, 456–469. https://doi.org/10.1016/j.ijggc.2012.07.010.

Lamotte, B., Guillaume, B., Rim, J., Bireglah, B., 2014. Modeling cumulative effects in life cycle assessment: The case of fertilizer in wheat production contributing to the global warming potential. Sci. Total Environ. 481, 588–595. https://doi.org/10.1016/j.scitotenv.2014.02.020.

Lathuillière, M.J., Miranda, E.J., Bulle, C., Couto, E.G., Johnson, M.S., 2017. Land occupation and transformation impacts of soybean production in Southern Amazonia, Brazil. J. Cleaner Prod. 149, 680–689. https://doi.org/10.1016/j.jclepro.2017.02.125.

Liu, X., Wang, B., Wang, J., Zuo, J., Peng, P., Wu, J., Sun, E., 2019. Carbon dioxide fixation coupled With ammonium uptake by immobilized scenedesmus obliquus and its potential for protein production. Bioresour. Technol. 289, 121685. https://doi.org/10.1016/j.biortech.2019.121685.

Maroneze, M.M., Siqueira, S.F., Vendruscolo, R.G., Wagner, R., Menezes De, C.R., Zepka, L.Q., Jacob-Lopes, E., 2016. The role of photoperiods on photobioreactors – a potential strategy to reduce costs. Bioresour. Technol. 219, 493–499. https://doi.org/10.1016/j.biortech.2016.08.003.

Nascimento, T.C., Nass, P.P., Fernandes, A.S., Vieira, K.R., Wagner, R., Jacob-Lopes, E., Zepka, L.Q., 2020. Exploratory data of the microalgae compounds for food purposes. Data in Brief 29, 105182. https://doi.org/10.1016/j.dib.2020.105182.

Nwoba, E.G., Parlevliet, D.A., Laird, D.W., Alameh, K., Moheimani, N.R., 2020. Pilot-scale self-cooling microalgal closed photobioreactor for biomass production and electricity generation. Algal Research 45, 101731. https://doi.org/10.1016/j.algal.2019.101731.

Patel, A.K., Choi, Y.Y., Sim, S.J., 2020. Emerging prospects of mixotrophic microalgae: way forward to sustainable bioprocess for environmental remediation and cost-effective biofuels. Bioresour. Technol. https://doi.org/10.1016/j.biortech.2020.122741, 122741.

Pérez-Fortes, M., Schöneberger, J.C., Boulamanti, A., Tzimas, E., 2016. Methanol synthesis using captured CO_2 as raw material: techno-economic and environmental assessment. Appl. Energy 161, 718–732. https://doi.org/10.1016/j.apenergy.2015.07.067.

Porcelli, S., Dotto, F., Pezzolesi, L., Morazza, B., Greggio, N., Righi, S., 2020. Comparative life cycle assessment of microalgae cultivation for bio-energy purposes using different carbon dioxide sources. Sci. Total Environ. 137714. https://doi.org/10.1016/j.scitotenv.2020.137714.

Qian, L., Wu, L., Yang, L., Zhang, Z., 2020. Inoculation concentration modulating the secretion and accumulation pattern of exopolysaccharides in desert cyanobacterium Microcoleus vaginatus. Biotechnol. Appl. Biochem. https://doi.org/10.1002/bab.1930.

Ramos-Suárez, J.R., Snell-Castro, R., Neris-Castillo, J.A., Choix, F.J., 2019. Biotechnological potential of Chlorella sp. and Scenedesmus sp. microalgae to endure high CO_2 and methane concentrations from biogas. Bioprocess Biosyst. Eng. 42 (10), 1603–1610. https://doi.org/10.1007/s00449-019-02157-y.

Rippka, R., Deruelles, J., Waterbury, J.B., Herdman, M., Stanier, R.Y., 1979. Generic assignments, strain histories and properties of pure cultures of cyanobacteria. Microbiology 111 (1), 1–61. https://doi.org/10.1099/00221287-111-1-1.

Santos, A.M., Santos, A.M., Sartori, R.B., Vieira, K.R., Zepka, L.Q., Queiroz, M.I., Jacob-Lopes, E., 2017. Heterotrophic cultivation of cyanobacteria: study of effect of exogenous sources of organic carbon, absolute amount of nutrients and stirring speed on biomass and lipid productivity. Front. Bioeng. Biotechnol. 5, 1–7. https://doi.org/10.3389/fbioe.2017.00012.

Severo, I.A., Deprá, M.C., Barin, J.S., Wagner, R., de Menezes, C.R., Zepka, L.Q., Jacob-Lopes, E., 2018. Bio-combustion of petroleum coke: the process integration with photobioreactors. Chem. Eng. Sci. 177, 422–430. https://doi.org/10.1016/j.ces.2017.12.001.

Severo, I.A., Deprá, M.C., Dias, R.R., Barin, J.S., de Menezes, C.R., Wagner, R., Zepka, L.Q., Jacob-Lopes, E., 2020. Bio-combustion of petroleum coke: the process integration with photobioreactors. Part II–Sustainability metrics and bioeconomy. Chem. Eng. Sci. 213, 115412. https://doi.org/10.1016/j.ces.2019.115412.

R. Sivaramakrishnan, S. Suresh, A. Pugazhendhi, J.M.N. Pauline, A. Incharoensakdi, Response of Scenedesmus sp. to microwave treatment: enhancement of lipid, exopolysaccharide and biomass production. Bioresour. Technol., 123562. DOI: j.biortech.2020.123562.

Tang, D., Han, W., Li, P., Miao, X., Zhong, J., 2011. CO_2 biofixation and fatty acid composition of *Scenedesmus obliquus* and *Chlorella pyrenoidosa* in response to different CO_2 levels. Bioresour. Technol. 102 (3), 3071–3076. https://doi.org/10.1016/j.biortech.2010.10.047.

Toro-Huertas, E.I., Franco-Morgado, M., de los Cobos Vasconcelos, D., González-Sánchez, A., 2019. Photorespiration in an outdoor alkaline open-photobioreactor used for biogas upgrading. Sci. Total Environ. 667, 613–621. https://doi.org/10.1016/j.scitotenv.2019.02.374.

Unduraga, D., Poirrier, P., Chamy, R., 2016. Microalgae growth kinetic model based on the PSII quantum yield and its utilization in the operational curves construction. Algal Res. 17, 330–340. https://doi.org/10.1016/j.algal.2016.05.020.

Vidyashankar, S., Deviprasad, K., Chauhan, V.S., Ravishankar, G.A., Sarada, R., 2013. Selection and evaluation of CO_2 tolerant indigenous microalga *Scenedesmus dimorphus* for unsaturated fatty acid rich lipid production under different culture conditions. Bioresour. Technol. 144, 28–37. https://doi.org/10.1016/j.biortech.2013.06.054.

Vieira, K.R., Pinheiro, P.N., Santos, A.B., Cichoski, A.J., de Menezes, C.R., Wagner, R., Zepka, L.Q., Jacob-Lopes, E., 2019. The role of microalgae based systems in the dynamics of odors compounds in the meat processing industry. Desalin. Water Treat. 150, 282–292. https://doi.org/10.5004/dwt.2019.23730.

Watt, B.K., Merrill, A.L., 1963. Agriculture Handbook no 8: Agricultural Research Service. USDA, pp. 161.

World Bank and Ecofys, 2019. State and Trends of Carbon Pricing 2019. World Bank, Washington, DC. DOI: 10.1596/978-1-4648-1435-8.

Chemical Engineering Science 213 (2020) 115412

Contents lists available at ScienceDirect

Chemical Engineering Science

journal homepage: www.elsevier.com/locate/ces

Bio-combustion of petroleum coke: The process integration with photobioreactors. Part II – Sustainability metrics and bioeconomy

Ihana A. Severo, Mariany C. Deprá, Rosangela R. Dias, Juliano S. Barin, Cristiano R. de Menezes, Roger Wagner, Leila Q. Zepka, Eduardo Jacob-Lopes *

Bioprocess Intensification Group, Federal University of Santa Maria, UFSM, Roraima Avenue 1000, Santa Maria, RS 97105-900, Brazil

HIGHLIGHTS

- Process integration of a photobioreactor with a combustion furnace was demonstrated.
- The most widely-deployed sustainability metrics evidenced improved performance.
- Fuel consumption cost during the bio-combustion was reduced.
- The process utilities have the potential to generate substantial revenues.
- The BCCU approach further extend the system revenues through carbon credits trading.

ARTICLE INFO

Article history:
Received 29 July 2019
Received in revised form 28 November 2019
Accepted 2 December 2019
Available online 4 December 2019

Keywords:
Biological carbon capture and utilization
Microalgae
Combustion
Life cycle assessment
Circular bioeconomy
Carbon credits

ABSTRACT

In this study, we evaluated the sustainability metrics and bioeconomy of the integrated bio-combustion system. Based on previous experiments, inventory data were standardized for a functional unit of 1 kg of mass, 1 MJ of energy, 1 m^3 of water, and a stream factor of 0.90. The impact categories resulted in a net energy ratio of 0.71, greenhouse gas emissions of 0.70 kg_{CHG}/kg_{fuel}, global warming potential of 12,523.60 $kgCO_{2eq}/yr$, water footprint of 56.40 $m^3/m^3/yr$, acidification potential of 33 $kgSO_{2eq}/yr$, eutrophication potential of 4.42×10^{-3} kgN_{eq}/yr, and ozone depletion potential of 2.15×10^{-6} $kgCFC\text{-}11_{eq}/yr$. Regarding the utilities, fuel consumption cost was reduced close to 40%, and the oxygen and volatile organic compounds productions were responsible for the majority revenue generation. Besides, both avoided and captured carbons obtained potential revenues through carbon credits. The current contribution of the integrated process has shown improved environmental performance and is a promising approach towards circular bioeconomy.

© 2019 Elsevier Ltd. All rights reserved.

1. Introduction

The global energy crisis, based on overexploitation of non-renewable resources, has propelled a tremendous advance for the industry, resulting in improvements in energy efficiency. But at the same time, several technical, environmental, economic, and political challenges have arisen in manufacturing processes. Today, decision-makers' primary concern is to expand further the energy supply and use it in a carbon-constrained era (World Energy Council, 2016).

Taking this into account, power generation, petrochemical, basic chemicals, and food sectors, are the most representative manufacturing industries that require intensive amounts of energy resources and produce massive emissions, exerting profound environmental impacts (EPA, 2016). These traditional plants are composed of combustion equipment, such as furnaces, kilns, boilers, heaters, thermal oxidizers, or any other type of burning machinery, which are the basic building block to produce practically everything that our society needs (IHEA, 2015). However, these burners are still exceedingly energy inefficient because they use high excess air and elevated temperatures without heat recovery from combustion products (Turns, 2011). Therefore, to withstand the massive industry workloads, there are substantial fuel requirements. Due to environmental issues, mainly CO_2 emissions, related to the type and quantity of fuel used, regulatory constraint, environmental taxes, and charges, will have a significant effect on overall process costs. It is noteworthy that the primary role of any combustor is to produce with the minimal operational expense, which is based on capital costs, costs incurred with fuel and other

* Corresponding author.
E-mail address: jacoblopes@pq.cnpq.br (E. Jacob-Lopes).

https://doi.org/10.1016/j.ces.2019.115412
0009-2509/© 2019 Elsevier Ltd. All rights reserved.

utilities, as well as maintenance costs (Mullinger and Jenkins, 2014).

Thereby, process integration emerged as a response to energy-savings, and it was a leap toward troubleshooting on large-scale. This concept is based on the adoption of chemical engineering methods, supported by energy and material balances, to couple unit operations, equipment, or processing techniques. Thus, it is possible to reduce resource consumption, emissions, process time, product losses, as well as maximize productivity and efficiency (Baleta et al., 2019). An integrated process takes advantage of thermal energy (waste heat recovery from heating or cooling streams), mass (effluent reuse), and water (recycling of reuse water and wastewater) surpluses. Still, the main reason for these integrations has been the realization of entrepreneurs and industrial engineers that this is a strategy for upgrading a plant site with better capital gains (Klemeš, 2013).

The numerous advantages of process integration motivate increasingly sustainable projects. This is all thanks to the research and development (R&D) partnerships between academic and industrial sectors, which are now joining an even more intense wake-up call in an attempt to pursue smart technology routes to attach with conventional plants (Varbanov et al., 2018).

Biological carbon capture and utilization (BCCU) is a robust technology with potential applicability for this purpose. The BCCU is mediated by microalgae-based processes, which can be developed in both open and closed systems. However, the first has many limitations that are overcome by the second culture system, called photobioreactors (Verma and Srivastava, 2018). These equipment are designed with parameters that allow adequate and controlled conditions for efficient CO_2 capture and conversion into biomass and other bioproducts of commercial interest (Jacob-Lopes et al., 2017; Severo et al., 2018a, 2018b; Merchuk et al., 2019). New photobioreactor designs have been claimed to meet scaling requirements. Such attributes should enable high operating volumes to obtain commodity products proportionally to industrial demands (Deprá et al., 2019).

The BCCU technology in an integrated process of biologically-assisted combustion was first demonstrated in Severo et al. (2018b), referring to Part I of this sequential research. The process recovers photobioreactor exhaust gas and injects them into a bio-combustion furnace. More specifically, gaseous bioproducts of the photosynthetic metabolism, such as volatile organic compounds (VOCs), oxygen, and part of unconverted CO_2, are reused as gaseous biofuels, oxidizer, and nitrogen diluent, respectively. Through bio-combustion, it was possible to increase the furnace efficiency close to 30% with parallel energy savings of 25%, compared to conventional combustion. In addition to being able to be retrofitted to existing combustion systems rather than newly built units, increasing the thermal performance parameters of this potential process indicates a crucial advantage concerning the reduction in fuel consumption and greenhouse gas emissions.

Considering these aspects, the process integration approach proposed here provides a broad view of industrial systems that lead to sustainability and circular bioeconomy (Walmsley et al., 2019). First, because we are dealing with a bio-based structure that increases cyclic flows in a combustion process. Afterward, these two indicators serve as powerful extensive project planning tools. They can guide them in the detailed evaluation of its future performance. Nevertheless, many industries still do not see the advance of engineering and technology innovation towards a sustainable economy pathway (Arastoopour, 2019). The actual development of environmentally and economically viable systems has been held back by the lack of a comprehensive metric methodology (Batterham, 2006). In this sense, the integrated bio-combustion system now needs to be subjected to a set of meaningful metrics to deal with this gap and highlight how this target can be achieved.

This is what we propose in Part II of this current research. Here, we evaluate the sustainability metrics and bioeconomy of the photobioreactor integrated into the bio-combustion furnace. We consider the most critical aspects that will determine the viability of the microalgae-based processes, such as life cycle assessment (LCA), assigned by the indicators of six environmental impact categories (net energy ratio, global warming potential, water footprint, acidification potential, eutrophication potential, and ozone depletion potential). As one of the typical steps that support the bioeconomy, we estimate utility costs and carbon credits. Moreover, according to the best of our knowledge, a theoretical-experimental approach of LCA oriented to this type of process has not yet been reported in the scientific literature.

2. Material and methods

The LCA tool was used to evaluate the environmental aspects and potential impacts of the microalgae-based process. According to the International Organization for Standardization (ISO) 14,000 series, there are four sequential phases in the LCA study: (i) goal and scope definition, (ii) Life Cycle Inventory (LCI), (iii) Life Cycle Impact Assessment (LCIA), and (iv) interpretation of results (ISO, 2006). The procedures considered in each step are detailed below.

2.1. Goal and scope definition

The goal of the LCA in this study was to evaluate the environmental profile of the integrated process, which consisting of the photobioreactor and bio-combustion furnace, whose data were previously obtained in Part I (Severo et al., 2018b). The system boundaries of gate-to-gate have been performed based on the integrated process (Fig. 1). The main steps included are the microalgae cultivation and the petroleum coke bio-combustion. Essential inputs for these operations include electricity, fuels, water, and greenhouse gas. The laboratory-scale experiments provided all the requirements for data inventory, which were then standardized for a functional unit of 1 kg of mass, 1 MJ of energy, and 1 m^3 of water. Besides, a total of 330 days per year was considered, resulting in a stream factor (SF) of 0.90.

2.2. Summary of the integrated bio-combustion system

The process developed was based on the biological CO_2 capture inside the leading equipment, consisting of a bubble column photobioreactor, which served as a reaction vessel for the *Scenedesmus obliquus* microalgae cultivated in synthetic BG-11 medium, fed with 15% of industrial CO_2 in the airstream. The microorganism metabolic activity allowed the CO_2 conversion into gaseous products of photosynthesis such as O_2 and VOCs, which were recovered and reused as an oxidizer and gaseous biofuels, respectively, for injection in the bio-combustion furnace. Additionally, the unconverted CO_2 fraction injected into the photobioreactor was regenerated for use as a nitrogen diluent. The bio-combustion furnace built on a laboratory scale consisted of a system for thermal energy generation with sufficient operational capacity to be coupled to the photobioreactor. The furnace was fed with O_2, VOCs, and unconverted CO_2 through a recirculation channel, in addition to the use of petroleum coke as the primary fuel (see Fig. 1, Part I). The specifications of the technique we described in patent WO2017/112984A1 (Jacob-Lopes et al., 2017). Besides, obtaining the kinetic data and the analytical methods used to control the photobioreactor and furnace are reported in detail in Part I of this study (Severo et al., 2018b).

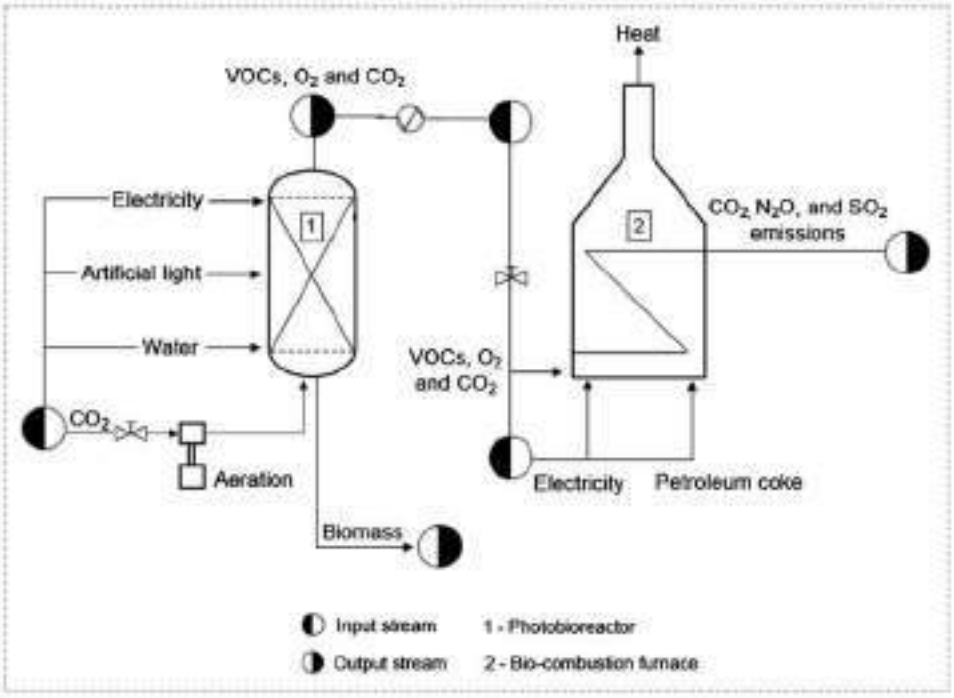


Fig. 1. Integrated bio-combustion system boundary based on the process flow diagram. Adapted from Severo et al. (2018b).

2.3. Experimental determination of greenhouse gas emissions

The GHGs emissions were daily measured in the bio-combustion furnace. A gas chromatograph (GC) was used to determine the CO_2 and N_2O. The equipment used was a GC Greenhouse Gas Analyzer (Shimadzu GC-2014, Kyoto, Japan), equipped with six-packed chromatographic columns (Supelco, Bellefonte-PA, USA) connected to the following detectors: thermal conductivity detector (TCD), flame ionization detector (FID), and electron capture detector (ECD). The FID and ECD were used for the determination of the CO_2 and N_2O, respectively. Helium was used as a carrier gas. Gaseous samples at the furnace output were collected in previously evacuated vials; 5 mL of sample was injected using a gas-tight syringe. The peak areas obtained using the integrator Software GC solution were compared with reference curves to determine the gas concentrations (Jacob-Lopes and Franco, 2013).

2.4. Life cycle inventory (LCI)

Table 1 summarizes the primary data sources and information involved in the operation of the integrated process. Most of the data were based on the identification and quantification of consumption flows and production (input and output) of each step of the process.

2.5. Life cycle impact assessment (LCIA)

The LCIA method is related to elementary flows, which considers the implementation of combined mid-point parameters. Thus, it is possible to derive the characterization factors and express the significance of the emissions with a higher level of reliability. The selected impact categories were: net energy ratio, global warming potential, water footprint, acidification potential, eutrophication potential, and ozone depletion potential, and their characterization factors are shown in Supporting Information (Table S1).

2.5.1. Impact categories

2.5.1.1. Energy balance and net energy ratio (NER). The energy balance (MJ) of the bio-combustion furnace was established from Eq. (1), and subsequently, the NER (dimensionless) was calculated (Turns, 2011; Jorquera et al., 2010).

$$Q = m\, c_p (T_{out} - T_{in}) \quad (1)$$

Table 1
Inputs and outputs of process data inventory.

Stage	Input/output	Materials/consumables	Unit	Value
Photobioreactor	In	Electricity	kWh	15,840
		Artificial light	kWh	81.97
		Aeration	kWh	104.54
		Water	m^3	2×10^{-3}
	Out	VOCs	MJ	5,031.76
		CO_2	MJ	1.10
		Biomass	MJ	58,990
Bio-combustion furnace	In	Electricity	kWh	7,128
		Petroleum coke	MJ	35.12
		VOCs	MJ	805.08
	Out	Heat	MJ	0.65
		GHGs emissions	MJ	0.28

where Q is the amount of heat loss in the exhaust gas, m is the fuel mass, Cp is the average specific heat of fuel, T_{out} is the combustion temperature of the exhaust gas, and T_{in} is the temperature before the fuel is burned.

The NER, which is defined as the ratio of the total renewable energy produced over the fossil-energy required, was calculated for the photobioreactor from Eq. (2):

$$NER = \frac{\sum E_{out}}{\sum E_{in}} \quad (2)$$

where E_{out} is the sum of the total energy produced, and E_{in} is the sum of the total energy required.

Afterward, the NER of the integrated process was calculated considering the ratio between the total quantification of output energy of the photobioreactor plus the furnace over the input energy thereof.

2.5.1.2. Global warming potential (GWP). The determination of the GWP ($kgCO_{2eq}/yr$) was evaluated according to the CO_2 and N_2O emissions measured from the experimental data. These values of GHGs were integrated with their respective emission factors and expressed as CO_2 equivalence ($kgCO_{2eq}$), based on a time horizon of 100 years, as described in Eq. (3) (Laratte et al., 2014):

$$GWP = GWP_i \times m_i \quad (3)$$

where GWP_i is the equivalence factor for the substance i and m_i is the emission of the substance i.

2.5.1.3. Water footprint (WF). The WF ($m^3/m^3/yr$) was quantified considering direct and indirect water consumption, according to Eq. (4) (Hoekstra, 2011):

$$WF = \sum WF_{blue} + WF_{green} + WF_{gray} \quad (4)$$

where WF_{blue}, WF_{green}, and WF_{gray} correspond to blue, green, and gray water footprints, respectively.

2.5.1.4. Acidification potential (AP). The AP ($kgSO_{2eq}$) was quantified using the AP of substances such as sulfur, as described in Eq. (5) (Hauschild and Wenzel, 1998):

$$AP = \sum_i AP_i \times m_i \quad (5)$$

where AP_i is the equivalence factor for the substance i, and m_i is the emission of substance i.

2.5.1.5. Eutrophication potential (EP). The EP ($kgPO_{4eq}$) can be measured according to Eq. (6) (Hauschild and Wenzel, 1998):

$$EP = \sum_i EP_i \times m_i \quad (6)$$

where EP_i is the equivalence factor for the substance i and m_i is the emission of the substance i.

2.5.1.6. Ozone depletion potential (ODP). The ODP (kgCFC-11) was estimated through Eq. (7), where the values are related to the equivalence factor relative to chlorofluorocarbons-11 (Hauschild and Wenzel, 1998).

$$ODP = \sum ODP_i \times m_i \quad (7)$$

where ODP_i is the equivalency factor for the substance i and m_i is the mass of the emission substance i.

2.6. Normalization

The normalization was determined according to Eq. (8) described by ILDC (2010). During this step, each of the environmental impact potentials was divided by reference value, corresponding to the world environmental impact normalization factor (Table S1).

$$N_k = \frac{S_k}{R_k} \quad (8)$$

where k denotes the impact category, N is the normalized indicator, S is the category indicator from the characterization phase, and R is the reference value or the normalization factor.

2.7. Bioeconomy of the integrated system

2.7.1. Estimation of manufacturing costs

For estimating operating costs associated with supplying utilities to the bio-combustion system, the approach taken here was to assume that the capital investment required to build a facility to supply the utility has already been made. The costs associated with providing a given utility were obtained by calculating the operational costs to generate it. The manufacturing and related expenses were reported in terms of USD per unit time, according to the methodology proposed by Turton (2009). An SF of 0.90 was considered to calculate the yearly cost of utilities. The elements of manufacturing expenses and revenues were focused on the utility streams required by the bio-combustion process. In this regard, the primary fuel (petroleum coke), the oxidizer (oxygen), and the additional biofuel (VOCs) were considered. The selling prices of the utilities were obtained from Chemical Market Reporter (CMR, 2019). The selling price of VOCs was estimated based on the prices of petroleum coke equivalent.

2.7.2. Estimation of carbon credits

The carbon credits were estimated according to the carbon footprint of the bio-combustion system, and the current average carbon prices suggested by the World Bank Group (World Bank, 2018). The streams of carbon dioxide not produced and avoided (Eqs. (9)–(10)) were considered, according to the methodology proposed by Pérez-Fortes et al. (2016).

$$CO_{2notproduced} = CO_{2conventional} - CO_{2emitted} \quad (9)$$

$$CO_{2avoided} = CO_{2_{sequestered}} + CO_{2_{ethanol}} \quad (10)$$

where $CO_{2conventional}$ is the amount of CO_2 released in the conventional process, while $CO_{2emitted}$ and $CO_{2captured}$ refer to the bio-combustion system.

3. Results and discussion

3.1. Net energy ratio and energy balance

The NER is an essential indicator that, in addition to investigating the global energy balance and the net income of a given process, it also assesses the feasibility of industrial scaling. Thus, Table 2 shows the energy balance and the NER for each life cycle stage of the process.

As shown in Table 2, the NER of the photobioreactor resulted in 1.04. This indicates that the amount of renewable energy produced during the cultivation stage is 3.7% greater than the fossil energy consumed. The output energy, related to the production of VOCs and biomass, has considerable potential to sustain a positive energy balance in the photobioreactor (Slade and Bauen, 2013).

Table 2
Energy balance and NER for life cycle stages of the integrated bio-combustion system.

Stage	Input (MJ)	Output (MJ)	NER
Photobioreactor	57,696.43	59,795.88	1.04
Bio-combustion furnace	26,501.00	0.93	0.000035
Integrated process	82,719.92	59,796.16	0.71

The sustainability of microalgae-based processes strongly depends on the value of NER. Most of the research reports very extreme values, ranging from less than 0.05 to greater than 19, since the energy requirements are directly influenced by the type of photobioreactor and the downstream steps involved (Hullat and Thomas, 2011; Tredici et al., 2015; Jacob et al., 2015). In this context, many attempts have been made in recent years to improve the NER of these bioprocesses. Deprá et al. (2019) showed a new hybrid photobioreactor design with an NER of 2.49, which, despite the relative energy consumption, presents considerable return energy in parallel to the superior volumetric productivity. This trade-off is favorable to the energetic bioreactor viability, which can still be enhanced by optimizing operational parameters.

Regarding the bio-combustion furnace, the energy balance resulted in a very low NER (0.000035). Thus, it should be considered that thermal energy consumed in furnaces represents the major part of the total energy consumption of traditional industrial combustion processes. This is because these devices typically depend on higher fuel mass input associated with superior temperatures (IHEA, 2015). From the chemical point of view, these processes are characterized by exothermic reactions, where the combustion products are less energetic than the reactants, that is, the losses of substantial amounts of heat are frequent, dissipating it through the chamber walls by conduction and thermal radiation (Glassman et al., 2015).

Finally, regarding the integrated process, there was a reduction in the energy input requirements of the furnace, resulting in an NER of 0.71. This means that the photobioreactor exhaust gas integration into the bio-combustion furnace, associated with petroleum coke as the primary fuel, providing substantial improvements in the energy performance of the whole system. By way of comparison, Tredici et al. (2015) showed the benefit of process integration, whose NER value doubled in the microalgae-based process. Therefore, the photobioreactor integration could be an advanced technique to energy retrofit existing combustion systems.

3.2. Greenhouse gas emissions

Harmful gas emissions from combustion processes are among the most critical aspects to reverse the trends of global warming. So, the environmental impact category related to greenhouse gas is the most addressed in the LCA studies. However, the theoretical values that are often extrapolated can provide unrealistic and imprecise data (Collet et al., 2015). In this research, this is overcome because we perform experimental measurements for the quantification of GHGs emissions of the bio-combustion system, as shown in Figs. 2 and 3.

Based on Figs. 2 and 3, the GHGs emissions profile shows that in a hydraulic retention time of 120 h, considered the best experimental condition, 0.70 kg of CO_2 is released for every 1 kg of petroleum coke burned. Similar behavior was obtained for N_2O emissions, however, in an extremely deficient range, with a value of 1.03×10^{-4} kg_{N2O}/kg_{fuel}.

The results obtained for both GHGs emissions corroborate, firstly, with the microalgae cell growth kinetics, following a bell-shaped curve pattern. In the initial and final cultivation stages, there is less production of the metabolites. In the intermediate steps, in hydraulic retention times between 96 and 120 h, there

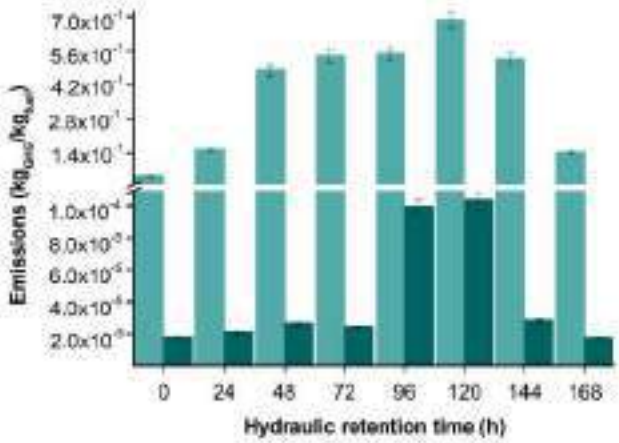


Fig. 2. Kinetics of gaseous emissions in the bio-combustion furnace at different hydraulic retention times.

is the maximum production of these bioproducts (Jacob-Lopes et al., 2010). This means that the furnace emissions vary to the same extent as substances such as VOCs, O_2, and unconverted CO_2 are desorbed in the photobioreactor exhaust gas and subsequently injected into the combustion chamber. As described in our previous work (Fig. 4, Part I), this profile is also co-related to the rates of CO_2 consumption and O_2 and VOCs release, which corresponds to values of 0.44, 0.38, and 3.42 kg/m^3/d, respectively (Severo et al., 2018b).

Secondly, about CO_2 and N_2O emissions, low concentrations in the furnace exhaust gas is related to the impact of oxygen-enrichment on the intake air and amount of fuel burned. Regarding CO_2, in this study, the values were substantially below that established by the stoichiometry of petroleum coke air-combustion, whose value is 3.30 kg_{CO2}/kg_{fuel}. This demonstrates that the integrated bio-combustion system emits 78.8% less CO_2 when compared to conventional combustion.

Such a phenomenon can be explained by the fact that when feeding the furnace inlet air with 12% of biological O_2 from the photobioreactor (Fig. 6, Part I), there is a change in the thermodynamic properties of the gas inside the combustion chamber. The inert N_2 is diluted by the volumetric increase of O_2, causing the heat loss by radiation in the furnace to be reduced. This increases the temperature and intensifies the faster fuel combustion, so a higher thermal-efficiency is obtained. Such an effect allows less fuel to be expended to maintain the same performance as in the air-combustion and, as a result, less CO_2 is formed (Yin and Yan, 2016).

In terms of N_2O emissions, they can also be justified for reasons similar to the CO_2. As O_2 partial pressure and local temperature increase, N_2 is displaced from air-combustion and, consequently, reduces its formation. Besides, the typical conversion of solid fuels, such as petroleum coke, to N_2O is about 1% under certain temperature conditions; this means that N_2O emissions are often in trace values (below 0.1 ppm) (Wang et al., 2019), which corroborates the data of this study.

According to the U. S. Department of Energy and the Industrial Heating Equipment Association, emissions from combustion devices depend directly on three variables: fuel consumption, oxidizer concentration in the combustion air, and system temperature. Enriching a furnace with 12% O_2 and operating at a constant temperature of 1000 °C, immediate fuel savings results are expected, generally exceeding 15%. Therefore, the emissions would be reduced proportionally to the reduction of fuel requirements. By spending less fuel per unit of production, decreasing incidences of emission-related penalties (IHEA, 2015; DOE, 2019).

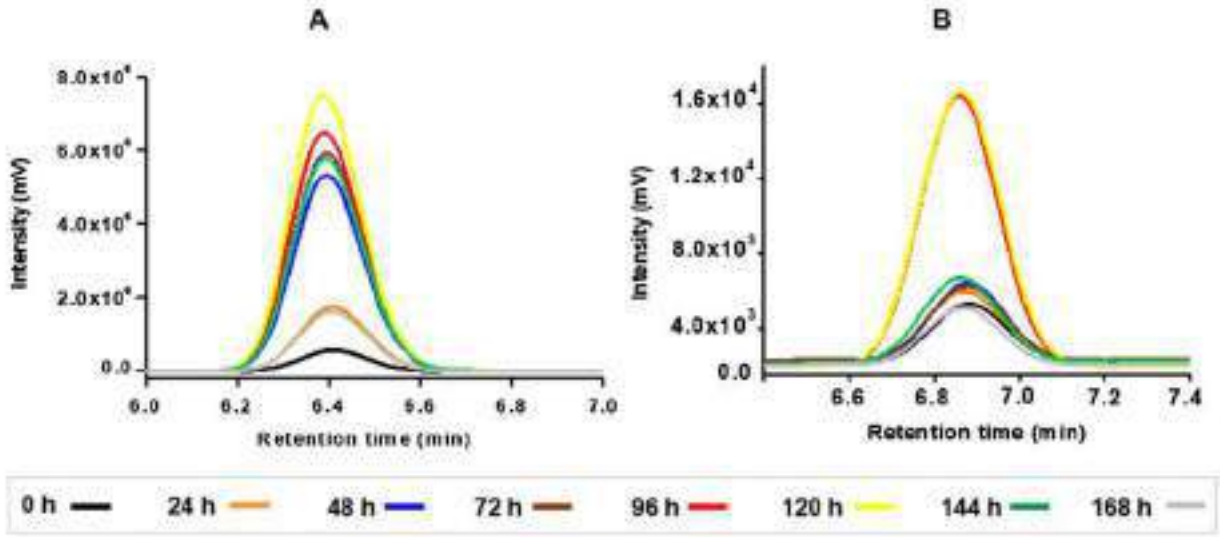


Fig. 3. Chromatogram detail representing gas release in the bio-combustion furnace. Greenhouse gas emissions: (A) CO_2 and (B) N_2O. The color of each peak represents the different hydraulic retention times. (For interpretation of the references to colour in this figure legend, the reader is referred to the web version of this article.)

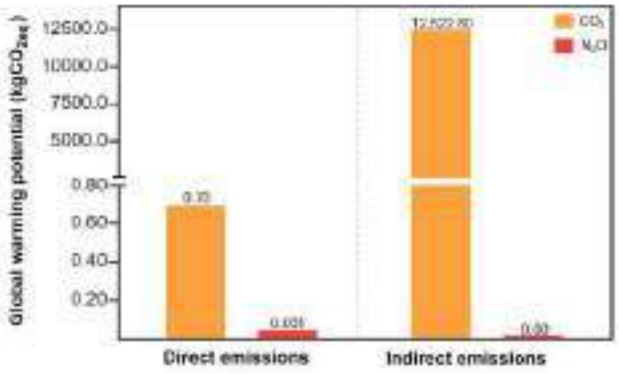


Fig. 4. Distribution of direct and indirect emissions contributors to the global warming potential.

Another essential factor to be considered about emissions is inferred not only to oxygen-enrichment but also to the joint injection of renewable energy from additional biofuels (VOCs) and nitrogen diluent (unconverted CO_2). All of them, when combined, lead to even more significant savings, close to 25%. The VOCs of microalgae are the main products of CO_2 biotransformation in the photobioreactor, accounting for about 90%. For this reason, their substantial quantities are released into the exhaust gas (Jacob-Lopes and Franco, 2013; Deprá et al., 2019). These metabolites belong to different chemical classes of low molecular weight carbonic chain compounds like alcohols, aldehydes, esters, hydrocarbons, ketones, terpenes, and sulfur compounds, which have the potential to be recovered as gaseous biofuels from microalgae cultivation (Santos et al., 2016). They have a high energy density, around 86.32 MJ/kg, which enhances the petroleum coke burning in the bio-combustion furnace, as reported in Part I of this study (Severo et al., 2018b). That is, if this source of renewable energy boosts combustion, it is expected that the fuel requirements and GHGs emissions are restricted.

3.2.1. Global warming potential analysis

In addition to the quantitative determination of each of the evaluated gas, it is essential to adopt a way of comparing them in a single unit. So, the direct and indirect GHGs emissions were estimated through the Global Warming Potential (GWP), whose sustainability metric provides a fundamental link between the process and the environmental impact caused by them. Besides, the accumulative GHGs emissions of microalgae-based processes are usually determined by each process step, which includes the production and consumption of electricity and materials production (Sun et al., 2019). Fig. 4 shows the distribution of GHGs emissions in the bio-combustion system.

Based on Fig. 4, the process indicated a GWP of 12,523.60 $kgCO_{2eq}$. Notably, direct GHGs emissions were practically negligible due to the low quantification of the gaseous compounds in furnace exhaustion. On the other hand, 99% of the indirect emissions accounted for virtually the entire GWP of the process, due to activities related to electricity consumption and fuel use heat. The cultivation stage by itself required a primary energy expenditure of 16,026.50 kWh. It is noteworthy that despite the energy outlay of the photobioreactor, it also generates a substantial fraction of renewable energy, contained in the VOCs, which assists the petroleum coke burning. Energy integration, in this case, allows higher indirect emissions to be converted into lower direct emissions, which minimizes GWP effects. Thus, the system could be adopted as a low-emission technology.

3.3. Water footprint

The Water Footprint (WF) usually includes the water consumed in the whole process, whose spending volume is not returned to the source for reuse. The WF analysis helps identify the intensive operations in the consumption of different water types: blue, green, and grey (Hoekstra, 2011). In microalgae-based processes, blue water is associated with the removal of freshwater in operations per temporal functional unit; green water refers to the evaporation rate and the volume incorporated into biomass; and grey water is related to the amount of water used to dilute a pollutant load which reaches a water body, taking as basis its natural conditions (Farooq et al., 2015). In this study, however, only the blue and green water footprint were considered because the water requirements in the integrated bio-combustion system solely come from the photobioreactor. Table 3 shows the water footprints evaluated.

According to Table 3, the blue water footprint of the process is approximately 47 $m^3/m^3/yr$. Considering that an average of 20% of cultivation water is incorporated into biomass, about 9.4 $m^3/m^3/yr$ of green water is spent in the process. The evaporation resulted in a water loss of 0.094 $m^3/m^3/yr$, which is attributed to the aeration rate. The total water footprint was estimated close to 56.4 $m^3/m^3/yr$.

Table 3
Water footprints of the integrated bio-combustion system.

Water footprint	Cultivation stage (m^3/m^3/yr)
Blue	47
Green	9.4
Grey	nc
Evaporation	0.084
Total water footprint	56.4

All values are expressed in 1 m^3 of water demand per 1 m^3 of reactor operating continuously with seven daily cycles and considering an SF of 0.90.
*nc: denotes a parameter not considered in the study.

Regarding the WF evaluation of microalgae-based processes, few studies are available in the literature, and the results of impacts differ greatly depending on the different cultivation systems, conversion methods, climatic, and geographical variations. Regardless, although the focus here is on a combustion system, there is a freshwater displacement, even minimal, to support this technological route. The results obtained show that about 79% of the water footprint could be reduced through partial or total integration of the volume of water demanded in the process, or still allocated as water credits, as suggested by Batan et al. (2013).

3.4. Potential of acidification, eutrophication, and ozone depletion

The mid-point impact related to the acidification (AP) and eutrophication potential (EP) is attributed to the SO_x and NO_x emissions. Both come entirely from the furnace due to the petroleum coke burning, which could cause a wide range of damages on terrestrial and aquatic ecosystems, organisms, and materials (Valderrama et al., 2012).

In this specific case, the AP refers to the SO_2 released in the combustion, which combines with the air humidity and forms sulfuric acid, the main compound responsible for the climatic phenomenon of acid rain (Ye et al., 2018). Therefore, the AP of the bio-combustion furnace was estimated in 33 $kgSO_{2eq}$/yr. The impact of this acidifying substance is minimal when compared to microalgae-based processes for biofuels and bioenergy production (Grierson et al., 2013).

On the other hand, the EP was 4.42×10^{-3} kgN_{eq}/yr, which is represented by small N_2O concentrations emitted in the bio-combustion furnace. The EP is due to the terrestrial eutrophication as a function of air nitrogenous compounds deposition. Usually, eutrophication is also related to phosphorus surplus and other nitrogen compounds released into marine and freshwater ecosystems (Czyrnek-Delêtre et al., 2017). In addition, NO_x contributes to the smog formation potential, whose impact category examines the mass of O_{3eq} released into the troposphere (Ye et al., 2018). However, it was disregarded because the concentrations would be insignificant during the bio-combustion.

Concerning ozone depletion potential (ODP), it is an impact related to the chlorofluorocarbons (CFCs) emissions and other halogenated ozone layer depleting substances in the atmosphere. Although ozone (O_3) plays a crucial role in the stratosphere, it is harmful in the troposphere and can cause damage to human health and change ecosystems (Koiwanit et al., 2014). The ODP of the integrated bio-combustion system was 2.15×10^{-8} $kgCFC\text{-}11_{eq}$/yr, whose environmental impact is mainly due to indirect emissions from electric power requirements. Direct emissions of CFCs in the system were insignificant.

3.5. Impact categories

Environmental profiles comparison reveals the absolute performance in the context of each metric analyzed. Although it seems simple, such patterns cannot be easily interpreted. For a better understanding between scores and emissions magnitude, all categories were normalized (ILDC, 2010). The environmental impacts of the integrated bio-combustion system are compared in Fig. 5.

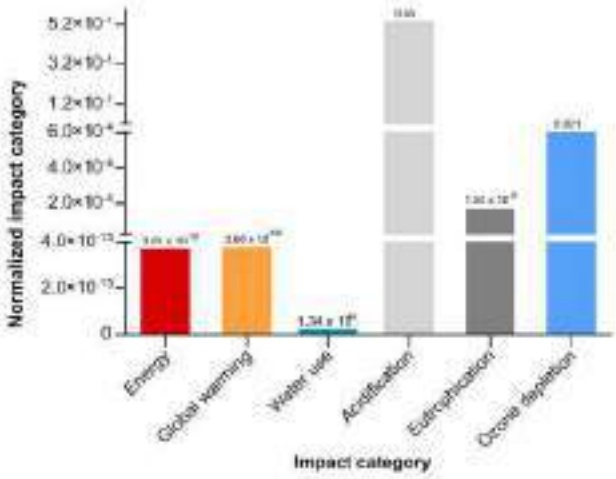


Fig. 5. Normalized impact categories of integrated bio-combustion system.

As shown in Fig. 5, acidification was the most representative impact category in the process (0.55), followed by ozone depletion (0.021). Even so, these values are much lower when compared to the microalgae-based processes with multiple unit operations. In the same tendency, other evaluated categories, such as eutrophication (1.84×10^{-4}), global warming (3.86×10^{-10}), energy (3.81×10^{-10}), and water use (1.34^{-14}), practically did not have any environmental impact.

About the acidification, data normalization indicated that this category is more expressive due to the release of sulfur dioxide (SO_2) from the petroleum coke combustion, accounting for 56% of the environmental impact when compared to the reference (ILDC, 2010). In contrast, the ozone depletion represents 20.3% of the total impact and is attributed exclusively to electricity consumption.

In most cases, the role played by the energy requirements, whether from fossil fuel or electricity use, accounts for more than 90% of the total environmental burden. As expected, the photobioreactor is the central hotspot of this study. This means that the electricity consumption impact during the cultivation stage comprises the environmental onus for almost all categories analyzed. This fact is consistent with other studies; however, with contributions significantly higher than that of the bio-combustion system (Pérez-López et al., 2017).

Given this scenario, the broad adoption of renewable energy sources is imperative. But although electricity has been produced efficiently from wind, solar, hydro, and geothermal power in recent years, the fact is that coal sustains, predominantly, the global energetic matrix. At this moment, alternative approaches, including the drastic reduction in non-renewable energy demand, would be needed. However, the main bottleneck persists in the economic unfeasibility for the full implementation of these alternative technologies worldwide.

3.6. Bioeconomy

3.6.1. Estimation of manufacturing costs and revenues

The fundamental components of manufacturing costs are raw materials, utilities, and waste treatment. The costs related to a day-to-day facility procedure must be estimates before the economic feasibility of a process can be evaluated. Regarding this, Fig. 6 shows the fuel consumption and production of oxygen and

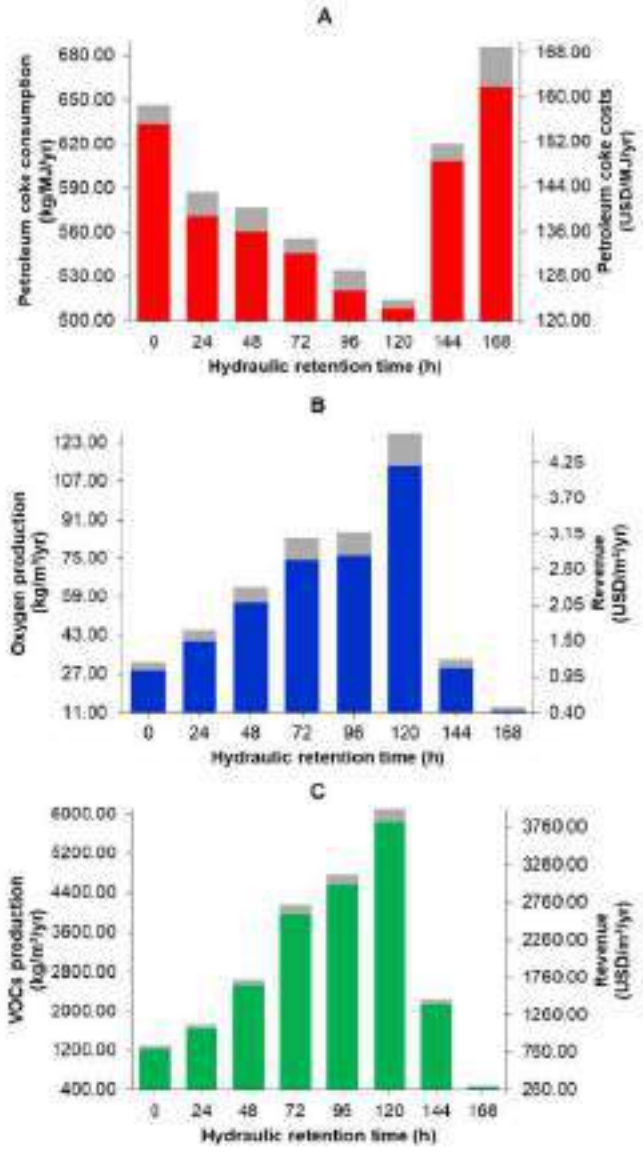


Fig. 6. Utility costs and revenues of the integrated bio-combustion system. (A) Petroleum coke, (B) Oxygen*, and (C) Volatile organic compounds**. Note: The left y-axis represents materials mass (gray bars), and the right y-axis represents the costs (red bars) and revenues (blue and green bars). *Considering oxygen selling price of 33 USD/metric ton (CMR, 2019). **Considering fuel selling price of 240 USD/metric ton and expressed in petroleum coke equivalents (CMR, 2019). (For interpretation of the references to colour in this figure legend, the reader is referred to the web version of this article.)

volatile organic compounds with their costs and revenues generated in the integrated bio-combustion system.

The main direct manufacturing costs of the bio-combustion system is related to fuel consumption, which is estimated close to 514.8 kg of petroleum coke per MJ of energy generated yearly, resulting in a utility cost of 122.1 USD/MJ/yr (Fig. 6A). Compared with other experimentally tested conditions (data from Table 1, Part I), fuel consumption and its costs in the combustion with the atmospheric air enrichment and with the simulated industrial gas stream (composition of 5.5% O_2, 17% CO_2, and 76.5% N_2) were estimated in values of 594 and 726 kg/MJ/yr, and 141.9 and 171.6 USD/MJ/yr, respectively. This represents more than 16% and 40%, respectively, of expenses concerning bio-combustion. The main parameter in the differentiation of these values is related to the concentration of oxygen injected into the furnace (IHEA, 2015). At the industrial level, combustion systems, in general, are highly energy-intensive. By way of exemplification, the typical fuel expenditure in a clinker furnace can reach up to 3.5 MJ/ton of processed clinker. Nonetheless, energy use has always been enhanced by economic reasons. In contrast, there are few options available for further optimization (Oliveira et al., 2019).

Besides, the integrated bio-combustion system generates two materials that can be classified as utilities (oxygen as oxidizer and VOCs as additional biofuel), and these revenues are demonstrated in Fig. 6B and 6C. Data analysis indicates that the system has the potential to produce 125.4 kg/m³/yr of oxygen that results in a revenue of 4.2 USD/m³/yr (data from Fig. 4, Part I). The impact of the volumetric oxygen productivity is not very representative in the process.

Regarding the VOCs, an energy potential of 5,029.20 MJ/m³/yr is generated in the photobioreactor. Associated with this, about 6,107.40 kg/m³/yr of VOCs are produced (data from Table 2 and Fig. 6, Part I), and this energetic fraction results in a possible revenue of 3,817 USD/m³/yr in terms of petroleum coke equivalents. These compounds represent a substantial net energy gain and can expand the revenues of the integrated system.

3.6.2. Carbon credits

Equally impactful to leverage the bioeconomy of the present process is the CO_2 capture and utilization in the photobioreactor, which would provide a new opportunity to generate additional revenues through the sale of carbon credits. Ultimately, this relevant economic aspect, which is often overlooked, could reduce other costs in the facility (Wiesberg et al., 2017). In this sense, Table 4 shows carbon credits associated with the integrated process.

According to Table 4, the relative mass of carbon captured in the photobioreactor was predicted to be 145 kg/m³/yr. While the carbon avoided from bio-combustion was close to 221.2 kg per MJ of energy produced yearly. In this sense, the bioeconomy of the integrated process showed that the facility could earn in terms of yearly carbon credits around 3.2 USD. This additional value represents only the 0.09% share of total revenue projected in the system. It is worth noting that the majority revenue (3,821.2 USD/m³/yr), related to utilities produced VOCs and oxygen, when accounted for together, forecast a possible amount that surpasses the fuel consumption expenses. Therefore, this is the point at which microalgae-based processes, primarily represented by photobioreactors, come into focus. If these BCCU technologies could be integrated, even partially and without any modernization into the retrofitting existing thermal system, they would be considered as ancillary equipment in utility costs.

However, while potential revenues are evident, the bioeconomy of the integrated system still does not hold up in practice. To date, there is no photobioreactor design, among other aspects, with operational capacity for CO_2 capture and bioconversion into bulk or commodity products (Severo et al., 2018a). This is also due to industrial combustion processes that would require such utilities in quantities high enough to withstand the daily workload. The same probably would not apply to the achievement of economic

Table 4
Carbon credits generated from the integrated process of biological carbon capture and utilization.

BCCU	Relative carbon mass	Carbon credits
Carbon captured	145 kg/m³/yr	1.30 USD/m³/yr
Carbon avoided	221.2 kg/MJ/yr	1.90 USD/MJ/yr

*The values were based on the experimental condition represented by the simulated industrial gas stream, assuming it as a conventional process (Severo et al., 2018b).

profits in combustion processes. Overall expenses of these facilities are undoubtedly more expressive, since they face much higher demand for other utilities, typically including process steam, electricity, compressed air, hot oil, and cooling and heating water. And this without taking into account the other elements of determining manufacturing costs, such as capital, labor, and general expenses (Ulrich and Vasudevan, 2006). Thus, the preliminary estimates of the integrated bio-combustion system could be used merely to further direct R&D efforts to cost-cutting improvement opportunities.

4. Conclusion

The integrated bio-combustion system based on BCCU has subjected a rigorous analysis across sustainability metrics and bioeconomy. Following the life cycle assessment, all scores had enhanced environmental performance. The normalization indicated that the most impacting factor in the categories evaluated is attributed often to non-renewable energy requirements, accounting 90% of the environmental burden. From the engineering costs analysis standpoint, fuel consumption was substantially inferior compared to air-enriched combustion and simulated industrial gas stream, reducing the cost of this utility by 16% and 40%, respectively. Besides, although the revenue obtained from oxygen productivity is not very expressive, the process generates jointly the VOCs, whose utilities represent 99% of the total revenue. Finally, carbon captured and avoided could further improve the bioeconomy earning additional revenues through potential carbon credits sale. These highlights seem hopeful, yet still problematic. Today, microalgae-based processes face a myriad of obstacles that need to be overcome, some of which have already been pointed out. This would require a combined effort among researchers, entrepreneurs, and policymakers to make these technologies viable in the future.

CRediT authorship contribution statement

Ihana A. Severo: Formal analysis, Data curation. **Mariany C. Deprá:** Methodology, Validation. **Rosangela R. Dias:** Methodology, Validation. **Juliano S. Barin:** Resources. **Cristiano R. de Menezes:** Writing - review & editing. **Roger Wagner:** Resources. **Leila Q. Zepka:** Supervision, Funding acquisition. **Eduardo Jacob-Lopes:** Conceptualization, Writing - review & editing.

Declaration of Competing Interest

We declare that we have no conflict of interest.

Acknowledgment

Funding for this research has been provided by the National Council for Scientific and Technological Development (CNPq), Coordination of Improvement of Higher Education Personnel (CAPES), Finance Code 001 (Brazil), and InterCement Brazil S/A. The authors are grateful to Seiiti Suzuki for technical support.

Appendix A. Supplementary material

Supplementary data to this article can be found online at https://doi.org/10.1016/j.ces.2019.115412.

References

Arastoopour, H., 2019. The critical contribution of chemical engineering to a pathway to sustainability. Chem. Eng. Sci. 203, 247–258. https://doi.org/10.1016/j.ces.2019.03.059.

Baleta, J., Mikulčić, H., Klemeš, J.J., Urbaniec, K., Duić, N., 2019. Integration of energy, water and environmental systems for a sustainable development. J. Clean. Prod. 215, 1424–1436. https://doi.org/10.1016/j.jclepro.2019.01.035.

Batcheham, R.J., 2006. Sustainability – the next chapter. Chem. Eng. Sci. 61, 4188–4193. https://doi.org/10.1016/j.ces.2005.10.016.

Batan, L., Quinn, J.C., Bradley, T.H., 2013. Analysis of water footprint of a photobioreactor microalgae biofuel production system from blue, green and lifecycle perspectives. Algal Res. 2, 196–203. https://doi.org/10.1016/j.algal.2013.02.003.

CMR. Chemical Market Reporter, 2019. Indicative chemical prices A–Z. Available at: <http://www.icis.com/chemicals/channel-info-chemicals-a-z/> (Accessed in: 06.13.2019).

Collet, P., Hélias, A., Lardon, L., Steyer, J.-P., Bernard, O., 2015. Recommendations for life cycle assessment of algal fuels. Appl. Energy 154, 1089–1102. https://doi.org/10.1016/j.apenergy.2015.03.008.

Czyrnek-Delêtre, M.M., Smyth, B.M., Murphy, J.D., 2017. Beyond carbon and energy: the challenge in setting guidelines for life cycle assessment of biofuel systems. Renew. Energy 105, 436–448. https://doi.org/10.1016/j.renene.2016.11.043.

Deprá, M.C., Mérida, L.G.R., de Menezes, C.R., Zepka, L.Q., Jacob-Lopes, E., 2019. A new hybrid photobioreactor design for microalgae culture. Chem. Eng. Res. Des. 144, 1–10. https://doi.org/10.1016/j.cherd.2019.01.023.

DOE. U.S. Department of Energy. Office of Energy Efficiency and Renewable Energy. Advanced Manufacturing Office. Available at: <https://www.energy.gov/eere/amo/advanced-manufacturing-office> (Accessed in: 01.16.2019).

EPA. Environmental Protection Agency of United States. Greenhouse Gas Inventory Guidance Direct Emissions from Stationary Combustion Sources, 2016. Available at: <www.epa.gov/sites/production/files/2016-03/documents/stationaryemissions_3_2016.pdf> (Accessed in: 01.16.2019).

Farooq, W., Suh, W.I., Park, M.S., Yang, J.-W., 2015. Water use and its recycling in microalgae cultivation for biofuel application. Bioresour. Technol. 184, 73–81. https://doi.org/10.1016/j.biortech.2014.10.148.

Glassman, I., Yetter, R.A., Glumac, N.G., 2015. Combustion. Academic Press Elsevier, p. 774p.

Grierson, S., Strezov, V., Bengtsson, J., 2013. Life cycle assessment of a microalgae biomass cultivation, bio-oil extraction and pyrolysis processing regime. Algal Res. 2, 299–311. https://doi.org/10.1016/j.algal.2013.04.004.

Hauschild, M. Z., Wenzel, H., 1998. Environmental Assessment of Products. Volume 2: Scientific Background. first ed., Springer US, 566p.

Hoekstra, A.Y., 2011. The global dimension of water governance: why the river basin approach is no longer sufficient and why cooperative action at global level is needed. Water 3 (1), 21–46. https://doi.org/10.3390/w3010021.

Hulatt, C.J., Thomas, D.N., 2011. Productivity, carbon dioxide uptake and net energy return of microalgal bubble column photobioreactors. Bioresour. Technol. 102, 5775–5787. https://doi.org/10.1016/j.biortech.2011.02.025.

IHEA. Improving Process Heating System Performance: A Sourcebook for Industry, 2015. Third edition, Prepared for the United States Department of Energy Office of Energy Efficiency and Renewable Energy. Advanced Manufacturing Office.

ILCD. International Reference Life Cycle Data System handbook: General guide for life cycle assessment – Detailed guidance, 2010. First ed., Luxembourg. Institute for Environment and Sustainability. Joint Research Centre, European Commission.

ISO. International Standardization Organization. Environmental management–life cycle assessment-principles and framework. ISO 14040, 2006. Available at: <http://www.iso.org/iso/catalogue_detail?csnumber=37456> (Accessed in: 12.12.2018).

Jacob, A., Xia, A., Murphy, J.D., 2015. A perspective on gaseous biofuel production from micro-algae generated from CO_2 from a coal-fired power plant. Appl. Energy 148, 398–402. https://doi.org/10.1016/j.apenergy.2015.03.077.

Jacob-Lopes, E., Scoparo, C.H.G., Queiroz, M.I., Franco, T.T., 2010. Biotransformations of carbon dioxide in photobioreactors. Energy Convers. Manage. 51, 894–900. https://doi.org/10.1016/j.enconman.2009.11.027.

Jacob-Lopes, E., Severo, I.A., Bizello, R.S., Barin, J.S., Menezes, C.R.D., Cichoski, A.J., et al., 2017. Process and system for re-using carbon dioxide transformed by photosynthesis into oxygen and hydrocarbons used in an integrated manner to increase the thermal efficiency of combustion systems. Patent WO2017/112984 A1, 2017.

Jacob-Lopes, E., Franco, T.T., 2013. From oil refinery to microalgal biorefinery. J. CO_2 Util. 2, 1–7. https://doi.org/10.1016/j.jcou.2013.06.001.

Jorquera, O., Kiperstok, A., Sales, E.A., Embiruçu, M., Ghirardi, M.L., 2010. Comparative energy life-cycle analyses of microalgal biomass production in open ponds and photobioreactors. Bioresour. Technol. 101, 1406–1413. https://doi.org/10.1016/j.biortech.2009.09.038.

Klemeš, J.J., 2013. Handbook of Process Integration (PI): Minimisation of Energy and Water Use, Waste and Emissions. Woodhead/Elsevier, Cambridge, UK.

Koiwanit, J., Manuilova, A., Chan, C., Wilson, M., Tontiwachwuthikul, P., 2014. A life cycle assessment study of a hypothetical Canadian oxy-fuel combustion carbon dioxide capture process. Int. J. Greenhouse Gas Control 28, 257–274. https://doi.org/10.1016/j.ijggc.2014.07.001.

Lasatte, B., Guillaume, B., Kim, J., Breregah, B., 2014. Modeling cumulative effects in life cycle assessment: the case of fertilizer in wheat production contributing to the global warming potential. Sci. Total Environ. 481, 588–595. https://doi.org/10.1016/j.scitotenv.2014.02.020.

Merchuk, J. C., Garcia-Camacho, F., Molina-Grima, E., 2019. Chapter 2.25 - Photobioreactors – Models of Photosynthesis and Related Effects. In: Moo-Young, M. (Ed.), Comprehensive Biotechnology (third ed.), pp. 320–360. DOI: 10.1016/B978-0-444-64046-8.00081-1.

Mullinger, P., Jenkins, B., 2014. Industrial and Process Furnaces. Principles, Design and Operation. Butterworth-Heinemann publications, Elsevier, Oxford, UK, p. 676p.

Oliveira, F.A.C., Fernandes, J.C., Calindo, J., Rodríguez, J., Cañadas, I., Vermelhudo, V., et al., 2019. Portland cement clinker production using concentrated solar energy – a proof-of-concept approach. Sol. Energy 183, 677–688. https://doi.org/10.1016/j.solener.2019.03.064.

Pérez-Fortes, M., Schöneberger, J.C., Boulamanti, A., Tzimas, E., 2016. Methanol synthesis using captured CO_2 as raw material: techno-economic and environmental assessment. Appl. Energy 161, 718–732. https://doi.org/10.1016/j.apenergy.2015.07.067.

Pérez-Lopez, P., de Vree, J.H., Feijoo, G., Bosma, R., Barbosa, M.J., Moreira, M.T., et al., 2017. Comparative life cycle assessment of real pilot reactors for microalgae cultivation in different seasons. Appl. Energy 205, 1151–1164. https://doi.org/10.1016/j.apenergy.2017.08.102.

Santos, A.B., Fernandes, A.S., Wagner, R., Jacob-Lopes, E., Zepka, L.Q., 2016. Biogeneration of volatile organic compounds produced by *Phormidium autumnale* in heterotrophic bioreactor. J. Appl. Phycol. 28, 1561–1570. https://doi.org/10.1007/s10811-015-0740-0.

Severo, I.A., Barin, J.S., Wagner, R., Zepka, L.Q., Jacob-Lopes, E., 2018a. Biofuels from Microalgae: Photobioreactor Exhaust Gases in Oxycombustion Systems. In: Jacob-Lopes, E., Zepka, L.Q., Queiroz, M.I. (Eds.), Energy from Microalgae. Green Energy and Technology. Springer, pp. 271–290. https://doi.org/10.1007/978-3-319-69093-3_13.

Severo, I.A., Deprá, M.C., Barin, J.S., Wagner, R., Menezes, C.R.de., Zepka, L.Q., Jacob-Lopes, E., 2018b. Bio-combustion of petroleum coke: The process integration with photobioreactors. Chemical Engineering Science, 177, 422–430. DOI: 10.1016/j.ces.2017.12.001.

Slade, R., Bauen, A., 2013. Micro-algae cultivation for biofuels: cost, energy balance, environmental impacts and future prospects. Biomass Bioenergy 53, 29–38. https://doi.org/10.1016/j.biombioe.2012.12.019.

Sun, C.-H., Fu, Q., Liao, Q., Xia, A., Huang, Y., Zhu, X., Reungsang, A., Chang, H.-X., 2019. Life-cycle assessment of biofuel production from microalgae via various bioenergy conversion systems. Energy 171, 1033–1045. https://doi.org/10.1016/j.energy.2019.01.074.

Tredici, M.R., Bassi, N., Prussi, M., Biondi, N., Rodolfi, L., Chini Zittelli, G., et al., 2015. Energy balance of algal biomass production in a 1-ha "Green Wall Panel" plant: how to produce algal biomass in a closed reactor achieving a high Net Energy Ratio. Appl. Energy 154, 1103–1111. https://doi.org/10.1016/j.apenergy.2015.01.086.

Turns, S.R., 2011. An Introduction to Combustion: Concepts and Applications. Mc Graw-Hill Education, Europe, p. 752p.

Turton, R., 2009. Analysis, Synthesis, and Design of Chemical Processes. Prentice-Hall, Upper Saddle River, p. 1144p.

Ulrich, G.D., Vasudevan, P.T., 2006. How to estimate utility costs. Chem. Eng. 113, 66–69.

Valderrama, C., Granados, R., Cortina, J.L., Gasol, C.M., Guillem, M., Josa, A., 2012. Implementation of best available techniques in cement manufacturing: a life-cycle assessment study. J. Clean. Prod. 25, 60–67. https://doi.org/10.1016/j.jclepro.2011.11.055.

Varbanov, P.S., Klemeš, J.J., Wang, X., 2018. Methods optimisation, process integration and modelling for energy saving and pollution reduction. Energy 146, 1–3. https://doi.org/10.1016/j.energy.2018.01.122.

Verma, R., Srivastava, A., 2018. Carbon dioxide sequestration and its enhanced utilization by photoautotroph microalgae. Environ. Develop. 27, 95–106. https://doi.org/10.1016/j.envdev.2018.07.004.

Walmsley, T.G., Ong, B.H.Y., Klemeš, J.J., Tan, R.R., Varbanov, P.S., 2019. Circular integration of processes, industries, and economies. Renew. Sustain. Energy Rev. 107, 507–515. https://doi.org/10.1016/j.rser.2019.03.039.

Wang, C., Wang, P., Du, Y., Che, D., 2019. Experimental study on effects of combustion atmosphere and coal char on NO_2 reduction under oxy-fuel condition. J. Energy Inst. 92, 1023–1031. https://doi.org/10.1016/j.joei.2018.07.004.

Westerg, I.L., Brigagão, G.V., de Medeiros, J.L., Araújo, O.Q.F., 2017. Carbon dioxide utilization in a microalga-based biorefinery: efficiency of carbon removal and economic performance under carbon taxation. J. Environ. Manage. 203, 988–998. https://doi.org/10.1016/j.jenvman.2017.03.005.

World Bank and Ecofys, 2018. State and Trends of Carbon Pricing. World Bank, Washington, DC. DOI: 10.1596/978-1-4648-1292-7.

World Energy Council. World Energy Resources, 2016. Available at: <https://www.worldenergy.org/assets/images/imported/2016/10/World-Energy-Resources-Full-report-2016.10.03.pdf> Accessed in: 05.18.2019.

Ye, C., Mu, D., Horowitz, N., Xue, Z., Chen, J., Xue, M., Zhou, Y., Klatts, M., Zhou, W., 2018. Life cycle assessment of industrial scale production of spirulina tablets. Algal Res. 34, 154–163. https://doi.org/10.1016/j.algal.2018.07.013.

Yin, C., Yan, J., 2016. Oxy-fuel combustion of pulverized fuels: combustion fundamentals and modeling. Appl. Energy 162, 742–762. https://doi.org/10.1016/j.apenergy.2015.10.149.

WOODHEAD SERIES IN BIOENERGY



ALGAL BIOREACTORS

SCIENCE, ENGINEERING AND TECHNOLOGY OF UPSTREAM PROCESSES

VOLUME 1

Edited by
EDUARDO JACOB-LOPES
LEILA QUEIROZ ZEPKA
MARIANY COSTA DEPRÁ

Series Editor
YVES GAGNON

ELSEVIER

Algal Bioreactors

This page intentionally left blank

Woodhead Series in Bioenergy

Algal Bioreactors

Science, Engineering and Technology of Upstream Processes

VOLUME 1

Series Editor

Yves Gagnon
Université de Moncton, Moncton, Canada

Edited by

Eduardo Jacob-Lopes
Department of Food Technology and Science, Federal University of Santa Maria, Santa Maria, Brazil

Leila Queiroz Zepka
Department of Food Technology and Science, Federal University of Santa Maria, Santa Maria, Brazil

Mariany Costa Deprá
Department of Food Technology and Science, Federal University of Santa Maria, Santa Maria, Brazil

ELSEVIER
WP
WOODHEAD PUBLISHING
An imprint of Elsevier

Woodhead Publishing is an imprint of Elsevier
50 Hampshire Street, 5th Floor, Cambridge, MA 02139, United States
125 London Wall, London EC2Y 5AS, United Kingdom

Copyright © 2025 Elsevier Ltd. All rights are reserved, including those for text and data mining, AI training, and similar technologies.

Publisher's note: Elsevier takes a neutral position with respect to territorial disputes or jurisdictional claims in its published content, including in maps and institutional affiliations.

No part of this publication may be reproduced or transmitted in any form or by any means, electronic or mechanical, including photocopying, recording, or any information storage and retrieval system, without permission in writing from the publisher. Details on how to seek permission, further information about the Publisher's permissions policies and our arrangements with organizations such as the Copyright Clearance Center and the Copyright Licensing Agency, can be found at our website: www.elsevier.com/permissions.

This book and the individual contributions contained in it are protected under copyright by the Publisher (other than as may be noted herein).

Notices
Knowledge and best practice in this field are constantly changing. As new research and experience broaden our understanding, changes in research methods, professional practices, or medical treatment may become necessary.

Practitioners and researchers must always rely on their own experience and knowledge in evaluating and using any information, methods, compounds, or experiments described herein. In using such information or methods they should be mindful of their own safety and the safety of others, including parties for whom they have a professional responsibility.

To the fullest extent of the law, neither the Publisher nor the authors, contributors, or editors, assume any liability for any injury and/or damage to persons or property as a matter of products liability, negligence or otherwise, or from any use or operation of any methods, products, instructions, or ideas contained in the material herein.

ISBN: 978-0-443-14058-7

For information on all Woodhead Publishing publications visit our website at https://www.elsevier.com/books-and-journals

Publisher: Megan Ball
Acquisitions Editor: Peter Adamson
Editorial Project Manager: Ellie Barnett
Production Project Manager: Kamesh R.
Cover Designer: Mark Rogers

Typeset by TNQ Technologies



Contents

Contributors xvii
About the editors xxiii
Foreword xxv
Preface xxvii

Part I
Fundamentals of algal bioreactors

1. Algal bioreactors: The core of the microalgae-based processes and products

Michael A. Borowitzka

1.1 Introduction 3
1.2 History 3
1.3 Basic considerations for the design and operational of algal bioreactors 4
1.3.1 Requirements from the perspective of the algae 4
1.3.2 Requirements from the perspective of the operator 7
1.3.3 Requirements from a commercial perspective 7
1.4 Conclusion 8
References 8

2. Global market and future trends of microalgae-based products

Kricelle Mosquera Deamici, Daniel Figueiredo, Inês Guerra, Pedro Letras and Hugo Pereira

2.1 Introduction 11
2.2 Microalgae as a sustainable environmental resource 12
2.2.1 Sustainable production of valuable biochemical compounds 12
2.3 Biotechnological applications of microalgae biomass 13
2.3.1 Human nutrition 13
2.3.2 Feed nutrition 15
2.3.3 Bioactive compounds 16
2.3.4 Biofuels 17
2.3.5 Other applications 18
2.4 Market insights: Industrial production and compounds of microalgal biomass 19
2.4.1 Overview of the world microalgae production 19
2.4.2 The growing microalgae market 19
2.5 Challenges and future directions 20
References 21

3. Innovation management on microalgae-based processes and products

José Moleiro Martins, Mário Nuno Mata, Rui Dantas, António Abreu and Kateryna Boichenko

3.1 Introduction 27
3.2 State-of-the-art 29
3.2.1 Systematic literature review 29
3.2.2 The common research trends and meta-analysis 31
3.3 Conclusions 36
References 37

4. Circular bio-based economy of microalgae-based processes and products

Doljit Borah, Khalifa S.H. Eldiehy, Rupam Kataki and Dhanapati Deka

4.1 Introduction 39
4.2 Bio-based products from microalgae 43
4.2.1 Microalgae as food source 43
4.2.2 Microalgae as biofuel feedstock 44
4.2.3 Microalgae-based fish and animal feed production 47
4.2.4 Microalgae bioplastics 48
4.3 Principles of circular economy and their application in microalgae-based processes and products 49

4.4 Closed-loop cultivation systems 50
4.4.1 Biorefineries for resource optimization 50
4.4.2 Synergy with other industries 51
4.4.3 Valorization of waste and by-products 53
4.4.4 Eco-friendly harvesting techniques 53
4.4.5 Extending product life and reusability 55
4.4.6 Collaboration and knowledge sharing 56
4.5 Challenges and prospects of commercializing microalgae-based processes and products 56
4.5.1 Challenges of scaling up microalgae-based processes 57
4.5.2 Opportunities of scaling up microalgae-based processes 58
4.6 Case studies of microalgae-based processes and products in the circular economy 59
4.6.1 Case study 1 59
4.6.2 Case study 2 60
4.6.3 Case study 3 61
4.7 Microalgae-based processes and products' future in a sustainable and circular bio-based economy 61
4.8 Conclusion and recommendations for further research 62
References 62

Part II
Science and engineering of algal bioreactors

5. Optimal growth and culture conditions for algae in bioreactors

Gabriela Filipini Ferreira, Bianca Ramos Estevam, Fernanda Palmeira Beatriz and Luisa Fernanda Ríos Pinto

5.1 Introduction 71
5.2 Cultivation systems 71
5.2.1 Open systems 72
5.2.2 Closed systems 72
5.2.3 Other configurations of bioreactors 74
5.2.4 Hybrid cultivation systems 74
5.3 Microalgae cultivation parameters 75
5.3.1 Light 75
5.3.2 Temperature 75
5.3.3 Nutrient availability 75
5.3.4 pH 75
5.3.5 Manipulation of cultivation parameters 76
5.4 Growth regime and carbon source 76
5.4.1 Inorganic carbon 76
5.4.2 Organic carbon 78
5.5 Conclusions and recommendations 80
References 80

6. Predictive models of algal growth in bioreactors

Reinaldo G. Bastos and Mariana A. da Silva

6.1 Introduction 83
6.2 Kinetic parameters for microalgae growth 84
6.3 Mass and energy balances 86
6.4 Predictive mathematical models 87
6.5 Conclusions and outlook 91
References 91

7. Transport phenomena assessment in algal bioreactors

Liliana Ardila Forero

7.1 Introduction 93
7.2 Type of algal bioreactors and their characteristics 93
7.3 Design aspects of photobioreactors related to transport phenomena 95
7.3.1 Rheological properties 95
7.3.2 Mechanical and pneumatic mixing and their flow patterns 96
7.3.3 Mass transport in phototrophic cultures 99
7.3.4 Heat and light transport in algal bioreactors 101
7.4 Recommendations 102
References 102

8. Mixing and agitation requirements in algal bioreactors

Marcio B. Machado and Inci Ayranci

8.1 Introduction 105
8.2 Mixing devices 106
8.3 Stirred tank—terminology and nomenclature 107
8.4 Dimensionless numbers 107
8.5 Impeller selection 109
8.5.1 Hydrofoils 110
8.5.2 Mixed-flow impellers 110
8.5.3 Radial flow impellers 111
8.6 Scale-up/down of stirred tanks 111
8.7 Oxygen transfer rate and scale-up 112
8.8 Bioreactor design recommendations 114
Nomenclature 116
References 116

9. Hydrodynamic performance of algal bioreactors

Zahra Zarei, Peyman Malekshahi, Mohammad Hossein Morowvat and Antoine P. Trzcinski

9.1 Introduction 121
9.2 Photobioreactor hydrodynamics 122
9.2.1 Mixing 122
9.2.2 Superficial gas velocity (or gas flow rate) 123
9.2.3 Bubble size and velocity 125
9.2.4 Gas holdup 126
9.2.5 Liquid velocity 127
9.2.6 Mass transfer coefficient 128
9.3 Conclusions 131
References 131

10. Heat transfer in algal bioreactors

Sarang Tamhankar, Manishkumar Dinesh Yadav and Channamallikarjun Sidramayya Mathpati

10.1 Introduction 135
10.2 Mechanisms of heat transfer 136
10.2.1 Conduction 136
10.2.2 Convection 136
10.2.3 Radiation 137
10.2.4 Heat generation during microbial growth 137
10.2.5 Model equation for the batch system (ideal scenario) 140
10.2.6 Design equations for continuous system 140
10.2.7 Case study 141
10.2.8 Steam sterilization 143
10.2.9 Sterilization of gases 143
10.3 Conclusions 144
References 144

11. Thermodynamic principles applied to exergy analysis of algal bioreactors: Enhanced-efficiency approaches for microalgae-based processes

Po-Chih Kuo, Zhuang Sun, Xiangxiang Chen, Du Wen and Muhammad Aziz

11.1 Introduction 147
11.2 The basic concept of exergy 148
11.2.1 Exergy balance 148
11.2.2 Physical exergy 148
11.2.3 Chemical exergy 148
11.2.4 Heat exergy 149
11.3 Case studies 149
11.3.1 Case I 150
11.3.2 Case II 153
11.3.3 Exergy analysis 155
11.4 Conclusions 158
References 158

12. Oxygen outgassing and hydrodynamics analysis in microalgal photobioreactors

Eleftherios Touloupakis, Isabela Calegari Moia, Cecilia Faraloni and Pietro Carlozzi

12.1 Introduction 159
12.2 State of the art 160
12.2.1 Photobioreactors 160
12.2.2 Tubular photobioreactors 160
12.2.3 Flat-plate photobioreactors 161
12.2.4 PBR with internal radiation systems 162
12.2.5 Oxygen build-up and outgassing in photobioreactors 163
12.2.6 Hydrodynamic aspects in PBRs 165
12.2.7 Photosynthetic efficiency, mixing and cell damage relationship 166
12.3 Conclusions 168
Acknowledgments 168
References 169

13. Light optimization and management technologies for increasing algal bioreactors efficiency

Lisa Borella, Nicola Trivellin and Eleonora Sforza

13.1 Introduction 173
13.2 Bottlenecks for light exploitation by microalgae 174
13.2.1 Theoretical photosynthetic efficiency 174
13.2.2 Light extinction profile in a PBR and operation at the compensation point 175
13.3 Strategies for sunlight exploitation and management 175
13.3.1 State of the art of microalgae outdoor production 175
13.3.2 Solar trackers 176
13.3.3 Light guides 177
13.3.4 Luminescent solar concentrators and spectral converters 177
13.3.5 Photovoltaics 178
13.4 Artificial light supply 180

13.4.1 State of the art of microalgae production using artificial light 180
13.4.2 Technologies for illumination: A comparison 181
13.5 Hybrid systems 184
Recommendations 185
References 185

14. Computational analysis and modeling of algal bioreactors performance

Fernando Z. Sierra-Espinosa, Francisco Carrillo and Dulce M. Graciano

14.1 Introduction 189
14.2 State-of-the-art 190
14.2.1 Bioreactors 190
14.2.2 Kinetics of algal growth 191
14.2.3 Photosynthesis and radiation 192
14.2.4 Turbulence 193
14.2.5 Experimental data 194
14.2.6 Numerical prediction for square section reactor 195
14.3 Recommendations 200
References 202

15. Internet of things (IoT) use for remote monitoring of algal bioreactors

Pavel Gotovtsev, Yana Sergeeva, Daniil Sukhinov, Maria Petrova, Maria Vishnevskaya, Alexandra Shestakova, Anton Rogov, Alexander Romanov, Kirill Gorin and Raif Vasilov

15.1 Introduction 205
15.1.1 Sensors network organization and data protocols 207
15.1.2 Data handling and machine learning approaches 209
15.1.3 Augmented and virtual reality IoT-based approaches 209
15.1.4 Recommendations 210
15.2 Conclusion 211
Acknowledgments 211
References 211

16. Process integration approaches applied to algal bioreactors

Jalelys Liceth Leones-Cerpa, Freyle A. Maza-Madera, Eduardo Luis Sánchez-Tuirán and Karina A. Ojeda-Delgado

16.1 Introduction 215
16.2 Technologies for algal bioreactors 215
16.2.1 Types and characteristics of algal bioreactors 215
16.2.2 Conventional approach to the algal production process 217
16.3 Process integration 218
16.3.1 Overview and importance of process integration 218
16.3.2 Fundamental concepts of process integration 218
16.3.3 Main concepts of mass integration 219
16.4 Mass integration applied to algal bioreactors 219
16.4.1 Latest research in mass integration 219
16.4.2 Mass integration focused on processes with aquatic biomasses 220
16.5 Case studies 221
16.5.1 Freshwater 223
16.5.2 Wastewater 223
References 223

17. Process intensification approaches applied to microalgae bioreactors

Valeria Caltzontzin-Rabell, Juan Manuel Vera Morales, Carlos Eduardo Guzmán-Martínez, Salvador Hernández, Sergio Iván Martínez-Guido and Claudia Gutiérrez-Antonio

17.1 Introduction 227
17.2 Microalgae generalities 228
17.3 Conventional bioreactors for microalgae cultivation 231
17.3.1 Types of photobioreactors 231
17.4 Intensified bioreactors for microalgae cultivation 232
17.5 Future trends on for microalgae cultivation 234
17.6 Concluding remarks 235
Acknowledgments 235
References 235

18. Control of biological contamination in microalgae cultures

Valeria Flores-Tinoco, Alethia A. Brito-Bello, Vy P. Le and Damar Lopez-Arredondo

Abbreviations 239
18.1 Introduction 239
18.2 Major biological contaminants and sources of contamination 240

18.3 Detection of biological contaminants 241
18.3.1 Agar plating 241
18.3.2 Microscopy 241
18.3.3 Flow cytometry 244
18.3.4 Marker gene and whole-genome sequencing 245
18.3.5 Artificial intelligence and machine learning 245
18.4 Strategies to avoid and control biological contamination 246
18.4.1 Physical control 246
18.4.2 Environmental pressure 248
18.4.3 Chemical control 249
18.4.4 Biological control 251
18.4.5 Genetic engineering approaches to enhance contamination control 252
18.5 Highlights and recommendations 255
References 256

19. Installations of algal bioreactors: Design and operational issues in commercial plants

Wei Han Khor and Hooi Siang Kang

19.1 Introduction 263
19.1.1 Microalgae and its application 263
19.1.2 Microalgae cultivation systems 263
19.1.3 Purpose of this chapter 267
19.2 Design considerations in photobioreactors 267
19.2.1 Key design parameters 267
19.2.2 State-of-art of commercial microalgae cultivation 269
19.3 Operational challenges in photobioreactors 271
19.3.1 Cleaning and sterilization 271
19.3.2 High operational cost 272
19.3.3 Nutrient supply 273
19.4 Scale up considerations 273
19.4.1 Scale-up strategies 274
19.5 Conclusion and recommendations 276
References 276

20. Scale-up of algal bioreactors for renewable resource production

Ombretta Paladino and Matteo Neviani

20.1 Complexity of scale-up for algal bioreactors 281
20.1.1 The microalgae growing modes 281
20.1.2 The algal bioreactors 282
20.1.3 The operating modes 284
20.2 Photobioreactors at the different scales 286
20.2.1 From lab-scale to pilot-scale 286
20.2.2 From pilot scale to industrial scale: Batteries of photobioreactors 287
20.3 Rigorous scale-up of photobioreactors 287
20.3.1 Theoretical background 287
20.3.2 Rigorous scale-up based on Buckingham's π-theorem 291
20.3.3 Scale-up of mixed fed-batch and semicontinuous photobioreactors 291
20.3.4 Scale-up of bubble and airlift photobioreactors 295
20.3.5 Organization of the π-space variables 297
20.3.6 Experimental determination of the π-space variables 298
20.4 Conclusions 299
References 299

Part III
Trends in algal bioreactors design for renewable resource production

21. Raceway ponds for microalgae production

Arturo Cadena Ramírez, Maria de los Angeles Baños Orozco and Miguel Angel Anducho Reyes

21.1 Introduction 305
21.2 Microalgae 305
21.3 Bioreactors 309
21.3.1 Open pond photobioreactors 310
21.3.2 Industrial relevance of raceway ponds 311
21.3.3 Process scaling 312
21.3.4 Hydrodynamic study 314
21.3.5 Artificial vision and image segmentation 314
21.3.6 Dead zones 322
21.3.7 Tracer particles 323
21.3.8 Imaging and preprocessing 323
21.3.9 Image processing and segmentation using the Fast Distance Transform 324
21.3.10 General factors that affect raceway productivity 326
References 326
Further reading 330

22. Heterotrophic microalgal bioreactors

Carlos A. Montenegro-Herrera, Viyils Sangregorio-Soto and Mariana Manzoni Maroneze

22.1 Introduction 331
22.2 Design, geometry, and operation conditions of heterotrophic microalgae bioreactors 331
22.2.1 Heterotrophic microalgae bioreactors 332
22.2.2 General features of bioreactor design 333
22.2.3 Recent trends in designing and operating bioreactors 333
22.3 Scaling-up criteria of heterotrophic bioreactors 336
22.3.1 Challenges during scale-up 337
22.3.2 Control of bioreactors 337
22.3.3 Dissolved oxygen and *pH* control 337
22.4 Heterotrophic reactors versus photobioreactors 338
22.5 Prospects and challenges 341
Nomenclature 341
References 342

23. The application of bubble column photobioreactor for algal cultivation

Linda O'Higgins, Muhammad Nabeel Haider, Nikita Verma and Archishman Bose

23.1 Introduction 345
23.2 Bottlenecks in the upstream processing 345
23.3 Microalgal cultivation systems 346
23.3.1 Open raceway pond cultivation and its downsides 347
23.3.2 Cultivation of microalgae in closed photobioreactors 347
23.4 Factors affecting microalgae growth in photobioreactors 348
23.4.1 Light intensity and photoperiod 348
23.4.2 Microalgae concentration 349
23.4.3 Mixing and mass transfer 349
23.4.4 Temperature 349
23.5 CO_2 and nutrient availability 349
23.6 Bubble column photobioreactor 350
23.6.1 Introduction 350
23.6.2 Hydrodynamics of the bubble column bioreactor 353
23.6.3 Parameter control and optimization 354
23.7 Conclusion 356
References 356

24. Airlift photobioreactors applied to algal production

Bahar Aslanbay Guler, Çağla Yarkent, Suphi S. Oncel and Esra Imamoglu

24.1 Introduction 361
24.2 Key factors for microalgae cultivation 362
24.3 ALPBRs applied to microalgae cultivation 364
24.3.1 Design principles 364
24.3.2 Scaling up 366
24.3.3 Common applications in lab and pilot scale 369
24.4 Technological perspectives applied to airlift PBRs 369
24.4.1 Novel design strategies 369
24.4.2 Modeling and simulation with computational fluid dynamics 371
24.5 Challenges, recommendations, and conclusion 373
References 374

25. Column photobioreactors applied to algal production: Design, assembly, and operation

Saeid Samipour, Payam Setoodeh and Amin Reza Rajabzadeh

25.1 Introduction 379
25.2 Modeling and analysis of CPBRs 383
25.3 Column photobioreactors design and operation 387
25.3.1 Principles of column photobioreactor design 388
25.3.2 Column photobioreactor types 388
25.3.3 Construction of column photobioreactors 391
25.3.4 Lighting strategy 392
25.3.5 Thermal design and temperature control 395
25.3.6 Aeration 396
25.3.7 Mixing and agitation 398
25.4 Conclusion 400
Nomenclature 400
Acknowledgments 401
References 401

26. Tubular photobioreactors applied to algal production

Priscila Santos Corrêa, Wilson Galvão de Morais Júnior and Nídia de Sá Caetano

26.1 Introduction 407
26.2 State-of-the-art 408
26.2.1 Microalgae growth: Limiting factors 408
26.2.2 Design of tubular PBRs 409
26.2.3 Modeling tubular PBRs to algal production 412
26.3 Recommendations 417
Acknowledgments 417
References 417

27. Flat-plate photobioreactors for renewable resources production

Mohammad Redwanur Rahman and Klaus Hellgardt

27.1 Introduction 423
27.2 State of the art in FP-PBR technology 431
27.2.1 State of the art 431
27.2.2 Components of FP-PBR 432
27.2.3 Construction mechanism of FP-PBR 433
27.2.4 FP-PBR design 433
27.2.5 Technical challenges associated with FP-PBR 434
27.2.6 Challenges associated with light in FP-PBR 435
27.2.7 Large-scale FP-PBRs for commercial production 436
27.2.8 Batch versus continuous production in FP-PBR 437
27.2.9 Why FB-PBR is most convenient for renewable resources production? 439
27.3 Future trends in FP-PBR design and development 440
27.4 Upstream and downstream integration of renewable resources production in FP-PBR 440
27.5 Recommendations 442
Acknowledgments 443
References 443

28. Plastic bag photobioreactors applied to algal production

Masatoshi Kishi and Yoshiki Takayama

28.1 Introduction 449
28.2 General characteristics of plastic bag photobioreactors 451
28.2.1 Materials 451
28.2.2 Bag longevity and sterilization methods 452
28.3 Advantages and disadvantages of plastic bag reactors 452
28.3.1 Advantages 452
28.3.2 Challenges and potential solutions 455
28.4 Existing plastic bag reactors (classified by the shape) 456
28.4.1 Tubular and flat bag reactors 456
28.4.2 Column and flat-panel reactors 458
28.4.3 Floating reactors 461
28.4.4 Membrane reactors 464
28.5 Future perspectives 465
28.5.1 Functionality by shape 465
28.5.2 Functionality by material 465
28.6 Conclusions 465
Acknowledgments 466
References 466

29. Membrane photobioreactors applied to microalgae-based processes

Enrique González, Elisabet Segredo-Morales and Oliver Díaz

29.1 Introduction 469
29.2 State of the art 471
29.2.1 Biomass retention membrane photobioreactors: Main configurations 471
29.2.2 Factors affecting process performance in MF/UF-MPBRs for wastewater treatment 472
29.3 Recommendations 478
References 478

30. Hybrid and nonconventional photobioreactors applied to microalgae production

Richard A. Rodríguez Padrón and Luis G. Ramírez Mérida

30.1 Introduction 483
30.2 Processing parameters to take into account in the design of photobioreactors 484
30.2.1 Light supply 484
30.2.2 Supply and transfer of gases 485
30.2.3 Mixture 485

30.2.4 Other factors 486
30.3 Types of photobioreactors 486
30.3.1 Tubular photobioreactors 486
30.3.2 Flat-plate photobioreactors 486
30.3.3 Stirred tank fermenter type photobioreactors 488
30.3.4 Nonconventional and hybrid photobioreactors 488
30.4 Final considerations 488
Acknowledgments 489
References 489

Part IV
Bioproducts and bioenergy obtained from algal bioreactors

31. Intensive biomass production in algal bioreactors

Rosa Olivia Cañizares–Villanueva and Alfredo de Jesús Martínez–Roldán

31.1 Introduction 495
31.2 Open systems 495
31.2.1 Raceways 496
31.2.2 Thin layers 497
31.3 Closed systems 497
31.3.1 Tubular PBR 498
31.3.2 Flat panel photobioreactors 500
31.4 Conclusions 502
References 502

32. Protein and amino acid production in algal bioreactors

Tomás Lafarga, Ana Sánchez-Zurano, Silvia Villaró and Luisa Gouveia

32.1 Introduction 507
32.2 State of the art 508
32.2.1 Protein content of microalgae 508
32.2.2 Production of algal proteins 512
32.2.3 Uses of microalgal protein 513
32.2.4 Commercially available products 514
32.3 Recommendations 516
Acknowledgments 516
References 516

33. Lipids, sterols, and fatty acids production in algal bioreactors

Mariane Bittencourt Fagundes, Mariana Miranda Moutinho and José Diogo Cruz

33.1 Introduction 521
33.2 Lipids, sterols, and fatty acids in microalgae 521
33.3 Trophic modes and their influence on the lipid fraction 522
33.4 Abiotic factors and their influence on the lipid fraction 523
33.5 Optimization strategies to enhance lipid metabolites in microalgae 525
33.6 Extraction methods: Emergent technologies 527
33.7 Prospects and recommendations: Future and challenges in algal bioreactors for lipids, sterols, and fatty acids production 528
Acknowledgments 529
References 529

34. Natural pigments production in algal bioreactors

Darissa Alves Dutra, Pricila Nass Pinheiro, Patrícia Acosta Caetano, Mariany Costa Deprá, Rosangela Rodrigues Dias, Tatiele C. do Nascimento and Leila Queiroz Zepka

34.1 Introduction 535
34.2 Commercial microalgae culture systems: Pigment production 535
34.3 Exploring the unique aspects of manufacturing pigments based on microalgae 537
34.3.1 *Dunaliella salina* for β-carotene production 537
34.3.2 *Haematococcus pluvialis* for astaxanthin production 538
34.3.3 *Arthrospira platensis* for phycocyanin production 538
34.3.4 *Chlorella* sp. for chlorophyll production 539
34.4 Biosynthesis of pigments in microalgae 540
34.5 Challenges 540
34.6 Conclusion 543
References 543

35. Algal bioreactors for phycoprospecting: An emphasis on algae culturing

Vasumathi Krishnan, Kanmani Shanmugam, Winfred Sofi Beaula, Rathinam Raja, Pujithaa Singaravelu, Jayappriyan Kothilmozhian Ranishree and Ouafa Cherifi

35.1 Introduction 549
35.2 Algae source 549

35.3 Isolation and establishment of monocultures 550
35.3.1 Single cell isolation 550
35.3.2 Agar-based methods 550
35.4 Axenic culture 551
35.5 Density gradient centrifugation 551
35.6 Antibiotics treatment 551
35.6.1 Antimicrobial agents 551
35.7 Ultraviolet radiation 551
35.8 Flow cytometer cell sorter–based isolation 552
35.8.1 Media 552
35.8.2 Freshwater culture media (Table 35.1) 552
35.8.3 Marine culture media (Table 35.2) 552
35.8.4 Photobioreactor and its types 552
35.8.5 Open pond systems 552
35.8.6 Circular ponds 555
35.8.7 Inclined surface system/thin film systems 556
35.8.8 Tubular photobioreactor 557
35.9 Vertical column photobioreactor 557
35.9.1 Airlift photobioreactors 558
35.9.2 Crucial factors influencing photobioreactor efficiency 558
35.9.3 Light utilization 559
35.9.4 pH control 559
35.9.5 Temperature 560
35.9.6 Carbon dioxide uptake 560
35.9.7 Agitation and mixing 560
35.9.8 Microalgae as potential food supplements 560
35.9.9 Nutraceuticals from microalgae 561
35.9.10 Microalgae as lipid source 561
35.9.11 Microalgae in animal feeds 561
References 562

36. Biomedical applications of algal-based products

Ming-Li Teoh, Wu-Thong Choo, Hazel Jing-Yi Leong and Peter Convey

36.1 Introduction 567
36.2 Bioactive compounds 567
36.2.1 Polysaccharides 568
36.2.2 Amino acids, peptides and proteins 568
36.2.3 Fatty acids 570
36.2.4 Pigments 571
36.2.5 Minerals and vitamins 571
36.2.6 Enzymes 572
36.3 Anticancer and immunomodulatory properties 572
36.4 Antidiabetic activity 573
36.5 Cardioprotective activities 573
36.6 Drug delivery 574
36.7 Tissue engineering 574
36.8 Conclusions 575
References 575

37. Animal feed production from algal bioreactors

Khondokar M. Rahman, Lynsey Melville and Alla Silkina

37.1 Introduction 581
37.2 Upstream and downstream processes 581
37.2.1 Upstream process 581
37.2.2 Harvesting and downstream processes 583
37.2.3 Algal biomass characterization 584
37.3 Policy and regulatory factor to algae cultivation 585
37.3.1 Industrial relevant micro-algae and their safety 585
37.3.2 Food safety of human consumption of *Spirulina* 585
37.3.3 European regulation on marketing of micro-algae for food and feed 585
37.3.4 Regulation on novel foods and novel food ingredients 585
37.4 Economic considerations of microalgae cultivation for animal food and feed 586
37.4.1 Market demand and market value 586
37.4.2 Cost of production 587
37.4.3 Future prospects 589
37.5 Conclusion 589
References 590
Further reading 592

38. Biofertilizers, soil conditioners, and biostimulants from microalgae

Najib EL Mernissi and Hicham EL Arroussi

38.1 Introduction 593
38.2 Microalgae as biofertilizers 594
38.2.1 Overview of biofertilizers 594
38.2.2 Types of biofertilizers that can be used to increase soil fertility 594
38.2.3 Benefits of microalgae as biofertilizers 595
38.3 Microalgae as biostimulants 596
38.3.1 Overview of biostimulants 596

38.3.2 Presentation of the categories of biostimulants 597
38.3.3 Benefits of microalgae as biostimulants 598
38.4 Microalgae as soil conditioners 599
38.4.1 Benefits of microalgae as soil conditioners 600
References 600

39. Biohydrogen production in microalgal bioreactors

Ramachandran Sivaramakrishnan and Aran Incharoensakdi

39.1 Introduction 603
39.2 Photobioreactors 603
39.3 Tubular photobioreactor 604
39.4 Flat-panel photobioreactors 605
39.5 Column photobioreactors 606
39.6 Soft frame photobioreactors 607
39.7 Hybrid photobioreactors 608
39.8 Conclusions 610
Acknowledgments 610
References 610

40. Biodiesel production from algal bioreactors

Islam Md Rizwanul Fattah, Md Mofijur Rahman, Fitranto Kusumo, Oyetola Ogunkunle, Arslan Ahmed, Md Abul Kalam and Teuku Meurah Indra Mahlia

40.1 Introduction 615
40.2 Algal biodiesel production steps 616
40.2.1 Algal strain selection 616
40.2.2 Site selection 617
40.3 Algal bioreactor systems 618
40.4 Algal growth in bioreactors 620
40.4.1 Open-pond bioreactor systems 622
40.4.2 Photobioreactors 622
40.4.3 Hybrid systems 624
40.5 Algae oil production steps in algal bioreactor 624
40.6 Lipid content of algal oil 626
40.7 Steps in microalgae biodiesel production 626
40.7.1 Biomass dewatering, thickening, and drying 626
40.7.2 Pretreatment of algal biomass 628
40.7.3 Lipid extraction 628
40.7.4 Biodiesel production using transesterification 629
40.8 Biodiesel standards 630
40.9 The biorefinery approach and genetic engineering 630
40.10 Conclusion 631
References 632

41. Bioethanol production in algal bioreactors

Melih Onay and Aytun Onay

41.1 Introduction 639
41.2 State of the art 639
41.2.1 Experimental studies for bioethanol production 639
41.2.2 Bioethanol production using microalgae: Machine learning applications and optimization methods 643
41.2.3 Literature survey: Modeling and optimization techniques for enhanced production of bioethanol 644
41.3 Recommendation and future direction 647
References 647

42. Biomethane production in algal bioreactors

Bárbara Rincón

42.1 Introduction 649
42.2 Anaerobic digestion of microalgae. State-of-the-art 650
42.2.1 Factors influencing biogas yields, bottlenecks in the process 652
42.2.2 Biomethane production 655
42.3 Recommendations 655
References 655

Part V
Environmental issues for algal bioreactors

43. Wastewater treatment in algal bioreactors

Sameh S. Ali, Konstantinos Pispas, Tamer Elsamahy, Eirini Sventzouri, Rania Al-Tohamy, Georgios Manthos, Jianzhong Sun and Michael Kornaros

43.1 Introduction 661
43.2 Algal bioreactor systems 663

43.2.1 Types of algal bioreactors 663
43.2.2 Design considerations for algal bioreactors 665
43.3 Wastewater characterization and pretreatment 673
43.3.1 Composition of wastewater 673
43.3.2 Pretreatment requirements 673
43.3.3 Removal of toxic compounds 674
43.3.4 Nutrient removal and recovery 674
43.4 Pollutant removal mechanisms 675
43.4.1 Nutrient uptake and assimilation 675
43.4.2 Removal of organic matter 675
43.4.3 Heavy metal and pollutant sequestration 676
43.4.4 Pathogen removal and disinfection 678
43.5 Challenges and future perspectives 678
43.5.1 Technological challenges and limitations 678
43.5.2 Future research directions and opportunities 679
43.6 Conclusion 680
References 680

44. Emerging pollutants treatment in algal bioreactors

Xiaoyan Wang and Yu Hong

44.1 Introduction 685
44.2 Emerging pollutants 686
44.2.1 Emerging pollutants types and characteristics 686
44.2.2 Emerging pollutants treatment approaches 687
44.2.3 Emerging pollutants analytical method 687
44.3 Algal-based system for removal of emerging pollutants 687
44.3.1 Working mechanism 687
44.3.2 Algae screening 688
44.3.3 Removal performance 688
44.4 Algal bioreactors for emerging pollutants treatment 689
44.4.1 Open bioreactors 690
44.4.2 Closed bioreactors 690
44.4.3 Influencing factors 690
44.5 Research challenges and future perspectives 691
44.6 Conclusion 692
Acknowledgments 692
References 692

45. Algal bioreactors as strategies for heavy metal phycoremediation

Karina G. Coronado-Apodaca, Celestino García-Gómez, David A. Buentello-Montoya and Manuel Martínez-Ruiz

45.1 Introduction 695
45.2 State-of-the-art 696
45.2.1 Mechanisms of heavy metal removal by microalgae 697
45.2.2 Operational factors that influence heavy metal removal by microalgae 699
45.2.3 Bioreactor configurations used for pilot-scale microalgae-based heavy metal removal processes 703
45.3 Recommendations 707
References 707

46. Greenhouse gas control in algal bioreactors

Rosangela Rodrigues Dias, Mariany Costa Deprá, Darissa A. Dutra, Adriane T. Schneider, Richard L.S. Machado and Eduardo Jacob-Lopes

46.1 Introduction 711
46.2 Carbon dioxide mitigation technologies 711
46.3 Microalgae-mediated carbon dioxide capture and utilization 713
46.3.1 Microalgae bioreactors for carbon dioxide capture 713
46.4 Approaches to improve carbon capture by microalgae 714
46.5 Conclusion 715
References 715

47. Carbon neutral in algal bioreactors: Is this possible?

Rosangela Rodrigues Dias, Mariany Costa Deprá and Eduardo Jacob-Lopes

47.1 Introduction to the climate emergency 717
47.2 Carbon footprint in microalgae-based systems 717
47.3 Roadmap to net-zero emissions in microalgae-based systems 718
47.4 Deficits in microalgae-based systems 719
47.5 Conclusion 720
References 720

48. Avoiding snowballs in algal biotechnology: How can the environmental assessment of bioreactors predict black swans in sustainable bioprocesses? 723

Mariany Costa Deprá, Adriane Terezinha Schneider, Darissa Alves Dutra, Richard Luan Silva Machado and Eduardo Jacob-Lopes

48.1 Introduction 723

48.2 Bioreactors—the core of algal biotechnology 724

48.3 Environmental performance of algal bioreactors 725

48.4 Conclusion, research gaps, and way forward 727

References 727

Index 731

WOODHEAD SERIES IN BIOENERGY

Algal Bioreactors, Volume 1: Science, Engineering and Technology of Upstream Processes is the first book of a two-volume set that provides all the knowledge needed to design, develop, and operate algal bioreactors for bioenergy and renewable resource production. Supported by critical parameters and properties, mathematical models and calculations, methods, and practical real-world case studies, readers will find everything they need to know about algal bioreactors' upstream and downstream processes for renewable resource production.

Divided into five parts, Volume 1 addresses all the fields of upstream processes in algal bioreactors. Part I explains the fundamental aspects of algal bioreactors, focusing on the global market potential and innovation for algal bioenergy and bioproducts. Part II examines the science and engineering features of algal bioreactors, with models and practical examples of the optimal conditions for algae growth, kinetic parameters, hydrodynamic performance, contamination control, and all other considerations for the development and operation of bioreactors. Part III analyzes the trends in algal bioreactor design for algal upstream processes, including consolidated models such as raceway ponds, industrial fermenters, air-lifts, columns, tubular, and flat-plates, and further variances, as well as emerging designs as hybrid and non-conventional photobioreactors. Part IV discusses the bioproducts and bioenergy obtained from algal bioreactors, while Part V explores the key criteria for operating algal bioreactors from an environmental and sustainable point of view.

Bringing together renowned experts in microalgal biotechnology, *Algal Bioreactors, Volume 1: Science, Engineering and Technology of Upstream Processes* will help researchers, scientists, and engineers from academia and industry to overcome barriers and advance the production of bioenergy and renewable resources from algae. Students will also find invaluable explanations of the fundamentals and key principles of algal bioreactors, making it an accessible read for engineering, microbiology, biochemistry, biotechnology, and environmental sciences students.

Key features:

- Explains scientific, engineering, and technology aspects for main configurations and designs of algal bioreactors, presenting recent innovations and future trends
- Covers the major research streams obtaining bioenergy and bioproducts from algal bioreactors
- Provides state-of-the-art research at various scales to demonstrate the practical implementation of the various technologies and bioreactor designs discussed
- Includes recent findings and often excluded areas in algal bioreactors research available in a single source

About the Editors:

Eduardo Jacob-Lopes

Food Science and Technology Department, Federal University of Santa Maria, Santa Maria, Brazil

Leila Queiroz Zepka

Food Science and Technology Department, Federal University of Santa Maria, Santa Maria, Brazil

Mariany Costa Deprá

Food Science and Technology Department, Federal University of Santa Maria, Santa Maria, Brazil

ELSEVIER

WP
WOODHEAD PUBLISHING
An imprint of Elsevier
elsevier.com/books-and-journals

ISBN 978-0-443-14058-7

9 780443 140587

WOODHEAD SERIES IN BIOENERGY



ALGAL BIOREACTORS

SCIENCE, ENGINEERING AND TECHNOLOGY OF DOWNSTREAM PROCESSES

VOLUME 2

Edited by
EDUARDO JACOB-LOPES
LEILA QUEIROZ ZEPKA
MARIANY COSTA DEPRÁ

Series Editor
YVES GAGNON

ELSEVIER

Algal Bioreactors

This page intentionally left blank

Woodhead Series in Bioenergy

Algal Bioreactors

Science, Engineering and Technology of Downstream Processes

VOLUME 2

Series Editor

Yves Gagnon
Université de Moncton, Moncton, Canada

Edited by

Eduardo Jacob-Lopes
Department of Food Technology and Science, Federal University of Santa Maria, Santa Maria, Brazil

Leila Queiroz Zepka
Department of Food Technology and Science, Federal University of Santa Maria, Santa Maria, Brazil

Mariany Costa Deprá
Department of Food Technology and Science, Federal University of Santa Maria, Santa Maria, Brazil



WP
WOODHEAD PUBLISHING
An imprint of Elsevier

Woodhead Publishing is an imprint of Elsevier
50 Hampshire Street, 5th Floor, Cambridge, MA 02139, United States
125 London Wall, London EC2Y 5AS, United Kingdom

Copyright © 2025 Elsevier Ltd. All rights are reserved, including those for text and data mining, AI training, and similar technologies.

Publisher's note: Elsevier takes a neutral position with respect to territorial disputes or jurisdictional claims in its published content, including in maps and institutional affiliations.

No part of this publication may be reproduced or transmitted in any form or by any means, electronic or mechanical, including photocopying, recording, or any information storage and retrieval system, without permission in writing from the publisher. Details on how to seek permission, further information about the Publisher's permissions policies and our arrangements with organizations such as the Copyright Clearance Center and the Copyright Licensing Agency, can be found at our website: www.elsevier.com/permissions.

This book and the individual contributions contained in it are protected under copyright by the Publisher (other than as may be noted herein).

Notices
Knowledge and best practice in this field are constantly changing. As new research and experience broaden our understanding, changes in research methods, professional practices, or medical treatment may become necessary.

Practitioners and researchers must always rely on their own experience and knowledge in evaluating and using any information, methods, compounds, or experiments described herein. In using such information or methods they should be mindful of their own safety and the safety of others, including parties for whom they have a professional responsibility.

To the fullest extent of the law, neither the Publisher nor the authors, contributors, or editors, assume any liability for any injury and/or damage to persons or property as a matter of products liability, negligence or otherwise, or from any use or operation of any methods, products, instructions, or ideas contained in the material herein.

ISBN: 978-0-443-14059-4

For information on all Woodhead Publishing publications visit our website at https://www.elsevier.com/books-and-journals

Publisher: Megan Ball
Acquisitions Editor: Peter Adamson
Editorial Project Manager: Ellie Barnett
Production Project Manager: Kamesh R.
Cover Designer: Mark Rogers

Typeset by TNQ Technologies



Contents

Contributors xiii
About the editors xvii
Foreword xix
Preface xxi

Part I
Fundamentals of algal downstream processes

1. Conventional and advances approaches in algal downstream processes

Richard Luan Silva Machado, Adriane Terezinha Schneider, Rosangela Rodrigues Dias, Mariany Costa Deprá, Leila Queiroz Zepka and Eduardo Jacob-Lopes

1.1 Introduction 3
1.2 Technologies for harvesting microalgae 3
1.2.1 Sedimentation 4
1.2.2 Coagulation–flocculation 4
1.2.3 Centrifugation 5
1.2.4 Flotation 5
1.2.5 Filtration membranes 5
1.3 Pretreatment and extraction of specific molecules from microalgae biomass 6
1.3.1 Drying 6
1.3.2 Cellular rupture mechanisms 7
1.3.3 Pigment extraction 8
1.3.4 Protein extraction 9
1.3.5 Fatty acid extraction 9
1.3.6 Carbohydrate extraction 10
1.4 Encompassing the downstream cost of employing dry versus wet biomass from microalgae 10
1.5 Pondering downstream processing and its environmental impact 11
1.6 Future perspectives and conclusion 11
References 12

2. Importance of biological knowledge in the downstream of microalgae-based processes and products

Bunushree Behera, Supraja Kolli Venkata, Mari Selvam S. and Prangya Ranjan Rout

2.1 Introduction 17
2.2 Framework of downstream techniques for microalgae-based biorefinery 19
2.2.1 Algal harvesting strategies 19
2.2.2 Processing of algal biomass into biofuel and value-added products 22
2.3 Factors influencing the selection of microalgal downstream strategies 25
2.3.1 Algal morpho-physiology and biochemical properties 25
2.3.2 Operational process parameters during algal cultivation 25
2.4 Scale-up of microalgal downstream strategies 26
2.4.1 Biological constraints in algal processes 26
2.4.2 Insights into enviro-economic constraints in algal processes 27
2.5 Conclusion and future perspectives 29
Acknowledgment 31
References 31

3. The importance of downstream processes in algal biorefinery concept

Benan İnan, Anıl Tevfik Koçer, Gülcan Ayşin Karaca, Beyza Karacaoğlu and Didem Balkanlı

3.1 Introduction 37
3.2 Algal biorefinery 38
3.3 Downstream processes in algal biorefinery 40
3.3.1 Cell disruption 40
3.3.2 Harvesting 44
3.3.3 Drying 45
3.3.4 Extraction 46

3.3.5 Separation and purification 48
3.4 Challenges and future prospects 49
3.5 Conclusions 49
References 49

Part II
Engineering and technology approach to harvesting, dewatering, and drying in algal processes

4. Implementation of gravity sedimentation in microalgae downstream processes: Principles, advances, and challenges

Zahra Shokravi and Hoofar Shokravi

List of abbreviations 59
4.1 Introduction 59
4.2 Basic principle, advantage, and disadvantages of gravity sedimentation 60
4.3 Factors influencing on sedimentation process efficiency 61
4.3.1 Size and shape of microalgae cells 61
4.3.2 Particles density 61
4.3.3 Zeta potential 62
4.3.4 pH 62
4.3.5 Ionic strength 62
4.3.6 Growth phase of microalgae 62
4.4 Enhancing sedimentation process 63
4.4.1 Improving sedimentation process with flocculation 63
4.4.2 Enhancing sedimentation process with floatation 65
4.4.3 Enhancing settling velocity with sedimentation tanks 65
4.4.4 Enhancing sedimentation process with lamellar separators 66
4.4.5 Enhancing sedimentation process with biomass recycling 67
4.5 Conclusion 67
References 67

5. Current progress on filtration techniques for recovery of microalgae-based products

Zubair Hashmi, Fahrurrozi, Juliana Zaini, Jun Wei Lim, Muhammad Saifullah Abu Bakar, Asep Bayu Dani Nandiyanto and Muhammad Roil Bilad

5.1 Introduction 71
5.2 Membrane photobioreactors 72
5.2.1 Carbonation membrane photobioreactor (C-MPBR) 72
5.2.2 Gas–liquid membrane contactor 73
5.2.3 Oxygen permeation membrane photobioreactor 75
5.2.4 Biomass retention membrane photobioreactor 76
5.2.5 Bacteria–microalgae consortia 77
5.2.6 Dialysis membrane photobioreactor 78
5.3 Microalgae harvesting 78
5.3.1 Membrane technology for microalgae harvesting 80
5.3.2 Pressure-driven membrane process 81
5.3.3 Filtration processes 82
5.4 Influential factors in microalgae filtration 86
5.4.1 Membrane pore size 86
5.4.2 Membrane surface properties 87
5.4.3 Pore interconnection 87
5.4.4 Membrane modifications 87
5.4.5 Surface patterning 88
5.4.6 Membrane materials 88
5.4.7 Microalgae species 89
5.5 Membrane fouling in microalgae filtration 89
5.6 Conclusion 91
References 91

6. Existing and emerging flotation methods for harvesting algae

Corey A. Laamanen, Claire A. Fawcett, Gerusa N.A. Senhorinho and John A. Scott

6.1 Introduction 99
6.2 Bulk harvesting 100
6.2.1 Centrifugation 100
6.2.2 Filtration and membrane separation 101
6.2.3 Gravity sedimentation 101
6.3 Flotation 101
6.4 Types of flotation 102
6.4.1 Dissolved air flotation 102
6.4.2 Dispersed air flotation 102
6.4.3 Electro-coagulation-flotation 105
6.4.4 Ballasted flotation 105
6.4.5 Modifications of flotation systems 106
6.4.6 Other methods of increasing efficiency 106
6.5 Coagulants 106

6.5.1 Metallic salts 107
6.5.2 Polymers 107
6.5.3 Cetyl trimethyl ammonium bromide 107
6.5.4 Autoflocculation 107
6.5.5 Bioflocculation 108
6.5.6 Cocultivation 108
6.5.7 Heating 108
6.5.8 Physical coagulation 108
6.6 Operational parameters 109
6.6.1 pH 109
6.6.2 Salinity 109
6.6.3 Bubbles 109
6.6.4 Microalgae cells 110
6.7 Recommendations 110
References 110

7. Recent advancements of coagulation–flocculation in microalgal downstream processes

Sabeela Beevi Ummalyma

7.1 Introduction 115
7.2 Different flocculation process 116
7.2.1 Physicochemical flocculation 116
7.3 Bioflocculation 118
7.3.1 Flocculation by algae–algae interaction 118
7.3.2 Bioflocculation induced by microorganism 119
7.4 Future perspectives 121
7.5 Conclusion 121
References 122

8. Advances in primary recovery for algae bioreactors: The centrifugation role

Jiajiang Zhou, Li Tong and Haixin Guo

8.1 Introduction 125
8.2 Algae harvesting methods 126
8.2.1 Centrifugation 126
8.2.2 Flotation 128
8.2.3 Flocculation 128
8.2.4 Sedimentation 129
8.2.5 Filtration 129
8.2.6 Screening 130
8.3 Centrifugation 131
8.3.1 Centrifuge type 131
8.3.2 Energy consumption and the economy 132
8.4 Challenges and opportunities 133
8.5 Conclusion 134
References 134

9. Conventional drying methods to algal biomass: Their applications and recent advances

Al Rey C. Villagracia, Hui Lin Ong, Alvin B. Culaba and Joel L. Cuello

9.1 Introduction 139
9.2 Drying algal biomass 140
9.2.1 Moisture ratio and drying rate 142
9.2.2 Advantages and disadvantages 143
References 147
Further reading 147

Part III
Cell rupture, extraction, and separation/purification methods of algal target molecules

10. Bead milling for algal cell disruption

Wanida Pan-utai, Penjit Srinophakun, Anusith Thanapimmetha and Hataichanok Kantrong

10.1 Introduction 151
10.2 Principle of algal cell disruption by bead milling 151
10.2.1 Types of bead mill 152
10.2.2 Energy consumption 155
10.3 Bead milling reactor 156
10.3.1 Factors affecting the cell disintegration process 157
10.4 Bioproducts from algal bead milling 158
10.5 Final consideration 161
References 162

11. Applications of pulsed electric field treatment in downstream processing of microalgae biomass

Christian (Adrian) Gusbeth

List of abbreviations 165
11.1 Introduction 165
11.2 Application of PEF technology in biotechnology 167
11.3 PEF technology in the algal biorefinery 169
11.4 Biological mechanisms involved in protein recovery and lipid extraction after PEF pretreatment 171
11.5 Recovery of carbohydrates and pigments 173
11.6 Upscaling from lab-scale to 200 L PBR pilot plant 175
11.7 Summary 176
References 176

12. Cycles of freeze-thawing as an efficient method to microalgal cell disruption

Supenya Chittapun, Theppanya Charoenrat and Chatchol Kongsinkaew

12.1 Introduction 181
12.2 Cell disruption methods 181
12.2.1 Limitations and challenges in cell disruption methods 181
12.3 Freeze-thawing: Principle and mechanism 183
12.3.1 Impact of freezing and thawing on microalgal cells 183
12.3.2 Benefits of freeze-thawing cell disruption 185
12.3.3 Limitations and challenges 185
12.4 Improving the extraction efficiency of freeze-thawing by increasing the number of cycles 186
12.4.1 Frequency of freeze-thaw cycles depending on cell wall structure 186
12.4.2 C-PC determination after freeze-thaw approach 188
12.4.3 Experimental setting up for the optimal number of freeze-thaw cycles 188
12.5 Increase cell disruption efficacy via the combination of freeze-thawing with other methods 189
12.5.1 Mechanical cell disruption methods combined with freeze-thawing 190
12.5.2 Nonmechanical cell disruption method combined with freeze-thawing 191
12.6 Conclusion 192
Acknowledgments 193
References 193

13. Osmotic shock pretreatment: an alternative cell disruption for extraction from wet microalgal biomass

Vandana Radhakrishnan, Sandu Sai Ranjith, K. Anaswara, Tharunkumar Jayakumar, Bobita Ray, Dolly Wattal Dhar and Suchitra Rakesh

13.1 Introduction 197
13.2 Cell disruption techniques 198
13.3 Comparison of various cell disruption methods 198
13.4 Osmotic shock pretreatment in freshwater microalgae 201
13.5 Osmotic shock pretreatment in marine microalgae 201
13.6 Impact of osmotic shock on cell physiology and cell wall integrity 202
13.7 Effect of osmotic shock on the yield of biomolecules 202
13.7.1 Carbohydrates 202
13.7.2 Lipids 203
13.7.3 Proteins 203
13.8 Merits and demerits of osmotic shock pretreatment 204
13.9 Perspectives and future directions 204
13.10 Conclusions 205
References 205

14. Enzymatic treatment for biological disruption of algal cells

Antonio Zuorro, Jefferson E. Contreras-Ropero, Janet B. Garcíá-Martínez and Andrés F. Barajas-Solano

14.1 Introduction 209
14.2 Enzyme selectivity and efficiency 210
14.3 Reaction conditions 211
14.4 Comparison between traditional methods and enzymatic hydrolysis 211
References 212

15. Surface-active agents for the disruption of algal cell walls: An alternative for lipid extraction

Sharmin Yousuf Rikta, Hosney Jahan Sraboni and Ehsanur Rahman

15.1 Introduction 215
15.2 Existing methods of microalgal cell disruption and lipid extractions 216
15.2.1 Microalgal cell disruption methods 216
15.2.2 Limitations of existing cell disruption methods 218
15.2.3 Lipid extraction methods 219
15.3 Surface-active agents: New alternative approach of lipid extraction 221
15.3.1 Mechanism of microalgal cell disruption by surface-active agents/ surfactants 222
15.3.2 Advantages of surfactant-assisted lipid extraction method 223

15.3.3 Cationic surface-active agents for lipid extraction 223
15.3.4 Anionic and nonionic surface-active agents for lipid extraction 224
15.4 Future prospects of surface-active agents for microalgal lipid extraction 226
15.5 Conclusion 227
References 227

16. Microwave pretreatment: A promising strategy to improve the clean extraction yield of microalgae-based products

Mary Leema J. Thilakan, Sakkarapani Amsaveni and Gopal Dharani

List of abbreviations 233
16.1 Introduction 233
16.2 Microwave-assisted extraction instrumentation and operation parameters 234
16.3 MAE pretreatment of algal biomass with water and water-based buffers 236
16.3.1 Phycobiliproteins 236
16.3.2 Alkali-assisted MW pretreatment 236
16.3.3 MAE treatment with solvents 238
16.4 MAE treatment with ionic liquids 242
16.5 Combination of MAE with other green processes for microalgal pretreatment 242
16.6 Recent trends and future perspectives for MAE pretreatment of microalgae 243
16.7 Challenges in MAE pretreatment of microalgae 243
16.8 Summary 243
Acknowledgments 245
References 245

17. Ultrasound-assisted extraction: Benefits and drawbacks in obtaining algal extracts

María Janeth Rodríguez-Roque, Ndahita de Dios-Ávila, Mayra Cristina Soto-Caballero, David Neder-Suarez and Rogelio Sánchez-Vega

17.1 Introduction 249
17.2 Overview of the extraction techniques and algal extracts 250
17.3 Ultrasound-assisted extraction 251
17.3.1 Principle and working mechanism 251
17.3.2 Factors influencing the UAE 251
17.3.3 Equipment to carry out the UAE 255
17.4 Application of UAE in algae 255
17.4.1 Examples of the application of UAE in algae 255
17.4.2 Advantages 255
17.4.3 Drawbacks 256
17.5 Comparison of UAE with other extraction techniques 256
17.6 Innovations in UAE and future trends 257
17.7 Conclusions and recommendations 258
References 258

18. Supercritical fluids for extraction of microalgae-based products

Rabinder Singh, Mohammed Rehmanji, Neeru Gupta, Gourav Kumar, Asha Arumugam Nesamma and Pannaga Pavan Jutur

18.1 Introduction 261
18.2 Supercritical fluid extraction of pigments from microalgae 262
18.3 Extraction of total lipid from microalgae using supercritical fluid extraction 263
18.3.1 Downstream processing of EPA and DHA via SFE 265
18.4 Recent advancement in extraction methods of HVRs 265
18.4.1 Traditional extraction methodologies 265
18.4.2 Emerging extraction methodologies 266
18.5 Conclusions 268
Acknowledgments 268
References 269

19. Principles and applications of hydrothermal liquefaction of microalgae

Amarjeet Bassi

19.1 Introduction 273
19.2 Principles of hydrothermal liquefaction 273
19.2.1 Products from HTL 274
19.2.2 Hydrothermal processing 274
19.2.3 The HTL reactor 274
19.2.4 Microalgae 275

19.2.5 Microalgae pretreatment 275
19.2.6 Parameters affecting HTL processing of microalgae 276
19.2.7 Solvent 276
19.2.8 Catalysts 276
19.3 Process schematic for HTL of microalage 277
19.4 Current studies of hydrothermal liquefaction of microalgae 277
19.4.1 Wastewater and mixed substrates 277
19.4.2 Upgrading of biocrude 278
19.5 Modeling of HTL kinetics 278
19.6 Life cycle analysis 278
19.7 Conclusions and future directions 278
References 279
Further reading 280

20. Techniques of adsorption, partition, ion exchange, and molecular exclusion for separation of microalgal extracts: Chromatography approaches

Raquel Guidetti Vendruscolo and Nathália de Andrade Neves

20.1 Introduction 281
20.2 Adsorption 282
20.3 Partition 283
20.4 Ion exchange and molecular exclusion 285
20.5 Conclusion 287
References 287

21. Advances in separation by ionic strength: Association of chromatography and ionic liquids or deep eutectic solvents for the purification of microalgae-based products

Nathalia Vieira Porphirio Veríssimo, Cassamo Usemane Mussagy, Júlio Gabriel Oliveira de Lima and Valéria de Carvalho Santos-Ebinuma

21.1 Introduction 291
21.2 ILs and DESs for bioseparations 292
21.3 Supported ILs and DESs for chromatographic matrices 293
21.3.1 ILs in chromatographic matrices 295
21.3.2 DESs in chromatographic matrices 297
21.4 Recovery of bioproducts from algae biomass using ILs and DESs integrated with chromatography 299
21.5 Recommendations 301
References 302

Part IV
Techno-economic, sustainable strategies, and innovations for algal downstream processes

22. Techno-economic analysis of downstream processing of microalgae

Maame A. Korsah, Theophilus Gyau, Daron Lyon and Michael K. Danquah

22.1 Introduction 309
22.2 Large-scale microalgae upstream cultivation methods 310
22.3 Downstream processing methods 311
22.4 Economic analysis of the process technology 315
22.5 Conclusion 318
References 318

23. Process intensification approaches applied to the extraction of microalgae-based molecules

Carolina E. Demaman Oro, Maicon Sérgio N. dos Santos, João Henrique C. Wancura, Marcus V. Tres and Giovani L. Zabot

23.1 Introduction 323
23.2 Compounds of interest in microalgae and applications 324
23.3 Extraction methods 325
23.4 Technological development of the considered platforms 325
23.5 Final considerations and future perspectives 326
References 327

24. Recent patents and relevant innovations in downstream processes of the microalgae

Cao Xupeng

24.1 Introduction 331
24.2 Brief review of recent patents related to microalgae 332
24.3 Downstream processing–related patents 332
24.3.1 Enzymes for easy biomass utilization 332
24.3.2 Introduction of deep eutectic solvent (DES) and other new solvents 332
24.3.3 The successive or recycled productions of microalgae and bacteria 336
24.3.4 Some instruments for microalgae biomass treatments 337
24.4 Summary 337
References 337

Index 339

WOODHEAD SERIES IN BIOENERGY

Algal Bioreactors, Volume 2: Science, Engineering and Technology of Downstream Processes is the second book of a two-volume set that provides the knowledge needed to design, develop, and operate algal bioreactors for bioenergy and renewable resource production. Supported by critical parameters and properties, mathematical models and calculations, methods, and practical real-world case studies, readers will find everything they need to know about algal bioreactors' upstream and downstream processes for renewable resource production.

Divided into four parts, Volume 2 addresses all fields of the downstream processes in algal bioreactors. Part I explains the scientific fundamentals of downstream processes, including principles of basic biological knowledge and conventional and advanced procedures. Part II examines the engineering and technology approaches to harvesting, dewatering, and drying in algal processes, discussing conventional and alternative methods. Part III critically evaluates a range of methods for cell rupture, extraction, and separation/purification methods of algal target-molecules. Finally, Part IV discusses techno-economic, sustainable strategies, and innovations for algal downstream processes.

Bringing together renowned experts in microalgal biotechnology, *Algal Bioreactors, Volume 2: Science, Engineering and Technology of Downstream Processes* will help researchers, scientists, and engineers from academia and industry to overcome barriers and advance the production of bioenergy and renewable resources from algae. Students will also find invaluable explanations of the fundamentals and key principles of algal bioreactors, making it an accessible read for engineering, microbiology, biochemistry, biotechnology, and environmental sciences students.

Key features:

- Explains the physical, biological, environmental, and economic parameters of downstream processes in the operation and development of algal bioreactors
- Critically reviews the techniques for harvesting, dewatering, and drying, as well as extraction and purification methods, and process yields
- Enlists the less explored areas of extraction and recovery of algal target-molecules for bioenergy and renewable resource production
- Provides state-of-art research for techno-economic and sustainable strategies, beyond innovations for algal downstream processes

About the Editors:

Eduardo Jacob-Lopes

Food Science and Technology Department, Federal University of Santa Maria, Santa Maria, Brazil

Leila Queiroz Zepka

Food Science and Technology Department, Federal University of Santa Maria, Santa Maria, Brazil

Mariany Costa Deprá

Food Science and Technology Department, Federal University of Santa Maria, Santa Maria, Brazil

ELSEVIER

WP
WOODHEAD PUBLISHING
An imprint of Elsevier
elsevier.com/books-and-journals

ISBN 978-0-443-14058-4

9 780443 140594